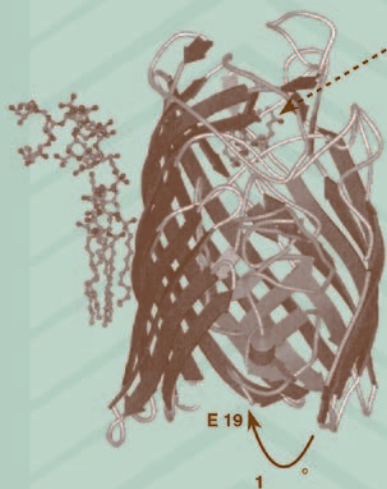


MOLECULAR AND CELLULAR IRON TRANSPORT



edited by
Douglas M. Templeton

ISBN: 0-8247-0621-8

This book is printed on acid-free paper.

Headquarters

Marcel Dekker, Inc.
270 Madison Avenue, New York, NY 10016
tel: 212-696-9000; fax: 212-685-4540

Eastern Hemisphere Distribution

Marcel Dekker AG
Hutgasse 4, Postfach 812, CH-4001 Basel, Switzerland
tel: 41-61-261-8482; fax: 41-61-261-8896

World Wide Web

<http://www.dekker.com>

The publisher offers discounts on this book when ordered in bulk quantities. For more information, write to Special Sales/Professional Marketing at the headquarters address above.

Copyright © 2002 by Marcel Dekker, Inc. All Rights Reserved.

Neither this book nor any part may be reproduced or transmitted in any form or by any means, electronic or mechanical, including photocopying, microfilming, and recording, or by any information storage and retrieval system, without permission in writing from the publisher.

Current printing (last digit):

10 9 8 7 6 5 4 3 2 1

PRINTED IN THE UNITED STATES OF AMERICA

Preface

Iron is essential for life but presents the living organism with a number of challenges. It is prone to oxidation and hydrolysis in the environment, and this severely restricts its bioavailability. Its low solubility creates difficulties for acquisition and transport. The rich redox chemistry that underlies many of iron's essential biological functions at the same time poses a hazard that has resulted in highly evolved mechanisms of transport. The problem of providing iron safely at the intracellular sites where it is needed has been solved in various ways throughout evolution, from binding by bacterial siderophores, to redox-dependent transport across cell membranes, to transport through the circulatory systems of higher animals in a protein-bound form.

Over the past several years, remarkable new insights have been gained into the molecular mechanisms and physiological regulation of iron transport. Details of release of iron from transferrin have become known, and transferrin-independent mechanisms of iron uptake in mammalian cells have been widely studied. Work with iron transport systems in bacteria and yeast has revealed surprising homologies with those operating in higher organisms, and among other issues has helped to elucidate the role of copper in iron transport. Identification of the gene mutated in human hereditary hemochromatosis provided the first new insights to emerge in several decades into regulation of intestinal iron transport, and heralded the identification of other molecular participants in the process. Animal models, both naturally occurring and genetically engineered, have been exploited with great effect to elucidate the phenotypic importance of the molecules of iron transport, and to gain insight into a number of related human diseases. It is timely to bring together in this volume the present state of our knowledge of how living organisms deal successfully—and at times unsuccessfully—with the problems of iron transport.

Initial chapters deal with chemical aspects of iron as they influence its role in biology. The molecules of iron transport, from microbial siderophores and cation pumps to mammalian transferrins, are presented; recently identified iron transport

proteins of the cell membrane, such as DMT1/Nramp2, hephaestin, Ireg1/ferroportin, and mitochondrial frataxin are dealt with in detail. Cellular features of iron transport are covered, including uptake by plant cells, bacteria, and yeast, through siderophore-mediated and non-siderophore-dependent processes. Transferrin-dependent and independent mechanisms in mammalian cells and various organ systems are considered. Several chapters deal with the physiology of human iron transport and its delivery to target tissues, both erythroid and nonerythroid. Subsequent chapters address animal models and several human disorders that are caused by, or result in, altered iron transport. These include hemochromatosis, in which transport of iron across the intestinal epithelium is dysregulated; transfusional iron overload, in which transferrin may become saturated and transport of non-transferrin-bound iron becomes important; and aceruloplasminemia, in which iron transport to the bone marrow is impaired. Therapeutic chelators are used to transport iron out of the body in some of these disorders; in part, their design has been based on structures of the siderophores that bacteria use to acquire iron.

The chapters in this book were written by experts who have contributed seminal findings that have given us a much more sophisticated understanding of iron transport than we had a decade ago. I am grateful that their thoughtful input has allowed us to produce a work on the subject that is definitive at this time. Nevertheless, the rapid pace of discovery in the field of iron transport continues, and this is evidenced by several studies that appeared while this book was in production. Of note are the recent discussions of hepcidin (1), SFT (2), and *Dcytb* (3). It seems that iron biology still holds secrets that will challenge and fascinate us for some time to come.

Doug Templeton

REFERENCES

1. Nicolas G, Bennoun M, Devaux I, Beaumont C, Grandchamp B, Kahn A, Vaulont S. Lack of hepcidin gene expression and severe tissue overload in upstream stimulator factor (USF2) knockout mice. *Proc Natl Acad Sci* 2001; 98:8780–8785.
2. Knutson MD, Levy JE, Andrews NC, Wessling-Resnick M. Expression of SFT in HFE knockout mice. *J Nutr* 2001; 131:1459–1464.
3. McKie AT, Barrow D, Latunde-Dada GO, Rolfs A, Sager G, Mudaly E, Mudaly M, Richardson C, Barlow D, Bomford A, Peters TJ, Raja KB, Shirali S, Hediger MA, Farzaneh F, Simpson RJ. An iron-regulated ferric reductase associated with the absorption of dietary iron. *Science* 2001; 291:1755–1759.

Contents

<i>Preface</i>	<i>iii</i>
<i>Contributors</i>	<i>ix</i>
I. Molecular Aspects of Iron Transport	
1. Iron Chemistry <i>Wesley R. Harris</i>	1
2. Transferrins <i>Ross T. A. MacGillivray and Anne B. Mason</i>	41
3. The Transferrin Receptor <i>Caroline A. Enns</i>	71
4. Molecular Aspects of Release of Iron from Transferrin <i>Qing-Yu He and Anne B. Mason</i>	95
5. Ferritins: Structural and Functional Aspects <i>Paolo Arosio and Sonia Levi</i>	125
6. The Divalent Metal-Ion Transporter (DCT1/DMT1/Nramp2) <i>Hiromi Gunshin and Matthias A. Hediger</i>	155
7. Basolateral Transport of Iron in Mammalian Intestine: From Physiology to Molecules <i>Andrew T. McKie and Robert J. Simpson</i>	175
8. HFE <i>Robert E. Fleming, Robert S. Britton, Abdul Waheed, William S. Sly, and Bruce R. Bacon</i>	189

9.	Regulation of Iron Homeostasis by Iron Regulatory Proteins 1 and 2	207
	<i>Eric S. Hanson and Elizabeth A. Leibold</i>	
10.	Iron-Response Element (IRE) Structure and Combinatorial RNA Regulation	237
	<i>Hans E. Johansson and Elizabeth C. Theil</i>	
11.	Frataxin and Mitochondrial Iron	255
	<i>Pierre Rustin</i>	
12.	Siderophore Chemistry	273
	<i>Alain Stintzi and Kenneth N. Raymond</i>	
13.	Iron Chelator Chemistry	321
	<i>Zu D. Liu and Robert C. Hider</i>	
II. Cellular Iron Transport		
14.	Iron Acquisition in Plants	359
	<i>Elizabeth E. Rogers and Mary Lou Guerinot</i>	
15.	Iron Uptake in Yeast	375
	<i>Orly Ardon, Jerry Kaplan, and Brooke D. Martin</i>	
16.	Bacterial Iron Transport	395
	<i>Volkmar Braun and Klaus Hantke</i>	
17.	Uptake of Transferrin-Bound Iron by Mammalian Cells	427
	<i>Deborah Trinder and Evan Morgan</i>	
18.	Transport of Non-Transferrin-Bound Iron by Hepatocytes	451
	<i>Joel G. Parkes and Douglas M. Templeton</i>	
19.	Iron Acquisition by the Reticuloendothelial System	467
	<i>Günter Weiss</i>	
20.	Iron Transport in the Central Nervous System	487
	<i>Joseph R. Burdo and James R. Connor</i>	
21.	Iron Uptake by Neoplastic Cells	509
	<i>Des R. Richardson</i>	
22.	Novel Methods for Assessing Transport of Iron Across Biological Membranes	539
	<i>Z. Ioav Cabantchik, Silvina Epsztejn, and William Breuer</i>	
III. Physiology of Iron Transport		
23.	Regulation of Intestinal Iron Transport	559
	<i>Gregory J. Anderson and Christopher D. Vulpe</i>	
24.	Regulation of Systemic Iron Transport and Storage	597
	<i>Pierre Brissot, Christelle Pigeon, and Olivier Loréal</i>	

25.	Regulation of Liver Iron Metabolism <i>Gaetano Cairo</i>	613
26.	Iron Utilization in Erythrocyte Formation and Hemoglobin Synthesis <i>Prem Ponka</i>	643
IV. Disorders of Iron Transport		
27.	Animal Models of Iron Transport and Storage Disorders <i>Nancy C. Andrews</i>	679
28.	Hemochromatosis: Diagnosis and Management Following the Discovery of the Gene <i>Paul C. Adams</i>	699
29.	Transfusional Iron Overload <i>Nancy F. Olivieri</i>	725
30.	Aceruloplasminemia <i>Nathan E. Hellman and Z. Leah Harris</i>	749
31.	Hereditary Hyperferritinemia Cataract Syndrome <i>Carole Beaumont and Domenico Girelli</i>	761
32.	Other Disorders of Increased Iron Absorption: Iron Overload in Africans and African Americans <i>Fitzroy W. Dawkins and Victor R. Gordeuk</i>	775
33.	Iron Chelation <i>Chaim Hershko, Gabriela Link, and Avraham M. Konijn</i>	787
	<i>Index</i>	817

Contributors

Paul C. Adams, M.D. Professor, Department of Medicine, London Health Sciences Centre, University of Western Ontario, London, Ontario, Canada

Gregory J. Anderson, Ph.D. Senior Research Officer, Iron Metabolism Laboratory, Queensland Institute of Medical Research, Brisbane, Queensland, Australia

Nancy C. Andrews, M.D., Ph.D. Associate Investigator, Howard Hughes Medical Institute, and Associate Professor, Department of Pediatrics, Children's Hospital and Harvard Medical School, Boston, Massachusetts

Orly Ardon, Ph.D. Department of Pathology, University of Utah, Salt Lake City, Utah

Paolo Arosio, Ph.D. Professor, Department of Chemistry, Faculty of Medicine, University of Brescia, Brescia, Italy

Bruce R. Bacon, M.D. Director, Division of Gastroenterology and Hepatology, and Professor, Department of Internal Medicine, Saint Louis University School of Medicine, St. Louis, Missouri

Carole Beaumont, Ph.D. Director of Research, INSERM U409, Faculté de Médecine Xavier Bichat, Paris, France

Volkmar Braun, Ph.D. Professor, Department of Microbiology/Membrane Physiology, University of Tübingen, Tübingen, Germany

William Breuer, Ph.D. Department of Biological Chemistry, Hebrew University of Jerusalem, Jerusalem, Israel

Pierre Brissot, M.D. Professor of Hepatology, Service des Maladies du Foie et INSERM U-522, University Hospital Pontchaillou, Rennes, France

Robert S. Britton, Ph.D. Associate Research Professor, Department of Internal Medicine, Saint Louis University School of Medicine, St. Louis, Missouri

Joseph R. Burdo, B.S. Department of Neuroscience and Anatomy, Pennsylvania State University College of Medicine/Milton S. Hershey Medical Center, Hershey, Pennsylvania

Z. Ioav Cabantchik, Ph.D. Professor of Biochemistry and Biophysics, Department of Biological Chemistry, Hebrew University of Jerusalem, Jerusalem, Israel

Gaetano Cairo, Ph.D. Professor, Institute of General Pathology and CNR Center of Cellular Pathology, University of Milan, Milan, Italy

James R. Connor, Ph.D. Director, George M. Leader Family Laboratory for Alzheimer's Disease, and Professor and Vice Chair, Department of Neuroscience and Anatomy, Pennsylvania State University College of Medicine/Milton S. Hershey Medical Center, Hershey, Pennsylvania

Fitzroy W. Dawkins, M.D. Associate Professor and Interim Chief, Hematology/Oncology, Department of Medicine, Howard University College of Medicine, Washington, D.C.

Caroline A. Enns, Ph.D. Professor, Department of Cell and Developmental Biology, Oregon Health Sciences University, Portland, Oregon

Silvina Epsztejn, M.Sc. Department of Biological Chemistry, Hebrew University of Jerusalem, Jerusalem, Israel

Robert E. Fleming, M.D. Associate Professor, Department of Pediatrics, Saint Louis University School of Medicine, St. Louis, Missouri

Domenico Girelli, M.D., Ph.D. Assistant, Internal Medicine, Department of Clinical and Experimental Medicine, University of Verona, Verona, Italy

Victor R. Gordeuk, M.D. Center for Sickle Cell Disease, Howard University College of Medicine, Washington, D.C.

Mary Lou Guerinot, Ph.D. Professor, Department of Biological Sciences, Dartmouth College, Hanover, New Hampshire

Hiromi Gunshin, Ph.D. Instructor in Pediatrics, Department of Medicine, Children's Hospital, Harvard Medical School, Boston, Massachusetts

Eric S. Hanson, Ph.D. Instructor, Division of Hematology, Department of Medicine, University of Utah, Salt Lake City, Utah

Klaus Hantke, Ph.D. Department of Microbiology/Membrane Physiology, University of Tübingen, Tübingen, Germany

Wesley R. Harris, Ph.D. Professor, Department of Chemistry, University of Missouri-St. Louis, St. Louis, Missouri

Z. Leah Harris, M.D. Assistant Professor, Department of Anesthesiology and Critical Care Medicine, Johns Hopkins University, Baltimore, Maryland

Qing-Yu He, Ph.D. Research Associate, Department of Biochemistry, College of Medicine, University of Vermont, Burlington, Vermont

Matthias A. Hediger, Ph.D. Associate Professor, Department of Medicine, Brigham and Women's Hospital and Harvard Medical School, Boston, Massachusetts

Nathan E. Hellman, B.Sc. Department of Pediatrics, Washington University School of Medicine, St. Louis, Missouri

Chaim Hershko, M.D. Professor and Chairman, Department of Medicine, Shaare Zedek Medical Center, Jerusalem, Israel

Robert C. Hider, Ph.D. Professor, Department of Pharmacy, King's College London, London, England

Hans E. Johansson, Ph.D. Assistant Research Scientist, Children's Hospital Oakland Research Institute, Oakland, California, and Uppsala University, Uppsala, Sweden

Jerry Kaplan, Ph.D. Department of Pathology, University of Utah, Salt Lake City, Utah

Avraham M. Konijn, Ph.D. Professor, Department of Human Nutrition and Metabolism, Faculty of Medicine, Hebrew University, Jerusalem, Israel

Elizabeth A. Leibold, Ph.D. Associate Professor of Medicine, Divisions of Hematology and Oncology, Eccles Program in Human Molecular Biology and Genetics and Department of Medicine, University of Utah, Salt Lake City, Utah

Sonia Levi, Ph.D. Protein Engineering Unit, IRCCS, H. San Raffaele, Milan, Italy

Gabriela Link, Ph.D. Research Associate, Department of Human Nutrition and Metabolism, Faculty of Medicine, Hebrew University, Jerusalem, Israel

Zu D. Liu, Ph.D. Department of Pharmacy, King's College London, London, England

Olivier Loréal, M.D., Ph.D. Service des Maladies du Foie et INSERM U-522, University Hospital Pontchaillou, Rennes, France

Ross T. A. MacGillivray, Ph.D. Professor, Department of Biochemistry and Molecular Biology, University of British Columbia, Vancouver, British Columbia, Canada

Brooke D. Martin, Ph.D. Department of Pathology, University of Utah, Salt Lake City, Utah

Anne B. Mason, Ph.D. Research Associate Professor, Department of Biochemistry, College of Medicine, University of Vermont, Burlington, Vermont

Andrew T. McKie, Ph.D. Department of Molecular Medicine, King's College London, London, England

Evan Morgan, M.D., Ph.D., D.Sc. Professor Emeritus, Department of Physiology, University of Western Australia, Nedlands, Western Australia, Australia

Nancy F. Olivieri, M.D. Professor, Departments of Pediatrics and Medicine, University of Toronto, Toronto, Ontario, Canada

Joel G. Parkes, Ph.D. Department of Laboratory Medicine and Pathobiology, University of Toronto, Toronto, Ontario, Canada

Christelle Pigeon, Ph.D. Service des Maladies du Foie et INSERM U-522, University Hospital Pontchaillou, Rennes, France

Prem Ponka, M.D., Ph.D. Professor, Lady Davis Institute for Medical Research, Jewish General Hospital, and Departments of Physiology and Medicine, McGill University, Montreal, Quebec, Canada

Kenneth N. Raymond, Ph.D. Professor, Department of Chemistry, University of California, Berkeley, California

Des R. Richardson, Ph.D. Associate Professor of Medicine, Iron Metabolism and Chelation Group, The Heart Research Institute, Sydney, New South Wales, Australia

Elizabeth E. Rogers, Ph.D. Department of Biological Sciences, Dartmouth College, Hanover, New Hampshire

Pierre Rustin, Ph.D. Research Director, CNRS, INSERM U393, Hôpital Necker—Enfants Malades, Paris, France

Robert J. Simpson, D.Phil. Department of Endocrinology, Diabetes, and Internal Medicine, GKT School of Medicine, King's College London, London, England

William S. Sly, M.D. Professor and Chairman, Doisy Department of Biochemistry and Molecular Biology, Saint Louis University School of Medicine, St. Louis, Missouri

Alain Stintzi, Ph.D. Department of Chemistry, University of California, Berkeley, California

Douglas M. Templeton, Ph.D., M.D. Professor, Department of Laboratory Medicine and Pathobiology, University of Toronto, Toronto, Ontario, Canada

Elizabeth C. Theil, Ph.D. Senior Research Scientist, Children's Hospital Oakland Research Institute, Oakland, California

Deborah Trinder, Ph.D. Department of Medicine, Fremantle Hospital, University of Western Australia, Fremantle, Western Australia, Australia

Christopher D. Vulpe, M.D., Ph.D. Department of Nutritional Sciences, University of California, Berkeley, California

Abdul Waheed, Ph.D. Research Professor, Doisy Department of Biochemistry and Molecular Biology, Saint Louis University School of Medicine, St. Louis, Missouri

Günter Weiss, M.D. Professor, Department of Internal Medicine, University Hospital, Innsbruck, Austria

1

Iron Chemistry

WESLEY R. HARRIS

University of Missouri-St. Louis, St. Louis, Missouri

I.	INTRODUCTION	2
A.	Cosmochemistry	2
B.	Geochemistry	3
II.	ELECTRONIC CONFIGURATIONS OF IRON(II) AND IRON(III)	5
A.	<i>d</i> -Orbital Splittings	6
B.	Spin States	7
C.	Ionic Radii	8
D.	Iron Porphyrin Complexes	9
III.	MAGNETIC PROPERTIES	10
A.	Spin Equilibrium	10
B.	Superexchange	11
IV.	ELECTRONIC SPECTRA	13
V.	COMPLEXATION EQUILIBRIA	16
A.	Hard–Soft Acid–Base Characteristics	16
B.	Equilibrium Constants	16
C.	Hydrolysis	18
D.	Chelate Hydrolysis	20
E.	Stability Constants for Ferric Complexes	20
F.	Low-Molecular-Weight Physiological Iron Chelators	22
G.	Ferrous Complexes	24
VI.	ELECTROCHEMISTRY	27
A.	Formal Potentials	27
B.	Effect of Hydrolysis on Redox Chemistry	29
C.	Fenton Chemistry	29

VII.	LIGAND-EXCHANGE KINETICS	31
A.	Reaction Mechanisms	31
B.	Ligand Field Activation Energy	32
C.	Reactions with Multidentate Ligands	33
VIII.	SUMMARY	34
	REFERENCES	35

I. INTRODUCTION

Iron is involved in a wide variety of critical biological functions. The importance of this element in biological systems is such that this entire volume is devoted to only one aspect of iron biochemistry: its transport in biological systems. This chapter does not deal directly with iron transport. Instead, it is intended to serve the reader as a more general primer to aid in understanding the chemical behavior of iron and the methods used in studying this element. Specific information, e.g., on solubility, hydrolysis, and redox activity, is of direct significance to biological transport.

The first and broadest question one might ask is why iron is used so extensively in biological systems. One obvious factor is that the ferric/ferrous redox couple operates within the potential range accessible to organisms in a neutral aqueous environment. This redox chemistry is involved not only in simple electron-transfer reactions, but also in a variety of reactions with molecular oxygen, which range from reversible binding of dioxygen in hemoglobin to oxygen reduction by cytochrome oxidase to the chemical insertion of oxygen into substances by cytochrome P-450. The ferric iron is also an excellent electrophile and is used to activate coordinated waters or substances in hydrolase enzymes such as the purple acid phosphatases. However, these properties are not unique to iron. Both Co^{2+} and Cu^+ have accessible one-electron redox couples and form reversible dioxygen complexes, and Zn^{2+} is used as a Lewis acid in a variety of enzymes. It is likely that the extensive utilization of iron in biological systems is due in large part to the simple fact that there is so much of it in the terrestrial environment.

A. Cosmochemistry

All the elements except hydrogen and helium have been formed by various nuclear reactions that take place within stars (1–4). In a typical star like our sun, energy is produced by the fusion of hydrogen into helium at about 10^7 K, with little formation of heavier elements (5). After about 10 billion years, the accumulation of helium in the core leads to an increase in core density and temperature, and the star changes into a short-lived red giant (2,4). As the core temperature increases to about 10^8 K, the fusion of helium to form large amounts of carbon and oxygen becomes the principal source of energy (1,4).

For stars that are much larger than the sun, the larger mass and resulting higher temperatures cause them to burn their initial hydrogen fuel very quickly and reach the red-giant stage in only about 10 million years (2,5). The core temperatures for these larger stars reach 10^9 K, which is high enough to promote additional exothermic

fusion reactions (1,5). Iron represents the maximum in nuclear binding energy. Thus, only elements up to iron can be produced by these exothermic reactions, and large amounts of iron accumulate in the core of the star (1,4,5). As a result, iron is much more abundant than its transition-metal neighbors: 20 times more abundant than nickel; 100 times more abundant than Cr, Mn, and Co; and 1000 times more abundant than Cu and Zn (Fig. 1) (6).

During the red-giant stage of stellar development, slow neutron capture reactions begin to generate small amounts of elements heavier than iron. Eventually the core collapses and the star explodes to produce a supernova, at which time a series of rapid neutron and proton capture reactions complete the synthesis of the relatively low-abundance, heavier elements from iron to uranium (1,4,5).

B. Geochemistry

Except for a few light elements that can escape the Earth's gravitational field, the composition of the Earth reflects the general cosmic abundances (2). However, due to their different chemical properties, the terrestrial distribution of the elements is very heterogeneous. The Earth consists of three major regions: the core, the mantle, and the crust (7). The central core has a radius of 3471 km and represents 32% of the Earth's total mass (7). It contains 86% iron and 7% nickel as an iron–nickel alloy identified by seismological data. Since it is impossible to actually sample the core, it is difficult to characterize its minor components.

The second layer, the mantle, is 2880 km thick and represents 67% of the Earth's mass. The major elemental components are oxygen (43.7%), silicon (22.5%),

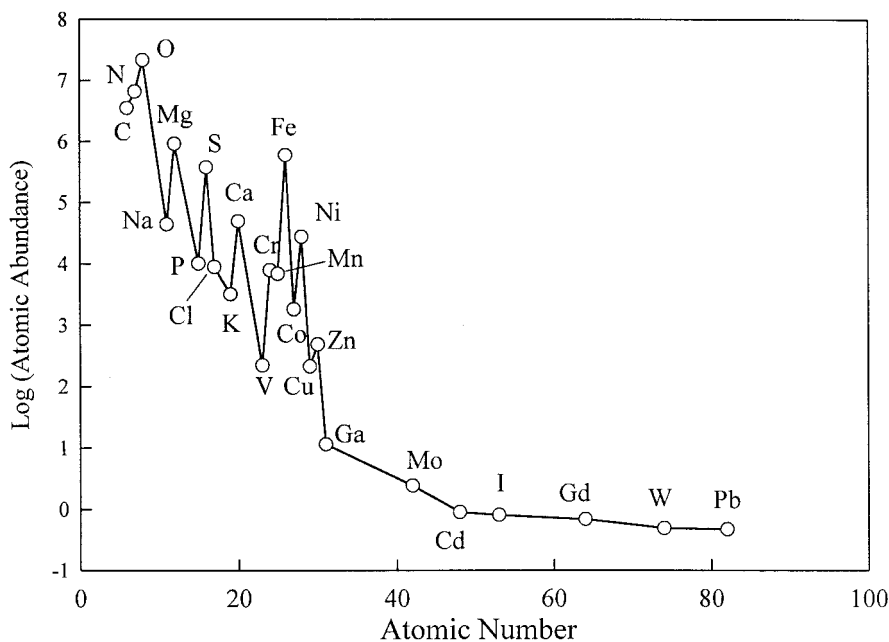


Figure 1 Relative atomic abundances in the universe for selected elements. Values represent the number of atoms of each element per 10^6 silicon atoms. (Based on data from Ref. 6.)

and magnesium (18.8%) (6), which are present primarily as Mg_2SiO_4 (olivine) and MgSiO_3 (pyroxene) (7). The mantle also contains 9.9% iron, 1.7% Ca, and 1.6% Al (6). The crust is a thin, 17-km outer layer. Since the deepest penetration humans have made into the Earth is only about 7 km (7), all of our activities are restricted to this thin coating, and any connection between elemental abundances and biological processes are based on the composition of the crust.

The concentration of selected elements in the crust is shown in Fig. 2 (6). Despite the enormous enrichment of iron in the core, iron remains by far the most abundant transition metal in the crust. Iron is about 100 times more abundant than Mn or Cr, about 350 times more abundant than V, Co, Ni, or Cu, and about 1200 times more abundant than Zn. Thus there is an obvious advantage to the use of iron in biological systems, particularly for oxygen transport, which is not a catalytic process and requires one or two iron atoms for each molecule of dioxygen transported.

In the earliest stages of life on Earth, about 3.5 billion years ago, iron was readily available as Fe^{2+} (8). The atmosphere, produced in large part by volcanic activity, consisted primarily of N_2 , with small amounts of carbon dioxide (8,9). The equilibration of volcanic gases with metallic iron at high temperatures prior to eruption introduced enough H_2 to maintain a steady-state atmospheric concentration of about 0.001 atm, which was enough to ensure that there was essentially no free O_2 (8). High-temperature reactions with volcanic iron and seawater may also have been an important mechanism for reducing CO_2 to CH_4 and N_2 to NH_3 (8). The presence of these reduced forms of carbon and nitrogen is a critical factor in the synthesis of

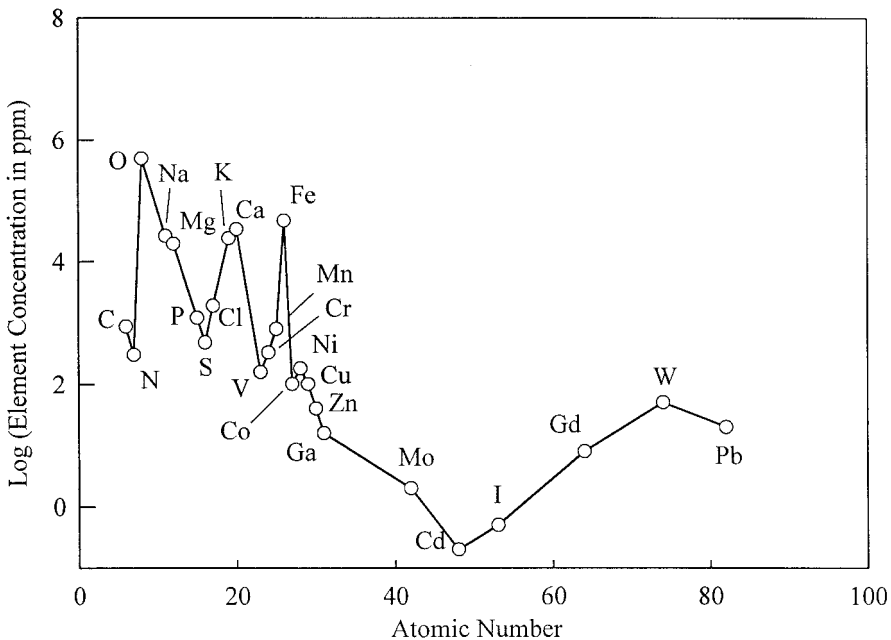


Figure 2 Concentrations (in ppm) of selected elements in the Earth's crust. (Based on data from Ref. 6.)

more complex organic compounds needed for the evolution of living systems by abiotic processes involving electrical discharges and ultraviolet (UV) radiation (8).

In a reducing atmosphere, iron solubility was determined primarily by precipitation reactions involving sulfide and carbonate. Ferrous ion was present at a concentration of about 50 μM (8) in the oceans, where it may have been involved in photochemical reactions that produced additional H_2 and helped maintain an anoxic atmosphere (9). These photochemical reactions would have produced the insoluble Fe^{3+} ion, which may account for the formation of iron deposits between 3.5 and 3 billion years ago.

The course of life on Earth changed dramatically about 3 billion years ago with the appearance of photosynthetic cyanobacteria that could utilize solar energy and in the process liberate molecular oxygen (10). The production of oxygen led to the precipitation of massive amounts of iron between 2.5 and 2 billion years ago (8) to give the deposits of magnetite (Fe_3O_4) and hematite (Fe_2O_3) that today provide the primary commercial iron ores.

By 2 billion years ago, the concentration of atmospheric oxygen was nearing its present level of about 23% (11), and ferrous ion was no longer stable in the oceans. Currently the oceans contain only about 23 nM dissolved iron, primarily as $\text{Fe}(\text{OH})_2^+$ and $\text{Fe}(\text{OH})_4^-$ (12), although they may contain 0.1 mg Fe/L (18 μM) as a suspension of insoluble $\text{Fe}(\text{OH})_3$ (7). Because of the very limited solubility of ferric ion, organisms have been forced to evolve elaborate mechanisms for solubilizing and transporting iron (10,13).

II. ELECTRONIC CONFIGURATIONS OF IRON(II) AND IRON(III)

The oxidation state of iron can vary from $-II$ to $+VI$. The lowest oxidation state is found in the $\text{Fe}(\text{CO})_4^{2-}$ anion, where there is considerable back-donation of negative charge from the metal ion to the π -acceptor carbonyl ligands (14). The highest oxidation state is found in the ferrate anion, FeO_4^{2-} , where extensive π donation occurs from the oxo ligands (15).

Within biological systems, the important oxidation states are iron(II), iron(III), and iron(IV). Iron(IV) is very reactive and is restricted to intermediates formed during enzyme catalytic cycles. The most common form of iron(IV) is the ferryl ion ($\text{Fe}=\text{O}^{2+}$) (16–18). Ferryl porphyrin complexes are formed when ferric–porphyrin–peroxide complexes undergo heterolytic cleavage of the $\text{O}-\text{O}$ bond. This releases O^{2-} and leaves behind a coordinated oxygen atom, which requires two electrons for reduction to a stable O^{2-} ligand. One electron comes from oxidation of Fe(III) to Fe(IV), and the other is obtained by oxidizing either the porphyrin ring or a nearby amino acid side chain to form a cation radical.

Other enzymes such as methane monooxygenase and ribonucleotide reductase contain nonheme dinuclear iron(IV) sites (19). In the active diferrous form, the two irons are five-coordinate and bridged by two carboxylate groups (20,21). Reaction with molecular oxygen gives a reactive intermediate that is thought to contain the so-called diamond core, which consists of two six-coordinate Fe^{4+} ions connected by two bridging oxo ligands and one bridging carboxylate group (22).

These highly reactive iron(IV) compounds can either insert atomic oxygen into a substrate (oxygenase activity) or oxidize a substrate by two electrons (oxidase activity) (16,17,20). The mechanism for oxygen insertion is still not clear, especially

for the binuclear, nonheme enzymes (23–25). The iron center in ribonucleotide reductase has an unusual function, which is to utilize molecular oxygen to form a stable tyrosyl radical (26).

Although these iron(IV) compounds are very interesting and important in understanding the catalytic activity of a number of enzymes, there is no indication that these highly reactive species play any role in iron transport and storage. Thus the discussion in this chapter will be restricted largely to the two more stable oxidation states: iron(II) (ferrous, 6 d electrons) and iron(III) (ferric, 5 d electrons).

A. d -Orbital Splittings

The splitting of the five $3d$ orbitals in iron complexes is most easily understood in terms of ligand field theory (LFT). In the absence of ligands, the $3d$ orbitals are degenerate. Upon complexation, the electrons residing in these $3d$ orbitals are raised in energy by electrostatic repulsion from the lone pairs of electrons from the ligands. The ligands present a set of point charges that do not have spherical symmetry with respect to the metal ion, which results in a splitting of the d orbitals into symmetry-related groups that change depending on the specific coordination geometry of the complex.

The two most common geometries for ferric and ferrous ion are octahedral for 6-coordinate complexes and tetrahedral for 4-coordinate complexes. In an octahedral complex, the lobes of the $d_{x^2-y^2}$ and the d_{z^2} orbitals point directly toward ligand lone pairs. This maximizes the electrostatic repulsions between the d electrons on the metal and the ligand lone-pair electrons, and these d orbitals are raised in energy by a relatively large amount. Conversely, the other three orbitals, the d_{xy} , d_{xz} , and d_{yz} , point to regions between the ligand lone pairs and are lowered in energy. This leads to the octahedral splitting diagram shown in Fig. 3. The symmetry-related d_{xy} , d_{xz} , and d_{yz} orbitals are referred to as the t_{2g} orbitals, while the $d_{x^2-y^2}$ and the d_{z^2} are referred to as the e_g orbitals. The energy gap between these two sets of orbitals is Δ_o , the crystal field splitting parameter for an octahedral complex.

The tetrahedral d -orbital splitting diagram is also shown in Fig. 3. The e orbitals ($d_{x^2-y^2}$ and the d_{z^2}) are now at lower energy, while the t_2 orbitals (d_{xy} , d_{xz} , and d_{yz}) are

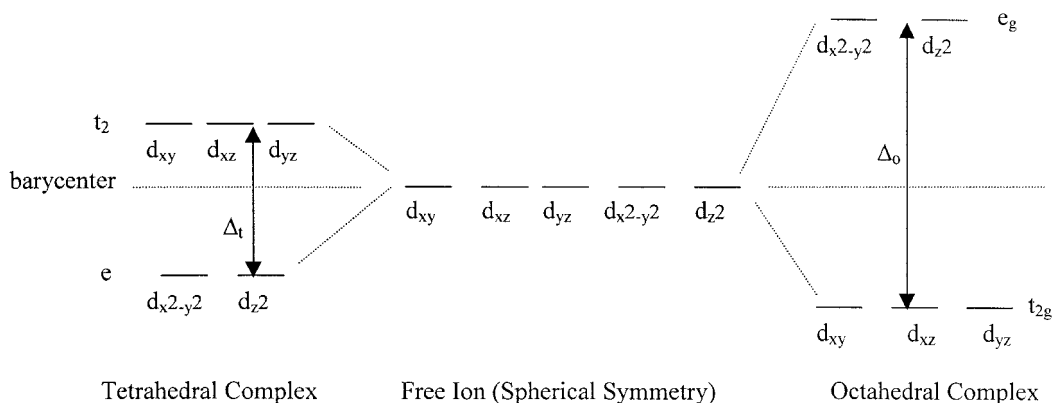


Figure 3 d -Orbital splitting diagram for tetrahedral and octahedral iron complexes.

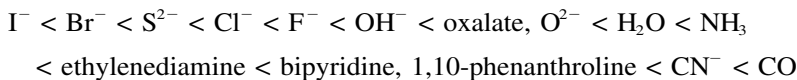
at higher energy. The gap between these two sets of orbitals is Δ_t . Because there are only four ligands instead of six, and because the ligands do not line up on the primary Cartesian axes of the d orbitals, the crystal field splitting (Δ_t) is smaller in tetrahedral complexes, typically only $\sim \frac{4}{9}\Delta_o$ for a comparable set of ligands.

The d -orbital splittings shown in Fig. 3 are referenced to the barycenter, which corresponds to the d -orbital energy associated with a spherical charge distribution. In octahedral symmetry, the e_g orbitals increase by $\frac{3}{5}\Delta_o$, while the t_{2g} orbitals decrease by $\frac{2}{5}\Delta_o$. Similarly, the energy of the t_2 orbitals in tetrahedral complexes will increase by $\frac{3}{5}\Delta_t$, while the energy of the e orbitals will decrease by $\frac{3}{5}\Delta_t$.

B. Spin States

It costs energy to force two electrons into the same d orbital. Because a higher ionic charge leads to a contraction of the d orbitals, the pairing energy increases from $17,600\text{ cm}^{-1}$ for Fe^{2+} to $30,000\text{ cm}^{-1}$ for Fe^{3+} (27). In the free ions the electrons follow Hund's rule and are distributed so as to maximize the total spin and avoid any unnecessary pairing. With the splitting of the d orbitals by an octahedral ligand field, the distribution of electrons depends on the crystal field splitting parameter. If Δ_o is smaller than the pairing energy, then the complex will adopt the high-spin configuration that has the fewest number of paired electrons ($t_{2g}^3 e_g^2$ for Fe^{3+} , $t_{2g}^4 e_g^2$ for Fe^{2+}). If Δ_o is greater than the pairing energy, then the complex will adopt the low-spin configuration (t_{2g}^5 for Fe^{3+} and t_{2g}^6 for Fe^{2+}).

The magnitude of Δ_o for a particular metal ion depends on the identity of the ligands. The spectrochemical series is an empirical ranking of ligands according to their ligand field strength, defined as the degree to which they split the d orbitals (28). Some ligands in this series follow the order



I^- leading to the lowest splitting and CO to the highest.

The values of Δ_o for the hexaquo ions are $14,000\text{ cm}^{-1}$ for $\text{Fe}(\text{H}_2\text{O})_6^{3+}$ and $10,000\text{ cm}^{-1}$ for $\text{Fe}(\text{H}_2\text{O})_6^{2+}$ (27). These values are less than the respective pairing energies, so both aquo ions are high-spin. Since halide, sulfide and oxygen donor ligands are lower than water in the spectrochemical series, they are also likely to form high-spin complexes. Strong field ligands such as bipyridine, phenanthroline, and cyanide increase Δ_o to the point that low-spin iron complexes are formed (14).

One should note that the ligand field strength is not closely correlated with the binding affinity of the ligand. For example, OH^- has a weaker ligand field strength than H_2O , even though hydroxide binds to the metal ion much more strongly than water. As a result, even every stable iron complexes of oxygen-donor ligands such as ferric enterobactin form high-spin complexes (13). For both ferric and ferrous ions, the value for Δ_t is too small to cause electron pairing even for high-field ligands. Thus tetrahedral complexes are almost invariably high-spin (28).

A simple electrostatic crystal field model cannot explain the observed order of the ligands in the spectrochemical series. For example, the neutral ligand CO is much higher in the series than charged ligands such as OH^- and F^- . The ranking of ligands also depends on π bonding between the metal and the ligands. In octahedral complexes, the lower-energy t_{2g} metal orbitals are formally nonbonding with respect to

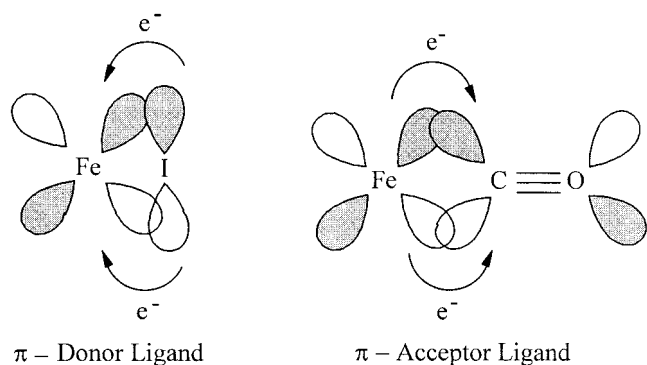


Figure 4 Orbital overlaps involved in metal–ligand bonding with π -donor and π -acceptor ligands.

M-L σ bonding, but they have the appropriate symmetry to form π bonds. Overlap with lower-energy, filled p orbitals of ligands such as I^- allows the donation of ligand electron density into the metal t_{2g} orbitals as shown in Fig. 4. This raises the energy of the metal t_{2g} orbitals, leading to a decrease in Δ_o and a position low in the spectrochemical series. Ligands that are purely σ bonding, e.g., H_2O , NH_3 , tend to fall in the center of the series. Ligands such as CO and CN^- have empty, higher-energy C–O and C–N π^* orbitals that can accept electron density from the metal t_{2g} orbitals (Fig. 4). This lowers the energy of the t_{2g} orbitals and increases Δ_o , leading to a ligand position high in the spectrochemical series.

C. Ionic Radii

The effective ionic radius of a metal cation depends on three properties: oxidation state, spin state, and coordination number (29). Ionic radii for ferric and ferrous ions are shown in Table 1. An increase in cationic charge contracts the radial distribution of the valence atomic orbitals and leads to a smaller ionic radius. Thus, for a given coordination number and spin state, Fe^{3+} is always smaller than Fe^{2+} .

In octahedral complexes the effect of spin state on ionic radius is linked to the electron density in the e_g set of metal orbitals. Electrons in these orbitals repel the electron lone pairs from the ligands, leading to a slight elongation of the metal–ligand bond. Therefore, the high-spin ions, in which the $d_{x^2-y^2}$ and d_{z^2} orbitals are half-occupied, have larger effective ionic radii than the low-spin ions. When the

Table 1 Ionic Radii for Ferric and Ferrous Ions (in Å)^a

	Fe^{3+}	Fe^{2+}
Octahedral, high-spin	0.645	0.780
Octahedral, low-spin	0.55	0.610
Tetrahedral, high-spin	0.490	0.630
Square planar, high-spin	—	0.640

^aData from Ref. 29.

coordination number decreases, there is a decrease in both electrostatic and steric interactions between adjacent ligands and an increase in the electrostatic attraction of the metal ion for the remaining ligand lone pairs. Thus the ligands are drawn closer to the metal, and there is a decrease in the effective ionic radius.

D. Iron Porphyrin Complexes

In porphyrin complexes, the axial ligands are necessarily different from the four nitrogens of the equatorial porphyrin ring, and this produces a tetragonal distortion from octahedral symmetry. Since the d_{z^2} orbital points directly at the two axial ligands, the energy of this orbital is strongly affected by the combined ligand field strength of the axial ligands. Weak axial ligands lead to a significant decrease in the energy of the d_{z^2} orbital. This decrease in the axial field strength also leads to a stronger σ -bonding interaction between the metal and the porphyrin, which raises the energy of the $d_{x^2-y^2}$ orbital (30). A set of general splitting diagrams for ferrous porphyrin complexes with different axial ligand field strengths is shown in Fig. 5. Most porphyrin complexes adopt either a high-spin or a low-spin configuration, but a very weak axial ligand field can result in an unusual intermediate spin state due to the large splitting between the d_{z^2} and the $d_{x^2-y^2}$ orbitals.

The porphyrin ligand provides a rather rigid cavity for the binding of the metal ion. The distance from the pyrrole nitrogen to the center of the porphyrin ring is 2.05 Å (31). If the metal ion does not fit well within the plane of the porphyrin ring,

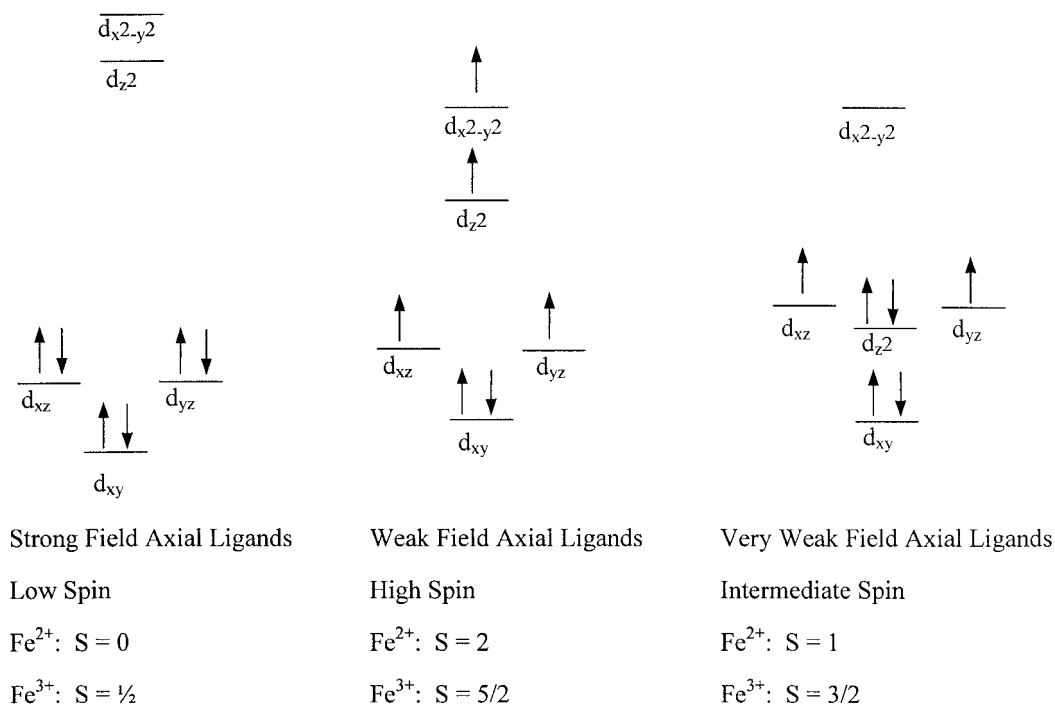


Figure 5 Crystal field splitting diagrams for ferrous porphyrin complexes with different axial ligand field strength. (Adapted from Ref. 30.)

it can still bind, but it will be displaced from the center of the ring to form an out-of-plane complex. In 5-coordinate complexes, the metal ion is displaced out of the ligand plane in the direction of the one axial ligand (30,31). The effect of spin state on the metal ionic radius is reflected in the displacement of the ferrous ion from the plane of the porphyrin ligand in 5-coordinate Fe(porphyrin)L complexes. The larger, high-spin ion is displaced by 0.4–0.6 Å from the plane of the ligand, while the smaller, low-spin ion is displaced by only 0.2–0.25 Å (30).

Six-coordinate Fe(porphyrin)L₂ complexes are close to planar for both ferrous and ferric ions (30). Thus the addition of a second axial ligand to a high-spin, 5-coordinate ferrous complex to form a planar, low-spin 6-coordinate complex causes the iron to move about 0.5 Å. This movement has been extensively discussed with respect to the conformational changes in hemoglobin caused by oxygen binding and the role of these conformational changes in the cooperativity of oxygen binding (32).

III. MAGNETIC PROPERTIES

Metal ions with total spin $S > 0$ are paramagnetic and have an intrinsic magnetic moment. The *spin-only* magnetic moment can be easily calculated as

$$\mu_{\text{SO}} = \sqrt{n(n + 2)} \quad (1)$$

where n is the number of unpaired electrons. This estimation of the total magnetic moment is typically quite accurate for high-spin ferric ions, which have five unpaired electrons and $\mu \approx 5.9$ Bohr magnetons (B.M.). For ions that have unequally populated t_{2g} orbitals, there is an orbital contribution to the magnetic moment, and the spin and orbital moments interact (33). This spin-orbit coupling can either decrease or increase the observed magnetic moment relative to the spin-only value. For both low-spin Fe³⁺ ($S = \frac{1}{2}$) and high-spin Fe²⁺ ($S = 2$), spin-orbit coupling adds to the spin only magnetic moment. For octahedral, low-spin Fe³⁺, $\mu_{\text{SO}} = 1.73$ B.M., while the observed values fall in the range 2.0–2.5 B.M. (33). For octahedral high-spin Fe²⁺, $\mu_{\text{SO}} = 4.9$ B.M., while the observed values fall in the range 5.1–5.7 B.M. (33). In low-spin, octahedral Fe²⁺, all the electrons are paired and the complex is diamagnetic.

A. Spin Equilibrium

In most complexes, one spin state is strongly preferred. However, it is possible to have a very close match between Δ_o and the pairing energy, such that the difference between the high-spin and low-spin states is so small that both states can be populated to give what is referred to as a spin equilibrium or spin crossover. Such equilibria have been observed for both iron(II) and iron(III) complexes (14,33). The observed magnetic moment is the weighted average of the moments of the two states,

$$\mu_{\text{obs}}^2 = (1 - \alpha)\mu_{\text{H}}^2 + \alpha\mu_{\text{L}}^2 \quad (2)$$

where α is the fraction of molecules in the low-spin state, and μ_{H} and μ_{L} are the moments of the high- and low-spin states (34). The relative population of the two states and thus the observed magnetic moment are temperature-dependent. A good example of this is provided by the bis complex of iron(III) with the Schiff-base ligand N-(2-(benzylamino)ethyl)-salicylaldimine. This complex goes from 97% low-spin at 10 K ($\mu \approx 2.1$ B.M.) to 93% high-spin at 300 K ($\mu \approx 5.7$ B.M.) (35).

The change from high-spin to low-spin is often accompanied by significant changes in metal–ligand bond lengths. In solution these changes are usual rapid and readily reversible. In solid samples the changes in the structure of the complex may be associated with changes in the crystal lattice. This can lead to highly cooperative spin state transitions and to marked hysteresis in the spin state populations when the samples is cycled between high and low temperatures (36).

B. Superexchange

The observed magnetic moment of ligand-bridged, polynuclear metal clusters can also be affected by the process of superexchange, in which the spins on the metal ions are coupled via a spin polarization of the electrons on the bridging ligands (33,37). Figure 6 shows the overlap between the metal $d_{x^2-y^2}$ orbitals and the p_x orbital on a bridging oxygen. The unpaired spin on Fe_A is arbitrarily assigned as positive. Covalent bonding between the metal and the ligand will polarize the spin in the adjacent lobe of the oxygen p orbital, leading to a net negative spin in this region. Since the net total spin within the oxygen p orbital is zero, an excess of negative spin adjacent to Fe_A leads to an accumulation of positive spin adjacent to Fe_B . Bonding between the oxygen and Fe_B will favor a negative orientation of the unpaired spin on Fe_B . The net result is that the spins on the two ferric ions tend to align in opposite directions and thus to cancel one another. This is an example of antiferromagnetic coupling. Similar types of spin polarization involving other ligand and metal orbitals can lead to ferromagnetic coupling, in which the metal spins are aligned in the same direction (33).

For a pair of antiferromagnetically coupled ferric ions, superexchange leads to a set of spin states ranging from fully paired ($S = 0$) to no pairing ($S = 5$). An energy-level diagram for the spin states of an antiferromagnetically coupled pair of ferric ions is shown in Fig. 7 (37). The separation between successive spin states S and $S - 1$ is $-2JS$, where J is the superexchange coupling constant. The value of J is negative for antiferromagnetic coupling, so the $S = 0$ state is the ground state. In ferromagnetic coupling J is positive, the order of the spin states inverts, and the $S = 5$ state becomes the ground state.

The net magnetic moment observed for a binuclear complex depends on the thermal population of the spin states shown in Fig. 7. Figure 8 shows the effective magnetic moment as a function of temperature calculated for different J values using the function from Murray (37). A significant decrease in the room-temperature magnetic moment is observed beginning at J values of about -10 cm^{-1} . For J values around -500 cm^{-1} , complexes are essentially diamagnetic at room temperature.

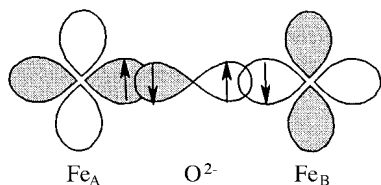


Figure 6 Orbital overlap for antiferromagnetic coupling in a μ -oxo binuclear iron(III) complex. (Adapted from Ref. 33.)

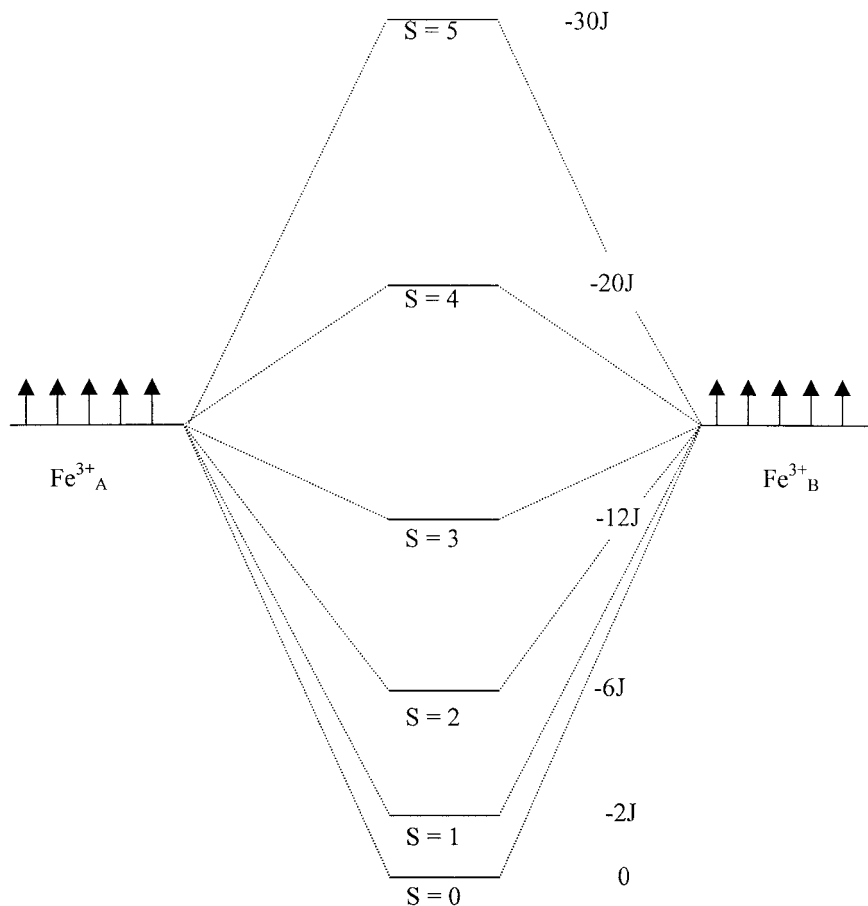


Figure 7 Energy-level diagram for the spin states in a binuclear iron(III) complex. (Adapted from Ref. 37.)

Oxo-bridged binuclear complexes of iron(III) with a variety of ligands form very readily in neutral aqueous solution, and the magnetic behavior of such complexes has been studied extensively (37). They are antiferromagnetically coupled, with J values around -100 cm^{-1} (19,37). The magnitude of J is not strongly dependent on the Fe–O–Fe bond angle, but protonation of the O^{2-} group to give a bridging hydroxyl group reduces the value of J to about -10 to -20 cm^{-1} (19).

Magnetically coupled binuclear iron(III) sites have been found in several proteins, such as oxyhemerythrin ($J = -90 \text{ cm}^{-1}$), diferric ribonucleotide reductase ($J = -110 \text{ cm}^{-1}$), and diferric uteroferrin ($J < -80 \text{ cm}^{-1}$), all of which appear to have a μ -oxo bridging ligand (19). The binuclear site in diferric methane monooxygenase is more weakly coupled, with $J = -7 \text{ cm}^{-1}$, which is consistent with OH^- bridging groups (20). This type of magnetic coupling is also a prominent feature of iron sulfur clusters. The magnetic behavior for the $2\text{Fe}-2\text{S}$ clusters can be described using the model discussed above for the μ -oxo-bridged complexes (38). The $2\text{Fe}-2\text{S}$ clusters tend to have J values of about -180 cm^{-1} for the oxidized diferric form, with a

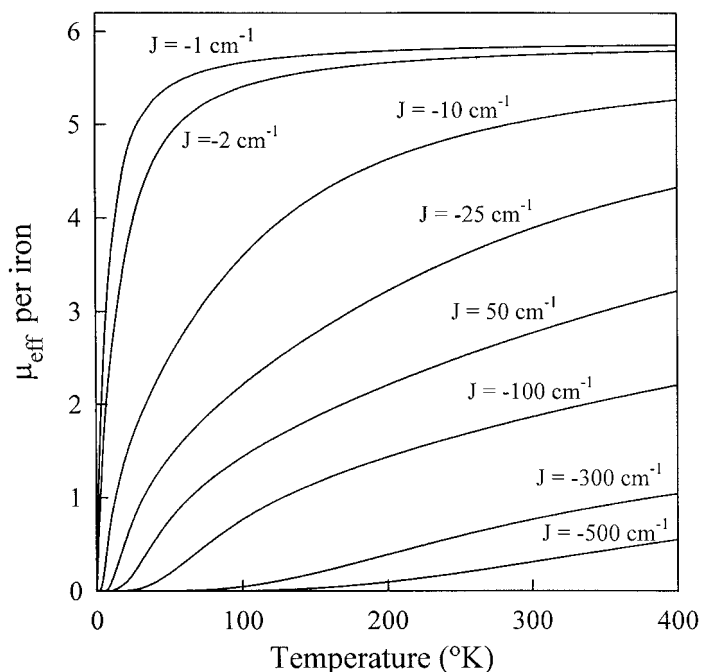


Figure 8 Effective magnetic moment for a binuclear iron(III) complex as a function of temperature for different values of the magnetic coupling parameter J .

lower value of about -100 cm^{-1} for the reduced $\text{Fe}^{3+}-\text{Fe}^{2+}$ form (38). Two or three J values are required to describe the more complex magnetic behavior of $4\text{Fe}-4\text{S}$ clusters (39–41), such as occur in the iron regulatory protein, IRP1 (see Chapter 9). There is a major change in the magnetic coupling for different cluster oxidation states. In the oxidized form ($2\text{Fe}^{3+}-2\text{Fe}^{2+}$), the J values are in the range -225 to -275 cm^{-1} , while in reduced clusters ($1\text{Fe}^{3+}-3\text{Fe}^{2+}$), the J values are in the range -40 to -60 cm^{-1} (39).

The diferrous $2\text{Fe}-2\text{S}$ clusters contain an even number of metal valence electrons, and the coupling between the irons is strong enough so that at low temperature, the clusters are diamagnetic with no electron paramagnetic resonance (EPR) signal. Oxidation to the ferric–ferrous state produces an odd electron system, which gives an $S = \frac{1}{2}$ state at low temperature and a characteristic EPR signal (42). For $4\text{Fe}-4\text{S}$ clusters, the $2\text{Fe}^{3+}-2\text{Fe}^{2+}$ form has an even electron count and is also diamagnetic at low temperature. Either oxidation or reduction by one electron produces an odd-electron system that is EPR-active (42,43). In proteins the reduced clusters tend to have an $S = \frac{1}{2}$ ground state, but a variety of other spin states are known for synthetic $4\text{Fe}-4\text{S}$ clusters (44).

IV. ELECTRONIC SPECTRA

Both iron(II) and iron(III) have partially filled d orbitals, and there are several possible $d-d$ electronic transitions for these ions. The energy (wavelength) of these

bands is related to the crystal field splitting parameter Δ_o , with larger values of Δ_o leading to higher-energy (lower-wavelength) absorbance bands. The intensity of the bands is independent of Δ_o and is determined by selection rules (45). One rule states that any transition that involves a change in spin state is “spin forbidden.” The second rule states that transitions within a given set of d or p orbitals are Laporte-forbidden or symmetry-forbidden if the complex has a center of symmetry. Thus all $d-d$ transitions in octahedral complexes are Laporte-forbidden. Tetrahedral complexes lack a center of inversion, and mixing of p and d orbitals leads to some weakening of the Laporte selection rule and a corresponding increase in band intensity (45).

Electronic absorption bands can also be associated with charge-transfer transitions. These transitions involve the movement of an electron between an orbital that is mainly metal in character to an orbital that is mainly ligand in character. The movement can be in either direction, a ligand-to-metal charge transfer (LMCT) or a metal-to-ligand charge transfer (MLCT) (33). Since these transitions are typically fully allowed, they tend to have very high intensities. The energy of charge-transfer transitions can be rationalized as an internal redox reaction. Since it is relatively easy to reduce Fe^{3+} to Fe^{2+} , LMCT bands are often observed in the visible spectrum when the ferric ion is coordinated to electron-rich ligands, e.g., oxide, phenolate, or catecholate. It is more difficult to reduce Fe^{2+} , so LMCT charge-transfer bands to ferrous ion tend to shift to much higher energy and are seldom observed in the visible region. However, when ferrous ion forms low-spin complexes with aromatic ligands such as 2,2'-bipyridine and 1,10-phenanthroline, visible MLCT bands are observed due to the movement of a metal t_{2g} electron to a π^* orbital on the ligand.

The magnitude of the absorbance band for an electronic transition is related by Beer's law to the concentration of the complex and to the molar extinction coefficient, ϵ , which represents the intrinsic intensity of the absorption. As a general rule, ϵ decreases by about a factor of 100 for each violation of a selection rule (45). Typical values for ϵ for various types of transitions are listed in Table 2. Spin-forbidden bands of octahedral complexes are too weak to be observed except in very concentrated solutions. The spin-allowed octahedral bands and both types of tetrahedral bands, with ϵ values in the range of 1 to 1000 $\text{M}^{-1} \text{cm}^{-1}$, can be routinely measured for low-molecular-weight complexes, for which one can prepare concentrated solutions if necessary.

Table 2 Molar Extinction Coefficients for Different Types of Electronic Transitions for Fe^{3+} and Fe^{2+}

Type of band	$\epsilon(\text{M}^{-1} \text{cm}^{-1})^a$	Examples
Charge transfer	2,000–10,000	Fe^{3+} -phenolate, Fe^{2+} (bipy) ₃
$d-d$, Tetrahedral, spin-allowed	100–1,000	Tetrahedral Fe^{2+}
$d-d$, Tetrahedral, spin-forbidden	1–10	Tetrahedral Fe^{3+}
$d-d$, Octahedral, spin-allowed	1–10	Octahedral Fe^{2+}
$d-d$, Octahedral, spin-forbidden	0.01–0.1	Octahedral Fe^{3+}

^aValues from Ref. 45.

The relatively few spin-allowed transitions for Fe^{3+} and Fe^{2+} that fall in the ultraviolet-visible-infrared region of the spectrum are listed in Table 3, along with the approximate band positions calculated from Tanabe-Sugano diagrams (28). The band positions for the high-spin octahedral and tetrahedral complexes reflect the ligand field strength of the aquo complexes. The bands for low-spin complexes were calculated for ligand field strengths slightly greater than the minimum required to cause spin pairing. There are no visible bands associated with the tetrahedral or high-spin octahedral complexes of either Fe^{2+} or Fe^{3+} . The high-spin, octahedral ferrous ion has only one spin-allowed band in the near-IR, at ~ 1000 nm. In tetrahedral ferrous complexes the spin-allowed band shifts even farther into the IR region to about 2300 nm. High-spin Fe^{3+} has no spin-allowed bands in either octahedral or tetrahedral symmetry. The low-spin Fe^{2+} and Fe^{3+} have a series of three bands in the UV-visible region, which should be observable unless obscured by more intense charge-transfer bands.

UV-visible studies on proteins typically involve concentrations of 1 mM or less, and often much less, so even spin-allowed $d-d$ bands are very often too weak to be observed. In addition, any $d-d$ bands falling in the UV will be buried under the more intense $\pi-\pi^*$ bands of the aromatic groups in the protein. Thus the visible spectra of iron-protein complexes usually consist of charge-transfer bands, e.g., $\text{Fe}^{3+} \rightarrow$ phenolate in transferrin and $\text{Fe}^{3+} \rightarrow \text{O}^{2-}$ in ferritin. The only notable exception is the intense bands between ~ 400 and 600 nm due to $\pi-\pi^*$ transitions in the porphyrin ring of heme proteins (46).

The presence of roughly tetrahedral metal-binding sites in proteins such as metallothionein has been detected from the appearance of a relatively intense $d-d$ band for the Co^{2+} -protein complex at about 700 nm (47). Thus it might be expected that similar information could be obtained for tetrahedral Fe^{2+} . The observed transition for the cobalt(II) ion is from the ${}^4\text{A}_{2g}$ ground state to the ${}^4\text{T}_{1g}(\text{P})$ excited state (47). Because this excited state is derived from the ${}^4\text{P}$ excited state of the free ion, the absorbance band appears at higher energy in the visible region in spite of the small crystal field splitting associated with tetrahedral complexes. In contrast, the spin-allowed band in the spectrum of tetrahedral Fe^{2+} is derived from the crystal field splitting of the ${}^5\text{D}$ ground state of the free ion. Thus, as noted above, the Fe^{2+}

Table 3 Spin-Allowed Transitions for Fe^{3+} and Fe^{2+}

Fe^{2+} high-spin, octahedral	${}^5\text{T}_{2g} \rightarrow {}^5\text{E}_g$	(~ 1000 nm, near-IR)
Fe^{2+} low-spin, octahedral	${}^1\text{A}_{1g} \rightarrow {}^1\text{T}_{1g}$	(~ 600 nm, vis)
	${}^1\text{A}_{1g} \rightarrow {}^1\text{T}_{2g}$	(~ 350 nm, UV)
	${}^1\text{A}_{1g} \rightarrow {}^1\text{E}_g$	(~ 270 nm, UV)
Fe^{2+} tetrahedral	${}^5\text{E} \rightarrow {}^5\text{T}_2$	(~ 2300 nm, IR)
Fe^{3+} high-spin, octahedral	None	
Fe^{3+} low-spin, octahedral	${}^2\text{T}_{2g} \rightarrow {}^2\text{A}_{2g}$	(~ 450 nm, vis)
	${}^2\text{T}_{2g} \rightarrow {}^2\text{E}_g$	(~ 300 nm, UV)
	${}^2\text{T}_{2g} \rightarrow {}^2\text{A}_{1g}$	(~ 250 nm, UV)
Fe^{3+} tetrahedral	None	

d-d band appears in the IR region at 2300 nm, where it is completely obscured by protein and solvent bands.

V. COMPLEXATION EQUILIBRIA

A. Hard–Soft Acid–Base Characteristics

The reversible binding of metal ions to both proteins and to low-molecular-weight ligands is obviously a central issue with respect to the biological transport and storage of metals. The simplest, qualitative way to understand and predict the complexation reactions of iron is by use of hard–soft acid–base (HSAB) theory (28). The ferric ion, with its relatively small radius and high ionic charge, is a prototypical hard metal ion, and thus is expected to form stable complexes with hard donors. In biological systems, the most readily available hard donors include the hydroxide and oxo anions, the phenolate side chains of tyrosine, phosphate groups, alkoxide groups (e.g., citrate, sugars), and carboxylate groups.

The ferrous ion is classified as a borderline metal ion. In terms of HSAB theory, it can be matched with the borderline imidazole side chains of histidine and with the soft sulfur donor atoms in methionine and especially cysteine. Porphyrins are also borderline ligands, which should favor coordination of ferrous ion.

The higher charge on the ferric ion makes it a much stronger Lewis acid than ferrous ion. A softer ligand may show relative preference for ferrous ion, but the preference may not be strong enough to overcome the differences in Lewis acidity of the two metal ions. For example, based just on HSAB theory, one might predict that the relatively soft ligand 1,10-phenanthroline will prefer to bind the softer ferrous ion over the harder ferric ion. However, the stability constants are $\log K_1 = 5.85$ for ferrous ion and $\log K_1 = 6.5$ for ferric ion (48).

B. Equilibrium Constants

Complexation equilibria in aqueous solutions usually involve three basic components, the metal, the ligand, and H^+ , which combine in various stoichiometric ratios to form a series of complex species. Each species is characterized by an equilibrium constant defined as



with the corresponding overall binding constant

$$\beta_{ijk} = \frac{[M_iL_jH_k]}{[M]^i[L]^j[H]^k} \quad (4)$$

The number of indices associated with β can be expanded to include as many components as necessary, although it is seldom necessary to have more than four components.

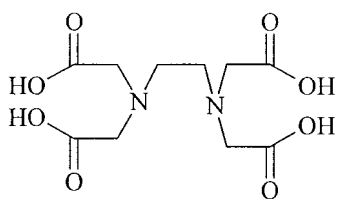
In a formal stability constant such as Eq. (4), the standard convention is that the symbol L refers to the fully deprotonated form of the ligand. For a ligand such as 1,10-phenanthroline, with a pK_a of only 4.93 (48), the ligand is fully deprotonated above pH 7 and the formal stability constants accurately reflect the metal-binding affinity of this ligand at physiological pH. For a ligand such as catechol, with $pK_{a1} = 13$ and $pK_{a2} = 9.23$, only one of every 10^7 molecules of the free ligand will be

present as the fully deprotonated catechololate dianion at pH 7, and the effective binding affinity of the ligand will be reduced proportionately.

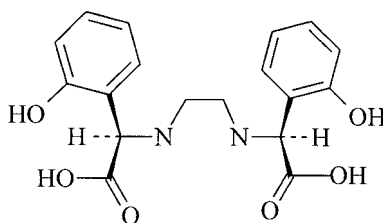
To take this pH dependence into account, investigators often define *effective* binding constants. The definitions vary, but a typical definition is

$$K_{\text{eff}} = \frac{\sum_k [\text{MLH}_k]}{[\text{M}] \sum_i [\text{H}_i\text{L}]} \quad (5)$$

The summation term in the numerator accounts for protonated complexes ($k > 0$) and for hydrolyzed complexes ($k < 0$). The summation term in the denominator accounts for the degree of protonation of the uncomplexed ligand. The impact of chelate protonation and/or hydrolysis is usually limited to two or three orders of magnitude. The impact of ligand protonation can be much larger. This is an important factor when comparing the metal binding by two ligands that have very different $\text{p}K_a$ values. As an example, consider the two ligands edta (**I**) and meso-ehpg (**II**).



I. edta



II. meso-ehpg

The formal stability constants are $10^{25.1}$ for ferric-edta (48) and $10^{33.28}$ for ferric-ehpg (49). The K_{eff} values as a function of pH for these two ligands are plotted in Fig. 9. At high pH, ehpg is the better ligand. As the pH is lowered, the high $\text{p}K_a$'s for ehpg result in a much more rapid decrease in K_{eff} , so that at pH 2, the K_{eff} for edta is almost 10 log units greater than that for ehpg.

Most metal–protein-binding constants are measured at a single pH and do not take into account the specific state of protonation of the ligating groups. These effective binding constants are valid only at the pH at which they were measured. The ferric binding constant for the C-terminal site of serum transferrin is $10^{19.5}$ at pH 7.4 (50). To calculate the competition between transferrin and edta, one would use the edta effective binding constant at pH 7.4 of $10^{23.9}$, not the formal stability constant of $10^{25.1}$.

Note that Eq. (5) is written specifically for 1:1 metal:ligand complexes. If the system contains a mixture of complexes with different metal:ligand stoichiometries, then this method of defining effective stability constants becomes cumbersome. One common alternative is first to define a set of standard solution conditions by specifying the pH and the total concentrations of ligand and metal, and then to use the complete set of equilibrium constants to calculate the concentration of free metal ion. This concentration is then expressed as pM , $-\log[\text{M}]$. A smaller concentration of free metal ion gives a larger pM , which denotes a more effective iron-complexing agent. This calculation easily takes into account the effects of ligand protonation, chelate protonation/hydrolysis, and the formation of a mixture of complexes with differing metal:ligand stoichiometry.

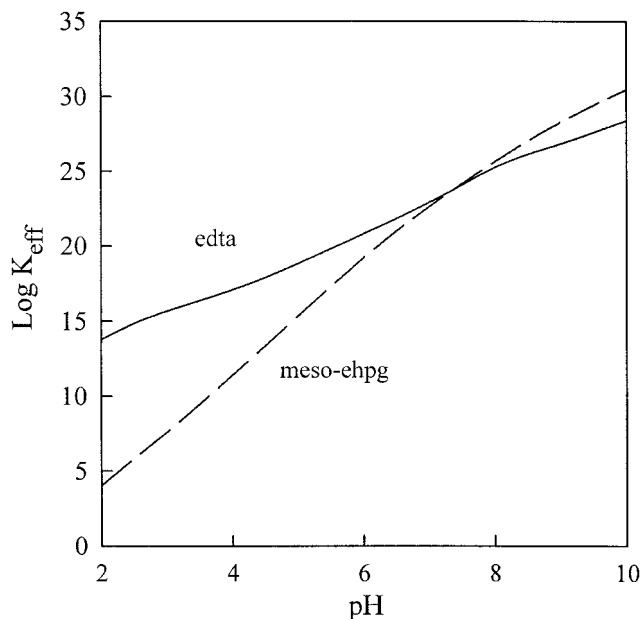
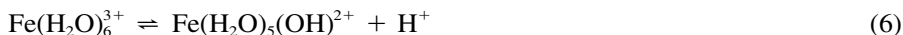


Figure 9 Effective binding constants [defined in Eq. (5)] for the ferric complexes of edta and meso-ehpg as a function of pH.

C. Hydrolysis

The fundamental complexation reaction in an aqueous solution is the formation of hydroxo complexes by hydrolysis of the aquated metal ion. The reaction can be described as the deprotonation of a coordinated water molecule, e.g.,



The general equilibrium constant for hydrolysis corresponds to Eq. (4) with a ligand index of $j = 0$, as shown in Eq. (7), where the metal ionic charge and the aquo ligands of the metal have been omitted for clarity.

$$\beta_{i_0-k} = \frac{[\text{M}_i(\text{OH}^-)_k][\text{H}^+]^k}{[\text{M}]^i} \quad (7)$$

Baes and Mesmer (51) have proposed a model for the first hydrolysis reaction of metal ions that is described by the equation

$$\log \beta_{1_0-1} = -19.8 + 11 \left(\frac{z}{d} \right) \quad (8)$$

The constant 19.8 reflects primarily the energy cost associated with ionizing the water molecule to H^+ and OH^- . The second term represents the energy gained by electrostatic attraction between the hydroxide anion and the metal cation, where z is the charge on the cation and d is the metal–hydroxide bond distance (51). This simple equation works quite well for most divalent and trivalent transition metal ions, including Fe^{2+} and Fe^{3+} . Because of its higher charge and smaller ionic radius, Fe^{3+}

($\log \beta_{10^{-1}} = -2.77$) begins to hydrolyze slightly below pH 2, while the ferrous ion ($\log \beta_{10^{-1}} = -9.79$) does not begin to hydrolyze until pH ~ 8.5 .

Many sources list hydrolysis constants for zero ionic strength, which reflect the maximum possible degree of hydrolysis. The value for $\log \beta_{10^{-1}}$ for the ferric ion changes from -2.19 at $\mu = 0$ to -2.68 at $\mu = 0.1$ to -3.21 at $\mu = 1.0$ (48). Table 4 shows a compilation of ferrous and ferric hydrolysis constants calculated from the empirical parameters from Baes and Mesmer (51) for $\mu = 0.15$, which approximates the ionic strength of human serum. Table 4 also lists the stepwise hydrolysis pK_a 's for the mononuclear hydroxide complexes.

Because there is no significant hydrolysis of Fe^{2+} at physiological pH, free ferrous ion has a solubility of about 0.1 M in a neutral aqueous solution. Between pH 9 and 12, hydrolysis proceeds rapidly through $\text{Fe}(\text{OH})^+$, $\text{Fe}(\text{OH})_2$, and $\text{Fe}(\text{OH})_3^-$. The $\text{Fe}(\text{OH})_4^{2-}$ complex is formed only in very strongly basic solutions. There is an anomaly in the stepwise hydrolysis reactions of ferrous ion in that the $\text{Fe}(\text{OH})_2$ complex hydrolyzes more readily than $\text{Fe}(\text{OH})^+$. Thus very little $\text{Fe}(\text{OH})_2$ accumulates in solution, and the system goes almost directly from $\text{Fe}(\text{OH})^+$ to $\text{Fe}(\text{OH})_3^-$ (51). This type of anomaly has also been observed for the hydrolysis of Al^{3+} and has been attributed to a change in coordination number from 6 to 4 as hydrolysis proceeds (52).

The hydrolysis of ferric ion is a dominating factor over a very wide pH range. Hydrolysis begins at about pH 2, and goes through a regular progression of 1:1, 1:2, 1:3, and 1:4 complexes that ends with the formation of $\text{Fe}(\text{OH})_4^-$ at pH 10 (51). At physiological pH, the dominant mononuclear species is $\text{Fe}(\text{OH})_3$, which has a solubility of only 10^{-12} M (51). Based on the K_{sp} for this species, the concentration of the free Fe^{3+} aquo ion is limited to about 10^{-20} M, or to $\text{pM} = 20$. The transport

Table 4 Hydrolysis Constants for Ferrous and Ferric Ion for 0.15 M Ionic Strength^a

Species	$\log \beta_{10^{-1}}^b$	Stepwise pK_a^c
Ferrous ion		
$\text{Fe}(\text{OH})^+$	-9.79	9.79
$\text{Fe}(\text{OH})_2$	-20.89	11.10
$\text{Fe}(\text{OH})_3^-$	-31.0	10.11
$\text{Fe}(\text{OH})_4^{2-}$	-46.48	15.5
$\log K_{\text{sp}} = -14.40$		
Ferric ion		
$\text{Fe}(\text{OH})^{2+}$	-2.77	2.77
$\text{Fe}(\text{OH})_2^+$	-6.53	3.76
$\text{Fe}(\text{OH})_3$	-12.86	6.33
$\text{Fe}(\text{OH})_4^-$	-22.18	9.32
$\text{Fe}_2(\text{OH})_2^{4+}$	-2.95	
$\text{Fe}_3(\text{OH})_4^{5+}$	-6.59	
$\log K_{\text{sp}} = -38.75$		

^aCalculated from the empirical equation reported in Ref. 51.

^b $\beta_{10^{-1}}$ defined in Eq. (7).

^cDefined as $-(\log \beta_{10^n} - \log \beta_{10^{(n-1)}})$.

of any appreciable mass of ferric ion must involve a chelating agent to increase the concentration of soluble iron. Microorganisms synthesize and secrete low-molecular-weight chelating agents called siderophores to mobilize iron in the environment (13,53), and these compounds are discussed in detail in Chapter 12. Higher organisms transport iron through blood bound to the protein transferrin (10,54), which is discussed in Chapter 2.

At higher iron concentrations the hydrolysis of ferric ion also involves the formation of the polynuclear $\text{Fe}_2(\text{OH})_2^{4+}$ and $\text{Fe}_3(\text{OH})_4^{5+}$ species. These species appear in significant concentrations at total ferric ion concentrations of about 10 mM and $\text{pH} < 6$ (51). Thus they are of little direct relevance to dilute solutions at physiological pH.

D. Chelate Hydrolysis

Even when ferric ion is complexed with a multidentate ligand, it retains a strong tendency to hydrolyze. Chelate hydrolysis can be expressed as an acid dissociation reaction:



Chelate hydrolysis can also be described by Eq. (4) by assigning the $\text{ML}(\text{OH})$ species stoichiometric coefficients of 1, 1, and -1 for metal, ligand, and hydrogen ion, respectively. The tendency of the chelate to hydrolyze is inversely related to the stability of the chelate. This is illustrated by the plot in Fig. 10, which shows a roughly linear relationship between the $\log \beta_{110}$ value for the unhydrolyzed chelate and the $\text{p}K_a$ for the chelate as defined in Eq. (11). The graph shows that an amino-carboxylate ligand must have a stability constant of about 10^{30} to prevent chelate hydrolysis at physiological pH. The monohydroxo ferric chelates tend to dimerize to μ -oxo-bridged binuclear complexes. Thus even the relatively stable ferric-edta complex exists at physiological pH as a mixture of $\text{Fe}(\text{edta})^-$, $\text{Fe}(\text{edta})(\text{OH})^{2-}$, and $(\text{Fe}-\text{edta})_2\text{O}^{4-}$ (37,48).

E. Stability Constants for Ferric Complexes

Table 5 lists $\log \beta$ and pM values for the binding of ferric ion by selected ligands. A ligand must bind iron strongly enough to raise the pM above the lower limit of 20 set by hydrolysis to prevent precipitation of ferric hydroxide from a 1 μM iron solution. Complexation by the smaller aminocarboxylates such as NTA does not meet this criterion. The larger aminocarboxylates such as edta and dtpa form reasonably stable complexes, but there is a very dramatic increase in stability for N,N'-bis(*o*-hydroxybenzyl)-ethylenediamine-N,N'-diacetic acid (HBED, **III**), where two of the carboxylate groups of edta have been replaced by *o*-phenolate donors (55). This illustrates the strong affinity of ferric ion for the hard, strongly basic phenolate oxygen. An even higher binding affinity is observed for 1,4,7-tris(3-hydroxy-6-methyl-2-pyridylmethyl)-1,4,7-triazanonane (TACN-HP, **IV**). The macrocyclic base contributes to a very high $\log \beta_{110}$ value of 49.98 (56). In addition, the introduction of nitrogen into the aromatic ring lowers the $\text{p}K_a$'s for the dissociation of the phenolic protons and makes the ligand more effective at physiological pH. As a result, this ligand has a pM of 40.3, which is the largest value yet reported.

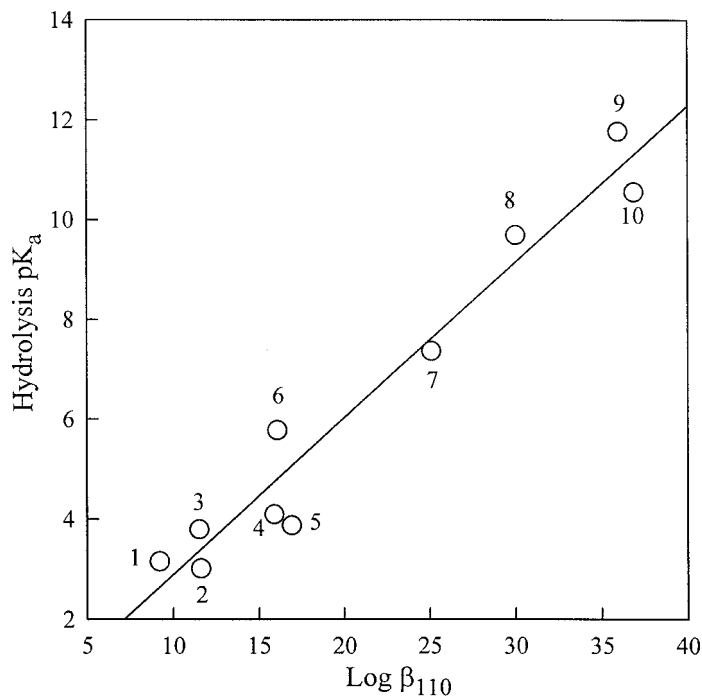
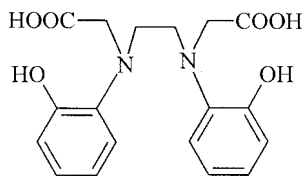
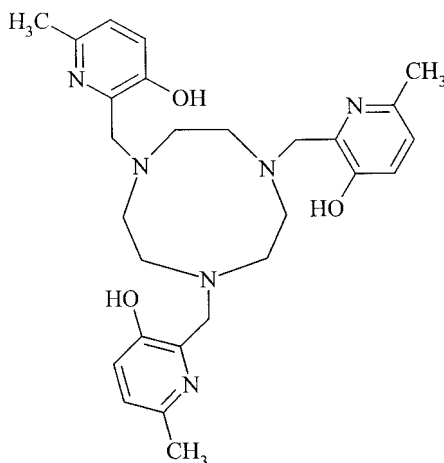


Figure 10 Linear free-energy relationship between the log β_{110} for a metal chelate and the chelate hydrolysis constant: (1) kojic acid; (2) sulfoxine; (3) maltol; (4) nitrilotriacetic acid; (5) ethylenediamine-*N,N*-diacetic acid; (6) *N*-phosphonomethylglycine; (7) edta; (8) *trans*-1,2-diaminocyclohexane-*N,N,N',N'*-tetraacetic acid; (9) *rac*-ethylenedis(2-hydroxyphenylglycine); (10) *N,N'*-(2-hydroxy-5-sulfobenzyl)ethylenediamine-*N,N'*-diacetic acid.



III. HBED



IV. TACN-HP

The pM values for the simple bidentate ligands catechol and acetohydroxamic acid are below the hydrolysis pM . However, there is a dramatic increase in pM when

Table 5 Stability Constants of Selected Ferric Chelates^a

Ligand	$\log \beta_{110}$	$\log \beta_{120}$	$\log \beta_{130}$	pM
Glycine	10.0			
Aspartic acid	11.4			
1,10-Phenanthroline	6.5	11.4	14.1	7.67
Oxalic acid	7.53	13.64	18.49	11.54
Iminodiacetic acid (VI)	10.72	20.12		12.04
Acetohydroxamic acid	11.42	21.10	28.33	13.29
Catechol	20.0	34.7	43.80	15.50
Citric acid (V)	11.40	18.2		16.73
Nitrilotriacetic acid (VII)	15.9	23.97		18.05
Deferiprone	15.10	26.61	35.88	19.31
Transferrin	21.39			22.34
Ethylenediaminetetraacetic acid (I)	25.1			23.52
Desferrioxamine B	30.5			26.60
Diethylenetriaminepentaacetic acid	28.0			28.24
MECAMS	41.00			29.40
HBED (III)	39.7			31.00
Enterobactin	49			34.0
TACN-HP (IV)	49.98			40.3

^a $\log \beta$ defined in Eq. (4). Values for 0.1 M ionic strength and 25°C from Refs. 48 and 73.

these functional groups are incorporated into multidentate ligands. This is shown by the pM values of 26.6 for the trihydroxamate siderophore desferrioxamine B (DFO) and 29.4 for N,N',N''-tris(2,3-dihydroxy-5-sulfobenzoyl)-1,3,5-tris(aminomethyl)-benzene (MECAMS) (57). A pM of 35.6 was reported for the catechol siderophore enterobactin based on estimated ligand protonation constants (58). Protonation constants for the three ortho-hydroxyl groups have now been determined (59), and these values lead to a slightly lower pM of 34.0.

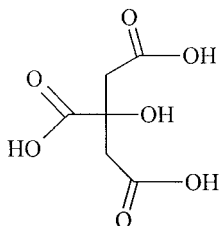
Hydroxypyridinone ligands such as 1,2-dimethyl-3-hydroxy-4-pyridinone (deferiprone) provide a bidentate-binding group similar to catechol but with a much lower ligand pK_a . This leads to improved binding at physiological pH, as shown by the pM of 19.3 for deferiprone compared to 15.5 for catechol. These compounds have been investigated very extensively as therapeutic chelating agents (60–62), as discussed in Chapter 13.

The traditional polyamine ligands such as ethylenediamine and triethylenetetramine are missing from Table 5 because these ligands cannot compete with hydrolysis for ferric ion. One can get more effective complexation using the more acidic pyridine functional group, and binding constants have been measured for the mono, bis, and tris chelates of 1,10-phenanthroline (48).

F. Low-Molecular-Weight Physiological Iron Chelators

May et al. have calculated the speciation of low-molecular-weight ferric ion in a computer model for human serum (63). They concluded that essentially all the low-molecular-weight iron in serum would be bound to citric acid (V), including low concentrations of mixed ligand complexes involving citrate in combination with sa-

licylate, glutamate, and oxalate (63). The model showed no significant concentrations of binary ferric complexes with simple amino acids, phosphate, lactate, malate, oxalate, salicylate, pyruvate or succinate.



V. Citric Acid

Citric acid (cta) has ligand pK_a 's of 5.69, 4.35, and 2.87, corresponding to the three carboxylic acid groups (48). The central $-\text{OH}$ group does not deprotonate over the normal pH range and has no assigned pK_a . Thus citrate is defined as an H_3L ligand. The ferric–citrate equilibria over the acidic pH range of 2–4 have been reasonably well characterized (64–66). At pH ~ 2 the neutral 1:1 complex $\text{Fe}(\text{cta})$ is the major species in solution. This complex loses an additional proton with a pK_a of 2.78, which is attributed not to hydrolysis, but to the deprotonation and coordination of the citrate hydroxyl group. Since this represents the loss of a fourth proton from an H_3L ligand, this complex is typically described as $\text{Fe}(\text{H}_{-1}\text{cta})^-$. The reported binding constants are $\log \beta_{111} = 12.4$ for $\text{Fe}(\text{Hcta})^+$, $\log \beta_{110} = 11.2$ for $\text{Fe}(\text{cta})$, and $\log \beta_{11-1} = 8.5$ for $\text{Fe}(\text{H}_{-1}\text{cta})^-$ (65). A binding constant for the 2:1 complex $\text{Fe}(\text{cta})_2^{3-}$ of $\log \beta_{120} = 18.2$ has been estimated by Martin based on aluminum-binding constants (66).

Potentiometric titrations of ferric–citrate solutions are characterized by slow, long-term drift above pH 3.5 to 4 (64,67), and the complexation reactions at higher pH have been difficult to characterize. At equimolar metal and ligand concentrations there is a slow hydrolytic polymerization reaction that leads to the formation of a spherical ferric–hydroxide polymer coated with citrate molecules (67). These soluble spheres have an average molecular weight of about 210,000 Da and a diameter of $\sim 72 \text{ \AA}$.

The presence of excess citrate reduces the degree of ferric–hydroxide polymer formation, and no polymer is formed in the presence of a 20-fold excess of citrate (68). Spiro et al. (68) established that this was due to the formation of a deprotonated bis complex, $\text{Fe}(\text{H}_{-1}\text{cta})_2^{5-}$, and this complex has recently been structurally characterized (69). The citrate is tridentate, binding through the central carboxylate, the deprotonated RO^- group, and one of the terminal carboxylate groups to form one five-membered and one six-membered chelate ring. Essentially the same structure has been observed for the 2:1 citrate complex of Al^{3+} (70).

Based on the available constants, a pM value of 16.75 has been calculated for citrate. Under the stated conditions for the pM calculation, the stable species at neutral pH is $\text{Fe}(\text{H}_{-1}\text{cta})^-$, not $\text{Fe}(\text{cta})_2^{3-}$, even though there is a 10-fold excess of ligand. Although there is ample evidence that the $\text{Fe}(\text{H}_{-1}\text{cit})_2^{5-}$ complex is likely to be an important species at neutral pH, no binding constant for this complex has been reported. Since this species cannot be included in the calculation, the pM value listed in Table 5 should be regarded as a lower limit.

Polyphosphates such as pyrophosphate, ADP, and ATP also bind ferric ion. All these ligands are capable of mediating the exchange of ferric ion between transferrin and desferrioxamine B (DFO), presumably by forming a small pool of labile complexes (71,72). The binding of ferric ion by pyrophosphate at acidic pH has been evaluated (73). A complex mixture of 1:1 and 2:1 complexes is present from pH 0 to 3. At higher pH the system is complicated by the formation of insoluble complexes of pyrophosphate and hydroxide. High concentrations of pyrophosphate can solubilize micromolar concentrations of Fe^{3+} , and 5 mM pyrophosphate will completely remove ferric ion from serum transferrin (74).

G. Ferrous Complexes

Binding constants for selected ferrous complexes are listed in Table 6. Because of its lower charge, the ferrous ion forms much less stable complexes than ferric ion with most ligands. For example, the binding constant with edta drops from $\log \beta_{110} = 25.1$ for ferric ion to 14.3 for ferrous ion (48), and it is difficult to find 1:1 ferrous complexes with $\log \beta$ values >15 . The Irving-Williams order predicts that for a typical ligand involving oxygen and/or nitrogen donor atoms, the stability constants for divalent metal ions will fall in the order $\text{Mn}^{2+} < \text{Fe}^{2+} < \text{Ni}^{2+} < \text{Cu}^{2+} > \text{Zn}^{2+}$. Thus ferrous complexes tend to be less stable than the complexes of most other first-row divalent metal ions.

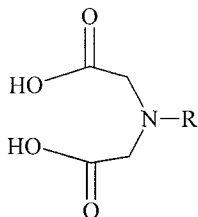
The softer nature of the ferrous ion can be seen in the comparison of the binding constants of iminodiacetic acid (VI), nitrilotriacetic acid (VII), and N-(2-

Table 6 Stability Constants for Selected Ferrous Chelates^a

Ligand	$\log \beta_1$	$\log \beta_2$	$\log \beta$	Percent Fe binding	pM
Ethylenediamine	4.34	7.66	9.72	0.01	6.00
Diethylenetriamine	6.23	10.53		0.02	6.00
Catechol	7.95	13.50		0.06	6.00
Glycine	4.13			0.15	6.00
Cysteine	6.2	11.77		0.40	6.00
Oxalic acid	3.05	5.15		1.17	6.01
Triethylenetetramine	7.76			4.6	6.02
Iminodiacetic acid (VI)	5.8			6.7	6.03
Histidine	5.88	10.43		13.0	6.06
Citric acid (V)	4.40			19.50	6.09
Picolinic acid	4.90	9.00	12.30	45.7	6.27
Nitrilotriacetic acid (VII)	8.33	12.80		91.6	7.07
Bipyridine	4.20	7.90	17.2	98.2	7.75
2-Mercaptoethyl-ida (VIII)	11.72			99.6	7.40
1,10-Phenanthroline	5.85	11.15	21.0	99.94	11.53
edta (I)	14.27			100	12.40
dtpa	16.40			100	13.25

^a $\log \beta$ defined in Eq. (4). Values for 0.1 M ionic strength and 25°C from Refs. 48 and 73.

mercaptoethyl)-iminodiacetic acid (**VIII**). Addition of an acetate group to **VI** to form **VII** raises the $\log \beta_{110}$ value from 5.8 to 8.33, while addition of the mercaptoethyl group to form **VIII** leads to a much larger $\log \beta_{110}$ value of 11.72. There is also an increase in β_{110} of two log units between glycine and cysteine due to coordination of the thiol side chain of cysteine.



	R	
VI.	H	(ida)
VII.	CH ₂ COOH	(nta)
VIII.	CH ₂ CH ₂ -SH	(meida)

The tris complexes of the aromatic amines bipy and phen with Fe^{2+} have unusually large stability constants. The stepwise binding constant for the binding of the third ligand is in fact much larger than the binding constant for the first ligand (48). This reversal in the usual trend in binding constants is associated with a change from a high-spin to a low-spin complex and the resulting change in ligand field stabilization energy (LFSE). The LFSE can be understood in terms of the d -orbital splitting diagram shown in Fig. 3. Each time an electron is placed in one of the lower t_{2g} orbitals, the complex is stabilized by $0.4\Delta_o$. Conversely, when an electron occupies one of the higher energy e_g orbitals, the complex is destabilized by $0.6\Delta_o$. In a high-spin ferrous complex, the d -orbital occupancy is $t_{2g}^4 e_g^2$, which results in a net LSFE of only $0.4\Delta_o$. In a low-spin ferrous complex, the configuration is t_{2g}^6 , which gives the maximum LFSE of $2.4\Delta_o$, and the complex is stabilized by $2\Delta_o - 2$ (pairing energy). This spin-state change occurs upon the formation of the tris chelates of both bipy and phen. The effect can be clearly seen in the linear free-energy relationship between Fe^{2+} and Mn^{2+} shown in Fig. 11. The open symbols represent the $\log \beta$ values for a series of ligands that bind through some combination of nitrogen donors. There is a very good linear relationship between the stability constants for Fe^{2+} and Mn^{2+} , which forms high-spin complexes with all these ligands. The filled symbols represent the β_{110} , β_{120} , and β_{130} values for bipy and phen. The points for the high-spin 1:1 and 2:1 complexes fall near the regression line for the LFER. The two points that deviate strongly from this line represent the β_{130} values for the low-spin tris complexes. From the figure one can see that the change in spin state increases β_{130} by about 10 log units.

Values for pM have been calculated using the same conditions as for the ferric ion calculations ($1 \mu\text{M Fe}^{2+}$, $10 \mu\text{M}$ ligand, pH 7.4) and are listed in Table 6. Hexadentate ligands such as edta and dtpa produce moderate pM values of ~ 13 . However, the majority of the ligands listed in Table 6 have pM values between 6 and 8. Since the total iron concentration is 10^{-6} M, a pM of 6.00 corresponds to no binding whatsoever. Table 6 also lists the percentage of the ferrous ion that is bound by each ligand.

None of the common physiological ligands listed in Table 6 (glycine, histidine, cysteine, oxalate, citrate, or phosphate) binds a substantial fraction of the ferrous ion under the conditions selected for the pM calculations. The strongest binding is associated with histidine (13% binding) and citrate (20% binding). Complexation by histidine is favored over that of the aliphatic polyamines such as en and dien by the

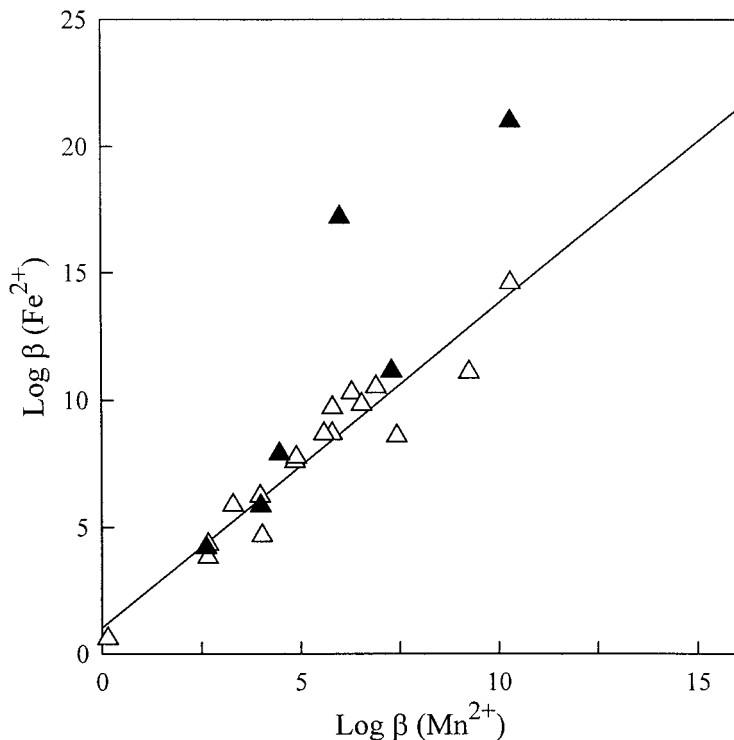


Figure 11 Linear free-energy relationship between the $\log \beta$ values for Mn^{2+} and Fe^{2+} with a series of amine and pyridyl ligands. The filled symbols represent the binding constants for 2,2'-bipyridine and 1,10-phenanthroline. The two points for the tris chelates deviate from the line because of the large ligand field stabilization energy associated with the change to a low-spin configuration for these complexes.

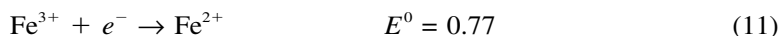
higher binding affinity and lower pK_a for the softer imidazole donor group. The ferrous ion shows a similar affinity for the softer pyridine nitrogen, as shown by the stronger complexation by bipy, phen, and picolinic acid.

The effectiveness of citric acid at neutral pH can be attributed in large part to the fact that the three carboxylate groups are fully deprotonated and thus fully available for binding metal ions. Citrate forms a 1:1 complex $\text{Fe}(\text{cta})^-$. Unlike the ferric ion discussed above, ferrous ion is not able to promote the further deprotonation of the central ROH group of the ligand. Nevertheless, it appears that the neutral ROH group still serves as a donor in the ferrous complex. The crystal structure has been determined for the complex $[\text{Fe}(\text{II})(\text{H}_2\text{O})_6][\text{Fe}(\text{II})(\text{cta})(\text{H}_2\text{O})_2]$ (75). Each citrate molecule binds one ferrous ion as a tridentate ligand via the central carboxylate, the central R-OH group, and one terminal carboxylate group. Each oxygen of the other terminal carboxylate is coordinated to an adjacent ferrous-citrate complex. The hexa-aquo iron(II) complex is present as a counterion. Essentially the same structure has been observed for the citrate complexes with both Mg^{2+} (76) and Mn^{2+} (77).

VI. ELECTROCHEMISTRY

A. Formal Potentials

By convention, formal potentials describe reductions taking place at 298 K in an aqueous solution in which all reagents (including H^+) are present at unit activity, or approximately 1 M concentration. The standard potentials for iron, referenced to the normal hydrogen electrode at 0.0 V (78), are

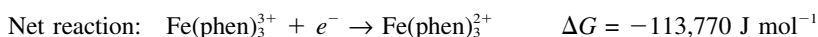


Reduction potentials are easily related to ΔG^0 values for each reaction by the equation

$$\Delta G = -nFE^0 \quad (13)$$

where n is the number of electrons involved in the reaction and F is Faraday's constant ($96,500 \text{ C mol}^{-1} \text{ K}^{-1}$). Thus a positive reduction potential corresponds to a negative ΔG^0 and a thermodynamically favorable reaction. The potentials in Eqs. (10) and (11) illustrate that in acidic solutions, the ferrate anion is an extremely powerful oxidizing agent, and Fe^{3+} is a modest oxidizing agent. The most stable form of iron under standard conditions is the hexaquo ferrous ion.

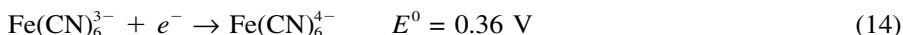
The addition of complexing agents can have a significant effect on the reduction potentials. As discussed above, the tris(phenanthroline)iron(II) complex is exceptionally stable due to the enhanced ligand field stabilization energy for the low-spin ferrous ion. This shifts the electrochemical potential between $Fe(phen)_3^{3+}$ and $Fe(phen)_3^{2+}$ in favor of the ferrous complex. The reduction potential for $Fe(phen)_3^{3+} \rightarrow Fe(phen)_3^{2+}$ can be calculated from the standard ferric ion reduction potential and the binding constants of $Fe(phen)_3^{3+}$ and $Fe(phen)_3^{2+}$. A simple method for this calculation when there are only two species involved is to break the overall reduction reaction down into individual steps and then sum the ΔG values for each step:



$$E^0 = \frac{\Delta G}{-nF} = 1.18 \text{ V}$$

Thus complexation by phenanthroline shifts the ferric reduction potential by +0.41 V from the potential of the aquo ions.

Reduction potentials are also affected by the accumulation of charge and changes in solvation energy. For example, the reduction potential for ferricyanide is



This potential is less than the standard ferric ion reduction potential, indicating that CN^- is stabilizing the harder Fe^{3+} ion even though it is a soft, π -receptor ligand. The reduction of the ferric complex leads to the formation of a tetra-anion. This high

charge leads to very strong solvation and a very unfavorable entropy change for this reaction (78), and electrostatic repulsion among the CN ligands further weakens the complexation, especially of the ferrous complex.

The presence of hard ligands is expected to favor the ferric oxidation state and shift the reduction potential to more negative values. For example, the reduction potential of the ferric complex of DFO at pH 7 is -0.468 V (53). The formal reduction potential for ferric enterobactin is even more negative, -0.99 V at pH 10 (79). At lower pH, one of the catecholate groups in the ferrous–enterobactin complex is protonated and the reduction potential increases to -0.790 V at physiological pH (79).

The ferric \rightarrow ferrous reduction potentials for several iron proteins are listed in Table 7. These are effective reduction potentials for pH 7, rather than standard potentials. The protein reduction potentials vary by more than 0.9 V. Some of this variation can be attributed to changes in the HSAB character of the ligands. For example, transferrin binds through a rather hard set of donor atoms, in particular two tyrosine side chains, that strongly prefer coordination to ferric ion and result in a low reduction potential of -0.526 V (80). Similarly, the heme group in catalase, which has a hard tyrosine axial ligand, has a more negative reduction potential than the heme group in proteins such as myoglobin and horseradish peroxidase, which have softer histidine axial ligands.

Unlike small molecules, proteins also have the capability to vary the local solvent and electrostatic environment around the redox center, and this provides an additional means of tuning the reduction potential (81). The reduction potential for

Table 7 Effective $\text{Fe}^{3+} \rightarrow \text{Fe}^{2+}$ Reduction Potentials at pH 7 for a Series of Iron Proteins

	$E_{\text{eff}}^{\text{a}}$	Axial ligands	Reference
Heme proteins			
Cytochrome c oxidase (heme a_3)	0.40	his	(119)
Cytochrome oxidase (heme a)	0.20	his, his	(119)
Cytochrome c	0.26	his, met	(18)
Methemoglobin	0.17	his	(18)
Metmyoglobin	0.05	his	(18)
Horseradish peroxidase	-0.17	his	(18)
Cytochrome c_3	-0.20	his, his	(81)
Cytochrome P450	-0.30	cys	(43)
Catalase	-0.42	tyr	(18)
Nonheme proteins			
HiPip ^b	0.350		(81)
Methane monooxygenase	0.350		(19)
Methemerythrin	0.110		(19)
Rubredoxin	-0.05 to $+0.05$		(43)
2Fe–2S ferredoxin	-0.270 to -0.420		(119)
4Fe–4S ferredoxin	-0.280 to -0.450		(119)
Serum transferrin	-0.526 (pH = 5.8)		(80)

^aVolts versus normal hydrogen electrode.

^bHigh-potential 4Fe–4S proteins.

hemoglobin, myoglobin, horseradish peroxidase, and cytochrome c oxidase vary by 0.57 V, even though all these proteins contain a 5-coordinate heme group with a histidine axial ligand. There is very little electrochemical data available for Fe^{4+} . No formal reduction potential for an Fe^{4+} aquo ion has been reported. The ferryl porphyrin complex has an effective reduction potential of about +1 V at pH 7 (82).

B. Effect of Hydrolysis on Redox Chemistry

Since no explicit protons are involved in Eq. (11), it is not obvious that the reduction potential for free Fe^{3+} will be pH-dependent. However, increasing the pH corresponds to the addition of a good ferric ion-complexing agent, the OH^- anion. As the pH increases, the population of ferric ion in solution is partitioned between the true aquo ion, Fe^{3+} , and its hydrolysis products, $\text{Fe}(\text{OH})^{2+}$, $\text{Fe}(\text{OH})_2^+$, $\text{Fe}(\text{OH})_3$, and $\text{Fe}(\text{OH})_4^-$. Hydrolysis stabilizes ferric ion relative to ferrous ion and reduces the reduction potential.

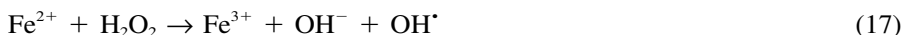
To calculate an effective reduction potential for ferric ion at a specified pH, the full range of hydrolyzed species of both ferric and ferrous ion should be considered. At pH 7.4, over 90% of the soluble ferric ion is present as $\text{Fe}(\text{OH})_3$ while hydrolysis of the ferrous ion is negligible, so the reaction at this pH can be approximated as



A formal potential of +0.913 V can be calculated for Eq. (15) using the summation of ΔG° 's, as described above for the phenanthroline system. The effective potential for Eq. (15) at pH 7.4 is +0.216 V. Aggregation of $\text{Fe}(\text{OH})_3(\text{aq})$ into a solid stabilizes the ferric ion by an additional 59 kJ mol⁻¹. This reduces the effective reduction potential that relates solid $\text{Fe}(\text{OH})_3$ to the aquated ferrous ion even further, to -0.391 V. Thus, while acidic solutions of ferrous ion are stable to air oxidation, neutral solutions are not.

C. Fenton Chemistry

The reactions of dioxygen species and $\text{Fe}^{3+/2+}$ has received considerable attention because they produce the very reactive hydroxyl radical (83–85). The use of iron to catalyze the oxidation of a wide variety of organic compounds under nonbiological conditions has been studied (83,86), but the interest here stems primarily from the potential for generating hydroxyl radical in vivo and the tissue damage that can result (84,85,87). The basic Fenton reaction system can be described as



In the first step, the superoxide anion reduces ferric to ferrous ion. In biological systems, ascorbate can substitute to some extent for superoxide as the reducing agent (84,88). In the second step this ferrous ion promotes the fission of the O–O bond in peroxide to generate a hydroxyl anion and a hydroxyl radical. The overall effect is that iron catalyzes the reaction



This reaction is very rapid under acidic conditions, where the superoxide anion is protonated, but is very slow at neutral pH in the absence of a catalyst (87).

The hydroxyl radical is extremely reactive and will not survive long enough to diffuse far from the site of generation (84,88,89). It will abstract a hydrogen atom from virtually any type of biological molecule to form water and an organic radical R[•]. A considerable amount of attention has been focused on the formation of lipid peroxides and on DNA base modification and strand breakages (85,87,88,90).

Both superoxide and peroxide are produced in a variety of biological reactions (84,87,88,91). The presence of free iron provides the catalyst needed for Fenton chemistry and the resulting oxidative damage. There is a poorly defined labile iron pool within cells that provides the normal supply of iron for the synthesis of enzymes (84,87,88,90). Since this free iron pool is essential to the cell, protection against intracellular oxidative damage is mediated primarily by the use of superoxide dismutase and catalase to quickly disproportionate the reactive oxygen species (85).

Extracellular fluids are also exposed to O₂⁻ and H₂O₂ from reactions such as the respiratory burst associated with activated phagocytes (84,88,89), but these fluids in general lack enzymatic protection (84). Instead, protection against oxidative damage is provided by binding the free iron very tightly, primarily to serum transferrin (85,92). In addition to limiting the concentration of free iron, it is essential that the iron complexes have reduction potentials that are low enough to avoid reduction by peroxide and superoxide. As shown in Table 7, transferrin has a very negative reduction potential and thus provides good protection against iron-catalyzed oxidative damage.

In contrast, the ferric complex of edta, with a reduction potential of about 0.1 V at pH 7.4, is an effective Fenton catalyst (91,93). The low-molecular-weight physiological ligands ATP and citrate also form soluble ferric complexes that catalyze Fenton chemistry. A comparison of transferrin and edta illustrates the important point that antioxidant protection is not due simply to the strong binding of the ferric ion. At neutral pH, edta binds ferric ion more strongly than transferrin (see pM values in Table 5). The key is that transferrin is very selective for ferric ion over ferrous ion and thus produces a much larger decrease in the ferric reduction potential.

The problem of iron-catalyzed oxidative damage becomes serious when hypoxic tissues are reoxygenated (88,89,94). This problem can be addressed using chelation therapy with DFO (84,87,88,95). Like transferrin, this hydroxamate siderophore has a high selectivity for ferric ion [$E_{\text{eff}} = -0.468 \text{ V}$ (53)], and thus stops the catalytic production of hydroxyl radical by preventing the reduction of ferric ion. It is also possible to break the Fenton catalytic cycle by using chelators such as bathophenanthroline sulfonate that are selective for ferrous ion (93,96).

Although the general view is that Fenton chemistry is based on the production of hydroxyl radicals, this has been a point of some continuing controversy. An alternative view is that the reaction of ferrous ion with peroxide involves a heterolytic cleavage of the O–O bond to produce one molecule of water and a highly reactive ferryl ion (87,88,97):



In this model of Fenton chemistry, the FeO²⁺ functions in place of the OH[•] and

abstracts a hydrogen atom from a biological molecule to initiate the observed free-radical chemistry. It has also been proposed that Fenton chemistry in organic solvents and with an excess of molecular oxygen involves no free radicals, but rather proceeds via a series of nucleophilic addition reactions (86), but this hypothesis has been severely criticized by workers who favor the more traditional mechanism involving HO[•] (98,99).

VII. LIGAND-EXCHANGE KINETICS

A. Reaction Mechanisms

Metal ions are routinely referred to as either “inert” or “labile,” although these terms have no strict quantitative definitions. A general definition is that complexes with a half-life for ligand-substitution reactions of less than 30 s are labile, while those with longer half-lives are inert (100). A simple way to compare the lability of a series of metals is to compare the rate for the exchange of water molecules in the aquo ions. Some representative water-exchange rate constants are listed in Table 8.

In general, water-exchange rates are inversely related to the charge/radius ratio of the metal ion. A higher charge density leads to stronger metal–ligand bonds and slower water-exchange reactions. Thus trivalent ions tend to react more slowly than divalent ions, and for a given ionic charge, smaller ions react more slowly than larger ions. For ions such as Ca²⁺, which have a low charge density and very weak covalent bonding, the water-exchange rates approach the diffusion limit. The water-exchange rates for iron are $4.4 \times 10^6 \text{ s}^{-1}$ for ferrous ion and $1.6 \times 10^2 \text{ s}^{-1}$ for ferric ion (101). Although the ferric ion reacts more slowly, both ions are considered labile.

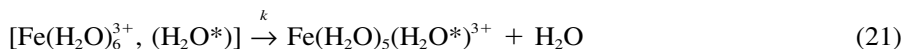
One can envision ligand substitution as proceeding by two simple pathways. In the dissociative (D) pathway, one water ligand dissociates, leaving a 5-coordinate intermediate that then reacts with another water molecule to return to the octahedral hexaaquo ion. In an associative mechanism (A), the hexaaquo complex adds a water molecule to go to a 7-coordinate intermediate, which then loses a water to return to the hexaaquo ion.

Table 8 Water-Exchange Rate Constants for Selected Hexaaquo Metal Ions^a

Metal ion	$k \text{ (s}^{-1}\text{)}$
Ca ²⁺	$\sim 5 \times 10^8$
Mn ²⁺	2.1×10^7
Fe ²⁺	4.4×10^6
Ni ²⁺	3.2×10^4
In ³⁺	$\sim 1 \times 10^6$
Fe ³⁺	1.6×10^2
Al ³⁺	~ 1
Cr ³⁺	2.4×10^{-6}

^aData from Ref. 101.

The exchange of coordinated waters on different metal ions generally falls between the extremes of the pure A and pure D pathways and follows an interchange mechanism (14,101). In this mechanism, there is a weak pre-equilibrium association of the reactants into an outer-sphere complex, followed by ligand exchange within the complex. This process for water exchange on a ferric ion can be described as



where the brackets are used to identify the outer-sphere complex. If the interchange process is dominated by breaking the M–L bond of the leaving group, the mechanism is dissociative interchange (I_d). If the process is governed primarily by the formation of the new M–L bond with the entering group, the mechanism is associative interchange (I_a). Volumes of activation indicate that water exchange at the ferrous ion follows an I_d mechanism, while water exchange at the ferric ion follows an I_a mechanism (101).

Based on the mechanism shown in Eqs. (20) and (21), the overall rate law for the displacement of a coordinated water by an incoming ligand (L) is

$$\text{Rate} = \frac{kK_{\text{OS}}[\text{Fe}(\text{H}_2\text{O})_6^{3+}][\text{L}]}{1 + K_{\text{OS}}[\text{L}]} \quad (22)$$

Since $K_{\text{OS}}[\text{L}]$ is usually $\ll 1$, the rate law reduces to

$$\text{Rate} = kK_{\text{OS}}[\text{Fe}(\text{H}_2\text{O})_6^{3+}][\text{L}] \quad (23)$$

so that the apparent rate constant is $k_{\text{obs}} = kK_{\text{OS}}$ (102). Values for K_{OS} can be approximated from a simple electrostatic model of ion pairing described by the Fousse-Eigen equation (102,103), and this allows one to estimate values for k .

Because of the strong hydrolytic tendency of the ferric ion, even acidic aqueous solutions contain a mixture of $\text{Fe}(\text{H}_2\text{O})_6^{3+}$ and $\text{Fe}(\text{H}_2\text{O})_5(\text{OH})^{2+}$. The presence of the hydroxide ligand increases the rate of water exchange from 160 s^{-1} to $\sim 140,000 \text{ s}^{-1}$ (104). This change in the water-exchange rates directly impacts the rate at which other ligands bind to the ferric ion. For example, the rate constant for the binding of ferric ion by acetohydroxamic acid increases from $1.2 \text{ M}^{-1} \text{ s}^{-1}$ for the unhydrolyzed aquo ion to $2000 \text{ M}^{-1} \text{ s}^{-1}$ for the $\text{Fe}(\text{H}_2\text{O})_5(\text{OH})^{2+}$ ion (53). Most of this increase is due to the enhanced lability of the water ligands. In addition, hydrogen bonding between the coordinated hydroxyl group and the incoming acetohydroxamic acid enhances the formation of the outer-sphere complex between the reactants, and the increase in K_{OS} contributes to the faster rate (53). Since the fraction of hydrolyzed ferric ion increases with pH, the rates of ligand substitution also tend to increase with pH.

B. Ligand Field Activation Energy

Ligand substitution at the Cr^{3+} ion is much slower than for the other ions in Table 8. Such very slow exchange kinetics are associated with a large contribution to the activation energy from changes in ligand field stabilization energies (LFSE). Ligand-exchange reactions all involve some type of distortion of the octahedral coordination geometry of the aquo ion. The change toward either a 5-coordinate or a 7-coordinate

intermediate involves a decrease in the ligand field stabilization energy. The loss of LFSE associated with the formation of the reaction intermediate is referred to as the ligand field activation energy (LFAE). It is particularly high for metal ions with a d^3 or a low-spin d^6 electron configuration. Thus the low-spin ferrous ion will undergo ligand-exchange reactions much more slowly than the high-spin ion. For example, the rate constants for the displacement of the lone aquo ligand in the low-spin $\text{Fe}(\text{CN})_5(\text{H}_2\text{O})^{3-}$ complex are in the range of 300–500 s^{-1} for several different entering ligands (105). This is about four orders of magnitude slower than water exchange on the high-spin ferrous aquo ion. The relative insensitivity to the identity of the entering group is consistent with a dissociative mechanism. The exchange of the tightly bound CN^- ligands in the low-spin $\text{Fe}(\text{CN})_6^{2-}$ ion has a half-life of approximately 4 days at pH 3.5 (106).

Ligand field activation energy is also important for low-spin Fe^{3+} . The replacement of the aquo ligand in the low-spin $\text{Fe}(\text{CN})_5(\text{H}_2\text{O})^{2-}$ complex by 0.1 M SCN^- has a pseudo-first-order rate constant of about 0.04 s^{-1} (107), which is about four orders of magnitude slower than the water-exchange rate for the ferric aquo ion. Even this rate may be high due to catalysis by traces of the ferrous $\text{Fe}(\text{CN})_5(\text{H}_2\text{O})^{3-}$ complex (108). Cyanide exchange for $\text{Fe}(\text{CN})_6^{3-}$ has a half-life at pH 9 of more than 10 days (106).

Porphyry ligands tend to accelerate the rate of exchange of the axial ligands in $\text{Fe}(\text{porphyrin})\text{L}_2$ complexes (109). The exchange of axial water ligands on the high-spin ferric complex with mesotetrakis(*p*-sulfonatophenyl)porphine has a rate constant of 10^7 s^{-1} (110), which is substantially faster than the rate of water exchange for the ferric aquo ion. This is attributed to a cis effect due to π donation from the porphyrin ring into the d_{zx} and d_{yx} orbitals on the metal ion.

C. Reactions with Multidentate Ligands

The reaction between Fe^{3+} and DFO has been studied extensively by Crumbliss and co-workers (53,111,112), and this system serves as an excellent example of the mechanisms of reactions involving strong, multidentate ligands. First consider the acid-promoted dissociation of ferric-DFO,



(DFO is defined here as the form of the ligand where the primary amine is protonated and the three hydroxamate groups are ionized). The three bidentate hydroxamate groups dissociate from the iron in discrete steps, and it is possible to detect spectroscopically the partially coordinated $\text{Fe}(\text{HDFO})(\text{H}_2\text{O})_2^+$ and $\text{Fe}(\text{H}_2\text{DFO})(\text{H}_2\text{O})_4^{2+}$ reaction intermediates. The first hydroxamate group dissociates with a rate constant of 290 $\text{M}^{-1} \text{ s}^{-1}$. The loss of the second hydroxamate ring is slower ($k = 0.34 \text{ M}^{-1} \text{ s}^{-1}$), and the loss of the third and final hydroxamate group is even slower ($k = 0.0019 \text{ M}^{-1} \text{ s}^{-1}$) (53). In the reverse of Eq. (24), the complexation of Fe^{3+} by H_3DFO , the formation of the first chelate ring is the slow, rate-determining step ($k = 0.2 \text{ M}^{-1} \text{ s}^{-1}$) (53). The subsequent chelate ring closures of the other two hydroxamate groups to form the final, hexacoordinate complex are too rapid to be detected.

The ferric–DFO dissociation reactions described above take place in very acidic solutions. At neutral pH, the strong binding of ferric ion by ligands such as edta or DFO reduces the free iron concentration to such extremely low values that

it is impossible to obtain meaningful rates of iron exchange between these ligands by a mechanism in which one complex first dissociates completely, followed by binding of the free iron to a new ligand. It is now well established that the exchange of metal ions between strong multidentate ligands proceeds by a mechanism involving (a) the loss of one or more chelate rings in the initial complex, which exposes aquated coordination sites, (b) the formation of a ternary complex by the binding of donor groups from the incoming ligand to these aquated sites, and (c) the loss of the initial ligand and rapid chelate ring closure reactions of the incoming ligand to form the final complex (53,111,113–115).

Metal exchange between strong multidentate ligands can be very slow. The reactions are first-order in both the donating metal complex and the receiving ligand (113), so the exchange half-lives are concentration-dependent. Based on the data in Refs. (113) and (116), the half-lives for the donation of iron from 1 mM ferric–edta to 1 mM DFO and 1 mM HBED are estimated to be 42 h and 14 h, respectively. The exchange of iron between DFO and edta can be accelerated by the addition of a bidentate hydroxamate ligand that creates a small labile pool of iron (111).

The rates at which multidentate ligands dissociate from a metal ion are also influenced by the rigidity of the chelate ring structure. A more rigid chelate ring increases the probability that a dissociated donor group will return to its original coordination site on the metal ion before the other end of the chelate ring dissociates, so that no net reaction takes place. Consider the rate of dissociation of the two ligands 2,2'-bipyridine (bipy) and 1,10-phenanthroline (phen). The donor atoms are very similar, but there is relatively free rotation between the two rings in bipy, while the phen ligand is rigidly planar. As a result, bipy dissociates from low-spin iron(II) about 10 times faster than phen (117).

This type of steric effect can be quite large for macrocyclic ligands. In the formation of a metal–macrocyclic complex, the rate-limiting step is often shifted from the first bond formation to a later chelate ring closure (118). Once the metal ion is bound inside the cavity of the ligand, the more rigid ligand structure makes it very difficult for a single donor group to dissociate and make room for attack by an incoming ligand. Thus the rates of metal ion dissociation from macrocycles can be very slow (118). This macrocyclic kinetic effect becomes even stronger with increasing rigidity of the ligand, and it follows that the rates of iron dissociation from porphyrins are extremely slow. In biological systems, iron is inserted into the porphyrin ring by ferrochelatase, after which there is no significant metal exchange (119).

VIII. SUMMARY

Iron is the most abundant transition metal, both in terms of cosmic abundance and in terms of its concentration in the Earth's crust. It is found in biological systems as Fe(II), Fe(III), and Fe(IV). Iron(IV) occurs in reactive intermediates in enzyme catalytic cycles, and is not important in terms of iron storage and transport. The *d–d* electronic spectra and magnetic properties of mononuclear ferrous and ferric complexes are determined by the spin state of the metal ion, with characteristic features for the high- and low-spin states. Most of the *d–d* electronic absorption bands for ferric and ferrous ions are either very weak or fall outside the visible region of the spectra, so that the visible spectra of iron compounds tend to be dominated by intense

charge-transfer bands. For polynuclear ferric and ferrous complexes, the magnetic properties can include the effects of either ferromagnetic or antiferromagnetic coupling between the metal ions. This type of magnetic superexchange is typically larger for ferric ions.

Ferric ion forms strong complexes with hard, oxygen-donor ligands, while ferrous ion forms less stable complexes with a preference for softer ligands. Hydrolysis severely restricts the solubility of ferric ion at neutral pH, while the ferrous ion is quite soluble. The stable oxidation state of iron in acidic solutions is Fe^{2+} , but complexation reactions can shift the ferric \rightarrow ferrous reduction potential over a wide range. Hydrolysis reactions strongly stabilize the ferric state such that the hexaquo ferrous ion is unstable to air oxidation at physiological pH. Ferric ion must be strongly chelated at physiological pH to prevent the precipitation of ferric hydroxide and to avoid the catalysis of redox reactions that generate hydroxyl radical. Both high-spin aquo ions are labile, and the water-exchange reactions follow I_d and I_a mechanisms for Fe^{2+} and Fe^{3+} , respectively. The exchange of iron between two strong polydentate ligands must proceed via the formation of an intermediate ternary complex of the metal with both ligands, and these reactions can be quite slow. In addition, the formation of low-spin complexes for both Fe^{3+} and Fe^{2+} leads to a sharp reduction in ligand-exchange rates.

REFERENCES

1. Selbin J. The origin of the chemical elements, 2. J Chem Ed 1973; 50:380–387.
2. Kirshner RP. The Earth's elements. Sci Am 1994; 59–65.
3. Selbin J. The origin of the chemical elements, 1. J Chem Ed 1973; 50:306–310.
4. Burbridge EM, Burbridge GR, Fowler WA, Hoyle F. Synthesis of the elements in stars. Rev Mod Phys 1957; 29:547–650.
5. Mason SF. Chemical Evolution. Origin of the Elements, Molecules, and Living Systems. Oxford, UK: Clarendon Press, 1991.
6. Rösler HJ, Lange H. Geochemical Tables. Amsterdam: Elsevier, 1972.
7. Mason B. Principles of Geochemistry. 3d ed. New York: Wiley, 1966.
8. Holland HD. The Chemical Evolution of the Atmosphere and Oceans. Princeton, NJ: Princeton University Press, 1984.
9. Cairns-Smith AG. Precambrian solution photochemistry, inverse segregation, and banded iron formation. Nature 1978; 276:807–808.
10. Aisen P. Iron metabolism: An evolutionary perspective. In: Brock JH, Halliday JW, Pippard MJ, Powell LW, eds. Iron Metabolism in Health and Disease. London: Saunders, 1994:1–30.
11. Allègre CJ, Schneider SH. The evolution of the earth. Sci Am 1994; 66–75.
12. Silver J. Introduction to iron chemistry. In: Silver J, ed. Chemistry of Iron. New York: Blackie, 1993:1–29.
13. Matzanke BF, Müller-Matsanke G, Raymond KN. Siderophore-mediated iron transport. In: Loehr TM, ed. Iron Carrier and Iron Proteins. New York: VCH, 1989:1–121.
14. Cotton FA, Wilkinson G. Advanced Inorganic Chemistry. 5th ed. New York: Wiley, 1988.
15. Viste A, Gray HB. The electronic structure of permanganate ion. Inorg Chem 1964; 3: 1113–1123.
16. Porter TD, Coon MJ. Cytochrome P-450. J Biol Chem 1991; 266:13469–13472.
17. Dawson JH. Probing structure-function relations in heme-containing oxygenases and peroxidases. Science 1988; 240:433–439.

18. Cowan JA. Inorganic Biochemistry. New York: VCH, 1993.
19. Sanders-Loehr J. Binuclear iron proteins. In: Loehr TM, ed. Iron Carrier and Iron Proteins. New York: VCH, 2000:373–466.
20. Waller BJ, Lipscomb JD. Dioxygen activation by enzymes containing binuclear non-heme iron clusters. Chem Rev 1996; 96:2625–2657.
21. Eriksson M, Jordan A, Eklund H. Structure of *Salmonella typhimurium* nrdF ribonucleotide reductase in its oxidized and reduced forms. Biochemistry 1998; 37:13359–13369.
22. Dunietz BD, Beachy MD, Cao Y, Whittington DA, Lippard SJ, Friesner RA. Large scale ab initio quantum mechanical calculation of the intermediates in the soluble methane monooxygenase catalytic cycle. J Am Chem Soc 2000; 122:2828–2839.
23. Choi SJ, Eaton PE, Kopp DA, Lippard SJ, Newcomb M, Shen R. Cationic species can be produced in soluble methane monooxygenase-catalyzed hydroxylation reactions; Radical intermediates are not formed. J Am Chem Soc 1999; 121:12198–12199.
24. Jin Y, Lipscomb JD. Probing the mechanism of C-H activation: Oxidation of methylcubane by soluble methane monooxygenase from *Methylosinus trichosporium* OB3b. Biochemistry 1999; 38:6178–6186.
25. Newcomb M, Shen R, Choi SJ, Toy PH, Hollenberg PF, Vaz ADF, Coon MJ. Cytochrome P450-catalyzed hydroxylation of mechanistic probes that distinguish between radicals and cations. Evidence for cationic but not for radical intermediates. J Am Chem Soc 2000; 122:2677–2686.
26. Jordan A, Reichard P. Ribonucleotide reductases. Ann Rev Biochem 1998; 1998:71–98.
27. Miessler GL, Tarr DA. Inorganic Chemistry. 2d ed. Upper Saddle River, NJ: Prentice-Hall, 1991.
28. Huheey JE. Inorganic Chemistry. 4th ed. New York: Harper & Row, 1993.
29. Shannon RD. Revised effective ionic radii and systematic studies of interatomic distances in halides and chalcogenides. Acta Crystallogr 1976; A32:751–767.
30. Scheidt WR, Reed CR. Spin-state/stereochemical relationships in iron porphyrins: Implications for the heme proteins. Chem Rev 1981; 81:543–555.
31. Fleischer EB. The structure of porphyrins and metalloporphyrins. Acc Chem Res 1970; 3:105–112.
32. Perutz MF, Fermi G, Luisi B, Shaanan B, Liddington RC. Stereochemistry of cooperative mechanisms in hemoglobin. Acc Chem Res 1987; 20:309–321.
33. Kettle SFA. Physical Inorganic Chemistry. Oxford, UK: Spektrum, 1996.
34. Ellison MK, Nasri H, Xia Y-M, Marchon J-C, Schulz CE, Debrunner PG, Scheidt WR. Characterization of the bis(azido)(meso-tetraphenylporphinato)ferrate(III) anion. An unusual spin-equilibrium system. Inorg Chem 1997; 36:4804–4811.
35. Timken MD, Hendrickson DN, Sinn E. Dynamics of spin-state interconversion and cooperativity for spin-crossover complexes in the solid state. 3. Bis(N-(2-(benzylamino)ethyl)salicylaldimato)iron(III) complexes. Inorg Chem 1985; 24:3947–3955.
36. König E, Ritter G, Irlner W, Goodwin HA. The high-spin (5T_2) \leftrightarrow low spin (1A_1) transition in solid bis(1,10-phenanthroline-2-carbaldehyde phenylhydrazone)iron(II) dichlorate. Simultaneous change of molecular spin state and crystallographic structure. J Am Chem Soc 1980; 102:4681–4687.
37. Murray KS. Binuclear oxo-bridged iron(III) complexes. Coord Chem Rev 1974; 12: 1–35.
38. Petersson L, Cammack R, Rao KK. Antiferromagnetic exchange interaction in the two-iron-two-sulfur ferredoxin from the blue-green alga *Spirulina maxima* studied with a highly sensitive magnetic balance. Biochim Biophys Acta 1980; 622:18–24.
39. Papaefthymiou GC, Laskowski EJ, Frota-Pressôa S, Frankel RB, Holm RH. Antiferromagnetic exchange interactions in $[\text{Fe}_4\text{S}_4(\text{SR})_4]^{2-3-}$ clusters. Inorg Chem 1982; 21: 1723–1728.

40. Noodleman L, Case DA. Density-functional theory of spin polarization and spin coupling in iron-sulfur clusters. *Adv Inorg Chem* 1992; 38:423–470.
41. Belinskii M. Spin coupling model for tetrameric iron clusters in ferredoxins. II. Hyperfine interactions, magnetism, high-spin systems. *Chem Phys* 1993; 172:213–238.
42. Moura I, Moura JGG. Simple iron-sulfur proteins. Methodology for establishing the type of center. In: Dunford HB, Dolphin D, Raymond KN, Sieker L, eds. *The Biological Chemistry of Iron*. Boston: Reidel, 1982:179–192.
43. Lippard SJ, Berg JM. *Principles of Bioinorganic Chemistry*. Mill Valley, CA: University Science Books, 1994.
44. Carney MJ, Papaefthymiou GC, Spartalian K, Frankel RB, Holm RH. Ground spin state variability in $[\text{Fe}_4\text{S}_4(\text{SR})_4]^{3-}$. Synthetic analogues of the reduced clusters in ferredoxins and other iron-sulfur proteins: Cases of extreme sensitivity of electronic state and structure to extrinsic factors. *J Am Chem Soc* 1988; 110:6084–6095.
45. Ebsworth EA, Rankin DWH, Craddock S. *Structural Methods in Inorganic Chemistry*. 2d ed. Boca Raton, FL: CRC Press, 1991.
46. Ochiai EI. *Bioinorganic Chemistry*. Boston: Allyn & Bacon, 1977.
47. Vasák M, Kägi JHR, Homquist B, Vallee BL. Spectral studies of cobalt(II)- and nickel(II)-metallothionein. *Biochemistry* 1981; 20:6659–6664.
48. Martell AE, Smith RM. *Critical Stability Constants*. New York: Plenum Press, 1974.
49. Bannochie CJ, Martell AE. Synthesis, separation and equilibrium characterization of racemic and meso forms of a new multidentate ligand: N,N'-trimethylenebis[2-(2-hydroxy-3,5-dimethylphenyl)glycine], TMPHPG. *Inorg Chem* 1991; 30:1385–1392.
50. Aisen P, Leibman A, Zweier J. Stoichiometric and site characteristics of the binding of iron to human transferrin. *J Biol Chem* 1978; 253:1930–1937.
51. Baes CF, Mesmer RE. *The Hydrolysis of Cations*. New York: Wiley, 1976.
52. Martin RB. Aluminum: A neurotoxic product of acid rain. *Acc Chem Res* 1994; 27: 204–210.
53. Albretch-Gary A-M, Crumbliss AL. Coordination chemistry of siderophores: Thermodynamics and kinetics of iron chelation and release. *Metal Ions Biol Syst* 1998; 35: 239–327.
54. Aisen P. Transferrin, the transferrin receptor, and the uptake of iron by cells. In: Sigel A, Sigel H, eds. *Metal Ions in Biological Systems*. New York: Marcel Dekker, 1998: 585–631.
55. L'Epplattenier F, Murase I, Martell AE. New multidentate ligands. VI. Chelating tendencies of N,N'-di(2-hydroxybenzyl)ethylenediamine-N,N'-diacetic acid. *J Am Chem Soc* 1967; 89:837–843.
56. Motekaitis RJ, Sun Y, Martell AE. New synthetic, selective, high-affinity ligands for effective trivalent metal ion binding and transport. *Inorg Chim Acta* 1992; 198–200, 421–428.
57. Harris WR, Raymond KN, Weilt FW. Ferric ion sequestering agents. 6. The spectrophotometric and potentiometric evaluation of sulfonated tricatecholate ligands. *J Am Chem Soc* 1981; 103:2667–2675.
58. Harris WR, Carrano CJ, Cooper SR, Sofen SR, Avdeef AE, McArdle JV, Raymond KN. Coordination chemistry of microbial iron transport compounds. 19. Stability constants and electrochemical behavior of ferric enterobactin and model compounds. *J Am Chem Soc* 1979; 101:6097–6104.
59. Loomis LD, Raymond KN. Solution equilibria of enterobactin and metal-enterobactin complexes. *Inorg Chem* 1991; 30:906–911.
60. Dobbin PS, Hider RC. Iron chelation therapy. *Chem Brit* 1990; 26:565–568.
61. Hider RC, Hall AD. Clinically useful chelators of tripositive elements. *Prog Med Chem* 1991; 28:43–173.

62. Porter JB, Huehns ER, Hider RC. The development of iron chelating drugs. *Baillière's Clin Haematol* 1989; 2:257–292.
63. May PM, Linder PW, Williams DR. Computer simulation of metal-ion equilibria in biofluids: Models for the low-molecular-weight complex distribution of calcium(II), magnesium(II), manganese(II), iron(III), copper(II), zinc(II), and lead(II) ions in human blood plasma. *J Chem Soc Dalton* 1977; 588–595.
64. Timberlake CF. Iron-malate and iron-citrate complexes. *J Chem Soc* 1964; 5078–5085.
65. Field TB, McCourt JL, McBryde WAE. Composition and stability of iron and copper citrate complexes in aqueous solution. *Can J Chem* 1974; 52:3119–3124.
66. Martin RB. Citrate binding of Al^{3+} and Fe^{3+} . *J Inorg Biochem* 1986; 28:181–187.
67. Spiro TG, Pape L, Saltman P. The hydrolytic polymerization of ferric citrate. I. The chemistry of the polymer. *J Am Chem Soc* 1967; 89:5555–5559.
68. Spiro TG, Bates GW, Saltman P. The hydrolytic polymerization of ferric citrate. II. The influence of excess citrate. *J Am Chem Soc* 1967; 89:55–62.
69. Matzapetakis M, Raptopoulou CP, Tsohos A, Papaefthymiou V, Moon N, Salifoglou A. Synthesis, spectroscopic and structural characterization of the first mononuclear, water soluble iron-citrate complex, $(NH_4)_5Fe(C_6H_4O_7)_2 \cdot 2H_2O$. *J Am Chem Soc* 1998; 120:13266–13267.
70. Matzapetakis M, Raptopoulou CP, Terzis A, Lakatos A, Kiss T, Salifoglou A. Synthesis, structural characterization, and solution behavior of the first mononuclear, aqueous aluminum citrate complex. *Inorg Chem* 1999; 38:618–619.
71. Pollack S, Vanderhoff G, Lasky F. Iron removal from transferrin. An experimental study. *Biochim Biophys Acta* 1977; 481–487.
72. Morgan EH. Iron exchange between transferrin molecules mediated by phosphate compounds and other cell metabolites. *Biochim Biophys Acta* 1977; 499:169–177.
73. Pettit LD, Powell KJ. Stability Constants Database, SC-Database for Windows. 2d ed. Trimble, Otley, UK: Academic Software, 1997.
74. Bali PK, Harris WR. Cooperativity and heterogeneity between the two binding sites of diferric transferrin during iron removal by pyrophosphate. *J Am Chem Soc* 1989; 111:4457–4461.
75. Strouse J, Layten SW, Strouse CE. Structural studies of transition metal complexes of triionized and tetraionized citrate. Models for the coordination of the citrate ion to transition metal ions in solution and at the active site of aconitase. *J Am Chem Soc* 1977; 99:562–572.
76. Johnson CK. X-ray crystal analysis of the substrates of aconitase. V. Magnesium citrate decahydrate $[Mg(H_2O)_6][MgC_6H_5O_7(H_2O)_2] \cdot 2H_2O$. *Acta Crystallogr* 1965; 18:1004–1018.
77. Glusker JP, Carrell HL. X-ray crystal analysis of the substrates of aconitase XI. Manganous citrate decahydrate. *J Mol Struct* 1973; 15:151–159.
78. Rayner-Canham G. *Descriptive Inorganic Chemistry*. New York: Freeman, 2000.
79. Lee C-W, Ecker DJ, Raymond KN. The pH-dependent reduction of ferric enterobactin probed by electrochemical methods and its implications for microbial iron transport. *J Am Chem Soc* 1985; 1985:6920–6923.
80. Kraiter DC, Zak O, Aisen P, Crumbliss AL. A determination of the reduction potential for diferric and C- and N-lobe monoferric transferrins at endosomal pH (5.8). *Inorg Chem* 1998; 37:964–968.
81. Reed CR. Oxidation states, redox potentials and spin states. In: Dunford HB, Dolphin D, Raymond KN, Sieker L, eds. *The Biological Chemistry of Iron*. Boston: Reidel, 1982:25–42.
82. Wikström M, Morgan JE. The dioxygen cycle. Spectral, kinetic, and thermodynamic characteristics of ferryl and peroxy intermediates observed by reversal of the cytochrome oxidase reaction. *J Biol Chem* 1992; 267:10266–10273.

83. Walling C. Fenton's reagent revisited. *Acc Chem Res* 1974; 8:125–131.
84. Halliwell B, Gutteridge JMC. Oxygen free radicals and iron in relation to biology and medicine: Some problems and concepts. *Arch Biochem Biophys* 1986; 246:501–514.
85. Gutteridge JMC. Hydroxyl radicals, iron, oxidative stress, and neurodegeneration. *Ann NY Acad Sci* 1994; 738:201–213.
86. Sawyer DT. Metal [Fe(II), Cu(I), Co(II), Mn(II)]/hydroperoxide-induced activation of dioxygen (O_2) for ketonization of hydrocarbons: Oxygenated Fenton chemistry. *Coord Chem Rev* 1997; 165:297–313.
87. Halliwell B, Gutteridge JMC. Oxygen toxicity, oxygen radicals, transition metals and disease. *Biochem J* 1984; 219:1–14.
88. Halliwell B, Gutteridge JMC. Role of free radicals and catalytic metal ions in human disease. *Methods Enzymol* 1990; 199:1–85.
89. Hershko C. Iron chelators. In: Brock JH, Halliday JW, Pippard MJ, Powell LW, eds. *Iron Metabolism in Health and Disease*. London: Saunders, 1994:392–436.
90. Hershko C, Link G, Cabantchik I. Pathophysiology of iron overload. *Ann NY Acad Sci* 1998; 850:191–201.
91. Winterbourn CC. Hydroxyl radical production in body fluids. *Biochem J* 1981; 198:125–131.
92. Gutteridge JMC, Quinlan GJ. Antioxidant protection against organic and inorganic oxygen radicals by normal human plasma: The important primary role for iron-binding and iron-oxidizing proteins. *Biochim Biophys Acta* 1993; 1156:144–150.
93. Butler J, Halliwell B. Reaction of iron-edta chelates with the superoxide radical. *Arch Biochem Biophys* 1982; 218:174–178.
94. Tilbrook GS, Hider RC. Iron chelators for clinical use. In: Sigel A, Sigel H, eds. *Iron Transport and Storage in Microorganisms, Plants, and Animals*. New York: Marcel Dekker, 1998:691–730.
95. Williams RE, Zweier JL, Flaherty JT. Treatment with deferoxamine during ischemia improves functional and metabolic recovery and reduces reperfusion-induced oxygen radical generation in rabbit hearts. *Circulation* 1991; 83:1006–1014.
96. Halliwell B. Superoxide-dependent formation of hydroxyl radicals in the presence of iron salts. *FEBS Lett* 1978; 96:238–242.
97. Halliwell B, Gutteridge JMC. Biologically relevant metal ion-dependent hydroxyl radical generation. An update. *FEBS Lett* 1992; 307:108–112.
98. MacFaul PA, Wayner DDM, Ingold KU. A radical account of “oxygenated Fenton chemistry.” *Acc Chem Res* 1998; 31:159–162.
99. Walling C. Intermediates in the reactions of Fenton type reagents. *Acc Chem Res* 1998; 31:155–157.
100. Douglas B, McDaniel D, Alexander J. *Concepts and Models of Inorganic Chemistry*. 3d ed. New York: Wiley, 1994.
101. Helm L, Merbach AE. Water exchange on metal ions: Experiments and simulations. *Coord Chem Rev* 1999; 187:151–181.
102. Shriver D, Atkins P. *Inorganic Chemistry*. 3d ed. New York: Freeman, 1999.
103. Moore JW, Pearson RG. *Kinetics and Mechanism*. 3d ed. New York: Wiley, 1981.
104. Crumbliss AL, Garrison JM. A comparison of some aspects of the aqueous coordination chemistry of aluminum(III) and iron(III). *Commun Inorg Chem* 1998; 8:1–26.
105. Toma HE, Malin JM. Kinetics of formation and stability constants of some pentacyanoferrate(II) complexes of aromatic nitrogen heterocycles. *Inorg Chem* 1973; 12:2080–2083.
106. MacDiarmid AG, Hall NF. Complex cyanide-simple cyanide exchange systems. *J Am Chem Soc* 1954; 76:4222–4228.
107. Espenson JH, Wolenuk SG. Kinetics and mechanisms of some substitution reactions of pentacyanoferrate(III) complexes. *Inorg Chem* 1972; 11:2034–2041.

108. James AD, Murray RS, Higginson CE. Iron(II) catalysis in substitution reactions of amminepentacyano- and aquopentacyano-ferrate(III) ions. *J Chem Soc Dalton* 1974; 1273–1278.
109. Holloway CE, Stynes DV, Vuik CPJ. Kinetics of ligand exchange in iron(II) complexes of 2,3,9,10-tetramethyl-1,4,8,11-tetra-azacyclotetradeca-1,3,8,10-tetraene. *J Chem Soc Dalton* 1979; 124–130.
110. Ostrich IJ, Liu G, Dodgen HW, Hunt JP. Oxygen-17 nuclear magnetic resonance study of water exchange on water-soluble iron(III) porphyrins. *Inorg Chem* 1980; 19:619–621.
111. Monzyk B, Crumbliss AL. Factors that influence siderophore mediated iron bioavailability: Catalysis of interligand iron(III) transfer from ferrioxamine B to EDTA by hydroxamic acids. *J Inorg Biochem* 1983; 19:19–39.
112. Monzyk B, Crumbliss AL. Kinetics and mechanism of the stepwise dissociation of iron(III) from ferrioxamine B in aqueous acid. *J Am Chem Soc* 1982; 104:4921–4929.
113. Tufano TP, Raymond KN. Coordination chemistry of microbial iron transport compounds. 21. Kinetics and mechanism of iron exchange in hydroxamate siderophore complexes. *J Am Chem Soc* 1981; 103:6617–6624.
114. Crumbliss AL. Iron bioavailability and the coordination chemistry of hydroxamic acids. *Coord Chem Rev* 1990; 105:155–179.
115. Margerum DW, Rosen HM. Multidentate ligand kinetics. XII. Ethylenediaminetetraacetate ion reaction with mono- and bis(diethylenetriamine)nickel(II) complexes. *Inorg Chem* 1968; 7:299–305.
116. Ma R, Motekaitis RJ, Martell AE. Stability of metal ion complexes of N,N'-bis(2-hydroxybenzyl)ethylenediamine-N,N'-diacetic acid. *Inorg Chim Acta* 1994; 224:151–155.
117. Basolo F, Hayes JC, Neuman HM. Mechanism of racemization of complex ions. II. Kinetics of the dissociation and racemization of tris-(1,10-phenanthroline)-iron(II) and tris-(2,2'-dipyridyl)-iron(II) complexes. *J Am Chem Soc* 1954; 76:3807–3809.
118. Lindoy LF. *The Chemistry of Macrocyclic Ligand Complexes*. Cambridge, UK: Cambridge University Press, 1989.
119. Fraústo da Silva JJR, Williams RJP. *The Biological Chemistry of the Elements*. Oxford, UK: Clarendon Press, 1991.

2

Transferrins

ROSS T. A. MACGILLIVRAY

University of British Columbia, Vancouver, British Columbia, Canada

ANNE B. MASON

University of Vermont, Burlington, Vermont

I.	INTRODUCTION	42
II.	CLASSES OF TRANSFERRINS	42
	A. Serum Transferrins	42
	B. Ovotransferrins	43
	C. Lactoferrins	44
	D. Melanotransferrins	45
	E. Other Transferrin-Like Proteins	45
III.	GENETICS OF TRANSFERRINS	46
IV.	STRUCTURE OF TRANSFERRINS	46
V.	EXPRESSION SYSTEMS FOR RECOMBINANT TRANSFERRINS	51
	A. <i>Escherichia coli</i>	52
	B. Filamentous Fungi	53
	C. Yeast Cells	53
	D. Insect Cells	54
	E. Mammalian Cells	54
	F. Other Systems	56
	G. Mutants of Transferrins	56
	ACKNOWLEDGMENTS	56
	REFERENCES	56

I. INTRODUCTION

Since their discovery over 50 years ago by Schade (1,2) and Laurell (3,4), the transferrins have attracted much scientific interest due to their ability to bind Fe(III) and other metals tightly and yet reversibly. The exact chemical nature of these high-affinity metal-binding sites was revealed by the ground-breaking structural work on lactoferrin by Baker and his colleagues in the 1980s (5). These structural studies, together with the availability of large amounts of recombinant transferrins (6) and site-directed mutants (7), have extended our understanding of structure–function relationships in the transferrins, including the mechanisms of iron binding and release. Other major advances include the determination of the structure of the transferrin receptor (8), the identification of a second transferrin receptor (9), the identification of the hemochromatosis gene product (10) and its interaction with the transferrin receptor (11,12), and the identification of the intracellular iron-binding protein Nramp2/DMT1 (13,14); see also Chapter 6. Each of these advances has given new insight into the complex pathways of iron metabolism.

In this chapter, we will review recent advances in transferrin biology. Several excellent reviews on transferrins have been published recently, describing the role of transferrin and the transferrin receptor in iron uptake by cells (15), iron metabolism (16), iron homeostasis (17), transferrin as an iron–protein (18), transferrin as a metal-ion mediator (19), the involvement of transferrin in iron overload (20), and the function and regulation of transferrin and ferritin (21). Because the transferrin field is advancing so rapidly, we will emphasize recent developments, with particular attention to structure–function studies of recombinant transferrins.

II. CLASSES OF TRANSFERRINS

Based on amino acid sequence identity, putative functions, and their occurrence in nature, the transferrins can be divided into several classes, including the serum transferrins, the ovotransferrins, the lactoferrins, the melanotransferrins, the saxophilins, and other transferrin-like proteins. In most cases, the transferrins are encoded as a single polypeptide chain of $M_r \sim 80,000$ that is consistent with the bilobal crystal structures of rabbit transferrin (22) and human lactoferrin (23).

A. Serum Transferrins

The serum transferrins were originally thought to be restricted to the blood of higher vertebrates, where they function in iron transport (24,25). Transferrins were then found in the hemolymph of the tobacco hornworm (*Manduca sexta*, also known as the sphinx moth) (26), and in the hemolymph of the cockroach (*Blaberus discoidalis*) (27). Recently, transferrin cDNAs have been isolated from a variety of other species, including the common brushtail possum (*Trichosurus vulpecula*) (28), several species of fish including Atlantic cod (29), rainbow trout (*Oncorhynchus mykiss*) (30), makata (31), and some salmonids (32,33), and invertebrates such as the mosquito (*Aedes aegypti*) (34), fruit fly (*Drosophila melanogaster*) (35), and silk moth [*Bombyx mori* (36)]. In each case, the cDNA encoded a polypeptide chain of $M_r \sim 80,000$ that shares extensive sequence identity with the amino acid sequence of human transferrin (37–39). In the possum, the fish species, and the cockroach, the sequence identity extends to the residues involved in the two iron-binding sites (Asp-63, Tyr-95, Tyr-

188, His-249 in the N lobe of human transferrin; Asp-392, Tyr-426, Tyr-517, His-585 in the C lobe of human transferrin), suggesting that these transferrins have retained the two metal-binding sites found in mammalian transferrins. In *M. sexta*, *Drosophila*, mosquito, and *B. mori* transferrins, however, the liganding residues are conserved in the N lobe but are not conserved in the C lobe (which also has large deletions in mosquito and *Drosophila* transferrin). This has led to the suggestion (34,36) that in some insects, transferrin plays a role similar to vertebrate lactoferrin in sequestering iron from invading organisms. Degradation of the C-lobe structure might be a mechanism for evading pathogens that use surface-bound transferrin receptors to capture sequestered iron from the diferric form of the host transferrin (34).

In addition to its role in iron transport including interaction with the transferrin receptor (see other chapters for detailed discussions), transferrin has been implicated in other functions including myelination (40). Transferrin has been found complexed with tubulin (41,42) and butyrylcholinesterase (43), and has been identified as a constituent of the platelet-derived activators of phagocytosis (44). Transferrin has also been exploited for a number of applications. It has been conjugated with polycations (such as polyamines or polylysine sequences) that bind DNA, and used as a tool to deliver the bound DNA to cells (45,46). Transferrin has also been conjugated to the anticancer drug chlorambucil for delivery to specific cells (47). Recently, it has also been used as a scaffold to engineer a peptide into a surface-exposed loop (48,49). The transferrin retained its iron-binding functions, but the peptide was immunoreactive and could be cleaved from the loop by HIV protease, suggesting that this could be used as a novel method for peptide delivery in vivo. Parise and colleagues (50) constructed a chimeric gene containing parts of the low-density lipoprotein (LDL) receptor and transferrin with the expectation that LDL would bind to the chimeric protein, and the complex would be internalized and processed using the transferrin receptor pathway. Preliminary results show that this may be a promising therapeutic tool in treating individuals with familial hypercholesterolemia (50).

B. Ovotransferrins

Although the ovotransferrins are found in avian egg whites, their polypeptide chains are encoded by the serum transferrin gene (51); ovotransferrins differ from serum transferrins only in their glycosylation pattern (52) and by their different transcriptional regulation (53–55). Ovotransferrins are believed to play an antimicrobial role in egg whites by chelating the trace amounts of Fe(III) required for microbial growth (56). In turn, some pathogens have circumvented this mechanism by either secreting siderophores that are capable of stripping the Fe(III) from transferrins (57), or by possessing surface-bound transferrin receptors that can sequester the Fe(III) from the host transferrin (58). In addition, an antibacterial domain has been identified in the N lobe of ovotransferrin (59). The antibiotic activity resides in a cationic peptide corresponding to residues 109–200 of ovotransferrin. The activity was abolished when the disulfide bonds in the peptide were reduced, suggesting that the conformation of the peptide was important for its biological activity. Hen ovotransferrin has also been used in detailed kinetic studies of iron uptake (60) and iron release (61). Recently, several crystal structures of ovotransferrins have been determined in both the Fe(III) and apo forms (see next section).

C. Lactoferrins

The lactoferrins represent a discrete gene family that encode metal-binding polypeptides that are distinct from the serum transferrins. Lactoferrin is found in human milk, tears, saliva, seminal fluid, and other secretions, where it is also thought to play an antimicrobial role (62–65). The ~40% sequence identity between human lactoferrin (66,67) and human serum transferrin (37–39) extends throughout the polypeptide chains, including the residues involved in iron binding. It is believed that the lactoferrin molecule has adapted to its antimicrobial role by binding iron more tightly and through a wider pH range than transferrins (68).

In addition to this general iron-dependent antimicrobial function, lactoferrin has been implicated in several other functions, including immunomodulation, regulation of cell growth, and iron-independent antimicrobial activity (69,70). This bactericidal effect of lactoferrin is contained within a peptide from a pepsin digest of lactoferrin (71–75). The active peptide is called lactoferricin and consists of a loop of 18–25 amino acid residues from the N-terminal region of lactoferrin. Lactoferricin is a potent antimicrobial peptide that is effective against a wide range of Gram-negative and Gram-positive bacteria, yeast, and filamentous fungi (75,76). The active center of lactoferricin consists of six residues with an amphipathic structure (77) that is consistent with the membrane disruption properties of the peptide (78). Native lactoferrin does not exhibit this antimicrobial activity, whereas synthetic peptides (79) and homologs (80) of the amphipathic alpha-helix loop of lactoferrin do show antimicrobial activity. Thus, this antimicrobial activity appears to be more complex than the simple chelation of iron required for microbial growth. Recently, lactoferrin has been detected in mouse brain tissue, and (together with other antioxidant enzymes) is elevated in the mouse model of Parkinson's disease after treatment with 1-methyl-4-phenyl-1,2,3,6-tetrahydropyridine (MPTP), presumably to protect brain tissue from oxidative damage induced by the drug (81).

Lactoferrin also binds to specific sequences of DNA (82,83), suggesting a further function for lactoferrin in transcriptional activation (84); however, the significance of lactoferrin as a transcriptional activator remains unclear. Lactoferrin has been implicated as an antiviral agent in the protection against infection by herpes simplex virus type 1 (85) and hepatitis C virus (86). Lactoferrin has also been shown to interact with ceruloplasmin in serum (87), although the physiological significance of this interaction is unclear. Lastly, binding studies have suggested the presence of a surface-bound lactoferrin receptor on several types of cells, including enterocytes (88), hepatocytes (89), intestinal brush border cells (90), lymphocytes (91,92), epithelial mammary cell lines (93), human airway epithelial cells (94), and platelets (95). These binding studies are complicated by the finding that a basic region in the N-terminal region of lactoferrin is involved in binding to heparin, bacterial lipopolysaccharide, human lysozyme, and DNA (96). The identification of the putative receptor remained elusive until 1997, when McAbee and colleagues identified a calcium-dependent lactoferrin receptor from rat hepatocytes (97). The receptor was of *M*_r 45,000, and was identified as the receptor by a combination of cross-linking, blot analysis, and affinity chromatography. Subsequent studies demonstrated that lactoferrin binds to the *M*_r 45,000 protein via noncarbohydrate determinants contained within its C lobe (98). To date, however, no amino acid or cDNA sequence data have been reported for this or any other putative lactoferrin receptor. The identity of

the receptor protein(s) and indeed the physiological significance of lactoferrins (63) remain to be determined.

D. Melanotransferrins

Human melanotransferrin (also known as p97) was originally isolated from the cell surface of melanoma cells (99); subsequent amino acid (100) and cDNA (101) sequence analyses revealed homology with human serum transferrin. Further studies showed that human melanotransferrin contains a single iron-binding site (in the N lobe) (102) and is anchored to the cell membrane surface through a glycosylphosphatidyl inositol (GPI) linkage (103–105). Melanotransferrin has now been identified in a number of different human tissues, including liver (106), intestinal epithelial cells (103), and thyroid tumors (107). Melanotransferrin appears to be involved in a transferrin-independent mechanism for uptake of iron by cells (104,108). Much excitement greeted the discovery of melanotransferrin in human brain endothelium (109). The observation that reactive microglia associated with amyloid plaques in Alzheimer's disease brain tissue express melanotransferrin (110,111), and that Alzheimer's patients have elevated levels of serum melanotransferrin (112), have provided a link between iron accumulation in the brain and neuronal death in neurodegenerative diseases (113).

Several interesting variants of melanotransferrin have been described, including a structural variant that is shed by human melanoma cell lines (114), a porcine GPI-anchored melanotransferrin homolog isolated from intestinal epithelial cells (115), the chicken homolog of melanotransferrin that appears to be a stage-specific marker for eosinophils (116), and the murine homolog of melanotransferrin (also known as membrane-bound transferrin-like protein or MTF) isolated from embryonic cells (117).

E. Other Transferrin-Like Proteins

Several newly discovered cDNAs and proteins share sequence identity with the transferrins but may represent different classes of transferrin (aside from the serum transferrin, ovotransferrin, lactoferrin, and melanotransferrin groups). Fisher et al. (118) isolated a novel transferrin-like protein (p150) from the plasma membranes of the unicellular green alga *Dunaliella salina* grown on high salinity. The p150 has a molecular weight of 150,000 and shares sequence identity with transferrin; however, the protein has three repeats rather than the two found in other transferrin molecules. The p150 appears to bind iron and is induced by conditions of iron deficiency, suggesting a role in iron accumulation under conditions of high salinity.

Saxiphilin is a soluble transferrin-like protein isolated initially from the North American bullfrog *Rana catesbeiana* based on its ability to bind saxitoxin (119–122). The larger size of saxiphilin (M_r 89,000) compared to transferrin (M_r 78,000) is due to an insertion of 144 residues in the saxiphilin sequence, including a 49-residue domain classified as a type 1 repetitive element of thyroglobulin (121). The remainder of the saxiphilin polypeptide shares 51% sequence identity with human transferrin, although mutation of metal-liganding residues in both lobes suggest that saxiphilin is unable to bind Fe(III) (121). Saxiphilins have now been found in a variety of arthropods, fish, amphibians, and reptiles (123), although their function(s), other than their ability to bind saxitoxin, remains to be elucidated.

A porcine inhibitor of carbonic anhydrase (named pICA) also has amino acid sequence homology with transferrin (124). The protein pICA was isolated from porcine plasma, and has a molecular weight of 79,000. Partial amino acid and cDNA sequence analyses revealed 64% sequence identity with transferrins (124), although again, mutations to liganding residues and anion-binding residues suggest that pICA is unable to bind Fe(III) (124). Aside from its ability to bind carbonic anhydrase with nanomolar affinity (124), the precise physiological role of pICA remains to be elucidated.

III. GENETICS OF TRANSFERRINS

The transferrin gene has been mapped to human chromosome 3q21-25 (38,125). This region of human chromosome 3 also contains the genes for melanotransferrin (126), the transferrin receptor (127), and lactoferrin (128). The detailed organization of this region of human chromosome 3 must await the completion of the human genome project; further DNA sequence analysis may also reveal additional transferrin-like genes in this and other regions of the genome. The human transferrin gene spans 33.5 kb (129), and is comprised of 17 exons interrupted by 16 introns (129,130). The organization of the human transferrin gene is very similar to the organization of the chicken transferrin gene (51). The human transferrin gene is expressed mainly in liver (131), but small amounts of transferrin are also expressed in other organs such as testis (132–137) and brain (138). Transferrin gene expression in the rabbit has also been studied (139,140).

In addition to these transcriptional regulation studies, recent genetic studies of transferrins have involved variant (141) and haplotype analysis (142) using restriction fragment length polymorphisms (142–144) and other polymorphisms (145,146), including the mutation that is responsible for the C1 and C2 electrophoretic variants of transferrin (146). The C2 allele of transferrin has been linked to late-onset Alzheimer's disease (147), while the C3 allele may have a protective effect in lung cancer (148). However, these electrophoretic variants of transferrin are fully functional, and are the result of genetically silent mutations. Perhaps reflecting the importance of iron metabolism for survival, no completely dysfunctional mutants of the human transferrin gene (affecting the iron-binding sites of both lobes) have been reported. As such, characterization of a G394R mutation in the C lobe of a British patient (149) remains the only functional variant of transferrin protein reported to date.

IV. STRUCTURE OF TRANSFERRINS

Since the determination of the amino acid sequence (37) and cDNA sequence (38,39) of human transferrin, the amino acid sequences of many different transferrins and transferrin-like polypeptides have been determined. These analyses revealed that the transferrins contain an extensive region of internal sequence homology; the N-terminal half is homologous to the C-terminal half. This structure is consistent with the idea that modern-day transferrins evolved through the duplication of an ancestral gene that coded for a polypeptide of $M_r \sim 40,000$ containing a single metal-binding site. Subsequent gene duplication events have given rise to the different classes of

transferrins, consisting mostly of a polypeptide of M_r 80,000 containing two metal-binding sites [see (117) for a recent evolutionary scheme for the transferrins].

Although the amino acid sequence data revealed the homology between the two halves of transferrin, it was really the initial structural studies of Baker and his colleagues that led to our current understanding of the bilobal structure of the transferrin-like family of proteins. In a series of elegant studies, Baker and colleagues determined the structures of human diferric-lactoferrin (5) and apo-lactoferrin (150). Concurrently, Lindley and colleagues obtained a low-resolution structure of rabbit serum transferrin (22). Using these structures as models for molecular replacement, many other transferrin structures have now been determined by a number of different investigators (Table 1). These structures include naturally occurring transferrins with a variety of metals and anions, recombinant transferrins, site-directed mutants, and individual lobes expressed in a variety of systems. The metal-bound structures reveal that the transferrins consist of two globular lobes (the N lobe and the C lobe) joined by a connecting peptide (Fig. 1). The polypeptide folding pattern is very similar in the N and C lobes. The two lobes of lactoferrin can be superimposed by a rotation of 179.5° and a translation of 24.5 \AA , resulting in 300 (of ~ 330) residues from each lobe being matched with a root-mean-square deviation in Ca positions of 1.28 \AA (151). In turn, each lobe consists of two domains (N-1, N-2 and C-1, C-2) that are joined by two antiparallel β sheets; the metal-binding site is located in the cleft that is formed at the interface of these two domains in each lobe. The metal-binding site is made up of four liganding residues from the polypeptide chain and two oxygen ligands from the synergistically bound anion. In hTf/2N (Fig. 2), the liganding residues are Asp-63, Tyr-95, and His-249 from the N-1 domain, and Tyr-188 from the N-2 domain (152). The anion is stabilized by hydrogen bonding to the side chains of Thr-120 and Arg-124, and to the main-chain nitrogen atoms of Ala-126 and Gly-127 (152). Although the two metal-binding sites of transferrin contain the same ligands, the two sites bind and release iron differently, with the N-lobe site generally releasing iron more readily than the C-lobe site (15). Details of release of iron from transferrin are given in Chapter 4. Metal binding to each of the two lobes of transferrin can be detected using nuclear magnetic resonance (NMR) (153).

The crystal structure of diferric ovotransferrin showed that the N lobe contains an interesting pair of lysine residues whose ϵ -amino groups are only 2.3 \AA apart (154). The two lysines are from different domains, and stretch across the cleft. As the normal pK_a of a lysine side-chain amino group is ~ 10 , Dewan and colleagues suggested that one or both may have an abnormally low pK_a such that the two residues form a hydrogen-bonded dilysine pair. As the pH decreases below 6, both lysine residues may become protonated, leading to charge repulsion and cleft opening. As such, Dewan suggested that these lysine residues may constitute a pH-sensitive dilysine trigger that is involved in metal release (154). Subsequent mutagenesis studies have confirmed the importance of the dilysine pair in iron release (see later section), and a functional role is consistent with their conservation in the N lobes of transferrins from different species (25). However, the dilysine pair is not found in the C lobe of transferrins—instead, Dewan and colleagues noted a Lys-Asp-Arg triplet in the C lobe, and suggested that this triplet may represent a second type of pH-sensitive trigger (154). However, the N lobe of human lactoferrin does not have a dilysine pair (66), but the N lobe of bovine lactoferrin does have a dilysine pair (155). The functional significance of these structural differences between the N and

Table 1 Crystal Structures of Transferrin-like Proteins

Species	Protein	Anion	Source	pH	Resolution (Å)	References
Human	Fe2-Lf	Carbonate	Milk	7.8	2.2	(151)
Human	Fe2-Lf	Carbonate	<i>Aspergillus</i>	8.0	2.2	(173)
Human	Fe2-Lf	Oxalate	Milk	8.0	2.4	(197)
Human	Cu2-Lf	Carbonate	Milk	7.8	2.1	(198)
Human	Cu2-Lf	Carbonate/oxalate	Milk	7.8	2.5	(199)
Human	apo-Lf	N/A	Milk	8.2	2.0	(156)
Human	Fe-Lf/2N	Carbonate	BHK	8.0	2.0	(200)
Human	Fe-Lf/2N D60S	Carbonate	BHK	8.0	2.05	(201)
Human	Fe-Lf/2N R121S	Carbonate	BHK	8.0	2.3	(202)
Human	Fe-Lf/2N R121E	Carbonate	BHK	8.0	2.5	(202)
Human	Fe-Lf/2N H253M	Carbonate	BHK	8.0	2.5	(203)
Human	Fe-Lf/2N R121D	Carbonate	BHK	8.0	3.0	(204)
Bovine	Fe2-Lf	Carbonate	Milk	7.7	2.8	(155)
Mare	Sm2-Lf	Carbonate	Milk	8.0	3.4	(205)
Mare	Fe2-Lf	Carbonate	Milk	8.0, 8.5	2.6	(206)
Mare	Fe2-Lf	Oxalate	Milk	8.5	2.7	(207)
Mare	apo-Lf	N/A	Milk	8.5	3.8	(158)
Buffalo	Fe2-Lf	Carbonate	Milk	8.0	2.5	(208)
Chicken	Fe2-ovoTf	Carbonate	Egg	5.9	2.4	(209)
Chicken	apo-ovoTf	N/A	Egg	6.0	3.0	(160)
Chicken	Fe-ovoTf/2N	Carbonate	Egg	5.9	2.3	(154, 162)
Duck	Fe2-ovoTf	Carbonate	Egg	5.8	2.3	(210)
Duck	Fe-ovoTf/4N	Carbonate	Egg	7.8	2.3	(211)
Duck	apo-ovoTf	N/A	Egg	6.0	4.0	(159)
Rabbit	Fe2-Tf	Carbonate	Serum	6.0	3.3	(22)
Rabbit ^a	Fe-hTf/2N	Carbonate	Serum	6.0	1.8	(212)
Human	Fe-Tf	Carbonate	Serum	5.75	2.6	(213)
Human	Fe-Tf/2N	Carbonate	BHK	5.75	1.6	(152)
Human	Fe-Tf/2N	Carbonate	BHK	6.1	1.8	(152)
Human	Fe-Tf/2N	Carbonate	<i>Pichia</i>	6.25	2.5	(177)
Human	apo-hTf/2N	N/A	BHK	5.3	2.2	(157)
Human	Fe-Tf/2N K206Q	Carbonate	BHK	5.75	1.8	(214)
Human	Fe-Tf/2N H207E	Carbonate	BHK	5.75	2.0	(214)
Human	Fe-Tf/2N H249E	Carbonate	BHK	6.1	2.4	(215)

References for lower-resolution structures of the same proteins are not given in this table but can be found in the references cited above.

Abbreviations used: N/A, not applicable; Lf, lactoferrin; Tf, transferrin; BHK, baby hamster kidney cells; *Aspergillus*, *Aspergillus awamori*; *Pichia*, *Pichia pastoris*. Fe-ovoTf/4N refers to the iron-binding fragment of the N2 domain of duck ovotransferrin.

^aPreliminary structural data only.

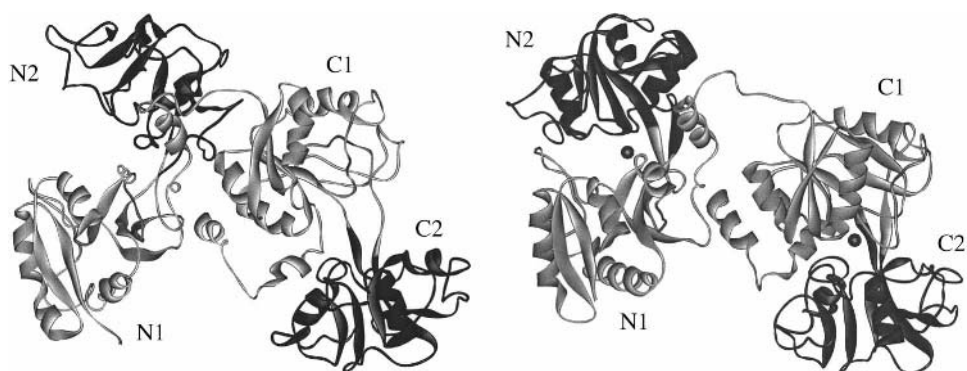


Figure 1 Structures of the diferric and apo forms of ovotransferrin. (Left) Diferric ovotransferrin (209). The individual domains are labeled as N-1 (residues 1–93 plus 248–336), N-2 (residues 94–247), C-1 (residues 345–432 plus 590–686), and C-2 (residues 433–589). The N-2 and C-2 domains are shaded darker than the N-1 and C-1 domains. The Fe(III) atoms are shown by the black sphere at the bottom of the cleft that separates the domains. (Right) apo Ovotransferrin (160). The domains are labeled and shaded as on the left. The coordinates were obtained from the Protein Data Base, Research Collaboratory for Structural Bioinformatics, Rutgers University, New Brunswick, NJ (<http://www.rcsb.org>) under the identifiers 1OVT and 1AIV, respectively.

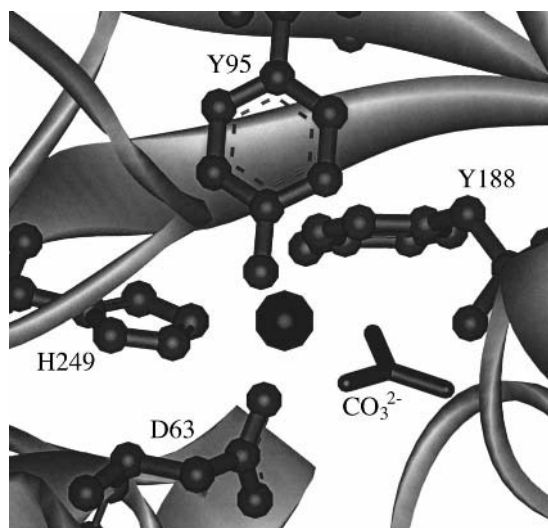


Figure 2 Structure of the metal-binding site of hTf/2N. The Fe(III) atom is shown as the black sphere; the ligands to the Fe(III) are labeled as D63, Y95, Y188, and H249. The bound carbonate is shown as CO_3^{2-} . Further details of the structure can be found in Ref. 152. The coordinates were obtained from the Protein Data Base under the identifier 1A8F.

C lobes of transferrin and lactoferrin must await further experimental characterization of the mechanism(s) of metal release.

The crystal structure of Fe(III)-hTf/2N revealed another interesting structural change (152). The protein was crystallized in two different space groups, and high-resolution X-ray diffraction data sets were obtained. The structures were solved by molecular replacement (using the rabbit transferrin N-lobe structure as the starting model). During the interpretation of the electron-density maps, it was noticed that the conventional placement of the liganding residues in the metal-binding site did not account for all of the observed electron density. To account for the additional electron density, it was suggested that the crystal contained hTf/2N in two conformations. Approximately two-thirds of the molecules had the liganding residues in positions that are similar to those found in lactoferrin and other transferrins. However, in one third of the molecules, the positions of Arg-124 and the carbonate were different—the side chain of Arg-124 had moved away from the carbonate, which in turn had rotated approximately 30° relative to the iron. The new conformation of the carbonate and Arg-124 were stabilized by hydrogen bonds. Because these two conformations were observed in the crystals of hTf/2N grown at pH ~6 and had not been seen in crystals of transferrins grown at higher pH, it was suggested that the carbonate may have become protonated to bicarbonate (152). This in turn leads to rotation of the bicarbonate such that it is monodentate to the Fe(III); as such, this structural observation may represent the first step in iron release—subsequent steps would include protonation of the dilysine pair, binding of the chelating anion, and cleft opening. Further experimentation is required to test this model of iron release (see Chapter 4).

As shown in Table 1, several structures of metal-free transferrins have been determined, albeit at different resolutions. The first such structure was apo-lactoferrin determined by Anderson et al. in 1990 (150) and subsequently refined to 2.0-Å resolution (156). As is also found with the N lobe of human transferrin (157), domain opening involves a rigid body movement of the two domains by 54–63° about a hinge made up of the two antiparallel beta sheets that join the domains. Surprisingly, although the apo structures are devoid of metals, the apo-lactoferrin structure shows the N lobe in an open conformation and the C lobe in a closed conformation. A chloride ion was found in both anion-binding sites. The closed conformation of the C lobe was attributed partly to weak stabilization by crystal packing interactions (156). In contrast, the lower-resolution structures of mare apo-lactoferrin (158) revealed both lobes in the closed conformation, while duck (159) and hen (160) apo-ovotransferrins have both lobes in the open conformation. In the higher-resolution hen apo-ovotransferrin structure, the N-lobe domains open by 53° while the C-lobe domains open by 35° (160). While some differences in lobe opening may be caused by crystal packing and functional differences between transferrins (which have to bind to a receptor to effect iron release) and lactoferrins (which do not necessarily have to release iron), Baker and colleagues (150,156) have postulated that an equilibrium exists between the open and closed states of an apo-transferrin in solution (with the observed state selected by the crystal packing of the particular protein). Using X-ray absorption fine structure spectroscopy and X-ray solution scattering, Grossmann et al. found evidence also for the existence of an intermediate conformation, and suggested that transferrin does not sample all intermediate states between the fully opened and fully closed conformations (161). A further complication is the

occurrence of an iron-loaded form of the N lobe of ovotransferrin in the open conformation (162). This was achieved by soaking a crystal of apo-oTf/2N with Fe(III) nitrilotriacetate. The high-resolution structure (2.1-Å) shows the domains open, and the Fe(III) bound by the regular two tyrosine ligands and the nitrilotriacetate anion. Further experiments are required to clarify the different conformational states of apo-transferrins.

V. EXPRESSION SYSTEMS FOR RECOMBINANT TRANSFERRINS

The production of recombinant transferrins is not a trivial undertaking, due in large part to the extensive number of disulfide bonds in these proteins. For example, human serum transferrin has 38 cysteine residues, all of which are involved in disulfide linkages (there are 8 in the N lobe and 11 in the C lobe). This makes the production of a correctly folded protein challenging. In addition, the presence of one or more carbohydrate attachment sites and the requirement to remove the signal sequence increase the difficulty.

In contrast to the challenges faced in producing recombinant transferrins, verifying the functionality of the proteins once produced and isolated is relatively straightforward. Benchmarks of function include the ability to reversibly bind iron as demonstrated by spectral analysis. In the case of human serum transferrin, for example, iron binding gives rise to a characteristic salmon-pink color with a maximum in the visible spectrum of 465 nm. The ratio of the absorbance at 280 nm to the visible maximum is a measure of purity, along with the absence of significant absorbance at 410, which traditionally has indicated contamination by hemopexin. For a pure, Fe(III)-bound transferrin, the A_{280}/A_{\max} should be around 20 and the A_{465}/A_{410} approximately 1.4. For serum transferrins, additional criteria include the ability to bind to the transferrin receptor and to deliver iron to cells. To ensure that the recombinant protein has been expressed correctly, both the determination of an N-terminal sequence and a high-resolution mass spectrum analysis should be used. Antibody reactivity and determination of the rates of iron uptake and release from recombinant proteins are two other parameters that are relatively simple to measure and provide valuable quantitative information.

The transferrins are abundant, making purification of the naturally occurring proteins relatively facile. Obviously, the compelling reason to produce these proteins by recombinant expression is to allow the mutation of individual amino acid residues to determine their specific contribution to function. Added bonuses include the ability to produce large amounts of homogeneous proteins, which can be used to obtain high-resolution crystal structures. In the case of serum transferrin, avoidance of blood-borne pathogens is also an important consideration. For all of these reasons, a concerted effort to develop and to optimize expression systems has been made. The robust nature of the transferrins proteins, combined with their importance in iron metabolism, has led to the development of a remarkable and possibly unprecedented number of different expression systems (Table 2). However, it is important to realize that there are both advantages and disadvantages to each expression system, as discussed in the following sections. It is often difficult to compare the value of expression systems because of a lack of accurate quantification of recombinant protein produced and an absence of information with regard to recovery following purification. A critical component of any expression and purification protocol should

Table 2 Expression of Recombinant Transferrins

Host cells	Protein	Level (mg/L)	References
<i>E. coli</i>	hTf	15	(163)
<i>E. coli</i>	hTf	Not given	(164)
<i>E. coli</i>	hTf/2N, hTf/2C	Not given	(165)
<i>E. coli</i>	hTf, hTf/2N, hTf/2C	60 ^a	(166,167)
<i>P. pastoris</i>	hTf/2N	50	(174)
<i>P. pastoris</i>	hTf/2N	240–1,000	(175,178)
<i>A. nidulans</i>	hLf	5	(169)
<i>A. oryzae</i>	hLf	25	(170)
<i>A. awamori</i>	hLf	5,000 ^b	(171)
<i>A. awamori</i>	mLf	12	(216)
Insect cells	hTf, bTf	20	(180)
Insect cells	hTf	20	(181)
Insect cells	hLf	10–15	(217)
BHK cells	hTf/2N	55–120	(6)
BHK cells	hTf/2C	12	(186)
BHK cells	hTf	125	(183,186)
BHK cells	hTf (nonglycosylated)	25–95	(183,186)
BHK cells	hLf	20	(188,218)
HEK293 cells	hLf	0.015	(219)
HEK293 cells	hLf (nonglycosylated)	Not detectable	(219)
Transgenic mouse milk	hLf	0.6–13,000	(192,193)
BHK cells	hLf/2N	35	(189)
BHK cells	oTf (nonglycosylated)	80	(187)
BHK cells	oTf/2N	30–55	(187)
Tobacco plants	hLf	0.3% leaf protein	(194)

Abbreviations used: hTf, human transferrin; hLf, human lactoferrin; bTf, bovine transferrin; oTf, ovotransferrin; hTf/2N, N lobe of human transferrin; hTf/2C, C lobe of human transferrin; hLf/2N, N lobe of human lactoferrin; oTF/2N, N lobe of ovotransferrin; BHK, baby hamster kidney; HEK, human embryonic kidney.

^aYield after renaturation was ~3 mg/mL.

^bYield quoted in Ref. 173.

be the concurrent development of an accurate assay to monitor the amount of recombinant protein produced and isolated at each step.

A. *Escherichia coli*

Initial efforts to express human serum transferrin in *Escherichia coli* failed (6), although several laboratories subsequently reported success (163–167). Production of human serum transferrin and/or the N and C lobes of transferrin in bacterial systems yield very limited amounts of functional protein. No convincing demonstration of iron binding has been provided in any of the studies. Problems encountered include both proteolysis and inhibition of bacterial growth; the well-documented antibacterial activity of the transferrins may be responsible for such inhibition. A more recent

study (167) reported a maximum of 60 mg/L of hTF, of which 3 mg was recovered following efforts to renature the protein found in insoluble inclusion bodies. Barring a technological breakthrough, production of recombinant transferrins in bacteria is not practical, given the poor yield of functional protein.

B. Filamentous Fungi

Functional human lactoferrin has been produced by Ward et al. in several different strains of *Aspergillus*, a filamentous fungus (168). Modest amounts of protein (5 mg/L) were produced by *A. nidulans*, but only about 30% was secreted into the growth medium, and characterization of the recombinant protein was cursory (169). Production was increased to 25 mg/L when a different strain, *A. oryzae*, was used (170). The recombinant protein appears to be glycosylated and able to bind iron. A far more promising expression system was developed using the *A. awamori* strain (171). Although few experimental details were provided, production levels in excess of 2000 mg/L were reported, with a recovery of 85% of the protein secreted into the medium. The recombinant lactoferrin was judged to be fully functional by a number of standard criteria, including iron binding and release, binding to human enterocyte cells, and antimicrobial activity. N-terminal sequence analysis established that the protein was processed correctly, and immunoreactivity was identical to that of native lactoferrin. The recombinant lactoferrin was glycosylated, although the precise composition of the carbohydrates appears to be different from that found in native lactoferrin. A subsequent study demonstrated the utility of this expression system for production of site-directed mutants of lactoferrin (172). Recently, crystals were grown from this recombinant protein, and the structure was determined (173); the polypeptide fold in the recombinant protein was found to be the same as that in native lactoferrin.

Advantages of the *Aspergillus* system include high-level expression, ability of the cells to carry out posttranslational modifications, easy scale-up, and low cost.

C. Yeast Cells

Functional human serum transferrin N lobe has been successfully produced from the methylotrophic yeast, *Pichia pastoris*, in shaker flasks at levels of 50 mg/L (174), and at 250 mg/L (175) in our laboratory. Recovery of the secreted protein following purification was 28% and 70%, respectively. In a subsequent report by Steinlein et al. (176), production levels were increased to 80–100 mg/L and a hexa-histidine tag was added, presumably increasing both the speed of recovery and yield of the recombinant protein. Analysis by electrospray mass spectrometry revealed that 80% of the N lobe produced by these yeast cells contained an additional one or two hexose residues (175), although no effect on function was noted. Proteolytic studies followed by further mass spectrometry identified Ser-32 as the site of the O-linked hexose (177). A crystal structure of the recombinant human N lobe (177) attests to its homogeneity and reveals a folding pattern that is identical to that of native human serum transferrin and an N lobe produced in a mammalian cell system (see below).

Advantages of the yeast cell system include simple purification and high recovery of the secreted N lobe, which is really the only protein present in the basal medium. The system is relatively inexpensive in cost and labor, and scale-up is easily achieved. A fermentor equipped with a methanol sensor was used to produce over

1000-mg/L quantities of protein (178). Because protein production is induced by methanol, but methanol is toxic to the yeast cells, optimization of this parameter maximizes production levels. The *P. pastoris* system has also been used to produce completely $^{13}\text{C}/^{15}\text{N}$ -labeled protein, useful for NMR studies (179). The only disadvantage thus far identified has been failure to express reasonable amounts of full-length transferrin in this system.

D. Insect Cells

Production of human serum transferrin by insect cells infected with a baculovirus has been reported by two different laboratories (180,181). Both achieved similar production levels (20 mg/L), although two different insect cell lines were used. Retzer et al. (180) isolated recombinant human and bovine serum transferrins using a concanavalin A column, giving an indication that the recombinant proteins were glycosylated. The carbohydrate was not analyzed further. However, an electroblot of a gel stained with amido black indicated that the proteins were of approximately the correct molecular weight. Further characterization indicated that for the most part the recombinant proteins were immunoreactive to a panel of monoclonal antibodies (180). In the second study, Ali et al. (181) isolated recombinant human transferrin using phenyl sepharose followed by Q-sepharose chromatography (181). Their characterization was more extensive and included N-terminal sequence analysis, a CD spectrum, cell binding, SDS/PAGE, and urea/PAGE analysis to verify size and ability to bind iron (181). By all criteria, the recombinant transferrin was equivalent to the native protein.

Insect cells can perform posttranslational modifications while sharing the faster growth rates of yeast, bacteria, and filamentous fungi. Insect cells can be grown in suspension cultures and do not require CO_2 incubators. Several different baculovirus expression systems and both lepidopteran and dipteran cell lines (182) were developed and optimized in the 1990s and are commercially available.

E. Mammalian Cells

The most utilized and best characterized system to date seems to be that developed in the authors' laboratories. The cDNAs of the transferrin-related proteins are inserted into a pNUT vector and transfected into baby hamster kidney (BHK) cells. The pNUT vector features a mutated dihydrofolate reductase gene allowing selection of cells containing the plasmid with a single high dose of methotrexate. This system has been used by other laboratories to produce significant quantities of functional recombinant protein and mutated transferrins containing single, double, and triple point mutations. Both glycosylated and nonglycosylated human serum transferrins have been expressed (183) and were shown by many criteria to be entirely equivalent to native protein in iron binding and interaction with cellular transferrin receptors. Interestingly, neither extensive and varied glycosylation of the protein produced in the BHK system nor the complete absence of glycosylation had an effect on the receptor binding affinity (183).

Mutated human serum transferrins have been used to probe the role of specific residues in function (184,185). The most comprehensive studies have involved the human serum transferrin N lobe, resulting in yields of up to 200 mg/L (Table 2). Expression of modest amounts (12 mg/L) of human transferrin C lobe has also been

Table 3 Mutant Forms of the N Lobes of Human Transferrin and Lactoferrin

Mutant	Molecule	References
Liganding residues		
D63S	hTf/2N	(7,220–224)
D63C	hTf/2N	(7,220–222)
D63N	hTf/2N	(224)
D63E	hTf/2N	(224)
D63A	hTf/2N	(224)
Y95F	hTf/2N	(225)
Y95H	hTf/2N	(161,226)
Y188F	hTf/2N	(225)
H249Q	hTf/2N	(215,222,223,227,228)
H249E	hTf/2N	(215,222,228)
H249A	hTf/2N	(215,228)
H249Y	hTf/2N	(226)
D60S	hLf/2N	(201)
H253G, A, P, T, L, F, M, Y, E, Q, C	hLf/2N	(203)
Second-shell residues		
G65R	hTf/2N	(7,221,222)
E83A	hTf/2N	(227)
Y85F	hTf/2N	(227)
R124A	hTf/2N	(229,230)
R124E	hTf/2N	(229)
R124S	hTf/2N	(161,226)
R124K	hTf/2N	(161,226)
K206A	hTf/2N	(176,229,230)
K206E	hTf/2N	(231)
K206E-K296E (double mutant)	hTf/2N	(231)
K206Q	hTf/2N	(7,214,221,222,231)
K206R	hTf/2N	(226)
K296A	hTf/2N	(176,229,230)
K296E	hTf/2N	(222,231)
K296Q	hTf/2N	(222,231)
R121S	hLf/2N	(202)
R121E	hLf/2N	(202)
Other residues		
W8Y, W128Y	hTf/2N	(232,233)
H207E	hTf/2N	(7,214,221,222,226,232)
K233Q	hTf/2N	(184)
M109L, M256V, M26I, M309I, M313I	hTf/2N	(191,234)

reported (186). Full-length ovotransferrin (80 mg/L) and the N lobe of ovotransferrin (55 mg/L) have also been expressed in the BHK system in high yields, and have been used to investigate the molecular details of receptor interaction (187). The production of human lactoferrin (maximum of 20 mg/L) and the N lobe of lactoferrin (35 mg/L) have also been reported using this system (188,189).

We favor this system because of its continuous production feature. Cells can be maintained in expanded-surface roller bottles for up to 60 days, and immunoassay allows monitoring of the recombinant protein expression level to determine the duration of the collection (190). From transfection of the cells with the plasmid to passage of cells into roller bottles typically takes less than 3 weeks. Both human transferrin and its N lobe in which the methionine residues are labeled with ^{13}C have been prepared for use in NMR experiments (191).

F. Other Systems

As shown in Table 2, lactoferrin has been expressed in very high yields in the milk of transgenic mice (192,193) and in leaves of tobacco plants (194). Although functional protein was produced in both cases, the absolute yield of purified protein was not given. It is therefore difficult to judge the suitability of this expression system for the production of large amounts of lactoferrin and its site-directed mutants, and the technologies are not readily available in many laboratories.

G. Mutants of Transferrins

By using in-vitro mutagenesis combined with production of the recombinant protein, many different transferrin mutants have been expressed (Table 3). These mutants include residues involved directly in iron binding (such as the liganding residues), second-shell residues that have a dramatic effect on iron binding and release although they are not directly involved as ligands, and other residues. As discussed in detail in Chapter 4, most of these mutants have been used to study the binding and release of metal under controlled conditions.

ACKNOWLEDGMENTS

Studies in the authors' laboratories are supported in part by grants from the Medical Research Council of Canada (MT-7716) and the National Institutes of Health (DK-21739). The authors wish to thank R. C. Woodworth for his support and collaboration over the past 20 years, and Michael Page for help with the figures.

REFERENCES

1. Schade AL, Caroline L. An iron-binding component in human blood plasma. *Science* 1946; 104:340–341.
2. Schade AL, Reinhart R, Levy H. Carbon dioxide and oxygen in complex formation with iron and siderophilin, the iron-binding component of human plasma. *Arch Biochem* 1949; 20:170–172.
3. Holmberg CG, Laurell C-B. Investigations in serum copper. I. Nature of serum copper and its relation to the iron-binding protein in human serum. *Acta Chem Scand* 1947; 1:944–950.
4. Laurell C-B, Ingelman B. The iron-binding protein of swine serum. *Acta Chem Scand* 1947; 1:770–776.
5. Anderson BF, Baker HM, Dodson EJ, Norris GE, Rumball SV, Waters JM, Baker EN. Structure of human lactoferrin at 3.2 Å resolution. *Proc Natl Acad Sci USA* 1987; 84: 1769–1773.

6. Funk WD, MacGillivray RTA, Mason AB, Brown SA, Woodworth RC. Expression of the amino-terminal half-molecule of human serum transferrin in cultured cells and characterization of the recombinant protein. *Biochemistry* 1990; 29:1654–1660.
7. Woodworth RC, Mason AB, Funk WD, MacGillivray RTA. Expression and initial characterization of five site-directed mutants of the N-terminal half-molecule of human transferrin. *Biochemistry* 1991; 30:10824–18029.
8. Lawrence CM, Ray S, Babyonyshev M, Galluser R, Borhani DW, Harrison SC. Crystal structure of the ectodomain of human transferrin receptor. *Science* 1999; 286:779–782.
9. Kawabata H, Yang R, Hirama T, Vuong PT, Kawano S, Gombart AF, Koeffler HP. Molecular cloning of transferrin receptor 2. A new member of the transferrin receptor-like family. *J Biol Chem* 1999; 274:20826–20832.
10. Feder JN, Gnirke A, Thomas W, Tsuchihashi Z, Ruddy DA, Basava A, et al. A novel MHC class I-like gene is mutated in patients with hereditary haemochromatosis [see comments]. *Nature Genet* 1996; 13:399–408.
11. Feder JN, Penny DM, Irrinki A, Lee VK, Lebron JA, Watson N, Tsuchihashi Z, Sigal E, Bjorkman PJ, Schatzman RC. The hemochromatosis gene product complexes with the transferrin receptor and lowers its affinity for ligand binding. *Proc Natl Acad Sci USA* 1998; 95:1472–1477.
12. Bennett MJ, Lebron JA, Bjorkman PJ. Crystal structure of the hereditary haemochromatosis protein HFE complexed with transferrin receptor. *Nature* 2000; 403:46–53.
13. Fleming MD, Andrews NC. Mammalian iron transport: An unexpected link between metal homeostasis and host defense. *J Lab Clin Med* 1998; 132:464–468.
14. Gruenheid S, Canonne-Hergaux F, Gauthier S, Hackam DJ, Grinstein S, Gros P. The iron transport protein NRAMP2 is an integral membrane glycoprotein that colocalizes with transferrin in recycling endosomes. *J Exp Med* 1999; 189:831–841.
15. Aisen P. Transferrin, the transferrin receptor, and the uptake of iron by cells. *Met Ions Biol Syst* 1998; 35:585–631.
16. Aisen P, Wessling-Resnick M, Leibold EA. Iron metabolism. *Curr Opin Chem Biol* 1999; 3:200–206.
17. Sherwood RA, Pippard MJ, Peters TJ. Iron homeostasis and the assessment of iron status. *Ann Clin Biochem* 1998; 35:693–708.
18. Evans RW, Crawley JB, Joannou CL, Sharma ND. Iron proteins. In: Bulen JJ, Griffiths E, eds. *Iron and Infection: Molecular, Physiological and Clinical Aspects*. Chichester, UK: Wiley, 1999:27–86.
19. Sun H, Li H, Sadler PJ. Transferrin as a metal ion mediator. *Chem Rev* 1999; 99: 2817–2842.
20. Kühn LC. Iron overload: Molecular clues to its cause. *Trends Biochem Sci* 1999; 24: 164–166.
21. Ponka P, Beaumont C, Richardson DR. Function and regulation of transferrin and ferritin. *Sem Hematol* 1998; 35:35–54.
22. Bailey S, Evans RW, Garratt RC, Gorinsky B, Hasnain S, Horsburgh C, Jhoti H, Lindley PF, Mydin A, Sarra R, Watson JL. Molecular structure of serum transferrin at 3.3-Å resolution. *Biochemistry* 1988; 27:5804–5812.
23. Anderson BF, Baker HM, Norris GE, Rice DW, Baker EN. Structure of human lactoferrin: Crystallographic structure analysis and refinement at 2.8 Å resolution. *J Mol Biol* 1989; 209:711–734.
24. Welch S. A comparison of the structure and properties of serum transferrin from 17 animal species. *Comp Biochem Physiol* 1990; B97:417–428.
25. Baldwin GS. Comparison of transferrin sequences from different species. *Comp Biochem Physiol* 1993; 106B:203–218.
26. Bartfield NS, Law J. Isolation and molecular cloning of transferrin from the tobacco hornworm *Manduca sexta*. Sequence similarity to the vertebrate transferrins. *J Biol Chem* 1990; 265:21684–21691.

27. Jamroz RC, Gasdaska JR, Bradfield JY, Law JH. Transferrin in a cockroach: Molecular cloning, characterization, and suppression by juvenile hormone. *Proc Natl Acad Sci USA* 1993; 90:1320–1324.
28. Demmer J, Stasiuk SJ, Adamski FM, Grigor MR. Cloning and expression of the transferrin and ferritin genes in a marsupial, the brushtail possum (*Trichosurus vulpecula*). *Biochim Biophys Acta* 1999; 1445:65–74.
29. Denovan-Wright EM, Ramsey NB, McCormick CJ, Lazier CB, Wright JM. Nucleotide sequence of transferrin cDNAs and tissue-specific expression of the transferrin gene in Atlantic cod (*Gadus morhua*). *Comp Biochem Physiol B* 1996; 113:269–273.
30. Tange N, Jong-Young L, Mikawa N, Hirono I, Aoki T. Cloning and characterization of transferrin cDNA and rapid detection of transferrin gene polymorphism in rainbow trout (*Oncorhynchus mykiss*). *Mol Marine Biol Biotechnol* 1997; 6:351–356.
31. Mikawa N, Hirono I, Aoki T. Structure of mekata transferrin gene and its 5' flanking region. *Mol Marine Biol Biotechnol* 1996; 5:225–229.
32. Lee JY, Tada T, Hirono I, Aoki T. Molecular cloning and evolution of transferrin cDNAs in salmonids. *Mol Marine Biol Biotechnol* 1998; 7:287–93.
33. Ford MJ, Thornton PJ, Park LK. Natural selection promotes divergence of transferrin among salmonid species. *Mol Ecol* 1999; 8:1055–1061.
34. Yoshiga T, Hernandez VP, Fallon AM, Law JH. Mosquito transferrin, an acute-phase protein that is up-regulated upon infection. *Proc Natl Acad Sci USA* 1997; 94:12337–12342.
35. Yoshiga T, Georgieva T, Dunkov BC, Harizanova N, Ralchev K, Law JH. *Drosophila melanogaster* transferrin. Cloning, deduced protein sequence, expression during the life cycle, gene localization and up-regulation on bacterial infection. *Eur J Biochem* 1999; 260:414–420.
36. Yun EY, Kang SW, Hwang JS, Goo TW, Kim SH, Jin BR, Kwon O-Y, Kim KY. Molecular cloning and characterization of a cDNA encoding a transferrin homolog from *Bombyx mori*. *Biol Chem* 1999; 380:1455–1459.
37. MacGillivray RTA, Mendez E, Shewale JG, Sinha SK, Lineback-Zins J, Brew K. The primary structure of human serum transferrin. The structures of seven cyanogen bromide fragments and the assembly of the complete structure. *J Biol Chem* 1983; 258:3543–3553.
38. Yang F, Lum JB, McGill JR, Moore CM, Naylor SL, van Bragt PH, Baldwin WD, Bowman BH. Human transferrin: cDNA characterization and chromosomal localization. *Proc Natl Acad Sci USA* 1984; 81:2752–2756.
39. Uzan G, Frain M, Park I, Besmond C, Maessen G, Trepast JS, Zakin MM, Kahn A. Molecular cloning and sequence analysis of cDNA for human transferrin. *Biochem Biophys Res Commun* 1984; 119:273–281.
40. Espinosa de los Monteros A, Kumar S, Zhao P, Huang CJ, Nazarian R, Pan T, Scully S, Chang R, de Vellis J. Transferrin is an essential factor for myelination. *Neurochem Res* 1999; 24:235–248.
41. Kondo T, Sakaguchi M, Namba M. Characteristics of intracellular transferrin produced by human fibroblasts: Its posttranscriptional regulation and association with tubulin. *Exp Cell Res* 1998; 242:38–44.
42. Sakaguchi M, Kondo T, Pu H, Namba M. Transferrin synthesized in cultured human fibroblasts is associated with tubulins and has iron binding capacity. *Cell Struct Funct* 1999; 24:5–9.
43. Weitnauer E, Ebert C, Hucho F, Robitzki A, Weise C, Layer PG. Butyrylcholinesterase is complexed with transferrin in chicken serum. *J Protein Chem* 1999; 18:205–214.
44. Sakamoto H, Sakamoto N, Oryu M, Kobayashi T, Ogawa Y, Ueno M, Shinnou M. A novel function of transferrin as a constituent of macromolecular activators of phago-

- cytosis from platelets and their precursors. *Biochem Biophys Res Commun* 1997; 230: 270–274.
45. Wagner E, Zenke M, Cotten M, Beug H, Birnstiel ML. Transferrin-polycation conjugates as carriers for DNA uptake into cells. *Proc Natl Acad Sci USA* 1990; 87:3410–3414.
 46. Wightman L, Patzelt E, Wagner E, Kircheis R. Development of transferrin-polycation/DNA based vectors for gene delivery into melanoma cells. *J Drug Target* 1999; 7:293–303.
 47. Beyer U, Roth T, Schumacher P, Maier G, Unold A, Frahm AW, Fiebig HH, Unger C, Kratz F. Synthesis and in vitro efficacy of transferrin conjugates of the anticancer drug chlorambucil. *J Med Chem* 1998; 41:2701–2708.
 48. Ali SA, Joao HC, Hammerschmid F, Eder J, Steinkasserer A. An antigenic HIV-1 peptide sequence engineered into the surface structure of transferrin does not elicit an antibody response. *FEBS Lett* 1999; 459:230–232.
 49. Ali SA, Joao HC, Hammerschmid F, Eder J, Steinkasserer A. Transferrin Trojan horses as a rational approach for the biological delivery of therapeutic peptide domains. *J Biol Chem* 1999; 274:24066–24073.
 50. Parise F, Simone L, Croce MA, Ghisellini M, Battini R, Borghi S, Tiozzo R, Ferrari S, Calandra S, Ferrari S, Calandra S, Ferrari S. Construction and in vitro functional evaluation of a low-density lipoprotein receptor/transferrin fusion protein as a therapeutic tool for familial hypercholesterolemia. *Hum Gene Ther* 1999; 10:1219–1228.
 51. Cochet M, Gannon F, Hen R, Maroteaux L, Perrin F, Chambon P. Organization and sequence studies of the 17-piece conalbumin gene. *Nature* 1979; 282:567–574.
 52. Graham I, Williams J. A comparison of glycopeptides from the transferrins of several species. *Biochem J* 1975; 145:263–279.
 53. McKnight GS, Palmiter RD. Transcriptional regulation of the ovalbumin and conalbumin genes by steroid hormones in chick oviduct. *J Biol Chem* 1979; 254:9050–9058.
 54. McKnight GS, Lee DC, Hemmaphard D, Finch CA, Palmiter RD. Transferrin gene expression. Effects of nutritional iron deficiency. *J Biol Chem* 1980; 255:144–147.
 55. McKnight GS, Lee DC, Palmiter RD. Transferrin gene expression. Regulation of mRNA transcription in chick liver by steroid hormones and iron deficiency. *J Biol Chem* 1980; 255:148–153.
 56. Weinberg ED. Iron and susceptibility to infectious disease. *Science* 1974; 184:952–956.
 57. Braun V, Killmann H. Bacterial solutions to the iron-supply problem. *Trends Biochem Sci* 1999; 24:104–109.
 58. Schryvers AB, Stojiljkovic I. Iron acquisition systems in the pathogenic *Neisseria*. *Mol Microbiol* 1999; 32:1117–1123.
 59. Ibrahim HR, Iwamori E, Sugimoto Y, Aoki T. Identification of a distinct antibacterial domain within the N-lobe of ovotransferrin. *Biochim Biophys Acta* 1998; 1401:289–303.
 60. Abdallah FB, el Hage Chahine JM. Transferrins. Hen ovo-transferrin, interaction with bicarbonate and iron uptake. *Eur J Biochem* 1998; 258:1022–1031.
 61. Abdallah FB, El Hage Chahine J-M. Transferrins, the mechanism of iron release by ovotransferrin. *Eur J Biochem* 1999; 263:912–920.
 62. Weinberg ED. Iron and infection. *Microbiol Rev* 1978; 42:45–66.
 63. Brock JH. Lactoferrin structure-function relationships. In: Hutchens TW, Lonnerdal B, eds. *Lactoferrin. Interactions and Biological Functions*. Totowa, NJ: Humana Press, 1997:3–23.
 64. Jurado RL. Iron, infections, and anemia of inflammation. *Clin Infect Dis* 1997; 25: 888–895.

65. Bhimani RS, Vendrov Y, Furmanski P. Influence of lactoferrin feeding and injection against systemic staphylococcal infections in mice. *J Appl Microbiol* 1999; 86:135–144.
66. Metz-Boutigue MH, Jolles J, Mazurier J, Schoentgen F, Legrand D, Spik G, Montreuil J, Jolles P. Human lactoferrin: Amino acid sequence and structural comparisons with other transferrins. *Eur J Biochem* 1984; 145:659–676.
67. Powell MJ, Ogden JE. Nucleotide sequence of human lactoferrin cDNA. *Nucleic Acids Res* 1990; 18:4013.
68. Baker EN. Structure and reactivity of transferrins. *Adv Inorg Chem* 1994; 41:389–463.
69. Iyer S, Lonnerdal B. Lactoferrin, lactoferrin receptors and iron metabolism. *Eur J Clin Nutr* 1993; 47:232–241.
70. Vorland LH. Lactoferrin: A multifunctional glycoprotein. *Acta Pathologica, Microbiologica et Immunologica Scandinavica* 1999; 107:971–981.
71. Arnold RR, Cole MF, McGhee JR. A bactericidal effect for human lactoferrin. *Science* 1977; 197:263–265.
72. Bellamy W, Tkase M, Wakabayashi H, Kawase K, Tomita M. Antibacterial spectrum of lactoferricin B, a potent bactericidal peptide derived from the N-terminal region of bovine lactoferrin. *J Appl Bacteriol* 1992; 73:472–479.
73. Yamauchi K, Tomita M, Giehl TJ, Ellison RT. Antibacterial activity of lactoferrin and a pepsin-derived lactoferrin peptide fragment. *Infect Immun* 1993; 61:719–728.
74. Jones EM, Smart A, Bloomberg G, Burgess L, Millar MR. Lactoferricin, a new antimicrobial peptide. *J Appl Microbiol* 1994; 77:208–214.
75. Tomita M, Takase M, Bellamy W, Shimamura S. A review: The active peptide of lactoferrin. *Acta Paediatr Jpn* 1994; 36:585–591.
76. Vorland LH, Ulvatne H, Andersen J, Haukland HH, Rekdal O, Svendsen JS, Gutteberg TJ. Antibacterial effects of lactoferricin B. *Scand J Infect Dis* 1999; 31:179–184.
77. Schibli DJ, Hwang PM, Vogel HJ. The structure of the antimicrobial active center of lactoferricin B bound to sodium dodecyl sulfate micelles. *FEBS Lett* 1999; 446:213–217.
78. Aguilera O, Ostolaza H, Quiros LM, Fierro JF. Permeabilizing action of an antimicrobial lactoferricin-derived peptide on bacterial and artificial membranes. *FEBS Lett* 1999; 462:273–277.
79. Groenink J, Walgreen-Weterings E, van't Hof W, Veerman EC, Nieuw Amerongen AV. Cationic amphiphathic peptides, derived from bovine and human lactoferrins, with antimicrobial activity against oral pathogens. *FEMS Microbiol Lett* 1999; 179:217–222.
80. Azuma M, Kojima T, Yokoyama I, Tajiri H, Yoshikawa K, Saga S, Del Carpio CA. Antibacterial activity of multiple antigen peptides homologous to a loop region in human lactoferrin. *J Peptide Res* 1999; 54:237–241.
81. Fillebeen C, Mitchell V, Dexter D, Benaissa M, Beauvillain J, Spik G, Pierce A. Lactoferrin is synthesized by mouse brain tissue and its expression is enhanced after MPTP treatment. *Brain Res Mol Brain Res* 1999; 72:183–194.
82. He J, Furmanski P. Sequence specificity and transcriptional activation in the binding of lactoferrin to DNA. *Nature* 1995; 373:721–724.
83. Kanyshkova TG, Semenov DV, Buneva VN, Nevinsky GA. Human milk lactoferrin binds two DNA molecules with different affinities. *FEBS Lett* 1999; 451:235–237.
84. Fleet JC. A new role for lactoferrin: DNA binding and transcription activation. *Nutr Rev* 1995; 53:226–227.
85. Siciliano R, Rega B, Marchetti M, Seganti L, Antonini G, Valenti P. Bovine lactoferrin peptidic fragments involved in inhibition of herpes simplex virus type 1 infection. *Biochem Biophys Res Commun* 1999; 264:19–23.
86. Ikeda M, Nozaki A, Sugiyama K, Tanaka T, Naganuma A, Tanaka K, Sekihara H, Shimotohno K, Saito M, Kato N. Characterization of antiviral activity of lactoferrin against hepatitis C virus infection in human cultured cells. *Virus Res* 2000; 66:51–63.

87. Zakharova ET, Shavovski MM, Bass MG, Gridasova AA, Pulina MO, De Filippis V, Beltramini M, Di Muro P, Salvato B, Fontana A, Vasilyev VB, Gaitskhoki VS. Interaction of lactoferrin with ceruloplasmin. *Arch Biochem Biophys* 2000; 374:222–228.
88. Gislason J, Douglas GC, Hutchens TW, Lonnerdal B. Receptor-mediated binding of milk lactoferrin to nursing piglet enterocytes: A model for studies on absorption of lactoferrin-bound iron. *J Ped Gastroenterol Nutr* 1995; 21:37–43.
89. Hu WL, Regoezi E, Chindemi PA, Bolyos M. Lactoferrin interferes with uptake of iron from transferrin and asialotransferrin by the rat liver. *Am J Physiol* 1993; 264: G112–G117.
90. Hu WL, Mazurier J, Montreuil J, Spik G. Isolation and partial characterization of a lactotransferrin receptor from mouse intestinal brush border. *Biochemistry* 1990; 29: 535–541.
91. Crouch SP, Slater KJ, Fletcher J. Regulation of cytokine release from mononuclear cells by the iron-binding protein lactoferrin. *Blood* 1992; 80:235–240.
92. Bi BY, Leveugle B, Liu JL, Collard A, Coppe P, Roche A-C, Nillesse N, Capron M, Spik G, Mazurier J. Immunolocalization of the lactotransferrin receptor on the human T lymphoblastic cell line Jurkat. *Eur J Cell Biol* 1994; 65:164–171.
93. Rochard E, Legrand D, Lecocq M, Hamelin R, Crepin M, Montreuil J, Spik G. Characterization of lactotransferrin receptor in epithelial cell lines from non-malignant human breast, benign mastopathies and breast carcinomas. *Anticancer Res* 1992; 12: 2047–2051.
94. Ghio AJ, Carter JD, Dailey LA, Devlin RB, Samet JM. Respiratory epithelial cells demonstrate lactoferrin receptors that increase after metal exposure. *Am J Physiol* 1999; 276:L933–L940.
95. Leveugle B, Mazurier J, Legrand D, Mazurier C, Montreuil J, Spik G. Lactotransferrin binding to its platelet receptor inhibits platelet aggregation. *Eur J Biochem* 1993; 213: 1205–1211.
96. van Berkel PH, Geerts ME, van Veen HA, Mericskay M, de Boer HA, Nuijens JH. N-terminal stretch Arg2, Arg3, Arg4 and Arg5 of human lactoferrin is essential for binding to heparin, bacterial lipopolysaccharide, human lysozyme and DNA. *Biochem J* 1997; 328:145–151.
97. Bennett DJ, McAbee DD. Identification and isolation of a 45-kDa calcium-dependent lactoferrin receptor from rat hepatocytes. *Biochemistry* 1997; 36:8359–8366.
98. Sitaram MP, Moloney B, McAbee DD. Prokaryotic expression of bovine lactoferrin deletion mutants that bind to the Ca^{2+} -dependent lactoferrin receptor on isolated rat hepatocytes. *Protein Exp Purif* 1998; 14:229–236.
99. Woodbury RG, Brown JP, Yeh MY, Hellstrom I, Hellstrom KE. Identification of a cell surface protein, p97, in human melanomas and certain other neoplasms. *Proc Natl Acad Sci USA* 1980; 77:2183–2187.
100. Brown JP, Hewick RM, Hellstrom I, Hellstrom KE, Doolittle RF, Dreyer WJ. Human melanoma-associated antigen p97 is structurally and functionally related to transferrin. *Nature* 1982; 296:171–173.
101. Rose TM, Plowman GD, Teplow DB, Dreyer WJ, Hellstrom KE, Brown JP. Primary structure of the human melanoma-associated antigen p97 (melanotransferrin) deduced from the mRNA sequence. *Proc Natl Acad Sci USA* 1986; 83:1261–1265.
102. Baker EN, Baker HM, Smith CA, Stebbins MR, Kahn M, Hellstrom KE, Hellstrom I. Human melanotransferrin (p97) has only one functional iron-binding site. *FEBS Lett* 1992; 298:215–218.
103. Alemany R, Vila MR, Franci C, Egea G, Real FX, Thomson TM. Glycosyl phosphatidylinositol membrane anchoring of melanotransferrin (p97): Apical compartmentalization in intestinal epithelial cells. *J Cell Sci* 1993; 104:1155–1162.

104. Kennard ML, Richardson DR, Gabathuler R, Ponka P, Jefferies WA. A novel iron uptake mechanism mediated by GPI-anchored human p97. *EMBO J* 1995; 14:4178–4186.
105. Food MR, Rothenberger S, Gabathuler R, Haidl ID, Reid G, Jefferies WA. Transport and expression in human melanomas of a transferrin-like glycosylphosphatidylinositol-anchored protein. *J Biol Chem* 1994; 269:3034–3040.
106. Sciot R, de Vos R, van Eyken P, van der Steen K, Moerman P, Desmet VJ. In situ localization of melanotransferrin (melanoma-associated antigen P97) in human liver. A light- and electronmicroscopic immunohistochemical study. *Liver* 1989; 9:110–119.
107. Barresi G, Tuccari G. Immunocytochemical demonstration of melanotransferrin (p97) in thyroid tumors of follicular cell origin. *Pathology* 1994; 26:127–129.
108. Food MR, Rothenberger S, Gabathuler R, Haidl ID, Reid G, Jefferies WA. Transport and expression in human melanomas of a transferrin-like glycosylphosphatidylinositol-anchored protein. *J Biol Chem* 1994; 269:3034–3040.
109. Rothenberger S, Food MR, Gabathuler R, Kennard ML, Yamada T, Yasuhara O, McGeer PL, Jefferies WA. Coincident expression and distribution of melanotransferrin and transferrin receptor in human brain capillary endothelium. *Brain Res* 1996; 712:117–121.
110. Jefferies WA, Food MR, Gabathuler R, Rothenberger S, Yamada T, Yasuhara O, McGeer PL. Reactive microglia specifically associated with amyloid plaques in Alzheimer's disease brain tissue express melanotransferrin. *Brain Res* 1996; 712:122–126.
111. Yamada T, Tsujioka Y, Taguchi J, Takahashi M, Tsuboi Y, Moroo I, Yang J, Jefferies WA. Melanotransferrin is produced by senile plaque-associated reactive microglia in Alzheimer's disease. *Brain Res* 1999; 845:1–5.
112. Kennard ML, Feldman H, Yamada T, Jefferies WA. Serum levels of the iron binding protein p97 are elevated in Alzheimer's disease. *Nature Med* 1996; 2:1230–1235.
113. Qian ZM, Wang Q. Expression of iron transport proteins and excessive iron accumulation in the brain in neurodegenerative disorders. *Brain Res Rev* 1998; 27:257–267.
114. Liao SK. Identification with monoclonal antibody 140.240 of a structural variant of melanotransferrin shed by human melanoma cell lines in vitro. *Anticancer Res* 1996; 16:171–176.
115. Danielsen EM, Van Deurs B. A transferrin-like GPI-linked iron-binding protein in detergent-insoluble noncaveolar microdomains at the apical surface of fetal intestinal epithelial cells. *J Cell Biol* 1995; 131:939–950.
116. McNagny KM, Rossi F, Smith G, Graf T. The eosinophil-specific cell surface antigen, EOS47, is a chicken homologue of the oncofetal antigen melanotransferrin. *Blood* 1996; 87:1343–1352.
117. Nakamasu K, Kawamoto T, Shen M, Gotoh O, Teramoto M, Noshiro M, Kato Y. Membrane-bound transferrin-like protein (MTf): Structure, evolution and selective pressure during chondrogenic differentiation of mouse embryonic cells. *Biochim Biophys Acta* 1999; 1447:258–264.
118. Fisher M, Gokhman I, Pick U, Zamir A. A structurally novel transferrin-like protein accumulates in the plasma membrane of the unicellular green alga *Dunaliella salina* grown in high salinities. *J Biol Chem* 1997; 272:1565–1570.
119. Li Y, Moczydlowski E. Purification and partial sequencing of saxiphilin, a saxitoxin-binding protein from the bullfrog, reveals homology to transferrin. *J Biol Chem* 1991; 266:15481–15487.
120. Li Y, Llewellyn L, Moczydlowski E. Biochemical and immunochemical comparison of saxiphilin and transferrin, two structurally related plasma proteins from *Rana catesbeiana*. *Mol Pharmacol* 1993; 44:742–748.
121. Morabito MA, Moczydlowski E. Molecular cloning of bullfrog saxiphilin: A unique relative of the transferrin family that binds saxitoxin. *Proc Natl Acad Sci USA* 1994; 91:2478–2482.

122. Morabito MA, Moczydlowski E. Molecular cloning of bullfrog saxiphilin: A unique relative of the transferrin family that binds saxitoxin. *Proc Natl Acad Sci USA* 1995; 92:6651.
123. Llewellyn LE, Bell PM, Moczydlowski EG. Phylogenetic survey of soluble saxitoxin-binding activity in pursuit of the function and molecular evolution of saxiphilin, a relative of transferrin. *Proc Roy Soc (Lond) B* 1997; 264:891–902.
124. Wuebbens MW, Roush ED, Decastro CM, Fierke CA. Cloning, sequencing, and recombinant expression of the porcine inhibitor of carbonic anhydrase: A novel member of the transferrin family. *Biochemistry* 1997; 36:4327–4336.
125. Baranov VS, Schwartzman AL, Gorbunova VN, Gaitskhoki VS, Rubtsov NB, Timchenko NA, Neifakh SA. Chromosomal localization of ceruloplasmin and transferrin genes in laboratory rats, mice and in man by hybridization with specific DNA probes. *Chromosoma* 1987; 96:60–66.
126. Plowman GD, Brown JP, Enns CA, Schroder J, Nikinmaa B, Sussman HH, Hellstrom KE, Hellstrom I. Assignment of the gene for human melanoma-associated antigen p97 to chromosome 3. *Nature* 1983; 303:70–72.
127. Rabin M, McClelland A, Kuhn L, Ruddle FH. Regional localization of the human transferrin receptor gene to 3q26.2—qter. *Am J Hum Genet* 1985; 37:1112–1116.
128. McCombs JL, Teng CL, Pentecost BT, Magnuson VL, Moore CM, McGill JR. Chromosomal localization of human lactotransferrin gene (LTF) by in situ hybridization. *Cytogenet Cell Genet* 1988; 47:16–17.
129. Schaeffer E, Lucero MA, Jeltsch JM, Py MC, Levin MJ, Chambon P, Cohen GN, Zakin MM. Complete structure of the human transferrin gene. Comparison with analogous chicken gene and human pseudogene. *Gene* 1987; 56:109–116.
130. Park I, Schaeffer E, Sidoli A, Baralle FE, Cohen GN, Zakin MM. Organization of the human transferrin gene: Direct evidence that it originated by gene duplication. *Proc Natl Acad Sci USA* 1985; 82:3149–3153.
131. Zakin MM. Regulation of transferrin gene expression. *FASEB J* 1992; 6:3253–3258.
132. Schaeffer E, Guillou F, Part D, Zakin MM. A different combination of transcription factors modulates the expression of the human transferrin promoter in liver and Sertoli cells. *J Biol Chem* 1993; 268:23399–23408.
133. Suire S, Fontaine I, Guillou F. Transferrin gene expression and secretion in rat sertoli cells. *Mol Reprod Dev* 1997; 48:168–175.
134. Maguire SM, Millar MR, Sharpe RM, Gaughan J, Saunders PT. Investigation of the potential role of the germ cell complement in control of the expression of transferrin mRNA in the prepubertal and adult rat testis. *J Mol Endocrinol* 1997; 19:67–77.
135. Chaudhary J, Cupp AS, Skinner MK. Role of basic-helix-loop-helix transcription factors in Sertoli cell differentiation: Identification of an E-box response element in the transferrin promoter. *Endocrinology* 1997; 138:667–675.
136. Chaudhary J, Skinner MK. Comparative sequence analysis of the mouse and human transferrin promoters: Hormonal regulation of the transferrin promoter in Sertoli cells. *Mol Reprod Dev* 1998; 50:273–283.
137. Sigillo F, Guillou F, Fontaine I, Benahmed M, Le Magueresse-Battistoni B. In vitro regulation of rat Sertoli cell transferrin expression by tumor necrosis factor alpha and retinoic acid. *Mol Cell Endocrinol* 1999; 148:163–170.
138. Espinosa de los Monteros A, Sawaya BE, Guillou F, Zakin MM, de Vellis J, Schaeffer E. Brain-specific expression of the human transferrin gene. Similar elements govern transcription in oligodendrocytes and in a neuronal cell line. *J Biol Chem* 1994; 269:24504–24510.
139. Ghareeb BA, Thepot D, Puissant C, Cajero-Juarez M, Houdebine LM. Cloning, structural organization and tissue-specific expression of the rabbit transferrin gene. *Biochim Biophys Acta* 1998; 1398:387–392.

140. Ghareeb BA, Thepot D, Delville-Giraud C, Houdebine LM. Cloning and functional expression of the rabbit transferrin gene promoter. *Gene* 1998; 211:301–310.
141. Guo Y, Li X, Zhu H, Shen Z. Subtyping of transferrin by isoelectric focusing in immobilized pH gradients. *Electrophoresis* 1998; 19:1314–1316.
142. Beckman L, Sikstrom C, Mikelsaar AV, Krumina A, Ambraisiene D, Kucinskas V, Beckman G. Transferrin variants as markers of migrations and admixture between populations in the Baltic Sea region. *Hum Hered* 1998; 48:185–191.
143. Tsuchida S, Ikemoto S, Kajii E. AvaI polymorphism in the human transferrin gene. *Hum Hered* 1997; 47:338–341.
144. Beckman LE, Van Lendeghem GF, Sikstrom C, Beckman L. DNA polymorphisms and haplotypes in the human transferrin gene. *Hum Genet* 1998; 102:141–144.
145. Pang H, Koda Y, Soejima M, Kimura H. Identification of a mutation (A1879G) of transferrin from cDNA prepared from peripheral blood cells. *Ann Hum Genet* 1998; 62:271–274.
146. Namekata K, Oyama F, Imagawa M, Ihara Y. Human transferrin (Tf): A single mutation at codon 570 determines Tf C1 or Tf C2 variant. *Hum Genet* 1997; 100:457–458.
147. Namekata K, Imagawa M, Terashi A, Ohta S, Oyama F, Ihara Y. Association of transferrin C2 allele with late-onset Alzheimer's disease. *Hum Genet* 1997; 101:126–129.
148. Beckman LE, Van Landeghem GF, Sikstrom C, Lundgren R, Beckman L. Protective effect of transferrin C3 in lung cancer? *Oncology* 1999; 56:328–331.
149. Evans RW, Crawley JB, Garratt RC, Grossmann JG, Neu M, Aitken A, Patel KJ, Meilak A, Wong C, Singh J, Bomford A, Hasnain SS. Characterization and structural analysis of a functional human serum transferrin variant and implications for receptor recognition. *Biochemistry* 1994; 33:12512–12520.
150. Anderson BF, Baker HM, Norris GE, Rumball SV, Baker E. Apolactoferrin structure demonstrates ligand-induced conformational change in transferrins. *Nature* 1990; 344:784–786.
151. Haridas M, Anderson BF, Baker EN. Structure of human diferric lactoferrin refined at 2.2 Å resolution. *Acta Crystallogr* 1995; D51:629–646.
152. MacGillivray RTA, Moore SA, Chen J, Anderson BF, Baker H, Luo Y, Bewley M, Smith CA, Murphy MEP, Wang Y, Mason AB, Woodworth RC, Brayer GD, Baker EN. Two high resolution crystal structures of the recombinant N-lobe of human transferrin reveal a structural change implicated in iron release. *Biochemistry* 1998; 37:7919–7928.
153. Sun H, Cox MC, Li H, Mason AB, Woodworth RC, Sadler PJ. [¹H, ¹³C] NMR determination of the order of lobe loading of human transferrin with iron: comparison with other metal ions. *FEBS Lett* 1998; 422:315–320.
154. Dewan JC, Mikami B, Hirose M, Sacchettini JC. Structural evidence for a pH-sensitive dilysine trigger in the hen ovotransferrin N-lobe: Implications for transferrin iron release. *Biochemistry* 1993; 32:11963–11968.
155. Moore SA, Anderson BF, Groom CR, Haridas M, Baker EN. Three dimensional structure of diferric bovine lactoferrin at 2.8 Å resolution. *J Mol Biol* 1997; 274:222–236.
156. Jameson GB, Anderson BF, Norris GE, Thomas DH, Baker EN. Structure of human apolactoferrin at 2.0 Å resolution. Refinement and analysis of ligand-induced conformational change. *Acta Crystallogr* 1998; D54:1319–1335.
157. Jeffrey PD, Bewley MC, MacGillivray RTA, Mason AB, Woodworth RC, Baker EN. Ligand-induced conformational change in transferrins: Crystal structure of the open form of the N-terminal half-molecule of human transferrin. *Biochemistry* 1998; 37:13978–13986.
158. Sharma AK, Rajashankar KR, Yadav MP, Singh TP. Structure of mare apolactoferrin: The N and C lobes are in the closed form. *Acta Crystallogr* 1999; D55:1152–1157.

159. Rawas A, Muirhead H, Williams J. Structure of apo duck ovotransferrin: The structures of the N and C lobes are in the open form. *Acta Crystallogr* 1997; D53:464–468.
160. Kurokawa H, Dewan JC, Mikami B, Sacchettini JC, Hirose M. Crystal structure of hen apo-ovotransferrin. Both lobes adopt an open conformation upon loss of iron. *J Biol Chem* 1999; 274:28445–28452.
161. Grossmann JG, Crawley JB, Strange RW, Patel KJ, Murphy LM, Neu M, Evans RW, Hasnain SS. The nature of ligand-induced conformational change in transferrin in solution. An investigation using X-ray scattering, XAFS and site-directed mutants. *J Mol Biol* 1998; 279:461–472.
162. Mizutani K, Yamashita H, Kurokawa H, Mikami B, Hirose M. Alternative structural state of transferrin. The crystallographic analysis of iron-loaded but domain-opened ovotransferrin N-lobe. *J Biol Chem* 1999; 274:10190–10194.
163. Hershberger CL, Larson JL, Arnold B, Rosteck PR, Williams P, DeHoff B, Dunn P, O'Neal KL, Riemen MW, Tice PA, Crofts R, Ivancic J. A cloned gene for human transferrin. *Ann NY Acad Sci* 1991; 646:140–154.
164. Ikeda RA, Bowman BH, Yang F, Lokey LK. Production of human serum transferrin in *Escherichia coli*. *Gene* 1992; 117:265–269.
165. Steinlein LM, Ikeda RA. Production of N-terminal and C-terminal human serum transferrin in *Escherichia coli*. *Enzyme Microbiol Technol* 1993; 15:193–199.
166. de Smit DH, Hoefkens P, de Jong G, van Duin J, van Knippenberg PH, van Eijk HG. Optimized bacterial production of nonglycosylated human transferrin and its half-molecules. *Int J Biochem Cell Biol* 1995; 27:839–850.
167. Hoefkens P, de Smit MH, de Jeu-Jaspars NMH, Huijskes-Heins MIE, de Jong G, van Eijk HG. Isolation, renaturation and partial characterization of recombinant human transferrin and its half molecules from *Escherichia coli*. *Int J Biochem Cell Biol* 1996; 28:975–982.
168. Ward PP, Cunningham GA, Conneely OM. Commercial production of lactoferrin, a multifunctional iron-binding glycoprotein. *Biotechnol Genet Eng Rev* 1997; 14:303–319.
169. Ward PP, May GS, Headon DR, Conneely OM. An inducible expression system for the production of human lactoferrin in *Aspergillus nidulans*. *Gene* 1992; 122:219–223.
170. Ward PP, Lo J-Y, Duke M, May GS, Headon DR, Conneely OM. Production of biologically active recombinant human lactoferrin in *Aspergillus oryzae*. *Bio/Technology* 1992; 10:784–789.
171. Ward PP, Piddington CS, Cunningham GA, Zhou X, Wyatt RD, Conneely OM. A system for production of commercial quantities of human lactoferrin: A broad spectrum natural antibiotic. *Bio/Technology* 1995; 13:498–503.
172. Ward PP, Zhou X, Conneely OM. Cooperative interactions between the amino- and carboxyl-terminal lobes contribute to the unique iron-binding stability of lactoferrin. *J Biol Chem* 1996; 271:12790–12794.
173. Sun XL, Baker HM, Shewry SC, Jameson BG, Baker EN. Structure of recombinant human lactoferrin expressed in *Aspergillus awamori*. *Acta Crystallogr* 1999; D55:403–407.
174. Steinlein LM, Graf TN, Ikeda RA. Production and purification of N-terminal half-transferrin in *Pichia pastoris*. *Protein Exp Purif* 1995; 6:619–624.
175. Mason AB, Woodworth RC, Oliver RWA, Green BN, Lin LN, Brandts JF, Tam BM, Maxwell A, MacGillivray RTA. Production and isolation of the recombinant N-lobe of human serum transferrin from the methylotrophic yeast *Pichia pastoris*. *Protein Exp Purif* 1996; 8:119–125.
176. Steinlein LM, Ligan CM, Kessler S, Ikeda RA. Iron release is reduced by mutations of lysines 206 and 296 in recombinant N-terminal half-transferrin. *Biochemistry* 1998; 37:13696–13703.

177. Bewley MC, Tam BM, Grewal J, He S, Shewry S, Murphy MEP, Mason AB, Woodworth RC, Baker EN, MacGillivray RTA. X-ray crystallography and mass spectroscopy reveal that the N-lobe of human transferrin expressed in *Pichia pastoris* is folded correctly but is glycosylated on Serine-32. *Biochemistry* 1999; 38:2535–2541.
178. Guarna M, Lesnicki GL, Tam B, Robinson J, Radziminski CZ, Hasenwinkle D, Boraston A, Jervis E, MacGillivray RTA, Turner RFB, Kilburn DG. On-line monitoring and control of methanol concentration in shake-flask cultures of *Pichia pastoris*. *Biotechnol Bioeng* 1997; 56:279–286.
179. Laroche Y, Storme V, De Meutter J, Messens J, Lauwereys M. High-level secretion and very efficient isotopic labeling of tick anticoagulant peptide (TAP) expressed in the methylotrophic yeast, *Pichia pastoris*. *Biotechnology* 1994; 12:1119–1126.
180. Retzer MD, Kabani A, Button LL, Yu RH, Schryvers AB. Production and characterization of chimeric transferrins for the determination of the binding domains for bacterial transferrin receptors. *J Biol Chem* 1996; 271:1166–1173.
181. Ali SA, Joao HC, Csonga R, Hammerschmid F, Steinkasserer A. High-yield production of functionally active human serum transferrin using a baculovirus expression system, and its structural characterization. *Biochem J* 1996; 319:191–195.
182. Hegedus DD, Pfeifer TA, Theilmann DA, Kennard ML, Gabathuler R, Jefferies WA, Grigliatti TA. Differences in the expression and localization of human melanotransferrin in lepidopteran and dipteran insect cell lines. *Protein Exp Purif* 1999; 15:296–307.
183. Mason AB, Miller MK, Funk WD, Banfield DK, Savage KJ, Oliver RWA, Green BN, MacGillivray RTA, Woodworth RC. Expression of glycosylated and nonglycosylated human transferrin in mammalian cells. Characterization of the recombinant proteins with comparison to three commercially available transferrins. *Biochemistry* 1993; 32:5472–5479.
184. Zak O, Tam B, MacGillivray RTA, Aisen P. A kinetically active site in the C-lobe of human transferrin. *Biochemistry* 1997; 36:11036–11043.
185. Mason AB, He Q-Y, Tam BM, MacGillivray RTA, Woodworth RC. Mutagenesis of the aspartic acid ligands in human serum transferrin: Lobe-lobe interaction and conformation as revealed by antibody, receptor binding and iron release studies. *Biochem J* 1998; 330:35–40.
186. Mason AB, Tam BM, Woodworth RC, Oliver RA, Green BA, Lin L-N, Brandts JF, Savage KJ, Lineback JA, MacGillivray RTA. Receptor recognition sites reside in both lobes of human serum transferrin. *Biochem J* 1997; 326:77–85.
187. Mason AB, Woodworth RC, Oliver RW, Green BN, Lin LN, Brandts JF, Savage KJ, Tam BM, MacGillivray RTA. Association of the two lobes of ovotransferrin is a prerequisite for receptor recognition. Studies with recombinant ovotransferrins. *Biochem J* 1996; 319:361–368.
188. Stowell KM, Rado TA, Funk WD, Tweedie JW. Expression of cloned human lactoferrin in baby-hamster kidney cells. *Biochem J* 1991; 276:349–355.
189. Day CL, Stowell KM, Baker EN, Tweedie JW. Studies of the N-terminal half of human lactoferrin produced from the cloned cDNA demonstrate that interlobe interactions modulate iron release. *J Biol Chem* 1992; 267:13857–13862.
190. Mason AB, Funk WD, MacGillivray RTA, Woodworth RC. Efficient production and isolation of recombinant amino-terminal half-molecule of human serum transferrin from baby hamster kidney cells. *Protein Exp Purif* 1991; 2:214–220.
191. Beatty EJ, Cox MC, Frenkiel TA, Tam BM, Mason AB, MacGillivray RT, Sadler PJ, Woodworth RC. Interlobe communication in ¹³C-methionine-labeled human transferrin. *Biochemistry* 1996; 35:7635–7642.
192. Nuijens JH, van Berkel PH, Geerts ME, Hartevelt PP, de Boer HA, van Veen HA, Pieper FR. Characterization of recombinant human lactoferrin secreted in milk of transgenic mice. *J Biol Chem* 1997; 272:8802–8807.

193. Kim SJ, Sohn BH, Jeong S, Pak KW, Park JS, Park IY, Lee TH, Choi YH, Lee CS, Han YM, Yu DY, Lee KK. High-level expression of human lactoferrin in milk of transgenic mice using genomic lactoferrin sequence. *J Biochem* 1999; 126:320–325.
194. Salmon V, Legrand D, Sloomianny MC, el Yazidi I, Spik G, Gruber V, Bournat P, Olgarnier B, Mison D, Theisen M, Merot B. Production of human lactoferrin in transgenic tobacco plants. *Protein Exp Purif* 1998; 13:127–135.
195. Bali PK, Zak O, Aisen P. A new role for the transferrin receptor in the release of iron from transferrin. *Biochemistry* 1991; 30:324–328.
196. Bali PK, Aisen P. Receptor-modulated iron release from transferrin: Differential effects on N- and C-terminal sites. *Biochemistry* 1991; 30:9947–9952.
197. Baker HM, Anderson BF, Brodie AM, Shongwe MS, Smith CA, Baker EN. Anion binding by transferrins: Importance of second-shell effects revealed by the crystal structure of oxalate-substituted diferric lactoferrin. *Biochemistry* 1996; 35:9007–9013.
198. Smith CA, Anderson BF, Baker HM, Baker EN. Metal substitution in transferrins: The crystal structure of human copper lactoferrin at 2.1 Å resolution. *Biochemistry* 1992; 31:4527–4533.
199. Smith CA, Baker HM, Baker EN. Preliminary crystallographic studies of copper(II)- and oxalate-substituted human lactoferrin. *J Mol Biol* 1991; 219:155–159.
200. Day CL, Anderson BF, Tweedie JW, Baker EN. Structure of the recombinant N-terminal lobe of human lactoferrin at 2.0 Å resolution. *J Mol Biol* 1993; 232:1084–1100.
201. Faber HR, Bland T, Day CL, Norris GE, Tweedie JW, Baker EN. Altered domain closure and iron binding in transferrins: The crystal structure of the Asp60Ser mutant of the amino-terminal half-molecule of human lactoferrin. *J Mol Biol* 1996; 256:352–363.
202. Faber HR, Baker CJ, Day CL, Tweedie JW, Baker EN. Mutation of arginine 121 in lactoferrin destabilizes iron binding by disruption of anion binding: Crystal structures of R121S and R121E mutants. *Biochemistry* 1996; 35:14473–14479.
203. Nicholson H, Anderson BF, Bland T, Shewry SC, Tweedie JW, Baker EN. Mutagenesis of the histidine ligand in human lactoferrin: Iron binding properties and crystal structure of the histidine-253→methionine mutant. *Biochemistry* 1997; 36:341–346.
204. Breyer WA, Kingston RL, Anderson BF, Baker EN. On the molecular-replacement problem in the presence of merohedral twinning: Structure of the N-terminal half-molecule of human lactoferrin. *Acta Crystallogr* 1999; D55:129–138.
205. Sharma AK, Singh TP. Lactoferrin-metal interactions: First crystal structure of a complex of lactoferrin with a lanthanide ion (Sm³⁺) at 3.4 Å resolution. *Acta Crystallogr* 1999; D55:1799–1804.
206. Sharma AK, Paramasivam M, Yadav MP, Srinivasan A, Singh TP. Three-dimensional structure of mare diferric lactoferrin at 2.6 Å resolution. *J Mol Biol* 1999; 289:303–317.
207. Sharma AK, Singh TP. Structure of oxalate-substituted diferric mare lactoferrin at 2.7 Å resolution. *Acta Crystallogr* 1999; D55:1792–1798.
208. Karthikeyan S, Paramasivam SY, Srinivasan A, Singh TP. Structure of buffalo lactoferrin at 2.5 Å resolution using crystals grown at 303 K shows different orientations of the N and C lobes. *Acta Crystallogr* 1999; D55:1805–1813.
209. Kurokawa H, Mikami B, Hirose M. Crystal structure of diferric hen ovotransferrin at 2.4 Å resolution. *J Mol Biol* 1995; 254:196–207.
210. Rawas A, Muirhead H, Williams J. Structure of diferric duck ovotransferrin at 2.35 Å resolution. *Acta Crystallogr* 1996; D52:631–640.
211. Lindley PF, Bajaj M, Evans RW, Garratt RC, Hasnain SS, Jhoti H, Kuser P, Neu M, Patel K, Sarrar R, Strange R, Walton A. The mechanism of iron uptake by transferrins: The structure of an 18 kDa NII-domain fragment from duck ovotransferrin at 2.3 Å resolution. *Acta Crystallogr* 1993; D49:292–304.

212. Sarra R, Lindley PF. Preliminary x-ray data for an N-terminal fragment of rabbit serum transferrin. *J Mol Biol* 1986; 188:727–728.
213. Zuccola HJ. The crystal structure of monoferric human serum transferrin. PhD dissertation, Georgia Institute of Technology, Atlanta, GA, 1993.
214. Yang AH-W, MacGillivray RTA, Chen J, Luo Y, Wang Y, Brayer GD, Mason AB, Woodworth RC, Murphy MEP. Crystal structures of two mutants (K206Q, H207E) of the N-lobe of human transferrin with increased affinity for iron. *Protein Sci* 2000; 9: 49–52.
215. MacGillivray RTA, Bewley MC, Smith CA, He Q-Y, Mason AB, Woodworth RC, Baker EN. Mutation of the iron ligand His 249 to Glu in the N-lobe of human transferrin abolishes the dilysine “trigger” but does not significantly affect iron release. *Biochemistry* 2000; 39:1211–1216.
216. Ward PP, Chu H, Zhou X, Conneely OM. Expression and characterization of recombinant murine lactoferrin. *Gene* 1997; 204:171–176.
217. Salmon V, Legrand D, Georges B, Slomianny MC, Coddeville B, Spik G. Characterization of human lactoferrin produced in the baculovirus expression system. *Protein Exp Purif* 1997; 9:203–210.
218. Legrand D, Salmon V, Coddeville B, Benaissa M, Plancke Y, Spik G. Structural determination of two N-linked glycans isolated from recombinant human lactoferrin expressed in BHK cells. *FEBS Lett* 1995; 365:57–60.
219. van Berkel PH, van Veen HA, Geerts ME, de Boer HA, Nuijens JH. Heterogeneity in utilization of N-glycosylation sites Asn624 and Asn138 in human lactoferrin: A study with glycosylation-site mutants. *Biochem J* 1996; 319:117–122.
220. Grossmann JG, Mason AB, Woodworth RC, Neu M, Lindley PF, Hasnain SS. Asp ligand provides the trigger for closure of transferrin molecules. Direct evidence from X-ray scattering studies of site-specific mutants of the N-terminal half-molecule of human transferrin. *J Mol Biol* 1993; 231:554–558.
221. Lin L-N, Mason AB, Woodworth RC, Brandts JF. Calorimetric studies of the N-terminal half-molecule of transferrin and mutant forms modified near the Fe³⁺-binding site. *Biochem J* 1994; 293:517–522.
222. Grady JK, Mason AB, Woodworth RC, Chasteen ND. The effect of salt and site-directed mutations on the iron(III)-binding site of human serum transferrin as probed by EPR spectroscopy. *Biochem J* 1995; 309:403–410.
223. Mecklenburg SL, Mason AB, Woodworth RC, Donohoe RJ. Distinction of the two binding sites of serum transferrin by resonance Raman spectroscopy. *Biospectroscopy* 1997; 3:435–444.
224. He QY, Mason AB, Woodworth RC, Tam BM, Wadsworth T, MacGillivray RTA. Effects of mutations of aspartic acid 63 on the metal-binding properties of the recombinant N-lobe of human serum transferrin. *Biochemistry* 1997; 36:5522–5528.
225. He QY, Mason AB, Woodworth RC, Tam BM, MacGillivray RTA, Grady JK, Chasteen ND. Inequivalence of the two tyrosine ligands in the N-lobe of human serum transferrin. *Biochemistry* 1997; 36:14853–14860.
226. Zak O, Aisen P, Crawley JB, Joannou CL, Patel KJ, Rafiq M, Evans RW. Iron release from recombinant N-lobe and mutants of human transferrin. *Biochemistry* 1995; 34: 14428–14434.
227. He QY, Mason AB, Woodworth RC, Tam BM, MacGillivray RTA, Grady JK, Chasteen ND. Mutations at nonliganding residues Tyr-85 and Glu-83 in the N-lobe of human serum transferrin. Functional second shell effects. *J Biol Chem* 1998; 273:17018–17024.
228. He Q-Y, Mason AB, Pakdaman R, Chasteen ND, Dixon BK, Tam BM, Nguyen V, MacGillivray RTA, Woodworth RC. Mutations at the histidine 249 ligand profoundly

- alter the spectral and iron-binding properties of human serum transferrin. *Biochemistry* 2000; 39:1205–1210.
229. Li Y, Harris WR, Maxwell A, MacGillivray RTA, Brown T. Kinetic studies on the removal of iron and aluminum from recombinant and site-directed mutant N-lobe half transferrins. *Biochemistry* 1998; 37:14157–14166.
230. Harris WR, Cafferty AM, Trankler K, Maxwell A, MacGillivray RTA. Thermodynamic studies on anion binding to apotransferrin and recombinant transferrin N-lobe half molecules. *Biochim Biophys Acta* 1999; 1430:269–280.
231. He QY, Mason AB, Tam BM, MacGillivray RTA, Woodworth RC. Dual role of Lys206-Lys296 interaction in human transferrin N-lobe: Iron-release trigger and anion-binding site. *Biochemistry* 1999; 38:9704–9711.
232. Luck LA, Mason AB, Savage KJ, MacGillivray RTA, Woodworth RC. ^{19}F NMR studies of the recombinant human transferrin N-lobe and three single point mutants. *Magn Reson Chem* 1997; 35:477–481.
233. Beatty EJ, Cox MC, Frenkiel TA, He QY, Mason AB, Sadler PJ, Tucker A, Woodworth RC. Trp128Tyr mutation in the N-lobe of recombinant human serum transferrin: ^1H - and ^{15}N -NMR and metal binding studies. *Protein Eng* 1997; 10:583–591.
234. He Q-Y, Mason AB, Tam BM, MacGillivray RTA, Woodworth RC. [^{13}C] Methionine NMR and metal-binding studies of recombinant human transferrin N-lobe and five methionine mutants: Conformational changes and increased sensitivity to chloride. *Biochem J* 1999; 344:881–887.

3

The Transferrin Receptor

CAROLINE A. ENNS

Oregon Health Sciences University, Portland, Oregon

I.	INTRODUCTION	72
II.	FUNCTION AND TRAFFICKING OF THE HUMAN TfR	72
	A. Overview of the TfR Endocytosis and Recycling	72
	B. The TfR Concentrates in Coated Pits	72
	C. Exocytosis of the TfR	74
	D. Other Pathways Taken by the TfR	74
	E. TfR Sorting in Polarized Cells	74
	F. Biosynthesis of the TfR	74
	G. Posttranslational Modifications	75
	H. Tf–TfR Interactions	77
	I. Association of the TfR with the Hereditary Hemochromatosis Protein	78
	J. Soluble TfR	79
III.	STRUCTURE OF THE Tf RECEPTOR	80
	A. Crystal Structure of the TfR	80
	B. Crystal Structure of the TfR/HFE Complex	80
	C. Structure of the TfR Gene	82
IV.	REGULATION OF THE Tf RECEPTOR	83
	A. Regulation of TfR mRNA Stability by Iron	83
	B. Non-Iron Regulation of TfR mRNA Stability	84
	C. Limitations of mRNA Stability	84
	D. Transcriptional Regulation	85
V.	TfR2	85
VI.	CONCLUSIONS	87
	REFERENCES	87

I. INTRODUCTION

One of the principle ways by which cells in the body take up iron is through the transferrin (Tf) receptor-mediated pathway. Most extracellular iron found in the blood is bound to Tf, an abundant glycoprotein that binds iron with extraordinary affinity at the nearly neutral pH of the blood. The Tf receptor (TfR) acts as the gatekeeper for Tf uptake by cells. Along with a recently identified hereditary hemochromatosis protein, HFE, it regulates the amount of Tf-bound iron taken up by cells. The TfR is tightly regulated at the levels of transcription, mRNA production, and protein synthesis by the iron, metabolic, and proliferative needs of the cell. The function, structure, and regulation of the TfR will be discussed in this chapter.

II. FUNCTION AND TRAFFICKING OF THE HUMAN TfR

A. Overview of the TfR Endocytosis and Recycling

The endocytic cycle of the TfR has been extensively characterized. At the cell surface the TfR binds iron-bound transferrin present in the extracellular medium with nM affinity ($K_d \sim 1-5$ nM) (1-6). The receptor undergoes constitutive endocytosis, that is, it cycles into the cell and back to the plasma membrane in the presence or absence of bound Tf (1,3,7). Internalization occurs via concentration into clathrin-coated pits, which bud off from the cell membrane (8,9). After losing their coats, the vesicles fuse with other internalized vesicles, forming an endosome. As the pH is lowered to 5.5-6.5, Fe^{3+} dissociates from Tf; the apo-Tf remains associated with the receptor (1,2,10). Acidification is essential for the dissociation of Fe^{3+} from Tf. Agents that raise endosomal pH, such as chloroquine and monensin, inhibit Fe^{3+} uptake into cells (11,12). Upon recycling of the apo-Tf-TfR complex to the cell surface, the apo-Tf/TfR complex dissociates once it encounters the near-neutral, slightly basic pH (1,3,13-16). This cycle is repeated many times during the lifetime of the TfR and is summarized in Fig. 1.

B. The TfR Concentrates in Coated Pits

Early estimates of the proportion of TfR in these structures at the cell surface ran as high as 70% (8,9), but more recent studies indicate a much lower proportion, perhaps 10-15% (17,18). Coated pits occupy only 1-2% of the cell surface (17). Thus the TfR is concentrated 5-15-fold in coated pits. The internalization rates of Tf for a number of cell lines are about 10% of surface-bound ligand per minute. The coated pit containing the Tf-TfR complex buds off from the plasma membrane, becomes uncoated, and enters the tubulo-vesicular endosomal system (19-21). A H^+ -adenosine triphosphatase acidifies the endosome (22,23), the Tf-TfR complex releases its iron, is sorted away from the co-endocytosed proteins that are not recycled, and returns to the cell surface as an apo-Tf-TfR complex.

The cytoplasmic domain of the receptor possesses the signal for endocytosis. Removal of the cytoplasmic domain of the TfR reduces the rate of endocytosis 10-20-fold and reduces its concentration in coated pits [(18,24); reviewed in Ref. 25]. The endocytic signal has been more precisely localized, by site-directed mutagenesis, to the YTRF sequence at positions 20-23, and the tyrosine at position 20 appears to be particularly critical for endocytosis (26). The type of amino acid at position

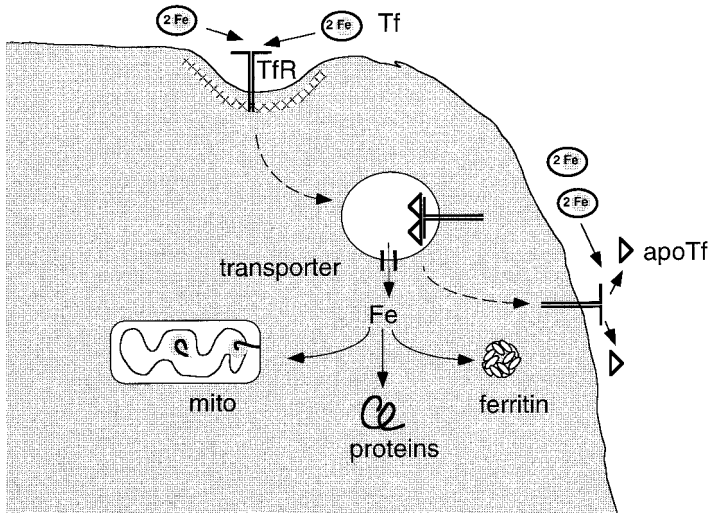


Figure 1 Tf-mediated iron transport into cells. Iron-laden Tf binds to the Tf receptor at the cell surface. The complex is taken into cells via clathrin-coated vesicles. Within the cell the endocytic vesicle acidifies, facilitating the release of iron from Tf. Iron is transported into the cytoplasm, where it can be incorporated into proteins, transported into mitochondria, or stored in ferritin. Apo-Tf remains bound to the Tf receptor, and both are transported back to the cell surface. At the near-neutral pH of the extracellular medium, apo-Tf is rapidly displaced by iron-laden Tf, and the cycle repeats.

21 does not appear to be critical for endocytosis, leading to a generalized motif of YXRF for internalization. A tyrosine is also a key ingredient in the internalization motif (NPVY) of the LDL receptor (27,28). Similar motifs have been identified in several other receptors (reviewed in Ref. 25). Mutations of phenylalanines at positions 13 and 23 of the TfR have a negative effect on endocytosis, suggesting that sequence information extending beyond tyrosine 20 contributes to efficient endocytosis. Also, substitution of tyrosine at position 34 for the normal serine causes reversion of an internalization-defective receptor (29). Therefore, cryptic internalization signals, in addition to the major motif, may be present.

Studies of endosomal sorting using density-shift techniques with Tf-horseradish peroxidase conjugates and diaminobenzidine in the presence of ^{125}I -labeled TfR, asialoglycoprotein receptor (ASGPR), and mannose-6-phosphate receptor (MPR) indicate that all three receptors are at least transiently present in the same compartment (30). TfR and ASGPR are rapidly recycled back to the surface from early endosomes, while MPR is largely transported to the trans-Golgi network, and shuttles back and forth to late endosomes.

The endocytic pathway used by the TfR is saturable. Overexpression of a number of receptors containing Tyr-internalization motifs, including the TfR, can saturate this pathway (31–33). As receptor numbers increase, the rate of endocytosis per cell surface receptor decreases. Thus, a redistribution of the overexpressed receptor to the cell surface occurs (31,33,34). Surprisingly, not all Tyr motifs compete with each other. Overexpression of the TfR does not compete with the internalization or result

in the redistribution of either the low-density lipoprotein receptor or the epidermal growth factor receptor pathway (32,33). The TfR receptor does compete with lysosomal-associated membrane protein 1 (LAMP1) (31,33). These results suggest that the different classes of Tyr-motif endocytic signals compete for different components of the endocytic machinery.

C. Exocytosis of the TfR

The kinetics of Tf cycling from the cell surface through the endosomes and back to the cell surface is identical to that of three membrane lipids, *N*-[*N*-(7-nitro-2,1,3-benzoxadiazol-4-yl)- ϵ -amino-hexanoyl]-sphingosylphosphorylcholine, C₆-NBD-phosphatidylcholine, and galactosylceramide. These results indicate that the receptor complex moves through the endocytic pathway by a bulk flow mechanism, and that proteins, which sort to the other compartments such as the late endosome or lysosome, are selectively sequestered (35).

D. Other Pathways Taken by the TfR

The TfR can also cycle back to the trans-Golgi compartment. Neuraminidase treatment of cells indicates that TfRs pass through the trans-Golgi network, where they can be resialylated with a half-life of 1.5 h (36). The extent of this pathway has been a matter of some controversy (36–38) and may correspond to the long recycling pathways described previously (9,39).

E. TfR Sorting in Polarized Cells

Most plasma membrane proteins are sorted preferentially to either the basolateral or the apical side of polarized cells. This phenomenon has been studied extensively in MDCK cells, where at least 95% of the TfR is sorted to the basolateral portion of the cell (40). Polarity of the TfR is maintained by the accurate recycling of the TfR to the basolateral membrane (40). The cytoplasmic domain of the TfR was examined to determine whether it played a role in sorting. Like the poly-Ig receptor, proper targeting of the TfR to the basolateral surface did not require phosphorylation (41). Deletion of 36 amino acids including the internalization sequence (6–41) resulted in 20% of the TfR being redirected to the apical membrane (41). Thus, basolateral targeting was not solely dependent on the internalization signal of the TfR but rather on other sequences or structural elements adopted by the cytoplasmic domain of the TfR. Therefore the TfR falls into the class of receptors with distinct sorting and internalization signals. The TfR is also found on the basolateral side of hepatocytes and Caco2 cells, an intestinal cell line, but the sorting in these cells has not been as extensively studied.

F. Biosynthesis of the TfR

Biosynthesis of the TfR has been examined, both in vivo and in vitro, in the presence of rabbit reticulocyte lysate and microsomes (42–44). The receptor is a type II transmembrane protein; that is, the N terminus is cytoplasmic and the C terminus is extracellular. The sequence that signals translocation through the endoplasmic reticulum membrane is within the transmembrane domain (45,46). Deletion of the trans-

membrane region results in the failure of the TfR to undergo translocation and glycosylation *in vitro*. Attachment of the transmembrane domain of the TfR onto the N terminus of mouse dihydrofolate reductase and chimpanzee α -globulin results in the insertion of these normally cytosolic proteins into the microsomal membrane in the same orientation as the TfR (45,46). Asn-linked glycosylation of the TfR occurs co-translationally (42,43).

The newly synthesized TfR is unable to bind Tf and is a monomer (42). Dimer formation and the ability to bind Tf occur rapidly. Disulfide-bond formation between subunits is a slower process, which occurs with a $t_{1/2}$ of approximately 30 min. The presence of inter-subunit disulfide bonds, however, is not required for dimer formation or for binding of Tf, because a mutated form of the TfR lacking disulfide bonds binds Tf with normal affinity (47).

G. Posttranslational Modifications

The human TfR undergoes several posttranslational modifications: (a) intermolecular disulfide-bond formation, (b) phosphorylation, (c) fatty acylation with palmitate, (d) addition of three Asn-linked oligosaccharides, (e) addition of one Ser/Thr-linked oligosaccharide, and (f) proteolytic cleavage (Fig. 2). The functions of many of these modifications are not known, however.

The sulfhydryls of Cys89 and Cys98 form intermolecular disulfide bonds. When only Cys98 is mutated to Ser, only about half of the TfRs have inter-subunit

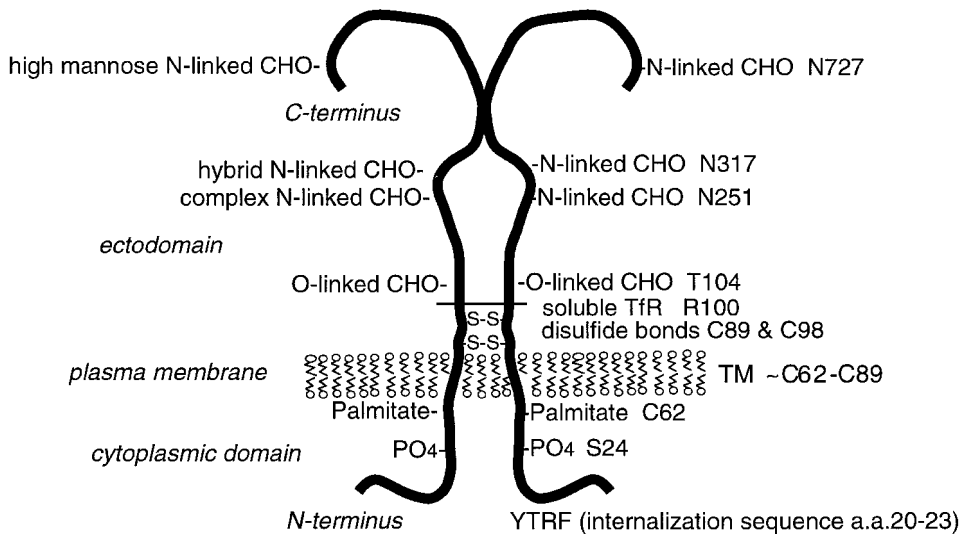


Figure 2 Key features of the human Tf receptor. The Tf receptor is extensively modified during and after its synthesis. On the ectodomain it contains three Asn-linked oligosaccharides at positions 251, 317, and 727. It has one O-linked glycosylation site on Thr 104 and two inter-subunit disulfide bonds at Cys89 and Cys98. The cytoplasmic domain contains a palmitate at Cys62 and Ser24 can be phosphorylated in response to activation of protein kinase C. The internalization motif is at amino acids 20–23.

disulfide bonds, indicating that in this mutant Cys89 does not always form disulfide bonds. Mutation of both Cys89 and Cys98 to Ser eliminates the disulfide bonds (48). These bonds are not necessary for normal endocytosis, recycling, iron accumulation, or the dimeric state. Rather, the dimeric state is maintained by the 70-kDa external domain of the TfR that can be isolated after trypsin treatment (49). It can also be isolated in an insect cell line secreting a soluble form of the TfR, which completely lacks any inter-subunit disulfide bonds (50).

Ser24 is the only known cytoplasmic domain phosphorylation site on the TfR. TfR is phosphorylated both *in vivo* and *in vitro* by protein kinase C (24,51,52). Phosphorylation of human TfR is not important for endocytosis in mouse L cells (24,29,53), nor is it important for the basolateral targeting of the TfR in polarized epithelial cells (41).

The fatty acid, palmitate, was shown to be attached to TfR (54,55) at Cys62 (48) and/or Cys67 (56). Acylation does not appear to be necessary for efficient endocytosis of human TfR expressed in chicken embryo fibroblasts (Jing and Trowbridge, 1990), but its presence may cause a 20% decrease in endocytosis rate in Chinese hamster ovary (CHO) cells (56). The palmitate of TfR has a higher turnover rate than TfR itself, and palmitate can be added to mature TfR as long as 48 hours after synthesis (55). The precise fraction of mature TfRs that are modified with palmitate is not known. The turnover of the palmitate is too slow for it to be involved in the endocytic cycle, although trafficking through slower pathways, such as to the trans Golgi network are not excluded (55).

The Asn-linked carbohydrate groups are added to TfR during synthesis and are further processed in the Golgi to yield one complex-type and two high-mannose oligosaccharides (57). In human TfR the modified sites are at Asn251, Asn317, and Asn727 (43,44,58,59). When the human TfR is either expressed in mouse 3T3 cells or isolated from human placentae, the complex-type oligosaccharide is at Asn251, and the other two Asn residues at 317 and 727 are of the high-mannose type (57). Mutation of each of these sites revealed that glycosylation of Asn727 is essential for TfR transport to the cell surface. Without this oligosaccharide, the TfR remains localized to the endoplasmic reticulum and is associated with an endoplasmic reticulum chaperone protein, binding immunoglobulin protein (BiP) (60,61). Transport of the TfR lacking the Asn727 glycosylation site to the plasma membrane can be partially recovered by generation of a glycosylation site at Asn722 (61). Mutation of the other two glycosylation sites had little effect on the TfR trafficking (60,61). A different mutation of the carbohydrate attachment site at Asn251 resulted in a TfR that was retained and cleaved in the endoplasmic reticulum (62). These results are in contrast to those mentioned above in which elimination of the carbohydrate at Asn251 did not significantly affect transport of TfR to the cell surface. They imply that the amino acid substitution rather than the lack of glycosylation resulted in a misfolded TfR and created a cleavage site.

The effect of Asn-linked glycosylation on TfR transport is the most dramatic of any of the posttranslational modifications thus far observed. The structure of the Asn-linked carbohydrates of the TfR shows considerable heterogeneity and varies with the cell line (63) and among individuals (64), and displays blood-group antigens (63). The possible physiological consequence of this heterogeneity is not known.

A single Ser/Thr (*O*-linked) carbohydrate of the human TfR has been characterized recently (63) and localized to Thr 104 (65,66). As with the variable structure

of Asn-linked oligosaccharides, the structure of the *O*-linked carbohydrate from different human cell lines varies also (63). The *O*-linked carbohydrate at Thr104 protects the TfR from efficient cellular proteolytic cleavage near the plasma membrane (67). When Thr104 is mutated to Asp, no *O*-linked oligosaccharide is attached, and an 80-kDa soluble TfR form accumulates in the growth medium. Sequencing of the soluble TfR at the cleavage site revealed that cleavage occurs between residues Arg100 and Leu101, only four amino acids from the normal site of *O*-linked carbohydrate attachment at Thr104, near the membrane (67). These results suggest that the carbohydrate inhibits access of a protease to this site. The cleavage of the TfR in cell culture is enhanced by treatment with neuraminidase, implying that removal of sialic acid from the *O*-linked carbohydrate is sufficient for efficient cleavage of the TfR (68). Since a soluble form of TfR has been observed in human blood with the same cleavage site (69), cleavage of the TfR appears to be an additional way to downregulate the TfR on the surface of cells.

H. Tf–TfR Interactions

The interaction of Tf with its receptor plays an important role in the delivery of iron to cells. At neutral pH, Tf has an extremely high avidity for two ferric ions ($K_a \approx 10^{20} - 10^{23} \text{ M}^{-1}$) (70,71), whereas at pH 5 the binding constant falls to a K_a of $\sim 10^7 \text{ M}^{-1}$. During its intracellular transit, the receptor cycles from the plasma membrane to an acidic compartment with a pH of $\sim 5.4 - 6.5$ depending on the cell type (12,22,23). This low pH and the rapid recycling of the receptor back to the cell surface are not sufficient to explain the release of iron from Tf inside the endosomal compartment (see Chapter 4). Evidence from two separate laboratories shows that the binding of Tf to its receptor facilitates the loss of iron at endosomal pH (72–74). In contrast, at pH 6.2 or higher, the receptor actually stabilizes the interaction between ferric ion and Tf, making it more difficult to remove iron from Tf bound to the receptor than from unbound Tf (73). The cycle is completed when the apo-Tf-TfR complex returns to the cell surface. At neutral pH the binding constant of apo-Tf for the receptor is ~ 2000 fold lower than that of diferric Tf (15) and consequently the apo-Tf readily dissociates from the receptor. For more insight into the release of iron from Tf, again see Chapter 4.

The structural features of the TfR that are involved in the binding of Tf are not known. Initial studies using tunicamycin-treated cells indicated that blocking Asn-linked glycosylation resulted in a form of the TfR that was unable to bind Tf (75,76) and greatly inhibited the ability of both the murine and human TfR to reach the cell surface (43,75–77). Site-directed mutagenesis of all of the consensus sequences for Asn-linked glycosylation confirmed the initial observations using tunicamycin (60,78). The third glycosylation at Asn727 appears to be the most critical site for Tf binding and transport to the cell surface (61). A TfR lacking a glycosylation site at Asn727 is still predominantly a disulfide-bonded dimer, and therefore retains much of its quaternary structure (61). Inhibition of Asn-linked processing of the core oligosaccharides of the human and murine TfRs by treatment of cells with swainsonine or deoxynojiramicin does not affect the ability of the TfR to reach the cell surface (42,77). It also does not have a substantial effect on its ability to bind Tf (42). Likewise, the binding of Tf to a soluble form of the TfR produced in

baculovirus-infected insect cells gives similar Tf binding affinities, even though these cells do not synthesize complex oligosaccharides (50).

Two features of the TfR have been identified as being critical for Tf binding. Using human/chicken chimeric TfR, Buchegger and colleagues demonstrated that the 50 C-terminal amino acids of the human TfR are critical for the binding of human Tf (79). Dubljevic and colleagues showed that the mutation of the RGD sequence in the TfR resulted in a loss of Tf binding implying that this sequence was critical (80).

The structural features of Tf required for TfR binding have been partially defined. As discussed above, apo-Tf is easily displaced by diferric Tf at neutral pH. Vertebrate Tfs have arisen from a gene duplication (reviewed in Ref. 81). Each lobe binds a single ferric ion with similar affinities. Tf can be cleaved by mild protease digestion into two peptides (82). Each peptide retains its ability to bind its ferric ion, but the peptides do not bind well to the TfR (83). Mutation of the iron-binding site of either lobe results in a three–four-fold lower binding affinity, but mutation of both lobes decreases the binding affinity ~30-fold (84). These results support the idea that the receptor-recognition site lies in both lobes of Tf. The C-terminal domain of Tf contains the two Asn-linked oligosaccharides (reviewed in Ref. 85), which are not necessary for binding to the receptor. Deglycosylation of Tf with glycosidases or elimination of the Asn-linked glycosyl groups by site-directed mutagenesis does not diminish the binding of Tf to the human (86) or bacterial TfRs (87).

I. Association of the TfR with the Hereditary Hemochromatosis Protein

The first link between HFE, the hereditary hemochromatosis protein, and its effect on iron metabolism in the cell came with the discovery that they form a tight complex and co-precipitate when co-expressed in tissue culture cells (88), and also form a tight complex when isolated from tissues such as the placenta and intestine (88–90). Association of the wild-type HFE with the TfR negatively regulates iron uptake into most tissue culture cells (91). The mechanism by which this is accomplished is not fully understood (but see Chapter 8). HFE decreases the affinity of Tf for the TfR approximately 10-fold (50,88,92). The lower affinity of Tf for the TfR is not a satisfactory explanation for the lower iron uptake because the concentration of diferric Tf in the serum is ~5 μM and the binding constant (K_d) of Tf for its receptor is ~1–2 nM. Indeed, even at 100 nM diferric Tf, no difference in the rates of Tf endocytosis are detected in cells expressing or not expressing TfR (91).

Different groups differ in terms of the effect of HFE on the cycling of the TfR. The first report did not detect any change in the cycling or distribution of TfRs in the presence of HFE (91). One group reports that TfR internalization is impaired (93). Another group reports that the rate of exocytosis decreases (94). All agree that expression of HFE results in a low ferritin phenotype. Consistent with this finding is the report that IRP mRNA-binding activity is increased in HFE-expressing cells (95,96). Together, the findings that Tf-mediated ^{55}Fe uptake is decreased, low ferritin levels are detected, and IRP mRNA binding activity is increased indicate that HFE expression leads to a low labile iron pool within nonpolarized cells.

Several lines of evidence suggest that the binding of HFE to the TfR appears to be essential for the low ferritin phenotype. Mutant forms of HFE which do not

interact with the TfR, such as C260Y HFE,* the most common mutation in hereditary hemochromatosis, or with W81A HFE, which has over a 1000-fold lower affinity for TfR when expressed in tissue culture cells, fail to lower ferritin levels (97). Soluble HFE lacking the transmembrane and cytoplasmic domains, when added to cells expressing TfR, are able to lower ferritin levels (97). These results indicate that the cytoplasmic domain does not participate directly in signaling events. The human HFE has no recognizable endocytic sequence and in cells lacking the human Tf receptor HFE remains on the cell surface. Addition of an internalization sequence to HFE lowers ferritin levels only if HFE interacts with the TfR and does not in the W81A HFE mutant (97). These results imply that HFE internalization alone is not sufficient for the low ferritin phenotype, but rather that the interaction of HFE with TfR is important.

J. Soluble TfR

The remarkable finding by Johnstone and colleagues (98,99) that when sheep reticulocytes mature they shed selected membrane proteins including the TfR led Kohgo and colleagues (100) to look for evidence of TfR in human serum. Not only was the TfR detectable, it appeared to be in a soluble form of ~85 kDa rather than the full-length form found in vesicles. Subsequent sequencing of the N terminus indicated that soluble TfR arises from the cleavage of the full-length TfR after Arg100 (69).

The mechanism by which the soluble TfR is generated is not completely understood, but several interesting observations have been made. Shedding of Tf receptors occurs in both erythroid and nonerythroid cells and cell lines (101–103). Endocytosis of the TfR is required for shedding of the TfR in both cases. In erythroid cells, endocytosis leads to formation of multivesicular structures and release of the vesicles into the medium (104). During this process (and subsequent to it), the receptor is cleaved and released from the vesicles. The identification of an *O*-linked glycosylation site at Thr104 led to the hypothesis that modification of this glycosylation site four amino acids away from the cleavage site could play a role in the cleavage at Arg100 (105). In nonerythroid cell lines, either elimination of the *O*-linked site or desialylation of the site does indeed result in increased cleavage and release of soluble TfR (68). Again, endocytosis is required and the cleaved TfR is released into the medium. In this case cleavage appears to take place in endosomal compartments, and no released vesicles are detectable.

The assay for serum TfR refined by Skikne and colleagues (106) has become generally accepted as an accurate method in conjunction with serum ferritin levels in the diagnosis of iron-deficiency anemia. The basis of the assay comes from the observation that ~50% of the serum TfR is the result of hematopoiesis (101). Thus, in patients with iron-deficiency anemia the amount of erythropoiesis is greatly expanded, leading to increased concentrations of soluble TfR. The assay is good at distinguishing between the anemias of chronic inflammation, where soluble TfR is not increased, and iron deficiency, where soluble TfR levels are high (107). In conjunction with serum ferritin levels, it can distinguish between anemias resulting from

*The numbering system for HFE used in this manuscript is in accordance with that published by Lebron and colleagues (50). The 22-amino acid signal sequence that is cleaved upon processing is not included in this numbering system.

thalassemias, hemolytic anemias, and polycythemias where both serum TfR and ferritin levels are elevated, and iron-deficiency anemias, where only serum TfR is high.

III. STRUCTURE OF THE Tf RECEPTOR

Even before the TfR was cloned, a great deal about the general topology and structure of the TfR had been deduced using biochemical analysis. Mild trypsin cleavage at the surface of cells released an 80-kDa fragment indicating that the majority of its amino acids were in the ectodomain. A combination of nonreducing sodium dodecylsulfate (SDS) gel electrophoresis, sedimentation velocity, and column chromatography indicated that the solubilized receptor was a dimer containing at least one inter-subunit disulfide bond (43,108,109). The dimer was capable of binding two Tf molecules (108). Binding studies indicated that Tf bound to each subunit with almost equal affinity (1,3,110). The cloning and sequencing of the TfR cDNA indicated that the receptor was a type 2 membrane protein with no signal sequence on the N terminus; rather, it possessed a transmembrane domain that served as a signal sequence (58,59).

More recently, image reconstruction from electron microscopy on the full-length TfR reconstituted into vesicles confirmed that the full-length TfR is indeed a dimer in the phospholipid membrane and consists of a large globular domain ($6.4 \times 7.5 \times 10.5$ nm) on a 2.9-nm stalk (111). Fuchs and colleagues (111) also observed the tendency of the TfR to aggregate into proteoparticles consisting predominantly of 6–12 receptor dimers. This ability to self-associate and propensity to preferentially integrate into smaller vesicles (60–90 nm) rather than into larger vesicles was suggested by the authors to account for TfR's ability to concentrate into similarly sized clathrin-coated vesicles and to recycle to the cell surface. Further stabilization of TfR clusters by incubation of cells with multimeric Tf causes the TfR traffic to later compartments and increases the degradation of the TfR (112,113).

A. Crystal Structure of the TfR

The crystal structure of the ectodomain of the TfR has provided a more detailed view of the TfR ectodomain (114) (Fig. 3). Each monomer is composed of three distinct domains: a protease domain, an apical domain, and a helical domain. The protease domain (residues 122–188 and 384–606) is 28% identical in sequence to membrane glutamate carboxylase II. This domain in the TfR is not catalytically active because the critical residues in the active site of the protease are not conserved. The sequence and structural similarities indicate that this domain most likely evolved from an ancestral carboxy- or amino-peptidase. The apical domain (residues 189–383) is composed of a beta sandwich and is farthest from the membrane. The helical domain (residues 607–760) consists of a four-helix bundle. This region forms the dimer interface between the two monomers. Under the crystallization conditions used by Lawrence and colleagues (114), each dimer had significant contact with other dimers burying 2600 \AA^2 of surface area, consistent with the propensity of the TfR to form higher-ordered structures as observed in the EM reconstruction studies.

B. Crystal Structure of the TfR/HFE Complex

Within a year and a half of cloning HFE, the crystal structure of the ectodomain of this molecule was solved (50), and less than two years later the structure of the HFE/

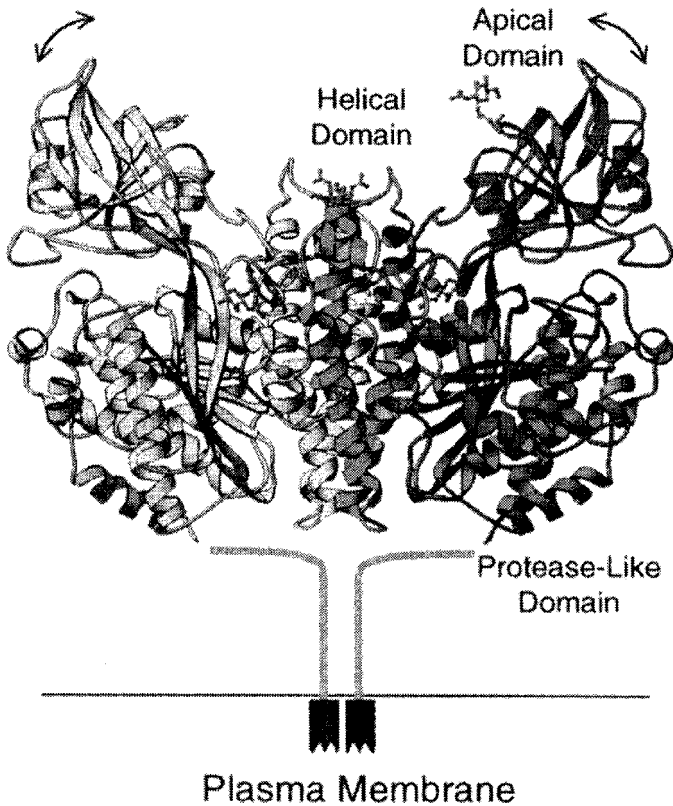


Figure 3 Structure of the ectodomain of the human transferrin receptor. The crystal structure of the ectodomain of the transferrin receptor reveals three domains, the apical domain, the helical domain, which is involved in the dimer interface and the protease domain, which is structurally similar to carboxypeptidase C. (Reprinted from Ref. 114.)

β_2 m TfR complex was published (115) (Fig. 4). The co-crystal structure reveals the sites of interaction between the HFE/ β_2 -microglobulin (β_2 m) complex and the TfR and possible conformational changes induced in the TfR by HFE binding. The main sites of interaction are between the $\alpha 1$ - $\alpha 2$ platform of HFE and the helical domain of TfR. The β_2 m subunit does not contribute directly to the binding interface. TfR and HFE have a large surface area of interaction ($\sim 1000 \text{ \AA}^2$ per subunit), whereas there is little conformational change between the crystal structure of HFE complexed with TfR and not much greater conformational change occurs in the TfR. The backbone structure in either case of the protease and apical domains do not change. In contrast, the helical domain in the lower-pH crystal uncomplexes TfR with respect to the other domains. This movement alters the shape of the cleft between the helical and protease-like domains. Bennett and colleagues (115) speculate that this change could alter the ability of Tf to bind to the TfR. In addition, three loops at the TfR dimer interface shift, changing the geometry of the histidine cluster found in this region. The histidine cluster is postulated to modulate TfR-facilitated release of iron from Tf.

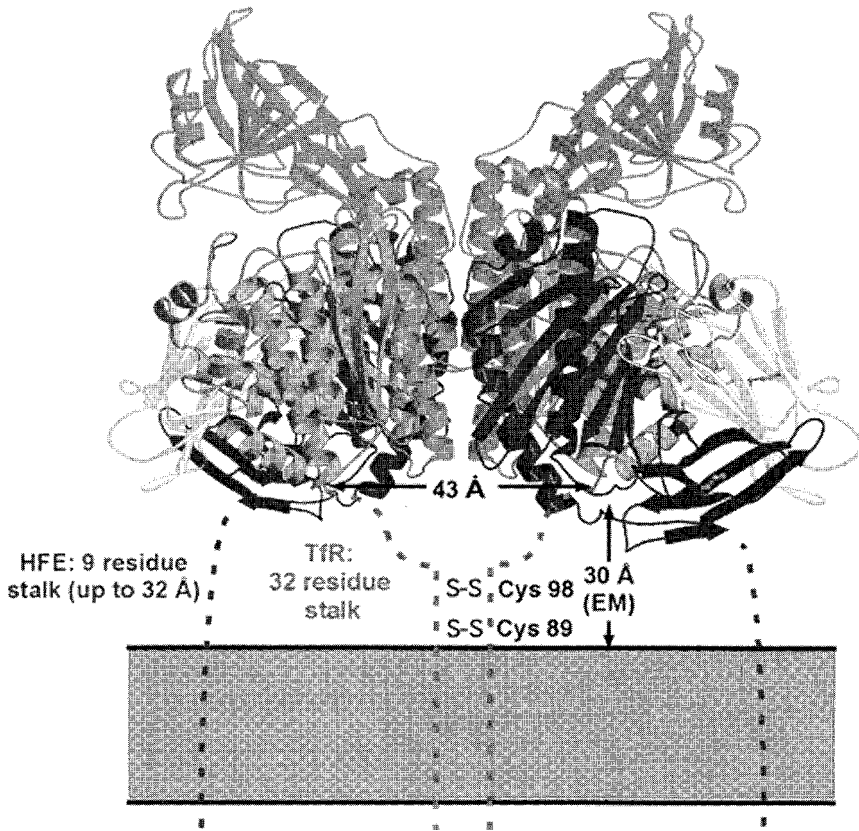


Figure 4 Crystal structure of the transferrin receptor-HFE/ β_2 microglobulin complex. A ribbon diagram of the transferrin receptor-HFE/ β_2 microglobulin complex shows the large region of interaction between these molecules. In this case the transferrin receptor is in medium gray. HFE is denoted in dark gray and β_2 microglobulin in light gray. (Reprinted from Ref. 50.)

Sorting out whether the changes are due to the interaction between HFE and TfR or the crystallization conditions remains to be determined. The TfR was crystallized at pH 6.5–7 and the HFE/ β_2 m TfR complex at pH 8.0. The TfR is known to undergo a measurable conformational change below pH 6 (72,74). Whether the TfR does so at higher pH is critical in order to interpret these results.

C. Structure of the TfR Gene

The TfR gene is over 30 kb in length (58). Early mapping of the intron–exon boundaries by heteroduplex mapping indicated that there were 19 exons and 18 introns length (58). More detailed and precise mapping of the intron–exon boundaries were later accomplished by Evans and Kemp (116). The exon–intron boundaries do not at all correspond to the five domains of the protein, the cytoplasmic, transmembrane, carboxy peptidase-like, apical, and helical domains. In fact, the relatively short (63-amino acid) cytoplasmic domain of the TfR is encoded by two

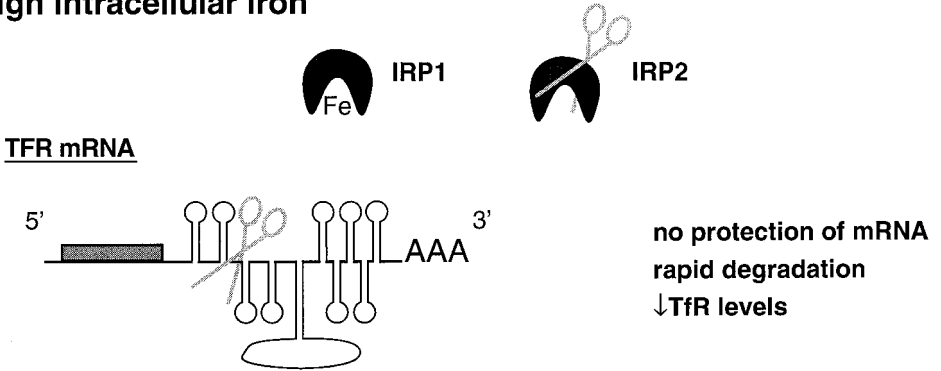
exons, the even shorter transmembrane domain (27 amino acids) is encoded by two exons, and 15 exons encode the ectodomain.

IV. REGULATION OF THE Tf RECEPTOR

A. Regulation of TfR mRNA Stability by Iron

The uptake of Tf into cells within the body is exquisitely regulated. This is accomplished, in part, via intracellular iron pools that regulate the stability of the TfR mRNA (reviewed in Refs. 117–119; see also Chapters 9 and 10). The 3' untranslated portion of the TfR mRNA is capable of forming secondary structure that consists of distinctive stem–loop structures called iron response elements (IREs) (Fig. 5). Iron regulatory proteins (IRPs) work in conjunction with these elements to sense and respond to changes in the regulatory iron pool, i.e., the amount of chelatable iron found inside the cell. Under low iron conditions, the IRPs bind to the stem–loop

high intracellular iron



low intracellular iron

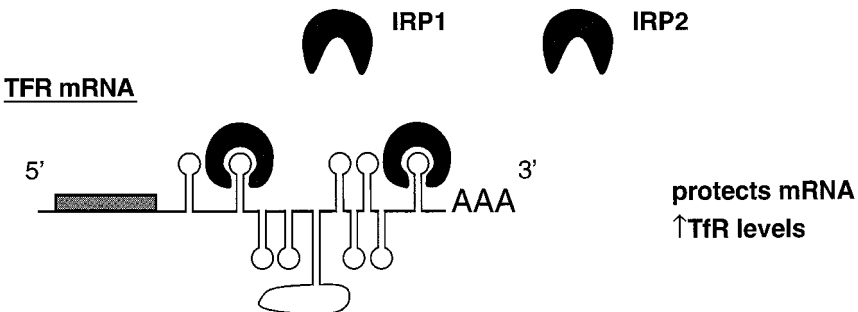


Figure 5 Iron control of Tf receptor mRNA stability. At low intracellular iron levels both IRP1 and IRP2 bind to the stem–loop IRE’s iron-responsive elements on the 3’ portion of the Tf receptor mRNA and protect the mRNA from degradation. At high intracellular iron concentrations IRP1 binds iron, rendering it unable to bind mRNA. IRP2 is oxidized, ubiquitinated, and degraded via proteasomes. The Tf receptor mRNA with no IRP bound to it is rapidly degraded, resulting in low steady-state levels of TfR mRNA. Consequently, less Tf receptor is synthesized.

structure in the TfR mRNA and protect it from degradation, resulting in increased TfR synthesis. Under high iron conditions, IRP1 binds iron in the form of a Fe–S complex, preventing interaction with the IRE. The TfR mRNA becomes less stable, resulting in less synthesis of TfR (recently reviewed in Ref. 120).

Iron levels within the cell regulate the levels of other iron-related proteins via the IRP. Ferritin is an intracellular iron storage protein. Under low intracellular conditions, the IRP binds to the IRE stem–loop structure on 5' of the translation start site of ferritin mRNA and prevents translation. Under high intracellular iron concentrations, when it is desirable to synthesize ferritin to sequester iron and prevent iron-catalyzed oxidative damage to the cell, IRP binds iron and no longer binds to the IRE. As a result, ferritin synthesis increases. Other iron metabolism-related proteins which possess stem–loop structures on either the 5' or 3' untranslated portion of their mRNA include: 5-amino levulinic acid synthetase, which is involved in heme biosynthesis; mitochondrial aconitase (121,122); and the iron–sulfur subunit of succinate dehydrogenase (121). They are all regulated by intracellular iron concentrations through the IRPs. The recently cloned iron transporter, Nramp2/DMT1, is regulated by intracellular iron concentrations and has a putative IRE structure in the 3' untranslated region similar to the TfR (123; see Chapter 6).

A second IRP has been identified (124). In contrast to IRP1, the activity of which is regulated by iron, the levels of IRP2 vary inversely to intracellular iron (125). IRP2 does not bind an iron sulfur complex, but rather its binding to mRNA is controlled at the level of protein stability. Excess intracellular iron results in oxidation, ubiquitination, and degradation of IRP2 by the proteasome (126).

B. Non-Iron Regulation of TfR mRNA Stability

Factors other than the intracellular iron pools can also affect TfR mRNA stability through IRP-regulatory mechanisms. Since the stability of the TfR mRNA is controlled by the binding of IRP1 and IRP2, agents which affect the levels of IRP2 or the ability of IRP2 to bind the Fe–S cluster will alter TfR mRNA levels. For example, cMyc was recently shown to be a transcriptional factor for the IRP2 gene. Thus, activation of cMyc leads to increases in IRP2 levels, which in turn result in increased TfR mRNA levels. Oxidative stress appears to regulate IRP activity. Signaling molecules such as NO and molecules such as H₂O₂ play a role in this process. NO can activate both IRP1 and IRP2 mRNA-binding activity. In contrast, treatment of cells with H₂O₂ in cells activates IRP1 but not IRP2. The response to H₂O₂ can be blocked by okadaic acid, a protein phosphatase inhibitor, raising the possibility that the signal is transduced by a phosphatase/kinase signal transduction pathway (127).

C. Limitations of mRNA Stability

The IRP-mediated regulation of TfR mRNA stability is able to regulate TfR levels over only a limited range. In mice containing only one gene for the TfR, the IRP system cannot compensate for the loss of one gene (128). These animals have severe hypochromic microcytic anemia, presumably resulting from lack of the ability to compensate for the lower gene dosage.

D. Transcriptional Regulation

In addition to the elegant control of TfR mRNA stability exerted by the IRPs, TfR expression can be controlled at the transcriptional level. Dramatic increases in TfR levels are seen when B and T cells are stimulated to proliferate and hence need a net uptake of iron for the synthesis of ribonucleotide reductase, a key enzyme in initiation of DNA synthesis (129,130). Increases in TfR mRNA levels are also detected during erythroid differentiation when cells need to take up large amounts of iron to be incorporated into hemoglobin (131,132). Finally, TfR mRNA levels increase during hypoxia (133–136). At least part of the increase in mRNA levels in all of these processes is the result of transcriptional activation of the TfR gene.

The transcription factors involved in TfR gene regulation have not been extensively studied as the regulation of mRNA stability. Mutagenesis of the 5' portion of the first 100 nucleotides upstream of the transcriptional start site revealed that this region is critical in promoter activity (reviewed in Ref. 137). An 8-bp element, TRA, (nucleotides -77 to -70) binds a heterodimeric protein complex (82 kDa and 62 kDa) called TRAC (138,139). This factor appears to allow the TfR gene to respond to mitogen-induced stimulation and has similar nucleic acid specificity to factors such as PIF (parvovirus initiation factor) isolated from HeLa extracts and Ku, a DNA-binding component of a DNA-dependent protein kinase (140). Ku, PIF, and perhaps TRAC belong to an emerging KDWK family of combinatorial transcription modulators, which are common in promoter regions of ATF/CREB and E-box motifs.

The observation that hypoxia induces erythropoiesis led to the question of whether the transcription factor HIF-1 (hypoxia-inducible factor) induces the transcription of the TfR gene. Hypoxia does indeed increase the transcription of the TfR gene two- to fourfold in nuclear run-on assays (133,135,136). A HIF-1 binding site at -93 to -73 was identified in the TfR promoter region by gel shift analysis and HIF-1's ability to activate the promoter region fused to reporter genes (133).

A dramatic increase in TfR levels occurs during erythroid differentiation (131,132). Hemoglobin iron accounts for nearly 80% of bodily iron, so the fact that Tf receptor levels are highest in cells that are actively synthesizing hemoglobin is not surprising. Part of the increase in mRNA levels is due to transcriptional activation. Transforming-specific protein-1 (Ets-1) is a transcription factor that is active in erythropoietic cells. An EBS, Ets-binding site, motif was identified in the promoter region of the TfR gene and appears to promote a four- to eightfold increase in TfR transcription (131,132).

V. TfR2

One of the unexpected entries into the field of iron uptake recently was the discovery and cloning of transferrin receptor 2 (TfR2) by Kawabata and colleagues in 1999 (141). Like the original TfR, TfR2 is a type 2 transmembrane protein with the N terminus in the cytoplasm and the C-terminal seven-eighths of the protein forming the ectodomain, although it shares only 45% sequence identity and 66% similarity with the ectodomain of the classical TfR (Fig. 6). The human TfR2 is less similar to TfR than human TfR is to chicken TfR, indicating that TfR2 represents a new family of Tf-binding proteins. Similar to TfR, it is a dimer that possesses at least one inter-subunit disulfide bond. It has four potential N-linked glycosylation sites.

```

TfR : 68 YGTIAVIVFFLIGFMIGYLGYCKGVEPKTECERLAGTESPVRE----EPGEDFPAARRLY 123
      Y + ++ F F++GY+ + + C+ + V E EP DF R LY
TfR2 : 84 YLVLTALLIFTGAFLLGYVAF-----RGSCQACGSDVLLVSEEDVNYEPDLDFHQGR-LY 136

TfR : 124 WDDLKRKLSEKLDSTDFSTIKLLNENSYPVREAGSQKDENLALYVENQFREFKLSKVWR 183
      W DL+ + L TI+ + S R AGS L + KL VW
TfR2 : 137 WSDLQAMFLQFLGEGRLEDTIR---QTSLRERVAGSAGMAALTQDIFRAALSRQKLDHVWT 193

TfR : 184 DQHFVKIQVKDSAQ-NSVIIVDKNGRL--VYLVENPGGYVAYSKAATVTGKLVHANFGTK 240
      D H+V +Q D A N++ VD+ G++ +E+P Y YS VTG+LV+A++G
TfR2 : 194 DTHYVGLQFPDPAHPNTLHWVDEAGKVGEQLPLEDDPVYCPYSAIGNVTGELVYAHYGRP 253

TfR : 241 KDFEDLYT----PVNGSIVIVRAGKITFAEKVANAESLNAIGVLIYMDQTKF-----PI 290
      +D +DL PV G +++VR G I+FA+KV NA+ A GVLIY + F P
TfR2 : 254 EDLQDLRARGVDPV-GRLLLVRVGVISFAQKVTAQDFGAQGVLIYEPEDFSQDPPKPS 312

TfR : 291 VNAELSFFGHAHLGTGDPYTPGFPSFNHTQFPFSPRSGLPNIPVQTISRAAAEKLFNGME 350
      ++++ + +GH HLTGDPYTPGFPSFN TQ KL G +
TfR2 : 313 LSSQQAVYGVHHLGTGDPYTPGFPSFNQTQ-----KLGKPV- 348

TfR : 351 GDCPSDWKTDSTCRMV-TSESKNVKLTVSNVLKEIKILNIFGVIKGFVEPDHYVVVGAQR 409
      P +W+ ++L V+N I NIFG I+G EPDHYVV+GAQR
TfR2 : 349 --APQEWQGSLLGSPYHLGPGPRLRLVNNHRTSTPINNIFGCIERGSEPDHYVVVGAQR 406

TfR : 410 DAWGPGAAGSGVGTALLLKLQAMFSDMVLKDGFPQSRSIIFASWSAGDFGSVGAWEWLEG 469
      DAWGPGAAGS VGTA+LL+L + FS MV +GF+P RS++F SW GDFGSVG+TEWLEG
TfR2 : 407 DAWGPGAAGSAVGTAIILLELVRTFSSMV-SNGFRPRRSLLFISWDGGDFGSVGSTEWLEG 465

TfR : 470 YLSSLHLKAFTYINLDKAVLGTSNFKVSASPLLYTLIEKTMQNVKHP-VTGQFLYQ---- 524
      YLS LHLKA Y++LD AVLG F SPLL +LIE ++ V P +GQ LY+
TfR2 : 466 YLSVLHLKAVVYVSLDNVAVLGDGDKFHAKTSPLLTSLIESVLKQVDSPNHSGQTLYEQVVF 525

TfR : 525 -DSNW-ASKVEKLTLDNAAFPFLAYSGIPAVSFCFCEDTD-YPYLGTTMDTYKELIERIP 581
      + +W A + L +D++A+ F A+ G+FAV F F ED YP+L T DTY+ L + +
TfR2 : 526 TNPSWDAEVIRPLEMDSSAYSFTAFVGVPAVEFSFMEDDQAYPFLHTKEDTYENLHKVLQ 585

Query: 582 -ELNKVARAAAEVAGQFVIKLTHTDVELNLDYERYNSQLLSFVRDLNQYRADIKEMGLSLQ 640
      L VA+A A++AGQ +I+L+HD L LD+ RY +L + +LN++ D+K GL+LQ
TfR2 : 586 GRLPAVAQAVAQLAGQLLIRLSHDRLPLDFGRYGDVVLRHIGNLNEFSGDLKARGTLTQ 645

TfR : 641 WLYSARGDFFRATSRLTTDFGNAEKTRDFVMKKLNDVRMR-----VEYHFLSPYVSPKE 694
      W+YSARGD+ RA +L + ++E+ D + + N R+MR VE++FLS YVSP +
TfR2 : 646 WVYSARGDYIRAAEKLRQEIYSSEERDERLTRMYNVRIMRIPLSAQVEFYFLSQYVSPAD 705

TfR : 695 SPFRHVFWGSGSHTLPALLENLKLKQKQNG-----AFNETLFRNQLALATWTIQGA 745
      SPFRH+F G G HTL ALL++L+L + N+ F E+ FR QLAL TWT+QGA
TfR2 : 706 SPFRHIFMGRGDHTLGALLDHLRLLRNSSSGTPGATSSTGFQESRFRRLALLTWTLQGA 765

TfR : 746 ANALSGDVWDIDNEF 760
      ANALSGDVW+IDN F
TfR2 : 766 ANALSGDVWNIDNNEF 780

```

Figure 6 Similarities between the TfR and TfR2. A BLAST analysis comparing the amino acid sequences of the classical Tf receptor and Tf receptor 2 reveals an overall 39% identity. The identity increases to 45% starting at the transmembrane region going through the ectodomain.

Three of these sites are close in position to those of TfR. TfR2 binds Tf with a 25- to 30-fold lower affinity than that of TfR (142,143) and has no demonstrable affinity for HFE (143). Indeed, about half the amino acids in TfR that interact with HFE are not conserved in TfR2. Some of the substitutions change the hydrophobicity of the interface, change the charge, or destroy hydrogen bonds.

Two additional features distinguish TfR2 from TfR. Unlike TfR, which is expressed ubiquitously on dividing cells and cells specialized for iron transport or utilization, TfR2 is expressed predominantly in the liver, a small amount in the kidney, and in a limited number of specific cell lines such as a human hepatoma cell line (HepG2), an erythroleukemia cell line (K563), and a prostate cell line (LNCaP) (141,144). Second, the TfR2 mRNA levels do not appear to be sensitive to the iron status of the cells, in that deprivation of intracellular iron with desferrioxamine treatment does not result in increased TfR2 mRNA levels (141,144). Consistent with this finding is the absence of potential IRE structures in the mRNA.

Intriguingly, a mutation in TfR2 (Y250Stop) has been implicated in a rare form of hereditary hemochromatosis associated with human chromosome 7 (*HFE3*) (145). How the presumed lack of function of this protein, which is expressed predominantly in the liver, and perhaps the bone marrow, increases iron uptake through the intestine will surely be an interesting and evolving story.

VI. CONCLUSIONS

In summary, the uptake of Tf into cells appears to be tightly regulated by the number of Tf receptors on the cell surface. The number of classical TfRs on the cell surface appears to be regulated at the level of transcription, mRNA stability, and the shedding of the receptor from the cell. Intracellular iron levels, proliferation factors, signaling molecules, and differentiation factors all participate in the control of TfR levels. The physiological significance and control mechanisms of the newly identified TfR2 are only beginning to be studied.

REFERENCES

1. Dautry-Varsat A, Ciechanover A, Lodish HF. pH and the recycling of Tf during receptor-mediated endocytosis. *Proc Natl Acad Sci USA* 1983; 80:2258–2262.
2. Karin M, Mintz B. Receptor-mediated endocytosis of Tf in developmentally totipotent mouse teratocarcinoma stem cells. *J Bio Chem* 1981; 256:3245–3252.
3. Klausner RD, Ashwell G, van Renswoude J, Harford JB, Bridges KR. Binding of apoTf to K562 cells: Explanation of the Tf cycle. *Proc Natl Acad Sci USA* 1983; 80:2263–2266.
4. Morgan EH. Passage of Tf, albumin and gamma globulin from maternal plasma to foetus in the rat and rabbit. *J Physiol* 1964; 171:26–41.
5. Wada HG, Hass PE, Sussman HH. Tf receptor in human placental brush border membranes: Studies on the binding of Tf to placental membrane vesicles and the identification of a placental brush border glycoprotein with high affinity for Tf. *J Biol Chem* 1979; 254:12629–12635.
6. Ward JH, Kushner JP, Kaplan J. Regulation of HeLa cell Tf receptors. *J Biol Chem* 1982; 257:10317–10323.
7. Schulman HM, Wilczynska A, Ponka P. Tf and iron uptake by human lymphoblastoid and K562 cells. *Biochem Biophys Res Commun* 1981; 100:1523–1530.

8. Hopkins C, Trowbridge IS. Internalization and processing of Tf and the Tf receptor in human carcinoma A431 cells. *J Cell Biol* 1983; 97:508–521.
9. Hopkins CR. Intracellular routing of Tf and Tf receptors in epidermoid carcinoma A431 cells. *Cell* 1983; 35:321–330.
10. Morgan EH. Studies on the mechanism of iron release from Tf. *Biochim Biophys Acta* 1979; 580:312–326.
11. Harding C, Heuser J, Stahl P. Receptor-mediated endocytosis of Tf and recycling of the Tf receptor in rat reticulocytes. *J Cell Biol* 1983; 97:329–339.
12. Paterson S, Armstrong NJ, Iacopetta BJ, McArdle HF, Morgan EH. Intravesicular pH and iron uptake by immature erythroid cells. *J Cell Physiol* 1984; 120:225–232.
13. Morgan EH. Inhibition of reticulocyte iron uptake by NH_4Cl and CH_3NH_2 . *Biochim Biophys Acta* 1981; 642:119–134.
14. Morgan EH. Effect of pH and iron content of Tf on its binding to reticulocyte receptors. *Biochim Biophys Acta* 1983; 62:498–502.
15. Tsunoo H, Sussman HH. Characterization of Tf binding and specificity of the placental Tf receptor. *Arch Biochem Biophys* 1983; 225:42–54.
16. Young SP, Aisen P. Tf receptors and the uptake and release of iron by isolated hepatocytes. *Hepatology* 1981; 1:114–119.
17. Hansen SH, Sandvig K, van Deurs B. Internalization efficiency of the Tf receptor. *Exp Cell Res* 1992; 199:19–28.
18. Iacopetta BJ, Rothenberger S, Kuhn LC. A role for the cytoplasmic domain in Tf receptor sorting and coated pit formation during endocytosis. *Cell* 1988; 54:485–489.
19. Geuze HJ, Slot JW, Strous GJAM, Lodish HF, Schwartz AL. Intracellular site of asialoglycoprotein receptor-ligand uncoupling: Double-label immunoelectron microscopy during receptor-mediated endocytosis. *Cell* 1983; 32:277–287.
20. Gruenberg J, Griffiths G, Howell KE. Characterization of the early endosome and putative endocytic carrier vesicles *in vivo* and with an assay of vesicle fusion *in vitro*. *J Cell Biol* 1989; 108:1301–1316.
21. Schmid SL. The mechanism of receptor-mediated endocytosis; more questions than answers. *Bioessays* 1992; 14:589–596.
22. Yamashiro DJ, Fluss SR, Maxfield FR. Acidification of endocytic vesicles by an ATP-dependent proton pump. *J Cell Biol* 1983; 97:929–934.
23. Yamashiro DJ, Maxfield FR. Acidification of endocytic compartments and the intracellular pathways of ligands and receptors. *J Cell Biol* 1983; 231–245.
24. Rothenberger S, Iacopetta BJ, Kuhn LC. Endocytosis of the Tf receptor requires the cytoplasmic domain but not its phosphorylation site. *Cell* 1987; 49:423–431.
25. Trowbridge IS, Collawn JF, Hopkins CR. Signal-dependent membrane protein trafficking in the endocytic pathway [review]. *Annu Rev Cell Biol* 1993; 9:129–161.
26. Jing S, Trowbridge IS. Nonacylated human Tf receptors are rapidly internalized and mediate iron uptake. *J Biol Chem* 1990; 265:11555–11559.
27. Chen WJ, Goldstein JL, Brown MS. NPXY, a sequence often found in cytoplasmic tails, is required for coated pit-mediated internalization of the low density lipoprotein receptor. *J Biol Chem* 1990; 265:3116–3123.
28. Davis CG, Elhammer A, Russell DW, Schneider WJ, Kornfeld S, Brown MS, Goldstein JL. Deletion of clustered O-linked carbohydrates does not impair function of low density lipoprotein receptor in transfected fibroblasts. *J Biol Chem* 1986; 261:2828–2838.
29. McGraw TE, Dunn KW, Maxfield FR. Phorbol ester treatment increases the exocytic rate of the Tf receptor recycling pathway independent of serine-24 phosphorylation. *J Cell Biol* 1988; 106:1061–1066.
30. Stoorvogel W, Geuze HJ, Griffith JM, Schwartz AL, Strous GJ. Relations between the intracellular pathways of the receptors for Tf, asialoglycoprotein, and mannose 6-phosphate in human hepatoma cells. *J Cell Biol* 1989; 108:2137–2148.

31. Marks MS, Woodruff L, Ohno H, Bonifacino JS. Protein targeting by tyrosine- and dileucine-based signals: Evidence for distinct saturable components. *J Cell Biol* 1996; 135:341–354.
32. Warren RA, Green FA, Enns CA. Saturation of the endocytic pathway for the Tf receptor does not affect the endocytosis of the epidermal growth factor receptor. *J Biol Chem* 1997; 272:2116–2121.
33. Warren RA, Green FA, Stenberg PE, Enns CA. Distinct saturable pathways for the endocytosis of different tyrosine motifs. *J Biol Chem* 1998; 273:17056–17063.
34. Marks MS, Ohno H, Kirchhausen T, Bonifacino JS. Protein sorting by tyrosine-based signals: Adapting to the Ys and wherefores. *Trends Cell Biol* 1997; 7:124–128.
35. Mayor S, Presley JF, Maxfield FR. Sorting of membrane components from endosomes and subsequent recycling to the cell surface occurs by a bulk flow process. *J Cell Biol* 1993; 121:1257–1269.
36. Snider MD, Rogers OC. Intracellular movement of cell surface receptors after endocytosis: Resialylation of asialo-Tf receptor in human erythroleukemia cells. *J Cell Biol* 1985; 100:826–834.
37. Neefjes JJ, Verkerk JMG, van der Marcel GA, van Boom JH, Ploegh HL. Recycling glycoproteins do not return to the cis-Golgi. *J Cell Biol* 1988; 107:79–87.
38. Robertson BJ, Park RD, Snider M. Role of vesicular traffic in the transport of surface Tf receptor to the Golgi complex in cultured human cells. *Arch Biochem Biophys* 1992; 292:190–198.
39. Stein BS, Sussman HH. Demonstration of two distinct Tf receptor recycling pathways and Tf-independent receptor internalization in K562 cells. *J Biol Chem* 1986; 261:10319–10331.
40. Fuller SD, Simons K. Tf receptor polarity and recycling accuracy in “tight” and “leaky” strains of Madin-Darby canine kidney cells. *J Cell Biol* 1986; 103:1767–1779.
41. Dargemont C, Le Bivic A, Rothenberger S, Iacopetta B, Kuhn LC. The internalization signal and the phosphorylation site of Tf receptor are distinct from the main basolateral sorting information. *EMBO J* 1993; 12:1713–1721.
42. Enns CA, Clinton EM, Reckhow CL, Root BJ, Do S-I, Cook C. Acquisition of the functional properties of the Tf receptor during its biosynthesis. *J Biol Chem* 1991; 266:13272–13277.
43. Omary MB, Trowbridge IS. Biosynthesis of the human Tf receptor in cultured cells. *J Biol Chem* 1981; 256:12888–12892.
44. Schneider C, Asser U, Sutherland DR, Greaves MF. *In vitro* biosynthesis of the human cell surface receptor for Tf. *FEBS Lett* 1983; 158:259–264.
45. Zerial M, Huylebroeck D, Garoff H. Foreign transmembrane peptides replacing the internal signal sequence of Tf receptor allow its translocation and membrane binding. *Cell* 1987; 48:147–155.
46. Zerial M, Melancon P, Schneider C, Garoff H. The transmembrane segment of the human Tf receptor functions as a signal peptide. *EMBO J* 1986; 5:1543–1550.
47. Alvarez E, Gironès N, Davis RJ. Intermolecular disulfide bonds are not required for the expression of the dimeric state and functional activity of the Tf receptor. *EMBO J* 1989; 8:2231–2240.
48. Jing S, Trowbridge IS. Identification of the intermolecular disulfide bonds of the human Tf receptor and its lipid attachment site. *EMBO J* 1987; 6:327–331.
49. Turkewitz AP, Amatruda JF, Borhani D, Harrison SC, Schwartz AL. A high yield purification of the human Tf receptor and properties of its major extracellular fragment. *J Biol Chem* 1988; 263:8318–8325.
50. Lebron JA, Bennett MJ, Vaughn DE, Chirino AJ, Snow PM, Mintier GA, Feder JN, Bjorkman PJ. Crystal structure of the hemochromatosis protein HFE and characterization of its interaction with Tf receptor. *Cell* 1998; 93:111–123.

51. Davis RJ, Johnson GL, Kelleher DJ, Anderson JK, Mole JE, Czech MP. Identification of serine 24 as the unique site on the Tf receptor phosphorylated by protein kinase C. *J Biol Chem* 1986; 261:9034–9041.
52. May WS, Sahyoun N, Jacobs S, Wolf M, Cuatrecasas P. Mechanism of phorbol diester-induced regulation of surface Tf receptor involves the action of activated protein kinase C and an intact cytoskeleton. *J Biol Chem* 1985; 260:9419–9426.
53. Davis RJ, Meisner H. Regulation of Tf receptor cycling by protein kinase C is independent of receptor phosphorylation at serine 24 in Swiss 3T3 fibroblasts. *J Biol Chem* 1987; 262:16041–16047.
54. Adam M, Rodriguez A, Turbide C, Larrick J, Meighen E, Johnstone RM. *In vitro* acylation of the Tf receptor. *J Biol Chem* 1984; 259:15460–15463.
55. Omary MB, Trowbridge IS. Covalent binding of fatty acid to the Tf receptor in cultured human cells. *J Biol Chem* 1981; 256:4715–4718.
56. Alvarez E, Gironès N, Davis RJ. Inhibition of the receptor-mediated endocytosis of diferric Tf is associated with the covalent modification of the Tf receptor with palmitic acid. *J Biol Chem* 1990; 265:16644–16655.
57. Hayes GR, Williams AM, Lucas JJ, Enns CA. Structure of human Tf receptor oligosaccharides: Conservation of site-specific processing. *Biochemistry* 1997; 36:5276–5284.
58. McClelland A, Kuhn LC, Ruddle FH. The human Tf receptor gene: Genomic organization, and the complete primary structure of the receptor deduced from a cDNA sequence. *Cell* 1984; 39:267–274.
59. Schneider C, Owen MJ, Banville D, Williams JG. Primary structure of human Tf receptor deduced from the mRNA sequence. *Nature* 1984; 311:675–678.
60. Williams AM, Enns CA. A mutated Tf receptor lacking asparagine-linked glycosylation sites shows reduced functionality and an association with binding immunoglobulin protein. *J Biol Chem* 1991; 266:17648–17654.
61. Williams AM, Enns CA. A region of the C-terminal portion of the human Tf receptor contains an asparagine-linked glycosylation site critical for receptor structure and function. *J Biol Chem* 1993; 268:12780–12786.
62. Hoe MH, Hunt RC. Loss of one asparagine-linked oligosaccharide from human Tf receptors results in specific cleavage and association with the endoplasmic reticulum. *J Biol Chem* 1992; 267:4916–4929.
63. Do S-I, Enns CA, Cummings RD. Human Tf receptor contains O-linked oligosaccharides. *J Biol Chem* 1990; 265:114–125.
64. Orberger G, Geyer R, Stirn S, Tauber R. Structure of the N-linked oligosaccharides of the human Tf receptor. *Eur J Biochem* 1992; 205:257–267.
65. Do SI, Cummings RD. Presence of O-linked oligosaccharide on a threonine residue in the human Tf receptor. *Glycobiology* 1992; 2:345–353.
66. Hayes GR, Williams A, Costello CE, Enns CA, Lucas JJ. The critical glycosylation site of human Tf receptor contains a high-mannose oligosaccharide. *Glycobiology* 1995; 5:227–232.
67. Rutledge EA, Green FA, Enns CA. Generation of the soluble Tf receptor requires cycling through an endosomal compartment. *J Biol Chem* 1994; 269:31864–31868.
68. Rutledge EA, Enns CA. Cleavage of the Tf receptor is influenced by the composition of the O-linked carbohydrate at position 104. *J Cell Physiol* 1996; 168:284–293.
69. Shih YJ, Baynes RD, Hudson BG, Flowers CH, Skikne BS, Cook JD. Serum Tf receptor is a truncated form of tissue receptor. *J Biol Chem* 1990; 265:19077–19081.
70. Aisen P, Leibman A, Zweier J. Stoichiometric and site characteristics of the binding of iron to human Tf. *J Biol Chem* 1978; 253:1930–1937.
71. Evans RW, Williams J. Studies of the binding of different iron donors to human serum Tf and isolation of iron-binding fragments from the N- and C-terminal regions of the protein. *Biochem J* 1978; 173:5442–5452.

72. Bali PK, Aisen P. Receptor-modulated iron release from Tf: Differential effects on N- and C-terminal sites. *Biochemistry* 1991; 9947–9952.
73. Bali PK, Zak O, Aizen P. A new role for the Tf receptor in the release of iron from Tf. *Biochemistry* 1991; 30:324–328.
74. Sipe DM, Murphy RF. Binding to cellular receptor results in increased iron release from Tf at mildly acidic pH. *J Biol Chem* 1991; 266:8002–8007.
75. Hunt RC, Riegler R, Davis AA. Changes in glycosylation alter the affinity of the human Tf receptor for its ligand. *J Biol Chem* 1989; 264:9643–9648.
76. Reckhow CL, Enns CA. Characterization of the Tf receptor in tunicamycin-treated A431 cells. *J Biol Chem* 1988; 263:7297–7301.
77. Ralton JE, Jackson HJ, Zanoni M, Gleeson PA. Effect of glycosylation inhibitors on the structure and function of the murine Tf receptor. *Eur J Biochem* 1989; 186:637–647.
78. Yang B, Hoe MH, Black P, Hunt RC. Role of oligosaccharides in the processing and function of human Tf receptors. *J Biol Chem* 1993; 268:7435–7441.
79. Buchegger F, Trowbridge IS, Liu L, White S, Collawn JF. Functional analysis of human/chicken Tf receptor chimeras indicates that the carboxy-terminal region is important for ligand binding. *Eur J Biochem* 1996; 235:9–17.
80. Dubljevic V, Sali A, Goding JW. A conserved RGD (Arg-Gly-Asp) motif in the Tf receptor is required for binding to Tf. *Biochemistry J* 1999; 341:11–14.
81. Williams J. The evolution of Tf. *Trends Biochem Sci* 1982; 7:394–397.
82. Williams J. The formation of iron-binding fragments of hen ovoTf by limited proteolysis. *Biochem J* 1974; 141:745–752.
83. Mason AB, Tam BM, Woodworth RC, Oliver RW, Green BN, Brandts JF, Savage KJ, Lineback JA, MacGillivray RT. Receptor recognition sites reside in both lobes of human serum Tf. *Biochem J* 1997; 326:77–85.
84. Mason A, He QY, Tam B, MacGillivray RA, Woodworth R. Mutagenesis of the aspartic acid ligands in human serum Tf: Lobe-lobe interaction and conformation as revealed by antibody, receptor-binding and iron-release studies. *Biochem J* 1998; 330:35–40.
85. De Jong G, Van Eijk HG. Functional properties of the carbohydrate moiety of human Tf. *Int J Biochem* 1989; 21:353–263.
86. Mason A, Miller M, Funk W, Banfield D, Savage K, Oliver R, Green BN. Expression of glycosylated and nonglycosylated human Tf in mammalian cells. Characterization of the recombinant proteins with comparison to three commercially available Tfs. *Biochemistry* 1993; 32:5472–5479.
87. Alcantara J, Yu RH, Schryvers AB. The region of human Tf involved in binding to bacterial Tf receptors is localized in the C-lobe. *Mol Microbiol* 1993; 8:1135–1143.
88. Feder JN, Penny DM, Irrinki A, Lee VK, Lebron JA, Watson N, Tsuchihashi Z, Sigal E, Bjorkman PJ, Schatzman RC. The hemochromatosis gene product complexes with the Tf receptor and lowers its affinity for ligand binding. *Proc Natl Acad Sci USA* 1998; 95:1472–1477.
89. Parkkila S, Waheed A, Britton RS, Bacon BR, Zhou XY, Tomatsu S, Fleming RE, Sly WS. Association of the Tf receptor in human placenta with HFE, the protein defective in hereditary hemochromatosis. *Proc Natl Acad Sci USA* 1997; 94:13198–13202.
90. Waheed A, Parkkila S, Saarnio J, Fleming RE, Zhou XY, Tomatsu S, Britton RS, Bacon BR, Sly WS. Association of HFE protein with Tf receptor in crypt enterocytes of human duodenum. *Proc Natl Acad Sci USA* 1999; 96:1579–1584.
91. Roy CN, Penny DM, Feder JN, Enns CA. The hereditary hemochromatosis protein, HFE, specifically regulates Tf-mediated iron uptake in HeLa cells. *J Biol Chem* 1999; 274:9022–9028.
92. Gross CN, Irrinki A, Feder JN, Enns CA. Co-trafficking of HFE, a nonclassical major histocompatibility complex class I protein, with the Tf receptor implies a role in intracellular iron regulation. *J Biol Chem* 1998; 273:22068–22074.

93. Salter-Cid L, Brunmark A, Li Y, Leturcq D, Peterson PA, Jackson MR, Yang Y. Tf receptor is negatively modulated by the hemochromatosis protein HFE: Implications for cellular iron homeostasis. *Proc Natl Acad Sci USA* 1999; 96:5434–5439.
94. Ikuta K, Fujimoto Y, Suzuki Y, Tanaka K, Saito H, Ohhira M, Sasaki K, Kohgo Y. Overexpression of hemochromatosis protein, HFE, alters Tf recycling process in human hepatoma cells. *Biochim Biophys Acta* 2000; 1496:221–231.
95. Corsi B, Levi S, Cozzi A, Corti A, Altimare D, Albertini A, Arosio P. Overexpression of the hereditary hemochromatosis protein, HFE, in HeLa cells induces an iron-deficient phenotype. *FEBS Lett* 1999; 460:149–152.
96. Riedel HD, Muckenthaler MU, Gehrke SG, Mohr I, Brennan K, Herrmann T, Fitscher BA, Hentze MW, Stremmel W. HFE downregulates iron uptake from Tf and induces iron-regulatory protein activity in stably transfected cells. *Blood* 1999; 94:3915–3921.
97. Ramalingam TS, West AP, Lebron JA, Nangiana JS, Hogan TS, Enns CA, Bjorkman PJ. Tf receptor binding is required for HFE to enter endosomes and regulate iron homeostasis. *Nature Cell Biol* 2000.
98. Pan B-T, Johnstone RM. Fate of the Tf receptor during maturation of sheep reticulocytes in vitro: Selective externalization of the receptor. *Cell* 1983; 33:967–977.
99. Pan BT, Johnstone R. Selective externalization of the Tf receptor by sheep reticulocytes in vitro. *J Biol Chem* 1984; 259:9776–9782.
100. Kohgo Y, Nishisato T, Kondo H, Tsushima N, Niitsu Y, Urushizaki I. Circulating Tf receptor in human serum. *Br J Haematol* 1986; 64:277–281.
101. Cook JD, Skikne MS, Baynes RD. Serum Tf receptor. *Annu Rev Med* 1993; 44:63–74.
102. Kohgo T, Niitsu Y, Nishisato T, Kato J, Kondo H, Sasaki K, Urushizaki I. Quantitation and characterization of serum Tf receptor in patients with anemias and polycythemias. *Jpn J Med* 1988; 27:54–70.
103. Singhal A, Cook JD, Skikne BS, Thomas P, Serjeant B, Serjeant G. The clinical significance of serum Tf receptor levels in sickle cell disease. *Br J Haematol* 1993; 84:301–304.
104. Johnstone RM. Maturation of reticulocytes: Formation of exosomes as a mechanism for shedding membrane proteins. *Biochem Cell Biol* 1992; 70:179–190.
105. Rutledge EA, Root BJ, Lucas JJ, Enns CA. Elimination of the O-linked glycosylation site at Thr 104 results in the generation of a soluble human Tf receptor. *Blood* 1994; 83:580–586.
106. Skikne BS, Flowers CH, Cook JD. Serum Tf receptor: A quantitative measure of tissue iron deficiency. *Blood* 1990; 75:1870–1876.
107. Ferguson BJ, Skikne BS, Simpson KM, Baynes RD, Cook JD. Serum Tf receptor distinguishes the anemia of chronic disease from iron deficiency anemia. *J Lab Clin Med* 1992; 19:385–390.
108. Enns CA, Sussman HH. Physical characterization of the Tf receptor in human placenta. *J Biol Chem* 1981; 256:9820–9823.
109. Goding JW, Harris AW. Subunit structure of cell surface proteins: Disulfide bonding in antigen receptors, Ly-2/3 antigens, and Tf receptors of murine T and B lymphocytes. *Proc Natl Acad Sci USA* 1981; 78:4530–4534.
110. Tsunoo H, Sussman HH. Placental Tf receptor. Evaluation of the presence of endogenous ligand on specific binding. *J Biol Chem* 1983; 258:4118–4122.
111. Fuchs H, Lucken U, Tauber R, Engel A, Gessner R. Structural model of phospholipid-reconstituted human Tf receptor derived by electron microscopy. *Structure* 1998; 6:1235–1243.
112. Marsh EW, Leopold PL, Jones NL, Maxfield FR. Oligomerized Tf receptors are selectively retained by a luminal sorting signal in a long-lived endocytic recycling compartment. *J Cell Biol* 1995; 129:1509–1522.

113. Weissman AM, Klausner RD, Rao K, Harford JB. Exposure of K562 cells to anti-receptor monoclonal antibody OKT9 results in rapid redistribution and enhanced degradation of the Tf receptor. *J Cell Biol* 1986; 102:951–958.
114. Lawrence CM, Ray S, Babyonyshev M, Galluser R, Borhani DW, Harrison SC. Crystal structure of the ectodomain of human Tf receptor. *Science* 1999; 286:779–782.
115. Bennett MJ, Lebron JA, Bjorkman PJ. Crystal structure of the hereditary haemochromatosis protein HFE complexed with Tf receptor. *Nature* 2000; 403:46–53.
116. Evans P, Kemp J. Exon/intron structure of the human Tf receptor gene. *Gene* 1997; 199:123–131.
117. Hentze MW, Kuhn LC. Molecular control of vertebrate iron metabolism: mRNA-based regulatory circuits operated by iron, nitric oxide, and oxidative stress. *Proc Natl Acad Sci USA* 1996; 93:8175–8182.
118. Klausner RD, Rousault TA, Harford JB. Regulating the fate of mRNA: The control of cellular iron metabolism. *Cell* 1993; 72:19–28.
119. Theil EC. Iron regulatory elements (IREs): A family of mRNA non-coding sequences. *Biochem J* 1994; 304:1–11.
120. Eisenstein RS. Iron regulatory proteins and the molecular control of mammalian iron metabolism [in process citation]. *Annu Rev Nutr* 2000; 20:627–662.
121. Gray NK, Pantopoulous K, Dandekar T, Ackrell BA, Hentze MW. Translational regulation of mammalian and *Drosophila* citric acid cycle enzymes via iron-responsive elements. *Proc Natl Acad Sci USA* 1996; 93:4925–4930.
122. Kim HY, LaVaute T, Iwai K, Klausner RD, Rouault TA. Identification of a conserved and functional iron-responsive element in the 5'-untranslated region of mammalian mitochondrial aconitase. *J Biol Chem* 1996; 271:24226–24230.
123. Gunshin H, Mackenzie B, Berger UV, Gunshin Y, Romero MF, Boron WF, Nussberger S, Gollan JL, Hediger MA. Cloning and characterization of a mammalian proton-coupled metal-ion transporter. *Nature* 1997; 388:482–488.
124. Henderson BR, Seiser C, Kuhn LC. Characterization of a second RNA-binding protein in rodents with specificity for iron-responsive elements. *J Biol Chem* 1993; 268:27327–27334.
125. Henderson BR, Kuhn LC. Differential modulation of the RNA-binding proteins IRP-1 and IRP-2 in response to iron. IRP-2 inactivation requires translation of another protein. *J Biol Chem* 1995; 270:20509–20515.
126. Iwai K, Drake SK, Wehr NB, Weissman AM, LaVaute T, Minato N, Klausner RD, Levine RL, Rouault TA. Iron-dependent oxidation, ubiquitination, and degradation of iron regulatory protein 2: Implications for degradation of oxidized proteins. *Proc Natl Acad Sci USA* 1998; 95:4924–4928.
127. Pantopoulos K, Hentze MW. Rapid responses to oxidative stress mediated by iron regulatory protein. *EMBO J* 1995; 14:2917–2924.
128. Levy JE, Jin O, Fujiwara Y, Kuo F, Andrews NC. Tf receptor is necessary for development of erythrocytes and the nervous system. *Nature Genet* 1999; 21:396–399.
129. Larrick JW, Cresswell P. Modulation of cell surface iron Tf receptors by cellular density and state of activation. *J Supramol Struct* 1979; 11:579–586.
130. Larrick JW, Cresswell P. Tf receptors on human B and T lymphoblastoid cell lines. *Biochim Biophys Acta* 1979; 583:483–490.
131. Busfield SJ, Tilbrook PA, Callus BA, Spadaccini A, Kuhn L, Klinken SP. Complex regulation of Tf receptors during erythropoietin-induced differentiation of J2E erythroid cells—Elevated transcription and mRNA stabilisation produce only a modest rise in protein content. *Eur J Biochem* 1997; 249:77–84.
132. Lok CN, Ponka P. Identification of an erythroid active element in the Tf receptor gene. *J Biol Chem* 2000; 275:24185–24190.

133. Bianchi L, Tacchini L, Cairo G. HIF-1-mediated activation of Tf receptor gene transcription by iron chelation. *Nucleic Acids Res* 1999; 27:4223–4227.
134. Kling PJ, Dragsten PR, Roberts RA, Dossantos B, Brooks DJ, Hedlund BE, Taetle R. Iron deprivation increases erythropoietin production in vitro, in normal subjects and patients with malignancy. *Br J Haematol* 1996; 95:241–248.
135. Lok CN, Ponka P. Identification of a hypoxia response element in the Tf receptor gene. *J Biol Chem* 1999; 274:24147–24152.
136. Tacchini L, Bianchi L, Bernelli-Zazzera A, Cairo G. Tf receptor induction by hypoxia. HIF-1-mediated transcriptional activation and cell-specific post-transcriptional regulation. *J Biol Chem* 1999; 274:24142–24146.
137. Ponka P, Lok CN. The Tf receptor: Role in health and disease. *Int J Biochem Cell Biol* 1999; 31:1111–1137.
138. Roberts MR, Miskimins WK, Ruddle FH. Nuclear proteins TREF1 and TREF2 bind to the transcriptional control element of the Tf receptor gene and appear to be associated as a heterodimer. *Cell Regulation* 1989; 1:151–164.
139. Roberts MR, Han Y, Fienberg A, Hunihan L, Ruddle FH. A DNA-binding activity, TRAC, specific for the TRA element of the Tf receptor gene copurifies with the Ku autoantigen. *Proc Natl Acad Sci USA* 1994; 91:6354–6358.
140. Christensen J, Cotmore SF, Tattersall P. Two new members of the emerging KDWK family of combinatorial transcription modulators bind as a heterodimer to flexibly spaced PuCGPy half-sites. *Mol Cell Biol* 1999; 19:7741–7750.
141. Kawabata H, Yang R, Hirama T, Vuong PT, Kawano S, Gombart AF, Koeffler HP. Molecular cloning of Tf receptor 2. A new member of the Tf receptor-like family. *J Biol Chem* 1999; 274:20826–20832.
142. Kawabata H, Germain RS, Vuong PT, Nakamaki T, Said JW, Koeffler HP. Tf receptor 2- α supports cell growth both in iron-chelated cultured cells and in vivo. *J Biol Chem* 2000; 274:16618–16625.
143. West AP Jr, Bennett MJ, Sellers VM, Andrews NC, Enns CA, Bjorkman PJ. Comparison of the interactions of Tf receptor and Tf receptor 2 with Tf and the hereditary hemochromatosis protein HFE. *J Biol Chem*. In press.
144. Fleming RE, Migas MC, Holden CC, Waheed A, Britton RS, Tomatsu S, Bacon BR, Sly WS. Tf receptor 2: Continued expression in mouse liver in the face of iron overload and in hereditary hemochromatosis. *Proc Natl Acad Sci USA* 2000; 97:2214–2219.
145. Camaschella C, Roetto A, Cali A, De Gobbi M, Garozzo G, Carella M, Majorano N, Totaro A, Gasparini P. The gene TFR2 is mutated in a new type of haemochromatosis mapping to 7q22. *Nature Genet* 2000; 25:13–15.

4

Molecular Aspects of Release of Iron from Transferrin

QING-YU HE and ANNE B. MASON

University of Vermont, Burlington, Vermont

I. INTRODUCTION	96
II. IRON RELEASE FROM TRANSFERRIN IN VIVO	96
III. MODULATING FACTORS AFFECTING IRON RELEASE FROM TRANSFERRIN	98
A. The Role of Receptor in Iron Release	99
B. The Role of Intralobe Interaction in Iron Release	100
C. The Role of Chelators in Iron Release	101
D. Anion Effect	103
E. pH Effect	106
IV. HUMAN SERUM TRANSFERRIN N LOBE: THE ROLE OF SPECIFIC AMINO ACID RESIDUES	107
A. Iron-Binding Ligands	109
B. Second-Shell Residues	111
C. Residues That Participate in Anion Binding	113
V. MOLECULAR MECHANISM OF IRON RELEASE FROM HUMAN TRANSFERRIN N LOBE	115
ACKNOWLEDGMENTS	116
REFERENCES	116

I. INTRODUCTION

The transferrins are a group of homologous iron-binding glycoproteins that include serum transferrin, lactoferrin (primarily from milk), ovotransferrin from egg white, and melanotransferrin from melanoma cells (see Chapter 2). Serum transferrins tightly and reversibly bind iron with a high affinity, approximate $K_d = 10^{-22}$ M (1). The specific function of serum transferrin is to sequester extracellular iron and to deliver it to cells. The function of all transferrins may be to prevent the damaging effects of free radicals, and to inhibit bacterial growth by assuring the absence of exchangeable or Fenton-active iron in bodily fluids.

A transferrin molecule consists of a single-chain polypeptide with approximately 680 amino acids and a molecular mass of 80 kDa. Crystal structures for lactoferrin (2,3), serum transferrin (4–6), and ovotransferrin (7) have confirmed that holo-transferrin is comprised of two halves, designated the N lobe and the C lobe, linked by a short peptide; each lobe contains a single iron-binding site located in a deep cleft (except melanotransferrin, which has an iron-binding site only in the N lobe (8)). The iron atom is octahedrally coordinated to four amino acid residues, Asp63, Tyr95, Tyr188, and His249, in the N lobe of human serum transferrin, and to two oxygens from the synergistic anion, carbonate (6,9) (Fig. 1). The carbonate is bound to the Arg at position 124. The transferrin structure is unusual in that the ligands of the bound metal are so widely separated in the primary sequence.

When iron is released, the two subdomains of each lobe, termed the N-1 and N-2 domains and the C-1 and C-2 domains, rotate and open approximately 60° around a hinge to convert the protein conformation from “closed” to “open” (see apo-hTF/2N in Fig. 1) (6,10). While the iron ligands play a primary role in iron binding, other residues have been identified that contribute to the stabilization of the iron-binding site. These residues (including Gly65, Glu83, Tyr85, Arg124, Lys206, Ser248, and Lys296 in hTF/2N) form a hydrogen-bonded network that has been termed the second shell (Fig. 1) (6,11,12).

Among transferrins, only serum transferrin is known to have the ability to transport iron from the blood stream to cells through receptor-mediated endocytosis. For this reason, most studies seeking insight into the detailed mechanism of iron release have been carried out using human serum transferrin. For the most part, this chapter will discuss experimental results from studies utilizing human transferrin. Brief discussions of possible mechanisms of iron release from human serum transferrin are found in three recent reviews (9,13,14). This chapter will summarize these studies, and then focus on the N lobe of human serum transferrin. A new model of iron release is presented in Section V, which is based on the recent studies of this single lobe.

The following abbreviations are used in this chapter: hTF for human serum transferrin, Fe_N -hTF and Fe_C -hTF for N- and C-terminal monoferric human transferrin, respectively, and hTF/2N for the recombinant N lobe of human transferrin.

II. IRON RELEASE FROM TRANSFERRIN IN VIVO

In the circulation, a hTF molecule undergoes about 100–200 cycles of iron binding, transport, and release during its lifetime (15), with a release time for iron from the protein to cells of 2–3 min (16). At the extracellular pH of 7.4, iron-loaded hTF

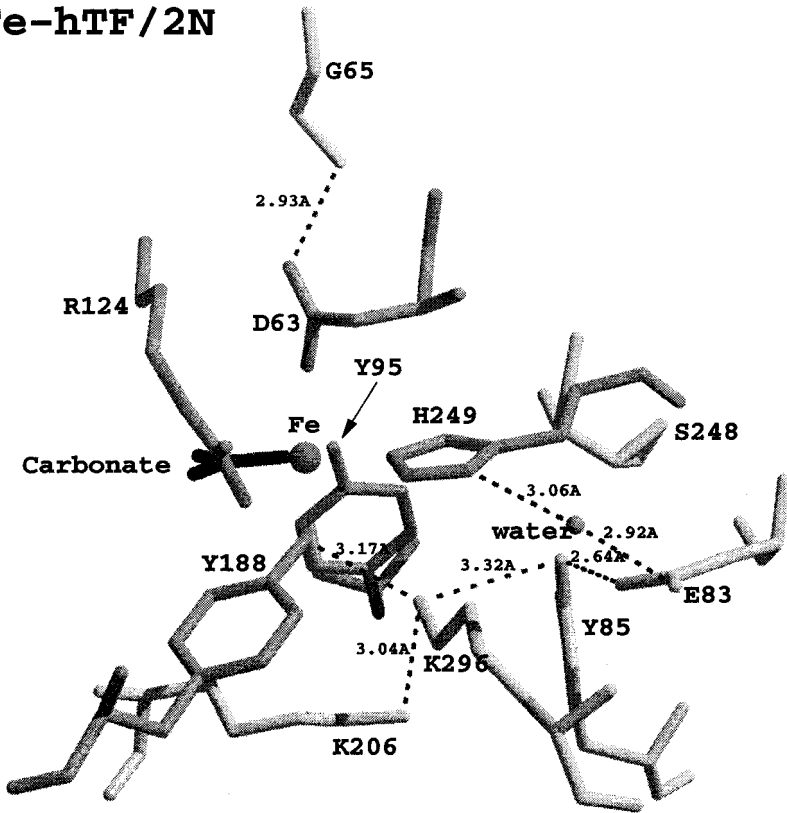
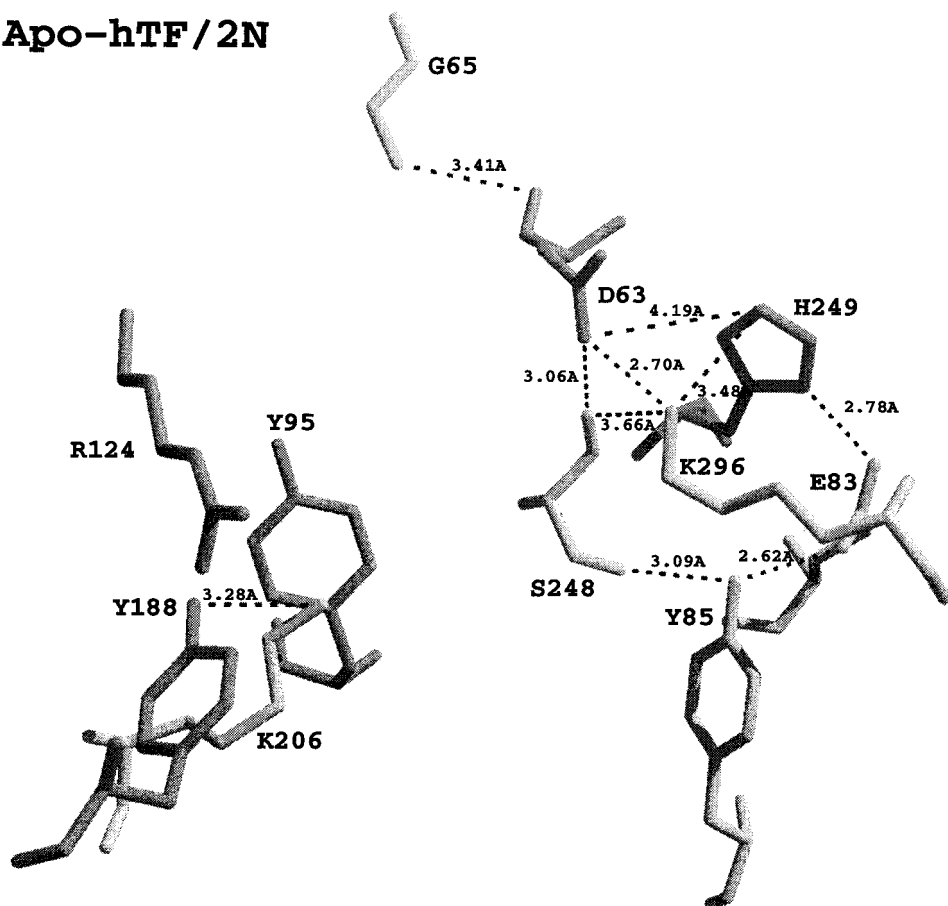
Fe-hTF/2N

Figure 1 The iron-binding site and hydrogen-bond network around the metal-binding site in the wild-type hTF/2N (1A8E & 1BP5) (6,10). The four iron-binding ligands are Asp63, Tyr95, Tyr188, and His249. Backbone atoms of residues 95–245 were used in a least-squares fit between the equivalent residues in apo-hTF/2N (1BP5). The molecules were then just translated in y to separate them. Figure was created using BOBSCRIPT and Raster3D.

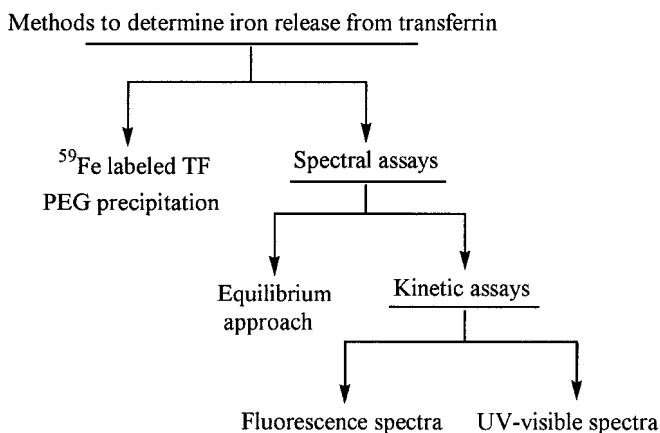
readily binds to the transferrin receptor on the cell surface and the entire complex is internalized into an endosomal vesicle (see the review in Ref 17 for more details). In the intracellular environment, an ATP-dependent proton pump produces a H^+ flow, decreasing the endosomal pH to about 5.5; this induces transferrin to assume an “open” conformation partially through protonation of critical residues within the cleft. Iron is then released for heme synthesis or storage in ferritin. The apo-transferrin still in the open conformation remains bound to the receptor and the complex is returned to the plasma membrane via a process of exocytosis (17). The apo-transferrin is released from the receptor at the surface, allowing it once again to sequester iron. The receptor binds another molecule of iron-loaded transferrin, thereby allowing the iron-transport cycle to continue. A tremendous amount of research effort has been devoted to understanding the mechanism of iron release from transferrin in the context of this pH-dependent cycle. The challenge now is to describe iron uptake and release in terms of responsible structural elements. Extensive biochemical and physical chemical analysis of a series of site-directed mutants of

Apo-hTF / 2N**Figure 1** Continued

the hTF N lobe, in combination with high-resolution crystal structures, allow us to begin to meet this challenge.

III. MODULATING FACTORS AFFECTING IRON RELEASE FROM TRANSFERRIN

In order to define the exact mechanism for iron release from transferrin, numerous in-vitro experiments have been performed over many years. As indicated in Scheme 1, different methods have been used to monitor iron release from transferrin. In one procedure, transferrin is saturated with ^{59}Fe . Following addition of a chelator, aliquots of the sample are removed at various time points and precipitated with poly(ethylene glycol) (PEG). The iron release rate is calculated by determining the amount of radiolabeled iron still associated with the protein as a function of time (18–20). The majority of iron release studies track changes in the spectral properties of the protein. When iron binds to transferrin, the intrinsic fluorescence is quenched (21,22) but the absorbance in both the ultraviolet and visible spectra increases due to energy transfer



Scheme 1 Methods to determine iron release from transferrin.

between Fe(III) and the two tyrosine ligands (23,24). Conversely, when iron is released there is an increase in fluorescence and a decrease in absorbance. A comparison of the original to the final spectral absorbance, at equilibrium, yields an estimate of the percentage of iron that is no longer associated with the transferrin (equilibrium method). By monitoring the increase in the intensity of the fluorescence or the decrease in the intensity of the absorbance in the electronic spectrum as a function of time, the kinetic rate of iron release can be determined (kinetic assay).

There is no question that iron release is complex and involves many factors that may, or may not, be independent of each other. These factors include receptor binding, lobe–lobe interaction, chelator type and concentration, pH, anion concentration, and ionic strength, as well as functional residues (9,11,12,25). It is important to emphasize that in all cases where iron is specifically bound, the actual amino acid ligands are identical. Nevertheless, substantial differences in the strength of iron binding exist both between lobes and between the various transferrins. Lactoferrin, for example, binds iron with an affinity that is considerably higher than hTF (26).

A. The Role of Receptor in Iron Release

As stated previously, iron delivery by transferrin into cells requires binding to the specific transferrin receptor. The transferrin receptor (Chapter 3) recognizes and binds an iron-saturated transferrin molecule on the cell surface and moves it into the cell to release iron. Thus the receptor serves as a “gatekeeper” in controlling iron transport from transferrin to the cells (13). At the physiological pH of 7.4, the transferrin receptor binds iron-saturated hTF with an affinity two orders of magnitude higher than iron-free hTF (27). Conversely, at the endosomal pH of 5.5, the receptor binds apo-hTF more tightly than iron-containing hTF (28). Although an accurate description of the receptor-modulated iron-delivery cycle exists, the specific details regarding the binding of transferrin to its receptor under different pH conditions remain elusive.

The transferrin receptor apparently modulates iron release from transferrin directly (29,30). As described by Aisen and co-workers, at the neutral pH of 7.4, iron

release to pyrophosphate (PP_i) from receptor-bound holo-hTF occurs at a rate only one-tenth that from free holo-hTF (18). However, at a pH of approximately 5.6, receptor-bound hTF releases iron much faster than free hTF (18). This receptor-mediated iron release also displays site selectivity. The receptor inhibits iron release from both the N and C lobes at pH 7.4; at pH 5.6, however, it has little effect on the N lobe but accelerates iron release from the C lobe (19,20). An intermediate point for the C lobe, at which the receptor has no effect on iron release, is pH 6.1 (22). The fact that this point is close to the isotropic pH ~ 6.2 for the chloride effect (see Sec. III.E) may be functionally significant.

Identifying the location of the binding site between transferrin and its receptor is critical to understanding exactly how the receptor is able to modulate iron release from transferrin. Zak et al. suggest that the primary receptor-recognition site of hTF is in the C-terminal lobe (31). Several studies with both hTF and ovotransferrin in our laboratory have provided evidence that regions in both the N and C lobes of transferrin are involved in receptor binding (32–35). In either case, identification of the exact regions involved awaits further work. Two recently published crystal structures of the ectodomain of the transferrin receptor (36,37) provide hope that a structure of the receptor–transferrin complex will soon be forthcoming and that these regions will be identified.

B. The Role of Intralobe Interaction in Iron Release

Major differences between the two iron-binding sites in regard to both metal uptake and release have been reported (14,38). Although different approaches may account for some of the discrepant results, it is generally accepted that the binding site in the N lobe of hTF binds and releases iron more easily than the C lobe; the C lobe both holds iron more tightly thermodynamically and releases iron more slowly kinetically (14). El Hage Chahine et al. suggest that, at acidic pH, removal of iron from the N lobe precedes removal of iron from the C lobe for both hTF (39) and ovotransferrin (40). Obviously, the functional difference between the two lobes must be accounted for by variation in other parts of the structure, given that the iron-binding ligands of each lobe are identical. As will be discussed in detail in Sec. III.E, a structural basis has in fact been proposed by Dewan et al. (41), who noted the presence of two lysines within hydrogen-bonding distance in the closed form of the N lobe of ovotransferrin. A similar dilysine pair exists in the N lobe of hTF (Fig. 1), but is absent in the C lobe and in both lobes of lactoferrin.

Complicating our understanding of iron release from the N and C lobes is the evidence of interaction between the two lobes. Iron release from the C lobe of transferrin is accelerated by the presence of metal in the N lobe, but the presence or absence of the metal in the C lobe has only a small influence on the iron release from the N lobe (42,43). However, these effects vary depending on which chelator is used to abstract the released iron (43). Similarly, differences have been noted in other studies. The rate of iron release from a mutant in which the Asp63 ligand was changed to a serine differed when the mutation was in the N lobe versus holo-hTF, implying an effect of the C lobe on the rate (44). An influence of one lobe on the other has also been observed in NMR studies of hTF (45), absorption spectra of ovotransferrin (46), pH-dependent iron-release studies of lactoferrin (47), and calorimetric studies of both hTF and ovotransferrin (48,49).

C. The Role of Chelators in Iron Release

Compared to the 2–3 min time frame for physiological iron release, release from holo-hTF in a self-buffered solution without any iron-chelating ligand is very slow, with a half-life greater than 3 h at pH 5.6 and even slower at pH 7.4 (13). Obviously, an iron-sequestering agent (chelator) must exist in the endosome to mediate iron removal from transferrin. Since transferrin binds Fe(III) so tightly, it has been proposed that a reduction from Fe(III) to Fe(II) prior to release might occur to help destabilize the iron binding. A number of earlier studies focused on the effect of reducing agents which were found to increase the rate of iron release (50–53).

Bates and co-workers initiated studies with iron chelators which are able to remove iron from transferrin directly. Since then, many chelators with various thermodynamic and kinetic properties have been used to sequester iron in release reactions (see Table 1). These chelators include, in the order of their iron-removal effectiveness (taking into consideration concentration and the rate of removal), synthetic and natural catecholates (54–59), PP_i (25,42,58,60–68), EDTA (69–73), other phosphonates (43,61,63,66,74,75), acetohydroxamic acid (AHA) (76,77), citrate (69,78), pyridonates (68,77), and nitrilotriacetic acid (NTA) (43,61,68,69). This order of effectiveness probably stems from a chelators' binding affinity for iron as well as its chemical configuration and charge (58,69). The size of a chelator seems unlikely to play a role, since bulky ligands such as synthetic tricatechols can remove iron from hTF as efficiently as small ligands (54,58).

In addition, as summarized in Table 1, different chelators release iron with different modes of action. In many cases, a simple saturation kinetic mode with respect to the chelator concentration has been found. Bates et al. proposed an iron release mechanism with a conformational change of the protein as the rate-limiting step (60,76). Equation (1) has been used to describe this mechanism (60,61):

$$k_{\text{obs}} = \frac{k'[\text{C}]}{1 + k''[\text{C}]} \quad (1)$$

It is assumed that even if an intermediate exists during the reaction and regardless of the chelator concentration, $[\text{C}]$, the iron release rate cannot exceed the rate of the conformational change of the transferrin molecule from the closed to the open form (56,60,76).

However, the complexity of the chelator effect on iron release from transferrin has been increasingly noted (Table 1). In particular, a study by Harris et al. using three types of chelators, phosphonates, NTA, and PP_i , demonstrated how different kinetic modes govern the same iron release reaction depending on the chelator (61). With respect to chelator concentration, phosphonic acids remove iron from hTF with a saturation mode, while NTA removes iron from hTF exclusively through a linear pathway. Interestingly, iron release from hTF by PP_i shows a combination mechanism of the saturation and linear pathways, with the saturation mode predominating at low chelator concentration and the linear mode predominating at higher chelator concentrations (61). The same dual-pathway kinetic mode was also reported by Bertini et al. for the identical protocol with PP_i as the chelator, and moreover, the two-pathway mode is true for both the N- and C-lobe sites in holo-hTF (62). Iron release studies with monoferric transferrins, designed to simplify the interpretation, have also shown

Table 1 Chelators Used for the Kinetics of Iron Release from Transferrin and the Different Kinetic Modes with Respect to the Chelator Concentration

Chelator ^a	Chelator type	Protein type	References
First-order (linear) kinetics			
EDTA	EDTA	hTF	(69)
NTA	NTA	Fe _N -hTF, Fe _C -hTF	(43)
NTA	NTA	hTF/2N, Fe _N -hTF	(61,68)
DTPA		Fe _N -hTF, Fe _C -hTF	(75)
Hyperbolic (saturation) kinetics			
EDTA	EDTA	hTF	(70,72)
EDTA	EDTA	hTF/2N	(73)
3,4-LICAMS	Catecholate	hTF	(54,56)
3,4-LICAMS, Tiron	Catecholate	hTF	(58)
Tiron	Catecholate	hTF/2N	(59)
AHA		hTF	(76)
PP _i	Phosphonate	hTF	(60)
EDTP, NTP, HEDP	Phosphonate	hTF	(74)
PP _i	Phosphonate	hTF/2N	(67)
L-Mimosine	Pyridonate	hTF	(58)
Deferiprone, 1H2P, AHA	Pyridinone	Fe _N -hTF, Fe _C -hTF	(77)
Deferiprone	Pyridinone	hTF/2N, Fe _N -hTF	(68)
Dual-pathway (saturation-linear) kinetics			
PP _i , NTP, DPG, PIDA	Phosphonate	hTF	(61)
PP _i , NTP	Phosphonate	hTF	(63)
PP _i	Phosphonate	hTF	(62)
PP _i	Phosphonate	Fe _C -hTF	(42)
PP _i	Phosphonate	Fe _N -hTF	(64)
NTP	Phosphonate	Fe _N -hTF, Fe _C -hTF	(43)
PP _i	Phosphonate	Fe _C -hTF	(65)
DTPP	Phosphonate	Fe _N -hTF, Fe _C -hTF	(75)
PP _i , phosphate	Phosphonate	Fe _C -hTF	(66)
PP _i	Phosphonate	hTF/2N	(68)
Citrate	Citrate	Fe _N -hTF, Fe _C -hTF	(78)

^aEDTA, ethylenediaminetetraacetic acid; NTA, nitrilotriacetic acid; DTPA, diethylenetriaminepentaacetic acid; 3,4-LICAMS, 1,5,10-N,N',N''-tris(5-sulfo-2,3-dihydroxybenzoyl)triazadecane; Tiron, 1,2-dihydroxybenzene-3,5-disulfonic acid; AHA, acetohydroxamic acid; PP_i, pyrophosphate; EDTP, ethylenediamine-N,N'-tetra(methylenephosphonic acid); HEDP, 1-hydroxyethane-1,1-diphosphonic acid; L-Mimosine, β-[N-(3-hydroxy-4-pyridone)]-(α-amino-propionic acid); Deferiprone, 1,2-dimethyl-3-hydroxypyridin-4-one; 1H2P, 1-hydroxypyridin-2-one; NTP, nitrilotris(methylenephosphonic acid); DPG, N,N-bis(phosphonomethyl) glycine; PIDA, N-(phosphonomethyl)iminodiacetic acid; DTPP, diethylenetriaminepenta (methylenephosphonic acid).

different kinetics with different chelators, providing further evidence for the complexity of the chelator effect (see Table 1 for details).

As shown in Table 1, in most cases, PP_i and phosphonate ligands release iron from either site of hTF through more than one pathway. This is true for the isolated recombinant half-molecule Fe-hTF/2N as well. While iron release from hTF/2N by NTA takes place with a simple linear mode (68) and Tiron (59) with a simple saturation mode, iron release from hTF/2N by PP_i follows the dual-pathway mechanism (68). A report by Zak et al. for iron release from hTF/2N by PP_i showed that the reaction occurs with a simple saturation pattern with respect to the PP_i concentration (67). This observed difference may be explained by the fact that an equimolar concentration of chloride (an effecting factor, see Sec. III.D) already existed in the PP_i stock solution, hampering the observation of a pure chelating effect (64,68).

To explain the dual-pathway mode, Harris et al. have suggested that, parallel to the saturation pathway, the linear pathway proceeds due to the substitution of the synergistic carbonate by an anionic moiety from the incoming chelator (43,75). Equation (1) has been modified to add a term that is first-order in chelator, resulting in Eq. (2) (43,61):

$$k_{\text{obs}} = \frac{k'[C]}{1 + k''[C]} + k'''[C] \quad (2)$$

According to this mechanism, synergistic-like anions such as NTA may simply replace carbonate prior to removing iron, leading to a strict linear pathway with respect to the ligand concentration ($k' = k'' = 0$). Other chelators such as synthetic catecholes cannot replace the synergistic anion and thus remove iron from transferrin through the simple saturation pathway ($k''' = 0$). The kinetics for the dual pathway of iron release by PP_i are related to the combination of PP_i binding to transferrin and formation of an unstable Fe-hTF- PP_i complex. The synergistic anion-substitution mode is supported in a study by Bailey et al. with ovotransferrin, in which an affinity-label analog of the synergistic anion is irreversibly and covalently attached to the protein (79). Results showed that a pure saturation mode with respect to chelator concentration was obtained.

D. Anion Effect

It is well established that anions bind to transferrins. There are at least two classes of anions. The first is the so-called synergistic anion, which must be bound for high-affinity iron binding to occur. As summarized in a review by Baker (9), a synergistic anion has a carboxylate group available to bind to an amino acid residue in the protein (Arg124) and an electron-donor group one or two carbon atoms away which binds to iron. The second class is the nonsynergistic anions. A nonsynergistic anion, by definition, is unable to participate in high-affinity iron binding. Anion or salt effects on iron release from transferrin have been noted for many years (38,70,71,80,81). An important finding, first reported by Kretchmar and Raymond, indicated the absolute necessity of an anion for any iron release to occur; iron release rates go to zero when the ionic strength is extrapolated to zero (57). The anion requirement for iron release has also been demonstrated in experiments with both free and receptor-bound Fe_c -hTF at pH 5.6 (22).

Anions affect iron release from transferrin in two different ways: by binding to active sites in the protein and by actually participating in iron removal. Binding of nonsynergistic anions can be observed by spectroscopic techniques such as electron paramagnetic resonance (EPR) (82–84) and difference UV spectra (85–90). Using difference UV, Harris observed that titrating an anion into apo-transferrin results in negative electronic absorbance bands, resembling in reverse the spectral change for iron binding (85). Using this titration technique, the binding strength of several different anions to apo-transferrins has been measured. The binding strength to transferrin based on the binding constants follows the order $PP_i > \text{other phosphonates} > \text{phosphate} > SO_4^{2-} > HCO_3^- > Cl^- > ClO_4^-$ (85,86,89,90).

Arginine and lysine residues have been repeatedly suggested as obvious anion-binding sites (9,85,91). Use of site-directed mutagenesis of hTF/2N has indeed confirmed that Arg124, Lys206, and Lys296 make important contributions to anion binding (see Sec. IV.C) (12,88,90). The fact that anions still have some effect on metal removal from the lysine mutants has led to the conclusion that they do not serve as anion-binding sites (67,90,92). We believe that the small negative anion effects on metal removal from the lysine mutants could be due to either the anion-binding ability of the remaining lysine residue or the existence of anion-binding site(s) other than the dilysine pair (see Sec. IV.C) (12). It has been proposed that anion binding to transferrin helps to induce conformational change and thus facilitates iron release from the protein (9,93).

An important finding, which is not always remembered, is that nonsynergistic anions themselves can remove iron from transferrin, especially at pH 5.6. Foley and Bates conducted a comprehensive study on the mobilization of iron from hTF by different inorganic anions at pH 5.5 (94). The results showed that every anion tested was able to remove iron from hTF to some extent, with the effectiveness following the order $H_2P_2O_7^- > H_2PO_4^- > SO_4^{2-} > NO_3^- > Cl^- > ClO_4^-$, approximately the same order as the anion-binding strength described above. Clearly, the properties of the anions, such as their chelation ability, charge, and geometry, play important roles in establishing both of these series. Marques et al. showed that chloride alone removes iron from Fe_C -hTF at pH 5.5 (66). The kinetic rate of removal linearly increased when the chloride concentration went from 0.04 to 1.04 M.

Removal of iron by chloride has also been demonstrated for hTF/2N in our laboratory. In a study measuring the pH stability of hTF/2N (pH profile) using an equilibrium approach, we found that iron release from hTF/2N is shifted about one pH unit higher when chloride is present at the physiological concentration of 0.14 M (95). Also, chloride itself removes iron from hTF/2N at pH 5.6 in a pseudo-single exponential mode, with the rate constants increasing from 0.052 to 0.087 min^{-1} when chloride concentration is increased from 0.05 to 0.5 M (unpublished results). Obviously, these rates for iron release by chloride are very low compared with those of “real” chelators such as PP_i and EDTA (see Table 2).

It is clear that anions can influence iron release from transferrin by chelators. Although the anion effect on iron release from transferrin has been extensively studied, different results have been reported. The discrepancies probably result from the use of different conditions and measurement techniques. In the majority of cases at neutral pH, an anion retards iron release from transferrin N lobe, but enhances iron release from the C lobe (12,22,57,59,63,68,70,71,77,82). However, Marques et al. reported that anions (except perchlorate) accelerated iron release from Fe_N -hTF by

Table 2 Rate Constants (min^{-1}) for Iron Release from Transferrin N-Lobe Fe-hTF/2N-CO₃^a

	[Tiron] = 12 mM, pH 7.4		[EDTA] = 4 mM, pH 5.6	
	[Cl ⁻] = 0	[Cl ⁻] = 50 mM ^b	[Cl ⁻] = 0	[Cl ⁻] = 50 mM
hTF/2N (WT)	0.0225	0.0205	4.99	22.6
Faster iron releasers				
D63A	314	377	5570/527	8290/618
D63E	126	160	6.36	10.6
D63N	163	188	4080/293	7320/295
D63S	153	172	3530/372	8910/384
H249A	295	499	3580	5760
H249E	0.0736	0.0680	11.5	11.9
H249Q	261	327	2320	5090
Y95F	51.1	190	476	1060
Y95H	16.3	40.3	224	438
E83A	318/37.8	715/25.4	1020/107	598/71.4
G65R	23.2/3.18	32.8/3.43	245/6.65	498/14.5
R124A	2.21	1.68	255	270
R124A(NTA)	1.81	1.30	2.01	4.32
Y85F	0.137	0.391	5.03	32.3/5.36
Slower iron releasers				
H207A	0.00971			
H207E	0.00147	7.01×10^{-4}	0.367	1.17
K206A			0.00403	
K296A			0.00410	
K206A/K296A	4.36×10^{-4}	1.36×10^{-4}	0.0248	0.0188
K206E	6.42×10^{-5}		1.61×10^{-4}	
K206Q	8.82×10^{-5}		0.0105	0.00891
K296E	1.28×10^{-4}		0.0149	0.00709
K296Q	2.04×10^{-4}		0.0375	0.0260
K206E/K296E	6.11×10^{-4}		0.0899	0.0628
S248A	0.00519	0.00333	0.436	2.38
Minor-affected mutants				
H119Q	0.0363	0.0269		
M26I	0.0243	0.00840		
M109L	0.0130	0.00450		
M256V	0.0280	0.00760		
M309I	0.0215	0.00790		
M313I	0.0286	0.00660		
W8Y	0.0998	0.0364		
W128Y	0.0625	0.0331		
W264Y	0.0236	0.0082		
Y96F	0.0270	0.0150		

^aIron release from some mutants has two rates, probably corresponding to two forms of these proteins (see text).

^bFor Y85F, [Cl⁻] = 0.14 M; for the Met and Trp mutants, [Cl⁻] = 0.50 M; for WT hTF/2N, these rates are 0.0165 and 0.0126 min^{-1} at [Cl⁻] = 0.14 and 0.50 M, respectively (59).

both PP_i and citrate (64,78), and Zak et al. showed that chloride had almost no effect on iron release from hTF/2N by PP_i at pH 7.4 (67). However, as mentioned previously, the findings in these studies are compromised by the presence of chloride in the samples. Controversial findings have also been reported for the anion effect on iron release at pH \sim 5.6. Studies by Aisen and co-workers showed that chloride accelerates iron release from Fe_C -hTF but retards the release from hTF/2N by PP_i (22,25,67). Conversely, Foley and Bates reported that chloride greatly enhanced iron removal from hTF by PP_i (94). Our recent experimental results show that both chloride and sulfate significantly accelerate iron release from hTF/2N by EDTA at pH 5.6 (12).

To account for the effect of anion binding, a model suggested by Egan et al. proposes that, in addition to the synergistic anion-binding site, at least one kinetically significant anion-binding (KISAB) site exists near the metal-binding center in each lobe and plays an important role in iron release from transferrin (22,64,65,78). According to this model, a KISAB site must be occupied by an anion such as chloride or a chelator such as PP_i before iron release can occur. Equation (3) describes the kinetic model:

$$k_{\text{obs}} = \frac{k'[C][X] + k''K[C]^2}{[X] + K[C]} \quad (3)$$

where K is an equilibrium constant for the competition between the chelator $[C]$ and the anion $[X]$ for the KISAB binding. The competition between anions and chelators for the binding to KISAB site(s) may result in a retarding anion effect at neutral pH. At the lower pH of 5.6, where the anion binding strength to the KISAB sites increases, anions may help chelators to remove iron synergistically, leading to an accelerating anion effect. This model can also be used to explain the combined saturation-linear pathway of iron release kinetics. If it is assumed that the occupation of KISAB sites results in a conformational change; this rate-determining step is accounted for by the saturation component in the kinetics. Iron release by the chelator then proceeds in a simple linear mode (22,64,65,78).

E. pH Effect

The importance of pH in affecting iron release has been well demonstrated in the iron delivery cycle in vivo: iron is sequestered at pH 7.4 and released at pH 5.6. In vitro, experimental data have demonstrated that with decreasing pH the extent and rate of iron release from transferrin increase (12,22,72,73,80,95-97). As mentioned in many of the studies described above, the pH effect on the iron release appears to have site selectivity. Studies of both hTF (72) and ovotransferrin (96) revealed that iron release from the N-terminal site is more facile at pH $<$ 8.2. Above this pH, iron release from the C site becomes faster. In the plot of $\log k_{\text{obs}}$ via pH, there is a transition point around pH 6.0, above and below which iron release occurs by different mechanisms (72). At low pH (less than 5.6), iron release from Fe_N -hTF is independent of the amount of the chelator and anion, whereas iron release from Fe_C -hTF increases with an increasing concentration of the chelator (72). Above pH 6.0, iron release from both sites has a positive correspondence to the chelator concentration (72).

It seems increasingly clear that the pH effect is closely correlated with the anion effect on iron release from transferrin. In one study, Chasteen and Williams

reported that chloride inhibited iron release from hTF at pH > 6.5 but has no effect in the pH range 6.0–6.5 (80). Our recent work further illustrates the pH-dependent iron release with the isolated hTF/2N (which eliminates possible effects from C lobe): chloride linearly enhances iron release at low pH and retards the release in a hyperbolic pattern at higher pH, with a transitional point at about pH = 6.3 (73). A more detailed determination has been carried out and shows that chloride affects iron release from hTF/2N in saturation modes with respect to the anion concentrations at both pH 7.4 and 5.6 (Fig. 2) (12). At pH 6.1, near the transitional point, as the anion concentration is increased, chloride significantly accelerates iron release, reaching a maximum point at $[Cl^-] = 0.1$ M, after which the rate slowly decreases (Fig. 2) (12).

Several explanations for the pH effect on iron release have been offered, and all focus on the pH-induced conformational change of transferrin. Obviously, the pH-related structural change must involve the protonation of various amino acid residues in the iron-binding cleft or the hinge area. As mentioned briefly, analysis of the crystal structure of hen ovotransferrin N lobe led Dewan et al. to propose that a pH-sensitive dilysine pair, made up of a lysine residue from domain NI and one from domain NII, might play a crucial role in the conformational change (41). The protonation of this dilysine pair at low pH would constitute a “driving force” to open the cleft for iron release. A similar dilysine pair, Lys206–Lys296, exists in the hTF N lobe but not in the C lobe (4,6). As shown in Fig. 1, K206 is 3.04 Å from K296 in the iron-containing N lobe, but 9 Å away in the apo-structure. The pH effect must involve other residues in addition to the two lysines. Analysis of the crystal structure of hTF/2N suggested that the histidine ligand at position 249 must be protonated for iron release to occur (10). A nuclear magnetic resonance (NMR) titration experiment by Kubal et al. predicted that certain histidine residues, in addition to His249 ligand, appear to be targets for protonation (98). In addition, the crystal structure for Fe-containing hTF/2N obtained at pH 6.1 showed that the synergistic carbonate anion exists in two positions, partially occupying both mono- and bidentate positions for iron binding (6). As a result of this observation, carbonate protonation has been proposed as a possible first step for cleft opening and iron release (6).

IV. HUMAN SERUM TRANSFERRIN N LOBE: THE ROLE OF SPECIFIC AMINO ACID RESIDUES

As mentioned previously, the technique of site-directed mutagenesis in conjunction with expression of functional protein has provided a powerful tool for investigating the intrinsic role that an individual amino acid residue plays in affecting the iron release property of transferrin. By mutating a target amino acid, the function of the side chain usually is altered or disabled. The resulting mutant often displays interesting iron-binding and release properties differing significantly from those for wild-type transferrin. To date, most mutations have been made in the N lobe of transferrin. Results have shown that recombinant hTF/2N is a good model for the N lobe of holo-hTF in terms of both iron binding and release (59,68). Compared to the wild-type hTF/2N, the single-point mutants demonstrate a wide range with respect to their rates of iron release. Table 2 contains a summary of the iron release rates for 34 single- and double-point mutants of hTF/2N determined in the absence or presence of chloride at both pH 7.4 and 5.6. It is clear that such mutations result in N lobes that release iron very much faster (faster iron releasers), substantially slower (slower iron releasers), or with rates only slightly different from those of wild-type hTF/2N

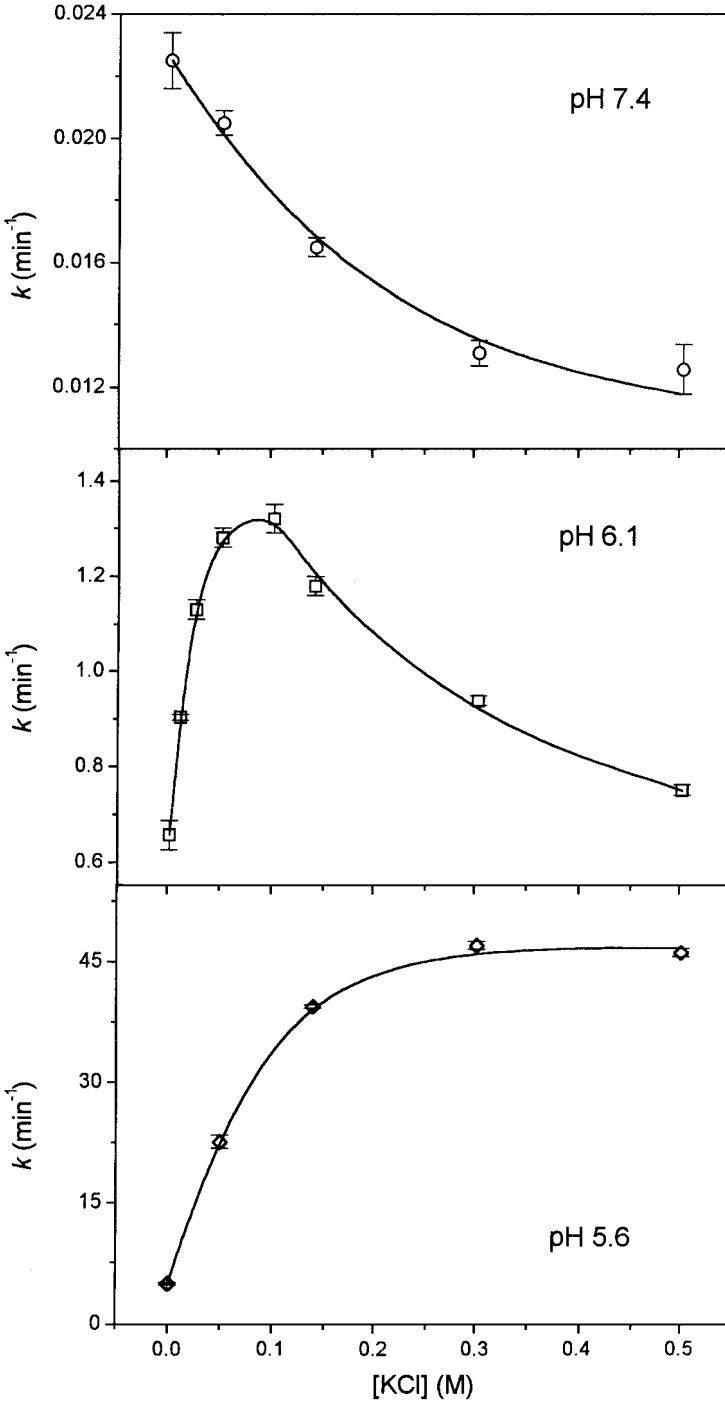


Figure 2 The chloride effect on iron release from wild-type hTF/2N at three different pH values (12). Tiron (12 mM) was the chelator for iron removal at pH 7.4 (HEPES 50 mM) and EDTA (4 mM) was the chelator at pH 6.1 and 5.6 (MES 50 mM), 25°C.

(Table 2). A graphic display of the tremendous differences in release rates is presented in Fig. 3. The 0 on the *Y* axis is the rate of release for the wild-type hTF/2N, taken as 1 under the conditions stated in each panel. The numbers given on the *Y* axis are the fold difference calculated by dividing the mutant release rate by the wild-type release rate for the positive rates or the wild-type divided by the mutant for the negative rates. In general, the effect that an individual residue exerts on iron release follows the order iron-binding ligands > second-shell residues > nonspecific function residues.

A. Iron-Binding Ligands

As might be expected, a very substantial impact on iron release results from the mutations at the iron-binding ligands, Asp63, His249, Tyr95, and Tyr188. Ligand Asp63 is from domain I, Tyr188 is from domain II, while ligands His249 and Tyr95 are from the hinge strands (6). Iron release from the D63, H249, and Y95 mutants occurs with rates four or five orders of magnitude higher than that of wild-type hTF/2N (Table 2 and Fig. 3). All ligand mutants feature a preference for the synergistic anion substitute, NTA, which has three potential ligands for iron, versus two for carbonate (59,99,100). These results imply the necessity of a full complement of ligands for stable iron binding and illustrate the flexibility in the binding cleft. In particular, the Y188F mutant is unable to bind iron in the presence of carbonate (99), suggesting that the Tyr188 ligand is absolutely critical. It is possible that iron binding to Tyr188 is the first step for iron uptake and the last step for iron release. A crystal structure for a domain II fragment of ovotransferrin showed that iron can be stably held by the two tyrosine ligands in the absence of the other two ligands (101). An alternative structure of the iron-loaded ovotransferrin N lobe also revealed that iron, in a complex with NTA, is bound by the two tyrosine ligands even when the cleft is wide open (102).

Asp63, the only ligand from domain I, was proposed to be the residue which triggered cleft opening (103). X-ray solution scattering data suggested that the D63S mutant has some degree of conformational opening (103). However, the crystal structure of the D60S mutant of lactoferrin actually showed a more closed conformation (104). Although hTF and lactoferrin differ substantially in the strength of iron binding, making comparisons uncertain, it seems logical that the absence of the aspartate ligand would make the cleft more flexible. Cell-binding studies with the D63S mutation in hTF clearly show that the cleft is open (44). The closed conformational structure may be a snapshot of the D60S mutant, and the half-open conformation may be the “sum” view of the “sampling” structure of the D63S mutant in solution. This flexibility appears to be the reason that iron release from the D63 mutants has two rates at pH 5.6, where the increasing anion-binding ability of the protein attracts the chelator EDTA. We hypothesize that the chelator EDTA enters the flexible cleft and binds to iron to form an intermediate; the disassociation of the intermediate gives rise to the second rate. In fact, an intermediate species has been identified in the anion-exchange reaction between the NTA and carbonate complexes of the mutant (59), suggesting that forming an intermediate with EDTA is also possible. The D63E mutant differs from the others; it seems likely that Glu63 may bind iron directly, resulting in a single rate of release which is similar to that for wild-type hTF/2N at pH 5.6. Crystal structures of these complexes are needed to verify these hypotheses.

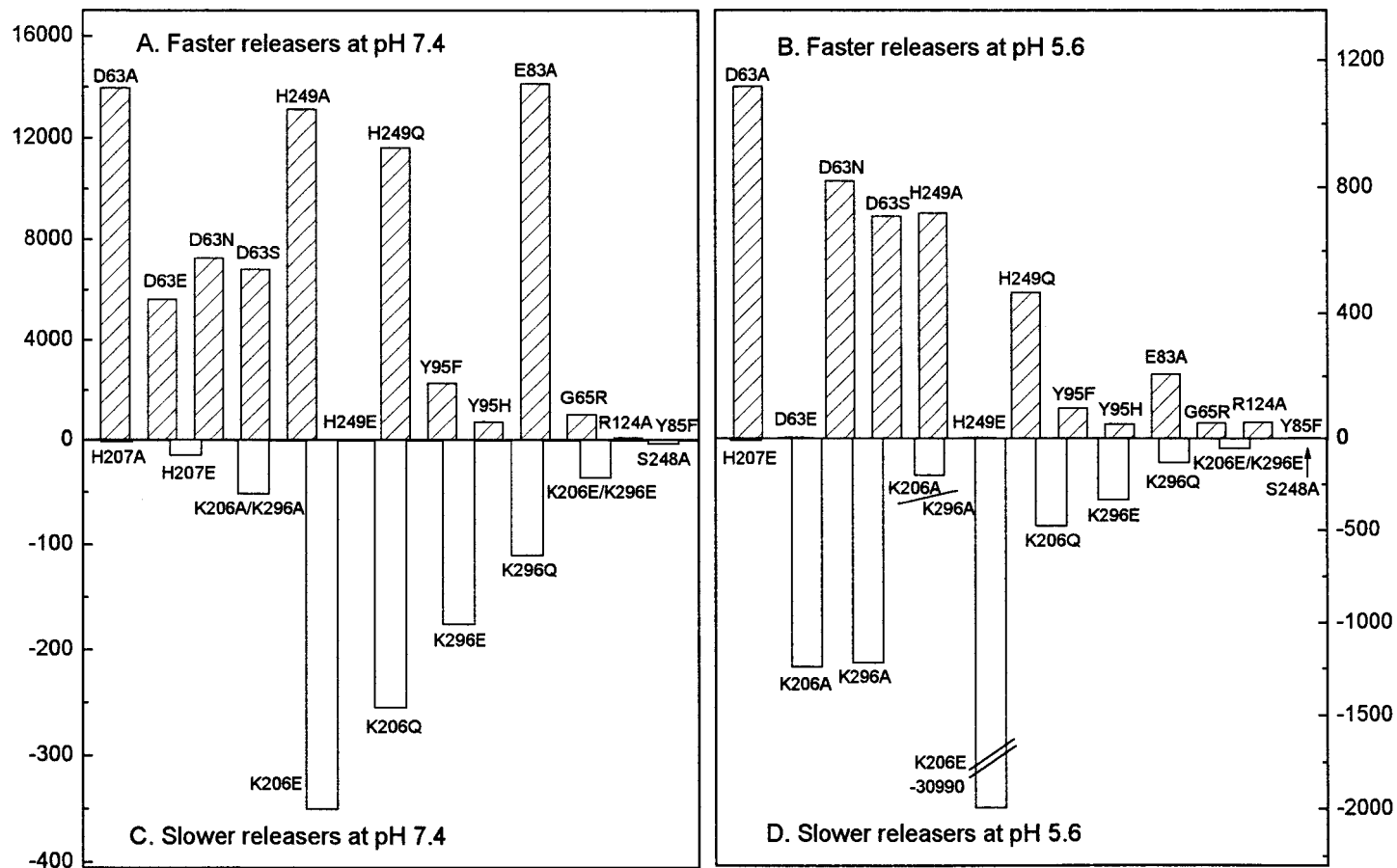


Figure 3 Fold difference of iron release rates for faster-releasing mutants (positive) and slower-releasing mutants (negative) in the absence of chloride (Table 2); the rate of iron release from wild-type hTF/2N is normalized to one. In mutants for which two rates were found, only the higher rate is shown.

Mutating the two hinge ligands, Tyr95 and His249, also dramatically impairs the iron binding ability of, and facilitates iron release from, the resulting mutants (99,100). It is apparent that, for the most part, mutation of His249 has a greater effect on iron release than mutation of Tyr95. Interestingly, the Y95H mutant releases iron very quickly, roughly similar to the Y95F mutant in which the Tyr95 ligand is disabled (Table 2 and unpublished results). It is therefore probable that His95 in the Y95H mutant does not act as a ligand for iron, perhaps due to unsuitable geometry. This finding conflicts with a previous report for the Y95H mutant (67), which showed little difference in the iron release rate relative to wild-type hTF/2N. Grossman et al. (105) suggest that the mutation of tyrosine-95 to histidine changes the geometry of the iron site such that the aspartic acid at position 63 is unable to bind to the iron. This idea would also account for the weak binding observed in this mutant.

When His249 is mutated to either an alanine or a glutamine, the effect on the rate of iron release is substantial (Fig. 3). In contrast, mutating His249 to a glutamic acid results in a small effect on iron release; the rate is only three times higher than that for the parent protein. As revealed by the crystal structure, Glu249 binds to the iron, but unexpectedly, the dilysine trigger in the mutant is completely disrupted by the interaction between Glu249 and Lys296 (95). The iron-binding and release behaviors of the H249E mutant are therefore the sum of these two opposite effects: the glutamic acid being a less stable ligand versus the stabilizing effect of disrupting the dilysine trigger.

It should be pointed out that chloride accelerates iron release from all the mutants in which a ligand is changed (except H249E) at both pH 5.6 and 7.4. This is in contrast to the wild-type protein, in which chloride enhances iron release at pH 5.6 but retards the reaction at pH 7.4 (Table 2). This suggests that mutations of the binding ligands cause labile iron binding or a “loose” conformation even at pH 7.4, and therefore chloride can enter the cleft to help remove iron.

B. Second-Shell Residues

As mentioned above, second-shell residues are those residues that form a hydrogen-bond network around the iron-binding center (see Fig. 1). We have examined mutants in which each of the second-shell residues has been changed to a different amino acid and found that the “native” residues exert profound effects on iron binding and release of transferrin. These mutants can be divided into two groups compared to wild-type hTF/2N: one group has faster iron release rates and includes the E83A, G65R, R124A, and Y85F mutants; the other group has slower iron release and includes the H207A, H207E, S248A, and all the K206 and K296 mutants (see Table 2 and Fig. 3).

Arg124 is the anchor for the synergistic carbonate binding. The fact that the R124A mutant features labile iron binding can be understood because the scaffolding support for the synergistic anion from Arg124 is eliminated. Interestingly, the favored Fe–R124A–NTA complex of the mutant is more acid-resistant; iron release at pH 5.6 from the mutant protein is slower than that from its parent protein. This suggests that the Arg124 residue, although important, is not crucial for stable iron binding in the presence of NTA. In the iron-containing but domain-open ovotransferrin N lobe, iron binding with NTA in the protein also showed no clear interaction between the NTA and the Arg124 anion-binding site (102). Also, all the Arg124 mutants generated

to date, including R124A, R124E, R124K, and R124S of hTF/2N, and R121E and R121S of lactoferrin N lobe, are able to bind iron with carbonate as the synergistic anion, although the binding is weak (67,68,106). A recent study showed that iron release from the R124A mutant by deferiprone follows simple linear kinetics with respect to the chelator concentration (68). This provides supporting evidence for the parallel linear model proposed by Harris, because without Arg124 the carbonate would be efficiently displaced by the chelator in a first-order process (68).

Glu83 is an important second-shell residue; it links to Tyr85 at one end and to His249 at the other end (Fig. 1) (6,10,11). It appears that Glu83 holds ligand His249 in a proper position for iron binding. Without it, the His249 moves away, leading to fast iron release from the mutant (11). Interestingly, we found that different monovalent anions were able to bind and restore the normal iron binding as revealed by EPR and electronic spectra (11), thereby slowing iron release to some extent. Logically, because of the connection to Glu83, mutating Tyr85 also destabilizes iron binding, although the effect is not as large as that for other second-shell residues (11).

Another mutant in this category, G65R, was made to mimic the natural mutation occurring at the equivalent position in the C lobe (107,108). Gly65 connects to ligand Asp63 in both apo- and iron-loaded hTF/2N (Fig. 1) (6,10). Mutating Gly65 to the large positively charged Arg65 disturbs the iron-binding sphere by its effect on the Asp63 ligand, resulting in much faster iron release (Fig. 3). The G65R mutant has two forms, a yellow form and a pink form, distinguishable by eye and by their visible electronic spectra (unpublished data). A modeling study by Evans et al. suggested that Asp63 should bind to the iron center but that the G65R mutant may have a partially open conformation due to the steric hindrance from the large Arg65 residue (109). This model probably only describes the pink form. The yellow form of the G65R mutant appears to have only three functional amino acid ligands given its UV-vis and EPR spectral similarity to the other known mutants including D63A, Y95F, and H249A, in which one of the ligands is disabled. The two forms account for the two different rates of iron release from the G65R mutant (Table 2). The two rates measured for iron release from the E83A mutant might also be explained due to the His249 ligand swinging between two conformations.

The slower iron releasers are the mutants (except S248A) with mutations directly or indirectly interrupting the dilysine pair, K206-K296 (Table 2). Mutating each or both lysines to Ala, Glu, or Gln dramatically increases the kinetic stability of the mutants (12,68,92). These observations directly confirm that the dilysine pair plays an important role in conformational opening, because changing them eliminates or decreases the driving force to open the cleft for iron release. Mutating Lys206 seems to have a bigger effect than mutating Lys296. Especially for the K206E mutant, the introduced negative residue Glu206 appears to form a locklike interaction by direct salt bonding to the Lys296, leading to extremely slow iron release, especially at pH 5.6 (Fig. 3) (12).

In addition, the slower iron release from mutants H207A and H207E is best explained by the effect of this neighboring residue on the dilysine trigger. This indirect effect would be expected to be weaker than the direct mutations at the Lys206 and Lys296. Ser248 has no direct connection to the dilysine pair. However, changing this residue to Ala unexpectedly slows down the iron release from the S248A mutant. Ser248 is located in the hinge area and is one of the pivots for cleft opening; a major movement of the Ser248-containing strand is evident between the

open and closed forms of hTF/2N (10). It is therefore possible that mutating Ser248 interrupts the hinge region and restricts the domain rotation, leading to slower iron release.

Mutation-induced effects on iron release behavior of transferrin have also been found by mutating even seemingly functionally “inert” side chains (see Table 2). It may be noteworthy that all of the Met mutants, especially in the apo form, show poor solubility in solutions that lack anions. This behavior implies a general effect of anion binding to surface residues (110).

C. Residues That Participate in Anion Binding

Mutations of functional residues also change the anion-binding ability of the mutant proteins, which accounts in part for their iron release behaviors. Binding constants (K) and maximum absorptivities ($\Delta\varepsilon_{\max}$) for binding of sulfate to apo-hTF/2N and 19 mutants are presented in Table 3. The data was obtained using the difference UV spectral titration technique developed by W. R. Harris. What is immediately obvious is that the ability to bind sulfate is completely eliminated for the mutants in which Lys296 is either mutated to a different amino acid or engaged in a bond to another amino acid. Much reduced sulfate-binding ability is found for the mutants K206A, K206Q, Y188F, and R124A (Table 3). These results indicate that Lys296 is critical

Table 3 Sulfate Binding to apo Wild-Type and Mutant hTF/2N Proteins

Protein	$\Delta\varepsilon_{\max}$ ($M^{-1} \text{ cm}^{-1}$)	K ($1/K_d$) (M^{-1})
hTF/2N (WT)	5,170	5,840
K206A	7,750	570
K296A		0
K206A/K296A		0
K206E		0
K296E		0
K296Q		0
K206Q	2,035	1,670
Y85F	6,265	8,835
Y95F	3,145	7,855
Y96F	5,370	5,815
Y188F	1,670	1,625
H249A	5,329	4,550
H249E		0
H249Q	3,910	2,355
D63A	1,530	14,715
E83A	3,070	9,220
G65R	5,510	10,440
R124A	4,870	425
S248A	5,230	4,505

Conditions: HEPES (50 mM), pH 7.4, 25°C, [Protein] \approx 13 μ M. The calculation of the binding constants was carried out using the equation, $\Delta\varepsilon_{\text{cat}} = \Delta\varepsilon_{\max} \times [X]/(K_d + [X])$, where X is sulfate anion.

for anion binding and that residues, Lys206, Tyr188, and Arg124 are also involved in some way in this binding (12,90,100). For the mutant H249E, the crystal structure shows that Lys296 is bound to Glu249, which concurrently binds the iron center (95). In addition, apo-K206E does not show any specific anion binding (12). We believe that the negatively charged glutamic acid binds to the positively charged lysine-296 to “lock” the protein in the closed conformation even in the absence of iron. A careful examination of the apo and iron structures shown in Fig. 1 reveals that only if the two domains of the apo protein come together could Glu206 have contact with Lys296. The two lysine ϵ -amino groups are 9 Å apart in the open conformation and 3.1 Å apart in the closed form (6,10). The logical explanation for our findings is that the two domains in the apo protein are sampling open and closed conformations (12).

Based on these findings and crystal structural data, we propose that there is a combination anion-binding site in which Lys296 and Tyr188 make up the binding core, with Lys296 as a primary binding residue and Tyr188 as a major reporting residue of spectral change (Fig. 4) (12). It appears that the spectral change occurring when an anion binds to apo-hTF/2N originates from the direct or indirect interaction with the liganding tyrosine residues, Tyr95 and Tyr188, and explains why no spectral absorbance is observed when anion is added to Fe-transferrin in which these tyrosine ligands are already bound to iron (12). It is important to mention that anion binding to the iron protein has been indirectly observed by changes in the EPR spectra (84).

As a result of the reduced anion-binding ability, iron release from the R124A, H249E, and Lys mutants shows unusual chloride effects (Table 2). Chloride exerts a retarding effect on iron release from mutants R124A and H249E at pH 7.4, opposite to the trend of the positive chloride effect for all other faster iron releasers. Chloride also has a negative effect on iron release from the Lys mutants and a very slight positive effect for the R124A and H249E mutants, totally different from the significantly positive effect found in all other cases at pH 5.6. These different behaviors are closely related to the anion-binding properties of the proteins. As shown in Fig. 5, the anion-binding ability of wild-type hTF/2N is considerably strengthened with

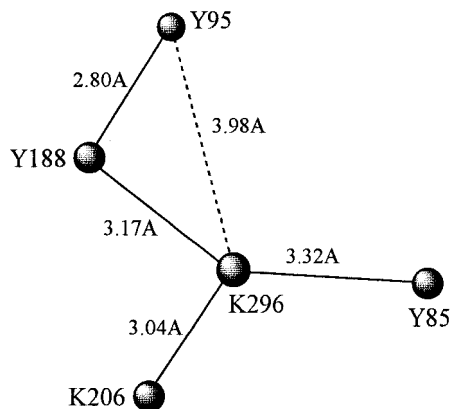


Figure 4 A schematic representation of the di-lysine anion-binding site. The distances between the residues were taken from their positions in the iron-loaded hTF/2N protein (6). In apo-hTF/2N, only Lys206 and Tyr188 are hydrogen-bonded to each other.

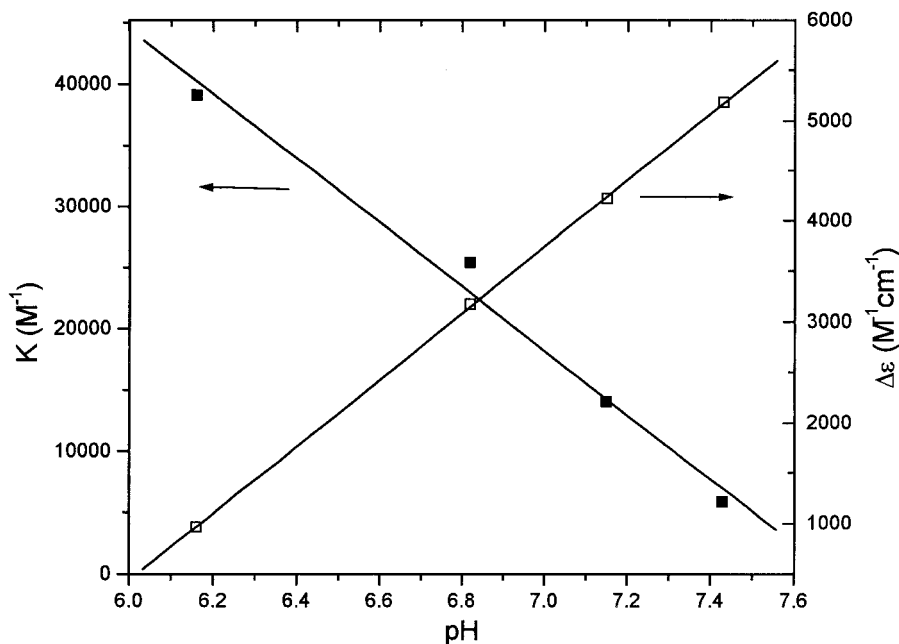


Figure 5 Linear dependence of sulfate-binding constant (K) and maximum absorptivity ($\Delta\epsilon$) of apo-hTF/2N on pH values (unpublished data).

decreasing pH (88) (unpublished data). Presumably, the increased anion-binding ability removes the competition between chloride and the chelator for the binding site(s), and chloride helps the chelator to remove iron from the labile cleft at low pH. However, because the important anion-binding residues, Arg124 and Lys296, are mutated or disrupted, the anion-binding ability of the R124A, H249E, and the Lys mutants would be sharply reduced even at low pH, leading to a negative or very small positive chloride effect on iron release.

V. MOLECULAR MECHANISM OF IRON RELEASE FROM HUMAN TRANSFERRIN N LOBE

As described above, several models have been proposed to interpret the mechanism for the iron release from transferrin. The three major tenets of these models are the following. (a) Conformational change is the rate-determining step which leads to saturation kinetics with respect to the chelator concentration. (b) A parallel linear pathway is accounted for by the replacement of the synergistic anion by the incoming chelator. (c) At least one KISAB site exists in each lobe and serves as a target for the binding of an anion or chelator. In addition, studies by El Hage Chahine and co-workers with both hTF and ovotransferrin in very acidic media (pH 3–6) suggest that iron release from transferrin involves slow proton exchange, possibly associated with the synergistic carbonate anion and/or an iron-binding ligand (39,40,111). This echoes the suggestion that the histidine ligand is protonated at low pH to destabilize

iron binding (10), and that carbonate and the lysine pair must also undergo protonation prior to iron release.

Although these models take into account most observations made for the kinetics of iron release, problems still remain. For example, the synergistic anion substitution model does not explain the anion effect or the complete loss of either the saturation or the linear component in the iron release kinetics. On the other hand, the linear portion predicted according to the KISAB mechanism does not appear for some iron release reactions, even when higher chelator concentrations are used. Part of the difficulty in defining the mechanism of iron release derives from the fact that the large conformational change which definitely occurs when the cleft opens is difficult to describe in mathematical terms.

Here, we present a model combining the essential points mentioned above and incorporating many recent observations. This model features the idea that the transferrin molecule is constantly “breathing” or sampling the open and closed conformations. As shown schematically in Fig. 6, we believe that the two domains making up the cleft of each lobe are in motion all the time, with the flexible domain I continually sampling open and closed structures. At neutral pH, the sampling is slow and the protein on average has a more closed conformation; with decreasing pH, some residues including binding ligands are protonated, leading to an increase in the sampling and favoring the open conformation. This breathing structure enables an anion or chelator or both to enter the cleft regardless of the pH. Entering is more difficult and restricted for the largely closed conformer at higher pH and easier in the largely open conformer at lower pH. Depending on its properties, the incoming

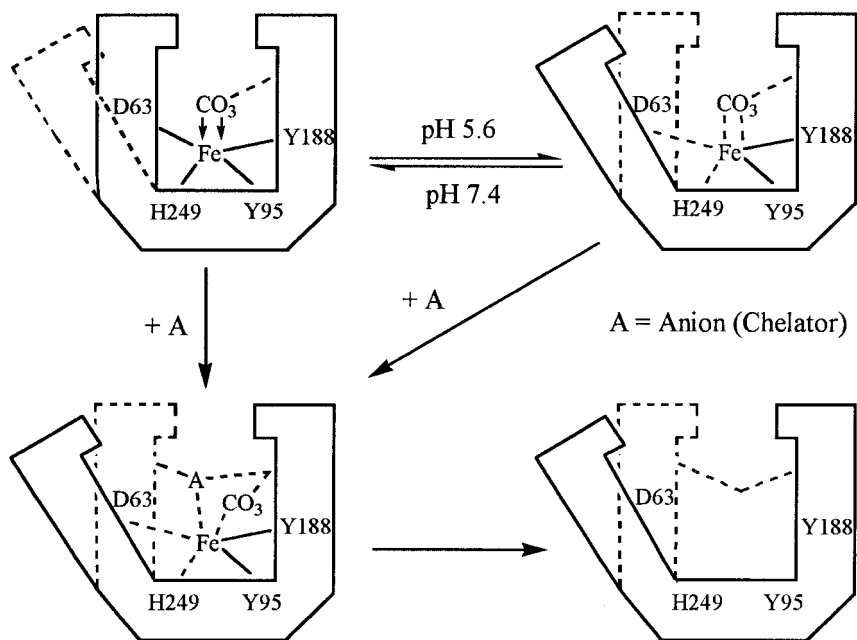


Figure 6 A “breathing” model for iron release from transferrin N lobe (see text for further explanation).

anion (chelator) may replace the synergistic anion, carbonate, or bind to KISAB site(s) and/or the iron center to form an intermediate. For those nonsynergistic inorganic anions such as chloride, the binding probably occurs at the KISAB site(s), resulting in a binding competition with the chelator at $\text{pH} > 6.3$ but helping to maintain the cleft in a more open conformation at $\text{pH} < 6.3$, where the protein has an increased anion-binding ability. With the two tyrosine ligands as the last iron-binding anchors, iron is eventually released as iron–chelator complexes or even hydro–iron–anion complexes, especially at low pH . The observed kinetic pathway varies depending on the nature of the chelators and anions in the cleft and depending on whether an intermediate species needs to be decomposed. And finally, the resulting apo protein is still sampling open and closed states, although on average the open form predominates; the two domains remain in communication at least through the dilysine pair for hTF/2N.

The breathing concept appears consistent with numerous experimental observations described throughout the text. Further support comes from an analysis of lactoferrin in which it was shown that the open and closed states of unliganded lactoferrin are similar in energy, implying a dynamic equilibrium between the two conformers in solution (112). The suggested breathing mechanism is a refinement of the conformational-change idea put forward by Bates et al. However, in our breathing model there is no gating conformational change in the iron release process, but saturation kinetics still exist in situations where the breathing is slower than iron release. A recent X-ray scattering study proposes the existence of an intermediate conformation between fully opened and fully closed. It is claimed that two separate events led to full closure: twisting around the hinge and bending at the hinge. The intermediate form was identified in two N-lobe mutants, D63S and Y95H, which apparently undergo the twist but are unable to bend (105). These ideas are compatible with the breathing model proposed.

We believe that there are no *nonchelating* anions, because a chelator is also an anion in nature and any anion can remove iron at low pH . An anion can synergistically and significantly help a chelator to remove iron from a more open conformer at low pH or from a loose conformer caused by mutating a critical iron-binding ligand. Our model also explains the reason why iron can be released from a *closed* conformation at $\text{pH} 7.4$, since even occasional breathing could be enough to allow a chelator to enter the cleft. The strength of the chelator would then dictate its effectiveness in removing iron. In addition, the domain sampling should be enhanced by increasing temperature, leading to fast iron release. This is supported by a temperature-dependence iron release study in which a positive proportion relationship between rate and temperature was found (57). We reiterate that this model may not explain the iron release process from the transferrin C lobe. Clearly, the reason for the difference between the two lobes lies within their structures. As our studies begin to focus on the C lobe of transferrin, increasing functional and structural information should help to understand the differences that exist. Additional crystal structures of the various N-lobe mutants are needed to validate the model.

ACKNOWLEDGMENTS

Support for this work was provided by U.S. Public Health Service Grant R01 DK 21739 from the National Institute of Diabetes and Digestive and Kidney Diseases.

We are indebted to R. C Woodworth for providing valuable suggestions with regard to the experimental design and research. We thank S. J. Everse for preparing Fig. 1 and for helpful comments in preparation of this chapter.

REFERENCES

1. Aisen P, Leibman A, Zweier J. Stoichiometric and site characteristics of the binding of iron to human transferrin. *J Biol Chem* 1978; 253:1930–1937.
2. Anderson BF, Baker HM, Dodson EJ, Norris GE, Rumball SV, Waters JM, Baker EN. Structure of human lactoferrin at 3.2 Å resolution. *Proc Natl Acad Sci USA* 1987; 84: 1769–1773.
3. Anderson BF, Baker HM, Norris GE, Rice DW, Baker EN. Structure of human lactoferrin: Crystallographic structure analysis and refinement at 2.8 Å resolution. *J Mol Biol* 1989; 209:711–734.
4. Zuccola HJ. The crystal structure of monoferric human serum transferrin. Ph.D. thesis, Georgia Institute of Technology, Atlanta, GA, 1993.
5. Bailey S, Evans RW, Garratt RC, Gorinsky B, Hasnain SS, Horsburgh C, Jhoti H, Lindley PF, Mydin A, Sarra R, Watson JL. Molecular structure of serum transferrin at 3.3-Å resolution. *Biochemistry* 1988; 27:5804–5812.
6. MacGillivray RTA, Moore SA, Chen J, Anderson BF, Baker H, Luo YG, Bewley M, Smith CA, Murphy ME, Wang Y, Mason AB, Woodworth RC, Brayer GD, Baker EN. Two high-resolution crystal structures of the recombinant N-lobe of human transferrin reveal a structural change implicated in iron release. *Biochemistry* 1998; 37:7919–7928.
7. Kurokawa H, Mikami B, Hirose M. Crystal structure of diferric hen ovotransferrin at 2.4 Å resolution. *J Mol Biol* 1995; 254:196–207.
8. Baker EN, Baker HM, Smith CA, Stebbins MR, Kahn M, Hellström KE, Hellström I. Human melanotransferrin (p97) has only one functional iron-binding site. *FEBS Lett* 1992; 298:215–218.
9. Baker EN. Structure and reactivity of transferrins. *Adv Inorg Chem* 1994; 41:389–463.
10. Jeffrey PD, Bewley MC, MacGillivray RTA, Mason AB, Woodworth RC, Baker EN. Ligand-induced conformational change in transferrins: Crystal structure of the open form of the N-terminal half-molecule of human transferrin. *Biochemistry* 1998; 37: 13978–13986.
11. He Q-Y, Mason AB, Woodworth RC, Tam BM, MacGillivray RTA, Grady JK, Chasteen ND. Mutations at nonliganding residues Tyr-85 and Glu-83 in the N-lobe of human serum transferrin—Functional second shell effects. *J Biol Chem* 1998; 273:17018–17024.
12. He Q-Y, Mason AB, Tam BM, MacGillivray RTA, Woodworth RC. Dual role of Lys206-Lys296 interaction in human transferrin N-lobe: Iron-release trigger and anion-binding site. *Biochemistry* 1999; 38:9704–9711.
13. Aisen P. Transferrin, the transferrin receptor, and the uptake of iron by cells. In: Sigel A, Sigel H, eds. *Iron Transport and Storage in Microorganisms, Plants and Animals*. New York: Marcel Dekker, 1998:585–631.
14. Evans RW, Crawley JB, Joannou CL, Sharma ND. Iron Proteins. In: Bullen JJ, Griffiths E, eds. *Iron and Infection: Molecular, Physiological and Clinical Aspects*. 2d ed. Chichester, UK: Wiley, 1999:27–86.
15. Jandl JH, Katz JH. The plasma-to-cell cycle of transferrin. *J Clin Invest* 1963; 42:314–346.
16. Aisen P, Leibman A. The role of the anion-binding site of transferrin in its interaction with the reticulocyte. *Biochim Biophys Acta* 1973; 304:797–804.

17. Wessling-Resnick M. Biochemistry of iron uptake. *Crit Rev Biochem Mol Biol* 1999; 34:285–314.
18. Bali PK, Zak O, Aisen P. A new role for the transferrin receptor in the release of iron from transferrin. *Biochemistry* 1991; 30:324–328.
19. Bali PK, Aisen P. Receptor-modulated iron release from transferrin: Differential effects on N- and C-terminal sites. *Biochemistry* 1991; 30:9947–9952.
20. Bali PK, Aisen P. Receptor-induced switch in site-site cooperativity during iron release by transferrin. *Biochemistry* 1992; 31:3963–3967.
21. Lehrer SS. Fluorescence and absorption studies of the binding of copper and iron to transferrin. *J Biol Chem* 1969; 244:3613–3617.
22. Egan TJ, Zak O, Aisen P. The anion requirement for iron release from transferrin is preserved in the receptor-transferrin complex. *Biochemistry* 1993; 32:8162–8167.
23. Gaber BP, Miskowski V, Spiro TG. Resonance Raman scattering from iron(III) and copper(II) transferrin and an iron(III) model compound. A spectroscopic interpretation of the transferrin binding site. *J Am Chem Soc* 1974; 96:6868–6873.
24. Patch MG, Carrano CJ. The origin of the visible absorption in metal transferrins. *Inorg Chim Acta* 1981; 56:L71–L73.
25. Zak O, Tam B, MacGillivray RTA, Aisen P. A kinetically active site in the C-lobe of human transferrin. *Biochemistry* 1997; 36:11036–11043.
26. Aisen P, Leibman A. Lactoferrin and transferrin: A comparative study. *Biochim Biophys Acta* 1972; 257:314–323.
27. Young SP, Bomford A, Williams R. The effect of the iron saturation of transferrin on its binding and uptake by rabbit reticulocytes. *Biochem J* 1984; 219:505–510.
28. Dautry-Varsat A, Ciechanover A, Lodish HF. pH and the recycling of transferrin during receptor-mediated endocytosis. *Proc Natl Acad Sci USA* 1983; 80:2258–2262.
29. Aisen P. Entry of iron into cells: A new role for the transferrin receptor in modulating iron release from transferrin. *Ann Neurol* 1992; 32(suppl):S62–S68.
30. Aisen P. The transferrin receptor and the release of iron from transferrin. *Adv Exp Med Biol* 1994; 356:31–40.
31. Zak O, Trinder D, Aisen P. Primary receptor-recognition site of human transferrin is in the C-terminal lobe. *J Biol Chem* 1994; 269:7110–7114.
32. Brown-Mason A, Woodworth RC. Physiological levels of binding and iron donation by complementary half-molecules of ovotransferrin to transferrin receptors on chick reticulocytes. *J Biol Chem* 1984; 259:1866–1873.
33. Mason AB, Brown SA, Butcher ND, Woodworth RC. Reversible association of half-molecules of ovotransferrin in solution: Basis of cooperative binding to reticulocytes. *Biochem J* 1987; 245:103–109.
34. Mason AB, Woodworth RC, Oliver RWA, Green BN, Lin L-N, Brandts JF, Savage KJ, Tam BM, MacGillivray RTA. Association of the two lobes of ovotransferrin is a prerequisite for receptor recognition. Studies with recombinant ovotransferrins. *Biochem J* 1996; 319:361–368.
35. Mason AB, Tam BM, Woodworth RC, Oliver RWA, Green BN, Lin L-N, Brandts JF, Savage KJ, Lineback JA, MacGillivray RTA. Receptor recognition sites reside in both lobes of human serum transferrin. *Biochem J* 1997; 326:77–85.
36. Lawrence CM, Ray S, Babyonyshev M, Galluser R, Borhani DW, Harrison SC. Crystal structure of the ectodomain of human transferrin receptor. *Science* 1999; 286:779–782.
37. Bennett MJ, Lebrón JA, Bjorkman PJ. Crystal structure of the hereditary haemochromatosis protein HFE complexed with transferrin receptor. *Nature* 2000; 403:46–53.
38. Brock JH. Transferrins. In: Harrison P, ed. *Metalloproteins Part II Metal Proteins with Non-redox Roles*. London: Macmillan, 1985:183–262.
39. El Hage Chahine JM, Pakdaman R. Transferrin, a mechanism for iron release. *Eur J Biochem* 1995; 230:1102–1110.

40. Abdallah FB, Chahine JM. Transferrins, the mechanism of iron release by ovotransferrin. *Eur J Biochem* 1999; 263:912–920.
41. Dewan JC, Mikami B, Hirose M, Sacchettini JC. Structural evidence for a pH-sensitive dilysine trigger in the hen ovotransferrin N-lobe: Implications for transferrin iron release. *Biochemistry* 1993; 32:11963–11968.
42. Bali PK, Harris WR. Cooperativity and heterogeneity between the two binding sites of diferric transferrin during iron removal by pyrophosphate. *J Am Chem Soc* 1989; 111:4457–4461.
43. Bali PK, Harris WR, Nessel-Tollefson D. Kinetics of iron removal from monoferric and cobalt-labeled monoferric human serum transferrin by nitrilotris(methylene-phosphonic acid) and nitrilotriacetic acid. *Inorg Chem* 1991; 30:502–508.
44. Mason AB, He Q-Y, Tam BM, MacGillivray RTA, Woodworth RC. Mutagenesis of the aspartic acid ligands in human serum transferrin: Lobe-lobe interaction and conformation as revealed by antibody, receptor-binding and iron-release studies. *Biochem J* 1998; 330:35–40.
45. Beatty EJ, Cox MC, Frenkiel TA, Tam BM, Mason AB, MacGillivray RTA, Sadler PJ, Woodworth RC. Interlobe communication in ¹³C-methionine-labeled human transferrin. *Biochemistry* 1996; 35:7635–7642.
46. Kurokawa H, Mikami B, Hirose M. Crucial role of intralobe peptide-peptide interactions in the uptake and release of iron by ovotransferrin. *J Biol Chem* 1994; 269:6671–6676.
47. Day CL, Stowell KM, Baker EN, Tweedie JW. Studies of the N-terminal half of human lactoferrin produced from the cloned cDNA demonstrate that interlobe interactions modulate iron release. *J Biol Chem* 1992; 267:13857–13862.
48. Lin L, Mason AB, Woodworth RC, Brandts JF. Calorimetric studies of the binding of ferric ions to ovotransferrin and interactions between binding sites. *Biochemistry* 1991; 30:11660–11669.
49. Lin L-N, Mason AB, Woodworth RC, Brandts JF. Calorimetric studies of serum transferrin and ovotransferrin. Estimates of domain interactions, and study of the kinetic complexities of ferric ion binding. *Biochemistry* 1994; 33:1881–1888.
50. Carver FJ, Frieden E. Factors affecting the adenosine triphosphate induced release of iron from transferrin. *Biochemistry* 1978; 17:167–172.
51. Kojima N, Bates GW. The reduction and release of iron from Fe(III)-transferrin-CO₃²⁻. *J Biol Chem* 1979; 254:8847–8854.
52. Ankel E, Petering DH. Iron-chelating agents and the reductive removal of iron from transferrin. *Biochem Pharmacol* 1979; 29:1833–1837.
53. Baldwin DA, Egan TJ, Marques HM. The effects of anions on the kinetics of reductive elimination of iron from monoferrictransferrins by thiols. *Biochim Biophys Acta Protein Struct Mol Enzymol* 1990; 1038:1–9.
54. Carrano CJ, Raymond KN. Ferric ion sequestering agents. 2. Kinetics and mechanism of iron removal from transferrin by enterobactin and synthetic triccatechols. *J Am Chem Soc* 1979; 101:5401–5404.
55. Rodgers SJ, Raymond KN. Ferric ion sequestering agents 11. Synthesis and kinetics of iron removal from transferrin of catechoyl derivatives of desferrioxamine B1. *J Med Chem* 1983; 26:439–442.
56. Kretchmar SA, Raymond KN. Biphasic kinetics and temperature dependence of iron removal from transferrin by 3,4-LICAMS. *J Am Chem Soc* 1986; 108:6212–6218.
57. Kretchmar SA, Raymond KN. Effects of ionic strength on iron removal from the monoferric transferrins. *Inorg Chem* 1988; 27:1436–1441.
58. Nguyen SAK, Craig A, Raymond KN. Transferrin: The role of conformational changes in iron removal by chelators. *J Am Chem Soc* 1993; 115:6758–6764.

59. He Q-Y, Mason AB, Woodworth RC, Tam BM, Wadsworth T, MacGillivray RTA. Effects of mutations of aspartic acid 63 on the metal-binding properties of the recombinant N-lobe of human serum transferrin. *Biochemistry* 1997; 36:5522–5528.
60. Cowart RE, Swope S, Loh TT, Chasteen ND, Bates GW. The exchange of Fe^{3+} between pyrophosphate and transferrin. *J Biol Chem* 1986; 261:4607–4614.
61. Harris WR, Rezvani AB, Bali PK. Removal of iron from transferrin by pyrophosphate and tripodal phosphonate ligands. *Inorg Chem* 1987; 26:2711–2716.
62. Bertini I, Hirose J, Luchinat C, Messori L, Piccioli M, Scozzafava A. Kinetic studies on metal removal from transferrins by pyrophosphate. Investigation on iron(III) and manganese(III) derivatives. *Inorg Chem* 1988; 27:2405–2409.
63. Harris WR, Bali PK. Effects of anions on the removal of iron from transferrin by phosphonic acids and pyrophosphate. *Inorg Chem* 1988; 27:2687–2691.
64. Marques HM, Egan TJ, Patrick G. The non-reductive removal of iron from human serum N-terminal monoferric transferrin by pyrophosphate. *S Afr J Sci* 1990; 86: 21–24.
65. Egan TJ, Ross DC, Purves LR, Adams PA. Mechanism of iron release from human serum C-terminal monoferric transferrin to pyrophosphate: Kinetic discrimination between alternative mechanisms. *Inorg Chem* 1992; 31:1994–1998.
66. Marques HM, Walton T, Egan TJ. Release of iron from C-terminal monoferric transferrin to phosphate and pyrophosphate at pH 5.5 proceeds through two pathways. *J Inorg Biochem* 1995; 57:11–21.
67. Zak O, Aisen P, Crawley JB, Joannou CL, Patel KJ, Rafiq M, Evans RW. Iron release from recombinant N-lobe and mutants of human transferrin. *Biochemistry* 1995; 34: 14428–14434.
68. Li YJ, Harris WR, Maxwell A, MacGillivray RTA, Brown T. Kinetic studies on the removal of iron and aluminum from recombinant and site-directed mutant N-lobe half transferrins. *Biochemistry* 1998; 37:14157–14166.
69. Bates GW, Billups C, Saltman P. The kinetics and mechanism of iron(III) exchange between chelates and transferrin. II. The presentation and removal with EDTA. *J Biol Chem* 1967; 242:2816–2821.
70. Baldwin DA. The kinetics of iron release from human transferrin by EDTA. Effects of salts and detergents. *Biochim Biophys Acta* 1980; 623:183–198.
71. Baldwin DA, DeSousa DMR. The effect of salts on the kinetics of iron release from N-terminal and C-terminal monoferric transferrins. *Biochem Biophys Res Commun* 1981; 99:1101–1107.
72. Baldwin DA, De Sousa DMR, Von Wandruszka RMA. The effect of pH on the kinetics of iron release from human transferrin. *Biochim Biophys Acta* 1982; 719:140–146.
73. He Q-Y, Mason AB, Woodworth RC. Iron release from recombinant N-lobe and single point Asp 63 mutants of human transferrin by EDTA. *Biochem J* 1997; 328:439–445.
74. Harris WR. Kinetics of the removal of ferric ion from transferrin by aminoalkylphosphonic acids. *J Inorg Biochem* 1984; 21:263–276.
75. Harris WR, Bali PK, Crowley MM. Kinetics of iron removal from monoferric and cobalt-labeled monoferric transferrins by diethylenetriaminepenta (methyleephosphonic acid) and diethylenetriaminepentaacetic acid. *Inorg Chem* 1992; 31:2700–2705.
76. Cowart RE, Kojima N, Bates GW. The exchange of Fe^{3+} between acetohydroxamic acid and transferrin. *J Biol Chem* 1982; 257:7560–7565.
77. Li YJ, Harris WR. Iron removal from monoferric human serum transferrins by 1,2-dimethyl-3-hydroxypyridin-4-one, 1-hydroxypyridin-2-one and acetohydroxamic acid. *Biochim Biophys Acta: Protein Struct Mol Enzymol* 1998; 1387:89–102.
78. Marques HM, Watson DL, Egan TJ. Kinetics of iron removal from human serum monoferric transferrins by citrate. *Inorg Chem* 1991; 30:3758–3762.

79. Bailey CT, Byrne C, Chrispell K, Molkenbur C, Sackett M, Reid K, McCollum K, Vibbard D, Catelli R. Effect of a covalently attached synergistic anion on chelator-mediated iron-release from ovotransferrin: Additional evidence for two concurrent pathways. *Biochemistry* 1997; 36:10105–10108.
80. Chasteen ND, Williams J. The influence of pH on the equilibrium distribution of iron between the metal-binding sites of transferrin. *Biochem J* 1981; 193:717–727.
81. Williams J, Chasteen ND, Moreton K. The effect of salt concentration on the iron-binding properties of human transferrin. *Biochem J* 1982; 201:527–532.
82. Thompson CP, McCarty BM, Chasteen ND. The effects of salts and amino group modification on the iron binding domains of transferrin. *Biochim Biophys Acta* 1986; 870:530–537.
83. Chasteen ND, Grady JK, Woodworth RC, Mason AB. Salt effects on the physical properties of the transferrins. *Adv Exp Med Biol* 1994; 357:45–52.
84. Grady JK, Mason AB, Woodworth RC, Chasteen ND. The effect of salt and site-directed mutations on the iron(III)-binding site of human serum transferrin as probed by EPR spectroscopy. *Biochem J* 1995; 309:403–410.
85. Harris WR. Thermodynamics of anion binding to human serum transferrin. *Biochemistry* 1985; 24:7412–7418.
86. Harris WR, Nettet-Tollefson D, Stenback JZ, Mohamed-Hani N. Site selectivity in the binding of inorganic anions to serum transferrin. *J Inorg Biochem* 1990; 38:175–183.
87. Harris WR, Nettet-Tollefson D. Binding of phosphonate chelating agents and pyrophosphate to apotransferrin. *Biochemistry* 1991; 30:6930–6936.
88. Cheng YG, Mason AB, Woodworth RC. pH dependence of specific divalent anion binding to the N-lobe of recombinant human transferrin. *Biochemistry* 1995; 34:14879–14884.
89. Harris WR, Cafferty AM, Abdollahi S, Trankler K. Binding of monovalent anions to human serum transferrin. *Biochim Biophys Acta: Protein Struct Mol Enzymol* 1998; 1383:197–210.
90. Harris WR, Cafferty AM, Trankler K, Maxwell A, MacGillivray RTA. Thermodynamic studies on anion binding to apotransferrin and to recombinant transferrin N-lobe half molecules. *Biochim Biophys Acta: Protein Struct Mol Enzymol* 1999; 1430:269–280.
91. Campbell RF, Chasteen ND. An anion binding study of vanadyl(IV) and human serotransferrin. *J Biol Chem* 1977; 252:5996–6001.
92. Steinlein LM, Ligman CM, Kessler S, Ikeda RA. Iron release is reduced by mutations of lysine 206 and 296 in recombinant N-terminal half-transferrin. *Biochemistry* 1998; 37:13696–13703.
93. Foltajtar DA, Chasteen ND. Measurement of nonsynergistic anion binding to transferrin by EPR difference spectroscopy. *J Am Chem Soc* 1982; 104:5775–5780.
94. Foley AA, Bates GW. The influence of inorganic anions on the formation and the stability of Fe(3+)-transferrin-anion complexes. *Biochim Biophys Acta* 1988; 965:154–162.
95. MacGillivray RTA, Bewley MC, Smith CA, He Q-Y, Mason AB, Woodworth RC, Baker EN. Mutation of the iron ligand His249 to Glu in the N-lobe of human transferrin abolishes the dilysine “trigger” but does not significantly affect iron release. *Biochemistry* 2000; 39:1211–1216.
96. Cheuk MS, Keung WM, Loh TT. The effect of pH on the kinetics of iron release from diferric ovotransferrin induced by pyrophosphate. *J Inorg Biochem* 1987; 30:121–131.
97. Lee DA, Goodfellow JM. The pH-induced release of iron from transferrin investigated with a continuum electrostatic model. *Biophys J* 1998; 74:2747–2759.
98. Kubal G, Sadler PJ, Tucker A. pH-induced structural changes in human serum apotransferrin—pKa values of histidine residues and N-terminal amino group determined by ¹H-NMR spectroscopy. *Eur J Biochem* 1994; 220:781–787.

99. He Q-Y, Mason AB, Woodworth RC, Tam BM, MacGillivray RTA, Grady JK, Chasteen ND. Inequivalence of the two tyrosine ligands in the N-lobe of human serum transferrin. *Biochemistry* 1997; 36:14853–14860.
100. He Q-Y, Mason AB, Pakdaman R, Chasteen ND, Dixon BL, Tam BM, Nguyen V, MacGillivray RTA, Woodworth RC. Mutations at the histidine 249 ligand profoundly alter the spectral and iron-binding properties of human serum transferrin N-lobe. *Biochemistry* 2000; 39:1205–1210.
101. Lindley PF, Bajaj M, Evans RW, Garratt RC, Hasnain SS, Jhoti H, Kuser P, Neu M, Patel K, Sarra R, Strange R, Walton A. The mechanism of iron uptake by transferrin—The structure of an 18 kDa NII-domain fragment of duck ovotransferrin at 2.3 Å resolution. *Acta Crystallogr* 1993; D49:292–304.
102. Mizutani K, Yamashita H, Kurokawa H, Mikami B, Hirose M. Alternative structural state of transferrin—The crystallographic analysis of iron-loaded but domain-opened ovotransferrin N-lobe. *J Biol Chem* 1999; 274:10190–10194.
103. Grossmann JG, Mason AB, Woodworth RC, Neu M, Lindley PF, Hasnain SS. Asp ligand provides the trigger for closure of transferrin molecules. Direct evidence from X-ray scattering studies of site-specific mutants of the N-terminal half-molecule of human transferrin. *J Mol Biol* 1993; 231:554–558.
104. Faber HR, Bland T, Day CL, Norris GE, Tweedie JW, Baker EN. Altered domain closure and iron binding in transferrins: The crystal structure of the Asp60Ser mutant of the amino-terminal half-molecule of human lactoferrin. *J Mol Biol* 1996; 256:352–363.
105. Grossmann JG, Crawley JB, Strange RW, Patel KJ, Murphy LM, Neu M, Evans RW, Hasnain SS. The nature of ligand-induced conformational change in transferrin in solution. An investigation using X-ray scattering, XAFS and site-directed mutants. *J Mol Biol* 1998; 279:461–472.
106. Faber HR, Baker CJ, Day CL, Tweedie JW, Baker EN. Mutation of arginine 121 in lactoferrin destabilizes iron binding by disruption of anion binding: Crystal structures of R121S and R121E mutants. *Biochemistry* 1996; 35:14473–14479.
107. Evans RW, Williams J, Moreton K. A variant of human transferrin with abnormal properties. *Biochem J* 1982; 201:19–26.
108. Evans RW, Meilak A, Aitken A, Patel KJ, Wong C, Garratt RC, Chitnavis B. Characterization of the amino acid change in a transferrin variant. *Biochem Soc Trans* 1988; 16:834–835.
109. Evans RW, Crawley JB, Garratt RC, Grossmann JG, Neu M, Aitken A, Patel KJ, Meilak A, Wong C, Singh J, Bomford A, Hasnain SS. Characterization and structural analysis of a functional human serum transferrin variant and implications for receptor recognition. *Biochemistry* 1994; 33:12512–12520.
110. He Q-Y, Mason AB, Tam BM, MacGillivray RTA, Woodworth RC. [¹³C]methionine NMR and metal-binding studies of recombinant human transferrin N-lobe and five methionine mutants: conformational changes and increased sensitivity to chloride. *Biochem J* 1999; 344:881–887.
111. El Hage Chahine J-M, Fain D. The mechanism of iron release from transferrin—Slow-proton-transfer-induced loss of nitrilotriacetatoiron(III) complex in acidic media. *Eur J Biochem* 1994; 223:581–587.
112. Gerstein M, Anderson BF, Norris GE, Baker EN, Lesk AM, Chothia C. Domain closure in lactoferrin. Two hinges produce a see-saw motion between alternative close-packed interfaces. *J Mol Biol* 1993; 234:357–372.

5

Ferritins Structural and Functional Aspects

PAOLO AROSIO

University of Brescia, Brescia, Italy

SONIA LEVI

H. San Raffaele, Milan, Italy

I.	INTRODUCTION	126
II.	FERRITINS IN ANIMALS, PLANTS, AND BACTERIA	126
	A. General	126
	B. Animals	128
	C. Plants	129
	D. Bacteria	129
III.	STRUCTURAL ASPECTS	130
	A. General	130
	B. Iron-Binding Sites	133
	C. The Mineral Core	133
IV.	THE IN-VITRO PROCESS OF IRON STORAGE	135
	A. Iron Entry	135
	B. Iron Oxidation	136
	C. Turnover at the Ferroxidase Center	137
	D. Redox Centers on Mammalian Ferritins	138
V.	FERRITIN GENE STRUCTURE AND EXPRESSION	139
	A. Gene Structures	139
	B. Regulation of Ferritin Expression in Mammals	140
	C. Regulation of Ferritin Expression in Other Animals	142
	D. Regulation of Ferritin Expression in Higher Plants	142

VI.	BIOLOGICAL ROLES OF FERRITINS	142
A.	Functions in Microorganisms	142
B.	Functions in Plants	143
C.	Functions in Mammals	144
VII.	FERRITIN AS AN IRON TRANSPORTER	147
VIII.	CONCLUSIONS AND PERSPECTIVES	147
	ACKNOWLEDGMENTS	148
	REFERENCES	148

I. INTRODUCTION

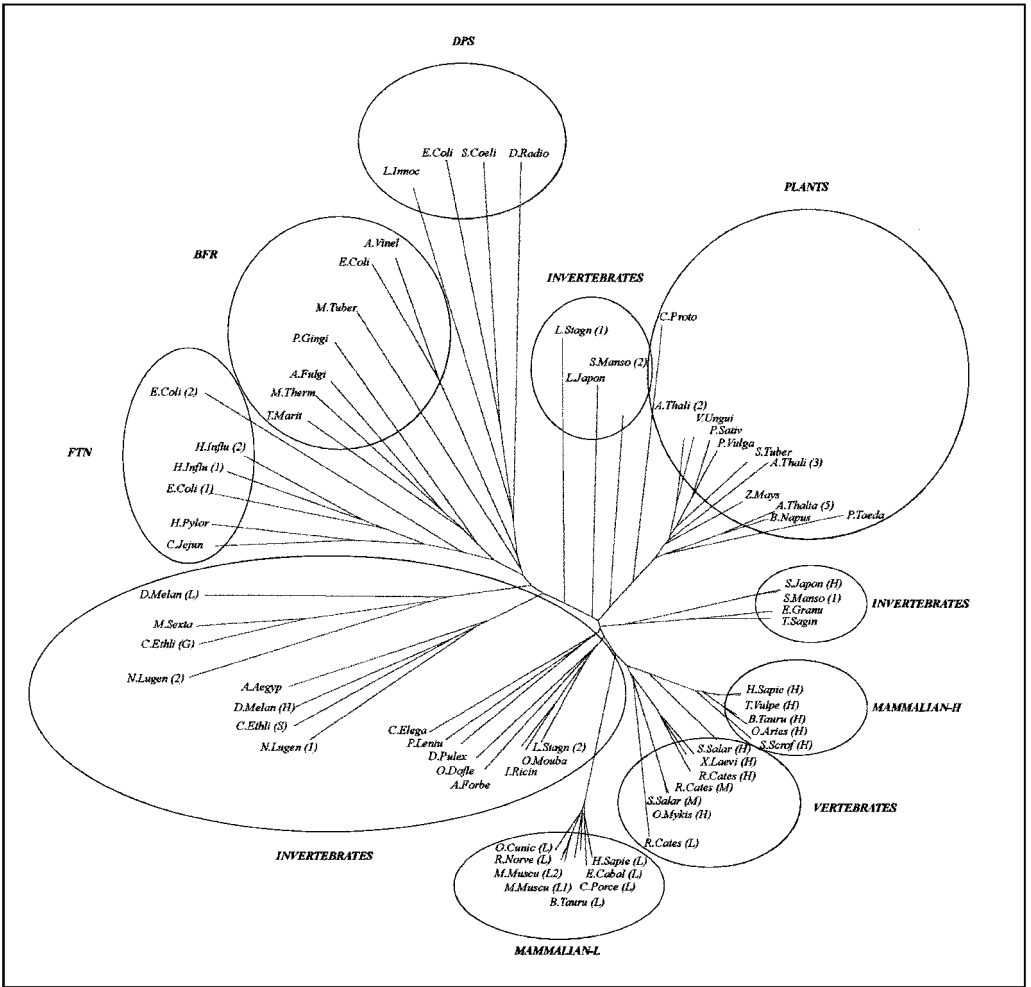
Iron is an essential nutrient for organisms, but in the presence of oxygen it becomes insoluble and potentially toxic. Ferritins are an ancient and widely distributed group of proteins which evolved to store and concentrate biological iron while limiting its toxic effects. The protein has catalytic sites that facilitate its interaction with iron and oxygen, and it has a unique hollow structure that serves to direct the formation of mineralized iron particles and maintain them in solution. These properties are common to most ferritins found in bacteria, plants, and animals, but significant functional and structural differences are now becoming apparent in different organisms that suit their different biological needs and access to iron. A comparison of ferritins from various sources may allow a better understanding of the biological function of these proteins and their role in iron metabolism.

II. FERRITINS IN ANIMALS, PLANTS, AND BACTERIA

A. General

Ferritins are a rather large class of proteins, normally composed of subunits of 150–190 amino acids that fold into a bundle of four α -helices (A, B, C, and D). (A fifth short C-terminal helix (E) is present in all but the dodecameric ferritins.) These usually assemble into a 450- to 500-kDa protein containing 24 chains that has characteristically a cavity for iron storage, catalytic sites for iron oxidation, and hydrophilic pores for solvent exchange. The helices A–B and C–D are connected by short turns and the helices B–C by a long loop. The complete amino acid (cDNA) sequences of more than 80 members of the ferritin family are available in data banks (1). Many of these originated from genome projects, including examples from archaeobacteria, proteobacteria, plants, invertebrates, vertebrates, and mammals (Fig. 1).

Figure 1 Phylogenetic tree showing the relationship among members of the ferritin superfamily, which includes ferritins, bacterioferritins, and dodecameric DPS-like ferritins. The programs ClustalX, Draw N-J Tree, and NJ Plot (116) were used to create the phylogenetic tree. The input consisted of complete sequences which included N-terminal leaders and extension peptides. Compact clusters are evident for the mammalian H and L ferritins, the ferritins of higher plants, and bacterial FTN, BFR, and DPS-like ferritins, while the distribution of invertebrate ferritins is dispersed. Abbreviations: *A.Aegypt* = *Aedes Aegypti*; *A.Forbe*



= *Asteria Forbesii*; *A.Fulgi* = *Archaeoglobus Fulgidus*; *A.Thali* = *Arabidopsis Thaliana*; *A.Vineli* = *Azotobacter Vinelandii*; *B.Napus* = *Brassica Napus*; *B.Tauru* = *Bos Taurus*; *C.Elega* = *Caenorhabditis Elegans*; *C.Ethli* = *Calpodes Ethlius*; *C.Jejuni* = *Campylobacter Jejuni*; *C.Porce* = *Cavia Porcellus*; *C.Proto* = *Chlorella Protothecoides*; *D.Melan* = *Drosophila Melanogaster*; *D.Pulex* = *Daphnia Pulex*; *D.Radio* = *Deinococcus Radiodurans*; *E.Cabal* = *Equus Caballus*; *E.Coli* = *Escherichia Coli*; *E.Granu* = *Echinococcus Granulosus*; *H.Influ* = *Haemophilus Influenzae*; *H.Pylori* = *Helicobacter Pylori*; *H.Sapie* = *Homo Sapiens*; *I.Ricin* = *Iodex Ricinus*; *L.Innoc* = *Listeria Innocua*; *L.Japon* = *Liolophura Japonica*; *L.Stagn* = *Lymnaea Stagnalis*; *M.Muscu* = *Mus Musculus*; *M.Sexta* = *Maduca Sexta*; *M.Therm* = *Methanobacterium Thermoautotrophicum*; *M.Tuber* = *Mycobacterium Tuberculosis*; *N.Lugen* = *Nilaparata Lugens*; *O.Aries* = *Ovis Aries*; *O.Cunic* = *Oryctolagus Cuniculus*; *O.Dofle* = *Octopus Dofleini*; *O.Mouba* = *Ornithodoros Moubata*; *O.Mykis* = *Oncorhynchus Mykiss*; *P.Gingi* = *Porphyromonas Gingivalis*; *P.Lenin* = *Pacifastacus Leniusculus*; *P.Sativ* = *Pisum Sativum*; *P.Taeda* = *Pinus Taeda*; *P.Vulga* = *Phaseolus Vulgaris*; *R.Cates* = *Rana Catesbeiana*; *R.Norve* = *Rattus Norvegicus*; *S.Coeli* = *Streptomyces Coelicor*; *S.Japon* = *Schistosoma Japonicum*; *S.Manso* = *Schistosoma Mansoni*; *S.Salar* = *Salmo Salar*; *S.Scrof* = *Sus Scrofa Domestica*; *S.Tuber* = *Solanum Tuberosum*; *T.Marit* = *Thermotoga Maritima*; *T.Sagn* = *Taenia Saginata*; *T.Vulpe* = *Trichosurus Vulpecula*; *V.Ungui* = *Vigna Unguiculata*; *X.Laevi* = *Xenopus Laevis*; *Z.Mays* = *Zea Mays*.

Although the three-dimensional structures are highly conserved, sequence identities as low as 15% are found between humans and bacteria. The ferritins of the different kingdoms have structural specificities, and they will be discussed separately.

B. Animals

Mammalian ferritins have been characterized from human, mouse, rat, rabbit, cow, Chinese hamster, and horse (2). They are composed of two subunit types, named H and L, encoded on distinct chromosomes, and with a sequence identity of about 50%. The H chains are highly conserved in the five mammalian examples, with identities above 82%. All have seven residues which are ligands in the ferroxidase center, the catalytic iron-binding site of the subunit. These are Glu27, Tyr34, Glu61, Glu62, His65, Glu107, and Gln142 in the human H-chain numeration that will be used throughout the text (3). The six known mammalian L-chain sequences are also highly conserved, with identities above 80%. These show substitutions of four ligands of the ferroxidase center (His, Gln, or Tyr in position 27, Lys62, Gly65, and Glu142) and have two critical conserved residues, Glu57 and Glu60, that correspond to His residues in the H chains (4). These latter are important in promoting the formation of the iron core. L chains from mouse and rat have an extra octapeptide located in the D–E turn (5). The H and L chains assemble in different proportions to form tissue-specific hybrid molecules with distinct functional properties (see below). Human H-chain cDNA hybridizes with many loci on various human chromosomes, but only that on chromosome 11 has been shown to be functional. The others appear to represent processed pseudo-genes, although the functionality of some of them cannot be totally excluded. The L chain hybridizes with fewer loci, and that on chromosome 19 is functional. In mouse the gene pattern is slightly less complex, with fewer H-chain and more L-chain loci than in humans. The representative crystallographic structures of the mammalian ferritins are human H and horse L chains, and their properties have been recently reviewed (6).

In lower vertebrates, complete cDNA sequences have been obtained for the frog *Xenopus laevis* (7), where two similar H ferritin homolog sequences were identified, and the bullfrog *Rana catesbeiana* (8), where three distinct sequences were found. One of them has substitutions in the ferroxidase center (K27 and Q107), and was therefore named L chain. The other two chains, named H and M, have 80% identity between them, and 65% with the human H chain. They have been produced in a recombinant form and analyzed in detail (9). It is unclear if these ferritins form hybrid molecules, and their functional specificity is also unknown. Fishes also contain multiple copies of H-like ferritins. Two were found in salmon (10) and three in trout (11,12). They are similar and possess the residues of the ferroxidase center, but no functional specificity has been attributed to them. In contrast, the snails *Limnea stagnalis* (13), *Schistosoma mansoni* (14), and *Schistosoma Japonicum* contain at least two largely different ferritin subunits. One is named yolk ferritin and is secreted and preferentially expressed by the females in *S. mansoni*. The other subunit, soma ferritin, has a sequence closer to the typical H chain without a leader sequence. In the complete genome of the insect *Drosophila melanogaster*, five loci for putative ferritins have been identified. Two of them are closely located and encode for secretory ferritins with leader sequences. One has a putative ferroxidase center, (Fer1HCH), and the other contains mutations and is more similar to the L-type

subunit type (Fer2LCH) (15,16). A third gene encodes an intracellular ferritin of the H type (17). Similar secretory ferritins are found in the insect *Aedes aegypti* (18). Two ferritin genes have been identified in the complete genome sequence of the nematode *Caenorhabditis elegans*. They are located on chromosomes I and V, and encode intracellular ferritin subunits with a putative ferroxidase center similar to the vertebrate H chains (19). One copy of H-type ferritin has been found in *Echinococcus granulosus* (20) and *Taenia saginata* (21), and in the parasites *Ixodes ricinus* and *Onithodoros moubata*.

C. Plants

In plants, the ferritins consistently have a leader transit sequence for targeting to the plastids where they accumulate. In addition, they have an N-terminal extension peptide which undergoes a free-radical-mediated cleavage during iron exchange, leading to protein degradation (22). This structure has been found in all complete cDNAs encoding ferritins of alfalfa, pea, soybean, bean, cowpea, maize, and *A. thaliana*. Up to four copies of ferritin genes have been found in plant genomes. They encode for very similar proteins, with the conserved residues of the ferroxidase center and a cluster of acidic residues exposed on the cavity, which resembles that of the mammalian L chains. The sequence identities among the plant ferritins are high and those with mammalian ferritin are around 40%, while they have no significant homology with bacterial ferritins. A model of the pea ferritin predicts a three-dimensional structure very similar to that of the human ferritins (23).

D. Bacteria

Bacteria can express a variety of ferritins and ferritin-like proteins. The typical 24-mer nonheme ferritin is designated FTN. Heme-binding bacterioferritins (BFR) and DPS-like dodecameric ferritin molecules also occur. BFR and dodecameric ferritins have no evident sequence similarity with vertebrate or plant ferritins, and the homology is at the structural levels; they form spherical structures with a cavity and pores analogous to that of the ferritins. Complete FTN sequences have been derived from *Hemophilus influenza* (two copies), *Escherichia coli* (two copies), *Helicobacter pylori* (three copies), *Campylobacter jejuni*, *Mycobacterium tuberculosis*, *Porphyromonas gingivalis*, and from the anaerobic Archaeobacteriae *Archeoglobus fulgidus* and *Methanobacteron thermoautrophicum*. Their sequences have about 20% identity with those of the human ferritins, and they retain the residues of the ferroxidase center, except one of the two ferritins of *E.coli* (FtnB), which is probably nonfunctional (24). The bacterioferritins (BFR, also known as cytochrome b₁ or cytochrome b₅₅₇) bind up to 12 molecules of heme per protein shell. Complete cDNA sequences have been obtained from *Magnetospirillum magnetotaticum* (two copies), *Brucella melitensis*, *Rhodobacter capsulatus*, *Neisseria gonorrhoeae* (two copies), *Azotobacter vinelandi*, *E. coli*, *Salmonella typhimurium*, *Serratia marcescens*, *Pseudomonas putida*, *Pseudomonas aeruginosa*, *Mycobacterium avium*, *M. leprae*, *M. tuberculosis*, and *Synechcystis sp.* (two copies). They encode peptides with about 40% sequence identity and have only 14% identity with the bacterial FTN ferritins. The residues of the ferroxidase center are conserved in most sequences (2). An example of BFR has been reported in the fungus *Absidia spinosa* (25), suggesting that these proteins may not be exclusive to bacteria. The resolution of the structure of a 19-kDa DNA-

binding protein which is expressed in *E. coli* under stressed conditions and named DPS (26) showed it to be composed of 12 subunits, each folded in a four-helix bundle analogous to that of the ferritins. In addition, the assembled protein delimits a cavity 0.4 nm across, half the size of the vertebrate ferritins, but has hydrophilic pores like the ferritins. The DNA-binding property is probably associated with the basic N-terminal sequence, which is disordered and therefore not visible in the crystal structure. The sequence is not conserved in all DPS-like proteins. Thus it is uncertain whether all proteins of this group have the capacity to bind DNA as does the one from *E. coli* (26). A possible ferritin-like function in iron binding is suggested by the structure but is not yet supported by biochemical evidence. However, a protein from *Listeria innocua* which purified as an iron-containing ferritin was found to have a dodecameric structure analogous to *E. coli* DPS (27). The residues of the ferroxidase center are not present in this protein, but evidence for an alternative site exposed in the protein cavity has been presented (28). Complete cDNAs for ortholog proteins found in *Synechocystis*, *Bacillus subtilis*, *Haemophilus influenzae*, *Borrelia burgdorferi*, *Treponema pallidum*, and *Rickettsia prowazekii*, and the protein from *Helicobacter pylori*, have been characterized (29). Since the residues involved in iron oxidation are highly conserved, it is not unlikely that most of these proteins have iron storage functions similar to that of ferritin.

III. STRUCTURAL ASPECTS

A. General

The resolved ferritin and ferritin-like three-dimensional structures include human H chain (access code 2FHA), horse L chain (1DAT), bullfrog L chain (1RCC) and M chain (1MFR), *E. coli* BFR (1BFR), *Listeria innocua* ferritin (1QGH), and *E. coli* DPS (1BG7). Each consists of a bundle of four long helices and a long extended loop connecting helices B and C. A fifth short C-terminal helix is present in all but the dodecameric ferritins (Fig. 2). The structures of the 24-mer ferritins are closely similar; most of the main-chain atoms of the vertebrate and *E. coli* FTN ferritins (EcFTN) superimpose within about 1 Å, and those of horse spleen ferritin and

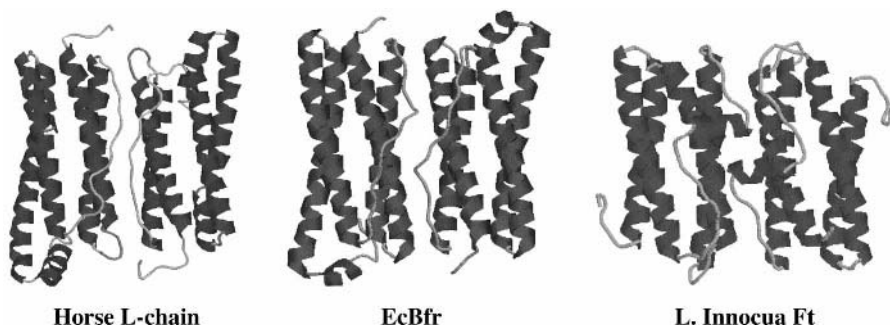


Figure 2 Cartoon representation of the subunit dimers of horse L-chain, *E. coli* BFR, and *Listeria innocua* ferritins. The similarity of the four-helical bundles and the differences at the twofold axes are evident. Coordinates from PDB files code 1IES, 1BFR, and 1QGH, respectively.

EcBFR within 2 Å (2). A similar conservation of the helical bundle structure is observed in the dodecameric ferritins of *Listeria* and EcDPS, the α of which have a root-mean-square deviation from EcBFR and horse L chain below 1.6 Å. The inner core of the bundle is hydrophilic in all ferritins, while it is hydrophobic in the dodecameric ferritins. In the 24-mer ferritins the assembled subunits are related by fourfold, threefold, and twofold symmetry axes (432 symmetry), while the dodecameric ferritins have different architecture with twofold axes similar to those of ferritin and two types of threefold axes, one similar to ferritin and the other specific to DPS (23 symmetry). At the twofold symmetry axes the antiparallel subunits pair with a long apolar interface (Fig. 2). In mammalian H and L chains the interface residues are highly conserved and involve a short β strand on the BC loop. The interaction is important in stabilizing subunit folding during the initial steps of protein assembly (30). Subunit dimers can be isolated from EcBFR ferritin preparations and also from human ferritins after specific modifications of the interfaces of the threefold and fourfold symmetry axes, indicating that the interactions along the twofold axes are essential for protein stability (30). These subassembly species are properly folded and functionally active in reacting with iron, while the subunits in which assembly was prevented by chemical modifications at the twofold axes' surface were poorly soluble and only partially folded (31). In the dodecameric ferritins the β strand is substituted by a short helix in the middle of the loop, which interacts with that of the symmetry-related subunit burying a hydrophobic cluster (28). The packing along the threefold axis is made by the coming together of the N-terminal portion of the D helix, and occurs similarly in all ferritins including the dodecameric ones (Fig. 3). This determines the formation of a funnel-like channel with hydrophilic characteristics in the ferritins of higher organisms. In vertebrate and plant ferritins the narrowest part of the channels is lined by three symmetry-related and conserved aspartate (D131) and glutamates (E134) which form a metal-binding site that is probably important for facilitating iron entry into the cavity (32). These properties are conserved in the BFRs and the dodecameric ferritins, where the equivalent threefold

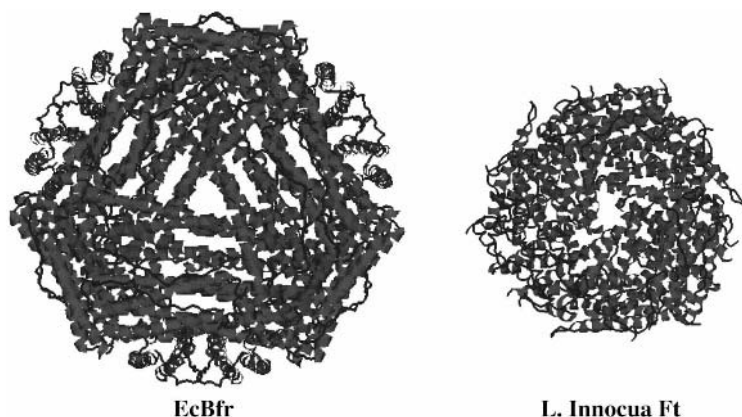


Figure 3 Cartoon representation of the *E. coli* Bfr and of the dodecameric *Listeria innocua* ferritins looking down the similar threefold axes. The shapes of the channels are similar, and both are surrounded by hydrophilic residues.

channels are surrounded by aspartates, while in bacterial FTNs the channels are surrounded by hydrophobic residues. The fourfold interface made by the coming together of the short C-terminal E helices is strongly hydrophobic in mammalian L chains, being lined by three leucines per subunit, and a little less hydrophobic in the H chains for the substitution of a leucine on the cavity side with a histidine (Fig. 4). In the model of pea seed ferritin as well as in EcBFR, these channels are more hydrophilic and are lined by His and Arg or by Asn and Gln. In vertebrate ferritins there is very little space around these axes, while in EcBFR it is less tightly packed and permeation is possible. The dodecameric ferritins do not have the C-terminal E helix and form a second type of threefold symmetry axis by the coming together of the N terminus of the B helix (Fig. 4). These channels have also hydrophobic characteristics and are tighter than those on the ferritin-like threefold channels. The mammalian L ferritins expose a high number of carboxyl groups on the cavity surface. The conserved Glu57 and 60 (His in the H chains), which have a major role in favoring iron mineralization, are particularly important (33). In mouse L ferritin, one of the conserved glutamates (E140) exposed on the cavity surface is substituted with a lysine, and this substitution makes the ferritin less efficient in iron incorporation than its human counterpart (5). Plant ferritins expose a number of acidic residues on the cavity surface and resemble the mammalian L chains, while the cavity of bacterial ferritins is less acidic. In the dodecameric *Listeria* ferritin the cavity exposes clusters of negative charges from aspartic and glutamic acids on the B and D helices, which are probably important for the formation of the iron cores, and are mostly conserved in the EcDPS. A calculation of the electrostatic potential in human H ferritin showed a positive potential at the outer entrance of the threefold channels, creating an electrostatic field directed toward the cavity which provides guidance for cations entering the protein. A large electrostatic potential at the fourfold channel produces a field directed outward from the cavity, suggesting a pathway for the efflux of the protons

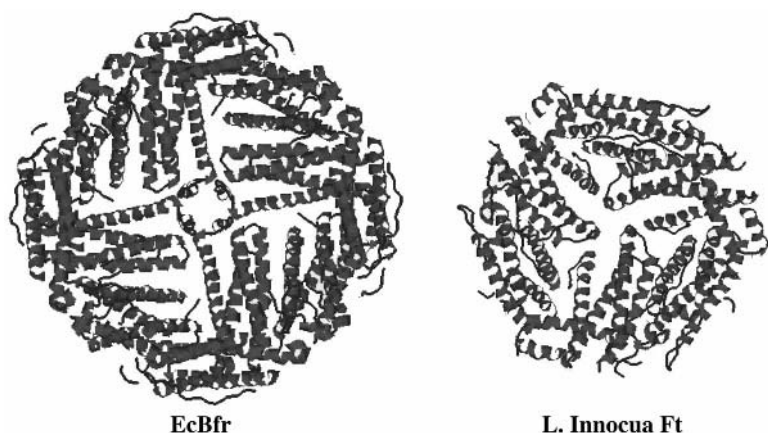


Figure 4 Cartoon representation of the *E. coli* Bfr and of the dodecameric *Listeria innocua* ferritins looking down the fourfold axes for the EcBfr and the DPS-type threefold axes of *L. innocua* ferritin. View from the inside. The two channels have different structure and shape, but both are hydrophobic and narrow.

generated during iron oxidation and deposition (34). A similar inward electrostatic field is also present in the dodecameric ferritins (28).

B. Iron-Binding Sites

The four-helix bundles of the 24-mer ferritins contain a central hydrophilic core which, in the mammalian L chains, contains a salt bridge that contributes to the protein stability (35). In the bullfrog L chain the region contains a water molecule (8), and in the human H chain it contains the metal-binding site referred to as the ferroxidase center. The metal ligands (Glu27, Tyr34, Glu61, Glu62, His65, Glu107, and Gln141) are highly conserved in mammalian H chains and in ferritins from plants and bacteria (Fig. 5). The structure of the site is remarkably similar to that of di-iron enzymes which activate dioxygen, such as the R2 subunit of *E. coli* ribonucleotide reductase and the hydroxylase component of methane monooxygenase (9). The enzymes use iron as a catalyst and the di-iron complex is stable, whereas ferritin uses iron as a substrate and the complex is transient. In EcFTN a third iron-binding site has been identified in a nearby position (36). In the EcBFR, five of the eight residues are conserved and bind metal in a structure slightly different from the one of EcFTN (2). In the dodecameric ferritin from *L. innocua*, the core of the helical bundle is hydrophobic and no metal-binding sites are present. However, two symmetry-related iron-binding sites have been identified toward the inner surface of the molecule along the dimer interface (28). Each iron is coordinated by a Glu and an Asp on the B helix, by a His on the A helix of the facing subunit, and by a water molecule. It is suggested that these sites may act as ferroxidase centers, and a model of a di-iron similar to that of the human H ferritin has been proposed. The ligands are conserved in the members of the DPS family, implying that the ferroxidase activity may be associated with all these proteins.

The BFRs, as isolated, contain heme with a unique bis-methionine coordination (2). The crystallographic structure of EcBFR showed that the heme is located at the twofold axis interface with two Met52 of the neighboring subunits as ligands. Interestingly, horse spleen ferritin can also bind protoporphyrin IX at the same interface in the similar inter-subunit cleft (37), and the site was found to be occupied by betaine in the crystallographic structure of bullfrog L ferritin (8), a compound added during the purification procedure. It is unclear how these molecules reach this site—whether the protein shell is sufficiently flexible to allow their passage or if the molecule partially dissociates. Horse ferritin was shown to demetallate heme before the incorporation of protoporphyrin IX, but the physiological significance of this is unclear (37). The presence of heme in BFR seems to facilitate reductive iron release from the ferritin, but it does not seem to have an effect on iron oxidation.

C. The Mineral Core

The mineral core of natural ferritins is highly variable both in size and in the content of inorganic phosphate. The electron-dense cores seen in transmission electron microscopy can reach up to 8 nm in diameter, which is close to the diameter of the protein shell cavity. They are mostly single crystallites, but multiple granules and amorphous regions are also observed. The cores of mammalian ferritins are made of ferrihydrite ($5\text{Fe}_2\text{O}_3 \cdot 9\text{H}_2\text{O}$) with various degrees of crystallinity. This is a precursor to more stable minerals which are formed after the loss of water or which may

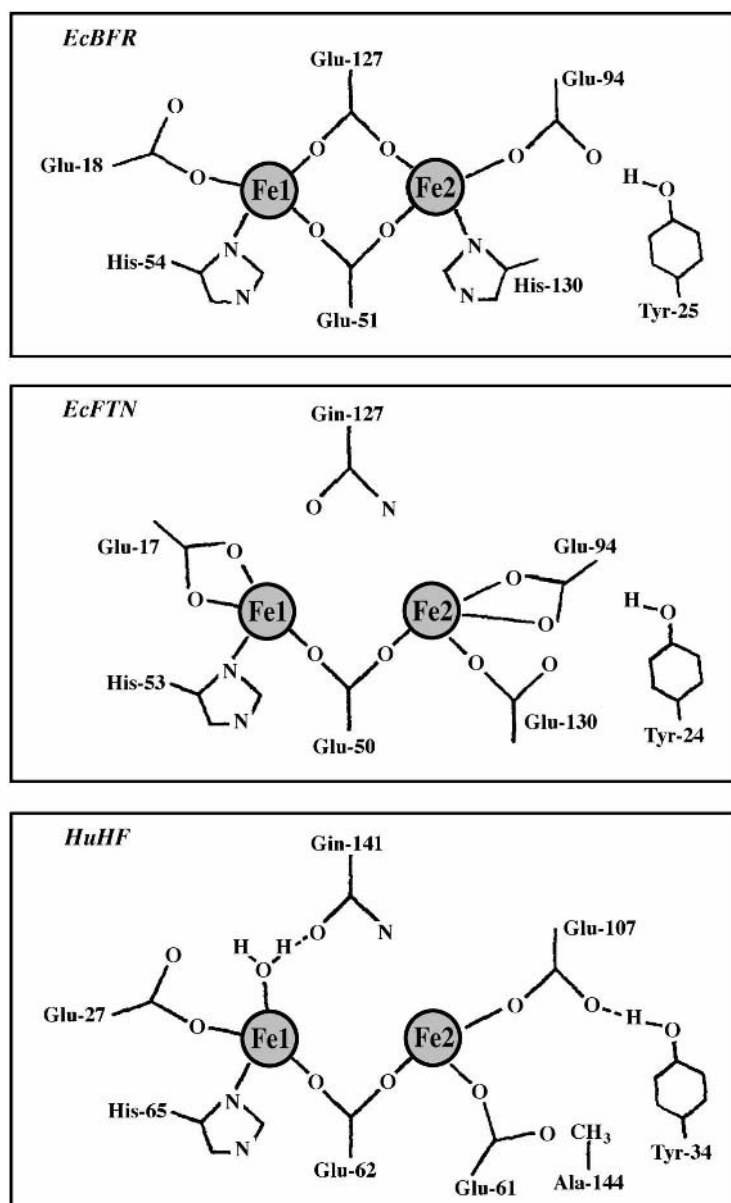


Figure 5 Schematic drawing of the dinuclear metal sites of human H, EcBfr, and EcFtnA ferritins. (From Ref. 2.)

precipitate from solution in the absence of ferritins. In the ferritin core each iron is surrounded by 5–6 oxygen atoms at a distance of 0.193 nm (38), suggesting that some iron atoms are tetracoordinate. The hydration and the rather disordered structure of the ferrihydrite structure probably account for the lower stability compared to that of other iron oxides and is probably important for the mobilization of ferritin iron (39). It was calculated that in a half-replenished ferritin (2000 iron atoms per mol-

ecule), about 40% of the atoms are exposed on the surface. This may further facilitate iron mobilization.

Most natural ferritins contain phosphate in an amount that is dependent on the biological source, and ranges from 44 Fe/Pi in the limpet *Patella laticosata* to 1.7 Fe/Pi for that of the bacterium *Pseudomonas aeruginosa* (40). Horse spleen ferritin has an intermediate ratio of about 1 phosphate per 10 iron atoms, with the phosphate bound on the surface of the core (41). In contrast, in the phosphate-rich bacterial ferritins the phosphate is uniformly distributed in the mineral core, which has a less ordered structure. The iron-to-phosphate ratio appears to reflect the composition of the medium from which it was formed and is not a property of the protein itself, since all ferritin types form ferrihydrite cores when reconstituted in vitro in the absence of phosphate. In fact, the phosphate content can provide an indication of the site of synthesis of the core. The low content in mammalian ferritin may suggest specific cellular compartmentalization, while the high phosphate of plant ferritin indicates that iron is incorporated into the protein when inside the plastids (42). It was found that under specific and anaerobic conditions a constant layer with P:Fe 3:1 can be deposited on the surface of the mineral core of horse spleen ferritin, which is remarkably similar to that of the natural protein. The layer was found to “float” on the surface of the mineral core after core enlargement and shrinking under nonreducing conditions (41). This layer may protect the ferrihydrite mineral core from transformation to other iron oxyhydroxides, and its iron seem to be more easily available to reductive mobilization. Thus, phosphate is a biological component of ferritin which may regulate its bioavailability and create new binding sites for Fe(II), but its biological role has not yet been assessed.

IV. THE IN-VITRO PROCESS OF IRON STORAGE

A. Iron Entry

Ferritins are designed to accommodate and maintain in solution iron granules which are otherwise insoluble. To accomplish this function they must be able to attract iron inside the cavity and induce its precipitation. Iron(III) complexed to citrate or other chelators binds ferritin up to 1 atom per subunit (32), but is not competent to form the mineral core. Iron(II), which is more soluble and unstable at physiological pH in the presence of oxygen, is readily taken up by the ferritins in vitro to form a product which is similar to the natural ferritins. This reaction has been studied extensively as a model of ferritin functionality. The aerobic formation of the iron core is a complex process which involves iron entry into the cavity, its oxidation, and mineralization. The most likely main sites of entrance of iron to the cavity are the hydrophilic channels on the threefold axes, which in most ferritins are lined in the narrowest part by conserved hydrophilic residues (Asp131 and Glu134 in the human H-chain sequence). The entry can be facilitated by the electrostatic field pointing to the channels and directed toward the interior cavity (34). This hypothesis is supported by experimental evidence: Fe(II) ions were found to compete with Cd(II) bound in the channels in horse spleen ferritin (43), Tb(III) was found to bind specifically to the site and reduce iron incorporation, and various mutational studies in which the two carboxyls were substituted with basic (His or Lys) or hydrophobic (Ile and Phe) residues resulted in about 50% reduction in efficiency of iron incorporation into

human H and L ferritins (32). In addition, closer to physiological conditions, when iron was supplied as Fe(II) citrate, the mutations of the metal-binding site on the channels totally prevented iron incorporation (44). Thus, the metal-binding sites on the threefold channel seems to have an active role in sequestering iron from solution and transporting it into the cavity.

Besides iron, other species may exchange with the cavity. These include protons which are generated during the reactions of iron oxidation and hydrolysis, phosphate, and negative ions, and possibly also chelating agents which mobilize iron. In addition, it has been shown that heme can gain access to the cavity to bind to a specific site along the twofold axis between two subunits (37). This may imply a large flexibility of the channels, although they are made by the contacts of α helices. A direct approach to studying ferritin permeability used electron paramagnetic resonance spectroscopy and gel permeation chromatography (45). Negatively charged, small nitroxide spin probes do not penetrate the molecule, whereas positively charged ones do, and apolar ones bind to ferritin but do not enter. The diffusion is not passive, the driving force being the concentration and charge interactions between the diffusant and the protein. The kinetics of diffusion are notably slow, with a half-time of 21–26 min. The analysis has been extended to recombinant proteins and to the study of efflux out of as well as influx into the molecule (46). They showed that the selective modification of two residues (D131H and E134H), which alter the electrostatic properties of the threefold channels, also allowed the entry of negatively charged probes, confirming that this is the entry to the protein cavity. Kinetic measurements demonstrated that the diffusion across the protein is slow, implying that ferritin is relatively impermeant to small molecules. The high energy for probe influx–efflux indicates a considerable frictional drag to transversing the channel. It was also observed that the rate of efflux is highly dependent on temperature and time of preincubation, an observation that indicates the presence of two populations of probes inside the protein, one likely associated with the iron core and the second probably engaged in transversing the channels. Thus, exchanges with the protein cavity are governed by the restrictive nature of the channels and by the binding properties of the mineral core (46).

B. Iron Oxidation

Under the conditions used to study ferritin functionality *in vitro*, Fe(II) spontaneously undergoes oxidation, with the formation of oxyhydroxide products structurally different from the ferrihydrite formed inside the ferritin. The reaction is affected by the type of buffer and pH of the reaction, and is strongly accelerated by the presence of Fe(III) due to surface catalysis of the ferric hydroxide (47). Ferritins of the L type do not significantly affect the reaction rate, but confine it specifically to the cavity (33). On the other hand, H-type ferritins accelerate the reaction several fold and, more important, change the stoichiometry of the reaction, with the oxidation of two Fe(II) atoms per dioxygen molecule and the transient production of hydrogen peroxide (48). In the absence of the ferritin catalytic site, four Fe(II) atoms are oxidized per dioxygen molecule, and water is produced. The spontaneous and the ferritin-catalyzed iron oxidations compete, and to observe the ferritin ferroxidase reaction the Fe(II) concentration must be low (100 μ M or lower) and comparable to that of

the ferroxidase sites (47). However, the two may both contribute to the deposition of the iron core because at high Fe(II)-to-protein ratios and when the incipient iron core has been formed, the reaction pathways shift from the ferroxidase to the mineral surface mechanism, at least under the conditions studied *in vitro*. The stoichiometry of iron oxidation for the human and horse ferritin has been recently determined by Yang et al. (48), who developed a system to follow proton release and oxygen consumption during the progress of the reaction. One proton per Fe(II) atom was released at the ferroxidation step on the ferroxidase center. A second proton was released at the hydrolysis step of iron in the cavity, and the ferroxidase center was then liberated. Once the core of about 100 atoms was formed, the iron oxidation and hydrolysis reaction proceeded directly on the core surface with the formation of water and a stoichiometry of 4 Fe(II) per oxygen.

Some of the intermediates of the oxidation reaction have been identified. The first event, which occurs rapidly after the addition of 48 Fe(II) atoms to human H or bullfrog H and M ferritins, is the transient formation of a blue intermediate which forms and decays within a few seconds. That produced by the bullfrog M ferritin was subjected to extensive examination by trapping with freeze-quenching techniques at 25 ms and 1 s after iron addition. It was originally attributed to an Fe-tyrosyl complex, but was later found to consist of a peroxodiferric complex with spectroscopic properties similar to those of other di-iron enzymes (9). Further analyses with X-ray absorption spectroscopy revealed an Fe-Fe separation of 0.23 nm, which is much shorter than that observed in other enzymes (0.31–0.4 nm). The short Fe-Fe distance implies differences in bond angles which should weaken the Fe-O bond and strengthen the O-O bonds, thus favoring the release of hydrogen peroxide and the formation of μ -oxo diferric mineral precursor (49). This helps to explain how ferritins use the binuclear iron centers as a substrate, while the structurally similar di-iron centers act as catalytic cofactors in dioxygen activation in enzymes, such as methane monooxygenase, the R2 subunit of ribonucleotide reductase, and the stearyl-acyl carrier protein Δ -9 desaturase. More subtle structural differences at the site may explain the different rates of the formation and decay of the peroxodiferric intermediate, such as the ones observed between tadpole H and M ferritins (49).

A second intermediate of the reaction was observed within 30–60 s after Fe(II) addition and had absorption bands at 305–310 nm and 340–350 nm, typical of the μ -oxo-bridged Fe(II) dimers expected to occur after the initial oxidation step (48,50). Studies on human H and horse spleen ferritins have shown that the Fe(III) dimers spilt before moving to the cavity. This may occur by the addition of water to the oxo bridge, and the mobility of the monomeric iron complexes may be increased. Initiation of the building of the core involves iron binding to exposed residues at the putative nucleation site in the cavity, which is located in the proximity of the ferroxidase center. Addition of further Fe(III) ions produced at the ferroxidase center allows the buildup of a single core per cavity.

C. Turnover at the Ferroxidase Center

The activity of the ferroxidase center is regenerated only after the iron has moved to the cavity, and this is a slow process. It was found that human H ferritin regained total activity several hours after a first Fe(II) addition (51), or after 10 min or longer,

if the reaction was done at 37°C (48). The rate of regeneration measured by oximetry was faster in molecules containing L chains, such as horse spleen ferritin, with a preformed iron core (48). Thus, the presence of L subunits in the ferritin hybrids not only facilitates iron nucleation-hydrolysis, but also promotes the reutilization of the H-chain ferroxidase center.

The reaction of iron oxidation in EcBFR seems to be analogous to that of vertebrate ferritins, although a mononuclear Fe(III) product was observed soon after Fe(II) addition (52), whereas that in EcFTN differs in some crucial aspects. The protein shows three iron-binding sites per subunit. Two of them, called A and B, are localized at the dinuclear center within the four-helix bundle like the H chains. The third, C, is nearby, on the inner surface of the protein (36,53). The presence of this third iron-binding site is not essential for fast iron oxidation, but causes the Fe-to-O₂ ratio to increase from 2, as in the H-ferritins, to 4, with the production of water instead of hydrogen peroxide. This probably occurs because some of the iron remains at the oxidation site. A study with variants in which the site had been abolished by site-directed mutagenesis showed that the C site binds the iron oxidized at the A–B sites and does not participate in iron nucleation, and probably retards it (36). In addition, by tightly binding the oxidized iron, the site also delays return of the activity of the ferroxidase site. Thus, the C site reduces, without abolishing, ferritins efficiency at building up an iron core and functioning as an iron storage protein. In fact, the protein incorporates iron *in vivo* (54). The site also achieves iron oxidation in a safer manner without the production of hydrogen peroxide, which may induce oxidative damage in the cells.

D. Redox Centers on Mammalian Ferritins

Fe(II) inside the cavity of natural mammalian ferritins can be oxidized under anaerobic conditions by large molecules such as oxidized cytochrome *c*, a result that implies a redox mechanism in the protein itself (55). Microcoulometric titrations indicated that apo-horse spleen ferritin contains six redox centers that can be fully oxidized or fully reduced. The sites are slowly re-oxidized by dioxygen, or more readily by ferric cyanide or cytochrome *c*, and can react with Fe(II) and Fe(III) depending on their redox status (55). A more recent analysis of various preparations of horse spleen and rat liver ferritins with different H-subunit content showed that their redox reactivity correlated with the H-subunit composition. However, the redox reactivity was absent in the recombinant ferritin homopolymers made of H and L chains, and was present in the heteropolymers reconstituted by *in-vitro* renaturation of different proportions of H and L chains. The redox activity reached a maximum in molecules with an H:L ratio of 1:1, suggesting it occurs as a result of interactions along the twofold axes of the H–L subunit dimers, with the assumption that heterodimers are made preferentially over homodimers. This hypothesis is supported by the finding that the single and conserved tryptophan in the H chain, which is located near the twofold axis, is essential for redox activity (56). The structural localization of the redox sites on the twofold axis is similar to that of heme in BFRs, and it was speculated that they may have a similar function in facilitating ferritin iron release. Alternatively, they may assist the ferroxidase activity in transporting electrons away during iron oxidation.

V. FERRITIN GENE STRUCTURE AND EXPRESSION

A. Gene Structures

1. Human Genes

About 15–20 H ferritin gene homologs have been identified on chromosomes 1, 2, 3, 6, 13, 17, 19, 20, and X. The functional gene is localized in the q13 region of chromosome 11, and is composed of four exons and three introns. It produces a transcript of 1.1 kb, although a second transcript of 1.4 kb has been found in the brain, probably produced by alternative splicing (57,58). Most or all of the remaining ferritin-like sequences are intron-less pseudo-genes probably produced by retrotranscription. Those located on chromosome 3, in the region of many iron-binding proteins such as transferrin, lactoferrin, and transferrin receptor, and on chromosome 6, near the gene for hereditary hemochromatosis, appeared particularly interesting for their strategic position, but their functionality has not been demonstrated (59). The functional gene for L ferritin is on chromosome 19q13.3-q13.4 (60). It has structural properties similar to the H gene. An additional seven ferritin-like genes, probably pseudo-genes, are on chromosomes 20 and X.

2. Mouse Genes

The mouse genome contains four sequences homologous to the H ferritin gene, located on chromosomes 3, 6, and 19 (61). The functional one is probably on 19, and it has been cloned and characterized. It is very similar to the human gene, with four exons and three introns. The functional L gene has also been cloned and characterized (62). It covers a length of 1.8 kb and has four exons and three introns, like the human gene. Its chromosomal location has not been identified. Another 10–14 L-ferritin-like sequences are present in the genome on different chromosomes. All are probably pseudo-genes.

3. Other Ferritin Genes

The genomic structure of the mammalian ferritins so far characterized is highly conserved, with three exons in the coding sequence that correspond to secondary structure domains of the protein, but this is not a general feature of ferritin genes. In higher plants (soybean, maize, and *A. thaliana*) the ferritin genes contain seven introns, none of which is in the same position as the corresponding mammalian ones, and in the plant genes the intron position is not related to triplet codon or to protein structure (63). In *Drosophila melanogaster* the Fer1HCH and Fer2LCH genes which encode homologs of the H and L chain, respectively, are closely clustered. Fer1HCH has three introns and Fer2LCH has two introns in positions that interrupt the coding region differently from those in other known ferritin genes. They also have putative metal-responsive elements and NF- κ B-like binding sites (19). The two ferritin genes in the nematode *Caenorhabditis elegans* are located on chromosomes I and V, and have two introns, one of which interrupts the coding sequence in the same position as the sixth intron of maize ferritin genes. They lack iron-responsive elements (IREs) (19). The data indicate a large divergence in gene organization and mechanisms of regulation of ferritin synthesis in the phyla.

B. Regulation of Ferritin Expression in Mammals

The iron-dependent regulation of H and L ferritin expression acts mainly at a post-transcriptional level through the interaction of the IRE structures on the transcripts with iron regulatory proteins (IRPs), as described elsewhere in this book (see Chapters 9 and 10). The different ratios of H-to-L chains in the various tissues is determined mainly at a transcriptional level, although posttranscriptional regulatory steps also cannot be ruled out.

1. Regulatory Elements of the H Chain

The mouse ferritin H gene has received much attention from various laboratories. It contains a minimal promoter of 140 bp, which includes a TATAA box (at -28 bp), a CCAAT box in reverse orientation (at -61 bp), and two Spl sites (at -84 and -128 bp) (64). This promoter is sufficient to induce strong expression of the gene. A similar promoter structure has been found in the human H gene (65). An additional regulatory site has been localized between -5000 and -300 bp (64,66). A transcriptional activator has been found in a 160-bp fragment 4.1 kb upstream from the transcription start site, with five binding sites for different factors. It contains, in the proximal part, a perfect consensus sequence for the erythroid specific factor NF-E2. The site binds NF-E2, but its mutations did not affect gene expression in differentiating mouse erythroleukemic (MEL) cells, and its functionality is unclear (66). The central part of the 160-bp fragment contains an element of transcriptional repression of the adenovirus E1A which includes two sequences, one of AP1 type, and the other an element with a symmetric dyad of 22 bp (67). The dyad binds a complex sp1/sp3, and the AP1-type sequence binds the activation complex junD/fosB/ATF1 (68). A study with reporter genes for the regulating sequences and mutated proteins E1A and P300 proposed a model for repression by the oncogenes (69). It suggests that in the absence of E1A the complex sp1/sp3 and junD/fosB/ATF1 binds the distal regulatory element and associates with P300 and CBP, with the formation of a complex with the initiation of transcription complex (ITC) on the TATAA box of the minimal promoter. This determines a strong expression of the H genes due to the secondary recruitment of a histone acetylase at the level of the P300/CBP complex. The presence of E1A limits the formation of the complex between distal and proximal promoters and reduces ferritin expression.

Another zone of transcriptional activation is on a 40-bp fragment -4.7 kb upstream of the transcription initiation site. It carries a response element to tumor necrosis factor- α (TNF- α), which corresponds to members of the NF- κ B family (70). The proximal site has a perfect consensus sequence which may bind a dimer P66/P50, while the other site has a sequence that differs from a consensus and may bind another dimer of the family Rel/NF- κ B, such as Rel/P50.

The distal regulatory region of the human H gene has not been investigated, but other relevant regions have been identified. Studying differentiating Caco2 cells, a transcriptional activation element was found in the region -62 to -45 of the promoter, and named Bdf (65). It binds a complex of 120 kDa which contains the trimeric factor NFY which binds the CCAAT box, and recruits the proteins P300 and CBP. The association is stimulated by cAMP (71,72). The complex P300/CBP recruits the histone acetylase P/CAF, which destabilizes the structure of nucleosomes and activates transcription. This mechanism explains the upregulation of H ferritin

expression in response to cAMP. The proposed mechanisms for human and mouse H-chain regulation involve the acetylation of histones in the proximal promoter involving the complex P300/CBP/histone acetylase, which seems a key point for the control of H-ferritin transcription in the two species. The distal regulatory site of the human gene has not been studied.

Another regulatory element which confers transcriptional regulation by heme in Friend leukemia cells and in monocyte-macrophages is located -77 nucleotides upstream from the TATA box. This element binds a heme-responsive factor (HRF) protein complex which contains the ubiquitous transcription factor NFY (73). It was shown that subunit A of NFY is necessary for transcriptional heme activation and is differentially expressed in heme-treated cells. Human H-ferritin promoter was found to contain an Inr element, the domain involved in the transcriptional repression by the proto-oncogene *c-myc* (74). Point mutations in the Inr element or modifications of the *c-myc* protein abolished the suppressive effect of *c-myc* on H-ferritin expression, and it has been shown that the suppression is required for cellular transformation by *c-myc*.

2. Regulatory Elements of the L Chain

The mouse gene has an organization similar to that of the H gene, with a TATA box -34 bases from the transcription site, two CCAAT boxes in opposite orientation at -84 and -127 , and a consensus site for SP1 at -232 . Deletion experiments suggest the presence of a distal regulatory element between -450 and -1200 upstream from the transcription start site (62). An antioxidant-responsive element (ARE) was found in the promoter of the mouse gene, consisting of 20 base pairs that bind a protein dimer named ARE-BP1 and mediate induction of transcription by antioxidant agents (75). A similar element is found in the promoters of hemoglobin and heme oxygenase genes, and may be present in the distal promoter of the mouse H-ferritin gene.

The identified regulatory elements in ferritin genes partially explain the distinct transcriptional regulation of the two subunits in the same tissue, such as TNF- α -induced upregulation of H ferritin in myoblasts (76), the increase in H ferritin during MEL cell differentiation induced by dimethylsulfoxide (DMSO) (77), and the alteration of ferritin expression in various organs of the rat following chemically induced oxidative stress (78). The relative increase in L-chain content in liver following iron loading is partially explained by a liver-specific L-ferritin upregulation at a transcriptional level reported in rat (79). The responsible promoter element was not analyzed in detail.

3. Translational Regulation

Undoubtedly, the well-characterized IRE-IRP system is the major translational regulatory mechanism for ferritin, but others have been reported. Rogers reported that the ferritin upregulation induced by interleukin- 1β in hepatoma cells was conferred by 60 nucleotide translational enhancer elements which are 39% identical in H- and L-chain transcripts and located in the 5' untranslated flanking regions of the transcripts. The motif is similar to that found in the 5' leaders of other acute-response mRNAs (80). More recently it was found that human ferritin H-chain mRNA contains in the 3' untranslated region a pyrimidine-rich sequence that interacts with protein factors present in monocytic THP-1 cell lines (81). The binding protein, of about 43 kDa, is a mRNA destabilizer, and its downregulation following PMA treat-

ment of THP-1 cells partially explains the observed increase of H-ferritin synthesis. The factor, which is absent from HeLa or hepatoma PLC cells, may be important in the regulation of H-ferritin expression in myeloid cells (81), suggesting tissue specificity.

C. Regulation of Ferritin Expression in Other Animals

The translational IRE-IRP system seems to be important for the iron-dependent ferritin expression in most animal ferritins, with some exceptions, such as the yolk ferritins from *Lymnaea stagnalis* and *Schistosoma mansoni* (2). However, other mechanisms also operate. For instance, in the yellow fever mosquito, iron also seems to induce also ferritin transcription (82), and in *Drosophila melanogaster*, iron and development regulate the alternative splicing of the ferritin H-chain homolog mRNA with the accumulation of forms that lack the IRE element (15,83).

D. Regulation of Ferritin Expression in Higher Plants

In plants, ferritin accumulates mainly in nongreen plastids of roots and leaves of young plantlets, and its expression is regulated by development and by iron. Detailed studies on the iron-dependent regulation showed that it acts at a transcriptional level, and that the activity may not be a direct one, but possibly mediated by chemical factors. In maize, a class of ferritin genes responds to abscisic acid, a hormone involved in stress response. Another class of ferritin genes responds to iron in the presence of H₂O₂, and the response is antagonized by antioxidants such as N-acetylcysteine or by Ser/Thr phosphatase inhibitors (84). This suggests that ferritin expression is tightly regulated by reactive oxygen species and oxidative stress. The identification of an iron-responsive element which controls the iron-mediated derepression of the soybean ferritin gene was recently reported (85). The element has no obvious homology with other promoters and binds trans-acting factors of cell extracts. Interestingly, this element responded to the physiological iron citrate complexes, but not nonphysiological Fe(III) ethylenediammetetracetic acid (EDTA). Thus, in higher plants and animals, mechanisms of iron-dependent ferritin regulation, as well as ferritin's cellular localization, are very different.

VI. BIOLOGICAL ROLES OF FERRITINS

A. Functions in Microorganisms

The easy recognition and isolation of ferritins from a large number of different organisms led to the suggestion that they are ubiquitous and possibly essential for all living cells that use iron. The suggestion may now be verified by analyzing the data produced by the genome projects. In the present complete and annotated genomic sequences of 21 representative unicellular organisms, FTN-like or BFR-like genes are found in nine species, and four other species have DPS-like sequences (86). Some organisms have multiple copies of genes for ferritin-like molecules, while eight have none, among which is notable *Saccharomyces cerevisiae*. Thus, ferritins are neither essential nor ubiquitous, at least in microorganisms, and alternative mechanisms may be used for protection from iron excess, such as limiting its uptake or depositing it inside vacuoles, as occurs in *S. cerevisiae* (87).

In some species, ferritins may have important biological functions, and they have been studied mainly in *E. coli*. Its genome contains one copy of Bfr, one of FtnA, and an additional gene for FtnB which is probably not functional. Bfr and FtnA were overexpressed up to 14–18% of total cellular protein content, and this determined an increase in total cellular iron content of 2.5- to 2.6-fold, in agreement with the proposed function of iron storage molecules (88). Bfr in vivo accumulates more iron than FtnA, although FtnA has faster rates of iron uptake in vitro. This suggests that FtnA and Bfr may act in short- and long-term iron storage, respectively. The two genes were inactivated singly and in combination to study their relative functions (24). Inactivation of Bfr alone did not produce an evident phenotype, while the inactivation of FtnA alone or in combination with Bfr reduced the iron content of cells grown in the stationary phase of growth. It had no effect in the log phase of growth or in iron-low medium. The reduction in total iron content was attributed to Fe(III) associated with ferritin. The work indicated that only a minor proportion of iron was associated to Bfr. The iron stored in FtnA appeared important to promote cell growth in iron-poor medium, particularly when the cells were precultured to stationary phase in iron-rich medium. The capacity should be important for bacteria, such as *E. coli*, that occupy environments where iron availability is variable, and is fully consistent with the role of storage of iron for future needs. Neither the deletion of the two genes nor their overexpression affected the sensitivity of the cells to the damaging effects of H₂O₂. However, when the level of redox-active iron was increased by the inactivation of the *fur* gene, the sensitivity to hydrogen peroxide increased following the deletion of FtnA and Bfr (24). These data are in partial agreement with the observation that inactivation of bacterioferritin in *Brucella melitensis* had no effect on survival and growth in human macrophages (89), while inactivation of ferritin in *Campylobacter jejuni* reduced resistance to redox stress and growth under iron-limiting conditions (90). The data support the hypothesis that ferritin in bacteria acts as an iron storage protein which releases iron upon demand when needed, and it also interferes with cellular iron toxicity, although the pool of redox iron may be small and the balance between the iron storage and iron detoxification roles may differ largely depending on the environmental niche of the microorganism and the specific properties of the protein. The functions of Bfr remain obscure.

B. Functions in Plants

In plants, most of the iron storage needs are covered by the apoplast, the network of cell walls forming the extracellular free space of plant cells. In fact, up to 90% of iron taken up by the root is trapped inside the apoplast, and this can be utilized in a period of iron deprivation (22). In addition, plants may store iron inside the vacuoles, as has been shown for *Saccharomyces cerevisiae* (87), although this has not been studied in detail. Plant ferritin accumulates inside the plastids, including chloroplasts which are heavily exposed to oxidative stress during photosynthesis. This may suggest a role in the protection against oxidative stress, a hypothesis supported by the finding that its synthesis is stimulated in response to various stresses involving abscisic acid and by H₂O₂ in the presence of iron (84). In derooted maize and in *A. thaliana* plantlets, an oxidation step is sufficient to increase ferritin transcripts (91).

More direct evidence on the role of ferritins came from approaches aimed at deregulating ferritin synthesis by overexpressing them in transgenic plants either in the plastids or in the cytoplasm. The soybean ferritin gene was introduced into rice plants under the glutelin promoter to address protein accumulation specifically to the seeds (92). The exogenous ferritin was properly processed and accumulated in the endosperm at levels of 0.01–0.3% of total protein. This was accompanied by a threefold increase in seed iron content, without evident morphological modification of the seeds. This supports a role for ferritin in iron storage in the seeds, and leads to the speculation that ‘ferritin rice’ may be used as an iron supplement in the human diet (92). Transgenic tobacco plants expressing ferritin were produced by various groups. The complete cDNA of alfalfa ferritin was placed under the rubisco and the viral CAMV 35S promoters for expression in vegetative tissues. It was found that the protein was correctly processed and accumulated in the chloroplasts, while that modified by a Flag tag accumulated in the cell extract (93). The transgenes exhibited a higher resistance to high levels of iron, to paraquat toxicity, and to necrotrophic pathogens, indicating that ferritin overproduction in leaves increases tolerance to oxidative damage. No evident effects on photosynthetic activity were reported (93).

In other studies, soybean ferritin cDNA, with or without the transit peptide sequence, was placed under the control of the CAMV 35S promoter, and in the tobacco transgenics ferritin accumulated inside the leaves (94,95). This was accompanied by an increase in leaf iron content and by increased root ferric reductase activity, which is an index of increased iron uptake and of plant iron starvation. The ferritin overproduction produced leaf yellowing, decreased chlorophyll content, and increased resistance to methyl viologen, a free-iron-dependent herbicide (96). The effects were comparable in the transgenics in which ferritin was directed to the chloroplasts or to the cytosol. Ultrastructural examination of the transgenics revealed chloroplast alterations similar to those observed in iron-deficient control plants, despite the increase in iron content. In addition, an increase in the activity of enzymes involved in oxygen detoxification (catalase, ascorbate peroxidase, guaiacol peroxidase) was observed, with a remarkable two- to threefold increase in glutathione reductase activity (96). This finding suggests that the protective effect of ferritin against oxidative damage may not be linked simply to iron sequestration, but may also be secondary to the activation of these protective enzymes, possibly triggered by iron starvation.

C. Functions in Mammals

In mammals, ferritin retains a large proportion of total body iron, and acts mainly as an iron storage protein that withholds iron excess and releases it upon demand. Its localization is mainly cytosolic. Thus, it is in contact with the small labile iron pool necessary for the synthesis of iron enzymes, and which is potentially toxic for its capacity to catalyze reactive oxygen species through Fenton-like reactions. Ferritin readily sequesters iron from the labile iron pool, and slowly recycles it back to the cytosol after degradation in the lysosomes (97). Thus, an approach to studying the relationship between ferritin and the labile iron pool was to expose cells to acute iron loads, which upregulated ferritin synthesis, and determine accumulation over the immediate needs of iron storage for a period of one or two days. Using this approach, it was shown that ferritin overexpression had a protective effect against

the oxidative damage induced by H_2O_2 and heme on endothelial cells (98). Similar results were obtained with murine and human leukemia cells using various different types of oxidative insults (99). Cells enriched in apoferritin via pinocytotic uptake showed similar hyperresistance to oxidative stress, and artificial downregulation of the H ferritin using antisense oligonucleotide resulted in the diminution of the hyperresistance to the stress (100). The data indicated that ferritin, particularly the H chain, when produced in excess, has the capacity to sequester and incapacitate the redox-active iron pool. It was also shown that ultraviolet A radiation upregulated heme oxygenase, and this liberated heme iron which eventually upregulated ferritin synthesis, with the effect of lowering the prooxidant state of the cell (101). However, simple ultraviolet A irradiation was also reported to induce immediate proteolytic ferritin degradation and release of prooxidant ferritin iron in a human primary fibroblast cell culture (102), although it seems unlikely that the insoluble iron of the ferritin core is readily available to enter the labile iron pool. In summary, ferritin seems to act normally as an antioxidant, but under stress conditions it may have prooxidant activity.

A peculiarity of the mammalian ferritins is the occurrence of hybrids of H and L chains that cooperate functionally. This complicates the study of the specific roles of the two gene products. In fact, one may consider that ferritin functionality is related both to the total number of ferritin molecules, or ferritin cavities, which determines the total cellular iron storage capacity, and also to the number of H chains containing the catalytic ferroxidase centers that can regulate cellular iron redox activity. In addition, in-vitro data suggest that the relative activity of the ferroxidase centers is higher in L-chain-rich molecules (35,48), and thus the presence of L chains should attenuate the biological effects of the variations in total H-chain content (31). Moreover, the iron-dependent IRE-IRP system acts equally on both subunits. These observations suggest that the artificial deregulation of the expression of the two chains may provide more direct evidence of their specific biological roles. When COS cells were transiently transfected with human ferritin H- and L-chain cDNAs, the ferritins accumulated in large amounts, up to 1000-fold over background, without signs of toxicity, but this did not determine any evident effect on cellular iron metabolism, monitored by cellular and ferritin iron uptake and by IRP activity (103). In addition, the exogenous subunits did not co-assemble with the endogenous one. Possibly the fast synthesis of the deregulated ferritin did not allow equilibration with the pool of endogenous ferritin subunits, or the time scale to observe ferritin effects is longer than that allowed by the system. It was concluded that the transient transfection approach is not informative about the biological functions of ferritins.

An opportunity to analyze the biological roles of the isoferritins came from the identification of the hereditary hyperferritinemia cataract syndrome (HHCS), in which mutations of the IRE sequence of L-chain mRNA determine a constitutive upregulation of L-ferritin synthesis in all tissues (104; see also Chapter 31). This does not cause apparent abnormalities in iron metabolism in the subjects, and cells derived from these patients have normal iron uptake and accumulation, despite a 10-fold enlargement of the ferritin compartment and cellular iron storage capacity (105). The tissues accumulate large amount of L-chain homopolymers which do not incorporate any iron. This is consistent with the in-vitro evidence that the L chain has no catalytic activity and does not perturb iron metabolism, and it also indicates that cellular iron availability is regulated by the total amount of H subunit, which is

unchanged in the HHCS cells, rather than by the iso-ferritin amount and concentration.

Beaumont's group produced stable lines of MEL cells transfected with mouse ferritin H-chain cDNA in which the IRE sequence was mutated in order to overexpress the ferritin constitutively (106). The cells accumulated H ferritin up to five- to sixfold over background. This was accompanied by a downregulation of the L subunit, leading to a large shift in iso-ferritin composition. The cells showed an iron-deficient phenotype, with a significant increase in IRP activity, upregulation of transferrin receptor synthesis, and repression of heme and hemoglobin synthesis. Analysis with the fluorescent metal sensor calcein showed that in the transfected cells the intracellular labile iron pool decreased from 1.3 μM to 0.56 μM , and they had a higher iron-buffering capacity following iron loading (107). Total iron content was comparable in the transfected and untransfected cells, and in the cells with higher H ferritin content a challenge with H_2O_2 induced a lower production of reactive oxygen species and lower cell mortality than in the cells with normal ferritin content (108). In addition, it was reported that the overexpression of H ferritin induced multidrug resistance properties to the cells, increasing cell resistance to cyclosporin. The significance of this is unclear.

We have subcloned the cDNAs for human L, H, and H mutated (with an inactivated ferroxidase site due to the substitutions E62K and H65G) under the inducible Tet-off promoter and obtained stably transfectant HeLa cell lines (108a). Under repressed conditions, in the presence of doxycycline, the cells behaved like the controls, but when ferritin synthesis was induced by the withdrawal of the drug, ferritin levels increased to 14- to 16-fold over background. This resulted in no evident phenotype for the L- and the H-ferritin mutant cells lines, while the H-ferritin clone exhibited a marked increase in IRP activity, of transferrin receptor, and of Fe-transferrin uptake, indices of cellular iron deficiency. In addition, they showed strongly reduced cell growth and higher resistance to H_2O_2 . All these effects were abolished by a prolonged growth in medium supplemented with ferric ammonium citrate to circumvent iron deficiency. The data suggest that the H-ferritin role in HeLa cells is tightly linked to the ferroxidase activity and this regulates iron availability for oxidative damage and enzymes related to cell proliferation. They also confirm that H-subunit homopolymers, although competent in incorporating iron inside the cell, are about fivefold less efficient than the H/L heteropolymers. This finding is in agreement with the in-vitro data, and confirms the evolutionary advantage of having two subunit types.

Overexpression of H ferritin in human lymphoid cells was shown to inhibit the clonogenic effect of the protooncogene *c-myc*, and overexpression of *c-myc* itself reduced H-ferritin expression at a transcriptional level (74). The finding that *c-myc* also upregulates IRP2, which is a ferritin suppressor and a regulator of the labile iron pool, suggests that the ferritin effect is also iron-mediated in this case.

Another way to study ferritin functionality is to reduce or abolish its expression. This was done for the H subunit by producing knockout mice (109). The observation that H-ferritin subunits are expressed in embryonic stem cells (ES) allowed the use of a promoterless targeting vector which increased the efficiency of selection. The mice that were heterozygous for the deletion were healthy, without evident alteration of iron metabolism, while the H-ferritin knockout mice died at an early stage of embryonic development, between day 3.5 and day 9.5. This indicates that the H-

ferritin function is nonredundant and cannot be substituted by the L chain. It also indirectly confirms that the various H-ferritin-like genes in the genome are nonfunctional pseudo-genes. In addition, the finding demonstrates that H ferritin is necessary in some essential steps of early embryonic development. The step has not been identified, and we can postulate that it may involve iron compartmentalization and (or) toxicity caused by the lack of a functional iron storage function, or to a possible role of H ferritin in iron transfer to the embryo. A complete analyses of ferritin functionality awaits the inactivation of the L-ferritin gene, and work is in progress in this direction.

VII. FERRITIN AS AN IRON TRANSPORTER

The high iron-binding capacity of ferritin makes it potentially a very efficient vehicle for iron, and it is apparently used as such in insects. In mammals, ferritin can be actively secreted, as shown by the presence of glycosylated ferritin in the serum and body fluids, but biochemical analyses show that serum ferritin is an iron-poor molecule (110). Serum ferritin is composed mainly of the L subunit, a portion of which is glycosylated, and this may explain its low capacity to incorporate iron. The hypothesis that serum ferritin is not a major iron transporter is also supported by the finding that patients with HHCS have normal iron distribution.

A binding factor for ferritin which is not specific for either subunit has been identified as H-kininogen. Its function is unclear, although it may be involved in the clearance of serum ferritin (111). A membrane receptor for H ferritin has been identified on various cell lines, and up to 20,000 receptor sites have been found on K562 cells (112). Its expression is regulated by iron in the same direction as the transferrin receptor, leading to speculation that its mRNA may carry an IRE sequence. Erythroid precursor K562 cells are able to bind and incorporate H-chain-containing ferritins and can use the ferritin iron for heme synthesis (113). This suggests that the ferritin-bound iron is taken up and probably follows the same degradation pathways as the endogenous ferritin. Availability of the iron is decreased or blocked by addition of protease inhibitors to the cells (113,114). The receptor may be important for the local exchange of iron in the bone marrow or the liver, and it has been suggested that ferritin may be a necessary nutrient for embryonic development. More intriguing is the demonstration that in the brain the cells which are richer in ferritin and iron, the astrocytes, do not express transferrin receptor, but express a high density of ferritin receptor (115). This raises the possibility that this molecule plays a major role in iron redistribution in the brain, and could be involved in the altered distribution found in neurodegenerative diseases (115).

VIII. CONCLUSIONS AND PERSPECTIVES

The conserved three-dimensional structure, the capacity to incorporate iron into the cavity, and a close relation with oxidative stress seem to be the major shared properties of all ferritins. Recent data have shown large variability within these common themes: amino acid sequences diverge notably between prokaryotes and eukaryotes, and also the gene structure of the few, but representative, examples so far characterized reveal an unexpected variability, with number and localization of introns that differ in plants, invertebrates, and vertebrates. Also, cellular localization varies, being

cytoplasmic in most organisms, but within the plastids in higher plants and secretory in many insects and molluscs. In addition, the identification of ferritin-like proteins with a new structural architecture, i.e., 12- instead of the usual 24-subunit assembly, indicates a remarkable plasticity of the structural motif. Biochemical analyses have revealed notable differences in the iron uptake mechanisms between prokaryotic and eukaryotic ferritins that until recently were considered essentially analogous. Thus, ferritins appear to be interesting examples of proteins that evolved under strong structural constraints to accomplish functional needs which vary with the complexity of the organisms. The basic function seems to be conserved: withdrawal of excess iron from the cell in order to detoxify it and store it for future needs. In mammals, the presence of two subunit types which form hybrid molecules seems an interesting mechanism to regulate independently the cellular iron storage capacity and the number of catalytic ferroxidase sites for regulation of cellular redox status. How this regulation is achieved remains to be clarified. In other eukaryotes it is unclear whether hybrid molecules are formed and whether the different subunit types have functional specificity comparable to those of the mammalian H and L chains. Even more intriguing is the reason for the multiple functional ferritin genes observed in most animals and plants, which somehow contradicts the occurrence of a single nonredundant H-ferritin gene in mammals. The presence of multiple copies of ferritin or ferritin-like genes in prokaryotes, where ferritin does not appear to be essential, is puzzling. In-vitro studies have provided a wealth of information on how ferritin interacts with iron to sequester it and concentrate it in the cavity; these are probably relevant to its physiological function. Less is known of how this protein “nanobox” exchanges reagents with the solvent, and in particular how it can release iron and protons. Possibly the most interesting aspect is how ferritin regulates iron–oxygen interactions and their potentially devastating effects. In-vitro and in-vivo data indicate that ferritins play an important role in this, and the elucidation of how they achieve this difficult task in the different organisms is a challenge for the future.

ACKNOWLEDGMENTS

The work was partially supported by a CNR targeted project in Biotechnology and by Murst Cofin to Paolo Arosio. We are grateful to Gianluigi Biagetti for assistance in the study of the ferritin phylogenetic trees.

REFERENCES

1. <http://www.sanger.ac.uk/Software/Pfam/>. www-1 2000.
2. Harrison PM, Arosio P. The ferritins: Molecular properties, iron storage function and cellular regulation. *Biochim Biophys Acta* 1996; 1275(3):161–203.
3. Lawson DM, Artymiuk PJ, Yewdall SJ, Smith JM, Livingstone JC, Treffry A, et al. Solving the structure of human H ferritin by genetically engineering intermolecular crystal contacts. *Nature* 1991; 349(6309):541–544.
4. Levi S, Yewdall SJ, Harrison PM, Santambrogio P, Cozzi A, Rovida E, et al. Evidence that H and L ferritins have co-operative roles in the iron uptake mechanism of human ferritin. *Biochem J* 1992; 288(Pt 2):591–596.
5. Santambrogio P, Cozzi A, Levi S, Rovida E, Magni F, Albertini A, et al. Functional and immunological analysis of recombinant mouse H- and L-ferritins from *Escherichia coli*. *Protein Expression Purif* 2000; 19(1):212–218.

6. Harrison PM, Hempstead PD, Artymiuk PJ, Andrews SC. Structure-function relationships in the ferritins. *Met Ions Biol Syst* 1998; 35:435–477.
7. Holland LJ, Wall AA, Bhattacharya A. Xenopus liver ferritin H subunit: cDNA sequence and mRNA production in the liver following estrogen treatment. *Biochemistry* 1991; 30(7):1965–1972.
8. Trikha J, Theil EC, Allewell NM. High resolution crystal structures of amphibian red-cell L ferritin: Potential roles for structural plasticity and solvation in function. *J Mol Biol* 1995; 248(5):949–967.
9. Pereira AS, Small W, Krebs C, Tavares P, Edmondson DE, Theil EC, et al. Direct spectroscopic and kinetic evidence for the involvement of a peroxodiferric intermediate during the ferroxidase reaction in fast ferritin mineralization. *Biochemistry* 1998; 37(28):9871–9876.
10. Andersen O, Dehli A, Standal H, Giskegjerde TA, Karstensen R, Rorvik KA. Two ferritin subunits of Atlantic salmon (*Salmo salar*): Cloning of the liver cDNAs and antibody preparation. *Mol Marine Biol Biotechnol* 1995; 4(2):164–170.
11. Miguel JL, Pablos MI, Agapito MT, Recio JM. Isolation and characterization of ferritin from the liver of the rainbow trout (*Salmo gairdneri* R.). *Biochem Cell Biol* 1991; 69(10–11):735–741.
12. Yamashita M, Ojima N, Sakamoto T. Molecular cloning and cold-inducible gene expression of ferritin H subunit isoforms in rainbow trout cells. *J Biol Chem* 1996; 271(43):26908–26913.
13. von Darl M, Harrison PM, Bottke W. cDNA cloning and deduced amino acid sequence of two ferritins: Soma ferritin and yolk ferritin, from the snail *Lymnaea stagnalis* L. *Eur J Biochem* 1994; 222(2):353–366.
14. Schussler P, Potters E, Winnen R, Michel A, Bottke W, Kunz W. Ferritin mRNAs in *Schistosoma mansoni* do not have iron-responsive elements for post-transcriptional regulation. *Eur J Biochem* 1996; 241(1):64–69.
15. Lind MI, Ekengren S, Melefors O, Soderhall K. *Drosophila* ferritin mRNA: Alternative RNA splicing regulates the presence of the iron-responsive element. *FEBS Lett* 1998; 436(3):476–482.
16. Charlesworth A, Georgieva T, Gospodov I, Law JH, Dunkov BC, Ralcheva N, et al. Isolation and properties of *Drosophila melanogaster* ferritin—Molecular cloning of a cDNA that encodes one subunit, and localization of the gene on the third chromosome. *Eur J Biochem* 1997; 247(2):470–475.
17. Adams MD, Celniker SE, Holt RA, Evans CA, Gocayne JD, Amanatides PG, et al. The genome sequence of *Drosophila melanogaster*. *Science* 2000; 287(5461):2185–2195.
18. Dunkov BC, Zhang D, Choumarov K, Winzerling JJ, Law JH. Isolation and characterization of mosquito ferritin and cloning of a cDNA that encodes one subunit. *Arch Insect Biochem Physiol* 1995; 29(3):293–307.
19. Dunkov BC, Georgieva T. Organization of the ferritin genes in *Drosophila melanogaster*. *DNA Cell Biol* 1999; 18(12):937–944.
20. Ersfeld K, Craig PS. Cloning and immunological characterisation of *Echinococcus granulosis* ferritin. *Parasitol Res* 1995; 81(5):382–387.
21. Benitez L, Harrison LJ, Parkhouse RM, Garate T. Sequence and immunogenicity of *Taenia saginata* ferritin. *Mol Biochem Parasitol* 1996; 82(1):113–116.
22. Briat JF, Lobreaux S. Iron storage and ferritin in plants. *Met Ions Biol Syst* 1998; 35: 563–584.
23. Lobreaux S, Yewdall SJ, Briat JF, Harrison PM. Amino-acid sequence and predicted three-dimensional structure of pea seed (*Pisum sativum*) ferritin. *Biochem J* 1992; 288(Pt 3):931–939.

24. Abdul-Tehrani H, Hudson AJ, Chang YS, Timms AR, Hawkins C, Williams JM, et al. Ferritin mutants of *Escherichia coli* are iron deficient and growth impaired, and fur mutants are iron deficient. *J Bacteriol* 1999; 181(5):1415–1428.
25. Carrano CJ, Bohnke R, Matzanke BF. Fungal ferritins: The ferritin from mycelia of *Absidia spinosa* is a bacterioferritin. *FEBS Lett* 1996; 390(3):261–264.
26. Grant RA, Filman DJ, Finkel SE, Kolter R, Hogle JM. The crystal structure of Dps, a ferritin homolog that binds and protects DNA. *Nature Struct Biol* 1998; 5(4):294–303.
27. Bozzi M, Mignogna G, Stefanini S, Barra D, Longhi C, Valenti P, et al. A novel non-heme iron-binding ferritin related to the DNA-binding proteins of the Dps family in *Listeria innocua*. *J Biol Chem* 1997; 272(6):3259–3265.
28. Ilari A, Stefanini S, Chiancone E, Tsernoglou D. The dodecameric ferritin from *Listeria innocua* contains a novel intersubunit iron-binding site. *Nature Struct Biol* 2000; 7(1):38–43.
29. Tonello F, Dundon WG, Satin B, Molinari M, Tognon G, Grandi G, et al. The *Helicobacter pylori* neutrophil-activating protein is an iron-binding protein with dodecameric structure. *Mol Microbiol* 1999; 34(2):238–246.
30. Santambrogio P, Pinto P, Levi S, Cozzi A, Rovida E, Albertini A, et al. Effects of modifications near the 2-,3- and 4-fold symmetry axes on human ferritin renaturation. *Biochem J* 1997; 322(Pt 2):461–468.
31. Levi S, Santambrogio P, Albertini A, Arosio P. Human ferritin H-chains can be obtained in non-assembled stable forms which have ferroxidase activity. *FEBS Lett* 1993; 336(2):309–312.
32. Levi S, Santambrogio P, Corsi B, Cozzi A, Arosio P. Evidence that residues exposed on the three-fold channels have active roles in the mechanism of ferritin iron incorporation. *Biochem J* 1996; 317(Pt 2):467–473.
33. Levi S, Santambrogio P, Cozzi A, Rovida E, Corsi B, Tamborini E, et al. The role of the L-chain in ferritin iron incorporation. Studies of homo and heteropolymers. *J Mol Biol* 1994; 238(5):649–654.
34. Douglas T, Ripoll DR. Calculated electrostatic gradients in recombinant human H-chain ferritin. *Protein Sci* 1998; 7(5):1083–1091.
35. Santambrogio P, Levi S, Cozzi A, Rovida E, Albertini A, Arosio P. Production and characterization of recombinant heteropolymers of human ferritin H and L chains. *J Biol Chem* 1993; 268(17):12744–12748.
36. Treffry A, Zhao Z, Quail MA, Guest JR, Harrison PM. How the presence of three iron binding sites affects the iron storage function of the ferritin (EcFtnA) of *Escherichia coli*. *FEBS Lett* 1998; 432(3):213–218.
37. Granier T, Comberton G, Gallois B, d'Estaintot BL, Dautant A, Crichton RR, et al. Evidence of new cadmium binding sites in recombinant horse L-chain ferritin by anomalous Fourier difference map calculation. *Proteins* 1998; 31(4):477–485.
38. Islam QT, Sayers DE, Gorun SM, Theil EC. A comparison of an undecairon(III) complex with the ferritin iron core. *J Inorg Biochem* 1989; 36(1):51–62.
39. Powell AK. Ferritin. Its mineralization. *Met Ions Biol Syst* 1998; 35:515–561.
40. Chasteen ND. Ferritin. Uptake, storage, and release of iron. *Met Ions Biol Syst* 1998; 35:479–514.
41. Johnson JL, Cannon M, Watt RK, Frankel RB, Watt GD. Forming the phosphate layer in reconstituted horse spleen ferritin and the role of phosphate in promoting core surface redox reactions. *Biochemistry* 1999; 38(20):6706–6713.
42. Waldo GS, Wright E, Whang ZH, Briat JF, Theil EC, Sayers DE. Formation of the ferritin iron mineral occurs in plastids. *Plant Physiol* 1995; 109(3):797–802.
43. Stefanini S, Desideri A, Vecchini P, Drakenberg T, Chiancone E. Identification of the iron entry channels in apoferritin. Chemical modification and spectroscopic studies. *Biochemistry* 1989; 28(1):378–382.

44. Santambrogio P, Levi S, Cozzi A, Corsi B, Arosio P. Evidence that the specificity of iron incorporation into homopolymers of human ferritin. *Biochem J* 1996; 314(Pt 1): 139–144.
45. Yang X, Chasteen ND. Molecular diffusion into horse spleen ferritin: A nitroxide radical spin probe study. *Biophys J* 1996; 71(3):1587–1595.
46. Yang X, Arosio P, Chasteen ND. Molecular diffusion into ferritin: Pathways, temperature dependence, incubation time, and concentration effects. *Biophys J* 2000; 78(4): 2049–2059.
47. Yang X, Chasteen ND. Ferroxidase activity of ferritin: Effects of pH, buffer and Fe(II) and Fe(III) concentrations on Fe(II) autoxidation and ferroxidation. *Biochem J* 1999; 338(Pt 3):615–618.
48. Yang X, Chen-Barrett Y, Arosio P, Chasteen ND. Reaction paths of iron oxidation and hydrolysis in horse spleen and recombinant human ferritins. *Biochemistry* 1998; 37(27):9743–9750.
49. Hwang J, Krebs C, Huynh BH, Edmondson DE, Theil EC, Penner-Hahn JE. A short Fe-Fe distance in peroxodiferric ferritin: control of Fe substrate versus cofactor decay? *Science* 2000; 287(5450):122–125.
50. Bauminger ER, Harrison PM, Hechel D, Hodson NW, Nowik I, Treffry A, et al. Iron (II) oxidation and early intermediates of iron-core formation in recombinant human H-chain ferritin. *Biochem J* 1993; 296(Pt 3):709–719.
51. Treffry A, Bauminger ER, Hechel D, Hodson NW, Nowik I, Yewdall SJ, et al. Defining the roles of the threefold channels in iron uptake, iron oxidation and iron-core formation in ferritin: A study aided by site-directed mutagenesis. *Biochem J* 1993; 296 (Pt 3):721–728.
52. Le Brun NE, Andrews SC, Moore GR, Thomson AJ. Interaction of nitric oxide with non-haem iron sites of *Escherichia coli* bacterioferritin: Reduction of nitric oxide to nitrous oxide and oxidation of iron(II) to iron(III). *Biochem J* 1997; 326(Pt 1):173–179.
53. Treffry A, Zhao Z, Quail MA, Guest JR, Harrison PM. Dinuclear center of ferritin: Studies of iron binding and oxidation show differences in the two iron sites. *Biochemistry* 1997; 36(2):432–441.
54. Thomson AJ, Le Brun NE, Keech A, Andrews SC, Moore GR. Pumping iron: Does bacterioferritin contain a redox-driven iron pump? *Biochem Soc Trans* 1997; 25(1): 96–101.
55. Watt RK, Frankel RB, Watt GD. Redox reactions of apo mammalian ferritin. *Biochemistry* 1992; 31(40):9673–9679.
56. Johnson JL, Copeland ND, Arosio P, Frankel RB, Watt GD. Redox reactivity of animal apoferritins and apoheteropolymers assembled from recombinant heavy and light human chain ferritins. *Biochemistry* 1999; 38(13):4089–4096.
57. Percy ME, Wong S, Bauer S, Liaghati-Nasseri N, Perry MD, Chauthaiwale VM, et al. Iron metabolism and human ferritin heavy chain cDNA from adult brain with an elongated untranslated region: New findings and insights. *Analyst* 1998; 123(1):41–50.
58. Dhar MS, Joshi JG. Detection and quantitation of the novel ferritin heavy chain message in human tissues. *Biofactors* 1994; 4(3–4):147–149.
59. Zheng H, Bhavsar D, Dugast I, Zappone E, Drysdale J. Conserved mutations in human ferritin H pseudogenes: A second functional sequence or an evolutionary quirk? *Biochim Biophys Acta* 1997; 1351(1–2):150–156.
60. Gasparini P, Calvano S, Memeo E, Bisceglia L, Zelante L. Assignment of ferritin L gene (FTL) to human chromosome band 19q13.3 by in situ hybridization. *Ann Genet* 1997; 40(4):227–228.
61. Yachou AK, Renaudie F, Guenet JL, Simon-Chazottes D, Jones R, Grandchamp B, et al. Mouse ferritin H multigene family is polymorphic and contains a single multiallelic functional gene located on chromosome 19. *Genomics* 1991; 10(3):531–538.

62. Renaudie F, Boulanger L, Grandchamp B, Beaumont C. [Cloning, characterization and expression of mouse ferritin L subunit gene]. *C R Acad Sci III* 1995; 318(4): 431–437.
63. Proudhon D, Wei J, Briat J, Theil EC. Ferritin gene organization: Differences between plants and animals suggest possible kingdom-specific selective constraints. *J Mol Evol* 1996; 42(3):325–336.
64. Beaumont C, Seyhan A, Yachou AK, Grandchamp B, Jones R. Mouse ferritin H subunit gene. Functional analysis of the promoter and identification of an upstream regulatory element active in erythroid cells. *J Biol Chem* 1994; 269(32):20281–20288.
65. Bevilacqua MA, Faniello MC, D'Agostino P, Quaresima B, Tiano MT, Pignata S, et al. Transcriptional activation of the H-ferritin gene in differentiated Caco-2 cells parallels a change in the activity of the nuclear factor Bbf. *Biochem J* 1995; 311(Pt 3): 769–773.
66. Beaumont C, Jones R, Seyhan A, Grandchamp B. A hemin-inducible enhancer lies 4.5 kb upstream of the mouse ferritin H subunit gene. *Adv Exp Med Biol* 1994; 356: 211–218.
67. Tsuji Y, Akebi N, Lam TK, Nakabeppu Y, Torti SV, Torti FM. FER-1, an enhancer of the ferritin H gene and a target of E1A-mediated transcriptional repression. *Mol Cell Biol* 1995; 15(9):5152–5164.
68. Tsuji Y, Torti SV, Torti FM. Activation of the ferritin H enhancer, FER-1, by the cooperative action of members of the AP1 and Sp1 transcription factor families. *J Biol Chem* 1998; 273(5):2984–2992.
69. Tsuji Y, Moran E, Torti SV, Torti FM. Transcriptional regulation of the mouse ferritin H gene. Involvement of p300/CBP adaptor proteins in FER-1 enhancer activity. *J Biol Chem* 1999; 274(11):7501–7507.
70. Kwak EL, Laroche DA, Beaumont C, Torti SV, Torti FM. Role for NF-kappa B in the regulation of ferritin H by tumor necrosis factor-alpha. *J Biol Chem* 1995; 270(25): 15285–15293.
71. Bevilacqua MA, Faniello MC, Quaresima B, Tiano MT, Giuliano P, Felicciello A, et al. A common mechanism underlying the E1A repression and the cAMP stimulation of the H ferritin transcription. *J Biol Chem* 1997; 272(33):20736–20741.
72. Faniello MC, Bevilacqua MA, Condorelli G, de Crombrugge B, Maity SN, Avvedimento VE, et al. The B subunit of the CAAT-binding factor NFY binds the central segment of the Co-activator p300. *J Biol Chem* 1999; 274(12):7623–7626.
73. Marziali G, Perrotti E, Ilari R, Testa U, Coccia EM, Battistini A. Transcriptional regulation of the ferritin heavy-chain gene: The activity of the CCAAT binding factor NFY is modulated in heme-treated Friend leukemia cells and during monocyte-to-macrophage differentiation. *Mol Cell Biol* 1997; 17(3):1387–1395.
74. Wu KJ, Polack A, Dalla-Favera R. Coordinated regulation of iron-controlling genes, H-ferritin and IRP2, by c-MYC. *Science* 1999; 283(5402):676–679.
75. Wasserman WW, Fahl WE. Functional antioxidant responsive elements. *Proc Natl Acad Sci USA* 1997; 94(10):5361–5366.
76. Miller LL, Miller SC, Torti SV, Tsuji Y, Torti FM. Iron-independent induction of ferritin H chain by tumor necrosis factor. *Proc Natl Acad Sci USA* 1991; 88(11): 4946–4950.
77. Beaumont C, Dugast I, Renaudie F, Souroujon M, Grandchamp B. Transcriptional regulation of ferritin H and L subunits in adult erythroid and liver cells from the mouse. Unambiguous identification of mouse ferritin subunits and in vitro formation of the ferritin shells. *J Biol Chem* 1989; 264(13):7498–7504.
78. Cairo G, Tacchini L, Pogliaghi G, Anzon E, Tomasi A, Bernelli-Zazzera A. Induction of ferritin synthesis by oxidative stress. Transcriptional and post-transcriptional regulation by expansion of the “free” iron pool. *J Biol Chem* 1995; 270(2):700–703.
79. White K, Munro HN. Induction of ferritin subunit synthesis by iron is regulated at

- both the transcriptional and translational levels. *J Biol Chem* 1988; 263(18):8938–8942.
80. Rogers JT, Andriotakis JL, Lacroix L, Durmowicz GP, Kasschau KD, Bridges KR. Translational enhancement of H-ferritin mRNA by interleukin-1 beta acts through 5' leader sequences distinct from the iron responsive element. *Nucleic Acids Res* 1994; 22(13):2678–2686.
 81. Ai LS, Chau LY. Post-transcriptional regulation of H-ferritin mRNA. Identification of a pyrimidine-rich sequence in the 3'-untranslated region associated with message stability in human monocytic THP-1 cells. *J Biol Chem* 1999; 274(42):30209–30214.
 82. Pham DQ, Winzerling JJ, Dodson MS, Law JH. Transcriptional control is relevant in the modulation of mosquito ferritin synthesis by iron. *Eur J Biochem* 1999; 266(1):236–240.
 83. Georgieva T, Dunkov BC, Harizanova N, Ralchev K, Law JH. Iron availability dramatically alters the distribution of ferritin subunit messages in *Drosophila melanogaster*. *Proc Natl Acad Sci USA* 1999; 96(6):2716–2721.
 84. Savino G, Briat JF, Lobreaux S. Inhibition of the iron-induced ZmFer1 maize ferritin gene expression by antioxidants and serine/threonine phosphatase inhibitors. *J Biol Chem* 1997; 272(52):33319–33326.
 85. Wei J, Theil EC. Identification and characterization of the iron regulatory element (FRE) of the ferritin gene of a plant (soybean). *J Biol Chem* 2000; 275(23):17488–17493.
 86. <http://www.ncbi.nlm.nih.gov:80/COG/>. www-2 2000.
 87. Eide DJ, Bridgham JT, Zhao Z, Mattoon JR. The vacuolar H(+)-ATPase of *Saccharomyces cerevisiae* is required for efficient copper detoxification, mitochondrial function, and iron metabolism. *Mol Gen Genet* 1993; 241(3–4):447–456.
 88. Hudson AJ, Andrews SC, Hawkins C, Williams JM, Izuhara M, Meldrum FC, et al. Overproduction, purification and characterization of the *Escherichia coli* ferritin. *Eur J Biochem* 1993; 218(3):985–995.
 89. Denoel PA, Crawford RM, Zygmunt MS, Tibor A, Weynants VE, Godfroid F, et al. Survival of a bacterioferritin deletion mutant of *Brucella melitensis* 16M in human monocyte-derived macrophages. *Infect Immun* 1997; 65(10):4337–4340.
 90. Wai SN, Nakayama K, Umene K, Moriya T, Amako K. Construction of a ferritin-deficient mutant of *Campylobacter jejuni*: Contribution of ferritin to iron storage and protection against oxidative stress. *Mol Microbiol* 1996; 20(6):1127–1134.
 91. Gaynard F, Boucherez J, Briat JF. Characterization of a ferritin mRNA from *Arabidopsis thaliana* accumulated in response to iron through an oxidative pathway independent of abscisic acid. *Biochem J* 1996; 318(Pt 1):67–73.
 92. Goto F, Yoshihara T, Shigemoto N, Toki S, Takaiwa F. Iron fortification of rice seed by the soybean ferritin gene [see comments]. *Nature Biotechnol* 1999; 17(3):282–286.
 93. Deak M, Horvath GV, Davletova S, Torok K, Sass L, Vass I, et al. Plants ectopically expressing the iron-binding protein, ferritin, are tolerant to oxidative damage and pathogens. *Nature Biotechnol* 1999; 17(2):192–196.
 94. Goto F, Yoshihara T, Saiki H. Iron accumulation in tobacco plants expressing soybean ferritin gene. *Transgenic Res* 1998; 7:173–180.
 95. van Wuytswinkel O, Vansuyt G, Grignon N, Fourcroy P, Briat JF. Iron homeostasis alteration in transgenic tobacco overexpressing ferritin. *Plant J* 1999; 17(1):93–97.
 96. Briat JF, Lobreaux S, Grignon N, Vansuyt G. Regulation of plant ferritin synthesis: how and why. *Cell Mol Life Sci* 1999; 56(1-2):155–166.
 97. Radisky DC, Kaplan J. Iron in cytosolic ferritin can be recycled through lysosomal degradation in human fibroblasts. *Biochem J* 1998; 336(Pt 1):201–205.
 98. Balla G, Jacob HS, Balla J, Rosenberg M, Nath K, Apple F, et al. Ferritin: A cytoprotective antioxidant strategem of endothelium. *J Biol Chem* 1992; 267(25):18148–18153.

99. Lin F, Girotti AW. Elevated ferritin production, iron containment, and oxidant resistance in hemin-treated leukemia cells. *Arch Biochem Biophys* 1997; 346(1):131–141.
100. Lin F, Girotti AW. Hemin-enhanced resistance of human leukemia cells to oxidative killing: Antisense determination of ferritin involvement. *Arch Biochem Biophys* 1998; 352(1):51–58.
101. Vile GF, Tyrrell RM. Oxidative stress resulting from ultraviolet A irradiation of human skin fibroblasts leads to a heme oxygenase-dependent increase in ferritin. *J Biol Chem* 1993; 268(20):14678–14681.
102. Pourzand C, Watkin RD, Brown JE, Tyrrell RM. Ultraviolet A radiation induces immediate release of iron in human primary skin fibroblasts: The role of ferritin. *Proc Natl Acad Sci USA* 1999; 96(12):6751–6756.
103. Corsi B, Perrone F, Bourgeois M, Beaumont C, Panzeri MC, Cozzi A, et al. Transient overexpression of human H and L ferritin chains in COS cells. *Biochem J* 1998; 330(Pt 1):315–320.
104. Beaumont C, Leneuve P, Devaux I, Scoazec JY, Berthier M, Loiseau MN, et al. Mutation in the iron responsive element of the L ferritin mRNA in a family with dominant hyperferritinaemia and cataract. *Nature Genet* 1995; 11(4):444–446.
105. Levi S, Girelli D, Perrone F, Pasti M, Beaumont C, Corrocher R, et al. Analysis of ferritins in lymphoblastoid cell lines and in the lens of subjects with hereditary hyperferritinemia-cataract syndrome. *Blood* 1998; 91(11):4180–4187.
106. Picard V, Renaudie F, Porcher C, Hentze MW, Grandchamp B, Beaumont C. Overexpression of the ferritin H subunit in cultured erythroid cells changes the intracellular iron distribution. *Blood* 1996; 87(5):2057–2064.
107. Picard V, Epsztejn S, Santambrogio P, Cabantchik ZI, Beaumont C. Role of ferritin in the control of the labile iron pool in murine erythroleukemia cells. *J Biol Chem* 1998; 273(25):15382–15386.
108. Konijn AM, Glickstein H, Vaisman B, Meyron-Holtz EG, Slotki IN, Cabantchik ZI. The cellular labile iron pool and intracellular ferritin in K562 cells. *Blood* 1999; 94(6):2128–2134.
- 108a. Cozzi A, Corsi B, Levi S, Santambrogio P, Albertini A, Arosio P. Overexpression of wild type and mutated ferritin H-chain in HeLa cells: in vivo role of ferritin ferroxidase activity. *J Biol Chem* 2000; 275(33):251222–251229.
109. Ferreira C, Bucchini D, Martin ME, Levi S, Arosio P, Grandchamp B, et al. Early embryonic lethality of H ferritin gene deletion in mice. *J Biol Chem* 2000; 275(5):3021–3024.
110. Santambrogio P, Cozzi A, Levi S, Arosio P. Human serum ferritin G-peptide is recognized by anti-L ferritin subunit antibodies and concanavalin-A. *Br J Haematol* 1987; 65(2):235–237.
111. Torti SV, Torti FM. Human H-kininogen is a ferritin-binding protein. *J Biol Chem* 1998; 273(22):13630–13635.
112. Fargion S, Fracanzani AL, Brando B, Arosio P, Levi S, Fiorelli G. Specific binding sites for H-ferritin on human lymphocytes: Modulation during cellular proliferation and potential implication in cell growth control. *Blood* 1991; 78(4):1056–1061.
113. Gelvan D, Fibach E, Meyron-Holtz EG, Konijn AM. Ferritin uptake by human erythroid precursors is a regulated iron uptake pathway. *Blood* 1996; 88(8):3200–3207.
114. Meyron-Holtz EG, Vaisman B, Cabantchik ZI, Fibach E, Rouault TA, Hershko C, et al. Regulation of intracellular iron metabolism in human erythroid precursors by internalized extracellular ferritin. *Blood* 1999; 94(9):3205–3211.
115. Hulet SW, Hess EJ, Debinski W, Arosio P, Bruce K, Powers S, et al. Characterization and distribution of ferritin binding sites in the adult mouse brain. *J Neurochem* 1999; 72(2):868–874.
116. Jeanmougin F, Thompson JD, Gouy M, Higgins DG, Gibson TJ. Multiple sequence alignment with Clustal X. *Trends Biochem Sci* 1998, 23, 403–405.

6

The Divalent Metal-Ion Transporter (DCT1/DMT1/Nramp2)

HIROMI GUNSHIN

Children's Hospital, Harvard Medical School, Boston, Massachusetts

MATTHIAS A. HEDIGER

*Brigham and Women's Hospital and Harvard Medical School,
Boston, Massachusetts*

I. OVERVIEW	156
II. INTRODUCTION	156
III. EXPRESSION CLONING AND CHARACTERIZATION OF DCT1/DMT1 IN <i>XENOPUS</i> OOCYTES	157
IV. POSITIONAL CLONING OF Nramp2 FROM RODENT MUTANTS WITH DEFECTS IN IRON METABOLISM	159
V. THE Nramp (NATURAL RESISTANCE-ASSOCIATED MACROPHAGE PROTEIN) FAMILY	159
VI. ANALYSIS OF DCT1/DMT1 REGULATION	162
VII. ROLE OF DCT1/DMT1 IN THE UPTAKE OF IRON FROM TRANSFERRIN	165
VIII. HEMOCHROMATOSIS GENE (HFE) AND DCT1/DMT1	166
IX. OTHER MOLECULES INVOLVED IN INTESTINAL IRON TRANSPORT	167
X. SUMMARY	168
ACKNOWLEDGMENTS	170
REFERENCES	170

I. OVERVIEW

Divalent metals play a crucial role in the catalytic function of numerous enzymes, and are involved in many key physiological processes. Despite extensive studies, there is sparse molecular information available on how divalent cations are actively absorbed by mammalian cells. We have cloned a divalent metal transporter DMT1 (previously known as DCT1 and Nramp2) from iron-deficient rat duodenum by expression cloning with *Xenopus* oocytes (1). The transport characteristics of DCT1/DMT1 were determined based on oocyte expression studies measuring $^{55}\text{Fe}^{2+}$ uptake and by two-microelectrode voltage-clamp analysis. DCT1/DMT1 transported Fe^{2+} , Zn^{2+} , Mn^{2+} , Co^{2+} , Cd^{2+} , Cu^{2+} , Ni^{2+} , and Pb^{2+} . Moreover, divalent cation transport mediated by DCT1/DMT1 is electrogenic, voltage-dependent, and H^{+} -coupled. DCT1/DMT1 mRNA was primarily expressed in duodenum, and mRNA levels increased dramatically in response to dietary iron depletion. DCT1/DMT1 mRNA also was expressed at lower levels in most other tissues examined, including kidney, liver, brain, and heart, and expression was again consistently higher in iron-deficient rats. The 3' untranslated region (UTR) of DCT1/DMT1 mRNA contained a stem-loop-like structure that resembles the iron-responsive element (IRE) of ferritin and transferrin receptor. Therefore, we hypothesized that DCT1/DMT1 might be regulated through IRE/IRP regulatory system. The observed regulation of DCT1/DMT1 mRNA may involve posttranscriptional regulation through binding of IRPs to the putative IRE in DCT1/DMT1. However, this DCT1/DMT1 regulatory system needs further investigation along with other molecules reported recently, such as HFE [(2); see also Chapter 8], hephaestin (3), IREG1/ferroportin1 [(4,5); see also Chapter 7], and ferrireductase (Dcytb) (6).

II. INTRODUCTION

Little is known regarding the uptake of essential metal ions, such as Fe^{2+} , Zn^{2+} , Co^{2+} , Mn^{2+} , Cu^{2+} , and Ni^{2+} , despite their vital roles in the catalytic function of many enzymes, their structural role in zinc-finger proteins, and their involvement in free-radical homeostasis. Furthermore, mammalian absorption of toxic divalent cations, such as Cd^{2+} and Pb^{2+} , is poorly understood.

Iron is an essential nutrient, yet it is toxic in excess. Disorders of iron metabolism are among the most prevalent causes of human morbidity and mortality worldwide. Iron deficiency affects up to a third of the world's population; women and children are particularly susceptible. The severe deficiency state presents with anemia. In contrast, iron overload can be due to genetic defects predisposing to iron accumulation, such as hereditary hemochromatosis (HH), one of the most common genetic disorders among Caucasoid populations. One key strategy to elucidate those common human diseases is to understand iron absorption in the body. Until recently, little molecular information was available on the mechanisms whereby mammalian cells actively absorb iron, in spite of the fact that iron is the most abundant metal in animal tissues. In particular, mammalian intestinal iron transport mechanisms were not elucidated at the molecular level until recently.

Iron uptake is generally facilitated by transferrin receptor (TfR)-mediated endocytosis in mammals. However, there is no available apo-transferrin in the intestinal lumen (7,8). Because this pathway is insufficient to account for dietary iron absorp-

tion, it is likely that other non-transferrin-mediated uptake systems exist in the intestine. Although there may be a paracellular ion transport pathway, such as PCLN1 (9) for Mg^{2+} , here we focus on transcellular passage of divalent metal ions, especially iron, through the plasma membrane. Two distinct forms of iron are present in foods: nonheme iron and heme iron. The bulk of intestinal nonheme iron is known to be absorbed in the first portion of the duodenum, where an acidic environment promotes the solubilization of iron and enhances reduction by ferrireductase (10,11), and/or ascorbate (12,13). The mechanism of Fe^{2+} absorption from the intestine had not been understood in detail. It is now clear that DMT1 (formerly DCT1, Nramp2) is the major apical intestinal iron transporter (1,14). Here we describe the expression cloning, characterization, and regulation of DCT1/DMT1, focusing on molecular insights into intestinal iron transport mechanisms.

III. EXPRESSION CLONING AND CHARACTERIZATION OF DCT1/DMT1 IN *XENOPUS* OOCYTES

We isolated the divalent metal transporter DCT1/DMT1 using an expression cloning strategy in *Xenopus* oocytes (1,15). Duodenal mRNA from rats fed a low-iron diet stimulated radiolabeled iron accumulation sevenfold compared to water-injected oocytes. Size-fractionated mRNA of 3.8–4.5 kb contained the stimulatory activity, and was used to prepare a cDNA library. DCT1/DMT1 was isolated by screening this cDNA library using a similar radiotracer assay of $^{55}Fe^{2+}$ uptake in cRNA-injected *Xenopus* oocytes. When expressed in the oocytes, a single DCT1/DMT1 clone stimulated the uptake of $^{55}Fe^{2+}$ 200-fold compared with water-injected control oocytes (Fig. 1). DCT1/DMT1 is a 561-amino acid protein with 12 putative membrane-spanning domains (Fig. 2A).

Using high-stringency Northern analysis and in-situ hybridization, we confirmed that DCT1/DMT1 was expressed ubiquitously. However, DCT1/DMT1 message was particularly abundant in the duodenum, where it was localized primarily in the lower segments of the villi, close to the crypts but not at the villus tips. The expression gradually decreased in jejunum, ileum, and colon. A remarkable finding was that mRNA levels increased dramatically in duodenum in iron-deficient rats. Expression was also consistently higher in all other tissues examined in iron-deficient rats. We concluded that there is a marked regulation of DCT1/DMT1 mRNA by dietary iron, suggesting that DCT1/DMT1 plays an important role in iron homeostasis.

In kidney, DCT1/DMT1 mRNA labeling was most prominent in proximal tubule S3 segments and the entire collecting duct. DCT1/DMT1 may be involved in iron reabsorption in these parts of the kidney (1). DCT1/DMT1 message was found in neurons throughout the brain. More intense labeling was present in densely packed cell groups, such as the hippocampus and cerebellum. One cell group, the ventral portion of the anterior olfactory nucleus, displayed very high levels of DCT1/DMT1 mRNA. DCT1/DMT1 message was also localized in the choroid plexus, and was present at moderate intensity in the substantia nigra. Interestingly, in Parkinson's disease there is substantial accumulation of iron in affected neurons in this part of brain (16). The increased iron content may contribute to neuronal death by catalyzing the production of harmful hydroxyl radicals. The precise roles of DCT1/DMT1 throughout the central nervous system (CNS) will require much investigation; how-

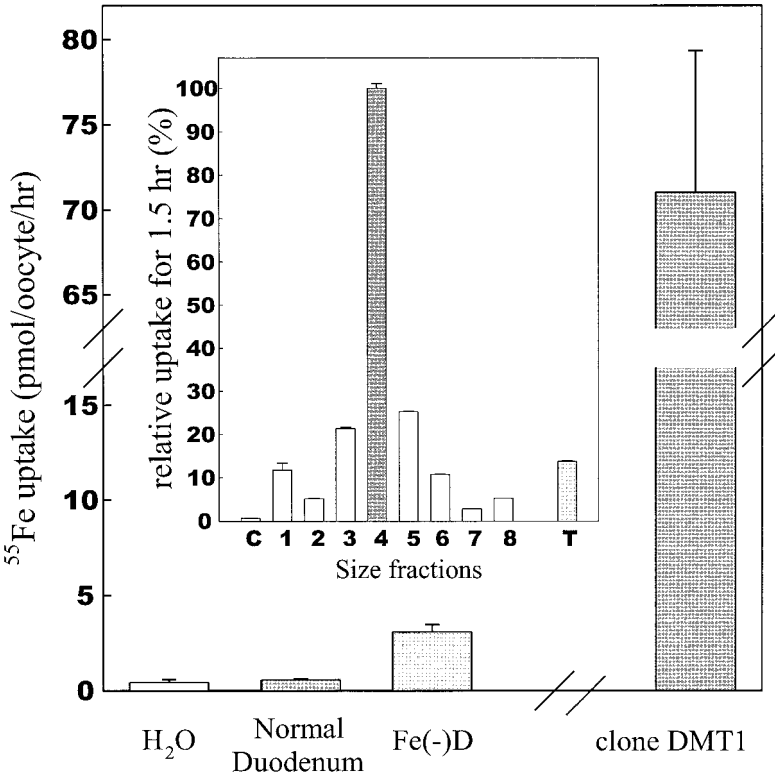


Figure 1 Uptake of $10\ \mu\text{M}$ ^{55}Fe in *Xenopus* oocytes injected with poly (A) + RNA from normal or iron-deficient [$\text{Fe}(-)\text{D}$] rat duodenum or with RNA synthesized from DCT1/DMT1 cDNA. Data are mean + SEM from 6–10 oocytes. Inset, relative ^{55}Fe uptake in oocytes injected with size-fractionated poly (A) + $\text{Fe}(-)\text{D}$ RNA. C, control water-injected oocytes; 1, 2.0–3.0 kb poly (A) + RNA; 2, 2.5–3.5 kb; 3, 3.3–4.0 kb; 4, 3.8–4.5 kb; 5, 4.4–5.7 kb; 6, 4.5–6.0 kb; 8, 5.5–7.0 kb; and T, unfractionated poly (A) + $\text{Fe}(-)\text{D}$ RNA. (From Ref. 1. Reprinted with permission from Nature. Copyright (1997) Macmillan Magazine Limited.)

ever, DCT1/DMT1 may play a role in the etiology of certain neurodegenerative diseases by promoting the generation of reactive oxygen species by divalent metals.

Two-microelectrode voltage-clamp analysis in oocytes clearly revealed that divalent cation transport mediated by DCT1/DMT1 is electrogenic, with currents of up to $-1000\ \text{nA}$. DCT1/DMT1 transports not only Fe^{2+} but also Zn^{2+} , Mn^{2+} , Cu^{2+} , Co^{2+} . It even transports the toxic metals Cd^{2+} and Pb^{2+} . Fe^{2+} uptake mediated by DCT1/DMT1 expressed in oocytes proceeded with a high affinity; the Fe^{2+} concentration at which current was half-maximal ($K_{0.5}^{\text{Fe}}$) was $2\ \mu\text{M}$ at $-50\ \text{mV}$. Superfusion of Fe^{2+} resulted in a profound intracellular acidification in oocytes expressing DCT1/DMT1; iron transport mediated by DCT1/DMT1 is proton-coupled. H^+ activation of the Fe^{2+} -evoked currents revealed Hill coefficients (n_H) for H^+ of approximately 1, suggesting that the transport stoichiometry for DCT1/DMT1 is $1\text{H}^+ : 1\text{Fe}^{2+}$ (see Fig. 5).

IV. POSITIONAL CLONING OF Nramp2 FROM RODENT MUTANTS WITH DEFECTS IN IRON METABOLISM

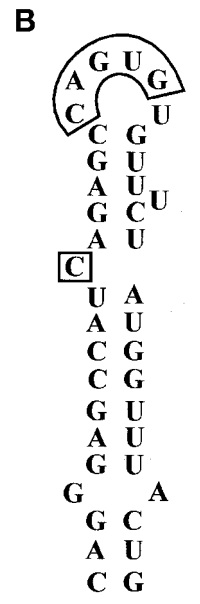
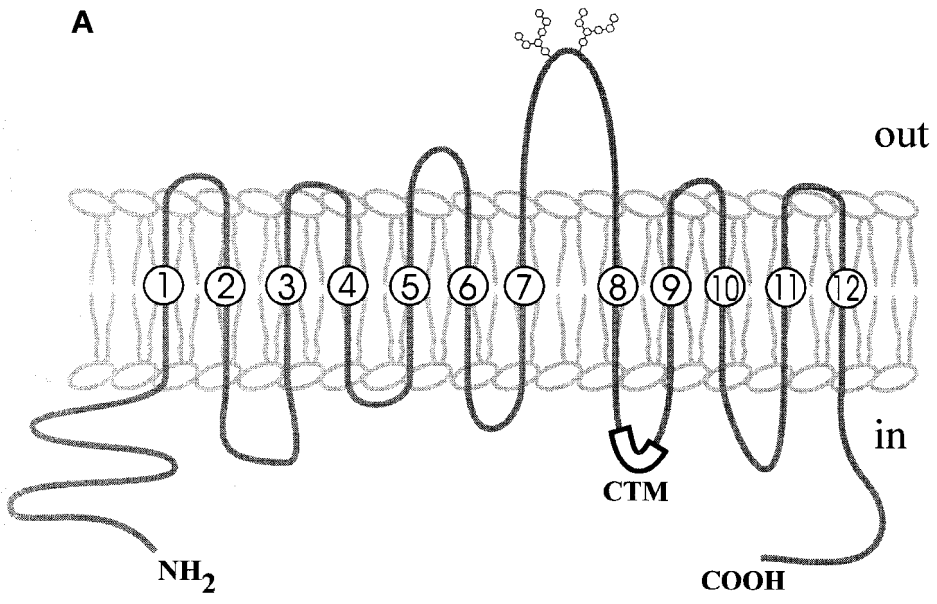
Fleming et al. have taken a genetic approach toward understanding iron transport in mice, subscribing to the idea that the most powerful biological tools for the study of metabolism are genetic defects in key metabolic pathways. They initiated genetic mapping and positional cloning experiments to identify the genes defective in rodents with autosomal recessive disorders of iron metabolism. Two of these mutants, the microcytic mouse (gene symbol *mk*), and the Belgrade rat (gene symbol *b*), have given important insight into transmembrane iron transport in vivo. These animals have severe iron deficiency anemia, due to impairment of iron transport in the intestine, the bone marrow, and other tissues.

The severe anemia in *mk* and *b* animals was not responsive to high dietary iron. An in-situ ligated duodenal loop experiment revealed that these mutant animals had an intestinal blockage for iron entry from the lumen, especially at the apical membrane. Also, these mutant animals did not recover from the anemic condition by i.p. or i.m. iron injection, suggesting a block of iron entry into red blood cell precursors. Furthermore, the *b* rats showed a defect in the transport of iron across the endosomal membrane as part of the Tf cycle. Fleming et al. found that both animals have identical missense mutations (G185R) in the DCT1/DMT1 gene (14,17). This phenotypic characterization of *mk* mice and *b* rats, coupled with biochemical data on DCT1/DMT1 activity in oocytes (1), provides compelling evidence that DCT1/DMT1 is a major mammalian transmembrane iron transporter, and the gateway for the entry of dietary iron into the body.

V. THE Nramp (NATURAL RESISTANCE-ASSOCIATED MACROPHAGE PROTEIN) FAMILY

DCT1/DMT1 was originally named Nramp2 after it was identified as a homolog to Nramp1, a gene involved in resistance to intracellular pathogens. Nramp1 was the first member of this family to be described. Its gene was identified by positional cloning of a murine locus and found to encode an integral membrane protein of unknown function (18). The locus, variably termed *Bcg*, *Lsh*, or *Ity*, mediates resistance to infection by intracellular pathogens such as *Mycobacteria sp. (bovis, avium, and lepraemurium)*, *Leishmania donovani*, and *Salmonella typhimurium* (18,19). The mechanism of action of Nramp1 in host defense remains unknown. At the time of our DCT1/DMT1 cloning experiments, no mechanisms of action had been demonstrated for either protein (18,20).

Nramp1 and Nramp2 belong to a small, highly conserved family of putative transmembrane transporters (Fig. 2C). Members of this family have been identified in mycobacteria, fungi, plants, insects, nematodes, fishes (21), and mammals (22). The common features include 10–12 predicted transmembrane domains, an extracytoplasmic loop with potential glycosylation sites, and a highly conserved, intracellular 20-amino acid motif. This last motif shows weak homology both to bacterial sequences known as binding-protein-dependent transport system inner membrane component signatures (BPPTS) or consensus transport motif (CTM) (Fig. 2A) and to a conserved region of voltage-gated glutamate and K⁺ transporters (20,22). The function of this motif in Nramp-related proteins has not been determined. Prior to



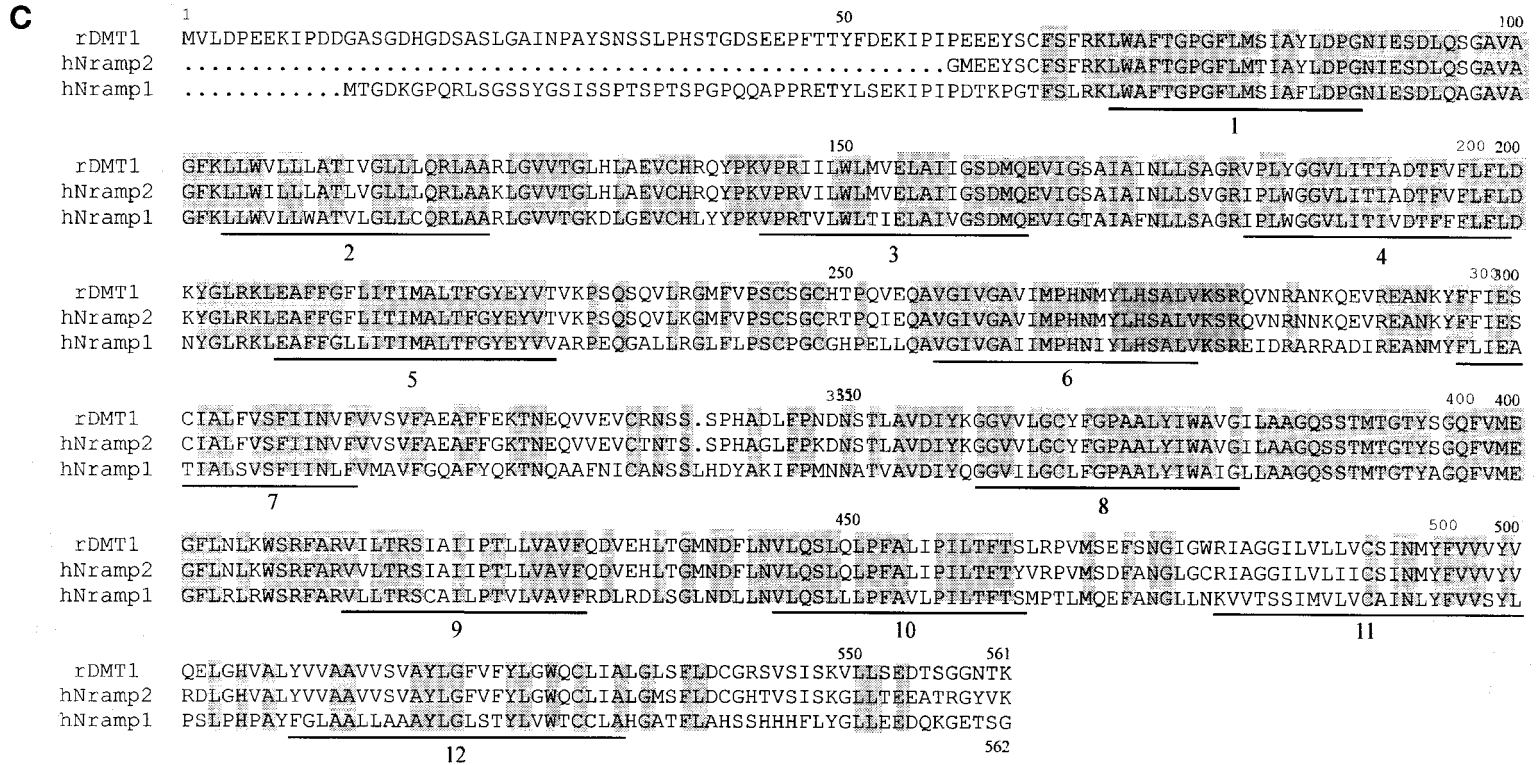


Figure 2 (A) Predicted topology of DCT1/DMT1 protein. Putative transmembrane domains 1 to 12 are indicated. The “consensus transport motif” (CTM) is indicated in the fourth intracellular loop, and putative N-linked glycosylation sites are identified in the fourth extracellular loop. (B) The potential iron-responsive element (IRE) is indicated. (C) Sequence alignment of rat DCT1/DMT1 and human Nramp1 and human Nramp2 (GeneBank accession numbers AF008439, L32185, and L37347). The 12 putative transmembrane regions are underlined and numbered 1 to 12. Identical residues are indicated by shading. (From Ref. 1. Reprinted with permission from Nature. Copyright (1997) Macmillan Magazine Limited.)

our studies, a yeast homolog called SMF1 was shown to function as a Mn^{2+} transporter (23). This result raised the possibility that other members of the Nramp family might transport metal ions, rather than anions as had been originally postulated.

Since mammalian Nramp1 and DCT1/DMT1/Nramp2 proteins share almost 80% sequence identity within their hydrophobic cores, it is likely that Nramp1 is involved in the transport of divalent cations as well. The available data suggest that Nramp1 expressing cells increase iron flux into the cytoplasm from a calcein-inaccessible cellular compartment (24). We also observed that Nramp1 could transport $^{55}Fe^{2+}$ in oocytes, but with a lower affinity than DCT1/DMT1/Nramp2 in oocytes expressing Nramp1 (1). Nramp1 is observed in the membrane of the pathogen-containing phagosomes as well as in the endosomal-lysosomal compartment of macrophages. Nramp1 is also recruited to the phagosomal membrane following phagocytosis (25). We postulate the mechanism for Nramp1-mediated pathogen resistance in the macrophages is the depletion from the phagosome by Nramp1 of Fe^{2+} , Mn^{2+} , Cu^{2+} , and (or) other divalent metal cations, resulting in a lack of essential metal ions for use by the pathogen.

VI. ANALYSIS OF DCT1/DMT1 REGULATION

DCT1/DMT1 is expressed ubiquitously, with highest levels observed in the duodenum. As described above, dietary iron deficiency upregulates DCT1/DMT1 mRNA levels in all tissues. DCT1/DMT1 may be regulated at the level of mRNA stability, because it has a stem-loop-like structure in the 3' untranslated region (UTR) (1), which resembles an iron-responsive element (IRE) present in the 3' UTR of TfR mRNA and the 5' UTR of ferritin mRNA. This DCT1/DMT1 IRE-like structure has a consensus sequence of a stem and a six-nucleotide (CAGUGN) loop, a single unpaired nucleotide bulge C, and an additional unpaired bulge U (Figs. 2B and 3). Since we found that the DCT1/DMT1-IRE sequence is conserved among rat, mouse, rabbit, and human, it is reasonable to speculate that this is an important regulatory

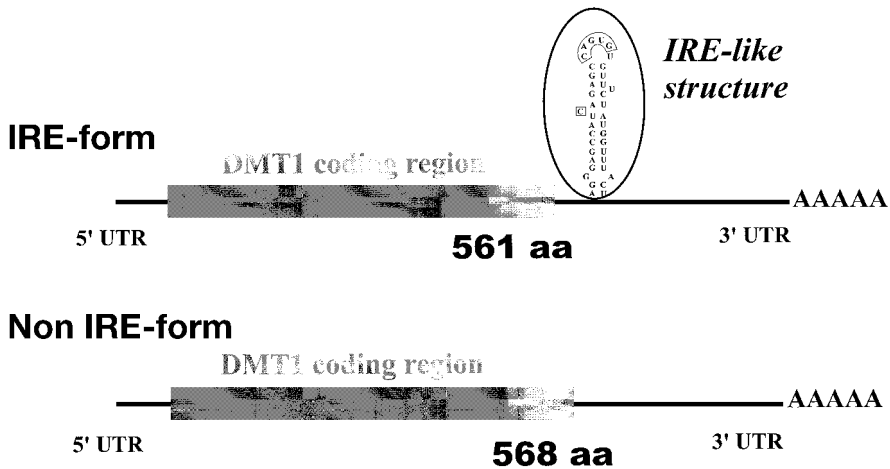


Figure 3 Two alternatively spliced isoforms of DCT1/DMT1. Details of the two isoforms are described in the text.

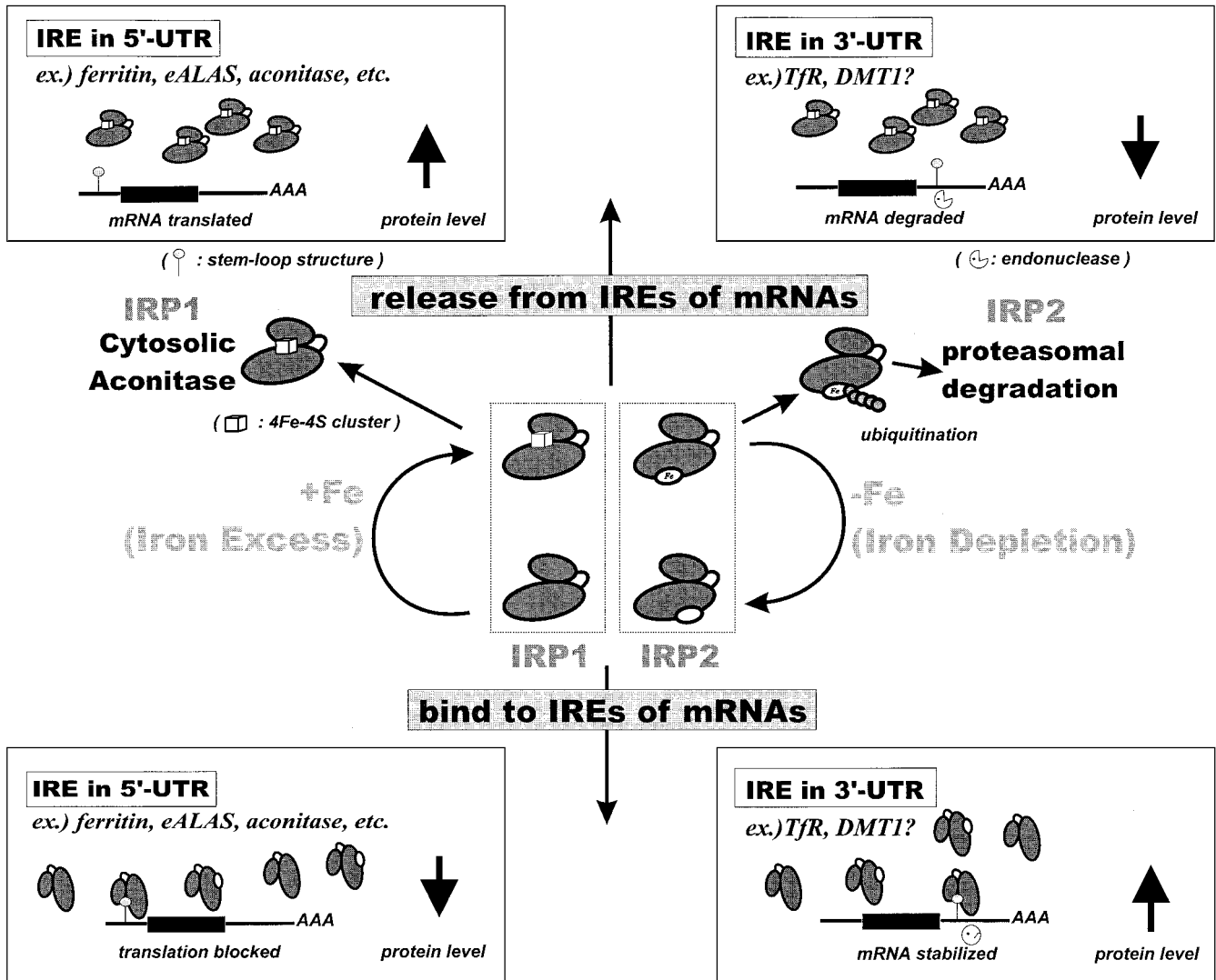
element and that DCT1/DMT1 is regulated by the IRE/iron regulatory protein (IRP) system (26). A schematic model of IRE/IRP mediated regulation is shown in Fig. 4 (and see Chapter 9). In the case of iron depletion, the IRE in the 3' UTR of DCT1/DMT1 mRNA may associate with IRPs (Fig. 4) to inhibit rapid mRNA degradation, which is a similar regulatory system to TfR. In contrast, the binding of IRPs to IRE in 5' UTR (such as ferritin) blocks the translation of mRNAs under this condition. Conversely, the addition of iron to cells results in loss of IRE/IRP binding, allowing degradation of the mRNA with IRE in 3' UTR and causing less of this protein to be made. When IRPs are released from the IREs in the 5' UTR, the mRNAs are translated under this condition.

To further study DCT1/DMT1 mRNA regulation, we first demonstrated that endogenous DCT1/DMT1 mRNAs from Hep3B and Caco2 cells were upregulated 10-fold to 50-fold in response to an iron chelator (desferrioxamine, Df), and diminished in response to iron (ferric ammonium citrate, FAC) addition (26). However, Wardrop et al. reported that there was no significant change in the expression of Nramp2/DCT1/DMT1 mRNA in LMTK fibroblasts after preincubation with Df or FAC, whereas TfR mRNA showed marked changes under the same conditions (27). It appears that DCT1/DMT1 may be regulated differently in different cell types.

Electrophoretic mobility shift assays demonstrated that the DCT1/DMT1-IRE is bound by both IRP1 and IRP2 (26). The affinity of the IRPs was lower for the DCT1/DMT1-IRE than for the ferritin IRE. Furthermore, IRP1 bound the DCT1/DMT1-IRE with greater affinity than did IRP2 (26). To examine whether RNA stability was involved in regulating DCT1/DMT1 expression *in vivo*, a portion of DMT1 mRNA containing the IRE was linked to a luciferase reporter gene. Following transient transfection into Hep3B cells, cells were treated for 30 h with Df or FAC. We found that addition of Df increased luciferase activity, whereas addition of FAC decreased luciferase activity. However, the magnitude of the changes in luciferase activity was insufficient to account fully for the regulation of endogenous DCT1/DMT1 mRNA levels that we observed in the Northern analysis in Hep3B and Caco2 cells (26) described above.

As shown in Fig. 3, DCT1/DMT1 has at least two alternatively spliced products. The cDNA that we originally identified encoded a 561-amino acid protein. This isoform has the potential IRE in its 3' UTR as described above. The other spliced isoform does not have an IRE-like structure and encodes a protein of 568 amino acids. These two proteins differ in a small portion of their C-terminal ends.

Regarding the DCT1/DMT1 protein distribution, antisera raised against Nramp2/DCT1/DMT1 were generated by Canonne-Hergaux et al. (28). Interestingly, they raised an antiserum against the N terminus of DCT1/DMT1 for both DCT1/DMT1 isoforms and another one against the C terminus of the non-IRE-containing isoform. DCT1/DMT1 was expressed as a broad band of molecular mass 80–100 kDa, which is larger than the predicted 60-kDa size due to extensive N-linked glycosylation of the protein. They showed that DCT1/DMT1 expression is very intense at the brush border of the apical pole of the enterocytes, whereas the basolateral membrane of these cells is negative for DCT1/DMT1. This is compatible with the demonstrated pH dependence of cation transport by DCT1/DMT1 (1). They also showed that protein expression of only the IRE isoform of DCT1/DMT1 was dramatically upregulated by dietary iron starvation in the proximal portion of the duodenum, but not in the rest of the small intestine and in kidney. This implies the



possibility of duodenum specificity that only the IRE isoform of DCT1/DMT1 may be spliced during dietary iron deficiency. However, this raises a discrepancy because DCT1/DMT1 transcript levels increase in dietary iron deficiency in all tissues that we examined (1). Lee et al. suggested that both splice variants of DCT1/DMT1 are ubiquitously expressed in human tissues, but brain appears to express the highest ratio of IRE to non-IRE forms, and spleen, thymus, and pancreas appear to have the highest ratio of non-IRE to IRE forms (29). There may be a difference between protein levels and mRNA levels, but this needs to be studied further.

Because DCT1/DMT1 transports not only iron but also other metals, we suggest that DCT1/DMT1 expression may be regulated by other metals through different regulatory mechanisms. Lee et al. showed that the DCT1/DMT1 5' regulatory region contains two CCAAT boxes, but no TATA box. This regulatory region also contains five potential metal response elements (MREs), three potential SP1 binding sites, and a single γ -interferon regulatory element (29). The promoter region that controls DCT1/DMT1 expression is still unknown. The observed regulation of DCT1/DMT1 mRNA by iron may involve posttranscriptional regulation through binding of IRPs to the putative IRE in DCT1/DMT1 and (or) transcriptional regulation, but this requires further investigation. It will be also interesting to identify functional differences between the two DCT1/DMT1 isoforms and to look for differences in their cellular/subcellular localization.

VII. ROLE OF DCT1/DMT1 IN THE UPTAKE OF IRON FROM TRANSFERRIN

Most iron in mammals exists either as heme, present in heme proteins, or as ferritin, a mobilizable storage form. Only a small fraction enters and leaves the body on a daily basis. Most iron is recycled from the breakdown of effete red cells by macrophages of the reticuloendothelial system. At any given time, approximately 0.1% (3 mg) of total body iron circulates in an exchangeable plasma pool. In normal individuals, essentially all circulating plasma iron is bound to Tf. Tf is a powerful chelator, binding iron with a dissociation constant of 10^{22} M^{-1} [(30); see also Chapter 2]. This chelation serves three purposes: it renders iron soluble under physiological conditions, it prevents iron-mediated free-radical toxicity, and it facilitates transport into cells. Radioactive tracer studies indicate that at least 70% of the iron bound to circulating Tf is delivered to the bone marrow (31).

Iron can be taken into cells by Tf receptor (TfR)-mediated endocytosis [(32); see also Chapter 3]. Specific TfRs on the outer face of the plasma membrane bind

←
Figure 4 Coordinated regulation by the IRE/IRP system. In the iron-depleted state, IRPs bind to the IREs on mRNA. Binding of the IRPs to mRNA in the 3' UTR results in stabilization of the RNA and production of more protein. Binding of IRPs to mRNA in the 5' UTR results in blockage of translation and thus less protein product. The opposite occurs in the iron-replete state. IRP1 presents aconitase activity converting citrate into isocitrate in the cytosol. In iron excess, holo-IRP1 (possessing a 4Fe-4S cluster) predominates and exhibits aconitase activity. In contrast, apo-IRP1 is the major form in iron-depleted cells. This apo-IRP1 binds IRE with high affinity (58,59). IRP2 does not have aconitase activity. Unlike IRP1, IRP2 is specifically degraded in the presence of iron excess (60,61).

diferric-Tf with high affinity. Once internalized, endosomes are acidified to pH 5.5–6.0 through the action of an ATP-dependent proton pump (33). Endosomal acidification releases iron from Tf, and produces conformational changes in both Tf and TfR, strengthening their association [(34,35); see also Chapter 4]. Iron release may also be facilitated by a plasma membrane oxidoreductase (36).

After iron dissociates from Tf in recycling endosomes, it must traverse the plasma membrane to gain entry to the cytosol. Until recently, this process was not understood on a molecular level, but there was evidence that it was carrier-mediated (37). Insight has come from identification of the DCT1/DMT1 mutation in *b* rats. The *b* anemia is associated with defective cellular iron uptake (38). Dual-labeling studies have shown that diferric-Tf is taken up into *b* reticulocytes, but the iron is poorly retained, and much is inappropriately recycled to the extracellular space along with Tf (38). It is clear that this “futile” Tf cycle does not result simply from a failure to dissociate iron from Tf (39,40). Rather, there is a defect in transmembrane iron transport, which can be explained by the mutation in DCT1/DMT1 (17).

Further details of DCT1/DMT1 localization became clear recently. DCT1/DMT1 was found in Tf-containing endosomes using an antibody against Nramp2/DCT1/DMT1 (28) and GFP-DCT1/DMT1 (26). This subcellular localization is consistent with the activity of DCT1/DMT1 because endosomes offer a low-pH environment that provides protons necessary for DCT1/DMT1 to function as a proton-coupled metal-ion transporter (1). However, DCT1/DMT1 protein is absent in the intestinal crypt (28) where HFE and TfR reside, suggesting that iron may exit from the endosome in crypt cells through a non-DCT1/DMT1-related mechanism. Since the crypt cells appear to play a key role in sensing body iron status and controlling intestinal iron regulatory mechanisms, it will be interesting to elucidate iron transport in this part of the intestine.

VIII. HEMOCHROMATOSIS GENE (HFE) AND DCT1/DMT1

Hereditary hemochromatosis (HH) is characterized by increased iron absorption and progressive iron storage, and results in damage to major organs in the body (see Chapter 28). In individuals of Northern European descent, approximately 1 in 20 people carries a defective allele (41). Homozygotes develop iron overload by middle age, with iron stores up to 10 times normal. The HH gene is closely linked to the HLA complex on human chromosome 6p. A compelling candidate gene for HH, *HFE*, was identified in 1996 by positional cloning (2). *HFE* protein is similar to major histocompatibility complex (MHC) class I molecules. Eighty-three percent of HH patients in the original study were homozygous for the same single-point mutation (C282Y) in the *HFE* gene (2). Subsequent reports have confirmed the high frequency of this mutation in other HH patients (42–44). A second missense mutation, H63D, was reported to be enriched in HH patients who are heterozygous for the C282Y mutation (2,44). The C282Y mutation disrupts a critical disulfide bond in the $\alpha 3$ domain of the *HFE* protein, which prevents its binding to β_2 -microglobulin (β_2 M) and its presentation on the cell surface (45,46), whereas the H63D mutation does not alter either the interaction with β_2 M or the surface expression of the protein (45). Knockout mice that lack either *HFE* or β_2 M develop iron overload similar to that occurring in human HH patients (see Chapter 27). Deficient *HFE* surface expression appears to cause excessive iron absorption by the intestine. Furthermore,

HFE associates with the TfR (47,48) soon after biosynthesis in the rough ER and is brought to the cell surface as a complex (49). The mechanisms by which HFE regulates iron homeostasis remain unclear. It is clear that HFE, with only a single transmembrane domain, is not an iron transporter, but it must regulate the iron transport apparatus in some way.

HFE protein is prominently expressed in the deep crypt cells of the duodenum (50), and these cells may act as sensors of the level of body iron stores. Perhaps HFE regulates the uptake of Tf-bound iron in crypt cells, which may then act as sensors of body iron stores. The C282Y mutation may impair the TfR-mediated uptake of iron into crypt cells and thus provide a false signal that body iron stores are low. As a result of the lower levels of intracellular iron, the differentiating enterocytes migrating up to the villus tip would increase production of DCT1/DMT1 and consequently iron uptake. The precise mechanisms have yet to be determined, but support for this hypothesis comes from HFE-knockout mice. Sly et al. have shown that DCT1/DMT1 mRNA expression is upregulated in these mice despite iron overload (51,52). Consistent with these data, Zoller et al. reported that DCT1/DMT1 mRNA expression in duodenal mucosa is increased in HH patients who are homozygous for the C282Y mutation (53). Increased duodenal DCT1/DMT1 mRNA expression could promote duodenal iron uptake and lead to iron overload. Coincidentally, IRPs have been found to be more active in duodenal cells in HH patients. In fact, intestinal ferritin expression in HH patients is diminished (54), suggesting that the intracellular iron concentration is low and IRP activity is, therefore, appropriately high.

IX. OTHER MOLECULES INVOLVED IN INTESTINAL IRON TRANSPORT

At present, very little is known about the processes involved in iron exit from absorptive enterocytes. Iron appears to be released through the basolateral membrane in the reduced ferrous state by a temperature-dependent mechanism. Positional cloning of the gene defective in the sex-linked anemia (*sla*) mouse led to the identification of a novel protein, hephaestin, that must play a role in this process. Hephaestin is homologous to the multi-copper ferroxidase ceruloplasmin and the yeast ferroxidase FET3 (3). Under normal physiological conditions, Fe^{2+} exported from the intestinal epithelium must bind to plasma Tf as Fe^{3+} . Hephaestin may link the processes of intestinal iron export and iron loading of Tf by oxidation of Fe^{2+} to Fe^{3+} as Fe^{2+} exits from enterocytes. The homology between hephaestin and FET3 is particularly intriguing because FET3 serves as a required component of the high-affinity iron transport apparatus by interacting with FTR1 in yeast (55). It seems reasonable to speculate that hephaestin interacts similarly with a transmembrane iron transporter on the basolateral membrane in the enterocyte. Although FTR1 presumably transports Fe^{3+} , IREG1 transports Fe^{2+} . McKie et al. isolated IREG1 [(5); see also Chapter 7] from duodenum of the hypotransferrinemic mouse (trf *hpx*) by a suppression subtractive hybridization method. (For a description of this method, see Ref. 56.) The *hpx* mouse is a mutant strain exhibiting Tf deficiency, marked anemia, hyperabsorption of iron, and elevated hepatic iron stores. IREG1 is a candidate gene for the basolateral membrane iron transporter. Interestingly, the 5' UTR of IREG1 contains a consensus IRE-like structure that is conserved between the mouse and human gene.

The significance of this IRE-like structure is still not clear. Perhaps in systemic iron deficiency, DCT1/DMT1 leads to an increased iron concentration in the enterocyte, which may in turn increase IREG1 translation through its 5' UTR-IRE-like structure around the villus tips.

In the intestinal crypts, the HFE-TfR complex may be responsible for normal iron regulation by sensing body iron status. The mutated HFE may lead to an improperly formed complex and subsequently dysregulated iron absorption, or iron overload, although the details have yet to be carefully elucidated. It seems reasonable that IREs are located in the mRNAs of both the 3' UTR of DMT1, an apical iron transporter, and the 5' UTR of IREG1, a basolateral iron transporter. Regulation of both proteins may occur through IRPs while the crypt cells grow to mature vertically. We postulate that the regulation occurs as follows: Under conditions of iron deficiency DCT1/DMT1 mRNA is stabilized, and IREG1 translation is blocked in the immature enterocytes while cells are migrating toward the villus tip. Once DCT1/DMT1 protein has been synthesized in the villus tip area, iron enters from the brush border membrane of the enterocytes and sequentially triggers the initiation of IREG1 translation, resulting in iron exit through the basolateral membrane site.

Another important molecule in intestinal iron transport is ferrireductase. In the intestine, the major site of iron absorption is the first part of the duodenum. It is now known that reduced ferrous iron is transported across the apical membrane of the duodenal cells by DCT1/DMT1. The acidic pH in the proximal intestine helps to solubilize Fe^{2+} . McKie et al. (6), using the same technique that identified IREG1, implicated a cytochrome b_{558} from the duodenum of *hpx* mice as the first example of a mammalian ferrireductase called Dcytb. The ferric-reducing activity is also increased by hypoxia and iron deficiency. It is not known whether the ferrireductases in other organs and cell types have the same molecular characteristics and properties as that in the duodenum. An overview of this model is shown in Fig. 5.

X. SUMMARY

In recent years, several key molecules of mammalian iron metabolism have been discovered, DCT1/DMT1 being one example. DCT1/DMT1 transports iron driven by the proton electrochemical gradient in the apical site of the epithelium. The existence of a single transport mechanism for a variety of divalent metal cations may have profound nutritional, clinical, and toxicological implications. Also, DCT1/DMT1 mRNA localization in the CNS indicates the potential pathophysiological relevance of DCT1/DMT1 in neurodegenerative disorders. As a member of the Nrap family, the characterization of DCT1/DMT1/Nrap2 has suggested a possible mechanism by which Nrap1 confers resistance to infection. Furthermore, DCT1/DMT1 accounts for the inherited hypochromic, microcytic anemia in *mk* mice and *b* rats.

Dietary iron deficiency results in increased DCT1/DMT1 mRNA levels in all tissues examined to date. It is not known whether this is a result of increased transcriptional activity, mRNA stabilization, or both. Interestingly, however, one of two alternative splice forms of DCT1/DMT1 mRNA has a stem-loop structure in its 3' UTR that closely resembles an IRE.

Other molecules important in iron transport and homeostasis, such as HFE, hephaestin, IREG1/Ferroportin1, and duodenal ferrireductase, have been discovered

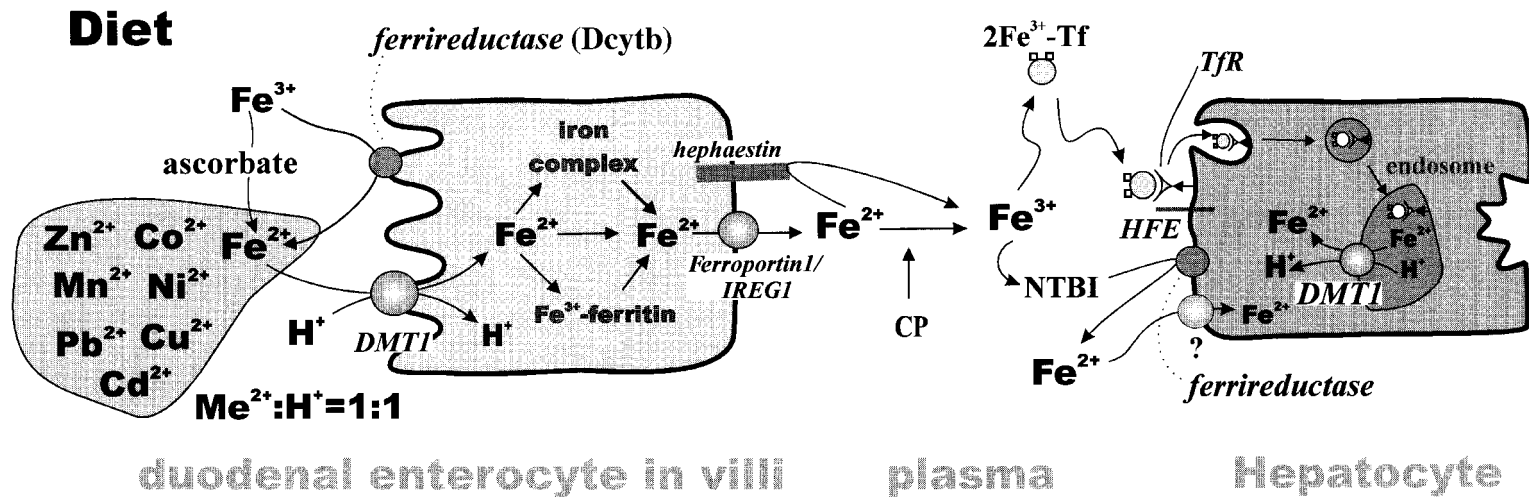


Figure 5 Diagram of divalent metal absorption in villus duodenal enterocyte and iron traversal to the hepatocyte. Key molecules, such as DCT1/DMT1, hephaestin, IREG1/Ferroportin1, TfR, and HFE are shown in italics. Ferric iron is reduced to the ferrous form by ascorbate or a ferrireductase localized to the enterocyte brush border membrane surface. Ferrous iron is then transported through DCT1/DMT1 energized by a proton. The transport stoichiometry for DCT1/DMT1 is predicted as $1Me^{2+}:1H^+$ (1). NTBI, non-Tf-bound-iron; CP, ceruloplasmin; Me, metal.

recently. The three-dimensional structure of soluble HFE has been determined (57). Some of these molecules may have direct or close interactions, as HFE physically associates with β_2M and TfR. This raises the question whether DCT1/DMT1 associates directly with or locates closely to ferrireductase in order to take up ferrous iron efficiently. Furthermore, are IREG1/ferroportin1 and hephaestin located next to each other? Crystal structures and mutational analyses may provide some insights into the normal function of those molecules. Given that yeast has several iron transporters, how many iron transporters will be found in mammals, and how are they regulated? Given the rapid recent progress, we may soon have a complete understanding of intestinal iron absorption and iron homeostasis.

ACKNOWLEDGMENTS

The authors thank Dr. Nancy Andrews for providing valuable advice during the research described in this review. The authors also thank Dr. David Eide for a critical reading and suggestions for the manuscript.

REFERENCES

1. Gunshin H, Mackenzie B, Berger UV, Gunshin Y, Romero MF, Boron WF, Hediger MA. Cloning and characterization of a mammalian proton-coupled metal-ion transporter. *Nature* 1997; 388:482–488.
2. Feder JN, Grirke A, Thomas W, Tsuchihashi Z, Ruddy DA, Basava A, Dormishian F, Domingo RJ, Ellis MC, Fullan A, Hinton LM, Jones NJ, Kimmel BE, Kronmal GS, Lauer P, Lee VK, Loeb DB, Mapa FA, McClelland E, Meyer NC, Mintier GA, Moeller N, Moore T, Morikang E, Prass CE, Quintana L, Starnes SM, Schatzman RC, Brunke KJ, Drayna DT, Risch NJ, Bacon BR, Wolff RK. A novel MHC class I-like gene is mutated in patients with hereditary haemochromatosis. *Nature Genet* 1996; 13:399–408.
3. Vulpe CD, Kuo YM, Murphy TL, Cowley L, Askwith C, Libina N, Gitschier J, Anderson GJ. Hephastin, a ceruloplasmin homologue implicated in intestinal iron transport, is defective in the sla mouse. *Nature Genet* 1999; 21:195–199.
4. Donovan A, Brownlie A, Zhou Y, Shepard J, Pratt SJ, Moynihan J, Paw BH, Drejer A, Barut B, Zapata A, Law TC, Brugnara C, Lux SE, Pinkus GS, Pinkus JL, Kingsley PD, Palis J, Fleming MD, Andrews NC, Zon LI. Positional cloning of zebrafish ferroportin1 identifies a conserved vertebrate iron exporter. *Nature* 2000; 403:776–781.
5. McKie AT, Marciani P, Rolfs A, Brennan K, Wehr K, Barrow D, Miret S, Bomford A, Peters TJ, Farzaneh F, Hediger MA, Hentze MW, Simpson RJ. A novel duodenal iron-regulated transporter, IREG1, implicated in the basolateral transfer of iron to the circulation. *Mol Cell* 2000; 5:299–309.
6. McKie AT, Barrow D, Latunde-Dada GO, Rolfs A, Sager G, Mudaly E, Mudaly M, Richardson C, Barlow D, Bomford A, Peters TJ, Raja KB, Shirali S, Hediger MA, Farzaneh F, Simpson RJ. An iron-regulated ferric reductase associated with the absorption of dietary iron. *Science* 2001; 291(5509):1755–1759.
7. Idzerda RL, Huebers H, Finch CA, McKnight GS. Rat transferrin gene expression: Tissue-specific regulation by iron deficiency. *Proc Natl Acad Sci USA* 1986; 83:3723–3727.
8. Conrad ME, Umbreit JN, Moore EG, Heiman D. Mobilferrin is an intermediate in iron transport between transferrin and hemoglobin in K562 cells. *J Clin Invest* 1996; 98: 1449–1454.
9. Simon D, Lu Y, Choate K, Velazquez H, Al-Sabban E, Praga M, Casari G, Bettinelli A, Colussi G, Rodriguez-Soriano J, McCredie D, Milford D, Sanjad S, Lifton R. Paracellin-

- 1, a renal tight junction protein required for paracellular Mg^{2+} resorption. *Science* 1999; 285:103–106.
10. Raja KB, Simpson RJ, Peters TJ. Investigation of a role for reduction in ferric iron uptake by mouse duodenum. *Biochim Biophys Acta* 1992; 1135:141–146.
 11. Jordan I, Kaplan J. The mammalian transferrin-independent iron transport system may involve a surface ferrireductase activity. *Biochem J* 1994; 302:875–879.
 12. Han O, Failla ML, Hill AD, Morris ER, Smith JC Jr. Reduction of Fe(III) is required for uptake of nonheme iron by Caco-2 cells. *J Nutr* 1995; 125:1291–1299.
 13. Dorey C, Cooper C, Dickson DPE, Gibson J, Simpson RJ, Peters TJ. Iron speciation at physiological pH in media containing ascorbate and oxygen. *Br J Nutr* 1993; 70:157–169.
 14. Fleming MD, Trenor CC, Su MA, Foernzler D, Beier DR, Dietrich WF, Andrews NC. Microcytic anaemia mice have a mutation in Nramp2, a candidate iron transporter gene. *Nature Genet* 1997; 16:383–386.
 15. Romero MF, Kanai Y, Gunshin H, Hediger MA. Expression cloning using *Xenopus laevis* oocytes. In: Amara SG, ed. *Methods in Enzymology, Neurotransmitter Transporters*. 1998; 296:17–52.
 16. Hirsch EC, Faucheux BA. Iron metabolism and Parkinson's disease. *Movement Disord* 1998; 13(suppl 1):39–45.
 17. Fleming MD, Romano MA, Su MA, Garrick LM, Garrick MD, Andrews NC. Nramp2 is mutated in the anemic Belgrade (b) rat: Evidence of a role for Nramp2 in endosomal iron transport. *Proc Natl Acad Sci USA* 1998; 95:1148–1153.
 18. Vidal S, Malo D, Vogan K, Skamene E, Gros P. Natural resistance to infection with intracellular parasites: Isolation of a candidate for Bcg. *Cell* 1993; 73:469–485.
 19. Vidal S, Gros P, Skamene E. Natural resistance to infection with intracellular parasites: Molecular genetics identifies Nramp1 as the *Bcg/Ity/Lsh* locus. *J Leukocyte Biol* 1995; 58:382–390.
 20. Gruenheid S, Cellier M, Vidal S, Gros P. Identification and characterization of a second mouse Nramp gene. *Genomics* 1995; 25:514–525.
 21. Dorschner MO, Phillips RB. Comparative analysis of two Nramp loci from rainbow trout. *DNA Cell Biol* 1999; 18:573–583.
 22. Cellier M, Privè GG, Belouchi Am, Kwan T, Gros P. Nramp defines a family of membrane proteins. *Proc Natl Acad Sci USA* 1995; 92:10089–10093.
 23. Supek F, Supekova L, Nelson H, Nelson N. A yeast manganese transporter related to the macrophage protein involved in conferring resistance to mycobacteria. *Proc Natl Acad Sci USA* 1996; 93:5105–5110.
 24. Atkinson P, Barton C. High level expression of Nramp1G169 in RAW264.7 cell transfectants: Analysis of intracellular iron transport. *Immunology* 1999; 656–662.
 25. Searle S, Bright N, Roach T, Atkinson P, Barton C, Meloen R, Blackwell J. Localisation of Nramp1 in macrophages: Modulation with activation and infection. *J Cell Sci* 1998; 111:2855–2866.
 26. Gunshin H, Rouault TA, Rogers J, Allerson C, Gollan JL, Andrews NC. Subcellular localization and regulation of the divalent metal-ion transporter, DMT1 (abstr). World Congress on Iron Metabolism BioIron'99, Sorrento, Italy, May 23–28, 1999.
 27. Wardrop S, Richardson D. The effect of intracellular iron concentration and nitrogen monoxide on Nramp2 expression and non-transferrin-bound iron uptake. *Eur J Biochem* 1999; 263:41–49.
 28. Canonne-Hergaux F, Gruenheid S, Ponka P, Gros P. Cellular and subcellular localization of the Nramp2 iron transporter in the intestinal brush border and regulation by dietary iron. *Blood* 1999; 93:4406–4417.
 29. Lee PL, Gelbart T, West C, Halloran C, Beutler E. The human Nramp2 gene: Characterization of the gene structure, alternative splicing, promoter region and polymorphisms. *Blood Cells, Mol Dis* 1998; 24:199–215.

30. Aisen P, Listowsky I. Iron transport and storage proteins. *Annu Rev Biochem* 1980; 49: 357–393.
31. Finch C, Huebers H. Perspectives in iron metabolism. *N Engl J Med* 1982; 1520–1528.
32. Harford JB, Rouault TA, Huebers H, Klausner RD. Molecular mechanisms of iron metabolism. In: Stamatoyannopoulos G, Neinhuis A, Majerus P, Varmus H, eds. *The Molecular Basis of Blood Diseases*. London: Saunders, 1994:351–378.
33. Dautry-Varsat A, Ciechanover A, Lodish H. pH and the recycling of transferrin during receptor-mediated endocytosis. *Proc Natl Acad Sci USA* 1983; 80:2258–2262.
34. Sipe D, Jesurum A, Murphy R. Absence of Na⁺,K⁺-ATPase regulation of endosomal acidification in K562 erythroleukemia cells. Analysis via inhibition of transferrin recycling by low temperatures. *J Biol Chem* 1991; 266:3469–3474.
35. Bali P, Zak O, Aisen P. A new role for the transferrin receptor in the release of iron from transferrin. *Biochemistry* 1991; 30:324–328.
36. Nunez M, Gaete V, Watkins J, Glass J. Mobilization of iron from endocytic vesicles. The effects of acidification and reduction. *J Biol Chem* 1990; 265:6688–6692.
37. Egyed A. Carrier mediated iron transport through erythroid cell membrane. *Br J Haematol* 1988; 68:483–486.
38. Garrick M, Gniecko K, Liu Y, Cohan D, Garrick L. Transferrin and the transferrin cycle in Belgrade rat reticulocytes. *J Biol Chem* 1993; 268:14867–14874.
39. Farcich E, Morgan E. Uptake of transferrin-bound and nontransferrin-bound iron by reticulocytes from the Belgrade laboratory rat: Comparison with Wistar rat transferrin and reticulocytes. *Am J Hematol* 1992; 39:9–14.
40. Hodgson L, Quail E, Morgan E. Iron transport mechanisms in reticulocytes and mature erythrocytes. *J Cell Physiol* 1995; 162:181–190.
41. Powell LW, Jazwinska E, Halliday JW. Primary iron overload. In: Powell LW, Jazwinska E, Halliday JW, eds. *Iron Metabolism in Health and Disease*. London: Saunders, 1994: 227–270.
42. Jouanolle AM, Gandon G, Jezequel P, Blayau M, Campion ML, Yaouanq J, Mosser J, Fergelot P, Chauvel B, Bouric P, Carn G, Andrieux N, Gicquel I, Le Gall JY, David V. Haemochromatosis and HLA-H. *Nature Genet* 1996; 14:251–252.
43. Jazwinska EC, Cullen LM, Busfield F, Pyper WR, Webb SI, Powell LW, Morris CP, Walsh TP. Haemochromatosis and HLA-H. *Nature Genet* 1996; 14:249–251.
44. Beutler E, Gelbart T, West C, Lee P, Adams M, Blackstone R, Pockros P, Kosty M, Venditti CP, Phatak PD, Seese NK, Chorney KA, Ten Elshof AE, Gerhard GS, Chorney M. Mutation analysis in hereditary hemochromatosis. *Blood Cells Mol Dis* 1996; 22: 187–194.
45. Feder JN, Tsuchihashi Z, Irrinki A, Lee VK, Mapa FA, Morikang E, Prass CE, Starnes SM, Wolff RK, Parkkila S, Sly WS, Schatzman RC. The hemochromatosis founder mutation in HLA-H disrupts beta2-microglobulin interaction and cell surface expression. *J Biol Chem* 1997; 272:14025–14028.
46. Waheed A, Parkkila S, Zhou XY, Tomatsu S, Tsuchihashi Z, Feder JN, Schatzman RC, Britton RS, Bacon BR, Sly WS. Hereditary hemochromatosis: Effects of C282Y and H63D mutations on association with beta2-microglobulin, intracellular processing, and cell surface expression of the HFE protein in COS-7 cells. *Proc Natl Acad Sci USA* 1997; 94:12384–12389.
47. Feder JN, Penny DM, Irrinki A, Lee V, Lebron J, Watson N, Tsuchihashi Z, Sigal E, Bjorkman PJ, Schatzman RC. The hemochromatosis gene product complexes with the transferrin receptor and lowers its affinity for ligand binding. *Proc Natl Acad Sci USA* 1998; 95:1472–1477.
48. Parkkila S, Waheed A, Britton RS, Bacon BR, Zhou XY, Tomatsu S, Fleming RYD, Sly WS. Association of the transferrin receptor in human placenta with HFE, the protein

- defective in hereditary hemochromatosis. *Proc Natl Acad Sci USA* 1997; 94:13198–13202.
49. Gross CN, Irrinki A, Feder JN, Enns CA. Co-trafficking of HFE, a nonclassical major histocompatibility complex class I protein, with the transferrin receptor implies a role in intracellular iron regulation. *J Biol Chem* 1998; 273:22068–22074.
 50. Parkkila S, Waheed A, Britton RS, Feder JN, Tsuchihashi Z, Schatzman RC, Bacon BR, Sly WS. Immunohistochemistry of HLA-H, the protein defective in patients with hereditary hemochromatosis, reveals unique pattern of expression in gastrointestinal tract. *Proc Natl Acad Sci USA* 1997; 94:2534–2539.
 51. Zhou XY, Tomatsu S, Fleming RE, Parkkila S, Waheed A, Jiang J, Fei Y, Brunt EM, Ruddy DA, Prass CE, Schatzman RC, O'Neill R, Britton RS, Bacon BR, Sly WS. HFE gene knockout produces mouse model of hereditary hemochromatosis. *Proc Natl Acad Sci USA* 1998; 95:2492–2497.
 52. Fleming RE, Migas MC, Zhou XY, Jiang J, Britton RS, Brunt EM, Tomatsu S, Waheed A, Bacon BR, Sly WS. Mechanism of increased iron absorption in murine model of hereditary hemochromatosis: Increased duodenal expression of the iron transporter DMT1. *Proc Natl Acad Sci USA* 1999; 96:3143–3148.
 53. Zoller H, Pietrangelo A, Vogel W, Weiss G. Duodenal metal-transporter (DMT-1, NRAMP-2) expression in patients with hereditary haemochromatosis. *Lancet* 1999; 353: 2120–2123.
 54. Pietrangelo A, Casalgrandi G, Quaglino D, Gualdi R, Conte D, Milani S, Montosi G, Cesarini L, Ventura E, Cairo G. Duodenal ferritin synthesis in genetic hemochromatosis. *Gastroenterology* 1995; 108:208–217.
 55. Stearman R, Yuan DS, Yamaguchi-Iwai Y, Klausner RD, Dancis A. A permease-oxidase complex involved in high-affinity iron uptake in yeast. *Science* 1996; 271:1552–1557.
 56. Diatchenko L, Lau YF, Campbell AP, Chenchik A, Moqadam F, Huang B, Lukyanov S, Lukyanov K, Gurskaya N, Sverdlov ED, Siebert PD. Suppression subtractive hybridization: A method for generating differentially regulated or tissue-specific cDNA probes and libraries. *Proc Natl Acad Sci USA* 1996; 93:6025–6030.
 57. Lebron JA, Bennett MJ, Vaughn DE, Chirino AJ, Snow PM, Mintier GA, Feder JN, Bjorkman PJ. Crystal structure of the hemochromatosis protein HFE and characterization of its interaction with transferrin receptor. *Cell* 1998; 93:111–123.
 58. Beinert H, Kennedy MC. Aconitase, a two-faced protein: enzyme and iron regulatory factor. *FASEB J* 1993; 7:1442–1449.
 59. Philpott CC, Haile D, Rouault TA, Klausner RD. Modification of a free Fe-S cluster cysteine residue in the active iron-responsive element-binding protein prevents RNA binding. *J Biol Chem* 1993; 268:17655–17658.
 60. Guo B, Phillips JD, Yu Y, Leibold EA. Iron regulates the intracellular degradation of iron regulatory protein 2 by the proteasome. *J Biol Chem* 1995; 270:21645–21651.
 61. Iwai K, Klausner RD, Rouault TA. Requirements for iron-regulated degradation of the RNA binding protein, iron regulatory protein 2. *EMBO J* 1995; 14:5350–5357.

7

Basolateral Transport of Iron in Mammalian Intestine From Physiology to Molecules

ANDREW T. McKIE and ROBERT J. SIMPSON

King's College London, London, England

I.	IRON ABSORPTION IS A TWO-STEP PROCESS	175
A.	Anatomical Location	175
B.	Kinetics of Mucosal Transfer: Two Phases Are Observed	176
C.	Regulation of the Transfer Step	176
D.	Cellular Studies	180
E.	Subcellular Studies	180
F.	Role of Ceruloplasmin in Transfer of Iron	181
II.	EXTRACELLULAR IRON MOVEMENT	182
III.	BASOLATERAL IRON TRANSPORTER, Ireg1	182
A.	Identification	182
B.	Evidence that Ireg1 Mediates Basolateral Iron Transport	183
C.	Ireg1 Expression Is Regulated by Iron Status	184
D.	Do Ireg1 and Hephaestin Interact Functionally?	185
	REFERENCES	185

I. IRON ABSORPTION IS A TWO-STEP PROCESS

A. Anatomical Location

Early studies of the iron absorption mechanism and its regulation established that this process is confined mainly to the duodenum and proximal jejunum, where the

small intestinal luminal pH is most suited to maintain iron in a soluble form (reviewed in Refs. 1–3). More recent data have strongly reinforced this view (4,5).

Manis and Schachter showed in 1962 that the absorption process in the proximal intestine can be divided into two steps, uptake of luminal iron into the mucosa and transfer of iron from mucosa to the blood (6). This terminology has been almost universally adopted in subsequent work, even though it is an oversimplification. The present review is confined to the second step, namely, mucosal transfer. This step can be equated to movement of iron from the epithelial cell interior to the circulation. Anatomical considerations suggest that the overall process of mucosal iron transfer involves several proteins and the traversing of such barriers as the epithelial cell cytosol, the basolateral membrane, the interstitial fluid space, epithelial basement membrane, lamina propria, and capillary wall. It is thought that the major influence on the rate of mucosal transfer is exerted by the cytoplasm and basolateral membrane. It is possible to obtain a measure of mucosal transfer *in vivo* as the appearance or retention of radioactive iron in the body of an animal or human. The process can also be measured with vascularly perfused intestine or *in vitro* with lumenally perfused intestinal segments or with everted sacs of intestine.

B. Kinetics of Mucosal Transfer: Two Phases Are Observed

Early work established that two kinetic phases of iron transfer can be identified. Once iron is introduced into the intestinal lumen, there is a rapid phase (within a few minutes) in which large amounts of the given dose of iron appear in the circulation. Then there is a slower phase (6–24 h) in which some iron, which was initially retained in the epithelial cells (1,2), is transferred to the circulation. Most studies of physiological regulatory mechanisms have focused on the rapid phase, but the presence of two distinguishable processes must be noted. Early kinetic studies also showed the presence of low- and high-affinity pathways for absorption, both of which are regulated by body iron stores (7).

C. Regulation of the Transfer Step

The importance of the transfer step in determining the overall rate of iron absorption remains a subject of debate. Many studies appear to show that the rate of iron transfer is regulated by body iron requirements (e.g., Refs. 1, 2, 8–10). On the other hand, two of the most sophisticated studies of this question concluded the opposite, namely, that iron stores do not regulate the rate of transfer, only the rate of uptake (11,14). Changes in transfer rates were observed in the latter studies, but they were consequential to changes in uptake—no change in iron carriers was needed. In other words, mucosal transfer *per se* is not a regulatory step. None of the above studies is without flaws. The *in-vivo* studies of Nathanson and McLaren (11,12) depend on computer-fitting data which seem to be underdetermined for flux of iron through the proximal intestinal lumen. Our own unpublished work shows that flux of iron through the proximal intestine in mice is very rapid and is a major determinant of iron absorption rates, and Nathanson and McLaren were not able to measure these flux rates accurately with their method. It is noteworthy that, when applying their method to human hemochromatosis, they came to the opposite conclusion, namely, that transfer is the major step affected, rather than mucosal uptake (13). On the other hand, all *in-vivo* work that supports a regulation of the transfer step involves the use

radioactive tracers, the specific activities of which are unknown after the iron has been taken into the mucosa. This makes quantitative comparison of flux rates difficult to interpret, especially when mucosal iron contents likely vary among different groups of people or experimental animals.

The careful *in-vitro* work of Schumann's group (14) does not suffer from the problem of transit, and precautions were taken to check on changes in specific activity of the iron transferred across the mucosa. Importantly, their data suggested that little or no isotope dilution occurred. They showed that the mucosal–serosal transfer rate constant is not altered in iron-deficient rat duodenal segments compared to controls, and that the process is not saturated by luminal iron concentrations up to 500 μM . If the basolateral membrane transfer step is the principal determinant of the mucosal–serosal transfer rate in their system, then their data suggest that this is not regulated by iron deficiency. They further show that it is unsaturated, having the properties of a facilitated diffusion process, though they assume that iron ions cannot cross membranes without the involvement of a carrier. This situation (i.e., an active uptake step at the brush border membrane with a high-capacity, facilitated diffusion at the basolateral membrane) resembles that initially proposed for other nutrients such as glucose and amino acids. It is noteworthy, however, that more recent data suggests that the basolateral membrane transport step can be regulated and (or) rate-determining for these nutrients (15).

The conclusions of Schumann and colleagues were weakened by the presence of a long lag phase (30 min) before iron transfer across the serosal wall begins. This lag is not seen *in vivo* (5), and it suggests that the slow, probably unregulated, serosal transfer step becomes rate-determining for overall iron transfer *in vitro*. Modeling studies of the two-step kinetic system for iron absorption can be used to illustrate the effects of uptake regulation versus transfer regulation (Fig. 1). These studies show that the quantity of iron present in the gut wall, or the percentage transfer of iron taken up by the duodenum, are useful indicators of whether mucosal transfer of iron has altered, provided that the absorption process is in a pseudo-steady state. Figure 1 illustrates the effect of selectively regulating mucosal uptake or mucosal transfer rates on the duodenal iron loading, percentage transfer, and actual amount of iron transferred to the body. The modeling demonstrates how regulation of the two steps has distinctive effects on duodenal iron loading or percentage of iron transfer. Figure 1 also illustrates that selectively regulating transfer is not a very efficient way to regulate the actual amount of iron transferred to the body. Thus, in the study of Schumann et al., the steady-state level of radioiron in the duodenal wall is increased in iron deficiency, due to the regulation occurring prior to the serosal transfer step.

Many *in-vivo* studies have documented changes that suggest mucosal transfer can be regulated (9,10,16–22). This is subject to the caveats that most of these studies were performed at single time points and none of them was able to measure the specific activity of the iron transferred to the blood. As an illustration of the type of changes seen, Figs. 2 and 3 display data from a study in which two regulators of iron absorption, dietary iron and hypoxia, were investigated. Figure 2 shows that a wide range of values for the percentage transfer of iron by the duodenum can be observed. Both dietary iron level and hypoxia can affect this parameter. Figure 3 shows that the duodenal loading with radio-iron can increase [effect of low iron diet at normal pressure, resembles findings of Schumann et al. (14)] or decrease (effect of low iron diet in hypoxic mice, or effect of hypoxia in low iron mice), an indicator

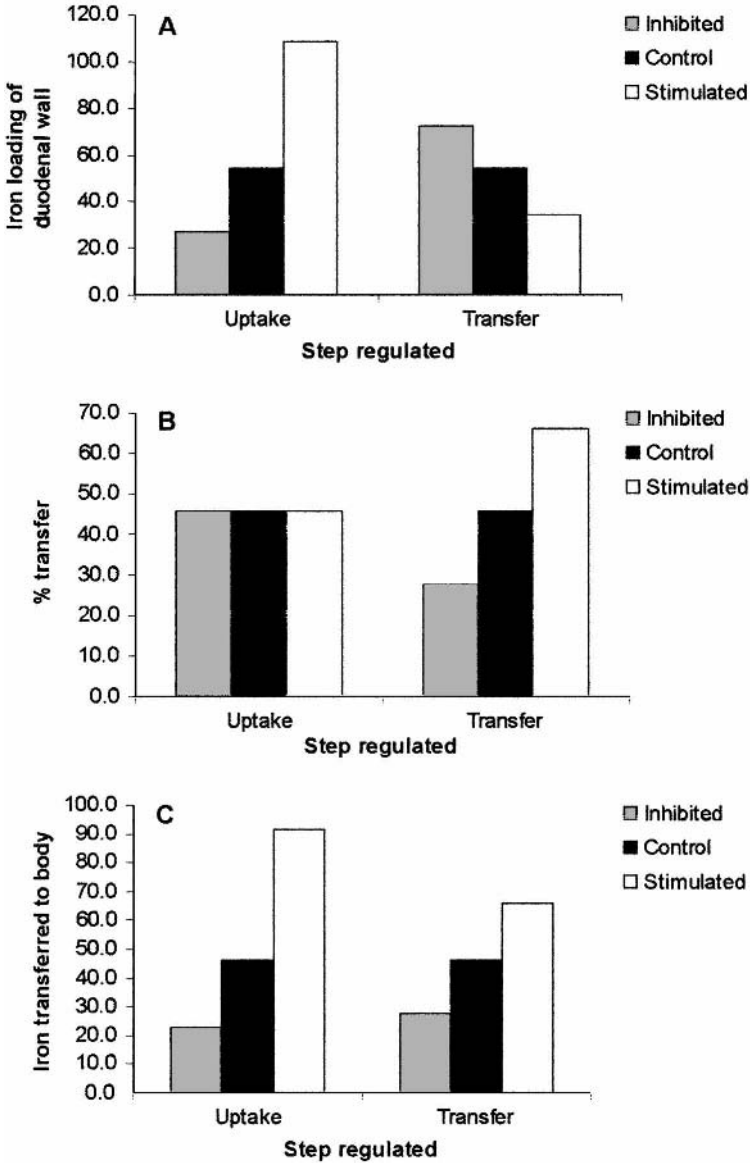


Figure 1 Modeling effect of regulation of mucosal uptake or mucosal transfer rates on iron absorption parameters. A simple two-step model (linear uptake rate, exponential transfer) for duodenal iron absorption, based on rates similar to those observed by Schumann et al. (14) with an incubation time of 1 h was simulated using a four-step Runge-Kutta integration method. Data for the effect of selective regulation of mucosal uptake or mucosal transfer on (A) duodenal iron loading, (B) % transfer, and (C) actual amount of iron transferred. Stimulated means the uptake or transfer step was increased $2 \times$ compound to control; inhibited means the rate was $0.5 \times$ control.

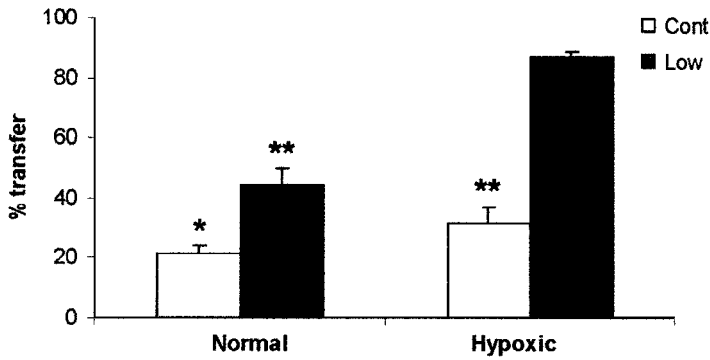


Figure 2 Effect of low-iron-diet feeding and hypoxia on duodenal mucosal transfer of iron in mice. Mice were fed low-iron or control diet for 4 days and exposed to normal or half-atmospheric pressure (hypoxia) for the latter 3 days as described by Simpson (10). Iron absorption was measured from tied-off duodenal segments in vivo after a 10-min incubation with 250 μM FeNTA₂. The quantity of radio-iron in the body is expressed as a percentage of the total radioactivity taken up from the lumen. * $p < 0.01$ versus normal, low iron; ** $p < 0.001$ versus hypoxic, low iron.

that mucosal transfer has increased to a greater extent than mucosal uptake. Some studies have shown increased iron uptake in the absence of increased iron transferred to the body (21), which suggests that the transfer rate constant had actually decreased. The majority of studies have shown both uptake and transfer to be regulated in parallel, although the relative degree to which the two steps are altered seems to vary. To conclude, there is evidence that basolateral transfer of iron is regulated and influences overall iron absorption, but this may not be true for all situations in which iron absorption is altered.

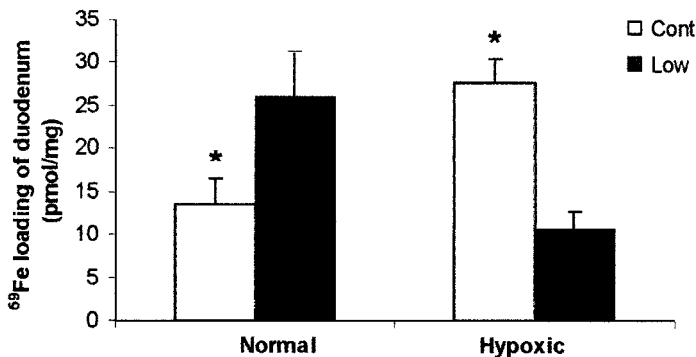


Figure 3 Effect of low-iron-diet feeding and hypoxia on duodenal loading of absorbed iron in mice. Mice were treated as in Fig. 1. The quantity of radio-iron in the duodenal wall after the 10-min tied-off segment incubation is shown. * $p < 0.05$ versus low iron.

D. Cellular Studies

In the last decade, cultured epithelial cell monolayers, especially CaCo cells derived from colonic carcinoma, have been used extensively to model intestinal iron absorption. The cultured epithelial cells are the only long-lived in-vitro model for intestinal transport which can allow investigation of regulatory processes in a controlled way, independent of corporeal factors. This makes them potentially decisive in establishing regulatory mechanisms. Some caution is necessary, however, in extrapolating mechanisms observed in these cells to whole duodenum. The differential expression of proteins along the crypt villus axis, e.g., transferrin receptor (26) or HFE (23), suggests that CaCo cells may represent emerging crypt cells or lower villus cells (24–26), rather than fully differentiated villus tip cells that express maximal activity of the iron-absorptive pathway (27,28). It is interesting to note that CaCo cells can synthesize transferrin (29), while small-intestinal mucosa in vivo is not thought to have this capability (30–32). This means that, although a useful tool, pathways for iron transport which operate in CaCo cells may not represent those operating at the villus tip. Furthermore, some groups have observed specific, regulated iron transfer with these cells (33,34) while others have not (35), emphasizing that results obtained with these cells must be interpreted with caution.

Alvarez-Hernandez et al. have suggested that basolaterally derived apotransferrin is involved in transfer of iron across CaCo cells (36). This finding echoes earlier work which showed that intestinal epithelial cells can bind apotransferrin (37), and many studies which suggested that transferrin or transferrin-like proteins were involved in iron transfer across the mucosa (4,38–40). Two groups of workers have suggested that vesicle movements are involved in iron transfer across CaCo cells (41,42). Another study failed to inhibit iron transfer with the cytoskeletal disruptor, cytochalasin B, but attributed this to effects on the tight junctions that increased paracellular transport (43). Most attempts to verify an involvement of apotransferrin in the rapid phase of in-vivo iron transfer have failed, however (37,44,45). A role of transferrin is also unlikely on kinetic grounds (see Sec. II). It should be noted that in-vivo iron absorption can be increased, even when transferrin is saturated [e.g., in hypoxia (46)] or absent (20). A role for apotransferrin, perhaps in the slower phase of iron absorption, remains a possibility. In-vivo work on the role of vesicles in iron absorption is more controversial (4,47).

E. Subcellular Studies

Ultrastructural studies in which movement of newly absorbed iron is followed across the epithelial cells showed that iron is associated with rough endoplasmic reticulum, ribosomes, and lateral cell membranes (48,49). Many early attempts to identify cytoplasmic intermediates in iron transfer found iron bound to transferrin and ferritin (e.g., Refs. 4, 38, and 39). It is accepted that at least some newly absorbed iron has access to ferritin, suggesting that it enters the cytosol at some point. The time course of loading ferritin with iron is relatively slow, showing that ferritin is not an intermediate in the rapid phase of iron absorption (1,2) and therefore cannot regulate the rapid phase of iron transfer. Ferritin likely plays some role in the slower phase of transfer, however. At one time, transferrin seemed an excellent candidate for the carrier for iron in the mucosal cells, perhaps exiting the cells by some process involving vesicle exocytosis at the basolateral membrane (see above).

Studies of the movement of iron between proteins in the mucosa have been performed and reviewed by Conrad and colleagues (50), who postulated a pathway explaining the movement of radioactive iron across the mucosa. This pathway involves binding of iron to mobilferrin, paraferitin, and an integrin. Mobilferrin has been reported to be a calcium-binding protein, calreticulin, while paraferitin is a multiprotein complex that includes mobilferrin, β_3 -integrin, and other proteins. Mobilferrin was proposed as the cytosolic “shuttle” for iron, while paraferitin was thought to be a ferric reductase which could provide ferrous iron for incorporation into, e.g., ferritin.

Early cell fractionation studies suggested that mitochondria were important in iron absorption, but later studies with high-resolution techniques confirmed the importance of the basolateral membrane (51).

F. Role of Ceruloplasmin in Transfer of Iron

The observation that copper deficiency leads to anemia and decreased iron absorption implicated copper or a copper-regulated protein in iron metabolism. The answer came with the recognized involvement of ceruloplasmin (Cp), a 132-kDa blue copper plasma protein (see Chapter 30). Cp binds 6 copper atoms and may play a role in copper transport. Cp has ferroxidase activity, readily converting Fe^{2+} to Fe^{3+} , and it was hypothesized that this reaction plays a role in loading circulating transferrin with iron (52,53). In copper deficiency, ceruloplasmin is still synthesized; however, copper incorporation is reduced, resulting in a lack of ferroxidase activity. Two different mutations have been found in the ceruloplasmin gene, both of which lead to aceruloplasminemia and neurological disorders caused by excessive iron deposition in the brain and other tissues including the liver (54,55). Other clinical features are low serum iron and elevated plasma ferritin. Recently, further evidence of the role of Cp in iron efflux has come from studies on mice with targeted disruption of the Cp gene (56). From these observations a reasonable working hypothesis is that iron is released from cells in the ferrous form and that the role of Cp is to convert ferrous iron to ferric iron, which can then be bound to transferrin. The lack of Cp leads to a failure to release iron, resulting in accumulation of iron in parenchymal cells. In the intestinal enterocytes, lack of Cp would be predicted to lead to reduced iron transfer to the circulation. The role of Cp in the mobilization of iron from the enterocyte has been studied in copper-deficient animals, with different results depending on the preparation used (57,58). Coppen and Davies saw no effect on transfer of iron from the mucosa to the circulation when they perfused intestinal preparations with four times the Cp activity normally present in the rat plasma (57). In these studies, however, iron transport was measured over a relatively long, 1-h period. Wollenberg, on the other hand, found a steep and rapid increase (within 1–2 min) in iron transfer when Cp was injected intravenously during the perfusion period (58). The increase was specific to Cp, as the response could not be elicited by other copper-containing protein complexes. The effect of Cp on iron transfer was transient and decreased to control levels within 30 min of injection. From these studies the authors concluded that iron is released from the basolateral membrane in the ferrous form and loading of transferrin is promoted by oxidation of ferrous iron by Cp. In this way a steep concentration gradient for ferrous iron is maintained. Thus iron can efflux from the mucosa when ceruloplasmin is absent, but its distribution to tissues will be affected.

II. EXTRACELLULAR IRON MOVEMENT

Morgan established that the final part of iron transfer involves iron entering the portal circulation, probably in a low-molecular-weight form (59), i.e., not bound to transferrin. There has been much conflicting data since 1980 on the matter of whether transferrin is involved directly in the transfer of iron to blood, or simply acts as the final acceptor for absorbed iron. Morgan based his conclusion on kinetics, and he acknowledged that other mechanisms likely coexist. This is something which should always be borne in mind when reading the literature of iron absorption—multiple mechanisms exist which may vary in importance in different pathological, experimental, or physiological circumstances.

Our own group has favored the lack of requirement for transferrin because of our experience with hypotransferrinaemic mice. These have very low levels of transferrin, but show the highest rate of iron absorption of any mouse model we have seen (20,60). Injecting these mice with transferrin decreases iron absorption rates (61). Other evidence against a role for transferrin has been summarized above. It is also noteworthy that humans with hemochromatosis lack apo-transferrin, but have high rates of iron absorption. Instead, transferrin seems to be required for distributing iron to cells requiring iron, especially the developing red cells in bone marrow. It is too early to provide a comprehensive mechanism for transfer which can account for all the above observations. It is quite clear that progress is ongoing and the cloning of new genes will illuminate this process.

A further argument in favor of a regulated transfer step came from the ferrokinetic study of SLA mice (62). It was apparent that these mice were able to take up iron into the mucosa but unable to transfer the iron to the circulation. A similar defect was observed in placental transfer of iron in these mice. Following a positional cloning strategy, the gene underlying the SLA phenotype was identified (63). Hephaestin, a ceruloplasmin homolog, multicopperoxidase, was isolated in 1999 and implicated a ferroxidase in the transfer of iron to the circulation.

III. BASOLATERAL IRON TRANSPORTER, Ireg1

A. Identification

In order to try to isolate genes involved in intestinal iron transport, we used hypotransferrinaemic mice (*hpx*) to make a subtracted duodenal cDNA library (Fig. 4). Homozygous *hpx* mice have a defect in the transferrin gene, and as a result become chronically anemic. As a result of the anemia they absorb iron up to 30 times faster than heterozygotes manipulated to have similar iron stores. We analyzed by Northern blots five clones picked at random from the subtracted library. The purpose of Northern analysis was to identify genes which were upregulated in the duodenal mucosa by various stimuli of the iron-absorption pathway, including iron deficiency and hypoxia. As a negative control RNA from ileum, which does not show regulated iron absorption to the same extent, was also blotted and probed. The clones were named oi1–oi5 (oi stands for obvious insert). All five cDNAs were highly expressed in the duodenum, and three of them (oi1, oi2 and oi5) were highly upregulated by both hypoxia and iron deficiency in the duodenum but showed low expression and no obvious iron regulation in ileum. Sequence analysis of oi1 identified the cDNA as mouse Nramp2. At this time, Nramp2 had already been described in the literature as a homolog of Nramp1 (64), but its function as an iron transporter had not yet

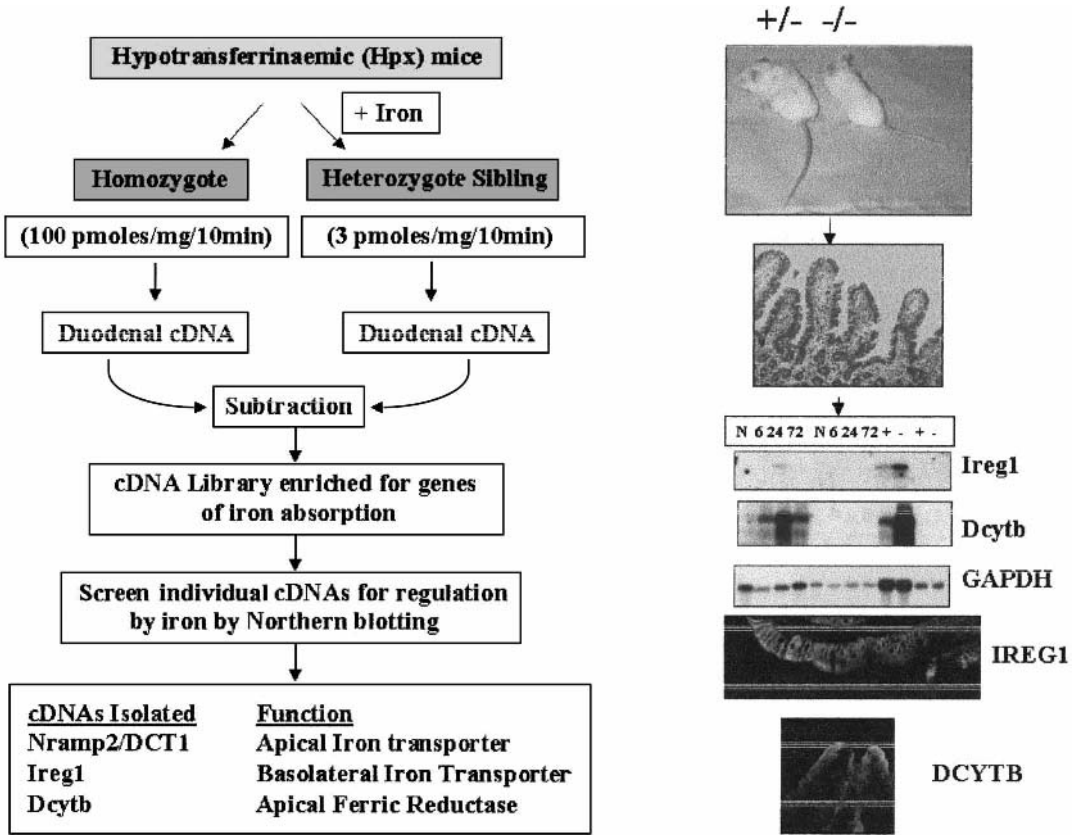


Figure 4 Outline of subtraction strategy (left-hand side). Right-hand side shows the representative Northern blots used to identify two iron-regulated genes (Ireg1 and Dcytb candidate basolateral transporter and apical ferric reductase, respectively); below this is immunocytochemistry using polyclonal peptide antibodies for Ireg1 and Dcytb showing that Ireg1 is expressed in basolateral membrane and Dcytb on the apical membrane.

been shown. The other two iron-regulated cDNAs, oi5 and oi2, were sequenced and appeared to encode novel membrane proteins. Further sequence analysis of oi5 revealed an iron-responsive element (IRE) in the 5' UTR of its mRNA, leading us to rename the gene Ireg1 (*Iron-regulated gene*) (65).

B. Evidence that Ireg1 Mediates Basolateral Iron Transport

Using a tagged Ireg1 construct, we found that the protein was targeted in polarized epithelial cells to the basolateral membrane, a finding which initially led us to hypothesize that Ireg1 is involved in the transfer of iron to the circulation across this membrane. By using the *Xenopus* oocyte expression system, Ireg1 is capable of inducing efflux of iron (66). We used a co-expression strategy with DMT1/Nramp2 (see Chapter 6) and Ireg1 expressed in the same oocyte. Oocytes were first loaded with iron by incubation in radio-iron solution at pH 6.2. These conditions are optimal for the uptake of ferrous iron via DMT1/Nramp2. Oocytes were then washed, and efflux of iron was measured in fresh buffer at pH 7.0. The efflux buffer also contained

ceruloplasmin and apo-transferrin. There was a significant efflux of iron in oocytes injected with DMT1/Nramp2 and Ireg1 cRNA, when compared to oocytes injected with DMT1/Nramp2 alone. We found that the efflux process required the presence of ceruloplasmin; in the absence of ceruloplasmin, little if any efflux was seen. These data support the idea that a ferroxidase is required for transfer of iron to the circulation. The gene Ireg1 has now been independently identified in two other laboratories and named ferroportin (67) and MTP1 (68). In the first of these reports, Donovan et al. used positional cloning to identify the gene responsible for the wiessherbst (*weh*; see Chapter 27) mutant phenotype in zebrafish, so-called because their lack of hemoglobin gives them a pale appearance. The gene they identified as responsible was the zebrafish homolog of Ireg1, named ferroportin. Ferroportin is expressed in the yolk sac and is likely to be responsible for transfer of iron from the maternally derived iron stores to the circulation. In the second report the authors used another approach, enriching for cDNA-containing IREs (68). In this way they found a cDNA identical to Ireg1 and named the gene MTP1 (for metal transport protein). It is interesting to note that three distinct approaches identified the same gene, and in each case the conclusions support the notion that Ireg1 is the basolateral iron transporter in intestinal cells. In addition, Ireg1 probably also plays an important role in iron transport in other organs, notably the placenta, where iron transfer between maternal and fetal circulations is critical, and in recycling iron into the circulation from the breakdown of hemoglobin in the Kupffer cells of the liver, and red pulp for the spleen.

C. Ireg1 Expression Is Regulated by Iron Status

By quantitation of mRNA and protein levels in mice with altered iron absorption, we observed a 2.4-fold increase in messenger RNA levels in mice fed an iron-deficient diet and a 3-fold increase in *hpx* mice compared to the appropriate controls (66). These increases in expression are similar in magnitude to increases in duodenal iron absorption in iron deficiency. It is noteworthy that Ireg1 is upregulated in both hypotransferrinemia (which causes elevated body iron stores) and iron deficiency. This indicates that Ireg1 can be regulated independently of iron stores. DMT1/Nramp2 mRNA levels are increased some 10-fold in iron deficiency, suggesting that transfer may be the limiting step for iron absorption (69). This makes sense, in that in iron deficiency an excess of iron can be rapidly acquired through uptake into the mucosa, but transfer could be more subtly adjusted to prevent all of the recently absorbed iron from reaching the circulation.

The mechanism of regulation of Ireg1 and DMT1/Nramp2 is not yet clear. Interestingly, they contain IREs in opposite ends of their mRNAs, DMT1/Nramp2 in the 3' UTR and Ireg1 in the 5' UTR. This is reminiscent of the transferrin receptor (IRE in 3' UTR) and ferritin (IRE in 5' UTR) couple, which are coordinately regulated by changes in intracellular iron (see Chapters 9 and 10). Is it possible that Ireg1 and DMT1/Nramp2 are also regulated in a coordinate manner by iron via the IRE/IRP system? In iron deficiency the mucosal cell would reduce Ireg1 translation and increase levels of DMT1/Nramp2 protein. As iron enters the cell via DMT1/Nramp2 and intracellular iron levels rise, IRE binding is reduced, thereby reducing DMT1/Nramp2 levels but allowing Ireg1 to be translated. This is an attractive model in many ways. However, how does one explain the increases in Ireg1 mRNA and

protein in iron deficiency? One possibility is that, in contrast to ferritin, the Ireg1 IRE is much farther from the starting ATG. This distance is enough that binding IRE-IRP would not likely inhibit translation (70). Binding of IRP to Ireg1 might actually stabilize the mRNA. Another proposed explanation (68) is that Ireg1 is regulated transcriptionally and the IRE is inactive. Clearly, further studies are required to address the role of these IREs in controlling the expression of Ireg1 and DMT1/Nramp2 transporters.

Interestingly, hephaestin does not appear to be regulated very strongly by iron deficiency, although we do not know whether regulators such as hypoxia or erythropoiesis regulate hephaestin. Our data on the regulation of Ireg1 by iron status supports the view that transfer of iron to the circulation is regulated and that this step may be the rate-limiting step in iron absorption.

D. Do Ireg1 and Hephaestin Interact Functionally?

An attractive mechanism envisaged is that Ireg1 transports ferrous iron, and that a ferroxidase is required for release and (or) binding of ferric iron to circulating transferrin. The recent cloning of hephaestin has also supported the idea that a ferroxidase is required for transfer of iron across the basolateral membrane (63). It is possible to speculate that Ireg1 and hephaestin, if in the same subcellular location, could work together in some way to provide ferrous transport and ferroxidase activity at the basolateral membrane. Whereas Ireg1 is expressed in the basolateral membrane of enterocytes, evidence for a similar location for hephaestin is lacking. Preliminary studies on the subcellular location of hephaestin using immunocytochemistry suggest that the protein is expressed in a perinuclear compartment (G. Anderson, personal communication). If this is the case, it suggests that oxidation of ferrous iron occurs in a compartment within the enterocyte, perhaps a transport vesicle. This vesicle could then be transported to the basolateral membrane, where Ireg1 could either transport ferric iron or reduce ferric iron and transport ferrous iron. The presence of a putative NADP/adenine binding site near the C-1 terminal end of Ireg1 would support this notion.

In summary, from these molecular studies, a ferroxidase is required for transfer of iron from the mucosa to the circulation. However, it is not yet clear how Ireg1 and hephaestin interact.

REFERENCES

1. Forth W, Rummel W. Iron absorption. *Physiol Rev* 1973; 53:724–792.
2. Turnbull A. Iron absorption. In: Jacobs A, Worwood M, eds. *Iron in Biochemistry and Medicine*. London: Academic Press, 1974:369–402.
3. Charlton RW, Bothwell TH. Iron absorption. *Annu Rev Med* 1983; 34:55–68.
4. Johnson G, Jacobs P, Purves LR. Iron binding proteins of iron absorbing rat intestinal mucosa. *J Clin Invest* 1983; 71:1467–1476.
5. Schumann K, Elsenhans B, Ehtechami C, Forth W. Rat intestinal iron transfer capacity and the longitudinal distribution of its adaptation to iron deficiency. *Digestion* 1990; 46: 35–45.
6. Manis JG, Schachter D. Active transport of iron by intestine: Features of the two-step mechanism. *Am J Physiol* 1962; 203:73–80.
7. Gitlin D, Cruchoad A. On the kinetics of iron absorption in mice. *J Clin Invest* 1962; 41:344–350.

8. Marx JJM, Stiekman J. Mucosal uptake, mucosal transfer and retention of a therapeutic dose of iron. *Eur J Clin Pharmacol* 1985; 23:335–338.
9. Raja KB, Duane PE, Ward RJ, Iancu TC, Simpson RJ, Peters TJ. In vitro and in vivo studies on Fe^{3+} absorption by mouse duodenum. Effect of iron loading on adaptive response to chronic hypoxia. *Biochem Pharmacol (Life Sci Adv)* 1990; 9:107–117.
10. Simpson RJ. Dietary iron levels and hypoxia independently affect iron absorption in mice. *J Nutr* 1996; 126:1858–1864.
11. Nathanson MH, Muir A, McLaren GD. Iron absorption in normal and iron-deficient beagle dogs: Mucosal iron kinetics. *Am J Physiol* 1985; 249:G439–448.
12. Nathanson MH, McLaren GD. Computer simulation of iron absorption: Regulation of mucosal and systemic iron kinetics in dogs. *J Nutr* 1987; 117:1067–1075.
13. McLaren GD, Nathanson MH, Jacobs A, Trevett D, Thomson W. Regulation of intestinal iron absorption and mucosal iron kinetics in hereditary hemochromatosis. *J Lab Clin Med* 1991; 117:390–401.
14. Schumann K, Elsenhans B, Forth W. Kinetic analysis of ^{59}Fe movement across the intestinal wall in duodenal rat segments *ex vivo*. *Am J Physiol* 1999; 276:G431–G440.
15. Cheeseman C. Role of intestinal basolateral membrane in absorption of nutrients. *Am J Physiol* 1992; 263:R482–R488.
16. Wheby MS, Jones LG, Crosby WH. Studies on iron absorption: Intestinal regulatory mechanisms. *J Clin Invest* 1964; 43:1433–1442.
17. Raja KB, Simpson RJ, Peters TJ. Comparison of $^{59}\text{Fe}^{3+}$ uptake in vitro and in vivo by mouse duodenum. *Biochim Biophys Acta* 1987; 901:52–60.
18. Raja KB, Simpson RJ, Pippard MJ, Peters TJ. In vivo studies of the relationship between intestinal iron (Fe^{3+}) absorption, hypoxia and erythropoiesis in the mouse. *Br J Haematol* 1988; 68:373–378.
19. Raja KB, Simpson RJ, Peters TJ. Effect of exchange transfusion of reticulocytes on in vitro and in vivo intestinal iron (Fe^{3+}) absorption in mice. *Br J Haematol* 1989; 73:254–259.
20. Simpson RJ, Lombard M, Raja KR, Thatcher R, Peters TJ. Iron absorption by hypotransferrinaemic mice. *Br J Haematol* 1991; 78:565–570.
21. Raja KB, Simpson RJ, Peters TJ. Intestinal iron absorption studies in mouse models of iron-overload. *Br J Haematol* 1994; 86:156–162.
22. Santos M, Wienk KJ, Schilham MW, Clevers H, de-Sousa M, Marx JJ. In vivo mucosal uptake, mucosal transfer and retention of iron in mice. *Lab Anim* 1997; 31:264–270.
23. Han O, Fleet JC, Wood RJ. Reciprocal regulation of HFE and Nramp2 gene expression by iron in human intestinal cells. *J Nutr* 1999; 129:98–104.
24. Bastin JM, Jones M, O'Callaghan CA, Schimanski L, Mason DY, Townsend ARM. Kupffer cell staining by an HFE-specific monoclonal antibody: Implications for hereditary haemochromatosis. *Br J Haematol* 1998; 103:931–941.
25. Parkkila S, Waheed A, Britton RS, Feder JN, Tsuchihashi Z, Schatzman RC, Bacon BR, Sly WS. Immunohistochemistry of HLA-H, the protein defective in patients with hereditary hemochromatosis, reveals unique pattern of expression in gastrointestinal tract. *Proc Natl Acad Sci USA* 1997; 94:2534–2539.
26. Anderson GJ, Powell LW, Halliday JW. Transferrin receptor distribution and regulation in the rat small intestine. Effect of iron stores and erythropoiesis. *Gastroenterology* 1990; 98:576–585.
27. O'Riordan DK, Sharp P, Sykes RM, Srai SK, Epstein O, Debnam ES. Cellular mechanisms underlying the increased duodenal iron absorption in rats in response to phenylhydrazine-induced haemolytic anaemia. *Eur J Clin Invest* 1995; 25:722–727.
28. O'Riordan DK, Debnam ES, Sharp PA, Simpson RJ, Taylor EM, Srai SKS. Mechanisms involved in increased iron uptake across rat duodenal brush border membrane during hypoxia. *J Physiol* 1997; 500:379–384.

29. Halleux C, Schneider YJ. Iron absorption by CaCo 2 cells cultivated in serum-free medium as in vitro model of the human intestinal epithelial barrier. *J Cell Physiol* 1994; 158:17–28.
30. Idzerda RL, Huebers H, Finch CA, McKnight GS. Rat transferrin gene expression: Tissue-specific regulation by iron deficiency. *Proc Natl Acad Sci USA* 1986; 83:3723–3727.
31. Bowman BH, Yang F, Adrian GS. Transferrin: Evolution and genetic regulation of expression. *Adv Genet* 1988; 25:1–38.
32. Pietrangelo A, Rocchi E, Casalgrandi G, Rigo G, Ferrari A, Perini M, Ventura E, Cairo G. Regulation of transferrin, transferrin receptor, and ferritin genes in human duodenum. *Gastroenterology* 1992; 102:802–809.
33. Tapia V, Arredondo M, Nunez MT. Regulation of Fe absorption by cultured intestinal epithelia (CACO-2) cell monolayers with varied Fe status. *Am J Physiol* 1996; 34: G443–G447.
34. Alvarez-Hernandez X, Nichols GM, Glass J. Caco-2 cell line: a system for studying intestinal iron transport across epithelial cell monolayers. *Biochim Biophys Acta* 1991; 1070:205–208.
35. Gangloff MB, Lai CD, Van-Campen DR, Miller DD, Norvell WA, Glahn RP. Ferrous iron uptake but not transfer is down-regulated in CACO-2 cells grown in high iron serum-free medium. *J Nutr* 1996; 126:3118–3127.
36. Alvarez-Hernandez X, Smith M, Glass J. The effect of apotransferrin on iron release from Caco-2 cells, an intestinal epithelial cell line. *Blood* 1998; 91:3974–3979.
37. Levine PH, Levine AJ, Weintraub LR. The role of transferrin in the control of iron absorption: Studies on a cellular level. *J Lab Clin Med* 1972; 80:333–341.
38. Huebers H, Huebers E, Rummel W, Crighton RR. Isolation and characterization of iron binding proteins from rat intestinal mucosa. *Eur J Biochem* 1976; 66:447–455.
39. Pollack S, Lasky FD. A new iron-binding protein isolated from intestinal mucosa. *J Lab Clin Med* 1976; 87:670–679.
40. Savin MA, Cook JD. Mucosal iron transport by rat intestine. *Blood* 1980; 56:1029–1035.
41. Halleux C, Schneider YJ. Iron absorption by intestinal epithelial cells: 1. CaCo2 cells cultivated in serum-free medium, on polyethyleneterephthalate microporous membranes, as an in vitro model. *In Vitro Cell Dev Biol* 1991; 27A:293–302.
42. Alvarez-Hernandez X, Smith M, Glass J. Regulation of iron uptake and transport by transferrin in Caco-2 cells, an intestinal cell line. *Biochim Biophys Acta* 1994; 1192: 215–222.
43. Nunez MT, Alvarez X, Smith M, Tapia V, Glass J. Role of redox systems on Fe³⁺ uptake by transformed human intestinal epithelial (Caco-2) cells. *Am J Physiol* 1994; 36: C1582–C1588.
44. Schade SG, Bernier GM, Conrad ME. Normal iron absorption in hypertransferrinaemic rats. *Br J Haematol* 1969; 17:187–190.
45. Wheby MS, Umpierre G. Effect of transferrin saturation on iron absorption in man. *N Engl J Med* 1964; 271:1391–1395.
46. Simpson RJ. Effect of hypoxic exposure on iron absorption in heterozygous hypotransferrinaemic mice. *Ann Haematol* 1992; 65:260–264.
47. Simpson RJ, Osterloh KRS, Raja KB, Snape S, Peters TJ. Studies on the role of transferrin and endocytosis in the uptake of Fe³⁺ from Fe-nitritolriacetate by mouse duodenum. *Biochim Biophys Acta* 1986; 884:166–171.
48. Humphrys J, Walpole B, Worwood M. Intracellular iron transport in rat intestinal epithelium: Biochemical and ultrastructural observations. *Br J Haematol* 1977; 36:209–217.

49. Bedard YC, Pinkerton PH, Simon GT. Radioautographic observations on iron absorption by the duodenum of mice with iron overload, iron deficiency and X-linked anaemia. *Blood* 1973; 42:131–140.
50. Umbreit JN, Conard ME, Moore EG, Latour LF. Iron absorption and cellular transport: The mobilferrin/paraferritin paradigm. *Semin Hematol* 1998; 35:13–26.
51. Snape S, Simpson RJ, Peters TJ. Subcellular localization of recently absorbed iron in mouse duodenal enterocytes: Identification of a basolateral membrane iron-binding site. *Cell Biochem Function* 1990; 8:107–115.
52. Osaki S. Kinetic studies of ferrous iron oxidation with crystalline human ferroxidase (ceruloplasmin). *J Biol Chem* 1966; 241:5053–5059.
53. Osaki S, Johnson DA, Frieden E. The possible significance of the ferrous oxidase activity of ceruloplasmin in normal human serum. *J Biol Chem* 1966; 241:2746–2751.
54. Yoshida K, Furihata K, Takeda S, et al. A mutation in the ceruloplasmin gene is associated with systemic hemosiderosis in humans. *Nature Genet* 1995; 9:267–272.
55. Harris ZL, Takahashi Y, Miyajima H, Serizawa M, MacGillivray RT, Gitlin JD. Aceruloplasminemia: Molecular characterization of this disorder of iron metabolism. *Proc Natl Acad Sci USA* 1995; 92:2539–2543.
56. Harris ZL, Durley AP, Man TK, Gitlin JD. Targeted gene disruption reveals an essential role for ceruloplasmin in cellular iron efflux. *Proc Natl Acad Sci USA* 1999; 96:10812–10817.
57. Copen DE, Davies NT. Studies on the roles of apotransferrin and caeruloplasmin (EC 1.16.3.1) on iron absorption in copper-deficient rats using an isolated vascularly- and lumenally-perfused intestinal preparation. *Br J Nutr* 1988; 60:361–373.
58. Wollenberg P, Mahlberg R, Rummel W. The valency state of absorbed iron appearing in the portal blood and ceruloplasmin substitution. *Biometals* 1990; 3:1–7.
59. Morgan EH. The role of plasma transferrin in iron absorption in the rat. *Quart J Exp Physiol* 1980; 65:239–252.
60. Bernstein SE. Hereditary hypotransferrinaemia with hemosiderosis. A murine disorder resembling human atransferrinemia. *J Lab Clin Med* 1987; 110:690–705.
61. Raja KB, Pountney DJ, Simpson RJ, Peters TJ. Importance of anaemia and transferrin levels in the regulation of intestinal iron absorption in hypotransferrinaemic mice. *Blood* 1999; 94:3185–3192.
62. Bannerman RM, Cooper RG. Sex-linked anemia: A hypochromic anemia of mice. *Science* 1966; 151:581–582.
63. Vulpe CD, Kuo YM, Murphy TL, et al. Hephaestin, a ceruloplasmin homologue implicated in intestinal iron transport, is defective in the *sla* mouse. *Nature Genet* 1999; 21:195–199.
64. Gruenheid S, Cellier M, Vidal S, Gros P. Identification and characterization of a second mouse Nramp gene. *Genomics* 1995; 25:514–525.
65. McKie AT, Wehr K, Simpson RJ, Peters TJ, Hentze MW, Farzaneh F. Molecular cloning and characterisation of a novel duodenal-specific gene implicated in iron absorption. *Biochem Soc Trans* 1998; 26:S264.
66. McKie AT, Marciani P, Rolfs, A, et al. A novel duodenal iron-regulated transporter, IREG1, implicated in the basolateral transfer of iron to the circulation. *Mol Cell* 2000; 5:299–309.
67. Donovan A, Brownlie A, Zhou Y, et al. Positional cloning of zebrafish ferroportin1 identifies a conserved vertebrate iron exporter. *Nature* 2000; 403:776–781.
68. Abboud S, Haile DJ. A novel mammalian iron-regulated protein involved in intracellular iron metabolism. *J Biol Chem* 2000; 275:19906–19912.
69. Gunshin H, Mackenzie B, Berger UV, et al. Cloning and characterization of a mammalian proton-coupled metal-ion transporter. *Nature* 1997; 388:482–488.
70. Goossen B, Hentze MW. Position is the critical determinant for function of iron-responsive elements as translational regulators. *Mol Cell Biol* 1992; 12:1959–1966.

8

HFE

**ROBERT E. FLEMING, ROBERT S. BRITTON, ABDUL WAHEED,
WILLIAM S. SLY, and BRUCE R. BACON**

Saint Louis University School of Medicine, St. Louis, Missouri

I.	INTRODUCTION	190
II.	<i>HFE</i> GENE	190
	A. Cloning the <i>HFE</i> Gene	190
	B. <i>HFE</i> Gene Structure	190
	C. <i>HFE</i> Gene Expression	191
	D. <i>HFE</i> Gene Regulation	191
	E. <i>HFE</i> Gene Splice Variants	192
III.	HFE PROTEIN	192
	A. HFE Protein Structure	192
	B. HFE Protein Expression	193
	C. Association of HFE with β_2 -Microglobulin	193
	D. Association of HFE with Transferrin Receptor	194
	E. Effect of HFE Protein on TfR-Mediated Iron Uptake in Cultured Cells	196
IV.	<i>HFE</i> MUTATIONS	197
	A. C282Y	197
	B. H63D	198
	C. Other Human <i>HFE</i> Mutations	198
	D. Effect of <i>HFE</i> Mutations on HFE–TfR Interaction	199
	E. Experimental <i>Hfe</i> Gene Disruption in Mice	199
V.	WORKING HYPOTHESIS FOR THE EFFECT OF HFE ON INTESTINAL IRON ABSORPTION	199
VI.	SUMMARY	201
	REFERENCES	201

I. INTRODUCTION

Hereditary hemochromatosis (HH) is a common inherited disorder of iron homeostasis characterized by increased gastrointestinal iron absorption and subsequent tissue iron deposition (see Chapter 28). While the autosomal recessive inheritance pattern of HH had long been recognized, identification of the gene responsible proved elusive until quite recently. Surprisingly, the gene, designated *HFE*, was found to encode a previously unidentified major histocompatibility complex (MHC) class I-like molecule (1), rather than a protein with metal-transport characteristics. The cloning of *HFE* has established a foundation for a better understanding of the molecular and cellular biology of iron homeostasis and its altered regulation in HH. Nonetheless, the molecular mechanism by which mutation of the *HFE* gene leads to increased intestinal iron absorption is still being determined. This chapter will review the current understanding of the biology of the *HFE* gene and HFE protein, and will present a working hypothesis to explain the effect of *HFE* mutation on intestinal iron absorption.

II. *HFE* GENE

A. Cloning the *HFE* Gene

An important breakthrough in identifying the gene responsible for HH occurred in 1976, when HH was found to be closely linked to the HLA-A3 region of the short arm of chromosome 6 (2). Not until 20 years later, however, were sufficient genetic markers available to allow successful positional cloning of the gene (1). Originally designated *HLA-H*, the gene was later renamed *HFE* to avoid confusion with an HLA pseudo-gene previously designated *HLA-H* (3). The major mutation associated with HH in this gene was a single base change in exon 4, resulting in the substitution of tyrosine for cysteine at amino acid 282 of the putative unprocessed protein (C282Y). Based on prior studies of other MHC class I molecules, this cysteine residue was predicted to be essential for the interaction of the HFE protein with β_2 -microglobulin (β_2m) (see below). The observation that mice lacking β_2m develop iron overload (4) provided a potential link between the C282Y *HFE* mutation and altered iron metabolism. Definitive proof that mutation of the *HFE* gene is responsible for HH was provided when knockout of the gene in the mouse resulted in iron overload (5).

B. *HFE* Gene Structure

The structure of the *HFE* gene is similar to that of other MHC class I genes. Seven exons have been identified, with each of the first six encoding a distinct domain of the HFE protein (Fig. 1). The seventh exon consists entirely of untranslated sequence. The sequence immediately upstream of the putative first exon contains no apparent cis-acting elements known to promote transcription, suggesting that the start of transcription is distant from the start of translation (6). This observation further suggests that additional exon(s) containing untranslated sequences may exist upstream of the putative first exon. The murine *Hfe* gene is structurally similar to the human gene (7). However, rather than being telomeric to the murine MHC complex (chromosome 17), the murine *Hfe* gene has been evolutionarily translocated to chromosome 13 (8), along with syntenic regions of the histone gene cluster (9).

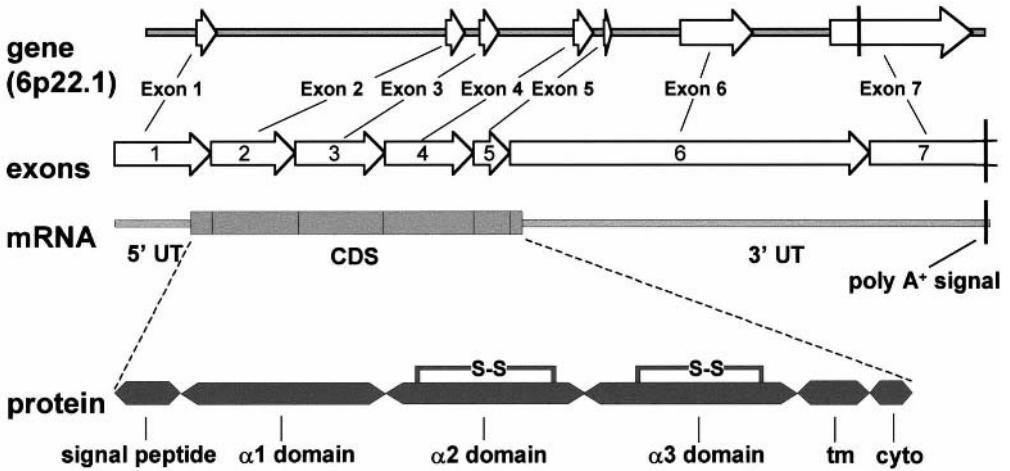


Figure 1 *HFE* gene structure. The *HFE* gene consists of seven (known) exons (top) which contribute to the major *HFE* mRNA transcript (middle). Each of the first six exons encodes a distinct domain of HFE protein (bottom). CDS = coding sequence, UT = untranslated sequence, tm = transmembrane domain, cyto = cytoplasmic domain.

C. *HFE* Gene Expression

The human *HFE* gene is expressed at relatively low levels in most human tissues (1) and in cell lines of epithelial or fibroblastic origin (7). Unlike other classical MHC class-I genes, however, little *HFE* expression is seen in lymphohematopoietic cells. The predominant *HFE* transcript is ~4.0 kb, with two minor transcripts of ~5.7 and ~2.4 kb (1). The largest *HFE* cDNA reported to date is a 2.7-kb clone that includes a single polyadenylation signal and polyA tail (Fig. 1). Analysis of the *HFE* gene and comparison with the *HFE* cDNA clones suggests that the 4.0- and 5.7-kb transcripts likely include additional 5' untranslated sequences (6). The derivation of the 2.4-kb transcript is unknown, although it is of sufficient size to include the entire coding sequence (1044 bp). The murine *Hfe* gene is expressed predominantly as an approximately 2-kb transcript in multiple tissues (8).

D. *HFE* Gene Regulation

Little is known of the regulation of *HFE* gene expression. In contrast to other MHC molecules, no induction of *HFE* expression with the use of various cytokines was observed in HEK 293 or HeLa cells (10). While one study found that *HFE* mRNA and HFE protein levels increase with increased iron status in a human intestinal cell line (CaCo2) (11), another study found that neither iron chelation nor iron replacement affected *HFE* mRNA levels in these cells (12). Sequences known to confer transcriptional regulation by cellular metal ion content have not been identified in the *HFE* gene. Furthermore, sequences homologous to iron-responsive elements have not been identified in either the 3' or 5' untranslated region of the *HFE* transcript.

E. HFE Gene Splice Variants

Several splice variants of the human *HFE* transcript have been identified. An *HFE* transcript lacking exons 6 and 7 has been detected (using reverse transcription followed by polymerase chain reaction) in human duodenum, spleen, breast, skin, and testicle (13). Because this transcript does not include the sequences encoding the transmembrane and cytoplasmic domains (see Fig. 1), it is predicted to encode a secretory form of HFE protein. *HFE* splice variant transcripts lacking exon 2 and/or a portion of exon 4 have been identified in a human liver cell line, colon carcinoma cell line, and ovarian cell line (14). Deletion of exon 2 would be predicted to eliminate the α_1 loop of HFE protein, while deletion of a portion of exon 4 would be predicted to affect the α_3 loop (see Fig. 1). The levels of protein expression and physiological roles of the splice variant *HFE* transcripts are unknown.

III. HFE PROTEIN

A. HFE Protein Structure

The *HFE* gene encodes a 343-amino acid protein consisting of a 22-amino acid signal peptide, a large extracellular domain, a single transmembrane domain, and a short cytoplasmic tail (Fig. 2). The extracellular domain of HFE protein consists of three loops (α_1 , α_2 , and α_3), with intramolecular disulfide bonds within the second and third loops. The structure of the HFE protein is thus similar to that of other MHC class I proteins. The two common HFE mutations, C282Y and H63D (see below), are in the extracellular domain. The deduced murine Hfe amino acid sequence is

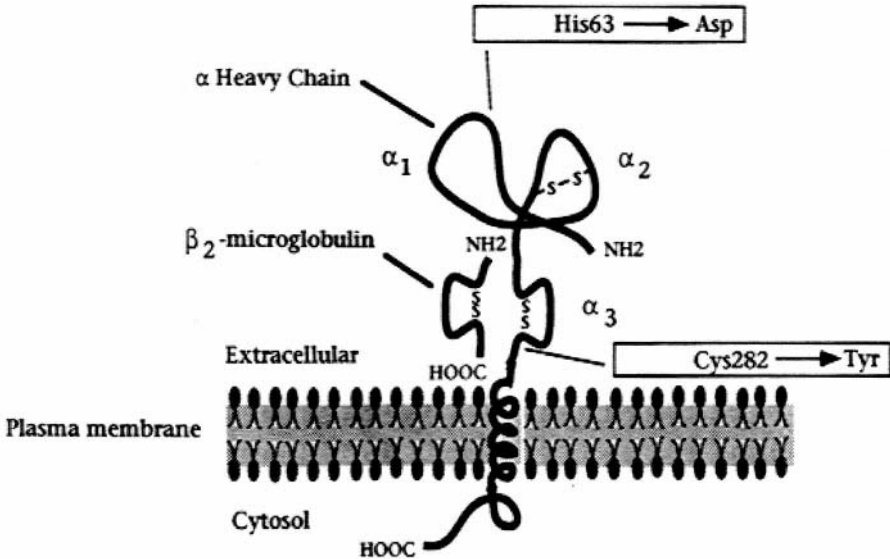


Figure 2 Representation of HFE protein in association with β_2 -microglobulin at the cell surface. The three extracellular domains of HFE are designated α_1 , α_2 , and α_3 . β_2 m is shown associated with the α_3 domain. Positions of the two common HFE mutations, C2824 and H63D, are noted. (Reprinted from Ref. 1, with permission.)

66% similar to the human, but includes additional amino acid residues between the $\alpha 1$ and $\alpha 2$ domains (8). These additional amino acids are attributable to the inclusion of nucleotide sequences in the murine transcript that are intronic in the human gene. Both C282 and H63 in the human *HFE* sequence are conserved in the mouse (C294 and H67).

Crystallographic studies demonstrate that the $\alpha 1$ and $\alpha 2$ loops of HFE form a superdomain consisting of antiparallel β strands topped by two antiparallel α helices (15). The groove between the antiparallel α helices is analogous to the peptide-binding groove in antigen-presenting MHC class I proteins. Several lines of evidence, however, suggest that HFE does not participate in antigen presentation. The groove between the α helices in HFE is physically narrower than in antigen-presenting MHC class I molecules, likely precluding peptide-binding capabilities. Two of four tyrosine residues necessary for antigen presentation by other MHC class I molecules (16) are absent in HFE. HFE is furthermore lacking CD8- and TAP-binding sites. Indeed, N-terminal sequencing performed on acid eluates from secreted soluble HFE found no evidence of peptide binding (15).

B. HFE Protein Expression

HFE protein has been detected by immunohistochemistry in the intestinal epithelium of esophagus, stomach, small intestine, and colon (17). However, the primary site of iron absorption, the duodenum, shows a distinctive pattern of HFE protein immunostaining. In this region of the intestine, HFE is highly expressed in crypt but not villus cells (Fig. 3, top) (17,18). Furthermore, the localization of HFE in the duodenal crypt cells is predominantly perinuclear, in contrast to the basolateral localization in other regions of the intestine. The perinuclear co-localization of HFE with TfR in these cells (Fig. 3, bottom) suggests their presence in the TfR recycling endosome (17). It has been postulated that HFE in duodenal crypt cells may play a key role in modulating dietary iron absorption (see Sec. V). HFE has also been detected immunohistochemically in liver (sinusoidal lining cells, bile duct epithelial cells, and Kupffer cells) (19), placenta (syncytiotrophoblasts) (20), tissue macrophages (21), and circulating monocytes and granulocytes (21).

C. Association of HFE with β_2 -Microglobulin

HFE, like other MHC class I molecules, is physically associated with β_2 m. The association between these molecules has been demonstrated in human duodenum (17) and placenta (20), as well as in cultured cells (22–24). Several lines of evidence suggest that this association is necessary for normal HFE function. The major mutation responsible for HH results in the substitution of tyrosine for cysteine at amino acid 282 in the $\alpha 3$ loop (C282Y) and abolishes the disulfide bond in this domain (Fig. 4) (1). As a consequence, C282Y mutant protein (expressed in HEK293 or COS7 cells) demonstrates diminished binding with β_2 m and decreased presentation at the cell surface (23,25). The C282Y mutant protein is retained in the endoplasmic reticulum and middle Golgi compartments, fails to undergo late Golgi processing, and is subject to accelerated degradation (23). C282Y mutant protein in patients with HH is detectable by immunohistochemistry at cell surfaces, albeit at reduced levels (21). The HH-like phenotype of β_2 m-knockout mice provides independent evidence

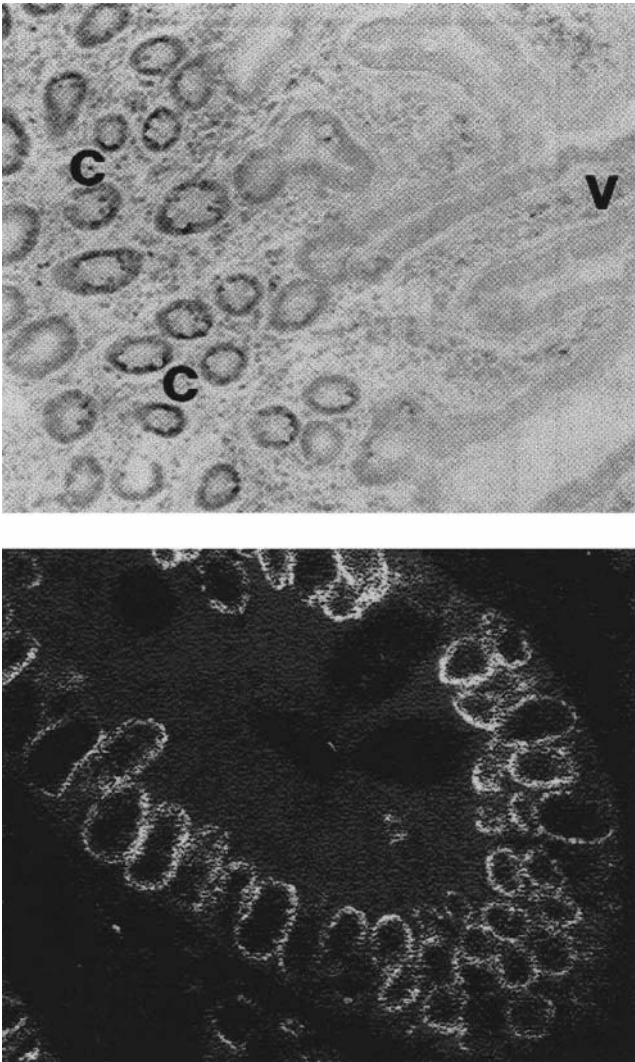


Figure 3 Immunohistochemistry of HFE in human duodenum. (Top) Most intense signal is confined to the crypt enterocytes (C), while signal in villus enterocytes (V) is minimal. (Bottom) Double immunofluorescence of HFE protein and TfR demonstrates that both proteins are expressed in the same crypt enterocytes. Co-localization of HFE and TfR is indicated by the bright white perinuclear signal. (Reprinted from Ref. 17, with permission.)

of the importance of the HFE- β_2m association for normal HFE function in the whole organism (4,26).

D. Association of HFE with Transferrin Receptor

The first mechanistic link between HFE and cellular iron metabolism was provided by the observation that HFE forms a complex with transferrin receptor (TfR). The physical association of HFE with TfR has been observed in placental syncytiotro-

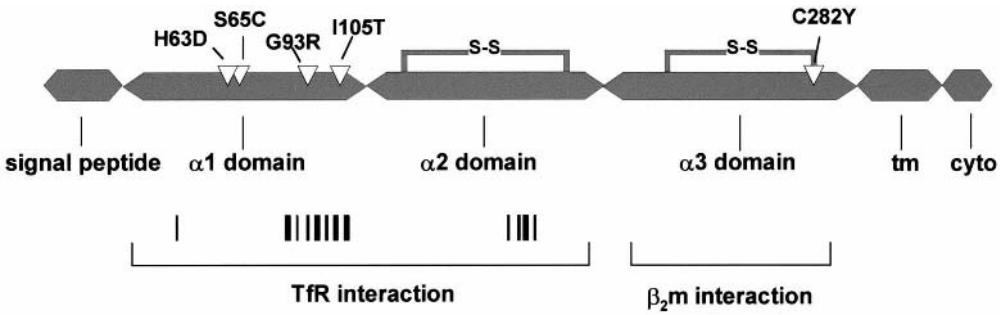


Figure 4 Representation of the structural domains of the HFE protein. The signal peptide is not present in the mature protein. Positions of mutations associated with iron overload in patients are noted. Positions of residues thought to participate in the interaction of HFE with TfR (27) are designated with vertical lines. tm = transmembrane domain, cyto = cytoplasmic domain.

phoblasts (20), the site of maternal–fetal iron transport, and in duodenal crypt enterocytes, the site of regulation of dietary iron absorption (17) (Fig. 3, bottom). Studies in transfected cell lines suggest that the HFE–TfR complex forms shortly after the biosynthesis of each protein (24). While free HFE protein was rapidly degraded in these studies, the HFE–TfR complex was found to be stable. HFE and TfR appeared to remain associated at the cell surface and in intracellular vesicles. This latter observation suggests that HFE, TfR, and diferric transferrin (FeTf) may undergo endocytosis as a complex. During the normal process of TfR endocytosis, the endosomal compartment is acidified to a pH of 5.5–6 and iron is released from FeTf (see Chapter 4). Experiments using soluble HFE and soluble TfR demonstrate that the HFE–TfR complex dissociates upon lowering the pH from 7.5 to 6.0 (15). This observation suggests that, upon acidification of the endocytotic vesicles, HFE protein might likewise dissociate from TfR. The effect, if any, of the dissociation of HFE from TfR on release of iron from FeTf in the endocytotic vesicle is unknown. Furthermore, the fate of the HFE protein after dissociation from TfR has not been determined.

Because TfR exists as a dimer at the cell surface, the stoichiometry of the relationship between TfR and HFE has been of particular interest. Studies have provided evidence for both a 1:2 and 2:2 (HFE:TfR monomer) relationship. A 2:2 relationship between HFE and TfR was demonstrated in crystallographic studies performed with high (millimolar) concentrations of soluble HFE and soluble TfR (27) (Fig. 5). If relevant *in vivo*, this observation suggests that the HFE–TfR complex would be unable to bind FeTf, as HFE and FeTf share a similar binding site on TfR. However, a ternary complex of HFE–TfR–FeTf with a stoichiometry of 1:2:1 has been observed in experiments using micromolar concentrations of soluble HFE and soluble TfR (28). The stoichiometry of the HFE–TfR complex at the cell membrane is unknown. However, it appears unlikely that all cell-surface TfR is complexed with two HFE molecules, as overexpression of HFE in transfected cells does not completely prevent FeTf binding to TfR.

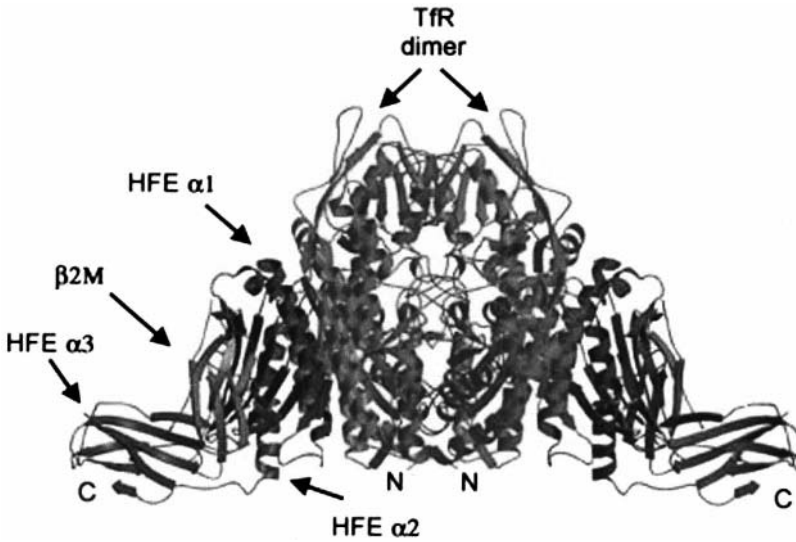


Figure 5 Ribbon diagram of HFE, β_2m , and TfR interacting as a complex. TfR is presented as a dimer with an HFE- β_2m complex interacting with each of the TfR monomers. While a 2:2 stoichiometry between HFE- β_2m and TfR monomer is depicted here, experimental evidence also supports a 1:2 relationship. (Modified from Ref. 27, with permission.)

E. Effect of HFE Protein on TfR-Mediated Iron Uptake in Cultured Cells

The observation that HFE and TfR are physically associated has led to a number of investigations on the effect of HFE expression on TfR-mediated iron uptake. Several studies have demonstrated that the overexpression of normal HFE protein in HeLa cells leads to a decrease in Tf-mediated uptake of iron by these cells (10,29–31). The decrease in Tf-mediated iron uptake is, in turn, associated with an increase in cellular iron-regulatory protein (IRP)-binding activity (30,31), a decrease in intracellular ferritin levels (24,29–31), and an increase in TfR expression (24,30). These observations are all consistent with a comparatively iron-deficient phenotype in HeLa cells overexpressing HFE.

The basis for the decreased uptake of Tf-bound iron in cells overexpressing HFE is unclear, and data have been conflicting. Decreased affinity of TfR for FeTf (i.e., an increased K_d) was observed upon overexpressing HFE (24,32) in HeLa cells, or upon addition of soluble HFE/ β_2m heterodimers (32) to these cells. However, the observed change in FeTf affinity for TfR would not be expected to have functional consequences under physiological conditions, where FeTf levels are well above that required to saturate TfR. Another study found no change in the affinity of FeTf for TfR upon overexpressing HFE in HeLa cells (10). Instead, it found that overexpressing HFE reduced the number of functional FeTf-binding sites and impaired TfR internalization. In contrast with the latter observation, another group (29) found that overexpression of HFE in HeLa cells had no effect on the rate of TfR endocytosis (or exocytosis). They instead proposed that normal HFE protein reduces cellular acquisition of iron from FeTf within endocytic compartments. Thus the basis for the

observed effects of overexpression of normal HFE on Tf-mediated iron uptake in HeLa cells is uncertain. It should further be noted that each of these studies was performed without overexpression of β_2m . It is thus possible that much of the HFE was abnormally processed in these cells (perhaps analogous to the situation in the β_2m knockout mouse), leading to otherwise unanticipated secondary consequences for iron homeostasis.

It is difficult to explain the pathophysiology of HH based entirely on the observed effects of overexpressing wild-type HFE in HeLa cells. It has been conjectured that since overexpression of HFE leads to relative cellular iron deficiency, loss of functional HFE (as in HH) might lead to cellular iron excess, and account for the iron deposition in HH. However, such a mechanism is unlikely to explain iron loading of the liver, as hepatocytes appear to express little (if any) HFE (19). More important, the *primary* defect in HH appears to be the excess uptake of iron by the duodenum. The duodenal enterocytes in HH demonstrate a relative iron-*deficient* phenotype (34–36). Likewise, the reticuloendothelial cells in HH patients are relatively iron-spared (33). Such findings would be better explained if functional loss of HFE protein caused a decrease rather than increase in Tf-mediated iron uptake in these cell populations. It has thus been proposed that loss of functional HFE in duodenal crypt cells (and reticuloendothelial cells) leads to a decrease rather than an increase in cellular iron (17,37,38). Such an effect in duodenal crypt cells could serve to alter the “set point” for iron uptake by daughter enterocytes and lead to an inappropriately high absorption of dietary iron by intestinal villus cells (see Sec. V).

IV. HFE MUTATIONS

A. C282Y

The *HFE* mutation found in the vast majority of HH patients is a single base change in exon 4, which results in the substitution of tyrosine for cysteine at amino acid 282 of the putative unprocessed protein (C282Y). Based on prior studies of other MHC class I molecules, this cysteine residue was predicted to be essential for the interaction of HFE protein with β_2m . The observation that mice lacking β_2m develop iron overload (4) provided a potential link between the C282Y *HFE* mutation and altered iron metabolism. Definitive proof that this mutation is responsible for HH was provided when knock-in of the C282Y mutation (39) in the mouse resulted in iron overload. As mentioned above, the impaired function of the C282Y mutant protein in HH appears to be due to loss of interaction of the protein with β_2m , with secondary block in intracellular transport, accelerated turnover, and decreased presentation on the cell surface. It should be noted, however, that the C282Y mutant protein was found to be detectable (although at reduced levels) on the surface of gastric epithelial cells and circulating leukocytes in C282Y-homozygous HH patients (21). In the duodenal crypt cells, C282Y protein was detected in supranuclear granular bodies (40), presumably representing abnormally processed protein.

The C282Y mutation is present in the vast majority, but not all, patients with a clinical diagnosis of HH. The proportion of HH patients who are homozygous for C282Y varies in different populations. While 100% of HH cases in a study from Australia were homozygous for the C282Y mutation, only 64% were in a study from Italy (41,42). In the United States, Britain, and France, 82–90% of patients with a

clinical diagnosis of HH are homozygous for C282Y (1,43–45). Conversely, individuals who are homozygous for C282Y frequently, but not universally, develop clinical findings of HH (46,47). This observation suggests incomplete penetrance of the C282Y mutation and raises the possibility that other genes involved in iron transport act as modifiers of the HH phenotype.

Prevalence of the C282Y mutation is greatest in Caucasian subjects of European ancestry. In this population, the carrier frequently is ~10–15% (47,48). In other ethnic populations, the C282Y mutation is less common and is always associated with the ancestral Caucasian haplotype (49,50). Such studies suggest that the C282Y mutation occurred once on an ancestral (possibly Celtic) haplotype that spread from Northern Europe to other regions of the world (44,51). The observation that the haplotype containing the C282Y mutation extends ~7 Mb suggests that the mutation arose during the past 2000 years (52). It has been proposed that the C282Y mutation, by leading to increased iron absorption and accumulation of body iron stores, provided a selective advantage to a population with limited dietary iron availability.

B. H63D

More common than the C282Y mutation in the general population is a missense mutation at nucleotide 187 of the *HFE* open reading frame, which results in the substitution of histidine for aspartate at amino acid 63 of the unprocessed protein (H63D) (1). The H63D mutation is found in 15–40% of Caucasians (53), a frequency too high to implicate this allele in most cases of HH. However, homozygosity for H63D appears to slightly increase (~fourfold) the risk for iron loading (54). Furthermore, compound heterozygosity for the H63D mutation with C282Y is found with an increased frequency in patients with iron overload over that predicted for the general population (1). The risk for iron loading in the C282Y/H63D compound heterozygote, however, is nearly 200-fold lower than in the C282Y homozygote (54). Interestingly, H63 appears to form a salt bridge with a residue in the $\alpha 2$ loop of *HFE* that binds to TfR, possibly providing a molecular basis for its effect on iron homeostasis.

The population distribution of the H63D mutation differs somewhat from that of C282Y. H63D is found at highest allele frequencies in Europe, in countries bordering the Mediterranean, in the Middle East, and in the Indian subcontinent. The H63D mutation has been found on many haplotypes, suggesting that this less consequential mutation may have arisen historically multiple times and in different populations. Because the H63D mutation occurs on a shorter haplotype (700 kb or less) than the C282Y mutation, it is thought to be evolutionarily older (52).

C. Other Human *HFE* Mutations

HFE mutations other than C282Y and H63D have been identified in isolated patients with iron overload (55). These mutations include S65C, G93R, and I105T (see Fig. 4). Interestingly, G93R and I105T are located in a TfR-binding region of the $\alpha 1$ domain of *HFE*. To date, each symptomatic patient carrying one of these mutations has carried the C282Y or H63D mutation on the other allele. The relative contribution of mutations other than C282Y (and perhaps H63D) to the overall incidence of HH, however, appears to be small.

D. Effect of *HFE* Mutations on HFE–TfR Interaction

Several observations suggest that alterations in the interaction between mutated HFE and TfR mediate the changes in iron homeostasis in HH patients. C282Y mutant HFE protein expressed in cell culture does not associate with TfR (32). H63, while remote from residues which interact with TfR (Fig. 2), appears to form a salt bridge with the TfR-binding region of the $\alpha 2$ loop of HFE (15). This observation suggests the possibility that the effects of the H63D mutation may be mediated by changes in HFE–TfR interaction. Nonetheless, expressed H63D protein is capable of forming a complex with TfR (32). As mentioned above, isolated patients with iron overload carry mutations in the region of *HFE* which binds TfR (see Fig. 4), suggesting that alteration in HFE–TfR interaction may be responsible. No TfR mutations have (to date) been identified in patients with iron overload but without mutations in *HFE* (56). Compound mutant mice hemizygous for TfR and lacking HFE do accumulate more liver iron than mice lacking HFE alone (58), supporting the concept that interaction between these two proteins is necessary in the normal control of iron absorption.

E. Experimental *Hfe* Gene Disruption in Mice

Transgenic methodology has provided important information about the functional consequences of *Hfe* gene disruption in the whole animal. Four different murine models have been generated: an exon 4 knockout (5), an exon 3 disruption/exon 4 knockout (39), an exon 2–3 knockout (57), and a C282Y knock-in (39). These mice manifest increased hepatic iron levels (5,39,57), elevated transferrin saturations (5), and increased intestinal iron absorption (57). No immunological consequences of *Hfe* disruption have been observed (57). Like HH patients, these mice demonstrate relative sparing of iron loading in reticuloendothelial cells (5,39). Interestingly, mice that are homozygous for the C282Y mutation have less severe iron loading than *Hfe*^{-/-} mice, indicating that the C282Y mutation is not a null allele (39). *Hfe*-knockout mice have been bred to strains carrying mutations in other genes involved in normal iron homeostasis (58). Studies using these animals suggest that the divalent metal transporter-1 (DMT1, also known as Nramp2), hephaestin, β_2m , and TfR play modifying roles in the HH phenotype.

V. WORKING HYPOTHESIS FOR THE EFFECT OF HFE ON INTESTINAL IRON ABSORPTION

The primary disorder in HH is the increased intestinal iron absorption relative to body iron stores. Sensing of body iron status is thought to occur in the duodenal crypt cells (59), which subsequently migrate and differentiate into absorptive enterocytes at the villus tip. HFE protein is highly expressed in these crypt cells (18), where it is physically associated with TfR (17). Dietary nonheme iron absorption occurs via the iron transport protein DMT1 at the villus tip. While DMT1 protein is predominantly expressed at the villus tip (62), the mRNA is predominantly expressed toward the crypts (60). DMT1 is upregulated in iron deficiency, through an increase in mRNA levels (60,61). Taken together, these observations led to the proposal (17,37,38) that loss of normal HFE leads to a relatively iron-deficient phenotype in the duodenal crypt cells, a relative increase in DMT1 mRNA in daughter enterocytes,

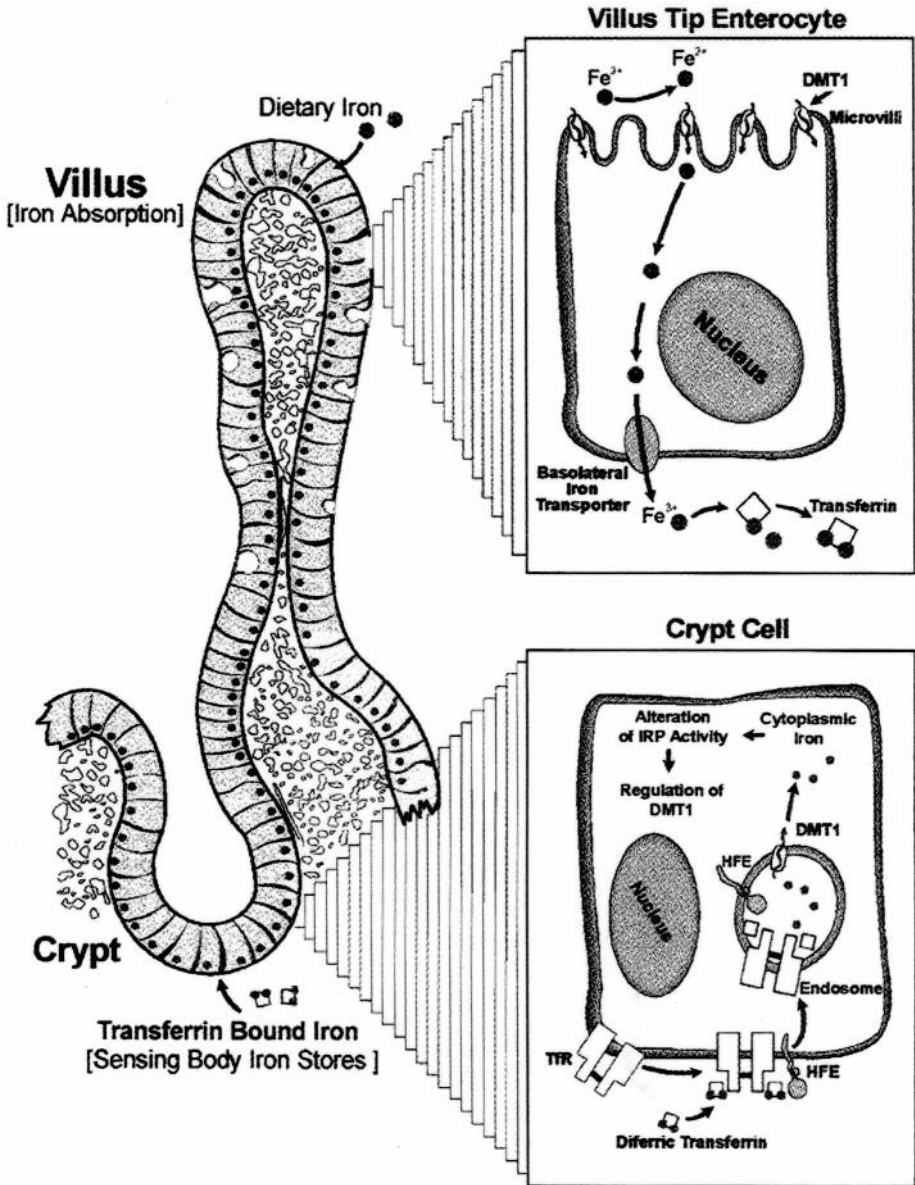


Figure 6 Proposed mechanism for effect of HFE on intestinal iron absorption. HFE is expressed in the crypt cells (bottom), where it may serve to increase uptake of serum Tf-bound iron via the TfR. Functional loss of HFE (as in HH) may impair the uptake of serum FeTf by crypt cells, leading to a relatively decreased intracellular free iron pool. The decreased free iron pool would lead to increased iron-regulatory protein activity in the crypt cells and daughter enterocytes. DMT1 mRNA in daughter enterocytes would be stabilized, and DMT1 protein expression increased in the villus. Increased DMT1 at the surface of the microvilli would mediate increased uptake of dietary iron. Other proteins involved in iron reduction and uptake at the luminal surface, and/or oxidation and transfer at the basolateral surface, may be similarly upregulated (relative to tissue iron stores) in HH. (Reprinted from Ref. 53, with permission.)

and relative increase in DMT1 protein at the villus tip. Loss of normal HFE in the crypt cells is proposed to lead to a decrease in Tf-mediated iron uptake, a decrease in the regulatory iron pool, an increase in the binding of iron regulatory protein to iron-responsive elements in the DMT1 mRNA, and stabilization of the mRNA (Fig. 6). Thus the proposed hypothesis predicts that the “set point” for dietary iron absorption in HH is altered, such that proteins involved in dietary iron absorption are increased relative to body iron stores.

The hypothesis is supported by the relatively iron-deficient phenotype (34–36) of the duodenum of HH patients, and by the increased DMT1 mRNA levels in HH patients (63) and *HFE*^{-/-} mice (37). The role for DMT1 in the altered iron homeostasis in HH is confirmed by the observation that compound mutant mice that are deficient in both HFE and DMT1 do not manifest iron loading (58). Other proteins involved in dietary iron absorption may be similarly dysregulated by the relatively iron-deficient phenotype of the duodenal crypt cells. The recent discoveries of other proteins participating in intestinal iron absorption allow for investigation into their roles as well. Current data suggest, however, that the primary defect in HH is the mis-sensing of body iron stores by HFE-expressing duodenal crypt cells. Ultimately, testing the proposed working hypothesis requires investigation of the consequences of *HFE* mutation on iron homeostasis in the duodenal crypt cell.

VI. SUMMARY

The recent identification and cloning of *HFE* has greatly expanded our understanding of many aspects of HH. The introduction of genetic tests for the C282Y and H63D mutations has allowed presymptomatic diagnosis, and added precision to studies of the population genetics of HH. Mouse models of HH and cell culture studies have increased our understanding of the normal physiology of HFE protein and the consequences of its disruption. Current data suggest that HFE exerts its effects on cellular iron homeostasis by complexing with TfR and influencing the level of Tf-mediated cellular iron uptake. The mechanism by which HFE mutation leads to increased intestinal iron uptake is incompletely understood; however, it appears to involve the missensing of body iron status by HFE-expressing duodenal crypt cells and an increase in the uptake of dietary iron by DMT1. It is anticipated that the recent discovery of other proteins involved in iron absorption will soon provide even further insights into the mechanisms by which *HFE* mutation leads to the pathogenesis of hereditary hemochromatosis.

REFERENCES

1. Feder JN, Gnirke A, Thomas W, Tsuchihashi Z, Ruddy DA, Basava A, et al. A novel MHC class I-like gene is mutated in patients with hereditary haemochromatosis. *Nature Genet* 1996; 13(4):399–408.
2. Simon M, Bourel M, Fauchet R, Genetet B. Association of HLA-A3 and HLA-B14 antigens with idiopathic haemochromatosis. *Gut* 1976; 17(5):332–334.
3. Mercier B, Mura C, Ferec C. Putting a hold on “HLA-H.” *Nature Genet* 1997; 15(3):234.
4. Santos M, Schilham MW, Rademakers LH, Marx JJ, de Sousa M, Clevers H. Defective iron homeostasis in β_2 -microglobulin knockout mice recapitulates hereditary hemochromatosis in man. *J Exp Med* 1996; 184(5):1975–1985.

5. Zhou XY, Tomatsu S, Fleming RE, Parkkila S, Waheed A, Jiang J, et al. *HFE* gene knockout produces mouse model of hereditary hemochromatosis. *Proc Natl Acad Sci USA* 1998; 95(5):2492–2497.
6. Feder JN. The hereditary hemochromatosis gene (*HFE*): A MHC class I-like gene that functions in the regulation of iron homeostasis. *Immunol Res* 1999; 20(2):175–185.
7. Riegert P, Gilfillan S, Nanda I, Schmid M, Bahram S. The mouse *HFE* gene. *Immunogenetics* 1998; 47(2):174–177.
8. Hashimoto K, Hirai M, Kurosawa Y. Identification of a mouse homolog for the human hereditary haemochromatosis candidate gene. *Biochem Biophys Res Commun* 1997; 230(1):35–39.
9. Albig W, Drabent B, Burmester N, Bode C, Doenecke D. The haemochromatosis candidate gene *HFE (HLA-H)* of man and mouse is located in syntenic regions within the histone gene cluster. *J Cell Biochem* 1998; 69(2):117–126.
10. Salter-Cid L, Brunmark A, Li Y, Leturcq D, Peterson PA, Jackson MR, et al. Transferrin receptor is negatively modulated by the hemochromatosis protein HFE: Implications for cellular iron homeostasis. *Proc Natl Acad Sci USA* 1999; 96(10):5434–5439.
11. Han O, Fleet JC, Wood RJ. Reciprocal regulation of HFE and Nramp2 gene expression by iron in human intestinal cells. *J Nutr* 1999; 129(1):98–104.
12. Feder JN, Penny DM, Irrinki A, Mintier GA, Lebron JA, Gross CN, et al. The hereditary hemochromatosis gene and iron homeostasis. *Mol Biol Hematopoiesis* 1999; 6.
13. Jeffrey GP, Basclain K, Hajek J, Chakrabarti S, Adams PC. Alternate splicing produces a soluble form of the hereditary hemochromatosis protein HFE. *Blood Cells Mol Dis* 1999; 25(1):61–67.
14. Rhodes DA, Trowsdale J. Alternate splice variants of the hemochromatosis gene *Hfe*. *Immunogenetics* 1999; 49(4):357–359.
15. Lebron JA, Bennett MJ, Vaughn DE, Chirino AJ, Snow PM, Mintier GA, et al. Crystal structure of the hemochromatosis protein HFE and characterization of its interaction with transferrin receptor. *Cell* 1998; 93(1):111–123.
16. Madden DR, Gorga JC, Strominger JL, Wiley DC. The three-dimensional structure of HLA-B27 at 2.1 Å resolution suggests a general mechanism for tight peptide binding to MHC. *Cell* 1992; 70(6):1035–1048.
17. Waheed A, Parkkila S, Saarnio J, Fleming RE, Zhou XY, Tomatsu S, et al. Association of HFE protein with transferrin receptor in crypt enterocytes of human duodenum. *Proc Natl Acad Sci USA* 1999; 96(4):1579–1584.
18. Parkkila S, Waheed A, Britton RS, Feder JN, Tsuchihashi Z, Schatzman RC, et al. Immunohistochemistry of HLA-H, the protein defective in patients with hereditary hemochromatosis, reveals unique pattern of expression in gastrointestinal tract. *Proc Natl Acad Sci USA* 1997; 94(6):2534–2539.
19. Bastin JM, Jones M, O'Callaghan CA, Schimanski L, Mason DY, Townsend AR. Kupfer cell staining by an HFE-specific monoclonal antibody: Implications for hereditary haemochromatosis. *Br J Haematol* 1998; 103(4):931–941.
20. Parkkila S, Waheed A, Britton RS, Bacon BR, Zhou XY, Tomatsu S, et al. Association of the transferrin receptor in human placenta with HFE, the protein defective in hereditary hemochromatosis. *Proc Natl Acad Sci USA* 1997; 94(24):13198–13202.
21. Parkkila S, Parkkila AK, Waheed A, Britton RS, Zhou XY, Fleming RE, et al. Cell surface expression of HFE protein in epithelial cells, macrophages, and monocytes. *Haematologica* 2000; 85(4):340–345.
22. Feder JN, Tsuchihashi Z, Irrinki A, Lee VK, Mapa FA, Morikang E, et al. The hemochromatosis founder mutation in HLA-H disrupts β_2 -microglobulin interaction and cell surface expression. *J Biol Chem* 1997; 272(22):14025–14028.
23. Waheed A, Parkkila S, Zhou XY, Tomatsu S, Tsuchihashi Z, Feder JN, et al. Hereditary hemochromatosis: Effects of C282Y and H63D mutations on association with β_2 -mi-

- croglobulin, intracellular processing, and cell surface expression of the HFE protein in COS-7 cells. *Proc Natl Acad Sci USA* 1997; 94(23):12384–12389.
24. Gross CN, Irrinki A, Feder JN, Enns CA. Co-trafficking of HFE, a nonclassical major histocompatibility complex class I protein, with the transferrin receptor implies a role in intracellular iron regulation. *J Biol Chem* 1998; 273(34):22068–22074.
 25. Feder JN, Tsuchihashi Z, Irrinki A, Lee VK, Mapa FA, Morikang E, et al. The hemochromatosis founder mutation in HLA-H disrupts β_2 -microglobulin interaction and cell surface expression. *J Biol Chem* 1997; 272(22):14025–14028.
 26. de Sousa M, Reimao R, Lacerda R, Hugo P, Kaufmann SH, Porto G. Iron overload in β_2 -microglobulin-deficient mice. *Immunol Lett* 1994; 39(2):105–111.
 27. Bennett MJ, Lebron JA, Bjorkman PJ. Crystal structure of the hereditary haemochromatosis protein HFE complexed with transferrin receptor. *Nature* 2000; 403(6765):46–53.
 28. Lebron JA, West AP Jr, Bjorkman PJ. The hemochromatosis protein HFE competes with transferrin for binding to the transferrin receptor. *J Mol Biol* 1999;294(1):239–245.
 29. Roy CN, Penny DM, Feder JN, Enns CA. The hereditary hemochromatosis protein, HFE, specifically regulates transferrin-mediated iron uptake in HeLa cells. *J Biol Chem* 1999; 274(13):9022–9028.
 30. Corsi B, Levi S, Cozzi A, Corti A, Altimare D, Albertini A, et al. Overexpression of the hereditary hemochromatosis protein, HFE, in HeLa cells induces an iron-deficient phenotype. *FEBS Lett* 1999; 460(1):149–152.
 31. Riedel HD, Muckenthaler MU, Gehrke SG, Mohr I, Brennan K, Herrmann T, et al. HFE downregulates iron uptake from transferrin and induces iron-regulatory protein activity in stably transfected cells. *Blood* 1999; 94(11):3915–3921.
 32. Feder JN, Penny DM, Irrinki A, Lee VK, Lebron JA, Watson N, et al. The hemochromatosis gene product complexes with the transferrin receptor and lowers its affinity for ligand binding. *Proc Natl Acad Sci USA* 1998; 95(4):1472–1477.
 33. McLaren GD. Reticuloendothelial iron stores and hereditary hemochromatosis: A paradox. *J Lab Clin Med* 1989; 113(2):137–138.
 34. Powell LW, Campbell CB, Wilson E. Intestinal mucosal uptake of iron and iron retention in idiopathic haemochromatosis as evidence for a mucosal abnormality. *Gut* 1970; 11: 727–731.
 35. Whittaker P, Skikne BS, Covell AM, Flowers C, Cooke A, Lynch SR, et al. Duodenal iron proteins in idiopathic hemochromatosis. *J Clin Invest* 1989; 83(1):261–267.
 36. Pietrangelo A, Casalgrandi G, Quaglino D, Gualdi R, Conte D, Milani S, et al. Duodenal ferritin synthesis in genetic hemochromatosis. *Gastroenterology* 1995; 108(1):208–217.
 37. Fleming RE, Migas MC, Zhou X, Jiang J, Britton RS, Brunt EM, et al. Mechanism of increased iron absorption in murine model of hereditary hemochromatosis: Increased duodenal expression of the iron transporter DMT1. *Proc Natl Acad Sci USA* 1999; 96(6): 3143–3148.
 38. Kuhn LC. Iron overload: Molecular clues to its cause. *Trends Biochem Sci* 1999; 24(5): 164–166.
 39. Levy JE, Montross LK, Cohen DE, Fleming MD, Andrews NC. The C282Y mutation causing hereditary hemochromatosis does not produce a null allele. *Blood* 1999; 94(1): 9–11.
 40. Zuccon L, Corsi B, Levi S, Mattioli M, Fracanzani AL, Corti A, et al. Immunohistochemistry of HFE in the duodenum of C282Y homozygotes with antisera for recombinant HFE protein. *Haematologica* 2000; 85(4):346–351.
 41. Jazwinska EC, Pyper WR, Burt MJ, Francis JL, Goldwurm S, Webb SI, et al. Haplotype analysis in Australian hemochromatosis patients: Evidence for a predominant ancestral haplotype exclusively associated with hemochromatosis. *Am J Hum Genet* 1995; 56(2): 428–433.

42. Carella M, D'Ambrosio L, Totaro A, Grifa A, Valentino MA, Piperno A, et al. Mutation analysis of the HLA-H gene in Italian hemochromatosis patients. *Am J Hum Genet* 1997; 60(4):828–832.
43. Beutler E, Gelbart T, West C, Lee P, Adams M, Blackstone R, et al. Mutation analysis in hereditary hemochromatosis. *Blood Cells Mol Dis* 1996; 22(2):187–194.
44. Merryweather-Clarke AT, Pointon JJ, Shearman JD, Robson KJ. Global prevalence of putative haemochromatosis mutations. *J Med Genet* 1997; 34(4):275–278.
45. Jouanolle AM, Fergelot P, Gandon G, Yaouanq J, Le Gall JY, David V. A candidate gene for hemochromatosis: Frequency of the C282Y and H63D mutations. *Hum Genet* 1997; 100(5–6):544–547.
46. Jouanolle AM, Fergelot P, Raoul ML, Gandon G, Roussey M, Deugnier Y, et al. Prevalence of the C282Y mutation in Brittany: Penetrance of genetic hemochromatosis? *Ann Genet* 1998; 41(4):195–198.
47. Olynyk JK, Cullen DJ, Aquilia S, Rossi E, Summerville L, Powell LW. A population-based study of the clinical expression of the hemochromatosis gene. *N Engl J Med* 1999; 341(10):718–724.
48. Beckman LE, Saha N, Spitsyn V, Van Landeghem G, Beckman L. Ethnic differences in the HFE codon 282 (Cys/Tyr) polymorphism. *Hum Hered* 1997; 47(5):263–267.
49. Chang JG, Liu TC, Lin SF. Rapid diagnosis of the HLA-H gene Cys 282 Tyr mutation in hemochromatosis by polymerase chain reaction—A very rare mutation in the Chinese population. *Blood* 1997; 89(9):3492–3493.
50. Cullen LM, Gao X, Eastaie S, Jazwinska EC. The hemochromatosis 845 G→A and 187 C→G mutations: Prevalence in non-Caucasian populations. *Am J Hum Genet* 1998; 62(6):1403–1407.
51. Jazwinska EC, Pyper WR, Burt MJ, Francis JL, Goldwurm S, Webb SI, et al. Haplotype analysis in Australian hemochromatosis patients: Evidence for a predominant ancestral haplotype exclusively associated with hemochromatosis. *Am J Hum Genet* 1995; 56(2):428–433.
52. Rochette J, Pointon JJ, Fisher CA, Perera G, Arambepola M, Arichchi DS, et al. Multicentric origin of hemochromatosis gene (HFE) mutations. *Am J Hum Genet* 1999; 64(4):1056–1062.
53. Bacon BR, Powell LW, Adams PC, Kresina TF, Hoofnagle JH. Molecular medicine and hemochromatosis: At the crossroads. *Gastroenterology* 1999; 116(1):193–207.
54. Risch N. Haemochromatosis, HFE and genetic complexity. *Nature Genet* 1997; 17(4):375–376.
55. Barton JC, Sawada-Hirai R, Rothenberg BE, Acton RT. Two novel missense mutations of the HFE gene (I105T and G93R) and identification of the S65C mutation in Alabama hemochromatosis probands. *Blood Cells Mol Dis* 1999; 25(3):147–155.
56. Tsuchihashi Z, Hansen L, Quintana L, Kronmal GS, Mapa FA, Feder JN, et al. Transferrin receptor mutation analysis in hereditary hemochromatosis patients. *Blood Cells Mol Dis* 1998; 24(3):317–321.
57. Bahram S, Gilfillan S, Kuhn LC, Moret R, Schulze JB, Lebeau A, et al. Experimental hemochromatosis due to MHC class I HFE deficiency: Immune status and iron metabolism. *Proc Natl Acad Sci USA* 1999; 96(23):13312–13317.
58. Levy JE, Montross LK, Andrews NC. Genes that modify the hemochromatosis phenotype in mice. *J Clin Invest* 2000; 105(9):1209–1216.
59. Anderson GJ. Control of iron absorption. *J Gastroenterol Hepatol* 1996; 11(11):1030–1032.
60. Gunshin H, Mackenzie B, Berger UV, Gunshin Y, Romero MF, Boron WF, et al. Cloning and characterization of a mammalian proton-coupled metal-ion transporter. *Nature* 1997; 388(6641):482–488.

61. Fleming MD, Trenor CC 3rd, Su MA, Foernzler D, Beier DR, Dietrich WF, et al. Microcytic anaemia mice have a mutation in Nramp2, a candidate iron transporter gene. *Nature Genet* 1997; 16(4):383–386.
62. Canonne-Hergaux F, Gruenheid S, Ponka P, Gros P. Cellular and subcellular localization of the Nramp2 iron transporter in the intestinal brush border and regulation by dietary iron. *Blood* 1999; 93(12):4406–4417.
63. Zoller H, Pietrangelo A, Vogel W, Weiss G. Duodenal metal-transporter (DMT-1, NRAMP-2) expression in patients with hereditary haemochromatosis. *Lancet* 1999; 353(9170):2120–2123.

9

Regulation of Iron Homeostasis by Iron Regulatory Proteins 1 and 2

ERIC S. HANSON and ELIZABETH A. LEIBOLD

University of Utah, Salt Lake City, Utah

I. INTRODUCTION	208
II. THE NEED TO TIGHTLY CONTROL CELLULAR IRON CONCENTRATION	208
III. IRPs INTERACT WITH mRNA THROUGH THE IRON-RESPECTIVE ELEMENT	209
IV. MECHANISMS BY WHICH IRP1 AND IRP2 POSTTRANSCRIPTIONALLY REGULATE GENE EXPRESSION	211
A. Regulation of mRNAs Containing 5' IREs	211
B. Regulation of mRNAs Containing 3' IREs	214
C. Coordinate Regulation of Iron Homeostasis by 5' and 3' IREs	214
V. IRON-DEPENDENT REGULATION OF IRP1 AND IRP2	215
A. Regulation of IRP1	215
B. Regulation of IRP2	218
VI. OTHER PHYSIOLOGICAL MODULATORS OF IRP ACTIVITY	220
A. Regulation of IRP1 by Reactive Oxygen Species	220
B. Regulation of IRPs by Reactive Nitrogen Species	221
C. Regulation of the IRPs by Hypoxia	223
VII. CONCLUSIONS	225
REFERENCES	225

I. INTRODUCTION

All mammalian cells have an absolute requirement for iron. Iron is indispensable to processes such as oxygen transport, Krebs cycle activity, oxidative phosphorylation, and DNA synthesis. These and many other fundamental processes require iron for incorporation into hemoproteins, formation of Fe–S clusters involved in redox reactions, and for insertion into enzyme active sites. Consequently, insufficient cellular iron negatively affects many cellular functions, and has profound consequences on the organism. Conversely, iron toxicity ensues when the concentration of iron exceeds the iron-binding capacity of the cell. To balance the requirement for iron with its toxicity, mammalian cells have evolved an elaborate posttranscriptional regulatory circuit with the RNA-binding iron-regulatory proteins 1 and 2 (IRP1 and IRP2) as the principal regulators. IRPs sense intracellular iron, and transduce this signal to alter their RNA-binding activities. This in turn regulates the expression of key proteins in iron homeostasis. The aim of this chapter is to describe our current understanding of the molecular mechanisms by which the RNA-binding activities of IRP1 and IRP2 posttranscriptionally regulate gene expression. Emphasis will be placed on recent work in the field that has identified other physiological signals that regulate IRP1 and IRP2, such as reactive oxygen and nitrogen species, and hypoxia. These observations illustrate that the IRP system is integrated with other cellular processes in addition to its classical role of iron sensing.

II. THE NEED TO TIGHTLY CONTROL CELLULAR IRON CONCENTRATION

Under physiological conditions, iron is found in one of two oxidation states, the reduced ferrous (Fe^{2+}) form or the oxidized ferric (Fe^{3+}) form. The ability of iron to exist in either of these two oxidation states is central to the many redox processes that are vital to cellular function. Paradoxically, it is this very redox property that renders iron inherently toxic, due to its ability to produce toxic oxygen radicals. Mitochondria have long been recognized as sites where reactive oxygen species are generated due to respiratory-chain electron carriers that univalently reduce oxygen to superoxide (O_2^-). It is estimated that under normal conditions up to 2% of the total oxygen consumed by a cell may be “leaked” from the electron-transport chain as O_2^- (1). Superoxide dismutase enzymatically converts O_2^- to hydrogen peroxide (H_2O_2) (1–4). Subsequently, through the Fenton reaction ($\text{Fe}^{2+} + \text{H}^+\text{H}_2\text{O}_2 \rightarrow \text{Fe}^{3+} + \cdot\text{OH} + \text{H}_2\text{O}$), “free” Fe^{2+} can react with H_2O_2 to generate the highly toxic hydroxyl radical ($\cdot\text{OH}$). The $\cdot\text{OH}$ radical is extremely reactive, and can oxidize proteins (5), lipids (6), and DNA (7), which leads to irreversible cellular damage. It is these oxidative processes that are major contributors to macromolecule dysfunction associated with many pathophysiological conditions and aging (5,8). Free Fe^{2+} can also be generated from the disintegration of Fe–S clusters by attack of O_2^- , further encouraging Fenton chemistry (3,4,9–11). To detoxify reactive oxygen species (ROS), mammalian cells have developed numerous antioxidant mechanisms, including enzymatic ROS scavengers such as superoxide dismutases, catalase, glutathione peroxidases, and nonenzymatic small antioxidant molecules (8). In addition to detoxification of ROS, the proper maintenance of free cellular iron is another important mechanism by which cells guard against oxidative damage.

Due to the nature of iron as a “double-edged sword,” aerobic organisms have been under strong evolutionary pressure to develop mechanisms to tightly control cellular iron uptake and storage (reviewed in Refs. 12–14). Cellular and systemic iron homeostasis is regulated in great part by posttranscriptional mechanisms involving IRP1 and IPR2. The IRPs are cytosolic RNA-binding proteins whose activities have been found in mammals, *Danio rerio* (Zebrafish), *Drosophila melanogaster*, *Caenorhabditis elegans*, and *Xenopus laevis* (15–17). More recently, IRP-like proteins have been described in the protozoan parasite *Trypanosoma brucei* (18), in tobacco (19), and IRP-like activity has been described in *Leishmania tarentolae* (20). In addition, a recent study has described an IRP-like activity in bacteria (see below) (21). It should be noted that IRPs or IRP-like activity have not been identified in yeast.

Shortly after their identification, it became clear that the IRPs play a central role in the regulation of cellular iron uptake and sequestration. Through their iron-regulated RNA-binding properties, the IRPs posttranscriptionally regulate the expression of mRNAs encoding proteins involved in both iron and energy homeostasis. The RNA-binding activities of IRP1 and IRP2 are inversely correlated with cellular iron concentration: RNA-binding activity decreases in iron-replete cells and increases in iron-depleted cells. The relationship between intracellular iron and IRP RNA-binding activity is the molecular basis for the control of cellular iron homeostasis.

III. IRPs INTERACT WITH mRNA THROUGH THE IRON-RESPONSIVE ELEMENT

IRP1 and IRP2 bind to RNA elements termed iron-responsive elements (IREs) (see Chapter 10). IREs are located in the 5' and 3' untranslated regions (UTRs) of mRNAs encoding proteins involved in iron homeostasis and energy production. Depending on the location of the IRE, the IRP–IRE interaction controls translational efficiency or mRNA stability, with prototypic examples represented by the ferritin and transferrin receptor (TfR) mRNAs, respectively. Phylogenetic analysis has defined a highly conserved ~30-nucleotide IRE consensus sequence (22–27) that binds to IRP1 and IRP2 with equally high affinities ($K_d = 30\text{--}50\text{ pM}$) (28,29). IREs harbor three structural components, including a hairpin structure with a six-membered nucleotide loop, a bipartite-stable base-paired stem, and an asymmetrical “bulge” (Fig. 1). The six-membered loop of bona-fide IREs has the invariant sequence 5'-CAGUGN-3', where N can be A, C, G, or U. In the consensus IRE, the bulge is located five base pairs to the 5' side of the first nucleotide of the loop. The importance of the IRE sequence/structure has been demonstrated by mutating nucleotides in the loop, in the bulge, or in the base-paired stem, all resulting in decreased IRP1 and IRP2 RNA binding (23–26,29,30). Although there are no sequence requirements for the stem per se, base-pair interactions must remain intact to stabilize the IRE structure. Therefore, compensatory mutations in the stem are tolerated, while destabilizing mutations decrease or ablate the IRP–IRE interaction (23,25,26,29).

To further examine the structural features of the IRE that are required for interaction with IRPs, in-vitro selection experiments using the technique of systematic evolution of ligands by exponential enrichment (SELEX) were performed. Starting with a random pool of permuted IREs, these experiments identified novel IRE-like structures that bound IRPs, although with suboptimal affinities (28,30,31).

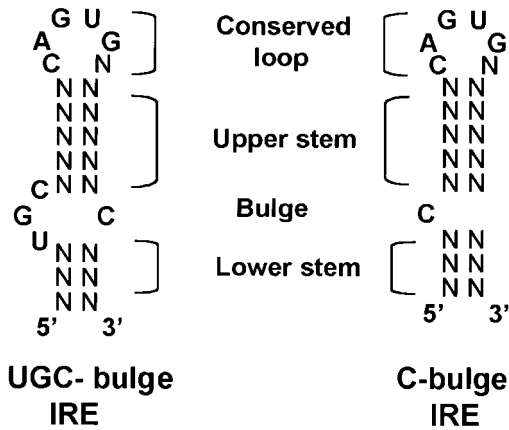


Figure 1 Structure of IREs. IRPs bind to IREs found in 5' or 3' untranslated regions of specific mRNAs. Known IREs are hairpin structures consisting of six-nucleotide loop with the invariant CAGUGN sequence, stable upper and lower base-paired stems, and a bulge created by unpaired UGC nucleotides (ferritin IRE) or a single C nucleotide (TfR, e-ALAS, and m-aconitase IREs).

Importantly, some IRE-like structures were identified that bound exclusively to IRP1 or to IRP2 *in vitro*, illustrating that the IRPs can recognize subtle differences in IRE structure (28,31). When placed in the 5' UTR of a reporter gene, IRE-like structures that bound only to IRP1 or to IRP2 *in vitro* conferred iron-regulated translational regulation *in vivo* (32). In addition to demonstrating that these IRE-like molecules are functional, these results demonstrate that IRP1 and IRP2 can function independently as translational regulators. Furthermore, a murine pro-B lymphocyte that does not express IRP1 regulates ferritin and TfR appropriately (33). Although no natural IRE sequences have been identified that match the *in-vitro* selected IRE-like structures, these results nonetheless suggest that IRPs can regulate specific IRE targets *in vivo*. The identification of IRE-like structures capable of binding IRPs suggests the possibility that novel IREs will be identified in the future.

Two types of bulges are found in IREs. The first can be modeled as having unpaired UGC nucleotides, and is represented by the ferritin IRE. The second results from a single unpaired cytosine that is found in other IREs (34) (Fig. 1). RNA band-shift assays revealed that the cytosine-bulged IREs represented in the TfR, mitochondrial (m) aconitase, and erythroid δ -aminolevulinate synthase (e-ALAS) mRNAs bound IRP1 with greater affinity than IRP2, suggesting the possibility that cytosine-bulged IREs might be regulated primarily by IRP1 *in vivo* (34). Taken together, these data suggest that one evolutionary selective force for the maintenance of two IRPs may relate to the potential differences in target specificity. A comprehensive understanding of the IRP-IRE system awaits the identification of the full repertoire of IRE-containing mRNAs, and *in-vivo* analysis of their specificity to IRP1 and/or IRP2.

To date one disorder has been identified that is attributed to dysregulation in the IRP-IRE system. Hereditary hyperferritinemia-cataract syndrome (HHCS) is an autosomal dominant disorder characterized by elevated levels of serum ferritin-L and

early onset of cataracts [(35,36); see also Chapter 31]. HHCS is associated with heterogeneous point and deletion mutations in the ferritin-L IRE. HHCS mutations have been identified in the loop, stem, and bulge (29,37–42). By decreasing the stability of the IRE, or by disrupting nucleotides that are important in IRP recognition, mutations in the ferritin-L IRE decrease or eliminate IRP1 and IRP2 IRE binding (29). Such mutations are coincident with a 5- to 20-fold increase in serum ferritin-L levels. Affected individuals, however, do not exhibit overall defects in iron homeostasis (43). The underlying mechanism by which aberrant levels of ferritin-L lead to this disorder is currently unknown.

IV. MECHANISMS BY WHICH IRP1 AND IRP2 POSTTRANSCRIPTIONALLY REGULATE GENE EXPRESSION

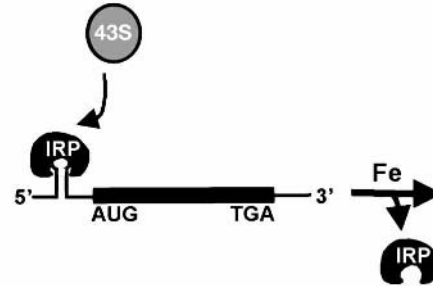
Although both IRP1 and IRP2 sense iron, their mechanisms of regulation differ. Iron regulates IRP1 by the conversion of the apo-RNA-binding form into a [4Fe–4S] cluster form without changes in IRP1 protein levels. In contrast, iron regulates IRP2 RNA binding through protein stability. Although the mechanisms of iron sensing are different, cellular iron concentration is inversely correlated with IRP RNA-binding activity. This serves as the molecular basis for regulating iron homeostasis.

A. Regulation of mRNAs Containing 5' IREs

The stimulation of ferritin synthesis in iron-replete cells represents a well-studied example of translational regulation. The first IRE structure identified was the 5' IRE found in the H- and L-ferritin subunit mRNAs (44–48) that was demonstrated to mediate inhibition of ferritin translation in iron-depleted cells (45,49). When this IRE is placed in the 5' UTR of chimeric mRNAs, it confers iron-dependent translational repression in both transient transfection assays and in cell-free translation systems (44,49–51). Therefore, the ferritin IRE represents a discrete RNA element containing all the information necessary and sufficient for translational regulation. Iron-induced derepression of ferritin translation is coincident with a shift of its mRNA from translationally inactive ribonucleoprotein complexes to translationally active polysomes (51–54). The IRE structure itself does not affect engagement or translocation of the ribosome. Rather, translational inhibition by the IRE is dependent on its interaction with IRP1 or IRP2. This interaction inhibits the recruitment of the small 43S ribosomal subunit to the mRNA, thus affecting translational initiation (Fig. 2) (51,53,55). For translational inhibition to occur, the IRE must be positioned within ~50 nucleotides of the 5' m⁷GpppN-cap structure (51,53,55). An IRE placed in the 5' UTR of a chimeric mRNA at a greater distance from the 5' cap has decreased efficiency in translational inhibition, demonstrating that a translating ribosome can displace the IRP (51,56,57).

The labile iron pool is a low-molecular-weight pool of weakly chelated iron that is believed to be sensed by IRPs (58,59). When the concentration of iron in the labile pool increases, IRP RNA-binding activity decreases. This results in translational derepression of the ferritin mRNA and increased ferritin synthesis, resulting in the sequestration of iron in a nontoxic form. The opposite occurs in iron-depleted cells, where high-affinity binding of the IRPs to the 5' ferritin IRE represses its synthesis. This mechanism of translational regulation of ferritin expression represents

Translational Repression



Translational Derepression



5' IREs:

Ferritin
e-ALAS
m-Aconitase
Succinate dehydrogenase
Ireg/ferroportin1/MTP

mRNA Stabilization



Fe-Induced mRNA degradation



3' IREs:

TfR
DMT1

Figure 2 Posttranscriptional regulation of iron homeostasis by the IRPs. The binding of IRPs to 5' IREs results in the inhibition of translation by sterically hindering the recruitment of the 43S translation pre-initiation complex. The binding of IRPs to 3' IREs stabilizes mRNA by preventing endonucleolytic attack by RNases. Increased intracellular iron concentration decreases IRP RNA binding activity, allowing translation to proceed and to destabilize IRE-containing mRNAs by exposing nucleolytic sensitive sites in the mRNA. IREs found in 5' and 3' UTRs are indicated.

the primary cellular defense against elevated iron levels. Because the IRPs can sense subtle changes in the labile iron pool, the regulation of their RNA-binding activity is not a simple on/off switch (60,61). Thus, there is tight regulation of IRE-containing mRNAs that is closely correlated with cellular iron concentration.

Since the identification of the ferritin IRE, similar IREs have been found in the 5' UTRs of mRNAs encoding m-aconitase (62–64), *Drosophila melanogaster* succinate dehydrogenase Fe-S subunit (65,66), e-ALAS (62,66–69), and most recently, the duodenal iron-regulated transporter IREG1 (also known as ferroportin-1 or MTP1) (70–72). Like the ferritin IRE, the 5' IREs in m-aconitase (73) and e-ALAS (53) mediate translational regulation. The function of the IREG1 IRE has not yet been thoroughly investigated.

The identification of IREs in mRNAs encoding proteins involved in cellular processes other than iron homeostasis expands the physiological function of the IRP–IRE regulatory network. The regulation of mammalian m-aconitase by the IRPs is particularly noteworthy, since it raises questions regarding the relationship between iron homeostasis and mitochondrial function. Mitochondrial aconitase is a [4Fe–4S] cluster-containing enzyme that participates in the Krebs cycle by catalyzing the dehydration/rehydration of citrate to isocitrate. The inhibition of mammalian m-aconitase translation by the IRPs has been demonstrated in in-vitro translation assays (64,66), in cultured cells (73), and in rats maintained on an iron-deficient diet (64,74,75). The role of IRE/IRP regulation of m-aconitase mRNA is unclear. It is possible, however, that during iron starvation the translational repression of m-aconitase mRNA could prevent the accumulation of apo-aconitase, which could be detrimental to Krebs cycle activity. Alternatively, since IRP1 RNA-binding activity is activated by ROS (discussed below), it is possible that an increase in mitochondrial ROS production might increase IRP1 RNA-binding activity and lead to repression of m-aconitase translation. If such a mechanism is operating, it could serve as a conduit between mitochondrial function and iron availability.

Since 60–70% of the total iron in humans is present in hemoglobin, it is not surprising that heme synthesis is coordinated with cellular iron availability. This is achieved through the IRP–IRE system that regulates heme synthesis in erythroid cells. Two different genes encode ALAS, one that is expressed ubiquitously (ALAS) and one that is specific to the erythroid lineage (e-ALAS) (76). ALAS is the first enzyme in the heme biosynthetic pathway, and is thought to constitute the rate-limiting step (77). The mRNA that encodes e-ALAS contains an IRE in its 5' UTR that mediates translational regulation by iron in a manner similar to ferritin regulation (62,66,67,69,78). The regulation of e-ALAS by the IRPs may provide a mechanism to decrease heme synthesis when there is insufficient iron for incorporation into protoporphyrin IX by ferrochelatase. This mechanism could also serve to decrease the concentration of toxic heme intermediates.

A novel duodenal membrane associated protein termed IREG1 has recently been cloned from mouse (70,72) and zebrafish (71). IREG1 is an iron transporter found on the basolateral surface of intestinal enterocytes, and is implicated in the export of iron from enterocytes into the bloodstream. Examination of the IREG1 nucleotide sequence reveals the presence of a single 5' IRE. Competition studies demonstrated that the IREG1 IRE specifically binds IRP1 and IRP2 with affinities equal to that of the ferritin IRE (70). Furthermore, transient transfection assays have demonstrated that the IREG1 5' IRE confers iron-regulated translational repression

on a reporter gene construct similar to the ferritin 5' IRE (72). It is not clear, however, how the IREG1 IRE functions in the context of the IREG1 mRNA, since IREG1 mRNA and protein levels increase in the duodenum of iron-deficient animals (70), a situation in which the IRPs would bind RNA and repress translation. Further studies are required to define the regulation of IREG1 expression at the transcriptional and translational levels.

B. Regulation of mRNAs Containing 3' IREs

To date, two mRNAs encoding proteins involved in iron transport, TfR and divalent metal transporter 1 (DMT1, also known as DCT1 or Nramp2), have been found to contain 3' IREs. The binding of the IRPs to the IREs located in the 3' UTRs protects mRNAs from endonucleolytic degradation. TfR is responsible for cellular iron acquisition through the endocytic uptake of diferric transferrin from the blood followed by intracellular release of iron (79). Early studies demonstrated that iron levels are inversely proportional to TfR levels (80,81), where the changes in TfR concentration could not be fully accounted for by an alteration in transcription (82). Subsequently, it was shown that iron significantly decreases the half-life of TfR mRNA in cultured cells (83–86). The modulation of TfR mRNA stability by iron is mediated by a nucleolytic region in the 3' UTR that contains five IREs (83,85,87). Mutation of the IRE loop sequences, or removal of three of the IREs, resulted in a constitutively unstable mRNA (85,87). Iron-mediated degradation of TfR mRNA occurs by the endonucleolytic cleavage at a site near one of the five IREs, and does not require deadenylation of the poly (A) tail (88). Furthermore, this approximately 250-base nucleolytic-sensitive region can transfer iron-dependent regulation on chimeric mRNAs (84,87,89).

DMT1 transports iron as well as other divalent metals [(90,91); see also Chapter 6]. The DMT1 protein is localized to the apical membrane of the enterocyte villi, where it is involved in the absorption of iron from the lumen, but it is not found in basolateral membranes or in crypt cells (92). Alternative splicing of the DMT1 mRNA generates two transcripts that differ in their 3' UTRs, one of which harbors a single IRE (93). The IRE form of DMT1 mRNA is increased in the duodenum of iron-starved mice, in *HFE* null mice (94), and in individuals with hereditary hemochromatosis (95). Although the DMT1 3' IRE has not been definitely shown to confer mRNA stability, the in-vivo data discussed above are consistent with the notion that the DMT1 mRNA is regulated by IRE-mediated stabilization.

A 3' IRE has been identified in mouse glycolate oxidase mRNA (96). This IRE binds IRPs in vitro; however, it contains a mismatch in its upper base-paired stem and does not confer iron-dependent regulation in vivo (96).

C. Coordinate Regulation of Iron Homeostasis by 5' and 3' IREs

Figure 2 summarizes the effects of iron on IRP RNA-binding activity, and the subsequent regulation of 5' and 3' IRE mRNAs. When cells are iron-depleted, IRP binding to TfR (and probably DMT1) 3' IREs stabilizes these mRNAs, while IRP binding to the ferritin 5' IRE (and to other 5' IRE mRNAs) represses translation. The activation of IRP RNA-binding activity decreases the cellular sequestration of iron by repressing ferritin synthesis while increasing iron uptake by elevating TfR

and DMT1 expression. Conversely, when cells are iron-replete, IRPs dissociate from 5' and 3' IREs, leading to an increase in ferritin synthesis and a decrease in TfR (and DMT1) mRNA stability. The net consequence from this regulation is an increase in iron sequestration and a decrease in iron uptake, thus preventing iron toxicity. Table 1 lists the known IRE-containing mRNAs (for more details, see Chapter 10). It is likely that others will be identified in the future.

V. IRON-DEPENDENT REGULATION OF IRP1 AND IRP2

A. Regulation of IRP1

IRP1 is found in one of two forms, an apo-RNA-binding form, and a [4Fe-4S] cluster form that has cytosolic aconitase (c-aconitase) activity (97–103). Iron levels dictate the form that predominates. An increase in cellular iron stimulates the assembly of the [4Fe-4S] cluster c-aconitase form, with a concomitant decrease in RNA-binding activity. Conversely, low cellular iron results in the accumulation of the apo-RNA-binding form at the expense of c-aconitase activity (98,100–104). Therefore, IRP1 is a bifunctional iron sensor that converts between its mutually exclusive apo-RNA-binding and c-aconitase forms, a process that is regulated by cellular iron. IRP1 protein levels are not affected by alterations in cellular iron concentration, indicating that iron affects IRP1 posttranslationally (105,106). Human, rat, mouse, and rabbit IRP1 share greater than 90% identity, and all have ~29% identity and ~59% similarity to mammalian m-aconitases (98). Although it is clear that the RNA-binding activity of IRP1 is central to the regulation of iron homeostasis, the function of c-aconitase activity is unknown.

Table 1 Functions of Proteins Encoded by IRE-Containing mRNAs

	Function/reaction	References
5' IREs		
Ferritin H and L	Iron sequestration, oxidation of Fe ⁺² to Fe ⁺³	22,47,48
m-Aconitase	Krebs cycle enzyme, interconverts citrate and isocitrate for energy production	62–64
Succinate dehydrogenase (<i>Drosophila</i>)	Krebs cycle enzyme, catalyzes succinate to fumarate for energy production	65,66
e-ALAS	Heme biosynthesis in erythroid cells, catalyzes the formation of 5-aminolevulinic acid from succinyl CoA and glycine	53,62,67–69
IREG1/ferroportin/MPT	Iron export	70–72
3' IREs		
TfR	Iron uptake of diferric transferrin	83,84,87,88
DMT1	Divalent metal transporter, uptake of iron and other divalent metals	91,93

Based on the conservation between IRP1 and m-aconitase, IRP1 is presumed to have a three-dimensional structure similar to that known for the porcine m-aconitase (107,108). Mitochondrial aconitase is arranged into four domains (98,107–109). Domains 1–3 form a compact, N-terminal core that is tethered to the larger C-terminus domain 4 via a flexible polypeptide linker (Fig. 3). This arrangement forms a cleft that accommodates the cubane [4Fe–4S] cluster, in addition to the 23 active-site residues that are located throughout all four domains. Domain 3 contains invariant active-site cysteines (437,503, and 506) that serve as ligands for three of the four iron atoms in the Fe–S cluster, while the fourth iron atom is coordinated by substrate, and is labile due to its exposure to solvent (110). When these three cysteines are mutated either singly or in combination, formation of the Fe–S cluster was blocked as determined by in-vitro reconstitution assays and by in-vivo transfection experiments (111–113). These mutants are constitutively active for RNA binding, even in the presence of high iron, demonstrating that the formation of the [4Fe–4S] cluster precludes RNA binding (112). When these cysteine mutants are stably expressed in cultured cells, ferritin and TfR expression are dysregulated, as would be predicted for an IRP1 whose RNA-binding activity cannot be downregulated by iron (114). These data indicate that the RNA-binding site and aconitase active site overlap, and account for the mutually exclusive activities of IRP1. Furthermore, these results suggest that the failure of m-aconitase to bind RNA is due to the absence of specific amino acids in the cleft that are important for RNA binding.

Until recently, IRP1-like RNA-binding activity was not thought to be present in prokaryotes. A recent study, however, has demonstrated that the *Bacillus subtilis* aconitase binds RNA (21). The single aconitase gene encoded by *B. subtilis* binds mammalian ferritin IRE, where RNA binding is regulated by the availability of iron both in vivo and in vitro (21). Examination of the *B. subtilis* genome revealed several IRE-like structures, two of which are found in UTRs of mRNAs encoding a cyto-

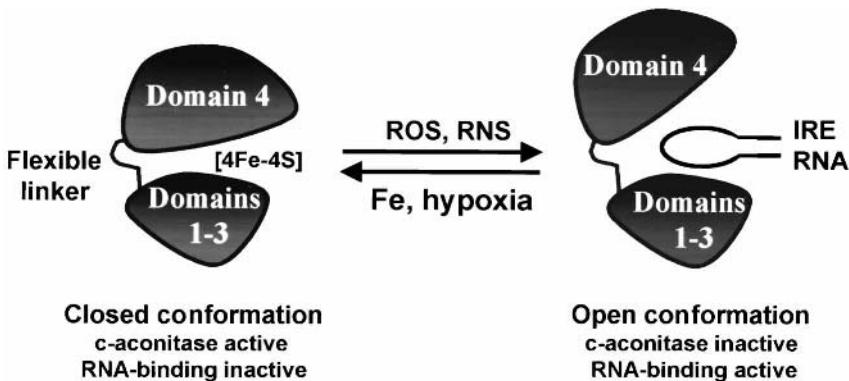


Figure 3 Model of IRP1 regulation by iron, ROS, RNS, and hypoxia. IRP1 is found in two mutually exclusive conformations, depending on the concentration of cellular iron, ROS, RNS, and oxygen. The closed conformation represents the c-aconitase form containing the [4Fe–4S] cluster but lacking RNA binding activity. The open conformation represents the RNA-binding form that lacks a [4Fe–4S] cluster and c-aconitase activity. Iron and hypoxia (see text) convert the RNA-binding form into the c-aconitase form, while ROS and RNS convert the c-aconitase form into the RNA-binding form.

chrome aa₃ oxidase subunit and one between two genes in the *feu* operon that encodes an iron uptake system. In both cases, the *B. subtilis* aconitase bound these novel IRE-like structures, whereas mammalian IRP1 did not. One *B. subtilis* strain expressing only a mutant form of aconitase, which lacks enzymatic activity but retains RNA-binding activity, sporulates 40 times more efficiently than the null mutant, demonstrating a physiological role for the RNA-binding activity of the *B. subtilis* aconitase.

IRP1 lacks classical RNA-binding motifs and does not appear to contain modular domains that are often found in nucleic acid-binding proteins. Biochemical analysis was therefore performed to characterize IRP1–RNA interactions. Chemical probing (111,112), UV cross-linking of IRP1 to radiolabeled IRE followed by peptide sequencing (115,116), and scanning mutagenesis (117) support the model in which the active-site cleft can conform to a “closed” or an “open” structure (Fig. 3). The linker peptide connecting domains 1–3 with domain 4 is believed to provide the necessary flexibility such that IRP1 can adopt to different structural conformations. In the closed conformation, IRP1 contains the [4Fe–4S] cluster and is enzymatically active, but RNA-binding incompetent. In the open conformation, IRP1 lacks the [4Fe–4S] cluster and is enzymatically inactive, but RNA-binding competent. The open conformation is predicted to accept the bulky IRE that is too large to fit into the closed conformation (118,119). More recently, mutagenesis experiments support this model by identifying regions in domain 4 that contact the IRE bulge (arginines 728 and 732) and that are necessary for recognition of the IRE loop (residues 685–689) (120). Lastly, limited in-vitro proteolysis demonstrated a decrease in protease sensitivity of the c-aconitase form versus the apo-IRP1, further indicating structural differences between the two forms (121,122). Understanding the precise nature of conformational changes in IRP1 between its two forms awaits the determination of the crystallographic structure of IRP1 with and without RNA bound.

It is becoming increasingly clear that the IRPs serve as focal points for a variety of extracellular and intracellular signals that act to integrate IRP function with other metabolic processes. In this regard, phosphorylation of IRP1 appears to be important in the regulation of its RNA-binding activity. IRP1 is phosphorylated when cultured HL60 cells are exposed to the protein kinase C (PKC) activator phorbol 12-myristate 13-acetate (PMA), where serine 138 and serine 711 were identified as the phosphorylated residues (123,124). IRP1 phosphorylation results in the accumulation of its RNA-binding form, although phosphorylation does not affect the K_d of IRP1-IRE interaction per se. Moreover, phosphorylation is not affected by exposure of cells to desferrioxamine or by the addition of hemin (124). Apo-IRP1 has about a fivefold increase in its phosphorylation in in-vitro experiments compared to its [4Fe–4S] form, suggesting that the [4Fe–4S] cluster sterically blocks PKC access to IRP1 (121). When wild-type IRP1 is introduced into an *aco1* aconitase-deficient yeast strain, the yeast are able to overcome glutamate auxotrophy (125). Using this yeast system with phosphomimetic mutants of serine 138, Brown et al. provided data indicating that phosphorylation of serine 138 negatively affects [4Fe–4S] cluster formation/stability (125). They suggested that by distorting the active-site cleft, serine 138 phosphorylation destabilizes the Fe–S cluster. This is in accord with the prediction that serine 138 lies near the entrance to the active-site cleft. Furthermore, by changing ROS levels by growth under aerobic and anaerobic conditions, data indicate that serine 138 phosphorylation enhances IRP1 sensitivity to ROS-mediated cluster

disassembly. These results may be relevant to hypoxic IRP1 regulation in mammalian cells (61,126–129) (see below).

The mechanism regulating the biosynthesis and assembly of the [4Fe–4S] cluster in c-aconitase/IRP1 is not known, but elucidation of this process will be required to understand IRP1 regulation fully. Recent studies have led to the identification of several proteins in bacteria, yeast, and mammals that are important in the maturation and stabilization of Fe–S clusters (130). In eukaryotes the proteins involved in Fe–S cluster biogenesis are best understood in *Saccharomyces cerevisiae*, where they have been localized to the mitochondria. These proteins include Nfs1p (cysteine desulfurase) (131–133), Yah1p (mitochondrial ferredoxin homolog) (134), Isa1p [proposed to be involved in Fe binding (135,136)], and Ssq1p and Jac1p (heat-shock proteins) (133). The mammalian *Nifs* gene has been cloned, and different proteins corresponding to alternative in-frame AUG start codons are differentially targeted to the mitochondria, cytoplasm, and nucleus (137). The role of mammalian *Nifs* in Fe–S cluster formation has yet to be established. Studies demonstrated that the *S. cerevisiae* mitochondrial ATP-binding cassette (ABC) transporter *Atm1p* is required for the mitochondrial export of Fe–S clusters required for the formation of cytosolic Fe–S cluster proteins (131). In light of these studies, it is interesting that the mammalian *ABC7* gene, which is an ortholog of yeast *ATM1*, is responsible for the human recessive disorder X-linked sideroblastic anemia and ataxia (138,139). It is tempting to speculate that the anemia in these patients might result from the constitutive activation of IRP1 RNA-binding activity due to a decrease in the export of Fe–S clusters from the mitochondria. This would lead to the repression of e-ALAS synthesis in erythroid cells. Although the processes involved in c-aconitase Fe–S cluster biogenesis are not known, it seems likely that they will involve a well-conserved biosynthetic pathway involving mitochondria. If so, this may tightly couple mitochondrial function with c-aconitase/IRP1 activity and cellular iron homeostasis.

B. Regulation of IRP2

IRP2 is ~57% identical and ~79% similar to IRP1 (140). Like IRP1, IRP2 is regulated by cellular iron, and thus functions as an iron sensor. Although structurally and functionally similar to IRP1, IRP2 does not contain a [4Fe–4S] cluster, and lacks aconitase activity (141). Furthermore, IRP2 has not been reported to bind iron directly. The regulation of IRP2 involves a change in protein stability that is related directly to cellular iron concentration, and studies with pharmacological inhibitors showed that iron targets the IRP2 protein for proteasomal destruction (141,142). The increase in IRP2 degradation in iron-replete cells parallels an increase in its ubiquitination (143), consistent with the proteasomal targeting function of ubiquitin. The process of iron-induced IRP2 degradation requires a unique 73-amino acid domain termed the degradation domain. This domain is encoded by an exon that is absent in IRP1 (16,142). Deletion of the degradation domain results in a mutant IRP2 protein that is constitutively stable and capable of binding RNA, even in the presence of high iron (144). Furthermore, the degradation domain can impart iron-dependent degradation on IRP1 when placed in the corresponding position in IRP1 (144). Therefore, the degradation domain is necessary and sufficient for iron-mediated IRP2 degradation.

Using the 2,4-dinitrophenylhydrazine assay (a common measure of protein oxidation), Iwai et al. showed that IRP2 is oxidized by iron both in vivo and in vitro

(143). In-vitro ubiquitination assays further demonstrated that IRP2 was an efficient substrate for ubiquitination only after it had first been iron-oxidized (143). Examination of the degradation domain revealed three invariant cysteines (168,174, and 178 in human IRP2), located in the sequence of CX₅CX₃C (Fig. 4). Since cysteines are often involved in the direct ligation of iron, each cysteine was individually or simultaneously mutated to serine(s) and examined for regulation by iron (143,144). These mutant proteins demonstrated decreased iron-catalyzed IRP2 oxidation and decreased ubiquitination, in vitro and in vivo, compared to wild-type IRP2 (143). Similar results were obtained using cell lines expressing wild-type and cysteine mutants of IRP2. Together these results support a model in which cysteines 168, 174, and 178 transiently coordinate iron that leads to a “caged” Fenton-like reaction resulting in IRP2 oxidation (143). The ubiquitination machinery specifically recognizes oxidized IRP2, resulting in its poly-ubiquitination and degradation by the proteasome (Fig. 4). The mechanism of ubiquitination of oxidized IRP2 is unclear, but it probably requires the activity of an E3 ubiquitin ligase. A comprehensive understanding of the IRP2 degradation pathway will help define how other stimuli regulate IRP2, such as hypoxia (126,127,129) and nitric oxide (145–150).

Our understanding of IRP2 (and IRP1) regulation at the transcriptional level is limited. Recent data, however, showed that the *c-myc* proto-oncogene gene product

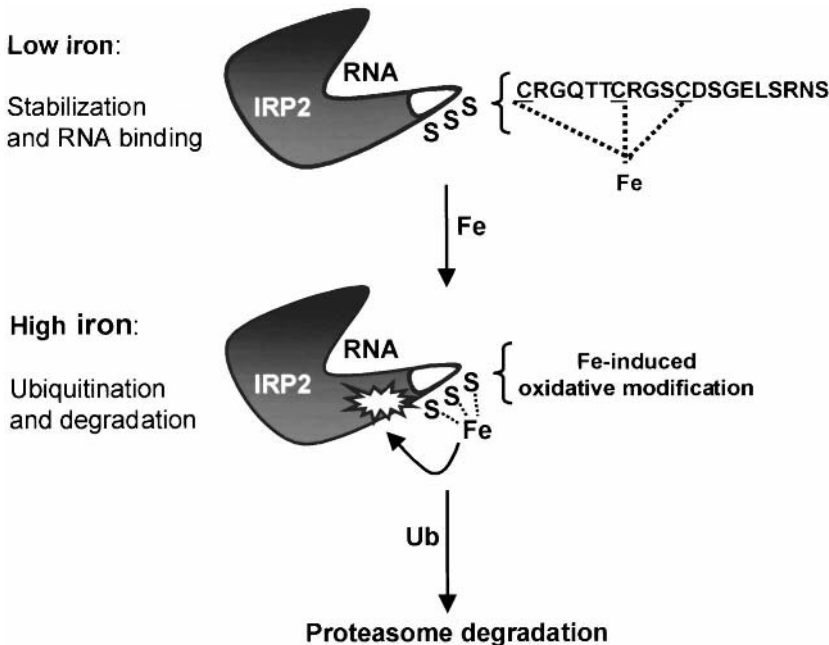


Figure 4 Model of IRP2 iron-induced degradation. In the model proposed by Iwai et al. (143), an increase in intracellular iron promotes IRP2 oxidation through a localized or “caged” Fenton-like reaction requiring the 73-amino acid degradation domain (shown in white). The degradation domain harbors three conserved cysteines presumed to be involved in coordinating iron. The oxidized IRP2 is then specifically ubiquitinated through an unknown mechanism, requiring a putative E3 ubiquitin ligase. Ubiquitinated IRP2 is then rapidly degraded by the proteasome. Low iron decreases this process and IRP2 is stabilized.

upregulates IRP2 transcription fivefold, without affecting IRP1 transcription (151). In addition, through its transcriptional repression activity, *c-myc* downregulates ferritin-H expression. Downregulation of ferritin-H gene expression was necessary for *c-myc* to induce cell proliferation and transformation of immortalized B cells (151). These results indicate that *c-myc* promotes an increase in cellular iron through increased iron uptake (by stabilizing TfR mRNA via increased IRP2) and decreased iron sequestration (by decreasing ferritin levels), a situation that would be favorable for cell proliferation.

VI. OTHER PHYSIOLOGICAL MODULATORS OF IRP ACTIVITY

A. Regulation of IRP1 by Reactive Oxygen Species

In addition to changes in cellular iron levels, other stimuli, such as reactive oxygen and nitrogen species (RNS), and oxygen tension, regulate IRP1/*c*-aconitase and IRP2 activities. Superoxide and H_2O_2 are natural by-products of cellular respiration, and are the major intermediates of oxygen reduction. Several Fe-S cluster-containing enzymes are targets of O_2^- -mediated inactivation, with aconitase the most extensively studied example (9–11,145,152–154). Treatment of IRP1/*c*-aconitase with O_2^- in vitro converts the [4Fe–4S] cluster to a [3Fe–4S] cluster, leading to the inactivation of both aconitase and RNA-binding activities (153,154). In-vivo data also support a role for O_2^- -mediated aconitase inactivation. For instance, in lung cells, 10–15% of total aconitase is inactive under normal growth conditions and was attributed to constant cluster disintegration by O_2^- (9). The inactivation of aconitase by O_2^- is a reversible and a cyclical process with inactivation/reactivation occurring every ~12 min (11). Reactivation is due to reincorporation of the fourth, labile Fe atom to form the complete [4Fe–4S] cluster. Since inactivation of *c*-aconitase by O_2^- in vitro does not result in complete cluster disintegration, the protein is not converted into its IRP1 RNA-binding form (145,154). Whether O_2^- activates IRP1 RNA-binding activity through cluster disintegration in vivo is unknown. The redox cycling drug menadione also regulates IRP1 by decreasing both IRP1 RNA-binding and *c*-aconitase activities (155). The effects of menadione are distinct from those of O_2^- and H_2O_2 (see below), and underscores the idea that IRP1 responds differently to diverse oxidative stress stimuli.

Hydrogen peroxide has been shown to repress ferritin synthesis and stabilize the TfR mRNA (156). This is achieved through the H_2O_2 -mediated activation of IRP1 RNA-binding activity (32,156–160). Physiological levels of extracellularly produced H_2O_2 (~10 μM) rapidly stimulate IRP1 RNA-binding activity by a mechanism that is not dependent on de-novo protein synthesis (156,160). Activation of IRP1 by H_2O_2 is accompanied by a decrease in *c*-aconitase activity, demonstrating that H_2O_2 results in the complete disassembly of the cluster that allows for RNA binding (156). The increase in IRP1 RNA-binding activity by H_2O_2 requires only a 15-min transient exposure to H_2O_2 to initiate (“induction phase”) a putative signaling pathway (“execution phase”) that results in IRP1 activation (160). IRP1 activation is faster in cells treated with H_2O_2 (0.5–1 h) compared to cells treated with the iron chelator desferrioxamine (8–12 h) (156–158), suggesting that the effect of H_2O_2 is distinct from iron depletion. Importantly, IRP1 activation by H_2O_2 requires cellular integrity, indicating that H_2O_2 does not work through a direct chemical mechanism (156,157,

160,161). The type I/IIa protein phosphatase inhibitor okadaic acid inhibits H_2O_2 -mediated IRP1 activation, indicating the involvement of a signaling pathway in the activation process (156). This is further supported by the work of Pantopoulos et al., who have reconstituted the H_2O_2 -induced activation of IRP1 in vitro using permeabilized cells (159). In this system, H_2O_2 -induced IRP1 activation requires an unidentified noncystolic component, possibly a plasma membrane-associated protein involved in “sensing” H_2O_2 (159). Activation is blocked in the presence of nonhydrolyzable ATP- γ -S or GTP- γ -S, indicating changes in phosphorylation or an energy requirement. One possibility is that H_2O_2 activates a signaling pathway that may involve changes in IRP1 phosphorylation, which in turn could destabilize the cluster (125).

The activation of IRP1 by H_2O_2 establishes a link between oxidative stress and iron homeostasis, although it is unclear what physiological function this plays. Activation and IRP1 RNA-binding activity would be expected to increase cellular iron concentration, a situation predicted to be deleterious when H_2O_2 levels are high. Consequently, the effect of H_2O_2 on IRP1 would be predicted to be pathophysiological. Alternatively, H_2O_2 activation of IRP1 may stimulate the expression of protein encoded by an unidentified IRE-containing mRNA that is involved in cellular adaptation to oxidative stress. Although significant inroads have been made in understanding the relationship between ROS and IRPs, more work is required to define the precise molecular mechanisms involved and the physiological significance of this regulation.

B. Regulation of IRPs by Reactive Nitrogen Species

In addition to iron and ROS, nitric oxide (NO) can modulate IRP activity, thereby influencing iron homeostasis (127,149). Nitric oxide is a key signaling molecule involved in a wide variety of cellular processes, including macrophage-mediated toxicity, vasodilation, neurotransmission, immune response, and adhesion. Nitric oxide mediates its effects by several mechanisms that include activation of guanylate cyclase, S-nitrosylation of thiol-containing proteins, or direct interaction with the Fe-S centers of nonheme proteins (162,163). By virtue of their [4Fe-4S] clusters, aconitases are major targets of NO. Mammalian c- (145,164–166) and m- (164) aconitases, as well as *Escherichia coli* (167) and plant (19) aconitases, are sensitive to inactivation by NO. Electron paramagnetic resonance (EPR) spectroscopy showed that inactivation of aconitases by NO was due to the disassembly of the [4Fe-4S] (168). Although the physiological role for the NO-mediated inactivation of m-aconitase is not certain, one notion is that it could serve as a mechanism to decrease oxidative stress by reducing electron flow through the mitochondrial electron-transport chain.

The sensitivity of m-aconitase to NO led to studies to determine the effects of NO on IRP1 RNA-binding activity in cultured cells and in-vitro cell extracts. When cell extracts are exposed to NO-generating chemicals, c-aconitase is converted from the [4Fe-4S] cluster form to the apo-RNA-binding form (145,165,166). The conversion to the RNA-binding form is enhanced by the presence of an endogenous reducing system, such as thioredoxin, suggesting that in-vivo thioredoxin might serve as a modulator of IRP activity during conditions at which RNS or ROS are generated (166). When the murine macrophage cell lines RAW264.7 (146,147,150,165) and

J774 (169–171) and a rat hepatoma cell line FTO2B (172) were stimulated with interferon- γ /lipopolysaccharide (γ -IFN/LPS) to produce NO, c-aconitase activity was inactivated concomitant with the activation of IRP1 RNA binding. IRP2 RNA-binding activity decreased in γ -IFN/LPS-stimulated macrophage cells (145,146,150), but not in FTO2B hepatoma cells (172). Treatment of RAW264.7 and J774 cells with γ -IFN/LPS in the presence of iron chelators prevented the decrease in IRP2 RNA-binding activity, indicating that iron is required for IRP2 inactivation (146,150). Specific inducible nitric oxide synthase inhibitors prevented the effects of NO, confirming that changes in IRP activity were NO-mediated. In some studies, the consequences of NO production on ferritin synthesis and TfR mRNA levels were measured, but with conflicting results. The NO-induced activation of IRP1 activity correlated with decreased ferritin synthesis in some studies (169,172,173), while in other studies ferritin synthesis increased (146,150). The latter two studies were carried out in RAW264.7 macrophages, where IRP2 activity dramatically decreased (146,150). Conflicting studies report both increases (173) and decreases (150,170) in TfR mRNA levels in γ -IFN/LPS-stimulated cells, and are complicated by the fact that TfR can be regulated by cytokines through NO-independent mechanisms (170). Taken together, these studies show that IRP1 and IRP2 are differentially regulated by NO in γ -IFN/LPS-stimulated cells. Whether the discrepant data regarding ferritin regulation in cytokine-stimulated macrophages is due to differences in growth condition or variations in experimental design remains to be determined.

Further studies were carried out to determine whether different redox forms of NO modulate IRP activity. Cells treated with S-nitroso-N-acetyl-pencillamine (SNAP), a NO \cdot generator, increased IRP1 RNA-binding activity (146,148,158, 172,174), while IRP2 RNA-binding activity was unaffected (148,172) or decreased (146). In contrast, RAW264.7 macrophage cells treated with sodium nitroprusside (SNP), a NO $^+$ generator, decreased IRP2 RNA-binding activity without significant changes in IRP1 RNA-binding activity (148). In another study, human erythroleukemia K562 cells treated with SNP decreased total IRP RNA-binding activity that was ascribed to IRP1 activity (174). [In human extracts, IRP1 and IRP2/IRE complexes co-migrate on RNA-bandshift gels (16).] Inactivation of IRP2 RNA-binding activity in SNP-treated cells is due to accelerated proteasomal degradation (148). In this study, the decrease in IRP2 activity correlated with a decrease in TfR mRNA level and an increase in ferritin synthesis, indicating that alterations in IRP2 activity regulated TfR expression (148). Kim and Ponka proposed a model whereby IRP1 and IRP2 are differently modulated by distinct NO-redox forms (148). For example, the cellular production of NO $^+$ would S-nitrosylate critical sulfhydryls in IRP2, targeting IRP2 for proteasomal degradation while NO \cdot targets the IRP1/c-aconitase [4Fe–4S] cluster, activating RNA binding. The three critical cysteines in the degradation domain of IRP2, which are required for iron-catalyzed degradation (144), might be targeted by S-nitrosylation, promoting IRP2 proteolysis. In cytokine-stimulated cells, the levels of nitrosoglutathione increase, and this species is known to mediate protein S-nitrosylation (148). The regulation of IRPs by NO may have implications for iron homeostasis during inflammatory conditions, when iron sequestration in reticuloendothelial cells is correlated with an increase in ferritin synthesis. The consequences of the differential regulation of IRP1 and IRP2 activities by NO for iron homeostasis remain to be determined.

C. Regulation of the IRPs by Hypoxia

The important relationship between oxygen-derived species and iron has prompted several investigations into the interplay between oxygen tension and iron homeostasis. Results from these studies have revealed that hypoxia affects iron homeostasis at different levels. At the transcriptional level, the genes for transferrin (175), TfR (128,129,176–179), and ceruloplasmin (180) are more highly expressed during hypoxia than during normoxia. The mechanism of hypoxic upregulation of these genes involves activation by the heterodimeric transcription factor termed hypoxia-inducible factor-1 (HIF-1). HIF-1 binds to hypoxic response elements found 5' or 3' to hypoxia-induced genes and stimulates their expression. Activation of hypoxia-induced genes is a central feature in cellular adaptation to a decreased oxygen environment [(181,182) and references therein]. At the posttranscriptional level, hypoxia has been shown to influence iron homeostasis through the regulation of IRP1 and IRP2 RNA-binding activities (61,126–129). The mRNA for the duodenal iron transporter IREG1 is also elevated during hypoxia, although the mechanism responsible for this regulation is not known (70). Taken together, these results indicate that hypoxia influences iron homeostasis in a complex manner that affects both cellular and physiological processes. The hypoxic regulation of iron homeostasis in response to low oxygen tension is relevant to normal physiological situations (such as embryonic development and changes in elevation), as well as during pathophysiological events (such as ischemia and tumor hypoxia).

Several reports have demonstrated that IRP RNA-binding activity is regulated during hypoxia (61,126–129). Physiological concentrations of oxygen (1–3% oxygen) were shown to decrease IRP1 RNA-binding activity in a variety of cell lines and in primary cardiac myocytes (61,126,127). These studies demonstrated that IRP1 RNA-binding activity decreases about threefold when cells are exposed to 6 h of hypoxia (61). The decrease in IRP1 RNA-binding activity is concomitant with an increase in its c-aconitase activity. Hypoxic IRP1 regulation appears to be posttranslational, since there are no changes in IRP1 protein levels (61). Lastly, hypoxic downregulation of IRP1 RNA-binding activity was blocked when cells were treated with desferrioxamine, demonstrating a requirement for iron in the IRP1 hypoxic response. These data indicate that hypoxia induces a shift from the IRP1 RNA-binding form to its c-aconitase form. One study claimed that hypoxia increases rather than decreases IRP1 RNA-binding activity (129). In that study, human cell lines were used in which IRP1 and IRP2 co-migrate in RNA bandshift analysis, and the experiments performed did not differentiate between IRP1 and IRP2 RNA binding. Because it has recently been shown that the IRP2 protein is stabilized during hypoxia (see below) (126), it seems likely that the increase in total IRP activity observed in the above studies was due to IRP2.

One possibility for the hypoxic inactivation of IRP1 RNA-binding activity is that hypoxia may increase cellular iron levels that would promote [4Fe–4S] cluster formation and increase c-aconitase activity. Activation of the TfR and transferrin genes in cell culture models of hypoxia supports the model whereby hypoxia increases iron uptake (128,175,177,178). A second mechanism by which IRP1 may be regulated during hypoxia is through [4Fe–4S] cluster stability. When oxygen is limiting, a decrease in cytosolic $O_2^{\cdot -}$ would reduce the rate of $O_2^{\cdot -}$ -mediated [4Fe–4S] cluster disassembly. Since the [4Fe–4S] cluster form of IRP1, like m-aconitase, is

sensitive to O_2^- disassembly (10), it is possible that hypoxia results in cluster stabilization. It should be noted, however, that there are conflicting reports on whether ROS decrease or increase during hypoxia [(182,183) and references therein]. The lack of consensus on this important issue is due to technical difficulties in measuring ROS during hypoxia.

Hypoxic downregulation of IRP1 RNA-binding activity is reversible (61). Since there is no change in IRP1 concentration during reoxygenation, reactivation may reflect a reversal in cluster stability. For instance, reoxygenation is predicted to increase ROS, a situation that could negatively affect cluster stability and lead to an increase in IRP1 RNA-binding activity. Alternatively, reoxygenation could induce IRP1 phosphorylation, or some other modification, that could decrease cluster stability. Importantly, reactivation of IRP1 during reoxygenation is completely blocked by cycloheximide and partially blocked by the phosphatase inhibitor okadaic acid (61). This suggests that de-novo synthesis of a protein may be required for IRP1 activation, such as a kinase or a phosphatase. It is also possible that de-novo synthesis of IRP1 may be required during reoxygenation, implying that the [4Fe-4S] c-aconitase form is not converted to the RNA-binding form. Because ROS generation during reoxygenation is thought to be an important component of ischemic-related diseases, it will be important to elucidate the consequences of IRP1 regulation during hypoxia/reoxygenation.

Hypoxia also regulates IRP2 RNA-binding activity, but in a direction opposite from that of IRP1 (126,127). IRP2 RNA-binding activity increases in cultured cells exposed to hypoxia, with an approximately threefold increase at 7 h and a sixfold increase at 19 h. This increase in RNA-binding activity results from an increase in IRP2 protein concentration without changes in IRP2 mRNA. The rise in IRP2 protein levels during hypoxia is due to increased protein stability (126), where the half-life of a myc-tagged IRP2 expressed in the human embryonic kidney 293 cell line increases from about 5 h during normoxia to more than 20 h during hypoxia. Interestingly, hypoxic regulation of IRP2 shares striking similarities to the hypoxia-regulated HIF-1 α subunit of HIF-1 transcription factor. First, both proteins accumulate during hypoxia by a posttranslational mechanism involving an increase in protein stability. In the case of HIF-1 α , hypoxic stabilization is achieved by a decrease in its rate of ubiquitination (184–186). Since the ubiquitin–proteasome pathway degrades IRP2, a decrease in ubiquitination during hypoxia seems a likely mechanism for IRP2 hypoxic stabilization. Second, exposure of cells to the hypoxic mimetics desferrioxamine and CoCl₂ results in the accumulation of the IRP2 (126,143, 144,187) and HIF-1 α proteins (188,189). It has been proposed that these agents interfere with the heme moiety of a hemoprotein oxygen sensor (190,191), although no such protein has yet been identified (see Ref. 183 for a discussion of oxygen sensing). More recent data demonstrated that iron is required for HIF-1 α interaction with the von Hippel-Lindau E3 ubiquitin ligase complex that is involved in HIF-1 α ubiquitination (192,193). This suggests that iron plays an important role in HIF-1 α degradation. Whether the function of iron in HIF-1 α regulation is similar to its role in IRP2 oxidation remains to be determined. Alternatively, an iron-containing protein may be involved in HIF-1 α ubiquitination. From the standpoint of hypoxic regulation of IRP2, it may be possible that iron has a role in mediating IRP2 degradation by facilitating its interaction with an as-yet-unidentified E3 ubiquitin ligase complex similar to HIF-1 α . Regardless of the mechanism, it appears that hypoxic regulation

of IRP2 and HIF-1 α is mediated through a similar oxygen-sensing/signaling pathway, allowing for the coordinated regulation of gene expression at the posttranscriptional and transcriptional levels, respectively.

VII. CONCLUSIONS

The 1990s witnessed considerable advances in our understanding of the regulation of IRP1 and IRP2 by iron, and by other stimuli, such as ROS, RNS, and hypoxia. Furthermore, the identification of novel IRE-mRNAs has broadened our understanding of iron homeostasis into other areas, including energy homeostasis. With this knowledge in hand, many questions can be posed regarding the detailed mechanisms of IRP1 and IRP2 regulation by iron, ROS, RNS, and hypoxia, and the physiological consequences of this regulation. In addition, the question of why two IRPs evolved, each regulated by different mechanisms, remains to be solved. The recent discovery of proteins involved in Fe–S cluster assembly will be important in unraveling the mechanism responsible for Fe–S cluster assembly in IRP1 and the function of c-*aconitase* in iron homeostasis. Over the next decade, as we obtain answers to these questions, we will increase our knowledge of the role in IRP regulation during pathophysiological disorders, such as tumor hypoxia, ischemia, and neurodegeneration.

REFERENCES

1. Boveris A, Oshino N, Chance B. The cellular production of hydrogen peroxide. *Biochem J* 1972; 128:617–630.
2. McCord JM, Fridovich I. Superoxide dismutase. An enzymatic function for erythrocyte hemocuprein (hemocuprein). *J Biol Chem* 1969; 244:6049–6055.
3. Fridovich I. Superoxide anion radical (O_2^-), superoxide dismutases, and related matters. *J Biol Chem* 1997; 272:18515–18517.
4. Fridovich I. Superoxide radical and superoxide dismutases. *Annu Rev Biochem* 1995; 64:97–112.
5. Berlett BS, Stadtman ER. Protein oxidation in aging, disease, and oxidative stress. *J Biol Chem* 1997; 272:20313–20316.
6. Steinberg D. Low density lipoprotein oxidation and its pathobiological significance. *J Biol Chem* 1997; 272:20963–20966.
7. Henle ES, Linn S. Formation, prevention, and repair of DNA damage by iron/hydrogen peroxide. *J Biol Chem* 1997; 272:19095–19098.
8. Beckman KB, Ames BN. The free radical theory of aging matures. *Physiol Rev* 1998; 78:547–581.
9. Gardner PR, Raineri I, Epstein LB, White CW. Superoxide radical and iron modulate aconitase activity in mammalian cells. *J Biol Chem* 1995; 270:13399–133405.
10. Gardner PR, Nguyen DH, White C. Aconitase is a sensitive and critical target of oxygen poisoning in cultured mammalian cells and in rat lungs. *Proc Natl Acad Sci USA* 1994; 91:12248–12252.
11. Gardner PR. Superoxide-driven aconitase Fe-S center cycling. *Biosci Rep* 1997; 17: 33–42.
12. Wessling-Resnick M. Biochemistry of iron uptake. *Crit Rev Biochem Mol Biol* 1999; 34:285–314.
13. Andrews NC, Fleming MD, Levy JE. Molecular insights into mechanisms of iron transport. *Curr Opin Hematol* 1999; 6:61–64.

14. Aisen P, Wessling-Resnick M, Leibold EA. Iron metabolism. *Curr Opin Chem Biol* 1999; 3:200–206.
15. Rothenberger S, Müllner EW, Kühn LC. The mRNA-binding protein which controls ferritin and transferrin receptor expression is conserved during evolution. *Nucleic Acids Res* 1990; 18:1175–1179.
16. Guo B, Brown FM, Phillips JD, Yu Y, Leibold EA. Characterization and expression of iron regulatory protein 2 (IRP2). *J Biol Chem* 1995; 270:16529–16535.
17. Muckenthaler M, Gunkel N, Frishman D, Cyrklaff A, Tomancak P, Hentze MW. Iron-regulatory protein-1 (IRP-1) is highly conserved in two invertebrate species—Characterization of IRP-1 homologues in *Drosophila melanogaster* and *Caenorhabditis elegans*. *Eur J Biochem* 1998; 254:230–237.
18. Saas J, Ziegelbauer K, von Haeseler A, Fast B, Boshart M. A developmentally regulated aconitase related to iron-regulatory protein-1 is localized in the cytoplasm and in the mitochondrion of *Trypanosoma brucei*. *J Biol Chem* 2000; 275:2745–2755.
19. Navarre DA, Wendehenne D, Durner J, Noad R, Klessig DF. Nitric oxide modulates the activity of tobacco aconitase. *Plant Physiol* 2000; 122:573–582.
20. Meehan HA, Lundberg RA, Connell GJ. A trypanosomatid protein specifically interacts with a mammalian iron-responsive element. *Parasitol Res* 2000; 86:109–114.
21. Alén C, Sonenshein AL. *Bacillus subtilis* aconitase is an RNA-binding protein. *Proc Natl Acad Sci USA* 1999; 96:10412–10417.
22. Leibold EA, Munro HN. Characterization and evolution of the expressed rat ferritin light subunit gene and its pseudogene family. Conservation of sequences within non-coding regions of ferritin genes. *J Biol Chem* 1987; 262:7335–7341.
23. Leibold EA, Laudano A, Yu Y. Structural requirements of iron-responsive elements for binding of the protein involved in both transferrin receptor and ferritin mRNA post-transcriptional regulation. *Nucleic Acids Res* 1990; 18:1819–1824.
24. Barton HA, Eisenstein RS, Bomford A, Munro HN. Determinants of the interaction between the iron-responsive element-binding protein and its binding site in rat L-ferritin mRNA. *J Biol Chem* 1990; 265:7000–7008.
25. Bettany AJ, Eisenstein RS, Munro HN. Mutagenesis of the iron-regulatory element further defines a role for RNA secondary structure in the regulation of ferritin and transferrin receptor expression. *J Biol Chem* 1992; 267:16531–16537.
26. Jaffrey SR, Haile DJ, Klausner RD, Harford JB. The interaction between the iron-responsive element binding protein and its cognate RNA is highly dependent upon both RNA sequence and structure. *Nucleic Acids Res* 1993; 21:4627–4631.
27. Theil EC. Iron regulatory element (IRE): A family of mRNA non-coding sequences. *Biochem J* 1994; 304:1–11.
28. Butt J, Kim H, Basilion J, Cohen S, Iwai K, Philpott C, Altschul S, Klausner R, Rouault T. Differences in the RNA binding sites of iron regulatory proteins and potential target diversity. *Proc Natl Acad Sci USA* 1996; 93:4345–4349.
29. Allerson CR, Cazzola M, Rouault TA. Clinical severity and thermodynamic effects of iron-responsive element mutations in hereditary hyperferritinemia-cataract syndrome. *J Biol Chem* 1999; 274:26439–26447.
30. Henderson BR, Menotti E, Bonnard C, Kühn LC. Optimal sequence and structure of iron-responsive elements. *J Biol Chem* 1994; 269:17481–17489.
31. Henderson BR, Menotti E, Kühn LC. Iron regulatory proteins 1 and 2 bind distinct sets of RNA target sequences. *J Biol Chem* 1996; 271:4900–4908.
32. Menotti E, Henderson BR, Kühn LC. Translational regulation of mRNAs with distinct IRE sequences by iron regulatory proteins 1 and 2. *J Biol Chem* 1998; 273:1821–1824.
33. Schalinske KL, Blemings KP, Steffen DW, Chen OS, Eisenstein RS. Iron regulatory protein 1 is not required for the modulation of ferritin and transferrin receptor expres-

- sion by iron in a murine pro-B lymphocyte cell line. *Proc Natl Acad Sci USA* 1997; 30:10681–10686.
34. Ke Y, Wu J, Leibold EA, Walden WE, Theil EC. Loops and bulge/loops in iron-responsive element isoforms influence iron regulatory protein binding. Fine-tuning of mRNA regulation? *J Biol Chem* 1998; 273:23637–23640.
 35. Bonneau D, Winter-Fuseau I, Loiseau MN, Amati P, Berthier M, Oriot D, Beaumont C. Bilateral cataract and high serum ferritin: A new dominant genetic disorder? *J Med Genet* 1995; 32:778–779.
 36. Girelli D, Olivieri O, De Franceschi L, Corrocher R, Bergamaschi G, Cazzola M. A linkage between hereditary hyperferritinaemia not related to iron overload and autosomal dominant congenital cataract. *Br J Haematol* 1995; 90:931–934.
 37. Beaumont C, Leneuve P, Devaux I, Scoazec JY, Berthier M, Loiseau MN, Grandchamp B, Bonneau D. Mutation in the iron responsive element of the L ferritin mRNA in a family with dominant hyperferritinaemia and cataract. *Nature Genet* 1995; 11:444–446.
 38. Girelli D, Corrocher R, Bisceglia L, Olivieri O, De Franceschi L, Zelante L, Gasparini P. Molecular basis for the recently described hereditary hyperferritinemia-cataract syndrome: A mutation in the iron-responsive element of ferritin L-subunit gene. *Blood* 1995; 86:4050–4053.
 39. Aguilar-Martinez P, Biron C, Masmejean C, Jeanjean P, Schved JF. A novel mutation in the iron responsive element of ferritin L-subunit gene as a cause for hereditary hyperferritinemia-cataract syndrome. *Blood* 1996; 88:1895.
 40. Martin ME, Fargion S, Brissot P, Pellat B, Beaumont C. A point mutation in the bulge of the iron-responsive element of the L ferritin gene in two families with the hereditary hyperferritinemia-cataract syndrome. *Blood* 1998; 91:319–323.
 41. Mumford AD, Vulliamy T, Lindsay J, Watson A. Hereditary hyperferritinemia-cataract syndrome: Two novel mutations in the L-ferritin iron-responsive element. *Blood* 1998; 91:367–368.
 42. Balas A, Aviles MJ, Garcia-Sanchez F, Vicario JL. Description of a new mutation in the L-ferritin iron-responsive element associated with hereditary hyperferritinemia-cataract syndrome in a Spanish family. *Blood* 1999; 93:4020–4021.
 43. Levi S, Girelli D, Perrone F, Pasti M, Beaumont C, Corrocher R, Albertini A, Arosio P. Analysis of ferritins in lymphoblastoid cell lines and in the lens of subjects with hereditary hyperferritinemia-cataract syndrome. *Blood* 1998; 91:4180–4187.
 44. Hentze MW, Caughman SW, Rouault TA, Barriocanal JG, Dancis A, Harford JB, Klausner RD. Identification of the iron-responsive element for the translational regulation of human ferritin mRNA. *Science* 1987; 238:1570–1573.
 45. Hentze MW, Rouault TA, Caughman SW, Dancis A, Harford JB, Klausner RD. A cis-acting element is necessary and sufficient for translational regulation of human ferritin expression in response to iron. *Proc Natl Acad Sci USA* 1987; 84:6730–6734.
 46. Leibold EA, Munro HN. Characterization and evolution of the expressed rat ferritin light subunit gene and its pseudogene family: Conservation of sequences within non-coding regions of ferritin genes. *J Biol Chem* 1987; 262:7335–7341.
 47. Leibold EA, Munro HN. Cytoplasmic protein binds in vitro to a highly conserved sequence in the 5' untranslated region of ferritin heavy- and light-subunit mRNAs. *Proc Natl Acad Sci USA* 1988; 85:2171–2175.
 48. Rouault TA, Hentze MW, Caughman SW, Harford J, Klausner RD. Binding of a cytosolic protein to the iron-responsive element of human ferritin messenger RNA. *Science* 1988; 241:1207–1210.
 49. Aziz N, Munro HN. Iron regulates ferritin mRNA through a segment of its 5' untranslated region. *Proc Natl Acad Sci USA* 1987; 84:8478–8482.

50. Caughman SW, Hentze MW, Rouault TA, Harford JB, Klausner RD. The iron-responsive element is the single element responsible for iron-dependent translational regulation of ferritin biosynthesis. Evidence for function as the binding site for a translational repressor. *J Biol Chem* 1988; 263:19048–19052.
51. Paraskeva E, Gray NK, Schlager B, Wehr K, Hentze MW. Ribosomal pausing and scanning arrest as mechanisms of translational regulation from cap-distal iron-responsive elements. *Mol Cell Biol* 1999; 19:807–816.
52. Zähringer J, Baliga BS, Munro HN. Novel mechanism for translational control in regulation of ferritin synthesis by iron. *Proc Natl Acad Sci USA* 1976; 73:857–861.
53. Gray NK, Hentz MW. Iron regulatory protein prevents binding of the 43S translation pre-initiation complex to ferritin and delta-ALAS mRNAs. *EMBO J* 1994; 13:3882–3891.
54. Mikulits W, Sauer T, Infante AA, Garcia-Sanz JA, Müllner EW. Structure and function of the iron-responsive element from human ferritin L chain mRNA. *Biochem Biophys Res Commun* 1997; 235:212–216.
55. Muckenthaler M, Gray NK, Hentze MW. IRP-1 binding to ferritin mRNA prevents the recruitment of the small ribosomal subunit by the cap-binding complex eIF4F. *Mol Cell* 1998; 2:383–388.
56. Goossen B, Caughman SW, Harford JB, Klausner RD, Hentze MW. Translational repression by a complex between the iron-responsive element of ferritin mRNA and its specific cytoplasmic binding protein is position-dependent in vivo. *EMBO J* 1990; 9:4127–4133.
57. Goossen B, Hentze MW. Position is the critical determinant for function of iron-responsive elements as translational regulators. *Mol Cell Biol* 1992; 12:1959–1966.
58. Breuer W, Epsztejn S, Cabantchik ZI. Iron acquired from transferrin by K562 cells is delivered into a cytoplasmic pool of chelatable iron(II). *J Biol Chem* 1995; 270:24209–24215.
59. Konijn AM, Glickstein H, Vaisman B, Meyron-Holtz EG, Slotki IN, Cabantchik ZI. The cellular labile iron pool and intracellular ferritin in K562 cells. *Blood* 1999; 94:2128–2134.
60. Seiser C, Posch M, Thompson N, Kühn LC. Effect of transcription inhibitors on the iron-dependent degradation of transferrin receptor mRNA. *J Biol Chem* 1995; 270:29400–29406.
61. Hanson ES, Leibold EA. Regulation of iron regulatory protein 1 during hypoxia and hypoxia/reoxygenation. *J Biol Chem* 1998; 273:7588–7593.
62. Dandekar T, Stripecke R, Gray NK, Goosen B, Constable A, Johansson HE, Hentze MW. Identification of a novel iron-responsive element in murine and human erythroid d-aminolevulinic acid synthase mRNA. *EMBO J* 1991; 10:1903–1909.
63. Zheng L, Kennedy MC, Blondin GA, Beinert H, Zalkin H. Binding of cytosolic aconitase to the iron responsive element of porcine mitochondrial aconitase mRNA. *Arch Biochem Biophys* 1992; 299:356–360.
64. Kim HY, LaVaute T, Iwai K, Klausner RD, Rouault TA. Identification of a conserved and functional iron-responsive element in the 5'-untranslated region of mammalian mitochondrial aconitase. *J Biol Chem* 1996; 271:24226–24230.
65. Kohler SA, Henderson BR, Kühn LC. Succinate dehydrogenase b mRNA of *Drosophila melanogaster* has a functional iron-responsive element in its 5'-untranslated region. *J Biol Chem* 1995; 270:30781–30786.
66. Gray NK, Pantopoulous K, Dandekar T, Ackrell BA, Hentz MW. Translational regulation of mammalian and *Drosophila* citric acid cycle enzymes via iron-responsive elements. *Proc Natl Acad Sci USA* 1996; 93:4925–4930.
67. Cox TC, Bawden MJ, Martin A, May BK. Human erythroid 5-aminolevulinic acid synthase: Promoter analysis and identification of an iron-responsive element in the mRNA. *EMBO J* 1991; 10:1891–1902.

68. Melefors O, Goossen B, Johansson HE, Stripecke R, Gray NK, Hentze MW. Translational control of 5-aminolevulinate synthase in mRNA by iron-responsive elements in erythroid cells. *J Biol Chem* 1993; 268:5974–5978.
69. Bhasker CR, Burgiel G, Neupert B, Emery-Goodman A, Kühn L, May BK. The putative iron-responsive element in the human erythroid 5-aminolevulinate synthase mRNA mediates translational control. *J Biol Chem* 1993; 268:12699–12705.
70. McKie AT, Marciani P, Rolfs A, Brennan K, Wehr K, Barrow D, Miret S, Bomford A, Peters TJ, Farzaneh F, Hediger MA, Hentze MW, Simpson RJ. A novel duodenal iron-regulated transporter, IREG1, implicated in the basolateral transfer of iron to the circulation. *Mol Cell* 2000; 5:299–309.
71. Donovan A, Brownlie A, Zhou Y, Shepard J, Pratt SJ, Moynihan J, Paw BH, Drejer A, Barut B, Zapata A, Law TC, Brugnara C, Lux SE, Pinkus GS, Pinkus JL, Kingsley PD, Palis J, Fleming MD, Andrews NC, Zon LI. Positional cloning of zebrafish ferroportin1 identifies a conserved vertebrate iron exporter. *Nature* 2000; 403:776–781.
72. Abboud S, Haile DJ. A novel mammalian iron-regulated protein involved in intracellular iron metabolism. *J Biol Chem* 2000; 275:19906–19912.
73. Schalinske KL, Chen OS, Eisenstein RS. Iron differentially stimulates translation of mitochondrial aconitase and ferritin mRNAs in mammalian cells. *J Biol Chem* 1998; 273:3740–3746.
74. Chen OS, Schalinske KL, Eisenstein RS. Dietary iron intake modulates the activity of iron regulatory proteins and the abundance of ferritin and mitochondrial aconitase in rat liver. *J Nutr* 1997; 127:238–248.
75. Chen OS, Blemings KP, Schalinske KL, Eisenstein RS. Dietary iron intake rapidly influences iron regulatory proteins, ferritin subunits and mitochondrial aconitase in rat liver. *J Nutr* 1998; 128:525–535.
76. Riddle RD, Yamamoto M, Engel JD. Expression of delta-aminolevulinate synthase in avian cells: Separate genes encode erythroid-specific and nonspecific isozymes. *Proc Natl Acad Sci USA* 1989; 86:792–796.
77. Ponka P. Tissue-specific regulation of iron metabolism and heme synthesis: Distinct control mechanisms in erythroid cells. *Blood* 1997; 89:1–25.
78. Melefors O, Hentze MW. Translational regulation by mRNA/protein interactions in eukaryotic cells: Ferritin and beyond. *Bioessays* 1993; 15:85–90.
79. Ponka P, Lok CN. The transferrin receptor: Role in health and disease. *Int J Biochem Cell Biol* 1999; 31:1111–1137.
80. Pelicci PG, Tabilio A, Thomopoulos P, Titeux M, Vainchenker W, Rochant H, Testa U. Hemin regulates the expression of transferrin receptors in human hematopoietic cell lines. *FEBS Lett* 1982; 145:350–354.
81. Mattia E, Rao K, Shapiro DS, Sussman HH, Klausner RD. Biosynthetic regulation of the human transferrin receptor by desferrioxamine in K562 cells. *J Biol Chem* 1984; 259:2689–2692.
82. Rao K, Harford JB, Rouault T, McClelland A, Ruddle FH, Klausner RD. Transcriptional regulation by iron of the gene for the transferrin receptor. *Mol Cell Biol* 1986; 6:236–240.
83. Owen D, Kühn LC. Noncoding 3' sequences of the transferrin receptor gene are required for mRNA regulation. *EMBO J* 1987; 6:1287–1293.
84. Casey JL, Hentze MW, Koeller DM, Caughman SW, Rouault TA, Klausner RD, Harford JB. Iron-responsive elements: Regulatory RNA sequences that control mRNA levels and translation. *Science* 1988; 240:924–928.
85. Casey JL, Koeller DM, Ramin VC, Klausner RD, Harford JB. Iron regulation of transferrin receptor mRNA levels requires iron-responsive elements and a rapid turnover determinant in the 3' untranslated region of the mRNA. *EMBO J* 1989; 8:3693–3699.

86. Casey JL, Di Jeso B, Rao K, Klausner RD, Harford JB. Two genetic loci participate in the regulation by iron of the gene for the human transferrin receptor. *Proc Natl Acad Sci USA* 1988; 85:1787–1791.
87. Müllner EW, Neupert B, Kühn LC. A specific mRNA binding factor regulates the iron-dependent stability of cytoplasmic transferrin receptor mRNA. *Cell* 1989; 58:373–382.
88. Binder R, Horowitz JA, Basilioni JP, Koeller DM, Klausner RD, Harford JB. Evidence that the pathway of transferrin receptor mRNA degradation involves an endonucleolytic cleavage within the 3' UTR and does not involve poly(A) tail shortening. *EMBO J* 1994; 13:1969–1980.
89. Posch M, Sutterluety H, Skern T, Seiser C. Characterization of the translation-dependent step during iron-regulated decay of transferrin receptor mRNA. *J Biol Chem* 1999; 274:16611–16618.
90. Fleming MD, Trenor CCr, Su MA, Foernzler D, Beier DR, Dietrich WF, Andrews NC. Microcytic anaemia mice have a mutation in Nramp2, a candidate iron transporter gene. *Nature Genet* 1997; 16:383–386.
91. Gunshin H, Mackenzie B, Berger UV, Gunshin Y, Romero MF, Boron WF, Nussberger S, Gollan JL, Hediger MA. Cloning and characterization of a mammalian proton-coupled metal-ion transporter. *Nature* 1997; 388:482–488.
92. Canonne-Hergaux F, Gruenheid S, Ponka P, Gros P. Cellular and subcellular localization of the Nramp2 iron transporter in the intestinal brush border and regulation by dietary iron. *Blood* 1999; 93:4406–4417.
93. Lee PK, Gelbart T, West C, Halloran C, Beutler E. The human Nramp2 gene: Characterization of the gene structure, alternative splicing, promoter region and polymorphisms. *Blood Cells Mol Dis* 1998; 2:199–215.
94. Fleming RE, Migas MC, Zhou XY, Jiang J, Britton RS, Brunt EM, Tomatsu S, Waheed A, Bacon BR, Sly WS. Mechanism of increased iron absorption in murine model of hereditary hemochromatosis: Increased duodenal expression of the iron transporter DMT1. *Proc Natl Acad Sci USA* 1999; 96:3143–3148.
95. Zoller H, Pietrangelo A, Vogel W, Weiss G. Duodenal metal-transporter (DMT-1, NRAMP-2) expression in patients with hereditary haemochromatosis. *Lancet* 1999; 353:2120–2123.
96. Kohler SA, Menotti E, Kühn LC. Molecular cloning of mouse glycolate oxidase. *J Biol Chem* 1999; 274:2401–2407.
97. Kaptain S, Downey WE, Tang C, Philpott C, Haile D, Orloff DG, Harford JB, Rouault TA, Klausner RD. A regulated RNA binding protein also possesses aconitase activity. *Proc Natl Acad Sci USA* 1991; 88:10109–10113.
98. Rouault TA, Stout CD, Kaptain S, Harford JB, Klausner RD. Structural relationship between an iron-regulated RNA-binding protein (IRE-BP) and aconitase: Functional implications. *Cell* 1991; 64:881–883.
99. Hentze MW, Argos P. Homology between IRE-BP, a regulatory RNA-binding protein, aconitase, and isopropylmalate isomerase. *Nucleic Acids Res* 1991; 19:1739–1740.
100. Haile DJ, Rouault TA, Tang CK, Chin J, Harford JB, Klausner RD. Reciprocal control of RNA-binding and aconitase activity in the regulation of the iron-responsive element binding protein: Role of the iron-sulfur cluster. *Proc Natl Acad Sci USA* 1992; 89: 7536–7540.
101. Kennedy MC, Mende-Mueller L, Blondin GA, Beinert H. Purification and characterization of cytosolic aconitase from beef liver and its relationship to the iron-responsive element binding protein. *Proc Natl Acad Sci USA* 1992; 89:11730–11734.
102. Hirling H, Emery-Goodman A, Thompson N, Neupert B, Seiser C, Kühn LC. Expression of active iron regulatory factor from a full-length human cDNA by in vitro transcription/translation. *Nucleic Acids Res* 1992; 20:33–39.

103. Emery-Goodman A, Hirling H, Scarpellino L, Henderson B, Kühn LC. Iron regulatory factor expressed from recombinant baculovirus: conversion between the RNA-binding apoprotein and Fe-S cluster containing aconitase. *Nucleic Acids Res* 1993; 21:1457–1461.
104. Kaptain S, Downey WE, Tang C, Philpott C, Haile D, Orloff DG, Harford JB, Rouault TA, Klausner RD. A regulated RNA binding protein also possesses aconitase activity. *Proc Natl Acad Sci USA* 1991; 88:10109–10113.
105. Tang CK, Chin J, Harford JB, Klausner RD, Rouault TA. Iron regulates the activity of the iron-responsive element binding protein without changing its rate of synthesis or degradation. *J Biol Chem* 1992; 267:24466–24470.
106. Yu Y, Radisky E, Leibold EA. The iron-responsive element binding protein. Purification, cloning, and regulation in rat liver. *J Biol Chem* 1992; 267:19005–19010.
107. Robbins AH, Stout CD. The structure of aconitase. *Proteins* 1989; 5:289–312.
108. Robbins AH, Stout CD. Structure of activated aconitase: Formation of the [4Fe-4S] cluster in the crystal. *Proc Natl Acad Sci USA* 1989; 86:3639–3643.
109. Gruer MJ, Artymiuk PJ, Guest JR. The aconitase family: Three structural variations on a common theme. *Trends Biochem Sci* 1997; 22:3–6.
110. Beinert H, Holm RH, Munck E. Iron-sulfur clusters: Nature's modular, multipurpose structures. *Science* 1997; 277:653–659.
111. Philpott CC, Haile D, Rouault TA, Klausner RD. Modification of a free Fe-S cluster cysteine residue in the active iron-responsive element-binding protein prevents RNA binding. *J Biol Chem* 1993; 268:17655–17658.
112. Hirling H, Henderson BR, Kühn LC. Mutational analysis of the [4Fe-4S]-cluster converting iron regulatory factor from its RNA-binding form to cytoplasmic aconitase. *EMBO J* 1994; 13:453–461.
113. Philpott CC, Klausner RD, Rouault TA. The bifunctional iron-responsive element binding protein/cytosolic aconitase: The role of active-site residues in ligand binding and regulation. *Proc Natl Acad Sci USA* 1994; 91:7321–7325.
114. DeRusso PA, Philpott CC, Iwai K, Mostowski HS, Klausner RD, Rouault TA. Expression of a constitutive mutant of iron regulatory protein 1 abolishes iron homeostasis in mammalian cells. *J Biol Chem* 1995; 270:15451–15454.
115. Basilion JP, Rouault TA, Massinople CM, Klausner RD, Burgess WH. The iron-responsive element binding protein: Localization of the RNA-binding site to the aconitase active-site cleft. *Proc Natl Acad Sci USA* 1994; 91:574–578.
116. Swenson GR, Walden WE. Localization of an RNA-binding element of the iron responsive element binding protein within a proteolytic fragment containing iron coordination ligands. *Nucleic Acids Res* 1994; 22:2627–2633.
117. Neupert B, Menotti E, Kühn LC. A novel method to identify nucleic acid binding sites in proteins by scanning mutagenesis: application to iron regulatory protein. *Nucleic Acids Res* 1995; 23:2579–2583.
118. Basilion JP, Rouault TA, Massinople CM, Klausner RD, Burgess WH. The iron-responsive element-binding protein: Localization of the RNA-binding site to the aconitase active-site cleft. *Proc Natl Acad Sci USA* 1994; 91:574–578.
119. Lauble H, Kennedy MC, Beinert H, Stout CD. Crystal structures of aconitase with isocitrate and nitroisocitrate bound. *Biochemistry* 1992; 31:2735–2748.
120. Kaldy P, Menotti E, Moret R, Kühn LC. Identification of RNA-binding surfaces in iron regulatory protein-1. *EMBO J* 1999; 18:6073–6083.
121. Schalinske KL, Anderson SA, Tuazon PT, Chen OS, Kennedy MC, Eisenstein RS. The iron-sulfur cluster of iron regulatory protein 1 modulates the accessibility of RNA binding and phosphorylation sites. *Biochemistry* 1997; 36:3950–3958.
122. Gegout V, Schlegl J, Schlager B, Hentze MW, Reinbolt J, Ehresmann B, Ehresmann C, Romby P. Ligand-induced structural alterations in human iron regulatory protein-1 revealed by protein footprinting. *J Biol Chem* 1999; 274:15052–15058.

123. Eisenstein RS, Tuazon PT, Schalinske KL, Anderson SA, Traugh JA. Iron responsive element binding protein: Phosphorylation by protein kinase C. *J Biol Chem* 1993; 268: 27363–27370.
124. Schalinske KL, Eisenstein RS. Phosphorylation and activation of both iron regulatory proteins 1 and 2 in HL-60 cells. *J Biol Chem* 1996; 271:7168–7176.
125. Brown NM, Anderson SA, Steffen DW, Carpenter TB, Kennedy MC, Walden WE, Eisenstein RS. Novel role of phosphorylation in Fe-S cluster stability revealed by phosphomimetic mutations at Ser-138 of iron regulatory protein 1. *Proc Natl Acad Sci USA* 1998; 95:15235–15240.
126. Hanson ES, Foot LM, Leibold EA. Hypoxia post-translationally activates iron regulatory protein 2. *J Biol Chem* 1999; 274:5047–5052.
127. Hanson ES, Leibold EA. Regulation of the iron regulatory proteins by reactive nitrogen and oxygen species. *Gene Expr* 1999; 7:367–376.
128. Tacchini L, Bianchi L, Bernelli-Zazzera A, Cairo G. Transferrin receptor induction by hypoxia. HIF-1-mediated transcriptional activation and cell-specific post-transcriptional regulation. *J Biol Chem* 1999; 274:24142–24146.
129. Toth I, Yuan L, Rogers JT, Boyce H, Bridges KR. Hypoxia alters iron-regulatory protein-1 binding capacity and modulates cellular iron homeostasis in human hepatoma and erythroleukemia cells. *J Biol Chem* 1999; 274:4467–4473.
130. Lill R, Diekert K, Kaut A, Lange H, Pelzer W, Prohl C, Kispal G. The essential role of mitochondria in the biogenesis of cellular iron-sulfur proteins. *J Biol Chem* 1999; 274:1157–1166.
131. Kispal G, Csere P, Prohl C, Lill R. The mitochondrial proteins Atm1p and Nfs1p are essential for biogenesis of cytosolic Fe/S proteins. *EMBO J* 1999; 18:3981–3989.
132. Li J, Kogan M, Knight SA, Pain D, Dancis A. Yeast mitochondrial protein, Nfs1p, coordinately regulates iron-sulfur cluster proteins, cellular iron uptake, and iron distribution. *J Biol Chem* 1999; 274:33025–33034.
133. Strain J, Lorenz CR, Bode J, Garland S, Smolen GA, Ta DT, Vickery LE, Culotta VC. Suppressors of superoxide dismutase (SOD1) deficiency in *Saccharomyces cerevisiae*. Identification of proteins predicted to mediate iron-sulfur cluster assembly. *J Biol Chem* 1998; 273:31138–31144.
134. Lange H, Kispal G, Kaut A, Lill R. A mitochondrial ferredoxin is essential for biogenesis of cellular iron-sulfur proteins. *Proc Natl Acad Sci USA* 2000; 97:1050–1055.
135. Kaut A, Lange H, Diekert K, Kispal G, Lill R. Isa1p is a component of the mitochondrial machinery for maturation of cellular iron-sulfur proteins and requires conserved cysteine residues for function. *J Biol Chem* 2000; 275:15955–15961.
136. Jensen LT, Culotta VC. Role of *Saccharomyces cerevisiae* ISA1 and ISA2 in iron homeostasis. *Mol Cell Biol* 2000; 20:3918–3927.
137. Land T, Rouault TA. Targeting of a human iron-sulfur cluster assembly enzyme, nifs, to different subcellular compartments is regulated through alternative AUG utilization. *Mol Cell* 1998; 6:807–815.
138. Csere P, Lill R, Kispal R. Identification of a human mitochondrial ABC transporter, the functional orthologue of yeast Atmp1. *FEBS Lett* 1998; 441:266–270.
139. Allikmets R, Raskind WH, Hutchinson A, Schueck ND, Dean M, Koeller DM. Mutation of a putative mitochondrial iron transporter gene (ABC7) in X-linked sideroblastic anemia and ataxia (XLSA/A). *Hum Mol Genet* 1999; 8:743–749.
140. Frishman D, Hentze MW. Conservation of aconitase residues revealed by multiple sequence analysis. Implications for structure/function relationships. *Eur J Biochem* 1996; 239:197–200.
141. Guo B, Yu Y, Leibold EA. Iron regulates cytoplasmic levels of a novel iron-responsive element binding protein without aconitase activity. *J Biol Chem* 1994; 269:24252–24260.

142. Samaniego F, Chin J, Iwai K, Rouault TA, Klausner RD. Molecular characterization of a second iron-responsive element binding protein, iron regulatory protein 2. Structure, function, and post-translational regulation. *J Biol Chem* 1994; 269:30904–30910.
143. Iwai K, Drake SK, Wehr NB, Weissman AM, LaVaute T, Minato N, Klausner RD, Levine RL, Rouault TA. Iron-dependent oxidation, ubiquitination, and degradation of iron regulatory protein 2: Implications for degradation of oxidized proteins. *Proc Natl Acad Sci USA* 1998; 95:4924–4928.
144. Iwai K, Klausner RD, Rouault TA. Requirements for iron-regulated degradation of the RNA binding protein, iron regulatory protein 2. *EMBO J* 1995; 14:5350–5357.
145. Bouton C, Raveau M, Drapier J. Modulation of iron regulatory protein functions. Further insights into the role of nitrogen- and oxygen-derived reactive species. *J Biol Chem* 1996; 271:2300–2306.
146. Recalcati S, Taramelli D, Conte D, Cairo G. Nitric oxide-mediated induction of ferritin synthesis in J774 macrophages by inflammatory cytokines: Role of selective iron regulatory protein-2 downregulation. *Blood* 1998; 91:1059–1066.
147. Bouton C, Oliveira L, Drapier J. Converse modulation of IRP1 and IRP2 by immunological stimuli in murine RAW 264.7 macrophages. *J Biol Chem* 1998; 273:9403–9408.
148. Kim S, Ponka P. Control of transferrin receptor expression via nitric oxide-mediated modulation of iron-regulatory protein 2. *J Biol Chem* 1999; 274:33035–33042.
149. Bouton C. Nitrosative and oxidative modulation of iron regulatory proteins. *Cell Mol Life Sci* 1999; 55:1043–1053.
150. Kim S, Ponka P. Effects of interferon-gamma and lipopolysaccharide on macrophage iron metabolism are mediated by nitric oxide-induced degradation of iron regulatory protein 2. *J Biol Chem* 2000; 275:6220–6226.
151. Wu KJ, Polack A, Dalla-Favera R. Coordinated regulation of iron-controlling genes, H-ferritin and IRP2, by c-MYC. *Science* 1999; 283:676–679.
152. Flint DH, Tuminello JF, Emptage MH. The inactivation of Fe-S cluster containing hydro-lyases by superoxide. *J Biol Chem* 1993; 268:22369–22376.
153. Hausladen A, Fridovich I. Superoxide and peroxynitrite inactivate aconitases, but nitric oxide does not. *J Biol Chem* 1994; 269:29405–29408.
154. Brazzolotto X, Gaillard J, Pantopoulos K, Hentze MW, Moulis JM. Human cytoplasmic aconitase (iron regulatory protein 1) is converted into its [3Fe-4S] form by hydrogen peroxide in vitro but is not activated for iron-responsive element binding. *J Biol Chem* 1999; 274:21625–21630.
155. Gehring NH, Hentze MW, Pantopoulos K. Inactivation of both RNA binding and aconitase activities of iron regulatory protein-1 by quinone-induced oxidative stress. *J Biol Chem* 1999; 274:6219–6225.
156. Pantopoulos K, Hentze MW. Rapid responses to oxidative stress mediated by iron regulatory protein. *EMBO J* 1995; 14:2917–2924.
157. Martins EA, Robalinho RL, Meneghini R. Oxidative stress induces activation of a cytosolic protein responsible for control of iron uptake. *Arch Biochem Biophys* 1995; 316:128–134.
158. Pantopoulos K, Weiss G, Hentze MW. Nitric oxide and oxidative stress (H₂O₂) control mammalian iron metabolism by different pathways. *Mol Cell Biol* 1996; 16:3781–3788.
159. Pantopoulos K, Hentze MW. Activation of iron regulatory protein-1 by oxidative stress in vitro. *Proc Natl Acad Sci USA* 1998; 95:10559–10563.
160. Pantopoulos K, Mueller S, Atzberger A, Ansorge W, Stremmel W, Hentze MW. Differences in the regulation of iron regulatory protein-1 (IRP-1) by extra- and intracellular oxidative stress. *J Biol Chem* 1997; 272:9802–9808.

161. Hentze MW. Letter-iron-sulfur clusters as biosensors of oxidants and iron. *TIBS* 1996; 248:282–283.
162. Stamler JS, Singel DJ, Loscalzo J. Biochemistry of nitric oxide and its redox-activated forms. *Science* 1992; 258:1898–1902.
163. Stamler JS. Redox signaling: Nitrosylation and related target interactions of nitric oxide. *Cell* 1994; 78:931–936.
164. Stadler J, Billiar TR, Curran RD, Stueher DJ, Ochoa JB, Simmons RL. Effect of exogenous and endogenous nitric oxide on mitochondrial respiration of rat hepatocytes. *Am J Physiol* 1991; 260:C910–C916.
165. Drapier JC, Hirling H, Wietzerbin J, Kaldy P, Kühn LC. Biosynthesis of nitric oxide activates iron regulatory factor in macrophages. *EMBO J* 1993; 12:3643–3649.
166. Oliveira L, Bouton C, Drapier J-C. Thioredoxin activation of iron regulatory proteins. *J Biol Chem* 1999; 274:516–521.
167. Gardner PR, Costantino G, Szabo C, Salzman AL. Nitric oxide sensitivity of the aconitases. *J Biol Chem* 1997; 272:25071–25076.
168. Kennedy MC, Antholine WE, Beinert H. An EPR investigation of the products of the reaction of cytosolic and mitochondrial aconitases with nitric oxide. *J Biol Chem* 1997; 272:20340–20347.
169. Weiss G, Goossen B, Doppler W, Fuchs D, Pantopoulos K, Werner-Felmayer G, Wächter H, Hentze MW. Translational regulation via iron-responsive elements by the nitric oxide/NO-synthase pathway. *EMBO J* 1993; 12:3651–3657.
170. Weiss G, Bogdan C, Hentze MW. Pathways for the regulation of macrophage iron metabolism by the anti-inflammatory cytokines IL-4 and IL-13. *J Immunol* 1997; 158: 420–425.
171. Mulero V, Brock JH. Regulation of iron metabolism in murine J774 macrophages: Role of nitric oxide-dependent and -independent pathways following activation with gamma interferon and lipopolysaccharide. *Blood* 1999; 94:2383–2389.
172. Phillips JD, Guo B, Yu Y, Brown FM, Leibold EA. Differential regulation of iron-regulatory proteins 1 and 2 by nitric oxide in hepatoma cells. *Blood* 1996; 50:1–10.
173. Pantopoulos K, Hentze MW. Nitric oxide signaling to iron regulatory protein: Direct control of ferritin mRNA translation and transferrin receptor mRNA stability in transfected fibroblasts. *Proc Natl Acad Sci USA* 1995; 92:1267–1271.
174. Richardson DR, Neumannova V, Nagy E, Ponka P. The effect of redox-related species of nitrogen monoxide on transferrin and iron uptake and cellular proliferation of erythroleukemia (K562) cells. *Blood* 1995; in press.
175. Rolfs A, Kvietikova I, Gassmann M, Wenger RH. Oxygen-regulated transferrin expression is mediated by hypoxia-inducible factor-1. *J Biol Chem* 1997; 272:20055–20062.
176. Kaur C, Ling EA. Increased expression of transferrin receptors and iron in amoeboid microglial cells in postnatal rats following an exposure to hypoxia. *Neurosci Lett* 1999; 262:183–186.
177. Lok CN, Ponka P. Identification of a hypoxia response element in the transferrin receptor gene. *J Biol Chem* 1999; 274:24147–24152.
178. Bianchi L, Tacchini L, Cairo G. HIF-1-mediated activation of transferrin receptor gene transcription by iron chelation. *Nucleic Acids Res* 1999; 27:4223–4227.
179. Dore-Duffy P, Balabanov R, Beaumont T, Hritz MA, Harik SI, LaManna JC. Endothelial activation following prolonged hypobaric hypoxia. *Microvasc Res* 1999; 57:75–85.
180. Mukhopadhyay CK, Mazumder B, Fox PL. Role of hypoxia inducible factor-1 in transcriptional activation of ceruloplasmin by iron deficiency. *J Biol Chem* 2000; 275: 21048–21054.

181. Semenza GL. HIF-1: Mediator of physiological and pathophysiological responses to hypoxia. *J Appl Physiol* 2000; 88:1474–1480.
182. Semenza GL. Perspectives on oxygen sensing. *Cell* 1999; 98:281–284.
183. Chandel NS, Schumacker PT. Cellular oxygen sensing by mitochondria: Old questions, new insight. *J Appl Physiol* 2000; 88:1880–1889.
184. Salceda S, Caro J. Hypoxia-inducible factor 1alpha (HIF-1alpha) protein is rapidly degraded by the ubiquitin-proteasome system under normoxic conditions. Its stabilization by hypoxia depends on redox-induced changes. *J Biol Chem* 1997; 272:22642–22647.
185. Huang LE, Gu J, Schau M, Bunn HF. Regulation of hypoxia-inducible factor 1alpha is mediated by an O₂-dependent degradation domain via the ubiquitin-proteasome pathway. *Proc Natl Acad Sci USA* 1998; 95:7987–7992.
186. Kallio PJ, Wilson WJ, O'Brien S, Makino Y, Poellinger L. Regulation of the hypoxia-inducible transcription factor 1alpha by the ubiquitin-proteasome pathway. *J Biol Chem* 1999; 274:6519–6525.
187. Guo B, Phillips JD, Yu Y, Leibold EA. Iron regulates the intracellular degradation of iron-regulatory protein 2 by the proteasome. *J Biol Chem* 1995; 270:21645–21651.
188. Wang GL, Semenza GL. Desferrioxamine induces erythropoietin expression and hypoxia-inducible factor 1 DNA-binding activity: Implications for models of hypoxia signal transduction. *Blood* 1993; 82:3610–3615.
189. Wang GL, Semenza GL. Purification and characterization of hypoxia-inducible factor 1. *J Biol Chem* 1995; 270:1230–1237.
190. Goldberg MA, Dunning SP, Bunn HF. Regulation of the erythropoietin gene: Evidence that the oxygen sensor is a heme protein. *Science* 1988; 242:1412–1415.
191. Ebert BL, Bunn HF. Regulation of the erythropoietin gene. *Blood* 1999; 94:1864–1877.
192. Maxwell PH, Wiesener MS, Chang GW, Clifford SC, Vaux EC, Cockman ME, Wykoff CC, Pugh CW, Maher ER, Ratcliffe PJ. The tumour suppressor protein VHL targets hypoxia-inducible factors for oxygen-dependent proteolysis. *Nature* 1999; 399:271–527.
193. Cockman ME, Masson N, Mole DR, Jaakkola P, Chang GW, Clifford SC, Maher ER, Pugh CW, Ratcliffe PJ, Maxwell PH. Hypoxia inducible factor-alpha binding and ubiquitylation by the von Hippel-Lindau tumor suppressor protein. *J Biol Chem* 2000; 275:25733–25741.

10

Iron-Response Element (IRE) Structure and Combinatorial RNA Regulation

HANS E. JOHANSSON

*Children's Hospital Oakland Research Institute, Oakland, California, and
Uppsala University, Uppsala, Sweden*

ELIZABETH C. THEIL

Children's Hospital Oakland Research Institute, Oakland, California

I. INTRODUCTION	237
II. PRIMARY STRUCTURE AND EVOLUTION OF IREs	238
III. SECONDARY IRE STRUCTURE—PAIRED AND UNPAIRED BASES	246
IV. TERTIARY IRE STRUCTURE—ISO-IRE LOOPS AND BULGES	246
V. PERSPECTIVE	249
ACKNOWLEDGMENTS	249
REFERENCES	249

I. INTRODUCTION

Combinatorial regulation is the use of multiple, related DNA/RNA elements with multiple recognition proteins to produce coordinated, differential control of gene expression. Two examples of combinatorial DNA regulation are known, and one is well characterized for RNA. In the first, a set of DNA promoters recognized by

glucocorticoid or thyroid hormone receptor and transcription factors combine for variable responses to hormones (1,2). In the second, a set of cell-specific REST proteins, created with different combinations of six enhancers, two repressors, and three promoters, differentially recognize the DNA neuron-restrictive silencer element (NRSE) to control differentiation and activity of neural cells (3). In the case of RNA, the best-characterized example of combinatorial regulation is the set of iso-IRE/iso-IRP interactions (recent reviews on IREs and IRPs include Refs. 4–10; see also Chapter 9). An emerging set of combinatorial interactions appears to be the differentiation control elements (DICE) in mRNAs encoding α -globin, and two lipoxygenases which recognize hnRNP proteins E1 and K to control the synthesis of the proteins at different stages of red cell maturation (11). Iron-responsive elements (IREs) are multiple, structurally related, noncoding sequences in a number of metabolically connected mRNAs which combine with IRE recognition proteins (IRPs, or iron-regulatory proteins) to produce a range of responses to iron, and possibly other (oxygen, anoxia, cytokines, nitric oxide) signals.

IREs have been found, to date, in mRNAs encoding both BioIRON and BioOXYGEN proteins. The BioIRON proteins are ferritin, transferrin receptor (TfR), DMT-1 (divalent metal transporter-1), and ferroportin1/Ireg1 (iron exporter). The BioOXYGEN proteins are m-aconitase, succinate dehydrogenase (both tricarboxylic acid cycle proteins), and erythroid cell aminolevulinic acid synthase (heme synthesis). The conservation between species for an IRE sequence in a particular mRNA is much higher (>95%) than for IRE sequences in the different IRE-containing mRNAs of the same species, where the sequence conservation varies from 36% to 80%. The isoforms of IREs found in different mRNAs show a range of responses to iron *in vivo* (12,13) and different interactions with one of the iso-IRP proteins, IRP2, *in vitro* (14). IREs act *in cis* together with iron regulatory proteins (IRPs) to confer iron-dependent regulation of the posttranscriptional fate of the host mRNA. This means that although there are numerous IRE-like sequences throughout the transcribed part of metazoan genomes, only those IRE sequences that do affect posttranscriptional processing, transport, translation, mRNA localization, or mRNA stability would be considered bona-fide IREs. Thus far, functional IREs that regulate translation and mRNA stability have been reported, while the functions of two newer candidate IREs (ferroportin-1 and DMT-1) remain to be clarified.

Here we will describe the IRE structural features that are shared among members of the iso-IRE family, as well as features that are specific to each member. Evolutionary and thermodynamic aspects are incorporated to help describe the structural variation of IREs.

II. PRIMARY STRUCTURE AND EVOLUTION OF IREs

Iso-IREs are defined as sequences of 25–30 nucleotides with a central pentamer, CAGUG, a conserved C five bases upstream of the C of the conserved CAGUG, and complementary sequences flanking the conserved C and CAGUG. The remarkable conservation of sequence among groups is apparent from the comparisons in Table 1. The specificity of an iso-IRE combines location in the 5' or 3' untranslated region (UTR) of its host mRNA, primary structure variation, and the incorporation of additional functions such as mRNA instability elements in the TfR mRNA and dual-level translational control elements in ferritin mRNAs (15). Iso-IRE specificity

leads to differential binding of IRP(s), which in turn allows IRE–IRP combinatorial regulation depending on the external stimulus that changes the RNA-binding status of IRP(s).

The minimal IRE sequence was first derived from phylogenetic and mutagenic analysis, primarily of ferritin and TfR IREs (16). Excluding the ferritin IREs from all animals but insects, it may be summarized as 5'-NNNNN C NNNNN CAGUGH N'N'N'N'N' N'N'N'N'N'-3' (N and N' are complementary nucleotides according to RNA base-pairing rules, and H is not G). The primary structure of noninsect ferritin IREs, 5'-NNNNN YGC NNNNN CAGUGH N'N'N'N'N' C N'N'N'N'N'-3', is very similar and differs only in the four nucleotides around the first conserved C.

Specific IRE–IRP complexes can form *in vitro* using an IRE trimmed to 21 nucleotides (17), whereas full-size IREs are required for full functionality *in vivo*. Several researchers have embarked on the active search for new and old iso-IREs using a variety of biochemical, genetic, and computational methods. The list presented in Table 1 summarizes the available sequences of IREs known, or at least strongly suggested, to act together with one or both IRPs to regulate the posttranscriptional fate(s) of the mRNAs in which they reside.

The IRE–IRP system arose early in metazoan evolution and may today be found in animals from nematodes to mammals. Recent studies in prokaryotes have revealed the presence of IRE-like sequences recognized by *Bacillus subtilis* aconitase (18). For a discussion of protein (IRP) evolution, see Refs. 19–21 and Chapter 9.

Ferritins are widely distributed in all kingdoms, but vertebrate ferritins differ from those in invertebrates, plants, and bacteria by having multiple genes that encode two protein subunit types: H, which is common to all ferritins; and L, which lacks an active catalytic site. In animals and plants, ferritins carry out unique and overlapping functions of iron concentration and storage, iron transport, and innate immunity. Ferritin mRNAs seem to have been equipped with IREs concomitant with the emergence of metazoans. IREs are absent in plant ferritin mRNA (23). In addition, the IRE in a plant–animal mRNA chimera functions poorly (22,23). Plant ferritin mRNA encodes an N-terminus protein sequence to target ferritin to plastids (22). IREs in ferritin mRNAs have been identified in the nematode *Brugia malayi*, arthropods [the ticks *Boophilus microplus*, *Ixodes ricinus*, and *Ornithodoros moubata* (24)], the crustacean signal crayfish *Pacifastacus leniusculus* (25), and insects such as the fruitfly *Drosophila melanogaster* (26–28), mosquito *Aedes aegypti* (29), and silkworm *Bombyx mori* [unpublished], echinodermata [starfish *Asterias forbesii* (29) and sea urchin *Strongylo-centrotus purpuratus* (both unpublished sequences)], and several vertebrates. The analyzed ferritin mRNAs of kinetoplastids (*Trypanosoma*), apicomplexa (*Plasmodium*), platyhelminthes (flatworms, *Schistosoma*) and the nematode *Caenorhabditis elegans*, however, lack IREs (30,31). This possibly reflects the use of trans-splicing to generate the mature mRNA 5' ends in these organisms. A non-ferritin, IRE-hybridizable sequence has been detected in soybean DNA (Ragland and Theil, unpublished observations). Only one out of three ferritin mRNAs in fruitfly (ferritin 1) contains an IRE that, in addition, is subject to tissue specific splicing (27,28). In contrast, all H-ferritin mRNAs have IREs, as do fish and amphibian M-ferritin mRNAs as well as mammalian L-ferritin mRNAs. All ferritin iso-IREs, except those of insects, have three additional conserved nucleotides. The conserved C that is isolated in the other IREs is, in vertebrate ferritin IRE, preceded by a con-

Table 1 Primary Structure of Iron-Responsive Elements^a

Species	mRNA	Sequence	Accession #/Reference #
5' UTR			
Mitochondrial aconitase			
<i>H. sapiens</i>	mt aconitase	CCUCAU C UUUGU CAGUGC ACAA AUGGCG	U80040, U87926, AF086788, AL021877
<i>B. taurus</i>	mt aconitase	CCUCAU C UUUGU CAGUGC ACAA AUGGCG	Z49931
<i>M. musculus</i>	mt aconitase	CCUCAU C UUUGU CAGUGC ACAA AUGGCG	Z78147, AI037103
<i>R. norvegicus</i>	mt aconitase	----- C UUUGU CAGUGC ACAA AUGGCG	AI235320
<i>S. scrofa</i>	mt aconitase	CCUCAU C UUUGU CAGUGC ACAA AUGGCG	J05224
<i>D. rerio</i>	mt aconitase	---CAU C UUUGU CAGUGA ACAA AUGGCG	AI722265
<i>X. laevis</i>	mt aconitase	----- - ---GU CAGUGA ACAA AUGGCG	AF186471
Erythroid aminolevulinatase synthase			
<i>H. sapiens</i>	e-ALAS	AUUCGUU C GUCCU CAGUGC AGGGC AACAGGU	X56352, X60364, AF068624, AL020991
<i>D. leucas</i>	e-ALAS	UUCGUU C GUCCU CAGUGC AGGUC AACAGA	AF086786
<i>M. musculus</i>	e-ALAS	UUGGUU C GUCCU CAGUGC AGGGC AACAGG	L08247, L08248, M15268, M63244
<i>R. norvegicus</i>	e-ALSA	----- - -----G	D86297
<i>G. gallus</i>	e-ALAS	GUGCUU C GUCCU CAGGGC GGGGC AACGGC	S57264, S69605
<i>D. rerio</i>	e-ALAS	GAAGUU C GUCCU CAGUGC AGGUC AACAGC	AF095747
<i>D. rerio</i>	e-ALAS	UCUCGUU C GUCCU CAGUGC AGGAU AACGACG	AW133872
<i>O. tau</i>	e-ALAS	--ACGUU C GUCCU CAGUGC AGGUC AACGAG	L02632
<i>O. tau</i>	h-ALAS	----- - ----- CAGUGC AGGAU AACGUC	L35915
Succinate dehydrogenase iron-sulfur protein			
<i>D. melanogaster</i>	SDH-1p	CGAUAAUUG C AAACG CAGUGC CGUUU CAUUGCAG	L27705
Vertebrate H- and M-ferritins			
<i>H. sapiens</i>	H-ferritin	GGGUUCC UGC UUCA CAGUGC UUGGA C GGAACCC	M18522, M14211
<i>B. taurus</i>	H-ferritin	GGUUUCC UGC UUCA CAGUGC UUGAA C GGAACC	AB003093, AW358499
<i>C. griseus</i>	H-ferritin	GGUUUCC UGC UUCA CAGUGC UUGAA C GGAACC	M99692, M89809
<i>M. musculus</i>	H-ferritin	GGUUUCC UGC UUCA CAGUGC UUGAA C GGAACC	X52561, X15404, X15405
<i>R. norvegicus</i>	H-ferritin	GGUUUCC UGC UUCA CAGUGC UUGAA C GGAACC	M18812, H35408

<i>S. scrofa</i>	H-ferritin	GGUUUC UGC UUCA CAGUGC UUGGA C GGAACCC	D15071
<i>G. gallus</i>	H-ferritin	GCGGGUUC UGC UUCA CAGUGC UUGGA C GGAACCGGC	M16343, Y14698
<i>R. catesbiana</i>	H-ferritin	AGUAGAUUCU UGC UUCA CAGUGU UUGAA C GGAACCCUCU	M12120, M15655
<i>R. catesbiana</i>	M-ferritin	GAGUUCU UGC UUCA CAGUGU UUGAA C GGAACCCUC	J02724, (64)
<i>X. laevis</i>	H-ferritin	GAGAGUUCU UGC UUCA CAGUGU UUGAA C GGAACCCUC	M55010, X51395, S64727
<i>C. carpio</i>	H-ferritin	GGUUACC UGC UUCA CAGUGC UUGAA C GGCAACC	C88364
<i>D. rerio</i>	H-ferritin	GGUUACC UGC UUCA CAGUGC UUGAA C GGCAACC	AA566838
<i>D. rerio</i>	M-ferritin	GAGGUUCU UGC UUCA CAGUGA UUGAA C GGAACUUC	AA566575, AW778401
<i>L. fluviatilis</i>	H-ferritin	-GUUC UGC UUCA CAGUGU UUGAA C GGAACG	(74)
<i>O. mykiss</i>	H1-ferritin	AGUUCU UGU UUCA CAGUGA UUGAA C GGAACU	D86625
<i>O. mykiss</i>	H2-ferritin	AGAAGU UGC UUCA CAGUGA UUGAA C GGAACU	D86626
<i>S. salar</i>	M-ferritin	GAAGUUCU UGC UUCA CAGUGA UUGAA C GGAACUCC	S77386

Mammalian L-ferritins

<i>H. sapiens</i>	L-ferritin	GGGUCUGUCUCU UGC UUCA CAGUGU UUGGA C GGAACAGAUC	Y09188, AC005913, AW966982
<i>B. taurus</i>	L-ferritin	GGAUCUGUCUCU UGC UUCA CAGUGC UUGGA C GGAACAGACC	AW307860, AW357264, AW632261
<i>M. musculus</i>	L-ferritin	GGAUCUGUGUCU UGC UUCA CAGUGU UUGAA C GGAACAGACC	J04716, L39879, AA869535
<i>O. cuniculus</i>	L-ferritin	GGACCUGUGUCU UGC UUCA CAGUGU UUGAA C GGAACAGGCC	X14578, X07830
<i>R. norvegicus</i>	L-ferritin	GGAUCUGUAUCU UGC UUCA CAGUGU UUGGA C GGAACAGACCC	M18812, J02741, C06732
<i>S. scrofa</i>	L-ferritin	GGAUCUGUCUCU UGC UUCA CAGUGU UUGGA C GGAACAGACC	AW347892, AW414939, AW619983

Invertebrate ferritins

<i>A. forbesii</i>	ferritin	UGUUUG UGC GUUCG CAGUGU CGGAA C CAAGCA	AF001984
<i>S. purpuratus</i>	ferritin	CUUG CGC UUUCG CAGUGU CGAAA C CAGG	R61991, R62056, R62084
<i>B. malayi</i>	L-ferritin	AUCUGCGUCC UGC UUCA CAGUGC UUGGA C GGAGCAGAC	N27315, A1105560, A1066024
<i>P. leniusculus</i>	ferritin	UAAGACGCU CGG GUCGC CAGUGU GUGAA C GAGCUCGCC	X90566
<i>B. microplis</i>	ferritin	----- -GCAA CAGUGA UUGAA C GAGCAUCGCC	U92787
<i>I. ricinus</i>	ferritin	UUU UGC UUCA CAGUGA UUGAA C GAGCAUCGCC	AF068224
<i>O. moubata</i>	ferritin	--- -GC UUCA CAGUGU UUGAA C GAGCAUCGCC	AF068225
<i>L. stagnalis</i>	S-ferritin	UGCU UGC UGCGU CAGUGA ACGUA C AGACA	X56778
<i>A. aegypti</i>	ferritin	GUCACCUU C UGUGC CAGUGU GUAUA AAGGUUGAC	L37082

Table 1 Continued

Species	mRNA	Sequence	Accession #/Reference #
<i>B. mori</i>	G-ferritin	GUCGCCUU C UGCGC CAGUGU GUGUA AAGGCAGU	AV399926, AV400149, AV400219
<i>C. ethlius</i>	G-ferritin	CGGCCUU C UGCGC CAGUGU GUGUA AAGGCUG	AF161709
<i>C. ethlius</i>	S-ferritin	GGCCUU C UGCGC CAGUGU GUGUA AAGGCU	AF161707
<i>D. melanogaster</i>	ferritin 1	GCCUU C UGCGC CAGUGU GUGUA AAGGC	Y15630, U91524
<i>M. sexta</i>	ferritin	GCCUU C UGCGC CAGUGU GUGUA AAGGC	L47123
<i>N. lugens</i>	ferritin	GCCUU C UAUAC CAGUGA GUGUA AAGGC	AJ251148
Ferroportin1			
<i>H. sapiens</i>	Fpn1	CUUUGCUUUCCAACUU C AGCUA CAGUGU UAGCU AAGUU U GGAAAGAAGG	AF215636, AF231121, AF226614
<i>M. musculus</i>	Fpn1	GCUUUGGCCUUUCCAACUU C AGCUA CAGUGU UAGCU AAGUU U GGAAAGAAGACAC	AF231120, AF226613
<i>R. norvegicus</i>	Fpn1	GCUUUAGCUUUCCAACUU C AGCUA CAGUGU UAGCU AAGUU U GGAAAGAAGACAC	U76714
<i>D. rerio</i>	Fpn1	UUAUUUCUCUCCGACUU C AGCUA CAGUGA UAGCU AAGUU U GGAGAGGAGAAA	AF22612
Bacterial IREs			
<i>B. subtilis</i>	qoxD (3' UTR)	AAAAAACCCUCUU CAGUGG AAGAGGGUUUUUUGCTGUGC	M86548
<i>B. subtilis</i>	feu (3' & 5' UTR)	CAA ACU AAUU CAGAGUA GGUUUUUG	L19954
3' UTR			
Divalent metal-ion transporter 1			
<i>H. sapiens</i>	DMT1	UGCAGGUAGCCAU C AGAGC CAGUGU GUUUC UAUGGUUUACUG	L37347, AB004857, AB015355, AF064482
<i>M. fascicularis</i>	DMT1	UGCAGGUAGCCAU C AGAGC CAGUGU GUUU- - - - -	AF153280
<i>M. musculus</i>	DMT1	UGCAGGGAGCCAU C AGAGC CAGUGU GUUUC UAUGGUUUACUG	L33415, AF029758
<i>R. norvegicus</i>	DMT1-A	UGCAGGGAGCCAU C AGAGC CAGUGU GUUUC UAUGGUUUACUG	AF008439
<i>R. norvegicus</i>	DMT1-B	UGUAGUAUGUU C GUUUA CAGUGA UAGAC GGUUCCAUUGUA	AF008439

Transferrin receptor

<i>H. sapiens</i>	TfR-A	UUAUUUUAU C AGUGA CAGAGU UCACU AUAAAUGG	M11507, X01060, AF187320
<i>M. musculus</i>	TfR-A	UUAUUUUAU C AGUGA CAGAGU UCACU AUAAAUAG	AA798416, AA656632
<i>R. norvegicus</i>	TfR-A	UUAUUUUAU C AGUGA CAGAGU UCACU AUAAAUAG	M58040
<i>G. gallus</i>	TfR-A	UUAUUUUAU C AGUGA CAGCGU UCACU AUAAAUGG	X13753, X55348
<i>D. rerio</i>	TfR-A	UUAUUUUAU C AGUGA CAGUGU UCACU AUAAAAG	AW454691
<i>H. sapiens</i>	TfR-B	AUAAUUUAU C GGAAG CAGUGC CUUCC AUAAUUAU	M11507, X01060, AF187320
<i>M. musculus</i>	TfR-B	AUAAUUUAU C GGAAG CAGUGC CUUCC AUAAUUUAU	AA656632
<i>R. norvegicus</i>	TfR-B	AUAAUUUAU C GGAAG CAGUGC CUUCC AUAAUUUAU	M58040
<i>G. gallus</i>	TfR-B	AUAAGGAG C GGAAG CAGUGC CUUCC AUAAUUUAU	X13753, X55348
<i>D. rerio</i>	TfR-B	UUAUUUUAU C GGAAG CAGUUC -----	AW454691
<i>H. sapiens</i>	TfR-C	ACAUUAU C GGGAG CAGUGU CUUCC AUAAUGU	M11507, X01060, AF187320
<i>M. musculus</i>	TfR-C	CAUUUAU C GGGAG CAGUGU CUUCC AUAAUG	AA919782, AA896927
<i>R. norvegicus</i>	TfR-C	ACAUUAU C GGGAG CAGUGU CUUCC AUAAUGU	M58040
<i>G. gallus</i>	TfR-C	ACAUUAU C GGGGG CAGUGU CUUCC AUAAUGU	X13753, X55348
<i>X. laevis</i>	TfR-C	CAUUUAU C GGAAG CCGUGU CUUCC AUAAUG	AW637789
<i>H. sapiens</i>	TfR-D	AGUGUAUGUAU C GGAGA CAGUGA UCUCU AUAUGUUACACU	M11507, X01060, AF187320
<i>M. musculus</i>	TfR-D	AGUGUCUAUAU C GGAGA CAGUGA UCUCU AUAUGUUACACU	AA919782, AA896927
<i>N. norvegicus</i>	TfR-D	AGUGUCUAUAU C GGAGA CAGUGA CCUCU AUAUGUUACACU	M58040
<i>G. gallus</i>	TfR-D	AGUGUUUAUAU C GGAGG CAGUGA CCUCU AUAUGUUGCACU	X13753, X55348
<i>X. laevis</i>	TfR-D	UGUGUGUUUAU C GGGGG CAGUGU UCCCU CAUUUACACUA	AW637789
<i>H. sapiens</i>	TfR-E	UAAAGUAAUUUAU C GGGAA CAGUGU UUCCC AUAAUU	M11507, X01060, AF187320
<i>M. musculus</i>	TfR-E	UAAAGUAAUUUAU C GGGAA CAGUGU UUCCC AUAAUUUUUCUUCAU	AA919782, AA896927
<i>R. norvegicus</i>	TfR-E	UAAAGUAAUUUAU C GGGAA CAGUGU UUCCC AUAAUU	M58040, AW914888
<i>G. gallus</i>	TfR-E	GUAUUUAU C GGGGA CAGUGU UUUCU AUAAUUUGU	X13753, X55348
<i>X. laevis</i>	TfR-E	AAUUUAU C GGGGA CAGUGU UUCCC AUAAUU	AW637789

^aShown are the RNA sequences of IREs identified in the 5' UTR of mRNAs for ferritins, succinate dehydrogenase iron protein subunit (SDH-Ip), mitochondrial aconitase, erythroid form of aminolevulinic acid synthase (e-ALAS), ferroportin, and in the 3' UTRs of divalent metal-ion transporter 1 (DMT-1) and transferrin receptor (TfR). Also shown are the RNAs that interact with bacterial aconitase (*B. subtilis* qoxD and feu). Due to space limitations, sequences are referred to either by the GenBank/EMBL accession numbers or, when lacking, the bibliographic reference.

served sequence U/CG. An additional conserved C is found six nucleotides downstream of the final G in the CAGUG (Table 1). The additional conserved bases create a specific protein (IRP2) and metal-binding motif (14,32,33). The ferritin IREs from crayfish (25) and starfish (GenBank: AF0001984) have unusual configurations around the internal loop bulge, but the first still binds IRP, supporting combinatorial IRE–IRP regulation. Ferritin IREs are positioned close to the 5' cap and are flanked by sequences that have retained partial complementarity through evolution.

Two independent solutions to directly couple energy and iron metabolism that involve the IRE–IRP system have been identified in vertebrates and in fruitfly. Vertebrate mRNAs encoding the evolutionarily ancient iron–sulfur cluster protein mitochondrial aconitase (mt-ACON) carry an IRE in the 5' UTR (34) that participates in iron-dependent translational regulation (35,36). Similarly, the 5' UTR IRE in the fruitfly's mRNA encoding the iron protein subunit (Ip) of the ancient succinate dehydrogenase (SDH) also serves to regulate translation in response to iron fluctuations (35,37,38). SDH-Ip and mt-ACON IREs function to repress translation in response to low iron. They are both of the unpaired C class of IREs and the 5' parts are U-rich, possibly to allow rapid helix untwining for efficient translation. However, devoid of flanking sequences, they are less efficient operators than ferritin IREs. The distinct primary structures and the phylogenetic distribution strongly suggest that the IREs arose independently. Further gene sequences of mt-ACON and SDH-Ip will be needed to further our understanding as to when these IRE appeared during metazoan evolution.

Vertebrate mRNAs encoding the erythroid form of the old enzyme 5-aminolevulinate synthase (e-ALAS) possess an IRE in the 5' UTR (34,39). This IRE also seems to have been added as an adapter to modulate the synthesis of e-ALAS in response to varying iron levels (40,41). The hepatic mRNA form for this enzyme (a separate gene) lacks an IRE and is unresponsive to variations in available iron. It appears that the housekeeping and erythroid forms of ALAS arose before the divergence of hagfish from the deuterostome line leading to the vertebrates, and that the addition of an IRE to eALAS mRNAs coincides with the proposed second genome duplication (and gene duplication of ALAS) as the vertebrates split from the chordates (42,43). The ALAS IRE is similar to mt-ACON and SDH-Ip IREs, and confers similar low-level regulation in response to changes in iron availability.

The membrane-bound divalent metal-ion transporter protein, DMT-1/Nramp2, is encoded by a gene that through differential splicing gives rise to two C-terminal protein variants (44–46). An IRE closely downstream of the stop codon in the human mRNA is found only in the mRNA encoding the shorter DMT-1 form. This IRE is conserved within vertebrates and may incorporate features that are important for the reversed posttranscriptional fate of the mRNA in duodenum as compared to that in other tissues (46). In analogy to eALAS, there are two genes encoding similar proteins in mammals, but the second, Nramp1, lacks an IRE and is more widely expressed. The human DMT-1 IRE has been shown to bind IRP *in vitro*, but a proposed function in mRNA stability remains unclear.

The recent cloning of three vertebrate cDNAs and genes for ferroportin (Fpn1/Ireg1/MTP1/Slc39a1) (47–49), an iron transport protein whose expression in duodenum is regulated by iron, revealed the presence of a single 5' UTR IRE close to the cap. It was first suggested that the IRE might be involved in regulation of iron uptake through the duodenum. The functionality of this IRE is supported by the

observation that the human IRE binds IRP (48), and seems to direct translational regulation in liver (49). However, the reciprocal regulation in response to iron in the duodenum remains to be clarified. The Fpn1 IRE is unusually long and possibly incorporates duodenum-specific regulatory elements. No ferroportin-like proteins have been reported for lower animals, although a highly similar open reading frame (GI:3395426) exists in the plant *Arabidopsis thaliana*.

The transferrin receptor (TfR) is ubiquitously expressed in vertebrates in response to iron deprivation. Proteins similar to TfR have been identified in nematodes and plants, which suggests that TfR-like proteins evolved early. However, only in vertebrates has the protein been demonstrated to form complexes with iron-charged transferrin. TfR genes encoding an mRNA with five IREs in the 3' UTR have been identified in several vertebrates. A second TfR gene (TfR2) has been identified in mammals (50,51). TfR2 mRNA expression is restricted to liver and kidney, where TfR2 seems to ensure a steady supply of iron despite bodily iron fluctuations. The TfR2 mRNA lacks IREs and remains stable at high levels of iron. In the TfR iso-IREs, multiple AU-rich sequences occur both within and between the five iso-IREs (52,53). The combined AU-rich sequences place the TfR regulatory element in the class of ARE (AU-rich elements) turnover elements (54) as well as in the IRE class.

The exploration of sequence space has also uncovered a number of IRE-like sequences. Some, such as the pseudo-IRE which resides in the 3' UTR of mouse (AI173821) and rat (AA945123) glycolate oxidase (55), even bind IRPs in vitro under certain conditions, whereas others, such as the 5' UTR of *Toll* mRNA from *D. melanogaster*, do not (34). The functionality of IRE-like structures in the 3' UTR of rabbit IRP1 [M95815, (56)] and at the 3' extreme of rat DMT-1 mRNA (DMT-1 IRE-B in Table 1) also remain to be tested. Transferrin expression varies in response to iron levels, and the apparent IRE-less 5' UTR of human transferrin mRNA has been shown to bind IRP1 weakly (57,58). Lastly, "IRE-like" sequences have been reported in a cytochrome oxidase mRNA and in a linker sequence between two *feu* genes for a polycistronic mRNA encoding iron uptake proteins in *B. subtilis*. The "IREs" either have a central CAGUG but no upstream C or a central CAGAG with the C five nucleotides upstream (Fig. 1). The bacterial "IRE"-binding protein is an aconitase homolog, as are the IRPs, and recognizes both the *B. subtilis* "IREs" and the rabbit ferritin IRE (18). *Escherichia coli* aconitases have similarly been reported to possess RNA-binding activity and act as posttranscriptional gene expression regulators (59,60).

There are several lines of evidence to support the idea that the iso-IREs arose independently of one another. The first is that an old (nematode) ferritin mRNA is substantially much more similar to a new (mammalian) one than the similarly old DMT-1 and eALAS IREs are. Second, although several IREs are found in individual exons that are subject to differential splicing, e.g., *D. melanogaster* ferritin 1 and mammalian DMT-1, there is no evidence for these exons to become associated with other coding sequences than that of the original host gene. Lastly, sequences in the TfR mRNAs (see *Xenopus* TfR-C and all but zebrafish TfR-A IREs in Table 1) may be seen as early variants of IREs such that some IREs display noncanonical features. A variant of the proposed independent origins of the iso-IREs is the proposed fusion between preexisting translation or mRNA-stability elements and the hairpin loop for IRP recognition and coordinated regulation of the IRE-containing mRNAs (61). In-

dependent evolution of IREs is also supported by the observation that in some duplicated genes only one member of the pair contains an IRE as in TfR and eALAS.

III. SECONDARY IRE STRUCTURE—PAIRED AND UNPAIRED BASES

All IRE sequences can be predicted to fold into hairpin loops (Fig. 1). Solution studies have confirmed the hairpin structure for ferritin, TfR, eALAS, and m-aconitase iso-IREs (17,32,62–68). Nuclear magnetic resonance (NMR) spectroscopy has shown that the paired bases in the IRE stem form a typical A helix (32,68).

The terminal loop of the IRE hairpin is always six nucleotides beginning with the invariant sequence CAGUG (Table 1). A CG base pair spans the hexaloop, based on nuclease reactivity, mutagenesis, and NMR spectroscopy (32,62,66,68,69). Substitution of C–G by U–A alters function (14,33,70) and does not occur in nature (Table 1). One full helix turn would be predicted from the number of base pairs generally found in iso-IRE hairpins.

All IREs have a distorted region in the middle of the helix, either a C bulge, a C in a two-nucleotide internal loop (DMT-1), or an internal loop/bulge (IL/B). On the NMR time scale, the IL/B is very dynamic, and the position of the loop relative to the helix in three-dimensional space is not fully understood. The H-ferritin and L-ferritin IREs have a G–C hydrogen bond that spans the IL/C adjacent to the conserved C residue and possibly selecting a favorable conformation of the conserved C (14,32).

The effect of the IL/B on IRE structure and function has been observed in several different ways. First, IL/B increases the distance between two protein cross-linking sites by 4 Å (32). Second, base substitutions or deletions in the internal bulge/bulge region alter protein binding and regulation (14,17,33,53,63,65). The RNA flexibility caused by the helix distortions at the loop/bulge could be important for the “best fit” of the RNA/protein-binding surfaces.

Many iso-IRPs have base-paired regions that flank the IRE and are outside the protein-binding site. For example, only 30 nucleotides of the ferritin IRE were protected by IRP1, using Fe-EDTA/radical cleavage as a probe (71). In addition, a base-paired flanking region of 10–15 base pairs occurs in the ferritin IRE, in which there is also a conserved set of three base pairs one helix turn from the end of the IRP-binding site (64). Other iso-IREs with base-paired flanking regions include TfR-IRE-A and TfR-IRE-B, ferroportin1/Ireg1, DMT-1 (Table 1), and qoxD of *B. subtilis* (18). The function of the flanking regions has been little studied, although it is known that structure around the conserved bases in the flanking region of the ferritin IRE is changed by IRP1 binding (71). Also, mutation of the conserved set of three base pairs weakens translational regulation (64). Genetic support for a second translational control element that flanks the primary structure of the IRE comes from the Pavia-2 mutations in human L-ferritin mRNA that decrease the complementarity of the flanking sequences (72).

IV. TERTIARY IRE STRUCTURE—ISO-IRE LOOPS AND BULGES

The three-dimensional structure of the iso-IREs creates remarkable specificity of protein binding. For example, no stem loops other than the known iso-IREs are

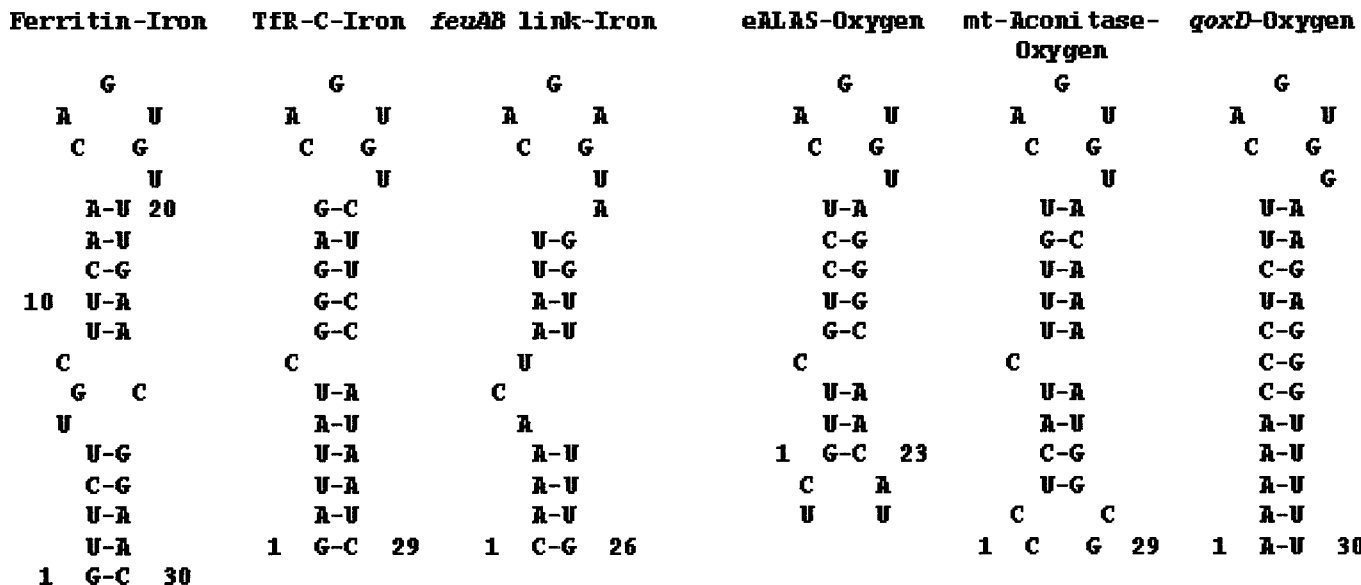


Figure 1 Predicted hairpins for iso IREs from vertebrates and bacteria. Comparisons of the secondary structure were made using sequences from Table 1 and M-fold (GCG version 8.1) and from *B. subtilis* (18). The *B. subtilis* sequences were found using a search for sequences we have copied as the canonical sequence in Table 1. A *B. subtilis* aconitase protein recognizes both the ferritin iso-IRE sequences and the iso-IRE sequences in an iron-dependent fashion (18). Note that ≤ 30 nucleotides are shown, since IRP1 binding “protects” up to 30 nucleotides in free-radical cleavage reactions (71); some iso-IRE sequences have longer base-paired flanking regions such as ferritin, *TFR-A/B*, DMT-1, ferroportin/Ireg1 (Table 1), and *goxD* of *B. subtilis* mRNA.

recognized by the IRPs. Within the IRE hairpin structure, further specificity is revealed by the differential binding of IRP2 and IRP2 in vitro, by binding of the shape selective complex $\text{Cu}(\text{phen})_2$ (33), and by the differential effects of iron on aconitase and ferritin mRNA activity in vivo (12).

Specific features of the C bulge or the internal loop bulge account for some of the structural and functional difference among iso-IREs such as ferritin iso-IRE, which has the internal loop/bulge and a C bulge iso-IRE such as TfR-IRE-C. The ferritin IRE is converted to the TfR-IRE in terms of translational regulation, $\text{Cu}(\text{phen})_2$ binding, and IRP2 binding, simply by deleting one nucleotide from the internal loop/bulge to form a C bulge in its place (14,33).

A pocket is formed in the center of the IRE hairpin by the disordered nucleotides (32,68). In the case of the ferritin IRE, metals such as Co(III) hexamine and Mg hexahydrate bind in the pocket formed by the internal loop/bulge and a widening in the major groove around the internal loop/bulge (32,33) (Fig. 2).

The terminal hairpin loop has, in addition to a base pair, significant base stacking (32,68,69,71). In a hairpin without the internal loop bulge, the hairpin loop would be 4 Å closer to the C bulge than in the ferritin IRE. Interestingly, the two loops in the ferritin IRE appear to be influencing each other, even though they are 22 Å apart, since mutations in one loop affect structure in the other (33).

Mg binding changes the environment in both loops and in the intervening helix, based on ^1H -NMR spectrum and the binding of $\text{Cu}(\text{phen})_2$ (33,62). Such data suggest that there is communication between the loops through the helix, possibly leading

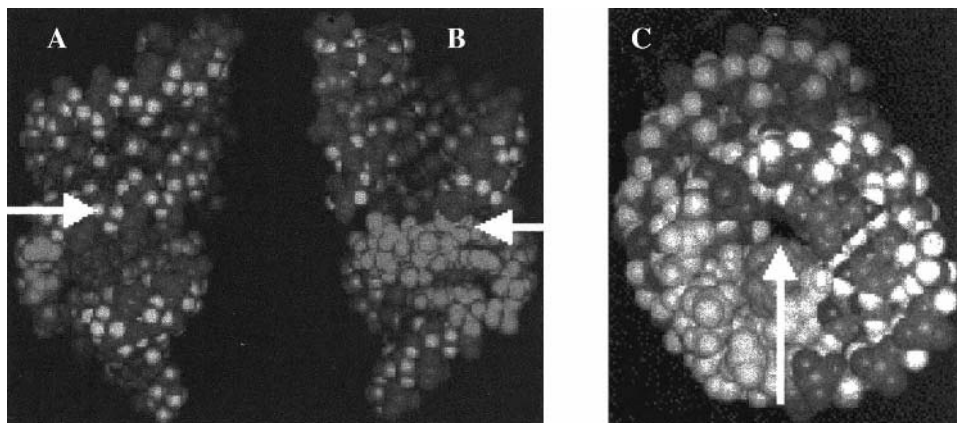


Figure 2 Co(III) hexamine in the pocket formed by the internal loop/bulge of the ferritin iso-IRE. Data from NMR spectroscopy, DOCKING, and MC-SYM were used to construct the model. Co(III) hexamine, indicated by the arrow, has size properties similar to Mg hexahydrate. Co(III) hexamine in the NMR spectrum (^1H) were localized to the internal loop/bulge itself, whereas Mg effects could be observed in the internal/loop bulge as well as the upper helix and the hairpin loop (32,33). After Docking, specific interactions occur between Co(III) hexamine (atom cluster at the arrow point) and G7, G27, G26, U5, U6, and C25 in the pocket of the internal loop/bulge (IL/B) region of the iso-IRE. (The atoms of the IL/B are lighter than the other atoms.) The same bases are affected in the ^1H -NMR spectrum of the IRE with Mg hexahydrate (33), whereas G7 and G27 were the most changed by Co(III) hexamine (32). (A) The view into the major groove. (B) The view into the minor groove. (C) The view from the bottom (5' and 3' termini). (Modified from Ref. 32, with permission.)

to enhanced ability of the binding proteins to induce the “best fit” in the RNA and the high efficiency of repression observed for ferritin mRNA. Among the iso-IREs, the tertiary structure of the ferritin iso-IRE is optimized for the best protein “fit” based on protein binding (33).

A physiological confirmation of the structural information encoded in the ferritin iso-IRE has come from studies of familial hyperferritinemia/cataract syndrome, where altered IRE sequences in human L-ferritin mRNA result in an altered balance between IRP binding and translation (72). The mutations change by base substitution or deletion the structure of the protein-binding site, based on the protein footprint (73). Abnormally high levels of L-ferritin are produced. There is a strong correlation between the type of mutation, the degree of the overexpression of ferritin, and the age of onset of cataracts. Mutations that affect the conserved hairpin loop sequence, CAGUG, or conserved C in the IL/B are associated with the most severe manifestations of the disease, while alterations in the helixes have milder symptoms.

V. PERSPECTIVE

IRE sequences occur in the noncoding region of mRNAs coding for BioIRON and BioOXYGEN proteins and are characterized by mRNA-specific isomeric hairpin loops which share the loop sequence CAGUG and a conserved C in a distorted region of the stem. No IRE in plant ferritin MRNAs has been identified to date, and the absence may relate to the N-terminal extension of plant ferritins with organellar protein targeting sequences. During evolution, the members of the iso-IRE family appear to have arisen independently of each other in bacteria and animals, to add regulatory functionality to preexisting mRNAs, and have since evolved very slowly in concert with IRPs to fine-tune mRNA regulation in a combinatorial manner.

Even with the detailed picture of the IRE structure now available, only a little is known about the protein/RNA interaction, or about the variations in iso-IRE structure that account for the differences in efficiency of iso-IRE function. What is clear is that the iso-IRE family of hairpin loop elements is derived from combinations of helix sequence and distortions selected throughout evolution to create a wide range of mRNA-specific responses to the same environmental signals. The fact that such a combinatorial array of mRNA regulatory elements is limited to BioIRON and BioOXYGEN genes indicates either that other such families of mRNA regulatory elements only await detection or that special regulatory mechanisms are required because of the central role of iron and oxygen in biology.

ACKNOWLEDGMENTS

We thank Dr. Öjar Melefors for help with Table 1. Work in the authors' laboratories is supported by the Swedish Cancer Society (H. E. J.) and NIH-DK20251; HL56169 (E.C.T.)

REFERENCES

1. Ding XF, Anderson CM, Ma H, Hong H, Uht RM, Kushner PJ, Stallcup MR. Nuclear receptor-binding sites of coactivators glucocorticoid receptor interacting protein 1 (GRIP1) and steroid receptor coactivator 1 (SRC-1): Multiple motifs with different binding specificities. *Mol Endocrinol* 1998; 12:302–313.

2. DeFranco D, Yamamoto KR. Two different factors act separately or together to specify functionally distinct activities at a single transcriptional enhancer. *Mol Cell Biol* 1986; 6:993–1001.
3. Koenigsberger C, Chicca JJ 2nd, Amoureux MC, Edelman GM, Jones FS. Differential regulation by multiple promoters of the gene encoding the neuron-restrictive silencer factor. *Proc Natl Acad Sci USA* 2000; 97:2291–2296.
4. Theil EC. The iron responsive element (IRE) family of mRNA regulators: regulation of iron transport and uptake compared in animals, plants, and microorganisms. In: Siegel A, Siegel H, eds. *Iron Transport and Storage in Microorganisms, Plants and Animals*. New York: Marcel Dekker, 1998:403–434.
5. Theil EC. Targeting mRNA to regulate iron and oxygen metabolism. *Biochem Pharmacol* 2000; 59:87–93.
6. Hanson ES, Leibold EA. Regulation of the iron regulatory proteins by reactive nitrogen and oxygen species. *Gene Expr* 1999; 7:367–376.
7. Aisen P, Wessling-Resnick M, Leibold EA. Iron metabolism. *Curr Opin Chem Biol* 1999; 3:200–206.
8. Eisenstein RS, Blemings KP. Iron regulatory proteins, iron responsive elements and iron homeostasis. *J Nutr* 1998; 128:2295–2298.
9. Hentze MW, Kühn LC. Molecular control of vertebrate iron metabolism: mRNA-based regulatory circuits operated by iron, nitric oxide, and oxidative stress. *Proc Natl Acad Sci USA* 1996; 93:8175–8182.
10. Rouault TA, Klausner RD. Translational control of ferritin. In: Hershey JWB, Mathews MB, Sonenberg N, eds. *Translational control*. Cold Spring Harbor, NY: Cold Spring Harbor Laboratory Press, 1996:335–362.
11. Ostareck-Lederer A, Ostareck DH, Hentze MW. Cytoplasmic regulatory functions of the KH-domain proteins hnRNPs K and E1/E2. *Trends Biochem Sci* 1998; 23:409–411.
12. Schalinske KL, Chen OS, Eisenstein RS. Iron differentially stimulates translation of mitochondrial aconitase and ferritin mRNAs in mammalian cells: Implications for iron regulatory proteins as regulators of mitochondrial citrate utilization. *J Biol Chem* 1998; 273:3740–3746.
13. Chen OS, Schalinske KL, Eisenstein RS. Dietary iron intake modulates the activity of iron regulatory proteins and the abundance of ferritin and mitochondrial aconitase in rat liver. *J Nutr* 1997; 127:238–248.
14. Ke Y, Wu J, Leibold EA, Walden WE, Theil EC. Loops and bulge/loops in iron-responsive element isoforms influence iron regulatory protein binding: Fine-tuning of mRNA regulation? *J Biol Chem* 1998; 273:23637–23640.
15. Dix DJ, Lin P-N, Kimata Y, Theil EC. The iron regulatory region of ferritin mRNA is also a positive control element for iron-independent translation. *Biochemistry* 1992; 31: 2818–2822.
16. Hentze MW, Caughman SW, Casey JL, Koeller DM, Rouault TA, Harford JB, Klausner RD. A model for the structure and function of iron-responsive elements. *Gene* 1988; 72: 201–208.
17. Leibold EA, Laudano A, Yu Y. Structural requirements of iron-responsive elements for binding of the protein involved in both transferrin receptor and ferritin mRNA posttranscriptional regulation. *Nucleic Acids Res* 1990; 18:1819–1824.
18. Alén C, Sonenshein AL. *Bacillus subtilis* aconitase is an RNA-binding protein. *Proc Natl Acad Sci USA* 1999; 96:10412–10417.
19. Frishman D, Hentze MW. Conservation of aconitase residues revealed by multiple sequence analysis: Implications for structure/function relationships. *Eur J Biochem* 1996; 239:197–200.
20. Gruer MJ, Artymiuk PJ, Guest JR. The aconitase family: Three structural variations on a common theme. *Trends Biochem Sci* 1997; 22:3–6.

21. Hentze MW, Argos P. Homology between IRE-BP, a regulatory RNA-binding protein, aconitase and isopropylmalate isomerase. *Nucleic Acids Res* 1991; 19:1739–1740.
22. Kimata Y, Theil EC. Posttranslational regulation of ferritin during nodule development in soybean. *Plant Physiol* 1994; 104:263–270.
23. Proudhon D, Wei J, Briat J, Theil EC. Ferritin gene organization: Differences between plants and animals suggest possible kingdom-specific selective constraints. *Mol Evol* 1996; 42:325–336.
24. Crampton AL, Miller C, Baxter GD, Barker SC. Expressed sequenced tags and new genes from the cattle tick. *Boophilus microplus*. *Exp Appl Acarol* 1998; 22:177–186.
25. Huang T, Melefors Ö, Lind MI, Söderhäll K. An atypical iron-responsive element (IRE) within crayfish ferritin mRNA and an iron regulatory protein 1 (IRP-1)-like protein from crayfish hepatopancreas. *Insect Biochem Mol Biol* 1999; 29:1–9.
26. Charlesworth A, Gerogieva T, Gospodov I, Law JH, Dunkov BC, Ralcheva N, Barillas-Mury C, Ralchev K, Kafatos FC. Isolation and properties of *Drosophila melanogaster* ferritin: Molecular cloning of a cDNA that encodes one subunit, and localization of the gene on the third chromosome. *Eur J Biochem* 1997; 247:470–475.
27. Lind MI, Ekengren S, Melefors Ö, Söderhäll K. *Drosophila* ferritin mRNA: Alternative RNA splicing regulates the presence of the iron-responsive element. *FEBS Lett* 1998; 436:476–482.
28. Georgieva T, Dunkov BC, Harizanova N, Ralchev K, Law JH. Iron availability dramatically alters the distribution of ferritin subunit messages in *Drosophila melanogaster*. *Proc Natl Acad Sci USA* 1999; 96:2716–2721.
29. Dunkov BC, Zhang D, Choumarov K, Winzerling JJ, Law JH. Isolation and characterization of mosquito ferritin and cloning of a cDNA that encodes one subunit. *Arch Insect Biochem Physiol* 1995; 29:293–307.
30. Schüssler P, Pötters E, Winnen R, Michel A, Bottke W, Kunz W. Ferritin mRNAs of the in *Schistosoma mansoni* do not have iron-responsive elements for post-transcriptional regulation. *Eur J Biochem* 1996; 241:64–69.
31. Dunkov BC, Georgieva T. Organization of the ferritin genes in *Drosophila melanogaster*. *DNA Cell Biol* 1999; 18:937–944.
32. Gdaniec Z, Sierzputowska-Graez H, Theil EC. Iron regulatory element and internal loop/bulge structure for ferritin mRNA studied by cobalt(III) hexammine binding, molecular modeling, and NMR spectroscopy. *Biochemistry* 1998; 37:1505–1512.
33. Ke Y, H. Sierzputowska-Graez, Gdaniec Z, Theil EC. Internal loop/bulge and hairpin loop of the iron-responsive element of ferritin mRNA contribute to maximal iron regulatory protein 2 binding and translational regulation in the iso-iron-responsive element/iso-iron regulatory protein family. *Biochemistry* 2000; 39:6235–6242.
34. Dandekar T, Stripecke R, Gray NK, Goossen B, Constable A, Johansson HE, Hentze MW. Identification of a novel iron-responsive element in murine and human erythroid δ -aminolevulinic acid synthase mRNA. *EMBO J* 1991; 10:1903–1909.
35. Gray NK, Pantopoulos K, Dandekar T, Ackrell BC, Hentze MW. Translational regulation of mammalian and *Drosophila* citric acid cycle enzymes via iron responsive-elements. *Proc Natl Acad Sci USA* 1996; 93:4925–4930.
36. Kim HY, LaVaute T, Klausner RD, Rouault TA. Identification of a conserved and functional iron-responsive element in the 5'-untranslated region of mammalian mitochondrial aconitase. *J Biol Chem* 1996; 271:24226–24230.
37. Kohler SA, Henderson BR, Kühn LC. Succinate dehydrogenase b mRNA of *Drosophila melanogaster* has a functional iron-responsive element in its 5'-untranslated region. *J Biol Chem* 1995; 270:30781–30786.
38. Melefors Ö. Translational regulation *in vivo* of the *Drosophila melanogaster* mRNA encoding succinate dehydrogenase iron protein via iron responsive elements. *Biochem Biophys Res Commun* 1996; 221:437–441.

39. Cox TC, Bawden MJ, Martin A, May BK. Human erythroid 5-aminolevulinate synthase: Promoter analysis and identification of an iron-responsive element in the mRNA. *EMBO J* 1991; 10:1891–1902.
40. Melefors Ö, Goossen B, Johansson HE, Striebeck R, Gray NK, Hentze MW. Translational control of 5-aminolevulinate synthase mRNA by iron-responsive elements in erythroid cells. *J Biol Chem* 1993; 268:5974–5978.
41. Bhasker CR, Burgiel G, Neupert B, Emery-Goodman A, Kühn LC, May BK. The putative iron-responsive element in the human erythroid 5-aminolevulinate synthase mRNA mediates translational control. *J Biol Chem* 1993; 268:12699–12705.
42. Kreiling JA, Duncan R, Faggart MA, Cornell NW. Comparison of the beluga whale (*Delphinapterus leucas*) expressed genes for 5-aminolevulinate synthase with those in other vertebrates. *Comp Biochem Physiol* 1999; 123B:163–174.
43. Duncan R, Faggart MA, Roger AJ, Cornell NW. Phylogenetic analysis of the 5-aminolevulinate synthase gene. *Mol Biol Evol* 1999; 16:383–396.
44. Vidal S, Belouchi AM, Cellier M, Beatty B, Gros P. Cloning and characterization of a second human NRAMP gene on chromosome 12q13. *Mamm Genome* 1995; 6:224–230.
45. Gunshin H, Mackenzie B, Berger UV, Gunshin Y, Romero MF, Boron WF, Nussberger S, Gollan JL, Hediger MA. Cloning and characterization of a mammalian proton-coupled metal-ion transporter. *Nature* 1997; 388:482–488.
46. Han O, Fleet JC, Wood RJ. Reciprocal regulation of HFE and nramp2 gene expression by iron in human intestinal cells. *J Nutr* 1999; 129:98–104.
47. Donovan A, Brownlie A, Zhou Y, Shepard J, Pratt SJ, Moynihan J, Paw BH, Drejer A, Barut B, Zapata A, Law TC, Brugnara C, Lux SE, Pinkus GS, Pinkus JL, Kingsley PD, Phalis J, Fleming MD, Andrews NC, Zon LI. Positional cloning of zebrafish ferroportin1 identifies a conserved vertebrate iron exporter. *Nature* 2000; 403:779–781.
48. McKie AT, Marciani P, Rolfs A, Brennan K, Wehr K, Barrow D, Miret S, Bomford A, Peters TJ, Farzaneh F, Hediger MA, Hentze MW, Simpson RJ. A novel duodenal iron-regulated transporter, IREG1, implicated in the basolateral transfer of iron to the circulation. *Mol Cell* 2000; 5:299–309.
49. Abboud S, Haile DJ. A novel mammalian iron-regulated protein involved in intracellular iron metabolism. *J Biol Chem* 2000; 275:19906–19912.
50. Kawabata H, Yang R, Hiramata T, Vuong PT, Kawano S, Gombart AF, Koeffler HP. Molecular cloning of transferrin receptor 2: A new member of the transferrin receptor-like family. *J Biol Chem* 1999; 274:20856–20832.
51. Fleming RF, Migas M, Holden CC, Waheed A, Britton RS, Tomatsu S, Bacon BR, Sly WS. Transferrin receptor 2: Continued expression in mouse liver in the face of iron overload and in hereditary hemochromatosis. *Proc Natl Acad Sci USA* 2000; 97:2214–2219.
52. Müllner EW, Kühn LC. A stem-loop in the 3' untranslated region mediates iron-dependent regulation of transferrin receptor mRNA stability in the cytoplasm. *Cell* 1988; 53:815–825.
53. Casey JL, Hentze MW, Koeller DM, Caughman SW, Rouault TA, Klausner RD, Harford JB. Iron-responsive elements: Regulatory RNA sequences that control mRNA levels and translation. *Science* 1988; 240:924–928.
54. Chen CY, Shyu AB. AU-rich elements: Characterization and importance in mRNA degradation. *Trends Biochem Sci* 1995; 20:465–470.
55. Kohler SA, Menotti E, Kühn LC. Molecular cloning of mouse glycolate oxidase. High evolutionary conservation and presence of an iron-responsive element-like sequence in the mRNA. *J Biol Chem* 1999; 274:2401–2407.
56. Patino MM, Walden WE. Cloning of a functional cDNA for the rabbit ferritin mRNA repressor protein. *J Biol Chem* 1992; 267:19011–19016.

57. Cox LA, Adrian GS. Posttranscriptional regulation of chimeric human transferrin genes by iron. *Biochemistry* 1993; 32:4738–4745.
58. Cox LA, Kennedy MC, Adrian GS. The 5' untranslated region of human transferrin mRNA, which contains a putative iron-regulatory element, is bound by purified iron regulatory protein in a sequence specific manner. *Biochem Biophys Res Commun* 1995; 212:925–932.
59. Dandekar T, Beyer K, Bork P, Kenealy MR, Pantopoulos K, Hentze M, Sonntag-Buck V, Flouriot G, Gannon F, Schreiber S. Systematic genomic screening and analysis of mRNA in untranslated region and mRNA precursors: Combining experimental and computational approaches. *Bioinformatics* 1998; 14:271–278.
60. Tang Y, Guest JR. Direct evidence for mRNA binding and post-transcriptional regulation by *Escherichia coli* aconitases. *Microbiology* 1999; 145:3069–3079.
61. Theil EC. Iron regulatory elements (IREs): A family of mRNA non-coding sequences. *Biochem J* 1994; 304:1–11.
62. Wang Y-H, Sczekan SR, Theil EC. Structure of the 5' untranslated regulatory region of ferritin mRNA studied in solution. *Nucleic Acids Res* 1990; 18:4463–4468.
63. Bettany AJE, Eisenstein RS, Munro HN. Mutagenesis of the iron-regulatory element further defines a role for RNA secondary structure in the regulation of ferritin and transferrin receptor expression. *J Biol Chem* 1992; 267:16531–16537.
64. Dix DJ, Lin P-N, McKenzie AR, Walden WE, Theil EC. The influence of the base-paired flanking region on structure and function of the ferritin mRNA iron regulatory element. *J Mol Biol* 1993; 231:230–240.
65. Jaffrey SR, Haile DJ, Klausner RD, Harford JB. The interaction between the iron-responsive element binding protein and its cognate RNA is highly dependent upon both RNA sequence and structure. *Nucleic Acids Res* 1993; 21:4627–4631.
66. Sierzputowska-Gracz H, McKenzie RA, Theil EC. The importance of a single G in the hairpin loop of the iron responsive element (IRE) in ferritin mRNA for structure: An NMR spectroscopy study. *Nucleic Acids Res* 1995; 23:145–153.
67. Schlegl J, Gegout V, Schläger B, Hentze MW, Westhof E, Ehresmann C, Ehresmann B, Romby P. Probing the structure of the regulatory region of human transferrin receptor messenger RNA and its interaction with iron regulatory protein-1. *RNA* 1997; 3:1159–1172.
68. Address KJ, Basilion JP, Klausner RD, Rouault TA, Pardi A. Structure and dynamics of the iron responsive element RNA: Implications for binding of the RNA by iron regulatory binding proteins. *J Mol Biol* 1997; 274:72–83.
69. Laing LG, Hall KB. A model of the iron responsive element RNA hairpin loop structure determined from NMR and thermodynamic data. *Biochemistry* 1996; 35:13586–13596.
70. Henderson BR, Menotti E, Kühn LC. Iron regulatory proteins 1 and 2 bind distinct sets of RNA target sequences. *J Biol Chem* 1996; 271:4900–4908.
71. Hall KB, Tang C. ¹³C relaxation and dynamics of the purine bases in the iron responsive element RNA hairpin. *Biochemistry* 1998; 37:9323–9332.
72. Allerson CR, Cazzola M, Rouault TA. Clinical severity and thermodynamic effects of iron-responsive element mutations in hereditary hyperferritinemia-cataract syndrome. *J Biol Chem* 1999; 274:26439–26447.
73. Harrell CM, McKenzie AR, Patino MM, Walden WE, Theil EC. Ferritin mRNA: Interactions of iron regulatory element with translational regulator protein P-90 and the effect on base-paired flanking regions. *Proc Natl Acad Sci USA* 1991; 88:4166–4170.
74. Andersen Ø, Pantopoulos K, Kao HT, Muckenthaler M, Youson JH, Pieribone V. Regulation of iron metabolism in the sanguivore lamprey *Lampetra fluviatilis*—Molecular cloning of two ferritin subunits and two iron-regulatory proteins (IRP) reveals evolutionary conservation of the iron-regulatory element (IRE)/IRP regulatory system. *Eur J Biochem* 1998; 254:223–229.

Frataxin and Mitochondrial Iron

PIERRE RUSTIN

Hôpital Necker—Enfants Malades, Paris, France

I. INTRODUCTION	255
II. FRATAXIN AND FRIEDREICH'S ATAXIA: MOLECULAR GENETICS	256
III. FRATAXIN: A MITOCHONDRIAL PROTEIN	257
IV. FRATAXIN AND MITOCHONDRIAL IRON	259
A. Frataxin and Mitochondrial Iron Transport	259
B. Frataxin and Mitochondrial Iron Storage and Utilization	262
V. PHENOTYPES ASSOCIATED WITH DECREASED OR ABSENT FRATAXIN	263
VI. FIGHTING FRIEDREICH'S ATAXIA	264
VII. CONCLUSIONS	266
REFERENCES	266

I. INTRODUCTION

Molecular linkage analysis and mutation screening have shown that mutations in the gene encoding frataxin are responsible for Friedreich's ataxia (FRDA) (1). FRDA is the most common inherited ataxia, with prevalence now estimated to be about 1/30,000 in Caucasians, being very much lower in Asians and Africans (2). As reported 137 years ago by Nikolaus Friedreich (3), the age of onset of the disease is typically around puberty, but some children develop symptoms earlier (4). The most common presenting symptom is gait ataxia. Most patients further present deep tendon areflexia, dysarthria, sensory loss, muscle weakness, scoliosis, foot deformity, and

cardiac symptoms (2,5). Hypertrophy of the myocardium is noted in most but not all (6) patients, often resulting in life-threatening cardiomyopathy in adulthood (2,7). Finally, diabetes (8) or glucose intolerance (9) is commonly observed, possibly related to pancreatic exocrine insufficiency.

The discovery of frataxin, the involvement of iron, and the further characterization of the mitochondrial origin of FRDA present an interesting chain of events. A metabolic defect in FRDA, particularly a mitochondrial enzyme deficiency, was long suspected (10). However, because biochemical studies performed on peripheral tissues (lymphocytes, skeletal muscle, skin fibroblasts) did not reveal any significant or reproducible mitochondrial anomalies, the hypothesis of mitochondrial involvement was finally discarded in the 1980s (11). On the other hand, the observation of iron deposits in a patient's heart, an observation reported in 1993 (12), remained completely unnoticed. Then, in the late 1990s, with the successive discoveries of mutations in the frataxin gene (1), of the mitochondrial location of frataxin (13–16), of its relationship to mitochondrial iron metabolism (16–18), of respiratory chain deficiency in yeast deleted for YFH1 (Δ YFH1), the yeast frataxin counterpart (18,19), and, finally, with the discovery of iron–sulfur protein (ISP) deficiency in the endomyocardial biopsies of patients with FRDA (19), much of the etiology has been elucidated and the mitochondrial origin of the disease unambiguously established (20).

Most of what little is known about frataxin function comes from studies carried out in yeast, as neither human cultured cells expressing the disease phenotype, i.e., ISP deficiency, nor a viable animal model are currently available (21,22). This example thus illustrates how the study of such a simple system as yeast can result in major advances in the understanding of human pathology. In less than 5 years, the gene was identified, its mutation characterized, and the protein function partially discovered. This has made therapeutic intervention possible, and preliminary results have been encouraging (23).

II. FRATAXIN AND FRIEDREICH'S ATAXIA: MOLECULAR GENETICS

The Friedreich ataxia-causing gene, encoding frataxin, maps to chromosome 9q13-q21.1 (24). The major form of frataxin mRNA results from the transcription of five exons spreading over 40 kb (exons 1 to 5a) (1). The corresponding open reading frame encodes a 210-amino acid protein. About 40 kb from exon 5a in the telomeric direction, there is an alternative exon 5b that also contains an in-frame stop codon. The alternative transcript differs from the main isoform by 11 C-terminal residues and results in a 171-amino acid protein. Finally, depending on the utilization of the donor splice site of the 5b exon, a third longer transcript may be found that includes a noncoding exon 6, 16 kb telomeric to exon 5b. Additional sequences with close similarity to the processed frataxin transcript have been found in the human genome, with at least one intron-free copy (1).

The major 1.3-kb transcript is differentially expressed in tissues, with highest expression in heart, intermediate levels in liver, skeletal muscle, pancreas, thymus, and brown fat, and minimal levels in other tissues (1,2). In the central nervous system, the highest level of expression is observed in dorsal root ganglia, where cell bodies of sensory nerves are found. These receive axons from the periphery and send

axons to the posterior columns up to the bulb. A much lower frataxin expression is observed in the spinal cord and in the cerebellum, and it is even lower in cerebral cortex. A detailed analysis of mouse frataxin expression has shown that the protein is developmentally regulated (25).

The FRDA-causing gene has been localized and identified as frataxin, but sequencing the coding exons initially failed to detect any mutation. However, the search for gross alterations of the gene revealed a massive expansion of a short GAA trinucleotide repeat (120 to 1700 bp in affected patients; 8 to 22 in controls) located in the middle of an Alu sequence on more than 90% of the alleles of the patients with typical FRDA (1,2,26–28). Expansion of CAG, CGG, and GAA repeats has been observed in 12 genetic diseases so far, both in coding and noncoding regions (29). Gain of function is observed as a result of expansions in coding regions leading to dominantly inherited diseases, such as Huntington's disease. Repeats in noncoding regions have been identified in fragile X syndrome, myotonic dystrophy, and FRDA (29). Among these, FRDA is the only one with autosomal recessive inheritance. A founder effect has been identified in this disease (30). Both meiotic and mitotic expansion has been found by DNA analysis in a FRDA premutation carrier (31), and somatic mosaicism has been observed in lymphocytes and nervous tissue (32). Rare heterozygous point mutations have also been identified in FRDA (missense, nonsense, and splicing mutations; Fig. 1) (33). Mutations have not been reported in the nonconserved N-terminal domain of the protein so far, which includes the 20-amino acid-long mitochondrial targeting sequence (1,26).

As a result of the trinucleotide expansion, the formation of a complex DNA structure (34–36), remarkably thermostable (sticky DNA), has been shown to occur depending on the length of the GAA*TTC tracts, with GAA repeats shorter than 59 being inert (37). This sticky conformation, highly sequence-specific (i.e., GAAGGA*TCCTTC tracts do not form such a sticky structure), may further generate interlocked DNA complexes and both potentially contribute to the blockade of transcription (34,36,38). This inhibition of transcription presumably accounts for the very low level of residual frataxin found in patients (1,39). Residual frataxin in lymphoblastoid cell lines from patients has been reported to range from 4% to 30% of controls. A correlation between the severity of the disease and the length of the expansion is generally observed (40–46; see, however, 47–49). The disease, therefore, appears to originate essentially from a loss of function of frataxin, with a few percent residual protein still present.

III. FRATAXIN: A MITOCHONDRIAL PROTEIN

Epitope tagging experiments, co-localization with well-known mitochondrial markers, subcellular fractionations, and computer prediction using the latest versions of sorting programs all establish a mitochondrial location for frataxin (13–15). The first 20 amino acids are sufficient to target a GFP protein to the mitochondria (14). Finally, immunoelectron microscopy performed on HeLa cells overexpressing full-length frataxin indicates that the protein localizes in the mitochondrial matrix at or near the inner membrane (39).

Homologs of the frataxin gene have been found in mouse, *Drosophila melanogaster*, *Caenorhabditis elegans*, *Saccharomyces cerevisiae*, and γ purple, a Gram-negative bacteria. Multiple alignment of frataxin genes from eukaryotic and bacterial

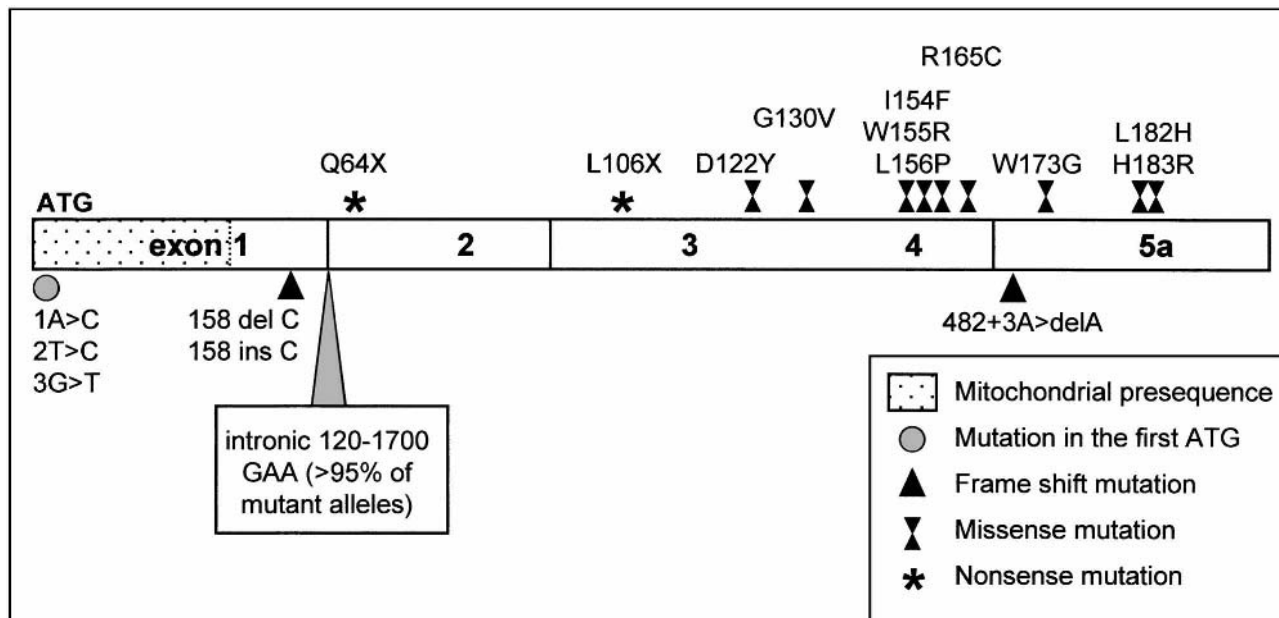


Figure 1 Disease-causing mutations in the frataxin gene.

source reveals the presence of a conserved C-terminal globular domain. Investigation of the three-dimensional solution structure of the 91 to 210 C-terminal sequence of frataxin has confirmed the presence of at least six stranded antiparallel β sheets flanked by two α helices packed with their hydrophobic residues into the β sheet (50).

No sequence homology with known proteins has yet been found, and analysis of the frataxin protein sequence did not give clues to its function, as no specific binding domain could be identified.

Mitochondrial processing peptidase (MPP) is the only partner identified so far for frataxin, but nevertheless this does not shed light on frataxin function (51). Frataxin is processed by this peptidase to a mature form in two sequential steps. In mammals, the intermediate form is processed by MPP much less efficiently than in yeast (52,53). This second step possibly involves additional species- and/or tissue-specific activating factors. Thus, in yeast, Ssq1P, a mitochondrial Hsp70 homolog, significantly improves the efficiency of the processing of Yfh1p, the yeast homolog of frataxin (54).

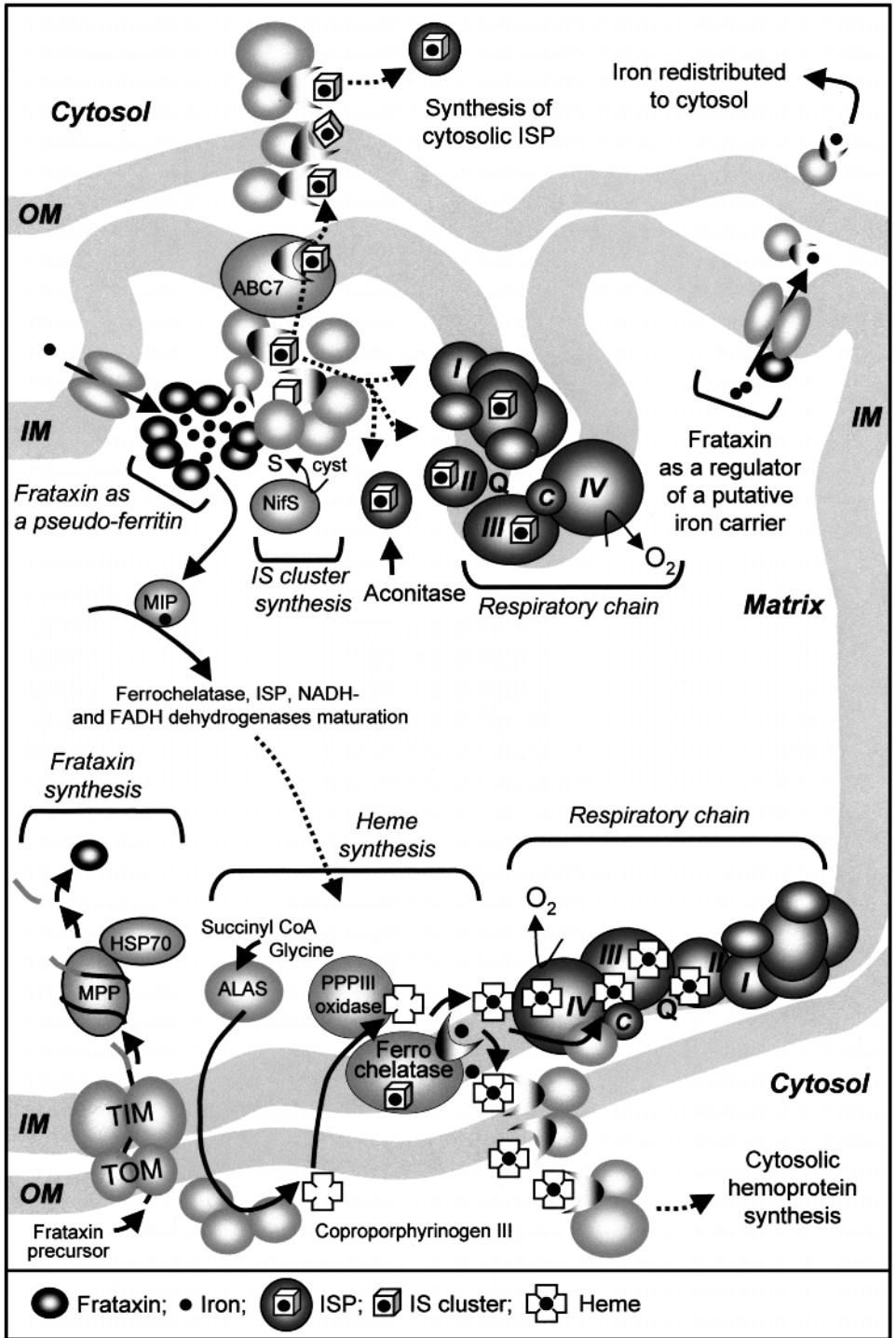
IV. FRATAXIN AND MITOCHONDRIAL IRON

Several hypotheses have been advanced for the function of frataxin, but yeast studies have conclusively established that frataxin is involved at one point in the transport, storage, and (or) handling of mitochondrial iron (Fig. 2) (16,17). In addition, direct evidence for mitochondrial iron accumulation has also been provided in FRDA patients (55,56).

Conclusions from yeast studies have been readily generalized to higher organisms and to pathological conditions in humans. However, it should be borne in mind that significant differences in the organization and control of iron homeostasis do exist between organisms. Regulation of cellular iron homeostasis has obviously evolved with the appearance of new specialized genes and (or) functions. Thus, cytosolic iron storage ferritin does not exist in yeast, nor does aconitase-iron-regulatory protein (IRP1) which is known to control iron homeostasis in mammalian cells (57,58). In addition, quite significant differences between mechanisms for transport of iron into cells have already been found between different tissues in human (59). All this shows that the precise organization and, a fortiori, the regulation, of cellular and possibly mitochondrial iron homeostasis may vary greatly from cell to cell, from tissue to tissue, and from one organism to another. As a result, it is probably too early to reach a firm conclusion on the actual function of frataxin in human cells based only on experiments carried out on yeast, particularly bearing in mind that even in yeast its function is still a matter of debate.

A. Frataxin and Mitochondrial Iron Transport

As mentioned above, frataxin is possibly involved in mitochondrial iron homeostasis through the regulation of iron transport into the organelle (16,60). Because of the multifaceted involvement of mitochondria in intermediary metabolism, in the commitment of cells to die, and in many other cell functions, the import/export through the impermeable mitochondrial membranes of numerous substrates, co-factors, proteins and their precursors, as well as metals, needs to be tightly controlled. Depending



on the specific metabolic requirements of each tissue, this import/export function of mitochondria varies considerably, and mitochondria are either freely permeable or have specific transport systems in order to permit efficient passage across their membranes. Being impermeable to polar compounds, anions, and cations, the mitochondrial inner membrane is equipped with various specialized carrier proteins, which can be energy-dependent (active transport) or not (facilitated diffusion). The permeability of the inner membrane to monovalent and divalent metals is too low to permit efficient simple diffusion, and transport systems for uptake of metals were the first to be recognized. Most divalent cations (Mg^{2+} , Ca^{2+} , Sr^{2+} , Mn^{2+}) require energy for import into the mitochondrial matrix. However, mechanisms of mitochondrial metal transport can differ markedly from tissue to tissue. Thus, regulation of steady-state cycling of calcium through the mitochondrial inner membrane relies on tissue-specific efflux pathways, which have been studied in great detail (61). Import of iron has been studied in isolated rat liver mitochondria, and reports suggest that different types of carriers are present on the inner mitochondrial membrane (62–64). However, surprisingly enough, apart from these few studies, mitochondrial iron transportation has received little attention until very recently. The recognition of frataxin as the disease-causing protein in Friedreich's ataxia and of its importance in mitochondrial iron homeostasis has been a strong incentive for studying the mechanisms of mitochondrial iron transportation and utilization. This has led to a major discovery on another aspect of iron utilization in mitochondria, i.e., the central role of mitochondria in the mechanism of both mitochondrial and cytosolic iron–sulfur cluster synthesis (65–66).

The idea that frataxin might be a protein involved in the control of mitochondrial iron transport stems from the observation that the $\Delta YFH1$ mutant accumulates iron in the mitochondrial matrix, presumably at the expense of cytosolic iron (16,17). The fact that in yeast, where no cytosolic ferritin can be found, mitochondria might represent a storage location for iron led to the idea that frataxin normally acts as a positive modulator of iron export and that its lack results in intramitochondrial iron accumulation (16,60). Indeed, an active export of iron from mitochondria infers that iron is normally stored in the organelle to be redistributed to the cytosol. Because mitochondria were not known to store iron in human cells (a function provided by cytosolic ferritin shells), we initially favored the idea that frataxin might rather exert a negative control on mitochondrial iron import (19). Whichever the case, either increased import or decreased export would deplete cytosolic iron and lead to mitochondrial iron accumulation. In human cells, depletion of cytosolic iron might in

←

Figure 2 Frataxin and mitochondrial iron utilization. Top: iron utilization for iron-sulfur cluster synthesis. Left, frataxin acting as a mitochondrial pseudo-ferritin allowing an adequate iron storage and utilization. Right, frataxin acting as a modulator of iron export. Bottom, iron utilization for heme synthesis. I, II, III, IV, the various respiratory chain complexes; ABC7, an ATP-binding cassette transporter, human counterpart of the yeast ATM1p; ALAS, 5-aminolevulinic acid synthase; c, cytochrome c; MIP, mitochondrial intermediate peptidase; MPP, mitochondrial processing peptidase; NifS, similar to the yeast Nfs1p; PPPIII, protoporphyrinogen III oxidase; Q, ubiquinone; TOM, TIM, protein import machinery through the outer and the inner mitochondrial membranes, respectively.

turn favor the conversion of cytosolic aconitase to its IRP1 form (57), thus favoring cellular iron import. However, both hypotheses require the existence of regulated iron import machinery interacting directly or indirectly with frataxin, and such a protein partner has not yet been identified.

The idea that frataxin in some way controls mitochondrial iron transport was based mostly on the hypothesis that the observed phenotype results from a quantitative accumulation of iron. However, two sets of data raise questions about this simple view. First, abnormally high mitochondrial iron accumulation (up to 75 pmol Fe/mg in yeast cultured with 50 μ M Fe, compared to 5 pmol/mg in controls) was reported in yeast with a missense *NFS1* allele (66). Nfs1p is a mitochondrial protein involved in the release of sulfur from cysteine for iron–sulfur cluster assembly (67). However, in this latter case, while an upregulation of the genes of the cellular iron system was noticed, increasing iron concentration in the yeast culture medium did not exacerbate the ISP deficiency (66). Similarly, accumulation of iron in mitochondria prepared from a yeast strain deleted for the gene encoding the ATP-binding cassette (ABC) transporter *Atm1p* of the inner mitochondrial membrane was found to be threefold higher than in Δ YFH1 (68). However, aconitase activity was only reduced by 50%, while it was decreased to less than 10% in Δ YFH1. Interestingly enough, mutations in *ABC7*, the gene encoding the human counterpart of yeast *Atm1p* (69), cause an X-linked sideroblastic anemia and ataxia (70). On the other hand, a loss of aconitase was reported in a specific Δ YFH1 strain grown with low iron concentration, but this was not associated with an intramitochondrial iron accumulation (71). Therefore, first, iron can accumulate in the mitochondria with only a mild ISP deficiency phenotype. Second, the lack of frataxin may lead to ISP deficiency without significant iron accumulation. This shows that no direct relationship exists between residual level of frataxin, degree of iron overload, or degree of ISP deficiency, suggesting that frataxin is not necessarily involved in the control of iron transport in the mitochondria. Accordingly, the biochemical phenotype, i.e., the loss of ISP activities, might well depend on the status of iron rather than on its actual amount, accumulation being possibly a secondary phenomenon. Then, it may be suggested that frataxin does not affect the transport of iron, but rather its storage or handling in the mitochondrial matrix (Fig. 2). In keeping with this, the embryonic death of homozygous frataxin-knock out mice was observed before any detectable iron accumulation (72). Similarly, the investigation of heart homogenates from conditional frataxin-knock out mice presenting a severely deficient activity of ISPs and a hypertrophic cardiomyopathy has shown that these were observed before any detectable iron accumulation, again suggesting that iron accumulation is a secondary phenomenon in Friedreich's ataxia (73).

B. Frataxin and Mitochondrial Iron Storage and Utilization

It is well known that unsequestered iron, as well as low-molecular-weight iron chelates, is quite toxic through Fenton reaction. Therefore, a lack of decreased content of any protein involved in storage of mitochondrial iron could lead to a mitochondrial phenotype such as the one observed in Δ YFH1 or *FRDA*, giving rise to the idea that frataxin may behave as a mitochondrial “pseudo-ferritin.” However, the absence of evidence for the formation of aggregates or precipitates, or of major conformational changes of frataxin even in the presence of high iron, together with the lack

of obvious specific iron-binding sites on the protein itself, prompted most authors to reject this hypothesis. Nevertheless, more recently it has been shown that aerobic addition of ferrous ammonium sulfate to the purified mature form of Yfh1p can result in the assembly of a regular spherical complex (diameter $176 \pm 10 \text{ \AA}$; molecular mass 1.1 MDa) (74). The resulting frataxin multimer consists of about 60 subunits, possibly sequestering up to 70 iron atoms per subunit in a polynuclear ferric core (74). According to this observation, frataxin would act as an iron storage protein, thus detoxifying iron. The lack of frataxin might then result in a phenotype, without requiring a significant increase in the amount of iron in the mitochondrial matrix, but rather through iron-catalyzed Fenton chemistry.

A particular feature of the mitochondrial phenotype observed both in $\Delta YFH1$ and FRDA is the loss of mitochondrial ISP activities, this loss being highly specific in the cardiomyocytes at the early stage of the disease (19). Several hypotheses might account for the specificity of iron-sulfur protein targeting.

First, by modulating mitochondrial iron transport, and therefore the amount of iron, frataxin might control iron-dependent oxidative reactions (19). As ISPs are exquisitely sensitive to free radicals (75), a specific loss of ISP activity might result from superoxide produced through iron-catalyzed Fenton chemistry. However, as discussed above, if frataxin acts only as a regulator of mitochondrial iron transport, then any similar intramitochondrial iron accumulation should be accompanied by a similar loss of ISP. This prediction is not verified, as neither NFS1 nor ATM1 yeast mutants, which accumulate high iron, present a similar decrease of ISP activities (66,68). Noticeably, in these latter mutants, accumulation takes place in the presence of frataxin, which might still be able to cope with the accumulated iron and to detoxify it.

Second, lack of frataxin may result in a similar ISP deficiency if frataxin acts as an iron-storage protein preventing the Fenton reaction.

Third, frataxin could be specifically involved in ISP biosynthesis. Nevertheless, there are no experimental data to support this view so far.

The idea that frataxin, functioning as an iron-storage protein, may also act to allow suitable presentation of iron for ISP biosynthesis may be relevant. Indeed, any iron targeted to mitochondria appears to enter for purposes of biosynthesis, either of heme, iron-sulfur clusters, or incorporation into iron-dependent proteins such as the mitochondrial intermediate protease involved in the processing of the ferrochelatase (MIP) (Fig. 2). Noteably, this latter protease may also link frataxin and mitochondrial iron homeostasis through the synthesis of heme (76). The synthesis of heme does not require import of iron into the mitochondrial matrix, but only to the inner membrane (77). This leaves matrix iron import required mostly for iron-sulfur cluster synthesis. It is therefore perhaps not surprising that disturbing mitochondrial iron homeostasis alters ISP synthesis specifically.

V. PHENOTYPES ASSOCIATED WITH DECREASED OR ABSENT FRATAXIN

Frataxin is highly conserved from *Escherichia coli* to humans, which suggests conserved function for the protein. However, noticeable differences between organisms

have been observed upon knockout or loss of function of the counterpart genes. For instance, knockout of the *cyaY* gene, the *E. coli* frataxin homolog, shows neither an effect on the cellular iron content nor any peculiar sensitivity to oxidants (78). In contrast, Δ YFH1 yeast strains grown under normal iron complement lose their mitochondrial function due to a generalized deficiency of the respiratory chain originating from the loss of mitochondrial DNA, and do not grow on nonfermentable sources of carbon (16–18). Notably, detailed phenotypic analysis revealed that mitochondrial ISPs were strongly deficient as well, particularly the matrix-localized aconitase (10–15% residual activity) (19).

In humans, a generalized deficiency of the activity of mitochondrial ISPs was detected in 2-mg endomyocardial biopsies of two FRDA patients (19). All other respiratory chain activities measured were normal. Such a biochemical phenotype has not been observed in more than 2000 patients suspected of mitochondrial dysfunction. We subsequently found an additional partial loss of complex IV activity in the biopsy of one additional patient with a more severe clinical presentation (unpublished). This might reflect progressive changes in the biochemical phenotype due to the progression of secondary peroxidative reactions. In addition, it is worth noting that ferrochelatase, which is involved in the synthesis of heme, also contains an iron–sulfur cluster that might be destroyed by free radicals at some stage of the disease (79). This would cause a worsening of the biochemical phenotype, with cytochromes possibly becoming deficient. These data were later confirmed on post-mortem samples of FRDA patients (27).

The quite characteristic phenotype observed in heart biopsies from FRDA patients, i.e., loss of ISP activity, cannot be observed in any peripheral tissues from the patients, including lymphocytes, skin fibroblasts, and skeletal muscle (19). As peripheral tissues had been used in the past to investigate mitochondrial function in FRDA, this key observation explains why it took so long to establish that FRDA is actually a mitochondrial disorder. As both the mitochondrial origin of the disease and the major features of the underlying mechanisms have been established, predictable changes in biochemical parameters can now be looked for (80), but above all it now appears possible to devise strategies to fight the disease (16,23,59).

VI. FIGHTING FRIEDREICH'S ATAXIA

Whatever the precise mechanism leading to mitochondrial iron toxicity in FRDA, it is now established that iron plays a major role in the pathophysiology of Friedreich's ataxia. Therefore, although serum iron and ferritin concentrations do not increase in patients with FRDA (81), the simplest idea would be to target iron by using a chelator, such as desferrioxamine (59,82). However, several potential drawbacks to this approach can be emphasized. First, mitochondrial iron accumulation is presumably at the expense of cytosolic iron (16,19). As a result, cytosol possibly lacks iron. Providing desferrioxamine might therefore further decrease cytosolic iron, while the few available data indicate a poor ability of desferrioxamine to decrease mitochondrial iron (83). Second, in-vitro experimentation has shown that in the presence of high iron, desferrioxamine, while protecting membrane components, caused a marked decrease in soluble aconitase activity, an enzyme already deficient in FRDA patients (84). Therefore, initial enthusiasm for trying iron chelators in FRDA vanished progressively (2).

Because of the increased load of free radicals, antioxidant therapy might slow the progression of the disease. Interestingly enough, an indication that the antioxidant system is challenged in FRDA is given by the abnormalities in antioxidant metabolism that can be observed in patients with FRDA (85). In addition, it is noteworthy that mutations in the α -tocopherol (vitamin E) transfer protein gene cause a Friedreich-like ataxia (86–88). Vitamin E being a powerful antioxidant component of the mitochondrial membranes, the overlap of the two clinical phenotypes also supports the view that a similar free-radical overproduction is occurring in both diseases.

A large choice of antioxidant drugs is available, allowing for immediate trials. In-vitro assays on human heart homogenates have emphasized the potential danger of using reducing antioxidants, which would tend to increase reduction of available iron (84). As a result of these in-vitro studies, idebenone, a short-chain homolog of ubiquinone (CoQ10), was selected for clinical trial (Fig. 3). Promising initial results obtained on three patients indicated major regression of heart hypertrophy upon idebenone oral supplementation with no adverse effect reported so far (23). These preliminary data were reinforced by additional observations showing that in 52 patients (children and adults) treated with idebenone, 41 had decreased cardiac hypertrophy and slight improvements of their muscular and neurological condition after 3–6 months of treatment (unpublished).

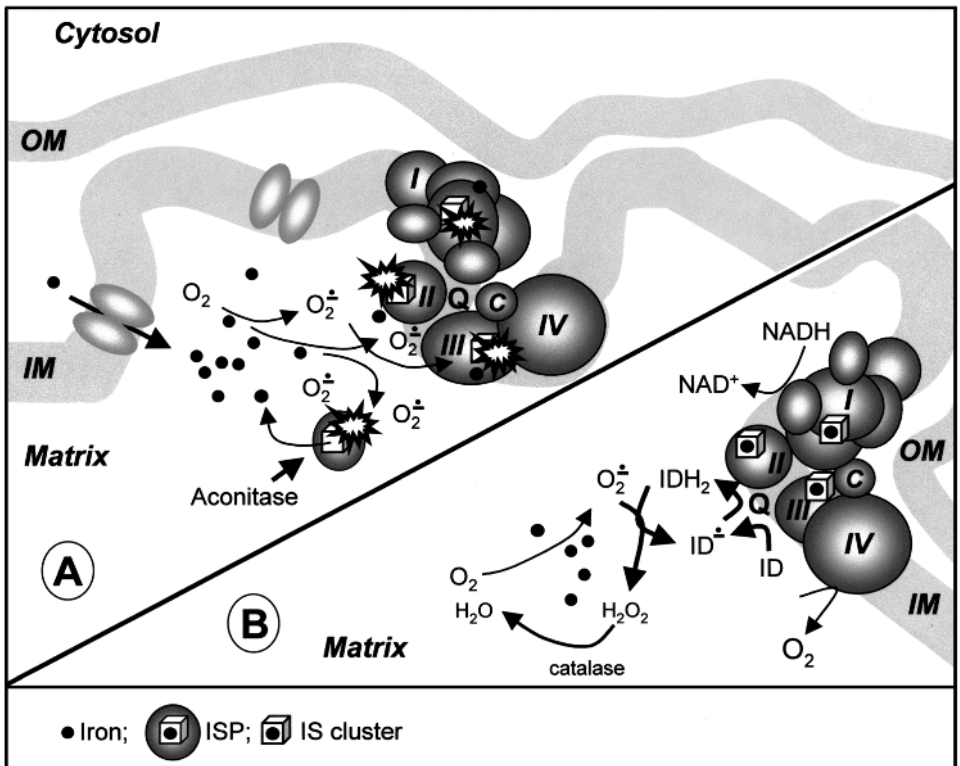


Figure 3 (A) Iron-induced iron-sulfur cluster damage in Friedreich's ataxia, and (B) protection by idebenone (ID).

VII. CONCLUSIONS

Although the exact function of frataxin, and the organization and regulation of mitochondrial iron transport and homeostasis, are still to be clarified, impressive progress has been made in understanding the disease resulting from mutation in the frataxin gene. In parallel, research into mitochondrial iron metabolism has been steadily increasing with positive consequences.

The description of the biosynthetic pathway for iron–sulfur clusters has uncovered a totally new domain of mitochondrial involvement in cell metabolism. Previously, mitochondria were known as the unique site of heme synthesis through the action of ferrochelatase. We now know that mitochondria are also probably the sole site of synthesis of iron–sulfur clusters, which are distributed in the mitochondria to the matrix and membrane ISP, and also to the cytosol ISP, presumably by an ATP-binding cassette transporter.

In yeast, two proteins localized to the mitochondria, Mmt1p and Mmt2p, may play a role in the redistribution of mitochondrial iron to the cytosol because overexpression of these genes tends to increase cytosolic iron (89). To date these two proteins have no known human counterparts. Interestingly, their simultaneous deletion leads to a yeast growth defect in low-iron medium but does not affect mitochondrial ISP and heme synthesis, or more generally mitochondrial function (68). The organization of iron transport through the mitochondrial inner membrane is therefore far from being understood, and the putative function of frataxin in this process is far from established. An alternative hypothesis of frataxin working as a mitochondrial pseudo-ferritin (74) accounts for most of the available data, and more will be required before any firm conclusion can be drawn.

Whatever the precise function of frataxin may be, the established fact that abnormal mitochondrial iron status causes overproduction of free radicals and is involved in FRDA has already provided clues for devising therapeutic strategies. Hopefully, the preliminary results obtained with antioxidant therapy will be confirmed, as this will change dramatically the fate of those affected by FRDA.

REFERENCES

1. Campuzano V, Montermini L, Molto MD, Pianese L, Cossee M, Cavalcanti F, Monros E, Rodius F, Duclos F, Monticelli A, Zara F, Canizares J, Koutnikova H, Bidichandani SI, Gellera C, Brice A, Trouillas P, de Michele G, Filla A, de Frutos R, Palau F, Patel PI, Di Donato S, Mandel JL, Coccozza S, Koenig M, Pandolfo M. Friedreich's ataxia: autosomal recessive disease caused by an intronic GAA triplet repeat expansion. *Science* 1996; 271:1423–1427.
2. Delatycki MB, Williamson R, Forrest SM. Friedreich ataxia: an overview. *J Med Genet* 2000; 37:1–8.
3. Friedreich N. Uber degenerative Atrophie der Spinalen hinterstrange. *Virchow's Arch Pathol Anat* 1863; 26:391–419.
4. De Michele G, Filla A, Criscuolo C, Scarano V, Cavalcanti F, Pianese L, Monticelli A, Coccozza S. Determinants of onset age in Friedreich's ataxia. *J Neurol* 1998; 245:166–168.
5. Harding AE. Friedreich's ataxia: a clinical and genetic study of 90 families with an analysis of early diagnostic criteria and interfamilial clustering of clinical features. *Brain* 1981; 104:589–620.

6. Dutka DP, Donnelly JE, Nihoyannopoulos P, Oakley CM, Nunez DJ. Marked variation in the cardiomyopathy associated with Friedreich's ataxia. *Heart* 1999; 81:141–147.
7. De Michele G, Perrone F, Filla A, Mirante E, Giordano M, De Placido S, Campanella G. Age of onset, sex, and cardiomyopathy as predictors of disability and survival in Friedreich's disease: a retrospective study on 119 patients. *Neurology* 1996; 47:1260–1264.
8. Ristow M, Giannakidou E, Hebinck J, Busch K, Vorgerd M, Kotzka J, Knebel B, Mueller-Berghaus J, Epplen C, Pfeiffer A, Kahn CR, Doria A, Krone W, Mueller-Wieand D. An association between NIDDM and a GAA trinucleotide repeat polymorphism in the X25/frataxin (Friedreich's ataxia) gene. *Diabetes* 1998; 47:851:854.
9. Hart LM, Ruige JB, Dekker JM, Stehouwer CD, Maassen JA, Heine RJ. Altered beta-cell characteristics in impaired glucose tolerant carriers of a GAA trinucleotide repeat polymorphism in the frataxin gene. *Diabetes* 1999; 48:924–926.
10. Barbeau A. Friedreich's ataxia 1980. An overview of the physiopathology. *Can J Neurol Sci* 1980; 7:455–468.
11. Chamberlain S, Lewis PD. Normal mitochondrial malic enzyme levels in Friedreich's ataxia fibroblasts. *J Neurol Neurosurg Psychiatry* 1983; 46:1050–1051.
12. Lamarche J, Shapcott D, Cote M, Lemieux B. Cardiac iron deposits in Friedreich's ataxia. In: Lechtenberg R, ed. *Handbook of Cerebellar Diseases*. New York: Marcel Dekker, 1993:453–457.
13. Koutnikova H, Campuzano V, Foury F, Dolle P, Cazzalini O, Koenig M. Studies of human, mouse and yeast homologues indicate a mitochondrial function for frataxin. *Nature Genet* 1997; 16:345–351.
14. Priller J, Scherzer CR, Faber PW, MacDonald ME, Young AB. Frataxin gene of Friedreich's ataxia is targeted to mitochondria. *Ann Neurol* 1997; 42:265–269.
15. Gibson TJ, Koonin EV, Musco G, Pastore A, Bork P. Friedreich's ataxia protein: phylogenetic evidence for mitochondrial dysfunction. *Trends Neurosci* 1996; 19:465–468.
16. Babcock M, de Silva D, Oaks R, Davis-Kaplan S, Jiralerspong S, Montermini L, Pandolfo M, Kaplan J. Regulation of mitochondrial iron accumulation by Yfh1p, a putative homolog of frataxin. *Science* 1997; 276:1709–1712.
17. Foury F, Cazzalini O. Deletion of the yeast homologue of the human gene associated with Friedreich's ataxia elicits iron accumulation in mitochondria. *FEBS Lett* 1997; 411:373–377.
18. Wilson RB, Roof DM. Respiratory deficiency due to loss of mitochondrial DNA in yeast lacking the frataxin homologue. *Nature Genet* 1997; 16:352–357.
19. Rötig A, de Lonlay P, Chretien D, Foury F, Koenig M, Sidi D, Munnich A, Rustin P. Aconitase and mitochondrial iron-sulphur protein deficiency in Friedreich ataxia. *Nature Genet* 1999; 17:215–217.
20. Koenig M, Mandel JL. Deciphering the cause of Friedreich ataxia. *Curr Opin Neurobiol* 1997; 7:689–694.
21. Knight SA, Kim R, Pain D, Dancis A. The yeast connection to Friedreich ataxia. *Am J Hum Genet* 1999; 64:365–371.
22. Askwith C, Kaplan J. Iron and copper transport in yeast and its relevance to human disease. *Trends Biochem Sci* 1998; 23:135–138.
23. Rustin P, von Kleist-Retzow JC, Chantrel-Groussard K, Sidi D, Munnich A, Rotig A. Effect of idebenone on cardiomyopathy in Friedreich's ataxia: a preliminary study. *Lancet* 1999; 354:477–479.
24. Chamberlain S, Shaw J, Rowland A, Wallis J, South S, Nakamura Y, von Gabain A, Farrall M, Williamson R. Mapping of mutation causing Friedreich's ataxia to human chromosome 9. *Nature* 1988; 334:248–250.
25. Jiralerspong S, Liu Y, Montermini L, Stifani S, Pandolfo M. Frataxin shows developmentally regulated tissue-specific expression in the mouse embryo. *Neurobiol Dis* 1997; 4:103–113.

26. Pandolfo M. Molecular pathogenesis of Friedreich ataxia. *Arch Neurol* 1999; 56:1201–1208.
27. Bradley JL, Blake JC, Chamberlain S, Thomas PK, Cooper JM, Schapira AH. Clinical, biochemical and molecular genetic correlations in Friedreich's ataxia. *Hum Mol Genet* 2000; 9:275–282.
28. Martin J, Martin L, Lofgren A, D'Hooghe M, Storm K, Balemans W, Palau F, Van Broeckhoven C. Classical Friedreich's ataxia and its genotype. *Eur Neurol* 1999; 42: 109–115.
29. Timchenko LT, Caskey CT. Triplet repeat disorders: discussion of molecular mechanisms. *Cell Mol Life Sci* 1999; 55:1432–1447.
30. Cossee M, Schmitt M, Campuzano V, Reutenauer L, Moutou C, Mandel JL, Koenig M. Evolution of the Friedreich's ataxia trinucleotide repeat expansion: founder effect and premutations. *Proc Natl Acad Sci USA* 1997; 94:7452–7457.
31. Delatycki MB, Paris D, Gardner RJ, Forshaw K, Nicholson GA, Nassif N, Williamson R, Forrest SM. Sperm DNA analysis in a Friedreich ataxia premutation carrier suggests both meiotic and mitotic expansion in the FRDA gene. *J Med Genet* 1998; 35:713–716.
32. Machkhas H, Bidichandani SI, Patel PI, Harati Y. A mild case of Friedreich ataxia: lymphocyte and sural nerve analysis for GAA repeat length reveals somatic mosaicism. *Muscle Nerve* 1998; 21:390–393.
33. Cossee M, Durr A, Schmitt M, Dahl N, Trouillas P, Allinson P, Kostrzewa M, Nivelon-Chevallier A, Gustavson KH, Kohlschutter A, Muller U, Mandel JL, Brice A, Koenig M, Cavalcanti F, Tammaro A, De Michele G, Filla A, Coccozza S, Labuda M, Montermini L, Poirier J, Pandolfo M. Friedreich's ataxia: point mutations and clinical presentation of compound heterozygotes. *Ann Neurol* 1999; 45:200–206.
34. Bidichandani SI, Ashizawa T, Patel PI. The GAA triplet-repeat expansion in Friedreich ataxia interferes with transcription and may be associated with an unusual DNA structure. *Am J Hum Genet* 1998; 62:111–121.
35. Mariappan SV, Catasti P, Silks LA 3rd, Bradbury EM, Gupta G. The high-resolution structure of the triplex formed by the GAA/TTC triplet repeat associated with Friedreich's ataxia. *J Mol Biol* 1999; 285:2035–2052.
36. Suen IS, Rhodes JN, Christy M, McEwen B, Gray DM, Mitas M. Structural properties of Friedreich's ataxia d(GAA) repeats. *Biochim Biophys Acta* 1999; 1444:14–24.
37. Sakamoto N, Chastain PD, Parniewski P, Ohshima K, Pandolfo M, Griffith JD, Wells RD. Sticky DNA: self-association properties of long GAA. TTC repeats in R.R.Y triplex structures from Friedreich's ataxia. *Mol Cell* 1999; 3:465–475.
38. Ohshima K, Montermini L, Wells RD, Pandolfo M. Inhibitory effects of expanded GAA. TTC triplet repeats from intron I of the Friedreich ataxia gene on transcription and replication in vivo. *J Biol Chem* 1998; 273:14588–14595.
39. Campuzano V, Montermini L, Lutz Y, Cova L, Hindelang C, Jiralerspong S, Trottier Y, Kish SJ, Fauchoux B, Trouillas P, Authier FJ, Durr A, Mandel JL, Vescovi A, Pandolfo M, Koenig M. Frataxin is reduced in Friedreich ataxia patients and is associated with mitochondrial membranes. *Hum Mol Genet* 1997; 6:1771–1780.
40. Durr A, Cossee M, Agid Y, Campuzano V, Mignard C, Penet C, Mandel JL, Brice A, Koenig M. Clinical and genetic abnormalities in patients with Friedreich's ataxia. *N Engl J Med* 1996; 335:1169–1175.
41. Filla A, De Michele G, Cavalcanti F, Pianese L, Monticelli A, Campanella G, Coccozza S. The relationship between trinucleotide (GAA) repeat length and clinical features in Friedreich ataxia. *Am J Hum Genet* 1996; 59:554–560.
42. Isnard R, Kalotka H, Durr A, Cossee M, Schmitt M, Pousset F, Thomas D, Brice A, Koenig M, Komajda M. Correlation between left ventricular hypertrophy and GAA trinucleotide repeat length in Friedreich's ataxia. *Circulation* 1997; 95:2247–2249.

43. Monros E, Molto MD, Martinez F, Canizares J, Blanca J, Vilchez JJ, Prieto F, de Frutos R, Palau F. Phenotype correlation and intergenerational dynamics of the Friedreich ataxia GAA trinucleotide repeat. *Am J Hum Genet* 1997; 61:101–110.
44. Montermini L, Richter A, Morgan K, Justice CM, Castellotti B, Mercier J, Poirier J, Czposoli F, Bouchard JP, Lemieux B, Mathieu J, Vanasse M, Seni MH, Graham G, Andermann F, Andermann E, Melancon SB, Keats BJ, DiDonato S, Pandolfo M. Phenotypic variability in Friedreich ataxia: role of the associated GAA triplet repeat expansion. *Ann Neurol* 1997; 41:675–682.
45. Alikasifoglu M, Topaloglu H, Tuncbilek E, Ceviz N, Anar B, Demir E, Ozme S. Clinical and genetic correlate in childhood onset Friedreich ataxia. *Neuropediatrics* 1999; 30:72–76.
46. Santoro L, De Michele G, Perretti A, Crisci C, Coccozza S, Cavalcanti F, Ragno M, Monticelli A, Filla A, Caruso G. Relation between trinucleotide GAA repeat length and sensory neuropathy in Friedreich's ataxia. *J Neurol Neurosurg Psychiatry* 1999; 66:93–96.
47. Webb S, Doudney K, Pook M, Chamberlain S, Hutchinson M. A family with pseudo-dominant Friedreich's ataxia showing marked variation of phenotype between affected siblings. *J Neurol Neurosurg Psychiatry* 1999; 67:217–219.
48. Klopstock T, Chahrokh-Zadeh S, Holinski-Feder E, Meindl A, Gasser T, Pongratz D, Muller-Felber W. Markedly different course of Friedreich's ataxia in sib pairs with similar GAA repeat expansions in the frataxin gene. *Acta Neuropathol (Berl)* 1999; 97:139–142.
49. Bidichandani SI, Garcia CA, Patel PI, Dimachkie MM. Very late-onset Friedreich ataxia despite large GAA triplet repeat expansions. *Arch Neurol* 2000; 57:246–251.
50. Musco G, de Tommasi T, Stier G, Kolmerer B, Bottomley M, Adinolfi S, Muskett FW, Gibson TJ, Frenkiel TA, Pastore A. Assignment of the 1H, 15N, and 13C resonances of the C-terminal domain of frataxin, the protein responsible for Friedreich ataxia. *J Biomol NMR*. 1999; 15:87–88.
51. Koutnikova H, Campuzano V, Koenig M. Maturation of wild-type and mutated frataxin by the mitochondrial processing peptidase. *Hum Mol Genet* 1998; 7:1485–1489.
52. Branda SS, Cavadini P, Adamec J, Kalousek F, Taroni F, Isaya G. Yeast and human frataxin are processed to mature form in two sequential steps by the mitochondrial processing peptidase. *J Biol Chem* 1999; 274:22763–22769.
53. Gordon DM, Shi Q, Dancis A, Pain D. Maturation of frataxin within mammalian and yeast mitochondria: one-step processing by matrix processing peptidase. *Hum Mol Genet* 1999; 8:2255–2262.
54. Knight SA, Sepuri NB, Pain D, Dancis A. Mt-Hsp70 homolog, Ssc2p, required for maturation of yeast frataxin and mitochondria iron homeostasis. *J Biol Chem* 1998; 273:18389–18393.
55. Delatycki MB, Camakaris J, Brooks H, Evans-Whipp T, Thorburn DR, Williamson R, Forrest SM. Direct evidence that mitochondrial iron accumulation occurs in Friedreich ataxia. *Ann Neurol* 1999; 45:673–675.
56. Waldvogel D, van Gelderen P, Hallett M. Increased iron in the dentate nucleus of patients with Friedreich's ataxia. *Ann Neurol* 1999; 46:123–125.
57. Hentze MW, Kuhn LC. Molecular control of vertebrate iron metabolism: mRNA-based regulatory circuits operated by iron, nitric oxide, and oxidative stress. *Proc Natl Acad Sci USA* 1996; 93:8175–8182.
58. Rouault TA, Klausner RD. Iron-sulfur clusters as biosensors of oxidants and iron. *Trends Biochem Sci* 1996; 21:174–177.
59. Richardson DR, Ponka P. The molecular mechanisms of the metabolism and transport of iron in normal and neoplastic cells. *Biochim Biophys Acta* 1997; 1331:1–40.

60. Radisky DC, Babcock MC, Kaplan J. The yeast frataxin homologue mediates mitochondrial efflux. Evidence for a mitochondrial iron cycle. *J Biol Chem* 1999; 274:4497–4499.
61. Nicholls DG, Crompton M. Mitochondrial calcium transport. *FEBS Lett* 1980; 111:261–268.
62. Weaver J, Pollack S. Two type of receptors for iron on mitochondria. *Biochem J* 1990; 271:463–466.
63. Flatmark T, Romslo I. Energy-dependent accumulation of iron by isolated rat liver mitochondria. Requirement of reducing equivalents and evidence for a unidirectional flux of Fe(II) across the inner membrane. *J Biol Chem* 1975; 250:6433–6438.
64. Konopka K, Romslo I. Studies on the mechanism of pyrophosphate-mediated uptake of iron from transferrin by isolated rat-liver mitochondria. *Eur J Biochem* 1981; 117:239–244.
65. Kispal G, Csere P, Prohl C, Lill R. The mitochondrial proteins Atm 1p and Nfs 1p are essential for biogenesis of cytosolic Fe/S proteins. *EMBO J* 1999; 18:3981–3989.
66. Lill R, Diekert K, Kaut A, Lange H, Pelzer W, Prohl C, Kispal G. The essential role of mitochondria in the biogenesis of cellular iron-sulfur proteins. *Biol Chem* 1999; 380: 1157–1166.
67. Nakai Y, Yoshihara Y, Hayashi H, Kagamiyama H. cDNA cloning and characterization of mouse nifS-like protein, m-Nfs1: mitochondrial localization of eukaryotic NifS-like proteins. *FEBS Lett* 1998; 433:143–148.
68. Kispal G, Csere P, Guiard B, Lill R. The ABC transporter Atm 1p is required for mitochondrial iron homeostasis. *FEBS Lett* 1997; 418:346–350.
69. Csere P, Lill R, Kispal G. Identification of a human mitochondrial ABC transporter, the functional orthologue of yeast Atm 1p. *FEBS Lett* 1998; 441:266–270.
70. Allikmets R, Raskind WH, Hutchinson A, Schueck ND, Dean M, Koeller DM. Mutation of a putative mitochondrial iron transporter gene (ABC7) in X-linked sideroblastic anemia and ataxia (XLSA/A). *Hum Mol Genet* 1999; 8:743–749.
71. Foury F. Low iron concentration and aconitase deficiency in a yeast frataxin homologue deficient strain. *FEBS Lett* 1999; 456:281–284.
72. Cossée M, Puccio H, Gansmuller A, Koutnikova H, Dierich A, LeMeur M, Fischbeck K, Dolle P, Koenig M. Inactivation of the Friedreich ataxia mouse gene leads to early embryonic lethality without iron accumulation. *Hum Mol Genet* 2000; 9:1219–1226.
73. Puccio H, Simon D, Cossée M, Criqui-Filippe P, Tiziano F, Melki J, Kahn R, Hindelang C, Matyas R, Rustin P, Koenig M. Mouse models for Friedreich ataxia exhibit cardiomyopathy, sensory nerve defect and Fe-S enzyme deficiency followed by intramitochondrial iron deposits. *Nature Genet* 2001; 27:181–186.
74. Isaya G, Adamec J, Rusnak F, Owen WG, Naylor S, Benson LM. Frataxin is an iron-storage protein. *Am J Hum Genet* 1999; 65:A167.
75. Fridovich I. Superoxide radical and superoxide dismutase. *Annu Rev Biochem* 1995; 64:97–112.
76. Branda SS, Yang ZY, Chew A, Isaya G. Mitochondrial intermediate peptidase and the yeast frataxin homolog together maintain mitochondrial iron homeostasis in *Saccharomyces cerevisiae*. *Hum Mol Genet* 1999; 8:1099–1110.
77. Lange H, Kispal G, Lill R. Mechanism of iron transport to the site of heme synthesis inside yeast mitochondria. *J Biol Chem* 1999; 274:18989–18996.
78. Li DS, Ohshima K, Jiralerspong S, Bojanowski MW, Pandolfo M. Knock-out of the *cyaY* gene in *Escherichia coli* does not affect cellular iron content and sensitivity to oxidants. *FEBS Lett* 1999; 456:13–16.
79. Furukawa T, Kohno H, Tokunaga R, Takeni S. Nitric oxide-mediated inactivation of mammalian ferrochelatase in vivo and in vitro: possible involvement of the iron-sulphur cluster of the enzyme. *Biochem J* 1995; 310:533–538.

80. Lodi R, Cooper JM, Bradley JL, Manners D, Styles P, Taylor DJ, Schapira AH. Deficit of in vivo mitochondrial ATP production in patients with Friedreich ataxia. *Proc Natl Acad Sci USA* 1999; 96:11492–11495.
81. Wilson RB, Lynch DR, Fischbeck KH. Normal serum iron and ferritin concentrations in patients with Friedreich's ataxia. *Ann Neurol* 1998; 44:132–134.
82. Wong A, Yang J, Cavadini P, Gellera C, Lonnerdal B, Taroni F, Cortopassi G. The Friedreich's ataxia mutation confers cellular sensitivity to oxidant stress which is rescued by chelators of iron and calcium and inhibitors of apoptosis. *Hum Mol Genet* 1999; 8: 425–430.
83. Hoyes KP, Porter JB. Subcellular distribution of desferrioxamine and hydroxypyridin-4-one chelators in K562 cells affects chelation of intracellular iron pools. *Br J Hematol* 1993; 85:393–400.
84. Rustin P, Munnich A, Rotig A. Quinone analogs prevent enzymes targeted in Friedreich ataxia from iron-induced injury in vitro. *Biofactors* 1999; 9:247–251.
85. Helveston W, Cibula JE, Hurd R, Uthman BM, Wilder BJ. Abnormalities of antioxidant metabolism in a case of Friedreich's disease. *Clin Neuropharmacol* 1996; 19:271–275.
86. Yokota T, Shiojiri T, Gotoda T, Arita M, Arai H, Ohga T, Kanda T, Suzuki J, Imai T, Matsumoto H, Harino S, Kiyosawa M, Mizusawa H, Inoue K. Friedreich-like ataxia with retinitis pigmentosa caused by the His101Gln mutation of the alpha-tocopherol transfer protein gene. *Ann Neurol* 1997; 41:826–832.
87. Hammans SR, Kennedy CR. Ataxia with isolated vitamin E deficiency presenting as mutation negative Friedreich's ataxia. *J Neurol Neurosurg Psychiatry* 1998; 64:368–370.
88. Cavalier L, Ouahchi K, Kayden HJ, Di Donato S, Reutenauer L, Mandel JL, Koenig M. Ataxia with isolated vitamin E deficiency: heterogeneity of mutations and phenotypic variability in a large number of families. *Am J Hum Genet* 1998; 62:301–310.
89. Li L, Kaplan J. Characterization of two homologous yeast genes that encode mitochondrial iron transporters. *J Biol Chem* 1997; 272:28485–28493.

12

Siderophore Chemistry

ALAIN STINTZI and KENNETH N. RAYMOND

University of California, Berkeley, California

I. INTRODUCTION	274
II. SIDEROPHORE STRUCTURES AND DIVERSITIES	274
A. Siderophores and Their Producers	274
B. Catecholate Siderophores	275
C. Hydroxamate Siderophores	279
D. Carboxylate Siderophores	284
E. Mixed Siderophores and Others	284
III. CHEMICAL SYNTHESIS OF NATURAL SIDEROPHORES	288
A. General Overview of Siderophore Synthesis	288
B. Synthesis of Catecholate Siderophores	289
C. Synthesis of Hydroxamate Siderophores	294
IV. METAL COMPLEXATION AND COORDINATION GEOMETRY	296
A. Thermodynamics of Siderophore Iron Binding	296
B. Coordination Geometry and Stereochemistry of Siderophores	298
V. SYNTHETIC MODELS FOR SIDEROPHORES AND THEIR USE AS PROBES OF FERRIC–SIDEROPHORE PROPERTIES AND TRANSPORT	299
A. Siderophore Analogs—A Powerful Tool to Study the Physicochemical Properties of Siderophores	300
B. Synthetic Models for Siderophores and Their Use in Probing Ferric–Siderophore Transport	303
VI. ISOLATION AND CHARACTERIZATION OF NEW SIDEROPHORES	306
VII. DRUG–SIDEROPHORE CONJUGATES AND THEIR POTENTIAL APPLICATIONS	307

VIII. CONCLUSION AND PERSPECTIVES	307
ACKNOWLEDGMENTS	308
REFERENCES	308

I. INTRODUCTION

In an aerobic neutral pH environment, the concentration of free $[\text{Fe}^{3+}]$ is limited to 10^{-18} M by the insolubility of $\text{Fe}(\text{OH})_3$. Similarly, the concentration of iron available to mammalian bacterial pathogens is low because it is sequestered by host proteins such as serum transferrin and lactoferrin (1,2), hence serum is bacteriostatic (3). Most microorganisms circumvent this nutritional limitation by producing siderophores, which are low-molecular-weight-compounds excreted under iron-limited conditions (4–7). These chelating agents strongly and specifically bind, solubilize, and deliver iron to microbial cells via specific cell surface receptors (4–10). The coordination geometry and chemical structure of these siderophores play a key role in ferric–siderophore recognition and transport (4,7). This chapter addresses only the chemistry of natural siderophores. However, this review will take into account the relevance of siderophore analogs to study the physicochemical properties of siderophores as well as their use in probing ferric–siderophore recognition.

II. SIDEROPHORE STRUCTURES AND DIVERSITIES

A. Siderophores and Their Producers

Siderophores commonly occur in three broad groups based on the chemical nature of the metal-binding functionality (4,5,7), catecholates, hydroxamates, or hydroxycarboxylates (Fig. 1). With the ongoing purification and characterization of new siderophores, the variety of resolved siderophore structures has greatly expanded and now includes siderophores with backbones of oxazoline, thiazoline, hydroxypyridinone, α - and β -hydroxy acids, and α -keto acids. The ligand denticity (number of coordinating atoms per molecule) constitutes an important feature of siderophores and ranges from bidentate to hexadentate chelators. Even though there is a great diversity among siderophores, there are also a few similarities. Siderophores contain hard donor atoms (often oxygen and to a lesser extent nitrogen or sulfur) and form thermodynamically stable, high-spin Fe^{3+} species, with a low reduction potential in the range of -0.33 V (for triacetylfulsarinin) to -0.75 V (for enterobactin) (11,12).

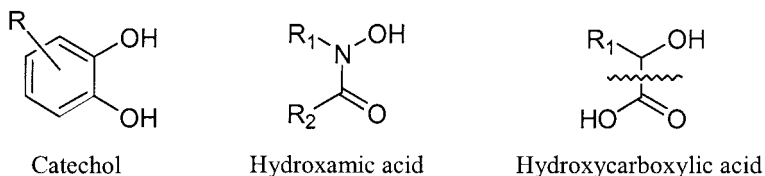


Figure 1 Principal functional groups in siderophores.

The preferred electronic configuration of Fe^{3+} in the ferric–siderophore complexes is the six-coordinate octahedron, in which each of the five $3d$ orbitals is occupied by one electron. This geometry is relatively easy to distort because the ferric ion does not have any directional preferences due to ligand-field stabilization.

A collection of siderophores produced by bacteria and fungi is presented in Tables 1 and 2, respectively. Although many siderophores and the microorganisms which produce them are listed in these two tables, we do not intend to give a complete synopsis of all known siderophores and their producers. Indeed, more than 200 siderophores have now been characterized. In addition, several bacteria excrete multiple siderophores, since specific siderophores may be more efficient than others under particular circumstances. For example, some *Escherichia coli* strains produce both enterobactin and aerobactin (Table 1). While aerobactin competes successfully in vivo for iron with the host iron-binding proteins, enterobactin cannot (due to its inactivation by serum albumin) (13). This is supported by conclusive experimental evidence which demonstrates the role of aerobactin as an associated virulence factor (14,15). The production of several siderophores may give the microbe the ability to colonize different environments. Enterobactin and aerobactin are exclusively synthesized by bacteria of the family Enterobacteriaceae, such as *E. coli* (16), *Shigella* (17), *Salmonella* (16,18), *Yersinia* (19), and *Klebsiella* (20) species. On the other hand, the ferrioxamine siderophores are produced by various microbes ranging from Gram-negative to Gram-positive bacteria, including *Streptomyces* species (21,22), *Erwinia herbicola* (23), or *Pseudomonas stutzeri* (24). Fungal siderophores commonly use hydroxamate groups as their iron-chelating functionality (Table 2). However, with the continuing characterization of new siderophores, other functional group types have been recently reported. Hydroxy carboxylate-containing siderophores—for example, rhizoferrin—are produced by fungi of the Zygomycete group (such as *Rhizopus* strains) (25,26). We also note that the production of phenolate-catecholate siderophores has been identified in wood-decaying basidiomycetes (27).

B. Catecholate Siderophores

Of all the catecholate siderophores, enterobactin, produced by Enterobacteriaceae such as *E. coli*, has received the most attention. Since its report in 1970 by O'Brien and Gibson (16) and Pollak and Neilands (18), enterobactin has been studied with regard to solution thermodynamics, microbial transport, catecholate siderophore synthesis, and biosynthetic pathways. The enterobactin molecule possesses threefold symmetry and is composed of three 2,3-dihydroxybenzoic acid groups, each one appended to an L-serine group. The three serines form a trilactone macrocycle backbone (Fig. 2). Metal coordination at neutral pH occurs through the six catecholate oxygens. A related siderophore, corynebactin, produced by *Corynebacterium glutamicum* (28), has also been characterized. Interestingly, corynebactin is the only other example of a siderophore containing a trilactone backbone. As shown in Fig. 2, corynebactin is composed of three identical units consisting of 2,3-dihydroxybenzoic acid, glycine, and L-threonine.

Several linear catecholate siderophores have also been identified, including protochelin, cepaciachelin, azotobactin, and aminochelin (Fig. 2). All of them, except cepaciachelin [from *Burkholderia cepacia* (29)], are produced by *Azotobacter vinelandii* (30–33). Protochelin contains three units of 2,3-dihydroxybenzoic acid at

Table 1 Bacterial Siderophores and Producing Organisms

Siderophores	Producing strains	Ref.
Acinetobactin	<i>Acinetobacter baumannii</i> , <i>A. haemolyticus</i>	76
Acinetoferrin	<i>Acinetobacter haemolyticus</i>	71
Aerobactin	<i>Aerobacter aerogenes</i> , <i>Escherichia coli</i> , <i>Shigella flexneri</i> , <i>S. boydii</i> , <i>Salmonella</i> spp., <i>Yersinia intermedia</i> , <i>Y. frederiksenii</i> , <i>Y. kristensii</i> , <i>Serratia</i> <i>ficaria</i> , <i>S. liquefaciens</i> , <i>Vibrio</i> <i>hollisae</i> , <i>V. mimicus</i>	14,19,66,173,194–197
Agrobactin	<i>Agrobacterium tumefaciens</i>	34
Alcaligin	<i>Alcaligenes xylooxidans</i> subsp. <i>xylooxidans</i> , <i>Bordetella pertussis</i> , <i>B. bronchiseptica</i>	52–54
Alterobactin A and B	<i>Alteromonas luteoviolacea</i>	73
Aminochelin	<i>Azotobacter vinelandii</i>	30
Amonabactin	<i>Aeromonas hydrophila</i>	40
Anguibactin	<i>Vibrio anguillarum</i>	77
Arthrobactin	<i>Arthrobacter pascens</i>	67
Azotobactin	<i>Azotobacter vinelandii</i>	31
Azotochelin	<i>Azotobacter vinelandii</i>	198
Azoverdin	<i>Azomonas macrocygenes</i>	199
Bisucaberin	<i>Alteromonas hyloplantis</i>	55
Cepabactin	<i>Pseudomonas cepacia</i>	58
Cepaciachelin	<i>Burkholderia cepacia</i>	29
Chryseomonin	<i>Chryseomonas luteola</i>	200
Chrysobactin	<i>Erwinia chrysanthemi</i> , <i>E. carotovora</i> subsp. <i>carotovora</i> , <i>Serratia</i> <i>marcescens</i> , <i>Chryseomonas luteola</i>	37,38
Corrugatin	<i>Pseudomonas corrugata</i>	201
Corynebactin	<i>Corynebacterium glutamicum</i>	28
Enterobactin	<i>Escherichia coli</i> , <i>Salmonella</i> <i>typhimurium</i> , <i>Shigella</i> spp., <i>Klebsiella</i> spp., <i>Aeromonas hydrophila</i> , <i>Aerobacter aerogenes</i> , <i>Serratia</i> <i>marcescens</i> W225	16–18,39
Exochelin MN	<i>Mycobacterium neoaurum</i>	85
Exochelin MS	<i>Mycobacterium smegmatis</i>	86
Exochelin MB	<i>Mycobacterium bovis</i>	202
Ferribactin	<i>Pseudomonas fluorescens</i>	92,203
Ferrioxamines (A ₁ , A ₂ , B, C, D ₁ , D ₂ , E, F, G, H)	<i>Streptomyces pilosus</i> , <i>S. griseus</i> , <i>S. griseoflavus</i> , <i>S. olivaceus</i> , <i>S. aureofaciens</i> , <i>S. galilaeus</i> , <i>S. lavendulae</i> , <i>Arthrobacter simplex</i> , <i>Streptomyces viridosporus</i> , <i>Pseudomonas stutzeri</i> , <i>Chromobacterium violaceum</i> , <i>Streptomyces ambocicus</i> , <i>Hafnia</i> <i>alvei</i> , <i>Streptomyces coelicolor</i> , <i>S. lividans</i>	7,173

Table 1 Continued

Siderophores	Producing strains	Ref.
Ferrithiocin	<i>Streptomyces</i>	78
Ferrosamine A	<i>Erwinia rapontici</i>	204
Fluvibactin	<i>Vibrio fluvialis</i>	36
Itoic acid (2,3-dihydroxy-benzoyl-glycine)	<i>Bacillus subtilis</i>	205
Maduraferrin	<i>Actinomadura madurae</i>	206
Mycobactins	<i>Mycobacteria</i>	83
Myxochelin	<i>Angiococcus disciformis</i>	207
Nannochelins	<i>Nannocystis excedens</i>	72
N-deoxyschizokinen	<i>Bacillus megaterium</i>	208
Nocobactin	<i>Nocardia asteroides</i> , <i>N. brasiliensis</i>	209
Ornibactin	<i>Burkholderia cepacia</i>	75
Parabactin	<i>Paracoccus denitrificans</i>	34
Protochelin	<i>Azotobacter vinelandii</i>	32
Putrebactin	<i>Shewanella putrefaciens</i>	56
Pyochelin	<i>Pseudomonas aeruginosa</i>	79
Pyoverdine	<i>Pseudomonas aeruginosa</i> , <i>P. putida</i> , <i>P. fluorescens</i> , <i>P. chlororaphis</i> , <i>P. tolaasii</i> , <i>P. aptata</i> , <i>P. B10</i> , <i>P. 7SR1</i>	24,210
Rhizobactin 1021	<i>Rhizobium meliloti</i>	211
Enantio-Rhizoferrin	<i>Ralstonia pickettii</i>	212
Schizokinen	<i>Bacillus megaterium</i> , <i>Ralstonia solanacearum</i>	68,69
Serratiochelin	<i>Serratia marcescens</i>	37
Spirillobactin	<i>Azospirillum brasiliense</i>	213
Staphyloferrin A and B	<i>Staphylococcus aureus</i> , <i>S. hyicus</i>	60,61
Vibriobactin	<i>Vibrio cholerae</i>	35
Vibrioferrin	<i>Vibrio parahaemolyticus</i>	214
Vicibactin	<i>Rhizobium leguminosarum</i>	215
Vulnibactin	<i>Vibrio vulnificus</i>	216
Yersiniabactin	<i>Yersinia pestis</i> , <i>Y. enterocolitica</i>	80,82

tached to a linear backbone formed by the amide of lysine with diaminobutane. Both cepaciachelin and azotochelin could be considered as either degradation products or precursors for protochelin. Aminochelin contains a single unit of 2,3-dihydroxybenzoic acid and can be regarded as the complementary part of azotochelin to form protochelin. Generally, the higher-denticity ligand forms a stronger ferric complex. Even when the formation constant for a ferric–siderophore complex is the same for ligands of different denticity, a hexadentate ferric–siderophore complex will be favored over a tetradentate or bidentate one (see Sec. IV) (7).

Catecholate siderophores containing triamine spermidine as a backbone include parabactin, from *Paracoccus denitrificans* (34), which contains two 2,3-dihydroxybenzoic acids and one hydroxyphenyl group linked to the backbone with a threonine residue, present as an oxazoline ring. Agrobactin, isolated from culture of *Agrobacterium tumefaciens* (34) differs from parabactin only in that it is composed of three

Table 2 Fungal Siderophores and Producing Organisms

Siderophores	Producing strains	Ref.
6-L-Alanineferrirubin	<i>Aspergillus ochraceus</i>	217
Coprogen	<i>Neurospora crassa</i> , <i>Penicillium camemberti</i> , <i>P. chrysogenum</i> , <i>P. citrinum</i> , <i>P. notatum</i> , <i>P. patulum</i> , <i>P. urticae</i> , <i>Curvularia lunata</i> , <i>Epicoccum purpurascens</i>	41,47,218,219
Coprogen B	<i>Histoplasma capsulatum</i> , <i>Fusarium</i> sp., <i>F. dimerum</i> , <i>Myrothecium striatisporium</i> , <i>M. verrucaria</i> , <i>Gliocladium virens</i> , <i>Stemphylium botryosum</i> , <i>Verticillium dahliae</i>	47,220
Dimerum acid	<i>Fusarium dimerum</i> , <i>Stemphylium botryosum</i> , <i>Verticillium dahliae</i> , <i>Gliocladium virens</i>	47,221,222
Ferrichrome	<i>Ustilago sphaerogena</i> , <i>U. maydis</i> , <i>Aspergillus niger</i> , <i>A. quadricinctus</i> , <i>Penicillium parvum</i> , <i>Neovossia indica</i> , <i>Trichophyton mentagrophytes</i>	41,173
Ferrichrysin	<i>Aspergillus melleus</i> , <i>A. ochraceus</i>	173,223
Ferricrocin	<i>Aspergillus</i> spp., <i>A. fumigatus</i> , <i>A. viridi-nutans</i> , <i>Neurospora crassa</i> , <i>Microsporum canis</i> , <i>Colletrichum gloeosporioides</i>	219,224,225
Ferrirhodin	<i>Aspergillus nidulans</i> , <i>A. versicolor</i> , <i>Botrytis cinerea</i> , <i>Verucobotrys</i>	226,227
Ferrirubin	<i>Penicillium variabile</i> , <i>P. rugulosum</i> , <i>Aspergillus ochraceus</i> , <i>Paecilomyces varioti</i>	173,223
Fusarinine (A, B)	<i>Fusarium roseum</i>	228
Fusarinine C	<i>Fusarium cubense</i> , <i>F. roseum</i> , <i>Aspergillus fumigatus</i> , <i>Giberella fujikuroi</i> , <i>Penicillium chrysogenum</i> , <i>Paecilomyces varioti</i>	41,173,229
Hydroxycorpogen	<i>Alternaria longipes</i>	50
Isotriornicin	<i>Epicoccum purpurascens</i>	230
Malonichrome	<i>Fusarium roseum</i>	231
N ^α -dimethylcoprogen	<i>Alternaria alternata</i>	49
N ^α -dimethylneocoprogen I	<i>Alternaria alternata</i>	49
N ^α -dimethylisoneocoprogen I	<i>Alternaria alternata</i>	49
Neocoprogen I	<i>Curvularia lunata</i>	232
Neocoprogen II	<i>Curvularia lunata</i>	232

Table 2 Continued

Siderophores	Producing strains	Ref.
Rhizoferrin	<i>Mucor mucedo</i> , <i>Chaetostylum fresenii</i> , <i>Cokeromyces recurvatus</i> , <i>Mycotypha africana</i> , <i>Cunninghamella elegans</i> , <i>Rhizopus</i> <i>microsporus</i> var. <i>rhizopodiformis</i>	25,26,233
Rhodotorulic acid	<i>Rhodotorula rubra</i> , <i>R. pilimanae</i> , <i>R. glutinis</i> , <i>Leucosporidium</i> spp., <i>Rhodosporidium</i> spp., <i>Sporidiobolus</i> spp., <i>Sporobolomyces</i> spp., <i>Microbotyrum violaceum</i> , <i>M. major</i> ; <i>Sphacelotheca</i> spp.	41,44,218
Siderochelin	<i>Nocardia</i>	243
Triacetylfusarine C	<i>Aspergillus fumigatus</i> , <i>A. deflectus</i> , <i>Mycelia sterilia</i>	234
Triornicin	<i>Epicoccum purpurascens</i>	235

2,3-dihydroxybenzoic acid groups. The two related compounds vibriobactin and flavibactin, isolated from *Vibrio cholerae* (35) and *V. vulnificus* (36), respectively, have nor-spermidine instead of spermidine as a backbone, and vibriobactin contains an additional oxazoline ring. *Serratia marcesens* produces two siderophores, chryso-bactin and serratiochelin (37). Serratiochelin could be considered a tetradentate analog of agrobactin. Chryso-bactin, also produced by *Erwinia chrysanthemii* (38), is composed of one unit of 2,3-dihydroxybenzoic acid attached to a backbone composed of lysine and serine residues with D and L configurations, respectively.

Amonabactins are a set of four bis-catecholate siderophores produced by *Aeromonas hydrophila* (39,40) and are composed of an amino acid backbone containing two lysines, one (L configuration) phenylalanine or tryptophan and an optional glycine.

C. Hydroxamate Siderophores

Hydroxamate siderophores are produced by both bacteria and fungi (7,41). The siderophores earlier characterized, such as ferrichromes, coprogens, ferrioxamines, fusarines, and mycobactins, have been intensively reviewed (7,41), so only a short description of their structures follows. Structures of the principal hydroxamate siderophores are presented in Fig. 3. The hydroxamate moiety is a bidentate ligand formed by an acyl group and a *N*-hydroxy group; all hydroxamate moieties originate from L-ornithine which is *N*⁸-hydroxylated or *N*⁶-acylated. In nature, hydroxamate siderophores are predominantly hexadentate (Tables 1 and 2) because of the concentration effect (7). Hydroxamate groups have two major resonance forms, one with a negative charge on a single oxygen atom, and one with a distributed negative charge over the two oxygen atoms. The nature of the carbonyl and nitrogen substituents, R₂ and R₁ (Fig. 1), plays an essential role in the charge distribution. The stability of the metal complex is enhanced when R₁ and R₂ promote donation of electron density

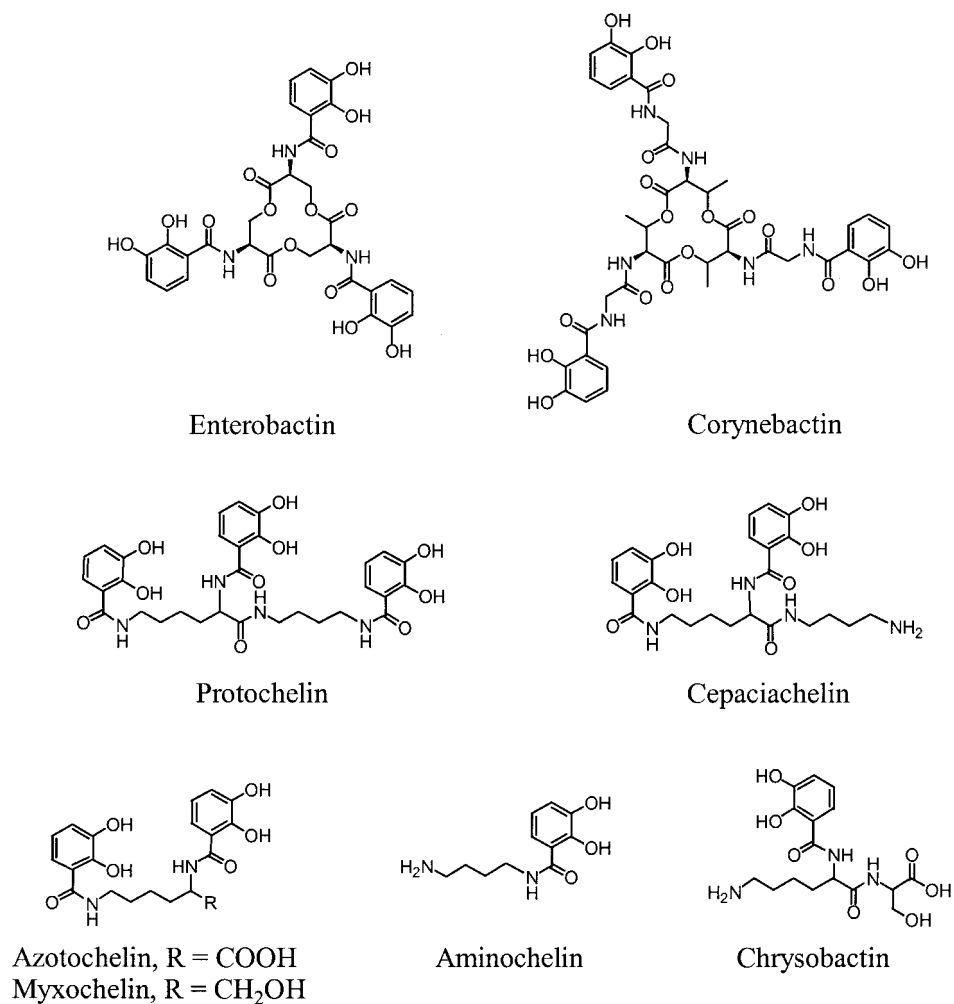
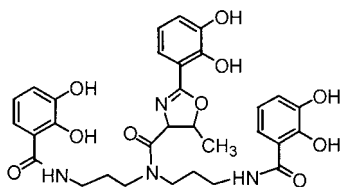


Figure 2 Catechololate (2,3-dihydroxybenzamide) siderophores.

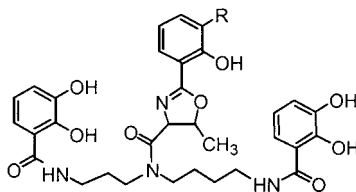
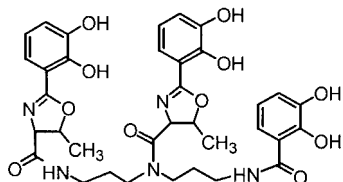
from the nitrogen lone pair to the carbonyl oxygen, so that both oxygen atoms are negatively charged.

Ferrichrome, isolated from the growth medium of *Ustilago sphaerogena*, was one of the first siderophores identified (42). Siderophores from the ferrichrome family are cyclic hexapeptides in which one tripeptide (of glycine, alanine, or serine) is linked to a second tripeptide of *N*^ε-acyl-*N*^δ-hydroxyornithine, and are exclusively produced by fungi, such as basidiomycetes and ascomycetes (43). Ferrichromes include various structural derivatives, such as ferricrocin, ferrichrome A, and ferrichrysin (41) (Fig. 3).

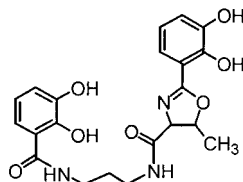
Rhodotorulic acid is also the primary siderophore of basidiomycetes (44). It is a dihydroxamate composed of the diketopiperazine of *N*^ε-acetyl-L-*N*^δ-hydroxyornithine. Dimerumic acid (45) is a derivative of rhodotorulic acid. Both siderophores form a 2:3 complex with two iron ions and three siderophore molecules.



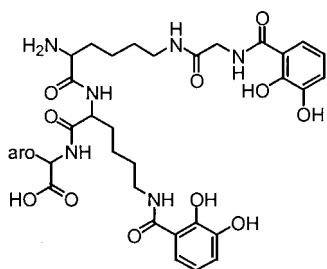
Fluvinbactin

Parabactin, R = H
Agrobactin, R = OH

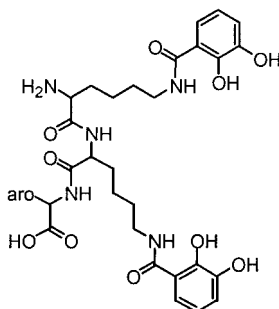
Vibriobactin



Serratiochelin



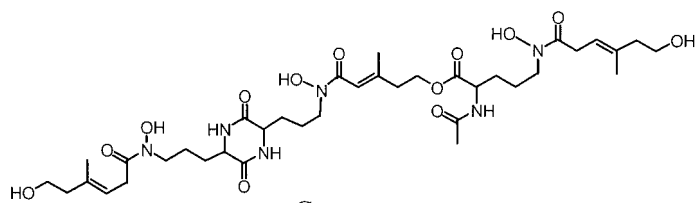
Amonabactins P750 and T789



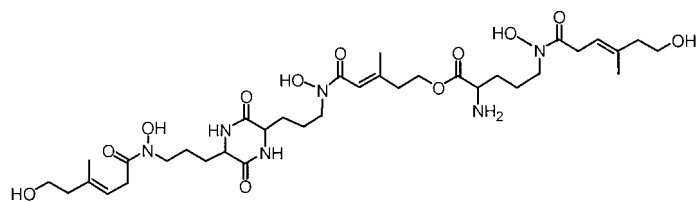
Amonabactins P693 and T732

Figure 2 Continued

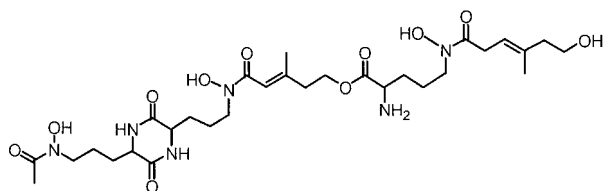
Since the first characterization of coprogen by Hesselstine in 1952 from the growth medium of *Penicillium* species and *Neurospora crassa* (46), several siderophores belonging to this family have been isolated from a number of different fungi (Table 2)—e.g., *Fusarium dimerum* (47), *Epicoccum purpurascens* (48), and *Aternaria longipes* (49,50). Only one coprogen-like siderophore, foxorymithine, has been shown to be produced by a bacterium, *Streptomyces nitrosporeus* (51). Coprogens are linear trihydroxamates composed of three units of N^{δ} -acyl- N^{β} -hydroxyornithine, three units of anhydromevalonic acid, and one unit of acetic acid. In the case of foxorymithine, the anhydromevalonyl group is replaced by a serine and the terminal N-hydroxy groups are formylated. Each fungus generally produces several coprogens, allowing the organism to adapt to various environments. All coprogens are hexadentate ligands, forming 1:1 complexes with Fe^{3+} .



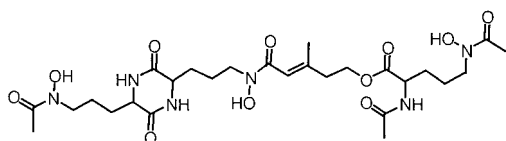
Coprogen



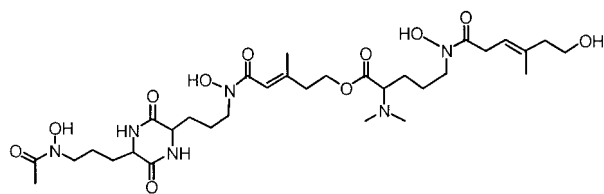
Desacetylcoprogen



Neocoprogen I



Neocoprogen II

N^α-dimethylcoprogen**Figure 3** Hydroxamate siderophores.

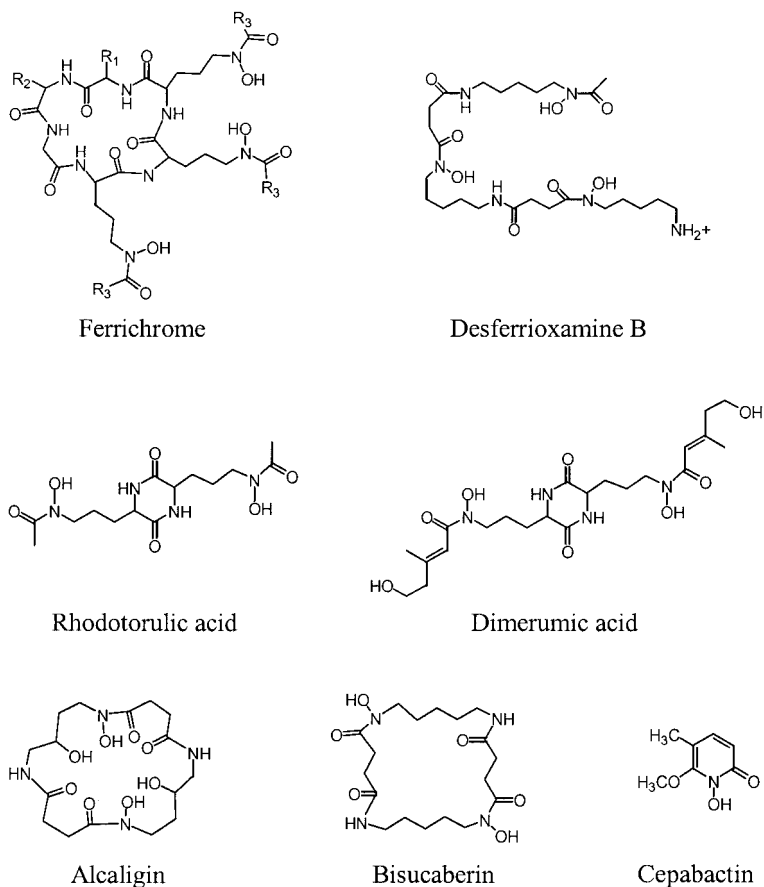


Figure 3 Continued

Among the hydroxamate siderophores identified, endocyclic ligands represent a distinctive structural family. Alcaligin is a cyclic bis-hydroxamate siderophore produced by an aquatic alga, *Alcaligenes xylosoxidans* subsp. *xylosoxidans* (52) as well as two mammalian pathogens, *Bordetella pertussis* (53), which causes whooping cough in humans, and *Bordetella bronchiseptica* (53,54), which is the agent of swine atrophic rhinitis and kennel cough in dogs. Bisucaberin and putrebactin, two structural analogs of alcaligin, are produced by the marine bacteria *Alteromonas hylolantis* (55) and *Shewanella putrefaciens* (56), respectively. Alcaligin and putrebactin are 20-membered macrocyclic dihydroxamate siderophores (Fig. 3), while bisucaberin is a 22-atom ring dihydroxamic acid. The tetradentate nature of these ligands is particularly interesting, since they need to form a binuclear metal complex with a stoichiometry Fe_2L_3 (L represents one dihydroxamate ligand). *Streptomyces pilosus* produces desferrioxamine E, a cyclic trihydroxamate siderophore (57), along with other desferrioxamine siderophores. Desferrioxamine E forms a FeL complex. All other desferrioxamine siderophores are linear trihydroxamates (Fig. 3), except des-

ferrioxamine H, which is an unusual pentadentate siderophore (21). The ferrioxamine siderophores are composed of acetate, succinate, and *o*-amino-*N*-hydroxyaminoalkane. Several ferrioxamine derivatives, named ferrimycins (7), display antibiotic activity. They are produced primarily by *Streptomyces* species and also by a few Gram-negative bacteria such as *Pseudomonas stutzeri* and *Herwinia herbicola* (4).

Cepabactin (1-hydroxy-5-methoxy-6-methylpyrid-6-one, Fig. 3) is a bidentate 1,2-hydroxypyridonate (aromatic hydroxamate) siderophore isolated from *Pseudomonas cepacia* (58). Cepabactin is also produced by some *Burkholderia cepacia* natural isolates and *Pseudomonas alcaligenes* strains (59). It is the only hydroxypyridinone known to be produced by a microorganism.

D. Carboxylate Siderophores

There are very few characterized siderophores containing an iron-chelating moiety composed of only carboxylate and α -hydroxy donor groups. Examples include staphyloferrin A and B, produced by staphylococci (60,61), rhizobactin, produced by *Rhizobium meliloti* (62), and rhizoferrin, produced by mucorales (25). The chemical structures of these siderophores are presented in Fig. 4. Staphyloferrin A, obtained from *Staphylococcus hyius* (60), is composed of D-ornithine substituted at N-1 and N-5 by amide bonds to the β -hydroxy groups of two citrate molecules. Staphyloferrin A forms a 1:1 complex with ferric ion. Staphyloferrin B has been isolated as a minor product from *Staphylococcus hyius* (61). This siderophore consists of a backbone of L-diaminopropionic acid, citrate, ethylenediamine, and α -oxoglutaric acid. Rhizoferrin is structurally similar to staphyloferrin A, lacking only a carboxylate residue on the backbone.

E. Mixed Siderophores and Others

Under this category we classify any siderophore that contains iron-binding groups different from those previously presented in this chapter. Some of these siderophores are represented in Fig. 5.

Several carboxylate/hydroxamate mixed siderophores have been isolated, including aerobactin, arthrobactin, shizokinen, acinetoferrin, and nannochelin. Aerobactin is a linear siderophore with a citrate backbone containing two hydroxamic acid chelating groups and one α -hydroxycarboxylic acid chelator. Aerobactin has

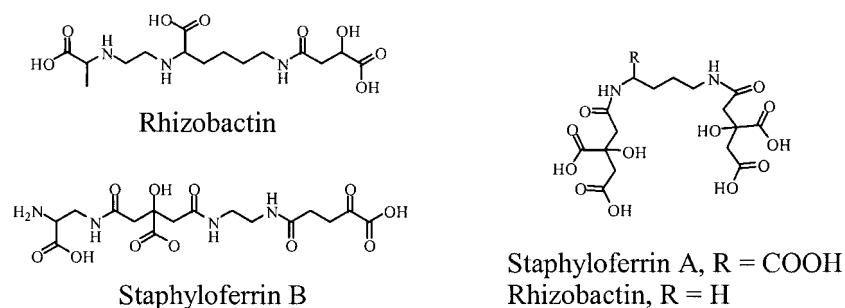
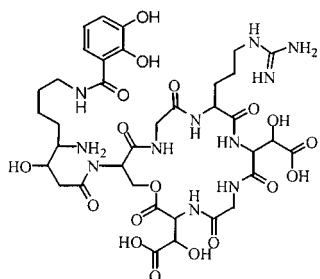
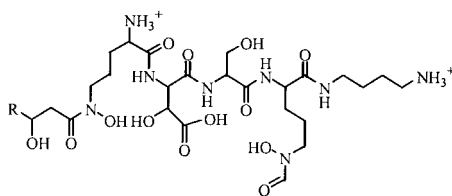


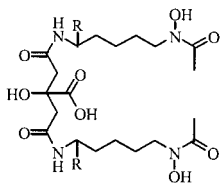
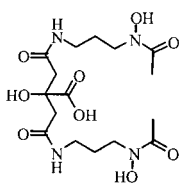
Figure 4 Hydroxycarboxylate siderophores.



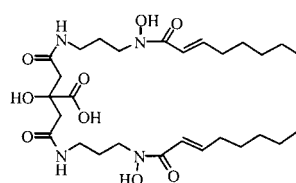
Alterobactin



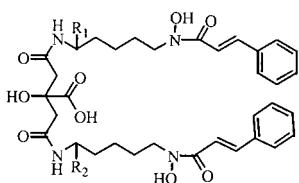
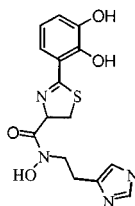
Ornibactin

Arthrobactin, R = H
Aerobactin, R = COOH

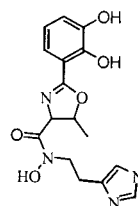
Schizokinen



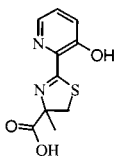
Acinetoferin

Nannochelin
A, R₁ = R₂ = COOMe
B, R₁ = COOMe, R₂ = COOH
C, R₁ = R₂ = COOH

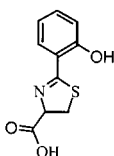
Anguibactin



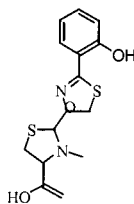
Acinetobactin



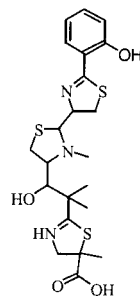
Desferrithiocin



Aeruginic acid



Pyochelin



Yersiniabactin

Figure 5 Mixed-ligand component siderophores.

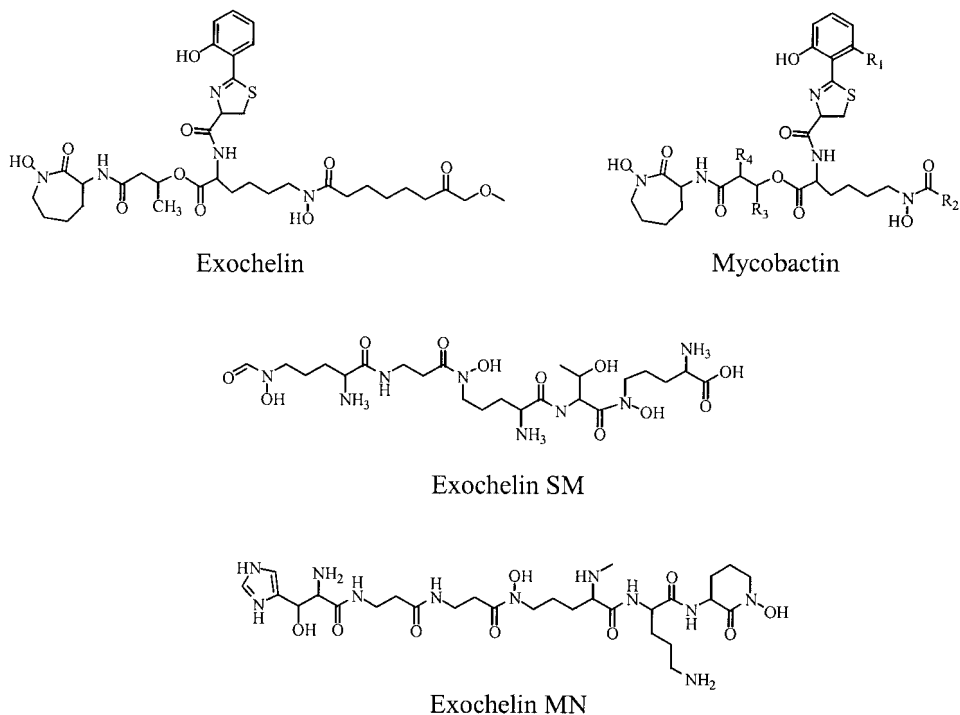


Figure 5 Continued

been isolated from *Aerobacter aerogenes* (63), *Escherichia* (64), *Salmonella* (65), *Shigella* (66), and many other bacteria. Arthrobactin, produced by *Arthrobacter* (67), differs from aerobactin only in that it lacks the two pendent carboxylates. Schizokinene is produced by *Bacillus megaterium* (68) as well as *Ralstonia solanacearum* (69) and *Anabaena* sp. strain 6411 (70). Schizokinene contains a citrate backbone substituted with 1-amino-3-(*N*-acetyl-*N*-hydroxylamino)propane. Acinetoferrin has been purified from the growth supernatant of *Acinetobacter haemolyticus* ATCC 17906 (71). It is a derivative of citric acid in which both carboxylic groups are symmetrically substituted with (*E*)-2-octanoic acid-*N*¹-hydroxy-*N*³-(*E*)-2-octenoyldiaminopropane. Nannochelin A, B, and C are three citrate-hydroxamate siderophores which are produced by the myxobacterium *Nannocystis exedens* strain Na e485 (72). Nannochelin contains a citric backbone symmetrically linked to two units of *N*⁶-cinnimoyl-*N*⁶-hydroxy-*L*-lysine.

Alterobactin siderophores (A and B) have been isolated from *Alteromonas luteoviolacea*, and are the first siderophore structurally characterized from an open-ocean bacterium (73). These have a cyclic peptide structure, with one catecholate and two hydroxycarboxylate units as iron-binding groups.

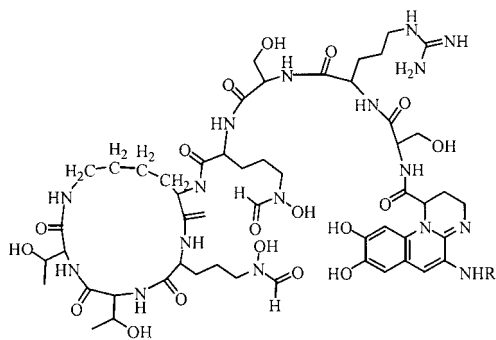
Ornibactin is another example of a mixed hydroxamate/carboxylate siderophore (Fig. 5). Ornibactin is produced by *Pseudomonas cepacia* (74), *Burkholderia vietnamiensis*, and *B. cepacia* (75). Ornibactins are modified tetrapeptide linear sidero-

phores containing a 1–4 diaminobutane (putrescine) residue and an acyl chain of 3-hydroxybutanoic acid, 3-hydroxyhexanoic acid, or 3-hydroxyoctanoic acid, giving three different ornibactin species: ornibactins C4, C6, and C8 (74).

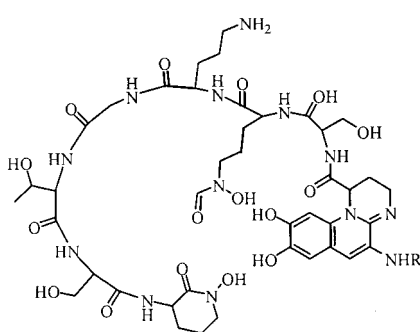
Acinetobactin has been identified in the growth supernatant of *Acinetobacter baumannii* ATCC 19606 and *A. haemolyticus* ATCC 17906 (76). It is composed of ω -*N*-hydroxyhistamine, threonine, and 2,3-dihydroxybenzoic acid, the last two components forming an oxazoline ring. Anguibactin, an analog of acinetobactin, has been isolated from *Vibrio anguillarum* (77). Both siderophores contain a catecholate and a hydroxamate iron-binding group. Desferrithiocin, an analog of aeruginosic acid, is produced by *Streptomyces* strains (78) and, like anguibactin, contains a diazoline ring. This siderophore complexes iron via the phenolate oxygen atom, the nitrogen atom of the diazoline ring, and the carboxylate oxygen atom. Pyochelin and yersiniabactin are produced by *Pseudomonas aeruginosa* (79) and *Yersinia* strains (80–82), respectively. Yersiniabactin contains a phenol and a thiazolidine ring, as well as two thiazoline rings. As seen in Fig. 5, pyochelin differs from yersiniabactin by the absence of a second thiazoline ring.

Mycobactins and exobactins are siderophores with complex peptidic backbones. Mycobactins are a family of siderophores which are produced by mycobacteria, including *Mycobacterium tuberculosis* and *M. plei* (83). All mycobactins contain a nearly identical molecular nucleus composed of two hydroxamic acid groups, a phenolate group, and one 2-(2-hydroxyphenyl)- Δ^2 -1,3-oxazoline residue, which constitute the iron chelating functionalities (Fig. 5). Mycobactins vary in the stereochemistry of the metal center and in the peripheral group, R₁₋₅ (Fig. 5). Siderophores from the exochelin family are also produced by mycobacteria species, such as *Mycobacterium tuberculosis* (84), *Mycobacterium neoaurum* (85), or *M. smegmatis* (86). Exochelin MN is the extracellular siderophore from *Mycobacterium neoaurum* (85). It has been characterized as a peptide, containing the unusual amino acid β -hydroxyhistidine and *N*-methyl groups. This siderophore coordinates iron(III) via two *cis*-hydroxamate units plus the hydroxyl and imidazole nitrogen of the β -hydroxyhistidine.

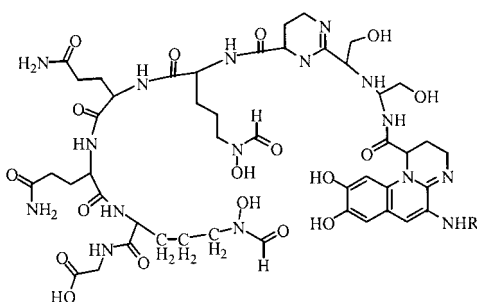
Fluorescent pseudomonad strains produce a number of related siderophores, termed pyoverdines and pseudobactins. Pyoverdine was the first siderophore to be characterized from the *Pseudomonas* species (87,88). Siderophores belonging to the pyoverdine family are heteropeptides composed of a linear or cyclic peptide, a small dicarboxylic acid (or its monoamide), and a quinoleinic chromophore (Fig. 6). The chromophore is identical for all pyoverdines characterized, except the one produced by *Pseudomonas putida* (89,90), which differs only in that the carboxylic group is attached to the C₃ instead of the C₁ of the quinoline cyclic ring. The chromophore structure is one of the binding sites for Fe³⁺ and confers the characteristic UV-visible spectrum and strong fluorescence to the molecule. Pyoverdine structures differ only in the amino acid composition of the peptidic part; these molecular structures have been thoroughly described (24,91). The peptidic structure provides the two other iron-binding groups (one β -hydroxy amino acid and one hydroxamic acid, or two hydroxamic acids) and plays an essential role in the mechanism of ferric-siderophore recognition with its cognate receptor. Ferribactin and azotobactin, produced by *Pseudomonas fluorescens* ATCC 13525 (91) and *Azotobacter vinelandii* (31), respectively, are similar to pyoverdine. Ferribactin is also produced by *Pseudomonas chlororaphis* (92) and has been proposed as a precursor of pyoverdine (91).



Pyoverdine group I

Pseudomonas aeruginosa ATCC15692

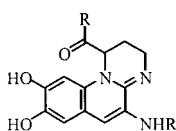
Pyoverdine group II

Pseudomonas aeruginosa ATCC27853

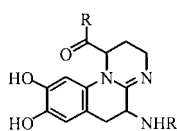
Pyoverdine group III

Pseudomonas aeruginosa R and Pa6

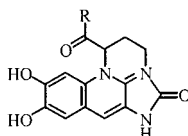
Chromophoric center of the pyoverdines and related siderophores



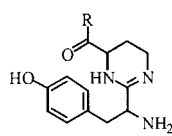
Pyoverdine



Pseudobactin A



Azotobactin



Ferribactin

Figure 6 Fluorescent siderophores of the pyoverdine type.

III. CHEMICAL SYNTHESIS OF NATURAL SIDEROPHORES

A. General Overview of Siderophore Synthesis

In the past two decades considerable effort has been devoted to the synthesis of natural siderophores and synthetic siderophore analogs, for several reasons. First, siderophores have been used as models for the design and synthesis of potential iron chelators in the treatment of iron overload [(93); see also Chapter 13]. In addition, the knowledge of siderophore synthesis is essential for the study of the relationship

between the structure and the physiochemical properties of the siderophore, and for the study of the mechanism of ferric–siderophore recognition and uptake by microbes. In this review we will discuss the synthesis of a selected number of siderophores rather than giving a complete synopsis of siderophore synthesis, since a considerable number of siderophores have been synthesized. These include, in alphabetical order, acinetoferrin (94), aerobactin (95), agrobactin (96,97), alcaligin (98), alterobactin A (99), amonabactin (40), arthrobactin (100), bisucaberin (101), chrysoactin (38,102), enterobactin (103–108), ferrichrome (109,110), desferrioxamine B (111,112), E (113), G (113), and H (114), mycobactin S2 (115,116), myxochelin B (117), nannochelin A (118,119), parabactin (120,121), rhizobactin (122), rhizoferrin (123), rhodotorulic acid (124–127), schizokinen (100), vibriobactin (128), and vibrioferrin (129,130).

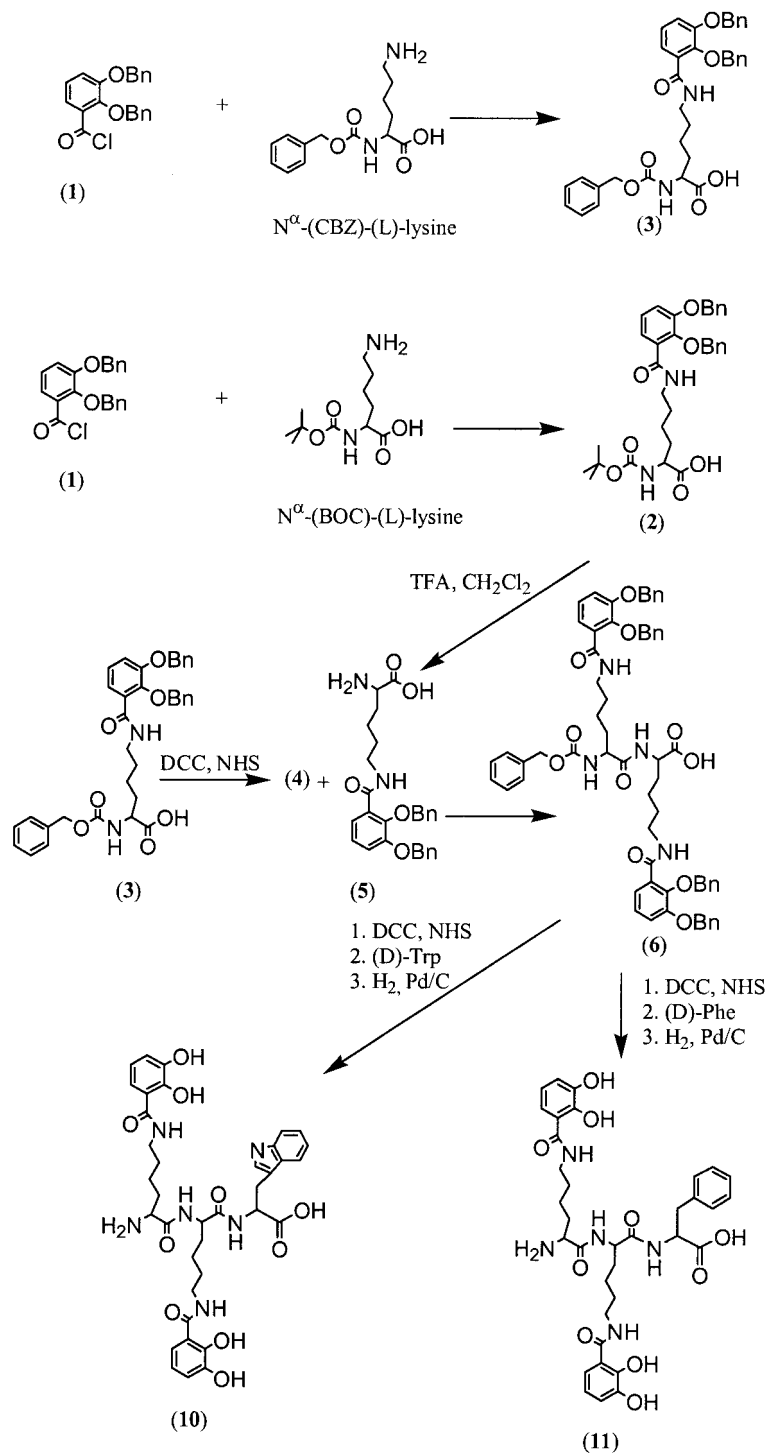
B. Synthesis of Catecholate Siderophores

Every catecholate siderophore has 2,3-dihydroxybenzoyl units attached via an amide linkage. The structure of the backbone can be a polyamine (for example, spermidine, nor-spermidine, or cadaverin), a peptidic, or a macrocyclic lactone. The synthesis of catecholate siderophores requires development of a method to couple the 2,3-dihydroxybenzoyl group to the appropriate backbone. This route for catecholate siderophore synthesis routinely involves protection of the phenolic oxygen (e.g., by butyl, benzyl, or acyl groups). Here we describe the synthesis of two representative catecholate siderophores: amonabactin and enterobactin. Amonabactin has its two 2,3-dihydroxybenzoyl groups fixed directly to a lysine–lysine or a glycine–lysine–lysine backbone, whereas the enterobactin structure is based on a macrocyclic serine backbone.

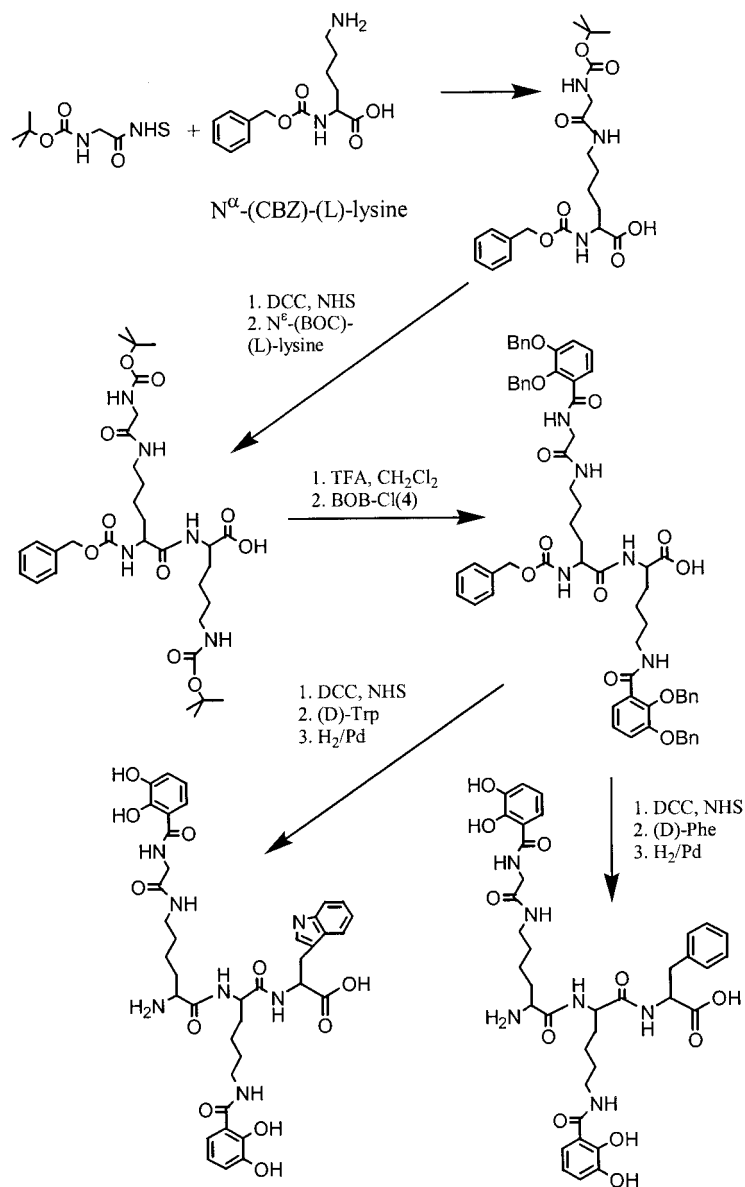
1. Synthesis of Amonabactins

The synthesis of the tripeptide amonabactin (40) begins by independently acylating the amine group of N^α -(CBZ)-(L)-lysine and N^α -(BOC)-(L)-lysine with 2,3-dibenzoyloxybenzoyl chloride (Scheme 1) under Schotten-Baumen conditions to produce (2) and (3). The protecting groups, carboxybenzoyloxy (CBZ) and *tert*-butoxycarbonyl (BOC), prevent unwanted reactions with the functional side chains of the amino acid. The advantage of using two protecting groups is that it allows selective deprotection and subsequent functionalization. The amine protecting group of (2) is removed by exposure to trifluoroacetic acid to yield (5). Compound 4, the activated ester of (3), formed by reaction with *N*-hydroxysuccinimide (NHS) and dicyclohexylcarbodiimide (DCC), is coupled to (5), giving compound (6). The free carboxyl group of (6), activated with DCC and NHS, is coupled to either D-tryptophan or D-phenylalanine. Finally, deprotection is accomplished by catalytic hydrogenation with hydrogen over palladium, resulting in the bis-catecholate siderophore with a final yield of 1–5%.

For the tetrapeptide siderophore, a more efficient synthesis has been developed (40). Typical solution-phase peptide techniques were employed to generate the tripeptide, glycine–lysine–lysine backbone (Scheme 2). The peptide synthesis proceeds by activation of the carboxy group of the N-terminus amino acid or peptide (by reaction with NHS and DCC) followed by coupling to the amine of the C-terminus amino acid. Unwanted reactions of the functional side chains of the amino acids are prevented by the use of protecting groups. The three-peptide backbone is then ac-



Scheme 1

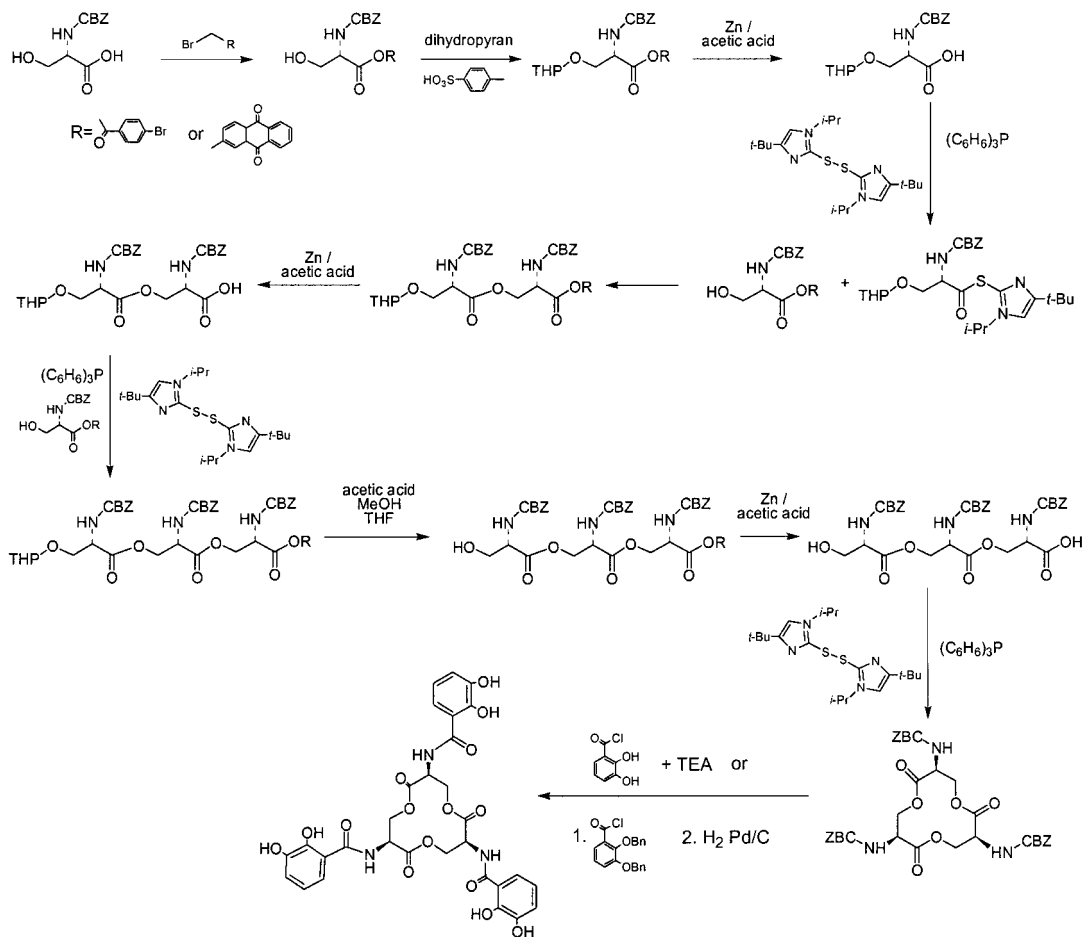


Scheme 2

ylated with 2,3-dibenzyloxybenzoyl chloride which is coupled to an aromatic amino acid, either D-tryptophan or D-phenylalanine. Finally, the product is deprotected by catalytic hydrogenation resulting in amonabactin T789 or P750.

2. Synthesis of Enterobactin

The first synthesis of enterobactin was reported in 1977 by Corey and Bhattacharya (103) (Scheme 3). The crucial step of the synthesis is the backbone cyclization which



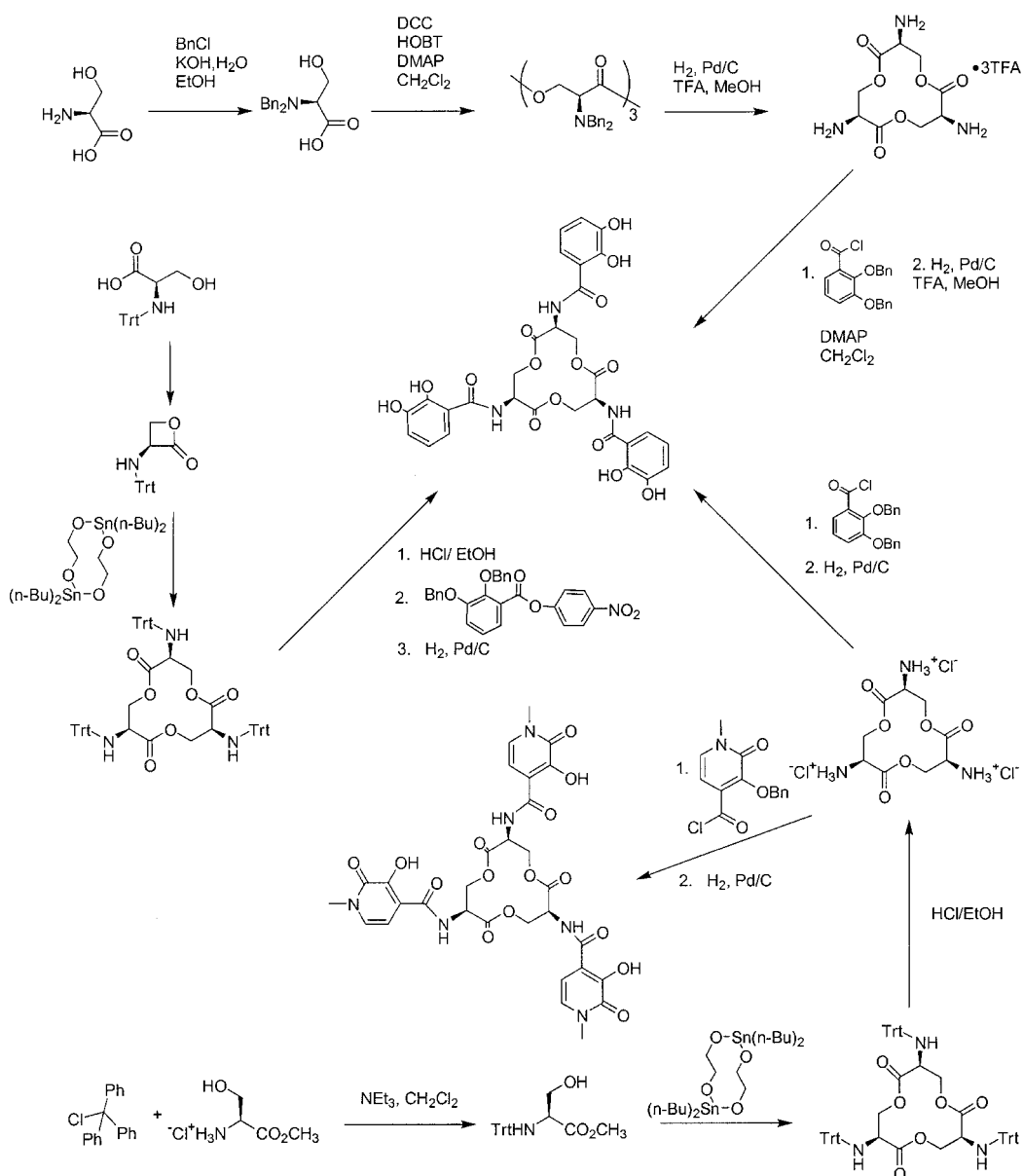
Scheme 3

generates the 12-member macrocycle. This approach involved first the formation of the cyclic triester L-serine backbone and then the attachment of the 2,3-dihydroxybenzoyl groups. The amino groups of the serine residues were protected with benzyloxycarbonyl. The *N*-benzyloxycarbonyl-serine units were converted to either the *p*-bromophenacyl esters or the *o*-tetrahydropyranyl thioester. The thioester was condensed with *N*-benzyloxycarbonyl-serine. Repetition of this procedure yields the cyclic trimer. In the final steps to synthesize the backbone, the *p*-bromophenacyl groups were removed and the product cyclized by carboxyl activation. Finally, deprotection of the amino groups and coupling with 2,3-dihydroxybenzoyl chloride gave enterobactin with a relatively low yield (~1%).

This synthetic approach was slightly modified by Rastetter et al. in order to synthesize both enterobactin and its mirror image, enantioenterobactin (104) (Scheme 3). The difference from the previous synthesis (103) is in the protecting groups used for the serine carboxyl and the catechol hydroxyl groups. The carboxy groups of the *N*-benzyloxycarbonyl-serine were alkylated with 2-(bromomethyl)anthraquinone,

and the hydroxyl groups of the catecholate were protected with benzyl groups. The 2,3-bis(benzyloxy)benzoyl chloride units were coupled to the amines and the benzyl groups were removed to produce enterobactin or enantioenterobactin, with 4% and 1.4% yields, respectively.

A completely different method was developed by Shanzer and Libman (105) to synthesize the siderophore enterobactin (Scheme 4). This approach was based on



Scheme 4

a single-step conversion of the *N*-tritylated-L-serine to the cyclic triester enterobactin backbone with the use of tin as a metal template, based on the reaction pioneered by Seebach (131). Finally, the trityl protecting groups were removed and replaced by catecholate units to yield enterobactin (~6%).

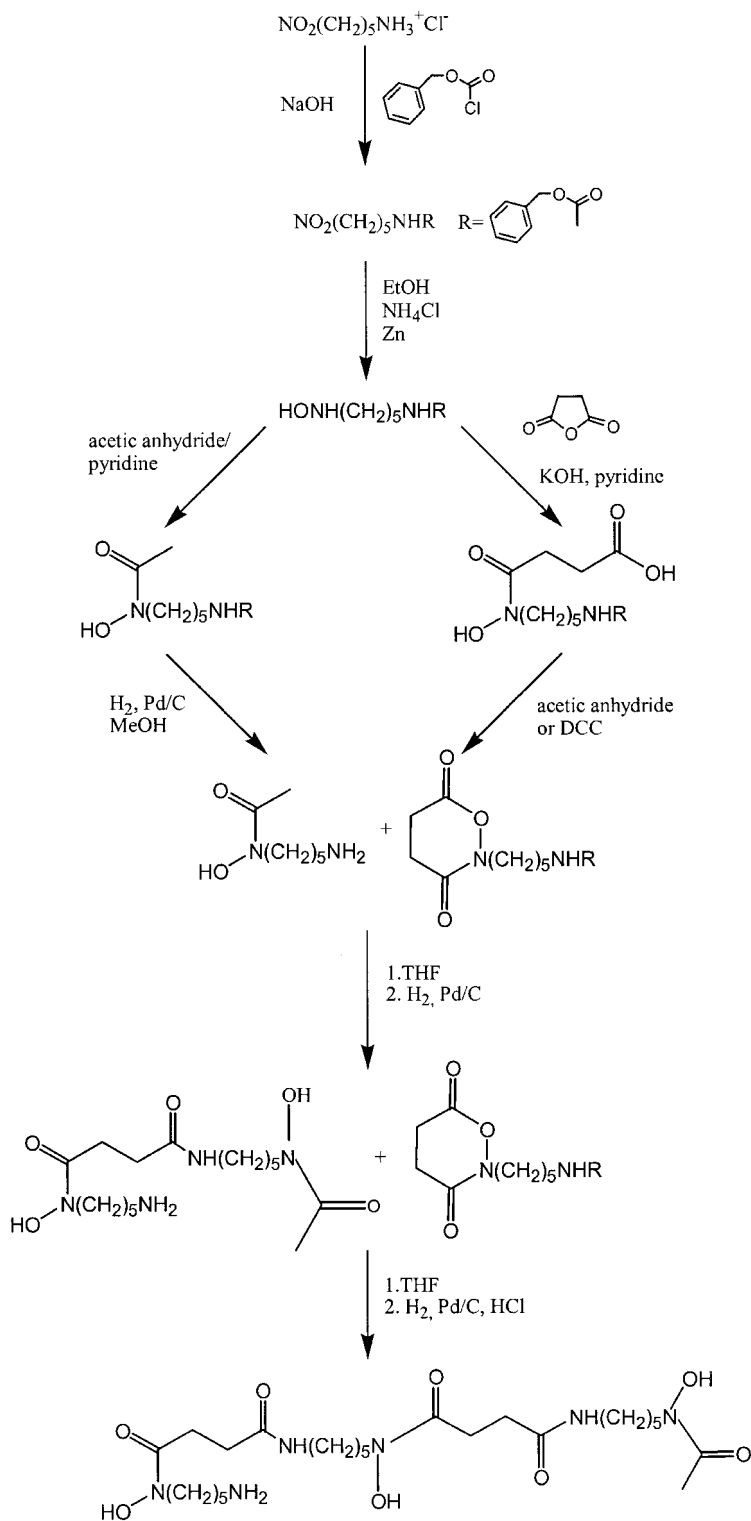
Rogers then described an enterobactin synthesis from *N,N*-dibenzyl-L-serine in four steps. First, the protected serine units were oligomerized using *N,N*-dicyclohexylcarbodiimide to yield a mixture of di-, tri-, and tetra-lactone. Then 2,3-dibenzoyloxybenzoyl chloride was added to the amines of the deprotected trilactone. Finally, deprotection of the catecholate hydroxy groups gave enterobactin with a still moderate yield (~4%).

More recently, Meyer et al. (108) described a high-yield synthesis of the enterobactin trilactone. A similar approach has also been presented by Ramirez et al. (107). This new strategy involves a single-step synthesis of the tri-serine lactone (Scheme 4). This synthesis relies on the fact that β -hydroxy acid derivatives can be oligomerized to macrocyclic lactones with the tri-lactone as the major product (132) using a stannoxane template, and leads to an overall yield of ~50%. Furthermore, this method enables the functionalization of the trilactone by attaching chelating groups other than catecholamides. After removal of the *N*-trityl protecting groups, the attachment of the chelating groups to the triamine scaffold via their acid chloride yielded enterobactin or enterobactin analogs (107) including hopobactin (108).

C. Synthesis of Hydroxamate Siderophores

The first synthesis of a hydroxamate siderophore was that of deferrioxamine B more than 30 years ago, which confirmed the chemical structure of the natural product (133) (Scheme 5). The key to the synthesis of hydroxamate siderophores is the ability to obtain *N*-protected hydroxydiamines or amino acids in an optically pure form. The most important *N*-hydroxy subunit in hydroxamate siderophores is the *N*-hydroxy-ornithine or *N*-hydroxy-lysine. This group of siderophores commonly are diketopiperazines (rhodotorulic acid, dimerum acid, coprogen) or other cyclic peptides (ferrichrome, fusarinine).

Standard peptide synthesis techniques were originally used in the synthesis of hydroxamate siderophores, such as rhodotorulic acid (125), dimerum acid (124), or ferrichrome (134). Hydroxamate siderophores were also synthesized by *N*-alkylation of simple *o*-substituted hydroxamic acid with a variety of alkylating agents (95). For example, during the course of the aerobactin synthesis, *o*-benzyl-protected hydroxamates were directly coupled to an activated amino acid; ϵ -hydroxynorleucine was transformed into a bromide reactive intermediate, which was used for the alkylation of *o*-benzylacetohydroxamic acid. After deprotection of the *N*¹-amino group and coupling with anhydromethylenecitryl chloride, the hydrolysis and deprotection of the remaining protecting groups yielded aerobactin. Unfortunately, this method is dependent on the difficult isolation of the starting material in its optical pure form, L- ϵ -hydroxynorleucine (95). To circumvent this limitation, an elegant synthesis of the key constituents of most hydroxamate siderophores, *N*⁵-acetyl-*N*⁵-hydroxy-L-ornithine (135) and *N* ^{ϵ} -acetyl-*N* ^{ϵ} -hydroxy-L-lysine (136), directly from the amino acids has been developed. Derivatives of *N* ^{ϵ} -acetyl-*N* ^{ϵ} -hydroxy-L-lysine are synthesized by direct oxidation of the ϵ -amino group of derivatives of L-lysine followed by hydrolysis and acetylation (136). This approach was used successfully to produce



Scheme 5

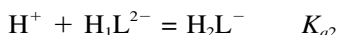
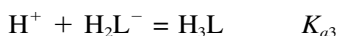
mycobactin (116). More recently, an indirect oxidation method has been used efficiently to synthesize hydroxylamine and hydroxamate siderophore components (137). This approach is based on the formation of stable nitrones by isomerization of the oxidation product of imines derived from L-ornithine. Subsequent hydrolysis of nitrones generates hydroxylamine that can be converted to the hydroxamate siderophore component.

IV. METAL COMPLEXATION AND COORDINATION GEOMETRY

A. Thermodynamics of Siderophore Iron Binding

Information about the potential effectiveness of a siderophore and its competition with other siderophores for Fe^{3+} requires solution thermodynamic characterization. The stability of an iron–siderophore complex must be greater than that of iron hydroxide. Siderophores involved in virulence must have a greater affinity for iron than the host iron storage or transport agents in order to be effective. This principle also applies to synthetic iron chelators designed to reduce corporal iron overload. Additionally, the stability of an iron–siderophore complex influences the Fe(III)–Fe(II) reduction potential and is a determinant of the mechanism of iron release from a siderophore.

Protonation and complexation equilibria can be expressed in a number of ways. Proton association constants ($\log K_a$) for a triprotic acid are expressed according to the following equations:



Note, in the corresponding stepwise equilibria, the most basic protonation reaction appears first. This follows the format for the stepwise equilibria involving a metal and a ligand, expressed as K :



By a standard convention (138), overall equilibria (139) are expressed as β_{mhl} values for the reaction $m\text{M} + l\text{L} + h\text{H} = \text{M}_m\text{L}_l\text{H}_h$. Hence $\beta_{110} = K_1$ and $\beta_{120} = K_1K_2$. Note that the above equilibria do not account for the fact that most ligands are protonated and hence H^+ and Fe^{3+} compete for the ligand. Hence the formal stability constant of a complex is not, by itself, a good measure of a ligand's ability to bind a metal. Differences in protonation constants and concentration dependence can lead to large differences in the magnitude of the overall formation constant among ligands which differ in pH dependence. To compare the true relative ability to bind a metal between differing ligands, some measure of the metal-ion free energy in the complex must be used. The pM value, analogous to pH value, is a convenient way to do this: $\text{pM} = -\log[\text{M}]$. The pM value is reported for a defined set of experimental conditions, usually $\text{pH} = 7.4$, $[\text{M}]_{\text{tot}} = 1 \mu\text{mol L}^{-1}$, $[\text{L}]_{\text{tot}} = 10 \mu\text{mol L}^{-1}$. The following example demonstrates the calculation of the pM value for the siderophore aerobactin (140).

Aerobactin has five dissociable protons from three carboxylate groups and two hydroxamate groups. The protonation constants are $\log K_1 = 9.44$, $\log K_2 = 8.93$,

$\log K_3 = 4.31$, $\log K_4 = 3.48$, and $\log K_5 = 3.11$. The hydroxy proton is not included, nor does it need to be, since it cannot be removed from the free ligand below pH 14. At pH 7.4, the fraction of the ligand in increasing protonation states can be calculated (defined as the α function). Hence L^{5-} represents the fully deprotonated ligand (excepting the hydroxy proton). In the following, the charges are not included for simplicity of the expressions.

$$\frac{[HL]}{[L]} = K_1[H^+] = 10^{9.44} \times 10^{-7.4} = 109.6$$

$$\frac{[H_2L]}{[L]} = K_1K_2[H^+]^2 = 3715.3$$

$$\frac{[H_3L]}{[L]} = K_1K_2K_3[H^+]^3 = 3.0$$

$$\alpha = 1 + 109.6 + 3715.3 + 3.0 = 3828.9$$

The concentrations of other species are so small that they can be neglected. The fractions (in percent) of the protonated forms of the ligand at pH 7.4 are thus $[L] = 0.03\%$, $[HL] = 2.86\%$, $[H_2L] = 97.0\%$, and $[H_3L] = 0.08\%$.



The last two reactions account for the two carboxylates which are not involved in metal binding and the second reaction corresponds to the loss of the hydroxy proton of the coordinated bidentate α -hydroxycarboxylate group. The acidity of this proton is increased by about 12 orders of magnitude (from a $\log K_a$ of about 16 to 4.27), owing to the hydroxy coordination to Fe^{3+} . If this were included in defining the fully deprotonated ligand, the formal formation constant for aerobactin would be $\log K_f = 34.6$ ($22.93 + 16 - 4.27$). However, this would be a meaningless description because a functional group with a pK_a of 16 cannot be significant in equilibria in any aqueous solutions. The pM value is calculated at $[L_{total}] = 10^{-5}$ mol/L, $[M_{total}] = 10^{-6}$ mol/L. If one assumes quantitative complex formation (as will be shown true), then $[L] = 10^{-5} - 10^{-6} = 9 \times 10^{-6}$ mol/L and the concentration of ligand that is fully deprotonated is given by

$$[L] = \left(\frac{1}{\alpha}\right) (9 \times 10^{-6}) = 2.35 \times 10^{-9} \text{ mol/L}$$

$$\frac{[MLH_{-1}]}{[ML]} = \frac{1}{(K_{MLH_{-1}})} ([H^+]) = 1348.96$$

$$\frac{[MHL]}{[ML]} = \frac{1}{(K_{MLH})} ([H^+]) = 1.2 \times 10^{-4}$$

$$\alpha_M = 1 + 1348.96 + 1.2 \times 10^{-4} = 1349.96$$

Again, the other forms of the protonated metal complex are present in insignificant concentrations. The percentages of deprotonated and monoprotonated com-

plex (these are the only forms considered here) at pH 7.4 are $[\text{MLH}_{-1}] = 99.93\%$ and $[\text{ML}] = 0.07\%$. Addition of the terms that describe the doubly and triply protonated metal complex and also the terms that describe the formation of hydroxide metal complex species are too small to affect the pM value (as shown below).

$$\frac{[\text{ML}]}{[\text{M}][\text{L}]} = K_f = 10^{22.93}$$

$$\frac{[\text{MLH}_{-1}]}{[\text{M}][\text{L}]} = K_f/K_{\text{MLH}_{-1}}[\text{H}^+] = 10^{26.06}$$

$$[\text{M}] = \frac{[\text{MLH}_{-1}]}{(10^{26.06})[\text{L}]} = 3.68 \times 10^{-24} \text{ mol/L}$$

$$\text{pM} = -\log(3.68 \times 10^{-24}) = 23.43$$

The overall ferric ion complex formation constants cannot be determined directly at neutral pH. The extremely high stability of siderophore complexes precludes direct measurement of the equilibrium of interest, which would yield the desired formation constant for the siderophore complex β_{110} . One method of circumventing this problem is the spectrophotometric measurement of competition for the metal by another thermodynamically well-characterized ligand, typically EDTA.



Using the known value for the formation constant of ferric EDTA, a value of the proton-dependent equilibrium constant can be calculated.

A number of ferric siderophores have had their electrochemistry studied; this has been reviewed previously and will not be repeated here (141). While reduction of Fe(III) to Fe(II) is a mechanism of recycling siderophore and locking up siderophore-transported Fe(III) inside the cell, such reduction has not been shown to be the rate-determining step in any microbial iron transport system yet studied. The shift in potential for a reversible couple is Nernstian:

$$E = E^0 - 0.059 \log \left(\frac{[\text{Fe}^{2+}]}{[\text{Fe}^{3+}]} \right)$$

Hence the shift of potential from the standard ferric/ferrous potential is just given by $0.059 (\text{pM}_{\text{Fe}^{3+}} - \text{pM}_{\text{Fe}^{2+}})$. Since both the ferrous and ferric pM values change from one ligand to another, both the ferrous and ferric stability constants must be known to calculate the redox potential. Conversely, the ferrous stability constant and the redox potential must both be known to determine the ferric siderophore stability constant. Figure 7 shows a plot of the pM values and redox potentials for a series of various siderophores.

B. Coordination Geometry and Stereochemistry of Siderophores

The stereochemistry of the siderophores has been extensively reviewed (4,142), including how UV/visible and circular dichroism spectra can provide useful geometric and electronic structure information. The geometry of the ferric siderophore complex (Fig. 8) is usually a key part of the recognition process of membrane siderophore receptors. This recognition has been shown to include chirality and geometric isomerism (4,7).

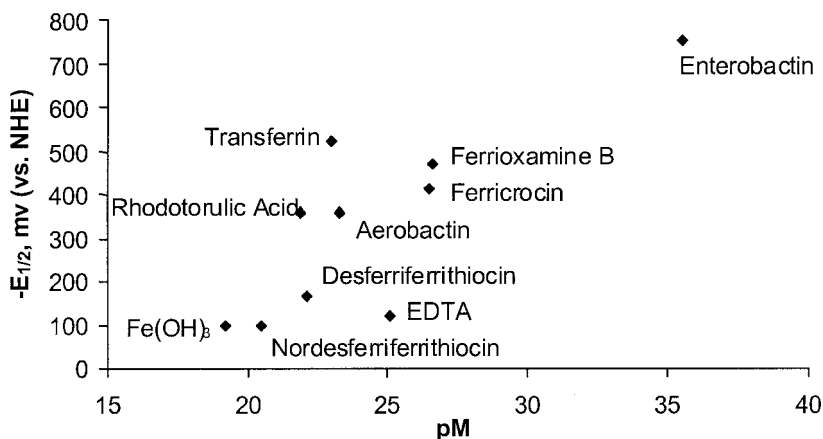


Figure 7 The pM and reduction potentials ($E_{1/2}$) for a variety of ferric siderophores and comparison species. Note that the scale is $-E$, such that the reduction potential decreases from bottom to top. While there is a general correlation of $E_{1/2}$ with pM, the several large exceptions show that the pM for both ferric and ferrous complexes must be known to predict the potential accurately. Enterobactin (140,236); Ferrioxamine (236,237); Ferricrocin (219); Transferrin (238,239); Rhodotorulic Acid (240); Aerobactin (240); Desferriferriethiocin and Nordesferriferriethiocin (176); EDTA (241,242); $\text{Fe}(\text{OH})_3$ is calculated using $\text{Fe}(\text{OH})_2k_{\text{sp}} = 10^{-16}$ and $\text{Fe}(\text{OH})_3k_{\text{sp}} = 10^{-39}$.

V. SYNTHETIC MODELS FOR SIDEROPHORES AND THEIR USE AS PROBES OF FERRIC-SIDEROPHORE PROPERTIES AND TRANSPORT

Mimics for siderophore molecules are useful for studying the physicochemical properties of siderophores and probing the recognition of a ferric-siderophore by its receptor. Other uses include producing drug-siderophore conjugates or efficient iron chelators for therapeutic applications. Here, we will briefly describe the design and potential use of drug-siderophores, while we refer the reader to a recent monograph (93) and Chapter 13.

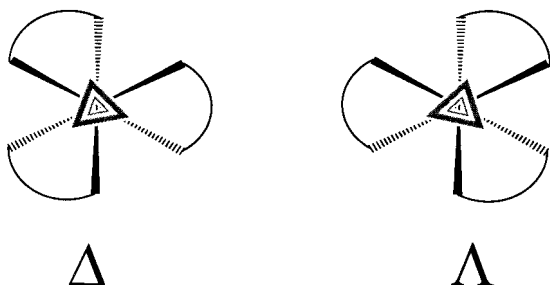
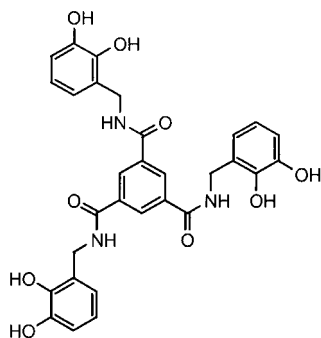


Figure 8 A schematic view of the pseudo octahedral geometry of $\text{Fe}(\text{III})$ in siderophores composed of bidentate chelating units (such as hydroxamate and catecholate). Chirality at the metal centers gives Δ or Λ stereochemistry and the sequence and orientation of the rings can give a number of geometric numbered isomers.

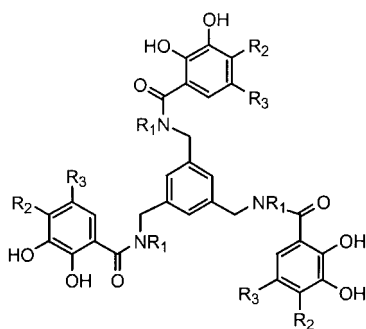
A. Siderophore Analogs—A Powerful Tool to Study the Physicochemical Properties of Siderophores

Enterobactin mimics have been widely used to examine the properties of this unique siderophore. Enterobactin forms a remarkably stable complex with iron ($K_f = 10^{49}$) and has a pM value of 35.5 at pH 7.4 (143). These features have prompted a range of studies of enterobactin's coordination chemistry and the structural origins of its unusual stability. Several synthetic analogs of enterobactin have been synthesized (Fig. 9), and in every case they have a much lower iron affinity. For example, MECAM (144) and TRENCAM (145) have iron-binding constants about 10^6 times smaller than enterobactin. X-ray crystallographic analysis of metal complexes of both enterobactin and synthetic analogs suggested that the major contributor to the stability of ferric enterobactin is the triester backbone of the molecule (142) which orients the catechol arms for complexation (Fig. 10). Furthermore, comparison of the backbone structure of enterobactin to comparable trilactones synthesized by Shanzer and co-workers (146) and Seebach and co-workers (131) shows very little reorganization of the backbone on metal complexation. A least-squares analysis of the overlay of the backbone in the vanadium(IV) enterobactin complex and Seebach's trilactone gave a root-mean-square (RMS) deviation of atom positions of only 0.133 Å. Direct calorimetric studies revealed that there is a decrease of six orders of magnitude in iron complex stability upon hydrolysis of the scaffold, which is about one-third enthalpic and two-thirds entropic in origin (147), confirming its importance. The contribution of the scaffold rigidity to enterobactin predisposition has been further investigated with the synthesis of other ligand analogs. Sterically constrained enterobactin analogs, MMECAM and EMECAM, were synthesized in which the ligating arms are held above the scaffold in a similar manner to enterobactin (148,149). A single-crystal structure of EMECAM confirmed the expected ligand conformation. The introduction of the three alkyl groups at the 2, 4, and 6 positions of the supporting aryl ring of MECAM acts to predispose the ligand conformation such that substituent groups alternate above and below the scaffold aryl ring due to steric interactions. Solution thermodynamic measurements have shown that this predisposition of these ligands for iron binding results in ferric complex stabilities of $10^{47.1}$ and $10^{45.8}$ for ferric EMECAM and ferric MMECAM, respectively (148), approaching that of enterobactin. This demonstrates the significance of the supporting scaffold conformation and size of enterobactin with respect to its superior metal-binding efficiency.

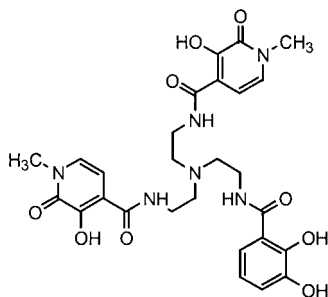
Recently, a high-yield synthesis for the enterobactin trilactone scaffold has been developed (108), enabling the predisposition of the enterobactin scaffold to be gauged with chelating groups other than catecholamides. To this end, an analog containing 3,2-HOPO (hydroxypyridinonate) binding groups was prepared (Scheme 4) and the X-ray structure of its ferric complex and its spectroscopic and thermodynamic properties determined (108). Since there is no change in hydrogen bonding of the amide linker in going from the free ligand to the metal complex, the trilactone scaffold does not contribute any predisposition for iron binding in this case. The hopobactin complex has a Δ configuration, imposed by the trilactone scaffold, making it the first reported chiral HOPO complex. Although at neutral pH the 3,2-HOPO ligands have a lower affinity for iron than do catecholates, hopobactin is an extraordinarily powerful iron-chelating agent under acidic conditions: no measurable dis-



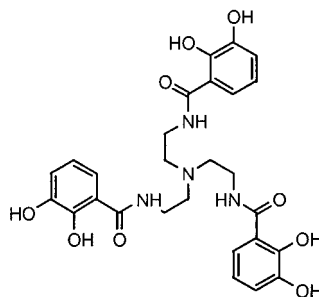
TRIMCAM



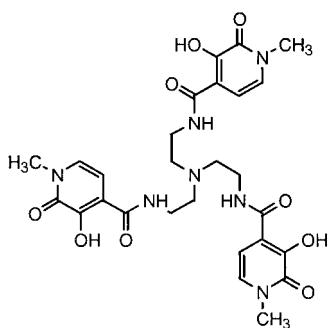
MECAM ($R_1=R_2=R_3=H$)
 MECAM-Me ($R_1=R_3=H, R_2=CH_3$)
 MECAMS ($R_1=R_2=H, R_3=SO_3^-$)
 Me₃MECAM ($R_2=R_3=H, R_1=CH_3$)



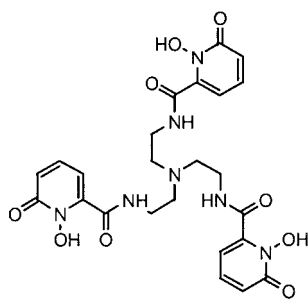
TREN-CAM-3,2-HOPO



TREN-CAM



TREN-Me-3,2-HOPO



TREN-1,2-HOPO

Figure 9 Synthetic analogs of enterobactin.

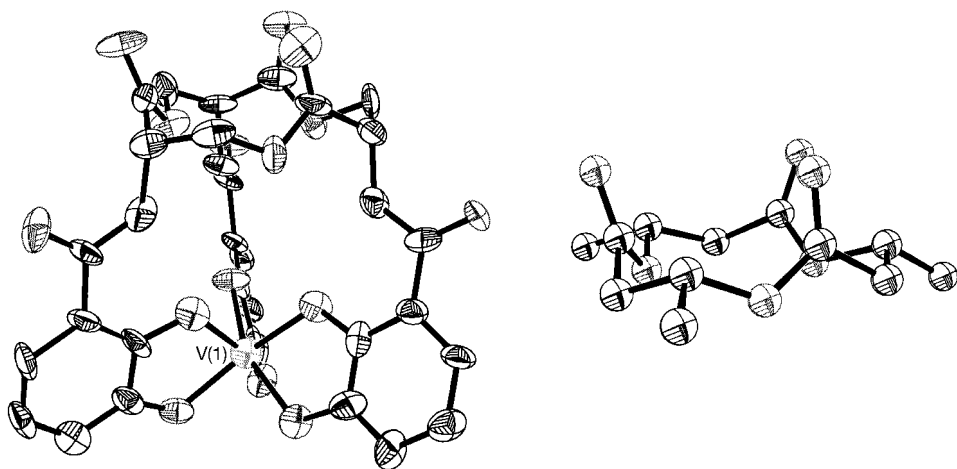


Figure 10 The structures (X-ray diffraction) of the enterobactin complex of vanadium(IV), considered to be essentially identical to the natural Fe(III) complex (left), and the Seebach trilactone (right). These show the importance of the trilactone in orienting all three catechol groups toward the metal ion center and the effect that this has on the stability of the complex.

sociation is observed even in 1.0 M HCl (pH 0). Indeed, hopobactin competes with enterobactin for iron at any pH below 6.

A series of ferrioxamine analogs has been produced by synthesis or fermentation. Directed fermentation of *Streptomyces olivaceus* in the presence of unnatural diamines and diamino acid precursors resulted in the production of 13 new desferrioxamine-type siderophores (150). The stability constants of the ferric complexes of these siderophore analogs were compared with that found for the natural siderophore desferrioxamine E produced by this bacterium. These studies showed that the stability of the ferric–trihydroxamate complex decreases monotonically as the structure of the ligand differs from that of desferrioxamine E.

It is clear from these two examples that analogs provide a powerful tool to study the physiochemical behavior of natural siderophores. This approach has been intensively used to investigate hydroxamate, catecholate, and hydroxypyridinate chemistry and has shed light on the properties governing formation and stability of the metal complex.

One striking characteristic of ferric–siderophore complexes is their intense red color, which is due to spin-allowed ligand-to-metal charge-transfer transitions, and which prompted the early name of siderochrome. Until recently, a detailed assignment of the observed transition was not available. Siderophore analogs have been used to assign these transitions. Single-crystal polarized absorption and magnetic circular dichroism (MCD) were employed to elucidate the electronic structure of the iron(III) tris(catecholate) complex $[\text{Fe}(\text{cat})_3]^{3-}$ and so to investigate the bonding in ferric enterobactin and similar catecholate siderophores (151) (Fig. 11). (Two related complexes were studied by MCD to provide a perturbation of the electronic structure of $[\text{Fe}(\text{cat})_3]^{3-}$ and also to determine differences in bonding between the three complexes.) Similar studies were performed on a series of bi-capped macrocycle analogs, which allowed for variation of the geometric, as well as electronic, structures of the

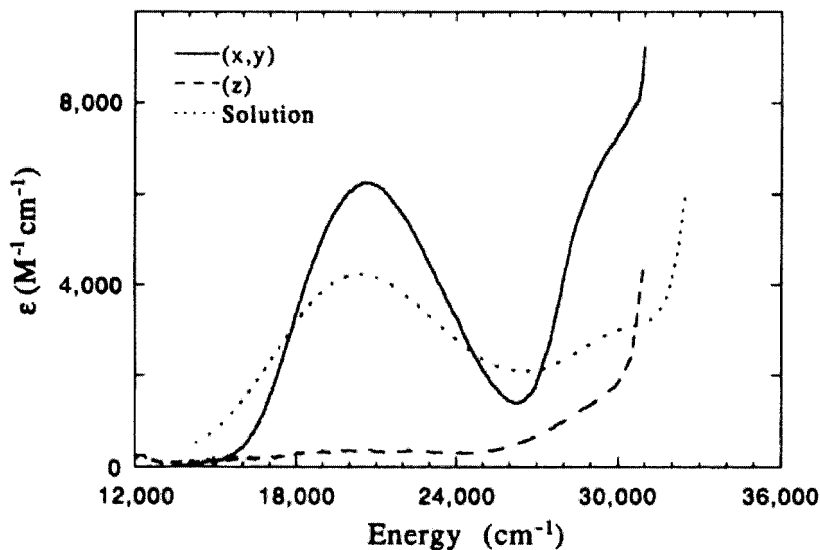


Figure 11 Single-crystal-polarized absorption spectra (110 face) of $K_3[Ga\{Fe\}(cat)_3] \cdot 1.5 H_2O$ ($[Fe] = 0.5\%$) at room temperature (Z and solution) and 6 K (x, y).

complexes (152). The ligand-to-metal charge-transfer band characteristic of the catecholate siderophores is found for $[Fe(cat)_3]^{3-}$ to be composed of two overlapping x, y polarized transitions at 18,414 and 22,018 cm^{-1} (152). These transitions are ligand π to metal d in nature; assignments of these and four other transitions and an experimental energy order for the molecular orbitals of the complexes have been made in D_3 symmetry (Fig. 12). The siderophore charge-transfer excited state is best described as a semiquinone Fe(II) species. A significant contribution to the Fe–O interaction is made by π bonding, and this accounts for the high stabilities of these complexes relative to similar Fe(III) complexes (e.g., oxalate).

B. Synthetic Models for Siderophores and Their Use in Probing Ferric–Siderophore Transport

Synthetic analogs of siderophores are also extremely useful in probing siderophore–receptor specificity in bacteria and fungi, i.e., the correlation between ferric–siderophore structure and recognition. These types of studies have shown that siderophore uptake in microorganisms is both receptor- and energy-dependent (6,153). The ferric–enterobactin and ferrichrome outer membrane receptors, FepA (154,155) and FhuA (155–157), respectively, have been intensively studied. Indeed, the crystal structures of both receptors have been recently resolved (154,156,157). Coverage of this information would be beyond the scope of this chapter; therefore, we will focus only on the structural recognition of the siderophore by the receptor protein. This recognition may be dependent on different parts and structural features of the siderophore: (a) the chirality or coordination geometry of the metal center, (b) the geometry of the backbone, (c) the chirality of the backbone, (d) the presence of peripheral groups, (e) the molecule as an entity, or (f) the nature or lability of the metal center.

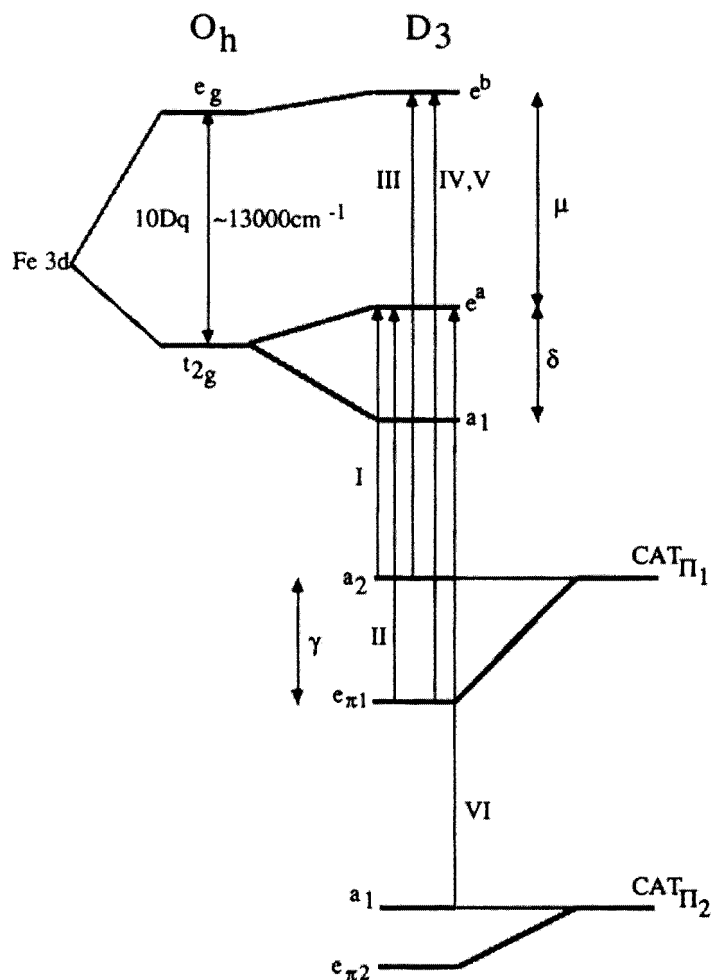


Figure 12 One-electron molecular-orbital energy-level diagram for iron(III) tris(catecholates). The observed charge-transfer transitions are indicated by arrows and labeled with appropriate Roman numerals.

Chiral ferric–siderophore complexes are common (7,141,142). Several studies by us and others have revealed important correlations between the coordination geometry of the metal center and ferric–siderophore recognition. Two clear examples of this are shown in studies of the uptake of ferric rhodotorulic acid (158) and ferrichrome (159). Rhodotorulic acid and desferrichrome form ferric complexes with preferred Δ -*cis* (right-hand propeller) and Λ -*cis* (left-handed propeller), respectively (Fig. 8). The enantiomeric forms of these siderophores were synthesized from the D-amino acid, instead of the L forms. Uptake of the rhodotorulic acid (158) and ferrichrome (159) enantiomers by *Rhodotorula pilimanae* and *E. coli*, respectively, has been shown to be much lower than uptake of the naturally occurring ferric siderophore. Hence, there is discrimination between the optically active siderophore complex and its synthetic enantiomer. Similar studies have been done with enterobactin and fer-

microcin (160,161). The ferric complex of enterobactin forms the Δ absolute configuration, and some time ago it was shown that the synthetic mirror image (Λ configuration, enantioenterobactin) does not promote the growth of *E. coli* (160). Subsequent studies have revealed that both enantiomers are transported into the bacterium, refuting the idea that chirality of the enterobactin metal center affects its recognition by the receptor FepA (162). Thus, chiral discrimination in iron delivery is not always due to chiral siderophore recognition during transport. The role of the metal–complex chirality can be probed directly by substitution of similar kinetically inert ions for the labile ferric ion in siderophores. Complexes of Cr(III) and Rh(III), which are nearly the same shape, charge, and size as Fe(III), are excellent probes for this study of siderophore–receptor recognition. Isomers of inert chromic desferrioxamine B complexes were used to probe the stereospecificity of the ferrioxamine uptake system in *Streptomyces pilosus* (22). The chromic complexes were separated into three fractions and characterized by their visible spectra as two cis and a (mixture of) trans geometric isomers. Each isomer competes equally for the uptake of iron via ^{55}Fe -ferrioxamine B, suggesting that there is no differentiation between cis and trans isomers by the ferrioxamine uptake system in *S. pilosus*. Since *S. pilosus* produces a great variety of desferrioxamines, desferrioxamines A₁, A₂, B, C, D₁, D₂, E, F, G, and H, the chromic isomers were also used to gain information about the structural recognition of ferrioxamine as well as the expression of one or more receptor sites. The chromic complex of desferrioxamine B (linear) was found to compete successfully with the transport of the ferric complex of the linear desferrioxamine D₁ and the two cyclic desferrioxamines E and D₂. These results suggest that all desferrioxamine-mediated iron transport occurs through the same system and that the receptor does not differentiate between cyclic and linear ferrioxamines (22). However, the positive charge of ferrioxamine B seems to play an important role in recognition, since the uptake rate of ferrioxamine D₁, which is acylated as the amino group and uncharged, is 40% lower.

The use of siderophore analogs is also a common strategy for probing the role of siderophore structure in the mechanism of recognition by its cognate receptor. A characteristic example of this approach is the one involving the receptor for enterobactin. Synthetic analogs of enterobactin have been used to probe the transport process. The features of the enterobactin structure recognized during the transport events have been studied with uptake experiments using the metal complex of several analogs. In an early investigation, Venuti et al. (163) showed that a synthetic analog of enterobactin, in which the triserine scaffold is replaced by a carbocyclic structure, still promotes the bacterial growth. Since the coordination environment about the iron center remains unchanged between enterobactin and its analog, this result suggests the primary importance of the catecholate portion of the ferric complex in receptor recognition. This hypothesis was later confirmed and the details investigated by both growth promotion and uptake experiments with a wide range of derivative ligands and various *E. coli* as well as other bacterial strains (162,164,165). The synthetic analogs used, with their abbreviation names, are shown in Fig. 9. These studies showed that MECAM mediates iron transport in *E. coli* at a rate comparable to that of enterobactin. The only structural difference between these two chelators is the replacement of the triserine lactone in enterobactin by a mesytilene ring in MECAM. Furthermore, the use of the MECAM analogs Me₃MECAM, TRICAM, and MECAMS led to a drastic reduction of iron transport. The sulfonated derivative

MECAMS was not transported at all. These experiments demonstrated that both the metal-binding unit and the amide linkage are necessary for recognition by FepA receptor. It is clear that the order of the amide linkage must be conserved, since reversal of the carbonyl and amine groups in TRINCAM greatly reduced iron uptake. These results show clearly that the enterobactin receptor, FepA, recognizes the catecholamide region of the ferric–enterobactin complex and that substitution of the catecholate or amide group prevents transport. More recently, the necessity of an unsubstituted catecholate iron complex has been reinvestigated and reconfirmed using other analogs. Thulasiraman et al. used enterobactin analogs with a different net charge (162) (such as TRENCAM-3,2-HOPO or TREN-Me-3,2-HOPO) for the uptake studies. In these complexes the catecholate groups were always substituted and therefore could not be used to probe the role of the overall charge of the complex on ferric–siderophore transport. Recently, we demonstrated that a neutral complex formed with unsubstituted HOPO ligand, TREN-1,2-HOPO (Fig. 9), does not mediate iron transport in *E. coli* through the receptor FepA (166). This result indicates that the overall charge of the ferric complex is important in FepA–siderophore recognition.

The use of siderophores labeled with fluorescent probes has been recently described for the spatial study of iron transport. The iron path in the fungus *Ustilago maydis* has been elegantly tracked with a fluorescently labeled ferrichrome or desferrioxamine B analog (167). The entry of the fluorescent ferrichrome into the fungal cells was followed; after 4 h incubation the fluorescence was found to be intracellular specifically inside two or three vesicles within each cell. In contrast, the fluorescence from the desferrioxamine analog, which exhibits fluorescence quenching upon iron binding, was visualized around the cell membrane, suggesting a removal of iron with the siderophore remaining outside. This study clearly demonstrated the use of fluorescent analogs of siderophores as a tool to directly track and discriminate between different pathways of iron uptake in cells.

VI. ISOLATION AND CHARACTERIZATION OF NEW SIDEROPHORES

Due to the structural diversity of siderophores, there is no standard method for their purification. As a preliminary step, cultures of bacterial strains of interest should be grown in a minimal medium. The supernatant, removed from these cultures, can be screened for the production of new siderophores by isoelectrofocusing (IEF) (168). This technique allows identification of new siderophores by comparison of pI values with those of already-known siderophores. Once bacteria producing new siderophores have been identified, the siderophores produced can be purified. The main steps of siderophore purification and identification are (a) growth of the microorganisms in an iron starved medium, (b) removal of the cells and characterization of siderophore production by either the universal Schwyn and Neilands (169) CAS shuttle assay or the Arnou (170) or Csaky (171) tests, and (c) extraction of the siderophores from the supernatant. Unfortunately, citrate, oxazoline, and carboxylate groups do not react in Arnou and Csaky tests. Furthermore, ferric complexes of several functional groups, such as hydroxy carboxylates, do not have easily detected spectroscopic features such as the intense red color associated with the ferric com-

plexes of catecholates and hydroxamates. The classical methods of siderophore purification have been the subject of numerous reviews (24,172–175).

Briefly, in siderophore purification, many separation techniques may be used, e.g., chloroform-phenol extraction, ethylacetate extraction, chromatography on XAD-4, LH-20 Sephadex, ion-exchange chromatography, or high-performance liquid chromatography (HPLC). These methodologies are well described and documented in the scientific literature (24,172–175). Following the isolation of a new siderophore, it remains to chemically characterize the molecule. Several examples exist in the literature of these characterizations by ourselves and by others (40,147,151,176–179).

We recently described investigations of the amonabactin family of siderophores (40) which outlined techniques such as multidimensional nuclear magnetic resonance (NMR) and chiral gas chromatography used to elucidate the structure of each member of the family. Complete chemical syntheses of the proposed structures were performed, and the synthesized siderophores showed chemical properties identical to the natural products (HPLC retention times, MSMS, NMR, UV/visible). A single-crystal structure analysis is probably the most complete method of characterization, giving important information about the ligand structure, conformation, and stereochemistry. Many crystal structures of siderophores have been solved, including alcaligin (180), ferrioxamine E (181), anguibactin (182), enterobactin (183), rhizoferrin (123), agrobactin (184), and ferrichrome (185).

VII. DRUG–SIDEROPHORE CONJUGATES AND THEIR POTENTIAL APPLICATIONS

Many pathogenic microorganisms acquire essential iron from their hosts by excreting siderophores. This ability correlates with their virulence (186). This correlation between high-affinity iron acquisition, colonization, and virulence *in vivo* makes these systems attractive targets for new approaches to antibiotics. Several reports describe the study of antibiotic–siderophore conjugates (135,187–192). These conjugates exploit their siderophore moiety for binding to ferric–siderophore receptors and transport through the outer membrane, delivering the antibiotic into the cell. Several types of conjugates have been synthesized to date. Typically, hydroxamate siderophores (similar to ferrichrome and arthrobactin) or catechol siderophores (derived from hydroxybenzoyl-based spermidine or lysine) are conjugated to carbacephalosporin, erythromycamine, or nalidixic acid (191). During these studies, bacteria resistant to the siderophore–antibiotic conjugates frequently arose and showed an absence of ferric–siderophore receptors (192). Nevertheless, receptor-deficient mutants can be subject to severe iron limitation and therefore be unable to develop their pathogenesis. While the idea of utilizing iron transport machineries for drug delivery is an old one (193), very few useful antimicrobial agents have been developed along these lines. These first attempts are promising and demonstrate the potential use of siderophore-mediated iron transport for drug delivery.

VIII. CONCLUSION AND PERSPECTIVES

In summary, the field of siderophore chemistry continues to grow rapidly, not just in the number of compounds known, but also, more importantly, in our understanding

of iron transport mediation and its impact for biology and medicine. Thirty years ago, this field comprised a few characterized compounds about which little was known of their metal-ion coordination chemistry, solution stability, and membrane transport processes. In contrast, it now constitutes a very substantial body of information. This field brings together chemists, microbiologists, and scientists from other disciplines who study various aspects of siderophore-mediated iron transport. We have tried similarly to assemble the different parts of the scientific literature related to siderophores in writing this review.

ACKNOWLEDGMENTS

We thank Jide Xu, Julia Brumaghim, and Emily Dertz for help in assembling this manuscript. We gratefully acknowledge the National Institutes of Health, which have supported our research in this field through grant AI11744.

REFERENCES

1. Otto BR, Verweij-van Vught AMJJ, MacLaren DM. Transferrins and heme-compounds as iron sources for pathogenic bacteria. *Crit Rev Microbiol* 1992; 18:217–233.
2. Neilands JB. A brief history of iron metabolism. *Biol Met* 1991; 4:1–6.
3. Weinberg ED. Cellular iron metabolism in health and disease. *Drug Metab Health* 1990; 22:531–579.
4. Telford JR, Raymond NK. In: Atwood JL, Davies JED, MacNicol DD, Vogtle F, eds. *Comprehensive Supramolecular Chemistry*. Oxford, U.K.: Elsevier, 1996:245–266.
5. Neilands JB. Siderophores: structure and function of microbial iron transport compounds. *J Biol Chem* 1995; 270:26723–26726.
6. Braun V, Hantke K. In: Winkelmann G, Carrano CJ, eds. *Transition Metals in Microbial Metabolism*. Amsterdam: Harwood, 1997:81–116.
7. Raymond KN, Müller G, Matzanke BF. In: Bosch FL, ed. *Topics in Current Chemistry*. Berlin: Springer-Verlag, 1984; 50–102.
8. Moeck GS, Coulton JW. TonB-dependent iron acquisition: mechanisms of siderophore-mediated active transport. *Mol Microbiol* 1998; 28:675–681.
9. Postle K. Active transport by customized beta-barrels. *Nature Struct Biol* 1999; 6:3–6.
10. Braun V. Pumping iron through cell membranes. *Science* 1998; 282:2202–2203.
11. Lee CW, Ecker DJ, Raymond KN. Coordination chemistry of microbial iron transport compounds. 34. The pH-dependent reduction of ferric enterobactin probed by electrochemical methods and its implications for microbial iron transport. *J Am Chem Soc* 1985; 107:6920–6923.
12. Pecoraro VI, Harris WR, Wong GB, Carrano CJ, Raymond KN. Coordination chemistry of microbial iron transport compounds. 23. Fourier-transform infrared-spectroscopy of ferric catecholamide analogs of enterobactin. *J Am Chem Soc* 1983; 105:4623–4633.
13. Konopka K, Neilands JB. Effect of serum-albumin on siderophore-mediated utilization of transferrin iron. *Biochemistry* 1984; 23:2122–2127.
14. Williams PH, Warner PJ. ColV plasmid-mediated, colicin V-independent iron uptake system of invasive strains of *Escherichia coli*. *Infect Immun* 1980; 29:411–416.
15. Nassif X, Sansonetti PJ. Correlation of the virulence of *Klebsiella-pneumoniae* K1 and K2 with the presence of a plasmid encoding aerobactin. *Infect Immun* 1986; 54:603–608.
16. O'Brien IG, Gibson F. Structure of enterochelin and related 2,3-dihydroxy- α -benzoyl-serine conjugates from *Escherichia coli*. *Biochim Biophys Acta* 1970; 215:393–397.

17. Schmitt MP, Payne SM. Genetic-analysis of the enterobactin gene-cluster in *Shigella flexneri*. J Bacteriol 1991; 173:816–825.
18. Pollack JR, Neilands JB. Enterobactin, an iron transport compound from *Salmonella typhimurium*. Biochem Biophys Res Commun 1970; 38:989–992.
19. Stuart SJ, Prpic JK, Robinsbrowne RM. Production of aerobactin by some species of the genus *Yersinia*. J Bacteriol 1986; 166:1131–1133.
20. Lodge JMT, Williams P, Brown MRW. Influence of growth-rate and iron limitation on the expression of outer-membrane proteins and enterobactin by *Klebsiella pneumoniae* in continuous culture. J Bacteriol 1986; 165:353–356.
21. Adapa S, Huber P, Kellerschierlein W. Metabolites of microorganisms. 216. Isolation, structure and synthesis of ferrioxamine H. Helv Chim Acta 1982; 65:1818–1824.
22. Muller G, Raymond KN. Specificity and mechanism of ferrioxamine mediated iron transport in *Streptomyces pilosus*. J Bacteriol 1984; 160:304–312.
23. Feistner GJ, Stahl DC, Gabrik AH. Proferrioxamine siderophores of *Erwinia amylovora*—a capillary liquid chromatographic electrospray tandem mass spectrometric study. Org Mass Spectrom 1993; 28:163–175.
24. Meyer JM, Stintzi A. Iron metabolism and siderophores in *Pseudomonas* and related species. Motie CT, ed. New York: Plenum Press, 1998.
25. Drechsel H, et al. Rhizoferrin—a novel siderophore from the fungus *Rhizopus microsporus* var *rhizopodiformis*. Biol Metals 1991; 4:238–243.
26. Thielen A, Winkelmann G. Rhizoferrin—a complexone type siderophore of the mucorales and entomophorales (Zygomycetes). FEMS Microbiol Lett 1992; 94:37–42.
27. Milagres AMF, Machuca A, Napoleao D. Detection of siderophore production from several fungi and bacteria by a modification of chrome azurol S (CAS) agar plate assay. J Microbiol Meth 1999; 37:1–6.
28. Budzikiewicz H, Bossenkamp A, Taraz K, Pandey A, Meyer JM. Bacterial constituents. 72. Corynebactin, a cyclic catechololate siderophore from *Corynebacterium glutamicum* ATCC 14067 (*Brevibacterium* sp. DSM 20411). Z Naturforsch 1997; C 52:551–554.
29. Barelmann I, Meyer JM, Taraz K, Budzikiewicz H. Cepaciachelin, a new catechololate siderophore from *Burholderia (Pseudomonas) cepacia*. Z Naturforsch 1996; C 51:627–630.
30. Page WJ, Vontigerstrom M. Aminochelin, a catecholamine siderophore produced by *Azotobacter vinelandii*. J Gen Microbiol 1988; 134:453–460.
31. Demange P, Bateman A, Dell A, Abdallah MA. Structure of azotobactin D, a siderophore of *Azotobacter vinelandii* strain D (CCM-289). Biochemistry 1988; 27:2745–2752.
32. Cornish AS, Page WJ. Production of the triscatechololate siderophore protochelin by *Azotobacter vinelandii*. Biometals 1995; 8:332–338.
33. Corbin JL, Bulen WA. The isolation and identification of 2,3-dihydroxybenzoic acid and 2-N, 6-N-di-(2,3-dihydroxybenzoyl)-L-lysine formed by iron-deficient *Azotobacter vinelandii*. Biochemistry 1969; 8:757–762.
34. Neilands JB. Isolation and assay of 2,3-dihydroxybenzoyl derivatives of polyamines—the siderophores agrobactin and parabactin from *Agrobacterium tumefaciens* and *Paracoccus denitrificans*. Meth Enzymol 1983; 94:437–441.
35. Griffiths GL, Sigel SP, Payne SM, Neilands JB. Vibriobactin, a siderophore from *Vibrio cholerae*. J Biol Chem 1984; 259:383–385.
36. Yamamoto S, et al. Structures of 2 polyamine containing catechololate siderophores from *Vibrio fluvialis*. J Biochem 1993; 113:538–544.
37. Ehlert G, Taraz K, Budzikiewicz H. Bacterial constituents. 59. Serratiochelin, a new catechololate siderophore from *Serratia marcescens*. Z Naturforsch 1994; C 49:11–17.
38. Persmark M, Expert N, Neilands JB. Isolation, characterization, and synthesis of chrysoactin, a compound with siderophore activity from *Erwinia-chrysanthemii*. J Biol Chem 1989; 264:3187–3193.

39. Barghouti S, et al. Amonabactin, a novel tryptophan-containing or phenylalanin-containing phenolate siderophore in *Aeromonas hydrophila*. J Bacteriol 1989; 171:1811–1816.
40. Telford JR, Raymond KN. Amonabactin: a family of novel siderophores from a pathogenic bacterium. J Biol Inorg Chem 1997; 2:750–761.
41. van der Helm D, Winkelmann G. In: Winkelmann G, Winge D, eds. Metals Ions in Fungi. New York: Marcel Dekker, 1994:39–98.
42. Neilands JB. A crystalline organo-iron pigment from the smut fungus. *Ustilago spheerogena*. J Am Chem Soc 1952; 74:4846–4847.
43. Emery T, Neilands JB. Structure of ferrichrome compounds. J Am Chem Soc 1961; 83:1626.
44. Atkin CL, Neilands JB, Phaff HJ. Rhodotorulic acid from species of *Leucosporidium*, *Rhodospiridium*, *Rhodotorula*, *Sporidiobolus* and *Sporobolomyces*, and a new alanine-containing ferrichrome from *Cryptococcus melibiosum*. J Bacteriol 1970; 103:722–733.
45. Diekmann H. Metabolic products of microorganisms. 81. Occurrence and structures of coprogen-B and dimerum acid. Archiv Mikrobiol 1970; 73:65–70.
46. Hesseltine CW, et al. Coprogen, a new growth factor for coprophilic fungi. J Chem Soc 1952; 74:1362.
47. Diekmann H. Metabolic products of microorganisms. 81. Occurrence and structures of coprogen B and dimerum acid. Arch Mikrobiol 1970; 73:65–76.
48. Frederick CB, Szanislo PJ, Vickrey PE, Bentley MD, Shive W. Production and isolation of siderophores from the soil fungus *Epicoccum purpurascens*. Biochemistry 1981; 28:2432–2436.
49. Jalal MA, Love SK, van der Helm D. N alpha-dimethylcoprogens. Three novel trihydroxamate siderophores from pathogenic fungi. Biol Medab 1988; 1:4–8.
50. Jalal MA, van der Helm D. Siderophores of highly phytopathogenic *Alternaria longipes*. Structures of hydroxycoprogens. Biol Metab 1989; 2:11–17.
51. Umezawa H, et al. Foroxymithine, a new inhibitor of angiotensin-converting enzyme, produced by Actinomycetes. J Antibiot 1985; 38:1813–1815.
52. Nishio T, et al. Isolation and structure of the novel dihydroxamate siderophore alcaligin. J Am Chem Soc 1988; 110:8733–8734.
53. Brickman TJ, Hansel JG, Miller MJ, Armstrong SK. Purification, spectroscopic analysis and biological activity of the macrocyclic dihydroxamate siderophore alcaligin produced by *Bordetella pertussis* and *Bordetella bronchiseptica*. Biometals 1996; 9:191–203.
54. Moore CH, Foster LA, Gerbig DGJ, Dyer DW, Gibson BW. Identification of alcaligin as the siderophore produced by *Bordetella pertussis* and *B. bronchiseptica*. J Bacteriol 1995; 177:1116–1118.
55. Takahashi A, et al. Bisucaberin, a new siderophore, sensitizing tumor-cells to macrophage-mediated cytolysis. 2. Physicochemical properties and structure determination. J Antibiot 1987; 40:1671–1676.
56. Ledyard KM, Butler A. Structure of putrebactin, a new dihydroxamate siderophore produced by *Shewanella putrefaciens*. J Biol Inorg Chem 1997; 2:93–97.
57. van der Helm D, Poling M. Crystal-structure of ferrioxamine E. J Am Chem Soc 1976; 98:82–86.
58. Meyer JM, Halle F, Hohnadel D. Cepabactin from *Pseudomonas cepacia*, a new type of siderophore. J Gen Microbiol 1989; 135:1479–1487.
59. Barker WR, et al. G1549, a new cyclic hydroxamic acid antibiotic, isolated from culture broth of *Pseudomonas alcaligenes*. J Antibiot 1979; 32:1096–1103.
60. Meiwes J, et al. Isolation and characterization of staphyloferrin-A, a compound with siderophore activity from *Staphylococcus hyicus* DSM-20459. FEMS Microbiol Lett 1990; 67:201–205.

61. Drechsel H, Friends S, Nicholson G. Purification and chemical characterization of staphyloferrin-B, a hydrophilic siderophore from Staphylococci. *Biometals* 1993; 6: 185–192.
62. Persmark M, et al. Isolation and structure of rhizobactin-1021, a siderophore from the alfalfa symbiont *Rhizobium meliloti* 1021. *J Am Chem Soc* 1993; 115:3950–3956.
63. Appanna DL, Grundy BJ, Szczepan EW, Viswanatha T. Aerobactin synthesis in a cell-free system of *Aerobacter aerogenes* 62-1. *Biochim Biophys Acta* 1984; 801:437–443.
64. Braun V. *Escherichia coli* cells containing the plasmid ColV produce the iron ionophore aerobactin. *FEMS Microbiol Lett* 1981; 11:225–228.
65. Visca P, et al. Siderophore production by *Salmonella* species isolated from different sources. *FEMS Microbiol Lett* 1991; 79:225–232.
66. Lawlor KM, Payne SM. Aerobactin genes in *Shigella* spp. *J Bacteriol* 1984; 160:266–272.
67. Linke WD, Diekmann H, Crueger A. Metabolic products of microorganisms. 106. Structure of terregens factor. *Archiv Mikrobiol* 1972; 85:44–50.
68. Mullis KB, Pollack JR, Neilands JB. Structure of schizokinen, an iron-transport compound from *Bacillus megaterium*. *Biochemistry* 1971; 21:4894–4898.
69. Budzikiewicz H, Munzinger M, Taraz K, Meyer JM. Bacterial constituents. 69. Schizokinen, the siderophore of the plant deleterious bacterium *Ralstonia (Pseudomonas) solanacearum* ATCC 11696. *Z Naturforsch* 1997; C 52:496–503.
70. Goldman SJ, Lammers PJ, Berman MS, Sanders-Loehr J. Siderophore-mediated iron uptake in different strains of *Anabaena* sp. *J Bacteriol* 1983; 156:1144–1150.
71. Okujo N, Sakakibara Y, Yoshida T, Yamamoto S. Structure of acinetoferrin, a new citrate-based dihydroxamate siderophore from *Acinetobacter haemolyticus*. *Biometals* 1994; 7:170–176.
72. Kunze B, Trowitzschkienast W, Hofle G, Reichenbach H. Antibiotics from bacteria. 46. Nannochelin-A, nannochelin-B and nannochelin-C new iron-chelating compounds from *Nannocystis-exedens* (myxobacteria) production, isolation, physicochemical and biological properties. *J Antibiot* 1992; 45:147–150.
73. Reid RT, Live DH, Faulkner DJ, Butler A. A siderophore from a marine bacterium with an exceptional ferric ion affinity constant. *Nature* 1993; 366:455–458.
74. Stephan H, et al. Ornibactins—a new family of siderophores from *Pseudomonas*. *Biometals* 1993; 6:93–100.
75. Meyer JM, Van TV, Stintzi A, Berge O, Winkelmann G. Ornibactin production and transport properties in strains of *Burkholderia vietnamiensis* and *Burkholderia cepacia* (formerly *Pseudomonas cepacia*). *Biometals* 1995; 8:309–317.
76. Yamamoto S, Okujo N, Sakakibara Y. Isolation and structure elucidation of acinetobactin, a novel siderophore from *Acinetobacter baumannii*. *Arch Microbiol* 1994; 162: 249–254.
77. Actis LA, et al. Characterization of anguibactin, a novel siderophore from *Vibrio anguillarum* 775 (PJM1). *J Bacteriol* 1986; 167:57–65.
78. Naegeli HU, Zahner H. Metabolites of microorganisms. 193. Ferrithiocin. *Helv Chim Acta* 1980; 63:1400–1406.
79. Cox CD, Rinehart KL, Moore ML, Cook JC. Pyochelin—a novel structure of an iron chelating growth promoter for *Pseudomonas aeruginosa*. *Proc Natl Acad Sci USA* 1981; 78:4256–4260.
80. Haag H, et al. Purification of yersiniabactin—a siderophore and possible virulence factor of *Yersinia enterocolitica*. *J Gen Microbiol* 1993; 139:2159–2165.
81. Drechsel H, et al. Structure elucidation of yersiniabactin, a siderophore from highly virulent *Yersinia* strains. *Lieb Ann* 1995; 10:1727–1733.
82. Perry RD, Balbo PB, Jones HA, Fetherston JD, DeMoll E. Yersiniabactin from *Yersinia pestis*: biochemical characterization of the siderophore and its role in transport and regulation. *Microbiology* 1999; 145:1181–1190.

83. Snow GA. Mycobactins: iron chelating growth factors from mycobacteria. *Microbiol Rev* 1970; 43:99–125.
84. Gobin J, Horwitz MA. Exochelins of *Mycobacterium tuberculosis* remove iron from human iron-binding proteins and donate iron to mycobactins in the *M-tuberculosis* cell wall. *J Exp Med* 1996; 183:1527–1532.
85. Sharman GJ, Williams DH, Ewing DF, Ratledge C. Determination of the structure of exochelin MN, the extracellular siderophore from *Mycobacterium-neoaurum*. *Chem Biol* 1995; 2:553–561.
86. Yu SW, Fiss E, Jacobs WR. Analysis of the exochelin locus in *Mycobacterium smegmatis*: biosynthesis genes have homology with genes of the peptide synthetase family. *J Bacteriol* 1998; 180:4676–4685.
87. Meyer JM, Abdallah MA. The fluorescent pigment of *Pseudomonas aeruginosa*: biosynthesis, purification, and physicochemical properties. *J Gen Microbiol* 1978; 118: 125–129.
88. Meyer JM, Hornsperger JM. Role of pyoverdinepf, the iron binding fluorescent pigment of *Pseudomonas fluorescens* in iron transport. *Appl Microbiol Biotech Mol* 1978; 37: 114–118.
89. Jacques P, et al. Isopyoverdin Pp BTP1, a biogenetically interesting novel siderophore from *Pseudomonas putida*. *Natural Prod Lett* 1993; 3:213–218.
90. Jacques P, et al. Structure and characterization of isopyoverdin from *Pseudomonas putida* BTP1 and its regulation to the biogenic pathway leading to pyoverdins. *Z Naturforsch* 1995; C 50C:622–629.
91. Budzikiewicz H. Siderophores of fluorescent pseudomonads. *Z Naturforsch* 1997; C 52:713–720.
92. Hohlneicher U, Hartmann R, Taraz K, Budzikiewicz H. Bacterial constituents. 62. Pyoverdine, ferribactin, azotobactin—a new triad of siderophores from *Pseudomonas chlororaphis* ATCC 9446 and its relation to *Pseudomonas fluorescens* ATCC 13525. *Z Naturforsch* 1995; C 50:337–344.
93. O'Sullivan B, Xu J, Raymond KN. In: *Iron Chelators: New Development Strategies*. Ponte Vedra: Saratoga, 2000:177–208.
94. Wang QXH, Phanstiel O. Total synthesis of acinetoferrin. *J Org Chem* 1998; 63:1491–1495.
95. Maurer PJ, Miller MJ. Microbial iron chelators: total synthesis of aerobactin and its constituent amino acid, N6-acetyl-N6-hydroxylysine. *J Am Chem Soc* 1982; 104:3096–3101.
96. Bergeron RJ, Stolowich NJ, Kline SJ. Synthesis and solution dynamics of agrobactin-A. *J Org Chem* 1983; 48:3432–3439.
97. Bergeron RJ, McManis JS, Dionis JB, Garlich JR. An efficient synthesis of agrobactin and its gallium(III) chelate. *J Org Chem* 1985; 50:2780–2782.
98. Bergeron RJ, McMani JS, Perumal PT, Algee SE. The total synthesis of alcaligin. *J Org Chem* 1991; 56:5560–5563.
99. Deng JG, Hamada Y, Shioiri T. Total synthesis of alterobactin A, a super siderophore from an open-ocean bacterium. *J Am chem Soc* 1995; 117:7824–7825.
100. Lee BH, Miller MJ. Natural ferric ionophores—total synthesis of schizokinen, schizokinen-A, and arthrobactin. *J Org Chem* 1983; 48:24–31.
101. Bergeron RJ, McManis JS. The total synthesis of bisucaberin. *Tetrahedron* 1989; 45: 4939–4944.
102. Lu C, Buyer JS, Okonya JF, Miller M. Synthesis of optically pure chrysobactin and immunoassay development. *Biometals* 1996; 9:377–383.
103. Corey EJ, Bhattacharyya S. Total synthesis of enterobactin, macrocyclic iron transporting agent of bacteria. *Tetrahedron Lett* 1977; 45:3919–3922.

104. Rastetter WH, Erickson TJ, Venuti MC. Synthesis of iron chelators—enterobactin, enantioenterobactin, and a chiral analog. *J Org Chem* 1981; 46:3579–3590.
105. Shanzer A, Libman J. Total synthesis of enterobactin via an organotin template. *J Chem Soc Chem Commun* 1983; 15:846–847.
106. Rogers HJ. Synthesis of enterobactin. *J Chem Soc—Perkin Trans* 1995; 1(24):3073–3075.
107. Ramirez RJA, Karamanukyan L, Ortiz S, Gutierrez CG. A much improved synthesis of the siderophore enterobactin. *Tetrahedron Lett* 1997; 38:749–752.
108. Meyer M, et al. High-yield synthesis of the enterobactin trilactone and evaluation of derivative siderophore analogs. *J Am Chem Soc* 1997; 119:10093–10103.
109. Isowa Y, Ohmori M, Kurita H. Total synthesis of ferrichrome. *J Chem Soc Jap* 1974; 47:215–220.
110. Naegeli H, Kellerschierlein W. Metabolites of microorganisms. 174. New synthesis of ferrichrome—enantio-ferrichrome. *Helv Chim Acta* 1978; 61:2088–2095.
111. Bergeron RJ, McManis JS, Phanstiel O, Vinson JRT. A versatile synthesis of desferrioxamine B. *J Org Chem* 1995; 60:109–114.
112. Bergeron RJ, Pegram JJ. An efficient total synthesis of desferrioxamine B. *J Org Chem* 1988; 53:3131–3134.
113. Bergeron RJ, McManis JS. The total synthesis of desferrioxamine E and desferrioxamine G. *Tetrahedron* 1990; 46:5881–5888.
114. Adapa S, Huber P, Kellerschierlein W. Metabolites of microorganisms. 216. Isolation, structure and synthesis of ferrioxamine-H. *Helv Chim Acta* 1982; 65:1818–1824.
115. Maurer PJ, Miller MJ. Total synthesis of a mycobactin—mycobactin S2. *J Am Chem Soc* 1983; 105:240–245.
116. Hu J, Miller MJ. Total synthesis of a mycobactin S, a siderophore and growth promoter of *Mycobacterium smegmatis*, and determination of its growth inhibitory activity against *Mycobacterium tuberculosis*. *J Am Chem Soc* 1997; 119:3462–3468.
117. Ambrosi HD, Hartmann V, Pistorius D, Reissbrodt R, Trowitzsch-Kienast W. Myxochelins B, C, D, E, and F: a new structural principle for powerful siderophores imitating nature. *Eur J Org Chem* 1998; 3:541–551.
118. Mulqueen GC, Pattenden G, Whiting DA. Synthesis of the hydroxamate siderophore nannochelin-A. *Tetrahedron* 1993; 49:9137–9142.
119. Sakamoto T, Li H, Kikugawa Y. A total synthesis of nannochelin A. A short route to optically active N-omega-hydroxy-alpha-amino acid derivatives. *J Org Chem* 1996; 61:8496–8499.
120. Bergeron RJ, Kline SJ. Short synthesis of parabactin. *J Am Chem Soc* 1982; 104:4489–4492.
121. Nagao Y, Miyasaka T, Hagiwara Y, Fujita E. Utilization of sulfur containing leaving group. 3. Total synthesis of parabactin, a spermidine siderophore. *J Am Chem Soc—Perkin Trans* 1984; 1(2):183–187.
122. Smith MJ. Total synthesis and absolute configuration of rhizobactin, a structurally novel siderophore. *Tetrahedron Lett* 1989; 30:313–316.
123. Bergeron RJ, et al. Total synthesis of rhizoferrin, an iron chelator. *Tetrahedron* 1997; 53:427–434.
124. Widmer J, Keller-Schierlein W. Metabolic products of microorganisms. 139. Synthesis in sideramine series-rhodotorulic acid and dimerumic acid. *Helv Chim Acta* 1974; 57:1904–1912.
125. Fujii T, Hatanaka Y. Synthesis of rhodotorulic acid. *Tetrahedron* 1973; 29:3825–3831.
126. Carrano CJ, Raymond KN. Synthesis and characterization of iron complexes of rhodotorulic acid—novel dihydroxamate siderophore and potential chelating drug. *J Am Chem Soc* 1978:12.

127. Lee BH, Gerfen GJ, Miller MJ. Constituents of microbial iron chelators—alternate syntheses of delta-N-hydroxy-L-ornithine derivatives and applications to the synthesis of rhodotorulic acid. *J Org Chem* 1984; 49:2418–2423.
128. Bergeron RJ, Garlich JR, McManis JS. Total synthesis of vibriobactin. *Tetrahedron* 1985; 41:507–510.
129. Takeuchi Y, et al. Synthesis and siderophore activity of vibrioferrin and one of its diastereomeric isomers. *Chem Pharm Bull* 1999; 47:1284–1287.
130. Takeuchi Y, Akiyama T, Harayama T. Total synthesis of the siderophore vibrioferrin. *Chem Pharm Bull* 1999; 47:459–460.
131. Seebach D, Muller HM, Burger HM, Plattner DA. The triolide of (R)-3-hydroxybutyric acid—direct preparation from polyhydroxybutyrate and formation of a crown ester carbonyl complex with Na irons. *Angew Chem Int Ed Engl* 1992; 31:434–435.
132. Marinez ER, Salmassian EK, Lau TT, Gutierrez CG. Enterobactin and enantioenterobactin. *J Org Chem* 1996; 61:3548–3550.
133. Bickel H, et al. *Helv Chim Acta* 1960; 43:2129.
134. Keller-Schierlein W. *Helv Chim Acta* 1969; 61:603.
135. Dolence EK, Lin CE, Miller MJ, Payne SM. Synthesis and siderophore activity of albomycin-like peptides derived from N5-acetyl-N5-hydroxy-L-ornithine. *J Med Chem* 1991; 34:956–968.
136. Hu JD, Miller MJ. A new method for the synthesis of Ne-acetyl-Ne-hydroxy-L-lysine, the iron-binding constituent of several important siderophores. *J Org Chem* 1994; 59:4858–4861.
137. Lin YM, Miller MJ. Practical synthesis of hydroxamate-derived siderophore components by an indirect oxidation method and syntheses of a DIG-siderophore conjugate and a biotin-siderophore conjugate. *J Org Chem* 1999; 64:7451–7458.
138. Martell AE. *The Determination and Use of Stability Constants*. New York: VCH, 1988.
139. Leggett DJ. *Computational Methods for the Determination of Formation Constants*. New York: Plenum Press, 1985.
140. Harris WR, Carrano CJ, Raymond KN. *J Am Chem Soc* 1979; 101:2722–2727.
141. Matzanke BF, Muller-Matzanke G, Raymond KN. In: Loehr TM, ed. *Iron Carriers and Iron Proteins*. New York: VCH, 1989:1–121.
142. Raymond KN, Telford JR. In: Kessissoglou D, ed. *Bioinorganic Chemistry*. Kluwer, 1995:25–37.
143. Loomis LD, Raymond KN. *Inorg Chem* 1991; 30:906–911.
144. Harris WR, Raymond KN. *J Am Chem Soc* 1979; 101:6534–6541.
145. Rodgers S, Lee C, Ng C, Raymond KN. *Inorg Chem* 1987; 26:1622–1625.
146. Shanzer A, Libman J, Lifson S. Multiple weak forces in ion-binding molecules. *Pure Appl Chem* 1992; 64:1421–1435.
147. Scarrow RC, Ecker DJ, Ng C, Liu S, Raymond KN. Iron(III) coordination chemistry of linear dihydroserine derived from enterobactin. *Inorg Chem* 1991; 30:900–906.
148. Hou Z, Stack TDP, Sunderland CJ, Raymond KN. Enhanced iron(III) chelation through ligand predisposition: synthesis, structures and stability of tris-catecholate enterobactin analogs. *Inorg Chim Acta* 1997; 263:341–355.
149. Stack TDP, Hou Z, Raymond KN. *J Am Chem Soc* 1993; 115:6466–6467.
150. Konetschny-Rapp S, Jung G, Raymond KN, Meiwes J, Zahner H. Solution thermodynamics of the ferric complexes of new desferrioxamine siderophore obtained by directed fermentation. *J Am Chem Soc* 1992; 114:2224–2230.
151. Karpishin TB, Gebhard MS, Solomon EI, Raymond KN. Spectroscopic studies of the electronic structure of iron(III) tris(catecholates). *J Am Chem Soc* 1991; 113:2977–2984.
152. Karpishin TB, Stack TDP, Raymond KN. Octahedral vs. trigonal prismatic geometry in a series of metal complexes with a macrobicyclic tris(catecholate) ligand. *J Am Chem Soc* 1993; 115:182–192.

153. Braun V. Energy-coupled transport and signal transduction through the gram-negative outer membrane via TonB-ExbB-ExbD-dependent receptor proteins. *FEMS Microbiol Rev* 1995; 16:295–307.
154. Buchanan SK, et al. Crystal structure of the outer membrane active transporter FepA from *Escherichia coli*. *Nat Struct Biol* 1999; 6:56–63.
155. van der Helm D. The physical chemistry of bacterial outer-membrane siderophore receptor proteins. *Met Ions Biol Syst* 1998; 35:355–401.
156. Locher KP, et al. Transmembrane signaling across the ligand-gated FhuA receptor: crystal structures of free and ferrichrome-bound states allosteric changes. *Cell* 1998; 95:771–778.
157. Ferguson AD, Hofmann E, Coulton J, Dieterichs K, Welte W. Siderophore-mediated iron transport: crystal structure of FhuA with bound lipopolysaccharide. *Science* 1998; 282:2215–2220.
158. Muller G, Isowa Y, Raymond KN. Stereospecificity of siderophore mediated iron uptake in *Rhodotorula pilimanae* as probed by enantiorhodotorulic acid and isomers of chronic rhodotorulate. *J Biol Chem* 1985; 260:13921–13926.
159. Winkelmann G, Braun V. Stereoselective recognition of ferrichrome by fungi and bacteria. *FEMS Microbiol Lett* 1981; 11:237–241.
160. Neilands JB, Erickson TJ, Rastetter WH. Stereospecificity of the ferric enterobactin receptor of *Escherichia coli*—12. *J Biol Chem* 1981; 26:3831–3832.
161. Huschka H, Naegeli HU, Leuenbegeryf H, Kellerschierlein W, Winkelmann G. Evidence for a common siderophore transport system but different siderophore receptors in *Neurospora crassa*. *J Bacteriol* 1985; 162:715–721.
162. Thulasiraman P, et al. Selectivity of ferric enterobactin binding and cooperativity of transport in gram-negative bacteria. *J Bacteriol* 1998; 180:6689–6696.
163. Venuti MC, Rastetter WH, Neilands JB. 1,3,5-tris(N,N',N''-2,3-dihydroxybenzoyl) amino-methylbenzene, a synthetic iron chelator related to enterobactin. *J Med Chem* 1979; 22:123–124.
164. Ecker DJ, Matzanke BF, Raymond KN. Coordination chemistry of microbial iron transport. 35. Recognition and transport of ferric enterobactin in *Escherichia coli*. *J Bacteriol* 1986; 167:666–673.
165. Ecker DJ, Loomis LD, Cass ME, Raymond KN. Coordination chemistry of microbial iron transport. 39. Substituted complexes of enterobactin and synthetic analogs as probes of the ferric enterobactin receptor in *Escherichia coli*. *J Am Chem Soc* 1988; 110:2457–2464.
166. Stüntzi A, Raymond KN. Unpublished data.
167. Ardon O, et al. Iron uptake in *Ustilago maydis*: tracking the iron path. *J Bacteriol* 1998; 180:2021–2026.
168. Koedam N, et al. Detection and differentiation of microbial siderophores by isoelectric focusing and chrome azurol S overlay. *Biometals* 1994; 7:287–291.
169. Schwyn B, Neilands JB. Universal chemical assay for the detection and determination of siderophore. *Anal Biochem* 1987; 160:47–56.
170. Arnow LE. Colorimetric determination of the components of 3,4-dihydroxyphenyl-alanine-tyrosine mixtures. *J Biol Chem* 1937; 118:531–541.
171. Csaky TZ. On the estimation of bound hydroxylamine in biological materials. *Acta Chem Scand* 1948; 2:450–454.
172. Neilands JB. Microbial iron compounds. *Annu Rev Biochem* 1981; 50:715–731.
173. Winkelmann G. In: Winkelmann G, ed. *CRC Handbook of Microbial Iron Chelates*. Boca Raton, FL: CRC Press, 1991:65–105.
174. Neilands JB, Nakamura K. In: Winkelmann G, ed. *CRC Handbook of Microbial Iron Chelates*. Boca Raton, FL: CRC Press, 1991:1–14.

175. Jalal MAF, van der Helm D. In: Winkelmann G, ed. CRC Handbook of Microbial Iron Chelates. Boca Raton, FL: CRC Press, 1991:235–269.
176. Langemann K, Heineke D, Rupprecht S, Raymond KN. Nordesferriferrithiocin. Comparative coordination chemistry of a prospective therapeutic iron chelating agent. *Inorg Chem* 1996; 35:5663–5673.
177. Stephan H, Freund S, Meyer JM, Winkelmann G, Jung G. Structure elucidation of the gallium-ornibactin complex by 2D-NMR spectroscopy. *Liebigs Ann Chem* 1993; 43–48.
178. Caudle MT, Stevens RD, Crumbliss AL. Electrospray mass spectrometry of 1:1 ferric dihydroxamates. *Inorg Chem* 1994; 33:6111–6115.
179. Kersting B, Telford JR, Meyer M, Raymond KN. Gallium(III) catecholate complexes as probes for the kinetics and mechanism of inversion and isomerization of siderophore complexes. *J Am Chem Soc* 1996; 118:5712–5721.
180. Hou ZG, Raymond KN, O'Sullivan B, Esker TW, Nishio T. A preorganized siderophore: thermodynamic and structural characterization of alcaligin and bisucaberin, microbial macrocycle dihydroxamate chelating agents. *Inorg Chem* 1998; 37:6630–6637.
181. Hossain MB, Jalal MAF, van der Helm D, Shimizu K, Akiyama M. Crystal structure of retro-isomer of the siderophore ferrioxamine E. *J Chem Crystallogr* 1998; 53–56.
182. Hossain MB, Jalal MAF, van der Helm D. Gallium-complex of anguibactin, a siderophore from fish pathogen *Vibrio anguillarum*. *J Chem Crystallogr* 1998; 28:57–60.
183. Karpishin TB, Raymond KN. The first structural characterization of metal-enterobactin complex: [V(enterobactin)]₂⁻. *Angew Chem Int Ed* 1992; 31:466–468.
184. Engwilmot DL, van der Helm D. Molecular and crystal-structure of the linear tri-catechol siderophore, agrobactin. *J Am Chem Soc* 1980; 102:7719–7725.
185. Zalkin A, Forrester JD, Templeton DH. Ferrichrome A tetrahydrate, determination of crystal and molecular structure. *J Am Chem Soc* 1966; 88:1810.
186. Crosa JH. The relationship of plasmid mediated iron transport and bacterial virulence. *Annu Rev Microbiol* 1984; 38:69–89.
187. Ramurthy S, Miller MJ. Framework-reactive siderophore analogs as potential cell-selective drugs. Design and syntheses of trimelamol-based iron chelators. *J Org Chem* 1996; 61:4120–4124.
188. Miller MJ, Malouin F. Microbial iron chelators as drug delivery agents—the rational design and synthesis of siderophore-antibiotic conjugates. *Acc Chem Res* 1993; 26:241–249.
189. Miller MJ, McKee JA, Minnick AA, Dolence EK. The design, synthesis and study of siderophore-antibiotic conjugates. Siderophore mediated drug transport. *Biometals* 1991; 4:62–69.
190. Minnick AA, McKee JA, Dolence EK, Miller MJ. Iron transport mediated antibacterial activity of and development of resistance to hydroxamate and catecholate siderophore-carbacephalosporin conjugates. *Antimicrobiol Agents Chemother* 1992; 36:840–850.
191. Diarra MS, et al. Species selectivity of new siderophore-drug conjugates that use specific iron uptake for entry into bacteria. *Antimicrob Agents Chemother* 1996; 40:2610–2617.
192. Brochu A, et al. Modes of action and inhibitory activities of new siderophore-beta-lactam conjugates that use specific iron uptake pathways for entry into bacteria. *Antimicrob Agents Chemother* 1992; 36:2166–2175.
193. Ames BN, Ames GF, Young JD, Tsuchiya D, Lecocq J. Illicit transport: the oligopeptide premease. *Proc Natl Acad Sci USA* 1973; 70:456–458.
194. Gibson F, Magrath D. The isolation and characterization of a hydroxamic acid (aerobactin) formed by *Aerobacter aerogenes*. *Biochim Biophys Acta* 1969; 192:175.
195. Rabsch W, Paul P, Reissbrodt R. A new hydroxamate siderophore for iron supply of *Salmonella*. *Acta Microbiol Hung* 1987; 34:85–92.

196. Murakami K, Fuse H, Takimura O, Kamimura K, Yamaoka Y. Phylogenetic analysis of marine environmental strains of *Vibrio* that produce aerobactin. *J Marine Biot* 1998; 6:76–79.
197. Okujo N, Yamamoto S. Identification of the siderophores from *Vibrio hollisae* and *Vibrio mimicus* as aerobactin. *FEMS Microbiol Lett* 1994; 118:187–192.
198. Sevinc MS, Page WJ. Generation of azotobacter vinelandii strains defective in siderophore production and characterization of a strain unable to produce known siderophores. *J Gen Microbiol* 1992; 138:587–596.
199. Linget C, et al. Structure of azoverdin, a pyoverdin-like siderophore of *Azomonas macrocytogenes* ATCC 12334. *Tetrahedron Lett* 1992; 33:1889–1892.
200. Adolphs M, Taraz K, Budzikiewicz H. Catechol siderophores from *Chryseomonas luteola*. *Z Naturforsch* 1996; C 51:281–285.
201. Risse D, Beiderbeck H, Taraz K, Budzikiewicz H, Gustine D. Bacterial constituents part LXXVII. Corrugatin, a lipopeptide siderophore from *Pseudomonas corrugata*. *Z Naturforsch* 1998; C 53:295–304.
202. Fiss EH, Yu SW, Jacobs WR. Identification of genes involved in the sequestration of iron in mycobacteria—the ferric exochelin biosynthetic and uptake pathways. *Mol Microbiol* 1994; 14:557–569.
203. Hohlneicher U, Hartmann R, Taraz K, Budzikiewicz H. The structure of ferribactin from *Pseudomonas fluorescens* ATCC 13525. 1. *Z Naturforsch* 1992; B 47:1633–1638.
204. Feistner G, Korth H, Ko H, Pulverer G, Budzikiewicz H. Ferrorsamine—a siderophore from *Erwinia rhapontici*. *Curr Microbiol* 1983; 8:239–243.
205. Ito T. Enzymatic determination of itoic acid, a *Bacillus subtilis* siderophore, and 2,3-dihydroxybenzoic acid. *App Env Microbiol* 1993; 59:2343–2345.
206. Keller-Schierlein W, Hagmann L, Zahner H, Huhn W. Metabolic products from microorganisms. 250. Maduraferrin, a novel siderophore from *Actinomadura madurae*. *Helv Chim Acta* 1988; 71:1528–1540.
207. Kunze B, Bedorf N, Kohl W, Hofle G, Reichenbach H. Myxochelin A, a new iron chelating compound from *Angiococcus disciformis* (myxobacterales)—production, isolation, physicochemical and biological properties. *J Antibiot* 1989; 42:14–17.
208. Hu XC, Boyer GL. Isolation and characterization of the siderophore N-deoxyschizokinene from *Bacillus megaterium* ATCC 19213. *Biometals* 1995; 8:357–364.
209. Ratledge C, Snow GA. Isolation and structure of nocobactin NA, a lipid-soluble iron binding compound from *Nocardia asteroides*. *Biochem J* 1974; 139:407–413.
210. Budzikiewicz H. Siderophores of fluorescent pseudomonads. *Z Naturforsch* 1997; C 52:713–720.
211. Smith MJ, Neilands JB. Rhizobactin, a siderophore from *Rhizobium meliloti*. *J Plant Nutr* 1984; 7:449–458.
212. Munzinger M, et al. S,S-rhizoferrin (enantiomer-rhizoferrin) a siderophore of *Ralstonia (Pseudomonas) pickettii* DSM 6297—the optical antipode of R,R-rhizoferrin isolated from fungi. *Biometals* 1999; 12:189–193.
213. Bachhawat AK, Ghosh S. Iron transport in *Azospirillum brasiliense*—role of the siderophore spirillobactin. *J Gen Microbiol* 1987; 133:1759–1765.
214. Yamamoto S, Okujo N, Yoshida T, Matsuura S, Shinoda S. Structure and iron transport activity of vibrioferrin, a new siderophore of *Vibrio parahaemolyticus*. *J Biochem* 1994; 115:868–974.
215. Dilworth MJ, Carson C, Giles RGF, Byrne LT, Gleen AR. *Rhizobium leguminosarum* bv. viciae produces a novel cyclic trihydroxamate siderophore, vicbactin. *Microbiology* 1998; 144:7481–791.
216. Okujo N, et al. Structure of vulnibactin, a new polyamine-containing siderophore from *Vibrio vulnificus*. *Biometals* 1994; 7:109–116.

217. Hossain MB, Jalal MAF, van der Helm D. 6-L-alanineferrirubin, a ferrichrome-type siderophore from the fungus *Aspergillus ochraceus*. *Acta Crystallogr* 1997; 15:716–718.
218. Howard DH. Acquisition, transport, and storage of iron by pathogenic fungi. *Clin Microbiol Rev* 1999; 12:394–404.
219. Wong GB, Kappel MJ, Raymond KN, Matzanke B, Winkelmann G. Coordination chemistry of microbial iron transport compounds. 24. Characterization of coprogen and ferricrocin, 2 ferric hydroxamate siderophores. *J Am Chem Soc* 1983; 105:810–815.
220. Burt WR. Identification of coprogen B and its breakdown products from *Histoplasma capsulatum*. *Infect Immun* 1982; 35:990–996.
221. Harrington GL, Neilands JB. Isolation and characterization of dimerum acid from *Verticillium dahliae*. *J Plant Nutr* 1982; 5:675–682.
222. Jalal MAF, Love SK, van der Helm D. Siderophore mediated iron(III) uptake in *Gliocladium virens*. 1. Properties of cis-fusarinine, trans-fusarinine, dimerum acid, and their ferric complexes. *J Inorg Biochem* 1986; 28:417–430.
223. Jalal MAF, et al. Extracellular siderophores from *Aspergillus ochraceus*. *J Bacteriol* 1984; 158:683–688.
224. Ohra J, et al. Production of the phytotoxic metabolite, ferricrocin, by the fungus *Colletrichum gloeosporioides*. *Biosci Biotechnol Biochem* 1995; 59:113–114.
225. Diekmann H, Krezdorn E. Metabolic products of microorganisms. 150. Ferricrocin, thiacythylfusigen and other sideramines from fungi of the genus *Aspergillus*, group *Fumigatus*. *Arch Microbiol* 1975; 106:191–194.
226. Diekmann H. Metabolic products of microorganisms. 83. Biosynthesis of sideramines in fungi—incorporation of ornithine and fusigen into ferrirhodin. *Archiv Mikrobiol* 1970; 74:301.
227. Jalal MAF, Galles JL, van der Helm D. Structure of des(diserylglycyl)ferrirhodin, DDF, a novel siderophore from *Aspergillus ochraceus*. *J Org Chem* 1985; 50:5642–5645.
228. Emery T. Isolation, characterization, and properties of fusarinine, a d-hydroxaminc acid derivative of ornithine. *Biochemistry* 1965; 4:1410.
229. Diekmann H. Stoffwechselprodukte von Mikroorganismen. 56. Mitteilung. Fusigen—ein neues Sideramin aus Pizlen. *Arch Microbiol* 1967; 58:1.
230. Frederick CB, Bentley MD, Shive W. The structure of the fungal siderophore, isotriornicin. *Biochem Biophys Res Commun* 1982; 105:133–138.
231. Emery T. Malonichrome, a new iron chelate from *Fusarium roseum*. *Biochim Biophys Acta* 1980; 7:382–390.
232. Hossain MB, Jalal MAF, Benson BA, Barnes CL, van der helm D. Structure and conformation of two coprogen-type siderophores—neocoprogen I and neocoprogen-II. *J Am Chem Soc* 1987; 109:4948–4954.
233. Shenker M, et al. Chemical structure and biological activity of a siderophore produced by *Rhizopus arrhizus*. *Soil Sci Soc Am J* 1995; 59:837–843.
234. Hossain MB, Engwilmot DL, Loghry RA, van der Helm D. Circular dichroism, crystal structure, and absolute configuration of the siderophore ferric N,N',N''-triacylfusarinine, FEC39H57N6O15. *J Am Chem Soc* 1980; 102:5766–5773.
235. Frederick CB, Bentley MD, Shive W. Structure of thriornicin, a new siderophore. *Biochemistry* 1981; 20:2436–2438.
236. Cooper SR, McArdle JW, Raymond KN. Siderophore electrochemistry: relation to intracellular iron release mechanism. *Proc Natl Acad Sci USA* 1978; 75:3551–3554.
237. Anderegg G, L'Eplattenier F, Schwarzenbach G. *Helv Chim Acta* 1963; 46:1409.
238. Kraiter DC, Zak O, Aisen P, Crumbliss AL. *Inorg Chem* 1998; 37:964–968.
239. Carrano CJ, Raymond KN. Ferric ion sequestering agents. 2. Kinetics and mechanism of iron removal from transferrin by enterobactin and synthetic triccatechols. *J Am Chem Soc* 1979; 101:5401–5404.

240. Carrano CJ, Cooper SR, Raymond KN. Coordination chemistry of microbial iron transport compounds. 11. Solution equilibria and electrochemistry of ferric rhodotorulate complexes. *J Am Chem Soc* 1979; 101:599–604.
241. Martell AE, Smith RM. *Critical Stability Constants*. New York: Plenum Press, 1977.
242. Harris DC. *Quantitative Chemical Analysis*. New York: Freeman, 1987.
243. Lin W-C, Fisher SM, Wells Jr JS, Ricca CS, Principe PA, Trejo WH, Bonner DP, Gougoutous JZ, Toeplitz BK, Sykes RB. Siderochelin, a new ferrous-ion chelating agent produced by "*Nocardia*." *J Antibiot* 1981; 34:791–799.

Iron Chelator Chemistry

ZU D. LIU and ROBERT C. HIDER

King's College London, London, England

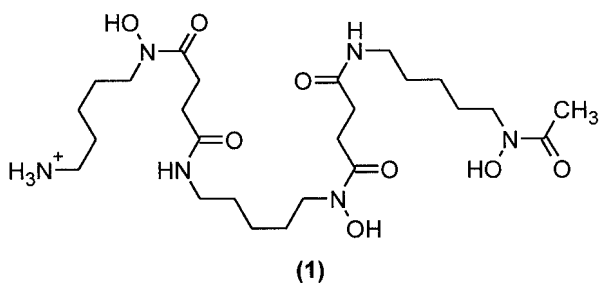
I. INTRODUCTION	321
II. DESIGN FEATURES OF IRON CHELATORS	322
A. Metal Selectivity and Affinity	322
B. Iron(III) Ligand Selection	324
C. Thermodynamic Stability of Iron(III) Complexes	328
III. CRITICAL FEATURES FOR CLINICAL APPLICATION	331
A. Lipophilicity and Molecular Weight	331
B. Drug Bioavailability and Disposition	334
C. Toxicity	334
IV. IRON CHELATORS CURRENTLY UNDER INVESTIGATION	336
A. Hexadentate Chelators	336
B. Tridentate Chelators	341
C. Bidentate Chelators	344
V. CONCLUSIONS	350
ACKNOWLEDGMENTS	351
REFERENCES	351

I. INTRODUCTION

Iron is a critically important metal for a wide variety of cellular events; indeed, no life form is possible without the presence of this element. Iron holds this central position in part by virtue of its facile redox chemistry and its high affinity for oxygen. It possesses incompletely filled *d* orbitals and can exist in various valencies, the most

common oxidation states in aqueous media being Fe(II) (d^6) and Fe(III) (d^5). The redox potential between these two states is such that oxidation processes centered on the iron can be coupled to a wide range of metabolic reactions.

Although iron is essential for the proper functioning of all living cells, it is toxic when present in excess. In the presence of molecular oxygen, “loosely bound” iron is able to redox-cycle between the two most stable oxidation states, thereby generating oxygen-derived free radicals such as the hydroxyl radical (1). Hydroxyl radicals are highly reactive and capable of interacting with most types of biological molecules, including sugars, lipids, proteins, and nucleic acids, resulting in peroxidative tissue damage. Indeed free radicals play a significant role in lipid peroxidation, protein degradation, and nucleic acid degradation (2). The production of such highly reactive species is undesirable, and thus a number of protective strategies are adopted by cells to prevent their formation. One of the most important strategies is the tight control of iron storage, transport, and distribution. In fact, iron metabolism in humans is highly conservative, with the majority of iron being recycled within the body. Since humans lack a physiological mechanism for eliminating iron, iron homeostasis is achieved by the regulation of iron absorption. In the normal individual, iron levels are under extremely tight control and there is little opportunity for iron-catalyzed free-radical-generating reactions to occur. However, there are situations when the iron status can change, either locally as in ischemic tissue, or systematically as with genetic hemochromatosis or transfusion-induced iron overload. In such circumstances, the elevated levels of iron ultimately lead to free-radical-mediated tissue/organ damage and eventual death (3). Although excess iron can be removed by venesection where adequate erythropoietic reserve exists, e.g., in cases of hemochromatosis, iron chelation is the only effective way to relieve iron overload in transfusion-dependent patients such as those suffering from β -thalassaemia. Desferrioxamine-B (DFO) (1), the most widely used iron chelator in hematology over the past 30 years, has a major disadvantage of being orally inactive (4). Consequently, there is an urgent need for an orally active iron chelating agent (5).



In order to identify an ideal iron chelator for clinical use, careful design consideration is essential; a range of specifications must be considered such as metal selectivity and affinity, kinetic stability of the complex, bioavailability, and toxicity.

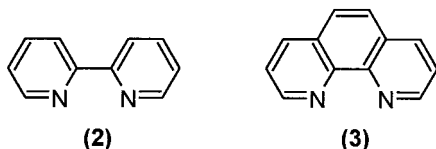
II. DESIGN FEATURES OF IRON CHELATORS

A. Metal Selectivity and Affinity

In designing iron chelators for clinical application, the properties for metal selectivity and resultant ligand–metal complex stability are paramount. The selection of an

appropriate ligand for metal complexation can be rationalized by classification of metals and ligands according to the concept of “hard” and “soft” acids and bases (6). Ligands which contain at least one electron pair to be donated for bond formation are generally considered as Lewis bases, and metal cations are regarded as Lewis acids. Hard metal cations retain their nonvalence electrons very strongly and as a result are of small size and high charge density. Such cations tend to form strong complexation with hard ligands which contain highly electronegative donor atoms. Correspondingly, soft metal cations are of low charge density and prefer to associate with soft ligands containing donor atoms which also possess low charge density.

In theory, chelating agents can be designed for either the iron(II) (ferrous) or iron(III) (ferric) oxidation state. High-spin iron(III) is a spherically symmetrical, tri-positive cation of radius 0.65 Å, and as such is classified as a hard Lewis acid by virtue of its high charge density. It forms the most stable bonds with “hard” ligands such as the charged hydroxamate oxygen atoms of DFO (1). In contrast, the iron(II) cation, which has relatively low charge density, prefers chelators containing “soft” donor atoms, exemplified by the nitrogen-containing ligands such as 2,2'-bipyridyl (2) and 1,10-phenanthroline (3).



Ligands that prefer iron(II) retain an appreciable affinity for other biologically important bivalent metals such as copper(II) and zinc(II) ions (Table 1), and thus the design of a nontoxic iron(II)-selective ligands is extremely difficult, and indeed may not be possible. In contrast, iron(III)-selective ligands, typically oxyanions and notably hydroxamates and catecholates, are generally more selective for tribasic metal cations over dibasic cations (Table 1). Most tribasic cations, for instance, aluminum(III) and gallium(III), are not essential for living cells and thus in practice iron(III) provides the best target for “iron chelator” design under biological conditions. An additional advantage of high-affinity iron(III) chelators is that, under aer-

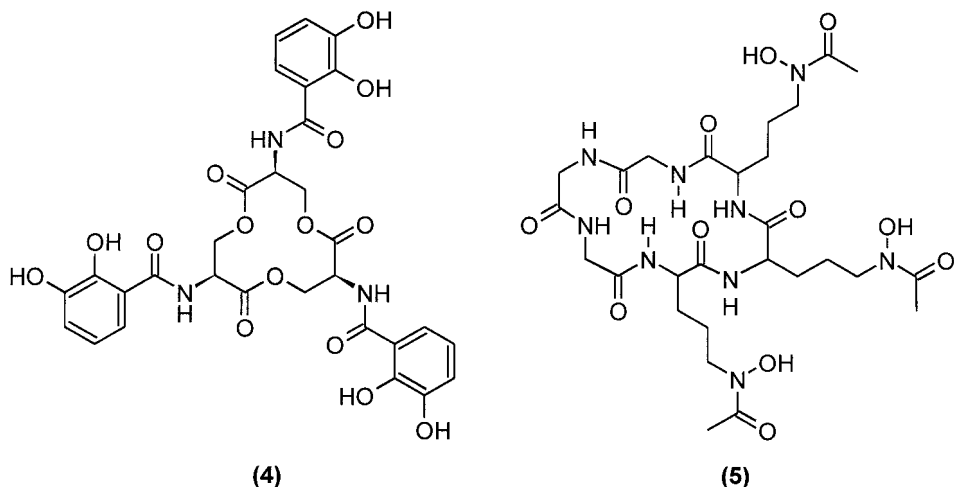
Table 1 Metal Affinity Constants for Selected Ligands

Ligand	Log cumulative stability constant					
	Fe(III)	Al(III)	Ga(III)	Cu(II)	Zn(II)	Fe(II)
DFO (1)	30.6	25.0	27.6	14.1	11.1	7.2
2,2'-Bipyridyl (2)	16.3	—	7.7	16.9	13.2	17.2
1,10-Phenanthroline (3)	14.1	—	9.2	21.4	17.5	21.0
DMB (6)	40.2	—	—	24.9	13.5	17.5
Acetohydroxamic acid (7)	28.3	21.5	—	7.9	9.6	8.5
Deferiprone (11)	37.2	35.8	32.6	21.7	13.5	12.1
EDTA (12)	25.1	16.5	21.0	18.8	16.5	14.3
DTPA (13)	28.0	18.6	25.5	21.6	18.4	16.5

Data from Ref. 7.

obic conditions, they will chelate iron(II) cations and autoxidize them to the iron(III) species (8). Thus, high-affinity iron(III)-selective ligands bind both iron(III) and iron(II) under most physiological conditions.

Siderophores (see Chapter 12), compounds possessing a high affinity for iron(III) and produced by microorganisms for scavenging iron from the environment, utilize the above principle (9). Typically they are hexadentate in design and utilize catechol or hydroxamate as ligands, for instance, enterobactin (4), deferriferrichrome (5), and DFO (1).

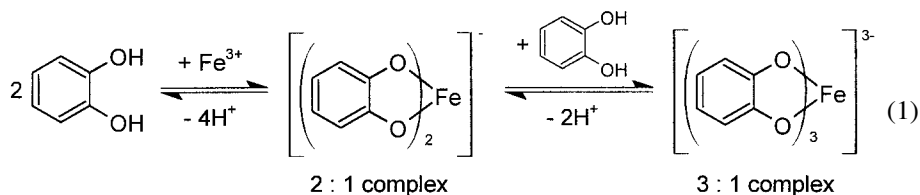


The stereochemistry of these molecules is such that the coordination sphere of iron(III) is completely occupied by the oxygen-containing ligands such as ferrioxamine B (Fig. 1). The selectivity of these molecules for iron(III) over iron(II) is enormous, leading to extremely low redox potentials—for example, enterobactin -750 mV and DFO -468 mV (10).

B. Iron(III) Ligand Selection

1. Catechols

Catechol moieties possess a high affinity for iron(III). This extremely strong interaction with tripositive metal cations results from the high electron density of both oxygen atoms. However, this high charge density is also associated with the high affinity for protons (pK_a values, 12.4 and 8.4). Thus the binding of cations by catechol has marked pH sensitivity (11). The complexes likely to form at pH 7.0 each bear a net charge [Eq. (1)] and consequently are unlikely to permeate membranes by simple diffusion.



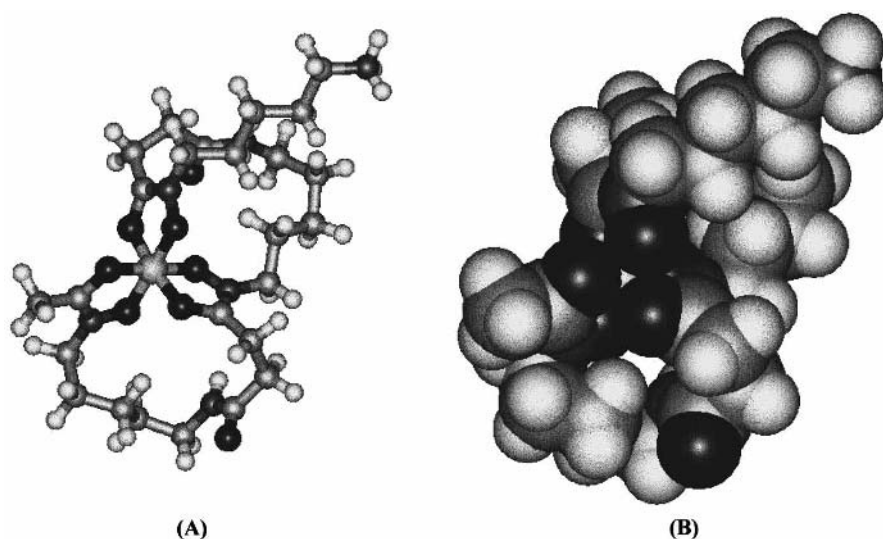
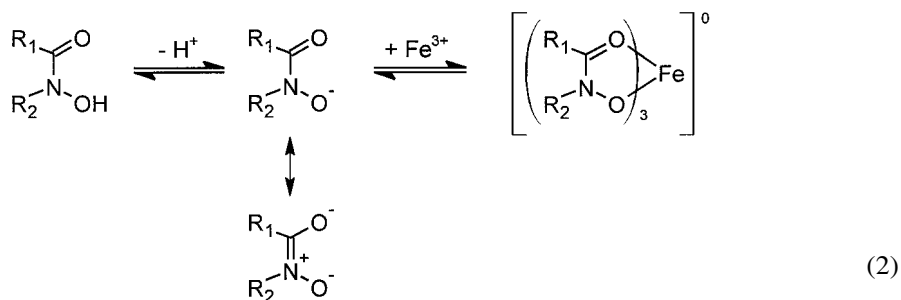


Figure 1 Energy-minimized structure of ferrioxamine B (Λ -C-trans, trans conformation): (A) ball-stick model; (B) space-filling model.

Therefore these charged iron complexes will tend to be trapped in intracellular compartments. For bidentate catechols, the 2:1 complex is the dominant form in the pH range 5.5–7.5, the 3:1 complex forming in appreciable quantities only above pH 8.0 (Fig. 2). With the 2:1 complexes, the iron atom is not completely protected from the solvent and consequently is able to interact with hydrogen peroxide or oxygen, resulting in the generation of hydroxyl radicals. A further problem with catechol-based ligands is their susceptibility toward oxidation (11). Although the oxidation products also possess the ability to coordinate cations, the affinity is generally reduced. To date, no catechol-based ligands have been identified as being suitable for clinical application (12).

2. Hydroxamates

The hydroxamate moiety possesses a lower affinity for iron than catechol. However, it has the advantage of forming neutral tris-complexes with iron(III) which are able to permeate membranes [Eq. (2)].



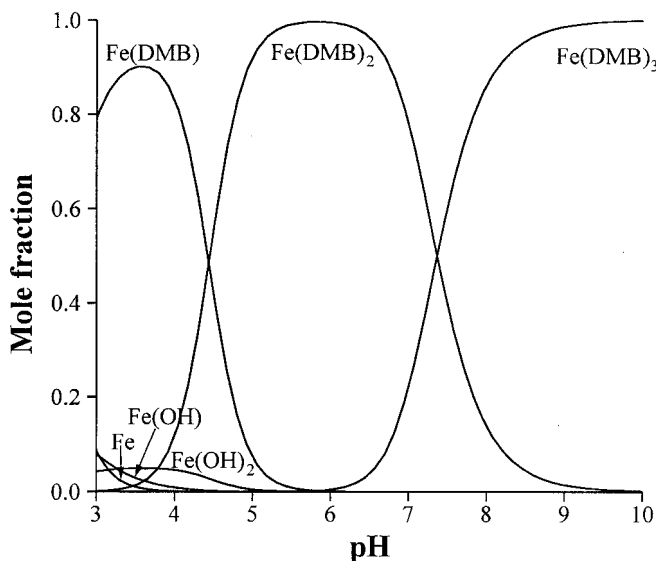
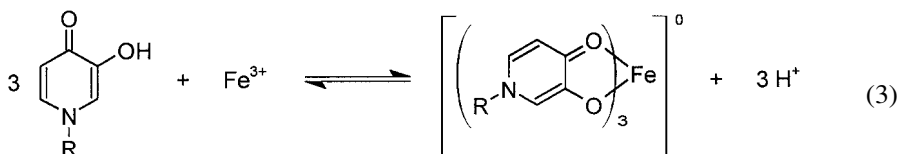


Figure 2 Speciation plot of iron(III) in the presence of N,N-dimethyl-2,3-dihydroxybenzamide (DMB); $[\text{Fe}^{3+}]_{\text{total}} = 1 \times 10^{-5} \text{ M}$; $[\text{DMB}] = 1 \times 10^{-4} \text{ M}$. Speciation plots display the relative concentration of different complex species as function of pH. Thus, at pH 6.0 $\text{Fe}(\text{DMB})_2$ totally dominates, whereas at pH 7.4 there is approximately equal concentration of $\text{Fe}(\text{DMB})_2$ and $\text{Fe}(\text{DMB})_3$.

The selectivity of hydroxamates, like catechols, favors tribasic cations over dibasic cations (Table 1). Because of the relatively low protonation constant ($\text{p}K_a \approx 9$), hydrogen-ion interference at physiological pH is less pronounced than for that of catechol ligands, and consequently the 3:1 complex predominates at pH 7.0 when sufficient ligand is present. Unfortunately, many hydroxamates are metabolically labile and are only poorly absorbed orally (13,14). Numerous approaches have been taken to address these problems. However, to date no suitable hydroxamate derivative with comparable activity to subcutaneous DFO has been identified (15,16).

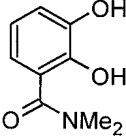
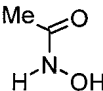
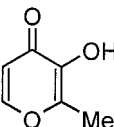
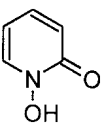
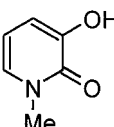
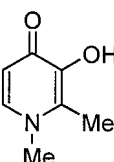
3. Hydroxypyridinones

Hydroxypyridinones (HPOs) have combined aspects of both hydroxamate and catechol groups. Like both catechol and hydroxamate, the HPOs form five-membered chelate rings in which the metal is coordinated by two vicinal oxygen atoms. The HPOs are monoprotic acids at pH 7.0, and thus form neutral tris-iron(III) complexes [Eq. (3)].

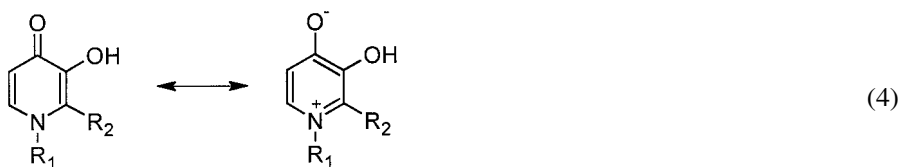


The affinity of such compounds for iron(III) reflects the $\text{p}K_a$ values of the chelating oxygen atoms: the higher the affinity for iron(III), the higher the $\text{p}K_a$ value (Table

Table 2 pK_a Values and Affinity Constants of Dioxobidentate Ligands for Iron(III). $pFe^{3+} = -\log[Fe^{3+}]$ when $[ligand] = 10 \mu M$ and $[Fe^{3+}] = 1 \mu M$

Ligand	Structure	pK_{a_1}	pK_{a_2}	Log β_3	pFe^{3+} (at pH 7.4)
<i>N,N</i> -Dimethyl-2,3-dihydroxybenzamide (DMB) (6)		8.4	12.1	40.2	15
Acetohydroxamic acid (7)		—	9.4	28.3	13
2-Methyl-3-hydroxy-pyran-4-one (maltol) (8)		—	8.7	28.5	15
1-Hydroxypyridin-2-one (9)		—	5.8	27	16
1-Methyl-3-hydroxy-pyridin-2-one (10)		0.2	8.6	32	16
1,2-Dimethyl-3-hydroxy-pyridin-4-one (deferiprone) (11)		3.6	9.9	37.2	20

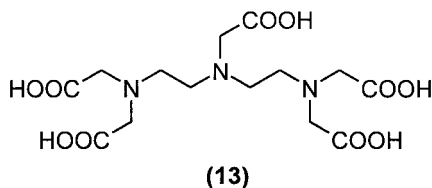
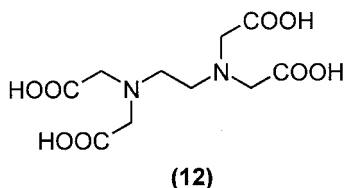
2). There are three classes of metal-chelating HPO ligands, 1-hydroxypyridin-2-one (**9**), 3-hydroxypyridin-2-one (**10**), and 3-hydroxypyridin-4-one (**11**) (Table 2). Of these three heterocyclic chelators, the pyridin-4-ones possess the highest affinity for iron(III) (Table 2) and are selective for tribasic metal cations over dibasic cations (Table 1). Thus, although such ligands also possess favorable affinities for aluminum(III), gallium(III), and indium(III), as these metals are not physiologically important, this property does not present a clinical problem. The surprisingly high pK_a value of the carbonyl function of 3-hydroxypyridin-4-one results from extensive delocalization of the lone pair associated with the ring nitrogen atom [Eq. (4)].



Although catechol derivatives possess higher β_3 values than that of 3-hydroxypyridin-4-one, the corresponding pFe^{3+} values are lower (Table 2). This difference is due to the relatively higher affinity of catechol for protons. Thus, of all dioxygen ligand classes, the 3-hydroxypyridin-4-ones possess the greatest affinity for iron(III) in the physiological pH range, as indicated by their respective pFe^{3+} values (Table 2).

4. Aminocarboxylates

Aminocarboxylate ligands are also excellent iron(III)-chelating agents. Several polycarboxylate ligands such as ethylenediaminetetraacetic acid (EDTA) (**12**) and diethylenetriaminepentaacetic acid (DTPA) (**13**), have been widely investigated for iron chelation.



However, the selectivity of these molecules for iron(III) is relatively poor (Table 1). This lack of selectivity leads to zinc depletion in patients receiving aminocarboxylate-based ligands such as DTPA (17).

C. Thermodynamic Stability of Iron(III) Complexes

Ligands can be structurally classified according to the number of donor atoms that each molecule possesses for coordinate bond formation. Ligands that contain one donor atom, such as NH_3 and H_2O , are termed monodentate. Ligands that contain two or more donor atoms are termed bidentate, tridentate, tetradentate, hexadentate, or generally multidentate.

The coordination requirements of iron(III) are best satisfied by six donor atoms ligating in an octahedral fashion to the metal center. A factor of great importance in the stability of a metal complex is the number of chelate rings formed in the resultant ligand-metal complex. The most favorable ring sizes consist of five or six atoms. The number of chelating rings can be increased by increasing the number of donor atoms attached to the ligand. For example, a metal ion with coordination number 6 may form three rings with a bidentate ligand or five rings with a hexadentate ligand (Fig. 3). In order to maximize the thermodynamic stability of the iron(III) complex it is necessary to incorporate all six donors into a single molecular structure, thereby creating a hexadentate ligand. This increase in thermodynamic chelate stability is largely associated with entropic changes that occur on going from free ligand and solvated free metal to ligand-metal complex [Eqs. (5)–(7)].

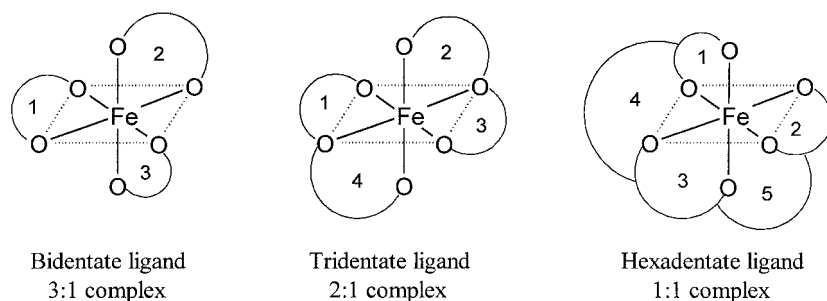
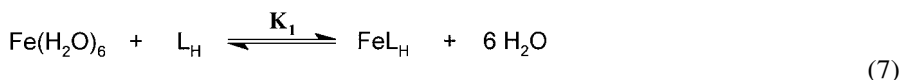
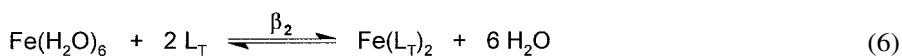
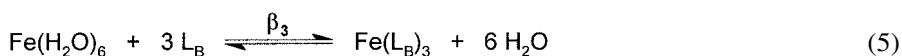


Figure 3 Schematic representation of chelate ring formation in metal–ligand complexes.



L_B , bidentate; L_T , tridentate; L_H , hexadentate ligand

Significantly, the majority of natural siderophores are hexadentate ligands. The overall stability constant trends for bidentate and hexadentate ligands are typified by the bidentate ligand *N,N*-dimethyl-2,3-dihydroxybenzamide (DMB) (**6**) and the hexadentate congener MECAM (**14**); a differential of three log units in stability is observed between them (Table 3). Similarly, comparison of the bidentate ligand acetohydroxamic acid (**7**) with the linear hexadentate ligand DFO (**1**) shows a positive increment of 2.3 log units (Table 3).

Although MECAM binds iron(III) three orders of magnitude more tightly than its bidentate analog DMB, other hexadentate catechols—for instance, enterobactin—bind iron(III) even more tightly (Table 4). Indeed, the smaller the conformational space of the free ligand, the higher the stability of the complex; as the difference between the flexibility of the ligand and its corresponding iron complex decreases, so does the difference in entropy. An extreme example would be the situation where no conformational change between free ligand and iron(III) complex occurs. Thus

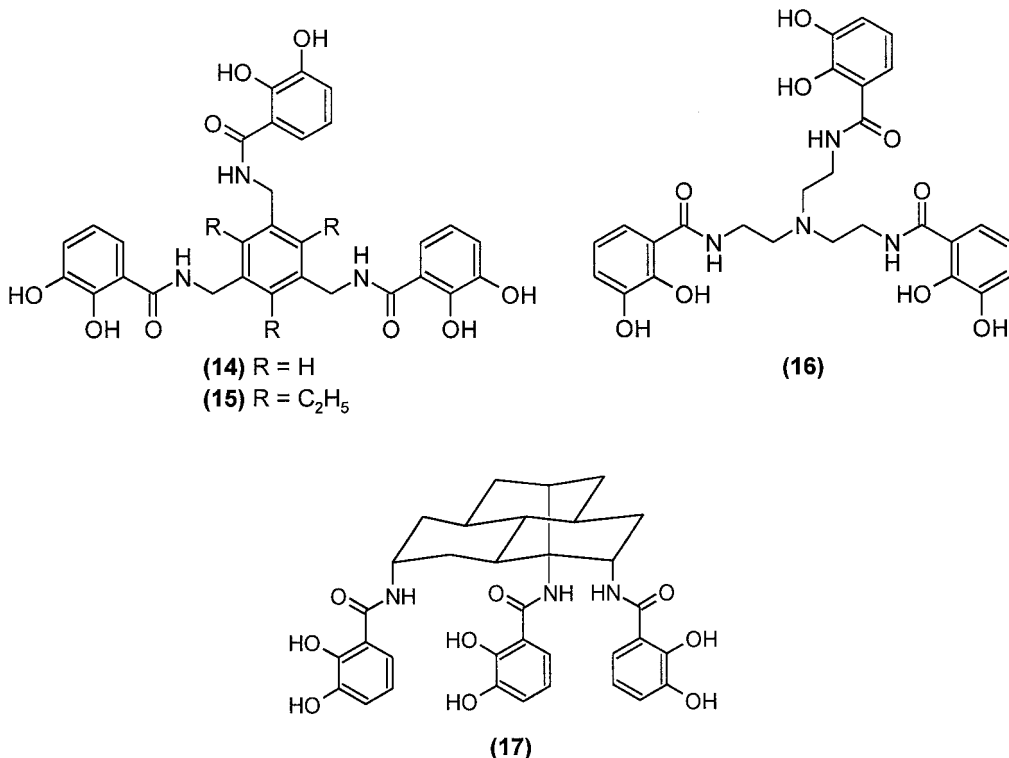
Table 3 Comparison of pFe^{3+} Values and Stability Constants for Bidentate and Hexadentate Ligands

Ligand	pFe^{3+} (at pH 7.4)	Log stability constant (Fe^{3+})
DMB (6)	15	40.2
MECAM (14)	28	43
Acetohydroxamic acid (7)	13	28.3
DFO (1)	26	30.6

Table 4 Stability Constants (Fe^{3+}) for a Range of Hexadentate Catechol Ligands

Ligand	Structure conformation	Log stability constant
Enterobactin (4)	Chiral monocyclic ring	49
(17)	Rigid tricyclic tripod	49
(Et) ₃ MECAM (15)	Planar ring with preorganised side chains	47
TRENCAM (16)	N-tripod	44
MECAM (14)	Planar ring	43

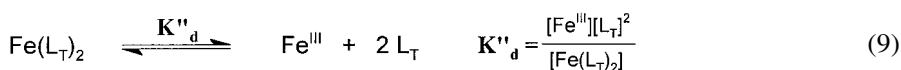
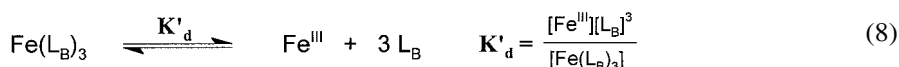
enterobactin, (Et)₃MECAM (**15**) (18), and (**17**) (19) can be considered to possess a degree of preorganization in contrast to MECAM (**14**) and TRENCAM (**16**) (20).



Under biological conditions, a comparison standard which is generally more useful than the stability constant is the pFe^{3+} value. The pFe^{3+} can be defined as the negative logarithm of the concentration of the free iron(III) in solution. Typically, pFe^{3+} values are calculated for total [ligand] = 10^{-5} M and total [iron] = 10^{-6} M at pH 7.4. The comparison of ligands under these conditions is useful, as the pFe^{3+} value, unlike the stability constant $\log K$ or $\log \beta_3$, takes into account the effects of ligand protonation and denticity as well as differences in metal–ligand stoichiometries. The comparison of pFe^{3+} values for hexadentate and bidentate ligands (Table 3) reveals that hexadentate ligands are far superior to their bidentate counterparts under in-vivo conditions. Indeed, when the influence of pH is monitored, the overall

shift in pFe^{3+} values is even clearer (Fig. 4A). The pFe^{3+} versus pH plot provides a useful method of comparing the ability of chelators to bind iron(III) at different pH values. Thus, for bidentate ligands 1-hydroxypyridin-2-one is relatively effective at acid pH values, whereas catechols dominate in the alkaline pH range (Fig. 4B). For a ligand to dominate iron(III) chelation in aqueous media, it must produce a pFe^{3+} curve above that of hydroxide anion. The larger the difference, the stronger is the chelator and the larger the pFe^{3+} value.

The formation of a complex will also depend on both free metal and free ligand concentrations, and as such will be sensitive to concentration changes. The degree of dissociation for a tris-bidentate ligand–metal complex is dependent on $[\text{ligand}]^3$, while the hexadentate ligand–metal complex dissociation is dependent only on $[\text{ligand}]$ [Eqs. (8)–(10)].



L_B , bidentate; L_T , tridentate; L_H , hexadentate ligand

Hence, the dilution sensitivity to complex dissociation for ligands follows the order hexadentate < tridentate < bidentate. It is for this reason that the majority of natural siderophores are hexadentate compounds and can therefore scavenge iron(III) efficiently at low metal concentrations (9).

III. CRITICAL FEATURES FOR CLINICAL APPLICATION

A. Lipophilicity and Molecular Weight

In order for a chelating agent to exert its pharmacological effect, it must be able to reach the target sites at sufficient concentration. Hence, a key property of an orally active iron chelator is its ability to be efficiently absorbed from the gastrointestinal tract and cross biological membranes to access the desired target sites such as liver, the major organ of iron storage. Three major factors influence a compound's ability to freely permeate a lipid membrane: lipophilicity, ionisation state, and molecular size.

Lipophilicity is a measure of the affinity of a molecule for a lipophilic environment, and is commonly assessed by measuring the distribution ratio of the solute (partition coefficient) between two phases, typically *n*-octanol and water. In order to achieve efficient oral absorption, the compound should possess appreciable lipid solubility which may facilitate the molecule to penetrate the gastrointestinal tract (partition coefficient greater than 0.2) (21). However, highly lipid-soluble molecules can also penetrate most cells and critical barriers such as the blood–brain barrier (BBB) and placental barrier, thereby possessing an increased potential to cause toxicity. The optimal partition coefficient for oral absorption of HPOs was found to be close to unity (21). Membrane permeability can also be affected by the ionic state

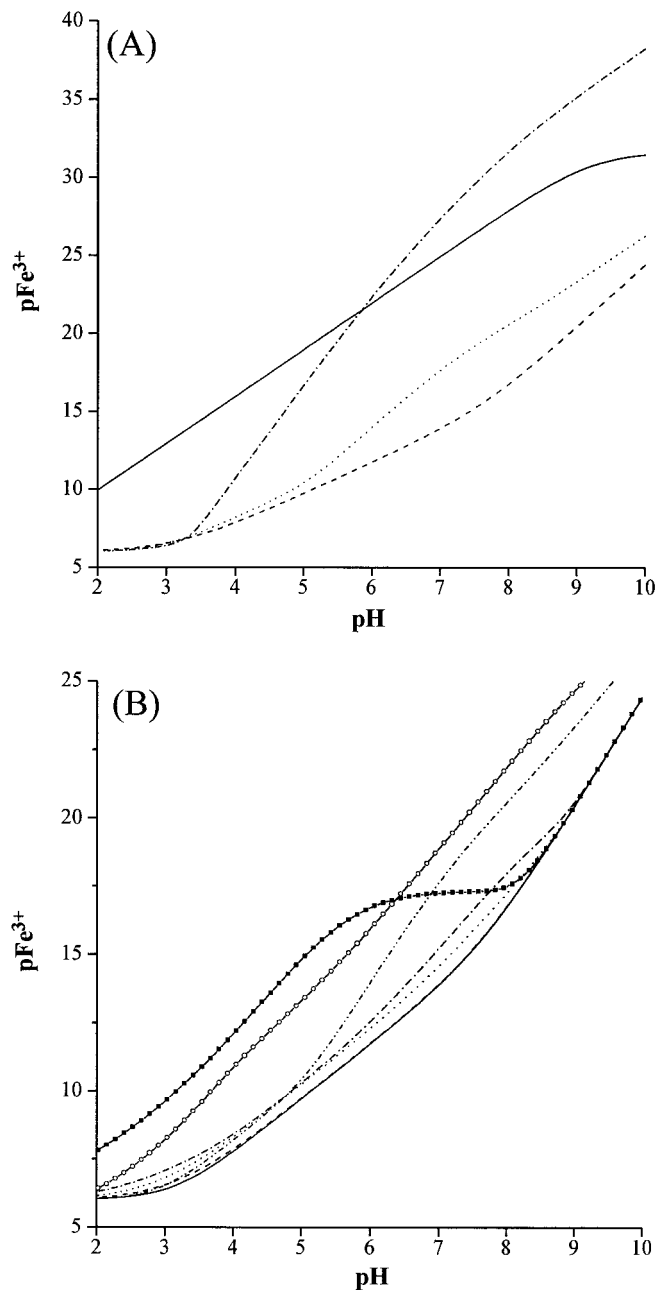


Figure 4 Influence of pH on $p\text{Fe}^{3+}$ values of (A) DFO, MECAM and (B) a range of bidentate ligands. $[\text{Fe}^{3+}]_{\text{total}} = 10^{-6}$ M; $[\text{Ligand}]_{\text{total}} = 10^{-5}$ M. (A) $\cdots\cdots\cdots$, N,N-dimethyl-2,3-dihydroxybenzamide (**6**); $-----$, acetohydroxamic acid (**7**); $-----$, DFO (**1**); $- \cdot - \cdot - \cdot - \cdot -$, MECAM (**14**). (B) $-----$, OH; $- \cdot - \cdot - \cdot - \cdot -$, N,N-dimethyl-2,3-dihydroxybenzamide (**6**); $-----$, acetohydroxamic acid (**7**); $\cdots\cdots\cdots$, 2-methyl-3-hydroxypyran-4-one (**8**); $-\blacksquare-$, 1-hydroxypyridin-2-one (**9**); $-\circ-$, 1,2-dimethyl-3-hydroxypyridin-4-one (**11**).

of the compound. Uncharged molecules penetrate cell membranes more rapidly than charged molecules (22). It is for this reason that aminocarboxylate-containing ligands are unlikely to be highly orally active. 3-Hydroxypyridin-4-ones are uncharged over the physiological pH range 5–9, both as free ligands and as the corresponding iron complexes. This property enables them to cross biological membranes more readily (23).

Molecular weight is another critical factor which influences the rate of oral drug absorption. Nonfacilitated diffusion is generally considered to be dominant for drugs with molecular weights below 200. The transcellular route involves diffusion into the enterocyte and thus utilizes some 95% of the surface area of the small intestine (Fig. 5). In contrast, the paracellular route utilizes only a small fraction of the total surface area, and the corresponding flux via this route is much smaller. The “cutoff” molecular weight for the paracellular route in the human small intestine is approximately 400 (24), and that for the corresponding transcellular route, as judged by polyethylene glycol permeability, is 500 (25). In order to achieve greater than 70% oral absorption, the chelator molecular weight probably needs to be less than 300 (25). This molecular weight limit provides a considerable restriction on the choice of chelator, and may effectively exclude hexadentate ligands from consideration. Most siderophores, including DFO, have molecular weights between 600 and 900. EDTA has a molecular weight of only 292; however, it is too small to fully encompass the chelated iron, thereby facilitating the potential toxicity of the metal (21). In contrast, bidentate and tridentate ligands, by virtue of their much lower molecular weights, are predicted to possess higher absorption efficiencies. The fraction of the absorbed dose for a range of bidentate 3-hydroxypyridin-4-ones has typically been found to fall between 50% and 70%, as assessed in the rabbit (26).

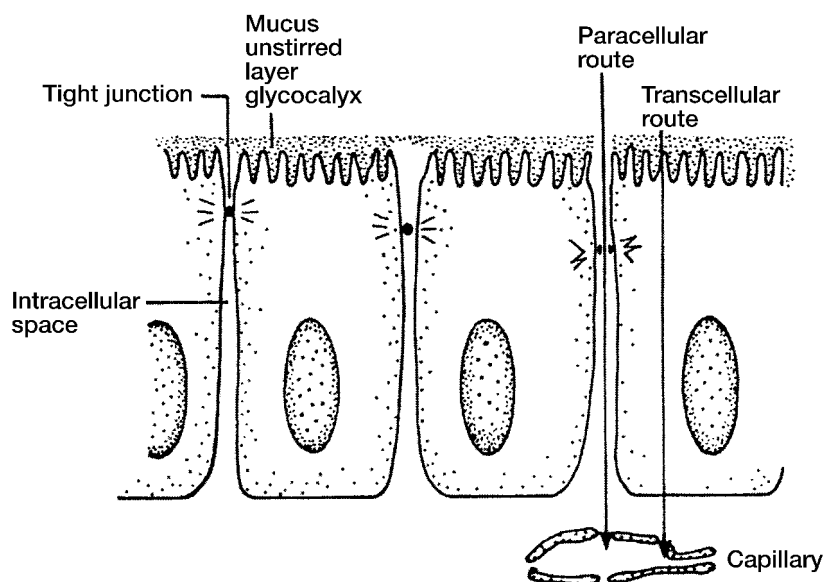


Figure 5 Intestinal epithelial barrier: routes of nonmediated permeation. Highly hydrophilic molecules utilize the paracellular pathway, whereas more lipophilic molecules permeate mainly through the transcellular pathway.

B. Drug Bioavailability and Disposition

Bioavailability can be defined as the percentage of absorbed dose which reaches the systemic blood circulation. It is not synonymous with absorption. If a compound is efficiently eliminated by hepatocytes, then a large fraction of the absorbed dose will be extracted from the portal blood supply, leading to so-called efficient first-pass kinetics and resulting low bioavailability. Thus, with orally active iron chelators, if general systemic delivery of the chelator is required, high bioavailability is ideal. However, if targeting of the chelator to the liver is sought (and the liver is the major iron storage organ), low bioavailability is required. In both cases, efficient absorption from the gastrointestinal tract is essential.

The metabolic properties of chelating agents also play a critical role in determining both their efficacy and toxicity. It is important to ensure that the agent is not metabolically degraded to metabolites which lack the ability to bind iron. This will inevitably require the use of higher drug levels, increasing the risk of inducing toxicity. Chelators are likely to be more resistant to metabolism if their backbones lack ester and amide links and to a lesser extent hydroxamate links (27). The catechol function is a disadvantage with respect to metabolism, numerous enzymes are designed specifically to modify the catechol entity—for instance, catechol-O-methyl transferase and tyrosinase (27).

Ideally, for maximal chelation, a chelator must be present within the extracellular fluids at both a reasonable concentration (10–25 μM) and length of time to ensure interception of iron from either the intracellular or extracellular pools. Compounds with short plasma half-lives are thus likely to be less effective due to the limited pool of chelatable iron present within the body at any one time. DFO possesses a very short plasma half-life, which is the reason for administration via an infusion pump (4,28).

C. Toxicity

The potential toxicity associated with iron chelators may originate from a number of factors other than intrinsic toxicity of the compound itself, including inhibition of iron-containing metalloenzymes, lack of metal selectivity which leads to the deficiency of other physiologically important metals such as zinc(II), redox cycling of the iron complex between iron(II) and iron(III), thereby generating free radicals, and the kinetic lability of the iron–complex, leading to iron redistribution.

1. Enzyme Inhibition

In general, iron chelators do not directly inhibit heme-containing enzymes, due to the inaccessibility of porphyrin-bound iron to chelating agents. In contrast, many nonheme iron-containing enzymes such as the lipoxygenase and aromatic hydroxylase families and ribonucleotide reductase are susceptible to chelator-induced inhibition (29,30). Clearly, the chemical nature of the ligand will have a dominant influence on its inhibitory potency; for instance, lipoxygenases are generally inhibited by hydrophobic chelators, and therefore the introduction of hydrophilic characteristics into a chelator tends to minimize inhibitory potential (31). The aromatic amino acid hydroxylases are particularly susceptible to inhibition by bidentate aromatic ligands—for instance, by catechols and HPOs—owing to the similar molecular characteristics of the inhibitor and the natural substrate. However, the introduction of a hy-

drophilic substituent at the 2-position of HPOs markedly reduces the inhibition, presumably due to steric interference of the chelation process at the enzyme active site (32,33). Thus, by careful modification of physicochemical properties and the molecular nature of the ligand, iron chelators can be designed which exert minimal inhibitory influence on most critical metalloenzymes (31,34).

2. Metal Selectivity

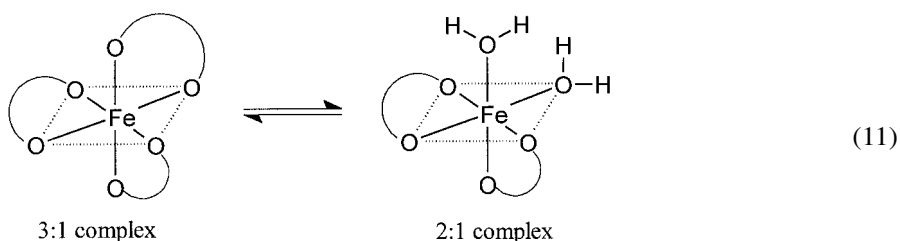
An ideal iron chelator should also be highly selective for iron(III), in order to prevent chelation of other biologically essential metal ions and leading to deficiency after prolonged usage. Unfortunately, many ligands that possess a high affinity for iron(III) may also have appreciable affinities for other metals such as zinc, especially in the case of carboxylate- and nitrogen-containing ligands. This is a minimal problem with the oxygen-containing bidentate catechol, hydroxamate, and HPO ligand families (Table 1).

3. Redox Activity

Chelators that bind both iron(II) and iron(III) are capable of redox cycling, a property that is utilized by a wide range of enzymes (35) and industrial catalysts (36). However, this is an undesirable property for iron-scavenging molecules, as redox cycling can lead to the production of hydroxyl radicals. Significantly, the high selectivity of siderophores for iron(III) over iron(II) renders redox cycling under biological conditions quite improbable (see Chapter 12). Chelators which utilize nitrogen as well as oxyanions as ligands possess lower redox potentials, and the coordinated iron can be reduced enzymatically under biological conditions. These complexes, therefore, can redox cycle under aerobic conditions, generating oxygen radicals. In order to avoid these undesirable properties, it is best to avoid using amines and carboxylates as ligands.

4. Complex Structure

In order to prevent free-radical production, iron should be coordinated by a ligand in such a manner as to avoid direct access of oxygen and hydrogen peroxide to the iron atom. Most hexadentate ligands such as DFO are kinetically inert and decrease hydroxyl radical production to a minimum by entirely masking the surface of the iron (Fig. 1). In contrast, bidentate and tridentate ligands are kinetically more labile, and therefore the resulting complexes tend to dissociate at low ligand concentrations [Eq. (11)].



Partial dissociation of bi- and tridentate ligand-iron complexes renders the iron(III) cation surface accessible to oxygen and hydrogen peroxide and thereby susceptible to the possible generation of hydroxyl radicals. The concentration dependence of 3-

hydroxypyridin-4-one iron complex species is minimal at pH 7.4 due to the relatively high affinity of the ligand for iron(III). Thus, bidentate 3-hydroxypyridin-4-ones behave more like hexadentate ligands as the 3:1 complex is the dominant species at pH 7.4, and the iron atom is completely protected from attack by oxygen in this form. Indeed, minimal hydroxyl radical production occurs in the presence of low levels of HPOs (37), especially in the presence of physiological levels of citrate and glutathione (38).

5. Hydrophilicity

Although bidentate and tridentate ligands possess a clear advantage over hexadentate ligands with respect to oral bioavailability, their enhanced ability to permeate membranes renders them potentially more toxic. Thus, the penetration of the BBB is one of the likely side effects associated with bidentate and tridentate ligands. The ability of a compound to penetrate the BBB is critically dependent on the partition coefficient as well as on the molecular weight (39). BBB permeability is predicted to be low for most hexadentate compounds, by virtue of their higher molecular weight (i.e., greater than 500). With low-molecular-weight molecules (below 300), penetration is largely dependent on the lipophilicity, and molecules with partition coefficients below 0.05 result in relatively poor penetration (40). Thus, chelators with partition coefficients lower than this critical value are predicted to show poor entry into the central nervous system. Indeed, brain penetration of 3-hydroxypyridin-4-ones is strongly dependent on their lipophilicity (Fig. 6) (41). Replacing a terminal hydrogen with a hydroxyl group further reduces BBB permeability (41). Comparative toxicities of iron(III) chelators are summarized in Table 5 (42,43).

IV. IRON CHELATORS CURRENTLY UNDER INVESTIGATION

A. Hexadentate Chelators

1. Desferrioxamine

Naturally occurring siderophores provide excellent models for the development of therapeutic useful iron chelators. Indeed, DFO (**1**), a growth-promoting agent secreted by the microorganism *Streptomyces pilosus* in order to scavenge iron from the environment, is the therapeutic agent of choice for the clinical treatment of chronic iron overload. DFO is a hexadentate tris-hydroxamic acid derivative and chelates ferric iron in an 1:1 molar ratio. It possesses an extremely high affinity for iron(III) and much lower affinity for other metal ions present in biological fluids, such as copper, zinc, calcium, and magnesium (Table 1). Although DFO is a large and highly hydrophilic molecule (the distribution coefficient at pH 7.4, $D_{7.4} = 0.01$), it gains entry into the liver via a facilitated transport system. Therefore, it can interact with both hepatocellular and extracellular iron, promoting both urinary and biliary iron excretion (44). Ferrioxamine, the DFO-iron complex (Fig. 1), is kinetically inert and possesses a relatively low lipophilicity, and thus is unlikely to enter cells. This property reduces the potential to redistribute iron to other sites. However, DFO is far from being an ideal therapeutic agent due to its oral inactivity; the only effective means of delivering this drug is by parenteral administration (see Chapter 33). Following intravenous bolus injection, DFO undergoes rapid metabolism and clearance by the kidney, with a plasma half-life of 5–10 min (45). In order to achieve

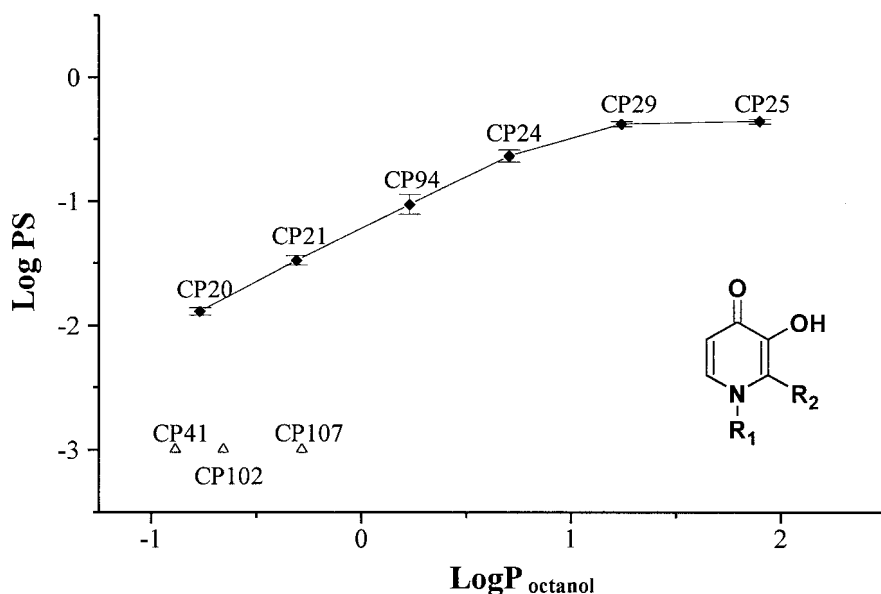


Figure 6 Relationship between blood–brain barrier permeability ($\log PS$) of the HPO family of iron chelators with $\log P_{\text{octanol}}$ in adult Wistar rats. Comparison of chelators with a hydroxyl group on the terminal carbon of the R1 chain (Δ) and simple N-alkyl chelators (\blacklozenge). The vascular perfusion time was 1 min. Values are expressed as means \pm SD ($n = 3$). CP20, $R_1 = R_2 = \text{CH}_3$; CP21, $R_1 = \text{C}_2\text{H}_5$, $R_2 = \text{CH}_3$; CP94, $R_1 = R_2 = \text{C}_2\text{H}_5$; CP24, $R_1 = (\text{CH}_2)_3\text{CH}_3$, $R_2 = \text{CH}_3$; CP29, $R_1 = (\text{CH}_2)_4\text{CH}_3$, $R_2 = \text{CH}_3$; CP25, $R_1 = (\text{CH}_2)_5\text{CH}_3$, $R_2 = \text{CH}_3$; CP41, $R_1 = (\text{CH}_2)_3\text{OH}$, $R_2 = \text{CH}_3$; CP102, $R_1 = \text{CH}_2\text{CH}_2\text{OH}$, $R_2 = \text{C}_2\text{H}_5$; CP107, $R_1 = (\text{CH}_2)_4\text{OH}$, $R_2 = \text{C}_2\text{H}_5$.

sufficient iron excretion, it has to be administered subcutaneously or intravenously for 8–12 h/day, 5–7 days/week (28). Consequently, patient compliance with this expensive and cumbersome regimen is often poor. Moreover, although DFO has been shown to be safe when administered in the presence of an elevated body iron burden, intensive therapy in young patients with relatively lower body iron stores may result in serious neurotoxicity, abnormalities of cartilage formation, and other serious adverse effects (46–49).

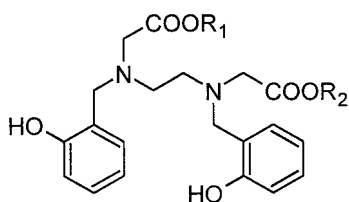
In an attempt to improve the oral bioavailability of the drug, a range of DFO prodrugs obtained via esterification of the labile hydroxamate functions has been investigated (50). However, only marginal improvement in oral activity was found with a range of tetra-acyl derivatives, and none have been identified which possess comparable activity to that of subcutaneous DFO (51). Several strategies centered on molecular modifications of the backbone of DFO have also been pursued (52,53). Unfortunately, no lead compound has yet emerged for further development as a potential oral iron chelator. Recently, a depot preparation of DFO was developed which, by delivering a smaller dose continuously over a longer period time (2–3 days), renders DFO more efficient and reduces the proportion of nonchelated DFO excreted (54–56). If successful, this preparation could obviate the requirement for portable infusion pumps. Local tolerability of this preparation is acceptable, but clinical trials have been disappointing (57).

Table 5 Comparative Toxicities of Bidentate, Tridentate, and Hexadentate Ligands

Bidentate ligands	Tridentate ligands	Hexadentate ligands
Possible for all coordinating atoms to be “hard” oxygen centers, which renders ligands highly selective for iron(III)	Very difficult for all coordinating atoms to be “hard” oxygen centers, which may lead to poor metal selectivity	Possible for all coordinating atoms to be “hard” oxygen centers, which renders ligands highly selective for iron(III)
Affinity for iron is concentration-dependent	Affinity for iron is concentration-dependent	Affinity for iron is concentration-dependent
Kinetically labile—iron redistribution is possible	Kinetically labile—iron redistribution is possible	Kinetically labile—iron redistribution is unlikely
Form partially coordinated 2:1 complexes, which could be toxic	Form partially coordinated 1:1 complexes, which could be toxic	Form only fully coordinated 1:1 complexes, which are generally nontoxic
Do not form polymeric complexes	Can form polymeric complexes which are likely to be trapped within cells	Do not form polymeric complexes
Penetration of BBB is dependent on lipophilicity	Penetration of BBB is dependent on lipophilicity	Generally low penetration of the BBB

2. Aminocarboxylates

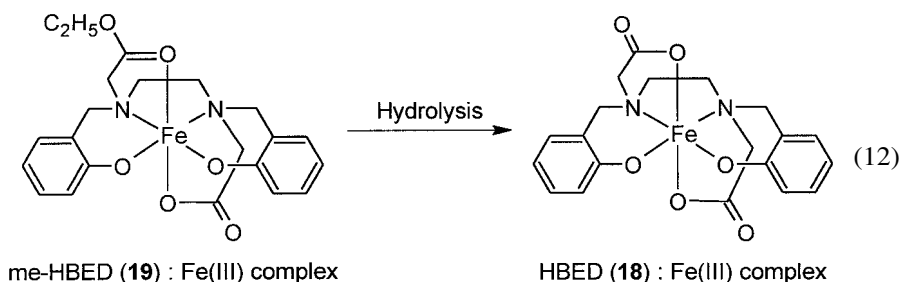
DTPA (**13**) is an aminocarboxylate hexadentate ligand and has been used in patients who develop toxic side effects with DFO (**58**). Due to its net charge at neutral pH, DTPA is largely confined to the extracellular compartment *in vivo* and is excreted in the urine within 24 h of administration (17,59). However, DTPA is not orally active, and due to its relative lack of selectivity for iron(III), it leads to zinc depletion (17). Consequently, zinc supplementation is required to prevent the toxic sequelae of such depletion. In order to enhance the selectivity of the aminocarboxylate ligands for iron(III), several analogs which contain both carboxyl and phenolic ligands have been designed (60,61). A particularly useful compound is *N,N'*-bis(2-hydroxybenzyl)-ethylenediamine-*N,N'*-diacetic acid (HBED) (**18**), which is significantly more effective than DFO when given intramuscularly to iron-overloaded rats (62,63).



(18) $R_1 = R_2 = \text{H}$

(19) $R_1 = \text{C}_2\text{H}_5$; $R_2 = \text{H}$

It binds ferric iron strongly with an overall stability constant ($\log K_1$) of 40 and a pFe^{3+} value of 31, rendering this molecule a potent ligand for chelation of ferric iron *in vivo*. Unfortunately, HBED is not efficiently absorbed via the oral route in either primates (63,64) or humans (65), because of the zwitterionic nature of the molecule. Considerable effort has been put into the design of HBED ester prodrugs (66,67). However, most of the compounds are of little use due to the slow rate of hydrolysis of the esters, particularly in primates (64). A compound of particular interest was found to be the monoethyl ester, me-HBED (**19**), which possesses good oral availability (68). This molecule has an appreciable affinity for iron(III) in its own right, and the resulting iron(III) complex activates the prodrug toward hydrolysis, leading to the formation of HBED [Eq. (12)] (69).

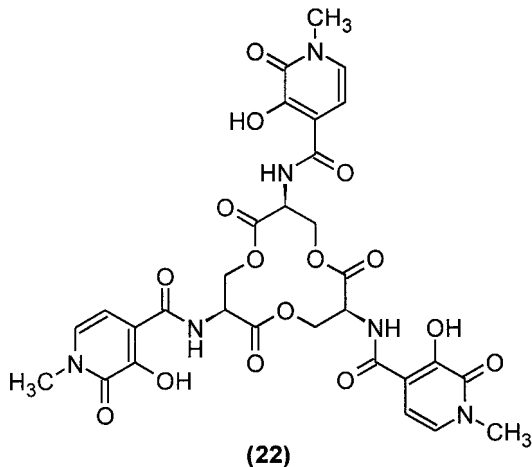
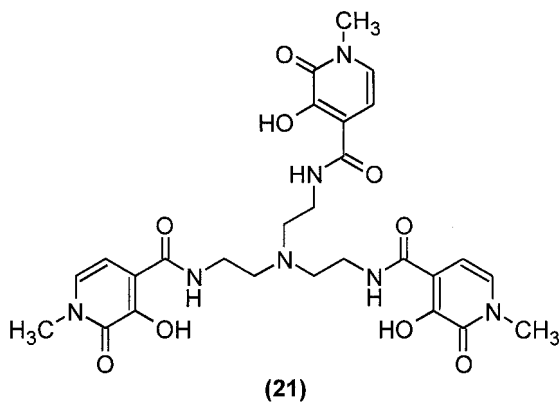
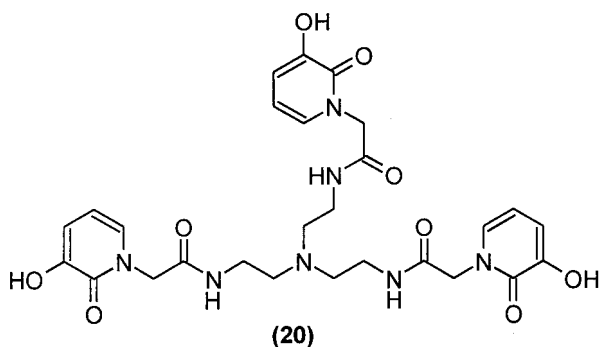


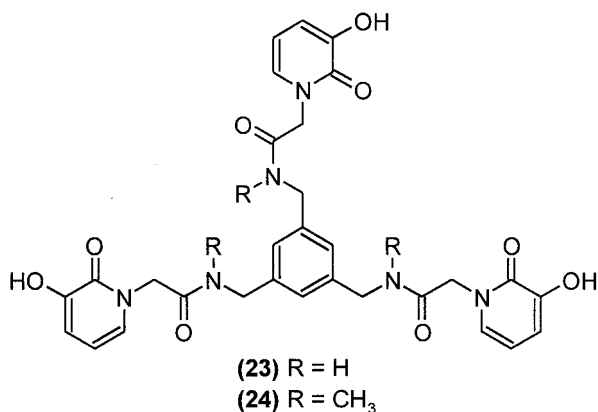
However, by virtue of the presence of the two nitrogen ligands, HBED retains a relatively high affinity for Zn^{2+} ($\log K_1 = 18.4$) and therefore would be predicted to induce similar side effects to those occurring with DTPA. Furthermore, it has been

demonstrated that HBED is capable of removing zinc from the zinc finger protein MTF-1 (70). Although the monoethyl ester of HBED was the lead orally active iron chelator for Novartis during 1998, it has not been taken forward for Phase I clinical trial.

3. Hydroxypyridinones

Several hexadentate ligands based on the HPO moiety have also been investigated, such as (20) (71), (21) (72), (22) (73), and (23) and (24) (74).

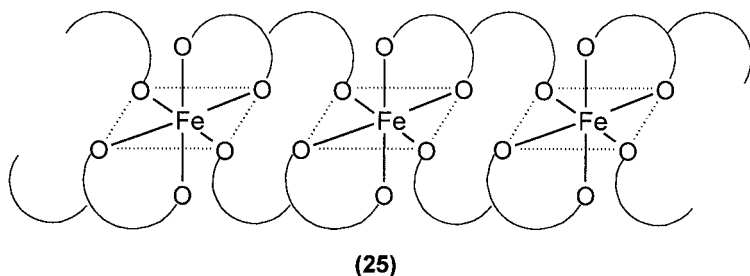




Hexadentate pyridinone molecules are likely to be less toxic than their bidentate analogs because of a more restricted biodistribution, and in particular, their failure to cross the BBB. However, by virtue of their higher molecular weight, such molecules, like siderophores, possess low oral bioavailability. The fraction of the oral dose absorbed for the hexadentate (21), for instance was found to be only 3.5% in mice (72).

B. Tridentate Chelators

A serious potential problem associated with tridentate ligands is that, unlike bidentate and most hexadentate compounds, there is a possibility of forming polymeric structures (25).



Such structures are difficult to clear via the kidney and are likely to become trapped within cells. Tridentate ligands fall into two major groups, class Y and class W (Fig. 7). In class W, one of the donor atoms (Z) is also part of the linking chain, and this atom is therefore limited to group V elements such as nitrogen. Such design leads to smaller chelating rings, and therefore to a reduction in the adverse change in entropy associated with chelation.

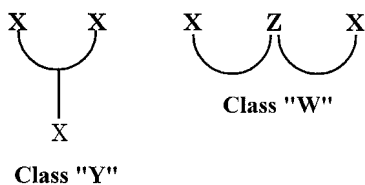
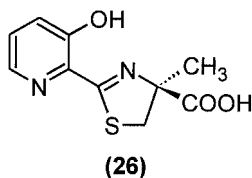


Figure 7 Two major classes of tridentate ligands: class Y, X = O, S, or NH; class W, X = O, S, or NH, Z limited to N.

1. Desferrithiocins

Desferrithiocin (DFT) (**26**), a siderophore isolated from *Streptomyces antibioticus*, belongs to class W.

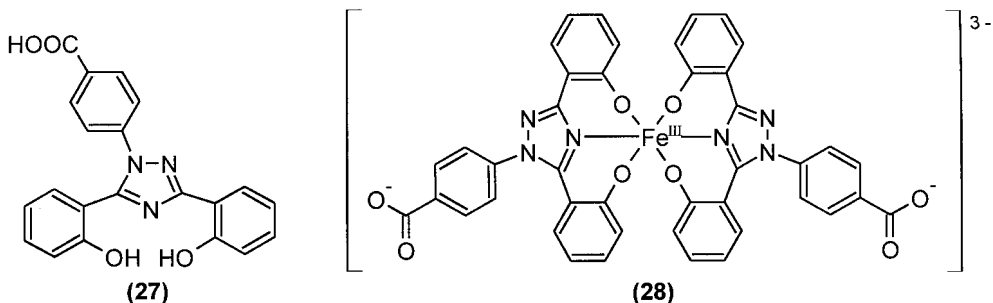


It forms a 2:1 complex with iron(III) at neutral pH using a phenolate oxygen, a carboxylate oxygen, and a nitrogen atom as ligands (75), and it possesses a high affinity for ferric iron ($\log \beta_2 = 29.6$). However, by virtue of the presence of the nitrogen and carboxylate ligands, it also binds other metals, particularly copper ($\log \beta_2 = 17.4$) and zinc ($\log \beta_2 = 15.3$) (76). Long-term studies of DFT in normal rodents and dogs have shown toxic side effects at low doses, such as reduced body weight and nerve damage (77). A range of synthetic analogs of DFT have been prepared (78). Such structure modification leads to the production of compounds with different activity profiles. However, to date no suitable candidates have been identified for the replacement of DFO, mainly because of the adverse toxicity of the iron complexes of this class of molecule (79), possibly associated with redox cycling.

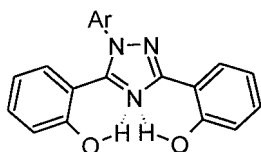
2. Triazoles

Recently, a novel class of tridentate ligand has been developed with the assistance of molecular modeling by Novartis (80). These also belong to the W class and chelate iron(III) with two phenolate oxygens and one triazolyl nitrogen. The lead compound (**27**) (81) possesses a $p\text{Fe}^{3+}$ value of 22.5. It is an extremely hydrophobic molecule with a $\log P$ value of 3.8 and a $\log D_{7.4}$ value of 1.0. As a result, it can penetrate membranes easily and possesses good oral availability. It has been found to be highly effective at removing iron from both the iron-loaded rats and marmosets. Compound (**27**) is the current lead orally active iron chelator of Novartis and has successfully completed Phase I clinical trials (82).

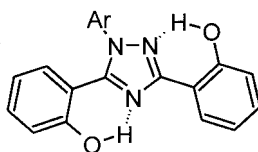
The high hydrophobicity of this chelator is undesirable; indeed, the $\log P$ value indicates that (**27**) is predicted to accumulate in tissue and to gain access to a wide variety of cells. However, the extremely high $\log P$ value also ensures that (**27**) binds tightly to plasma proteins and this property will, to some extent, limit body distribution. Compound (**27**) is efficiently extracted by the liver; indeed, virtually all induced iron excretion is via the bile, very little being excreted in the urine.



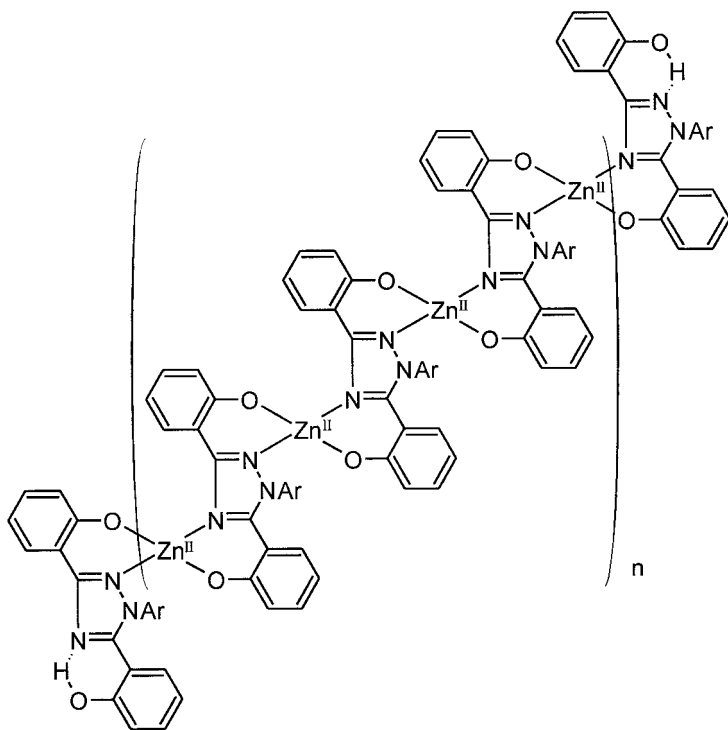
The triazole (27) forms a 2:1 iron complex (28) which possesses a net charge of 3^- and a molecular weight over 800 (81). Should such a complex form in muscle or endocrine tissue, it is likely that the iron would remain trapped within the cell. This chelator series utilizes nitrogen as one of the ligands and therefore is predicted to possess an appreciable affinity for zinc(II) and other divalent cations including iron(II). Indeed, the β_2 value for zinc(II) is reported as 17.5 as compared to 18.4 corresponding to HBED. When interacting with divalent metals such as zinc(II), the triazoles behave as tetradentate ligands (29b) and form insoluble polymers (30) (83).



Tridentate conformation
(29a)



Tetradentate conformation
(29b)



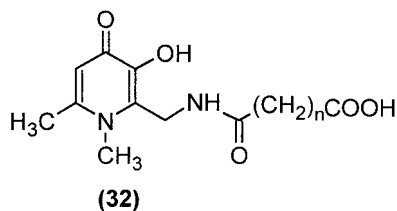
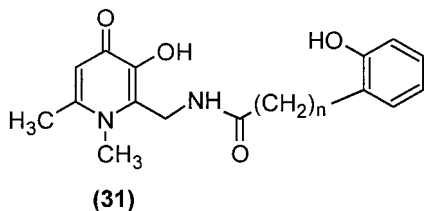
(30)

As with the rest of this group, (27) has been demonstrated to form insoluble complexes with zinc(II) (81); similar complexes with iron would undoubtedly undergo redox cycling.

3. Hydroxypyridinones

For optimal activity and selectivity with iron(III), the three ligating atoms in tridentate ligands should be anionic oxygen, which excludes class W. A series of class Y

tridentate ligands such as (31) and (32) based on the hydroxypyridin-4-one moiety have been synthesized.



However, the chelation entropy factor is such that these molecules behave as bidentate pyridinones and the potential ligating side arm plays no demonstrable role in the coordination of iron(III) (21,43,84).

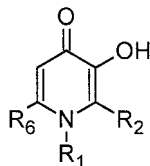
C. Bidentate Chelators

On the basis of selectivity and affinity, particularly considering the pFe^{3+} value, 3-hydroxypyridin-4-one is the optimal bidentate ligand for the chelation of iron(III) over the pH range of 6.0–9.0 (Fig. 4B). Indeed, the 3-hydroxypyridin-4-ones are currently among the leading candidates for an orally active alternative to DFO (21,27).

1. Dialkylhydroxypyridinones

The 1,2-dimethyl derivative (deferiprone, L1, CP20) (8) (Table 6) is the only orally active iron chelator currently available for clinical use (marketed by Apotex, Inc.,

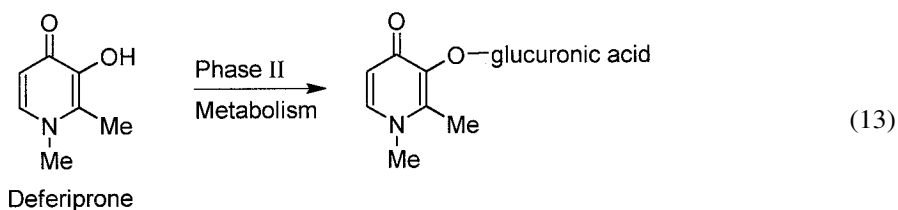
Table 6 Chemical Structure of Selected 3-Hydroxypyridin-4-ones



Ligand	R ₁	R ₂	R ₆	log P	pFe ³⁺ (at pH 7.4)	Iron mobilization efficacy (%) ^a
Deferiprone (8)	CH ₃	CH ₃	H	-0.77	19.4	9.5
CP94 (33)	CH ₂ CH ₃	CH ₂ CH ₃	H	0.25	19.7	55.8
CP102 (34)	CH ₂ CH ₂ OH	CH ₂ CH ₃	H	-0.66	Not determined	12.9
CP41 (35)	(CH ₂) ₃ OH	CH ₃	H	-0.89	Not determined	26.0
CP117 (36)	CH ₂ CH ₂ OOC(CH ₃) ₃	CH ₂ CH ₃	H	1.16	Not determined	19.1
CP283 (37)	(CH ₂) ₃ OOCCH ₆ H ₅	CH ₃	H	1.25	Not determined	32.5
CP412 (38)	-CH ₂ CH ₂	CH ₂ CH ₃	H	0.94	Not determined	26.5
CP365 (39)	CH ₂ CH ₃	CH(OH)CH ₃	H	-0.58	21.4	50.6
CP502 (44)	CH ₃	CONHCH ₃	CH ₃	-1.36	21.7	55.8

^aIron mobilization efficacy of chelators (450 μmol/kg) was measured using the ⁵⁹Fe-ferritin-loaded rat model (103).

Toronto, Canada, as Ferriprox). Unfortunately, the dose required to keep a previously well-chelated patient in negative iron balance with Ferriprox appears to be relatively high, in the region of 75–100 mg/kg/day (85). Not surprisingly, therefore, side effects have been observed in some patients receiving deferiprone (86,87), although these have been disputed (88) or maybe iron-induced (89). One of the major reasons for the limited efficacy of deferiprone in clinical use is that it undergoes extensive phase II metabolism in the liver. The 3-hydroxyl functionality, which is crucial for scavenging iron, is also a prime target for phase II conjugation [Eq. (13)].



Urinary recovery studies conducted on deferiprone in both rats and humans have shown that respectively >44% and >85% of the administered dose is recovered in the urine as the nonchelating 3-O-glucuronide conjugate (90). The use of deferiprone for the treatment of iron overload remains a hotly debated subject at the present time (87–89,91–94). However, until a superior orally active chelator becomes available, deferiprone remains in the unique position of being the only orally active chelator available for clinical use.

The 1,2-diethyl analogue CP94 (**33**) (Table 6) has also been widely investigated in animals (95–98). This chelator has been found to be more efficient at iron removal than deferiprone in several mammalian species, e.g., rat (95) and cebus monkey (98). One of the presumed reasons for the greater efficacy of CP94 in the rat is its unusual phase I metabolic pathway, which leads to the formation of the 2-(1'-hydroxyethyl) metabolite, CP365 (**39**) (Fig. 8) (88). This metabolite does not undergo further phase II metabolism to form a glucuronide conjugate, and hence it retains the ability to chelate iron. Promising results obtained in rat models led to the limited clinical evaluation of CP94 in thalassaemic patients (97). Unfortunately, the metabolism of CP94 in humans did not parallel that of the rat. The main urinary metabolite of CP94 in humans is the 3-O-glucuronide conjugate (>85%) (96). Extensive conversion to this metabolite was found to severely limit the clinical efficacy of CP94.

2. Hydroxypyridinone Prodrugs

The critical dependence of chelator efficacy on metabolic behavior has led to a concept of ligand design which minimizes conjugation reactions with glucuronic acid. Despite the limited efficacy of CP94 in humans, the superior extracellular and intracellular iron mobilization ability in the rat provided important information for chelator design. The lack of glucuronidation of the 2-(1'-hydroxyethyl) metabolite of CP94 led to the investigation of the possibility of developing structurally related compounds. Indeed, 1-hydroxyalkyl derivatives of HPOs such as CP102 (**34**) and CP41 (**35**) (Table 6), which are not extensively metabolized via phase II reactions, have been identified (99,100). Although the use of 1-hydroxyalkyl derivatives of HPO may offer a significant improvement over previously evaluated HPOs (101–103), a possible disadvantage of these compounds, especially with some of the more

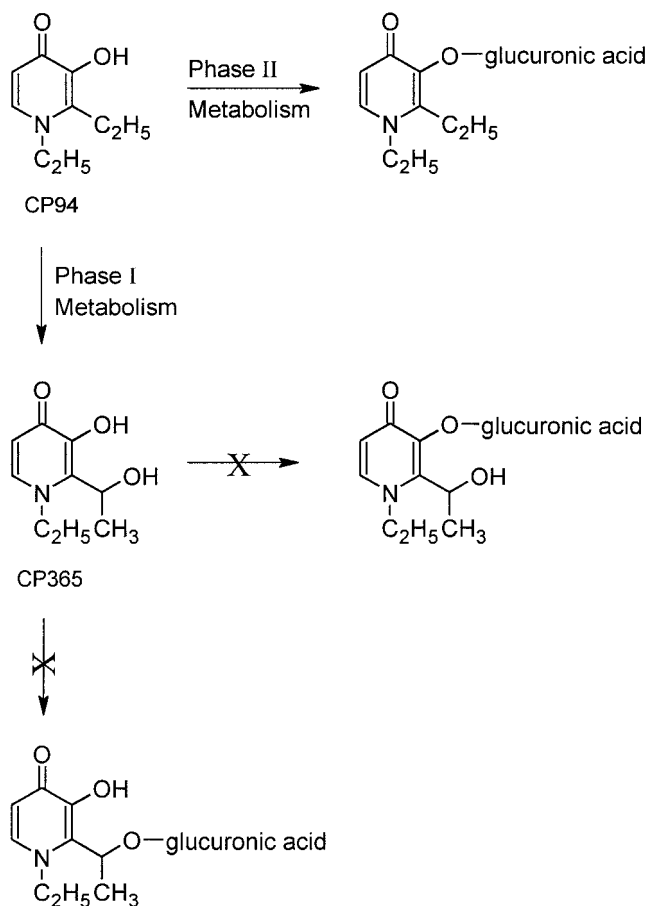


Figure 8 Metabolism of CP94 via phase I and phase II metabolic pathways. The 2-1'-hydroxylated metabolite (CP365) is the major metabolite in rat, whereas phase II glucuronidation is the major metabolic route of CP94 in humans.

hydrophilic analogs, is reduced extraction by the liver, which is the major iron storage organ.

One of the potential problems associated with orally active bidentate HPOs is that by virtue of their relatively low molecular weight and favorable distribution coefficients, they rapidly penetrate cells and critical barriers such as the BBB and placental barrier, thus potentially causing toxicity. Ideally, the distribution of iron chelators developed for the treatment of general iron overload, such as encountered in β -thalassemia major, is best limited to the extracellular space and liver. The anticipated distribution coefficient ($D_{7.4}$) requirements for an ideal iron chelator are outlined in Table 7 (43). Clearly, there is no single compound fulfilling these requirements, since the optimal distribution coefficient for absorption from the gastrointestinal tract is quite different from that necessary to limit access to the brain, placenta, and the peripheral cell. In principle this problem can be surmounted by using a prodrug strategy where a lipophilic prodrug P, by virtue of its distribution

Table 7 Anticipated Optimal Distribution Coefficients of an Ideal Iron Chelator

	$D_{7.4}$
Good absorption from the gastrointestinal tract	>0.2
Efficient liver extraction	>1.0
Poor entry into peripheral cells (thymus and bone marrow)	<0.001
Poor ability to penetrate the blood–brain and maternal/placental barriers	<0.001

coefficient, is rapidly absorbed from the gastrointestinal tract and is also efficiently extracted by the liver (Fig. 9). If, when gaining entry to the hepatocyte, the prodrug is rapidly converted to an iron-selective chelator L, which possesses a much lower distribution coefficient, this chelator L can scavenge iron in the hepatocyte, but also can efflux into the systemic circulation, thereby scavenging the extracellular iron pool. However, because L is hydrophilic, its ability to cross critical membrane bar-

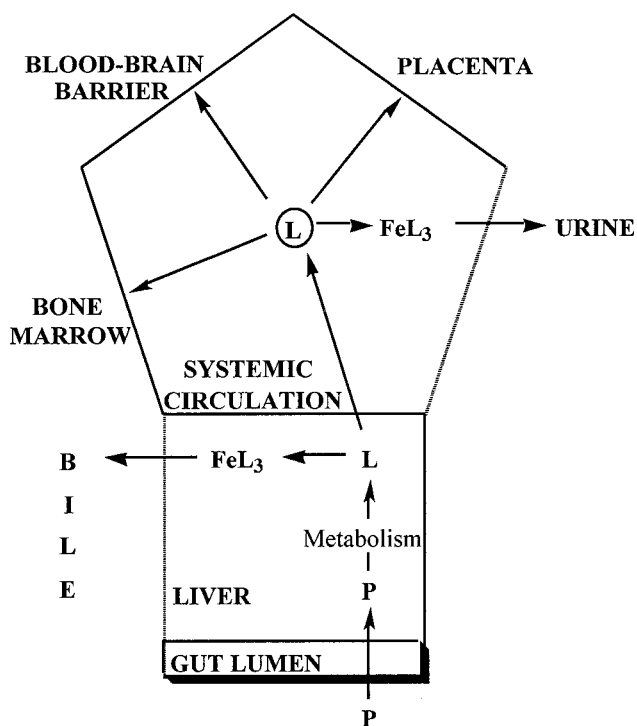


Figure 9 Major fluxes of a bidentate chelator prodrug (P) after oral administration. The lipophilic prodrug P ($D_{7.4} > 2$) is rapidly cleared from blood stream by the liver (first-pass kinetics). In the hepatocyte, the prodrug is rapidly converted to the iron-selective chelator L, which possesses a much lower distribution coefficient. The chelator L can scavenge iron in the hepatocyte and can efflux into the systemic circulation, thereby scavenging the extracellular iron pool. If the distribution coefficient of L is adjusted to be less than 0.001, the molecule will be expected not to readily penetrate either the blood–brain barrier or the placenta.

riers is markedly reduced, thereby minimizing toxicity problems. A wide range of ester prodrugs of 1-hydroxyalkyl HPOs, such as CP117 (**36**) and CP283 (**37**), has been investigated (104–106), and preliminary pharmacokinetic and efficacy studies have demonstrated that the selective delivery of HPO iron chelators to the target organs such as liver can be achieved using this strategy (104–107).

3. Lysosomotropic Hydroxypyridinones

The strategy of drug delivery can be further refined by targeting the chelator not only to the hepatocyte, but also to the lysosome located in the hepatocyte. Ferritin is constantly broken down in cells within lysosomes, and much of the liberated iron is reincorporated into new ferritin molecules (Fig. 10) (108,109). It is, therefore to be expected that the acidic lysosomal compartment possesses a relatively high concentration of iron in a chemical form suited to efficient chelation. This conclusion is further endorsed by the results of Laub et al. (110), who, by using radiolabeled DFO, showed that the likely source of chelatable iron in the hepatocyte is the lysosomal pool. Thus, the selective delivery of chelating agents to lysosomes may greatly improve their efficiency in iron removal from iron-overloaded patients. To investigate the possibility of targeting chelators into the lysosomal iron pool, a range of 3-hydroxypyridin-4-ones with basic chains have been synthesized (111). Such basic chelators are predicted to accumulate in acidic organelles such as lysosomes more efficiently than neutral compounds (112,113). Preliminary dose–response studies suggest that basic pyridinones are relatively more effective at lower doses when compared with N-alkylhydroxypyridinones. Optimal effects have been observed with the piperidine derivative CP412 (**38**). Thus, in the rat, CP412 at a dose of 150 $\mu\text{mol/kg}$ was found to be more effective than 450 $\mu\text{mol/kg}$ deferiprone, the widely adopted clinical dose.

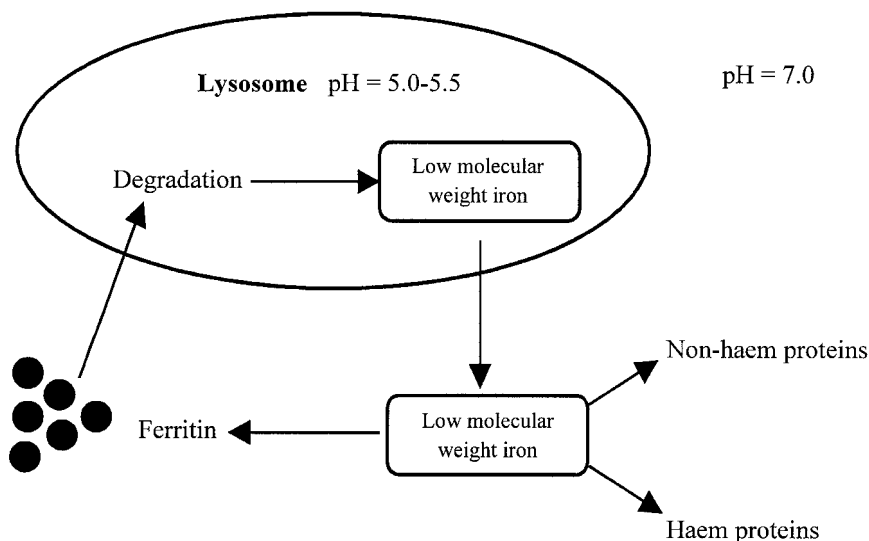
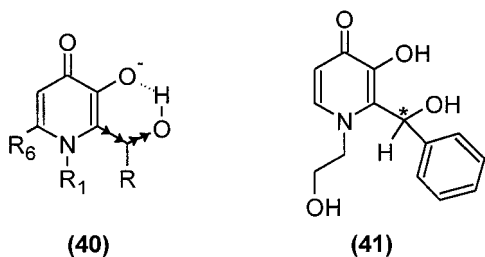


Figure 10 Schematic representation of the major intracellular iron fluxes in the hepatocyte. Chelators with basic substituents tend to be accumulated in the acidic lysosomal compartment more efficiently than neutral ligands.

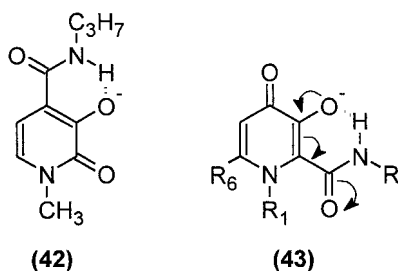
4. "High-pFe³⁺" Hydroxypyridinones

Despite the developments outlined above, which have centered on a wide range of derivatives, no HPO investigated prior to 1997 had been found to be more effective than CP94 in rats (102,114). The greater efficacy of CP94 in rats drew the authors' attention to its unusual 2-(1'-hydroxyethyl) metabolite, CP365 (**39**). Subsequent physicochemical characterization of CP365 indicated that the introduction of a 1'-hydroxyalkyl group at the 2-position significantly increases the pFe³⁺ value (115). This effect results from stabilizing the ionized species due to the combined effect of intramolecular hydrogen bonding between the 2-(1'-hydroxyl) group and the adjacent 3-hydroxyl function, and the negative inductive effect of the 2-(1'-hydroxyl) group from the pyridinone ring (**40**).



Although such an effect reduces the overall stability constants for iron(III), it also reduces the affinity of the chelating function for protons. These two changes result in an increase in the corresponding pFe³⁺ values at pH 7.4 (115). Such an enhancement of pFe³⁺ values is associated with a clear improvement in the ability of chelators to remove iron under in-vivo conditions (115). Thus it emerges from these studies that, in rats, CP94 acts as a "prodrug" of CP365, a chelator with a higher pFe³⁺ value, and this accounts for the particularly high efficacy of CP94. Recently, Novartis produced a range of bidentate HPO ligands which possess an aromatic substituent at the 2-position. The aromatic group is reported to stabilize the resulting iron complex and hence increase the pFe³⁺ values (116). Interestingly, the lead compound (**41**) (117) also possesses a 1'-hydroxyl group at the 2-position, and this is almost certainly responsible for the observed enhanced efficacy of (**41**) when compared with deferiprone.

It has been previously established that the introduction of an amide function at the 4-position of 3-hydroxypyridin-2-ones (**42**) reduces the pK_a values and hence increases the corresponding pFe³⁺ values, due to the formation of a stable intramolecular hydrogen bond between the amide proton and the adjacent oxygen donor (72).



Similarly, the introduction of an amido function at the 2-position of 3-hydroxypyridin-4-ones (**43**) increases the pFe^{3+} value (118). A potential advantage of such 2-amido derivatives over the 2-(1'-hydroxyalkyl) analogs, including the Novartis compound (**41**), is that they lack a chiral centre.

An undesirable feature associated with bidentate HPO chelators is the kinetic lability of the iron(III) complexes. Ideally, the dominant species under most physiological conditions should be the fully coordinated 3:1 species. Partial dissociation of the iron complex renders the iron(III) cation surface accessible to oxygen and hydrogen peroxide, and thereby susceptible to the possible generation of hydroxyl radicals (21). The enhancement of pFe^{3+} values has a dramatic effect on the speciation plot of the iron(III), the N-methyl amido derivative CP502 (**44**) dissociating less readily, leading to lower concentrations of the L_2Fe^+ complex when compared with deferiprone (Fig. 11). Clearly, chelators with high pFe^{3+} values are predicted not only to scavenge iron more effectively at low ligand concentrations, but also to dissociate less readily and therefore form lower concentrations of the partially coordinated complexes. These novel high- pFe^{3+} HPOs show great promise in their ability to remove iron under in-vivo conditions and thereby offer a realistic approach to the design of orally active iron chelators for clinical use.

V. CONCLUSIONS

Over the past 30 years many attempts have been directed at the design of nontoxic orally active iron chelators, but only one clinically useful compound, deferiprone, has emerged to date. Since 1995 a number of significant advances have been made,

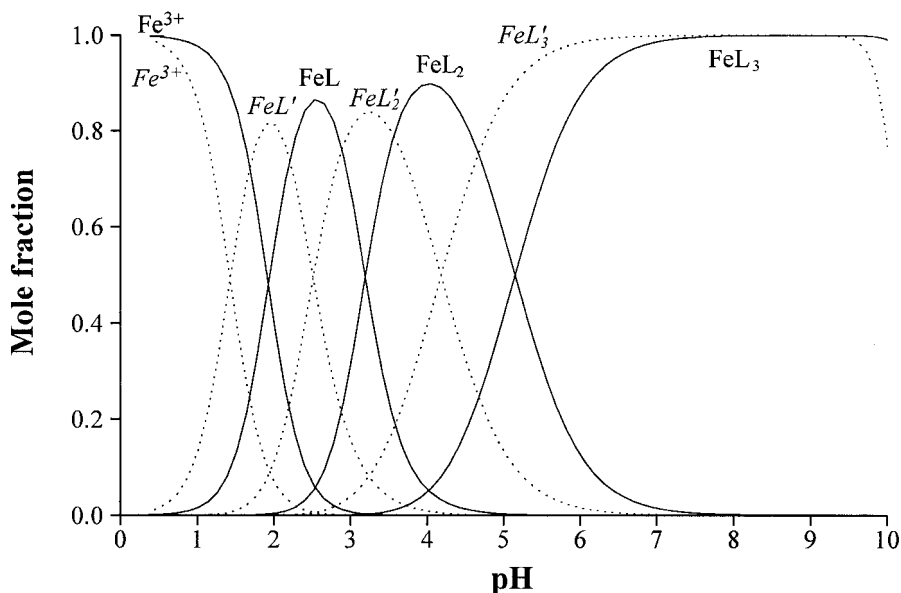


Figure 11 Comparison of the speciation plots of deferiprone and CP502 in the presence of iron(III); L = deferiprone; L' = CP502; $[Fe^{3+}]_{total} = 1 \times 10^{-6}$ M and $[Ligand] = 1 \times 10^{-5}$ M.

and the authors are confident that other more efficacious orally active chelators will soon join deferiprone. Several lead compounds have been identified and are under active development for the treatment of transfusional iron overload. The successful introduction of such compounds will impact considerably on the therapeutic outcome and quality of life for the thalassaemic population. There is a potential for iron chelation in a wide range of clinical situations. Once a chelator has been clinically proven in thalassaemic patients, such compounds will almost certainly find application for the treatment of other disease states, for instance, sickle-cell anaemia.

ACKNOWLEDGMENTS

The authors thank Apotex Research, Inc., Canada, and Biomed EC grant BMH4-CT97-2149 for financial support. Zu D. Liu would like to thank the KC Wong Education Foundation (Hong Kong) and the Committee of Vice-Chancellors and Principals of the Universities of the United Kingdom for joint scholarships.

REFERENCES

1. Halliwell B, Gutteridge JMC. *Free Radicals in Biology and Medicine*. 2d ed. Oxford, U.K.: Clarendon Press, 1989.
2. Crichton RR. *Inorganic Biochemistry of Iron Metabolism*. New York, London: Ellis Harwood, 1991.
3. Brittenham GM. Disorders of iron metabolism: deficiency and overload. In: Hoffman R, Benz E, Shattil S, Furie B, Cohen H, eds. *Hematology: Basic Principles and Practice*. New York: Churchill Livingstone, 1991:327–349.
4. Hershko C, Konijn AM, Link G. Iron chelators for thalassaemia. *Br J Haematol* 1998; 101:399–406.
5. Andrews NC. Medical progress: disorders of iron metabolism. *N Engl J Med* 1999; 341:1986–1995.
6. Pearson RG. Hard and soft acids and bases. *J Am Chem Soc* 1963; 85:3535–3539.
7. Martell AE, Smith RM. *Critical Stability Constants*. Vols. 1–6. London: Plenum Press, 1974–1989.
8. Harris DC, Aisen P. Facilitation of Fe(II) autoxidation by Fe(III) complexing agents. *Biochim Biophys Acta* 1973; 329:156–158.
9. Hider RC. Siderophore mediated absorption of iron. *Struct Bond* 1984; 38:25–87.
10. Raymond KN, Muller G, Matzanke BF. Complexation of iron by siderophores: a review of their solution and structural chemistry and biological function. *Top Curr Chem* 1984; 58:49–102.
11. Hider RC, Mohd-Nor AR, Silver J, Morrison IEG, Rees LVC. Model compounds for microbial iron-transport compounds. Part 1. Solution chemistry and mössbauer study of iron(II) and iron(III). Complexes from phenolic and catecholic system. *J Chem Soc Dalton Trans* 1981; 2:609–622.
12. Templeton DM. Therapeutic use of chelating agents in iron overload. In: Goyer RA, Cherian MG, eds. *Toxicology of Metals; Biochemical Aspects*. Berlin: Springer-Verlag, 1995:305–331.
13. Keberle H. The biochemistry of DFO and its relation to iron metabolism. *Ann NY Acad Sci* 1964; 119:758–768.
14. Summers JB, Gunn BP, Martin JG, Mazdiyasi H, Stewart AO, Young PR, Goetze AM, Bouska JB, Dyer RD, Brooks DW, Carter GW. Orally active hydroxamic acid inhibitors of leukotriene biosynthesis. *J Med Chem* 1988; 31:3–5.

15. Grady RW, Graziane JH, Alkers HA, Cerami A. The development of new iron-chelating drugs. *J Pharmacol Exp Ther* 1976; 196:478–485.
16. Winston A, Varaprasad Dvpr, Metterville JJ, Rosenkrantz H. Evaluation of polymeric hydroxamic acid iron chelators for treatment of iron overload. *J Pharmacol Exp Ther* 1985; 232:644–649.
17. Pippard MJ, Jackson MJ, Hoffman K, Petrou M, Model CB. Iron chelation using subcutaneous infusion of diethyl triaminopentaacetic acid (DTPA). *Scand J Haematol* 1986; 36:466–472.
18. Stack TDP, Hou ZG, Raymond KN. Rational reduction of the conformational space of a siderophore analog through nonbonded interactions: the role of entropy in enterobactin. *J Am Chem Soc* 1993; 115:6466–6467.
19. Tse B, Kishi Y. Conformationally rigid tricyclic tripods: synthesis and application to preparation of enterobactin analogs. *J Org Chem* 1994; 59:7807–7814.
20. Rodgers SJ, Lee CW, Ng CY, Raymond KN. Ferric ion sequestering agents 15. Synthesis, solution chemistry, and electrochemistry of a new cationic analog of enterobactin. *Inorg Chem* 1987; 26:1622–1625.
21. Tilbrook GS, Hider RC. Iron chelators for clinical use. In: Sigel A, Sigel H, eds. *Metal Ions in Biological Systems. Vol. 35: Iron Transport and Storage in Microorganisms, Plants and Animals*. New York: Marcel Dekker, 1998:691–730.
22. Florence AT, Attwood D. *Physicochemical Principles of Pharmacy*. 2d ed. London: Macmillan, 1988.
23. Hider RC, Hall AD. Clinically useful chelators of tripositive elements. *Prog Med Chem* 1991; 28:41–173.
24. Travis S, Menzies I. Intestinal permeability: functional assessment and significance. *Clin Sci* 1992; 82:471–488.
25. Maxton DG, Bjarnason I, Reynolds AP, Catt SD, Peters TJ, Menzies IS. Lactulose ⁵¹Cr-labelled ethylenediaminetetra-acetate, L-rhamnose and polyethyleneglycol 500 as probe markers for assessment in vivo of human intestinal permeability. *Clin Sci* 1986; 71:71–80.
26. Yokel RA, Fredenburg AM, Meurer KA, Skinner TL. Influence of lipophilicity on the bioavailability and disposition of orally active 3-hydroxypyridin-4-one metal chelators. *Drug Metab Disp* 1995; 23:1178–1180.
27. Porter JB, Huehns ER, Hider RC. The development of iron chelating drugs. *Bailliere's Clin Haematol* 1989; 2:257–292.
28. Pippard MJ, Callender ST, Weatherall DJ. Intensive iron-chelation therapy with desferrioxamine in iron-loading anaemias. *Clin Sci Mol Med* 1978; 54:99–106.
29. Hider RC. Potential protection from toxicity by oral iron chelators. *Toxicol Lett* 1995; 82–83:961–967.
30. Hider RC, Singh S, Porter JB. Iron chelating agents with clinical potential. *Proc R Soc Edin* 1992; 99B:137–168.
31. Abeyasinghe RD, Robert PJ, Cooper CE, MacLean KH, Hider RC, Porter JB. The environment of the lipoygenase iron binding site explored with novel hydroxypyridinone iron chelators. *J Biol Chem* 1996; 271:7965–7972.
32. Hider RC, Lerch K. The inhibition of tyrosinase by pyridinones. *Biochem J* 1989; 257: 289–290.
33. Liu ZD, Lockwood M, Rose S, Theobald AE, Hider RC. Structure-activity investigation of the inhibition of 3-hydroxypyridin-4-ones on mammalian tyrosine hydroxylase. *Biochem Pharmacol* 2001; 61:285–290.
34. Cooper CE, Lynagh GR, Hoyes KP, Hider RC, Cammack R, Porter JB. The relationship of intracellular iron chelation to the inhibition and regeneration of human ribonucleotide reductase. *J Biol Chem* 1996; 271:20291–20299.

35. Lippard SJ, Berg JM. Principles of Bioinorganic Chemistry. Sausalito, CA: University Science Books, 1994.
36. Britovsek GJP, Gibson VC, Wass DF. The search for new-generation olefin polymerization catalysts: life beyond metallocenes. *Angew Chem Int Ed* 1999; 38:428–447.
37. Singh S, Khodr H, Taylor MI, Hider RC. Therapeutic iron chelators and their potential side-effects. *Biochem Soc Symp* 1995; 61:127–137.
38. Hider RC, Kayyili R, Evans P. The production of hydroxyl radicals by Deferiprone-iron compounds under physiological conditions. *Blood* 1999; 94(suppl):406A–406A.
39. Levin VA. Relationship of octanol/water partition coefficient and molecular weight to rat brain capillary permeability. *J Med Chem* 1980; 23:682–684.
40. Oldendorf WH. Lipid solubility and drug penetration of the blood brain barrier. *Proc Soc Exp Bio Med* 1974; 147:813–816.
41. Habgood MD, Liu ZD, Dehkordi LS, Khodr HH, Abbott J, Hider RC. Investigation into the correlation between the structure of hydroxypyridinones and blood-brain barrier permeability. *Biochem Pharmacol* 1999; 57:1305–1310.
42. Hider RC, Porter JB, Singh S. The design of therapeutically useful iron chelators. In: Bergeron RJ, Brittenham GM, eds. *The Development of Iron Chelators for Clinical Use*. London: CRC Press, 1994; 353–371.
43. Hider RC, Choudhury R, Rai BL, Dekhordi LS, Singh S. Design of orally active iron chelators. *Acta Haematol* 1996; 95:6–12.
44. Hershko C, Grady RW, Cerami A. Mechanism of iron chelation in the hypertransfused rat: definition of two alternative pathways of iron mobilisation. *J Lab Clin Med* 1978; 92:144–149.
45. Summers MR, Jacobs A, Tudway D, Perera P, Ricketts C. Studies in desferrioxamine and ferrioxamine metabolism in normal and iron-loaded subjects. *Br J Haematol* 1979; 42:547–555.
46. Porter JB, Jawson MC, Huehns ER, East CA, Hazell JWP. Desferrioxamine toxicity: evaluation of risk factors in thalassaemic patients and guidelines for safe dosage. *Br J Haematol* 1989; 73:403–405.
47. Freedman MH, Grisaru D, Olivieri NF, MacLusky I, Thorner PS. Pulmonary syndrome in patients with thalassemia major receiving intravenous deferoxamine infusions. *Am J Dis Child* 1990; 144:565–569.
48. Olivieri NF, Buncic JR, Chew E, Gallant T, Harrison RV, Keenan N, Logan W, Mitchell D, Ricci G, Skarf B. Visual and auditory neurotoxicity in patients receiving subcutaneous desferrioxamine infusions. *N Engl J Med* 1986; 314:869–873.
49. Olivieri NF, Harris J, Koren G, Khattak S, Freedman MH, Templeton DM, Bailey JD, Reilly BJ. Growth failure and bony changes induced by deferoxamine. *Am J Pediatr Hematol Oncol* 1992; 14:48–56.
50. Peter HH. Industrial aspects of iron chelators: pharmaceutical application. In: Spik G, Montreuil J, Crichton RR, Mazurier J, eds. *Proteins of Iron Storage and Transport*. Amsterdam: Elsevier, 1985:293–303.
51. Fechtig B, Peter H. New O-acylhydroxamic acid derivatives. International Patent WO 8603745, 1984.
52. Bergeron Rj, Wiegand J, McManis JS, Perumal PT. Synthesis and biological evaluation of hydroxamate-based iron chelators. *J Med Chem* 1991; 34:3182–3187.
53. Bergeron RJ, Liu Z, McManis JS, Wiegand J. Structural alterations in desferrioxamine compatible with iron clearance in animals. *J Med Chem* 1992; 35:4739–4744.
54. Porter JB, Alberti D, Hassan I, Howes C, Stallibrass L, Racine A, Alexander E, Davis B, Voi V, Brookman L, Piga A. Subcutaneous depot desferrioxamine (CGH 749B): relationship of pharmacokinetics to efficacy and drug metabolism. *Blood* 1997; 90(suppl 1):1163.

55. Porter JB, Alberti D, Hassan I, Racine A, Davis B, Voi V, Piga A. Phase I, single dose trial on depot desferrioxamine (CGH 749B) in transfusion-dependent beta-thalassemic patients. *Br J Haematol* 1998; 102(suppl):280.
56. Porter JB, Wier DT, Davis B, Alexander E, McCombie RR, Walker SM, Osborne S, Lowe PJ. Iron balance and chelation efficiency following single dose depot desferrioxamine. *Blood* 1998; 92(suppl 1):325A.
57. Galanello R, Kattamis C, Athanassiou M, Quarta G, Ballati G, Zoumbos N, Capellini MD, Piga A, Porter J, Romeo MA, Racine A, Lowe P, Osborne S, Alberti D, Dimitrijevic S. A depot formulation of desferrioxamine (ICL749b): Update on the dose-finding program. *Blood* 1999; 94(suppl):32B.
58. Jackson MJ, Brenton DP, Modell B. DTPA in the management of iron overload in thalassaemia. *J Inher Metab Dis* 1983; 6(suppl 2):97–98.
59. Bannerman RM, Callender ST, Williams DL. Effect of desferrioxamine and DTPA in iron overload. *Br Med J* 1962; 2:1573–1577.
60. LfEplattenier F, Murase I, Martell AE. New multidentate ligands. IV. Chelating tendencies of N,N'-di(2-hydroxybenzyl)ethylenediamine-N,N'-diacetic acid. *J Am Chem Soc* 1967; 89:837–843.
61. Martell AE, Motekaitis RJ, Clarke ET. Synthesis of N,N'-di(2-hydroxybenzyl)ethylenediamine-N,N'-diacetic (HBED) derivatives. *Can J Chem* 1986; 64:449–456.
62. Lau EH, Cerny EA, Wright BJ, Rahman YE. Improvement of iron removal from the reticuloendothelial system by liposome encapsulation of N,N'-bis[2-hydroxybenzyl]ethylenediamine-N,N'-diacetic acid (HBED)—comparison with desferrioxamine. *J Lab Clin Med* 1983; 101:806–816.
63. Bergeron RJ, Wiegand J, Brittenham GM. HBED: a potential alternative to deferoxamine for iron-chelating therapy. *Blood* 1998; 91:1446–1452.
64. Peter HH, Bergeron RJ, Streiff RR, Wiegand J. A comparative evaluation of iron chelators in a primate model. In: Bergeron RJ, Brittenham GM, eds. *The Development of Iron Chelators for Clinical Use*. London: CRC Press, 1993:373–394.
65. Grady RW, Salbe AD, Hilgartner MW, Giardina PJ. Results from phase I clinical trial of HBED. *Adv Exp Med Biol* 1994; 356:351–359.
66. Pitt CG, Bao Y, Thompson J, Wani MC, Rosenkrantz H, Metterville J. Esters and lactones of phenolic amino carboxylic acids: prodrugs for iron chelation. *J Med Chem* 1986; 29:1231–1237.
67. Gasparini F, Leutert T, Farley DL. N,N'-bis(2-hydroxybenzyl)ethylenediamine-N,N'-diacetic acid derivatives as chelating agents. International Patent WO 95/16663, 1995.
68. Lowther N, Tomlinson B, Fox R, Faller B, Sergejew T, Donnelly H. Caco-2 cell permeability of a new (hydroxybenzyl)ethylenediamine oral iron chelator: correlation with physicochemical properties and oral activity. *J Pharm Sci* 1998; 87:1041–1045.
69. Faller B, Spanka C, Sergejew T, Tschinke V. Improving the oral bioavailability of the iron chelator HBED by breaking the symmetry of the intramolecular H-bond network. *J Med Chem* 2000; 43:1467–1475.
70. Hider RC, Bittel D, Andrews GK. Competition between iron(III)-selective chelators and zinc-finger domains for zinc(II). *Biochem Pharmacol* 1999; 57:1031–1035.
71. Streater M, Taylor PD, Hider RC, Porter JB. Novel 3-hydroxyl-2(1H)-pyridinones. Synthesis, iron(III) chelating properties and biological activity. *J Med Chem* 1990; 33:1749–1755.
72. Xu JD, Kullgren B, Durbin PW, Raymond KN. Specific sequestering agents for the actinides. 28: Synthesis and initial evaluation of multidentate 4-carbamoyl-3-hydroxy-1-methyl-2(1H)-pyridinone ligands for in vivo plutonium(IV) chelation. *J Med Chem* 1995; 38:2606–2614.
73. Meyer M, Telford JR, Cohen SM, White DJ, Xu J, Raymond KN. High-yield synthesis of the enterobactin trilactone and evaluation of derivative siderophore analogs. *J Am Chem Soc* 1997; 119:10093–10103.

74. Rai BL, Khodr H, Hider RC. Synthesis, physico-chemical and iron(III)-chelating properties of novel hexadentate 3-hydroxy-2(1H)pyridinone ligands. *Tetrahedron* 1999; 55: 1129–1142.
75. Hahn FN, McMurry TJ, Hugi A, Raymond KN. Coordination chemistry of microbial iron transport. 42: Structural and spectroscopic characterisation of diastereometric Cr(III) and Co(III) complexes of desferrithiocin. *J Am Chem Soc* 1990; 112:1854–1860.
76. Anderegg G, Raber M. Metal complex formation of a new siderophore desferrithiocin and of three related ligands. *J Chem Soc Chem Commun* 1990; 1194–1196.
77. Wolfe LC. Desferrithiocin. *Semin Haematol* 1990; 27:117–120.
78. Bergeron RJ, Wiegand J, Dionis JB, Egli-Karmakka M, Frei J, Huxley-Tencer A, Peter HH. Evaluation of desferrithiocin and its synthetic analogues as orally effective iron chelators. *J Med Chem* 1991; 34:2072–2078.
79. Baker E, Peter WH, Jacobs A. Desferrithiocin is an effective iron chelator in vivo and in vitro but ferrithiocin is toxic. *Br J Haematol* 1992; 81:424–431.
80. Lattmann R, Acklin P. Substituted 3,5-diphenyl-1,2,4-triazoles and their use as pharmaceutical metal chelators. International Patent WO 97/49395, 1997.
81. Heinz U, Hegetschweiler K, Acklin P, Faller B, Lattmann R, Schnebli HP. 4-[3,5-bis(2-hydroxyphenyl)-1,2,4-triazol-1-yl]benzoic acid: a novel efficient and selective iron(III) complexing agent. *Angew Chem Int Ed* 1999; 38:2568–2570.
82. Piga A, Galanello R, Dessi C, Sedaro M, Loehrer F, Sechaud R, Bigler H, Origa R, Tartaglia N, Alberti D. A novel oral iron chelator (ICL670A): results of a Phase I single-dose safety study. *Blood* 1999; 94(suppl 1):35B.
83. Ryabukhin YI, Shibaeva NV, Kuzharov AS, Korobkova VG, Khokhlov AV, Garnovskii AD. Synthesis and investigation of complex compounds of transition metals with di(o-hydroxyphenyl)-1,2,4-oxadiazole and its 1,2,4-triazole analogs. *Sov J Coord Chem* 1988; 493–499.
84. Moridani MY, Tilbrook GS, Khodr HH, Hider RC. Synthesis and physico-chemical assessment of novel 2-substituted-3-hydroxypyridin-4-ones. In press.
85. Balfour JAB, Foster RH. Deferiprone—a review of its clinical potential in iron overload in beta-thalassaemia major and other transfusion-dependent diseases. *Drugs* 1999; 58:553–578.
86. Brittenham GM. Development of iron-chelating agents for clinical use. *Blood* 1992; 80:569–574.
87. Olivieri NF, Brittenham GM, McLaren CE, Templeton DM, Cameron RG, McClelland RA, Burt AD, Fleming KA. Long-term safety and effectiveness of iron-chelation therapy with deferiprone for thalassemia major. *N Engl J Med* 1998; 339:417–423.
88. Callea F. Iron chelation with oral deferiprone in patients with thalassemia. *N Engl J Med* 1998; 339:1710–1711.
89. Kowdley KV, Kaplan MM. Iron-chelation therapy with oral deferiprone—toxicity or lack of efficacy? *N Engl J Med* 1998; 339:468–469.
90. Singh S, Epemolu O, Dobbin PS, Tilbrook GS, Ellis BL, Damani LA, Hider RC. Urinary metabolic profiles in man and rat of 1,2-dimethyl- and 1,2-diethyl substituted 3-hydroxypyridin-4-ones. *Drug Metab Disp* 1992; 20:256–261.
91. Nathan DG. An orally active iron chelator. *N Engl J Med* 1995; 332:953–954.
92. Tricta F, Spino M. Iron chelation with oral deferiprone in patients with thalassemia. *N Engl J Med* 1998; 339:1710.
93. Maggio A, Capra M, Ciaccio C, Magnano C, Rizzo M, et al. Evaluation of efficacy of L1 versus desferrioxamine by clinical randomized multicentric study. *Blood* 1999; 94(suppl):34B.
94. Cohen AR, Galanello R, Piga A, Gamberini R, DeSanctis V, Tricta F. Deferiprone and neutropenia: incidence and characteristics in a long-term safety study. *Blood* 1999; 94(suppl):406A.

95. Porter JB, Morgan J, Hoyes KP, Burke LC, Huehns ER, Hider RC. Relative oral efficacy and acute toxicity of hydroxypyridin-4-one iron chelators in mice. *Blood* 1990; 76:2389–2396.
96. Porter JB, Abeyasinghe RD, Hoyes KP, Barra C, Huehns ER, Brooks PN, Blackwell MP, Araneta M, Britenham G, Singh S, Dobbin P, Hider RC. Contrasting interspecies efficacy and toxicology of 1,2-diethyl-3-hydroxypyridin-4-one CP94, relates to differing metabolism of the iron chelating site. *Br J Haematol* 1993; 85:159–168.
97. Porter JB, Singh S, Katherine PH, Epemolu O, Abeyasinghe RD, Hider RC. Lessons from preclinical and clinical studies with 1,2-diethyl-3-hydroxypyridin-4-one, CP94 and related compounds. *Adv Exp Med Biol* 1994; 356:361–370.
98. Bergeron RJ, Streiff RR, Wiegand J, Luchetta G, Creary EA, Peter HH. A comparison of the iron-clearing properties of 1,2-dimethyl-3-hydroxypyrid-4-one, 1,2-diethyl-3-hydroxypyrid-4-one, and Deferoxamine. *Blood* 1992; 79:1882–1890.
99. Singh S, Epemolu RO, Ackerman R, Porter JB, Hider RC. Development of 3-hydroxypyridin-4-ones which do not undergo extensive phase II metabolism. 3rd NIH-Sponsored Symposium on the Development of Iron Chelators for Clinical Use, Gainesville, FL, 1992, abstr 52.
100. Singh S, Choudhury R, Epemolu RO, Hider RC. Metabolism and pharmacokinetics of 1-(2'-hydroxyethyl)- and 1-(3'-hydroxypropyl)-2-ethyl-3-hydroxypyridin-4-ones in the rat. *Eur J Drug Metab Pharmacokinet* 1996; 21:33–41.
101. Zanninelli G, Choudury R, Loreal O, Guyader D, Lescoat G, Arnaud J, Verna R, Cosson B, Singh S, Hider RC, Brissot P. Novel orally active iron chelators (3-hydroxypyridin-4-ones) enhance the biliary excretion of plasma non-transferrin-bound iron in rats. *J Hepatol* 1997; 27:176–184.
102. Rai BL, Dekhordi LS, Khodr H, Jin Y, Liu Z, Hider RC. Synthesis, physicochemical properties and evaluation of N-substituted-2-alkyl-3-hydroxy-4(1H)-pyridinones. *J Med Chem* 1998; 41:3347–3359.
103. Liu ZD, Lu SL, Hider RC. In vivo iron mobilisation evaluation of hydroxypyridinones in 59Fe-ferritin loaded rat model. *Biochem Pharmacol* 1999; 57:559–566.
104. Rai BL, Liu ZD, Liu DY, Lu SL, Hider RC. Synthesis, physicochemical properties and biological evaluation of ester prodrugs of 3-hydroxypyridin-4-ones: design of orally active chelators with clinical potential. *Eur J Med Chem* 1999; 34:475–485.
105. Liu ZD, Liu DY, Lu SL, Hider RC. Synthesis, physicochemical properties and biological evaluation of aromatic ester prodrugs of 1-(2'-hydroxyethyl)-2-ethyl-3-hydroxypyridin-4-one (CP102): orally active iron chelators with clinical potential. *J Pharm Pharmacol* 1999; 51:555–564.
106. Liu ZD, Liu DY, Lu SL, Hider RC. Design, synthesis, and biological evaluation of aromatic ester prodrugs of 1-(3'-hydroxypropyl)-2-methyl-3-hydroxypyridin-4-one (CP41) as orally active iron chelators. *Arzneim-Forsch/Drug Res* 2000; 50:461–470.
107. Choudhury R, Epemolu RO, Rai BL, Hider RC, Singh S. Metabolism and pharmacokinetics of 1-(2'-trimethylacetoxylethyl)-2-ethyl-3-hydroxypyridin-4-one (CP117) in the rat. *Drug Metab Disp* 1997; 25:332–339.
108. Pippard MJ, Tikerpae J, Peters TJ. Ferritin iron metabolism in the rat liver. *Br J Haematol* 1986; 64:839.
109. Radisky DC, Kaplan J. Iron in cytosolic ferritin can be recycled through lysosomal degradation in human fibroblasts. *Biochem J* 1998; 336:201–205.
110. Laub R, Schneider YJ, Octave JN, Trouet A, Crichton RR. Cellular pharmacology of desferrioxamine B. *Biochem Pharmacol* 1985; 34:1175–1182.
111. Liu ZD, Khodr HH, Lu SL, Hider RC. Design, Synthesis and evaluation of N-basic substituted 3-hydroxypyridin-4-ones: orally active iron chelators with lysosomotropic potential. *J Pharm Pharmacol* 2000; 52:263–272.

112. de Duve C. The lysosome concept. In: de Reuck AVA, Cameron MP, eds. *Lysosomes, a CIBA Foundation Symposium*. Boston: CIBA Foundation, 1963:1–35.
113. de Duve C, de Barse T, Poole B, Trouet A, Tulkens P, van Hoof F. Lysosomotropic agents. *Biochem Pharmacol* 1974; 23:2495–2531.
114. Dobbin PS, Hider RC, Hall AD, Taylor PD, Sarpong P, Porter JB, Xiao G, van der Helm D. Synthesis, physicochemical properties, and biological evaluation of N-substituted 2-alkyl-3-hydroxy-4(1H)-pyridinones: orally active iron chelators with clinical potential. *J Med Chem* 1993; 36:2448–2458.
115. Liu ZD, Khodr HH, Liu DY, Lu SL, Hider RC. Synthesis, physicochemical characterisation and biological evaluation of 2-(1'-hydroxyalkyl)-3-hydroxypyridin-4-ones: novel iron chelators with enhanced pFe^{3+} values. *J Med Chem* 1999; 42:4814–4823.
116. Zbinden P. Hydroxypyridinones. U.S. Patent 5,688,815, 1997.
117. Lowther N, Fox P, Faller B, Nick H, Jin Y, Sergejew T, Hirschberg Y, Oberle R, Donnelly H. In vitro and in situ permeability of a “second generation” hydroxypyridinone oral iron chelator: correlation with physico-chemical properties and oral activity. *Pharmaceut Res* 1999; 16:434–440.
118. Hider RC, Tilbrook GS, Liu ZD. Novel Orally Active Iron(III) Chelators. International Patent WO 98/54138, 1998.

Iron Acquisition in Plants

ELIZABETH E. ROGERS and MARY LOU GUERINOT

Dartmouth College, Hanover, New Hampshire

I. INTRODUCTION	359
II. STRATEGY I	360
A. Proton Release	360
B. Fe(III) Chelate Reductase	362
C. Fe(II) Transport	362
D. Plant Mutants with Altered Strategy I Responses	363
III. STRATEGY II	364
IV. WITHIN-PLANT IRON TRANSPORT	365
A. Root Structure	365
B. Root Iron Transport	366
C. Complexation in the Xylem and Phloem	366
D. Transporters	366
V. IRON STORAGE	367
VI. CONCLUSIONS	369
REFERENCES	369

I. INTRODUCTION

In any aerobic environment, iron exists primarily in the ferric [Fe(III)] form. This poses a problem for plants that need to acquire this essential nutrient, as Fe(III) is highly insoluble at neutral or basic pH, being found largely as polyhydroxide precipitates [Fe(OH)₃] (see Chapter 1 for further details). Furthermore, the little Fe(III) that is in solution is usually present in a chelated form. Given these constraints,

mechanisms that drive more Fe(III) into solution or that allow utilization of chelated forms of Fe(III) should allow for greater mobilization of iron from the soil. Not surprisingly, such mechanisms are employed by various plant species (Fig. 1). All plants except the grasses rely on a combination of proton release and reduction of Fe(III) chelates to help them acquire iron from the soil. This combination has been called Strategy I. The grasses rely on a chelation strategy, designated Strategy II, that involves the release and subsequent utilization of low-molecular-weight, Fe(III)-specific chelators called siderophores. This type of mechanism is also utilized by many species of bacteria and fungi [(1); see also Chapters 15 and 16]. Interestingly, the baker's yeast *Saccharomyces cerevisiae* uses both reduction and chelation strategies (2–4). Whether certain plant species might use reduction as well as chelation strategies remains to be determined. In addition, Fe(II) and Fe(III) can act catalytically to generate hydroxyl radicals, which are highly damaging to cellular components (5). Therefore, both Strategy I and Strategy II plants carefully regulate their iron uptake mechanisms to balance the need for this essential element against its potential toxicity.

This review will describe in some detail how the two main strategies used by plants facilitate iron uptake from the soil and outline what is known about iron transport and storage within plants. Such knowledge is important not only for improving plant nutrition but for making plants better sources of iron for humans. Iron deficiency is the most prevalent human nutritional disorder in the world today. Iron deficiency anemia affects an estimated 2.7 billion people (World Health Organization, <http://www.who.int/nut/>), and most of these people get their iron from eating plants.

II. STRATEGY I

When starved for iron, Strategy I plants induce proton release, Fe(III) chelate reductase activity, and Fe(II) transport activity (6).

A. Proton Release

Proton release serves two functions. First, like animals, plants use a transport system to generate an ion gradient whose electrochemical potential represents stored energy (7). However, unlike animals, which use Na^+ ions, plants use protons to generate this gradient, which then provides the energy for Fe(II) uptake across the root cell plasma membrane. In addition, the resulting acidification of the rhizosphere increases Fe(III) solubility. Specifically, as the pH decreases, the equilibrium is shifted in favor of the dissociation of Fe(OH)₃ complexes, driving more Fe(III) into solution. Indeed, the solubility of Fe(III) increases 1000-fold with each one-unit decrease in pH. The relative contribution of proton release to iron mobilization as part of the Strategy I response is still not known. Evidence from several subclover cultivars indicates that Fe deficiency-induced H^+ release can be the predominant factor conferring resistance to Fe deficiency (8). These cultivars differ in resistance to iron deficiency and have significantly different rates of H^+ release, whereas they have similar rates of Fe(III) chelate reduction. It is, of course, possible that other plants might differ in response to iron deficiency due to changes in their Fe(III) chelate reductase activity. We are now in a position to test whether acidification or reduction is more important in mounting an efficient iron deficiency response using mutants of the model plant *Arabidopsis thaliana*. A family of P-type H^+ -ATPases has been identified in *Arabi-*

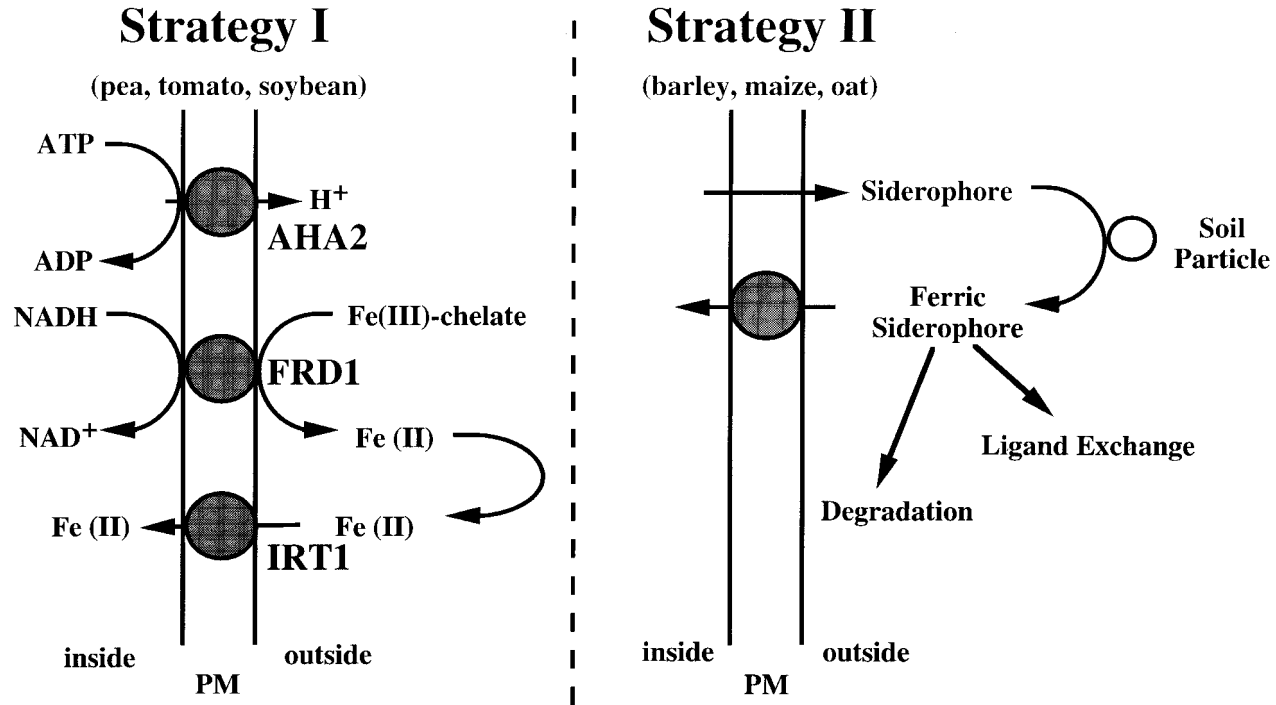


Figure 1 Models for iron acquisition by higher plants. Only the best-studied features are shown. (Modified from Ref. 94.)

dopsis and named the *AHA* gene family, for *Arabidopsis H⁺-ATPase* (9,10). One of these, *AHA2*, is expressed at high levels in root tissue (10), making it a candidate for the gene responsible for the observed proton extrusion activity. We are testing whether an *Arabidopsis aha2* mutant is impaired in iron acquisition relative to wild-type plants. As we have also identified a mutant for *Arabidopsis* that is deficient in Fe(III) chelate reductase activity (see Sec. II.B), we can compare each of the single mutants to a double mutant and assess the relative contribution of proton release and Fe(III) reduction to iron mobilization from the rhizosphere.

It is worth noting that proton release makes iron uptake by Strategy I plants more sensitive to soil pH than iron uptake by Strategy II plants. In well-buffered, high-pH soils, Strategy I plants have great difficulty in dropping the pH of the soil solution.

B. Fe(III) Chelate Reductase

Strategy I plants must reduce Fe(III) to Fe(II) before transport, as they appear to have a transport mechanism only for Fe(II). For some species, Fe(III) reduction is thought to be the rate-limiting step in iron uptake (11), and levels of Fe(III) chelate reductase activity correlate well with tolerance to iron deficiency (12). Biochemical evidence has shown this Fe(III) chelate reductase activity to be membrane-bound, passing electrons across the membrane from NAD(P)H to Fe(III) at the root surface, possibly by a member of the cytochrome b5 reductase flavoprotein family (13–16). To date, this activity has not been sufficiently purified to identify a single polypeptide responsible for the root ferric chelate reductase activity. An alternative approach to identifying the reductase gene was employed by Yi and Guerinot (17), who identified an *Arabidopsis* mutant, called *frd1* (for ferric reductase defective), which completely lacks the inducible Fe(III) chelate reductase activity, presumably due to a mutation in the Fe(III) chelate reductase gene (17). At that time, several candidate Fe(III) chelate reductase genes from *Arabidopsis* had been identified by similarity to the conserved flavin and NADPH-binding domains from yeast Fe(III) reductases and mammalian respiratory burst oxidase, *gp91^{phox}* (18–20). By sequence similarity, these group into two classes. The *Atrboh* (for *Arabidopsis thaliana* respiratory burst oxidase homolog) genes are more similar to mammalian *gp91^{phox}* and are predicted to be involved in the pathogen-associated oxidative burst (20). The other group is comprised of the *FRO* (for ferric reductase oxidase) genes. The *FRO* gene products are predicted to contain several transmembrane domains and contain conserved heme, NADPH, and FAD-binding sites (18). One of these, *FRO2*, mapped to the same location as *frd1*, and was more highly expressed in iron-deficient roots as compared to iron-sufficient roots. The *FRO2* gene was shown to complement the *frd1* mutant, and several *frd1* mutants contain mutations in their *FRO2* genes (21), proving that the *FRO2* gene does indeed encode the inducible Fe(III) chelate reductase in *Arabidopsis* roots.

C. Fe(II) Transport

The first plant iron transporter was cloned by Eide et al. (22), who used an *Arabidopsis* cDNA expression library to complement an iron uptake-defective *S. cerevisiae* mutant. This led to the identification of the *IRT1* gene (for iron regulated transporter), one of the founding members of a large family of metal transporters (23).

When expressed in yeast, *IRT1* confers novel iron, zinc, manganese, and cadmium uptake activities (22,24,25). This transporter shows a strong preference for Fe(II) over Fe(III) (22). In *Arabidopsis*, *IRT1* mRNA accumulates under iron deficiency (22).

D. Plant Mutants with Altered Strategy I Responses

In addition to the above-mentioned *frd1*, a number of other plant mutants with alterations in their Strategy I responses have been identified. The *chloronerva* (*chln*) mutant of tomato shows both constitutive iron deficiency symptoms and constitutive Strategy I iron deficiency responses (26). Surprisingly, it accumulates more iron than the wild type in its tissues, suggesting there may be a problem in iron sensing (27). This mutant is discussed more fully in Sec. IV.C. Briefly, the phenotypes of the *chln* mutant are completely reversed by the application of exogenous nicotianamine (28). Nicotianamine has been implicated in iron transport and storage in plants; *chln* completely lacks nicotianamine and nicotianamine synthase activity (29). The *chln* gene has recently been cloned by a map-based approach and shown to encode a nicotianamine synthase (30).

A second class of *Arabidopsis* Fe(III) reductase-defective mutants has been identified (31). In contrast to *frd1*, *frd3* mutants show constitutive Fe(III) chelate reductase activity (31). *frd3* is allelic to the *man1* mutant of *Arabidopsis* (Rogers and Guerinot, unpublished). *man1* was identified as a manganese overaccumulator, but it also accumulates a variety of metals and shows constitutive Fe(III) reductase activity (32). Plants carrying any of the *frd3* alleles show constitutive expression of the *FRO2* Fe(III) reductase gene and the *IRT1* transporter gene, and have higher levels of iron, zinc, and manganese in their shoot tissues than wild-type *Arabidopsis* (22) (Rogers and Guerinot, unpublished). Although some of these phenotypes are similar to the phenotypes of the tomato mutant *chln*, *frd3* is unaffected by exogenous nicotianamine and maps to a different chromosome than any of the three *Arabidopsis* nicotianamine synthase genes (Rogers and Guerinot, unpublished results). The fact that multiple Strategy I responses are constitutively active in a plant that has higher levels of iron than wild type indicates that the *FRD3* gene probably encodes some type of regulatory factor. The map-based cloning of *frd3* is in progress.

Two pea mutants also show constitutive iron deficiency responses and accumulate iron. These are the *bronze* (*brz*) (33,34) and *degenerative leaves* (*dgl*) (35,36) mutants. They are both recessive, nonallelic mutations (33). *brz* accumulates iron only in the leaves, while *dgl* accumulates iron in its leaves and translocates excess iron to the seeds (37,38). Grafting studies have shown that both *brz* and *dgl* express a shoot factor that leads to the constitutive expression of root ferric chelate reductase activity (36). Therefore, these mutations probably also affect a factor involved in the regulation of Strategy I responses. Unfortunately, the large size of the pea genome makes map-based cloning efforts impractical.

Another tomato mutant shows the opposite phenotype to the previously mentioned mutants. The *fer* mutant is unable to express Strategy I responses, such as proton release and Fe(III) chelate reductase activity, under iron-limiting conditions (39). The resulting iron deficiency makes this mutant chlorotic. Therefore, *FER* may encode a positive regulatory factor of these responses (40). Additional evidence of a regulatory role for *FER* comes from studies showing that *fer* is epistatic to *chlo-*

ronerva (41), indicating that *FER* regulates *CHLN*. A map-based cloning effort is underway to identify the *FER* gene (41).

III. STRATEGY II

Strategy II can be divided into four components: siderophore biosynthesis, release, iron solubilization, and uptake of the iron–siderophore complex (42).

Plant siderophores identified to date belong to the mugineic acid family and include mugineic acid, avenic acid, 3-hydroxymugineic acid, 3-epihydroxymugineic acid, 3-epihydroxy-2'-deoxymugineic acid, 2'-deoxymugineic acid, and distichonic acid (43,44). The biosynthetic pathway of mugineic acids in barley roots has been largely elucidated (12). Methionine is the predominant precursor (45), which is converted to nicotianamine by nicotianamine synthase (46,47). A nicotianamine synthase activity from barley was purified and used to identify several similar genes (47,47a), which confer nicotianamine synthase activity when expressed in *Escherichia coli*. The *nas1* protein from barley is 76% similar to the tomato protein identified by cloning the *chloronerva* gene (30). In monocots, nicotianamine is then converted to deoxymugineic acid by nicotianamine aminotransferase (48). Depending on the species, deoxymugineic acid is further modified to create other mugineic acid family siderophores. A number of genes, called *IDS* (for iron deficiency specific) have been identified and shown to catalyze some of these subsequent modifications (12,49,50). The biosynthesis of all mugineic acid family siderophores is tightly controlled by intracellular iron concentration, with iron deficiency increasing the levels of both phytosiderophores and the mRNAs of siderophore biosynthetic genes, although the mechanism of this regulation is not known (42). Secretion of phytosiderophores follows a diurnal rhythm; they are synthesized throughout the day and accumulated within the root cells for release the following morning (42). Recent electron microscope studies have identified vesicles in iron-deficient barley root cells which are larger in size just before dawn. These vesicles are studded with ribosomes and appear to be ER-derived. Immunoelectron microscopy shows that a number of siderophore biosynthetic enzymes are associated with these vesicles, implying that these are centers for siderophore biosynthesis and likely serve as storage sites (51).

After release, the phytosiderophores bind Fe(III) and then the iron–siderophore complex is transported into the root epidermal cells. Double labeling experiments have shown that Strategy II plants take up the siderophore as well as the Fe(III) (52). Unlike Strategy I plants, Strategy II plants do not reduce Fe(III) to Fe(II) prior to transport (52). As with phytosiderophore biosynthesis, uptake is enhanced several-fold under iron deficiency (52).

The maize *yellow stripe 1* (*ys1*) mutant exhibits interveinal chlorosis similar to the symptoms of iron deficiency in maize, hence the name. This mutant has been shown to produce wild-type levels of phytosiderophores but is defective in Fe(III)–siderophore uptake (53). A transposon tagged allele of *ys1* was recently identified, allowing the gene responsible to be cloned (54). *ys1* encodes a novel transporter, 705 amino acids in length with 12 to 14 predicted transmembrane domains. It is similar to a number of genes from other plants, including *Arabidopsis*. The *ys1* gene is expressed in maize at low levels in the roots under iron-sufficient conditions; iron deficiency induces high-level expression in both the roots and the leaves. The *ys1* cDNA complements the iron-limited growth defect of the *S. cerevisiae* iron uptake

mutant *fet3 fet4* when iron is supplied as Fe(III)-deoxymugineic acid but not when iron is supplied as Fe(III) citrate. This indicates that *ys1* may be involved in iron–siderophore uptake from the soil.

A second maize mutant showing constitutive iron deficiency symptoms has also been identified. *ys3* is less well characterized than *ys1*; however, it also appears to have alterations in its ability to utilize chelated Fe(III) (55). The iron deficiency of *ys3* can be rescued by spent media in which wild-type plants were grown, implying that *ys3* has a defect in siderophore biosynthesis or secretion rather than iron–siderophore uptake (55).

IV. WITHIN-PLANT IRON TRANSPORT

A. Root Structure

In plants, once iron is taken up by the root, it must be transported throughout the plant. Figure 2 shows a drawing of a typical plant root. There are three methods by which water and solutes may enter the root: apoplastic, symplastic, and transmembrane pathways. The apoplast refers to the intercellular spaces largely taken up by cell walls. Passive diffusion controls the movement of small molecules in the apoplast, since they do not have to cross a cell membrane. As shown in Figure 2, the Casparian strip is a layer of suberin-coated endodermal cells. Suberin is a waxy substance which together with the endodermal cells themselves form a water- and solute-impermeable barrier, separating the apoplast of the outer root (the cortex) from the apoplast in the stele and the rest of the plant. Therefore, all small molecules entering the stele, or central vascular tissue of the root, must use one of the other two pathways and cross a cell membrane. The symplast refers to the whole network of cell cytoplasm interconnected by plasmadesmata, extensions of plasma membrane that connect the cytoplasm of adjacent cells. Once a small molecule or ion, such as iron, has crossed a plasma membrane and entered one plant cell, it can move throughout the plant using the symplastic pathway. In the transmembrane pathway, small molecules sequentially enter one root cell, exit on the other side, enter the next cell, and so on. The majority of long-distance transport within the plant occurs through the vascular tissue, the xylem and the phloem. The phloem is responsible for transporting metabolites from the shoot to the root, while the xylem transports water and solutes to the shoot.

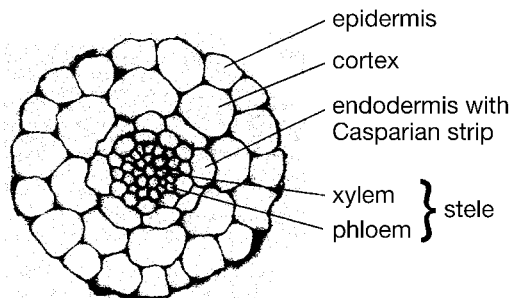


Figure 2 A cross section of the primary root of *Arabidopsis thaliana*. (Adapted from Ref. 95.)

B. Root Iron Transport

In contrast to iron uptake into the root, relatively little is known about the molecular basis of iron transport within the plant. It is not clear if transport within the plant differs significantly between Strategy I and II plants. Many metals appear to be in constant flux from one part of the plant to another throughout the lifespan of the plant (27). For example, in *Arabidopsis* copper levels drop by one-half several days after the onset of senescence and the copper chaperone CCH is upregulated in senescent leaves (56). Iron, among other metals, seems to be retranslocated through the phloem from mature organs to actively growing young tissues, a process intensified by iron deficiency (27). Iron has been shown to be transported from a cut portion of the leaf to other leaves and in iron-deficient plants to the root meristem, possibly through both the apoplast and the vascular system (57).

C. Complexation in the Xylem and Phloem

Within the xylem and phloem, iron presumably moves as Fe(III) chelates. Nicotianamine has been shown to chelate a variety of metals, including copper, zinc, manganese (58), and both Fe(II) and Fe(III), although the Fe(II)–nicotianamine complex is kinetically more stable than the Fe(III)N–nicotianamine complex (59). At the relatively low pH found in the xylem, all Fe(III) is predicted to be complexed to citrate, while at the higher pH of the phloem, both Fe(III) and Fe(II) will be complexed with nicotianamine (59). In grasses, 2'-deoxymungenic acid is the predominant chelator at acidic xylem pH, while again, nicotianamine dominates at alkaline pH (59). Immunolocalization of nicotianamine in the root tips of tomato reveals it in the vacuoles of stele cells in the root, implicating it in storage and detoxification of iron (60).

The tomato mutant *chloronerva* (*chl*n), a nicotianamine auxotroph, has also been useful in elucidating the role of nicotianamine in plant iron nutrition (27,61). Recently, the *chloronerva* gene has been cloned by a map-based approach (30). Based on in-vitro enzyme activity of bacterially expressed protein and sequence similarity to a nicotianamine synthase gene cloned from barley, this gene was shown to encode the tomato nicotianamine synthase (30). Since the *chl*n mutant exhibits both constitutive iron deficiency responses and higher levels of iron than wild type, the Fe(II)–nicotianamine complex has been hypothesized to be a signal molecule for iron status (28). Because the *chl*n mutant lacks nicotianamine and the Fe(II)–nicotianamine complex, it will constitutively act iron-deficient, even if it contains high levels of iron in its tissues.

D. Transporters

Iron, like any charged species, must be transported across membranes, whether into a cell or from the cytoplasm to a subcellular organelle. There are at least three families of genes that may be involved in the transport of iron in plants. These are the ZIP gene family (23), the Nramp family (62,63), and the ferroportins (64).

The ZIP gene family was named after the first two members to be discovered, the *IRT1* gene of *Arabidopsis* mentioned above, and the *ZRT1* and *ZRT2* genes, which are the high- and low-affinity zinc transporters in the yeast *S. cerevisiae*

(65,66). *IRT1*, *ZRT1*, and *ZRT2* are all predicted to contain eight transmembrane domains with the N and C termini extracellular and a histidine-rich loop located in the cytoplasm (22,65,66). To date, *ZIP* family members have been found in animals, plants, fungi, protists, and bacteria (23), making this an ancient and diverse family of metal transporters. There are at least 14 *ZIP* family members in *Arabidopsis*, a number of which have been shown to transport iron and/or zinc when expressed in yeast (22,24,67). Several *ZIP* genes from *Arabidopsis* have putative mitochondrial or chloroplast targeting sequences (23). This may explain why there are so many family members in a single plant species, if this family is involved in transporting multiple metals across multiple membranes.

Nramps (Natural resistance associated macrophage proteins) have been identified in mammals as divalent cation transporters involved in host resistance to certain pathogens and in iron metabolism (see Chapter 6). The first Nramp was discovered in mice, where it was shown to be responsible for mycobacteria resistance or sensitivity (68). Later, a second mammalian family member was shown to be a proton-coupled iron transporter and implicated in iron uptake in the duodenum (69). The original Nramp1 has been shown to transport iron from endosomes containing endocytosed transferrin receptors to the cell cytoplasm (70). A yeast Nramp has been identified and implicated in manganese transport (71), and several bacterial orthologs have been shown to be divalent metal ion transporters as well (72,73). There are several *Nramp*-like genes in *Arabidopsis*, which have been shown to play roles in transporting a number of metals, including iron, manganese, and cadmium (62,63). Two of the *Arabidopsis Nramp* genes complement a yeast iron uptake mutant and are expressed at higher levels under iron deficiency (62). The *Arabidopsis* genes are predicted to contain 12 transmembrane domains, with a highly conserved consensus transport motif, hypothesized to interact with ATP-coupling subunits, between transmembrane domains 8 and 9 (63). Another *Arabidopsis Nramp*-like gene, *EIN2*, has been identified based on its role in ethylene signaling (74). However, the protein is unable to confer iron transport activity when expressed in *S. cerevisiae*, *Xenopus* oocytes, or insect cells, and therefore appears to lack metal transport functions (63,74). *Nramp*-like genes have also been found in rice (63).

More recently, a third class of proteins implicated in iron transport has been discovered in plants. These are the ferroportins or *IREG1*-like genes, recently implicated in iron export in animals [(64,75,76); see also Chapter 7]. When iron is absorbed from the intestinal tract in animals, it must then exit the epidermal cells in order to be transported via transferrin throughout the organism. In plants, iron also must exit the epidermal cells, either through a process analogous to that in mammals or through intercellular pores called plasmodesmata. *ferroportin1* from zebrafish (75) and *IREG1* from mouse (64) have both been implicated in exporting iron from intestinal epidermal cells. There are three *Arabidopsis* genes with similarity to *ferroportin1* and *IREG1* (Grotz and Guerinot, unpublished), which are candidates for involvement in iron transport or xylem and phloem loading in plants.

V. IRON STORAGE

The primary sites of iron storage in plants are the apoplast, the extracellular free space around plant cells, and vacuoles, intracellular acidic organelles. Like animals, plants use ferritin for intracellular iron storage and detoxification [(77); see also

Chapter 5]. However, unlike animals, plant ferritins are localized to plastids, not the cytoplasm. Plant ferritins show 39–49% identity to animal ferritins, although they have a different intron number and position and lack a recognizable iron regulatory element (IRE), a characteristic of animal ferritins responsible for their translational control [(78); see also Chapter 9]. In plants, ferritin is most commonly found in seeds, cotyledons, and shoot apices, while levels in mature organs such as leaves and roots are very low (77). It is often present in etioplasts but rarely in mature chloroplasts. This suggests that at early stages of development, ferritin acts as an iron source, donating iron to necessary iron-containing proteins (79). Intracellular levels of the reductant ascorbate and intracellular pH appear to regulate the flux of iron in and out of ferritin cores (80). Ferritin also accumulates in response to iron overload, either as a result of a mutation as in the *brz* and *dgl* mutants (81), or as a result of high external iron supply (82,83).

Plant ferritin biosynthesis is regulated both transcriptionally and posttranscriptionally. There appear to be two pathways that transcriptionally control ferritin mRNA accumulation in maize and *Vigna mungo* (82,84). *ZmFer1* is regulated by an iron-mediated oxidative pathway, while *ZmFer2* is regulated by the plant hormone abscisic acid (82), and the same pathways act in *Vigna mungo* (84). In *Arabidopsis*, *AtFer1* accumulates only in response to the oxidative pathway, not to abscisic acid (83). However, there are other, divergent ferritin genes in *Arabidopsis* whose expression has not been investigated (83), although one was first sequenced as part of an abscisic acid-responsive gene cluster (85). Recently, an 86-base-pair iron regulatory element (FRE) was identified upstream of the soybean ferritin gene (86). Induction by iron and iron-mediated pathways implicates ferritin in detoxifying excess cytoplasmic iron. Plant ferritin protein levels are independent of mRNA levels, implicating posttranscriptional levels of control. It has been reported that ferritin mRNA levels are higher in mature soybean leaves than in young leaves, but ferritin protein was more abundant in young leaves (77). The maize iron–siderophore uptake mutant *ys1* has lower levels of iron and ferritin protein in its leaves than wild type, but similar levels of ferritin mRNA (87).

Ferritins have been overexpressed in transgenic plants, providing added insight into their roles. A soybean ferritin gene was expressed at high levels throughout transgenic tobacco plants (88). These plants overaccumulated functional ferritin, which led to illegitimate iron sequestration. Therefore, even though the leaf iron content was higher than in nontransgenic tobacco plants, the transgenic plants behaved as if iron-deficient, exhibiting chlorosis and activating iron transport systems (88). Transgenic tobacco plants expressing alfalfa ferritin were tolerant to a variety of oxidative stresses and pathogens, probably because the ferritin sequestered excess intracellular iron normally involved in the generation of reactive hydroxyl radicals (89). In an attempt to improve the iron content of rice and reduce dietary iron deficiency, a transgenic rice line was constructed which expresses a soybean ferritin gene only in the endosperm of the rice seed (90). This increased the iron content of the rice seed almost threefold, while no alterations in the physiology of the transgenic rice were reported (90). However, there is conflicting evidence on the bioavailability of iron complexed to plant ferritins (91,92), so the effect of ferritin-fortified rice on dietary iron deficiency is not clear.

VI. CONCLUSIONS

The ultimate goal is to understand metal transport on the level of the whole plant, which should allow the development of plants with enhanced nutritive value and plants that accumulate or exclude potentially toxic metals. The high cost and adverse environmental impact of heavy fertilizer use emphasize the need for plants with increased endogenous iron uptake mechanisms (93). In recent years, a number of genes involved in iron nutrition, especially in transport and phytosiderophore biosynthesis, have been identified. However, the signals regulating these genes and the system(s) responsible for sensing iron levels in the plant remain unknown. Because excess iron is toxic, uptake is tightly controlled. Therefore, successfully increasing plant iron content will require a thorough understanding of these sensing and regulatory mechanisms.

REFERENCES

1. Guerinot ML. Microbial iron transport. *Annu Rev Microbiol* 1994; 48:743–772.
2. Askwith C, Kaplan J. Iron and copper transport in yeast and its relevance to human disease. *Trends Biochem Sci* 1998; 23:135–138.
3. Yun C-W, Ferea T, Rashford J, Ardon O, Brown PO, Botstein D, Kaplan J, Philpott CC. Desferrioxamine-mediated iron uptake in *Saccharomyces cerevisiae*: evidence for two pathways of iron uptake. *J Biol Chem* 2000; 275:10709–10715.
4. Yun C-W, Tiedman JS, Moore RE, Philpott CC. Siderophore-iron uptake in *Saccharomyces cerevisiae*: identification of ferrichrome and fusarine transporters. *J Biol Chem* 2000; 275:16354–16359.
5. Halliwell B, Gutteridge JMC. Biologically relevant metal ion-dependent hydroxyl radical generation. *FEBS Lett* 1992; 307:108–112.
6. Römheld V, Marschner H. Mobilization of iron in the rhizosphere of different plant species. *Adv Plant Nutr* 1986; 2:155–204.
7. Sze H, Li X, Palmgren MG. Energization of plant cell membranes by H⁺-pumping ATPases: regulation and biosynthesis. *Plant Cell* 1999; 11:677–689.
8. Wei LC, Loeppert RH, Ocumpaugh WR. Fe-deficiency stress response in Fe-deficiency resistant and susceptible subterranean clover: importance of induced H⁺ release. *J Exp Bot* 1997; 48:239–246.
9. Harper JF, Surowy TK, Sussman MR. Molecular cloning and sequence of cDNA encoding the membrane proton pump (H⁺-ATPase) of *Arabidopsis thaliana*. *Proc Natl Acad Sci USA* 1989; 86:1234–1238.
10. Harper JF, Manney L, DeWitt ND, Yoo MH, Sussman MR. The *Arabidopsis thaliana* plasma membrane H⁺-ATPase multigene family. *J Biol Chem* 1990; 265:13601–13608.
11. Grusak MA, Welch RM, Kochian LV. Physiological characterization of a single-gene mutant of *Pisum sativum* exhibiting excess iron accumulation. I. Root iron reduction and iron uptake. *Plant Physiol* 1990; 93:976–981.
12. Mori S. Iron acquisition by plants. *Curr Opin Plant Biol* 1999; 2:250–253.
13. Buckhout TJ, Bell PF, Luster DG, Chaney RL. Iron-stress induced redox activity in tomato (*Lycopersicon esculentum* Mill.) is localized on the plasma membrane. *Plant Physiol* 1989; 90:151–156.
14. Holden MJ, Luster DG, Chaney RL. Enzymatic iron reduction at the root plasma membrane: partial purification of the NADH-Fe chelate reductase. In: Manthey J, Luster D, Crowley DE, eds. *Biochemistry of Metal Micronutrients in the Rhizosphere*. Chelsea, MI: Lewis, 1994: 284–294.

15. Bagnaresi P, Basso B, Pupillo P. The NADH-dependent Fe(III)-chelate reductases of tomato roots. *Planta* 1997; 202:427–434.
16. Bérczi A, Van Gestelen P, Pupillo P. NAD(P)H-utilizing oxidoreductases in the plant plasma membrane. In: Asgard H, Bérczi A, Caubergs RJ, eds. *Plasma Membrane Systems and Their Role in Biological Stress and Disease*. Dordrecht, The Netherlands: Kluwer, 1998:33–67.
17. Yi Y, Guerinot ML. Genetic evidence that induction of root Fe(III) chelate reductase activity is necessary for iron uptake under iron deficiency. *Plant J* 1996; 10:835–844.
18. Robinson NJ, Sadjuga MR, Groom QJ. The froh gene family from *Arabidopsis thaliana*: putative iron-chelate reductases. *Plant Soil* 1997; 196:245–248.
19. Sadjuga MR, Procter CM, Robinson NJ, Groom QJ. Isolation and analysis of genes encoding novel NAD(P)H oxidases from *Arabidopsis thaliana*: their putative role(s) as ferric/cupric reductases. *J Exp Bot* 1997; 48:101(suppl).
20. Torres MA, Onouchi H, Hamada S, Machida C, Hammond-Kosack KE, Jones JDG. Six *Arabidopsis thaliana* homologs of the human respiratory burst oxidase (gp91phox). *Plant J* 1998; 14:365–370.
21. Robinson NJ, Procter CM, Connolly EL, Guerinot ML. A ferric-chelate reductase for iron uptake from soils. *Nature* 1999; 397:694–697.
22. Eide D, Broderius M, Fett J, Guerinot ML. A novel iron-regulated metal transporter from plants identified by functional expression in yeast. *Proc Natl Acad Sci USA*. 1996; 93:5624–5628.
23. Guerinot ML. The ZIP family of metal transporters. *Biochim Biophys Acta* 2000; 1465: 190–198.
24. Korshunova Y, Eide D, Clark G, Guerinot M, Pakrasi H. The Irt1 protein from *Arabidopsis thaliana* is a metal transporter with broad specificity. *Plant Mol Biol* 1999; 40:37–44.
25. Rogers EE, Eide DJ, Guerinot ML. Altered selectivity in an *Arabidopsis* metal transporter. *Proc Natl Acad Sci USA* 2000; 97:12356–12360.
26. King J. *The genetic basis of plant physiological processes*. London: Oxford University Press, 1991.
27. Stephan UW, Scholz G. Nicotianamine: mediator of transport of iron and heavy metals in the phloem? *Physiol Plant* 1993; 88:522–529.
28. Scholz G, Schlesier G, Seifert K. Effect of nicotianamine on iron uptake by the tomato mutant “chloronerva.” *Physiol Plant* 1985; 63:99–104.
29. Higuchi K, Nishizawa N, Roemheld V, Marschner H, Mori S. Absence of nicotianamine synthase activity in the tomato mutant “chloronerva.” *J Plant Nutr* 1996; 19:1235–1239.
30. Ling H-Q, Koch G, Baumlein H, Ganai MW. Map-based cloning of *chloronerva*, a gene involved in iron uptake of higher plants encoding nicotianamine synthase. *Proc Natl Acad Sci USA* 1999; 96:7098–7103.
31. Yi Y. Iron uptake in *Arabidopsis thaliana*. Ph.D. dissertation, Dartmouth College, Hanover, NH, 1995.
32. Delhaize E. A metal-accumulator mutant of *Arabidopsis thaliana*. *Plant Physiol* 1996; 111:849–855.
33. Kneen BE, LaRue TA, Welch RM, Weeden NF. Pleiotropic effects of *brz*. *Plant Physiol* 1990; 93:717–722.
34. Welch RM, LaRue TA. Physiological characteristics of Fe accumulation in the “Bronze” mutant of *Pisum sativum* L., cv “Sparkle” E107 (*brz brz*). *Plant Physiol* 1990; 93:723–729.
35. Gottschalk W. Improvement in the selection value of gene *dgl* through recombination. *Pisum Newsl* 1987; 19:9–11.

36. Grusak MA, Pezeshgi S. Shoot-to-root signal transmission regulates root Fe(III) reductase activity in the *dgl* mutant of pea. *Plant Physiol* 1996; 110:329–334.
37. Grusak MA. Whole-root iron(III)-reductase activity throughout the life cycle of iron-grown *Pisum sativum* L. (Fabaceae): relevance to the iron nutrition of developing seeds. *Planta* 1995; 197:111–117.
38. Marentes E, Grusak MA. Iron transport and storage within the seed coat of developing embryos of pea (*Pisum sativum* L). *Seed Sci Res* 1998; 8:367–375.
39. Brown JC, Chaney RL, Ambler JE. A new tomato mutant inefficient in the transport of iron. *Physiol Plant* 1971; 25:48–53.
40. Bienfait HF. Proteins under the control of the gene for Fe efficiency in tomato. *Plant Physiol* 1988; 88:785–787.
41. Ling HQ, Pich A, Scholz G, Ganai MW. Genetic analysis of two tomato mutants affected in the regulation of iron metabolism. *Mol Gen Genet* 1996; 252:87–92.
42. Ma JF, Nomoto K. Effective regulation of iron acquisition in graminaceous plants. The role of mugineic acids as phytosiderophores. *Physiol Plant* 1996; 97:609–617.
43. Bughio N, Takahashi M, Yoshimura E, Nishizawa N-K, Mori S. Light-dependent iron transport into isolated barley chloroplasts. *Plant Cell Physiol* 1997; 38:101–105.
44. Ma J-F, Takeda S, Chong YC, Iwashita T, Matsumoto H, Takeda K, Nomoto K. Genes controlling hydroxylations of phytosiderophores are located on different chromosomes in barley. *Planta* 1999; 207:590–596.
45. Ma JF, Shinada T, Matsuda C, Nomoto N. Biosynthesis of phytosiderophores, mugeneic acid, associated with methionine cycle. *J Biol Chem* 1995; 270:16549–16554.
46. Herbig A, Koch G, Mock H-P, Dushkov D, Czihal A, Thielmann J, Stephan UW, Bäumlein H. Isolation, characterization and cDNA cloning of nicotianamine synthase from barley: a key enzyme for iron homeostasis in plants. *Eur J Biochem* 1999; 265:231–239.
47. Higuchi K, Suzuki K, Nakanishi H, Yamaguchi H, Nishizawa NK, Mori S. Cloning of nicotianamine synthase genes, novel genes involved in the biosynthesis of phytosiderophores. *Plant Physiol* 1999; 119:471–479.
- 47a. Herbig A, Koch G, Mock HP, Dushkov D, Czihal A, Thielmann J, Stephan UW, Baumlein H. Isolation, characterization and DNA cloning of nicotianamine synthase from barley. A key enzyme for iron homeostasis in plants. *Eur J Biochem* 1999; 265:231–239.
48. Takahashi M, Yamaguchi H, Nakanishi H, Shioiri T, Nishizawa N-K, Mori S. Cloning two genes for nicotianamine aminotransferase, a critical enzyme in iron acquisition (strategy II) in graminaceous plants. *Plant Physiol* 1999; 121:947–956.
49. Nakanishi H, Okumura N, Umehara Y, Nishizawa N-K, Chino M, Mori S. Expression of a gene specific for iron deficiency (*Ids3*) in the roots of *Hordeum vulgare*. *Plant Cell Physiol* 1993; 34:401–410.
50. Okumura N, Nishizawa N-K, Umehara Y, Ohata T, Nakanishi H, Yamaguchi T, Chino M, Mori S. A dioxygenase gene (*Ids2*) expressed under iron deficiency conditions in the roots of *Hordeum vulgare*. *Plant Mol Biol* 1994; 25:705–719.
51. Nishizawa NK, Negishi T, Higuchi K, Takahashi M, Itai R, Nakanishi H, Mori S. The secretion and biosynthesis of mugineic acid family phytosiderophores (MAs) in iron deficient barley roots. 10th International Symposium on Iron Nutrition and Interactions in Plants, Houston, Texas, USA, May 14–19, 2000.
52. Römheld V, Marschner H. Evidence for a specific uptake system for iron-phytosiderophores in roots of grasses. *Plant Physiol* 1986; 80:175–180.
53. von Wirén N, Mori S, Marschner H, Römheld V. Iron inefficiency in maize mutant *ysI* (*Zea mays* L. cv yellow-stripe) is caused by a defect in uptake of iron phytosiderophores. *Plant Physiol* 1994; 106:71–77.

54. Curie C, Panaviene Z, Loulergue C, Dellaporta SL, Briat JF, Walker EL. Maize yellow stripe 1 encodes a membrane protein directly involved in Fe(III) uptake. *Nature* 2001; 409:346–349.
55. Basso B, Bagnaresi P, Bracale M, Soave C. The yellow-stripe-1 and -3 mutants of maize: nutritional and biochemical studies. *Maydica* 1994; 39:97–105.
56. Himelblau E, Mira H, Lin SJ, Culotta VC, Penarrubia L, Amasino RM. Identification of a functional homolog of the yeast copper homeostasis gene *ATX1* from *Arabidopsis*. *Plant Physiol* 1998; 117:1227–1234.
57. Mori S. Iron transport in graminaceous plants. In: Sigel A, Sigel H, eds. *Metals Ions in Biological Systems*. New York: Marcel Dekker, 1998:216–238.
58. Stephan UW, Schmidke I, Stephan VW, Scholz G. The nicotianamine molecule is made-to-measure for complexation of metal micronutrients in plants. *BioMetals* 1996; 9:84–90.
59. von Wirén N, Klair S, Bansal S, Briat J-F, Khodr H, Shioiri T, Leigh RA, Hider RC. Nicotianamine chelates both Fe(III) and Fe(II). Implications for metal transport in plants. *Plant Physiol* 1999; 119:1107–1114.
60. Pich A, Hillmer S, Manteuffel R, Scholz G. First immunohistochemical localization of the endogenous Fe(II)-chelator nicotianamine. *J Exp Bot* 1997; 48:759–767.
61. Herbig A, Giritch A, Horstmann C, Becker R, Balzer H, Bäumlein H, Stephan UW. Iron and copper nutrition-dependent changes in protein expression in a tomato wild type and the nicotianamine-free mutant *chloronerva*. *Plant Physiol* 1996; 111:533–540.
62. Thomine S, Wang R, Ward JM, Crawford NM, Schroeder JI. Cadmium and iron transport by members of a plant metal transporter family in *Arabidopsis* with homology to *Nramp* genes. *Proc Natl Acad Sci USA* 2000; 97:4991–4996.
63. Curie C, Alonso JM, LeJean M, Ecker JR, Briat JF. Involvement of Nramp1 from *Arabidopsis thaliana* in iron transport. *Biochem J* 2000; 347:749–755.
64. McKie AT, Marciani P, Rolfs A, Brennan K, Wehr K, Barrow D, Miret S, Bomford A, Peters TJ, Farzaneh F, Hediger MA, Hentze MW, Simpson RJ. A novel duodenal iron-regulated transporter, IREG1, implicated in the basolateral transfer of iron to the circulation. *Mol Cell* 2000; 5:299–309.
65. Zhao H, Eide D. The yeast ZRT1 gene encodes the zinc transporter of a high affinity uptake system induced by zinc limitation. *Proc Natl Acad Sci USA* 1996; 93:2454–2458.
66. Zhao H, Eide D. The ZRT2 gene encodes the low affinity zinc transporter in *Saccharomyces cerevisiae*. *J Biol Chem* 1996; 271:23203–23210.
67. Grotz N, Fox T, Connolly EL, Park W, Guerinot ML, Eide D. Identification of a family of zinc transporter genes from *Arabidopsis* that respond to zinc deficiency. *Proc Natl Acad Sci USA* 1998; 95:7220–7224.
68. Vidal SM, Malo D, Vogan K, Skamene E, Gros P. Natural resistance to infection with intracellular parasites: isolation of a candidate for Bcg. *Cell* 1993; 73:469–485.
69. Gunshin H, Mackenzie B, Berger UV, Gunshin Y, Romero MF, Boron WF, Nussberger S, Gollan JL, Hediger MA. Cloning and characterization of a mammalian proton-coupled metal-ion transporter. *Nature* 1997; 388:482–488.
70. Nelson N. Metal ion transporters and homeostasis. *EMBO J* 1999; 18:4361–4371.
71. Supek F, Supekova L, Nelson H, Nelson N. A yeast manganese transporter related to the macrophage protein involved in conferring resistance to mycobacteria. *Proc Natl Acad Sci USA* 1996; 93:5105–5110.
72. Makui H, Roig E, Cole ST, Helmann JD, Gros P, Cellier MFM. Identification of the *Escherichia coli* K-12 Nramp ortholog (MntH) as a selective divalent metal ion transporter. *Mol Microbiol* 2000; 35:1065–1078.
73. Kehres DG, Zaharik ML, Finlay BB, Maguire ME. The NRAMP proteins of *Salmonella typhimurium* and *Escherichia coli* are selective manganese transporters involved in the response to reactive oxygen. *Mol Microbiol* 2000; 36:1085–1100.

74. Alonso JM, Hirayama T, Roman G, Nourizadeh S, Ecker JR. EIN2, a bifunctional transducer of ethylene and stress responses in *Arabidopsis*. *Science* 1999; 284:2148–2152.
75. Donovan A, Brownlie A, Zhou Y, Shepard J, Pratt SJ, Monyihan J, Paw BH, Drejer A, Barut B, Zapata A, Law TC, Brugnara C, Lux SE, Pinkas GS, Pinkas JL, Kingsley PD, Palis J, Fleming MD, Andrews NC, Zon LI. Positional cloning of zebrafish ferroportin1 identifies a conserved vertebrate iron exporter. *Nature* 2000; 403:776–781.
76. Abdoud S, Haile DJ. A novel mammalian iron-regulated protein involved in intracellular iron metabolism. *J Biol Chem* 2000; 275:19906–19912.
77. Briat JF, Lobreaux S. Iron storage and ferritin in plants. In: Sigel A, Sigel H, eds. *Metal Ions in Biological Systems*. Vol. 35. New York: Marcel Dekker, 1998:563–587.
78. Proudhon D, Wei J, Briat JF, Theil EC. Ferritin gene organization: differences between plants and animals suggest possible kingdom-specific selective constraints. *J Mol Evol* 1996; 42:325–336.
79. Briat JF, Lobreaux S, Grignon N, Vansuyt G. Regulation of plant ferritin synthesis: how and why. *Cell Mol Life Sci* 1999; 56:155–166.
80. Laulhere JP, Briat JF. Iron release and uptake by plant ferritin: effects of pH, reduction and chelation. *Biochem J* 1993; 290:693–699.
81. Becker R, Manteuffel R, Neumann D, Scholz G. Excessive iron accumulation in the pea mutants *dgl* and *brz*: subcellular localization of iron and ferritin. *Planta* 1998; 207.
82. Savino G, Briat JF, Lobreaux S. Inhibition of the iron-induced ZmFer1 maize ferritin gene expression by antioxidants and serine/threonine phosphatase inhibitors. *J Biol Chem* 1997; 272:33319–33326.
83. Gaymard F, Boucherez J, Briat JF. Characterization of ferritin mRNA from *Arabidopsis thaliana* accumulated in response to iron through an oxidative pathway independent of abscisic acid. *Biochem J* 1996; 318:67–73.
84. Kumar TR, Prasad MNV. Ferritin induction by iron mediated oxidative stress and ABA in *Vigna mungo* (L) Hepper seedlings: role of antioxidants and free radical scavengers. *J Plant Physiol* 1999; 155:652–655.
85. Wang ML, Belmonte S, Kim U, Dolan M, Morris JW, Goodman HM. A cluster of ABA-regulated genes on *Arabidopsis thaliana* BAC T07M07. *Genome Res* 1999; 9: 325–333.
86. Wei J, Theil EC. Identification and characterization of the iron regulatory element in the ferritin gene of a plant (soybean). *J Biol Chem* 2000; 275:17488–17493.
87. Fobis-Loisy I, Aussel L, Briat JF. Post-transcriptional regulation of plant ferritin accumulation in response to iron as observed in the maize mutant *ys1*. *FEBS Lett* 1996; 397:149–154.
88. Van Wuytswinkel O, Vansuyt G, Grignon N, Fourcroy P, Briat J. Iron homeostasis alteration in transgenic tobacco overexpressing ferritin. *Plant J* 1999; 17:93–97.
89. Deak M, Horvath GV, Davletova S, Torok K, Sass L, Vass I, Barna B, Kiraly Z, Dudits D. Plants ectopically expressing the iron-binding protein, ferritin, are tolerant to oxidative damage and pathogens. *Nature Biotechnol* 1999; 17:192–196.
90. Goto F, Yoshihara T, Shigemoto N, Toki S, Takaiwa F. Iron fortification of rice seed by the soybean ferritin gene. *Nature Biotechnol* 1999; 17:282–286.
91. Baynes RD, Bothwell TH. Iron deficiency. *Annu Rev Nutr* 1990; 10:133–148.
92. Beard JL, Burton JW, Theil EC. Purified ferritin and soybean meal can be sources of iron for treating iron deficiency in rats. *J Nutr* 1996; 126:154–160.
93. Hirsh RE, Sussman MR. Improving nutrient capture from soil by the genetic manipulation of crop plants. *Trends Biotechnol* 1999; 17:356–361.
94. Guerinot ML, Yi Y. Iron: nutritious, noxious, and not readily available. *Plant Physiol* 1994; 104:815–820.
95. Bowman J, ed. *Arabidopsis: An Atlas of Morphology and Development*. New York: Springer-Verlag, 1994.

Iron Uptake in Yeast

ORLY ARDON, JERRY KAPLAN, and BROOKE D. MARTIN

University of Utah, Salt Lake City, Utah

I. INTRODUCTION	375
II. CELLULAR IRON UPTAKE IN <i>SACCHAROMYCES CEREVISIAE</i>	376
A. Cell Surface Reductases	376
B. Iron Transport Across the Plasma Membrane	379
C. Intracellular Iron Metabolism	385
III. IRON TRANSPORT IN OTHER YEAST	388
A. <i>Candida albicans</i>	388
B. <i>Ustilago maydis</i>	388
C. <i>Cryptococcus neoformans</i>	389
D. <i>Histoplasma capsulatum</i>	389
ACKNOWLEDGMENTS	389
REFERENCES	389

I. INTRODUCTION

The extraordinary conservation of genetic material among eukaryotes is one of the major findings resulting from genome sequencing efforts. The more essential the biochemical process, the greater is the probability that genes encoding proteins for that process will be conserved between species. Such conservation of genetic material, along with a haploid genome, has made the budding yeast, *Saccharomyces cerevisiae*, an excellent system for the study of genes involved in iron metabolism. Several other features of yeast have contributed to a robust understanding of the metabolism of iron, as well as other transition metals. The yeast genome is small, at 6043 genes, and has been completely sequenced (1). Most yeast genes do not

have introns, which facilitates complementation analysis, as a genomic library is functionally equivalent to a cDNA library. Furthermore, yeast, unlike mammals, favor homologous recombination. It is comparatively easy to inactivate specific genes, permitting a rigorous test of gene function and fulfilling Koch's postulates for genetics. It is technically easy (and relatively inexpensive) to obtain significant yeast biomass through growth on defined media. Many of the mechanisms that govern iron uptake and metabolism, initially identified in mammalian cells, have homologous systems in *S. cerevisiae*. Further, many of the yeast iron transport and transport-protein assembly genes with homology to human genes define disease states in humans when they are functionally inactive. Investigations of yeast iron metabolism have also been used to identify genes or to effectively model homologous uptake systems in mammals (2,3), plants (4), and fungi (5).

Yeast, like most other organisms, have multiple transport systems for iron. Currently, five such systems are described for iron uptake in yeast in which the genes for the transporters have been identified. These transport systems include:

1. A high-affinity iron transport system that consists of the protein products of the *FET3* and *FTR1* genes.
2. A low-affinity iron transport system encoded by the *FET4* gene.
3. Divalent cation/H⁺ symporters comprising the *SMF* gene family, which are homologous to the mammalian iron transporter DMT1/Nramp2.
4. Two different transport mechanisms capable of utilizing xenosiderophores secreted by other organisms. One system uses the high-affinity iron transport system and the second requires the products of the *ARN* family of genes.
5. A transport system comprised of the *FET5* and *FTH1* genes, which can recover iron from the vacuole.

These multiple iron-acquisition systems satisfy the need for iron in different environments and under various growth conditions. A common feature of both yeast and mammals is that there is no excretory route for iron. Iron homeostasis is controlled by tightly regulating uptake and storage. This chapter will review the acquisition of iron by yeast cells, its regulation by the cell's nutritional demands, and its subsequent storage.

II. CELLULAR IRON UPTAKE IN *SACCHAROMYCES CEREVISIAE*

While there are multiple iron transport systems in yeast, most of these systems require reduced, ferrous iron (Fe²⁺) as a substrate. Extracellular iron is rarely present in this oxidation state, as atmospheric conditions are oxidizing with regard to iron (see Chapter 1). Environmental iron exists predominately as insoluble ferric polymers, usually ferric oxides or ferric hydroxides. Alternatively, as a result of biological activity, iron is found as Fe³⁺ surrounded by organic iron chelates, for example, Fe³⁺-citrate complexes. Thus, the first step required for iron transport is the reduction of Fe³⁺ to Fe²⁺.

A. Cell Surface Reductases

Plants can reduce extracellular iron through the secretion of organic molecules that are reductants or through the transport of electrons by membrane reductases. *S. cer-*

evisiae utilizes membrane-bound reductases that transport electrons across the cell surface. The presence of a cell surface ferrireductase was inferred from the observation that cells preferentially accumulate iron when given Fe^{2+} rather than Fe^{3+} , and that intact cells can reduce Fe^{3+} to Fe^{2+} (6). That this activity was an ectoenzyme was surmised from the ability of cells to reduce the impermeable substrate ferricyanide (6). One of the first genes identified in the iron uptake pathway was a ferrireductase. Dancis and co-workers (7) selected a yeast mutant lacking iron reductase activity, as measured by a colorimetric indicator specific for ferrous iron, bathophenanthroline disulfonate (BPS). The mutant strain did not turn pink when given ferric iron, indicating that the defects in iron uptake were due to an inability to reduce ferric iron. The gene responsible for the defect, termed *FRE1*, was identified through complementation of the phenotype using a genomic library. The original mutant (W103) showed a complete absence of ferrireductase activity. Yeast strains in which the *FRE1* gene was deleted showed significant, 30–40% residual ferrireductase activity. The residual activity was shown to result from a second ferrireductase gene termed *FRE2*. This second gene was discovered through its sequence homology to *FRE1* (8). In addition to sequence similarity (24.5% amino acid identity), *FRE2* also exhibits a similar hydropathy plot to *FRE1*, and contains an NADPH-binding motif in its carboxyl terminus. NADPH is required for activity of this enzyme (6). Deletion of both *FRE1* and *FRE2* resulted in a complete loss of reductase activity, while deletion of a single gene resulted in only partial loss of reductase activity. It is thought that the original mutant W103, which had been subjected to chemical mutagenesis, probably had mutations in both *FRE1* and *FRE2*. As these genes are functionally redundant, expression of either one will complement the double-deletion strain.

The protein encoded by *FRE1* is 78.8-kDa in mass and has several predicted membrane-spanning domains (9). The protein has sequence homology to the large gp91^{phox} subunit of a multicomponent NADPH oxidase localized on the plasma membrane (10) of human phagocytic cells. Together with a smaller subunit (p22^{phox}), the multicomponent oxidase proteins form a complex that comprises a flavocytochrome b₅₅₈ that takes electrons from NADPH and transfers them via flavin adenine dinucleotide (FAD) and heme groups across the cell membrane to an electron acceptor, molecular oxygen. The carboxyl terminal of Fre1p bears significant similarity (62%) to gp91^{phox}, with substantial similarity within a potential FAD-binding region and an NADPH-binding domain. Plasma membrane extracts of Fre1p show an absorption spectrum identical to that of the heme-containing purified neutrophil flavocytochrome b₅₅₈ (9).

Spectroscopic analysis of Fre1p revealed an intense Soret band characteristic of a heme moiety present at ~428 nm (9,11). Several histidine residues with defined spacing are highly conserved in b cytochromes and are believed to be the heme-binding moieties. Substitution of alanine for any one of the histidines results in the loss of ferric reductase activity. These mutations do not affect protein expression as shown by Western blot analysis. However, the characteristic heme absorption spectrum is significantly abrogated or absent. Independent confirmation of these results was provided by Lesuisse and colleagues (6), who found that insertion of an epitope tag in the middle of the heme-binding motif destroyed functional activity.

Shatwell and co-workers (9) found that Fre1p behaved like the human gp91^{phox} with regard to reactivity to CO and midpoint potential. They found, however, that

molecular oxygen, the natural substrate for gp91^{phox}, reacted only weakly with Fre1p if at all, and that this reactivity was insensitive to superoxide dismutase. Others found a very slight, SOD-inhibited superoxide production in purified Fre1p-containing extracts (6). A spectral trace generated by subtracting the absorbance spectrum of the oxidized, purified Fre1p complex from its purified, reduced form revealed a small trough at 450 nm consistent with the presence of flavin. Using a substrate reported to accept electrons directly from flavin, iodonitrotetrazolium violet (INT), Shatwell et al. (9) found that INT reductase activity did not require the addition of exogenous flavin, confirming that it is already present in the purified complex. Overexpression of Fre1p led to elevated levels of noncovalently bound FAD associated with the plasma membrane extracts. Calculation of the heme-to-FAD ratio, however, gave a number (18.6:1) about nine times higher than required for the two-electron transfer catalyzed by b-type flavocytochromes. The implication is that FAD had been lost during purification, or that another, unknown co-factor was required for full activity.

As NADPH is required for ferrireductase activity, its oxidation is implied as part of the enzymatic process. Therefore a second essential component of the ferrireductase system is measurable NADPH-dehydrogenase activity. When analyzed by native PAGE gel electrophoresis, the NADPH-dehydrogenase activity migrates differently than epitope-tagged Fre1p. In whole cells, reductase activity can be monitored by use of a membrane-permeable, synthetic substrate, resazurin, which becomes fluorescent upon reduction. The reduction of this substrate is both qualitatively and quantitatively different from the reduction of ferric citrate. Treatment of whole cells with the detergent Zwittergent almost completely inhibits the reduction of ferric citrate by the treated cells, whereas the reduction of the membrane permeable resazurin is reduced by only 50%. Such data provide evidence that the ferrireductase system is a multicomponent enzymatic process, with the *FRE* genes comprising only one component. In purified plasma membrane extracts, ferric iron appears able to access the electron source without first docking with the Fre1p protein. In whole cells, the ferrireductase activity of the *FRE* genes is absolutely required for ferric iron reduction, indicating that Fre1p (and Fre2p) may specify the substrate. The low-to-negligible reactivity with the preferred substrate for the macrophage NADPH oxidase, molecular oxygen, indicates that Fre1p may confer a high selectivity for metals over other substrates.

The NADPH oxidase to which Fre1p bears such similarity is assembled from three cytosolic components in addition to the two membrane subunits described above. The multisubunit nature of the mammalian reductases prompted studies of whether Fre1p also had a protein co-factor. Mutations in a gene of unknown function, *UTR1*, were found to affect ferrireductase activity (6). The *UTR1* gene encodes a 59.4-kDa hydrophilic protein with no predicted transmembrane regions, indicating that it is a cytosolic factor. Co-overexpression of Fre1p and Utr1p gave rise to significantly enhanced cell surface ferrireductase activity over that seen when each protein was expressed by itself. While these data indicate that Utr1p is involved somehow in the ferrireductase activity of Fre1p, its precise function remains elusive.

Examination of the yeast genome revealed five more genes with significant homology to *FRE1* and *FRE2*, which were named *FRE3*–*FRE7* (12), and two genes with lesser homology, *YGL160w* and *YLR047c* (13). Transcription of *FRE1* and *FRE7* is increased under conditions of copper deprivation, while transcripts for *FRE1*–*FRE6* are increased under conditions of iron deprivation. The expression of

YGL160w and *YLR047c* did not change under either condition. Examination of the 5'-upstream promoter region of the *FRE* genes revealed at least one Aft1p-binding site in *FRE1-6*, with *FRE3* containing three such binding sites and *FRE5* containing two. Aft1p is a transcription factor that binds to DNA under conditions of low iron and activates transcription of the gene immediately downstream. Though these genes are termed ferrireductases, they also reduce copper, and reduced copper is the substrate for the cell-surface copper transporters *CTR1* and *CTR3*.

The analogous transcription factor for copper is Mac1p, and two Mac1p-binding sites were found in the promoter region of *FRE1* (12). The promoter region of *FRE7* contains one consensus Mac1p-binding site and two imperfect palindromic sequences that act as Mac1p-binding sites (12). The fact that some *FRE* genes are regulated by both iron and copper underscores what is a consistent theme, that the physiology of these two metals is inextricably linked.

B. Iron Transport Across the Plasma Membrane

1. The High-Affinity Iron Transport System

The *FRE1/FRE2* ferrireductase system is not essential for cell survival, and providing cells with reduced iron can circumvent the need for a ferrireductase. Ferrireductase activity can be separated from iron transport activity by manipulation of experimental conditions. Inhibition of ferrireductase activity by Pt(II) did not prevent uptake of chemically reduced iron into the cell (14). Similarly, stationary phase cells inoculated into fresh culture exhibit ferrireductase activity that is independent of iron concentration in the fresh medium. Iron uptake activity, on the other hand, is dependent on the concentration of iron in the medium (14). Analysis of the concentration dependence (K_m) of iron uptake indicated that iron transport is mediated through (at least) two transport systems: a tightly regulated high-affinity system selective for iron, and a lower-affinity system in which iron transport is competed with by other transition metals (14).

A genetic screen was devised to select for mutant yeast strains with defects in the high-affinity iron transport system. The basis of the screen was the aminoquinone antibiotic streptonigrin, which reacts with intracellular iron to generate toxic hydroxyl radicals. Mutants that are unable to accumulate iron are resistant to its lethal effects but grow poorly on medium containing low levels of iron. The mutants, however, could be rescued by growth on high iron that enters cells through the low-affinity iron transport system. A mutant of *fet3* that showed normal cell surface ferrireductase activity, but was unable to grow on low-iron medium, was selected for further study. The mutant was shown to be unable to accumulate chemically reduced iron in low-iron conditions. This observation again indicated that ferrireductase activity was separable from iron transport (15). Complementation analysis using genomic libraries revealed a gene, designated *FET3*, which restored the ability of mutant cells to grow under low-iron conditions. Further genetic analysis, including gene deletion studies, confirmed that the identified gene was the normal allele of the mutant gene. The expression of the *FET3* transcript was inversely regulated by concentration of iron in the medium (15). Subsequently it was shown that *FET3* is regulated by *AFT1* and that the *FET3* promoter region contains a single Aft1p-binding site (16).

Fet3p shows extensive homology to the multicopper oxidase family, which includes ascorbate oxidase, laccase, and ceruloplasmin (15). These copper-containing

proteins couple the four-electron reduction of molecular oxygen to water with the oxidation of substrates. The enzymes oxidize substrates sequentially, storing each abstracted electron. When the fourth electron is removed from the substrate, the reduction of oxygen occurs in a concerted fashion that precludes the generation of reactive oxygen intermediates. The substrates oxidized by these enzymes are diverse, although the enzymes are conveniently assayed through the oxidation of paraphenyldiamine, yielding a colored substrate. Among these enzymes, ceruloplasmin was formerly considered unique in its ability to utilize iron as a substrate. Oxidation of iron by ceruloplasmin facilitates binding of iron to the mammalian plasma protein transferrin. That Fet3p also had ferroxidase activity was shown by several approaches, most directly by the oxidation of iron *in vitro* by a purified preparation of Fet3p (17). Further studies demonstrated that iron oxidation was stoichiometric with oxygen consumption: four atoms of iron were oxidized concomitant with the reduction of molecular oxygen. In the absence of oxygen, Fet3p is nonfunctional, and under anaerobic conditions, cells are unable to accumulate iron by the high-affinity iron transport system.

All multicopper oxidases contain copper in three different spectroscopic forms. The absorption and EPR spectra of a secreted form of Fet3p, in which the transmembrane domain has been deleted, indicates that it has one type 1 copper, one type 2 copper, and two type 3 coppers, consistent with all multicopper oxidases. The type 2 and type 3 coppers are assembled in a unit referred to as the trinuclear copper center. The sequence of the copper-binding regions is highly conserved between Fet3p and the other members of this protein family (18). Mutation of the type 1 or type 2 copper-binding regions results in a loss of the absorption spectrum characteristic of the metal center, as well as of iron uptake activity, paraphenyldiamine oxidase activity, and ferroxidase activity. This suggests that the multicopper oxidase activity is required for iron transport.

Although the role of Fet3p as a ferroxidase and its requirement for high-affinity iron uptake is established, it contains only a single transmembrane domain in its carboxyl terminus (17). The absence of significant transmembrane regions and any homology to known permeases indicate that this protein is unlikely to be a plasma membrane ion channel. In addition, overexpression of Fet3p from a high-copy plasmid produced only wild-type levels of iron transport. Based on the assumption that a component of the iron transport machinery remained unidentified, Stearman used a genetic screen which took advantage of the iron-dependent transcriptional regulation of many genes involved in iron metabolism (19). The promoter region of *FRE1*, known to contain Aft1p binding sites, was fused to the *HIS3* gene and integrated into the yeast genome. In a $\Delta his3$ mutant background, the *HIS3* gene would be transcribed only when cytosolic iron levels were low. When grown in iron-replete medium, most cells were histidine auxotrophs and would not grow in the absence of histidine. Cells with defects in surface iron transport, however, would induce transcription of *HIS3*, and become histidine prototrophs and survive the selection scheme. Using this approach, Stearman and co-workers identified a mutant that grew poorly in low-iron medium due to an inability to transport iron (19). Mutations in known genes (*CTR1*, *CCC2*, and *FET3*) were ruled out by creating diploids between the newly selected mutants and cells carrying a mutant copy of each of these genes. Complementation analysis identified *FTR1* (*Fe Transporter*) as the normal allele of the mutated gene. This gene encodes a protein containing six predicted transmem-

brane domains and a potential iron-binding site. The sequence REGLE is a known iron-binding motif in the mammalian light chain of ferritin. Site-specific mutagenesis of the REGLE sequence in *FTR1* demonstrated that these amino acids are required for iron transport, although it is yet to be shown that this region specifically binds iron. Like *FET3*, transcription of *FTR1* is increased under low-iron conditions through the action of the transcription factor *AFT1* and the promoter region contains a single Aft1p-binding site (19).

Immunofluorescence of epitope-tagged Ftr1p and Fet3p showed that both proteins localized to the plasma membrane (19). Further studies indicated that there is an interaction between Fet3p and Ftr1p. In the absence of either protein, the other protein did not localize to the cell surface, but rather accumulated and was degraded in an intracellular compartment. The localization to the cell surface does not require an active Fet3p or even an active Ftr1p: apoFet3p or Ftr1p with mutations in the REGLE domains still localize to the cell surface, even though high-affinity iron transport is inactive. These data suggest that Fet3p and Ftr1p must form a complex for translocation to the surface, although a physical interaction between the two proteins still has not been demonstrated.

An interaction between Fet3p and Ftr1p was confirmed, however, using a different genetic approach. *Schizosaccharomyces pombe*, the fission yeast, is quite evolutionarily distant from *S. cerevisiae*. Homologs of both *FET3* and *FTR1* were identified in *S. pombe* by sequence homology (20). Inactivation of the *S. pombe FET3* homolog, termed *fiol*⁺, resulted in the loss of high-affinity iron transport. Expression of *fiol*⁺ in a *FET3* deletion strain of *S. cerevisiae*, however, could not restore high-affinity iron transport, even though that strain had a functional *FTR1*. Iron transport could only be reconstituted when these cells were also transformed with the *S. pombe FTR1* homolog *fp1*⁺. That both the *S. pombe* oxidase and permease must be made at the same time to reconstitute transport provides further evidence that the two act as a pair. The other conclusion from this experiment is that the only plasma membrane proteins required for high-affinity iron transport are the oxidase and the permease.

The conclusion that Fet3p and Ftr1p are the only plasma membrane proteins required for high-affinity iron transport has not been challenged. What has been revealed by genetic studies is that a number of other genes are required for the proper assembly of these proteins. Most of the genes identified are required for the insertion of copper into the multicopper oxidase Fet3p. The copper requirement of this protein has led to the identification of mutants with iron uptake phenotypes that result from defects in copper metabolism. Indeed, one of the first genes detected by the Klausner group using the *FRE1-HIS* construct described above was actually the high-affinity copper transporter *CTR1* (21). This gene is not regulated by the iron-dependent transcription factor Aft1p, but is regulated by copper requirement through the copper-inhibitable transcription factor Mac1p (22). Defects in copper transport or intracellular copper metabolism result in a decreased ability to obtain iron through the high-affinity transport system and result in the appearance of an apoFet3p on the cell surface. The requirement for Fet3p to be copper-loaded for activity has led to the dissection of an intracellular pathway for copper metabolism. Copper loading of Fet3p requires the products of high-affinity cell-surface copper transporters, *CTR1* or *CTR3*. Three different copper chaperones bind copper once it enters the cell (23). These small proteins target copper to specific cellular locations: Lys7p targets copper

to cytosolic superoxide dismutase; Cox17p targets copper to the mitochondria (24); and Atx1p targets copper to an intracellular vesicle in which Fet3p becomes copper-loaded (25).

The copper chaperone Atx1p was discovered through a genetic screen as a suppressor of defects in superoxide dismutase (25). Deletion of *SOD1*, which encodes superoxide dismutase, results in an increased sensitivity to H_2O_2 . Overexpression of Atx1p, another copper-binding molecule, reduces that sensitivity. A deletion in *ATX1* results in reduced iron uptake through decreased Fet3p activity. Further study revealed that Atx1p was required to deliver copper to a post-Golgi compartment where Fet3p was copper-loaded. Cytosolic Atx1p delivers copper to a vesicular copper transporter, Ccc2p, a P-type ATPase that transports copper across the vesicle membrane. That the major function of Ccc2p is to copper-load Fet3p is suggested by the fact that transcription of *CCC2* is regulated by Aft1p (26).

The copper loading of Fet3p by Ccc2p occurs in an intracellular vesicle. The specific location of the vesicle is not known, but it is in the secretory pathway, most probably between the trans-Golgi network and the prevacuole. Many mutants in vesicular transport, termed *vps* mutants, show a phenotype of defective vacuole formation, inability to grow on low iron, and respiratory deficit. Defective vacuole formation can result from mutations in genes required to form the vacuole or to effectively target vacuolar proteins from the Golgi to the vacuole. A characteristic of *vps* mutants is that vacuolar proteins are appropriately glycosylated, as the processing defect is subsequent to passage through the Golgi (27). Many *vps* mutants result in the appearance of an appropriately glycosylated but inactive apoFet3p (28). Complementation cloning of the low-iron phenotype has resulted in the identification of two more genes whose effects provide insight into the mechanism of Fet3p assembly (29). One gene, *GEF2*, is a subunit of the H^+ -ATPase that acidifies both vacuoles and endosomes. The second gene, *GEF1*, encodes a voltage-regulated chloride channel (30). The requirement for an H^+ -ATPase for the copper loading of apoFet3p indicates that copper assembly requires an acidic pH (31). The requirement for the chloride channel is less obvious. There appear to be two reasons why a chloride channel is required. The first reason is that transport of cations, either H^+ or $Cu^{(n+)}$ into a bounded compartment, such as a vesicle, is limited by the generation of an unfavorable electrochemical potential: the transport of cations precludes the further transport of cations (31). Under normal conditions the electrochemical potential is dissipated because a voltage-regulated chloride channel is opened and the voltage-driven movement of chloride into the vesicle dissipates the potential gradient. The presence of chloride results in a lower pH and a higher $Cu^{(n+)}$ concentration. The second reason that a chloride channel is required may be that chloride is directly required for the insertion of copper atoms into apoFet3p (32). In the absence of chloride, even in the presence of high copper concentrations, the type 1 copper site can not be filled (Kaplan, unpublished results).

2. FET4, a Low-Affinity Iron Transport System

Deletion of the *FET3* gene does not result in a growth defect in yeast growing in an iron-rich medium, indicating the presence of alternative iron transport systems (15). A gene for a low-affinity iron transport system was identified through a screen designed to identify genes capable of restoring normal growth in a $\Delta fet3$ strain. A gene named *FET4*, when overexpressed, permitted the $\Delta fet3$ strain to grow in low-

iron medium (33). This gene encodes a 63-kDa integral membrane protein containing six transmembrane domains and, unlike Fet3p, is a candidate for a classic plasma membrane permease. Fet4p does not exhibit substantial homology to any other characterized cell-surface permease (34). Deletion of both *FET4* and *FET3* genes abolishes measurable iron accumulation and results in iron-limited growth. The ability to selectively delete *FET3* or *FET4* permitted a detailed investigation of the characteristics of the low-affinity iron transport system. The ensuing studies revealed that the K_m of Fet4p-mediated iron transport was 30 μM , substantially different from the *FET3/FTR1* transport system, which has a K_m of 0.15 μM . Whereas the *FET3/FTR1* transport system is absolutely selective for iron, Fet4p can transport other transition metals, including Cu^{2+} , Mn^{2+} , and Cd^{2+} (33,34). These metals will compete with each other for uptake, suggesting a common transport mechanism. Transcription of *FET4* is regulated by iron need, but is not regulated by Aft1p (34). *FET4* is not regulated, however, by other transition metals. Under conditions of low iron, particularly in the absence of *FET3*, *FET4* mRNA is increased, resulting in increased transport activity. In the presence of high concentrations of potentially toxic transition metals, such as Co^{2+} , Cu^{2+} , or Mn^{2+} , high levels of Fet4p will lead to cell death due to toxic metal accumulation (35).

A major function of the Fet4p iron transport system is to provide iron to cells under anaerobic conditions. In an anaerobic environment, a Δfet3 strain can grow on iron-containing medium, whereas a Δfet4 strain cannot grow. This observation indicates that Fet4p is the most important iron transport system under anaerobic conditions. Transcription of *FET3* and other Aft1p-regulated genes are decreased in anaerobic conditions (36), providing a rationale for the lack of Aft1p regulation of *FET4*.

3. The SMF Family of Transporters

The *SMF* family comprises three homologous genes, *SMF1*, *SMF2*, and *SMF3*. The proteins encoded by these genes share 45% identity and may have as many as 10 transmembrane domains. *SMF1* and *SMF2* were first identified as high-copy suppressors of a temperature-sensitive mutation in the manganese-dependent mitochondrial matrix protease (37). At the restrictive temperature the mutant protease cannot process mitochondrial protein precursors. Overexpression of *SMF1* or *SMF2* permitted the mutant protein to cleave mitochondrial precursors. The same two genes were identified as suppressors of a mutation in *CDC1*, a gene required for progression through the cell cycle (37). Analysis of a *cdc* mutation revealed that the mutant protein was defective in its ability to bind Mn^{2+} , as the mutant was isolated from medium low in Mn^{2+} . *SMF1/SMF2* were found to be cell-surface Mn^{2+} transporters, and their overexpression led to increased levels of cytosolic Mn^{2+} . Increased cellular Mn^{2+} could also explain how *SMF1* and *SMF2* complemented the phenotype of the mutant mitochondrial processing protease, because that enzyme is Mn^{2+} -dependent.

Although the *SMF* genes were identified initially as Mn^{2+} transporters, a role for iron was surmised based on their homology to the mammalian iron transporter DMT1/Nramp2. In vertebrates, uptake of iron into the absorptive intestinal epithelium and across the endosomal membrane within cells is mediated by a divalent cation transporter, initially referred to as Nramp2, or DCT1, but now termed DMT1 [(2,3); see also Chapter 6]. DMT1 encodes a ubiquitously expressed 561-amino acid protein with 12 putative membrane-spanning domains. It was found to have an un-

usually broad range of substrate specificity, accepting most divalent cations, in a pH-dependent manner (3). Mechanistically, the protein is considered to be a divalent cation/H⁺ symporter.

Deletion of both *SMF1* and *SMF2* results in hypersensitivity to EGTA under oxidative stress (methyl viologen) conditions and an inability to grow at alkaline pH (pH 7.9) (38). These phenotypes could be complemented by transformation of the deletion strains with a high-copy plasmid containing *DMT1*. The complementation of the high pH sensitivity required the presence of a divalent cation, and iron was capable of satisfying that requirement. Iron transport by *SMF1* and *SMF2* was demonstrated using an oocyte expression system (39). *SMF3*, however, was unable to mediate iron transport. The role played by the *SMF* genes in yeast iron transport is unclear. It is predicted that they may be responsible for some component of iron uptake as a $\Delta fet3/\Delta fet4$ strain can still grow on YPD, a rich medium containing moderate amounts of iron. Additional deletions in *SMF1* and *SMF2* compromise the ability to grow on this medium unless additional iron is added (Kaplan, unpublished results).

SMF1 and *SMF2* are not transcriptionally regulated by iron. They are post-translationally regulated by the product of the *BSD2* gene (40). In the presence of cobalt, manganese, or copper, Smf1p and Smf2p are degraded in the lysosome instead of being targeted to the plasma membrane. Under metal-deficient conditions the proteins are transported to the cell surface. In the absence of Bsd2p the proteins are targeted to the cell surface regardless of cellular metal levels. Whether iron can also affect organelle targeting has not been established.

4. Siderophore-Mediated Iron Uptake

S. cerevisiae does not secrete or synthesize its own iron-sequestering siderophores. It can, however, take up iron–siderophore complexes. A variety of siderophores can satisfy the cellular need for iron. The ability of yeast to utilize siderophore-chelated iron was shown most dramatically using a $\Delta fet3/\Delta fet4$ deletion mutant (41). This mutant cannot grow on minimal medium, but can grow when the medium is supplemented with the iron-containing siderophores. The hydroxamate-type siderophores (coprogen and ferricrocin), or catecholate-type siderophores [enterobactin and ferrioxamine B (FOB)] permit growth of cells on minimal medium. Both FOB and ferricrocin display saturable, glucose-dependent, energy-dependent, high-affinity uptake. Lessuisse et al. (41) took advantage of the siderophore-dependent growth of the $\Delta fet3/\Delta fet4$ strain to identify a mutant that was unable to utilize siderophore-chelated iron for growth. The mutant gene was identified by complementation of the phenotype using a genomic library. Gene deletion studies confirmed that the identified gene, *SITI1*, was responsible for FOB siderophore-mediated iron uptake.

Lesuisse et al. (41) reported that *SITI1* was iron-regulated but stated that regulation was not *AFT1*-mediated. Subsequently, however, another group identified *SITI1* as a target of *AFT1* by microarray analysis (42). There are five other genes in *S. cerevisiae* that are homologous to *SITI1*, and three of them are also iron-regulated. These four iron-regulated genes are termed *ARN* genes, (*AFT1 regulon*), where *ARN3* is *SITI1*. The *ARN* genes are highly homologous, and are members of the “Major Facilitator Superfamily.” Further studies indicated that other siderophores could be taken up by the *ARN* genes and that each transporter has a different affinity for different siderophores (43). For example, uptake of ferrichrome and ferrichrome A

is mediated by Arn1p and Arn3p, while uptake of triacetylfusarinine C is effected primarily by Arn2p, and to lesser extent by Arn1p and Arn3p.

Uptake of siderophore–iron was shown to occur by two different mechanisms (42). One mechanism requires the *FET3/FTR1* transport system. Reduction of siderophore–iron complexes by the ferrireductases results in release of iron and uptake by Fet3p/Ftr1p. A second transport system is seen only in the absence of Fet3p and requires members of the *ARN* family. A curious feature is that Arn3p is not localized on the cell surface but rather is present in an intracellular vesicle. How iron or iron–siderophore complexes gain access to the transporter, and how and where iron is extracted from the siderophore, are unresolved questions.

5. Recovery of Iron from the Vacuole

Examination of the yeast genome revealed a homolog of *FET3* termed *FET5*. The homology between the two proteins is extensive, and *FET5* shows all of the sequence features expected of a multicopper oxidase. High-copy expression of *FET5* can suppress the $\Delta fet3$ phenotype of low growth on iron-deficient medium (44). The Fet5p protein is not located at the plasma membrane but is found in an intracellular compartment. The fact that it is not localized on the cell surface and that a deletion strain showed no iron-deficiency phenotype suggested that it was not primarily involved in iron transport from the cell surface. More recent studies suggest that Fet5p may play a role in vacuolar iron metabolism. The protein was localized to the vacuole where it was found complexed to an *FTR1* homolog Fth1p (45). In the absence of Fet5p, Fth1p is not found in the vacuole, but rather is retained in the endoplasmic reticulum. Further studies showed a physical complex between Fth1p and Fet5p, as they could be co-immunoprecipitated. These results suggest that Fet5p and Fth1p form an oxidase/permease pair, analogous to Fet3p/Ftr1p. Studies indicate that this pair may mediate the transport of iron from the vacuole to the cytosol. Cells with a *fet5* deletion show an increased rate of transcription of *FET3* and a decreased ability to undergo respiratory activity when removed from glucose. Increased *FET3* transcription and a decreased ability to grow on respiratory substrates are thought to reflect a diminished pool of intracellular iron. These results suggest that Fet5p/Fth1p complex can mobilize iron from the vacuole to the cytosol.

These studies do not, however, address the means by which iron accumulates in the vacuole. One potential route is through endocytosis. Yeast show constitutive endocytic activity that results in the “capture” of extracellular fluid. Iron or any other substance that is membrane-impermeable will accumulate in the vacuole, the “terminal” organelle in the endocytic pathway. This iron is then available for recovery through the action of Fet5p/Fth1p.

C. Intracellular Iron Metabolism

Despite the advances in the characterization of the *S. cerevisiae* iron-uptake systems, much less is known about intracellular iron metabolism.

1. Mitochondrial Iron Transport

Iron must also be transported into the mitochondrion, as it is required for the synthesis of heme proteins and of iron–sulfur-cluster-containing proteins (Fe/S proteins), both of which occur within mitochondria. As important as mitochondrial iron is to

the cell, almost nothing is known about mitochondrial iron uptake systems. A technical problem hindering in-vitro studies of mitochondrial iron uptake is the high backgrounds that result when mitochondria are incubated with radiolabeled iron. The only published study on yeast mitochondrial iron transport employing an in-vitro analysis used the incorporation of iron into heme as an assay for mitochondrial iron transport (46). In the absence of an intact mitochondrial membrane, ferrochelatase, which is located in the mitochondrial matrix, will insert metals other than iron into the protoporphyrin ring. The presence of the mitochondrial membrane provides selectivity such that iron, as opposed to cobalt, zinc, or other metals, will be inserted into heme. Using heme synthesis and metal selectivity as an assay, it was found that Fe^{2+} is the preferred substrate for transport into mitochondria. Iron transport does not require ATP but does require a mitochondrial membrane potential. It was also discovered that heme synthesis requires exogenous iron for synthesis, as iron stored within mitochondria was not to be used for heme synthesis.

While the characteristics of mitochondrial iron transport are not known, recent studies indicate that there is a mitochondrial iron cycle. Mitochondria not only import but can also export iron. The discovery of a mitochondrial iron cycle was a novel finding and resulted from the analysis of the function of the gene *YFH1*, a homolog of a mammalian gene *Frataxin* [(47); see also Chapter 11]. Mutations in the *Frataxin* gene are responsible for the human disease Friedreich's ataxia. Yfh1p encodes a mitochondrial protein of 125 amino acids, which is localized to the mitochondrial matrix. Strains with a deletion in *yfh1* are unable to grow on respiratory substrates, such as glycerol-ethanol, and show poor growth on glucose media. Associated with these characteristics is increased expression of the high-affinity iron transport system. As *FET3* and *FTR1* are regulated by iron demand, increased expression suggests that the $\Delta yfh1$ deletion strain had low cytosolic iron despite functional cell surface transport systems. The phenotypes of respiratory incompetence and decreased cytosolic iron are the result of abnormal mitochondrial iron accumulation. In the absence of Yfh1p, iron accumulates in mitochondria at the expense of cytosolic iron. The accumulated iron reacts with H_2O_2 , which is a by-product of respiration, generating toxic oxygen radicals. These radicals may damage mitochondrial proteins, lipids, and DNA. Damaged mitochondrial DNA results in the generation of respiratory incompetent yeast termed petites. Petites can survive because *S. cerevisiae* can satisfy its needs for ATP through glycolysis. Indeed, respiratory-incompetent $\Delta yfh1$ yeast should have a selective growth advantage, as they no longer produce toxic oxygen radicals at the inner mitochondrial membrane.

Evidence that Yfh1p effects mitochondrial iron loss was shown by experiments in which a regulatable promoter controlled expression of *YFH1* (48). In the absence of Yfh1p expression, ^{59}Fe accumulated in mitochondria. When Yfh1p was turned on, there was an accelerated loss of mitochondrial iron. This result suggests that the accumulated mitochondrial iron found in $\Delta yfh1$ strains is bioavailable. The sequence of Yfh1p does not have any transmembrane domains, making it unlikely that it is a membrane transporter. Yfh1p either regulates iron transport or it maintains iron in a form that is recognized by the transporter. The transcription of *YFH1* is not iron-regulated, but it is not known whether protein concentration is iron-regulated.

Yfh1p is a mitochondrial protein and requires processing for localization in mitochondria. A yeast strain carrying a mutation in *SSQ1*, a homolog of HSP70 (a mitochondrial heat-shock protein), was found to be defective in Yfh1p activity and

also accumulated iron in the mitochondrion (49). Ssq1p is a chaperone and is required for the mitochondrial import of Yfh1p.

Deletions in nuclear genes that affect mitochondrial iron/iron–sulfur cluster metabolism also lead to mitochondrial iron accumulation. Many mitochondrial proteins, as well as a few cytosolic proteins, have as a catalytic site an iron–sulfur cluster. While there is some debate on the site of synthesis of mammalian iron–sulfur clusters, the preponderance of data suggests that in *S. cerevisiae*, iron–sulfur clusters are made in the mitochondria and are either used there or are exported to the cytosol (50). Genes involved in iron–sulfur cluster formation have been identified on the basis of homology to bacterial genes required for the individual steps in iron–sulfur cluster formation. Inactivation of these genes in yeast, either singly or in combination, results in respiratory incompetence and defects in leucine biosynthesis (51). One of the major cytosolic iron–sulfur enzymes is Leu1p, and deficits in iron–sulfur formation result in leucine auxotrophy. It is unclear why defects in individual enzymes involved in iron–sulfur clusters result in excessive deposition of iron in mitochondria. One suggestion is that a lack of iron–sulfur cluster synthesis affects regulation of iron transport, but the details of such regulatory circuits are unknown.

In at least one instance, however, there is an explanation as to how a defective gene affecting iron–sulfur cluster formation might result in abnormal iron accumulation. Deletion of *ATM1*, encoding a P-type ATPase, results in respiratory incompetence, excessive iron accumulation, and leucine auxotrophy (52). *ATM1* encodes a mitochondrial ABC transporter that appears to be responsible for the export of iron–sulfur clusters. In the absence of Atm1p, Leu1p is synthesized but does not have an iron–sulfur cluster and is enzymatically inactive. This observation suggests a role for Atm1p in the export of iron–sulfur clusters, although its relationship to Yfh1p is unclear. In $\Delta yfh1$ cells there are decrements in the activity of iron–sulfur-cluster-containing mitochondrial enzymes. The loss of activity is only partial, and cells are not leucine auxotrophs. This latter observation indicates that Yfh1p may not play a role in iron–sulfur formation or export.

2. Iron Storage in *S. cerevisiae*

Iron-storage molecules such as the mammalian ferritin, plant phytoferritin, or bacterial bacterioferritin are not found in *S. cerevisiae*, although this yeast possess DNA sequences that were predicted to encode sequences with homology to mammalian ferritin (53). To date, there is no evidence that these proteins act as iron storage molecules. It has been suggested that iron, as perhaps other transition metals, are stored within vacuoles. Yeast grown in media containing millimolar concentrations of iron localized iron to the vacuole (54). Since such superphysiological iron concentrations can fully repress both high- and low-affinity iron transport (26,35), vacuolar iron may be derived only from fluid-phase endocytosis, as the vacuole is the ultimate destination of such endocytosed material. Yeast mutants defective in vacuolar formation or function (55) have increased sensitivity to transition metals, suggesting that metals are stored in vacuoles. An alternative explanation for metal sensitivity in yeast vacuolar mutants, however, has been suggested. Yeast vacuolar mutants are incapable of assembling the high-affinity transport system (28,56) and compensate by overexpressing less selective divalent metal cation transporters such as Fet4p (35). Overexpression of Fet4p results in increased cellular accumulation of transition metals, resulting in increased toxicity. The same explanation, that vacuolar

mutants do not make a functional, high-affinity iron transport system, could also explain why such mutants may be respiratory incompetent, as they are iron-deficient.

Yet another alternative hypothesis is that yeast do not sequester excess iron in the vacuole, but rather retain iron in the cytoplasm. This hypothesis is consistent with experiments with cells lacking *YFHI*. These cells hyperaccumulate iron in their mitochondria. Reintroduction of Yfh1p results in export of the mitochondrial iron, but this iron remains in the cytosol and is not sequestered in the vacuole (48).

III. IRON TRANSPORT IN OTHER YEAST

Of all yeast, iron transport systems are best characterized for *S. cerevisiae* and to a lesser extent *S. pombe*. This is in large part because of the facile genetics of these particular fungi, which spend much of their life cycle in the haploid state. Most fungi of economic or pathogenic importance are diploid. Diploid organisms are much more difficult to work with genetically. What little work has been done on other fungi suggests that they may utilize similar iron transport systems as *S. cerevisiae*. Some characteristics of iron transport in fungi other than *S. cerevisiae* are discussed below.

A. *Candida albicans*

The dimorphic pathogenic yeast *Candida albicans* can secrete siderophores when grown in medium that is low in iron (57), though little is known about its secretion or uptake of siderophores. This fungus, however, is genetically related to *S. cerevisiae*, and recent studies have demonstrated homology between components of the elemental iron uptake systems in this yeast and *S. cerevisiae* (5,58,59).

As with most iron transport systems that require Fe^{2+} as a substrate, *C. albicans* has a ferrireductase that appears homologous to the *S. cerevisiae* *FRE* genes (58). Further, *C. albicans* also has an oxidase/permease-based high-affinity iron transport system (5). A *Candida* homolog of *S. cerevisiae* *FET3* (CaFET3) was identified and sequenced and was found to have 55% identity to Fet3p at the amino acid level.

The accumulation of iron in *C. albicans* cells is considered to be a virulence factor permitting it to infect mammalian hosts. Studies were conducted to test whether the *Cafet3* mutant had reduced pathogenicity due to its decreased ability to acquire the iron from the host organism (5). The pathogenicity of the *Cafet3* mutant was similar to the wild type in the mouse model of systemic candidiasis. This result suggests that additional iron uptake mechanisms must exist that mediate iron accumulation in the absence of the ferroxidase-based transport system.

B. *Ustilago maydis*

Ustilago maydis is a pathogen of maize (*Zea mays*). The fungus produces the siderophores ferrichrome and ferrichrome A under iron-limiting conditions (60). Using fluorescent biomimetic siderophore analogs of ferrichrome, and FOB (a xenosiderophore), studies revealed two different active mechanisms for iron uptake from these siderophores. The fungal cells take up ferrichrome-iron complexes, iron is removed from the siderophore, and the desferri-siderophore is secreted back into the medium (61). Examination by fluorescent microscopy showed that ferrichrome analogs accumulate in intracellular vesicles. Iron removal from the fluorescent siderophores lags behind ^{55}Fe uptake, suggesting a storage role for ferrichrome. Accumulation of

iron from xenosiderophores, such as FOB, involves an extracellular reduction mechanism, in which iron is delivered into the cell without the entry of the siderophore (62).

C. *Cryptococcus neoformans*

The pathogenic yeast *Cryptococcus neoformans* does not secrete siderophores, and many of the components of iron reduction and uptake in *C. neoformans* are similar to those of *S. cerevisiae*. *C. neoformans* and *S. cerevisiae* are evolutionary distinct members of the Basidiomycetes and Ascomycetes families, respectively (63–65). Under conditions of iron stress, *C. neoformans* also expresses a plasma membrane ferric reductase that supplies substrate to both low- and high-affinity Fe^{2+} transmembrane transporters (63). This ferric reductase can reduce both Fe^{3+} and Cu^{2+} and is regulated by four different genes (66).

C. neoformans can accumulate siderophore-bound iron using siderophores produced by other organisms, for example, FOB. Little is known, however, about the mechanisms of siderophore uptake.

D. *Histoplasma capsulatum*

Histoplasma capsulatum is known to secrete siderophores under iron-limiting conditions. As might be expected, siderophore synthesis is regulated by iron need and is produced in greatest amount under conditions of iron deprivation (67). Recently, five different hydroxamate siderophores of the dimerum acid, fusarinine, and coprogen B, families were identified in cultures of *H. capsulatum* (68). In addition, the fungus is thought to have a high-affinity ferric reductase system as well as an ability to utilize the host's holotransferrin for its iron requirements.

We fully suspect that as genomes for other fungi are sequenced, genes for iron transport systems will be identified on the basis of their sequence. We also expect that genes from other fungi can be studied and characterized when expressed in *S. cerevisiae*, as have been genes from *S. pombe* or *C. albicans*. This approach will result in a more robust understanding of cellular iron transport in yeast and other fungi.

ACKNOWLEDGMENTS

Orly Ardon is supported by postdoctoral award FI274-98 from BARD, the United States Israel Binational Agricultural Research and Development Fund. Work in the authors' lab was done during the tenure of a research fellowship from the American Heart Association, Western States Affiliate Research Fellowship, awarded to Brooke Martin. Jerry Kaplan acknowledges Grant NIDDK-30534 and Grant NIDDK-52380 from the National Institutes of Health.

REFERENCES

1. Goffeau A, Barrell BG, Bussey H, Davis RW, Dujon B, Feldmann H, Galibert F, Hoheisel JD, Jacq C, Johnston M, Louis EJ, Mewes HW, Murakami Y, Philippsen P, Tettelin H, Oliver SG. Life with 6000 genes. *Science* 1996; 274:563–567.

2. Fleming MD, Trenor CC 3rd, Su MA, Foernzler D, Beier DR, Dietrich WF, Andrews NC. Microcytic anaemia mice have a mutation in Nramp2, a candidate iron transporter gene. *Nature Genet* 1997; 16:383–386.
3. Gunshin H, Mackenzie B, Berger UV, Gunshin Y, Romero MF, Boron WF, Nussberger S, Gollan JL, Hediger MA. Cloning and characterization of a mammalian proton-coupled metal-ion transporter. *Nature* 1997; 388:482–488.
4. Eide D, Broderius M, Fett J, Guerinet ML. A novel iron-regulated metal transporter from plants identified by functional expression in yeast. *Proc Natl Acad Sci USA* 1996; 93:5624–5628.
5. Eck R, Hundt S, Hartl A, Roemer E, Kunkel W. A multicopper oxidase gene from *Candida albicans*: cloning, characterization and disruption. *Microbiology* 1999; 145: 2415–2422.
6. Lesuisse E, Casteras-Simon M, Labbe P. Evidence for the *Saccharomyces cerevisiae* ferrireductase system being a multicomponent electron transport chain. *J Biol Chem* 1996; 271:13578–13583.
7. Dancis A, Klausner RD, Hinnebusch AG, Barriocanal JG. Genetic evidence that ferric reductase is required for iron uptake in *Saccharomyces cerevisiae*. *Mol Cell Biol* 1990; 10:2294–2301.
8. Georgatsou E, Mavrogiannis LA, Fragiadakis GS, Alexandraki D. The yeast Fre1p/Fre2p cupric reductases facilitate copper uptake and are regulated by the copper-modulated Mac1p activator. *J Biol Chem* 1997; 272:13786–13792.
9. Shatwell KP, Dancis A, Cross AR, Klausner RD, Segal AW. The FRE1 ferric reductase of *Saccharomyces cerevisiae* is a cytochrome b similar to that of NADPH oxidase. *J Biol Chem* 1996; 271:14240–14244.
10. Thrasher AJ, Keep NH, Wientjes F, Segal AW. Chronic granulomatous disease. *Biochim Biophys Acta* 1994; 1227:1–24.
11. Finegold AA, Shatwell KP, Segal AW, Klausner RD, Dancis A. Intramembrane bis-heme motif for transmembrane electron transport conserved in a yeast iron reductase and the human NADPH oxidase. *J Biol Chem* 1996; 271:31021–31024.
12. Martins LJ, Jensen LT, Simons JR, Keller GL, Winge DR. Metalloregulation of FRE1 and FRE2 homologs in *Saccharomyces cerevisiae*. *J Biol Chem* 1998; 273:23716–23721.
13. Georgatsou E, Alexandraki D. Regulated expression of the *Saccharomyces cerevisiae* Fre1p/Fre2p Fe/Cu reductase related genes. *Yeast* 1999; 15:573–584.
14. Eide D, Davis-Kaplan S, Jordan I, Sipe D, Kaplan J. Regulation of iron uptake in *Saccharomyces cerevisiae*. The ferrireductase and Fe(II) transporter are regulated independently. *J Biol Chem* 1992; 267:20774–20781.
15. Askwith C, Eide D, Van Ho A, Bernard PS, Li L, Davis-Kaplan S, Sipe DM, Kaplan J. The *FET3* gene of *S. cerevisiae* encodes a multicopper oxidase required for ferrous iron uptake. *Cell* 1994; 76:403–410.
16. Yamaguchi-Iwai Y, Dancis A, Klausner RD. AFT1: a mediator of iron regulated transcriptional control in *Saccharomyces cerevisiae*. *EMBO J* 1995; 14:1231–1239.
17. De Silva DM, Askwith CC, Eide D, Kaplan J. The FET3 gene product required for high affinity iron transport in yeast is a cell surface ferroxidase. *J Biol Chem* 1995; 270: 1098–1101.
18. Hassett RF, Yuan DS, Kosman DJ. Spectral and kinetic properties of the Fet3 protein from *Saccharomyces cerevisiae*, a multinuclear copper ferroxidase enzyme. *J Biol Chem* 1998; 273:23274–23282.
19. Stearman R, Yuan DS, Yamaguchi-Iwai Y, Klausner RD, Dancis A. A permease-oxidase complex involved in high-affinity iron uptake in yeast. *Science* 1996; 271:1552–1557.
20. Askwith C, Kaplan J. An oxidase-permease-based iron transport system in *Schizosaccharomyces pombe* and its expression in *Saccharomyces cerevisiae*. *J Biol Chem* 1997; 272:401–405.

21. Dancis A, Haile D, Yuan DS, Klausner RD. The *Saccharomyces cerevisiae* copper transport protein (Ctr1p). Biochemical characterization, regulation by copper, and physiologic role in copper uptake. *J Biol Chem* 1994; 269:25660–25667.
22. Labbe S, Zhu Z, Thiele DJ. Copper-specific transcriptional repression of yeast genes encoding critical components in the copper transport pathway. *J Biol Chem* 1997; 272:15951–15958.
23. Culotta VC, Lin SJ, Schmidt P, Klomp LW, Casareno RL, Gitlin J. Intracellular pathways of copper trafficking in yeast and humans. *Adv Exp Med Biol* 1999; 448:247–254.
24. Srinivasan C, Posewitz MC, George GN, Winge DR. Characterization of the copper chaperone Cox17 of *Saccharomyces cerevisiae*. *Biochemistry* 1998; 37:7572–7577.
25. Lin SJ, Culotta VC. The *ATX1* gene of *Saccharomyces cerevisiae* encodes a small metal homeostasis factor that protects cells against reactive oxygen toxicity. *Proc Natl Acad Sci USA* 1995; 92:3748–3788.
26. Yamaguchi-Iwai Y, Stearman R, Dancis A, Klausner RD. Iron-regulated DNA binding by the AFT1 protein controls the iron regulon in yeast. *EMBO J* 1996; 15:3377–3384.
27. Stack JH, Horazdovsky B, Emr SD. Receptor-mediated protein sorting to the vacuole in yeast: roles for a protein kinase, a lipid kinase and GTP-binding proteins. *Annu Rev Cell Dev Biol* 1995; 11:1–33.
28. Radisky DC, Snyder WB, Emr SD, Kaplan J. Characterization of *VPS41*, a gene required for vacuolar trafficking and high-affinity iron transport in yeast. *Proc Natl Acad Sci USA* 1997; 94:5662–5666.
29. Eide DJ, Bridgham JT, Zhao Z, Mattoon JR. The vacuolar H⁽⁺⁾-ATPase of *Saccharomyces cerevisiae* is required for efficient copper detoxification, mitochondrial function, and iron metabolism. *Mol Gen Genet* 1993; 241:447–456.
30. Greene JR, Brown NH, DiDomenico BJ, Kaplan J, Eide DJ. The *GEF1* gene of *Saccharomyces cerevisiae* encodes an integral membrane protein; mutations in which have effects on respiration and iron-limited growth. *Mol Gen Genet* 1993; 241:542–553.
31. Gaxiola RA, Yuan DS, Klausner RD, Fink GR. The yeast CLC chloride channel functions in cation homeostasis. *Proc Natl Acad Sci USA* 1998; 95:4046–4050.
32. Davis-Kaplan SR, Askwith CC, Bengtzen AC, Radisky D, Kaplan J. Chloride is an allosteric effector of copper assembly for the yeast multicopper oxidase fet3p: An unexpected role for intracellular chloride channels. *Proc Natl Acad Sci USA* 1998; 95:13641–13645.
33. Dix DR, Bridgham JT, Broderius MA, Byersdorfer CA, Eide DJ. The *FET4* gene encodes the low affinity Fe(II) transport protein of *Saccharomyces cerevisiae*. *J Biol Chem* 1994; 269:26092–26099.
34. Dix D, Bridgham J, Broderis M, Eide D. Characterization of the FET4 protein of yeast. Evidence for a direct role in the transport of iron. *J Biol Chem* 1997; 272:11770–11777.
35. Li L, Kaplan J. Defects in the yeast high affinity iron transport system result in increased metal sensitivity because of the increased expression of transporters with a broad transition metal specificity. *J Biol Chem* 1998; 273:22181–22187.
36. Hassett RF, Romeo AM, Kosman DJ. Regulation of high affinity iron uptake in the yeast *Saccharomyces cerevisiae*. Role of dioxygen and Fe. *J Biol Chem* 1998; 273:7628–7636.
37. Supek F, Supekova L, Nelson H, Nelson N. Function of metal-ion homeostasis in the cell division cycle, mitochondrial protein processing, sensitivity to mycobacterial infection and brain function. *J Exp Biol* 1997; 200:321–330.
38. Pinner E, Gruenheid S, Raymond M, Gros P. Functional complementation of the yeast divalent cation transporter family SMF by NRAMP2, a member of the mammalian natural resistance-associated macrophage protein family. *J Biol Chem* 1997; 272:28933–28938.

39. Chen XZ, Peng JB, Cohen A, Nelson H, Nelson N, Hediger MA. Yeast SMF1 mediates H⁽⁺⁾-coupled iron uptake with concomitant uncoupled cation currents. *J Biol Chem* 1999; 274:35089–35094.
40. Liu XF, Supek F, Nelson N, Culotta VC. Negative control of heavy metal uptake by the *Saccharomyces cerevisiae* *BSD2* gene. *J Biol Chem* 1997; 272:11763–11769.
41. Lesuisse E, Simon-Casteras M, Labbe P. Siderophore-mediated iron uptake in *Saccharomyces cerevisiae*: the *SIT1* gene encodes a ferrioxamine B permease that belongs to the major facilitator superfamily. *Microbiology* 1998; 144:3455–3462.
42. Yun CW, Ferea T, Rashford J, Ardon O, Brown PO, Botstein D, Kaplan J, Philpott CC. Desferrioxamine-mediated iron uptake in *Saccharomyces cerevisiae*. Evidence for two pathways of iron uptake. *J Biol Chem* 2000; 275:10709–10715.
43. Yun CW, Tiedeman JS, Moore RE, Philpott CC. Siderophore-iron uptake in *Saccharomyces cerevisiae*: identification of ferrichrome and fusarinine transporters. *J Biol Chem* 2000; in press.
44. Spizzo T, Byersdorfer C, Duesterhoeft S, Eide D. The yeast *FET5* gene encodes a FET3-related multicopper oxidase implicated in iron transport. *Mol Gen Genet* 1997; 256: 547–556.
45. Urbanowski JL, Piper RC. The iron transporter Fth1p forms a complex with the Fet5 iron oxidase and resides on the vacuolar membrane. *J Biol Chem* 1999; 274:38061–38070.
46. Lange H, Kispal G, Lill R. Mechanism of iron transport to the site of heme synthesis inside yeast mitochondria. *J Biol Chem* 1999; 274:18989–18996.
47. Babcock M, de Silva D, Oaks R, Davis-Kaplan S, Jiralerspong S, Montermini L, Pandolfo M, Kaplan J. Regulation of mitochondrial iron accumulation by Yfh1p, a putative homolog of frataxin. *Science* 1997; 276:1709–1712.
48. Radisky DC, Babcock MC, Kaplan J. The yeast frataxin homologue mediates mitochondrial iron efflux. Evidence for a mitochondrial iron cycle. *J Biol Chem* 1999; 274: 4497–4499.
49. Knight SA, Sepuri NB, Pain D, Dancis A. Mt-Hsp70 homolog, Ssc2p, required for maturation of yeast frataxin and mitochondrial iron homeostasis. *J Biol Chem* 1998; 273:18389–18393.
50. Lill R, Diekert K, Kaut A, Lange H, Pelzer W, Prohl C, Kispal G. The essential role of mitochondria in the biogenesis of cellular iron-sulfur proteins. *Biol Chem* 1999; 380: 1157–1166.
51. Schilke B, Voisine C, Beinert H, Craig E. Evidence for a conserved system for iron metabolism in the mitochondria of *Saccharomyces cerevisiae*. *Proc Natl Acad Sci USA* 1999; 96:10206–10211.
52. Kispal G, Csere P, Prohl C, Lill R. The mitochondrial proteins Atm1p and Nfs1p are essential for biogenesis of cytosolic Fe/S proteins. *EMBO J* 1999; 18:3981–3989.
53. Andrews SC, Arosio P, Bottke W, Briat JF, von Darl M, Harrison PM, Laulhere JP, Levi S, Lobreaux S, Yewdall SJ. Structure, function, and evolution of ferritins. *J Inorg Biochem* 1992; 47:161–174.
54. Raguzzi F, Lesuisse E, Crichton RR. Iron storage in *Saccharomyces cerevisiae*. *FEBS Lett* 1988; 231:253–258.
55. Bode HP, Dumschat M, Garotti S, Fuhrmann GF. Iron sequestration by the yeast vacuole. A study with vacuolar mutants of *Saccharomyces cerevisiae*. *Eur J Biochem* 1995; 228: 337–342.
56. Yuan DS, Dancis A, Klausner RD. Restriction of copper export in *Saccharomyces cerevisiae* to a late Golgi or post-Golgi compartment in the secretory pathway. *J Biol Chem* 1997; 272:25787–25793.
57. Sweet SP, Douglas LJ. Effect of iron concentration on siderophore synthesis and pigment production by *Candida albicans*. *FEMS Microbiol Lett* 1991; 64:87–91.

58. Morrissey JA, Williams PH, Cashmore AM. *Candida albicans* has a cell-associated ferric-reductase activity which is regulated in response to levels of iron and copper. *Microbiology* 1996; 142:485–492.
59. Yamada-Okabe T, Shimmi O, Doi R, Mizumoto K, Arisawa M, Yamada-Okabe H. Isolation of the mRNA-capping enzyme and ferric-reductase-related genes from *Candida albicans*. *Microbiology* 1996; 142:2515–2523.
60. Budde AD, Leong SA. Characterization of siderophores from *Ustilago maydis*. *Mycopathologia* 1989; 108:125–133.
61. Ardon O, Nudelman R, Caris C, Libman J, Shanzer A, Chen Y, Hadar Y. Iron uptake in *Ustilago maydis*: tracking the iron path. *J Bacteriol* 1998; 180:2021–2026.
62. Ardon O, Weizman H, Libman J, Shanzer A, Chen Y, Hadar Y. Iron uptake in *Ustilago maydis*: studies with fluorescent ferrichrome analogues. *Microbiology* 1997; 143:3625–3631.
63. Nyhus KJ, Wilborn AT, Jacobson ES. Ferric iron reduction by *Cryptococcus neoformans*. *Infect Immun* 1997; 65:434–438.
64. Jacobson ES, Petro MJ. Extracellular iron chelation in *Cryptococcus neoformans*. *J Med Vet Mycol* 1987; 25:415–418.
65. Jacobson ES, Vartivarian SE. Iron assimilation in *Cryptococcus neoformans*. *J Med Vet Mycol* 1992; 30:443–450.
66. Nyhus KJ, Jacobson ES. Genetic and physiologic characterization of ferric/cupric reductase constitutive mutants of *Cryptococcus neoformans*. *Infect Immun* 1999; 67:2357–2365.
67. Burt WR. Identification of coprogen B and its breakdown products from *Histoplasma capsulatum*. *Infect Immun* 1982; 35:990–996.
68. Howard DH. Acquisition, transport, and storage of iron by pathogenic fungi. *Clin Microbiol Rev* 1999; 12:394–404.

16

Bacterial Iron Transport

VOLKMAR BRAUN and KLAUS HANTKE

University of Tübingen, Tübingen, Germany

I. INTRODUCTION	395
II. IRON TRANSPORT SYSTEMS	397
A. Siderophores	397
B. Transport Across the Cytoplasmic Membrane	397
C. Transport Across the Outer Membrane via Regulated Channel-Forming Proteins	406
III. REGULATION OF BACTERIAL IRON TRANSPORT	413
A. Regulation by the Fe ²⁺ -Fur Repressor Protein	413
B. Regulators Regulated by Fur	415
C. DtxR-Like Proteins Regulate Iron Uptake and Oxidative Stress Response in Gram-Positive Bacteria	415
D. Is There an Iron-Responsive RNA-Binding Protein in Bacteria?	416
E. Novel Mechanism of Transcriptional Control of the Ferric Citrate Transport System via Transmembrane Signaling	417
F. Regulatory Systems That Function Similar to the fec Device	418
ACKNOWLEDGMENTS	420
REFERENCES	420

I. INTRODUCTION

The interest in research on microbial iron supply lies in its multifaceted aspects: (a) iron plays an important role as co-factor in the active centers of soluble and membrane-bound redox enzymes, (b) bacteria have to be able to use the very different iron sources found in different environments, (c) cells have to overcome the insolubility of Fe³⁺, (d) iron supply is related to bacterial pathogenicity, (e) iron is taken

up by active transport mechanisms, (f) iron is metabolized inside the cells, and (g) iron uptake and iron metabolism are regulated to save bacterial resources and to avoid iron toxicity.

The concentration of Fe^{3+} in nature and the human body is orders of magnitude below the concentration microorganisms require for growth. Therefore, microorganisms have developed means to use a variety of different iron sources: Fe^{3+} siderophores derived from microbial and plant exudates, the polymeric Fe^{3+} hydroxide, heme, hemoglobin, haptoglobin, transferrin, and lactoferrin. Microbes acquire iron from Fe^{3+} hydroxide by synthesis and secretion of very strong and highly specific iron-complexing compounds, called siderophores (see Chapter 12). The Fe^{3+} -loaded siderophores are actively transported into the cells, where Fe^{3+} is released from the siderophores by reduction to Fe^{2+} and incorporated into heme and nonheme iron proteins. Some bacteria take up free heme and heme released from hemoglobin by heme-specific transport systems and use heme as such for the synthesis of heme proteins or release the iron from heme to synthesize their own heme and iron proteins. Some bacteria mobilize iron from transferrin and lactoferrin at the cell surface and transport the iron into the cytoplasm. Detailed reviews on certain aspects may be found in Refs. 1–4.

Iron is the only nutrient known to be generally in short supply to all bacteria growing aerobically at a pH around 7. Limitation of growth also means limitation of pathogenicity. Therefore, pathogens have adapted their iron-import mechanisms to the type of iron supply the hosts provide at the sites of infection. Host defense mechanisms against bacterial invaders may include active withdrawal of iron. For example, macrophages contain high amounts of lactoferrin, which can limit growth of ingested bacteria within macrophages and also growth around macrophages if lactoferrin is discharged from the macrophages. Iron bound by lactoferrin is unavailable for most pathogens. Another means of reducing the iron available for microbes is the increase in the synthesis of serum transferrin, which reduces the mobile iron pool. However, at a site of an infection, it is not known how much iron is in the Fe^{3+} form and how much is in the Fe^{2+} form. The latter is much more soluble than Fe^{3+} , but transport of Fe^{2+} has only been investigated in a few cases.

To save material and energy, bacteria usually synthesize proteins only when they are required. Therefore, the iron transport systems are only formed under iron-limiting growth conditions, when iron transport is needed to fulfill the growth requirements. The danger of iron overload is another reason to control the iron supply strictly; iron catalyzes the formation of oxygen and nitrogen radicals, which can damage DNA, membrane lipids, and proteins.

Very little is known about the intracellular iron metabolism in bacteria—whether iron is immediately incorporated into iron proteins or temporarily deposited in storage compounds from where it is mobilized when needed, and how it is distributed among the various pathways.

In the following, those aspects of iron transport for which the most advanced knowledge exists will be described. We will refer to reviews that cover data on many iron transport systems of bacteria that have not been studied in depth or that are closely related to the discussed iron transport mechanisms. Most publications have identified iron transport genes and analyzed similarities in amino acid sequence to that of well-described systems under the assumption that these reflect the iron source used and the mechanism of transport. The many genes identified in partially and

completely sequenced genomes that have been related to known iron transport genes based on sequence similarities will not be discussed. Siderophore biosynthesis is also not discussed; interested readers are referred to previous reviews on this subject (5–7).

II. IRON TRANSPORT SYSTEMS

A. Siderophores

Siderophores are iron-complexing compounds of microbial origin. They are synthesized and secreted by bacteria and fungi, and they are involved in cross-feeding. For example, *Escherichia coli* K-12 contains an iron transport system for ferrichrome, which is the product of the fungus *Ustilago sphaerogena*. Ferrichrome belongs to the hydroxamate siderophores, which form a large variety of structures (Fig. 1). In contrast, the catecholate siderophores display less variation. They are synthesized by bacteria, and the most prominent one is enterobactin, also designated enterochelin (Fig. 1), formed for example by *E. coli*. A third structural group is the carboxylates, to which belong citrate, exochelin, and mycobactin of mycobacteria, staphyloferrin, or staphylococci (Fig. 1), and rhizoferrin of mucorales (Fig. 1). There are also mixed-type siderophores, such as yersiniabactin (Fig. 1) of *Yersinia* strains, which contains a benzene, a thiazolidine ring, and two thiazoline rings (8). *Pseudomonas* species are particularly rich in siderophores with different iron ligands, as exemplified by pseudobactin 358 (Fig. 1). Mycobacteria synthesize the water-soluble exochelins and the membrane-associated mycobactins (Fig. 1). *Mycobacterium smegmatis* produces both types, *Mycobacterium tuberculosis* only mycobactins (9); the latter are important for survival in macrophage-like THP-1 cells (10). The marine bacteria *Halomonas aquamarina* and *Marinobacter* sp. synthesize aquachelins and marinobactins, respectively, which consist of a unique peptide head group that coordinates Fe^{3+} and a series of short-chain fatty acid residues (C2–C8). In contrast to the mycobactins with long-chain fatty acid groups (C16–C21), aquabactins and marinobactins form water-soluble micelles that form vesicles upon coordination of Fe^{3+} (11).

Siderophores are synthesized only when they are needed under iron-limiting growth conditions. It is not known how they are secreted by the producing strains. Since many of the siderophores are charged and therefore cannot escape the cytoplasm by diffusion through membranes, there should be secretion systems. Over 300 siderophores have been identified, and transport has been studied in many organisms to various degrees (12).

B. Transport Across the Cytoplasmic Membrane

All bacteria have the same kind of cytoplasmic membrane that encloses the cytoplasm. As far as is known, all types of iron sources that reach the cytoplasmic membrane— Fe^{3+} , Fe^{3+} siderophores, and heme—are transported across the cytoplasmic membrane basically by the same mechanism. The iron transport systems belong to the ATP-binding-cassette (ABC) transport systems, also called traffic ATPases, which are the most frequently occurring transport systems in bacteria. Bacterial ABC transporters not only import substrates, but also export biopolymers. ABC transporters constitute a superfamily to which also belong the multiple-drug transporter glycoproteins of eukaryotes. The glycoproteins consist of a single polypeptide

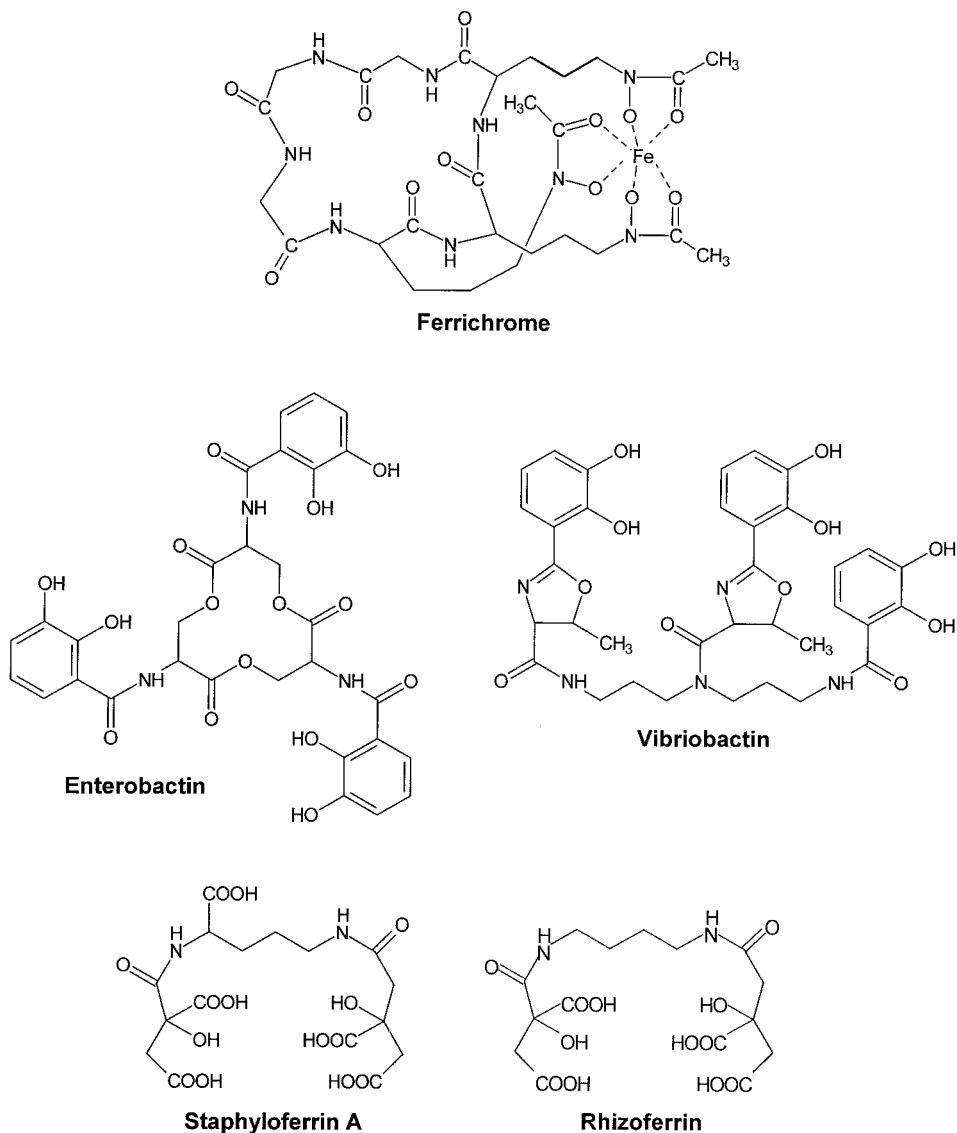


Figure 1 Selected siderophores synthesized by microorganisms. The conformation of ferrichrome loaded with Fe^{3+} is known and is as shown. For the other siderophores, only the chemical structures have been drawn.

chain with two ATPase domains linked by the transmembrane transporter domain. In bacteria, the ATPases are separate from the transmembrane transport proteins; they are located in the cytoplasm, but associate with the transport proteins. Most bacterial ABC substrate importers are composed of two transmembrane proteins. In those cases where there is only one protein, it has approximately twice the size and has evolved by fusion of two proteins, as evidenced by an internal sequence similarity between the two halves. The energy consumed by the active transport is derived

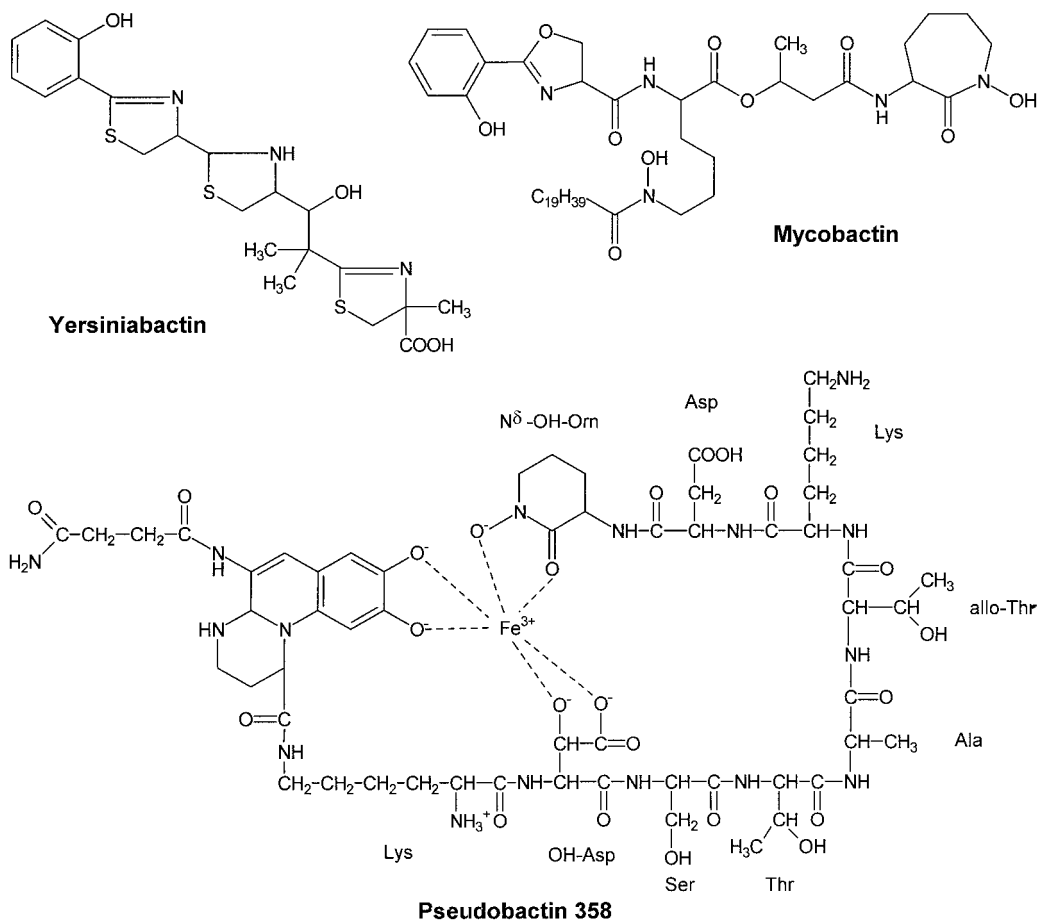


Figure 1 Continued

from ATP hydrolysis catalyzed by the ATPases (13). In the systems that transport maltose and histidine, two ATPases associate with the transport protein(s). The two transport proteins do not have identical functions, and the two ATPases may not fulfill the same role. It is feasible that one provides the energy and one exerts a regulatory role.

Substrates are delivered to the cytoplasmic membrane transporters by binding proteins. In Gram-negative bacteria, the binding proteins reside in the periplasm, the space between the outer membrane and the cytoplasmic membrane. The strict requirement for binding proteins for transport and their location in the periplasm resulted in the term “periplasmic-binding-protein-dependent transport system,” which is rapidly being abandoned in favor of the term “ABC transporter.” In Gram-positive bacteria, which lack a periplasm, the binding proteins are fixed to the cytoplasmic membrane by a lipid anchor of the murein lipoprotein type. The binding proteins confer specificity for the substrate to be transported; recognition of substrates by the membrane transporter has only been demonstrated for mutants that lack binding

proteins and in addition carry mutations in the membrane transporter (14). Binding of substrate-loaded binding protein to the cytoplasmic membrane transporters triggers ATP hydrolysis by the cytoplasmic ATPase. This finding, obtained with the maltose and histidine ABC transporters reconstituted in liposomes, may also apply for the iron transport systems.

1. Ferrichrome Transport of *E. coli* K-12 as an Example of Fe^{3+} –Siderophore Transport

Ferrichrome transport will be described in more detail, since it is the only Fe^{3+} –siderophore transport system in which studies on the interaction of the transport proteins and their substrates has been studied with the aim to understand the transport mechanism. As early as 1983, the genes of the entire ferrichrome transport system were cloned, the transcription polarity was determined, and the transport proteins were identified (15). The operon is composed of the genes *fhuA*, *fhuC*, *fhuD*, and *fhuB*, which are transcribed in this order. FhuD is located in the periplasm, FhuB is in the cytoplasmic membrane, and FhuC is associated with the cytoplasmic membrane, provided that this contains FhuB (16). The FhuB cytoplasmic membrane protein is difficult to observe in polyacrylamide gels because, as later shown by analysis of the primary structure deduced from the *fhuB* nucleotide sequence, it is very hydrophobic and does not enter gels after heating in 2% sodium dodecyl sulfate (17,18).

The transmembrane topology of FhuB was determined using fusion proteins of N-terminal FhuB fragments of increasing size and β -lactamase (19). Cells are protected against ampicillin only when the β -lactamase is in the periplasm. The fusion sites of the fusion proteins from ampicillin-resistant cells revealed the FhuB sites located in the periplasm (Fig. 2). FhuB is the transmembrane transporter and is twice the size of most ABC transporters. FhuB was genetically separated into two halves which, when co-synthesized, form an active transporter. Both halves are required for transport. FhuB apparently evolved by duplication of a gene and subsequent fusion of the two genes. Point mutations in FhuB at two sites have been proposed to be involved in binding of the FhuC ATPase inactivate FhuB (20,21). FhuC contains two nucleotide-binding domains (Walker motifs A and B), which are typical for ABC transporters (22,23). Replacement of lysine in domain I by glutamine or glutamate, and of aspartate in domain II by asparagine or glutamate, abolishes ferrichrome transport (24). Covalent binding of 5'-*p*-fluorosulfonylbenzoyl-[8- ^{14}C]adenosine to FhuC associated with membrane vesicles demonstrated that FhuC binds ATP (25). FhuC labeled with a His tag and purified on a Ni-agarose column displays ATPase activity with a K_m of 420 μM and a V_{max} of 0.54 $\mu\text{mol min}^{-1} \text{mg}^{-1}$, which is in the range of ATPase activities found for other ABC transporters (26).

Deletion of the *fhuD* gene inactivates ferrichrome transport. Addition of ferrichrome, aerobactin, or coprogen, all of which are siderophores of the hydroxamate type that are transported by the Fhu system, to a FhuD-containing periplasmic fraction renders FhuD resistant to proteinase K degradation. Ferrichrome A, which is not transported, does not protect FhuD (27). The dissociation constant of purified FhuD for ferric aerobactin is 0.4 μM , 1 μM for ferrichrome, 5.4 μM for the structurally related antibiotic albomycin, and 0.3 μM for ferric coprogen. Dissociation constants of FhuD for hydroxamate siderophores, which supply iron poorly via the Fhu system, are 100-fold higher than for ferric aerobactin. FhuD mutants with lower transport activities have higher dissociation constants (28).

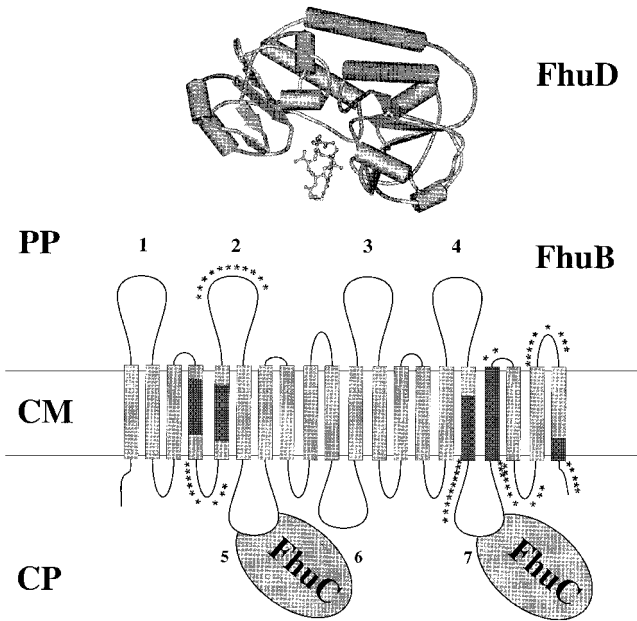


Figure 2 Predicted transmembrane topology of the FhuB protein in the cytoplasmic membrane of *E. coli* (19) and sites of interaction between the periplasmic FhuD protein and FhuB as determined by competitive peptide mapping (29,30; A. Mademidis, H. Killmann, and V. Braun, unpublished). The asterisks indicate sites of interaction outside the membrane; the black bars show sites of interaction within the membrane. However, some of the regions indicated by asterisks may fold back into a putative channel formed by FhuB (see text). The binding sites of the FhuC ATPase to FhuB are drawn based on a previous proposal (20). The folding of the FhuD protein is shown as determined for the *E. coli* FhuD occupied with gallichrome (32).

Interaction of FhuD with FhuB was demonstrated by chemical cross-linking of the two proteins and protection of FhuB from degradation by proteinase K and trypsin added to spheroplasts. The sites of interaction between FhuD and FhuB were determined by competitive peptide mapping. Synthetic peptides of 10 and 20 amino acids labeled with biotin that together spanned the entire FhuB sequence were incubated with isolated FhuD adsorbed to microtiter plates (29,30). Binding of the FhuB peptides to FhuD was monitored by measuring the activity of β -galactosidase linked to biotin via streptavidin. The results obtained are noteworthy in several respects. Peptides of only two of the periplasmic loops of FhuB interact with FhuD, and they are located in different segments of the two FhuB halves. In contrast, peptides from four transmembrane regions and three periplasmic loops of FhuB interact with FhuD, and they also differ in the two FhuB halves (Fig. 2). This implies that the periplasmic FhuD not only interacts with periplasmic loops of FhuB, but also inserts deeply into FhuB.

It is assumed that FhuB forms a channel that is closed at the inside. Such a model, derived from electron microscopy to 2.5-nm resolution and single-particle image analysis, has been proposed for the multiple-drug-resistance P-glycoprotein

(31). The model predicts that the FhuB transmembrane regions that interact with FhuD line the inner surface of the channel. The periplasmic loops that interact with FhuD in fact do not form periplasmic loops, but fold back into the channel. Consequently, triggering of ATP hydrolysis by FhuC does not require a transmembrane signal that goes across the entire cytoplasmic membrane from the periplasm to FhuC at the inner side of the cytoplasmic membrane. One of the interaction sites of FhuD at FhuB is very close to the proposed binding site of FhuC at FhuB, which suggests a direct interaction of FhuD with FhuC. The asymmetry of the interaction sites with regard to the two halves of FhuB indicates that both halves of FhuB, although they display an internal homology, have different functions in ferrichrome transport.

The crystal structure of FhuD with bound gallichrome was determined at 1.9 Å resolution (32). In gallichrome, Fe^{3+} of ferrichrome is replaced by Ga^{3+} , which has an ionic radius very similar to that of Fe^{3+} . Gallium is suitable for multiwavelength anomalous dispersion phasing techniques. The overall structure of FhuD resembles that of periplasmic binding protein transporters, many of which have been crystallized and the structures determined. They form two globular domains connected by short stretches of β strands. Like Venus's flytraps, which close when they have caught their prey, binding proteins are flexible around a hinge region and close when they bind the substrate. Although no crystal structure is available for FhuD free of substrate, it is inferred from the crystal structure that substrate-dependent opening and closing of FhuD is restricted. Unlike other binding proteins, the domain interface in FhuD is predominantly hydrophobic, which limits rotational movements between open and closed states. Nevertheless, it is likely that FhuD changes its conformation by a small-scale hinge-bending motion when it delivers its substrate to FhuB. The biophysical results agree with biochemical studies, which show that FhuD binds to FhuB independent of loading with ferrichrome, protects FhuB from being degraded by proteases, and becomes chemically cross-linked to FhuB (28). Since the active site of FhuD is not deeply buried in the protein, only 45% of the surface of gallichrome is immersed in the protein and a less pronounced conformational change upon gallichrome binding is likely. The open binding pocket also explains the rather broad specificity of FhuD for substrates which encompass ferrichrome, ferricrocin, ferrichrysin, albomycin, aerobactin, rhodotorulate, coprogen, and ferrioxamine B. Essential elements that are recognized by FhuD are the hydroxamate moieties and adjacent hydrophobic linkers. Rather bulky side chains, like that of albomycin, can be accommodated and may be exposed to the solvent.

2. Transport of Fe^{3+}

In 1989, it was shown that a DNA fragment of the chromosome of *Serratia marcescens* conferred to an *E. coli* K-12 mutant deficient in siderophore synthesis growth on iron-limited medium (33). No evidence for the involvement of a siderophore was found, and iron transport did not depend on an outer membrane receptor and the TonB activity (see Sec. II.C). Since Fe^{3+} could be solubilized with phosphate, citrate, or oxaloacetate for transport assays, no specific iron chelate was required. Analysis of the nucleotide sequence of the DNA fragment revealed three genes, *sfuA*, *B*, *C*, which encode proteins typical for ABC transporters (34). *SfuA* is a hydrophilic protein located in the periplasm, *SfuB* is a very hydrophobic protein found in the cytoplasmic membrane, and *SfuC* is a polar yet membrane-associated cytoplasmic protein with a nucleotide-binding site.

During studies on the growth of *Haemophilus influenzae* and pathogenic *Neisseria* with transferrin and lactoferrin as the iron source, the transport genes *fbpABC* and *hitABC*, respectively, were identified; these genes display strong sequence similarities to the *sfuA*, *B*, *C* genes (2). The genes that encode proteins involved in transport from the periplasm into the cytoplasm are not flanked by genes that encode outer membrane proteins. Various Fe^{3+} compounds that diffuse from the culture medium through the porins into the cytoplasm or Fe^{3+} released from transferrin and lactoferrin are transported by the Sfu-type system across the cytoplasmic membrane. The iron compounds tested do not tightly bind iron. Fe^{3+} is either transported across the cytoplasmic membrane as an ion or complexed by an unknown chelator of low molecular weight. The periplasmic FbpA and HitA proteins bind a single Fe^{3+} with as high an affinity (10^{19} M^{-1}) as they bind transferrin (10^{20} M^{-1}). Biochemical evidence indicates that the same set of amino acid residues that bind Fe^{3+} to transferrin also bind Fe^{3+} to FbpA. This result is confirmed by the crystal structure of HitA (also designated hFBP), which corresponds to the folding of the N lobe of transferrin (35). Although HitA, like FhuD, belongs to the transferrin superfamily, it probably evolved from an ancestor of the periplasmic binding proteins that transport anions. HitA contains a phosphate group bound to a conserved helix, which in transferrin binds carbonate. In HitA, unchelated Fe^{3+} is buried in a pocket more deeply than Fe^{3+} siderophores are buried in FhuD, which binds the substrate rather close to the protein surface. However, in both proteins the iron is exposed to the solvent more than in transferrin and lactoferrin.

An apparent ABC-type iron transport system of *Yersinia pestis* also transports Mn^{2+} (36). It belongs to a family of metal transporters that take up Mn^{2+} , Fe^{2+} , and Zn^{2+} , and *yfeABCDE* shows no sequence similarity to *sfuABC*, *hitABC*, or *fbpABC*. Transcription of *yfeABCD* (*yfeE* is transcribed divergently from *yfeABCD*) is regulated by iron and manganese via the Fur protein. A DNA fragment from *Salmonella typhimurium* homologous to *yfe* was cloned and sequenced and designated *sitABCD*, where *sitA* encodes a putative periplasmic binding protein, *sitB* an ATPase, and *sitC* and *sitD* two cytoplasmic membrane transport proteins (37).

Biochemical studies on the supply of iron by transferrin to the Gram-positive *Staphylococcus aureus* and *S. epidermidis* led to the identification of the transferrin binding protein Tpn. The Tpn protein (42 kDa) is located in the cell wall, is synthesized under iron-limiting growth conditions, and elicits antibody formation in the human serum and peritoneum upon staphylococcal infections (38). Tpn is a cell-wall glyceraldehyde-3-phosphate dehydrogenase that binds not only transferrin but also plasmin (39). Transferrin binds to Tpn with the N lobe, where iron is first released before it is mobilized from the C lobe (40). It is assumed that the released iron is taken up into the cytoplasm by ABC transporters.

3. Transport of Heme

For pathogenic and commensal bacteria, heme represents an iron source that is widely distributed throughout the human body in various forms, but is only available in low concentrations. Free heme in the serum is bound to hemopexin (12 μM) with a dissociation constant below 1 pM. Hemoglobin in the serum (80–800 nM) is released from lysed erythrocytes, rapidly bound to serum haptoglobin (5–20 μM), and removed by the liver. Bacteria have developed transport systems for heme de-

livered as heme, hemoglobin, hemoglobin-haptoglobin, heme-hemopexin, and myoglobin.

The first hemin transport system was characterized in *Yersinia enterocolitica* (41,42). In these experiments, the insolubility of hemin was overcome by binding hemin to serum albumin. A cosmid containing a fragment of the *Y. enterocolitica* genome conferred growth on hemin to an *E. coli* K-12 mutant unable to synthesize both its own siderophore enterobactin (*aroB*) and heme (*hemA*). The cosmid encoded six hemin-related genes, *hemPRSTUV*, which are transcribed in this order (Fig. 3). *hemR* encodes an outer membrane transport protein, *hemT* a periplasmic hemin-binding protein, *hemU* a cytoplasmic membrane transporter, and *hemV* an ATPase. HemR catalyzes the TonB-dependent transport across the outer membrane, and HemTUV catalyzes the ATP-dependent transport across the cytoplasmic membrane (ABC transporter). The small HemP protein is not essential for heme uptake. HemS seems to be essential for *Y. enterocolitica* metabolism, since no chromosomal mutant could be isolated. The *E. coli* K-12 *aroB hemA* mutant transformed with the *Y. enterocolitica hemR* gene uses hemin as a porphyrin source, but not as an iron source. *hemRS* transformants grow with hemin as the iron source. However, *hemR* on a low-copy-number plasmid confers growth to the *E. coli* K-12 *aroB hemA* transformant, which suggests that high amounts of hemin in the absence of HemS are toxic due to the promotion of lipid peroxidation. In fact, HemR on high-copy-number plasmids transports high amounts of hemin into the periplasm of *E. coli* K-12. Attempts to assign a hemin degradation activity to HemS are inconclusive (K. Hantke, unpublished). Hemin uptake by *E. coli* K-12 through the *Y. enterocolitica* HemR protein suggests that *E. coli* K-12 lacks an outer-membrane hemin transporter, but contains a cytoplasmic hemin transporter, or that diffusion of hemin, accumulated in the periplasm by the HemR activity, across the cytoplasmic membrane into the cytoplasm is sufficient to cover the hemin requirement.

Y. pestis contains a hemin transport system that is analogous to that of *Y. enterocolitica* (Fig. 3) (43). The HmuRTUV proteins are necessary for growth on hemin, hemin-albumin, and myoglobin, but not on hemoglobin, hemoglobin-haptoglobin, or heme-hemopexin. In *hmuTUV* mutants, HmuS substitutes the lacking HmuTUV for the use of hemoglobin and heme-hemopexin. *hmuP'RSTUV* deletion mutants of *Y. pestis* display a lethal dose of infection the same as *hmu* wild-type cells administered subcutaneously and retro-orbitally to mice (43a). This heme transport system is therefore not required for *Y. pestis* lethality in the mouse model.

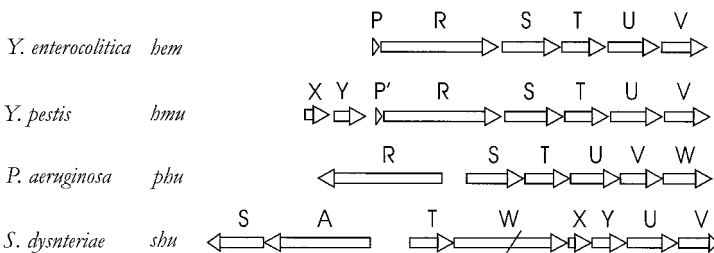


Figure 3 Organization of heme transport genes. The same designations indicate homologous genes, except in the case of *S. dysenteriae*, where the A gene is homologous to the R genes, and where *shuW* (incomplete gene) is not homologous to *phuW*.

Y. pestis also contains a heme storage system, which does not participate in iron nutrition. At 26°C, large amounts of hemin are located in the outer membrane and appear to play an important role in the transmission of bacteria from the flea to the mammalian host. Transmission of plague depends on blockage of the foregut of the flea by a mass of plague bacilli; this occurs only upon heme storage. Blockage leads to starvation of the flea, resulting in frequent attempts to feed (44).

Pseudomonas aeruginosa synthesizes siderophores and also exocytotoxins that damage eukaryotic cells and mobilize intracellular iron, secretes proteases to release protein-bound heme and iron, and contains transport systems for ferric siderophores and heme. Two heme transport systems, designated *phu* and *has*, have been found in *P. aeruginosa* (45). The *phuSTUVW* genes are co-transcribed, and *phuR* is transcribed divergently (Fig. 3). Sequence comparisons suggest that the PhuRSTUV proteins have the same functions as those of the HemRSTUV proteins of *Y. enterocolitica*, and the HumRSTUV proteins of *Y. pestis*. *has* encodes a heme transport system where heme is mobilized by a hemophore (see Sec. B.3.a).

The genome of *Shigella dysenteriae* contains the divergently transcribed genes *shuAS* and *shuTWXYUV* (46). ShuA is the outer-membrane transporter, ShuT the periplasmic binding protein, ShuU the cytoplasmic membrane transporter, and ShuV the ATPase of the ABC transporter. *shuW* seems to encode an inactive protein, and the functions of the *shuXY* gene products are unknown (Fig. 3).

Vibrio cholerae carries the genes for a heme transport system that are closely linked to one of two sets of *tonB*, *exbB*, and *exbC* genes (see Sec. B.3.1). *tonB1*, *exbB1*, and *exbD1*, together with the *hutBCD* genes, form an operon that is controlled by a single Fur-regulated promoter upstream of *tonB1*. By comparison with characterized proteins, HutB was assigned as a heme-binding protein and HutCD as a cytoplasmic membrane transporter. Together with the outer-membrane transporter HutA, the six proteins reconstituted a heme transport system in *E. coli* (47).

In *Hemophilus influenzae* type b, three hemoglobin and hemoglobin-haptoglobin-binding proteins, HgpA, HgpB, and HgpC, were identified, and a fourth hemoglobin acquisition system exists (48). Multiple repeats of CCAA units immediately follow the sequence that encodes the signal peptides of the three proteins. Spontaneous alteration in the CCAA repeat length is associated with variable transcription of the encoding genes, as has been demonstrated with an *hgpA-lacZ* fusion (49). This kind of phase variation is caused by an on-and-off switch.

A similar but mechanistically different translational frame shift governs the expression of hemoglobin utilization of *Neisseria gonorrhoeae*. Most *N. gonorrhoeae* isolates are unable to grow on human hemoglobin as the sole iron source, but a minor population is able to do so (50). Those cells able to grow on hemoglobin contain 10 G nucleotides within a sequence encoding the N-terminal amino acids of the mature HpuA protein, which serves as an outer-membrane hemoglobin receptor. Those cells that are not able to grow on hemoglobin contain 9 G nucleotides with a stop codon at the end of the G tract. The switch from hemoglobin nonutilization to hemoglobin utilization occurs at a frequency of 1×10^{-4} to 2×10^{-3} . In addition to HpuA, a second protein, HpuB, is involved in hemoglobin utilization and is co-synthesized with HpuA.

a. Involvement of Hemophores in Heme Transport

A novel kind of heme utilization system was discovered in *Serratia marcescens* (51). The HasA (heme acquisition system) protein is secreted, releases heme from he-

moglobin, and delivers the heme to the HasR outer-membrane transporter. HasA is a monomeric protein that binds one heme molecule (52). The crystal structure (53) reveals a new type of conformation, including the structure of the heme-binding site. The heme–apoHasA complex has an unusually low midpoint potential of -550 mV which indicates exposure of heme to the aqueous solvent. His32 and Tyr75 ligate the heme iron. Since the OH group of Tyr75 also forms a strong hydrogen bond to His83, control of the protonation of His83 would indirectly control the affinity of iron since protonated His83 would favor protonation of Tyr75 and concomitantly weaken iron binding. The *hasR* gene transferred into an *E. coli* mutant unable to utilize heme confers uptake of heme; this uptake is greatly improved when the mutant also carries the *hasA* gene. The minimum hemoglobin concentration required to satisfy the *hasA hasR* transformant's need for porphyrin was 100-fold lower than in the *hasR* transformant. HasA alone is not sufficient to deliver heme (54). Both heme-free and heme-loaded HasA binds to HasR independently of the TonB protein, which is involved in the subsequent translocation of heme across the outer membrane via HasR (55). It is not known how HasA releases iron from hemoglobin, which binds heme very tightly (association constant 10^{12} – 10^{15}). Has proteins have also been identified in *Pseudomonas aeruginosa* (45,55) and *P. fluorescens* (56).

Haemophilus influenzae type b secretes the HuxA protein, which acquires heme from the heme–hemopexin complex and delivers it to the HuxC outer-membrane transporter, from where it is taken up across the outer membrane by a TonB-dependent process (57,58).

A third type of heme uptake was identified in the human pathogenic *E. coli* strain EB1 (59). The strain secretes a protease that has a high affinity for hemoglobin, hydrolyses hemoglobin, and binds heme. It is not known how the heme bound to the HbP protease is transported into *E. coli*.

None of the heme transport systems have been completely characterized. The contiguous genes are iron-regulated via the Fur repressor, and therefore all are probably involved in heme transport. The function of the homologous HemS, HmuS, PhuS, and ShuS proteins is not clear. HemP and HmuP seem to be dispensible, and the role of the PhuW and ShuXY proteins is not known. In addition, two open reading frames were localized upstream of the transport genes. In *Y. enterocolitica*, the open reading frames encode proteins of 45 and 21 kDa; similar open reading frames in *Y. pestis* were designated *OrfXY*. It would be interesting to see whether they exert regulatory functions, for example, transcription induction of the heme transport genes by heme, as has been found for the ferric citrate transport system, which is induced by ferric citrate (see Sec. III.E). In a number of organisms, such as pathogenic *Neisseria* (3), outer-membrane transporters for heme have been identified, but the entire transport systems have not been cloned and characterized. Furthermore, mutants designated as heme transport mutants are generally leaky, which suggests the existence of additional unidentified heme transport systems.

C. Transport Across the Outer Membrane via Regulated Channel-Forming Proteins

In general, transport of structurally similar Fe^{3+} siderophores across the outer membrane of Gram-negative bacteria is more specific than transport across the cytoplasmic membrane. Examples are transport across the *E. coli* outer membrane of the

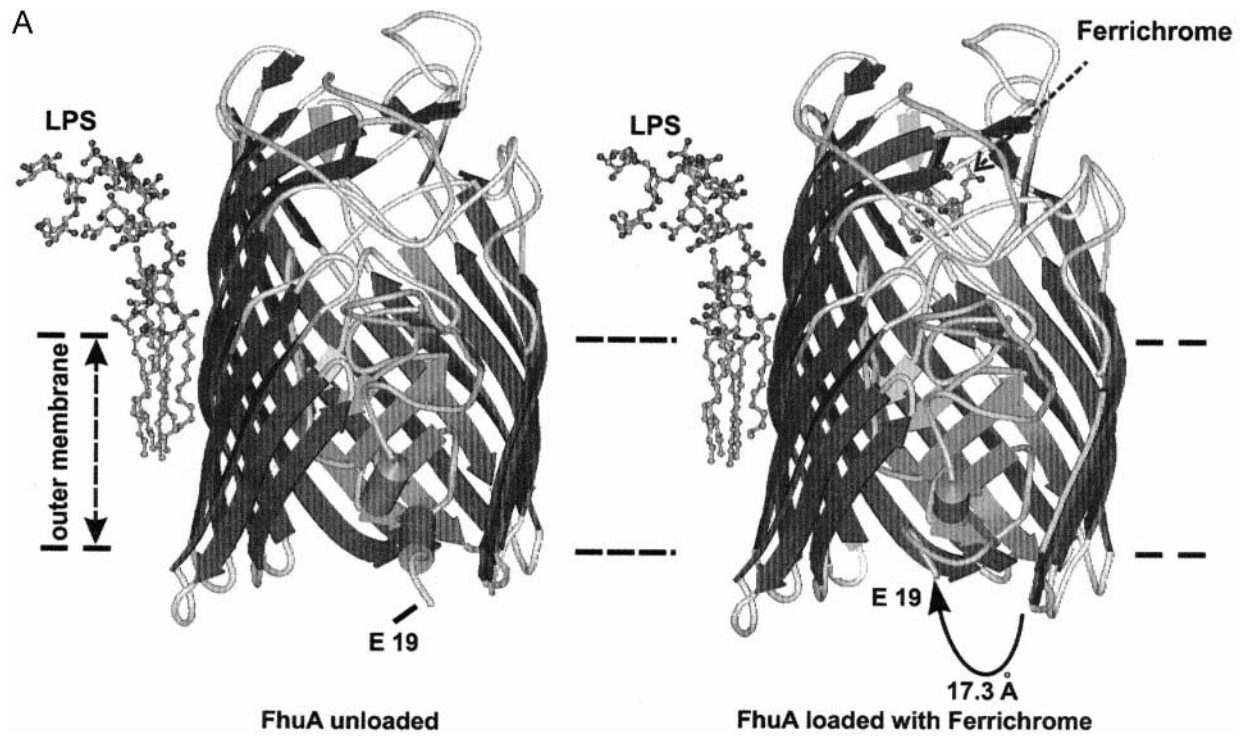
Fe^{3+} hydroxamates ferrichrome via the FhuA protein, coprogen via the FhuE protein, and aerobactin via the Iut protein. All three Fe^{3+} hydroxamates are transported across the cytoplasmic membrane by the single FhuBCD system. Another example is the transport of the catechol siderophores: enterobactin is transported by FepA, and dihydroxybenzoylserine and other catecholates are transported via the Fiu and Cir transporters across the outer membrane; all are transported across the cytoplasmic membrane by the single FepBCDE system. The two catecholate siderophores enterobactin and vibriobactin are transported across the outer membrane of *Vibrio cholerae* by the transport proteins VctA and ViuA, respectively, but can use either ViuCDP or VctCDG across the cytoplasmic membrane (60).

1. FhuA and FepA, Channel-Forming Outer-Membrane Transport Proteins

Recently, the crystal structures of the FhuA protein (61,62) and the FepA protein (63) were published. Since FhuA could be crystallized in the substrate-loaded and the unloaded form and in addition contains in one crystal a lipopolysaccharide (LPS) molecule (61), FhuA will be discussed in more detail. Only the structure of unloaded FepA without LPS has been described, and the structure is very similar to that of unloaded FhuA.

FhuA forms a β barrel, as has been found for all nine crystal structures of outer-membrane proteins determined to date (64). The FhuA β barrel is composed of 22 antiparallel β strands (residues 161–723). What is new in the crystal structure of FhuA and FepA is the N-proximal globular domain that tightly closes the β barrel; this domain is designated the cork or plug. The channels in FhuA and FepA have to be opened so that substrates can pass through. Opening requires input of energy, which is provided by the cytoplasmic membrane in the form of the proton-motive force. How the energy from the cytoplasmic membrane is transmitted to the outer membrane, and what effect this has on FhuA and FepA and all the other outer-membrane iron transport proteins that are thought to function similarly, regardless whether the available Fe^{3+} is complexed in siderophores, heme, heme–hemopexin, hemoglobin, hemoglobin–haptoglobin, transferrin or lactoferrin, is not known. For energetic reasons, it is unlikely that the entire cork domain leaves the β barrel to open the channel, since nine salt bridges and more than 60 hydrogen bonds tightly attach the cork to the β barrel. It seems that in the region separating one major cavity that extends to the cell surface and another major cavity that reaches the periplasm, rather small changes connect the cavities to form an open channel.

Bound LPS allows FhuA to be positioned in the outer membrane, since the fatty acids of LPS are inserted in the outer leaflet of the lipid bilayer membrane (Fig. 4). Half of the FhuA molecule is located above the membrane, where ferrichrome, the iron substrate, is bound in a pocket exposed to the aqueous environment. Binding of ferrichrome induces a small structural transition in FhuA, which moves apex B (Glu98–Gln100) of the cork 1.7 Å toward ferrichrome, and a large structural transition in the periplasm, where a short helix (residues 22–30) is converted into a coil in which Glu19 moves 17 Å away from its former α -carbon position. The structural change in FhuA does not open the channel. Apparently, input of energy is required, which is provided by the proton-motive force of the cytoplasmic membrane through the action of a protein complex composed of the proteins TonB, ExbB, and ExbD. These proteins are anchored in the cytoplasmic membrane (Fig. 4) and contain in



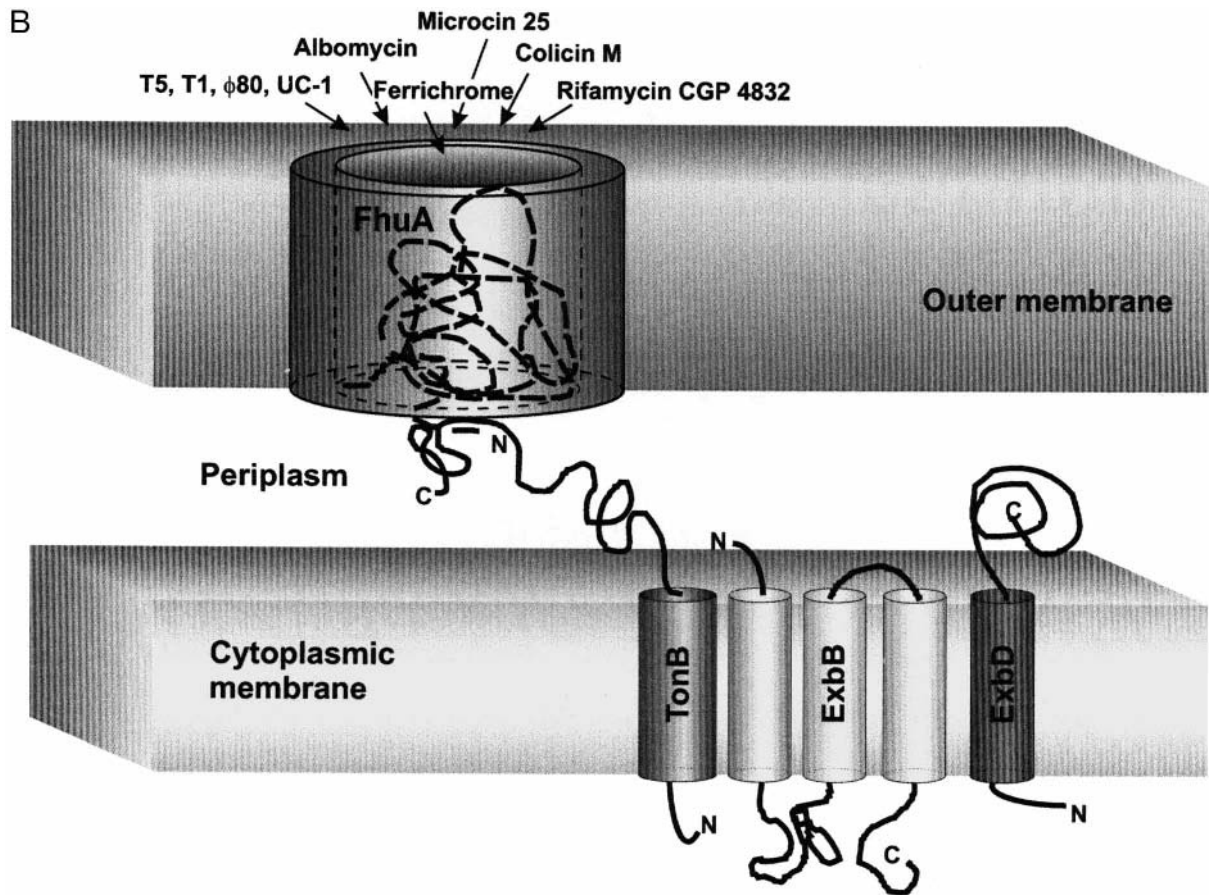


Figure 4 (A) Crystal structure of the FhuA protein in the unloaded (left) and the ferrichrome-loaded form (right). The ferrichrome-binding site is indicated by an arrow, and lipopolysaccharide bound to FhuA is drawn to the left structure. Some of the transmembrane β strands have been removed to improve the view of the cork domain. (B) Transmembrane topology of the TonB, ExbB, and ExbD proteins in the cytoplasmic membrane and site of interaction between the Glu160 region of TonB with the TonB box of FhuA. The figure is not meant to imply an equal number of TonB, ExbB, and ExbD molecules. In fact, when the proteins are synthesized from a single phase T7 promoter placed upstream of *tonB* in a plasmid-encoded *tonB exbB exbD* construct, ExbB is the most abundant protein, followed by ExbD and then by TonB (65,67).

the otherwise hydrophobic transmembrane segment polar amino acids that seem to play an important role in the functional interaction of the three proteins. Conversion of His20 to Arg in *E. coli* TonB abolishes nearly all TonB-dependent activities (65), and replacement of Asp25 by Asn in ExbD inactivates ExbD (66). It is feasible that His20 is protonated and changes the TonB conformation such that it interacts with FhuA in a way that opens the FhuA channel by a movement of the cork. Interaction of ExbB with TonB and ExbD was originally shown by a higher stability of TonB and ExbD to intrinsic proteolysis in the presence of ExbB (67). Deletion of Val17 in the transmembrane segment also inactivates TonB. TonB activity is partially restored by the transmembrane mutation Ala39 → Glu in ExbB, which suggests an interaction of TonB with ExbB within the transmembrane regions, although complementation is not allele-specific since ExbB-Val36 → Asp and ExbB-Val35 → Glu also complement TonB-ΔVal17. TonB alters the conformation upon energization; the proteinase K degradation products of TonB change when the proton-motive force is abolished by CCCP or by lysis of spheroplasts used in these experiments. In addition, the stability of TonB-ΔVal17 in the presence of ExbB-Ala39 → Glu is reduced in the presence of enterobactin, presumably through interaction of energized TonB-ΔVal17 with FepA loaded with enterobactin, which results in de-energization of TonB-ΔVal17 (68). These data indicate that TonB assumes an energized conformation and is de-energized upon interaction with substrate-loaded outer-membrane transporters. Energy transfer induces a conformational change in the outer-membrane transporters, as has been demonstrated by electron-spin resonance spectroscopy with a nitroxide spin label covalently linked to Cys280 of FepA. Spin-label relocation observed in metabolizing wild-type cells is not seen in energy-deprived cells and in TonB mutants (69).

Genetic evidence suggests that the TonB protein interacts with the N terminus of the outer-membrane transport proteins; this region, the so-called TonB box, of FhuA reads 7-Asp-Thr-Ile-Thr-Val-Thr-Ala-13. Single amino acid replacements in the TonB box of several transporters results in inactive transporters. Transport activity is restored by mutations in TonB; in all mutated transporters examined, the mutation is found at Gln160, which is mutated to Leu or Lys. A weak suppressor mutation contains a Leu residue instead of Arg158 (70). That the TonB box interacts with the region around residue 160 of TonB is supported by data obtained with mutants in the TonB box of the vitamin B₁₂ transporter BtuB and mutations in the region around residue 160 of TonB, in which the amino acid residues were replaced by cysteines. (Vitamin B₁₂ transport is very similar to Fe³⁺ transport.) The resulting functional proteins cross-link spontaneously in growing cells, and the preferentially cross-linked residues indicate a parallel N-to-C alignment of BtuB and TonB at this site of interaction. In addition, the preferential reaction of alternating amino acid residues with all three TonB cysteine residues suggest a β-sheet conformation of the BtuB TonB box. In the crystals, the TonB box of FhuA and FepA is located on the periplasmic side, where interaction with TonB most likely occurs. The TonB box of FhuA is not seen in the crystal presumably because it is flexible, and in FepA, it assumes an extended conformation without an obvious secondary structure.

An astounding result was obtained when the entire cork of FhuA (residues 5–160) was removed by genetic means (71). The rather stable FhuA Δ5–160 protein is synthesized in the cytoplasm, translocated across the cytoplasmic membrane, and inserted into the outer membrane. This multistep process requires recognition by the

secretion proteins of the Sec apparatus and proper folding of FhuA $\Delta 5$ –160. As expected, FhuA $\Delta 5$ –160 forms a rather small open channel; higher concentrations of ferrichrome supports growth independently of the Ton system, and the antibiotics erythromycin, rifamycin, bacitracin, and vancomycin, which are too large to diffuse fast enough through the porin channels, gain access to their intracellular targets and kill cells. FhuA $\Delta 5$ –160 confers infection by phage T5 (Fig. 4) for which FhuA serves as a receptor. Phage T5 infection is the only FhuA activity that occurs independently of the Ton system. However, ferrichrome delivered at low concentrations still supports growth and is actively transported across the outer membrane, since transport depends on the Ton system. Binding of ferrichrome to FhuA $\Delta 5$ –160 is less than 10% of the binding to FhuA, since FhuA $\Delta 5$ –160 lacks the cork binding sites that make up half of the total ferrichrome binding sites. The low affinity to FhuA $\Delta 5$ –160 allows the diffusion of ferrichrome through FhuA $\Delta 5$ –160 when ferrichrome is supplied at a concentration higher than is needed when ferrichrome is actively transported.

FhuA is a multifunctional protein that serves as a transporter for ferrichrome, the structurally related antibiotic albomycin, and the structurally different and iron-free antibiotic rifamycin CGP 4832, a synthetic derivative of rifamycin; as receptor for the unrelated phages T1, T5, $\phi 80$, and UC-1, which upon binding to FhuA release their DNA; and for the uptake of the colicin M protein toxin and the microcin 25 peptide toxin (Fig. 4). FhuA $\Delta 5$ –160 has activity with all the ligands of wild-type FhuA, except for microcin 25. This finding implies that TonB interacts with FhuA more than just through the TonB box, which is missing in FhuA $\Delta 5$ –160. TonB interacts also with the β barrel and induces a conformation in FhuA that leads to the release of ferrichrome from its residual binding sites at the β barrel and its diffusion into the periplasm; allows the binding of Ton-dependent phages to the most prominent loop (L4) at the cell surface (72) so that their DNA is released and taken up into the cells; and allows the import of colicin M into the cytoplasmic membrane, where it inhibits murein and LPS synthesis by interference with C₅₅-polyisoprenoid pyrophosphate regeneration. The crystal structure of albomycin bound to FhuA reveals that the iron-chelating portion of albomycin binds to the same site as ferrichrome and the antibiotic moiety is located in the cavity that is exposed to the cell surface. Surprisingly, albomycin can assume two conformations in FhuA—an extended and a bent conformation—that occur at about the same frequency (73). The binding site of the structurally very dissimilar rifamycin CGP 4832 overlaps with the ferrichrome-binding site and also extends into the surface cavity (74). Active transport of rifamycin CGP 4832 via FhuA decreases the minimal inhibitory concentration 200-fold as compared to unmodified rifamycin (75). In general, active transport of antibiotics into bacteria as compared to mere diffusion greatly decreases the concentration required to kill the cells (76).

The following tentative mechanism may be envisioned for the active transport of ferrichrome, albomycin, and rifamycin CGP 4832 across the outer membrane. The substrates bind to the active center of the FhuA transporter. Ferrichrome and albomycin cause a large structural change in the FhuA N terminus that brings the TonB box into position to interact productively with the TonB protein. No such structural change has been observed in the FhuA crystal loaded with rifamycin CGP 3847, but this could still occur *in vivo* prior to transport. Energized TonB alters the conformation of FhuA such that the substrates are released, a channel is opened in FhuA,

and the substrates enter the periplasm. FhuA $\Delta 5-160$ contains a channel that probably differs from the channel formed by wild-type FhuA. The conformational change in FhuA $\Delta 5-160$ induced by energized TonB occurs via the β barrel and weakens binding of ferrichrome to the amino acid residues on the β barrel, which results in the release of ferrichrome and diffusion into the cytoplasm. Translocation of ferrichrome may also occur via facilitated diffusion such that ferrichrome binds to amino acid residues on its way through FhuA into the periplasm. Energized TonB assumes a conformation that is different from that of the energetic ground state. TonB, together with ExbB and ExbD, could form a regulated channel in the cytoplasmic membrane through which protons flow from the outside to the inside of the membrane, as occurs in the F_0 portion of the F_1F_0 ATPase. Protonation of His20 in the TonB transmembrane region may trigger the conformational change from the ground state to the excited state. TonB can be considered as the regulatory entity of the FhuA transporter, like the regulatory subunit of an allosteric enzyme. As it activates FhuA, TonB loses its energized conformation and assumes the energetic ground state. This is accompanied by the dissociation of the proton from His20. The proton is discharged into the cytoplasm directly or through Asp25 in the transmembrane region of ExbD. As long as His20 is protonated, it is inaccessible to additional protons from the periplasm, thus avoiding a permanently open channel through which the proton gradient of the cytoplasmic membrane would collapse. After discharge of the proton, His20 is again accessible, allowing re-energization of TonB in preparation for another transport cycle.

2. Outer-Membrane Proteins That Bind Transferrin and Lactoferrin

Transferrin is contained in human serum (25–44 μM), and lactoferrin is found in mucosal secretions (6–13 μM) and leukocytes, from where it may be released at sites of microbial infections. Thus, throughout the human body, these iron-binding glycoproteins strongly reduce the free iron concentration for microbial invaders in the extracellular milieu (affinity for Fe^{3+} 10^{22} M^{-1}). Bacteria that can use transferrin and lactoferrin iron have a great advantage over those that cannot. Gram-negative bacteria such as *Neisseriaceae* and *Pasteurellaceae* synthesize two outer-membrane proteins, TbpA and TbpB, for binding of transferrin, and LbpA and LbpB for binding of lactoferrin (3). In-vitro studies with purified dimeric TbpA TbpB, or with TbpA or TbpB alone, demonstrate that no iron transfer occurs directly from transferrin to the periplasmic binding protein FbpA (see Sec. B.2), but through the activity of TbpA and TbpB, where the TbpA TbpB complex is the most active entity (77). These data indicate mobilization of transferrin iron by TbpA TbpB and transfer of iron to FbpA. In vivo, mutants lacking TbpB still take up transferrin iron, but much less efficiently than TbpA TbpB wild-type cells. In vivo, iron has to be transported across the outer membrane until it gains access to FbpA. It is not known whether FbpA interacts with TbpA TbpB, resulting in transfer of iron from one protein to the next; such an interaction would have the advantage that the iron released from TbpA TbpB does not precipitate in the periplasm. TbpA contains the TonB box through which TbpA receives the energy, as shown by transport-inactive TonB box mutants (78). TbpA interacts functionally with TbpB; TbpA prevents TbpB proteolysis when energized via TonB. TbpB is protease-sensitive in a TonB mutant, a TbpA TonB-box mutant, and in de-energized cells. The iron-binding sites of transferrin and lactoferrin may open upon binding to the bacterial outer-membrane transporters. Trans-

port of iron requires energy input by the Ton system, but it is not certain whether energy is required only for opening of the TbpA channel or whether it is also needed for a step prior to translocation across the outer membrane, such as transfer of iron from transferrin to TbpA TbpB.

In *Actinobacillus pleuropneumoniae*, the genes of the energy-transducing proteins TonB, ExbB, and ExbD and the outer-membrane transporters TbpA and TbpB are organized in an operon in the order *tonB exbB exbD tbpB tpbA*. Cotranscription of these genes under conditions of iron deprivation indicates that they form a functional unit in the transport of transferrin iron.

III. REGULATION OF BACTERIAL IRON TRANSPORT

A. Regulation by the Fe^{2+} –Fur Repressor Protein

The observation that expression of siderophore receptors is strongly regulated by the iron supply of the cells dates back to the 1970s. A 10- to 20-fold induction of siderophore receptors in the outer membranes of Gram-negative bacteria under iron-limiting growth conditions was observed. The Fur repressor protein (ferric iron uptake regulator) and Fe^{2+} as co-repressor were shown to direct the synthesis of siderophores and siderophore uptake systems in Gram-negative bacteria.

Iron supply is an important virulence determinant for many pathogenic bacteria (1), and also several bacterial toxins are expressed mainly under iron deficiency (79). This led to a continuous interest of medical microbiologists in iron uptake and regulation in pathogenic bacteria. In nearly every important pathogen, iron transport systems and their Fur regulators have been identified. However, most of these studies demonstrated the similarities to the well-studied *E. coli* Fur protein without adding new insights into its function (1).

Structural studies on the Fur protein identified the DNA-binding site in the N-terminal domain of the protein (80). The protein structure predicted from the amino acid sequence place this protein into the superfamily of CAP-like dimeric regulatory proteins (81). In these proteins, the N-terminal domain contains the DNA-binding site, while the C-terminal domain is important for dimerization; this is in agreement with the structural studies on Fur. It was surprising to find out that Fur contains one zinc ion in addition to the regulatory active Fe^{2+} . It is assumed that Cys92 and Cys95 in the C-terminal domain of Fur bind Zn^{2+} (82,83). The binding site of the regulatory Fe^{2+} is less well defined—it is certain from spectroscopic data that cysteine is not a binding partner. Rather, histidines and carboxylates seem to bind the iron (84).

The sequence of the Fur- Fe^{2+} DNA-binding sites was defined by DNase I footprinting experiments; the consensus sequence GATAATGATAATCATTATC was identified (85). Further studies led to the interesting suggestion that not this palindrome, but three tandem GATAAT hexanucleotides are recognized. The polarity of the hexanucleotides did not matter (86). Oligomerization and wrapping of Fur around the DNA strand site was observed at high Fur concentrations (87), which may be explained by the unusual type of Fur–DNA contact, which has not been observed for other members of the CAP superfamily of regulatory proteins. Unfortunately, no suitable crystals for an X-ray structure determination of Fur have been obtained.

In some bacterial species (*E. coli*, *Vibrio anguillarum*, *Yersinia pestis*, and others), it is possible to select Fur mutants on a complex medium that is low in

magnesium and high in manganese (88). Some of the manganese-resistant mutants are mutated in *fur*, and it is assumed that Mn^{2+} competes with Fe^{2+} for the binding site at Fur, which leads to a repression of the iron uptake genes needed for the iron supply of the cells. Fur mutants have a growth advantage on this type of medium since their iron uptake systems are derepressed. *E. coli* K-12 *fur* mutants have the following phenotype: high production of the siderophore enterochelin, expression of the outer-membrane siderophore receptors, and expression of iron-regulated reporter genes in iron-rich media. Fur not only regulates iron uptake, it also has a strong influence on the internal balance between Fe^{2+} and Fe^{3+} , which is normally about 50% Fe^{2+} /50% Fe^{3+} . According to results of Mössbauer spectroscopy studies, this changes in a *fur* mutant to 70% Fe^{2+} /30% Fe^{3+} (89). This imbalance may be the reason for the poorer functioning of the respiratory chain, as indicated by the finding that *fur* mutants do not grow well on minimal media with carbon sources such as acetate, succinate, or malate (88).

Cells with a *fur* mutation can cope with the oxidative stress generated by the Fenton reaction, in which Fe^{2+} is oxidized and highly reactive hydroxyl radicals are generated. However, their redox sensitivity is disclosed in certain double mutants. The high content of reactive Fe^{2+} seems to be the reason why a *fur recA* double mutation is lethal under oxic conditions (90). This lethality can be cured by a *tonB* mutation, which reduces iron uptake, or by a plasmid expressing the FtnA ferritin. Interestingly, *fur ftnA* or *fur bfr* (*bfr* codes for bacterioferritin) double mutants show an increased sensitivity to hydroperoxides, but not to superoxide or NO (91). The reason for the protective function of the ferritins may be their capacity to store iron in a safe environment, or their enzymatic activity to oxidize Fe^{2+} , which may help to balance the Fe^{2+}/Fe^{3+} ratio. The superoxide dismutases *sodA* and *sodB* are also regulated by Fur. The expression of the manganese-containing SodA is repressed by Fur-iron, while synthesis of the iron-containing SodB is activated by an unknown Fur-dependent mechanism.

The multifunctional properties of Fur are also apparent from the recently detected regulation of *fur* by the oxidative stress regulators OxyR and SoxRS. Hydrogen peroxide activates OxyR through the oxidation of two cysteines. At this stage, OxyR activates the transcription of peroxidases and other defense proteins. OxyR also binds to the *fur* promoter and activates its transcription (92). Superoxide activates the transcription factor SoxR by damaging the [2Fe-2S] cluster of this protein. The oxidized SoxR then induces the expression of a second transcription factor, SoxS, which activates the transcription of *sodA*, *fpr* (ferredoxin reductase), *zwf* (glucose-6-phosphate reductase), *acnA* (aconitase A), and the polycistronic messenger encompassing *fur* and its upstream gene *fldA*, which codes for a flavodoxin. In addition, SoxS binds to the *fldA* promoter (92). This demonstrates how intimately Fur is connected to the oxidative stress response of the cell.

In most Gram-positive bacteria, the DtxR regulator (see below) seems to regulate siderophore synthesis and iron uptake. However, *fur*-like genes have been found in all Gram-positive organisms whose genomes have been fully or partially sequenced. In mycobacteria, a *fur*-like gene, *furA*, is upstream of *katG* (encodes a catalase-peroxidase). It is not known whether *katG* is regulated by FurA (93). In a study of the very similar CpeB catalase-peroxidase of *Streptomyces reticuli*, the same gene order *furS cpeB* is found. FurS and FurA of *Mycobacterium tuberculosis* have 64% identity. In this case, it was demonstrated that the divalent metal chelators EDTA

and diethylenetriaminepentaacetic acid derepress the production of CpeB (94). CpeB is a mycelium-associated protein that is exported by an unknown route. The enzyme has a broad substrate specificity, and it is not known why it should be induced under low iron. It is feasible that CpeB protects cells against radicals generated by high amounts of flavins produced under low-iron stress by certain fungi.

B. subtilis contains three *fur*-like genes. One Fur-like protein seems to regulate siderophore biosynthesis and iron uptake, the second protein, PerR, is a peroxide regulon repressor (95), and the third protein regulates zinc uptake (96). *perR* mutants overproduce catalase KatA, alkyl-hydroperoxidase AhpC, and the protective DNA-binding protein MrgA. PerR does not seem to be very specific in its metal-binding properties. In the *perR*⁺ strain, H₂O₂ or limitation of iron and manganese derepress the regulon. These reports show that in Gram-positive bacteria some proteins of the Fur family are specialized in regulating particular oxidative stress responses, while other proteins regulate iron uptake or zinc uptake. This is a caveat to all who want to derive functions only from sequences.

Fur is not only a repressor; in some cases it seems to act in an unknown way as a positive regulator. Fur-iron activates production of SodB (iron-containing superoxide dismutase) in *E. coli*. Another, less characterized example in enterobacteria is found in the acid stress response regulon. In *Salmonella enterica*, eight gene products of the acid stress response are induced by Fur in an iron-independent manner (97,98). How this positive regulation is achieved by Fur is not known.

B. Regulators Regulated by Fur

Several iron transport systems and proteins are regulated by a Fur-regulated regulator; in most instances, this allows the integration of additional environmental signals into the regulatory circuit. One of the first and best-studied examples is the induction of ferric citrate uptake system in *E. coli* (see below).

It has long been known that in *Pseudomonas aeruginosa*, exotoxin A is regulated by iron. However, it has only in recent years become clear that a cascade of regulators, including Fur, controls toxin expression. In addition, a variety of different types of regulators of siderophore transport were found to be regulated by Fur: alternative sigma factors, two-component regulatory systems, and AraC-like regulators (99). Additional regulatory principles with Fur and iron in *Vibrio cholerae* and *V. anguillarum* have been described (1,4).

C. DtxR-Like Proteins Regulate Iron Uptake and Oxidative Stress Response in Gram-Positive Bacteria

The study of the long-known phenomenon of the iron regulation of diphtheria toxin production led to the detection of the diphtheria toxin regulator DtxR, which is a new type of iron regulator, found mainly in Gram-positive bacteria. The DtxR amino acid sequence is not related to that of Fur, although the 3-D structures show some similarities. DtxR and related proteins, such as IdeR from mycobacteria, regulate iron uptake and metabolism and have some less well characterized influence on oxidative stress response genes (100–102).

Results of footprinting experiments indicated that DtxR and iron repress the synthesis of HmuO, which is the first bacterial heme oxygenase identified in *C. diphtheriae*. Transcription of the gene is regulated by heme and by iron: only in the

presence of heme or hemoglobin under low-iron growth conditions is high expression achieved (103). In addition, a two-component system that transmits the heme signal was identified (104). This regulation indicates that heme–iron can be used by *C. diphtheriae* in the human host, where the bacteria are confronted with growth-limiting iron concentrations but with a sufficient supply of heme.

SirR, which is homologous to DtxR, was found in staphylococci during the study of the iron-regulated operon *sitABC*. Purified SirR protein bound in an iron-dependent or manganese-dependent manner to a synthetic oligonucleotide derived from a hypothetical Sir box of an iron-regulated operon. This provides indirect evidence that also in staphylococci a DtxR-like protein may regulate iron transport.

TroR is the first DtxR-like protein identified in a Gram-negative bacterium. In *Treponema pallidum*, TroR seems to regulate a binding protein-dependent ABC transporter that has similarity to manganese transporters. TroR is exceptionally specific, since it is activated only by Mn^{2+} and not by Fe^{2+} . It is interesting to note that the level of manganese in the brain is 100-fold higher than in the blood (105), which brings to mind that during the late stages of syphilis, the central nervous system is affected. *T. pallidum* is a highly adapted pathogen that possibly does not need iron for growth. In the sequence of the 1.3-Mb genome, no indications of genes for heme proteins, iron–sulfur proteins, and non-iron–sulfur nonheme proteins were found. The iron requirement of *T. pallidum* has not been tested because it is not possible to culture the organism in vitro.

Very little is known about iron transport and regulation in archaea. Putative genes encoding DtxR-like molecules have been found in the sequenced genomes. The regulation of the MDR1 operon by the MDR1 protein of *Archaeoglobus fulgidus* is metal-dependent. In vitro, MDR1 binds in a Me^{2+} -dependent way to three sites at the promoter of this operon (106).

The examples mentioned above show that DtxR-like proteins have a much wider distribution than expected at the time they were first detected.

The structures of DtxR and IdeR have been determined by X-ray studies (107,108). Crystals of two DtxR dimers with a DNA fragment of the binding site showed the binding of the N-terminal domain (residues 1–73) to DNA, the domain for dimerization (74–140), and the C-terminal domain with contacts to the N-terminal domain (109). The C-terminal domain has structural similarity to the three Scr domains that bind internally to proline-containing peptides. A similar binding function was suggested for the C-terminal domain of DtxR to the proline-containing peptide near residue 130 (110). It is proposed that this binding influences the monomer/dimer equilibrium.

D. Is There an Iron-Responsive RNA-Binding Protein in Bacteria?

In eukaryotic cells, the cytosolic enzyme aconitase has a central function in regulation of iron uptake, metabolism, and oxidative stress response. The enzymatically active enzyme contains an iron–sulfur center. Under low-iron conditions or under oxidative stress, the center is not present or is damaged, which allows binding of certain mRNAs to the inactive protein. The binding of mRNAs is controlled by certain stem–loop structures called iron-responsive elements (IREs) (see Chapter 9). Depending on their position in the mRNA, their binding may inhibit translation (IRE in the 5' untranslated region) or may stabilize the mRNA (IRE in the 3' untranslated region) and enhance the amount of product. Aconitases are well conserved in evo-

lution; the aconitase A of *E. coli* is 53% identical to the human aconitase IRP1. Apo-aconitase A stabilizes mRNA of aconitases A and B. The increase of aconitase A and B synthesis by apo-aconitase A was observed in vitro (111). Other iron and oxidative stress proteins are most likely also regulated by this posttranscriptional mechanism. Further evidence for this regulatory principle comes from studies with the aconitase from *B. subtilis*, which as an apo-enzyme binds IRE-like elements on mRNA of the major cytochrome oxidase and a putative iron transporter (112). In addition, the aconitase is important for the differentiation from vegetative cells to the spore forms. Similarly, in *Streptomyces coelicolor*, an *acnA* mutation impairs the ability to differentiate. The mutant is unable to develop an aerial mycelium, to sporulate, and to produce the antibiotic phosphinotricin (113). Further research is necessary to clarify the contribution of translational control to the overall regulation of iron transport and metabolism of the prokaryotic cell.

E. Novel Mechanism of Transcriptional Control of the Ferric Citrate Transport System via Transmembrane Signaling

E. coli K-12 uses ferric citrate as an iron source and contains a ferric citrate transport system. Transport of Fe^{3+} via citrate occurs after growth of the bacteria in an iron-limited medium in the presence of at least 0.1 mM citrate. Cells first recognize iron limitation, and then they synthesize the system that is appropriate for transport of the Fe^{3+} chelate contained in the growth medium. Regulation is achieved by six proteins, four of which are also involved in Fe^{3+} -citrate transport. The various parameters—synthesis of the transport system when it is needed, selection of the right system among the six transport systems available for *E. coli* K-12, and the use of transport components for regulation that does not involve transport—add to the highly economic and sophisticated process.

Seven genes, organized and transcribed in the order *fecIRABCDE*, are specific for Fe^{3+} -citrate transport and regulation. *fecIR* encode regulatory functions; *fecABCDE* encode transport functions. Upon iron starvation, repression of the *fecIR* regulatory genes by Fe^{2+} -Fur is relieved, and the genes are transcribed. The FecIR regulatory proteins formed are not active, but require Fe^{3+} -citrate for activation. What are the functions of the FecIR proteins and how are they activated?

Fe^{3+} -citrate is the inducer, as shown by trapping of iron by deferriferrichrome, which abolishes induction (114). Fe^{3+} -citrate binds to the FecA protein, but the transport activity of FecA across the outer membrane is not required for induction, as shown by a FecA deletion mutant in which residues 14–68 of the mature protein are removed. This derivative no longer induces *fec* transport gene transcription, but fully transports Fe^{3+} -citrate (115). FecA contains a longer N terminus than all the other *E. coli* Fe^{3+} -siderophore transporters, which are not involved in Fe^{3+} -siderophore-specific transcription induction. In addition, a *fecA* missense mutant (*fecA4*) constitutively induces *fec* transport gene transcription in the absence of Fe^{3+} -citrate and TonB (116). The entire Ton system (TonB, ExbB, and ExbD) is required for induction, as it is required for transport of Fe^{3+} -citrate across the outer membrane. Other *fecA* missense mutants display constitutive expression. This together with the phenotype of the deletion mutant prove beyond doubt the direct involvement of FecA in induction (116). FecA plays a dual role as a transporter and a regulator.

The question arises how Fe^{3+} -citrate induces when it does not enter the cells. The presence of Fe^{3+} -citrate is recognized by the cells through the binding to FecA.

Since FecA belongs to the outer-membrane iron transporters, it is legitimate to deduce that Fe^{3+} -citrate is bound close to the cell surface, as has been shown for binding of ferrichrome to FhuA (61,62). FecA must transmit its occupation with Fe^{3+} -citrate across the outer membrane into the periplasm. This may occur by a conformational change similar to that observed when ferrichrome binds to FhuA, which is propagated from the cell surface across the entire width of the outer membrane into the periplasm. By this means, an induction-competent conformation is assumed by the N terminus of FecA.

The Fe^{3+} -citrate signal is transmitted across the cytoplasmic membrane by the FecR regulatory protein, which is probably oriented such that residues 101–317 are in the periplasm, 85–100 form a hydrophobic transmembrane segment, and 1–84 are located in the cytoplasm (117). The transmembrane topology is perfectly suited for transduction of the Fe^{3+} -citrate signal that FecR receives from FecA. Interaction of the N terminus of FecA with FecR and of FecA_{1–79} with FecR_{101–317} has been demonstrated (118), which suggests that this interaction transmits the Fe^{3+} -citrate signal. The mechanism of how the signal is transmitted across the cytoplasmic membrane is not known. FecR forms a dimer or oligomer (A. Stiefel, S. Enz, and V. Braun, unpublished), but no evidence exists that the interconversion of monomers and oligomers forms the structural basis of the signal transmission.

In the cytoplasm, the signal must be transmitted to the FecI regulatory protein, which is an alternative sigma factor of the σ^{70} type. FecI only recognizes the promoter upstream of the *fecA* gene that controls transcription of all *fecABCDE* transport genes (119). FecI binds together with the RNA polymerase apoenzyme to the *fecA* promoter, as shown by DNA band shift with *fecA* promoter DNA and competition of a surplus of plasmid-encoded *fecA* promoter DNA, which prevents binding of FecI-RNA polymerase to the chromosomal *fecA* promoter. The *fecA* promoter extends to position +13, as was demonstrated by the lack of binding of FecI-RNA polymerase to *fecA* promoter DNA containing point mutations (119,120). Binding of FecR to FecI and of FecR_{1–85} to FecI_{1–173} has been shown (118), which indicates a direct interaction of the two regulatory proteins for signal transduction. It is not known by which mechanism FecI is activated. The finding that FecI in a crude extract of induction-competent cells grown in the presence of Fe^{3+} -citrate is active (119) argues in favor of a chemical modification of FecI. A test for phosphorylation was negative (A. Angerer and V. Braun, unpublished).

As long as there is sufficient iron in the medium, the Fe^{2+} -Fur protein represses transcription of the *fecIR* genes. Binding of Mn^{2+} -Fur (Mn^{2+} was used instead of Fe^{2+} since Fe^{2+} is easily oxidized) to the promoter of *fecIR* upstream of *fecI* has been demonstrated by DNase I footprint analysis (121). However, Mn^{2+} -Fur also bound to the *fecA* promoter, which indicates immediate repression of *fecABCDE* transcription after sufficient iron has been transported via citrate into the cells. If repression occurred only at the *fecI* promoter, the FecIR regulatory proteins would have to be diluted out during growth of the cells, which would take several generations until the regulatory proteins reached levels below the inducing concentration.

F. Regulatory Systems That Function Similar to the fec Device

Pseudomonas putida regulates synthesis of the PupB outer-membrane transport protein for Fe^{3+} -pseudobactin BN8 by a mechanism similar to that of the *E. coli fec*

system (122). Pseudobactin BN8 in the growth medium enhances the amount of PupB in the outer membrane. The direct involvement of PupB in induction was shown by the creation of a chimeric protein in which the N-terminal region of PupA, an outer-membrane transport protein similar to PupB, was replaced by the N-terminal region of PupB. In response to Fe^{3+} -pseudobactin 358 (Fig. 1), the siderophore specific for PupA, PupB synthesis was increased. PupA as such does not induce its own synthesis in response to pseudobactin 358 and BN8. *P. putida* contains genes homologous to the *E. coli fecIR* regulatory genes that are required for the induction of PupB synthesis. Deletion of *pupR* results in synthesis of PupB, in contrast to the deletion of *fecR*, which abolishes induction of *fecABCDE* transcription. In this system, PupR would serve as a repressor of PupI activity. More work on the *P. putida* system is required to resolve this apparent difference to the Fec system.

The genome of *P. aeruginosa* carries six pairs of genes homologous to *fecIR* (Table 1). In four of them (ORFs 6976, 8492, 9092, 10600), *fecA* homologs occurs adjacent to *fecIR*, but no additional transport genes homologous to the *E. coli fecBCDE* genes are located downstream of *fecA*. It is very likely that the FecIRA homologs function as regulatory proteins similar to the *E. coli* FecIRA proteins. Two of the FecA homologs probably function as heme transporters, as has been shown for one of them (see Sec. II.B.3).

The ferric pyoverdinin receptor FpvA of *P. aeruginosa* contains an extended N terminus like FecA, which suggests that it is, like FecA, not only a transporter but also a transcription regulator. The sequence of the N-terminus displays 23% identity to FecA and 30% to PupB. In a highly purified state, FpvA contains iron-free pyoverdinin, which binds to FpvA with the same affinity as iron-loaded pyoverdinin (123). For transport, Fe^{3+} either binds to pyoverdinin attached to FpvA, or Fe^{3+} -pyoverdinin

Table 1 Protein Homolog of FecI, FecR, and FecA in Other Bacterial Species

Organism	Percent identity (protein or ORF number ^a)			Function
	FecI	FecR	FecA	
<i>Pseudomonas aeruginosa</i>	47% (10598)	35% (10599)	64% (10600)	Putative iron citrate transporter
	46% (9094)	37% (9093)	24% (9092)	Putative ferrioxamine transporter
	43% (8494)	38% (8493)	25% (8492)	Unknown ferric siderophore transporter
	41% (6978)	29% (6977)	24% (6976)	Hydroxamate-type ferric siderophore transporter
	39% (11637)	36% (11636)	20% (HasR)	Heme transporter
	27% (10089)	34% (10088)	20% (HasR)	Heme transporter
<i>Pseudomonas putida</i>	41% (PupI)	35% (PupR)	20% (PupB)	Ferric pseudobactin transporter
<i>Serratia marcescens</i> ^b	35% (HasI)	28% (HasS)	20% (HasR)	Heme transporter

^aORF numbers represent the designation found in the *Pseudomonas* genome project database (<http://www.pseudomonas.com>).

^bJ.-M. Ghigo and C. Wandersmann, personal communication.

exchanges with unloaded pyoverdinin on FpvA. If binding of pyoverdinin, which is usually in excess over Fe³⁺-pyoverdinin in the growth medium, already triggers a conformation change in FpvA as is observed in FhuA when ferrichrome binds, and if substrate-loaded transporters preferentially interact with TonB, then TonB might accelerate Fe³⁺ loading of FpvA-bound pyoverdinin or the exchange reaction. In this case, TonB would act in a step prior to the release of Fe³⁺-pyoverdinin from the active centers and its translocation through the opened FpvA channel.

ACKNOWLEDGMENTS

The authors' work was supported by the Deutsche Forschungsgemeinschaft and the Fonds der Chemischen Industrie. We thank Michael Braun for computer drawings and Karen Brune for critical reading of the manuscript.

REFERENCES

1. Braun V, Hantke K, Köster W. Bacterial iron transport: mechanisms, genetics, and regulation. In: Sigel A, Sigel H, eds. *Metal Ions in Biological Systems*. Vol. 35, Iron Transport and Storage in Microorganisms, Plants and Animals. New York: Marcel Dekker, 1998:67–145.
2. Mietzner TA, Tencza SB, Adhikari P, Vaughan KG, Nowalk AJ. Fe(III) periplasm-to-cytosol transporters of gram-negative pathogens. *Curr Top Microbiol Immunol* 1998; 35:113–135.
3. Schryvers AB, Stojiljkovic I. Iron acquisition systems in the pathogenic *Neisseria*. *Mol Microbiol* 1999; 32:1117–1123.
4. Crosa JH. Signal transduction and transcriptional and posttranscriptional control of iron-regulated genes in bacteria. *Microbiol Mol Biol Rev* 1997; 61:319–336.
5. Earhart CF. Uptake and metabolism of iron and molybdenum. In: Neidhart FC, ed. *Escherichia coli and Salmonella typhimurium*. 2d ed. Washington, DC: ASM Press, 1996:1075–1090.
6. Braun V, Hantke K. Receptor-mediated bacterial iron transport. In: Winkelmann G, Carrano CJ, eds. *Transition Metals in Microbial Metabolism*. Amsterdam: Harwood, 1997:81–116.
7. Suo Z, Walsh CT, Miller DA. Tandem heterocyclization activity of the multidomain 230 kDa HMWP2 subunit of *Yersinia pestis* yersiniabactin synthetase: interaction of the 1-1382 and 1383-2035 fragments. *Biochemistry* 1999; 38:17000.
8. Drechsel H, Stephan H, Lotz R, Haag H, Zähler H, Hantke K, Jung G. Structure elucidation of yersiniabactin, a siderophore from highly virulent *Yersinia* strains. *Liebigs Ann* 1995:1727–1733.
9. De Voss JJ, Rutter K, Schroeder BG, Barry CE. Iron acquisition and metabolism by mycobacteria. *J Bacteriol* 1999; 181:4443–4451.
10. De Voss JJ, Rutter K, Schroeder BG, Su H, Zhu Y, Barry CE. The salicylate-derived mycobactin siderophores of *Mycobacterium tuberculosis* are essential for growth in macrophages. *Proc Natl Acad Sci USA* 2000; 97:1252–1257.
11. Martinez JS, Zhang GP, Holt PD, Jung HT, Carrano CJ, Haygood MG, Butler A. Self-assembling amphiphilic siderophores from marine bacteria. *Science* 2000; 287:1245–1247.
12. Drechsel H, Winkelmann G. Iron chelation and siderophores. In: Winkelmann G, Carrano CJ, eds. *Transition Metals in Microbial Metabolism*. Amsterdam: Harwood, 1997: 1–49.

13. Schneider E, Hunke S. ATP-binding-cassette (ABC) transport systems: functional and structural aspects of the ATP-hydrolyzing subunits/domains. *FEMS Microbiol Rev* 1998; 22:1–20.
14. Boos W, Shuman H. Maltose/maltodextrin system of *Escherichia coli*: transport, metabolism, and regulation. *Microbiol Mol Biol Rev* 1998; 62:204–229.
15. Fecker L, Braun V. Cloning and expression of the *fhu* genes involved in iron(III) hydroxamate uptake by *Escherichia coli*. *J Bacteriol* 1983; 156:1301–1314.
16. Schultz-Hauser G, Köster W, Schwarz H, Braun V. Iron(III) hydroxamate transport in *Escherichia coli* K-12: FhuB mediated membrane association of the FhuC protein and negative complementation of *FhuC* mutants. *J Bacteriol* 1992; 174:2305–2311.
17. Köster W, Braun V. Iron hydroxamate transport of *Escherichia coli*: nucleotide sequence of the *fhuB* gene and identification of the protein. *Mol Gen Genet* 1986; 204: 435–442.
18. Köster W, Braun V. Iron-hydroxamate transport into *Escherichia coli* K12: localization of FhuD in the periplasm and of FhuB in the cytoplasmic membrane. *Mol Gen Genet* 1989; 217:233–239.
19. Groeger W, Köster W. Transmembrane topology of the two *FhuB* domains representing the hydrophobic components of bacterial ABC transporters involved in the uptake of siderophores, haem and vitamin B12. *Microbiology* 1998; 144:2759–2769.
20. Böhm B, Boschert H, Köster W. Conserved amino acids in the N- and C-terminal domains of integral membrane transport FhuB define sites important for intra- and intermolecular interactions. *Mol Microbiol* 1996; 20:223–232.
21. Köster W, Böhm B. Point mutations in two conserved glycine residues within the integral membrane protein FhuB affect iron(III)hydroxamate transport. *Mol Gen Genet* 1992; 232:399–407.
22. Burkhardt R, Braun V. Nucleotide sequence of *fhuC* and *fhuD* genes involved in iron(III)-hydroxamate transport: domains in FhuC homologous to ATP binding proteins. *Mol Gen Genet* 1987; 209:49–55.
23. Coulton JW, Mason P, Allat DD. *fhuC* and *fhuD* genes for iron(III)-ferrichrome transport into *Escherichia coli* K-12. *J Bacteriol* 1987; 169:3844–3849.
24. Becker K, Köster W, Braun V. Iron(III)hydroxamate transport of *Escherichia coli* K-12: single amino acid replacements at potential ATP-binding sites inactivate the FhuC protein. *Mol Gen Genet* 1990; 223:159–162.
25. Schultz-Hauser. FhuC, die “konservierte Komponente” des Eisen(III)-Hydroxamat-Transports. Thesis, Tübingen, Germany, 1992.
26. Engel. Isolierung und Charakterisierung der FhuC ATPase des Eisen(III)-Hydroxamat-Transportsystems von *Escherichia coli*. Diplomarbeit, Tübingen, Germany, 1999.
27. Köster W, Braun V. Iron(III)hydroxamate transport into *Escherichia coli*. Substrate binding to the periplasmic FhuD protein. *J Biol Chem* 1990; 265:21407–21410.
28. Rohrbach MR, Braun V, Köster W. Ferrichrome transport in *Escherichia coli* K-12: altered substrate specificity of mutated periplasmic FhuD and interaction of FhuD with the integral membrane protein FhuB. *J Bacteriol* 1995; 177:7186–7193.
29. Mademidis A, Killmann H, Kraas W, Flechsner I, Jung G, Braun V. ATP-dependent ferric hydroxamate transport system in *Escherichia coli*: periplasmic FhuD interacts with a periplasmic and a transmembrane/cytoplasmic region of the integral membrane protein FhuB, as revealed by competitive peptide mapping. *Mol Microbiol* 1997; 26: 1109–1123.
30. Braun V, Killmann H. Bacterial solutions to the iron-supply problem. *Trends Biochem Sci* 1999; 24:104–109.
31. Rosenberg MF, Callaghan R, Ford RC, Higgins CF. Structure of the multidrug resistance P-glycoprotein to 2.5 nm resolution determined by electron microscopy and image analysis. *J Biol Chem* 1997; 272:10685–10694.

32. Clarke TE, Ku S-Y, Dougan DR, Vogel H, Tari LW. The structure of the *Escherichia coli* periplasmic ferric siderophore binding protein FhuD complexed with gallichrome. *Nat Struct Biol* 2000; 7:287–291.
33. Zimmermann L, Angerer A, Braun V. Mechanistically novel iron(III) transport system in *Serratia marcescens*. *J Bacteriol* 1989; 171:238–243.
34. Angerer A, Gaisser S, Braun V. Nucleotide sequences of the *sfuA*, *sfuB*, and *sfuC* genes of *Serratia marcescens* suggest a periplasmic-binding-protein-dependent iron transport mechanism. *J Bacteriol* 1990; 172:572–578.
35. Bruns CM, Nowalk AJ, Arvai AS, McTigue MA, Vaughan KG, Mietzner TA, McRee DE. Structure of *Haemophilus influenzae* Fe(+3)-binding protein reveals convergent evolution within a superfamily. *Nat Struct Biol* 1997; 4:919–924.
36. Bearden SW, Staggs TM, Perry RD. An ABC transporter system of *Yersinia pestis* allows utilization of chelated iron by *Escherichia coli* SAB11. *J Bacteriol* 1998; 180: 1135–1147.
37. Zhou D, Hardt WD, Galan JE. *Salmonella typhimurium* encodes a putative iron transport system within the centisome 63 pathogenicity island. *Infect Immun* 1999; 67: 1974–1981.
38. Modun BJ, Cockayne A, Finch R, Williams P. The *Staphylococcus aureus* and *Staphylococcus epidermidis* transferrin-binding proteins are expressed in vivo during infection. *Microbiology* 1998; 144:1005–1012.
39. Modun B, Williams P. The staphylococcal transferrin-binding protein is a cell wall glyceraldehyde-3-phosphate dehydrogenase. *Infect Immun* 1999; 67:1086–1092.
40. Modun B, Evans RW, Joannou CL, Williams P. Receptor-mediated recognition and uptake of iron from human transferrin by *Staphylococcus aureus* and *Staphylococcus epidermidis*. *Infect Immun* 1998; 66:3591–3596.
41. Stojiljkovic I, Hantke K. Hemin uptake system of *Yersinia enterocolitica*: similarities with other TonB-dependent systems in gram-negative bacteria. *EMBO J* 1992; 11: 4359–4367.
42. Stojiljkovic I, Hantke K. Transport of haemin across the cytoplasmic membrane through a haemin-specific periplasmic binding-protein-dependent transport system in *Yersinia enterocolitica*. *Mol Microbiol* 1994; 13:719–732.
43. Hornung JM, Jones HA, Perry RD. The *hmu* locus of *Yersinia pestis* is essential for utilization of free haemin and haem protein complexes as iron source. *Mol Microbiol* 1996; 20:725–739.
- 43a. Thompson JM, Jones HA, Perry RD. Molecular characterization of the hemin uptake locus (*hmu*) from *Yersinia pestis* and analysis of *hmu* mutants for hemin and hemo-protein utilization. *Infect Immun* 1999; 67:3879–3892.
44. Hinnebusch BJ, Perry RD, Schwan TG. Role of the *Yersinia pestis* hemin storage (*hms*) locus in the transmission of plague by fleas. *Science* 1996; 273:367–370.
45. Ochsner UA, Johnson Z, Vasil ML. Genetics and regulation of two distinct haem-uptake systems, *phu* and *has*, in *Pseudomonas aeruginosa*. *Microbiology* 2000; 146: 185–198.
46. Wyckoff EE, Duncan D, Torres AG, Mills M, Maase K, Payne SM. Structure of the *Shigella dysenteriae* haem transport locus and its phylogenetic distribution in enteric bacteria. *Mol Microbiol* 1998; 28:1139–1152.
47. Occhino DA, Wyckoff EE, Henderson DP, Wrona TJ, Payne SM. *Vibrio cholerae* iron transport: haem transport genes are linked to one of two sets of *tonB*, *exxB*, *exbD* genes. *Mol Microbiol* 1998; 29:1493–1507.
48. Morton DJ, Whitby PW, Jin H, Ren Z, Stull TL. Effect of multiple mutations in the hemoglobin- and hemoglobin-haptoglobin-binding proteins, HgpA, HgpB, and HgpC, of *Haemophilus influenzae* type b. *Infect Immun* 1999; 67:2729–2739.
49. Ren Z, Jin H, Whitby PW, Morton DJ, Stull TL. Role of CCAA nucleotide repeats in regulation of hemoglobin and hemoglobin-haptoglobin binding protein genes of *Haemophilus influenzae*. *J Bacteriol* 1999; 181:5865–5870.

50. Chen CJ, Elkins C, Sparling PF. Phase variation of hemoglobin utilization in *Neisseria gonorrhoeae*. *Infect Immun* 1998; 66:987–993.
51. Letoffe S, Ghigo JM, Wandersman C. Secretion of the *Serratia marcescens* HasA protein by an ABC transporter. *J Bacteriol* 1994; 176:5372–5377.
52. Izadi N, Henry Y, Haladjian J, Goldberg ME, Wandersman C, Delepierre M, et al. Purification and characterization of an extracellular heme-binding protein, HasA, involved in heme iron acquisition. *Biochemistry* 1997; 36:7050–7057.
53. Arnoux P, Haser R, Izadi N, Lecroisey A, Delepierre M, Wandersman C, Czjzek M. The crystal structure of HasA, a hemophore secreted by *Serratia marcescens*. *Nat Struct Biol* 1999; 6:516–520.
54. Ghigo J-M, Letoffe S, Wandersman C. A new type of hemophore-dependent heme acquisition system of *Serratia marcescens* reconstituted in *Escherichia coli*. *J Bacteriol* 1997; 179:3572–3579.
55. Letoffe S, Nato F, Goldberg ME, Wandersman C. Interactions of HasA, a bacterial haemophore, with haemoglobin and with its outer membrane receptor HasR. *Mol Microbiol* 1999; 33:546–555.
56. Idei A, Kawai E, Akatsuka H, Omori K. Cloning and characterization of the *Pseudomonas fluorescens* ATP-binding cassette exporter, HasDEF, for the heme acquisition protein HasA. *J Bacteriol* 1999; 181:7545–7551.
57. Hanson MS, Pelzel SE, Latimer J, Muller Eberhard U, Hansen EJ. Identification of a genetic locus of *Haemophilus influenzae* type b necessary for the binding and utilization of heme bound to human hemopexin. *Proc Natl Acad Sci USA* 1992; 89:1973–1977.
58. Jarosik GP, Maciver I, Hansen EJ. Utilization of transferrin-bound iron by *Haemophilus influenzae* requires an intact *tonB* gene. *Infect Immun* 1995; 63:710–713.
59. Otto BR, van Dooren SJ, Nuijens JH, Luirink J, Oudega B. Characterization of a hemoglobin protease secreted by the pathogenic *Escherichia coli* strain EB1. *J Exp Med* 1998; 188:1091–1103.
60. Wyckoff EE, Valle AM, Smith SL, Payne SM. A multifunctional ATP-binding cassette transporter system from *Vibrio cholerae* transports vibriobactin and enterobactin. *J Bacteriol* 1999; 181:7588–7596.
61. Ferguson AD, Hofmann E, Coulton JW, Diederichs K, Welte W. Siderophore-mediated iron transport: crystal structure of FhuA with bound lipopolysaccharide. *Science* 1998; 282:2215–2220.
62. Locher KP, Rees B, Koebnik R, Mitschler A, Moulinier L, Rosenbusch JP, Moras D. Transmembrane signaling across the ligand-gated FhuA receptor: crystal structures of free and ferrichrome-bound states reveal allosteric changes. *Cell* 1998; 95:771–778.
63. Buchanan SK, Smith BS, Venkatramani L, Xia D, Esser L, Palnitkar M, Chakraborty R, van der Helm D, Deisenhofer J. Crystal structure of the outer membrane active transporter FepA from *Escherichia coli*. *Nat Struct Biol* 1999; 6:56–63.
64. Koebnik R, Locher KP, van Gelder P. Barrels in a nutshell. *Mol Microbiol* 2000; 37: 239–253.
65. Traub I, Gaisser S, Braun V. Activity domains of the TonB protein. *Mol Microbiol* 1993; 8:409–423.
66. Braun V, Gaisser S, Herrmann C, Kampfenkel K, Killmann H, Traub I. Energy-coupled transport across the outer membrane of *Escherichia coli*: ExbB binds ExbD and TonB in vitro, and leucine 132 in the periplasmic region and aspartate 25 in the transmembrane region are important for ExbD activity. *J Bacteriol* 1996; 178:2836–2845.
67. Fischer E, Günter K, Braun V. Involvement of ExbB and TonB in transport across the outer membrane of *Escherichia coli*: phenotypic complementation of *exb* mutants by overexpressed *tonB* and physical stabilization of TonB by ExbB. *J Bacteriol* 1989; 171: 5127–5134.
68. Larsen RA, Thomas MG, Postle K. Protonmotive force, ExbB and ligand-bound FepA drive conformational changes in TonB. *Mol Microbiol* 1999; 31:1809–1824.

69. Jiang X, Payne MA, Cao Z, Foster SB, Feix JB, Newton SM, et al. Ligand-specific opening of a gated-porin channel in the outer membrane of living bacteria. *Science* 1997; 276:1261–1264.
70. Günter K, Braun V. In vivo evidence for FhuA outer membrane receptor interaction with the TonB inner membrane protein of *Escherichia coli*. *FEBS Lett* 1990; 274:85–88.
71. Braun M, Killmann H, Braun V. The beta-barrel domain of FhuDelta5-160 is sufficient for TonB-dependent FhuA activities of *Escherichia coli*. *Mol Microbiol* 1999; 33: 1037–1049.
72. Killmann H, Videnov G, Jung G, Schwarz H, Braun V. Identification of receptor binding sites by competitive peptide mapping: phages T1, T5, and phi 80 and colicin M bind to the gating loop of FhuA. *J Bacteriol* 1995; 177:694–698.
73. Ferguson AD, Braun V, Fiedler H-P, Coulton JW, Diederichs K, Welte W. Crystal structure of the antibiotic albomycin in complex with the outer membrane transporter FhuA. *Prot Sci* 2000; 9:956–963.
74. Ferguson AD, Braun V, K`dding J, Walker G, B` s C, Coulton JW, et al. Crystal structure of a semisynthetic rifamycin derivative in complex with the active outer membrane transporter FhuA from *E. coli* K-12. *Structure* 2001. In press.
75. Pugsley AP, Zimmerman W, Wehrli W. Highly efficient uptake of a rifamycin derivative via the FhuA-TonB-dependent uptake route in *Escherichia coli*. *J Gen Microbiol* 1987; 133:3505–3511.
76. Braun V. Active transport of siderophore-mimicking antibacterials across the outer membrane. *Drug Resistance Updates* 2000; 2:363–369.
77. Gomez JA, Criado MT, Ferreiros CM. Cooperation between the components of the meningococcal transferrin receptor, TbpA and TbpB, in the uptake of transferrin iron by the 37-kDa ferric-binding protein (FbpA). *Res Microbiol* 1998; 149:381–387.
78. Cornelissen CN, Anderson JE, Sparling PF. Energy-dependent changes in the gonococcal transferrin receptor. *Mol Microbiol* 1997; 26:25–35.
79. Litwin CM, Calderwood SB. Role of iron in regulation of virulence genes. *Clin Microbiol Rev* 1993; 6:137–149.
80. Stojiljkovic I, Hantke K. Functional domains of the *Escherichia coli* ferric uptake regulator protein (Fur). *Mol Gen Genet* 1995; 247:199–205.
81. Holm L, Sander C, Rüterjans H, Schnarr M, Fogh R, Boelens R, Kaptein R. LexA repressor and iron uptake regulator from *Escherichia coli*: new members of the CAP-like DNA binding domain superfamily. *Protein Eng* 1994; 7:1449–1453.
82. Jacquamet L, Aberdam D, Adrait A, Hazemann JL, Latour JM, Michaud-Soret I. X-ray absorption spectroscopy of a new zinc site in the Fur protein from *Escherichia coli*. *Biochemistry* 1998; 37:2564–2571.
83. Althaus EW, Outten CE, Olson KE, Cao H, O'Halloran TV. The ferric uptake regulation (Fur) repressor is a zinc metalloprotein. *Biochemistry* 1999; 38:6559–6569.
84. Saito T, Wormald MR, Williams RJ. Some structural features of the iron-uptake regulation protein. *Eur J Biochem* 1991; 197:29–38.
85. De Lorenzo V, Herrero M, Giovannini F, Neilands JB. Fur (ferric uptake regulation) protein and CAP (catabolite-activator protein) modulate transcription of *fur* gene in *Escherichia coli*. *Eur J Biochem* 1988; 173:537–546.
86. Escolar L, Perez-Martin J, De Lorenzo V. Binding of the fur (ferric uptake regulator) repressor of *Escherichia coli* to arrays of the GATAAT sequence. *J Mol Biol* 1998; 283:537–547.
87. Le Cam E, Frechon D, Barray M, Fourcade A, Delain E. Observation of binding and polymerization of Fur repressor onto operator-containing DNA with electron and atomic force microscopes. *Proc Natl Acad Sci USA* 1994; 91:11816–11820.

88. Hantke K. Selection procedure for deregulated iron transport mutants (*fur*) in *Escherichia coli* K-12: *fur* not only affects iron metabolism. *Mol Gen Genet* 1987; 210:135–139.
89. Matzanke B, Bill E, Trautwein AX. Main components of iron metabolism in microbial systems-analyzed by in vivo Mössbauer spectroscopy. *Hyperf Interact* 1992; 71:1259–1262.
90. Touati D, Jacques M, Tardat B, Bouchard L, Despied S. Lethal oxidative damage and mutagenesis are generated by iron in *fur* mutants of *Escherichia coli*: protective role of superoxide dismutase. *J Bacteriol* 1995; 177:2305–2314.
91. Abdul-Tehrani H, Hudson AJ, Chang YS, Timms AR, Hawkins C, Williams JM, Harrison PM, Guest JR, Andrews SC. Ferritin mutants of *Escherichia coli* are iron deficient and growth impaired, and *fur* mutants are iron deficient. *J Bacteriol* 1999; 181:1415–1428.
92. Zheng M, Doan B, Schneider TD, Storz G. OxyR and SoxRS regulation of *fur*. *J Bacteriol* 1999; 181:4639–4643.
93. Pagan-Ramos E, Song J, McFalone M, Mudd MH, Deretic V. Oxidative stress response and characterization of the *oxyR-ahpC* and *furA-katG* loci in *Mycobacterium marinum*. *J Bacteriol* 1998; 180:4856–4864.
94. Zou P, Borovok I, Lucana DO, Müller D, Schrepf H. The mycelium-associated *Streptomyces reticuli* catalase-peroxidase, its gene and regulation by FurS. *Microbiology* 1999; 145:549–559.
95. Bsai N, Herbig A, Casillas-Martinez L, Setlow P, Helmann JD. *Bacillus subtilis* contains multiple Fur homologues: identification of the iron uptake (Fur) and peroxide regulon (PerR) repressors. *Mol Microbiol* 1998; 29:189–198.
96. Gaballa A, Helmann JD. Identification of a zinc-specific metalloregulatory protein, Zur, controlling zinc transport operons in *Bacillus subtilis*. *J Bacteriol* 1998; 180:5815–5821.
97. Foster JW, Moreno M. Inducible acid tolerance mechanisms in enteric bacteria. *No-vartis Found Symp* 1999; 221:55–69.
98. Hall HK, Foster JW. The role of *fur* in the acid tolerance response of *Salmonella typhimurium* is physiologically and genetically separable from its role in iron acquisition. *J Bacteriol* 1996; 178:5683–5691.
99. Vasil ML, Ochsner UA. The response of *Pseudomonas aeruginosa* to iron: genetics, biochemistry and virulence. *Mol Microbiol* 1999; 34:399–413.
100. Schmitt MP, Holmes RK. Characterization of a defective diphtheria toxin repressor (*dtxR*) allele and analysis of *dtxR* transcription in wild-type and mutant strains of *Corynebacterium diphtheriae*. *Infect Immun* 1991; 59:3903–3908.
101. Dussurget O, Timm J, Gomez M, Gold B, Yu S, Sabol SZ, Holmes RK, Jacobs WR Jr, Smith I. Transcriptional control of the iron-responsive *fxbA* gene by the mycobacterial regulator IdeR. *J Bacteriol* 1999; 181:3402–3408.
102. Dussurget O, Rodriguez M, Smith I. An IdeR mutant of *Mycobacterium smegmatis* has derepressed siderophore production and altered oxidative stress response. *Mol Microbiol* 1996; 22:535–544.
103. Schmitt MP. Transcription of the *Corynebacterium diphtheriae hmuO* gene is regulated by iron and heme. *Infect Immun* 1997; 65:4634–4641.
104. Schmitt MP. Identification of a two-component signal transduction system from *Corynebacterium diphtheriae* that activates gene expression in response to the presence of heme and hemoglobin. *J Bacteriol* 1999; 181:5330–5340.
105. Posey JE, Hardham JM, Norris SJ, Gherardini FC. Characterization of a manganese-dependent regulatory protein, TroR, from *Treponema pallidum*. *Proc Natl Acad Sci USA* 1999; 96:10887–10892.

106. Bell SD, Cairns SS, Robson RL, Jackson SP. Transcriptional regulation of an archaeal operon in vivo and in vitro. *Mol Cell* 1999; 4:971–982.
107. White A, Ding X, vanderSpek JC, Murphy JR, Ringe D. Structure of the metal-ion-activated diphtheria toxin repressor/tox operator complex. *Nature* 1998; 394:502–506.
108. Pohl E, Holmes RK, Hol WGJ. Crystal structure of the iron-dependent regulator (IdeR) from *Mycobacterium tuberculosis* shows both metal binding sites fully occupied. *J Mol Biol* 1999; 285:1145–1156.
109. Pohl E, Holmes RK, Hol WG. Crystal structure of a cobalt-activated diphtheria toxin repressor-DNA complex reveals a metal-binding SH3-like domain. *J Mol Biol* 1999; 292:653–667.
110. Wang G, Wylie GP, Twigg PD, Caspar DL, Murphy JR, Logan TM. Solution structure and peptide binding studies of the C-terminal src homology 3-like domain of the diphtheria toxin repressor protein. *Proc Natl Acad Sci USA* 1999; 96:6119–6124.
111. Tang Y, Guest JR. Direct evidence for mRNA binding and post-transcriptional regulation by *Escherichia coli* aconitases. *Microbiology* 1999; 145:3069–3079.
112. Alen C, Sonenshein AL. *Bacillus subtilis* aconitase is an RNA-binding protein. *Proc Natl Acad Sci USA* 1999; 96:10412–10417.
113. Schwartz D, Kaspar S, Kienzlen G, Muschko K, Wohlleben W. Inactivation of the tricarboxylic acid cycle aconitase gene from *Streptomyces viridochromogenes* Tu494 impairs morphological and physiological differentiation. *J Bacteriol* 1999; 181:7131–7135.
114. Hussein S, Hantke K, Braun V. Citrate-dependent iron transport system in *Escherichia coli* K-12. *Eur J Biochem* 1981; 117:431–437.
115. Kim I, Stiefel A, Plantor S, Angerer A, Braun V. Transcription induction of the ferric citrate transport genes via the N-terminus of the FecA outer membrane protein, the Ton system and the electrochemical potential of the cytoplasmic membrane. *Mol Microbiol* 1997; 23:333–344.
116. Härle C, Kim I, Angerer A, Braun V. Signal transfer through three compartments: transcription initiation of the *Escherichia coli* ferric citrate transport system from the cell surface. *EMBO J* 1995; 14:1430–1438.
117. Welz D, Braun V. Ferric citrate transport of *Escherichia coli*: functional regions of the FecR transmembrane regulatory protein. *J Bacteriol* 1998; 180:2387–2394.
118. Enz S, Mahren S, Stroehrer UH, Braun V. Surface signaling in ferric citrate transport gene induction: interaction of the FecA, FecR, and FecI regulatory proteins. *J Bacteriol* 2000; 182:637–646.
119. Angerer A, Enz S, Ochs M, Braun V. Transcriptional regulation of ferric citrate transport in *Escherichia coli* K-12. FecI belongs to a new subfamily of sigma-type factors that respond to extracytoplasmic stimuli. *Mol Microbiol* 1995; 19:163–174.
120. Enz S, Braun V, Crosa J. Transcription of the region encoding the ferric dicitrate transport system in *Escherichia coli*: similarity between promoters for fecA and for extracytoplasmic function sigma factors. *Gene* 1995; 163:13–18.
121. Angerer A, Braun V. Iron regulates transcription of the *Escherichia coli* ferric citrate transport genes directly and through the transcription initiation proteins. *Arch Microbiol* 1998; 169:483–490.
122. Koster M, van Klompenburg W, Bitter W, Leong J, Weisbeek PJ. Role for the outer membrane ferric-siderophore receptor PupB in signal transduction across the bacterial cell envelope. *EMBO J* 1994; 13:2805–2813.
123. Schalk IJ, Kyslik P, Prome D, van Dorsselaer A, Poole K, Abdallah MA, Pattus F. Copurification of the FpvA ferric pyoverdinin receptor of *Pseudomonas aeruginosa* with its iron-free ligand: implications for siderophore-mediated iron transport. *Biochemistry* 1999; 38:9357–9365.

Uptake of Transferrin-Bound Iron by Mammalian Cells

DEBORAH TRINDER

University of Western Australia, Fremantle, Western Australia, Australia

EVAN MORGAN

University of Western Australia, Nedlands, Western Australia, Australia

I. INTRODUCTION	427
II. CELLULAR UPTAKE OF TRANSFERRIN-BOUND IRON	429
A. Transferrin–Transferrin Receptor Interaction	430
B. Endocytosis and Iron Release from Transferrin	431
C. Iron Transport Through the Endosomal Membrane	434
III. UPTAKE OF TRANSFERRIN-BOUND IRON IN SPECIFIC TISSUES	434
A. Erythroid Cells	434
B. Brain	435
C. Placenta	435
D. Duodenum	436
E. Liver	437
REFERENCES	442

I. INTRODUCTION

Iron is transported in the blood plasma and interstitial fluid of the body in a complexed form, which overcomes the problems arising from the high insolubility of ferric iron in aqueous media. Under normal circumstances nearly all of this transport iron is bound to transferrin, but minute amounts are also present in plasma ferritin,

in hemopexin–heme, and haptoglobin–haemoglobin complexes, and as non-protein-bound forms. In abnormal conditions such as those associated with iron overload a greater proportion of plasma iron may be present in nontransferrin forms. These forms are directed mainly to the liver, where they are processed and the iron either stored or released to the plasma, where it will bind to transferrin as long as this protein is not already saturated with iron. Due to the reversible nature of iron binding by transferrin, this protein can act as a true carrier of the metal, accepting it from sites of release such as intestinal absorptive cells, storage cells (e.g., hepatocytes), and sites of red cell destruction (macrophages), and donating it to most cells for iron utilization, particularly immature erythroid cells for hemoglobin synthesis. Transferrin also has a second function, that of participating in the body's defense mechanisms against infection.

Although it has been known since 1927 that plasma iron is protein-bound (1), it was not until the mid-1940s that the identity of transferrin was established and some of its functions described. This was achieved by Holmberg and Laurell in Sweden and Schade and Caroline in the United States, who were working independently on the two major functions of iron-binding proteins: plasma transport of iron (2,3) and inhibition of bacterial growth (4,5). Laurell's work led to the purification of swine transferrin (6,7) and to a clear demonstration of the role of transferrin in iron transport (5,8). In keeping with this function, Holmberg and Laurell proposed the name "transferrin" (9). Schade and Caroline's work with different Cohn fractions of serum finally resulted in the purification of human serum transferrin (10–14).

The transport of iron bound to transferrin has several important consequences. First, its extracellular distribution and circulation have the characteristics of a protein rather than a small molecule or ion, and its diffusion properties and rate of penetration through cellular membranes have the properties of the carrier protein. Second, loss of iron from the body by passage through surfaces such as the gut and kidney is greatly restricted. Third, the free iron concentration in body fluids is extremely low, so the injurious effects of ionic iron are largely avoided. Fourth, since spontaneous dissociation of iron from transferrin cannot occur at a significant rate under conditions present in extracellular fluids (15), the cellular acquisition of transferrin-bound iron requires specific, cell-mediated mechanisms. Usually these involve the function of specific transferrin receptors.

Transferrin, like other plasma proteins, is distributed throughout most of the extracellular fluid of the body and circulates continuously from plasma to interstitial fluid and then back to the plasma via the lymph (Fig. 1). Iron remains bound to transferrin during passage through most capillary walls (16), but not those of the blood–brain or blood–testis barriers (17–19). Here the iron dissociates from transferrin before being transported into the tissues, where locally synthesized transferrin probably takes over the function of iron transport. In contrast to the brain and testis, iron bound to transferrin has almost unrestricted access to cells of bone marrow, liver, and spleen, due to the fenestrated nature of the sinusoids in these tissues. This aids in the delivery of plasma iron to erythroid precursors and hepatocytes and the return of iron to the plasma from hepatocytes and macrophages. Another tissue with unrestricted access to transferrin-bound iron is the placenta in those species of animals which have a hemochorial type of placenta in which the trophoblast cells are bathed in maternal blood (20).

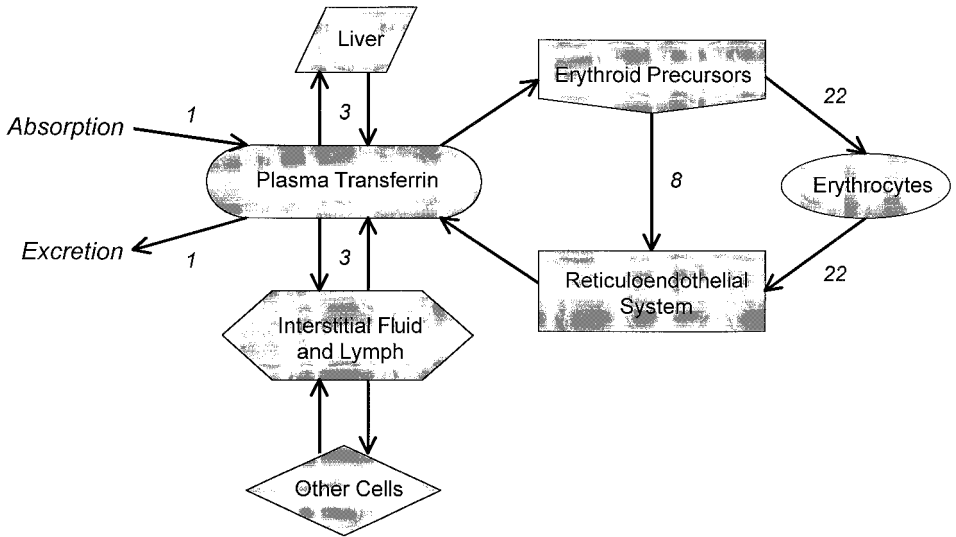


Figure 1 A model of iron exchanges in the human. The numerical values indicate approximately daily exchange of iron in mg.

In the normal human the plasma pool of transport iron (about 3 mg) is turned over approximately 10 times per day. This rate is far greater than that of transferrin catabolism, approximately 15% of the plasma pool per day (21), or its rate of circulation through the lymph, one plasma pool per day (22). Hence, it can be concluded that most of the plasma iron turnover occurs at sites which are in direct contact with plasma and that transferrin is not catabolized during the processes involved in iron exchange with cells (bone marrow, liver, spleen, and placenta).

About 80% of iron that leaves the plasma is taken up by immature erythroid cells in the bone marrow and returns to the plasma when the resultant circulating red blood cells are broken down in macrophages of the reticuloendothelial system at the end of their life span or within the marrow as a consequence of ineffective erythropoiesis (23–25). Much smaller fractions of plasma iron turnover are derived from the bidirectional exchange of iron with hepatocytes, iron absorption from the intestine, and iron exchange with almost all other types of cells. Of these, the cytotrophoblast cells of the placenta are the most active. Iron uptake by these cells can account for approximately 10% of the plasma iron turnover toward the end of pregnancy in humans and over 50% of the turnover in rats and rabbits (26–28). The major determinants of the cellular distribution of iron derived from plasma transferrin are the permeability of the capillaries of the various organs and the cellular content of membrane receptors for transferrin. Receptors are in greatest abundance in erythroid precursors and placental cells. See Fig. 1 for a model of iron exchange in humans.

II. CELLULAR UPTAKE OF TRANSFERRIN-BOUND IRON

The mechanism of cellular iron uptake from transferrin has aroused considerable interest because of the very high affinity of transferrin for iron, the impermeability

of cell membranes to proteins and cations, and the universal but varying requirements of cells for iron. Research over the last 40 years has dwelt on the steps involved in the iron uptake process and their regulation in order to meet the specific needs of different types of cells at the various stages of their life cycle. The steps involved in iron uptake are (a) interaction of the iron–transferrin complex with specific receptors on the cell membrane, (b) release of iron from transferrin, and (c) iron transport across the cell membrane. In most types of cells, iron release from transferrin occurs within endosomes following receptor-mediated endocytosis of the transferrin-iron–transferrin receptor complex, followed by transport across the endosomal membrane by a carrier-mediated process. However, in certain types of cells such as hepatocytes there is evidence that some iron is released from transferrin on the plasma membrane before transport into the cell, as described in Sec. III.E.4.

A. Transferrin–Transferrin Receptor Interaction

The concept that uptake for transferrin-bound iron involves interaction with specific cell membrane receptors was proposed by Jandl and Katz in 1963 (29). They demonstrated that radioiodinated transferrin binds to reticulocytes prior to donation of its iron, that these processes can be eliminated by treatment of the cells with trypsin to remove the receptors, that iron-saturated transferrin is taken up in greater amounts than iron-depleted transferrin, and that the binding of transferrin by the cells is reversible, the protein being released after it has donated its iron to the cell. Subsequent studies have led to the isolation, cloning, and determination of the molecular structure of the protein and regulation of its expression (see Chapters 3 and 9).

The interaction between transferrin and its receptor is reversible, pH-dependent, and influenced by the iron content of transferrin. At extracellular pH the receptor has a much higher affinity of diferric transferrin than for apotransferrin, and an intermediate affinity for monoferric transferrin (30–34). The dissociation constant, K_d , for the binding of diferric transferrin by receptors of various species and cell types has been reported to be 10^{-7} – 10^{-9} M, and that of monoferric transferrin about 10^{-6} M. As a consequence of the differences in affinity and iron content, diferric transferrin has approximately a 10-fold advantage over monoferric transferrin in delivering iron to cells when both proteins are present at concentrations sufficient to saturate the receptors (35). Apotransferrin does not compete with iron-transferrin for binding to the receptors (31). Hence cellular iron uptake from mixtures of the three forms of transferrin, such as from the extracellular fluids of the body, increases as the plasma iron concentration and percent saturation of plasma transferrin rises, as has been demonstrated in ferrokinetic studies in humans (36) and animals (37).

As the pH is lowered below about 6.5, the affinity of receptors for apotransferrin rises and at pH 5–6 is approximately as great as that for diferric transferrin at pH 7.4 (32,33,38,39). As a consequence, apotransferrin remains bound to the receptor after it has released its iron at acidic sites within the cell.

The prime and possibly the only function of the transferrin receptor is to mediate the cellular uptake of transferrin-bound iron by localizing and concentrating transferrin-iron to the cell surface and facilitating the release of the iron from its carrier protein. This has been demonstrated in a number of ways, such as by inactivating the receptor with proteases (29,40) or specific antibodies (41) and by the close correlation between the rate of iron uptake and the number of receptors present on cells (42–45).

B. Endocytosis and Iron Release from Transferrin

Receptor-mediated endocytosis of transferrin was first described in reticulocytes (46,47) and subsequently in a wide variety of other cells including nucleated erythroid precursors, hepatocytes, vascular endothelial cells, placental trophoblast cells, myocytes, lymphocytes, fibroblasts, and many different cell lines in culture (48). Evidence that the endocytosis is necessary for iron uptake by cells is derived from measurements of the rates of transferrin endocytosis and iron accumulation under control conditions and when the endocytic rate is varied by the use of inhibitors, alterations in cellular environment, and incubation temperature. In all such conditions a close correlation was found between the rates of the two processes (41).

After transferrin endocytosis and its role in iron uptake by cells was demonstrated, the question was asked why endocytosis is required for the process. It was proposed that endocytosis provides the microenvironment necessary for iron release from transferrin, probably as a consequence of the acidic nature of the endocytic vesicles or endosomes (49). This proved correct, as shown by many experiments in a variety of cells in which vesicular pH was elevated by use of weak bases, ionophores, inhibitors of endosomal H^+ -ATPase, and mutant cell lines which are incapable of acidifying their vesicles—with resultant loss of iron uptake by the cells (50–56).

Receptor-mediated endocytosis of transferrin occurs in several steps (Fig. 2). The receptors on the cell surface bind transferrin-iron and cluster into coated pits. This is followed by endocytosis, uncoating of the vesicles to form smooth vesicles or endosomes, and acidification by the action of an ATP-dependent proton pump to a pH of approximately 5.5 (57,58). The acidification of the vesicles is followed by release of iron from transferrin and its transport across the endosomal membrane. The apotransferrin remains bound to its receptors even at the low pH and recycles to the plasma membrane with the receptor. When exocytosis occurs, the apotransferrin, now exposed to the extracellular pH, is released from the receptor and is free to circulate in the blood and interstitial fluid to accept iron released from cells elsewhere in the body, while the receptors can bind more transferrin-iron so that the iron acquisition cycle continues (32,33,39,54). During the endocytic cycle, endosomes fuse with other intracellular vesicles and at least some of the receptor–transferrin complexes become associated with elements of the Golgi complex or are incorporated into multivesicular bodies (59–61). These bodies contain many small vesicles with receptors, including transferrin receptors, on their outer surface. They have been called exosomes and are lost from the cell by exocytosis. This provides a means of reducing the transferrin receptor content of cells and is probably the mechanism by which receptors are lost from erythroid cells during maturation into erythrocytes (62,63). Such a process would release intact, albeit membrane-bound, receptors into the blood plasma. However, although transferrin receptors are found in the blood plasma, they exist in a truncated form consisting only of the extracellular domain. This appears to result from cleavage from the membrane by a serine protease within the multivesicular bodies (63). Measurement of plasma transferrin receptor levels is used for evaluating iron status and erythropoietic rate in certain hematological conditions, presumably because the main source of the cell-free receptors is erythropoietic tissue and their expression increases in iron deficiency (Fig. 2).

Neither the dominant transferrin receptor cycle associated with rapid recycling to the plasma membrane nor the pathway through multivesicular bodies leads to

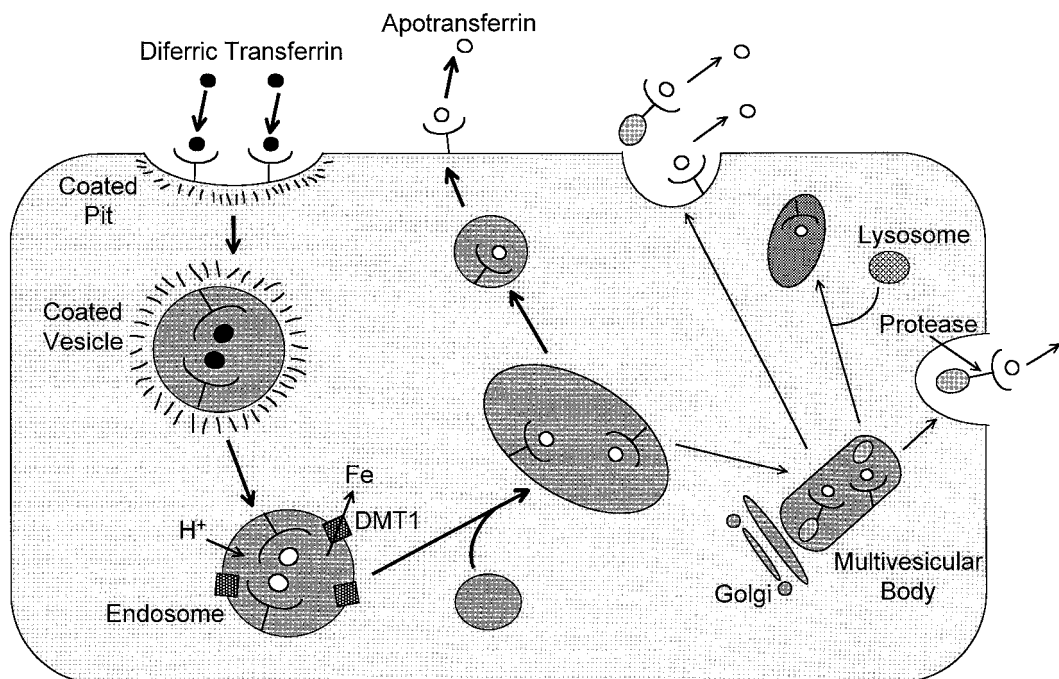


Figure 2 Diagrammatic representation of pathways involved in the endocytosis of transferrin and its receptor in mammalian cells. The figure shows diferric transferrin (●), apotransferrin (○), transferrin receptor (Y) and DMT1 (■). The shorter cycle occurs more frequently than the longer cycle in most types of cells, and fusion with lysosomes occurs infrequently if at all.

degradation of transferrin, which is in keeping with the much lower rate of plasma transferrin turnover than iron turnover mentioned above. This is true for erythropoietic tissue, the major utilizer of transferrin-iron, but degradation of transferrin does occur in some other tissues, particularly the liver and kidneys (64), which raises the possibility that in some types of cells a proportion of the receptors and bound transferrin is directed to lysosomes, where proteolytic degradation of both proteins can occur. Alternatively, transferrin degradation may occur only as a consequence of fluid-phase endocytosis, which accounts for very little iron uptake by erythroid cells but may be of greater significance in other types of cells.

Transferrin receptor endocytosis and uptake of transferrin-bound iron requires interaction between the cytoplasmic tail of the receptor and the endocytic machinery present in coated vesicles (45,65), but is not dependent on phosphorylation of the receptor (65). The internalization signal has been identified as a tetrapeptide sequence in the tail, $Y^{20}TRF^{23}$ (66). Separate signals in the cytoplasmic domain direct the receptor to the basolateral membrane of polarized cells (67). Another possible signal for endocytosis is interaction between the receptor and transferrin. However, endocytosis of the receptor can proceed in the absence of bound transferrin (68,69) although the rate may be somewhat lower than when transferrin is present (70).

Acidification of the endosome is undoubtedly the major determinant of iron release from transferrin. This is demonstrated by the highly significant correlation between the rate of iron uptake by reticulocytes and changes in endosomal pH produced by incubation of the cells with varying concentrations of ammonium chloride (58); (see Fig. 3). However, acidification is probably not the only factor involved, since even at pH 5.5 the rate of iron release from transferrin would probably not be sufficient to account for the rate at which iron is accumulated by the cell (and see Chapter 3). This is undoubtedly true of erythroid cells, in which the transferrin receptor cycle time is only 2–3 min (44,71) yet both iron atoms are released from transferrin and are taken up by the cell. Other possible factors include reduction of the iron, effects of interaction between transferrin and its receptor, and, in certain types of cells, interaction between the receptor and the hemochromatosis protein, HFE. Reduction of the iron released from transferrin certainly occurs, since the iron can be chelated by ferrous iron chelators (72), and the iron is probably transported across the endosomal membrane in the ferrous form (see below). Evidence for reductant processes in endocytic vesicles has been presented (73), but it is not known whether they play a direct role in the release of iron from transferrin. A second factor that is probably involved in iron release is the effect which binding to the receptor has on the conformation of the transferrin molecule. Several studies indicate that changes in conformation occur and accelerate the release of iron from transferrin at the acidic pH present in endosomes (74–77). The third factor that could modulate iron release from transferrin within endosomes is HFE. This protein binds to the transferrin receptor (78) and lowers its affinity for transferrin (79,80) in association with conformational changes in the receptor molecule (81). The interaction is strong at pH 7.5 but weak or nonexistent at pH 6.0 (82). One effect of this interaction could be reduced endocytosis of transferrin, as has been reported (83). However, other investigators, also using a cell line which had been induced to overexpress HFE were

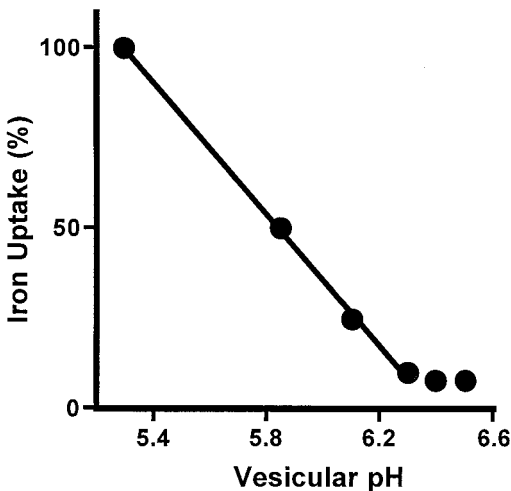


Figure 3 Relationship between rate of iron uptake and pH of endosome vesicles in rabbit reticulocytes incubated with transferrin-bound iron in the presence of varying concentrations of ammonium chloride (for details, see Ref. 51).

unable to find any evidence of an alteration in the rates of transferrin endocytosis and recycling even though the iron uptake by the cells was impaired (84). They concluded that the action of HFE was exerted within the endosomes, either by inhibiting iron release from transferrin or its transport across the endosomal membrane. Whether these conclusions are correct and, indeed, whether HFE exerts an effect on uptake of transferrin-bound iron by cells at any site except duodenal crypt enterocytes is yet to be determined.

C. Iron Transport Through the Endosomal Membrane

Once released from transferrin, the iron must be transported across the endosomal membrane. Studies using nontransferrin-bound iron led to the demonstration of a high-affinity carrier for ferrous iron in erythroid cells (85). It was shown to have an acidic pH optimum and many other properties which suggested that it is the endosomal carrier (86). The properties closely resemble those of the recently cloned metal-ion carrier, originally called Nramp2 or DCT1 (87) but now known as divalent metal transporter 1 (DMT1; see Chapter 6). Subsequent studies showed that two strains of laboratory animals with genetic defects of iron metabolism, microcytic anemic mice and the Belgrade rat, have a common mutation G185R in DMT1 (88,89). These animals suffer from a microcytic, hypochromic anemia due to impaired iron uptake by developing erythroid cells (90,91), which in the case of the Belgrade rat has been shown to be due to impaired iron transport across the endosomal membrane (92). Moreover, when mutant forms of DMT1 were expressed in human embryonic kidney cells in culture, the protein localized to the plasma membrane and to the membrane of the endosomes, and this was associated with impaired iron uptake from transferrin (93). Hence, there is compelling evidence that DMT1 can function as the endosomal iron transporter, but whether it is the only transporter and whether it functions at this site in all types of cells has yet to be determined. (For further discussion of animal models, see Chapter 27).

III. UPTAKE OF TRANSFERRIN-BOUND IRON IN SPECIFIC TISSUES

The mechanisms of cellular iron uptake from transferrin are similar in all tissues so far examined. The predominant mechanism, found in virtually all cells except mature erythrocytes, involves receptor-mediated transport of transferrin. Iron release from transferrin at the plasma membrane and uptake through this membrane probably also occurs in some types of cells, particularly hepatocytes, as discussed above. However, although there are general similarities among cells from all tissues, differences which have significance with respect to the overall iron metabolism of the body do exist. These are discussed here, concentrating on those tissues which have important functions in iron metabolism: erythroid cells, liver, brain, placenta, and duodenum. The phagocytes of the reticuloendothelial system also have a quantitatively important role, since all of the iron from effete erythrocytes is directed through them back to the plasma. However, they obtain little iron from transferrin.

A. Erythroid Cells

Immature erythroid cells, mainly in the bone marrow of adult animals, represent by far the greatest mass of transferrin receptor-containing cells in the body and account

for 70–80% of the plasma iron turnover. Iron uptake occurs entirely by receptor-mediated endocytosis, and its rate in individual cells is determined by the cell's complement of transferrin receptors. This changes during cellular development and maturation, rising as the cells develop into basophilic normoblasts and then falling during maturation into reticulocytes, mature erythrocytes having no receptors (42,43). Features of the endocytic cycle in erythroid cells are its rapidity and efficiency, each cycle taking only 2–3 min (44,71) and delivering both iron atoms from transferrin in each cycle (92). Considerably longer cycling times have been described for other types of cells, and it is not known whether the two iron atoms are taken up during each cycle. The regulation of transferrin receptor expression and rate of iron uptake by erythroid cells is discussed further below (see Chapter 26).

B. Brain

Two aspects of brain iron metabolism are of particular interest. One is how iron, while bound to transferrin, crosses the blood–brain barrier, which has extremely low permeability to plasma proteins, and the other is the mechanism of iron transport and uptake by cells within the brain. The demonstration of transferrin receptors on brain capillaries (94) and the ability of these cells to take up transferrin by endocytosis led to the idea that transferrin–iron complexes are transported across brain capillaries by transcytosis (95,96). However, measurement of the rates of transferrin and iron uptake by the brain showed that this could not be so, because uptake of iron greatly exceeded that of transferrin (97,98). It was concluded that the majority, but not all, of the transferrin endocytosed by the capillaries is returned to the plasma after release of its iron within the cells (in endosomes). The iron is then transported into the brain, where it is bound by transferrin derived mainly from local synthesis in oligodendrocytes and choroid plexus cells. Neurones express transferrin receptors and can, presumably, take up the iron by endocytosis. However, transferrin receptors have not been demonstrated on all types of glial cells. This raises the question that some of the iron transported across the blood–brain barrier is not bound by transferrin and that this iron may be the source used by glial cells (99).

The iron requirements of the brain are greatest during early stages of development, when cell proliferation and brain growth are occurring rapidly. In rats it has been shown that the number of receptors on brain capillary cells and the rate of iron transfer into the brain are maximal at the time of maximal growth of the brain (in the first 3 weeks of life), and also vary with iron status, increasing in iron deficiency (97,98). Hence, maximal supplies of iron are provided at the time when iron is needed most, and the brain is protected to some extent from the effects of iron deficiency. However, this protection is not complete, and deleterious effects of iron deficiency on brain function can occur.

C. Placenta

The mechanisms involved in placental transfer of iron provide an excellent example of the principle that permeability of blood capillaries to transferrin can limit the availability of iron to certain tissues. In the brain this problem has been overcome by the expression of transferrin receptors and of a receptor-mediated iron transport system in the capillary cells. A different solution has arisen in the placenta. In those

species with the hemochorial type of placenta, the maternal capillary wall breaks down and the trophoblast cells of the placenta are bathed in maternal blood, with no barrier between maternal plasma transferrin and the cells. However, in many mammalian species (e.g., cat, dog, sheep, goat, cow), the trophoblast is separated from maternal blood by one or more layers of maternal cells. In these species little maternal transferrin is bound by the placenta and little transferrin-bound iron is transferred to the fetus. The source of fetal iron appears to be maternal erythrocytes, which are extravasated into the lumen of the uterus and are taken up by phagocytosis in the chorionic epithelial cells (20).

In these species with the hemochorial type of placenta (e.g., human, rat, rabbit), the trophoblast cells are richly endowed with transferrin receptors and take up iron from maternal plasma by receptor-mediated endocytosis (100). The iron is released from transferrin in the endosomes and is transported into the fetal blood to be bound by fetal transferrin, while the maternal apotransferrin returns to maternal blood. Little transferrin crosses the placenta. The nature of the carrier which transports the iron to the fetus is unknown, but the trophoblast cells appear to be highly polarized, since transferrin binds only to the maternal side and the iron is transported only to the fetus. None returns to the maternal circulation (27,28). The number of transferrin receptors in the placenta and the rate of iron transfer to the fetus increase rapidly during the last one-third of pregnancy and keep up with fetal growth (27,28). The mechanisms responsible for these changes are unknown.

D. Duodenum

It is widely believed that iron absorption from the intestine, which occurs mainly in the duodenum, is regulated by the amount of iron taken up by enterocytes from plasma transferrin while they are in the crypts of Lieberkuhn (101). This determines their function when they migrate into the villi and develop into mature enterocytes, iron depletion in the crypts leading to increased absorptive ability, and iron overload to decrease absorption. Hence, the mechanism of iron uptake in the crypts is of considerable importance.

Isolated crypt cells have been shown to possess basolateral transferrin receptors and are capable of taking up iron by receptor-mediated endocytosis (102). Also, *in vivo*, crypt cells can take up plasma transferrin-bound iron in amounts proportional to plasma iron concentration (103). These observations are compatible with the above hypothesis. However, certain observations indicate that the iron uptake mechanism may differ from other types of cells. First, iron uptake from transferrin is not impaired in homozygous Belgrade rats (103), which suggests that DMT1 is not involved in the transport of iron into the cells. Second, HFE is highly expressed in crypt epithelial cells (104) and would be expected to impair the uptake of iron by these cells. Hence, increased membrane expression of HFE in crypt cells should accentuate iron absorption in the villi, and decreased expression diminish it. However, in hereditary hemochromatosis, where there is a mutation of HFE (104) which leads to reduced expression on cell membranes (105,106), iron absorption is enhanced, not diminished. Hence, further work is required to determine the role of HFE and iron uptake by crypt cells in the regulation of iron absorption.

E. Liver

1. Transferrin Receptor-Mediated Uptake

Two types of cells in the liver, hepatocytes and Kupffer cells, have important roles in iron metabolism. Hepatocytes are parenchymal cells of the liver, where 98% of the liver iron is stored mainly as ferritin (107). Kupffer cells are liver macrophages and, like splenic macrophages, are part of the reticuloendothelial system. They play a role in the recycling of iron from damaged or senescent erythrocytes.

Most of the transferrin-bound iron delivered to the liver is deposited in the hepatocyte (108,109). The mechanisms of transferrin-iron uptake by hepatocytes are complex and have been the subject of investigation for more than 25 years. Hepatocytes take up transferrin-iron by a number of mechanisms including a transferrin receptor-mediated process and at least three other mechanisms that are independent of the transferrin receptors which will be discussed in detail later in this chapter.

The uptake of transferrin-iron by hepatocytes and hepatoma cells mediated by transferrin receptors has many of the characteristics of the transferrin receptor-mediated process operating in the developing erythroid cells. Subcellular fractionation of rat liver (108,110–113) and the effects of proteolytic enzymes (110,114–117) and inhibitors (116–118) on transferrin and iron uptake indicate that this process is mediated by the endocytosis of transferrin. It involves internalisation into low-density vesicles, where the iron is released from transferrin by a pH-dependent process and the iron-deficient transferrin is recycled back to the cell surface. It is likely that, as found in other types of cells, the iron is reduced to its ferrous form in the endosome and transported across the endosomal membrane by the divalent metal transporter (DMT1) that is expressed in liver (87,89,119). In the cytosol, most of the iron is incorporated into ferritin or taken to the mitochondria for synthesis of heme proteins (Fig. 4).

The expression of transferrin receptors and the subsequent uptake of iron by hepatocytes is affected by a variety of conditions such as cellular proliferation rate, stages of development, iron status, and cytokines. After partial hepatectomy, proliferating hepatocytes express an increased number of receptors per cell when compared with hepatocytes in the stationary growth phase (120,121). The developing hepatocytes isolated from fetal rat livers express a high number of transferrin receptors and take up large amounts of iron (114). The level of receptor expression decreases rapidly in the early neonatal period, reaching a relatively low level in adult hepatocytes (122). This is likely to be due to the high iron requirements of the fetus and neonate for the synthesis of iron-containing proteins and enzymes.

The uptake of iron by the liver is dependent on hepatic iron levels. Iron-deficient hepatocytes express increased numbers of transferrin receptors and take up more iron (123–125), while the reverse occurs for the iron-loaded hepatocytes (124). In fact, a complete lack of receptor-positive hepatocytes was observed in hereditary hemochromatosis patients with liver iron overload (126,127). The effects of iron levels on transferrin receptor expression are reminiscent of control mechanisms that are operating in a number of other types of cells via the iron-responsive element (IRE)–iron regulatory protein (IRP) system discussed in detail in Chapters 9 and 10.

Nitric oxide and cytokines (tumor necrosis factor- α , interleukin-1 β , interleukin-6) have a key role in inflammatory responses and increase hepatic transferrin receptor

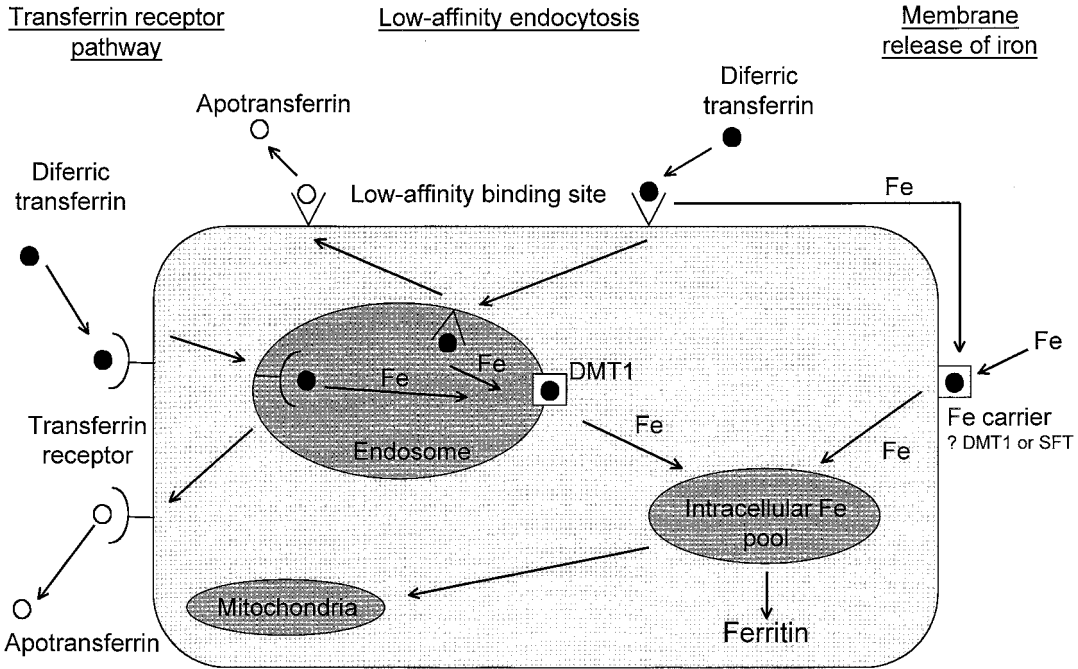


Figure 4 Model of the pathways of transferrin-iron uptake by hepatocytes. Uptake occurs by three pathways: transferrin receptor-mediated endocytosis, low-affinity endocytosis, and the release of iron from transferrin at the cell membrane. The figures show diferric transferrin (●), apotransferrin (○), transferrin receptor (Y), low-affinity transferrin-binding site (V), and DMT1 (□).

expression and iron uptake (128–130). The effects of nitric oxide are likely to be due to an increase in IRP-binding activity, but the mechanisms of regulation by the cytokines are unknown.

The nonparenchymal cells of the liver, the Kupffer cells and endothelial cells which line the sinusoids, both express transferrin receptors and take up transferrin-bound iron (109,131,132). Expression of receptors in Kupffer cells is heterogeneous, but on average they display only 25% as many receptors as hepatocytes (131). The level of expression of receptors by Kupffer cells is altered during development and by iron status of the cells (122). Tavassoli and co-workers showed that the endothelial cells expressed more receptors than hepatocytes, and they proposed that the endothelial cell rather than the hepatocyte plays the central role in regulating iron transport in the liver (133). These findings have not been confirmed by other investigators.

2. Transferrin Receptor-Independent Pathways

A number of types of cells, including hepatocytes, hepatoma cells, fibroblasts, Chinese hamster ovary cells, and melanoma cells, acquire transferrin-bound iron by pathways that do not involve transferrin receptors (111,114,116,118,134–139). The most well characterized example of this type of iron transport system is found in the

hepatocyte. Initial studies (111,114,116,118,134,135) identified that when the extracellular diferric transferrin concentration was elevated above that required to saturate the transferrin receptors, the uptake of transferrin and iron by hepatocytes increased with increasing extracellular transferrin concentration. This suggested the presence of at least two iron-uptake pathways. The first is a high-affinity, low-capacity process mediated by the limited number of transferrin receptors that saturate at relatively low extracellular transferrin concentrations, while the second is a low-affinity, high-capacity process that operates at higher transferrin concentrations. The relative importance of the second pathway increases as the transferrin concentration is raised. Findings from *in vitro* experiments indicate that at normal plasma transferrin concentrations the uptake of iron would occur primarily by the transferrin receptor-independent pathway. The NTR pathway is likely to be a particularly important mechanism for the delivery of iron to the hepatocyte in iron-overload conditions such as hereditary hemochromatosis, where hepatocytes lack transferrin receptors (126,127).

Strong evidence for the presence of transferrin receptor-independent pathways has been demonstrated using experimental techniques where either the binding of transferrin iron to the cell surface receptors has been eliminated or the expression of the transferrin receptors was reduced. First, the binding of transferrin to the transferrin receptor was blocked using an antibody to the transferrin receptor. When rat hepatocytes were treated with the antibody, the cells did not take up transferrin-iron by the receptor-mediated process, but the hepatocytes were still able to acquire iron and transferrin even in the presence of rat serum albumin (115). This indicates the presence of an NTR transport mechanism. Second, transferrin can be proteolytically cleaved into C- and N-terminal half-transferrin molecules. The C-terminal half-transferrin molecule binds to transferrin receptors and delivers iron to cells, but the N-terminal half-transferrin cannot (140). When rat hepatocytes were incubated with radiolabeled N-terminal half-molecules, the cells did not bind the protein specifically, indicating that the N-terminal half transferrin was not binding to the transferrin receptors but could donate iron to the cells by a NTR pathway (141).

Transferrin receptor expression was suppressed in a human HuH7 hepatoma cell line by transfecting the cells with a transferrin receptor antisense RNA expression vector. The uptake of transferrin and iron by the transfected cells was reduced significantly when compared with the wild-type cells. However, the uptake by a NTR pathway was not affected (116). Also, a mutant Chinese hamster ovary cell line that was selected by resistance to cholera toxin conjugated to transferrin does not express transferrin receptors. These cells were also able to acquire iron from transferrin (136).

The mechanisms involved in the uptake of transferrin-iron by the NTR processes are complex. Data has been published indicating that at least three pathways are involved. These include low-affinity endocytosis, fluid-phase endocytosis, and the release of iron from transferrin at the cell surface (142–144).

3. Low-Affinity Endocytosis

The NTR process involves the binding of transferrin to low-affinity binding sites on the cell surface of hepatocytes and hepatoma cells (114,116). The binding of transferrin to the cell surface is nonsaturable up to transferrin concentrations of at least

10 μM and occurs even in the presence of albumin (111). Transferrin-iron uptake by the low-affinity NTR process is mediated by the endocytosis of transferrin. Morgan et al. (111) demonstrated that radiolabeled transferrin is taken up by rat liver and internalised into low-density endosomal vesicles. Kinetics experiments using proteolytic enzymes to remove transferrin bound to the cell surface revealed that transferrin levels inside the cell reached a steady-state level, while the iron continued to accumulate (114,116). Transferrin endocytosis and iron uptake are both temperature- and energy-dependent, whereas uptake of iron, but not of transferrin, is reduced by weak bases (114,116).

Essentially, the NTR process is similar to the transferrin receptor-mediated process except that the transferrin binds to a low-affinity binding site rather than the high-affinity transferrin receptor. Transferrin is then endocytosed by an energy- and temperature-dependent process into low-density vesicles, where the iron is released from transferrin by a pH-dependent step and the protein is recycled to the extracellular medium (Fig. 4).

In contrast to the uptake of transferrin by the NTR process, iron uptake by human hepatoma and melanoma cell lines saturates with increasing concentrations of diferric transferrin, indicating that the uptake of iron by the NTR involves a carrier-mediated step (116,139,145). It is possible that this rate-limiting step in the uptake of iron reflects the transfer of iron across the endosomal membrane to the cell cytosol by iron transporters. Whether this iron transporter is the same as the endosomal iron transporter, DMT1, that mediates the transfer of iron across the endosomal membrane when iron is delivered into the endosome by the transferrin receptor is uncertain (89,93). Once the iron is delivered to the cytosol, it is stored either as ferritin or used for the synthesis of heme proteins (Fig. 4).

The identity of the membrane-binding protein that mediates the uptake of transferrin by the NTR is not known. Recently, a second human transferrin receptor (TfR2) has been cloned that has a high degree of sequence homology to the first transferrin receptor. It is highly expressed in the human liver, and the level of expression is not affected by iron status. When TfR2 is expressed in transferrin receptor-deficient Chinese hamster ovary cells, it can mediate uptake of transferrin and iron (146,147). There is also evidence that proteoglycans bind transferrin in a manner that is dependent on the pH and iron content of transferrin and promote the release of iron from transferrin (148–150). However, to date there is no direct evidence of a role for either TfR2 or proteoglycans in iron uptake by liver.

Fluid-phase endocytosis contributes to the uptake of transferrin iron by the cells. Fluid-phase endocytosis is the nonspecific uptake of molecules in the fluid phase of the endocytic vesicles. The contents of these vesicles are usually targeted to the lysosomes and degraded. The rate of fluid-phase endocytosis reported for hepatocytes is sufficient to account for less than 20% of observed uptake of transferrin iron (118,134,135,151). However, Bakoy and Thorstensen (152) suggest that recycling of the fluid from the endocytic vesicles to the extracellular medium rather than targeting to lysosomes would allow iron accumulation at a sufficient rate to account for NTR by hepatocytes.

4. Iron Release from Transferrin at the Plasma Membrane

It is now generally accepted that most types of cells acquire transferrin iron by the endocytosis of transferrin. In addition, there is evidence that hepatocytes are also

able to take up transferrin iron by a mechanism that does not involve transferrin endocytosis. Instead, it is proposed that the iron is reduced by a redox reaction and released from transferrin at the cell surface before the iron is transported across the cell membrane by an iron carrier (143). Evidence for the presence of a reductase in liver plasma membranes has been provided by the action of iron chelators on iron uptake. Both ferrous iron chelators and lipophilic iron chelators that cannot pass through the cell membrane have been reported to inhibit the uptake of iron from transferrin by hepatocytes (134,153,154), suggesting that the iron is reduced to its ferrous form outside the cell. Furthermore, ferricyanide can be reduced by hepatocytes and it in turn can inhibit transferrin-iron uptake while low oxygen levels increase hepatic iron uptake, implying that a reductive step is important (153). NADH is a likely electron donor, as it can release iron from transferrin in the presence of cell membranes (153–156). However, one of the main obstacles to this theory is that in a cell-free system the reduction potential of NADH is not sufficient to release iron from transferrin (157). However, it is possible that conformational changes to transferrin, reduction in pH, or the presence of iron chelators may make iron reduction more favorable, allowing the release of iron from transferrin at the cell membrane. Participation of the transferrin receptors in this process is unlikely, as monoclonal antibodies that recognized the receptor's transferrin-binding site did not interfere with the redox system (158), although it is possible that transferrin binds to the low-affinity sites on the hepatocyte membrane to facilitate the release of iron.

Further evidence for the release of iron at the cell membrane comes from the observation that the uptake of transferrin iron by hepatocytes and hepatoma cells is inhibited by non-transferrin-bound iron (145). Indeed the reverse, in which transferrin iron inhibits the uptake of non-transferrin-bound iron by hepatocytes, also occurs (159,160). Interestingly, in HuH7 human hepatoma cells, non-transferrin-bound iron has no effect on the uptake of iron by the transferrin receptor process, but it does competitively inhibit iron uptake by the NTR process. However, no changes in the rates of transferrin endocytosis by the NTR process are observed (145). This demonstrates that non-transferrin-bound iron does not inhibit the uptake of transferrin-iron by the NTR endocytic process but does diminish the uptake of iron released from transferrin at the cell surface.

The inhibitory effect of non-transferrin-bound iron on the uptake of transferrin iron at the cell surface indicates that the iron from both sources is taken up by the cell by a common pathway. Non-transferrin-bound iron is taken up avidly by many types of cells, including hepatic cells, by a mechanism that involves iron reduction and transport across the cell membrane by an iron carrier-mediated process [(161–165); see also Chapter 18]. Hence, it can be concluded that non-transferrin-bound iron and iron released from transferrin at the cell surface are transported across the hepatic cell membrane by a common iron transporter (Fig. 4). The identity of this iron transporter is unknown; a possibility is DMT1. As the endosomal membranes are constantly being recycled to the cell surface, it is possible that DMT1 could also operate at the cell surface.

Although a great deal of knowledge has been gained about the NTR-mediated processes, there are still many unanswered questions. Further studies are required to identify and characterize the low-affinity transferrin-binding sites, iron transporters, mechanisms of iron release from transferrin at the cell surface, and the regulatory mechanisms that control the NTR pathways.

REFERENCES

1. Barkan G. Eisenstudien. Die Verteilung des leicht abspaltbaren Eisens Zwischen Blutkörperchen und plasma und sein Verhalten unter experimentellen Bedingungen. *Z Physiol Chem* 1927; 171:194–221.
2. Holmberg CG, Laurell C-B. Studies on the capacity of serum to bind iron. A contribution to our knowledge of the regulation mechanism of serum iron. *Acta Physiol Scand* 1945; 10:307–319.
3. Laurell C-B. Studies on the transportation and metabolism of iron in the body with special reference to the iron-binding component of blood plasma. *Acta Med Scan* 1947; 14(Suppl 46):1–129.
4. Schade AL, Caroline L. Raw hen egg white and the role of iron in growth inhibition of *Shigella dysenteriae*, *Staphylococcus aureus*, *Escherichia coli* and *Saccharomyces cerevisial*. *Science* 1944; 100:14–15.
5. Schade AL, Caroline L. An iron-binding component in human blood plasma. *Science* 1946; 104:340–344.
6. Laurell C-B, Ingleman D. Fe-binding protein of swine serum. *Acta Chem Scand* 1947; 1:770–776.
7. Laurell C-B. Isolation and properties of crystalline Fe-transferrin from pigs serum. *Acta Chem Scand* 1953; 7:1407–1412.
8. Laurell C-B. Plasma iron and transport of iron in the organism. *Pharm Rev* 1952; 4: 371–395.
9. Holmberg CG, Laurell C-B. Investigations in serum copper. I. Nature of serum copper and its relation to the iron-binding protein in human serum. *Acta Chem Scand* 1947; 1:944–950.
10. Alderton G, Ward WH, Fevold HL. Identification of the bacteria-inhibiting, iron-binding protein of egg white as conalbumin. *Arch Biochem* 1946; 11:9–13.
11. Cohn EJ. Chemical, physiological and immunological properties and clinical uses of blood derivatives. *Experientia* 1947; 3:125–168.
12. Schade AL, Reinhart RW, Levy H. Carbon dioxide and oxygen in complex formation with iron and siderophilin, the iron-binding component of human plasma. *Arch Biochem* 1949; 20:170–172.
13. Surgenor DM, Koechlin BA, Strong LE. Chemical, clinical and immunological studies on the products of human plasma fractionation. XXXVII. The metal-combining globulin of human plasma. *J Clin Invest* 1949; 28:73–78.
14. Koechlin BA. Preparation and properties of serum and plasma proteins. XXXVIII. The b1-metal combining protein of human plasma. *J Am Chem Soc* 1952; 74:2649–2653.
15. Aisen P, Leibman A. Citrate-mediated exchange of Fe³⁺ among transferrin molecules. *Biochem Biophys Res Commun* 1968; 32:220–226.
16. Morgan EH. Exchange of iron and transferrin across endothelial surfaces in the rat and rabbit. *J Physiol* 1963; 169:339–352.
17. Taylor EM, Morgan EH. Developmental changes in transferrin and iron uptake by the brain in the rat. *Devel Brain Res* 1990; 55:35–42.
18. Taylor EM, Crowe A, Morgan EH. Transferrin and iron uptake by the brain: effects of altered iron status. *J Neurochem* 1992; 57:1584–1592.
19. Morales C, Sylvester SR, Griswold MD. Transport of iron and transferrin by the semiferous epithelium of the rat in vivo. *Biol Reprod* 1987; 37:995–1005.
20. Morgan EH. Placental transfer of iron. *Proc Austral Physiol Pharmacol Soc* 1982; 13: 11–17.
21. Awai M, Brown EB. Studies of the metabolism of I131-labelled human transferrin. *J Lab Clin Med* 1963; 63:363–396.
22. Wasserman LR, Sharney L, Gevirtz NR, Schwartz L, Weintraub LR, Tendler D, Du-

- mont AE, Drieling D, Witte M. The exchange of iron with interstitial fluid. *Proc Soc Exp Biol Med* 1964; 115:817–820.
23. Pollycove M, Mortimer R. The quantitative determination of iron kinetics and hemoglobin synthesis in human subjects. *J Clin Invest* 1961; 40:753–782.
 24. Bothwell TH, Charlton RW, Cook JD. *Iron Metabolism in Man*. Oxford: Blackwell, 1979.
 25. Cazzola M, Pootrakul P, Bergamaschi G, Huebers HA, Eng M, Finch CA. Adequacy or iron supply for erythropoiesis: in vivo observations in humans. *J Lab Clin Med* 1987; 110:734–739.
 26. Bothwell TH, Finch CA. *Iron Metabolism*. London: Churchill, 1962.
 27. Bothwell TH, Pribilla WF, Mebust W, Finch CA. Iron metabolism in the pregnant rabbit: iron transport across the placenta. *Am J Physiol* 1958; 193:615–622.
 28. McArdle HJ, Morgan EH. Transferrin and iron movements in the rat conceptus during gestation. *J Reprod Fertil* 1982; 66:529–536.
 29. Jandl JH, Katz JH. The plasma-to-cell cycle of transferrin. *J Clin Invest* 1963; 42:314–326.
 30. Kornfeld S. The effect of metal attachment to human apotransferrin on its binding to reticulocytes. *Biochim Biophys Acta* 1969; 194:25–33.
 31. Morgan EH. Transferrin, biochemistry, physiology and clinical significance. *Mol Aspects Med* 1981; 4:1–123.
 32. Dautry-Varsat A, Chiechanover A, Lodish HF. PH and the recycling of transferrin during receptor-mediated endocytosis. *Proc Natl Acad Sci USA* 1983; 80:2258–2262.
 33. Klausner RD, Ashwell G, van Renswoude J, Harford J, Bridges K. Binding of apotransferrin to K562 cells: explanation of the transferrin cycle. *Proc Natl Acad Sci USA* 1983; 80:2263–2266.
 34. Young SP, Bomford A, Williams R. The effect of the iron saturation of transferrin on its binding and uptake by rabbit reticulocytes. *Biochemistry* 1984; 219:505–510.
 35. Huebers H, Csiba E, Huebers E, Finch CA. Molecular advantage of diferric transferrin in delivering iron to reticulocytes: a comparative study. *Proc Soc Exp Biol Med* 1985; 179:222–226.
 36. Cook JD, Marsaglia G, Eschbach JW, Funk DD, Finch CA. Ferrokinetics: a biologic model for iron exchange in man. *J Clin Invest* 1970; 49:197–205.
 37. Christensen AC, Huebers H, Finch CA. Effect of transferrin saturation on iron delivery in rats. *Am J Physiol* 1978; 235:R18–R22.
 38. Ecarot-Charrier B, Grey VL, Wilczynska A, Schulman HM. Reticulocyte membrane transferrin receptors. *Can J Biochem* 1980; 58:418–426.
 39. Morgan EH. Effect of pH and iron content of transferrin on its binding to reticulocyte receptors. *Biochim Biophys Acta* 1983; 762:498–502.
 40. Hemnapharah D, Morgan EH. Transferrin uptake and release by reticulocytes treated with proteolytic enzymes and neuraminidase. *Biochim Biophys Acta* 1976; 426:385–398.
 41. Morgan EH, Baker E. Role of transferrin receptors and endocytosis in iron uptake by hepatic and erythroid cells. *Ann NY Acad Sci* 1988; 256:65–82.
 42. Iacopetta BJ, Morgan EH, Yeoh GCT. Transferrin receptors and iron uptake during erythroid cell development. *Biochim Biophys Acta* 1982; 687:204–210.
 43. Iacopetta BJ, Morgan EH. Transferrin endocytosis and iron uptake during erythroid cell development. *Biomed Biochim Acta* 1983; 42:S182–S186.
 44. Qian ZM, Morgan EH. Changes in the uptake of transferrin-free and transferrin-bound iron during reticulocyte maturation in vivo and in vitro. *Biochim Biophys Acta* 1992; 1135:35–43.
 45. Callus BA, Iacopetta BJ, Kühn LC, Morgan EH. Effects of overexpression of the transferrin receptor on the rates of transferrin recycling and uptake of non-transferrin

- recycling and uptake of non-transferrin-bound iron. *Eur J Biochem* 1996; 238:463–469.
46. Morgan EH, Appleton TC. Autoradiographic localization of 125I-labelled transferrin in rabbit reticulocytes. *Nature* 1969; 223:1371–1372.
 47. Appleton TC, Morgan EH, Baker E. A morphological study of transferrin uptake by reticulocytes. In: *The Regulation of Erythropoiesis and Haemoglobin Synthesis*. Prague: University Karlova, 1971:310–315.
 48. Hanover JA, Dickson RB. Transferrin: receptor-mediated endocytosis and iron delivery. In: *Endocytosis*. New York: Plenum Press, 1985:131–161.
 49. Baker E. General discussion II. In: *Iron Metabolism: Ciba Foundation Symposium 51 (new series)*. Amsterdam: Elsevier, 1977:364–369.
 50. Octave J-N, Schneider Y-J, Hoffman P, Trouet A, Crichton RR. Transferrin uptake by cultured rat embryo fibroblasts. The influence of lysomotropic agents, iron chelators and colchicine on the uptake of iron and transferrin. *Eur J Biochem* 1982; 123:235–240.
 51. Paterson S, Morgan EH. Effect of changes in the ionic environment of reticulocytes on the uptake of transferrin-bound iron. *J Cell Physiol* 1980; 105:484–502.
 52. Morgan EH. Inhibition of reticulocyte iron uptake by NH₄Cl and methylamine. *Biochim Biophys Acta* 1981; 642:119–134.
 53. Karin M, Mintz B. Receptor mediated endocytosis of transferrin in developmentally totipotent mouse teratocarcinoma stem cells. *J Biol Chem* 1981; 256:3245–3252.
 54. Harding C, Stahl P. Transferrin cycling in reticulocytes: pH and iron are important determinants of ligand binding and processing. *Biochem Biophys Res Commun* 1983; 113:650–658.
 55. Klausner RD, van Renswode J, Kempf C, Rao K, Bateman JL, Robbins AR. Failure to release iron from transferrin in a Chinese hamster ovary cell mutant pleiotropically defective in endocytosis. *J Cell Biol* 1984; 98:1098–1101.
 56. Savigni DL, Morgan EH. Use of inhibitors of ion transport to differentiate iron transporters in erythroid cells. *Biochem Pharmacol* 1996; 52:371–377.
 57. van Renswoude J, Bridges KR, Harford JB, Klausner RD. Receptor-mediated endocytosis of transferrin and the uptake of Fe in K562 cells: identification of a nonlysosomal acidic compartment. *Proc Natl Acad Sci USA* 1982; 79:5186–6190.
 58. Paterson S, Armstrong NJ, Iacopetta NJ, McArdle HJ, Morgan EH. Intravesicular pH and iron uptake by immature erythroid cells. *J Cell Physiol* 1984; 120:225–232.
 59. Iacopetta BJ, Morgan EH. An electron-microscope autoradiographic study of transferrin endocytosis by immature erythroid cells. *Eur J Cell Biol* 1983; 32:17–23.
 60. Stoorvogel W, Geuze HJ, Griffith JM, Strous GJ. The pathways of endocytosed transferrin and secretory proteins are connected in the trans-Golgi reticulum. *J Cell Biol* 1988; 106:1821–1829.
 61. Harding C, Heuser J, Stahl P. Endocytosis and intracellular processing of transferrin and colloidal gold-transferrin in rat reticulocytes: demonstration of a pathway for receptor shedding. *Eur J Cell Biol* 1984; 35:256–263.
 62. Johnstone RM. Maturation of reticulocytes: formation of exosomes as a mechanism for sledding membrane proteins. *Biochem Cell Biol* 1992; 70:179–190.
 63. Baynes RD, Skikne BS, Cook JD. Circulating transferrin receptors and assessment of iron status. *J Nutr Biochem* 1994; 5:322–330.
 64. Strahan ME, Crowe A, Morgan EH. Iron uptake in relation to transferrin degradation in brain and other tissues of rats. *Am J Physiol* 1992; 263:R924–R929.
 65. Rothenberger S, Iacopetta BJ, Juhn LC. Endocytosis of the transferrin receptor requires the cytoplasmic domain but not its phosphorylation site. *Cell* 1987; 49:423–431.
 66. Collawn JR, Lai A, Domingo D, Fitch M, Hatton S, Trowbridge IS. YTRF is the conserved internalization signal of the transferrin receptor, and a second YTRF signal at position 31–34 enhances endocytosis. *J Biol Chem* 1993; 268:21686–21692.

67. Odorizzi G, Trowbridge IS. Structural requirements for basolateral sorting of the human transferrin receptor in the biosynthetic and endocytic pathways of Madin-Darby canine kidney cells. *J Cell Biol* 1997; 137:1255–1264.
68. Watts C. Rapid endocytosis of the transferrin receptor in the absence of bound transferrin. *J Cell Biol* 1985; 100:633–637.
69. Stein BS, Sussman HH. Demonstration of two distinct transferrin receptor recycling pathways and transferrin-independent receptor internalization in K562 cells. *J Biol Chem* 1986; 261:10319–10331.
70. Girones N, Davis RJ. Comparison of the kinetics of cycling of the transferrin receptor in the presence or absence of bound transferrin. *Biochem J* 1989; 264:35–46.
71. Intragumtornchai T, Huebers HA, Finch CA. Transferrin-reticulocyte cycle time in rat reticulocytes. *Blut* 1990; 60:249–252.
72. Morgan EH. Chelator-mediated iron efflux from reticulocytes. *Biochem Biophys Acta* 1983; 733:39–50.
73. Watkins JA, Altazan JD, Elder P, Li C-Y, Nanez M-T, Cui X-X, Glass J. Kinetic characterization of reductant dependent processes in iron mobilization from endocytic vesicles. *Biochemistry* 1992; 31:5820–5830.
74. Teeters CL, Lodish HF, Ciechanover A, Wallace BA. Transferrin and apotransferrin: pH-dependent conformational changes associated with receptor-mediated uptake. *Ann NY Acad Sci* 1986; 463:403–407.
75. Bali PK, Aisen P. Receptor-modulated iron release from transferrin: differential effects on N- and C-terminal sites. *Biochemistry* 1991; 30:9947–9952.
76. Bali PK, Zak O, Aisen P. A new role for the transferrin receptor in the release of iron from transferrin. *Biochemistry* 1991; 30:324–328.
77. Sipe DM, Murphy RF. High-resolution kinetics of transferrin acidification in BALB/c3T3 cells: exposure to pH 6 followed by temperature-sensitive alkalization during recycling. *Proc Natl Acad Sci USA* 1987; 84:7119–7123.
78. Parkkila S, Waheed A, Britton RS, Bacon B, Zhou XY, Tomatsu S, Fleming RE, Sly WS. Association of the transferrin receptor in human placenta with HFE, the protein defective in hereditary hemochromatosis. *Proc Natl Acad Sci USA* 1997; 94:13198–13202.
79. Feder JN, Penny DM, Irrinki A, Lee VK, Lebron JA, Watson N, Tsuchihashi Z, Sigal E, Bjorkman PJ, Schatzman RC. The hemochromatosis gene product complexes with the transferrin receptor and lowers its affinity for ligand binding. *Proc Natl Acad Sci USA* 1998; 95:1472–1477.
80. Lebron J, West AP, Bjorkman PJ. The hemochromatosis protein HFE competes with transferrin for binding to the transferrin receptor. *J Mol Biol* 1999; 294:239–245.
81. Bennett MJ, Lebron JA, Bjorkman PJ. Crystal structure of the hereditary hemochromatosis protein HFE complexed with transferrin receptor. *Nature* 2000; 403:46–53.
82. Lebron J, Bennett MJ, Vaughn DE, Chirino A, Snow PM, Mintier GA, Feder JN, Bjorkman PJ. Crystal structure of the hemochromatosis protein HFE and characterization of its interaction with the transferrin receptor. *Cell* 1998; 93:111–123.
83. Salter-Cid L, Brunmark A, Li Y, Leturcq D, Peterson PA, Jackson MR, Yang Y. Transferrin receptor is negatively modulated by the hemochromatosis protein HFE: implication for cellular iron homeostasis. *Proc Natl Acad Sci USA* 1999; 96:5434–5439.
84. Roy CN, Penny DM, Feder JN, Erins C. The hereditary hemochromatosis protein, HFE, specifically regulates transferrin-mediated iron uptake in HeLa cells. *J Biol Chem* 1999; 274:9022–9028.
85. Morgan EH. Membrane transport of non-transferrin-bound iron by reticulocytes. *Biochim Biophys Acta* 1988; 943:428–439.
86. Savigni D, Morgan EH. Transport mechanisms for iron and other transition metals in rat and rabbit erythroid cells. *J Physiol* 1998; 508:837–850.

87. Gunshin H, MacKenzie B, Berger VV, Gunshin Y, Romero MF, Boron WF, Nussberger S, Gollan JL, Hediger MA. Cloning and characterization of a mammalian proton-coupled metal ion transporter. *Nature* 1997; 389:482–488.
88. Fleming MD, Trenor CC, Su MA, Foenzler D, Beier DR, Dietrich WF, Andrews NC. Microcytic anaemia mice have a mutation in Nramp2, a candidate ion transporter gene. *Nature Genet* 1997; 16:383–386.
89. Fleming MD, Romano MA, Su MA, Garric LM, Garrick MD, Andrews NC. Nramp2 is mutated in the anemic Belgrade(b) rat: evidence of a role for Nramp2 in endosomal iron transport. *Proc Natl Acad Sci USA* 1998; 95:1148–1153.
90. Edwards JA, Hoke JE. Red cell iron uptake in hereditary microcytic anemia. *Blood* 1975; 46:381–388.
91. Edwards JA, Garrick LM, Hoke JE. Defective iron uptake and globin synthesis by erythroid cells in the anemia of the Belgrade laboratory rat. *Blood* 1978; 51:347–357.
92. Bowen BJ, Morgan EH. Anemia of the Belgrade rat: evidence for defective membrane transport of iron. *Blood* 1987; 70:38–44.
93. Su MA, Trenor CC, Fleming JC, Fleming MD, Andrews NC. The G185R mutation disrupts function of the iron transporter Nramp2. *Blood* 1998; 92:2157–2163.
94. Jeffries WA, Brandon WR, Hunt SV, Williams AF, Galler KC, Mason DY. Transferrin receptor on endothelium of brain capillaries. *Nature* 1984; 312:162–163.
95. Fishman JB, Rubin JB, Handrahan JV, Connor JR, Fine RE. Receptor-mediated transcytosis of transferrin across the blood-brain barrier. *J Neuroscience Res* 1987; 18:288–304.
96. Pardridge WM. Recent advances in blood-brain barrier transport. *Ann Rev Pharmacol Toxicol* 1988; 28:25–39.
97. Taylor E, Morgan EH. Developmental changes in transferrin and iron uptake by the brain in the rat. *Devel Brain Res* 1990; 55:35–42.
98. Taylor E, Crowe A, Morgan EH. Transferrin and iron uptake by the brain: effects of altered iron status. *J Neurochem* 1991; 57:1584–1592.
99. Moos T, Morgan EH. Evidence for low molecular weight, non-transferrin-bound iron in rat brain and cerebrospinal fluid. *J Neurosci Res* 1998; 54:496–494.
100. Baker E, van Bockxmeer FM, Morgan EH. Distribution of transferrin and transferrin receptors in the rabbit placenta. *Q J Exp Physiol* 1983; 69:359–372.
101. Anderson GJ. Control of iron absorption. *J Gastroenterol Hepatol* 1996; 11:1030–1032.
102. Anderson GJ, Powell LW, Halliday JW. Transferrin receptor distribution and regulation in the rat small intestine. *Gastroenterology* 1990; 98:576–585.
103. Oates PS, Thomas C, Freitas E, Callow MJ, Morgan EH. Gene expression of divalent metal transporter and transferrin receptor in the duodenum of Belgrade rats. *Am J Physiol* 2000; 278:G930–G936.
104. Feder JN, Grirke A, Tsuchihashi Z, Ruddy DA, Basava A, Dormishian F, Domingo R, Ellis MC, Fullan A, Hinton LM, Jones NL, Kimmel BE, Kronmal GS, Lauer P, Lee VK, Loeb DB, Mapa FA, McClelland E, Meyer NC, Mintier GA, Moeller N, Moore T, Morikang E, Prass CE, Quintana L, Starnes SM, Schatzman RC, Brunke KJ, Drayna DT, Risch NJ, Bacon BR, Wolff RK. A novel MHC class 1-like gene is mutated in patients with hereditary hemochromatosis. *Nature Genet* 1996; 13:399–408.
105. Feder JN, Tsuchihashi Z, Irrinki A, Lee VK, Mapa FA, Morikang E, Prass CE, Starnes SM, Wolff RK, Parkkila S, Sly WS, Schatzman RC. The hemochromatosis founder mutation in HLA-H disrupts b2-microglobulin interaction and cell surface expression. *J Biol Chem* 1997; 272:14025–14028.
106. Waheed A, Parkkila S, Zhou XY, Tomatsu S, Tsuchihashi Z, Feder JN, Schatzman RC, Britton RS, Bacon BR, Sly WS. Hereditary hemochromatosis: effects of C282Y and H63D mutations on association with b2-microglobulin, intracellular processing, and

- cell surface expression of HFE protein in COS-7 cells. *Proc Natl Acad Sci USA* 1997; 94:12384–12389.
107. Van Wyke CP, Linder-Horowitz M, Munro HN. Effect of iron loading on heme-iron compounds in different liver cell populations. *J Biol Chem* 1971; 246:1025–1031.
 108. Sibille J-C, Octave J-N, Schneider Y-J, Trouet A, Crichton RR. Subcellular localization of transferrin protein and iron in the perfused rat liver. Effect of Triton WR 1339, digitonin and temperature. *Eur J Biochem* 1986; 155:47–55.
 109. van Berkel TJC, Dekker CJ, Kruijt JK, van Eijk HG. The interaction in vivo of transferrin and asialotransferrin with liver cells. 1987; 243:715–722.
 110. Young SP, Roberts S, Bomford A. Intracellular processing of transferrin and iron by isolated rat hepatocytes. *Biochem J* 1985; 232:819–823.
 111. Morgan EH, Smith GD, Peters TJ. Uptake and subcellular processing of ⁵⁹Fe-125I-labelled transferrin by rat liver. *Biochem J* 1986; 237:163–173.
 112. Goldenberg HM, Elder R, Pumm E, Wallner H, Retzek H, Huttinger M. Uptake and subcellular distribution of transferrin in rat liver. *Biochim Biophys Acta* 1988; 968:331–339.
 113. Goldenberg HM, Seelos C, Chatwani S, Chegini S, Pumm R. Uptake and endocytic pathway of transferrin and iron in perfused rat liver. *Biochim Biophys Acta* 1991; 1067:145–152.
 114. Trinder D, Morgan EH, Baker E. The mechanisms of iron uptake by fetal rat hepatocytes in culture. *Hepatology* 1986; 6:852–858.
 115. Trinder D, Morgan EH, Baker E. The effects of an antibody to the rat transferrin receptor and of serum albumin on the uptake of diferric transferrin by rat hepatocytes. *Biochim Biophys Acta* 1988; 943:440–446.
 116. Trinder D, Zak O, Aisen P. Transferrin receptor-independent uptake of diferric transferrin by human hepatoma cells with antisense inhibition of receptor expression. *Hepatology* 1996; 23:1512–1520.
 117. Ciechanover A, Schwartz AL, Dautry-Varsat A, Lodish HF. Kinetics of internalization and recycling of transferrin and the transferrin receptor in human hepatoma cell line. *J Biol Chem* 1983; 258:9681–9689.
 118. Sibille J-C, Octave J-N, Schneider Y-J, Trouet A, Crichton RR. Transferrin protein and iron uptake by cultured hepatocytes. *FEBS Lett* 1982; 150:365–369.
 119. Trinder D, Oates PS, Thomas C, Sadleir J, Morgan EH. Localisation of divalent metal transporter 1 (DMT1) to the microvillus membrane of rat duodenal enterocytes in iron deficiency, but to hepatocytes in iron overload. *Gut* 2000; 46:270–276.
 120. Tei I, Makino Y, Kadoofuku T, Kanamaru I, Konn K. Increase of transferrin receptors in regenerating rat liver cells after partial hepatectomy. *Biochem Biophys Res Commun* 1984; 121:717–721.
 121. Hirose-Kumagai A, Sakai H, Akamatsu N. Increase of transferrin receptors in hepatocytes during rat liver regeneration. *Int J Biochem* 1984; 16:601–605.
 122. Sciot R, Verhoeven G, van Eyken P, Cailleau J, Desmet VJ. Transferrin receptor expression in rat liver: immunohistochemical and biochemical analysis of the effect of age and iron storage. *Hepatology* 1990; 11:416–427.
 123. Muller-Eberhard U, Liem HH, Grasso JA, Giffhorn-Katz S, DeFalco MG, Katz NR. Increase in surface expression of transferrin receptors on cultured hepatocytes of adult rats in response to iron deficiency. 1989; 263:14753–14756.
 124. Trinder D, Batey RG, Morgan EH, Baker E. Effect of cellular iron concentration on iron uptake by hepatocytes. *Am J Physiol* 1990; 259:G611–G617.
 125. Holmes JM, Morgan EH. Uptake and distribution of transferrin and iron in perfused, iron-deficient liver. *Am J Physiol* 1990; 256:G1022–G1027.
 126. Sciot R, Paterson AC, van den Oord JJ, Desmet VJ. Lack of hepatic transferrin receptor expression in hemochromatosis. *Hepatology* 1987; 7:831–837.

127. Lombard M, Bomford A, Hynes M, Naumov NV, Roberts S, Crowe J, Williams R. Regulation of the hepatic transferrin receptor in hereditary hemochromatosis. *Hepatology* 1989; 9:1–5.
128. Barsini D, Cairo G, Ginelli E, Marozzi A, Conte D. Nitric oxide reduces nontransferrin-bound iron transport in HepG2 cells. *Hepatology* 1999; 29:464–470.
129. Hirayama M, Kohgo Y, Kondo H, Shintani N, Fujikawa K, Sasaki K, Kato J, Niitsu Y. Regulation of iron metabolism in HepG2 cells: a possible role for cytokines in the hepatic deposition of iron. *Hepatology* 1993; 18:874–880.
130. Kobune M, Konhgo Y, Kato J, Miyazaki E, Niitsu Y. Interleukin-6 enhances hepatic transferrin uptake and ferritin expression in rats. *Hepatology* 1994; 19:1468–1475.
131. Vogel W, Bomford A, Young S, Williams R. Heterogeneous distribution of transferrin receptors on parenchymal and non-parenchymal liver cells: biochemical and morphological evidence. *Blood* 1987; 69:264–270.
132. Soda R, Tavassoli M. Liver endothelium and not hepatocytes or Kupffer cells have transferrin receptors. *Blood* 1984; 63:270–276.
133. Tavassoli M. The role of liver endothelium in the transfer of iron from transferrin to the hepatocyte. *Ann NY Acad Sci* 1988; 526:83–92.
134. Cole ES, Glass J. Transferrin binding and iron uptake in mouse hepatocytes. *Biochim Biophys Acta* 1983; 762:102–110.
135. Page M, Baker E, Morgan EH. Transferrin and iron uptake by rat hepatocytes in culture. *Am J Physiol* 1984; 246:G26–G33.
136. Chan RYY, Ponka P, Schulman HM. Transferrin-receptor-independent but iron-dependent proliferation of variant Chinese hamster ovary cells. *Exp Cell Res* 1992; 202:326–336.
137. Oshira S, Nakajima H, Markello T, Krasnewich D, Bernaerding I, Gahl WA. Redox, transferrin-independent, and receptor-mediated endocytosis iron uptake systems in cultured human fibroblasts. *J Biol Chem* 1993; 268:21586–21591.
138. Richardson D, Baker E. The uptake of iron and transferrin by the human melanoma cell. *Biochim Biophys Acta* 1990; 1053:1–12.
139. Richardson D, Baker E. Two saturable mechanisms of iron uptake from transferrin in human melanoma cells: the effect of transferrin concentration, chelators, and metabolic probes on transferrin and iron uptake. *J Cell Physiol* 1994; 161:160–168.
140. Zak O, Trinder D, Aisen P. Primary receptor-recognition site of human transferrin is in the C-terminal lobe. *J Biol Chem* 1994; 269:7110–7114.
141. Thorstensen K, Trinder D, Zak O, Aisen P. Uptake of iron from N-terminal half-transferrin by isolated rat hepatocytes. Evidence of transferrin-receptor-independent iron uptake. *Eur J Biochem* 1995; 232:129–1331.
142. Baker E, Morgan EH. Iron transport. In: Brock JH, Halliday JW, Pippaed MJ, Powell LW, eds. *Iron Metabolism in Health and Disease*. London: Sanders, 1994:63–95.
143. Thorstensen K, Romslo I. The role of transferrin in the mechanism of cellular iron uptake. *Biochem J* 1990; 271:1–10.
144. Richardson D, Ponka P. The molecular mechanisms of the metabolism and transport of iron in normal and neoplastic cells. *Biochim Biophys Acta* 1997; 1331:1–40.
145. Trinder D, Morgan EH. Inhibition of uptake of transferrin-bound iron by human hepatoma cells by nontransferrin-bound iron. *Hepatology* 1997; 26:691–698.
146. Kawabata H, Yang R, Hirama T, Vuong PT, Kawano S, Gombart AF, Koeffler HP. Molecular cloning of transferrin receptor 2 a new member of the transferrin receptor-like family. *J Biol Chem* 1999; 274:20826–20832.
147. Fleming RE, Migas MC, Holden CC, Waheed A, Britton RS, Tomatsu S, Bacon BR, Sly WS. Transferrin receptor 2: continued expression in mouse liver in the face of iron overload and in hereditary hemochromatosis. *Proc Natl Acad Sci USA* 2000; 97:2214–2219.

148. Omoto E, Minguell JJ, Tavassoli MJ. Proteoglycan synthesis by cultured liver endothelium: the role of membrane-associated heparin sulphate in transferrin binding. *Exp Cell Res* 1990; 187:85–89.
149. Hu W-L, Reggoczi E. Hepatic heparan sulphate proteoglycan and the recycling of transferrin. *Biochem Cell Biol* 1992; 70:535–538.
150. Reggoczi E, Chindemi PA, Hu W-L. Interaction of transferrin and its iron-binding fragments with heparin. *Biochem J* 1994; 299:819–823.
151. Thorstensen K, Romslo I. Uptake of iron from transferrin by isolated hepatocytes. *Biochim Biophys Acta* 1984; 804:200–208.
152. Bakoy OE, Thorstensen K. The process of cellular uptake of iron from transferrin. A computer simulation program. *Eur J Biochem* 1994; 222:105–112.
153. Thorstensen K, Romslo I. Uptake of iron from transferrin by isolated rat hepatocytes. A redox-mediated plasma membrane process. *J Biol Chem* 1988; 263:8844–8850.
154. Thorstensen K, Romslo I. Hepatocytes and reticulocytes have different mechanisms for the uptake of iron from transferrin. *J Biol Chem* 1988; 263:16837–16841.
155. Low H, Sun IL, Navas P, Grebing C, Crane FL, Morre DJ. Transplasmalemma electron transport from cells is part of a diferric transferrin reductase system. *Biochem Biophys Res Commun* 1986; 139:1117–1123.
156. Sun IL, Navas P, Crane FL, Morre DJ, Low H. NADH diferric transferrin reductase in liver plasma membranes. *J Biol Chem* 1987; 262:15915–15921.
157. Thorstensen K, Aisen P. Release of iron from diferric transferrin in the presence of rat liver plasma membranes: no evidence of a plasma membrane diferric transferrin reductase. *Biochim Biophys Acta* 1990; 1052:29–35.
158. Toole-Simms W, Sun IL, Faulk WP, Low H, Lindgren A, Crane FL, Morre DJ. Inhibition of transplasma membrane electron transport by monoclonal antibodies to the transferrin receptor. *Biochem Biophys Res Commun* 1991; 176:1437–1442.
159. Scheiber B, Goldenberg H. Uptake of iron by isolated rat hepatocytes from hydrophilic impermeable ferric chelate Fe(III)-DPTA. *Arch Biochem Biophys* 1996; 326:185–192.
160. Graham RM, Morgan EH, Baker E. Ferric citrate uptake by cultured rat hepatocytes is inhibited in the presence of transferrin. *Eur J Biochem* 1998; 253:139–145.
161. Wright TL, Brissot P, Ma W-L, Weisiger RA. Characterization of non-transferrin-bound iron clearance by rat liver. *J Biol Chem* 1986; 261:10909–10914.
162. Randell EW, Parkes JG, Oliveri NF, Templeton DM. Uptake of non-transferrin-bound iron by both reductive and nonreductive processes is modulated by intracellular iron. *J Biol Chem* 1994; 269:16046–16053.
163. Sturrock A, Alexander J, Lamb J, Craven CM, Kaplan J. Characterization of a transferrin-independent uptake system for iron in Hela cells. *J Biol Chem* 1990; 265:3139–3145.
164. Baker E, Baker SM, Morgan EH. Characterisation of non-transferrin-bound iron (ferric citrate) uptake by rat hepatocytes in culture. *Biochim Biophys Acta* 1998; 1380:21–30.
165. Trinder D, Morgan EH. Mechanisms of ferric citrate uptake by human hepatoma cells. *Am J Physiol* 1998; 275:G279–G286.

Transport of Non-Transferrin-Bound Iron by Hepatocytes

JOEL G. PARKES and DOUGLAS M. TEMPLETON

University of Toronto, Toronto, Ontario, Canada

I. INTRODUCTION	451
II. THE NATURE OF NTBI	452
III. NTBI TRANSPORT IN LIVER	453
IV. NTBI TRANSPORT IN CULTURED HEPATOCYTES	453
V. REGULATION OF NTBI UPTAKE IN HEPATOCYTES	460
A. Transcriptional Regulation	460
B. Posttranscriptional Regulation	460
C. Intracellular Trafficking of NTBI Carrier Proteins	462
VI. CONCLUSIONS	462
ACKNOWLEDGMENTS	463
REFERENCES	463

I. INTRODUCTION

It has been long recognized that Fe occupies a pivotal role in mammalian metabolism due to its special redox properties, exhibiting a range of potentials that facilitate its participation in the one-electron catalysis of both oxidative and reductive reactions. In recent years the “dark” side of Fe has become increasingly apparent in view of its capacity through one-electron reactions to promote generation of toxic free radicals under physiological conditions. The dilemma for eukaryotic cells, therefore, is to exploit the beneficial effects of Fe while avoiding its harmful effects. Both these

objectives are achieved by regulating Fe supply in a variety of ways, including solubilization, dietary absorption, transport in the circulation, uptake by tissues, and incorporation into or as prosthetic groups, and storage. Since Fe excretion is minimal, dysfunction resulting in an increased supply of Fe can result in Fe overload, a condition that if left untreated can have fatal consequences. It was in situations such as these that the liver was recognized as one of the most important sites for Fe turnover and targets for Fe toxicity. In this chapter we will review transport of low-molecular-weight forms of Fe and the impact of these mechanisms on Fe-overload diseases, with particular emphasis on hepatic iron metabolism.

II. THE NATURE OF NTBI

The concept of non-transferrin-bound Fe (NTBI) first appeared to describe a form of Fe in transit, putatively identified as a plasma Fe pool capable of forming complexes with diethylenetriaminepentaacetic acid (DTPA) in rats whose transferrin was saturated by hypertransfusion or dietary Fe overload (1). Later, the term non-transferrin-bound iron (NTBI) was used to describe dialyzable Fe in patient serum with saturated latent Fe-binding capacity (2). While the existence of NTBI was not immediately accepted, improvements in methodology for its detection (3) and quantitation (4,5) have confirmed its existence as a true species of Fe.

The toxicity of NTBI depends on its availability in plasma, which in turn determines its uptake by vulnerable tissues. As seen in Table 1, high plasma NTBI is found in significant concentrations in plasma Fe overload associated with hereditary hemochromatosis or secondarily in patients being transfused for hemoglobinopathies such as thalassemia (5–8). NTBI also becomes significant in end-stage renal disease (5) and in patients undergoing chemotherapy for a variety of leukemic disorders (9,10). Clinical studies following plasma NTBI as a function of chelation therapy in patients with thalassemia major and thalassemia intermedia highlight the complex turnover of NTBI both during and after chelation therapy (8), possibly reflecting its varied structure and diverse origins.

Table 1 Serum NTBI Concentrations in Human Disease

Diagnosis	Serum NTBI (μM)	References	
Normal	≤ 0	(5,7,8,72)	
Thalassemia major	3.6	(7)	
	2.9	(8)	
	0.9–12.8	(5)	
Thalassemia intermedia	4.5	(8)	
Hereditary hemochromatosis	11.9	(5)	
	Homozygous (phlebotomized)	1.8	(72)
	Heterozygous (phlebotomized)	0.5	(72)
NHL, AML, HD, ALL ^a	3.1	(9)	

^aAll patients undergoing chemotherapy for non-Hodgkin's lymphoma (NHL), acute myeloid leukemia (AML), Hodgkin's disease (HD), or acute lymphoblastic leukemia (ALL).

The low molecular weight of NTBI was deduced from its dialyzability, and nuclear magnetic resonance (NMR) studies confirmed that complexes with citrate are the most likely species of NTBI found in plasma (11), although an Fe(III)-binding polypeptide in serum has been described (12). Complexation with higher-molecular-weight plasma proteins, such as albumin, may also contribute to the plasma NTBI pool. Although the bulk of studies of NTBI have dealt with the oxidized form [Fe(III) and its complexes], extending the definition to include the reduced state [Fe(II)] may be physiologically meaningful in the context of NTBI transport mechanisms. Therefore, in this chapter the definition of NTBI includes salts and low-molecular-weight complexes of both valence states of Fe.

III. NTBI TRANSPORT IN LIVER

Uptake of plasma NTBI by the liver was demonstrated by single-pass perfusion to be highly efficient (58–75%), with Fe(II) exhibiting a slightly greater uptake than Fe(III) [63% for Fe(II) versus 55% for Fe(III)] (13). Clearance of transferrin by the liver, which requires receptor-mediated endocytosis, was usually less than 1% (14). Efflux of Fe was negligible under these conditions (<1%), suggesting that intracellularly the bulk of NTBI may become incorporated into a high-molecular-weight impermeant pool such as ferritin. This notion was confirmed when particles resembling ferritin cores were observed in lysosomes of hepatic parenchymal cells 30 min postperfusion (15). This latter study also determined that Zn^{2+} , Co^{2+} , and Mn^{2+} competitively inhibited Fe(II) uptake, suggesting a common divalent metal-ion carrier might be involved. In addition, hepatic uptake was not energy-dependent and was the same regardless of iron status (Fe-loaded or -deficient); high activation energy (14.3 kcal/mol) was consistent with a carrier-mediated process.

IV. NTBI TRANSPORT IN CULTURED HEPATOCYTES

From this earlier work on whole liver, attention turned to in-vitro techniques with cultured hepatocytes to characterize hepatic NTBI uptake more fully. To this end, primary hepatocytes from chick embryo (16), as well as fetal (17) and adult rat liver (18–22), were used along with established cell lines of hepatic origin such as the human hepatocellular carcinoma cells HepG2 (23–25) and HuH7 (62). Table 2 summarizes the kinetic parameters reported for NTBI uptake in intact liver as well as by cultured cells. The variation in K_m for Fe(III) and Fe(II) uptake can be attributed to the variety of ligands utilized, but in general, cultured hepatocytes appear to exhibit a greater affinity for NTBI than does whole liver, perhaps in keeping with the localization of Fe to parenchymal cells in perfused liver (13). Because in vivo the fenestrated endothelium permits close contact between serum and parenchymal cells, Fe concentrations encountered by these cells are the same as those in serum. Comparing serum NTBI concentrations encountered in Fe overload (Table 1) with the K_m values in Table 2 shows that hepatic NTBI uptake is unlikely to be saturated because many of these concentrations are below the K_m for uptake by liver. Nevertheless, the relation between serum NTBI levels, NTBI transport processes, and hepatic iron deposition still remains to be determined. Complicating this relationship is the nature of the contribution of hepatocytes and other nonparenchymal cells as

Table 2 Kinetic Constants for NTBI Uptake in Mammalian Liver and Cultured Hepatocytes

	Ligand ^a	K_m (μM)	V_{max}	References
Fe(III)				
Liver	Tricine	14	24 ± 2 nmol/min/g liver	(13)
Cultured hepatocytes				
HepG2	NTA	4.3	2.6 fmol/min/ μg protein	(25)
HuH7	Citrate	1.1	1.9 fmol/min/ μg protein	(26)
Rat liver	NTA	1.25	241 pmol/min/ 10^6 cells	(24)
	DTPA	0.63	98 fmol/min/ 10^6 cells	(41)
	Citrate	7.2	2.3 pmol/min/ μg DNA	(19)
Fe(II)				
Liver	Tricine	22	38 nmol/min/g	(13)
Cultured hepatocytes				
HepG2	NTA	3.6	55 fmol/min/ μg protein	(23)

^aDTPA, diethylenetriamine pentaacetate; NTA, nitrilotriacetate

well as the contribution of the recently described transferrin receptor-2 (TfR2), which is not subject to downregulation by Fe loading (27).

The units used to express rates (V_{max}), whether based on protein, cell number, or DNA, vary from one laboratory to another, as does the use of different ligands. Table 3 lists a number of cellular and molecular factors that modulate NTBI transport in cultured liver cells. Broadly speaking, these data may be summarized according to a model depicted in Fig. 1. Low-molecular-weight forms of plasma NTBI, consisting exclusively of Fe(III) bound to some ligand (L) in a complex L-Fe(III), are taken up in a two step process. First, L-Fe(III) is bound by cell surface binding protein(s) (B) where dissociation of the ligand and Fe(III) takes place. Dissociation may require reduction by a cell surface reductase (R). The second step, translocation, may occur via either the Fe(II) (T2) or Fe(III) (T3) translocator, coupled with either cell surface binding proteins (B) or a ferrireductase (R). Oxidation of Fe(III) by plasma ceruloplasmin (Cp), secreted by the liver, may also generate Fe(III) and direct it to a trivalent metal-ion translocator (T3). A transmembrane homolog of a multi-copper oxidase, hephaestin, has been identified in intestine but not in liver and is not included in this model.

Trying to accommodate such a large number of experimental observations into a single model of NTBI transport necessarily leads to oversimplification and some assumptions. One of these assumptions is that the ligand plays no direct role in the response to any given parameter. Since comparisons are made to controls utilizing the same ligand, this is unlikely to be problematic, for example, when the use of metabolic inhibitors, alkylating agents, etc., are examined. The ligand may be more important, however, when divalent metal-ion specificity is being explored or when high-affinity processes in the micromolar range are being measured in balanced culture media (28). Cell surface binding of Fe(III) and its ligand is the first step, followed rapidly by dissociation of the ligand. Consistent with such a scheme is the observation that the uptake of Fe by HeLa cells from ferric citrate does not require

Table 3 Factors Affecting NTBI Uptake in Cultured Hepatocytes

Factor	Response	References
Degradative enzymes		
Trypsin	Inhibition	(23,41)
Neuraminidase	No effect	(23)
Heparin lyase III	No effect	(23)
Chondroitinase	No effect	(23)
Channel blockers		
Diltiazem	No effect	(23)
Verapamil	No effect	(23)
Nifedipine	No effect	(23)
Dicyclohexylcarbodiimide	No effect	(41)
Bafilomycin A1	No effect	(41)
Competition by divalent metals		
Co	Inhibition	(19,23)
Ni, Cu, Cd, Zn	No effect	(23)
Ni, Mg, Zn	Inhibition	(19)
Mn	No effect	(24)
Ca	Stimulation	(19,73)
Cellular Fe status		
Fe-loaded	Stimulation	(21,25)
	Inhibition	(53)
Fe chelators		
Deferoxamine	Inhibition	(25,41)
Deferiprone	Inhibition	(25)
Catechol disulfonate	Stimulation	(41)
Bathophenanthroline disulfonate	Inhibition	(26)
2,2'-bipyridine	Inhibition	(26,41)
Pyridoxal isonicotinoyl hydrazone	Inhibition	(26)
Transferrin	Inhibition	(18,22)
Apotransferrin	Inhibition	(18,22)
Sulfhydryl alkylation		
Dithionitrobenzene	No effect	(23)
N-ethylmaleimide	Inhibition	(23,41)
Iodoacetate	Inhibition	(23)
<i>p</i> -Mercuribenzoylsulfonate	No effect	(41)
Metabolic inhibitors		
Chloroquine	Inhibition	(23)
2,4-Dinitrophenol	Inhibition	(23)
Potassium cyanide	No effect	(23)
Sodium azide	No effect	(41)
Actinomycin D	Inhibition	(23)
Cycloheximide	Inhibition	(23)
Monensin	No effect	(23)
Reductants/oxidants		
Ascorbate	Stimulation	(23,26,41)
Ferricyanide (<20 μ M)	Stimulation	(26)
Ferricyanide (>100 mM)	Inhibition	(26,41)
Ferrocyanide (<10 μ M)	No effect	(26)
Ferrocyanide (>100 mM)	Stimulation	(26)
Ferrocyanide (1 mM)	Inhibition	(41)
Ceruloplasmin	Stimulation	(46)
Nitric oxide		
S-nitroso-N-acetylpenicillamine	Inhibition	(68)
Sodium nitroprusside	Inhibition	(68)

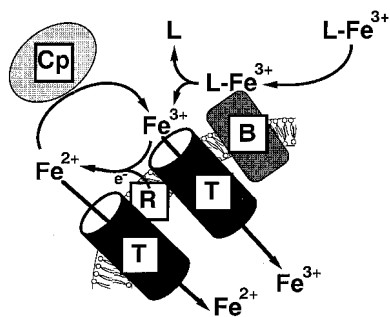


Figure 1 A two-step mechanism of NTBI uptake in hepatocytes. In the first step, ligand-bound plasma NTBI [L-Fe(III)] dissociates as a consequence of interacting with cell surface binding proteins (B) or reductase (R). Plasma ceruloplasmin (Cp) may function as a multicopper ferroxidase to oxidize Fe(II) prior to uptake. In the second stage, Fe enters the cell through either an Fe(II) (T2) or Fe(III) (T3) translocase.

the obligatory uptake of its ligand, citrate (29). Furthermore, the dissociation constant of ferric ion (provided as ferric citrate) binding to HeLa cell plasma membranes was an order of magnitude less than the K_m for transport (30), suggesting that a two-step process is involved in NTBI transport, the first being binding of ferric ion to specific cell surface sites, followed by a rapid translocation step. Scheiber et al. (22) report that the surfaces of hepatocytes promote the release of Fe from stable chelates with DTPA, and this Fe can be acquired by extracellular impermeant ligands such as hydroxyethyl-starch coupled deferoxamine (DFO). Direct transfer between DTPA and DFO is negligible in the absence of cells, suggesting that, in support of the two-step model, there are activities on the cell surface that can strip Fe from some ligands, presumably as a prelude to transport. A family of six polypeptides has been isolated from rat liver basolateral plasma membranes (31), and these may be candidates for Fe-binding proteins required for dissociating ligand from Fe(III), but as yet such a function remains to be established. A differential display analysis of control and Fe-loaded HepG2 cells failed to identify any potential NTBI carriers or binding proteins (32).

The question remains what criteria determine which ligands are suitable for studying NTBI uptake. Dissociation is a function of the ligand stability constant, and hexadentate chelators such as DFO have high Fe-binding affinity [$\log \beta = 31$ (33)]. DFO is also a poor ligand for NTBI uptake (J. G. Parkes and D. M. Templeton, unpublished observations), which may be due to its inability to dissociate from Fe at the cell surface. However, deferiprone [$\log \beta_3 = 35.9$ (33)] is able to participate in NTBI uptake (J. G. Parkes and D. M. Templeton, unpublished observations), suggesting that stability alone is not the determining factor. Alternatively, the Fenton activity of Fe(III) bound to its ligand may be an indication of its suitability as a substrate for NTBI uptake. It has been argued that this activity is dependent on the availability of a free coordination site on the metal to allow access to the oxygen species (34). Using relative Fenton activity as a correlate to dissociation prior to uptake by cells is certainly an oversimplification. However, it is consistent with the observation that ferrioxamine [Fe(III)-DFO] is a poor substrate for transport and

catalyzes virtually no free-radical formation. On the other hand, Fe complexes with DTPA, citrate, NTA, and deferiprone—ligands commonly employed in NTBI uptake studies (Table 2)—have much greater Fenton activity than ferrioxamine (34), suggesting that availability of a free coordination site may be the common factor linking Fenton activity of Fe/ligand complexes with their dissociation prior to NTBI uptake. This relationship may be especially true where reductase activity is involved in addition to dissociation.

In recent years considerable effort has been directed toward determining whether NTBI undergoes redox cycling prior to transport. Such a notion that Fe reduction is *sine qua non* for NTBI transport in mammalian cells is reminiscent of the multicomponent Fe transport system in *Saccharomyces sp.*, where separate genes, *FRE1* and *FRE2*, code for proteins that carry out an essential reduction step prior to Fe uptake (35). Cells with high reductase activity and *FRE1* gene copy number exhibit a heme absorption spectrum similar to that of flavocytochrome b₅₅₈, a heterodimer in phagocytic membranes capable of NADPH-dependent reduction of molecular oxygen to superoxide anion (36). One component of this complex, p22^{phox}, shows considerable sequence homology with *FRE1*, especially at sites associated with FAD and NADPH binding (36). Since many types of leukocytes can take up NTBI, it was suggested that gp91^{phox}, by its analogy with the *FRE1* gene product, could mediate the reductive uptake of NTBI. However, recent findings that lymphocytes from patients with chronic granulomatous disease that lack functional gp91^{phox} exhibit the same ability to acquire Fe as those with functional flavoprotein suggest that gp91^{phox} does not participate in NTBI uptake by leukocytes, despite its structural and functional similarity to fre1p (37).

In yeast (see Chapter 15) transport is carried out under aerobic conditions by a combination of a multicopper oxidase and a transmembrane permease, coded for by *FET3* and *FTR1* genes, respectively. No mammalian homologs to yeast *FTR1* have been identified with NTBI transport in hepatocytes. However, the *FET3* gene sequence predicts a protein with high sequence homology to a mammalian ferroxidase, ceruloplasmin (38,39), and a role for a ferroxidase activity in NTBI uptake in both yeast and humans has been proposed (40) (see below).

Iron reduction and NTBI transport have been addressed by the studies shown in Table 3. A key finding is that reduction by ascorbate (23,26,41) or low concentrations of impermeant ferricyanide ions (26) stimulate Fe(III) uptake, suggesting that, *in vivo*, a reduction step may contribute to NTBI uptake. In keeping with this suggestion is the observation that the impermeant Fe(II) chelator, bathophenanthroline disulfonate (BPS), was able to inhibit uptake of Fe(III). However, BPS may shift the redox equilibrium away from Fe(III) and thereby drive the formation of Fe(II) rather than act as a passive chelator of the reduced form of Fe (42). Reconciling a reductive step with the potential redox effects of BPS may lie with the kinetic properties of Fe(III) reductase, an enzyme that has yet to be identified in liver. In cardiac myocytes ferricyanide reductase kinetic parameters indicate that rates of Fe(III) reduction may be two- to sixfold greater than Fe(III) transport (43), suggesting that chelation by impermeant Fe(II) chelators may be able to compete for transport and thereby decrease uptake. Although there is an Fe(III) reductase in liver endosomal membranes (44) and an Fe(III) reductase in monocytes distinct from

ferricyanide reductase (45), the identity of a specific hepatic reductase for NTBI and its cofactors remains elusive.

At the opposite end of the redox spectrum are reports of the oxidation of Fe prior to transport by hepatocellular carcinoma HepG2 cells (46) and erythroleukemic K562 cells (47). These studies follow several reports of a well-known link between copper and iron metabolism through the serum protein ceruloplasmin, a copper-containing enzyme with ferroxidase activity (see Chapter 30). Of particular significance is the fact that patients with hereditary ceruloplasmin deficiency exhibit hemochromatosis and increased Fe deposition in organs including the liver (48). Early reports attributed tissue iron deposition in aceruloplasminemia to reduced Fe efflux, since it was demonstrated that ceruloplasmin promoted the release of Fe to transferrin in the perfused liver (49) and in HepG2 cultures (50). The identification of the *FET3* gene that encodes a multicopper oxidase involved in Fe uptake in yeast (38,39) implied that ceruloplasmin might perform an analogous function in mammalian cells (40). A transmembrane-bound intestinal ceruloplasmin homologue, hephaestin, may be necessary for the passage of Fe from the intestine into the circulation (51). Fox and co-workers have demonstrated that Fe(III) uptake by HepG2 cells is enhanced by the addition of ceruloplasmin but only in cells rendered Fe deficient by chelation with BPS, an impermeant Fe(II) chelator; there was no stimulation of Fe uptake in cells replete with Fe (46). These studies promote the notion of a trivalent metal-ion carrier that has yet to be identified but appears to be associated with ceruloplasmin and its ferroxidase activity. The requirement for Fe depletion of HepG2 cells before stimulation by ceruloplasmin remains the most difficult feature of the oxidation mechanism to fit into a physiological context. Processes resulting in Fe depletion in vivo are not well characterized and therefore difficult to envision, but if they occur there would be a prompt increase in transferrin receptor synthesis, mediated post-transcriptionally by iron-responsive element/iron regulatory protein (IRE/IRP) interactions at the 3' untranslated region of transferrin receptor mRNA (see Chapter 9). Iron depletion begs the question of where the substrate would come from for uptake via the ferroxidase activity of ceruloplasmin, since reduced plasma Fe is undetectable and plasma NTBI is elevated only in Fe overload (Table 1). A great deal more needs to be done to clarify the role of ferroxidase in NTBI transport, especially where there is an apparent "futile cycle," involving reduced Fe(II) arising from a cell surface ferrireductase in conjunction with an extracellular (ceruloplasmin?) or transmembrane (hephaestin?) ferroxidase. How these activities would optimize availability of Fe from a variety of non-transferrin-bound plasma sources, while at the same time controlling cellular entry via specific transporters or carriers, remains to be established.

The final stage in transport is translocation across the cell membrane. There is sufficient agreement that NTBI uptake is a carrier-mediated process. First, it is saturable (Table 1) and is inhibited by proteolytic enzymes, cycloheximide, and actinomycin D [Table 3; (22,23)]. No extracellular polyelectrolytes appear to be involved, as there is no effect of neuraminidase, heparin lyase III, or chondroitinase (23) on NTBI transport. Uptake in hepatocytes, as in a number of other cells, is upregulated by Fe loading (21,25,43,52), and this is reversed by chelation with DFO (25,41) and deferiprone (25). This suggests that an intracellular and chelatable regulatory Fe pool plays a role in expression of NTBI transport protein(s). Early work,

showing a 50% inhibition of NTBI uptake by iron loading in Chang liver cells, appears to contradict these findings (53), but in that study uptake was measured over 22 h, reflecting equilibrium processes, while initial rates were used in others (21,25,41).

To date none of the known ion channels seem to be involved in hepatic Fe uptake, although Fe(II) uptake by an L-type Ca^{2+} channel has been observed in adult rat myocardium and myocytes (54). As seen in Table 3, three structurally different Ca^{2+} channel blockers (diltiazem, verapamil, and nifedipene) are ineffective in blocking NTBI uptake (25), as is the proton channel blocker dicyclohexylcarbodiimide (41). However, a divalent cation carrier protein with broad metal-ion specificity, possibly coupled to proton transport and sharing 92% identity with human DMT1/Nramp2, was cloned from the cDNA library of rat intestine of Fe-deficient animals (55). DMT1/Nramp2 is responsible for the Fe transport defect in the Belgrade (*b*) rat and *mk* mouse suffering from microcytic anemia (56). Its role as a candidate NTBI transport protein was confirmed by expression in *Xenopus* oocytes, where it stimulated the uptake of Fe(II) by 200-fold. The greatest DMT1/Nramp2 mRNA expression was in the duodenum, but detectable message was demonstrated in liver (55). Dietary Fe deficiency increased DMT1 mRNA in duodenum dramatically, but lesser (55) or no (57) changes were reported for liver, suggesting that DMT1/Nramp2 may play a more significant role in intestinal Fe absorption than hepatic NTBI uptake. Nevertheless, immunohistochemical staining revealed increased DMT1/Nramp2 protein in Fe-loaded liver and in cell membranes of isolated hepatocytes (57), suggesting that DMT1/Nramp2 may contribute to the upregulation of NTBI transport in Fe-loaded hepatocytes.

Several observations argue against this thesis. First, as indicated in Table 3, the ability of divalent cations to compete with Fe for uptake by hepatocytes is variable. Thus, while Co^{2+} is an effective competitor, Ni^{2+} , Cu^{2+} , Cd^{2+} , Mn^{2+} , or Zn^{2+} have no effect on $\text{Fe}^{2+/3+}$ uptake, although all these divalent cations are reported to be transported equally with Fe(II) by DMT1 (55). [Parenthetically, Co^{2+} also mimics the increase in erythropoietin gene expression due to hypoxia in HepG2 cells (58), suggesting that its inhibitory effect may not be entirely due to competition.] Second, both Fe(II) and Fe(III) uptake are increased by Fe loading (23), and no evidence has come to light indicating that DMT1/Nramp2 can function as a carrier for Fe(III) in liver. Third, DMT1/Nramp2 is a proton-coupled activity and neither bafilomycin nor dicyclohexylcarbodiimide have any effect on NTBI uptake (41). Lastly, microcytic anemia in animals that lack functional DMT1/Nramp2, the Belgrade rat and the *mk* mouse, is due to defective intestinal Fe absorption rather than defective NTBI uptake in liver. To our knowledge NTBI uptake has not been investigated in the liver cells of DMT1/Nramp2-defective animals.

The data in Table 3 also point to the role of specific sulfhydryl groups that are required for NTBI transport by cultured hepatocytes. These are unreactive toward the well-known SH inactivators *p*-chloromercuribenzoate and dithio-*bis*-nitrobenzoate, but are sensitive to iodoacetic acid and *N*-ethylmaleimide. This may be explained by postulating differentially accessible —SH groups, the essential one(s) being more accessible to and/or reactive with the smaller alkylating reagents. These studies do not identify the location of these —SH groups and as such do not rule out the possibility of multiple polypeptide targets with susceptible —SH groups.

V. REGULATION OF NTBI UPTAKE IN HEPATOCYTES

Very little is known about the mechanisms by which NTBI uptake is regulated, but examining the number of different characteristics listed in Table 3 indicates that it is likely a complex process. A number of genes of iron metabolism (that are related to NTBI transport by the fact that their activities or expression are affected by Fe or by chelation) may provide some insights into possible regulatory pathways for NTBI uptake. For simplicity we will assume that these regulatory mechanisms apply to all polypeptides involved in NTBI uptake, including ligand-binding proteins, oxidoreductases, and translocases. A number of possible regulatory scenarios are considered in Fig. 2 and form the basis for a discussion of plausible although somewhat speculative schemes.

A. Transcriptional Regulation

One of the most common motifs for modulating gene expression is by regulating transcription by *trans*-activating transcription factors binding to *cis*-acting untranscribed sequences flanking genes on either the 3' or 5' side. The erythropoietin gene (Fig. 2A, Epo) is one such example whose expression is increased by hypoxia, and this increase is due to the binding of hypoxia inducible factor (HIF-1) to an enhancer site in the 3' flanking sequence (59). One of the protein components of HIF-1, HIF-1 α , is exquisitely sensitive to oxygen and through hypoxia-responsive elements (HRE) controls many different genes including glucose transporters, glycolytic enzymes (60), the inducible form of nitric oxide synthetase [iNOS (61)], and various growth factors (62). It is interesting that Co and Fe chelators such as DFO mimic the effects of hypoxia in Hep3B (59) and HepG2 (58) cells. Deferiprone was as effective as DFO in affecting growth-factor gene expression in one study (62). Recent studies indicate that in addition to the posttranscriptional mechanism of regulating transferrin receptor mRNA stability through IRE/IRP interactions (63), there is increased transcription of transferrin receptor genes by hypoxia (64) and by Fe chelation (65) in hepatoma cells (Hep 3B). In both these studies, a role for HIF-1 α in activating transcription through an HRE in the transferrin receptor gene was proposed (Fig. 2A, TfR). A similar mechanism was proposed for erythroid cells (66). A role for HIF-1 α in hepatic NTBI uptake has not been reported, but one study in neonatal cardiac myocytes indicated that hypoxia stimulated NTBI uptake over twofold (67). The physiological basis for this is unknown, but the increase in NTBI uptake parallels the stimulation of transferrin receptor mRNA in hepatocytes (64) and erythroid cells (66), suggesting that a common process is plausible. It may be significant that Fe chelation potentiates the effect of ceruloplasmin-stimulated NTBI uptake in HepG2 cells (46), but as yet no connection has been made between this mechanism and hypoxia.

B. Posttranscriptional Regulation

The data in Table 3 indicate that NTBI transport is stimulated by intracellular Fe in cultured cells (21,25), and such a relationship immediately suggests a posttranscriptional mechanism utilizing the proteins IRP-1 and IRP-2 and IREs in mRNA (Fig. 2A). If such a mechanism exists, stimulation of NTBI transporter synthesis by intracellular Fe accumulation would be modeled after the IRE/IRP-dependent process

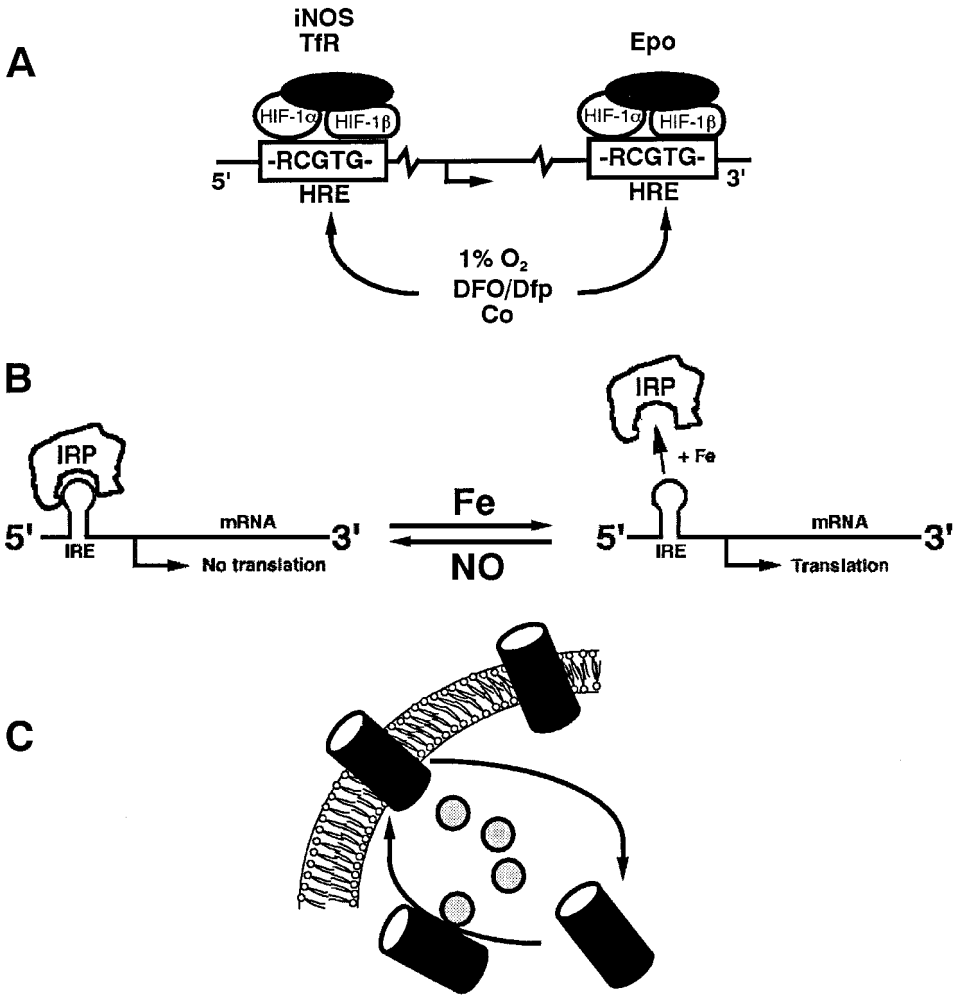


Figure 2 Potential mechanisms for regulation of hepatocyte NTBI uptake. (A) Transcriptional control of the protein components involved in NTBI uptake may occur through a mechanism similar to those utilizing the hypoxia response element (HRE). In this scheme, stimuli such as hypoxia (1% O₂), Fe chelation with deferroxamine (DFO) or deferiprone (Dfp), or addition of Co²⁺ ions results in the formation of a transcriptional activation complex consisting of a co-activator (p300/CBP), HIF-1 α , and HIF-1 β . This *trans*-acting complex binds to a *cis*-acting enhancer consensus sequence (5'-RCGTG-3') located either at the 3' untranslated region (as for erythropoietin, Epo) or the 5' untranslated region (as for transferrin receptor, TfR, and inducible form of nitric oxide synthetase, iNOS). (B) Posttranscriptional control of NTBI transport may occur by modulating translation through an iron response element (IRE), located in the 5' untranslated region of an appropriate mRNA. Binding of the iron-response-element-binding protein (IRP) is enhanced by low intracellular Fe or by nitric oxide (NO) and is reduced by high intracellular Fe. In the latter case, dissociation of the IRP allows translation to proceed, thereby increasing proteins involved in NTBI transport. (C) Modulation of NTBI transport may occur by modulating the intracellular movement of translocase proteins between cytosolic storage sites and the plasma membrane. Cycling of these proteins may require the assistance of small GTP-binding proteins (stippled circles) homologous to rab11 proteins involved in transferrin receptor trafficking.

governing ferritin synthesis. Thus, IRP-1 binding to an IRE located on the 5' side of the translation initiation site at low cellular Fe levels would dissociate with increased Fe, thus promoting translation (Fig. 2B). It may be significant in this regard that NO[•] donors decrease NTBI uptake in HepG2 cells [Table 3 (68)]. This reduction is due to a reduced number of transporters rather than a reduced affinity, suggesting an effect of NO[•] upon protein synthesis, possibly mediated by IRE/IRP interactions at the transcript level. In keeping with this notion, IRP binding to IRE is enhanced by NO[•] (63), suggesting that translation of transporter mRNA would be blocked by the presence of IRP at the IRE in the 5' untranslated region. Another study indicated that hypoxia enhanced the binding of IRP1 to the transferrin receptor transcript, and the resultant stabilization prompted a 10-fold increase in mRNA (69). The mechanism for this was not mentioned, but an increase in iNOS induced by hypoxia may account for the increased binding of IRP-1 to the IRE of transferrin receptor. It should be mentioned that NO can also react with low-molecular-weight intracellular Fe (70). Since NTBI transport seems to be coupled to the chelatable intracellular Fe pool (23), increased NO[•] could be depleting this pool, mimicking the effect of chelation and reducing NTBI uptake as a consequence. Thus, posttranscriptional processes regulating NTBI uptake may be multifactorial and involve other mechanisms in addition to IRE/IRP interactions.

C. Intracellular Trafficking of NTBI Carrier Proteins

The cycling of NTBI transport proteins between the cytosol and the cell surface may be considered an alternative means by which NTBI transport may be modulated. According to this model (Fig. 2C), high concentrations of intracellular Fe mobilize NTBI transport proteins to the cell surface, thereby increasing NTBI uptake. Kinetic studies showing no change in K_m but an increase in V_{max} are consistent with such a mechanism. In addition, recycling of receptors is an integral part of transferrin-bound Fe uptake by receptor-mediated endocytosis and small GTP-binding proteins belonging to the rab family appear to participate in receptor recycling. Recently a 912-Da polypeptide capable of binding to one member of the rab family, rab11, was found to be distributed between the cytosol and endosomal membranes (71). Proteins with similar effector activity may facilitate NTBI partitioning between the cytosol and the plasma membrane under appropriate stimuli.

VI. CONCLUSIONS

Plasma NTBI is particularly enigmatic, arising from different sources, entering a wide variety of tissues by carrier-mediated processes, and potentially contributing to the progression of diseases such as hepatocellular carcinoma and hepatic and cardiac fibrosis. Equally problematic is the means by which its transport into tissues is regulated. Unraveling the cellular and molecular details of NTBI transport awaits a clearer definition of the molecular species of Fe involved and the identification of additional specific genes or polypeptides that participate in the process. While NTBI transport into liver may serve in the short term to clear harmful redox-active species from the plasma, the physiological significance of this is unproven.

ACKNOWLEDGMENTS

Work in the authors' laboratory is supported by grants from the Medical Research Council of Canada and The Heart and Stroke Foundation of Ontario.

REFERENCES

1. Hershko C. A study of the chelating agent diethylenetriaminepentaacetic acid using selective radioiron probes of the reticuloendothelial and parenchymal iron stores. *J Lab Clin Med* 1975; 85:913–921.
2. Hershko C, Rachmilewitz EA. Non-transferrin plasma iron in patients with transfusional iron overload. In: RR Crichton, ed. *Proteins of Iron Storage and Transport in Biochemistry and Medicine*. Amsterdam: North-Holland, 1975:427–432.
3. Gutteridge JMC, Rowley DA, Griffiths E, Halliwell B. Low-molecular-weight iron complexes and oxygen radical reactions in idiopathic haemochromatosis. *Clin Sci* 1985; 68:463–467.
4. Singh S, Hider RC, Porter JB. A direct method for quantitation of non-transferrin-bound iron. *Anal Biochem* 1990; 186:320–323.
5. Breuer W, Ronson A, Slotki IN, Abramov A, Hershko C, Cabantchik ZI. The assessment of serum nontransferrin-bound iron in chelation therapy and iron supplementation. *Blood* 2000; 95:2975–2982.
6. Hershko C, Peto TEA. Non-transferrin plasma iron. *Br J Haematol* 1987; 66:149–151.
7. Al-Refaie FN, Wickens DG, Wonke B, Kontoghiorghe GJ, Hoffbrand AV. Serum non-transferrin-bound iron in beta-thalassemia major patients treated with desferrioxamine and L1. *Br J Haematol* 1992; 82:431–436.
8. Porter JB, Abeyasinghe RD, Marshall L, Hider RC, Singh S. Kinetics of removal and reappearance of non-transferrin-bound plasma iron with deferoxamine therapy. *Blood* 1996; 88:705–713.
9. Bradley SJ, Gosriwitana I, Srichairatanakool S, Hider RC, Porter JB. Non-transferrin-bound iron induced by myeloablative chemotherapy. *Br J Haematol* 1977; 99:337–343.
10. Halliwell B, Aruoma OI, Mufti G, Bomford A. Bleomycin-detectable iron in serum from leukaemic patients before and after chemotherapy. Therapeutic implications for treatment with oxidant-generating drugs. *FEBS Lett* 1988; 241:202–204.
11. Grootveld M, Bell JD, Halliwell B, Aruoma OI, Bomford A, Sadler PJ. Non-transferrin-bound iron in plasma or serum from patients with idiopathic hemochromatosis. Characterization by high performance liquid chromatography and nuclear magnetic resonance spectroscopy. *J Biol Chem* 1989; 264:4417–4422.
12. Stojkovski S, Goumakos W, Sarkar B. Iron(III)-binding polypeptide in human cord and adult serum: isolation, purification and partial characterization. *Biochim Biophys Acta* 1992; 1137:155–161.
13. Brissot P, Wright TL, Ma W-L, Weisiger RA. Efficient clearance of non-transferrin-bound iron by rat liver. Implications for hepatic iron loading in iron overload states. *J Clin Invest* 1985; 76:1463–1470.
14. Zimelman AP, Zimmerman HJ, McLean R, Weintraub LR. Effect of iron saturation of transferrin on hepatic iron uptake: an in vitro study. *Gastroenterology* 1977; 72:129–131.
15. Wright TL, Brissot P, Ma W-L, Weisiger RA. Characterization of non-transferrin-bound iron clearance by rat liver. *J Biol Chem* 1986; 261:10909–10914.
16. Shedlofsky SI, Bonkowsky HL, Sinclair PR, Sinclair JF, Bement WJ, Pomeroy S. Iron loading of cultured hepatocytes. Effect of iron on 5-aminolaevulinate synthase is independent of lipid peroxidation. *Biochem J* 1983; 212:321–330.

17. Trinder D, Batey RG, Morgan EH, Baker E. Effect of cellular iron concentration on iron uptake by hepatocytes. *Am J Physiol* 1990; 259:G611–G617.
18. Graham RM, Morgan EH, Baker E. Ferric citrate uptake by cultured rat hepatocytes is inhibited in the presence of transferrin. *Eur J Biochem* 1998; 253:139–145.
19. Baker E, Baker SM, Morgan EH. Characterisation of non-transferrin-bound iron (ferric citrate) uptake by rat hepatocytes in culture. *Biochim Biophys Acta* 1998; 1380:21–30.
20. Cable EE, Connor JR, Isom HC. Accumulation of iron by primary rat hepatocytes in long-term culture—changes in nuclear shape mediated by non-transferrin-bound forms of iron. *Am J Pathol* 1998; 152:781–792.
21. Richardson DR, Chua AG, Baker E. Activation of an iron uptake mechanism from transferrin in hepatocytes by small-molecular-weight iron complexes: implications for the pathogenesis of iron-overload disease. *J Lab Clin Med* 1999; 133:144–151.
22. Scheiber B, Goldenberg H. The surface of rat hepatocytes can transfer iron from stable chelates to external acceptors. *Hepatology* 1998; 27:1075–1080.
23. Randell EW, Parkes JG, Olivieri NF, Templeton DM. Uptake of non-transferrin-bound iron by both reductive and nonreductive processes is modulated by intracellular iron. *J Biol Chem* 1994; 269:16046–16053.
24. Barisani D, Berg CL, Wessling-Resnick M, Gollan JL. Evidence for a low K_m transporter for non-transferrin-bound iron in isolated rat hepatocytes. *Am J Physiol* 1995; 269:G570–G576.
25. Parkes J, Randell E, Olivieri N, Templeton D. Modulation by iron loading and chelation of the uptake of non-transferrin-bound iron by human liver cells. *Biochim Biophys Acta* 1995; 1243:373–380.
26. Trinder D, Morgan E. Mechanisms of ferric citrate uptake by human hepatoma cells. *Am J Physiol* 1998; 275:G279–G286.
27. Fleming RE, Migas MC, Holden CC, Waheed A, Britton RS, Tomatsu S, Bacon BR, Sly WS. Transferrin receptor 2: continued expression in mouse liver in the face of iron overload and in hereditary hemochromatosis. *Proc Natl Acad Sci USA* 2000; 97:2214–2219.
28. Brunner-Döpfer L, Kriegerbeckova K, Kovar J, Goldenberg H. Pitfalls in assessing specificity and affinity of non-transferrin-bound iron uptake. *Anal Biochem* 1998; 261:128–130.
29. Jordan I, Kaplan J. The mammalian transferrin-independent iron transport system may involve a surface ferrireductase activity. *Biochem J* 1994; 302:875–879.
30. Musílková J, Kriegerbecková K, Krusek J, Kovár J. Specific binding to plasma membrane is the first step in the uptake of non-transferrin iron by cultured cells. *Biochim Biophys Acta* 1998; 1369:103–108.
31. Barisani D, Wessling-Resnick M. Fe-nitritotriacetic acid-binding proteins associated with rat liver plasma membranes. *Hepatology* 1996; 24:934–938.
32. Barisani D, Meneveri R, Ginelli E, Cassani C, Conte D. Iron overload and gene expression in HepG2 cells: analysis by differential display. *FEBS Lett* 2000; 469:208–212.
33. Motekaitis RJ, Martell AE. Stabilities of the iron(III) chelates of the 1,2-dimethyl-3-hydroxy-4-pyridinone and related ligands. *Inorg Chim Acta* 1991; 183:71–80.
34. Singh S, Hider RC. Colorimetric detection of the hydroxyl radical: comparison of the hydroxyl-radical-generating ability of various iron complexes. *Anal Biochem* 1988; 171:47–54.
35. Radisky D, Kaplan J. Regulation of transition metal transport across the yeast plasma membrane. *J Biol Chem* 1999; 274:4481–4484.
36. Shatwell KP, Dancis A, Cross AR, Klausner RD, Segal AW. The FRE1 ferric reductase of *Saccharomyces cerevisiae* is a cytochrome b similar to that of NADPH oxidase. *J Biol Chem* 1996; 271:14240–14244.

37. DeLeo FR, Olakanmi O, Rasmussen GT, Lewis TS, McCormick SJ, Nauseef WM, Britigan BE. Despite structural similarities between gp91phox and FRE1, flavocytochrome b558 does not mediate iron uptake by myeloid cells. *J Lab Clin Med* 1999; 134:275–282.
38. Dancis A, Yuan DS, Haile D, Askwith C, Eide D, Moehle C, Kaplan J, Klausner RD. Molecular characterization of a copper transport protein in *S. cerevisiae*: an unexpected role for copper in iron transport. *Cell* 1994; 76:393–402.
39. Askwith C, Eide D, Van Ho A, Bernard PS, Li L, Davis-Kaplan S, Sipe DM, Kaplan J. The *FET3* gene of *S. cerevisiae* encodes a multicopper oxidase required for ferrous iron uptake. *Cell* 1994; 76:403–410.
40. Kaplan J, O'Halloran TV. Iron metabolism in eukaryotes: Mars and Venus at it again. *Science* 1996; 271:1510–1512.
41. Scheiber B, Goldenberg H. Uptake of iron by isolated rat hepatocytes from a hydrophilic impermeant ferric chelate, Fe(III)-DTPA. *Arch Biochem Biophys* 1996; 326:185–192.
42. Thorstensen K, Aisen P. Release of iron from diferric transferrin in the presence of rat liver plasma membranes: no evidence of a plasma membrane diferric transferrin reductase. *Biochim Biophys Acta* 1990; 1052:29–35.
43. Parkes JG, Olivieri NF, Templeton DM. Characterization of Fe²⁺ and Fe³⁺ transport by iron-loaded cardiac myocytes. *Toxicology* 1997; 117:141–151.
44. Scheiber B, Goldenberg H. NAD(P)H:ferric iron reductase in endosomal membranes from rat liver. *Arch Biochem Biophys* 1993; 305:225–230.
45. May JM, Qu ZC, Mendiratta S. Role of ascorbic acid in transferrin-independent reduction and uptake of iron by U-937 cells. *Biochem Pharmacol* 1999; 57:1275–1282.
46. Mukhopadhyay CK, Attieh ZK, Fox PL. Role of ceruloplasmin in cellular iron uptake. *Science* 1998; 279:714–717.
47. Attieh ZK, Mukhopadhyay CK, Seshadri V, Tripoulas NA. Ceruloplasmin ferroxidase activity stimulates cellular iron uptake by a trivalent cation-specific transport mechanism. *J Biol Chem* 1999; 274:1116–1123.
48. Harris ZL, Takahashi Y, Miyajima H, Seizawa M, MacGillivray RTA, Gitlin JD. Aceruloplasminemia: molecular characterization of this disorder of iron metabolism. *Proc Natl Acad Sci USA* 1995; 92:2539–2543.
49. Osaki S, Johnson DA, Frieden E. The mobilization of iron from the perfused mammalian liver by a serum copper enzyme, ferroxidase I. *J Biol Chem* 1971; 246:3018–3023.
50. Young SP, Fahmy M, Golding S. Ceruloplasmin, transferrin and apotransferrin facilitate iron release from human liver cells. *FEBS Lett* 1997; 411:93–96.
51. Vulpe CD, Kuo Y-M, Murphy TL, Cowley L, Askwith C, Libina N, Gitschier J, Anderson GJ. Hephaestin, a ceruloplasmin homologue implicated in intestinal iron transport, is defective in the *sla* mouse. *Nature Genet* 1999; 21:195–199.
52. Olakanmi O, Stokes JB, Pathan S, Britigan BE. Polyvalent cationic metals induce the rate of transferrin-independent iron acquisition by HL-60 cells. *J Biol Chem* 1997; 272:2599–2606.
53. White GP, Jacobs A. Iron uptake by Chang cells from transferrin, nitriloacetate and citrate complexes: the effect of iron-loading and chelation with desferrioxamine. *Biochim Biophys Acta* 1978; 543:217–225.
54. Tsushima RG, Wickenden AD, Bouchard RA, Oudit GY, Liu PP, Backx PH. Modulation of iron uptake in heart by L-type Ca²⁺ channel modifiers. Possible implications in iron overload. *Circ Res* 1999; 84:1302–1309.
55. Gunshin H, Mackenzie B, Berger U, Gunshin Y, Romero M, Boron W, Nussberger S, Gollan J, Hediger M. Cloning and characterization of a mammalian proton-coupled metal-ion transporter. *Nature* 1997; 388:482–488.
56. Su MA, Trenor III CC, Fleming JC, Fleming MD, Andrews NC. The G185R mutation disrupts function of the iron transporter Nramp2. *Blood* 1998; 92:2157–2163.

57. Trinder D, Oates PS, Thomas C, Sadleir J, Morgan EH. Localisation of divalent metal transporter I (DMT1) to the microvillus membrane of rat duodenal enterocytes in iron deficiency, but to hepatocytes in iron overload. *Gut* 2000; 46:270–276.
58. Ehleben W, Porwol T, Fandrey J, Kummer W, Acker H, Cobalt and desferrioxamine reveal crucial members of the oxygen sensing pathway in HepG2 cells. *Kidney Int* 1997; 51:483–491.
59. Wang GL, Semenza GL. Desferrioxamine induces erythropoietin gene expression and hypoxia-induced factor 1 DNA-binding activity: implications for models of hypoxia signal transduction. *Blood* 1993; 82:3610–3615.
60. Semenza GL. Expression of hypoxia inducible factor-1: mechanisms and consequences. *Biochem Pharmacol* 2000; 59:47–53.
61. Jung F, Palmer LA, Zhou N, Johns RA. Hypoxic regulation of inducible nitric oxide synthase via hypoxia inducible factor-1 in cardiac myocytes. *Circ Res* 2000; 86:319–325.
62. Gleadle JM, Ebert BL, Firth JD, Ratcliffe PJ. Regulation of angiogenic growth factor expression by hypoxia, transition metals, and chelating agents. *Am J Physiol* 1995; 268: C1362–C1368.
63. Hentze MW, Kühn LC. Molecular control of vertebrate iron metabolism: mRNA-based regulatory circuits operated by iron, nitric oxide, and oxidative stress. *Proc Natl Acad Sci USA* 1996; 93:8175–8182.
64. Tacchini L, Bianchi L, Bernelli-Zazzera A, Cairo G. Transferrin receptor induction by hypoxia—HIF-1-mediated transcriptional activation and cell-specific post-transcriptional regulation. *J Biol Chem* 1999; 274:24142–24146.
65. Bianchi L, Tacchini L, Cairo G. HIF-1-mediated activation of transferrin receptor gene transcription by iron chelation. *Nucleic Acids Res* 1999; 27:4223–4227.
66. Lok CN, Ponka P. Identification of a hypoxia response element in the transferrin receptor gene. *J Biol Chem* 1999; 274:24147–24152.
67. Hershko C, Link G, Pinson A. Modification of iron uptake and lipid peroxidation by hypoxia, ascorbic acid, and α -tocopherol in iron-loaded rat myocardial cell cultures. *J Lab Clin Med* 1987; 110:355–361.
68. Barisani D, Cairo G, Ginelli E, Marozzi A, Conte D. Nitric oxide reduces nontransferrin-bound iron transport in HepG2 cells. *Hepatology* 1999; 29:464–470.
69. Toth I, Yuan L, Rogers JT, Boyce H, Bridges KR. Hypoxia alters iron-regulatory protein-1 binding capacity and modulates cellular iron homeostasis in human hepatoma and erythroleukemic cells. *J Biol Chem* 1999; 274:4467–4473.
70. Sergeant O, Griffon B, Morel I, Chevanne M, Dubos M-P, Cillard P, Cillard J. Effect of nitric oxide on iron-mediated oxidative stress in primary rat hepatocyte culture. *Hepatology* 1996; 25:122–127.
71. Zeng JB, Ren MD, Gravotta D, De Lemos-Chiarandini C, Lui M, Erdjument-Bromage H, Tempst P, Xu GX, Shen TH, Morimoto T, Adesnik M, Sabatini DD. Identification of a putative effector protein for rab11 that participates in transferrin recycling. *Proc Natl Acad Sci USA* 1999; 96:2840–2845.
72. De Valk B, Addicks MA, Gosriwatana I, Lu S, Hider RC, Marx JM. Non-transferrin-bound iron is present in serum of hereditary haemochromatosis heterozygotes. *Eur J Clin Invest* 2000; 30:248–251.
73. Nilsen T. Effects of calcium on hepatocyte iron uptake from transferrin, iron-pyrophosphate and iron ascorbate. *Biochim Biophys Acta* 1991; 1095:39–45.

19

Iron Acquisition by the Reticuloendothelial System

GÜNTER WEISS

University Hospital, Innsbruck, Austria

I.	IRON HANDLING BY LYMPHOCYTES	467
A.	Iron Uptake via Transferrin Receptors	468
B.	Iron Uptake via Transferrin Receptor-Independent Systems	470
II.	IRON HANDLING BY MONOCYTES/MACROPHAGES	472
A.	Iron Uptake by Resident Monocytes/Macrophages	473
B.	Iron Acquisition by Activated Macrophages	475
III.	IRON HANDLING BY NEUTROPHILS	478
	ACKNOWLEDGMENT	479
	REFERENCES	479

Iron has proven to be an essential compound for immunosurveillance because of its growth-promoting and differentiation-inducing properties for immune cells, and its interference with cell-mediated immune effector pathways and cytokine activities. Thus, the reticuloendothelial system has evolved sophisticated strategies to control iron metabolism in general and the handling of the metal within cells of the immune system.

I. IRON HANDLING BY LYMPHOCYTES

Lymphocytes are the central regulatory cells of specific immunity. Thus, a sufficient capacity of these cells to proliferate and differentiate is a prerequisite for normal immune function. Iron has turned out to be centrally involved in these processes and

thus lymphocytes have evoked different mechanisms to acquire iron even under conditions when iron availability is limited.

A. Iron Uptake via Transferrin Receptors

It has been known for several years that the proliferation of lymphocytes—like that of many other cells—depends on their ability to take up iron via the transferrin/transferrin receptor pathway (1,2). Lymphocytes respond to a proliferative stimulus with increased formation and expression of transferrin receptors (TfR) on their cell surface. This has been shown in all lymphocyte subsets, i.e., B lymphocytes, T cells, and natural killer (NK) cells. Conversely, incubation of cells with an anti-TfR antibody results in inhibition of their proliferation and differentiation (1,3,4), in accordance with studies in animal models where induction of iron deficiency resulted in defect T-cell mitogen responses (5,6). The increased requirements of iron for proliferation may arise from the fact that iron is centrally involved in mitochondrial respiration, as it is an essential compound of enzymes in the citric acid cycle (aconitase) and the oxidative phosphorylation pathway, and because iron also takes part in DNA synthesis as a co-factor in ribonucleotide reductase (7).

The magnitude of upregulation of TfR upon induction of lymphocyte proliferation is very impressive; it increases approximately 10-fold on phytohemagglutinin-activated human peripheral lymphocytes (1). Interestingly, lymphocyte subsets differ with respect to the number of TfRs they express in response to mitogen stimulation. In a study measuring TfR expression on both proliferating T and B cells, it was demonstrated that T cells express higher amounts of TfR mRNA than do B cells (8). Moreover, a study performed with T-lymphoblastic cells revealed that TfRs expressed by T cells are hyperglycosylated and may thus differ from others with respect to iron uptake and signal transduction properties (9).

Only limited information is available on the regulatory pathways underlying increased TfR expression on mitogen-stimulated T cells. The published evidence available so far suggests that the metabolic changes responsible for TfR expression depend on the stimulus/mitogen used. As nicely reviewed by Brock (10), the activation of T cells with lectin-containing mitogens results in stimulation of TfR expression via an interleukin-2 (IL-2)-dependent pathway (11,12), while if phorbol esters are used for T-cell stimulation, the TfR expression occurs earlier and is IL-2-independent (8,13). A definite mechanism has not been identified for the latter pathway, but it would be reasonable to suggest that TfR expression in this setting may be due to posttranscriptional regulation of TfR mRNA via interaction of iron regulatory proteins (IRPs) with specific RNA iron responsive elements (IREs) within the 3' untranslated region of TfR mRNA (14,15). Such a fast activation of IRPs with a subsequent increase in TfR expression has been observed after challenging cells with oxygen radicals (16), a scenario which will also take place upon mitogen-mediated activation of immune cells.

Alternatively, mitogens may directly affect the binding affinities of IRPs, e.g., via induction of IRP phosphorylation (17), changes in intracellular iron trafficking, or stimulation of iron-consuming metabolic pathways which result in IRP activation due to intracellular iron restriction (for review, see Refs. 18 and 19). Finally, mitogens may induce IRP-independent mechanisms which regulate TfR, e.g., via the formation of cytokines such as interferon-gamma (IFN- γ), which is a major player in the regulation of iron metabolism in macrophages.

1. T-Lymphocyte Subsets and TfR-Mediated Iron Uptake

Lymphocyte subsets have been shown to differ in their dependence on iron in general and specifically on transferrin-mediated iron uptake. This is of great functional relevance for immunity in view of the reciprocal regulatory interactions between iron metabolism and T cells (2). The induction of experimental iron overload in rats resulted in a shift in the ratio between T-helper (CD4+) and T-suppressor/cytotoxic T-cells (CD8+) with a relative expansion of the latter population (20). Moreover, even T-helper (Th) subsets respond differently to iron perturbations.

In the past several years evidence has accumulated for the existence of two CD4+ T-helper cell subsets in humans, each producing a typical set of cytokines which regulate different immune effector functions, and which cross-react with each other (21,22). T-helper cells type 1 (Th-1) produce IFN- γ , IL-2, and tumor necrosis factor (TNF)- β . These cytokines activate macrophages, thus contributing to the formation of pro-inflammatory cytokines, such as TNF- α , IL-1, or IL-6, and the induction of cytotoxic immune effector mechanisms of macrophages. By contrast, Th-2 cells produce IL-4, IL-5, IL-10, and IL-13, which induce a strong antibody response but also exert anti-inflammatory actions via inhibition of various macrophage functions (21,22).

Thorson et al. (23) have shown that Th cell subsets differently respond to limitation of iron availability. While Th-1 clones are very sensitive to treatment with anti-TfR antibodies, resulting in inhibition of their DNA synthesis, Th-2 cells are resistant to this procedure. This is partly due to the fact that Th-2 clones exhibit larger chelatable iron storage pools than Th-1 cells. Thus, Th-1-mediated immune effector pathways may be much more sensitive to changes in iron homeostasis in vivo. The latter may be also due to the fact that iron perturbations affect the activity of cytokines secreted by Th-1 cells such as IFN- γ (24). This is of general importance because IFN- γ modulates (a) the expression of critical iron proteins, e.g., on monocytes (see below), and (b) because of the regulatory properties of this cytokine for the activation/proliferation of lymphocyte subsets according to the Th-1/Th-2 paradigm (22).

The above suggests that changes in iron homeostasis may exert subtle effects on cell-mediated immune effector function, which may be of clinical relevance in patients with iron deficiency due to anemia of chronic disease or with iron-deficient anemia. Opposite effects may also occur in patients with primary and secondary iron overload. Evidence for such an interaction in vivo has been provided in patients with iron overload due to hemochromatosis (25), β -thalassemia (2), and secondary siderosis (26), as well as upon pharmacological modulation of iron homeostasis (27–29).

Once TfRs are expressed, transferrin-bound iron is taken up effectively via endocytosis and subjected to storage (ferritin incorporation) or iron consumption (synthesis of iron-containing enzymes), while a certain percentage (10–20% of the iron) remains in the labile iron pool (30). Nevertheless, data have been presented demonstrating that different forms of iron, i.e., transferrin-bound versus chelatable iron, are handled differently by primary lymphocytes in terms of incorporation into ferritin and their effects on cell metabolism (31). Although no differentiation was made between T and B cells in this study, the results indicated that lymphocytes have only a limited capacity to sequester iron and that hydrophilic iron chelates such

as ferric nitrilotriacetate are toxic to these cells, and not available for metabolic use (31).

2. B Lymphocytes

While the importance of TfR-mediated iron uptake for T-cell proliferation and function is well documented, its role for B-cell proliferation is less clear. Studies have indicated that although proliferation of B cells in response to mitogen stimulation depends on iron availability, they appear to be less sensitive to changes of iron availability than T cells (32). This is in accordance with clinical studies indicating that iron overload or deficiency does not significantly affect B-cell-mediated immune effector mechanisms (for review, see Ref. 10). An increase of TfR expression is observed early in B-cell activation (33), but B lymphocytes rather than T cells may be able to take up iron also by non-transferrin-mediated uptake systems (see below). Most interestingly, an in-vivo study investigating iron traffic within mouse lymph nodes which had been previously stimulated with Freund's adjuvant revealed that macrophages, rather than lymphocytes, were able to synthesize and release iron-loaded transferrin (34). This paracrine delivery of transferrin iron by macrophages supports lymphocyte growth and proliferation, and may maintain a sufficient immune response under conditions when iron availability is limited, e.g., chronic immune activation in the case of hypoferremic anemia of chronic disease in the presence of a malignancy (35).

3. Natural Killer Cells

Little information is available on mechanisms of iron uptake by natural killer (NK) cells. However, their activity is significantly impaired by iron depletion (36) and iron overload, e.g., in β -thalassemia patients (37). This may be due on the one hand to the need of iron for proliferation, as found for T lymphocytes, or on the other hand partly due to the modulatory potential of iron on the activities of cytokines which are essential for NK differentiation and activation, such as IL-2, IFN- γ , or IL-12 (10,35).

B. Iron Uptake via Transferrin Receptor-Independent Systems

Apart from the "classical" iron uptake mechanism via Fe-Tf/TfR interactions, non-transferrin-mediated iron uptake mechanisms have been described in lymphocytes.

1. Uptake of Chelatable Iron

In a malignant B-lymphocytic, transformed cell line, a highly efficient uptake in transferrin-free medium was described that took up the metal by a high-capacity, low-affinity, temperature- and calcium-dependent mechanism (38). Limiting iron availability to these B cells by addition of desferrioxamine resulted in growth arrest (38). Similar observations have been made in phytohemagglutinin-stimulated human peripheral lymphocytes, and this iron uptake system was not influenced by addition of an excess of iron-transferrin (39).

A considerable number of new iron transporters has been identified in various organisms ranging from yeast to rodents and humans, and they are discussed extensively in other chapters of this volume. However, no studies have been undertaken so far to elucidate whether or not one of these transporters would account for the

transferrin-independent iron uptake system in lymphocytes. Putative iron transporters which are of special interest in connection with the immune system include natural resistance-associated macrophage proteins (NRAMP)-1 and NRAMP-2. NRAMP-2, now named divalent metal transporter, DMT-1, is ubiquitously expressed [(40,41); see Chapter 6]. DMT-1 has been identified in rat duodenum, where it transports iron and other divalent metals by a hydrogen-coupled transmembrane transport mechanism (40), and this protein may be a major gatekeeper for coordinating uptake of iron with the needs of the body. Moreover, DMT-1 is also of major importance for the release of iron from the endosome into erythroid cells and, thus, mutations of this transporter lead to the development of iron-deficient anemia (for a review, see Ref. 42). However, information is limited on both tissue distribution of DMT-1 in humans and other functions of this transmembrane protein.

NRAMP-1 has previously been identified as the gene which is associated with resistance toward infections with intracellular pathogens such as *Leishmania*, *Salmonella* or *Mycobacteria* species (43). Although NRAMP-1 expression appears to be regulated by iron perturbations, with increased NRAMP-1 mRNA and protein levels in macrophages loaded with iron (H. Zoller and G. Weiss, manuscript in preparation), clear-cut evidence for a role of NRAMP-1 as an iron transporter is still missing although some observations point to this notion (44) while others do not (45). NRAMP-1 is a lysosomal protein and most likely involved in acidification of the vesicles (45). Nevertheless, NRAMP-1 is primarily expressed in monocytes/macrophages and neutrophils (43) and thus—in contrast to a putative role for DMT-1—this protein may not be involved in iron acquisition by lymphocytes.

2. Ferritin Receptors

Lymphocytes of all subtypes express receptors which specifically bind H- but not L-ferritin (46,47). The expression of these receptors was observed on both B and T lymphocytes and peaked during S phase, suggesting that ferritin receptor expression may be associated with proliferation (48,49). However, it is not yet clear whether these receptors are involved in iron uptake by lymphocytes, or in iron exchange—as assumed for iron traffic between hepatocytes and macrophages (50)—or whether they have functions which are distinct from iron metabolism. The latter notion is supported by the finding that addition of H-ferritin to stimulated lymphocytes expressing H-ferritin receptors resulted in inhibition of cell proliferation and colony formation (50).

3. Lactoferrin

It has been known for several years that lymphocytes express receptors which are capable of interacting with lactoferrin, an iron-binding protein found in milk, mucosa, and neutrophil granules (51). Lactoferrin receptors are present on almost all lymphocyte types investigated so far, i.e., CD4+ and CD8+ T cells, B cells, and NK cells. The highest proportion of lactoferrin receptors has been found in gamma-delta T cells (52). The expression of lactoferrin receptors appears to be associated with lymphocyte activation, since they are hardly expressed by unstimulated blood lymphocytes (52). Moreover, lactoferrin receptors show similar expression kinetics to TfR, although a considerable number of lymphocytes express only lactoferrin receptors and no TfR. Addition of lactoferrin to such cells augments the proliferative response of $\gamma\delta$ T cells to mitogen stimulation (52). Whether this is due to the delivery

of iron to the cells or to other functions of lactoferrin not related to iron homeostasis remains to be shown (51).

Apart from the above, lactoferrin has various other immunoregulatory functions. These include modulation of cytokine formation, antibody and complement production, and NK function (51). The latter effect was not influenced by iron perturbations of NK cells in culture, suggesting that lactoferrin may interact with immunomodulatory target molecules rather than acting solely through regulation of the availability of iron to NK cells (53).

4. HFE

Another link between immunity and iron metabolism has been identified by the cloning and characterization of HFE, a nonclassical MHC class I molecule which is ubiquitously expressed on cell surfaces (54). Approximately 80–90% of patients with hereditary iron overload are homozygous for a point mutation in the HFE gene leading to an amino acid exchange from Cys to Tyr at position 282 (C282Y) [(54–56); see also Chapters 8 and 28]. This mutation results in loss of HFE function by disrupting its interaction with β_2 -microglobulin and cell surface expression (57). Further evidence for the importance these phenomena is provided by the observation that β_2 -microglobulin knockout mice develop parenchymal iron overload (58,59), and also lack CD8+ cells (60).

Additional data provide evidence for a functional interaction of HFE with transferrin/TfR-mediated iron uptake. HFE co-localizes with TfR in human placenta (61). Moreover, HFE forms a stoichiometric complex with TfR and lowers the affinity of TfR for iron loaded transferrin [(62,63); see also Chapter 3]. The role of these associations in iron uptake is not fully understood (42). However, the C282Y HFE mutant protein does not associated with β_2 -microglobulin, and is thus not expressed on the cell surface. Thus, the presence of this mutation in hereditary hemochromatosis may be associated with a diminished uptake and release of iron in duodenal crypt cells, which then results in activation of IRP (64). This will cause upregulation of DMT-1 expression (65,66) on the apical side of the enterocyte (presumably via stabilization of DMT-1 mRNA by IRPs) and a subsequent increase in iron uptake which is the underlying pathophysiological mechanism in hereditary hemochromatosis.

Most interestingly, evidence has been provided that γ,δ T cells may communicate with intestinal cells by a γ,δ -receptor/HFE antigen interaction (67). Such an intercellular communication between T lymphocytes and intestinal cells may induce immune effector pathways (e.g., TNF- α formation) and thus regulate intestinal cell differentiation/apoptosis, thus being of central importance for both the intestinal immune response and regulation of iron uptake. The most important pathways for iron uptake by lymphocytes are summarized in Fig. 1.

II. IRON HANDLING BY MONOCYTES/MACROPHAGES

As in lymphocytes, various pathways for iron acquisition by these cells have been described, but in contrast to lymphocytes, monocytes/macrophages not only acquire iron for their own needs but also act as a major storage pool of iron which is primarily expanded under inflammatory conditions or in the case of secondary iron overload.

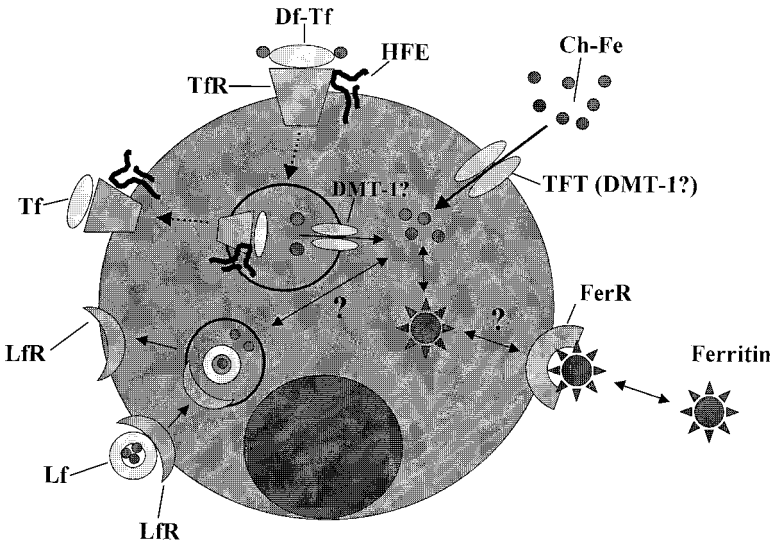


Figure 1 Pathways for iron acquisition by lymphocytes. A question mark indicates that either a pathway or a transport mechanism has not been fully elucidated so far. TfR, transferrin receptor; DMT-1, divalent metal transporter; Th, T-helper cells; NK, natural killer cells; Lf, lactoferrin; Ch-Fe, chelatable iron; FerR, ferritin receptor; LfR, lactoferrin receptor.

A. Iron Uptake by Resident Monocytes/Macrophages

1. Transferrin Receptor-Mediated Iron Uptake

In contrast to lymphocytes, monocyte/macrophages are differentiated and not proliferating cells. Thus TfR-mediated iron uptake is necessary to maintain basic cell functions and macrophage-mediated cytotoxicity. The cytotoxicity depends on iron-catalyzed formation of toxic oxygen radicals, e.g., $\text{HO}\cdot$ (68), which are centrally involved in macrophage effector function against invading pathogens. Not surprisingly, then, iron uptake by monocytes/macrophages very much differs between unstimulated, differentiating cells and inflammatory cells (69–71). On primary human monocytes, TfR expression is rather low or almost absent while it is enhanced in cultured macrophages, resulting in a progressive endosomal uptake of iron-transferrin complexes and rapid incorporation of iron into ferritin. In parallel with this, changes in IRP activity during differentiation of monocytes have been observed (72). IRP-binding affinity to IREs sharply increases during maturation of monocytes to macrophages, suggesting that increased TfR expression in macrophages as compared to resting monocytes may be due primarily to posttranscriptional regulation of TfR expression via stabilization of TfR mRNA following IRE/IRP interaction (14,15) and stimulation of IRP-binding activity during maturation.

The highly conserved IRE/IRP system, which is described in more detail elsewhere in this volume (see Chapters 9 and 10), enables cells to link their requirement for iron with the expression of the proteins for iron uptake (TfR), iron consumption [erythroid amino-levulinate synthase (e-ALAS); which is not expressed in macrophages], and iron storage (ferritin). The binding affinity of the two cytoplasmic pro-

teins, IRP-1 and IRP-2, to specific mRNA stem-loop structures, IREs, is increased during iron deficiency states and in cells exposed to oxidative stress (H_2O_2) or nitric oxide (NO) (for a review, see Refs. 18 and 19). IRP binding to IREs located within the 5' untranslated region of the mRNA for ferritin H chain and L chain causes their translational repression. Conversely, the high-affinity interaction between IRP and IREs within the 3' untranslated region of the TfR mRNA increases the stability of this mRNA by protecting it from endonucleolytic degradation, thus promoting iron uptake into cells. Conversely, increased cellular iron availability reduces the IRE-binding activity of IRP-1 and IRP-2, thus leading to enhanced translation of ferritin and e-ALAS mRNAs, and to a reduced half-life of TfR mRNA. This homeostatic response stimulates iron storage and consumption, whereas iron uptake is decreased (18,19).

Most recently, a second TfR has been cloned which is primarily expressed on hepatic and erythroid cells (73). This receptor subtype, TfR2, which shares 45% identity with TfR, has no IRE within its untranslated regions and is thus presumably not sensitive to regulation by iron (74). Thus, TfR2 may maintain continuous iron uptake into cells. Its importance for iron acquisition by cells of the immune system remains to be determined.

2. Uptake of Iron Chelates: A Role for Nramp3?

Although transferrin appears to be a major source of iron for resting monocytes/macrophages, these cells are also able to take up iron by various TfR-independent pathways (75,76). Studies with rat macrophages provided indirect evidence that transferrin-bound iron may be taken up by a non-receptor-mediated mechanism which is independent of the degree of transferrin saturation (77). Furthermore, human macrophages are able to take up iron chelates with a greater efficacy than they take up diferric-transferrin; they achieve this by a temperature-dependent, pH-independent process (78). The acquisition of the metal by these pathways is influenced by the nature of the iron chelate, with iron-ascorbate, iron-citrate and iron-nitrilotriacetate taken up most efficiently. Iron uptake by this pathway is inhibited by other divalent-metal chelates (78), which raises the question of whether DMT-1 may be centrally involved in this uptake mechanism of macrophages; this membrane protein has similar transport kinetics for iron and other divalent metal ions such as zinc, copper, lead, etc. (40). These observations are in accordance with the finding that blocking TfR in a human myelo-monocytic cell line upon competitive binding of α_1 -antitrypsin did not alter iron uptake or the proliferation kinetics of these cells (79), while the proliferation of erythroid progenitors was very much affected (80). Moreover, at least in alveolar macrophages, the uptake and sequestration of iron salts is dependent on the oxygen tension of the medium. Hyperoxia decreases iron uptake by macrophages, reduces the incorporation of iron into ferritin, and at the same time increases the hyperoxic injury toward other cells mediated by iron (81).

Macrophages express NRAMP-1 in phagolysosomes, and this protein may be able to transport iron across the lysosomal membrane. Ectopic expression of NRAMP-1 in COS-1 cells modulated intracellular levels of chelatable iron but did not influence iron uptake (44), suggesting that NRAMP-1 may be involved in intracellular iron trafficking and mobilization of iron from intracellular vesicles (82). This notion is supported by a recent investigation using virus-transformed murine macrophages (83). The attractive hypothesis that NRAMP-1 expression may confer re-

sistance toward intracellular pathogens, either by limiting the availability of iron to the microbes or by supplying iron for the formation of toxic radicals by the Haber-Weiss reaction, has yet to be confirmed, perhaps by studies using fluorescent probes detecting iron traffic within cells (84).

3. Lactoferrin Receptor

Although macrophages do not produce lactoferrin, they express lactoferrin receptors on their surface which then bind lactoferrin. Uptake of this protein by macrophages exerts subtle effects on their function and iron metabolism. Lactoferrin is internalized most likely via an endocytotic process and is then involved in the transfer of iron to ferritin (85). Lactoferrin does not interfere with the binding of transferrin to the surface of human monocytic cells, and vice versa. However, monocytes take up iron from transferrin approximately 10 times faster than from lactoferrin (86). While lactoferrin does not alter TfR-mediated iron uptake, the acquisition of chelatable iron by U937 human monocytic cells is inhibited by the protein, pointing to a regulatory effect of lactoferrin for uptake of non-transferrin-bound iron by monocytes (86). Interestingly, after incubation of macrophages in lactoferrin-free media, this milk-specific protein was released from cells which had been previously loaded with lactoferrin, providing good evidence for a recyclable pool of lactoferrin within macrophages (87). Once taken up, lactoferrin may play a regulatory role within the macrophages by modulating on the one hand iron-mediated cytotoxic effector mechanisms against intracellular pathogens via the formation of hydroxyl radicals (88), while on the other hand apo-lactoferrin may protect macrophages from membrane peroxidation (87).

4. Iron Export

Macrophages have been shown to be able to release iron into tissue culture supernatants. However, the TfR/transferrin system appears not to be involved in the release of iron from macrophages (89). Most recently, a new transporter, termed ferroportin 1 (see Chapter 7), has been identified, which exports iron from the basolateral site of the duodenum (90). High levels of this protein have also been detected in Kupffer cells and spleen macrophages (90), suggesting that this transmembrane transporter may be involved in iron export from monocytes/macrophages. Finally, at least in alveolar macrophages from smokers, iron is released by ferritin (91). The impact of erythrophagocytosis on the release of iron from the reticuloendothelial system is described below. The pathways for iron handling by resident monocytes/macrophages are summarized in Fig. 2.

B. Iron Acquisition by Activated Macrophages

1. Regulation of Iron Acquisition by Cytokines and Radicals

In inflammatory macrophages, many metabolic changes occur, not only involving iron metabolism. Upon activation, T cells, NK cells, and macrophages produce a number of cytokines which then influence iron metabolism via transcriptional and posttranscriptional alterations of ferritin and/or TfR expression through IRE/IRP-dependent and -independent pathways (for reviews, see Refs. 10 and 35). Some of these immunoproteins stimulate iron acquisition and storage by macrophages, thus leading to hypoferrremia, a major pathogenic mechanism contributing to the devel-

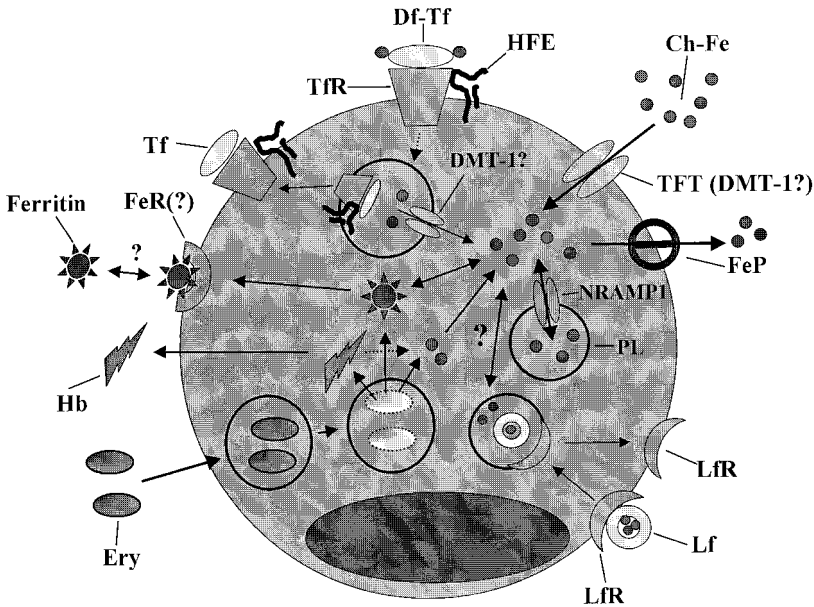


Figure 2 Pathways for iron acquisition by resident monocytes/macrophages. A question mark indicates that either a pathway or a transport mechanism has not been fully elucidated so far. TfR, transferrin receptor; DMT-1, divalent metal transporter; TFR, transmembrane iron transporter; NRAMP-1, natural resistance-associated macrophage protein-1; Fp, ferroportin; Ch-Fe, chelatable iron; Lf, lactoferrin; LfR, lactoferrin receptor; Ery, erythrocyte; Hb, hemoglobin; PL phagolysosome.

opment of anemia of chronic disease (ACD). ACD is thus frequently observed in patients suffering from diseases with activated cell-mediated immunity such as autoimmune diseases, chronic infections, or tumors (92–94).

It has been shown *in vitro* and *in vivo* that treatment of mice with TNF- α or IL-1 causes hypoferrremia (95), which may be a consequence of induction of ferritin synthesis by the cytokines (96). The underlying mechanism may be a direct stimulatory effect of TNF- α and IL-1 on ferritin transcription (97,98). Moreover, the pro-inflammatory cytokines IL-1 and IL-6 also regulate ferritin expression at the translational level by a mechanism independent of the IRP system (99,100), namely, via stimulation of an “acute-phase box” which is located in the 5' untranslated region of ferritin mRNA.

Only limited information is available on how the induction of ferritin synthesis may lead to hypoferrremia, as the pro-inflammatory cytokines (TNF α , IL-1, IL-6) rather downregulate TfR synthesis (101,102). A limitation of some of the studies investigating the effects of cytokines is that often cell lines other than macrophages and monocytes have been used, and thus—although suggestive—it remains to be shown whether or not these pro-inflammatory cytokines have similar regulatory effects on ferritin or TfR expression in monocytes as they do in, e.g., fibroblasts or adipocytes. Nevertheless, one could suggest that hyperferritinemia will decrease the concentration of metabolically available iron, resulting in stimulation of iron uptake

mechanisms other than TfR/diferric transferrin-mediated endocytosis, or alternatively, that ferritin may be directly involved in iron uptake via interaction with surface ferritin receptors.

The major regulatory Th-1-mediated cytokine IFN- γ has distinct effects on iron homeostasis. IFN- γ inhibits ferritin translation. This is due to stimulation of nitric oxide (NO) formation by IFN- γ (103,104). The radical then activates IRP-1 binding to the ferritin IRE, which downregulates ferritin translation (103,105), although ferritin mRNA transcription is upregulated by the cytokine. However, iron metabolism and NO pathways are functionally connected because iron also modulates the expression of NO via transcriptional regulation of the enzyme-inducible nitric oxide synthase (iNOS), which is responsible for high-output formation of NO by cytokine-stimulated macrophages (106,107). A major underlying mechanism for this regulatory function of iron is a direct effect of the metal on the binding affinity of the transcription factor NF-IL6 to the *iNOS* promoter which impairs *iNOS* transcription (108). This provided evidence for an auto-regulatory feedback mechanism in macrophages linking maintenance of iron homeostasis with optimal formation of NO for host defense (35). Such a “seesaw” principle may contribute to acquisition and incorporation of iron into ferritin by macrophages during chronic inflammatory processes. Currently ongoing studies investigating iron metabolism in iNOS knockout mice (C. Bogdan, G. Weiss, manuscript in preparation) may contribute to the clarification of this situation.

IFN- γ treatment of monocytes blocks a major iron uptake mechanism via downregulation of TfR expression (109–112), which is most likely due to induction of a proximal inhibitory factor by IFN- γ which inhibits *TfR* transcription. Withholding iron from macrophages would make sense in view of the inactivating effect of iron on IFN- γ activity, which in turn weakens the Th-1-mediated immune effector pathways in macrophages (24). Nevertheless, the effects of IFN- γ on TfR expression probably depend on cell differentiation and culture conditions, since just the opposite effect—upregulation of TfR expression by IFN- γ —has also been reported (113).

Interestingly, anti-inflammatory cytokines derived from Th-2 cells such as IL-4, IL-10, and IL-13 counteract effects of IFN- γ on iron homeostasis in activated macrophages (111). Treatment of macrophages with IL-4 and (or) IL-13 prior to stimulation with IFN- γ suppresses NO formation and subsequent IRP activation, and concomitantly enhances ferritin translation. Conversely, TfR mRNA levels increase following pretreatment of IFN- γ -stimulated macrophages with antiinflammatory cytokines. This may be due to IL-4/IL-13-mediated antagonism of the inhibitory signal which is induced by IFN- γ and inhibits TfR expression through an IRP-dependent pathway (111). Thus, Th-2-derived cytokines may increase TfR-mediated iron uptake and storage of iron in ferritin in activated macrophages, collaborating with pro-inflammatory cytokines (TNF- α , IL-1, IL-6) in the development of hypoferrremia observed during chronic inflammatory processes.

2. Erythrophagocytosis

Monocytes and macrophages are able to acquire and recirculate iron from erythrocytes. Erythrocytes are taken up by phagocytosis and then destroyed within the monocytes/macrophages. Macrophages have been shown to phagocytize about three times as many erythrocytes as monocytes (115,116). Moreover, upon stimulation of macrophages with TNF α , phagocytosis of sialidase-treated erythrocytes is further

increased—at least *in vitro*—which may be due to enhanced expression of C3b (CD11b/CD18) receptors following cytokine treatment (115). Within the macrophage, iron is then released from hemoglobin and rapidly shifted to reutilization via incorporation in iron proteins or storage by ferritin (115,117). Moreover, a high proportion of erythrocyte iron is released by macrophages in different forms, namely, as hemoglobin, ferritin, or low-molecular-weight iron which then binds to plasma transferrin (115,117).

III. IRON HANDLING BY NEUTROPHILS

Although information concerning iron uptake pathways in neutrophils is limited, the ability of neutrophil granulocytes to proliferate is closely associated with the expression of surface TfR. In a recent study, TfR-positive HL-60 cells had a tendency to proliferate rather than differentiate, while TfR-negative cells expressed markers of differentiation and activation such as superoxide radicals or formyl-Met-Leu-Phe receptors (118). Moreover, a balanced iron homeostasis is of central importance for many functions of neutrophil granulocytes such as phagocytosis or killing of intracellular pathogens via the formation of toxic radicals (68). The importance of this has been underscored by the observation that iron therapy of chronic hemodialysis patients for the correction of renal anemia impaired the potential of neutrophils to kill bacteria and reduced their capacity to phagocytose foreign particles (119). This is in accordance with observations made by others that iron overload both *in vitro* and *in vivo* resulted in dysfunction of neutrophils (120,121). Whether this can be explained by a negative regulatory interaction between iron and immune function comparable to that between iron and IFN- γ activity in macrophages remains to be discovered (35).

Interestingly, neutrophil granulocytes may contribute to the release of iron from transferrin via formation and release of superoxide. By this pathway, neutrophils may deliver metabolically active iron for cytotoxic effector functions such as hydroxyl radical formation or lipid peroxidation (122). On the other hand, neutrophils down-regulate the binding of diferric transferrin to their specific surface receptors via the release of myeloperoxidase, an enzyme involved in cellular radical formation (123). This suggests that activated neutrophils decrease iron uptake, which would make sense in view of the deactivating effects of iron on neutrophil function. Moreover, neutrophils may influence iron homeostasis in neighboring cells in a paracrine manner, since addition of hydrogen peroxide to cells has been shown to stimulate IRP-1 binding to IREs with the subsequent metabolic changes on TfR and ferritin expression described above (16).

Lactoferrin may also be centrally involved in iron handling by neutrophils, which have been shown to produce and release large amounts of this protein upon stimulation with infectious targets (51). Lactoferrin may on the one hand be directly toxic to bacteria by limiting iron availability to them, while at the same time it exerts distinct effects on overall immune function by regulating the proliferation and activation of lymphocytes, NK cells, and monocytes (51,124).

Like monocytes, neutrophils express the phagolysosomal protein NRAMP-1, which confers resistance to infections with intracellular pathogens but are putatively involved also in intracellular handling of iron and supply of iron for catalyzing the formation of radicals for the oxidative burst. Thus, although iron is an essential

component for neutrophil function and proliferation, much more work is needed to gain insight into the regulatory pathways for handling this metal within polymorphonuclear granulocytes.

ACKNOWLEDGMENT

Support by grant FWF-14215 from the Austrian Research Fund is gratefully acknowledged.

REFERENCES

1. Seligman PA, Kovar J, Gelfand EW. Lymphocyte proliferation is controlled both by iron availability and regulation of iron uptake pathways. *Pathobiology* 1992; 60:19–26.
2. De Sousa. Immune cell functions in iron overload. *Clin Exp Immunol* 1989; 75:1–6.
3. Keyna U, Nusslein I, Rohwer P, Kalden JR, Manger B. The role of the transferrin receptor for the activation of human lymphocytes. *Cell Immunol* 1991; 132:411–422.
4. Brekelmans P, van Soest P, Leenen PJ, van Ewijk W. Inhibition of proliferation and differentiation during early T cell development by anti-transferrin receptor antibody. *Eur J Immunol* 1994; 24:2896–2902.
5. Kuvibidila S, Dardenne M, Savino W, Lepault F. Influence of iron deficiency on selected thymus functions in mice: thymulin biological activity, T cells subsets and thymocyte proliferation. *Am J Clin Nutr* 1990; 51:228–232.
6. Mainou-Fowler T, Brock JH. Effect of iron deficiency on the response of mouse lymphocytes to concanavalin A: importance of transferrin bound iron. *Immunology* 1985; 54:325–332.
7. Laskey J, Webb I, Schulman HM, Ponka P. Evidence that transferrin supports cell proliferation by supplying iron for DNA synthesis. *Exp Cell Res* 1988; 176:87–93.
8. Kumagai N, Benedict SH, Mills GB, Gelfand EW. Comparison of phorbol ester/calcium ionophore and phytohemagglutinin induced signaling in human T lymphocytes. Demonstration of interleukin-2 independent transferrin receptor gene expression. *J Immunol* 1988; 140:37–43.
9. Petriani M, Pelos-Testa E, Sposi NM, Mastroberardino G, Camagna A, Bottero L, Mavillo F, Testa U, Peschle C. Constitutive expression and abnormal glycosylation of transferrin receptor in acute T-cell leukemia. *Cancer Res* 1989; 69:6989–6996.
10. Brock JH. Iron in infection, immunity, inflammation and neoplasia. In: Brock JH, Halliday JW, Pippard MJ, Powell LW, eds. *Iron Metabolism in Health and Disease*. Philadelphia: Saunders, 1994:353–391.
11. Neckers LM, Cossman J. Transferrin receptor induction in mitogen stimulated human T-lymphocytes is required for DNA synthesis and cell division and is regulated by interleukin-2. *Proc Natl Acad Sci USA* 1983; 80:3494–3497.
12. Seiser C, Teixeira S, Kühn LC. Interleukin-2 dependent transcriptional and posttranscriptional regulation of transferrin receptor mRNA. *J Biol Chem* 1993; 268:13074–13080.
13. Teixeira S, Kühn LC. Post-transcriptional regulation of transferrin receptor and 4F2 antigen heavy chain mRNA during growth activation of spleen cells. *Eur J Biochem* 1991; 202:819–826.
14. Casey JL, Koeller DM, Ramin VC, Klausner RD, Harford JB. Iron regulation of transferrin receptor mRNA levels requires iron-responsive elements and a rapid turnover determinant in the 3' untranslated region of the mRNA. *EMBO J* 1989; 8:3693–3699.

15. Moller EW, Neupert B, Kühn LC. A specific mRNA binding factor regulates the iron-dependent stability of cytoplasmic transferrin receptor mRNA. *Cell* 1989; 58:373–382.
16. Pantopoulos K, Hentze MW. Rapid responses to oxidative stress mediated by iron regulatory protein. *EMBO J* 1995; 14:2917–2924.
17. Schalinske KL, Eisenstein RS. Phosphorylation and activation of both iron regulatory proteins 1 and 2 in HL-60 cells. *J Biol Chem* 1996; 271:7168–7176.
18. Rouault TA, Klausner R. Regulation of iron metabolism in eukaryotes. *Curr Topics Cell Regul* 1997; 35:1–6.
19. Hentze MW, Kühn LC. Molecular control of vertebrate iron metabolism: mRNA based regulatory circuits operated by iron, nitric oxide and oxidative stress. *Proc Natl Acad Sci USA* 1996; 93:8175–8180.
20. De Sousa M, Reimao R, Porto G, Grady RW, Hilgartner MW, Giardina P. Iron and lymphocytes: reciprocal regulatory interactions. *Curr Stud Hematol Blood Transf* 1992; 58:171–177.
21. Mosmann TR, Coffman RL. Th1 and Th2 cells: different patterns of lymphokine secretion leads to different functional properties. *Annu Rev Immunol* 1989; 7:145–162.
22. Romagnani S. The Th1/Th2 paradigm. *Immunol Today* 1997; 18:263–267.
23. Thorson JA, Smith KM, Gomez F, Naumann PW, Kemp JD. Role of iron in T cell activation: Th-1 clones differ from Th-2 clones in their sensitivity to inhibition for DNA synthesis caused by IGG MAbs against transferrin receptor and the iron chelator desferrioxamine. *Cell Immunol* 1991; 14:126–127.
24. Weiss G, Fuchs D, Hausen A, Reibnegger G, Werner ER, Wern-Felmayer G, Wachter H. Iron modulates interferon- γ effects in the human myelomonocytic cell line THP-1. *Exp Hematol* 1992; 20:605–610.
25. Porto G, Reimao C, Goncalves C, Vincente B, Justica B, DeSousa M. Haemochromatosis as a window into the study of the immunological system in men: a novel correlation between CD8+ lymphocytes and iron overload. *Eur J Haematol* 1994; 52:283–288.
26. Gangaidzo IT, Gordeuk VR. Hepatocellular carcinoma and African iron overload. *Gut* 1995; 37:727–730.
27. Latunde-Dada GO, Young SP. Iron deficiency and immune response. *Scand J Immunol* 1992; 36:207–209.
28. Weiss G, Thuma PE, Mabeza F, Werner ER, Herold M, Gordeuk VR. Modulatory potential of iron chelation therapy on nitric oxide formation in cerebral malaria. *J Infect Dis* 1997; 175:226–230.
29. Menacci A, Cenci E, Boelaert JR, Bucci P, Mosci P, Fe'd Ostiani C, Bistoni F, Romain L. Iron overload alters T helper cell responses to *Candida albicans* in mice. *J Infect Dis* 1997; 175:1467–1476.
30. Bomford A, Young S, Williams R. Intracellular forms of iron during transferrin iron uptake by mitogen stimulated human lymphocytes. *Br J Haematol* 1986; 487–494.
31. Djeha A, Brock JH. Uptake and intracellular handling of iron from transferrin and iron chelates by mitogen stimulated mouse lymphocytes. *Biochim Biophys Acta* 1992; 1133:147–152.
32. Brock JH. The effect of iron and transferrin on the response of serum free cultures of mouse lymphocytes to concanavalin A and lipopolysaccharide. *Immunology* 1981; 43:387–392.
33. Futran J, Kemp JD, Field EH, Vora A, Ashman RF. Transferrin receptor synthesis is an early event in B-cell activation. *J Immunol* 1989; 143:787–792.
34. Djeha A, Perez-Arellano JL, Brock J. Transferrin synthesis by mouse lymph node and peritoneal macrophages: iron content and effect of lymphocyte proliferation. *Blood* 1993; 81:1046–1050.

35. Weiss G, Wachter H, Fuchs D. Linkage of cellular immunity to iron metabolism. *Immunol Today* 1995; 16:495–500.
36. Rothman-Sherman A, Lockwood JF. Impaired natural killer cell activity in iron deficient rat pups. *J Nutr* 1987; 117:567–571.
37. Kaplan J, Sarnaik S, Gitlin J, Lusher J. Diminished helper/suppressor lymphocyte ratios and natural killer activity in recipients of repeated blood donations. *Blood* 1984; 64:308–310.
38. Seligman PA, Kovar J, Schleicher RB, Gelfand EW. Transferrin-independent iron uptake supports B-lymphocyte growth. *Blood* 1991; 78:1526–1531.
39. Hamazaki S, Glass J. Non-transferrin dependent ⁵⁹Fe uptake in phytohemagglutinin-stimulated human peripheral lymphocytes. *Exp Hematol* 1992; 20:436–441.
40. Gunshin H, Mackenzie B, Gunshin H, Mackenzie B, Berger UV, Gunshin Y, Romero MF, Boron WF, Nussberger S, Gollan JL, Hediger MA. Cloning and characterization of a mammalian proton-coupled metal-ion transporter. *Nature* 1997; 388:482–488.
41. Vidal S, Belouchi AM, Cellier M, Beatty B, Gros P. Cloning and characterization of a second human NRAMP gene on chromosome 12q13. *Mammal Genome* 1995; 6:224–230.
42. Andrews NC, Levy JE. Iron is hot: update on the pathophysiology of hemochromatosis. *Blood* 1998; 92:1845–1852.
43. Vidal SM, Malo D, Vogan K, Skamene E, Gros P. Natural resistance to infections with intracellular parasites: isolation of a candidate for BCG. *Cell* 1993; 73:469–476.
44. Atkinson PG, Barton CH. Etoposide expression of NRAMP-1 in COS-1 cells modulates iron accumulation. *FEBS Lett* 1998; 425:239–242.
45. Hackam DJ, Rotstein O, Zhang D, Gruenheid S, Gros P, Grinstein S. Host resistance to intracellular infection: mutation of natural resistance associated macrophage protein 1 impairs phagosomal acidification. *J Exp Med* 1998; 188:351–364.
46. Anderson GJ, Faulk WP, Arosio P, Moss D, Powell LW, Halliday JW. Identification of H- and L-ferritin subunit binding sites on human T and B lymphoid cells. *Br J Haematol* 1989; 73:260–264.
47. Konijn AM, Meyron-Holtz EG, Levy R, Ben-Bassat H, Matzner Y. Specific binding of placental acidic isoferritins to cells of the T-cell line HD-MAR. *FEBS Lett* 1990; 263:229–234.
48. Farigon S, Fracanzani AL, Brando B, Arosio P, Levi S, Fiorelli G. Specific binding sites for H-ferritin on human lymphocytes: modulation during cellular proliferation and potential implication in cell growth control. *Blood* 1991; 78:1056–1061.
49. Moss D, Powell LW, Arosio P, Halliday LW. Effect of cell proliferation on H-ferritin receptor expression in human T lymphoid (MOLT-4) cells. *J Lab Clin Med* 1992; 120:239–243.
50. Moss D, Farigon S, Fracanzani AL, Levi S, Cappellini MD, Arosio P, Powell LW, Halliday JW. Functional roles of the ferritin receptors of human liver, hepatoma, lymphoid and erythroid cells. *J Inorg Biochem* 1992; 47:219–227.
51. Brock JH. Lactoferrin. A multifunctional immunoregulatory protein? *Immunol Today* 1995; 16:417–419.
52. Mincheva-Nilsson L, Hammarstrom S, Hammarstrom ML. Activated human gamma delta T-lymphocytes express functional lactoferrin receptors. *Scand J Immunol* 1997; 46:609–618.
53. Shau H, Kim A, Golub SH. Modulation of natural killer and lymphokine activated killer cell cytotoxicity by lactoferrin. *J Leukoc Biol* 1992; 51:343–349.
54. Feder JN, Gnirke A, Thomas W, Tsuchihashi Z, Ruudy DA, Basava A, Dormishian F, Domingo R, Ellis MC, Fullan LM, Hinton LM, Jones NL, Kimmel BE, Kronmal GS, Lauer P, Lee VK, Loeb DB, Mapa FA, McClelland E, Meyer NC, Mintier GA, Moeller N, Moore T, Morikang E, Prass CE, Quintana L, Starnes SM, Schatzman RC, Brunke

- KJ, Drayna DT, Risch NJ, Bacon BR, Wolff RK. A novel MHC class I like gene is mutated in patients with hereditary haemochromatosis. *Nature Genet* 1996; 13:399–408.
55. Jawinska EC, Cullen LM, Busfield F, Pyper WR, Webb SI, Powell LW, Morris CP, Walsh TP. Haemochromatosis and HLA-H. *Nature Genet* 1996; 14:249–251.
56. Jouanolle AM, Gandon G, Jezequel P, Blayau M, Campion ML, Yaouanq J, Moser J, Fergelot P, Chauvel B, Bouric P, Carn G, Andrieux N, Gicquel I, LeGall JY, David V. Haemochromatosis and HLA-H. *Nature Genet* 1996; 14:251–252.
57. Waheed AM, Parkkila S, Zhou XY, Tomatsu S, Tsuchihashi Z, Feder JN, Schatzman RC, Britton RS, Bacon BR, Sly WS. Hereditary hemochromatosis: effects of C282Y and H63D mutations on association with fl2-microglobulin, intracellular processing, and cell surface expression of the HFE protein in COS-7 cells. *Proc Natl Acad Sci USA* 1997; 94:12384–12389.
58. Santos M, Schilham MW, Rademakers LHPM, Marx JJM, de Sousa M, Clevers H. Defective iron homeostasis in β_2 -microglobulin knockout mice recapitulates hereditary hemochromatosis in man. *J Exp Med* 1996; 184:1975–1985.
59. Rothenberg BE, Volland JR. β_2 -Microglobulin knockout mice develop parenchymal iron overload: a putative role for class I genes of the major histocompatibility complex in iron metabolism. *Proc Natl Acad Sci USA* 1996; 93:1529–1534.
60. Koller BH, Marrack B, Kappler JW, Smithies O. Normal development of mice deficient in β_2m , MCHI proteins and CD8+ cells. *Science* 1990; 248:1227–1230.
61. Parkkila S, Waheed A, Britton RS, Bacon BR, Zhou XY, Tomatsu S, Fleming RE, Sly WS. Association of the transferrin receptor in human placenta with HFE, the protein defective in hereditary hemochromatosis. *Proc Natl Acad Sci USA* 1997; 94:13198–13202.
62. Feder JN, Penny DM, Irrinki A, Lee VK, Lebron JA, Watson N, Tschihashi Z, Sigal E, Bjorkman PJ, Schatzman RC. The hemochromatosis gene product complexes with the transferrin receptor and lowers its affinity for ligand binding. *Proc Natl Acad Sci USA* 1998; 95:1472–1477.
63. Lebron JA, Bennett MJ, Vaughn DE, Chirino AJ, Snow PM, Mintier GA, Feder JN, Bjorkman PJ. Crystal structure of the hemochromatosis protein HFE and characterization of its interaction with transferrin receptor. *Cell* 1998; 93:111–123.
64. Pietrangelo A, Casalgrandi G, Quaglino D, Gualdi R, Conte D, Milani S, Montosi G, Cesarini L, Ventura E, Cairo G. Duodenal ferritin synthesis in genetic hemochromatosis. *Gastroenterology* 1995; 108:208–217.
65. Fleming RE, Migas MC, Zhou X, Jiang J, Britton RS, Brunt EM, Tomatsu S, Waheed A, Bacon BR, Sly WS. Mechanism of increased iron absorption in murine model of hereditary hemochromatosis: increased duodenal expression of the iron transporter DMT-1. *Proc Natl Acad Sci USA* 1999; 96:3143–3148.
66. Zoller H, Pietrangelo A, Vogel W, Weiss G. Duodenal metal-transporter (DMT-1) expression in patients with hereditary hemochromatosis. *Lancet* 1999; 353:2120–2123.
67. TenElshof AE, Brittenham G, Chorney KA, Page MJ, Gerhard G, Cable EE, Chorney MJ. $\gamma\delta$ Intraepithelial lymphocytes drive tumor necrosis factor- α responsiveness to intestinal iron challenge: relevance to hemochromatosis. *Immunol Rev* 1999; 167:223–232.
68. Rosen GM, Pou S, Ramos CL, Cohen MS, Britigan BE. Free radicals and phagocytic cells. *FASEB J* 1995; 9:200–205.
69. Baynes R, Bukofzer G, Bothwell T, Bezwoda W, MacFarlane B. Transferrin receptors and transferrin uptake by culture human monocytes. *Eur J Cell Biol* 1987; 43:372–376.
70. Hamilton TA, Gray PW, Adams DO. Expression of the transferrin receptor on murine peritoneal macrophages in different stages of functional activation. *J Immunol* 1984; 132:2285–2290.

71. Andreesen R, Osterholz J, Bodemann H, Bross KJ, Costabel U, Löhner GW. Expression of transferrin receptors and intracellular ferritin during terminal differentiation of human monocytes. *Blut* 1984; 49:195–202.
72. Testa U, Kühn L, Petrini M, Quartana MT, Pelosi E, Peschle C. Differential regulation of iron regulatory element binding proteins in cell extracts of activated lymphocytes versus monocytes/macrophages. *J Biol Chem* 1991; 266:13925–13930.
73. Kawabata H, Yang R, Hirama T, Vuong PT, Kawano S, Gombart AF, Koeffler HP. Molecular cloning of transferrin receptor 2. A new member of the transferrin receptor family. *J Biol Chem* 1999; 274:20826–20832.
74. Fleming RE, Migas MC, Holden CC, Waheed A, Britton RS, Tomatsu S, Bacon BR, Sly WS. Transferrin receptor 2: continued expression in mouse liver in the face of iron overload and in hereditary hemochromatosis. *Proc Natl Acad Sci USA* 2000. In press.
75. Oria R, Alvarez-Hernandez X, Licega J, Brock JH. Uptake and handling of iron from transferrin, lactoferrin and immune complexes by a macrophage cell line. *Biochem J* 1988; 252:221–225.
76. Kaplan J, Jordan I, Sturrock. Regulation of the transferrin independent iron transport system in cultured cells. *J Biol Chem* 1991; 266:2997–3004.
77. Rama R, Sanchez J. Transferrin uptake by bone marrow macrophages is independent of the degree of iron saturation. *Br J Haematol* 1992; 82:455–459.
78. Olakamni O, Stokes JB, Britigan BE. Acquisition of iron bound to low molecular weight chelates by human monocyte derived macrophages. *J Immunol* 1994; 153: 2691–2703.
79. Weiss G, Graziadei I, Urbanek M, Grünwald K, Vogel W. Divergent effects of α_1 -antitrypsin on the regulation of iron metabolism in human erythroleukemic (K562) and myelomonocytic (THP-1) cells. *Biochem J* 1996; 319:897–902.
80. Graziadei I, Gaggl S, Kaserbacher R, Braunsteiner H, Vogel W. The acute phase protein alpha-1 antitrypsin inhibits growth and proliferation of human early erythroid progenitor cells and of human erythroleukemic cells by interfering with transferrin iron uptake. *Blood* 1994; 83:260–268.
81. Wesselius LJ, Williams WL, Bailey K, Vamos S, O'Brien-Ladner AR, Wiegmann T. Iron uptake promotes hyperoxic injury to alveolar macrophages. *Am J Respir Crit Care Med* 1999; 159:100–106.
82. Atkinson PG, Barton CH. High level expression of NRAMP1G169 in RAW264.7 cell transfectants: analysis of intracellular iron transport. *Immunology* 1999; 656–662.
83. Kuhn DE, Baker BD, Lafuse WP, Zwilling BS. Differential iron transport into phagosomes isolated from the RAW264.7 macrophage cell lines transfected with NRAMP-1 Gly169 or NRAMP1Asp169. *J Leukoc Biol* 1999; 66:113–119.
84. Cabantchik ZI, Glickstein H, Milgram P, Breuer W. 1996. A fluorescence assay for assessing chelation of intracellular iron in a membrane model system and in mammalian cells. *Anal Biochem* 233:221.
85. Birgens HS, Kristensen LO, Borregaard N, Karle H, Hansen NE. Lactoferrin-mediated transfer of iron to intracellular ferritin in human monocytes. *Exp Hematol* 1988; 41: 52–57.
86. Ismail M, Brock JH. Binding of lactoferrin and transferrin to the human promonocytic cell line U937. *J Biol Chem* 1993; 268:21618–21625.
87. Britigan BE, Serody JS, Hayek MB, Charniga LM, Cohen MS. Uptake of lactoferrin by mononuclear phagocytes inhibits their ability to form hydroxyl radical and protects them from membrane peroxidation. *J Immunol* 1991; 147:4271–4277.
88. Lima MF, Kierszenbaum F. Lactoferrin effects of phagocytic cell function. The presence of iron is required for the lactoferrin molecule to stimulate intracellular killing by macrophages but not to enhance the uptake of particles and microorganisms. *J Immunol* 1987; 1647–1651.

89. Baynes RD, Bukofzer G, Bothwell TH, Bezwoda WR. Apotransferrin receptors and the delivery of iron from cultured human blood monocytes. *Am J Hematol* 1987; 25: 417–425.
90. Donovan A, Brownlie A, Zhou Y, Shepard J, Pratt SJ, Moynihan J, Paw BH, Drejer A, Barut B, Zapata A, Law TC, Brugnara C, Lux SE, Pinkus GS, Pinkus JL, Kingsley PD, Palis J, Fleming MD, Andrews NC, Zon LI. Positional cloning of zebrafish ferroportin 1 identifies a conserved vertebrate iron exporter. *Nature* 2000; 403:776–781.
91. Wesselius LJ, Nelson ME, Skikne BS. Increased release of ferritin and iron by iron-loaded alveolar macrophages in cigarette smokers. *Am J Respir Crit Care Med* 1994; 150:690–695.
92. Konjin A, Hershko C. The anaemia of inflammation and chronic disease. In: DeSousa M, Brock JH, eds. *Iron in Immunity, Cancer and Inflammation*. Chichester, UK: Wiley, 1989:111–143.
93. Means RT, Krantz SB. Progress in understanding the pathogenesis of the anemia of chronic disease. *Blood* 1992; 80:1639–1647.
94. Weiss G. Iron and the anemia of chronic disease. *Kidney Int* 1999; 55(suppl 69):12–17.
95. Alvarez-Hernandez X, Licega J, McKay I, Brock JH. Induction of hypoferraemia and modulation of macrophage iron metabolism by tumor necrosis factor. *Lab Invest* 1989; 61:319–322.
96. Konjin AM, Carmel N, Levy R, Hershko C. Ferritin synthesis in inflammation. Mechanism of increased ferritin synthesis. *Br J Haematol* 1981; 49:361–368.
97. Torti SV, Kwak EL, Miller SC, Miller LL, Ringold GM, Myambo KB, Young AP, Torti FM. The molecular cloning and characterization of ferritin heavy chain, a tumor necrosis factor inducible gene. *J Biol Chem* 1988; 263:12638–12644.
98. Wei YS, Miller SC, Tsuji Y, Torti S, Torti FM. Interleukin 1 induces ferritin heavy chain in human muscle cells. *Biochem Biophys Res Commun* 1990; 169:288–296.
99. Rogers JT, Bridges KB, Durmowicz G, Glass J, Auron PR, Munro HN. Translational control during the acute phase response. Ferritin synthesis in response to interleukin 1. *J Biol Chem* 1990; 265:14572–14578.
100. Rogers JT. Ferritin translation by Interleukin-1 and interleukin-6: the role of sequences upstream of the start codons of the heavy and light subunit genes. *Blood* 1996; 87: 2525–2537.
101. Tsuji Y, Miller LL, Miller SC, Torti SV, Torti FM. Tumor necrosis factor- α and interleukin 1- α regulate transferrin receptor in human diploid fibroblasts. *J Biol Chem* 1991; 266:7257–7261.
102. Fahmy M, Young SP. Modulation of iron metabolism in the monocyte cell line U937 by inflammatory cytokines: changes in transferrin uptake, iron handling and ferritin mRNA. *Biochem J* 1993; 296:175–181.
103. Weiss G, Goossen B, Doppler W, Fuchs D, Pantopoulos K, Werner-Felmayer G, Wachter H, Hentze MW. Translational regulation via iron-responsive elements by the nitric oxide/NO-synthase pathway. *EMBO J* 1993; 12:3651–3657.
104. Drapier JC, Hirling H, Wietzerbin H, Kaldy P, Kühn LC. Biosynthesis of nitric oxide activates iron regulatory factor in macrophages. *EMBO J* 1993; 12:3643–3650.
105. Pantopoulos K, Hentze MW. Nitric oxide signaling to iron-regulatory protein. Direct control of ferritin mRNA translation and transferrin receptor mRNA stability in transfected fibroblasts. *Proc Natl Acad Sci USA* 1995; 92:1267–1271.
106. Weiss G, Werner-Felmayer G, Werner ER, Grünewald K, Wachter H, Hentze MW. Iron regulates nitric oxide synthase activity by controlling nuclear transcription. *J Exp Med* 1994; 180:969–976.
107. Mellilo G, Taylor LS, Brooks A, Musso T, Cox GW, Varesio L. Functional requirement

- of the hypoxia responsive element in the activation of the inducible nitric oxide synthase promoter by the iron chelator desferrioxamine. *J Biol Chem* 1997; 272:12236–12342.
108. Dlaska M, Weiss G. Central role of transcription factor NF-IL6 for cytokine and iron-mediated regulation of murine inducible nitric oxide synthase expression. *J Immunol* 1999; 162:6171–6177.
 109. Bourgeade MF, Silbermann F, Kühn L, Testa U, Peschle C, Memet S, Thang MN, Besancon F. Post-transcriptional regulation of transferrin receptor mRNA by IFN γ . *Nucleic Acids Res* 1992; 20:2997–3003.
 110. Byrd T, Horwitz MA. Regulation of transferrin receptor expression and ferritin content in human mononuclear macrophages. Coordinate upregulation by iron transferrin and down-regulation by interferon gamma. *J Clin Invest* 1993; 91:969–976.
 111. Weiss G, Bogdan C, Hentze MW. Pathways for the regulation of macrophage iron metabolism by the anti-inflammatory cytokines IL-4 and IL-13. *J Immunol* 1997; 158:420–425.
 112. Mulero V, Brock JH. Regulation of iron metabolism in murine J774 macrophages: role of nitric oxide dependent and independent pathways following activation with gamma interferon and lipopolysaccharide. *Blood* 1999; 94:2383–2389.
 113. Taetle R, Honeysett JM. γ -Interferon modulates human monocyte/macrophage transferrin receptor expression. *Blood* 1988; 71:1590–1595.
 114. Weiss G, Bogdan C, Hentze MW. 1997. Pathways for the regulation of macrophage iron metabolism by the anti-inflammatory cytokines IL-4 and IL-13. *J Immunol* 1997; 158:420–425.
 115. Custer G, Balcerzak S, Rinehart J. Human macrophage hemoglobin-iron metabolism in vitro. *Am J Hematol* 1982; 13:23–26.
 116. Kitagawa S, Yuo A, Yagisawa M, Azuma E, Yoshida M, Furukawa Y, Takahashi M, Masuyama J, Takaku F. Activation of human monocyte functions by tumor necrosis factor. Rapid priming for enhanced release of superoxide and erythrophagocytosis, but no direct triggering of superoxide release. *Exp Hematol* 1996; 24:559–567.
 117. Moura E, Noordermeer MA, Verhoeven N, Verheul AFM, Marx JJ. Iron release from human monocytes after erythrophagocytosis in vitro: an investigation in normal subjects and hereditary hemochromatosis patients. *Blood* 1998; 92:2511–2519.
 118. Kanayasu-Toyoda T, Yamaguchi T, Uchida E, Hayakawa T. Commitment of neutrophilic differentiation and proliferation of HL-60 cells coincides with expression of transferrin receptor. Effect of granulocyte colony stimulating factor on differentiation and proliferation. *J Biol Chem* 1999; 274:25471–25480.
 119. Patruta SI, Edlinger R, Sunder-Plassmann G, Horl WH. Neutrophil impairment associated with iron therapy in hemodialysis patients with functional deficiency. *J Am Soc Nephrol* 1998; 9:655–663.
 120. Hoepelman IM, Jaarsma EY, Verhoef J, Marx JJ. Effect of iron on polymorphnuclear granulocyte phagocytic capacity. Role of oxidation state and effect of ascorbic acid. *Br J Haematol* 1988; 70:495–500.
 121. Cantinieaux B, Janssens A, Boelaert JR, Lejeune M, Vermeylen C, Kerrels V, Cornu G, Winand J, Fondu P. Ferritin-associated iron induces neutrophil dysfunction in hemosiderosis. *J Lab Clin Med* 1999; 133:353–361.
 122. Brieland JK, Fantone JC. Ferrous iron release from transferrin by human neutrophil-derived superoxide anion: effect of pH and iron saturation. *Arch Biochem Biophys* 1991; 284:78–83.
 123. Clark RA, Pearson DW. Inactivation of transferrin iron binding capacity by the neutrophil myeloperoxidase system. *J Biol Chem* 1989; 264:9240–9247.

124. Crouch SPM, Slater KJ, Fletcher J. Regulation of cytokine release from mononuclear cells by iron binding protein lactoferrin. *Blood* 1992; 80:235–240.
125. VanAsbeck BS, Marx JJ, Struyvenberg A, vanKats JH, Verhoef J. Deferoxamine enhances phagocytic function of human polymorphonuclear phagocytes. *Blood* 1984; 714–720.
126. Clark RA, Pearson DW. Inactivation of transferrin iron binding capacity by the neutrophil myeloperoxidase system. *J Biol Chem* 1989; 264:9240–9247.

Iron Transport in the Central Nervous System

JOSEPH R. BURDO and JAMES R. CONNOR

Pennsylvania State University College of Medicine/Milton S. Hershey Medical Center, Hershey, Pennsylvania

I. INTRODUCTION	487
II. UPTAKE OF IRON INTO THE BRAIN	488
A. Development	490
B. Animal Models of Brain Iron Transport	491
C. Cell Culture	493
D. Cerebrospinal Fluid Iron Delivery	494
E. Iron Transport in Non-BBB Areas	496
III. IRON TRANSPORT WITHIN THE BRAIN	497
IV. IRON EXPORT FROM THE BRAIN	499
V. NEUROLOGICAL DISEASES	500
A. Demyelinating Disorders	501
VI. CONCLUSIONS	502
REFERENCES	502

I. INTRODUCTION

Iron is abundant in the brain and has a distinct regional and cellular pattern of distribution (1). The reason for this selective distribution involves differences in oxidative metabolism and in neurotransmitter concentration. The concentration of iron in some regions of the brain (e.g., the basal ganglia) can achieve levels found

in the liver, which historically has been considered the iron storage organ for the body. Thus, iron transport proteins can be expected to be abundant in brain, but can also be expected to vary in expression among brain regions and cell types. Because the brain is regionally and cellularly compartmentalized with regard to function, and hence regional shifts in metabolic activity occur, iron delivery to this organ has challenges not encountered in other organs. In addition, the brain presents challenges to iron transport because of the blood–brain barrier.

The importance of sufficient and timely iron delivery to the brain has been repeatedly demonstrated. There are numerous studies reporting cognitive and motor impairment in children and adults who are iron-deficient (2–4). Learning impairment at a young age has been demonstrated in both laboratory animals (5) and in humans (6) that were iron-deficient. Although iron deficiency in brain can have devastating and long-term neurological effects, iron accumulation is likewise associated with decreased function and cell loss in the brain. Damage associated with too much iron is presumably due to the direct relationship between iron and oxidative injury. Individuals with such common neurological diseases as Alzheimer's disease and Parkinson's disease invariably accumulate iron in the basal ganglia. Less common neurological diseases such as Huntington's disease (7) and Friederich's ataxia (8) are also associated with iron accumulation in the basal ganglia. Iron in the brain is used as a co-factor in ATP and DNA synthesis, as it is in the rest of the body. But brain iron also has unique functions in the synthesis of neurotransmitters and myelin, and unique consequences arise.

Transferrin (Tf) was the first iron delivery protein identified, and most cells express Tf receptor (TfR). In the brain, the majority of TfR are found on neurons (1,9). Autoradiographic analyses indicate relatively little detectable TfR expression in white matter (10,11). The concentration of TfR is highest in cortex, amygdala, hippocampus, and brainstem in the rat brain (86). Immunohistochemical studies on the adult brain show that neurons are the predominant cells that stain for TfR (9), although immunopositive astrocytes and oligodendrocytes are also found (100). The limited Tf receptor expression in white matter is inconsistent with the amount of iron in white matter and the constant iron requirement by oligodendrocytes. Our recent reports that ferritin receptors are predominantly expressed in white matter (10,11) indicate two nonoverlapping receptor systems for iron in the brain. Recently the divalent metal transporter 1 (Nramp2/DMT1; see Chapter 6) has been shown to be present in the brain (12,13). Receptors for lactoferrin, an iron transport protein normally associated with milk and neutrophils, have been reported in human brains and their expression is altered in Parkinson's disease (14). A homolog of Tf, p97, has also been reported in the brain (15,16).

II. UPTAKE OF IRON INTO THE BRAIN

Iron enters the brain through the vasculature, whether it be directly into the parenchyma from the blood or through the choroid plexus into the cerebrospinal fluid (CSF)-filled ventricles. In most areas of the brain, the plasma membranes of vasculature endothelial cells are in close apposition to one another, forming tight junctions. These tight junctions are also present in the endothelial cells lining the vasculature of the testes, but do not exist elsewhere in the periphery of the body. The blood–brain barrier (BBB) was thought to have developed to protect the brain from

large hydrophilic compounds that may have potentially harmful effects. While this function may spare the brain from unwanted effects, it also necessitates the presence of specific transporters for compounds that the brain needs to perform its daily functions. These transporters have already been described for compounds such as glucose (17,18) and insulin (19). In this section we will review studies into the mode of iron transport across the BBB, and speculate on some of the unknown points.

Nonheme iron circulates in the blood mainly in the form of (di)ferrous Tf iron (FeTf) complexes. In other parts of the body, FeTf can be transported from the vasculature paracellularly, due to the lack of endothelial cell tight junctions. But, as mentioned above, the tightness of the BBB precludes any significant paracellular transport. A specific TfR is necessary to accept the FeTf complex from the blood.

Transferrin receptors on brain endothelial cells were first demonstrated by injection of OX-26, a mouse anti-TfR antibody, intravenously into the rat (20). This study showed that TfR are present at the luminal surface of the rat brain blood vessels, while vascular staining of peripheral rat organs with the OX-26 antibody was not seen. Transferrin receptor was also localized to the human BBB in the same study using the B3/25 human TfR monoclonal antibody. There is a high density of TfR expression on the brain microvasculature in the adult brain, 6–10 times higher than the expression on the brain parenchyma (99). The kinetics of Tf binding to isolated human brain capillaries has been evaluated (21). Binding and endocytosis of Tf to its receptor were saturable and temperature-dependent, with a K_d of 448 ± 110 ng/mL, which is in the range of affinity shown previously for insulin and IGF receptors at the blood–brain barrier (22). It has been suggested that aluminum, a compound that is toxic to the CNS, enters the brain using the Tf-TfR system at the BBB (23). Transport of gallium into the brain, most likely bound to Tf, has also been noted (24).

The brain vasculature endothelial cell has a unique requirement to fulfill when it comes to iron transport. Certainly the cell itself has some requirement for iron, which necessitates unloading of iron from Tf within the cell. But due to the tight junctions of the blood–brain barrier, the endothelial cell is also responsible for passage of iron into the brain itself. Normally, iron is removed from Tf in an acidified vesicle, as has been shown for other cell types (25,26). Are there additional endosomal pathways in brain vasculature endothelial cells that are responsible for transcytosis of the Fe–Tf conjugate into the brain? Alternatively, perhaps iron is removed from the endosome and transported into the brain alone, with recycling of peripheral Tf to the blood vessel lumen.

One of the first studies designed to answer this question involved perfusion of [125 I]-Tf into the rat brain (27). A pulse of [125 I]-Tf was followed by a chase period, in which there was a decrease in radioactivity associated with the endothelial cells and an increase in radioactivity associated with the nonvascular elements of the brain. This finding seems to argue for transcytosis of a Fe–Tf complex. However, this study did not determine whether the iron bound to the radiolabeled Tf was transported into the brain parenchyma or it was removed and remained in the vasculature. Other studies using radiolabeled Tf contradict the above findings. Analysis of [125 I]-Tf perfused into the rat brain showed that, after correction for nonspecific binding, only 10% of the initial perfused radioactivity was associated with the brain after a 30-min perfusion with warm buffer (30). This small pool of remaining radioactivity is assumed to be either [125 I]-Tf that was transcytosed into the brain or

[¹²⁵I]-Tf that was not recycled in the endothelial cells and thus remained in the vasculature.

A subsequent study showed that iron is transported across the BBB at a greater rate than Tf (28). It was found that the brain-to-blood ratio was $14.7 \pm 0.9 \mu\text{L/g}$ brain for radiolabeled iron versus $11.7 \pm 0.6 \mu\text{L/g}$ brain for radiolabeled Tf. It is not clear what the iron saturation level of Tf used in this study was. For Tf fully saturated with iron, which is the form of Tf preferred by the TfR, one might expect a 2:1 stoichiometry if the Fe-Tf complex is transported across the blood-brain barrier intact. Because whole brain was analyzed for radioactivity after application of peripheral iron and/or Tf, it may be that transport of some Fe-Tf complex is taking place at the circumventricular organs, resulting in misleading Tf:Fe ratios. These organs are served by vasculature that does not have the normal tight junctions seen in the rest of the brain, leading to the possibility of paracellular transport.

Studies using a Tf-horseradish peroxidase (Tf-HRP) complex with subsequent electron microscopic evaluation have been performed to help evaluate transport of Tf across the BBB. Tf-HRP has been observed in coated vesicles within the vascular endothelial cells, although no evidence of Tf-HRP transcytosis was seen in the electron micrographs (29). Another study by Roberts et al. demonstrated similar findings (30). These findings seem to argue for removal of iron from Tf within the endothelial cell. However, HRP-conjugated compounds are not natural to the brain, and a previous study demonstrated HRP permeation into the brain only at the circumventricular organs (31).

Transport of iron on Tf-like molecules may also take place at the BBB. Melanotransferrin, or p97, has been localized to the capillary endothelia of the brain (16). This molecule is structurally similar to Tf but has an independent mechanism for iron uptake. Its distribution suggests that it may play a role in uptake of iron into the brain. Receptor-mediated transcytosis of lactoferrin (Lf), an iron-binding glycoprotein similar to Tf, has been demonstrated in primary cultures of bovine vascular endothelial cells (32). Binding of [¹²⁵I]-Lf to these cells is saturable, concentration-dependent, and inhibited by unlabeled Lf. Double labeling of Lf and Fe in this study demonstrated transcytosis of intact holo-Lf across the endothelial cell monolayer. An interesting aspect of this experiment is the fact that Lf transport was 70% inhibited by the receptor-associated protein (RAP), a specific antagonist of the low-density lipoprotein receptor-related protein (LRP). This indicates an involvement for LRP in lactoferrin transport. Lactoferrin is present in the normal human cortex, but is present at higher levels in neurodegenerative diseases such as Parkinson's disease (33). Parkinson's is one of many diseases associated with an alteration in iron and iron-management proteins. These alterations will be discussed later in this chapter.

A. Development

Because of the formation of the BBB, the mode of uptake of iron and Tf into the developing brain must be considered separately. In the rat brain, there is no evidence of histologically stainable iron at embryonic day 10 (E10) (34). But by E14, iron-containing endothelial cells line the blood vessels in the brain (34). The iron content in these endothelial cells as indicated by the Perl's-DAB histochemical reaction decreases to reach a low point by postnatal day 15 (P15). Closure of the BBB generally

occurs during the first few weeks of life in the rat, with some regional variation (35). The decrease in endothelial cell iron staining may represent increased iron movement into the brain. During the first two weeks of life, many processes requiring large amounts of energy are at their peaks, including replication of glial cells, myelogenesis, and mitochondriogenesis. Perhaps not coincidentally, uptake of iron and Tf in the rat both peak at approximately day 15 of life, as shown by uptake of peripherally injected ^{59}Fe -[^{125}I]-Tf (36). A slow accumulation of Tf occurs from the time of injection, but this accumulation is much less than that of iron. This latter observation indicates that the majority of iron that reaches the brain is removed from Tf within the endothelial cell, whereas the majority of Tf is recycled back into the plasma. It is possible that the mechanism of Fe–Tf transport changes during development, which may explain the evidence for Tf transcytosis seen by Fishman et al. (27) as noted above. This proposed mechanistic change during development may be triggered by, or reflected in, the decrease in stainable iron in endothelial cells as noted above.

Understanding the transport of Tf into the developing rat brain is complicated by the fact that mature oligodendrocytes, the main Tf-producing cells in the rat brain, do not appear until P10 (37). These cells secrete Tf and are responsible for 95% of the Tf in the brain (38). Choroid plexus is also a source of brain and CSF Tf in rats (39,40). The postnatal maturation of oligodendrocytes may require the transcytosis of Fe–Tf into the brain during the first weeks of development to meet the high growth requirements, with a switch to Tf recycling in the vascular endothelial cell and independent iron transport into the brain during the third developmental week when endogenous brain Tf is available. The brain is the only organ in which Tf mRNA continuously increases (41,42). Levels of Fe–Tf and ferritin in the brain are highest at birth, decreasing to the lowest measured levels during the third week of life. Iron and ferritin increase from this point on throughout the life of the animal, while Tf levels do not change significantly after day 24 (43). Perhaps it is the switch from transcytosed FeTf to endogenous production of brain Tf that keeps the brain concentrations of Tf relatively constant. This is still to be determined, as the regulation of Tf synthesis in brain is poorly understood. Recently, brain Tf levels have been shown to increase in animals fed an iron-deficient diet, but the source of the Tf is not known to be solely from the brain (44).

B. Animal Models of Brain Iron Transport

The hypotransferrinemic (hpx) mouse is an important model in discerning the mode of iron transport across the BBB. This mouse has less than 1% of normal circulating Tf levels in its blood (45), due to a defect in splicing of Tf precursor mRNA (46). These animals die within the first week of life unless they are supplemented with serum or purified Tf. Although the hpx mice also have no endogenous brain Tf, peripheral supplementation with human apo-Tf is sufficient for normal delivery of iron to the brain and for a normal oligodendrocytic Tf and iron staining (47). BBB integrity in these animals is reportedly normal (48), so it appears that peripheral Tf is being transcytosed across the brain vascular endothelial cells. This observation lends support to the concept of Fe–Tf transcytosis for use by the brain. Alternatively, transcytosis of Tf in the hpx mice may be the result of a compensatory mechanism that results from the lack of endogenous brain Tf, and may not be present in the

normal state. The compensatory mechanism apparently does not include increased TfR levels; heterozygotic hpx mice have approximately 50% of normal circulating Tf levels, but have no increase in BBB Tf receptors, which is also the case for homozygotic hpx mice supplemented with human apo-Tf (49). Transport studies using primary cultures of hpx brain microvascular endothelial cells may help to elucidate the mechanism of iron transport in these versus normal BBB cells.

The Belgrade (b) rat is another exciting model to apply to the problem of brain iron transport. This rat has a hypochromic, microcytic anemia (50), with only 20% of normal levels of iron uptake into reticulocytes (51). These b reticulocytes have twice the number of Tf receptors as normal reticulocytes, but return approximately twice as much iron to the cell surface as normals during endocytosis (52). The Belgrade defect is in *Nramp2/DMT1* (53), the transporter responsible for absorption of iron from the duodenum lumen and movement of iron out of endosomes. This transporter is discussed in detail elsewhere in this volume (see Chapter 6). The Belgrade rat provides the opportunity to determine if DMT1 is important for brain iron transport. We have recently shown DMT1 is present in the brain microvasculature (Fig. 1). Neurons and oligodendrocytes within the Belgrade brain have decreased levels of iron (54). It has also been shown that ^{59}Fe uptake in Belgrade rat brains is only 10% that of normal, while ^{125}I -Tf uptake is 40% that of normal after peripheral injection of ^{59}Fe - ^{125}I -Tf (55). The decrease in cellular iron within the brain may be due to a defect in transport at the neural cell level, but the decrease could also be at the level of the BBB. Although we have recently shown that DMT1 is present in the brain vascular endothelial cell, the near-100% saturation of plasma Tf in these rats could result in a downregulation of BBB Tf receptors.

Some of the iron being transported across the BBB in this nearly Tf-saturated state may be in the non-transferrin-bound iron (NTBI) form. NTBI has been demonstrated peripherally in pathological states such as hemochromatosis (56,57), in which Tf saturation is at or near 100%. Recent evidence suggests that iron may

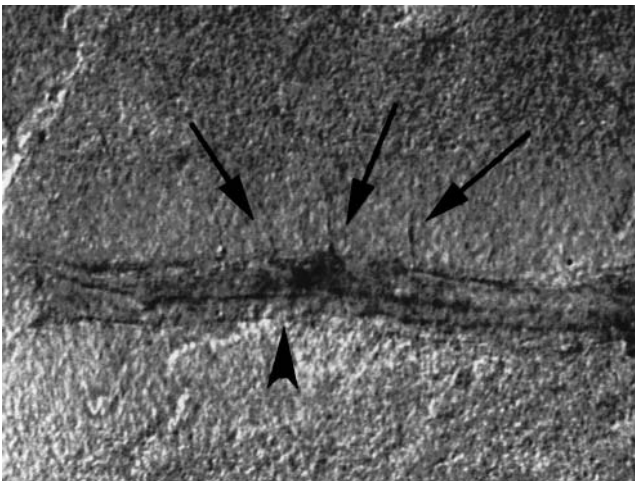


Figure 1 DMT1 staining in rat cortical vasculature. Astrocytic processes (arrows) are seen coursing to a blood vessel (arrowhead).

accumulate in brain in hemochromatotics (discussed below). Delivery of NTBI across the BBB may also be inducible in normal animals. Inhibition of TfR in mouse at levels sufficient to block iron uptake in the spleen blocks only 75% of brain iron uptake (48). The differences in iron versus Tf transport in the Belgrade rat could also be a consequence of missorted Tf being directed into the brain after removal of iron in the endosome, with the defect in DMT1-mediated iron transport resulting in a return of the iron to the luminal side of the endothelial cell instead of the brain side.

In the future, these animal mutants will provide us with the opportunity to elucidate aspects of iron transport into the brain that are still unclear. One way this may be possible is through the use of transport studies using in-vitro replication of the BBB. These types of studies have been performed using cultures from normal animals, as discussed below.

C. Cell Culture

Cultures of bovine brain microvessel endothelia have been utilized to address the question of iron transport across the blood–brain barrier. Raub and Newton have shown that Tf binding is saturable in these cells, with a K_d of 4.8 ± 0.8 nM and 100,000 receptors per cell (58). By studying binding of Tf at different temperatures and at different solubilization conditions, they also determined that approximately 90% of the total cellular TfR pool is located intracellularly. After growing the endothelial cells on filters, they incubated the cells with [125 I]-Tf for 1 h at 37°C. Approximately 15% of the total incubated radioactivity was associated with the basal media. Paracellular leakage, as measured by dextran support, was only 6%. This amount (15%) of specific transcytotic Tf transport agrees well with in-vivo estimates. One potential pitfall of these types of studies is the possibility that Tf may bind to the extracellular matrix or to the filter on which the cells are grown. In the Raub and Newton study, 37% of radioactivity remained associated with the cellular fraction during counting after a 1-h incubation. It is not known what fraction of this number represents intracellular Tf and what fraction may be associated with the substrate, but it may be a large enough percentage to significantly affect the amount of Tf thought to be transcytosed. It is also possible that the Tf that is transported to the basal media is missorted apo-Tf, and not due to a true transcytotic Fe–Tf pathway.

Another study of Tf transport in bovine vascular endothelial cells provided different results. Descamps et al. reported a K_d of 11.3 ± 2.1 nM with 35,000 TfR per cell (59), significantly different from the K_d and receptor number reported by Raub and Newton. Unlike the Raub and Newton study, Descamps et al. demonstrated approximately 75% transcytosis of [125 I]-Tf after a pulse-chase experiment, with only 10% recycled to the apical media. They also demonstrated that iron is transported across the endothelial cell monolayer in a 2:1 molar ratio as compared with Tf using an ^{59}Fe -[125 I]-Tf double-label transport experiment. This transcytotic transport was seen for holo-Tf, but no apo-Tf. As mentioned above, this is the ratio expected if Fe–Tf is transported intact across the monolayer. Also unlike the Raub and Newton study, Descamps et al. co-cultured the vascular endothelial cells in the presence of astrocytes. Astrocytes are normally in close apposition to the vascular endothelial cells in the brain, and are thought to induce many of the properties of the BBB. In fact, it has been shown that astrocytes can induce BBB properties even in non-brain

vascular endothelial cells (60). The co-culture system may induce a higher rate of endocytotic or transcytotic activity, which could explain the increased Tf seen in the basal media. Another interesting factor that may have led to the increased transcytosis seen in the Descamps et al. study is the fact that no saturation of [¹²⁵I]-holoTf transport was seen even with concentrations of Tf up to 1400 ng/mL. The lack of saturation may be due to recruitment of TfRs from the intracellular pool to the active endocytotic pool, with the purpose of maximum iron transport from a possibly iron deficient media, or influenced by iron-deficient astrocytes in the co-culture model.

Iron status of the brain vascular endothelial cells is an important factor in control of iron transport into the brain. Transferrin receptor numbers are increased in porcine endothelial cells grown in iron-depleted media as compared to normal media (61). The same study also showed that there are also more surface-bound TfR and more total TfR participating in the endocytotic cycle when these cells are grown in iron-deficient media. Previous work has shown that there is normally an inactive pool of TfR comprised of approximately 90% of the total cellular TfR (62). In an iron-deficient state, the total number of TfR remains constant, while the number of surface-bound TfR can be modulated by the cell. Thus, it appears that endothelial cells activate TfR from the inactive pool for use in the endocytotic cycle during an iron-deficient state. This activation would allow for a quicker response to iron need by the cell and by the brain than if new TfR had to be synthesized from mRNA. Also, greater iron accumulation was seen in endothelial cells grown in iron-enriched media as compared to iron-deficient media (61). This is an important finding, as it may allow the brain vasculature to act as a “buffer” against excessive iron accumulation in the brain. It may also allow the vascular cells to store iron that can be transported into the brain in the future if needed, during a period of iron deficiency, for example.

D. Cerebrospinal Fluid Iron Delivery

The role of the choroid plexus in maintaining brain iron homeostasis has received less attention than it probably should. The choroid plexus has a very high degree of vascularization compared to the rest of the brain, and is the source of CSF. One hour after a peripheral injection of ⁵⁹Fe, the majority of radioactivity is detected in the choroid plexus (63,64). Iron staining in the choroid plexus is robust (Fig. 2), as is staining for the iron-management proteins DMT1 and metal transport protein 1 (MTP-1) (unpublished observations). Ferritin is also abundant in the choroid plexus (65). As mentioned earlier, rat choroid plexus expresses the mRNA for Tf (39,40). Secretion of Tf into the ventricles may be an important delivery mechanism for iron to the rest of the brain. This is especially true during development, when the requirement for iron in the brain is high. In the pig (66) and sheep (67), CSF Tf levels are highest at one month gestation, and Tf is also found in the human fetal choroid plexus (68). Iron may also be transported from the CSF in a non-transferrin-bound state.

A review of iron status in the CSF has shown that previous measurements of iron and Tf concentration vary widely (69). Most of these measurements indicate that Tf in the CSF may be fully saturated. Sampling and analysis of CSF and brain tissue after peripheral ⁵⁹Fe-[¹²⁵I]-Tf injection indicates that a percentage of iron in the CSF and possibly brain interstitial space occurs as NTBI (70). Compounds in

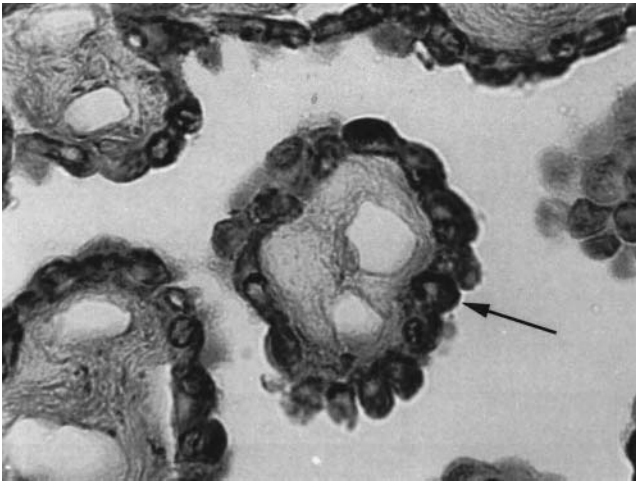


Figure 2 Iron staining in human choroid plexus. The arrow indicates the iron-containing epithelial cells.

the CSF that may also be responsible for transport of iron in the fully Tf-saturated state include citrate (71), ascorbate (72), and ferritin (70,73,74).

The levels of CSF ferritin are roughly 10% of the levels of ferritin found in the serum (75). Normal CSF contains approximately 3 ng/mL ferritin, but this concentration will increase during infectious meningoencephalitis, CNS vascular diseases, and dementia without vascular pathology (76). Marked elevations of CSF ferritin (30-fold) were observed in patients with bacterial or fungal meningitis in contrast to modest CSF ferritin elevations in patients with viral meningitis. Consequently, CSF ferritin could be a valuable early clinical tool for differential diagnosis (75). It is not known whether the CSF ferritin is first taken up from blood and secreted, or synthesized within the choroid plexus and secreted.

In contrast to serum ferritin, which is highly glycosylated (>70%), ferritin within the CSF is largely nonglycosylated (<20% glycosylated). Nonglycosylated ferritin is usually considered as “tissue ferritin,” suggesting that CSF ferritin is derived from cell death and subsequent ferritin release (77). However, the concentration of ferritin within the CSF of normal patients is significantly higher than that which would be expected to occur by passive diffusion across the blood–CSF barrier (78). This suggests that local synthesis and secretion of ferritin by brain cells occurs normally.

Because the total CSF volume is replaced approximately every 8 h, both iron and iron-carrying compounds are subject to nonspecific, rapid removal from the ventricles. After injection of ^{59}Fe -[^{125}I]-Tf into the rat ventricle, only 2.5% remains after 4 h (79). Within the brain parenchyma, the level of [^{125}I]-Tf declined steadily after intracerebroventricular (ICV) injection to less than 1% of dose after 24 h, while ^{59}Fe was retained at 18% of the initial dose even after 72 h. This indicates that iron may be removed from Tf within the ependymal cells lining the ventricles before it is transported into the brain. We have found that ependymal cells contain high levels of DMT1 (Fig. 3), supporting the idea of iron transport across ependymal cells. It

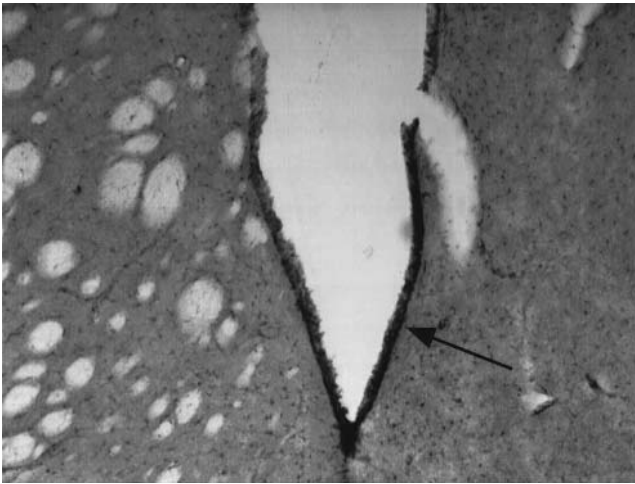


Figure 3 DMT1 staining in endepymal cells adjacent to the third ventricle. The immunostained endepymal cells are indicated by the arrow.

may be that endogenous brain Tf receives iron at the abluminal membrane of the endepymal cells for distribution throughout the brain. ICV injections of ^{59}Fe -[^{125}I]-Tf into 7-day-old rats led to a greater retention of radiolabeled Tf in both the CSF and the brain parenchyma as compared to adults, while radiolabeled iron was retained in the parenchyma to a higher degree than in the adult rats (79). The greater retention of Tf in the CSF of young rats probably is a result of lower turnover of CSF as compared to the adults, while the increased need for brain iron during development probably leads to a greater amount of transcytosis of Fe-Tf as well as endocytosis of iron to meet that need.

The high rate of blood flow (and thus of Fe-Tf) through the choroid plexus has led to the hypothesis that the majority of iron enters the brain through the CSF. This possibility was investigated by Ueda et al., who found that uptake of peripherally injected ^{59}Fe into the CSF was significantly less than uptake into the cerebral hemispheres, cerebellum, and brainstem (48). Although the choroid plexus may be more densely vascularized than other areas of the brain, the sheer size of the rest of the brain in comparison seems to allow more iron to accumulate directly into the brain parenchyma through the vasculature than that directed into the CSF. We propose that the CSF is useful for general distribution (and perhaps removal) of iron in the brain whereas the Tf receptors on the vasculature direct regional uptake.

E. Iron Transport in Non-BBB Areas

Finally, there is transport of iron to those brain regions that do not reside behind a conventional BBB. These areas are termed the circumventricular organs, and include the posterior pituitary and median eminence. Fenestrated capillaries in these regions are generally lacking in TfR (80). These fenestrations present a special problem when trying to determine how iron is transported into the brain. Whole-brain counts of peripherally injected radioactivity, whether it be [^{125}I]-Tf, ^{59}Fe , or both must take into account the possibility of nonspecific paracellular Tf transport or NTBI transport

across these fenestrated vessels. Free diffusion of iron into the CSF from the circumventricular organs though is prevented by the tight junctions that tanycytes (modified glial cells that line the ventricles) form between the circumventricular organs and the ventricles. Tanycytes stain intensely for iron (54,65,81), with one study demonstrating a localization of iron staining to tanycytes associated with the arcuate and posterior nuclei of the hypothalamus (47). This leads us to believe that tanycytes play a role in transport of iron into these two nuclei. This transport function apparently does not rely on DMT1 or Tf, as iron staining in the Belgrade rat (54) and hpx mouse (47) are normal.

III. IRON TRANSPORT WITHIN THE BRAIN

Iron transport within the brain has received relatively little study. The current thinking is that iron is transported across the BBB and then picked up by endogenous brain Tf. However, the considerable problems with this concept are reviewed in the previous section in this chapter. One problem with this concept is that astrocytes are thought to have end-feet that envelop the vasculature [(82) and Fig. 4]. Thus, iron entering the brain should necessarily pass through the glial end-feet. The mechanism and transport protein for this action are unknown. There are normally no Tf receptors on these astrocytes. A possible mechanism involves DMT1, which is found in astrocytes associated with the BBB, and the ferroxidase ceruloplasmin. In support of the

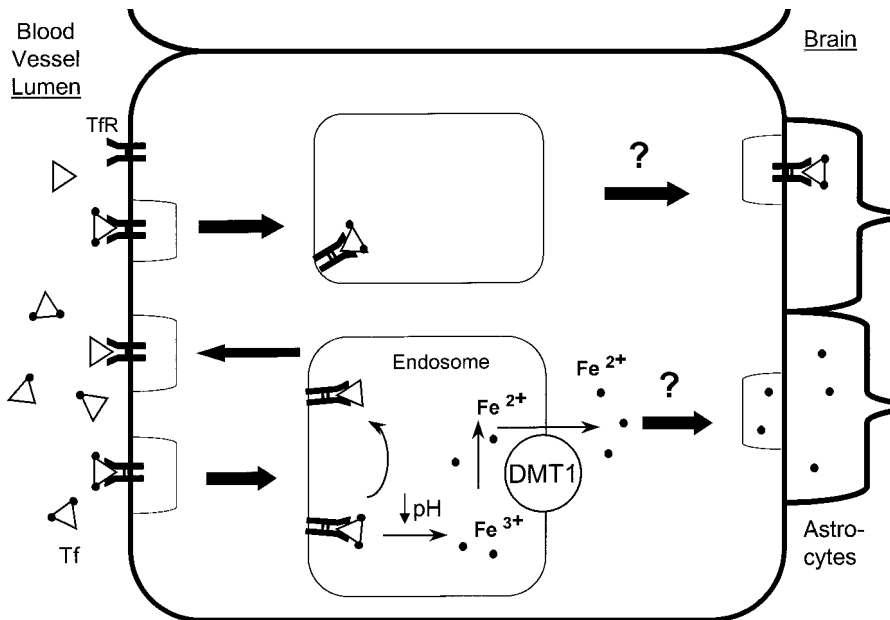


Figure 4 Schematic of iron transport in brain vascular endothelial cells. The question marks indicate our lack of certainty as to whether iron is transported into the brain as a complex with peripheral transferrin, or whether iron is removed from transferrin within the endosome and transported alone into the brain, with recycling of transferrin back into the blood vessel lumen. TfR, transferrin receptor; Tf, transferrin; DMT1, divalent metal transporter 1.

possibility that ceruloplasmin is involved in the transport of iron into the brain are the findings that a membrane-anchored form of ceruloplasmin is present in mammalian astrocytes (83), and the accumulation of iron in the brain in aceruloplasminemia [(84); see also Chapter 30]. Once released from astrocytes, iron would be available to bind to Tf. Indeed, hepatocytes process iron in a manner that makes it available to Tf, and astrocytes could mimic this function in the brain (85).

Iron in the parenchyma is likely associated with Tf or ferritin. Transferrin receptors are found throughout gray-matter regions of the brain in varying densities (86). Ferritin receptors are found selectively in white-matter regions of the brain (10,11). Cell culture studies have shown that Tf can deliver iron to neurons (87) and possibly glia (88,89), but Tf is not required for iron uptake or release from glia (90). Ferritin is easily transported around the brain in the extracellular space (91), and ferritin receptors have been shown on oligodendrocytes in culture (92).

Movement of iron in the brain from one region to another has been proposed. For example, brain regions that are normally high in iron are anatomically connected via neuronal axons to brain regions that are normally high in Tf receptors (86,81). For example, the nucleus accumbens and the caudate putamen (low-Fe areas) have high TfR densities. These regions connect with the globus pallidus and the substantia nigra (high-Fe areas); thus, there is the possibility of an uptake of iron in one area and delivery to storage/function in another through axonal transport (93). In support of this idea, anterograde transport of Tf and iron from the cell body/dendrite region to the axonal region has been demonstrated in cultured hippocampal neurons (94). Retrograde transport of iron-dextran has also been shown (95), but multiple particles including viruses are also retrogradely transported, so the physiological significance of this latter observation is unclear. Peripheral-type benzodiazepine receptors appear to play a role in transport of iron-containing compounds as well (96). The best evidence of iron redistribution in the brain comes from a study by Dwork et al., which demonstrated that iron enters the brain in a homogenous pattern and then redistributes to the basal ganglia over a period of 6 weeks (97).

Evidence exists for regulation of iron uptake and release specific to brain regions that may also be age-dependent. In a rat model of iron deficiency during weaning, the decline in brain iron concentration is not equal in all regions (44). At P21, cortex, deep and superficial cerebellum, pons, substantia nigra, and striatum in the iron-deficient rats lost significant amounts of iron compared to iron-fed controls, but not the hippocampus or thalamus. If an iron-fed rat is made iron-deficient post-weaning, significant iron loss is then seen in the thalamus, but still not in the hippocampus. Iron repletion after early iron deficiency normalized brain iron content in all regions except for the deep cerebellum and substantia nigra. These data are important not only because they show region-specific responses to systemic iron changes, but they also show that iron-repletion diets may selectively target brain regions. The selective targeting of brain regions in iron-replete diets could be relevant to the observations of iron accumulation in select brain regions in neurodegenerative diseases. We have already proposed that the brain may be targeted preferentially for iron delivery when dietary iron is insufficient (98).

The distribution of iron and iron-management proteins in the brain is heterogeneous with respect to cell type as well as brain area in the adult rat brain. This variable distribution indicates the presence of specificity of transport in the brain, which may operate at the level of the vasculature as well as at the level of the

Table 1 Cellular Distribution of Iron and Iron-Management Proteins in the Brain

	Region	Cell type
H-Ft	White matter, cortex	Oligodendrocytes, neurons
L-Ft	White matter	Oligodendrocytes, microglia
FtR	White matter	Oligodendrocytes
TfR	Cortex, striatum, hippocampus	Neurons, VECs
Tf	Ubiquitous	Oligodendrocytes, VECs, choroid plexus, ependyma
DMT1	Striatum, thalamus, choroid plexus, cerebellum	Neurons, astrocytes, ependymal cells, VECs, Purkinje cells
MTP-1	Cortex, cerebellum	Neurons, oligodendrocytes
Fe	Ubiquitous, high in motor areas	Oligodendrocytes, tanycytes, ependyma, neurons

Abbreviations: H-Ft (H-chain ferritin), L-Ft (L-chain ferritin), FtR (ferritin receptor), TfR (transferrin receptor), Tf (transferrin), DMT1 (divalent metal transporter 1), MTP-1 (metal transport protein 1).

individual cell. In Table 1, we summarize the data for cellular distribution of iron and the iron-management proteins. These data have been extensively reviewed elsewhere (1).

IV. IRON EXPORT FROM THE BRAIN

Export of iron from the brain is less well understood than the transport of iron into the brain. Control of iron transport is tightly regulated, as described above. This tight control over the amount of iron brought into the brain may keep to a minimum the amount of iron that it is necessary to transport out of the brain. Indeed, iron turnover in the brain is reportedly slow (101). However, because a number of studies provide more recent evidence that systematically injected iron can be demonstrated in brain within an hour, we have suggested that the notion of slow turnover of brain iron should be reconsidered (64). Dallman and Spirito (101) and Hallgren and Sourander (102) initially put forth the concept that brain iron turnover is slow. Dallman and Spirito saw minimal changes in levels of ^{59}Fe after peripheral infection at P15 in rat brains over a period of 14 weeks and concluded that iron went into the brain and remained there. We have suggested an alternative interpretation that the Dallman and Spirito data indicate that iron levels are maintained in a steady state and that radiolabeled iron (in their study) could have been initially stored in other organs and subsequently transported to the brain (98). Hallgren and Sourander (102) reported that brain iron accumulates throughout life in humans, but critical examination of their data reveals that most of the iron accumulates in the first two decades of life and remains at a plateau afterwards. These data also argue for an active efflux system.

Iron can either leave the brain parenchyma through reuptake into the vasculature or through transport across the ependymal cell lining into the ventricles. It has been demonstrated that transport of iron across the blood-brain barrier is bi-directional (28). Studies supporting removal of iron from brain via the ventricular system also exist. Radiolabeled Tf appears in the peripheral blood after injection into the (28,79), and the rate of Tf turnover through reabsorption of the CSF is near the rate

of uptake of iron into the brain (69,79). Because the complete reabsorption of CSF into the blood occurs approximately every 8 h in an adult human, the export of iron from the brain using CSF as a vehicle would possibly be more rapid than reuptake into brain parenchyma vasculature.

Transferrin synthesized in the choroid plexus may be useful in binding iron in the CSF to be reabsorbed into the blood. Penetration of radiolabeled Tf from the ventricles into the brain is lower than that of radiolabeled (79), so it seems unlikely that choroid plexus-derived Tf functions solely to import iron into the brain parenchyma. Also, as stated earlier, previous measurements indicate that Tf in the CSF is fully saturated, which may make newly imported Tf useful for binding iron for export.

As mentioned previously, we have recently demonstrated the presence of DMT1 in brain ependymal cells (Fig. 3). Indeed, the ependymal cells lining the ventricles stain more intensely for DMT1 than any other part of the brain. It is not possible from our immunohistochemical study to determine the direction of transport between the ventricles and brain parenchyma, but the presence of DMT1 strongly suggests transport occurs. The DMT1-defective Belgrade rats present a unique opportunity to analyze the role of ependymal cells in brain iron homeostasis.

V. NEUROLOGICAL DISEASES

Iron accumulation in specific brain regions is a consistent characteristic of a number of neurological diseases. This accumulation suggests disruption in brain iron transport. The disruptions in transport could be due to excessive uptake, limited movement within the brain, or inadequate efflux. Each of these topics has been specifically addressed in this chapter. One consequence of excess iron in the brain is the potential for iron-induced oxidative stress. Oxidative stress is a contributing factor in the neurological disorders associated with excess brain iron.

The neurological disorders associated with excess iron in the brain are presented in Table 2, and the major alterations in brain iron status are included. These diseases and their association with iron have recently been reviewed in detail (103). In Alzheimer's disease, iron is associated with neuritic plaques, the hallmark pathological change in Alzheimer's disease. The key component of neuritic plaques is amyloid. The production of amyloid may be influenced by cellular iron status (104,105). In addition, iron accumulates in Alzheimer's disease brains at a pace that is faster than ferritin production. This relative excess in iron compared to ferritin occurs in those regions of the Alzheimer's disease brain that undergo the most degeneration (106).

Another prominent neurological disease in which iron accumulation is excessive *vis à vis* ferritin expression is Parkinson's disease. Specifically, the substantia nigra and striatum appear to have increased levels of iron (107–110). Deficiencies in Fe-S-dependent enzyme activities, in cytochrome complexes I, II, and III, and in aconitase activity have been associated with Friedrich's ataxia, secondary to a mutation in the frataxin gene (111). Increased levels of iron are also present in the dentate nucleus of affected cerebelli in Friedrich's ataxia (8). In Hallervorden-Spatz, there are large amounts of iron in the globus pallidus and substantia nigra pars reticulata (112). In hereditary hemochromatosis, classically considered a peripheral disease, there are increased magnetic resonance image relaxation rate values in the

Table 2 Neurological Diseases and Their Associated Alterations in Iron Status

Neurological disease	Involvement of iron
Tardive dyskinesia	Increased striatal iron
Hereditary hemochromatosis	Increased iron in choroid plexus and pituitary, basal ganglia
Aceruloplasminemia	Increased basal ganglia and CSF iron
Restless legs syndrome	Decreased plasma and CSF ferritin Increased CSF transferrin Decreased iron in substantia nigra and putamen
Huntington's disease	Increased iron in striatum, occurs presymptomatically
Freidreich's ataxia	Increased mitochondrial iron in striatum and cerebellum
Multiple sclerosis	Loss of ferritin receptors in periplaque white matter
Parkinson's disease	Iron accumulation in substantia nigra, striatum, and in neuromelanin-containing cells Decreased levels of ferritin in substantia nigra, caudate, putamen
Alzheimer's disease	Iron accumulation in amygdala, hippocampus, frontal lobe, inferior parietal lobe, temporal cortex, nucleus basalis, globus pallidus, motor cortex Decreased iron in occipital cortex, substantia nigra Ferritin decreased in areas that accumulate iron Increased iron in amyloid plaques Changes in iron regulatory protein (IRP) distribution and activity TfR decreased in hippocampus
Hallervorden-Spatz	Iron accumulation in globus pallidus, substantia nigra

lentiform nucleus, which indicates increased levels of iron (113). In contrast to those diseases associated with an increase in iron accumulation, restless legs syndrome, a neurological disorder associated with an uncontrollable urgency to move the legs, appears to be related to iron deficiency.

Of particular note is that most of these diseases are movement disorders, and areas of the brain that are richest in iron are associated with motor systems. Given the number of diseases associated with iron and iron-management protein alteration, and the debilitating nature of these diseases, understanding mechanisms of iron transport in the brain should be given high priority.

A. Demyelinating Disorders

It is now accepted that iron acquisition by oligodendrocytes is essential for normal production of myelin. Iron concentration in white-matter regions of the brain consistently exceeds that of corresponding gray matter (114). Hypomyelination is a consistent and predominant effect of iron deficiency in humans and in animal models (103). The myelin-producing cells, oligodendrocytes, have developed a selective iron uptake system in the brain via ferritin (10,11,92). The expression of a ferritin receptor ensures that oligodendrocytes do not have to compete for Tf-delivered iron in the

brain, and also provides these cells with the opportunity to acquire much more iron than could be delivered by Tf. The uptake of ferritin into oligodendrocytes is ATP-dependent and clathrin-dependent (92). The selective presence of ferritin receptors on oligodendrocytes makes this protein attractive to pursue as the hypothetical auto-immune target in multiple sclerosis (11).

Other demyelinating diseases, such as Pelizaeous-Merzbacher (115,116), central pontine myelinolysis (117), and progressive rubella panencephalitis (118), reportedly have changes in iron and Tf. In experimental allergic encephalomyelitis, an animal model of demyelinating disorders, iron chelation therapy decreases both the severity of the histopathology and the clinical symptoms (119).

VI. CONCLUSIONS

The brain presents unique challenges to the study of iron transport because it resides behind an endothelial cell barrier, has multiple regions with differing metabolic requirements, and has a variety of cell types with specialized functions and hence specialized iron requirements. Critical review of the literature on mechanisms of brain iron uptake reveals numerous contradictory findings. Some of these apparently contradictory findings can be reconciled if transcytosis of the FeTf complex across the BBB and traditional release of iron in an acidified endosome are both considered possible. One type of transport may take precedence over the other under various conditions of iron status. It is essential to understand iron and (or) Tf transport across the BBB because the iron transport system could serve as a model for drug delivery into the brain. Efforts in this regard are already underway, as nerve growth factor has been conjugated to TfR antibodies to assist in delivery of this trophic substance to the brain (120).

Once the mechanism of iron transport into the brain has been elucidated, the daunting questions of regional regulation of transport and cellular transport remain. Two regional and cell selective mechanisms for iron acquisition have already been identified in the TfR and ferritin receptor. Regional regulation suggests there is input from the brain to the vasculature to indicate iron status. Identification of the factors involved in this system remain to be identified.

REFERENCES

1. Connor JR, Menzies SL. Cellular management of iron in the brain. *J Neurol Sci* 1995; 134(suppl):33–44.
2. Deinard AS, List A, Lindgren B, Hunt JV, Chang PN. Cognitive deficits in iron-deficient and iron-deficient anemic children. *J Pediatr* 1986; 108:681–689.
3. Tu JB, Shafey H, VanDewetering C. Iron deficiency in two adolescents with conduct, dysthymic and movement disorders. *Can J Psychiatr* 1994; 39:371–375.
4. Cook JD, Skikne BS, Baynes RD. Iron deficiency: the global perspective. *Adv Exp Med Biol* 1994; 356:219–228.
5. Yehuda S, Youdim ME, Mostofsky DI. Brain iron-deficiency causes reduced learning capacity in rats. *Pharmacol Biochem Behav* 1986; 25:141–144.
6. Palti H, Meijer A, Adler B. Learning achievement and behavior at school of anemic and non-anemic infants. *Early Hum Dev* 1985; 10:217–223.
7. Bartzokis G, Cummings J, Perlman S, Hance DB, Mintz J. Increased basal ganglia iron levels in Huntington disease. *Arch Neurol* 1999; 56:569–574.

8. Waldvogel D, van Gelderen P, Hallett M. Increased iron in the dentate nucleus of patients with Friedrich's ataxia. *Ann Neurol* 1999; 46:123–125.
9. Moos T. Immunohistochemical localization of intraneuronal transferrin receptor immunoreactivity in the adult mouse central nervous system. *J Comp Neurol* 1996; 375: 675–692.
10. Hulet SW, Hess EJ, Debinski W, Arosio P, Bruce K, Powers S, Connor JR. Characterization and distribution of ferritin binding sites in the adult mouse brain. *J Neurochem* 1999; 72:868–874.
11. Hulet SW, Powers S, Connor JR. Distribution of transferrin and ferritin binding in normal and multiple sclerotic human brains. *J Neurol Sci* 1999; 165:48–55.
12. Gunshin H, Mackenzie B, Berger U, Gunshin Y, Romero MF, Boron WF, Nussberger S, Gollan JL, Hediger MA. Cloning and characterization of a mammalian proton-coupled metal-ion transporter. *Nature* 1997; 388:482–488.
13. Moos T, Trinder D, Morgan EH. Cellular distribution of ferric iron, ferritin, transferrin and divalent metal transporter 1 (DAMT1) in substantia nigra and basal ganglia of normal and $\beta 2$ -microglobulin deficient mouse brain. *Cell Mol Biol* 2000; 46:549–561.
14. Faucheux BA, Nillesse N, Damier P, Spik G, Mouatt-Prigent A, Pierce A, Leveugle B, Kubis N, Hauw JJ, Agid Y. Expression of lactoferrin receptors is increased in the mesencephalon of patients with Parkinson disease. *Proc Natl Acad Sci USA* 1995; 92: 9603–9607.
15. Yamada T, Tsujioka Y, Taguchi J, Takahashi M, Tsuboi Y, Moroo I, Yang J, Jefferies WA. Melanotransferrin is produced by senile plaque-associated reactive microglia in Alzheimer's disease. *Brain Res* 1999; 845:1–5.
16. Rothenberger S, Food MR, Gabathuler R, Kennard ML, Yamada T, Yasuhara O, McGeer PL, Jefferies WA. Coincident expression and distribution of melanotransferrin and transferrin receptor in human brain capillary endothelium. *Brain Res* 1996; 712: 117–121.
17. Boado RJ, Pardridge WM. The brain-type glucose transporter mRNA is specifically expressed at the blood-brain barrier. *Biochem Biophys Res Commun* 1990; 166:174–179.
18. Rahner-Welsch S, Vogel J, Kuschinsky W. Regional congruence and divergence of glucose transporters (GLUT1) and capillaries in rat brains. *J Cereb Blood Flow Metab* 1995; 15:681–686.
19. Pardridge WM, Eisenberg J, Yang J. Human blood-brain barrier insulin receptor. *J Neurochem* 1985; 44:1771–1778.
20. Jefferies W, Brandon M, Hunt S, Williams A, Gatter K, Mason D. Transferrin receptor on endothelium of brain capillaries. *Nature* 1984; 312:162–163.
21. Pardridge WM, Eisenberg J, Yang J. Human blood-brain barrier transferrin receptor. *Metabolism* 1987; 36:892–895.
22. Frank HJ, Pardridge WM, Morris WL, Rosenfeld RG, Choi TB. Binding and internalization of insulin and insulin-like growth factors by isolated brain microvessels. *Diabetes* 1986; 35:654–661.
23. Roskams AJ, Connor JR. Aluminum access to the brain: a role for transferrin and its receptor. *Proc Natl Acad Sci USA* 1990; 87:9024–9027.
24. Murphy VA, Rapoport SI. Brain transfer coefficients for ^{67}Ga : comparison to ^{55}Fe and effect of calcium deficiency. *J Neurochem* 1992; 58:898–902.
25. Forsbeck K, Nilsson K. Iron metabolism of established human hematopoietic cell lines in vitro. *Exp Cell Res* 1983; 144:323–332.
26. Sipe DM, Murphy RF. Binding to cellular receptors results in increased iron release from transferrin at mildly acidic pH. *J Biol Chem* 1991; 266:8002–8007.
27. Fishman J, Rubin J, Handrahan J, Connor J, Fine R. Receptor-mediated transcytosis of transferrin across the blood-brain barrier. *J Neurosci Res* 1987; 18:299–304.

28. Banks WA, Kastin AJ, Fasold MB, Barrera CM, Augereau G. Studies of the slow bidirectional transport of iron and transferrin across the blood-brain barrier. *Brain Res Bull* 1988; 21:881–885.
29. Roberts R, Sandra A, Siek GC, Lucas JJ, Fine RE. Studies of the mechanism of iron transport across the blood-brain barrier. *Ann Neurol* 1992; 32(suppl):43–50.
30. Roberts RL, Fine RE, Sandra A. Receptor-mediated endocytosis of transferrin at the blood-brain barrier. *J Cell Sci* 1993; 104(Pt2):521–532.
31. Broadwell RD, Brightman MW. Entry of peroxidase into neurons of the central and peripheral nervous systems from extracerebral and cerebral blood. *J Comp Neurol* 1976; 166:257–283.
32. Fillebeen C, Descamps L, Dehouck MP, Fenart L, Benaissa M, Spik G, Cecchelli R, Pierce A. Receptor-mediated transcytosis of lactoferrin through the blood-brain barrier. *J Biol Chem* 1999; 274:7011–7017.
33. Leveugle B, Faucheux BA, Bouras C, Nillesse N, Spik G, Hirsch EC, Agid Y, Hof PR. Cellular distribution of the iron-binding protein lactotransferrin in the mesencephalon of Parkinson's disease cases. *Acta Neuropathol (Berl)* 1996; 91:566–572.
34. Moos T. Developmental profile of non-heme iron distribution in the rat brain during ontogenesis. *Brain Res Dev Brain Res* 1995; 87:203–213.
35. Dobbing J. The development of the blood-brain barrier. *Prog Brain Res* 1968; 29:417–427.
36. Taylor EM, Morgan EH. Developmental changes in transferrin and iron uptake by the brain in the rat. *Brain Res Dev Brain Res* 1990; 55:35–42.
37. Connor JR, Fine RE. Development of transferrin-positive oligodendrocytes in the rat central nervous system. *J Neurosci Res* 1987; 17:51–59.
38. Connor JR, Phillips TM, Lakshman MR, Barron KD, Fine RE, Csiza CK. Regional variation in the levels of transferrin in the CNS of normal and myelin-deficient rats. *J Neurochem* 1987; 49:1523–1529.
39. Aldred AR, Dickson PW, Marley PD, Schreiber G. Distribution of transferrin synthesis in brain and other tissues in the rat. *J Biol Chem* 1987; 262:5293–5297.
40. Dickson PW, Aldred AR, Marley PD, Tu GF, Howlett GJ, Schreiber G. High prealbumin and transferrin mRNA levels in the choroid plexus of rat brain. *Biochem Biophys Res Commun* 1985; 127:890–895.
41. Levin MJ, Tuil D, Uzan G, Dreyfus JC, Kahn A. Expression of the transferrin gene during development of non-hepatic tissues: high level of transferrin mRNA in fetal muscle and adult brain. *Biochem Biophys Res Commun* 1984; 122:212–217.
42. Bartlett WP, Li XS, Connor JR. Expression of transferrin mRNA in the CNS of normal and jimpy mice. *J Neurochem* 1991; 57:318–322.
43. Roskams AJ, Connor JR. Iron, transferrin, and ferritin in the rat brain during development and aging. *J Neurochem* 1994; 63:709–716.
44. Pinero DJ, Li NQ, Connor JR, Beard JL. Variations in dietary iron alter brain iron metabolism in developing rats. *J Nutr* 2000; 130:254–263.
45. Bernstein SE. Hereditary hypotransferrinemia with hemosiderosis, a murine disorder resembling human atransferrinemia. *J Lab Clin Med* 1987; 110:690–705.
46. Huggenvik JI, Craven CM, Idzerda RL, Bernstein S, Kaplan J, McKnight GS. A splicing defect in the mouse transferrin gene leads to congenital atransferrinemia. *Blood* 1989; 74:482–486.
47. Dickinson TK, Connor JR. Cellular distribution of iron, transferrin, and ferritin in the hypotransferrinemic (Hp) mouse brain. *J Comp Neurol* 1995; 355:67–80.
48. Ueda F, Raja KB, Simpson RJ, Trowbridge IS, Bradbury MW. Rate of ⁵⁹Fe uptake into brain and cerebrospinal fluid and the influence thereon of antibodies against the transferrin receptor. *J Neurochem* 1993; 60:106–113.

49. Dickinson TK, Connor JR. Immunohistochemical analysis of transferrin receptor: regional and cellular distribution in the hypotransferrinemic (hpx) mouse brain. *Brain Res* 1998; 801:171–181.
50. Sladic-Simic D, Martinovitch PN, Zivkovic N, Pavic D, Martinovic J, Kahn M, Ranney HM. A thalassemia-like disorder in Belgrade laboratory rats. *Ann NY Acad Sci* 1969; 165:93–99.
51. Edwards J, Garrick L, Hoke J. Defective iron uptake and globin synthesis by erythroid cells in the anemia of the Belgrade laboratory rat. *Blood* 1978; 51:347–357.
52. Garrick M, Gniecko K, Liu Y, Cohan D, Garrick L. Transferrin and the transferrin cycle in Belgrade rat reticulocytes. *J Biol Chem* 1993; 268:14867–14874.
53. Fleming MD, Romano MA, Su MA, Garrick LM, Garrick MD, Andrews NC. Nramp2 is mutated in the anemic Belgrade (b) rat: evidence of a role for Nramp2 in endosomal iron transport. *Proc Natl Acad Sci USA* 1998; 95:1148–1153.
54. Burdo JR, Martin J, Menzies SL, Dolan KG, Romano MA, Fletcher RJ, Garrick MD, Garrick LM, Connor JR. Cellular distribution of iron in the brain of the Belgrade rat. *Neuroscience* 1999; 93(3):1189–1196.
55. Farcich EA, Morgan EH. Diminished iron acquisition by cells and tissues of Belgrade laboratory rats. *Am J Physiol* 1992; 262:R220–R224.
56. Bacon BR, Fried MW, DiBisceglie AM. A 39-year-old man with chronic hepatitis, elevated serum ferritin values, and a family history of hemochromatosis. *Semin Liver Dis* 1993; 13:101–105.
57. de Valk B, Addicks MA, Gosriwatana I, Lu S, Hider RC, Marx JJ. Non-transferrin-bound iron is present in serum of hereditary haemochromatosis heterozygotes. *Eur J Clin Invest* 2000; 30:248–251.
58. Raub TJ, Newton CR. Recycling kinetics and transcytosis of transferrin in primary cultures of bovine brain microvessel endothelial cells. *J Cell Physiol* 1991; 149:141–151.
59. Descamps L, Dehouck MP, Torpier G, Cecchelli R. Receptor-mediated transcytosis of transferrin through blood-brain barrier endothelial cells. *Am J Physiol* 1996; 270:1149–1158.
60. Hayashi Y, Nomura M, Yamagishi S, Harada S, Yamashita J, Yamamoto H. Induction of various blood-brain barrier properties in non-neural endothelial cells by close apposition to co-cultured astrocytes. *Glia* 1997; 19:13–26.
61. van Gelder W, Huijskes-Heins MI, Cleton-Soeteman MI, van Dijk JP, van Eijk HG. Iron uptake in blood-brain barrier endothelial cells cultured in iron-depleted and iron-enriched media. *J Neurochem* 1998; 71:1134–1140.
62. van Gelder W, Huijskes-Heins MI, van Dijk JP, Cleton-Soeteman MI, van Eijk HG. Quantification of different transferrin receptor pools in primary cultures of porcine blood-brain barrier endothelial cells. *J Neurochem* 1995; 64:2708–2715.
63. Dwork AJ. Effects of diet and development upon the uptake and distribution of cerebral iron. *J Neurol Sci* 1995; 134(suppl):45–51.
64. Malecki EA, Cook BM, Devenyi AG, Beard JL, Connor JR. Transferrin is required for normal distribution of ⁵⁹Fe and ⁵⁴Mn in mouse brain. *J Neurol Sci* 1999; 170:112–118.
65. Benkovic SA, Connor JR. Ferritin, transferrin, and iron in selected regions of the adult and aged rat brain. *J Comp Neurol* 1993; 338:97–113.
66. Cavanagh ME, Cornelis ME, Dziegielewska KM, Luft AJ, Lai PC, Lorscheider FL, Saunders NR. Proteins in cerebrospinal fluid and plasma of fetal pigs during development. *Dev Neurosci* 1982; 5:492–502.
67. Cavanagh ME, Cornelis ME, Dziegielewska KM, Evans CA, Lorscheider FL, Mollgard K, Reynolds ML, Saunders NR. Comparison of proteins in CSF of lateral and IVth ventricles during early development of fetal sheep. *Brain Res* 1983; 313:159–167.

68. Mollgard K, Jacobsen M, Jacobsen GK, Clausen PP, Saunders NR. Immunohistochemical evidence for an intracellular localization of plasma proteins in human foetal choroid plexus and brain. *Neurosci Lett* 1979; 14:85–90.
69. Bradbury MW. Transport of iron in the blood-brain-cerebrospinal fluid system. *J Neurochem* 1997; 69:443–454.
70. Moos T, Morgan EH. Evidence for low molecular weight, non-transferrin-bound iron in rat brain and cerebrospinal fluid. *J Neurosci Res* 1998; 54:486–494.
71. Haerer AF. Citrate and alpha-ketoglutarate in cerebrospinal fluid and blood. *Neurology* 1971; 21:1059–1065.
72. Spector R, Spector AZ, Snodgrass SR. Model for transport in the central nervous system. *Am J Physiol* 1977; 232:R73–79.
73. Fehling C, Qvist I. Ferritin concentration in cerebrospinal fluid. *Acta Neurol Scand* 1985; 71:510–512.
74. Earley CJ, Connor JR, Beard JL, Malecki EA, Epstein DK, Allen RP. Abnormalities in CSF concentrations of ferritin and transferrin in restless legs syndrome. *Neurology* 2000; 54:1698–1700.
75. Campbell DR, Skikne BS, Cook JD. Cerebrospinal fluid ferritin levels in screening for meningism. *Arch Neurol* 1986; 43:1257–1260.
76. Sindic CJ, Collet-Cassart D, Cambiaso CL, Masson PL, Laterre EC. The clinical relevance of ferritin concentration in the cerebrospinal fluid. *J Neurol Neurosurg Psychiatr* 1981; 44:329–333.
77. Zappone E, Bellotti V, Cazzola M, Ceroni M, Meloni F, Pedrazzoli P, Perfetti V. Cerebrospinal fluid ferritin in human disease. *Haematologica* 1986; 71:103–107.
78. Keir G, Tasdemir N, Thompson EJ. Cerebrospinal fluid ferritin in brain necrosis: evidence for local synthesis. *Clin Chim Acta* 1993; 216:153–166.
79. Moos T, Morgan EH. Kinetics and distribution of [⁵⁹Fe-125I]transferrin injected into the ventricular system of the rat. *Brain Res* 1998; 790:115–128.
80. Broadwell RD, Baker-Cairns BJ, Friden PM, Oliver C, Villegas JC. Transcytosis of protein through the mammalian cerebral epithelium and endothelium. III. Receptor-mediated transcytosis through the blood-brain barrier of blood-borne transferrin and antibody against the transferrin receptor. *Exp Neurol* 1996; 142:47–65.
81. Hill J, Switzer RC. The regional distribution and cellular localization of iron in the rat brain. *Neuroscience* 1984; 11:595–603.
82. Xu J, Ling EA. Studies of the ultrastructure and permeability of the blood-brain barrier in the developing corpus callosum in postnatal rat brain using electron dense tracers. *J Anat* 1994; 184(Pt2):227–237.
83. Patel BN, David S. A novel glycosylphosphatidylinositol-anchored form of ceruloplasmin is expressed by mammalian astrocytes. *J Biol Chem* 1997; 272:20185–20190.
84. Harris ZL, Klomp LW, Gitlin JD. Aceruloplasminemia: an inherited neurodegenerative disease with impairment of iron homeostasis. *Am J Clin Nutr* 1998; 67:972S.
85. Harris ZL, Durley AP, Man TK, Gitlin JD. Targeted gene disruption reveals an essential role for ceruloplasmin in cellular iron efflux. *Proc Natl Acad Sci USA* 1999; 96:10812–10817.
86. Hill JM, Ruff MR, Weber RJ, Pert CB. Transferrin receptors in rat brain: neuropeptide-like pattern and relationship to iron distribution. *Proc Natl Acad Sci USA* 1985; 82:4553–4557.
87. Swaiman KF, Machen VL. Iron uptake by mammalian cortical neurons. *Ann Neurol* 1984; 16:66–70.
88. Swaiman KF, Machen VL. Iron uptake by glial cells. *Neurochem Res* 1985; 10:1635–1644.
89. Espinosa de los Monteros A, Foucaud B. Effect of iron and transferrin on pure oligodendrocytes in culture; characterization of a high-affinity transferrin receptor at different ages. *Brain Res* 1987; 432:123–130.

90. Takeda A, Devenyi A, Connor JR. Evidence for non-transferrin-mediated uptake and release of iron and manganese in glial cell cultures from hypotransferrinemic mice. *J Neurosci Res* 1998; 51:454–462.
91. Westergaard E, Brightman MW. Transport of proteins across normal cerebral arterioles. *J Comp Neurol* 1973; 152:17–44.
92. Hulet SW HS, Powers S, Connor JR. Oligodendrocyte progenitor cells internalize ferritin via clathrin-dependent receptor mediated endocytosis. *J Neurosci Res* 2000; 61(1): 52–60.
93. Mash DC, Pablo J, Flynn DD, Efang SM, Weiner WJ. Characterization and distribution of transferrin receptors in the rat brain. *J Neurochem* 1990; 55:1972–1979.
94. Hemar A, Olivo JC, Williamson E, Saffrich R, Dotti CG. Dendroaxonal transcytosis of transferrin in cultured hippocampal and sympathetic neurons. *J Neurosci* 1997; 17: 9026–9034.
95. Cesaro P, Nguyen-Legros J, Berger B, Alvarez C, Albe-Fessard D. Double labelling of blanchard neurons in the central nervous system of the rat by retrograde axonal transport of horseradish peroxidase and iron dextran complex. *Neurosci Lett* 1979; 15:1–7.
96. Taketani S, Kohno H, Furukawa T, Tokunaga R. Involvement of peripheral-type benzodiazepine receptors in the intracellular transport of heme and porphyrins. *J Biochem (Tokyo)* 1995; 117:875–880.
97. Dwork AJ, Lawler G, Zybert PA, Durkin M, Osman M, Willson N, Barkai AI. An autoradiographic study of the uptake and distribution of iron by the brain of the young rat. *Brain Res* 1990; 518:31–39.
98. Malecki EA, Devenyi AG, Beard JL, Connor JR. Transferrin response in normal and iron-deficient mice heterozygotic for hypotransferrinemia; effects on iron and manganese accumulation. *Biometals* 1998; 11:265–276.
99. Kalaria R, Sromek S, Grahovac I, Harik S. Transferrin receptors of rat and human brain and cerebral microvessels and their status in Alzheimer's disease. *Brain Res* 1992; 585:87–93.
100. Giometto B, Bozza F, Argentiero V, Gallo P, Pagni S, Piccinno MG, Tavolato B. Transferrin receptors in rat central nervous system. An immunocytochemical study. *J Neurol Sci* 1990; 98:81–90.
101. Dallman PR, Spirito RA. Brain iron in the rat: extremely slow turnover in normal rats may explain long-lasting effects of early iron deficiency. *J Nutr* 1977; 107:1075–1081.
102. Sourander B, Hallgren P. The effect of age on the non-haemin iron in the human brain. *J Neurochem* 1958; 3:41–51.
103. Pinero D, Connor JR. Iron in the brain: an important contributor in normal and diseased states. *Neuroscientist* 2000; 6:435–453.
104. Mantyh PW, Ghilardi JR, Rogers S, DeMaster E, Allen CJ, Stimson ER, Maggio JE. Aluminum, iron, and zinc ions promote aggregation of physiological concentrations of beta-amyloid peptide. *J Neurochem* 1993; 61:1171–1174.
105. Tanzi RE, Hyman BT. Alzheimer's mutation [letter; comment]. *Nature* 1991; 350:564.
106. Connor JR, Snyder BS, Beard JL, Fine RE, Mufson EJ. Regional distribution of iron and iron-regulatory proteins in the brain in aging and Alzheimer's disease. *J Neurosci Res* 1992; 31:327–335.
107. Earle KM. Studies on Parkinson's disease including X-ray fluorescent spectroscopy of formalin fixed brain tissue. *J Neuropathol Exp Neurol* 1968; 27:1–14.
108. Sofic E, Riederer P, Heinsen H, Beckmann H, Reynolds GP, Hebenstreit G, Youdim MB. Increased iron (III) and total iron content in post mortem substantia nigra of parkinsonian brain. *J Neural Transm* 1988; 74:199–205.
109. Dexter DT, Wells FR, Lees AJ, Agid F, Agid Y, Jenner P, Marsden CD. Increased nigral iron content and alterations in other metal ions occurring in brain in Parkinson's disease. *J Neurochem* 1989; 52:1830–1836.

110. Dexter DT, Carayon A, Javoy-Agid F, Agid Y, Wells FR, Daniel SE, Lees AJ, Jenner P, Marsden CD. Alterations in the levels of iron, ferritin and other trace metals in Parkinson's disease and other neurodegenerative diseases affecting the basal ganglia. *Brain* 1991; 114(Pt 4):1953-1975.
111. Rotig A, de Lonlay P, Chretien D, Foury F, Koenig M, Sidi D, Munnich A, Rustin P. Aconitase and mitochondrial iron-sulphur protein deficiency in Friedreich ataxia. *Nature Genet* 1997; 17:215-217.
112. Swaiman KF. Hallervorden-Spatz syndrome and brain iron metabolism. *Arch Neurol* 1991; 48:1285-1293.
113. Berg D, Hoggenmuller U, Hofmann E, Fischer R, Kraus M, Scheurlen M, Becker G. The basal ganglia in haemochromatosis. *Neuroradiology* 2000; 42:9-13.
114. Connor J. Proteins of iron regulation in the brain in Alzheimer's disease. In: Lauffer R, ed. *Iron and Human Disease*. Ann Arbor, MI: CRC Press, 1992:365-393.
115. Koeppen AH, Barron KD, Csiza CK, Greenfield EA. Comparative immunocytochemistry of Pelizaeus-Merzbacher disease, the jimpy mouse, and the myelin-deficient rat. *J Neurol Sci* 1988; 84:315-327.
116. Jaeken J, van Eijk HG, van der Heul C, Corbeel L, Eeckels R, Eggermont E. Sialic acid-deficient serum and cerebrospinal fluid transferrin in a newly recognized genetic syndrome. *Clin Chim Acta* 1984; 144:245-247.
117. Gocht A, Lohler J. Changes in glial cell markers in recent and old demyelinated lesions in central pontine myelinolysis. *Acta Neuropathol (Berl)* 1990; 80:46-58.
118. Valk J, van der Knaap MS. White matter disorders. *Curr Opin Neurol Neurosurg* 1991; 4(6):843-851.
119. Bowern N, Ramshaw IA, Clark IA, Doherty PC. Inhibition of autoimmune neuropathological process by treatment with an iron-chelating agent. *J Exp Med* 1984; 160:1532-1543.
120. Friden PM, Walus LR, Watson P, Doctrow SR, Kozarich JE, Backman C, Bergman H, Hoffer B, Bloom F, Granholm AC. Blood-brain barrier penetration and in vivo activity of an NGF conjugate. *Science* 1993; 259:373-377.

Iron Uptake by Neoplastic Cells

DES R. RICHARDSON

The Heart Research Institute, Sydney, New South Wales, Australia

I. INTRODUCTION	510
II. GENERAL OVERVIEW OF CELLULAR IRON UPTAKE AND METABOLISM	510
III. IRON UPTAKE MECHANISMS IN NEOPLASTIC CELLS	513
A. Transferrin	513
B. Transferrin Receptor (TfR) and Receptor-Mediated Endocytosis of Transferrin	514
C. A Second Process of Iron Uptake from Transferrin	514
D. Transferrin Receptor 2 (TfR2)	514
E. Estrogen-Inducible Transferrin-Receptor-Like Protein	515
F. Iron Uptake Mechanisms from Low-Molecular-Weight Iron Complexes	515
G. Natural Resistance-Associated Macrophage Proteins 1 and 2 (Nramp1 and 2)	516
H. Melanotransferrin	517
I. Does Ceruloplasmin Play a Role in Iron Uptake by Neoplastic Cells?	521
IV. FERRITIN AND NEOPLASIA	524
V. EFFECT OF IRON CHELATORS ON IRON UPTAKE AND METABOLISM IN CANCER CELLS: POTENTIAL ANTINEOPLASTIC AGENTS	526
ACKNOWLEDGMENTS	528
REFERENCES	529

I. INTRODUCTION

The use of neoplastic cell lines has been a major development in understanding a wide spectrum of biological processes. Needless to say, this has also been the case for understanding the metabolism of iron, where the use of these cells has provided a significant amount of new knowledge. Tumor cell lines provide a convenient model that can be manipulated under highly controlled conditions. The use of these cells has not only provided information on the mechanisms that underlie a variety of biological processes in neoplastic cells, but also enabled studies on the action of potential anticancer agents that chelate iron.

This chapter will review some of the features of cancer cell iron metabolism. Since neoplastic cells have a high metabolic rate and take up iron rapidly from transferrin (Tf), the molecules involved in iron uptake and their regulation will first be described. Changes in the way tumour cells metabolize iron may also be reflected in ferritin metabolism which is altered in some cancers, and this will also be examined. A final section reviews the use of Fe chelators to prevent Fe uptake and to act as potential antiproliferative agents.

II. GENERAL OVERVIEW OF CELLULAR IRON UPTAKE AND METABOLISM

The transport of Fe in the serum is mediated by Tf, which binds two atoms of Fe(III) with high affinity (for reviews see Refs. 1–3; and Chapter 2). Tf donates its bound Fe to cells by binding to the Tf receptor (TfR) (Chapter 3). Internalization of Tf bound to the TfR occurs by receptor-mediated endocytosis (RME) (1,4). Fe is released from Tf in the endocytotic vesicle via a decrease in pH (to 5.5), and is then transported through the membrane in the Fe(II) state (5) by DMT1 (see Sec. III.G, and Chapter 6) (6–8). In addition to the well-characterized RME process of Tf uptake, a number of cell types have been reported to take up Fe from Tf by another process that increases after saturation of the TfR (see Sec. III.C and Refs. 9–14). Apart from Fe uptake, there is evidence to indicate that Fe is also released from some cell types, and this process is accelerated by the serum ferroxidase ceruloplasmin (Cp) (15–19).

Once Fe is transported through the endosomal membrane, it enters a poorly characterized compartment known as the intracellular Fe pool. Despite many investigations (for a review, see Ref. 2), this pool remains the most enigmatic and difficult to characterize component of the Fe-uptake pathway. This pool of Fe appears to be in a reasonably labile form that can be bound by specific Fe chelators. For instance, chelators are far more effective at mobilizing intracellular Fe from neoplastic cells after short incubations with Tf than after longer labeling times (Fig. 1) (20,21). These latter data indicate that the pool is a transitory form of Fe that is incorporated into other compartments which are less easy to access, e.g., ferritin, cytochromes, and FeS proteins (20,21). It has been suggested that this Fe pool is composed of freely diffusible Fe complexes that could potentially be toxic (22). In contrast, studies examining erythroid cells have found very little low- M_r Fe not acting as an intermediate for heme synthesis (Fig. 2) (23).

An excess of Fe in the intracellular pool that is not used for metabolism is

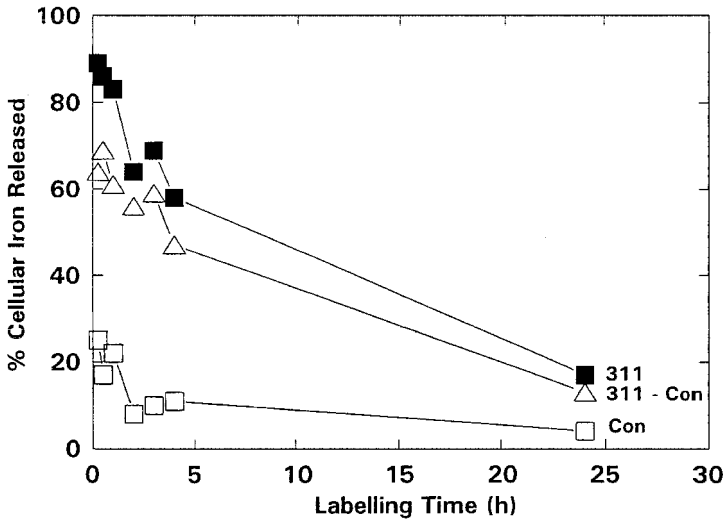


Figure 1 The ability of a lipophilic iron chelator (2-hydroxy-1-naphthylaldehyde isonicotinoyl hydrazine; 311) to mobilize ^{59}Fe from cells decreases as the incubation time with ^{59}Fe -transferrin increases. Similar results were also found for desferrioxamine (data not shown). The SK-N-MC neuroblastoma cells were preincubated for 15 min to 24 h with ^{59}Fe -transferrin ($1.25 \mu\text{M}$), washed, and then reincubated with either control medium or medium containing the chelator for 3 h at 37°C . The difference in ^{59}Fe release between 311 and the control (311-Con) has also been graphed to show clearly the difference in the 311-mediated ^{59}Fe efflux as a function of labeling time. Results are means from triplicate determinations in a typical experiment. (From Ref. 20.)

stored in ferritin. Ferritin is a high- M_r molecule (430–450 kDa) composed of two subunits (H and L) that can store about 4500 atoms of Fe (for reviews, see Refs. 24 and 25; and Chapter 5). While ferritin is mainly an intracellular protein, small amounts do occur in the serum, and this is usually proportional to the quantity of Fe in stores (26). It is controversial whether serum ferritin represents a different gene product or a glycosylated form of the intracellular protein that is routed along a secretory pathway (27,28).

The intracellular Fe pool regulates two mRNA-binding molecules known as the iron regulatory proteins (IRP) 1 and 2 (for reviews, see Refs. 2 and 29; and Chapters 9 and 10). Both IRP1 and IRP2 are trans-regulators that posttranscriptionally control the expression of a variety of molecules that play essential functions in Fe homeostasis (2,29). The IRPs bind to hairpin loop structures called iron-responsive elements (IREs) in the 5' and 3' untranslated regions (UTRs) of several mRNAs including those encoding the ferritin H and L subunits, and the TfR. The binding of the IRPs to the single IRE in the 5'-UTR of ferritin mRNA inhibits translation. In contrast, the binding of the IRPs to the five IREs in the 3'-UTR of TfR mRNA confers stability against degradation (for reviews, see Refs. 2 and 29). While the DMT1 IRE can bind the IRPs in cell lysates from a fibroblast cell line (30), the regulation of its mRNA by this mechanism remains uncertain (Sec. III.G).

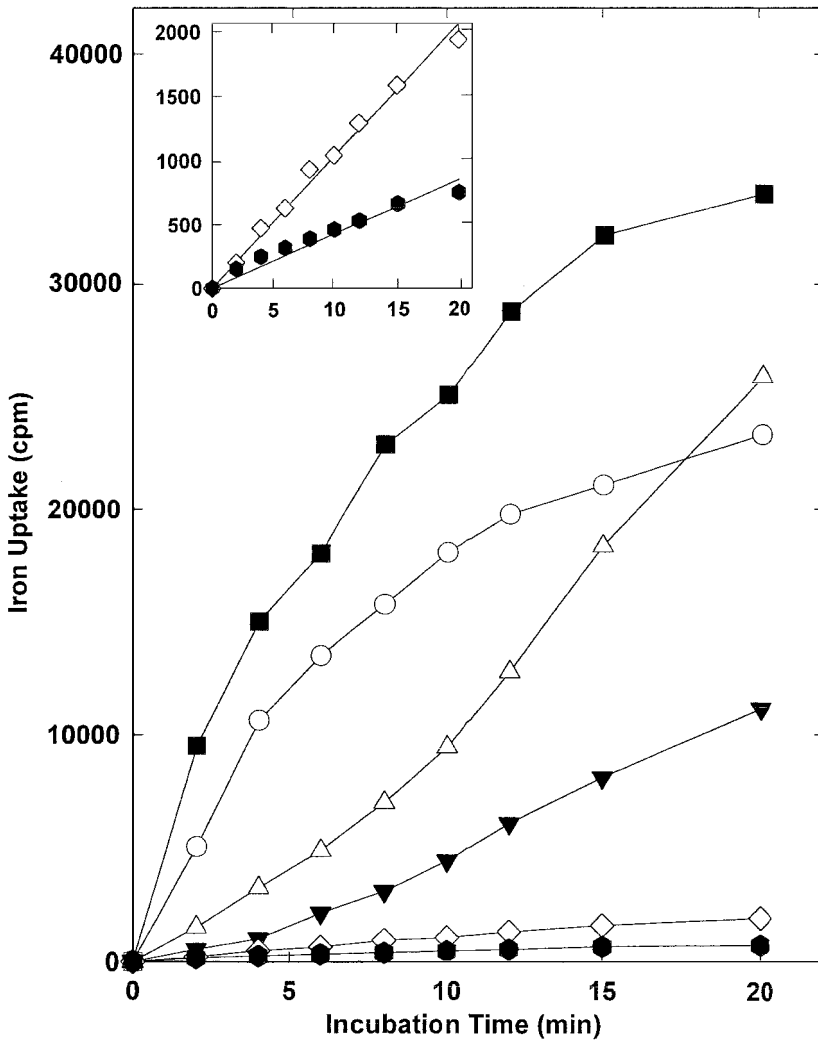


Figure 2 There is little low- M_r Fe in rabbit reticulocytes which does not act like an intermediate for heme synthesis. The distribution of ^{59}Fe in the stromal mitochondrial fraction (SMM) and the cytosolic high- M_r (>5-kDa) and low- M_r (<5-kDa) compartments. Results were compared between control reticulocytes and reticulocytes treated with the heme synthesis inhibitor succinylacetone (SA; 2 mM). Reticulocytes were incubated for 1–20 min with ^{59}Fe -Tf (3.75 μM) and the ^{59}Fe distribution assessed using the spinning column technique. Radioactivity in the SMM (○), cytosolic high- M_r compartment (Δ), and cytosolic low- M_r compartment of control reticulocytes (◇), and in the SMM (■), cytosolic high- M_r compartment (▼), and cytosolic low- M_r compartment (●) of SA-treated reticulocytes. Inset: incorporation of ^{59}Fe into the low- M_r compartment of control (◇) and SA-treated reticulocytes (●). Results are means of duplication determinations from a typical experiment. (From Ref. 23.)

Intracellular Fe levels regulate the binding of IRP1 and IRP2 to the IREs via different mechanisms [(2); Chapter 9]. High Fe levels within cells promote [4Fe–4S] cluster assembly in IRP1, with loss of IRE-binding activity. In cells depleted of Fe, the [4Fe–4S] cluster is not present, and under these conditions, IRP1 can bind to the IRE (2). In contrast to IRP1, IRP2 does not contain a [4Fe–4S] cluster, and is broken down in Fe-replete cells via proteasome-dependent degradation (Chapter 9).

The mechanisms of Fe uptake and acquisition by neoplastic cells show many similarities to those of normal cells, although there are some differences that will be described below.

III. IRON UPTAKE MECHANISMS IN NEOPLASTIC CELLS

A. Transferrin

Several studies have suggested that some proteins involved in Fe metabolism may play a role in the proliferation of breast cancer cells (BCCs) and other tumors. As described above, the major Fe-transport protein in the plasma is Tf that is synthesized by hepatocytes. Due to its Fe-binding properties, Tf is a growth factor required for all proliferating cells (1,2,31). In vitro, Tf is a vital requirement in defined medium (32). There is evidence that extrahepatic tissues synthesize Tf, which has been suggested to permit specialized proliferation and differentiation. For example, T4 lymphocytes synthesize Tf that has been implicated in an autocrine pathway functionally linked to the interleukin-2/interleukin-2-receptor autocrine loop (33). In addition, Sertoli cells of the testes synthesize Tf to provide proliferating spermatocytes with Fe (34).

Interestingly, the human BCC line MCF-7 secretes a factor which is immunologically identical to Tf, and its secretion is enhanced by 17- β -estradiol (ES) and reduced by the anti-estrogen 4-hydroxy-tamoxifen (35). It was suggested that Tf secreted by BCCs may act as an autocrine growth factor conferring selective advantages to rapidly proliferating BCCs and permitting tumor growth in poorly vascularized areas (35). Similarly, other cancer cell types also synthesize Tf, including small-cell carcinoma (36) and T-lymphoma cells (37), and in both of these reports an autocrine function of Tf was proposed. In small-cell carcinoma, Tf secretion was suggested to play a role in cell growth, since Tf secretion increased more than 10-fold when the cells entered the active phase of the cell cycle (36).

While it has been proposed that Tf may play an important role as an autocrine growth factor, it is difficult to understand how secretion of this molecule would specifically benefit cancer cells even in poorly vascularized areas. For instance, secretion of apoTf would have to bind free Fe in the vicinity of the tumor that is not thought to be readily available under physiological conditions (2). Whether free Fe does become accessible as a tumor invades normal tissues remains unclear. Further studies are necessary to determine whether Tf secretion may be important for proliferation or whether it represents a general upregulation of gene expression related to neoplastic transformation.

B. Transferrin Receptor (TfR) and Receptor-Mediated Endocytosis of Transferrin

Cancer cells as compared to their normal counterparts generally have higher numbers of TfRs (38,39) and take up Fe at a high rate (11–14). Indeed, this is reflected by the ability of tumors to be radiolocalized using ^{67}Ga (40), which binds to the Tf–Fe-binding site and is delivered by RME (1,41). The fact that the Fe chelator desferrioxamine (DFO) can inhibit the growth of a variety of aggressive tumors, including leukemia and neuroblastoma (NB), illustrates their high Fe requirement (see Sec. V). The importance of Fe in cancer cell proliferation is shown by the observation that the MoAb 42/6, which sterically inhibits Tf uptake by the TfR, also prevents cancer cell proliferation in vitro (42). It has been suggested that the host may withhold Fe during cancer cell proliferation, and this is observed in Hodgkins and non-Hodgkins lymphoma, where there is a decrease in the saturation of Tf with Fe (43).

C. A Second Process of Iron Uptake from Transferrin

The existence of a second process of Fe uptake from Tf was initially demonstrated in hepatocytes, where an increase in Fe uptake occurred after saturation of the TfR [(9,10); Chapter 17]. A very similar process was also identified in the human melanoma cell line SK-Mel-28 (11,13), and also in a hepatoma cell line (14). In SK-Mel-28 melanoma cells this second process of Fe uptake increased after saturation of the TfR and then plateaued at higher concentrations of Tf [0.3 mg/mL (13)]. Scatchard analysis of [^{125}I]-Tf binding demonstrated only one high-affinity Tf-binding site, and since the second process also required internalization of Tf, it was suggested to be consistent with adsorptive pinocytosis (13).

D. Transferrin Receptor 2 (TfR2)

Another TfR, termed TfR2, has recently been identified in normal and neoplastic cells (44). This molecule is mapped to chromosome 7q22 (in contrast to chromosome 3 for the TfR) and is expressed as two transcripts, α and β , both of which lack IREs in their UTRs. The predicted amino acid sequence of TfR2- α shares a 45% identity and 66% similarity in its extracellular domain with the TfR (44). In contrast, TfR2- β lacks the amino-terminal portion and putative transmembrane domain of TfR2- α . Northern blot analysis demonstrated that the *TfR2- α* transcript was found predominantly in the liver, and also in K562 erythroleukemia cells (44). Expression of this latter transcript was not well correlated to the expression of *TfR* mRNA. Sensitive RT-PCR analysis demonstrated that *TfR2- α* expression also occurs in the liver, lung, spleen, muscle, prostate, peripheral blood mononuclear cells, and most neoplastic cell lines (44). *TfR2- β* is expressed even more widely, being found in all human tissues tested, and in most cancer cells. Transfection of CHO cells which lack the TfR (CHO-TRVb) with TfR2- α demonstrated an increase in Tf-binding and Fe uptake (44).

As described above, it has long been known that a second process of Fe uptake from Tf exists in many cells (9–14). However, Scatchard analysis of [^{125}I]-Tf binding has indicated only one saturable high-affinity Tf-binding site, while clearly there are two saturable mechanisms of Fe uptake from Tf (13,14). However, the possibility exists that TfR2- α could have a low affinity for Tf, and may not be easily detected

via Scatchard analysis of [125 I]-Tf binding. Further studies are essential to determine the affinity of TfR2- α for diferric Tf, its possible role in Fe metabolism, and whether it may also bind other types of ligands.

E. Estrogen-Inducible Transferrin-Receptor-Like Protein

In several reports, Poola and colleagues (45–48) identified an ES-inducible Tf-binding protein in chick oviduct cells and BCCs that has limited homology (10%) to the TfR. This protein binds to diferric Tf affinity columns, as does the TfR (47). Furthermore, when Fe is removed from diferric Tf under mildly acidic conditions (pH 5), and the pH is then returned to neutrality, the TfR-like protein releases Tf in a very similar way to the TfR (47). These results indicate that the TfR-like protein could act like the TfR during RME (1,4), and may suggest a possible role in Fe uptake. The TfR-like protein in chick oviduct cells is present in two forms of M_r , 104 and 116 kDa (47), and appears to form a dimer (45) in a similar way to the TfR. Immunoprecipitation studies have demonstrated that the 104-kDa form of this TfR-like protein is present in the ES-sensitive human BCC lines, MCF-7 and T-47D (47). In those studies, no attempt was made to purify the protein from BCCs or to examine whether this molecule has a role in Fe uptake from Tf. Since Fe is a rate-limiting nutrient for growth (43,49), the expression of a molecule that can increase Fe uptake may have some implications for tumor cell proliferation.

Increased expression of Fe transport molecules after exposure to ES may have some significance, as the mechanism by which ES acts to stimulate BCC multiplication is unclear (50). Since ES-stimulated BCCs secrete Tf (35) and increase the expression of a TfR-like protein that can bind Tf, it can be hypothesized that this autocrine-loop mechanism may enhance Fe uptake by these cells. However, as stated above, additional experimentation is required to determine if this is the case.

Considering the presence of multiple Fe transport pathways in BCCs in addition to the TfR which is also found on these cells (51,52), it can be suggested that BCCs have a high Fe requirement. This demand for Fe may be exploited by the use of Fe chelators that prevent Fe uptake from Tf and inhibit the growth of tumor cells (see Sec. V).

F. Iron Uptake Mechanisms from Low-Molecular-Weight Iron Complexes

Apart from the uptake of Tf-bound Fe by RME and non-receptor-mediated pinocytosis, neoplastic and normal cells can also efficiently take up Fe from a variety of low- M_r Fe complexes, e.g., Fe-citrate and Fe-nitrilotriacetate (Fe-NTA) (53–58). This process is not restricted to cancer cells and has also been demonstrated in the liver (59,60), primary cultures of hepatocytes (9), and primary cultures of myocardiocytes (61).

Interestingly, preincubation of a wide variety of cell types with ferric ammonium citrate (FAC) can result in a marked increase in Fe uptake not only from low- M_r complexes [e.g., Fe-NTA or Fe-citrate (61–64)] but also from diferric Tf (12,63,65,66). The precise mechanism involved in this stimulation of Fe transport remains unknown, but in human melanoma cells, a variety of free-radical scavengers added together with FAC prevent the stimulation of Fe uptake (63). These studies suggested that the production of free radicals by FAC is necessary to increase Fe

uptake (63). Preincubation of neoplastic cells with gallium salts also increases Fe uptake from both Fe-NTA (64,67,68) and diferric Tf (66). Since Ga(III) does not redox cycle, the mechanism of stimulation induced by this metal ion remains to be explored.

G. Natural Resistance-Associated Macrophage Proteins 1 and 2 (Nramp1 and 2)

The Natural Resistance-Assoiated Macrophage Protein-2 (*Nramp2*) gene was identified as encoding a protein (now known as DMT-1; see Chapter 6) of unknown function, homologous to natural resistance-associated macrophage protein 1 (Nramp1) (69). Both of these molecules appear to act as metal-ion transporters, Nramp1 being involved in natural resistance to microbes and found only in macrophages. In contrast, Nramp2/DMT-1 is expressed in a wide variety of tissues (69). Gunshin and associates (6) have demonstrated that the protein product DMT-1 causes a marked increase in non-Tf-bound Fe uptake by *Xenopus* oocytes.

Interestingly, the expression of *DMT-1* mRNA is upregulated in the duodenum of Fe-deficient animals and was found to contain a putative IRE in its 3' UTR (6). This latter finding suggested that DMT-1 expression is controlled in an analogous way to the TfR via the binding of IRPs (6). In contrast to the single IRE in *DMT-1* mRNA (6), the *TfR* mRNA possesses five IREs in its 3' UTR (29,70,71). In addition, while the loop of the *DMT-1* IRE possesses the consensus 5'-CAGUGN-3' sequence (6), the bulge in the stem is somewhat different to the structure of other IREs. Thus, it was unclear whether the upregulation of *DMT-1* mRNA in Fe deficiency was via the IRP-IRE mechanism. Fleming and colleagues (7,8) have demonstrated that the product of the *DMT-1* gene plays an important role in both Fe uptake from Tf in the endosome and Fe absorption from the intestine (see Chapters 6 and 27). The DMT-1 molecule transports Fe from low- M_r Fe complexes as well as from Tf (7,72,73).

There is at least one splice variant of human *DMT-1* cDNA that has an UTR lacking the putative IRE (74). In addition, it has been suggested that the two splice forms are differentially expressed depending on the tissue type (74). Recent studies have shown that the IRE in Nramp2 mRNA does bind the IRPs in lysates from the LMTK⁻ fibroblast cell line (30). Moreover, reverse transcriptase-PCR (RT-PCR) demonstrated that both the IRE and non-IRE-containing transcripts were present within these cells. However, there was no change in *DMT-1* mRNA expression in LMTK⁻ cells after incubation with either the Fe chelator DFO, the Fe donor FAC, or the NO generator S-nitroso-N-acetylpenicillamine (SNAP). In contrast, these agents caused a marked change in the RNA-binding activity of the IRPs and TfR mRNA expression (30). In addition, both FAC and DFO caused an appropriate change in Fe uptake from diferric Tf, viz., an increase in Fe uptake after exposure to DFO and a decrease after treatment with FAC (Fig. 3). Since DMT-1 can transport Fe from non-Tf-bound Fe (7), the effect of preincubation with DFO and FAC was also examined on Fe uptake from [⁵⁹Fe]-NTA (Fig. 4) and [⁵⁹Fe]-citrate (30). However, in contrast to the results found for [⁵⁹Fe]-Tf, incubation with DFO and FAC did not result in appropriate regulation of Fe uptake from [⁵⁹Fe]-NTA (Fig. 4) or [⁵⁹Fe]-citrate (30). These data demonstrate that non-Tf-bound Fe uptake was not under control of the IRP-IRE system in these cells. Collectively, the results indicate that in LMTK⁻ fibroblasts, *DMT-1* mRNA expression was not regulated like *TfR*

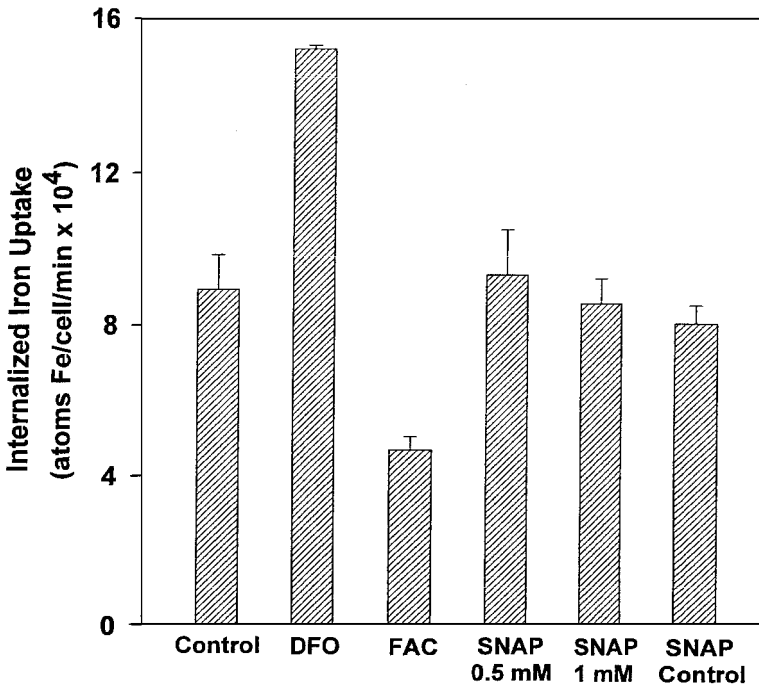


Figure 3 Internalized Fe uptake from [⁵⁹Fe]-transferrin (pH 7.4) by mouse LMTK⁻ fibroblasts after a 20-h preincubation with desferrioxamine (DFO), ferric ammonium citrate (FAC), or the NO generator, S-nitroso-N-acetylpenicillamine (SNAP). Cells were preincubated with DFO (100 μ M), FAC (100 μ g/mL), or SNAP (0.5 mM or 1 mM) for 20 h at 37°C. After this, the cells were washed extensively and incubated for 2 h at 37°C with [⁵⁹Fe]-transferrin (1.25 μ M; [Fe] = 2.5 μ M). The cells were then washed and internalized ⁵⁹Fe uptake determined by incubation with pronase. Results are mean \pm s.d. of 4–6 determinations from a typical experiment of two independent experiments performed. (From Ref. 30.)

mRNA (30). RNase protection assays suggested that the non-IRE-containing transcript predominated in these cells, which may be the reason for the lack of regulation of the mRNA transcripts by intracellular Fe levels (30).

H. Melanotransferrin

Considering altered pathways of Fe utilization in cancer cells, the malignant melanoma cell is of particular interest, as these tumors express a membrane-bound Tf homolog known as melanotransferrin (MTf) or p97 (78–83). During the early 1980s MTf was found to be either not expressed, or only slightly expressed in normal tissues, but was observed in larger amounts in tumor cells (but especially melanoma cells) and fetal tissues (78–80). In fact, anti-MTf MoAb bound to 90% of melanoma cell lines tested, varying from 80% to 0.3% of that found for the SK-Mel-28 melanoma cell line (78). Melanoma cells expressed the highest MTf levels of all cell types tested (78). Also, 55% of 35 other tumor cells also bound anti-MTf MoAb, although to 0.3–38% of that found for SK-Mel-28 cells (78).

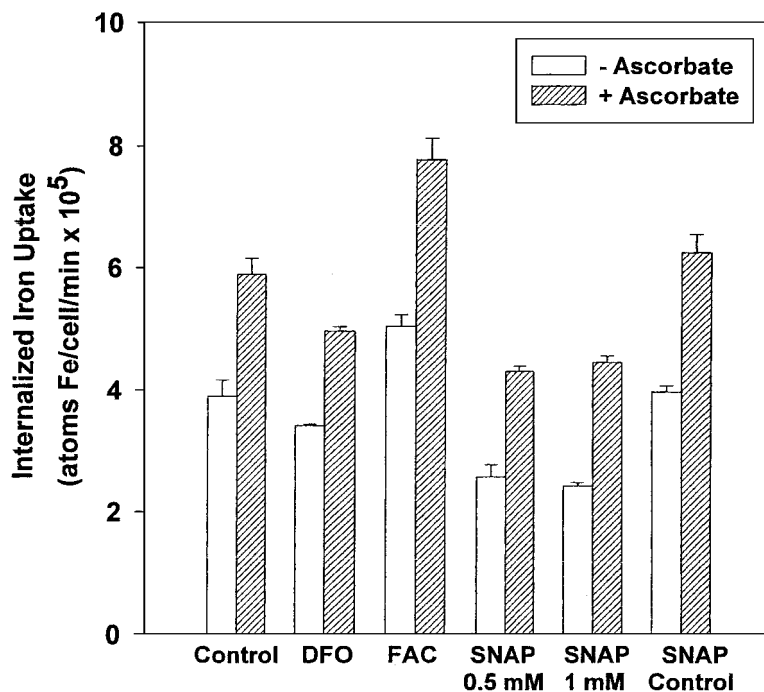


Figure 4 Internalized Fe uptake from [⁵⁹Fe]-nitrilotriacetic acid ([⁵⁹Fe]-NTA; pH 7.4) by mouse LMTK⁻ fibroblasts after a 20-h preincubation with desferrioxamine (DFO), ferric ammonium citrate (FAC), or the NO generator, S-nitroso-N-acetylpenicillamine (SNAP). Similar results were also found when the cells were incubated with [⁵⁹Fe]-NTA at pH 6.0 (data not shown). Cells were preincubated with DFO (100 μM), FAC (100 μg/mL), or SNAP (0.5 mM or 1 mM) for 20 h at 37°C. After this, the cells were washed extensively and incubated for 2 h at 37°C with [⁵⁹Fe]-NTA (5 μM; molar ratio Fe:NTA = 1:50, pH 7.4) + 1 mM ascorbate. The cells were then washed and internalized ⁵⁹Fe uptake determined by incubation with pronase. Results are mean ± s.d. of 4–6 determinations from a typical experiment of two independent experiments performed. (From Ref. 30.)

Human MTf is also found in normal tissues, including sweat gland ducts (84,85), endothelial cells of the liver (85,86), and the endothelium and reactive microglia of the brain (87,88). Normal serum contains very low amounts of MTf, and the levels of this molecule were not consistently increased in serum samples from patients with melanoma (80). An increase in the concentration of serum MTf has been described in Alzheimer's disease patients (89), but the significance of this observation remains unclear. MTf homologs have been identified on porcine fetal intestinal cells (90), avian eosinophils (91), and rabbit cartilage (92).

Melanotransferrin has a number of characteristics in common with serum Tf, including: (a) it has a 37–39% sequence identity to human serum Tf, human lactoferrin, and chicken Tf; (b) the MTf gene is on chromosome 3, as are those for Tf and the TfR; (c) many of the disulfide bonds present in serum Tf and lactoferrin are also present in MTf; (d) MTf has an N-terminal Fe-binding site that is very similar to that found in serum Tf; and (e) isolated and purified MTf can bind Fe from

Fe(III)-citrate complexes (81–83,93–95). These observations suggest that MTF plays some role in Fe transport. The greatest difference between MTf and serum Tf is that serum Tf is free in the plasma, while MTf is bound to the membrane by a glycosyl phosphatidylinositol anchor (85,96). Indeed, MTf can be removed from the cell membrane using phosphatidylinositol-specific phospholipase C (PI-PLC) (85,96,97).

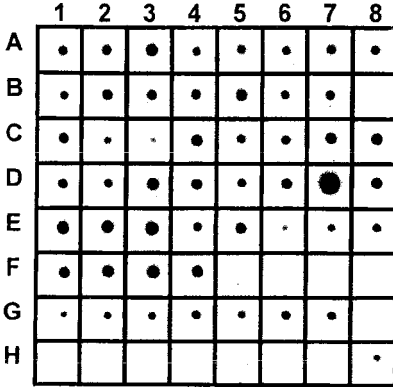
We have attempted to understand the relative roles of MTf compared to the TfR in Fe uptake by the human melanoma cell line SK-Mel-28 (11–13,55,98–100). Our investigations showed that SK-Mel-28 melanoma cells take up Fe from Tf by two processes, namely, RME and adsorptive pinocytosis of Tf (11,13,98). In addition, these cells could take up Fe from low- M_r Fe complexes by a process that was independent of the TfR (55). Of interest, a membrane-bound, pronase-sensitive, Fe-binding component was identified in SK-Mel-28 cells consistent with MTf (11,55,98,100). However, while this membrane Fe-binding component could bind Fe, it did not appear to donate it to the cell (98). Other experiments showed that MoAb 96.5 against MTf (but not control MoAbs) could modulate internalized Fe uptake from low- M_r complexes but not Tf by these cells (55). Our more recent studies using CHO cells transfected with the full-length MTf sequence (97) demonstrated that this molecule can transport Fe from Fe-citrate complexes but not Tf. As Fe is thought to be a rate-limiting nutrient for growth (43), and since rapidly replicating neoplastic cells have a high Fe requirement, MTf may act as an alternative pathway separate from the Tf-TfR system. However, again, the source of low- M_r Fe complexes for MTf remains unclear, as most Fe in the serum is bound to Tf.

It is important to note that the levels of MTf in the CHO cells transfected with this molecule were far greater (1.2×10^6 sites/cell) (97) than that found on the SK-Mel-28 cell line ($3-3.8 \times 10^5$ sites/cell) (80,81). Since Fe uptake by MTf-transfected CHO cells after a 4-h incubation with [^{59}Fe]-citrate was only 2.4-fold of that seen with control CHO cells, this questions the significance of MTf in Fe uptake by melanoma cells, where it is expressed at lower levels (80,81). To address this issue, we have further examined the role of MTf in Fe uptake by the melanoma cell line, SK-Mel-28, in an attempt to understand its function (101). Our results demonstrate that MTf expression was not regulated by Fe deprivation or Fe loading like the TfR. Moreover, while PI-PLC markedly decreased ^{125}I -labeled anti-MTf MoAb binding to 3% of the control, in parallel experiments it only slightly reduced ^{59}Fe uptake from [^{59}Fe]-citrate (101) that is bound by the MTf Fe-binding site (82,97). In addition, our studies using PI-PLC showed that MTf did not play a significant role in the uptake of Cu(II), Ga(III), or Zn(II) (101).

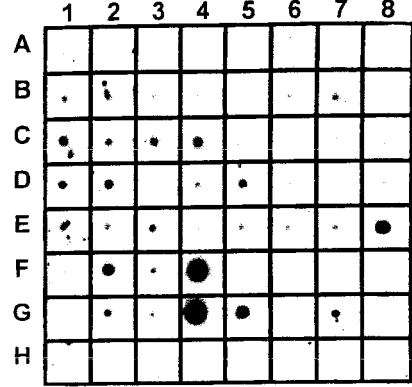
Examining the expression of *MTf* mRNA in a variety of human adult and fetal tissues, we found that the expression of this molecule was markedly different from either *Tf* mRNA or *TfR* mRNA (101) (Fig. 5). In fact, *MTf* mRNA expression was distributed among a wide variety of tissues, with the highest level being observed in the salivary gland (Fig. 5). In contrast to previous studies that suggested that MTf was an oncofetal antigen, *MTf* mRNA expression was generally greater in adult than in fetal tissues (Fig. 5). In conclusion, in the human melanoma cell line, SK-Mel-28, MTf does not play a major role in Fe uptake from [Fe]-citrate (101) or Tf (55,97).

Other evidence which suggests that MTf is not crucial for Fe uptake and proliferation includes the fact that MTf is not found in all melanoma cell lines, varying

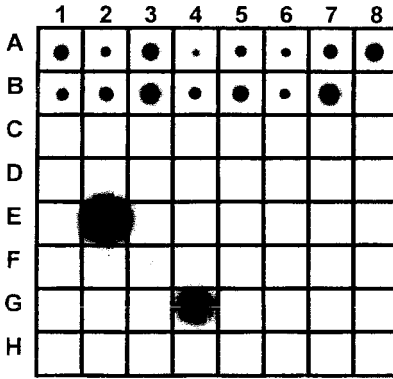
Melanotransferrin



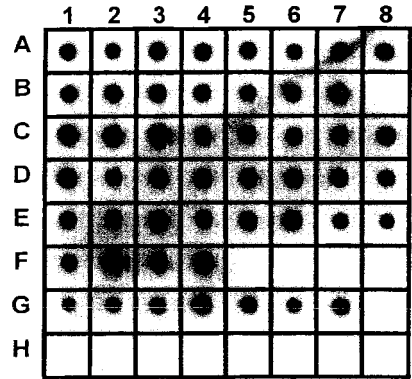
Transferrin Receptor



Transferrin



Ubiquitin



Blot Diagram

	1	2	3	4	5	6	7	8
A	whole brain	amygdala	caudate nucleus	cerebellum	cerebral cortex	frontal lobe	hippo-campus	medulla oblongata
B	occipital lobe	putamen	substantia nigra	temporal lobe	thalamus	nucleus accumbens	spinal cord	
C	heart	aorta	skeletal muscle	colon	bladder	uterus	prostate	stomach
D	testis	ovary	pancreas	pituitary gland	adrenal gland	thyroid gland	salivary gland	mammary gland
E	kidney	liver	small intestine	spleen	thymus	peripheral leukocyte	lymph node	bone marrow
F	appendix	lung	trachea	placenta				
G	fetal brain	fetal heart	fetal kidney	fetal liver	fetal spleen	fetal thymus	fetal lung	
H	yeast total RNA 100 ng	yeast tRNA 100 ng	<i>E. coli</i> rRNA 100 ng	<i>E. coli</i> DNA 100 ng	Poly r(A) DNA 100 ng	human C_{α} 1 DNA 100 ng	human DNA 100 ng	human DNA 500 ng

Figure 5 The expression of melanotransferrin (MTf) mRNA compared to Tf and TfR mRNA in a range of human tissues. The human mRNA (poly A+) Master Blot™ (CLONTECH Laboratories) was sequentially hybridized to human melanotransferrin cDNA, transferrin receptor cDNA, transferrin cDNA, and ubiquitin cDNA (control). Probes were labeled and hybridized to the blot. (From Ref. 101.)

from 0.3% to 80% of that found for SK-Mel-28 melanoma cells (78). In addition, MTf expression has not been consistently found on other proliferating neoplastic cells or normal tissues (78,101). Furthermore, while TfR numbers increase prior to DNA synthesis (102), due to the Fe requirement of ribonucleotide reductase (103,104), MTf density remains relatively constant throughout the cell cycle (105). Seligman et al. (106) have shown using HL-60 leukemic cells and FAMC 110 melanoma cells that MTf expression does not change when comparing confluent cells, growing cells, or cells grown in high concentrations of diferric Tf. These data were in marked contrast to observations for the TfR (106). Considering the results collectively, it appears that MTf is not vital for obtaining Fe for rapidly growing neoplasms (2,55,98). Nonetheless, MTf has an N-terminal Fe-binding site that binds Fe (82,95), and we demonstrated a membrane-bound Fe-binding component consistent with MTf in SK-Mel-28 melanoma cells (11,13,55,98). Thus, it can be speculated that MTf may act as a Fe scavenger that could bind Fe complexes that cause oxidative damage to the cell membrane.

I. Does Ceruloplasmin Play a Role in Iron Uptake by Neoplastic Cells?

Ceruloplasmin (Cp) is a blue α_2 -globulin of the serum that contains six atoms of copper with a M_r of 134 kD [(107); Chapter 30]. This molecule acts as a multi-copper oxidase that could have a role in Fe metabolism by oxidizing Fe(II) to Fe(III) (107). For instance, copper-deficient swine develop an anemia that can be overcome by injection of Cp (15,16,108). Further, Osaki et al. (17) demonstrated that Cp could increase Fe efflux from the perfused liver. It is well known that the ferroxidase activity of Cp accelerates Fe incorporation into apoTf (109). This effect may accelerate cellular Fe release by generating a concentration gradient across the cell membrane. Together, these data suggest that Cp plays some role in Fe mobilization.

Considering the probable role of Cp in Fe metabolism, Mukhopadhyay et al. (110) have examined the role of Cp in Fe uptake and Fe release by the HepG2 hepatoma cell line. In Fe-deficient HepG2 cells, Cp increased ^{55}Fe uptake from [^{55}Fe]-NTA, but had no effect at mobilizing Fe from cells prelabeled with this complex (110). These results were interpreted to indicate that Cp may act like the multi-copper oxidase (FET3p) involved in Fe uptake by *Saccharomyces cerevisiae* (111). However, the investigation of Mukhopadhyay and colleagues (110) used the non-physiological complex Fe-NTA to load cells with Fe at 25°C and high Cp concentration. The same investigators also used very similar conditions to demonstrate that Cp elevates Fe-NTA uptake by Fe-deficient K562 cells (112).

Due to the potential importance of Cp in cellular Fe uptake, the study of Mukhopadhyay et al. (110) was repeated using physiologically relevant conditions to determine the role of Cp in Fe uptake from Tf and Fe release from HepG2 cells (19). When cells were labeled at 37°C with [^{59}Fe]-Tf in the presence of a physiologically relevant Cp concentration (300 $\mu\text{g}/\text{mL}$), this latter protein had no effect on the uptake of ^{59}Fe from Tf in control cells or in cells depleted of Fe using DFO (Fig. 6). In addition, when Fe-replete or Fe-depleted cells were incubated with [^{59}Fe]-NTA at 25°C or 37°C, Cp had no effect on ^{59}Fe uptake compared to the control (Fig. 7). When the effect of Cp (10–500 $\mu\text{g}/\text{mL}$) on ^{59}Fe release was examined in cells prelabeled with [^{59}Fe]-Tf, a concentration-dependent increase in ^{59}Fe efflux was

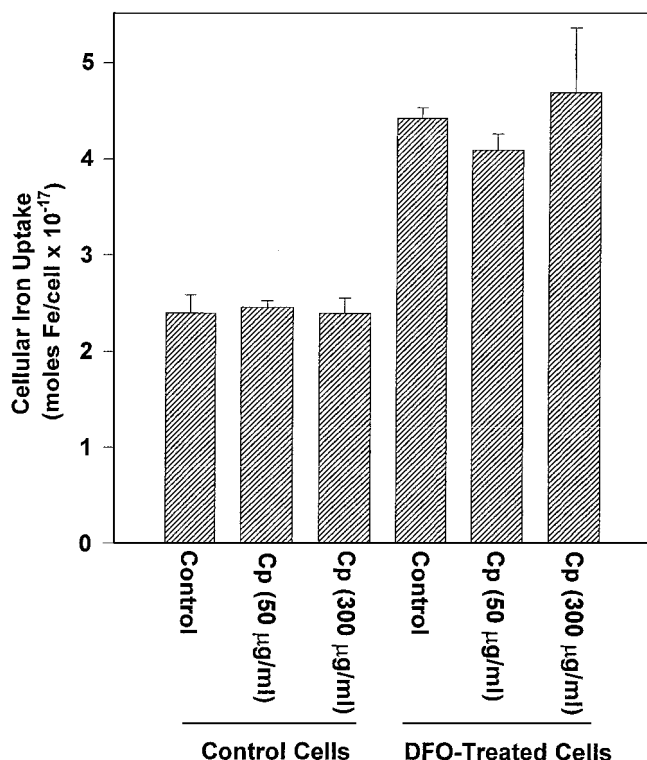
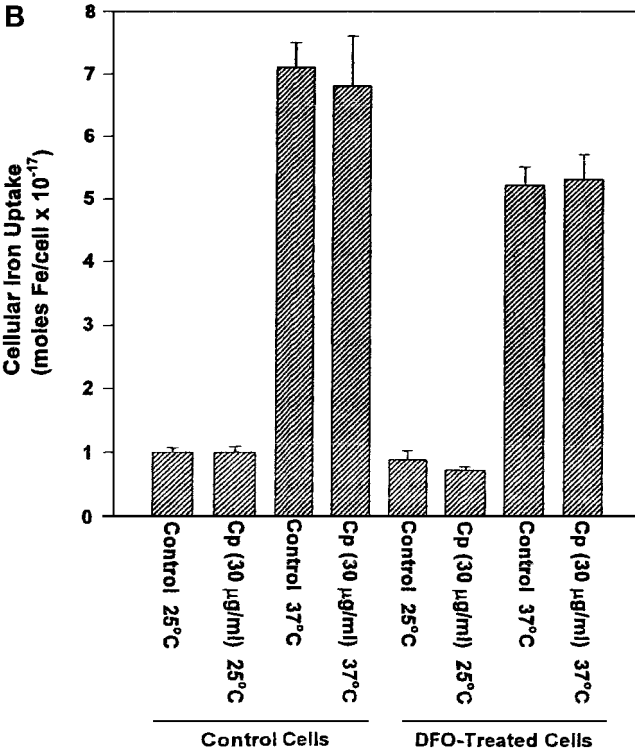
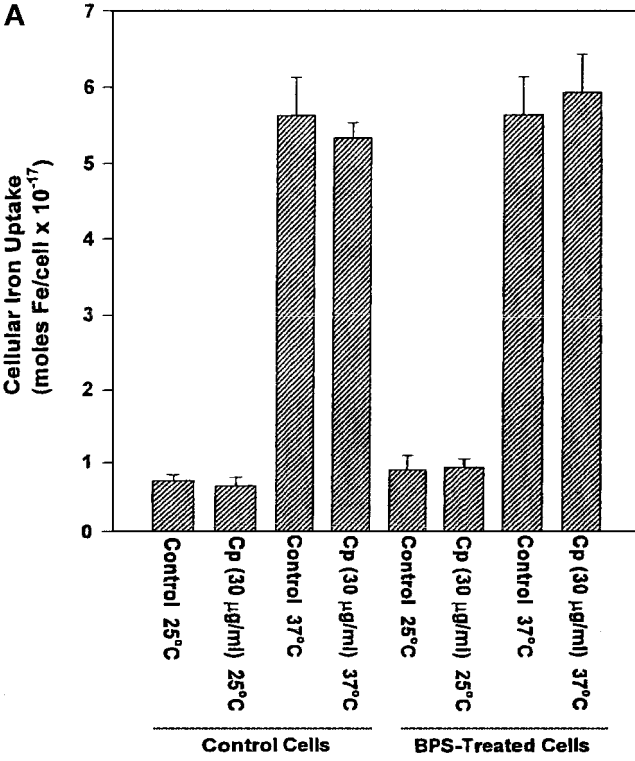


Figure 6 The effect of ceruloplasmin (Cp; 50 and 300 $\mu\text{g/ml}$) on Fe uptake from ^{59}Fe -labeled transferrin (^{59}Fe -Tf) by control and desferrioxamine (DFO)-treated HepG2 cells. Cells were preincubated with control medium alone or medium containing DFO (100 μM) for 20 h at 37°C. The cells were then extensively washed to remove DFO (see Ref. 19) and labeled with ^{59}Fe -Tf (0.75 μM) for 3 h at 37°C in the presence and absence of Cp at 50 or 300 $\mu\text{g/ml}$. Results are expressed as the mean \pm s.d. of three determinations from a typical experiment of four separate experiments performed. (From Ref. 19.)

Figure 7 The effect of ceruloplasmin (Cp) on Fe uptake from ^{59}Fe -nitrilotriacetic acid (^{59}Fe -NTA) at 25°C or 37°C by control cells or cells depleted of Fe using (A) bathophenanthroline disulphonate (BPS) or (B) desferrioxamine (DFO). (A) HepG2 cells were depleted of Fe using a 16-h incubation with 1 mM BPS, washed, and then incubated with ^{59}Fe -NTA (0.5 μM) for 15 min at 25°C or 37°C in the absence or presence of Cp (30 $\mu\text{g/ml}$). (B) HepG2 cells were depleted of Fe using a 20-h incubation with DFO (100 μM), the cells washed extensively, and then incubated with ^{59}Fe -NTA (0.5 μM) for 15 min at 25°C or 37°C in the absence or presence of Cp (30 $\mu\text{g/ml}$). Results are expressed as the mean \pm s.d. of 4–5 determinations from a typical experiment of three separate experiments performed. (From Ref. 19.)



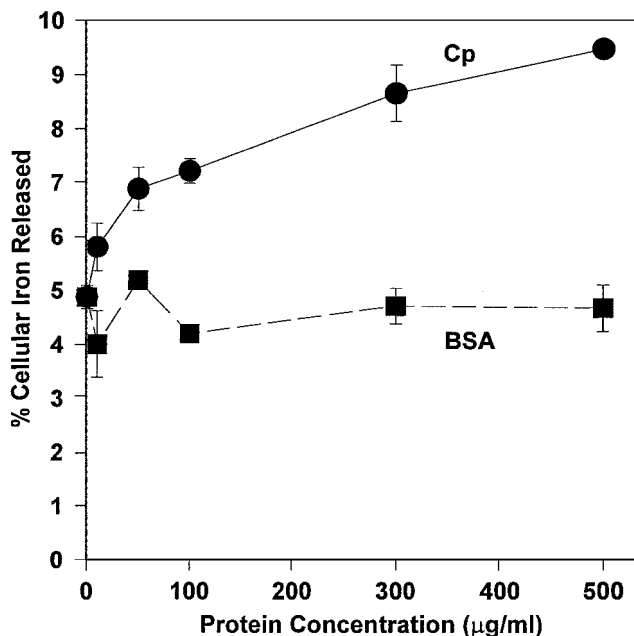


Figure 8 The effect of ceruloplasmin (Cp) or bovine serum albumin (BSA) concentration (10–500 $\mu\text{g}/\text{mL}$) on ^{59}Fe release from HepG2 cells prelabeled with [^{59}Fe]-transferrin (Tf). Cells were labeled for 3 h at 37°C with [^{59}Fe]-Tf (0.75 μM). The cells were then washed and reincubated for 3 h at 37°C in control medium alone or medium containing Cp or BSA (10–500 $\mu\text{g}/\text{mL}$). Results are expressed as the mean \pm s.d. of three determinations from a typical experiment of two separate experiments performed. (From Ref. 19.)

observed, while bovine serum albumin had no effect (Fig. 8). However, in contrast to membrane-permeable Fe chelators that caused a marked increase in Fe release, the effect of Cp on Fe efflux was far less impressive (19). Our studies suggest that Cp is involved in Fe mobilization but does not affect Fe uptake from Tf or Fe-NTA (19). Similarly, Young et al. (18) demonstrated that Cp in combination with apoTf (200–500 $\mu\text{g}/\text{mL}$) increased ^{59}Fe efflux from HepG2 cells, and this was potentiated under anoxic conditions. Collectively, considering the data on Cp function in vitro and in vivo (15–19), it can be suggested that Cp can increase Fe release but plays no role in Fe uptake.

IV. FERRITIN AND NEOPLASIA

Some relationship may exist between ferritin and cancer. In fact, despite no increase in Fe stores, serum ferritin is increased in patients suffering a number of neoplasms (113–116). Generally, neoplastic cells have been reported to contain low quantities of ferritin poor in Fe (24). In contrast, neuroblastoma (NB) cells have been reported to contain Fe-rich ferritin and hemosiderin (117,118). These latter properties, together with the fact that NB appears sensitive to Fe chelation with DFO (see Sec. V), suggest that the Fe metabolism of this tumor may be somewhat altered compared to other cell types. Serum ferritin is markedly elevated in NB at stages III and IV, but

not in stages I or II, and has been used as a prognostic indicator, high levels of ferritin indicating a poor prognosis and low levels a good prognosis (115,119,120). The neoplasm is the source of increased serum ferritin levels as (a) NB cells contain Fe-rich ferritin and patients with advanced NB have increased amounts of ferritin within the tumor (115,117,118); (b) nude mice bearing NB xenografts have human ferritin in their sera (121); (c) levels of serum ferritin become normal with remission (115); and (d) most ferritin released from NB is glycosylated, indicating active secretion (122).

H-type ferritins may suppress immunological responses (122,123), which may aid cancer cell proliferation. However, most ferritin secreted by NB cells is of the L type (124), suggesting that some other property may be important. Since NB cells contain ferritin rich in Fe (117,118), it can be hypothesized that ferritin secreted by NB cells could possibly be used as an Fe source by other NB cells in distant metastases, for example. However, Blatt and Wharton (125) demonstrated that ferritin added to serum-free medium only slightly stimulates NB proliferation and DNA synthesis. In addition, specific ferritin-binding sites were not identified on these cells (125). These latter authors suggest that ferritin has mitogenic activity for NB cells, but do not establish the mechanism of this stimulation.

Other studies have found that an autocrine growth factor secreted from human leukemia cells has immunological identity with ferritin (126,127). Furthermore, an antibody to ferritin inhibited the growth of these cells, suggesting a role for ferritin in stimulating cellular proliferation (126,127). Ferritin-binding sites (128–131) and the endocytosis of ferritin (132) have been identified in neoplastic cells, suggesting that ferritin Fe uptake could occur by RME.

Apart from ferritin secretion, there is some evidence that neoplastic transformation can result in changes in the expression of ferritin and other molecules involved in cellular Fe metabolism. For example, the potent E1A oncogene modulates ferritin-H chain expression at the transcriptional level (133). In proliferating cells the transcription factor encoded by the proto-oncogene *c-myc* represses *ferritin-H* expression and increases *IRP2* expression (134). Moreover, downregulation of *ferritin-H* expression was shown to be required for transformation via *c-myc*. The elevation in *IRP2* expression may enhance RNA-binding activity of this protein. Thus, a possible increase in TfR expression and Fe uptake from Tf may occur that is necessary for growth (134).

In contrast to the results above, Modjtahedi et al. (135) showed that transfection of cells with copies of the *c-myc* gene resulted in an overexpression of *ferritin-H* due to an increase in the rate of transcription. Furthermore, this latter study demonstrated that the expression of *ferritin-H* as well as *cytokeratin* was increased in tumorigenic compared to nontumorigenic clones of the SW 613-S human carcinoma cell line (135). Perhaps the role of *c-myc* in *ferritin-H* expression may be dependent on the cell type examined. Hence, at least some oncogenes modulate ferritin synthesis, and these results could possibly explain the changes in ferritin synthesis and secretion found in some tumors.

It is of interest that *N-myc* amplification correlates strongly with rapid NB progression and poor prognosis (136), and may play an important role in the malignant behavior of this neoplasm. The *N-myc* gene has some sequence homology to *c-myc* (137,138), and *N-myc* amplification and secretion of ferritin coexist in patients with advanced NB (120,136). Moreover, a study examining ferritin secretion and

synthesis in three NB cell lines found that the cell line synthesizing and secreting the highest concentration of ferritin also had the highest number of *N-myc* copies (139). In preliminary studies reported at conference meetings, DFO was shown to reduce *N-myc* expression, and this effect could be prevented by the addition of Fe (140). The decrease in *N-myc* expression was not due to a general decrease in gene expression, as *c-fos* was increased, whereas *c-jun* and β -*actin* were unchanged. There was no change in the half-life of *N-myc* mRNA, whereas DFO-treated NB cells failed to transcribe *N-myc* (140,141). In more recent studies using the BE-2 NB cell line, *N-myc* mRNA levels were not altered after incubation with a range of DFO concentrations (21). However, the transcription rate of the *N-myc* gene was not assessed, and further studies are required to determine the role of this proto-oncogene in ferritin gene expression.

V. EFFECT OF IRON CHELATORS ON IRON UPTAKE AND METABOLISM IN CANCER CELLS: POTENTIAL ANTINEOPLASTIC AGENTS

The clinically used Fe chelator, DFO, is capable of a cytotoxic effect on a variety of cancer cell types *in vitro* and *in vivo*, including NB (142–147), leukemia (148–150), melanoma (151), hepatoma (152), breast cancer (153), and Kaposi's sarcoma (151). For example, in a clinical trial, a single 5-day course of DFO given as an 8-h i.v. infusion at 150 mg/kg/day, resulted within 2 days in seven of the nine patients having more than a 50% decrease in bone marrow infiltration of tumor cells (144). In addition, in one patient, a 48% decrease of tumor size was found. In contrast to most cytotoxic drug treatments, there were no significant side effects (144). Further, when DFO therapy was combined with cytotoxic agents, very good responses were observed in NB patients (145–147; for reviews see 155,156). The fact that DFO can inhibit the growth of this aggressive tumor *in vivo* is probably related to the high rate of Fe uptake that is necessary for proliferation.

Unfortunately, treatment with DFO suffers a number of serious disadvantages, including its high cost, its requirement for long s.c. administration (12–24 h/day, 5–6 times per week), its short plasma half-life, and its poor absorption from the gut. Indeed, its less than optimal activity in some biological screens (157) may be due to its short plasma half-life and its low efficiency at permeating biological membranes in some cancer cell types (20,21,151). In fact, high concentrations of DFO are required to induce apoptosis and G₁/S arrest in several cell lines *in vitro* (20). The failure of DFO to prevent the growth of NB xenografts in one study (157) could be due to the chelator not reaching an appropriate concentration in the serum to inhibit proliferation. This latter study is isolated by a range of previous investigations *in vitro* and *in vivo* demonstrating the antiproliferative effects of DFO (for reviews, see Refs. 147, 155, and 156). These problems with DFO indicate the importance of developing more potent Fe chelators that may be effective at inhibiting the growth of NB cells and other tumors.

It has been shown that the lipophilic Fe chelator, pyridoxal isonicotinoyl hydrazone (PIH) (158–161), demonstrates activity against mammary tumors in mice (162), and in various neoplastic cell lines *in vitro* (163). In addition, some of the metal-ion complexes of these aroylhydrazone ligands [e.g., Ga(III)-PIH] display greater antiproliferative activity than the ligand alone (164–167). For instance, when

the Cu(II) complex of salicyladehyde benzoyl hydrazone was injected into a methylcholanthrene-induced fibrosarcoma in mice, the compound markedly inhibited tumor growth (168). Importantly, little effect of this compound was observed in normal control animals. We have done studies characterizing a series of PIH analogs as active Fe chelators (166,169–173). Our experiments with a number of human cancer cell lines have shown that these compounds effectively inhibit cellular proliferation, being far more effective than DFO or PIH (20,21,164,174). The most efficient group of ligands are those hydrazones derived from 2-hydroxy-1-naphthyladehyde benzoyl hydrazone, which markedly increase ^{59}Fe efflux from cells (Fig. 9) and prevent ^{59}Fe uptake from $[^{59}\text{Fe}]\text{-Tf}$ (Fig. 10) (20,21,164).

The potential of Fe chelators to inhibit Fe uptake and to prevent the proliferation of cancer cells cannot be dismissed lightly, as one of the most successful

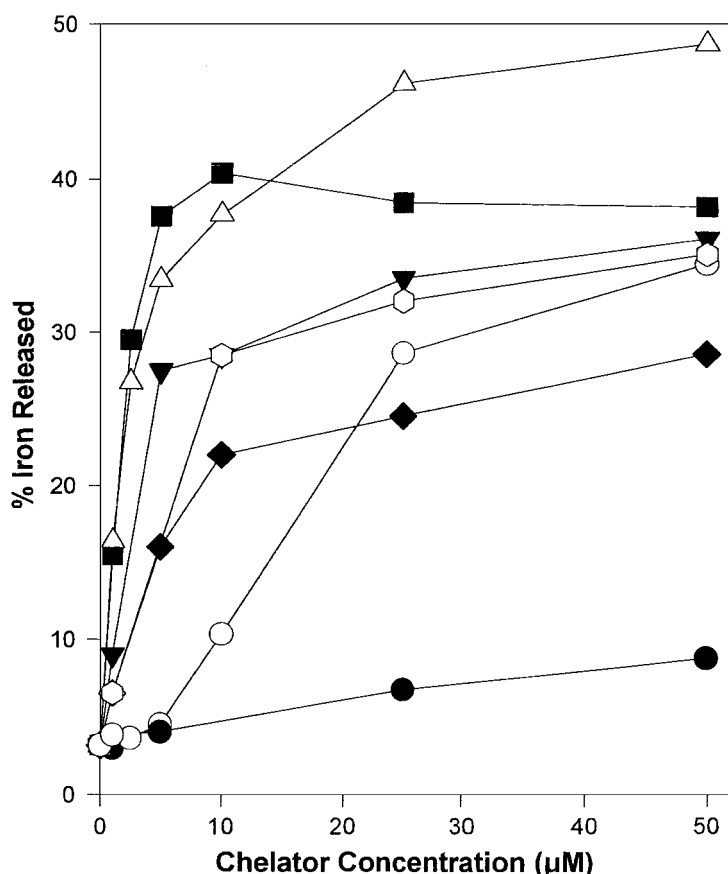


Figure 9 The effect of the concentration of the chelators DFO (●), PIH (○), and the PIH analogs 206 (▼), 308 (◇), 309 (◐), 311 (■), and 315 (△) on ^{59}Fe release from SK-N-MC neuroblastoma cells prelabeled with $[^{59}\text{Fe}]\text{-transferrin}$. In these experiments, the cells were prelabeled with $[^{59}\text{Fe}]\text{-transferrin}$ ($1.25\ \mu\text{M}$) for 3 h, washed, and then reincubated with either medium alone or medium containing the chelators ($2\text{--}50\ \mu\text{M}$) for 3 h at 37°C . Results are means of triplicate determinations in a typical experiment. (From Ref. 20.)

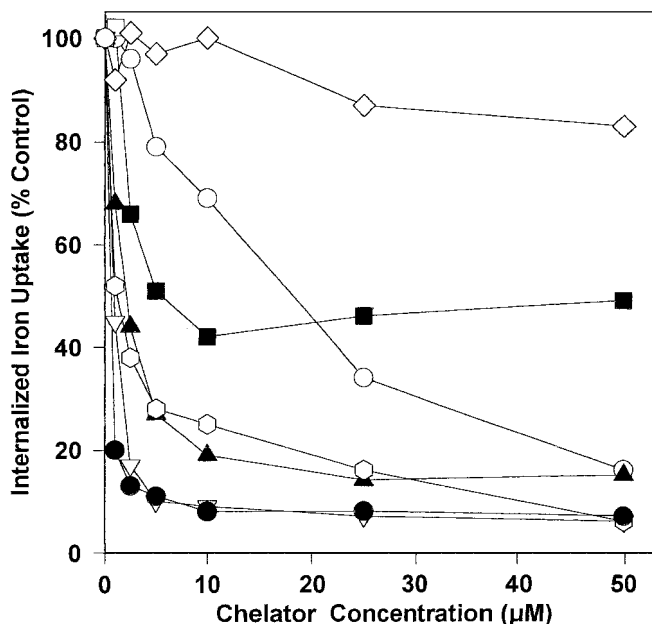


Figure 10 The effect of the concentration of DFO (◇), PIH (○), and the PIH analogs 206 (□), 308 (■), 309 (▲), 311 (●), and 315 (▽) on internalized ^{59}Fe uptake from $[^{59}\text{Fe}]$ -transferrin ($1.25 \mu\text{M}$) by SK-N-MC neuroblastoma cells over a 3-h incubation at 37°C . After this, the cells were washed and internalized ^{59}Fe was determined by incubation with pronase (1 mg/mL) for 30 min at 4°C . The results are means of duplicate determinations from a typical experiment. (From Ref. 20.)

antineoplastic drugs, doxorubicin, has been found to bind Fe (175–177). In fact, this latter agent probably inhibits neoplastic cell growth by a number of mechanisms, including its ability to generate free radicals via redox cycling of its Fe complex (177,178). Studies on the antitumor activity of a related group of chelators to the aroylhydrazones known as the thiosemicarbazones (179–182) may provide the basis for designing more effective chelators as antineoplastic agents.

Further studies on the mechanisms involved in the uptake of Fe by neoplastic cells are important in terms of understanding cellular proliferation and also in the development of Fe chelators as potential antitumor agents.

ACKNOWLEDGMENTS

Research work from the author's laboratory cited in this review was supported by grants from the Medical Research Council of Canada, National Cancer Institute of Canada, National Health and Medical Research Council of Australia (#970360 and 981826), Australian Research Council Large Grant, Kathleen Cunningham Foundation for Breast Cancer Research, and the Friedrich's Ataxia Support Group of Queensland. The author was supported by a Medical Research Council of Canada Scholarship and a Research Fellowship/Senior Research Fellowship from the Department of Medicine, University of Queensland.

REFERENCES

1. Morgan EH. Transferrin biochemistry, physiology and clinical significance. *Mol Aspects Med* 1981; 4:1–123.
2. Richardson DR, Ponka P. The molecular mechanisms of the metabolism and transport of iron in normal and neoplastic cells. *Biochim Biophys Acta* 1997; 1331:1–40.
3. Ponka P, Beaumont C, Richardson DR. Function and regulation of transferrin and ferritin. *Semin Hematol* 1998; 35:35–54.
4. Klausner RD, Ashwell G, Van Renswoude J, Harford JB, Bridges KR. Binding of apotransferrin to K562 cells: explanation of the transferrin cycle. *Proc Natl Acad Sci USA* 1983; 80:2263–2266.
5. Morgan EH. Membrane transport of non-transferrin-bound iron by reticulocytes. *Biochim Biophys Acta* 1988; 943:428–439.
6. Gunshin H, MacKenzie B, Berger UV, Gunshin Y, Romero MF, Boron WF, Nussberger S, Gollan JL, Hediger MA. Cloning and characterization of a mammalian proton-coupled metal-ion transporter. *Nature* 1997; 388:482–488.
7. Fleming MD, Romano MA, Su MA, Garrick LM, Garrick MD, Andrews NC. Nramp2 is mutated in the anemic Belgrade (b) rat: evidence of a role for Nramp2 in endosomal iron transport. *Proc Natl Acad Sci USA* 1998; 95:1148–1153.
8. Fleming MD, Trenor CC, Su MA, Foernzler D, Beier DR, Dietrich WF, Andrews NC. Microcytic anaemia mice have a mutation in Nramp2, a candidate iron transporter gene. *Nature Genet* 1997; 16:383–386.
9. Page MA, Baker E, Morgan EH. Transferrin and iron uptake by rat hepatocytes in culture. *Am J Physiol* 1984; 246:G26–G33.
10. Trinder D, Morgan E, Baker E. The mechanisms of iron uptake by rat fetal hepatocytes. *Hepatology* 1986; 6:852–858.
11. Richardson DR, Baker E. The uptake of iron and transferrin by the human melanoma cell. *Biochim Biophys Acta* 1990; 1053:1–12.
12. Richardson DR, Baker E. Two mechanisms of iron uptake from transferrin by melanoma cells. The effect of desferrioxamine and ferric ammonium citrate. *J Biol Chem* 1992; 267:13972–13979.
13. Richardson DR, Baker E. Two saturable mechanisms of iron uptake from transferrin in human melanoma cells: the effect of transferrin concentration, chelators, and metabolic probes on transferrin and iron uptake. *J Cell Physiol* 1994; 161:160–168.
14. Trinder D, Zak O, Aisen P. Transferrin receptor-independent uptake of diferric transferrin by human hepatoma cells with antisense inhibition of receptor expression. *Hepatology* 1996; 23:1512–1520.
15. Osaki S, Johnson DA. Mobilization of liver iron by ferroxidase (ceruloplasmin). *J Biol Chem* 1969; 244:5757–5758.
16. Roeser HP, Lee GR, Nacht S, Cartwright GE. The role of ceruloplasmin in iron metabolism. *J Clin Invest* 1970; 49:2408–2417.
17. Osaki S, Johnson DA, Frieden E. The mobilization of iron from the perfused mammalian liver by a serum copper enzyme, ferroxidase I. *J Biol Chem* 1971; 246:3018–3023.
18. Young SP, Fahmy M, Golding S. Ceruloplasmin, transferrin and apotransferrin facilitate iron release from human liver cells. *FEBS Lett* 1997; 411:93–96.
19. Richardson DR. The role of ceruloplasmin and ascorbate in cellular iron release. *J Lab Clin Med* 1999; 134:454–465.
20. Richardson DR, Milnes K. The potential of iron chelators of the pyridoxal isonicotinoyl hydrazone class as effective antiproliferative agents II. The mechanism of action of ligands derived from salicylaldehyde benzoyl hydrazone and 2-hydroxy-1-naphthylaldehyde benzoyl hydrazone. *Blood* 1997; 89:3025–3038.

21. Darnell G, Richardson DR. The potential of analogues of the pyridoxal isonicotinoyl hydrazone class as effective anti-proliferative agents III: the effect of the ligands on molecular targets involved in proliferation. *Blood* 1999; 94:781–792.
22. Jacobs A. Low molecular weight intracellular iron transport compounds. *Blood* 1977; 50:433–439.
23. Richardson DR, Ponka P, Vyoral D. Distribution of iron in reticulocytes after inhibition of heme synthesis with succinylacetone: examination of the intermediates involved in iron metabolism. *Blood* 1996; 87:3477–3488.
24. Munro HN, Linder MC. Ferritin: structure, biosynthesis and role in iron metabolism. *Physiol Rev* 1978; 58:317–396.
25. Harrison PM, Arosio P. The ferritins: molecular properties, iron storage function and cellular regulation. *Biochim Biophys Acta* 1996; 1275:161–203.
26. Jacobs A, Worwood M. Ferritin in serum. Clinical and biochemical implications. *N Engl J Med* 1975; 292:951–956.
27. Linder MC, Schaffer KJ, Hazegh-Azam M, Zhou CY, Tran TN, Nagel GM. Serum ferritin: does it differ from tissue ferritin. *J Gastroenterol Hepatol* 1996; 11:1033–1036.
28. Tran TN, Eubanks SK, Schaffer KJ, Zhou CY, Linder MC. Secretion of ferritin by rat hepatoma cells and its regulation by inflammatory cytokines and iron. *Blood* 1997; 90:4979–4986.
29. Hentze MW, Kühn LC. Molecular control of vertebrate iron metabolism: mRNA-based regulatory circuits operated by iron, nitric oxide, and oxidative stress. *Proc Natl Acad Sci USA* 1996; 93:8175–8182.
30. Wardrop SL, Richardson DR. The effect of intracellular iron concentration and nitrogen monoxide on Nramp2 expression and non-transferrin-bound iron uptake. *Eur J Biochem* 1999; 263:41–49.
31. Aisen P, Listowsky I. Iron transport and storage proteins. *Ann Rev Biochem* 1980; 49:357–393.
32. Barnes D, Sato G. Methods for growth of cultured cells in serum-free medium. *Anal Biochem* 1980; 102:255–270.
33. Lum JB, Infante AJ, Makker DM, Yang F, Bowman BH. Transferrin synthesis by inducer T lymphocytes. *J Clin Invest* 1986; 77:841–849.
34. Skinner MK, Griswold MD. Sertoli cells synthesize and secrete transferrin-like protein. *J Biol Chem* 1980; 255:9523–9525.
35. Vandewalle B, Hornez L, Revillion F, Lefebvre J. Secretion of transferrin by human breast cancer cells. *Biochem Biophys Res Commun* 1989; 163:149–154.
36. Vostrejs M, Moran PL, Seligman PA. Transferrin synthesis by small cell lung cancer cells acts as an autocrine regulator of cellular proliferation. *J Clin Invest* 1988; 82:331–339.
37. Morrone G, Corbo L, Turco MC, Pizzano R, De Felice M, Bridges S, Venuta S. Transferrin-like autocrine growth factor, derived from T-lymphoma cells, that inhibits normal T-cell proliferation. *Cancer Res* 1988; 48:3425–3429.
38. Larrick JW, Cresswell P. Modulation of cell surface iron transferrin receptors by cellular density and the state of activation. *J Supramol Struct* 1979; 11:579–586.
39. Chitambar CR, Massey EJ, Seligman PA. Regulation of transferrin receptor expression on human leukemic cells during proliferation and induction of differentiation. *J Clin Invest* 1983; 72:1314–1325.
40. Chan SM, Hoffer PB, Maric N, Duray P. Inhibition of gallium-67 uptake in melanoma by an anti-human transferrin receptor monoclonal antibody. *J Nuclear Med* 1987; 28:1303–1307.
41. Chitambar CR, Zivkovic Z. Uptake of gallium-67 by human leukemic cells: demonstration of transferrin receptor-dependent and transferrin receptor-independent mechanisms. *Cancer Res* 1987; 47:3929–3934.

42. Trowbridge IS, Lopez F. Monoclonal antibody to transferrin receptor blocks transferrin binding and inhibits tumor cell growth in vitro. *Proc Natl Acad Sci USA* 1982; 79: 1175–1179.
43. Weinberg ED. Iron withholding a defense against infection and neoplasia. *Physiol Rev* 1984; 64:65–102.
44. Kawabata H, Yang R, Hirama T, Vuong PT, Kawano S, Gombart AF, Koeffler HP. Molecular cloning of transferrin receptor 2: a new member of the transferrin receptor-like family. *J Biol Chem* 1999; 274:20826–20832.
45. Poola I, Lucas JJ. Purification and characterization of an estrogen-inducible membrane glycoprotein. Evidence that it is a transferrin receptor. *J Biol Chem* 1988; 263:19137–19146.
46. Poola I, Mason AB, Lucas JJ. The chicken oviduct and embryonic red blood cell transferrin receptors are distinct molecules. *Biochem Biophys Res Commun* 1990; 171: 26–32.
47. Poola I, Kiang JG. The estrogen-inducible transferrin receptor-like membrane glycoprotein is related to stress-regulated proteins. *J Biol Chem* 1994; 269:21762–21769.
48. Poola I. An estrogen inducible 104 kDa chaperone glycoprotein binds ferric iron containing proteins: a possible role in intracellular iron trafficking. *FEBS Lett* 1997; 416: 139–142.
49. Stevens RG, Jones DY, Micozzi MS, Taylor PR. Body iron stores and the risk of cancer. *N Engl J Med* 1988; 319:1047–1052.
50. Migliaccio A, Di Domenico M, Castoria G, de Falco A, Bontempo P, Nola E, Auricchio F. Tyrosine kinase/p21ras/MAP-kinase pathway activation by estradiol-receptor complex in MCF-7 cells. *EMBO J* 1996; 15:1292–1300.
51. Revillion F, Lassalle B, Vandewalle B, Lefebvre J. Cell kinetics (SAMBA200) of estradiol stimulated long-term phenol red withdrawn cultured breast cancer cells. *Anti-cancer Res* 1990; 10:1067–1070.
52. Raaf HN, Jacobsen DW, Savon S, Green R. Serum transferrin receptor level is not altered in invasive adenocarcinoma of the breast. *Am J Clin Pathol* 1993; 99:232–237.
53. Fuchs O, Borova J, Hradilek A, Neuwirt J. Non-transferrin donors of iron for heme synthesis in immature erythroid cells. *Biochim Biophys Acta* 1988; 969:158–165.
54. Sturrock A, Alexander J, Lamb J, Craven CM, Kaplan J. Characterization of a transferrin-independent uptake system for iron in HeLa cells. *J Biol Chem* 1990; 265:3139–3145.
55. Richardson D, Baker E. The uptake of inorganic iron complexes by human melanoma cells. *Biochim Biophys Acta* 1991; 1093:20–28.
56. Inman RS, Wessling-Resnick M. Characterization of transferrin-independent iron transport in K562 cells: unique properties provide evidence for multiple pathways of iron uptake. *J Biol Chem* 1993; 268:8521–8528.
57. Parkes JG, Randell EW, Olivieri NF, Templeton DM. Modulation by iron loading and chelation of the uptake of non-transferrin bound iron by human liver cells. *Biochim Biophys Acta* 1995; 1243:373–380.
58. Inman RS, Coughlan MM, Wessling-Resnick M. Extracellular ferrireductase activity in K562 cells is coupled to transferrin-independent transport. *Biochemistry* 1994; 33: 11850–11857.
59. Brissot P, Wright TL, Ma WL, Weisiger RA. Efficient clearance of non-transferrin-bound iron by rat liver. *J Clin Invest* 1985; 76:1463–1470.
60. Wright TL, Brissot P, Ma W-L, Weisiger RA. Characterization of non-transferrin-bound iron clearance by rat liver. *J Biol Chem* 1986; 261:10909–10914.
61. Parkes JG, Hussain RA. Effects of iron loading on uptake, speciation, and chelation of iron in cultured myocardial cells. *J Lab Clin Med* 1993; 122:36–47.

62. Kaplan J, Jordan I, Sturrock A. Regulation of the transferrin-independent iron transport system in cultured cells. *J Biol Chem* 1991; 266:2997–3004.
63. Richardson DR, Ponka P. Identification of a mechanism of iron uptake by cells that is stimulated by hydroxyl radicals generated via the iron-catalyzed Haber-Weiss reaction. *Biochim Biophys Acta* 1995; 1269:105–114.
64. DeLeo FR, Olakanmi O, Rasmussen GT, Lewis TS, McCormick SJ, Nauseef WM, Britigan BE. Despite structural similarities between gp91phox and FRE1, flavocytochrome b558 does not mediate iron uptake by myeloid cells. *J Lab Clin Med* 1999; 134:275–282.
65. Richardson DR, Chua A, Baker E. Activation of an iron-transport mechanism from transferrin in hepatocytes by preincubation with low molecular weight iron complexes. *J Lab Clin Med* 1999; 133:144–151.
66. Richardson DR. Iron and gallium increase iron uptake from transferrin by human melanoma cells. Further examination of the ferric ammonium citrate-activated iron uptake process. *Biochim Biophys Acta* 2001; 1536:133–140.
67. Chitambar CR, Sax D. Regulatory effects of gallium on transferrin-independent iron uptake by human leukemic HL60 cells. *Blood* 1992; 80:505–511.
68. Olakanmi O, Stokes JB, Pathan S, Britigan BE. Polyvalent cationic metals induce the rate of transferrin-independent iron acquisition by HL-60 cells. *J Biol Chem* 1997; 272:2599–2606.
69. Gruenheid S, Cellier M, Vidal S, Gros P. Identification and characterization of a second mouse Nramp gene. *Genomics* 1995; 25:514–525.
70. Müllner EW, Kühn LC. A stem-loop in the 3' untranslated region mediates iron-dependent regulation of transferrin receptor mRNA stability in the cytoplasm. *Cell* 1998; 53:815–825.
71. Müllner EW, Neupert B, Kühn LC. A specific mRNA-binding factor regulates the iron-dependent stability of the cytoplasmic transferrin receptor mRNA. *Cell* 1989; 58:373–382.
72. Bowen BJ, Morgan EH. Anaemia of the Belgrade rat: evidence for defective membrane transport of iron. *Blood* 1987; 70:38–44.
73. Farcich E, Morgan EH. Uptake of transferrin-bound and nontransferrin-bound iron by reticulocytes from the Belgrade laboratory rat: comparison with Wistar rat transferrin and reticulocytes. *Am J Hematol* 1992; 39:9–14.
74. Lee PL, Gelbart T, West C, Halloran C, Beutler E. The human Nramp2 gene: characterization of the gene structure, alternative splicing, promoter region and polymorphisms. *Blood Cells, Mol, Dis* 1998; 24:199–215.
78. Woodbury RG, Brown JP, Yeh M-Y, Hellström I, Hellström KE. Identification of a cell surface protein, p97, in human melanoma and certain other neoplasms. *Proc Natl Acad Sci USA* 1980; 77:2183–2187.
79. Woodbury RG, Brown JP, Loop SM, Hellström KE, Hellström I. Analysis of normal and neoplastic human tissues for the tumor-associated protein p97. *Int J Cancer* 1981; 27:145–149.
80. Brown JP, Woodbury RG, Hart CE, Hellström I, Hellström KE. Quantitative analysis of melanoma-associated antigen p97 in normal and neoplastic tissues. *Proc Natl Acad Sci USA* 1981; 78:539–543.
81. Brown JP, Nishiyama K, Hellström I, Hellström KE. Structural characterization of human melanoma-associated antigen p97 with monoclonal antibodies. *J Immunol* 1981; 127:539–546.
82. Brown JP, Hewick RH, Hellström I, Hellström KE, Doolittle RF, Dreyer WJ. Human melanoma antigen p97 is structurally and functionally related to transferrin. *Nature* 1982; 296:171–173.

83. Rose TM, Plowman GD, Teplow DB, Dreyer WJ, Hellström KE, Brown JP. Primary structure of human melanoma-associated antigen p97 (melanotransferrin) deduced from the mRNA sequence. *Proc Natl Acad Sci USA* 1986; 83:1261–1265.
84. Natali PG, Roberts JT, Difilippo F, Bigotti A, Dent PB, Ferrone S, Liao SK. Immunohistochemical detection of antigen in human primary and metastatic melanomas by the monoclonal antibody 140.240 and its possible prognostic significance. *Cancer* 1987; 59:55–63.
85. Alemany R, Rosa Vilá M, Franci C, Egea G, Real FX, Thompson JM. Glycosyl phosphatidylinositol membrane anchoring of melanotransferrin (p97): apical compartmentalization in intestinal epithelial cells. *J Cell Sci* 1993; 104:1155–1162.
86. Sciot R, De Vos R, van Eyken P, van der Steen K, Moerman P, Desmet VJ. In situ localization of melanotransferrin (melanoma-associated antigen P97) in human liver. A light- and electron-microscopic immunohistochemical study. *Liver* 1989; 9:110–119.
87. Jefferies WA, Food MR, Gabathuler R, Rothenberger S, Yamada T, Yasuhara O, McGeer PL. Reactive microglia specifically associated with amyloid plaques in Alzheimer's disease brain tissue express melanotransferrin. *Brain Res* 1996; 712:122–126.
88. Rothenberger S, Food MR, Gabathuler R, Kennard ML, Yamada T, Yasuhara O, McGeer PL, Jefferies WA. Coincident expression and distribution of melanotransferrin and transferrin receptor in human brain capillary endothelium. *Brain Res* 1996; 712: 117–121.
89. Kennard ML, Feldman H, Yamada T, Jefferies WA. Serum levels of the iron binding protein p97 are elevated in Alzheimer's disease. *Nature Med* 1996; 2:1230–1235.
90. Danielson EM, van Deurs B. A transferrin-like GPI-linked iron-binding protein in detergent-insoluble noncaveolar microdomains at the apical surface of fetal intestinal epithelial cells. *J Cell Biol* 1995; 131:939–950.
91. McNagny KM, Rossi F, Smith G, Graf T. The eosinophil-specific cell surface antigen, EOS47, is a chicken homologue of the oncofetal antigen melanotransferrin. *Blood* 1996; 87:1343–1352.
92. Kawamoto T, Pan H, Yan W, Ishida H, Usui E, Oda R, Nakamasu K, Noshiro M, Kawashima-Ohya Y, Fujii M, Shintani H, Okada Y, Kato Y. Expression of membrane-bound transferrin-like protein p97 on the cell surface of chondrocytes. *Eur J Biochem* 1998; 256:503–509.
93. Plowman GD, Brown JP, Enns CA, Schröder J, Nikinmaa B, Sussman HH, Hellström KE, Hellström I. Assignment of the gene for human melanoma-associated antigen p97 to chromosome 3. *Nature* 1983; 303:70–72.
94. Baker EN, Rumball SV, Anderson BF. Transferrins: insights into structure and function from studies on lactoferrin. *Trends Biochem Sci* 1987; 2:350–353.
95. Baker EN, Baker HM, Smith CA, Stebbins MR, Kahn M, Hellström KE, Hellström I. Human melanotransferrin (p97) has only one functional iron-binding site. *FEBS Lett* 1992; 298:215–218.
96. Food MR, Rothenberger S, Gabathuler R, Haidl ID, Reid G, Jefferies WA. Transport and expression in human melanomas of a transferrin-like glycosylphosphatidylinositol-anchored protein. *J Biol Chem* 1994; 269:3034–3040.
97. Kennard ML, Richardson DR, Gabathuler R, Ponka P, Jefferies WA. A novel iron uptake mechanism mediated by GPI-anchored human p97. *EMBO J* 1995; 14:4178–4186.
98. Richardson DR, Baker E. The release of iron and transferrin by the human melanoma cell. *Biochim Biophys Acta* 1991; 1091:294–304.
99. Richardson DR, Baker E. Intermediate steps in cellular iron uptake from transferrin. Detection of a cytoplasmic pool of iron free of transferrin. *J Biol Chem* 1992; 267: 21384–21389.

100. Richardson DR, Baker E. The effect of desferrioxamine and ferric ammonium citrate on the uptake of iron by the membrane iron-binding component of human melanoma cells. *Biochim Biophys Acta* 1992; 1103:275–280.
101. Richardson DR. The role of melanotransferrin (tumor antigen p97) in iron uptake by the human malignant melanoma cell. *Eur J Biochem* 2000; 267:1290–1298.
102. Neckers LM, Cossman J. Transferrin receptor induction in mitogen-stimulated human T lymphocytes is required for DNA synthesis and cell division and is regulated by interleukin 2. *Proc Natl Acad Sci USA* 1983; 80:3494–3498.
103. Thelander L, Reichard P. The reduction of ribonucleotides. *Annu Rev Biochem* 1979; 48:133–158.
104. Thelander L, Graslund A, Thelander M. Continual presence of oxygen and iron is required for mammalian ribonucleotide reduction: possible regulation mechanism. *Biochem Biophys Res Commun* 1983; 110:859–865.
105. Kameyama K, Takezaki S, Kanzaki T, Nishiyama S. HLA-DR and melanoma-associated antigen (p97) expression during the cell cycle in human melanoma cell lines, and the effects of recombinant gamma-interferon: two colour flow cytometric analysis. *J Invest Dermatol* 1986; 87:313–318.
106. Seligman PA, Butler CD, Massey EJ, Kaur EJ, Brown JP, Plowman GD, Miller Y, Jones C. The p97 antigen is mapped to the q24-qter region of chromosome 3; the same region as the transferrin receptor. *Am J Hum Genet* 1996; 38:540–548.
107. Kaplan J, O'Halloran TV. Iron metabolism in eukaryotes: Mars and Venus at it again. *Science* 1996; 271:1510–1512.
108. Ragan HA, Nacht S, Lee GR, Bishop CR, Cartwright GE. Effect of ceruloplasmin on plasma iron in copper-deficient swine. *Am J Physiol* 1969; 217:1320–1323.
109. Osaki S, Johnson DA, Frieden E. The possible significance of ferrous oxidase activity of ceruloplasmin in normal human serum. *J Biol Chem* 1966; 241:2746–2751.
110. Mukhopadhyay CK, Attieh ZK, Fox PL. Role of ceruloplasmin in cellular iron uptake. *Science* 1998; 279:714–717.
111. Yuan DS, Stearman R, Dancis A, Dunn T, Beeler T, Klausner RD. The Menkes/Wilson disease gene homologue in yeast provides copper to a ceruloplasmin-like oxidase required for iron uptake. *Proc Natl Acad Sci USA* 1995; 92:2632–2636.
112. Attieh ZK, Mukhopadhyay CK, Seshadri V, Tripoulas NA, Fox PL. Ceruloplasmin ferroxidase activity stimulates cellular iron uptake by a trivalent cation-specific transport mechanism. *J Biol Chem* 1999; 274:1116–1123.
113. Marcus DM, Zinberg M. Measurement of serum ferritin by radioimmunoassay: results in normal individuals and patients with breast cancer. *J Natl Cancer Inst* 1975; 55:791–795.
114. Kew MC, Torrance JD, Derman D, Simon M, Macnab GM, Charlton RW, Bothwell TH. Serum and tumour ferritins in primary liver cancer. *Gut* 1978; 19:294–299.
115. Hann HW, Levy HM, Evans AE. Serum ferritin as a guide to therapy in neuroblastoma. *Cancer Res* 1980; 40:1411–1413.
116. Zhou XD, Stahlhut MW, Hann HL, London WT. Serum ferritin in hepatocellular carcinoma. *Hepatogastroenterology* 1988; 35:1–4.
117. Iancu TC, Shiloh H, Kedar A. Neuroblastomas contain iron-rich ferritin. *Cancer* 1988; 61:2497–2502.
118. Iancu TC. Iron and neoplasia: ferritin and hemosiderin in tumor cells. *Ultrastruct Pathol* 1989; 13:573–584.
119. Hann HW, Evans AE, Cohen IJ, Leitmeyer JE. Biologic differences between neuroblastoma stages IV-S and IV. Measurement of serum ferritin and E-rosette inhibition in 30 children. *N Engl J Med* 1981; 305:425–429.
120. Hann HW, Evans AE, Siegel SE, Wong KY, Sather H, Dalton A, Hammond D, Seeger RC. Prognostic importance of serum ferritin in patients with stages III and IV neuro-

- blastoma: the Children's Cancer Study Group experience. *Cancer Res* 1985; 45:2843–2848.
121. Hann HL, Stahlhut MW, Millman I. Human ferritins present in the sera of nude mice transplanted with human neuroblastoma or hepatocellular carcinoma. *Cancer Res* 1984; 44:3898–3901.
 122. Broxmeyer HE, Cooper S, Levi S, Arosio P. Mutated recombinant human heavy-chain ferritins and myelosuppression in vitro and in vivo: a link between ferritin ferroxidase activity and biological function. *Proc Natl Acad Sci USA* 1991; 88:770–774.
 123. Broxmeyer HE, Bognack J, Dorner MH, de Sousa M. Identification of leukemia-associated inhibitory activity as acidic iso-ferritins. A regulatory role for acidic iso-ferritins in the production of granulocytes and macrophages. *J Exp Med* 1981; 153:1426–1444.
 124. Hann HW, Stahlhut MW, Evans AE. Basic and acid iso-ferritins in the sera of patients with neuroblastoma. *Cancer* 1988; 62:1179–1182.
 125. Blatt J, Wharton V. Stimulation of growth of neuroblastoma cells by ferritin in vitro. *J Lab Clin Med* 1992; 119:139–143.
 126. Kikyo N, Hagiwara K, Fujisawa M, Kikyo N, Yazaki Y, Okabe T. Purification of a cell growth factor from a human lung cancer cell line: its relationship with ferritin. *J Cell Physiol* 1994; 161:106–110.
 127. Kikyo N, Suda M, Kikyo N, Hagiwara K, Yasukawa K, Fujisawa M, Yazaki Y, Okabe T. Purification and characterization of a cell growth factor from a human leukemia cell line: immunological identity with ferritin. *Cancer Res* 1994; 54:268–271.
 128. Covell AM, Cook JD. Interaction of acidic iso-ferritins with human promyelocytic HL60 cells. *Br J Haematol* 1988; 69:559–563.
 129. Fargion S, Arosio P, Fracanzani AL, Cislighi V, Levi S, Cozzi A, Piperno A, Fiorelli G. Characteristics and expression of binding sites specific for ferritin H-chain on human cell lines. *Blood* 1988; 71:753–757.
 130. Anderson GJ, Faulk WP, Arosio P, Moss D, Powell LW, Halliday JW. Identification of H- and L-ferritin subunit binding sites on human T and B lymphoid cells. *Br J Haematol* 1989; 73:260–264.
 131. Konijn AM, Meyron-Holtz EG, Levy R, Ben-Bassat H, Matzner Y. Specific binding of placental acidic iso-ferritins to cells of the T-cell line HD-MAR. *FEBS Lett* 1990; 263:229–232.
 132. Bretscher MS, Thomson JN. Distribution of ferritin receptors and coated pits on giant HeLa cells. *EMBO J* 1983; 2:599–603.
 133. Tsuji Y, Kwak E, Saika T, Torti SV, Torti FM. Preferential repression of the H-subunit of ferritin by adenovirus E1A in NIH-3T3 mouse fibroblasts. *J Biol Chem* 1993; 268:7270–7275.
 134. Wu K, Polack A, Dalla-Favera R. Coordinated regulation of iron-controlling genes, H-ferritin and IRP2, by c-MYC. *Science* 1999; 283:676–679.
 135. Modjtahedi N, Frebourg T, Fossar N, Lavielle C, Cremisi C, Brison O. Increased expression of cytokeratin and ferritin-H genes in tumorigenic clones of the SW 613-S human colon carcinoma cell line. *Exp Cell Res* 1992; 201:74–82.
 136. Brodeur GM, Seeger RC, Schwab M, Varmus HE, Bishop JM. Amplification of N-myc in untreated neuroblastomas correlates with advanced disease stage. *Science* 1984; 224:1121–1124.
 137. Schwab M, Alitalo K, Klempnauer KH, Varmus HE, Bishop JM, Gilbert F, Brodeur G, Goldstein M, Trent J. Amplified DNA with limited homology to myc cellular oncogene is shared by human neuroblastoma cell lines and a neuroblastoma tumor. *Nature* 1983; 305:245–248.
 138. Schwab M, Varmus HE, Bishop JM, Grzeschik KH, Naylor SL, Sakaguchi AY, Brodeur G, Trent J. Chromosomal localization in normal human cells and neuroblastomas of a gene related to c-myc. *Nature* 1984; 308:288–291.

139. Selig RA, Madafiglio J, Haber M, Norris MD, White L, Stewart BW. Ferritin production and desferrioxamine cytotoxicity in human neuroblastoma cell lines. *Anticancer Res* 1993; 13:721–725.
140. Frantz CN, Iyer J, Frick KK, Eskenazi AE, Derg PE. Iron and N-myc expression in neuroblastoma. Proceedings of the Neuroblastoma Research Meeting, Philadelphia, PA. 1993.
141. Frantz CN, Eskenazi AE, Overman D. Iron chelation cancer therapy for neuroblastoma. Proceedings of the International Conference on Bioiron, Asheville, NC, 1995, p. 195.
142. Blatt J, Stitely S. Antineuroblastoma activity of desferrioxamine in human cell lines. *Cancer Res* 1987; 47:1749–1750.
143. Becton DL, Bryles P. Deferoxamine inhibition of human neuroblastoma viability and proliferation. *Cancer Res* 1988; 48:7189–7192.
144. Donfrancesco A, Deb G, Dominici C, Pileggi D, Castello MA, Helson L. Effects of a single course of deferoxamine in neuroblastoma patients. *Cancer Res* 1990; 50:4929–4930.
145. Donfrancesco A, Deb G, Dominici C, Angioni A, Caniglia M, De Sio L, Fidani P, Amici A, Helson L. Deferoxamine, cyclophosphamide, etoposide, carboplatin, and thiotepa (D-CECat): a new cytoreductive chelation-chemotherapy regimen in patients with advanced neuroblastoma. *Am J Clin Oncol* 1992; 15:319–322.
146. Donfrancesco A, De Bernardi B, Carli M, Mancini A, Nigro M, De Sio L, Casale F, Bagnulo S, Helson L, Deb G. Deferoxamine (D) followed by cytoxan (C), etoposide (E), carboplatin (Ca), thio-TEPA (T), induction regimen in advanced neuroblastoma. *Eur J Cancer* 1995; 31A:612–615.
147. Donfrancesco A, Deb G, De Sio L, Cozza R, Castellano A. Role of desferrioxamine in tumor therapy. *Acta Haematol* 1996; 95:66–69.
148. Estrov Z, Tawa A, Wang X-H, Dube ID, Sulh H, Cohen A, Gelfand EW, Freedman MH. In vivo and in vitro effects of desferrioxamine in neonatal acute leukemia. *Blood* 1987; 69:757–761.
149. Becton DL, Roberts B. Antileukemic effects of desferrioxamine on human myeloid leukemia cell lines. *Cancer Res* 1989; 49:4809–4812.
150. Dezza L, Cazzola M, Danova M, Carlo-Stella C, Bergamaschi G, Brugnattelli S, Invernizzi R, Mazzini G, Riccardi A, Ascari E. Effects of desferrioxamine on normal and leukemic human hematopoietic cell growth: in vitro and in vivo studies. *Leukemia* 1989; 3:104–107.
151. Richardson DR, Ponka P, Baker E. The effect of the iron(III) chelator, desferrioxamine, on iron and transferrin uptake by the human melanoma cell. *Cancer Res* 1994; 54: 685–689.
152. Hann H-WL, Stahlhut MW, Rubin R, Maddrey WC. Antitumor effect of deferoxamine on human hepatocellular carcinoma growing in athymic nude mice. *Cancer* 1992; 70: 2051–2056.
153. Voest EE, Rooth H, Neijt JP, van Asbeck BS, Marx JJ. The in vitro response of human tumour cells to desferrioxamine is growth medium dependent. *Cell Prolif* 1993; 26: 77–88.
154. Simonart T, Noel JC, Andrei G, Parent D, Van Vooren JP, Hermans P, Lunardi-Yskander Y, Lambert C, Dieye T, Farber CM, Liesnard C, Snoeck R, Heenen M, Boelaert JR. Iron as a potential co-factor in the pathogenesis of Kaposi's sarcoma. *Int J Cancer* 1998; 78:720–726.
155. Richardson DR. Iron chelators as effective anti-proliferative agents. *Can J Physiol Pharmacol* 1997; 75:1164–1180.
156. Richardson DR. Analogues of pyridoxal isonicotinoyl hydrazone (PIH) as potential iron chelators for the treatment of neoplasia. *Leukemia and Lymphoma* 1998; 31:47–60.

157. Selig RA, White L, Gramacho C, Sterlinglevis K, Fraser IW, Naidoo D. Failure of iron chelators to reduce tumor growth in human neuroblastoma xenografts. *Cancer Res* 1998; 58:473–478.
158. Ponka P, Borova J, Neuwirt J, Fuchs O. Mobilization of iron from reticulocytes. Identification of pyridoxal isonicotinoyl hydrazone as a new iron chelating agent. *FEBS Lett* 1979; 97:317–321.
159. Ponka P, Borova J, Neuwirt J, Fuchs O, Necas E. A study of intracellular iron metabolism using pyridoxal isonicotinoyl hydrazone and other synthetic chelating agents. *Biochim Biophys Acta* 1979; 586:278–297.
160. Cikrt M, Ponka P, Necas E, Neuwirt J. Biliary iron excretion in rats following pyridoxal isonicotinoyl hydrazone. *Br J Haematol* 1980; 45:275–283.
161. Richardson DR, Ponka P. Pyridoxal isonicotinoyl hydrazone and its analogues: potential orally effective iron-chelating agents for the treatment of iron overload disease. *J Lab Clin Med* 1998; 131:306–315.
162. Sah P. Nicotinoyl and isonicotinoyl hydrazones of pyridoxal. *J Am Chem Soc* 1954; 76:300.
163. Johnson DK, Murphy TB, Rose NJ, Goodwin WH, Pickart L. Cytotoxic chelators and chelates. 1. Inhibition of DNA synthesis in cultured rodent and human cells by aroylhydrazones and by a copper(II) complex of salicylaldehyde benzoyl hydrazone. *Inorg Chim Acta* 1982; 67:159–165.
164. Richardson DR, Tran E, Ponka P. The potential of iron chelators of the pyridoxal isonicotinoyl hydrazone class as effective antiproliferative agents. *Blood* 1995; 86:4295–4306.
165. Chitambar CR, Boon P, Wereley JP. Evaluation of transferrin and gallium-pyridoxal isonicotinoyl hydrazone as potential therapeutic agents to overcome lymphoid leukemic cell resistance to gallium nitrate. *Clin Cancer Res* 1996; 2:1009–1015.
166. Richardson DR. Cytotoxic analogues of the iron(III) chelator pyridoxal isonicotinoyl hydrazone: effect of complexation with copper(II), gallium(III), and iron(III) on their anti-proliferative activity. *Antimicrob Agents Chemother* 1997; 41:2061–2063.
167. Knorr GM, Chitambar CR. Gallium-pyridoxal isonicotinoyl hydrazone (Ga-PIH), a novel cytotoxic gallium complex. A comparable study with gallium nitrate. *Anticancer Res* 1998; 18:1733–1737.
168. Pickart L, Goodwin WH, Burgua W, Murphy TB, Johnson DK. Inhibition of the growth of cultured cells and an implanted fibrosarcoma by aroylhydrazone analogs of the Gly-His-Cu(II) complex. *Biochem Pharmacol* 1983; 32:3868–3871.
169. Richardson D, Baker E, Ponka P, Wilairat P, Vitolo ML, Webb J. Effects of pyridoxal isonicotinoyl hydrazone and analogs on iron metabolism in hepatocytes and macrophages in culture. *Birth Defects* 1988; 23:81–88.
170. Richardson DR, Hefter GT, May PM, Webb J, Baker E. Iron chelators of the pyridoxal isonicotinoyl hydrazone class III. Formation constants with calcium(II), magnesium(II), and zinc(II). *Biol Metals* 1989; 2:161–167.
171. Richardson DR, Wis Vitolo ML, Hefter GT, May PM, Clare BW, Webb J, Wilairat P. Iron chelators of the pyridoxal isonicotinoyl hydrazone class part 1. Ionisation characteristics of the ligands and their relevance to biological properties. *Inorg Chim Acta* 1990; 170:165–170.
172. Ponka P, Richardson D, Baker E, Schulman HM, Edward JT. Effect of pyridoxal isonicotinoyl hydrazone and other hydrazones on iron release from macrophages, reticulocytes and hepatocytes. *Biochim Biophys Acta* 1988; 967:122–129.
173. Baker E, Richardson DR, Gross S, Ponka P. Evaluation of the iron chelation potential of pyridoxal, salicylaldehyde and 2-hydroxy-1-naphthylaldehyde using the hepatocyte in culture. *Hepatology* 1992; 15:492–501.

174. Richardson DR, Ponka P. The iron metabolism of the human neuroblastoma cell. Lack of relationship between the efficacy of iron chelation and the inhibition of DNA synthesis. *J Lab Clin Med* 1994; 124:660–671.
175. May PM, Williams GK, Williams DR. Speciation studies of adriamycin, quelamycin, and their metal complexes. *Inorg Chim Acta* 1980; 46:221–228.
176. Minotti G. Adriamycin-dependent release of iron from microsomal membranes. *Arch Biochem Biophys* 1989; 268:398–403.
177. Hasinoff BB, Davey JP. The iron(III)-adriamycin complex inhibits cytochrome c oxidase before its inactivation. *Biochem J* 1998; 250:827–834.
178. Dorr RT. Cytoprotective agents for anthracyclines. *Semin Oncol* 1996; 23:23–34.
179. French FA, Blanz EJ Jr, Schaddix SC, Brockman RW. (–(N)-Formylheteroaromatic thiosemicarbazones. Inhibition of tumor derived ribonucleoside diphosphate reductase and correlation with in vivo anti-tumor activity. *J Med Chem* 1974; 17:172–181.
180. Krakoff IH, Etcubanas E, Tan C, Mayer K, Bethune V, Burchenal JH. Clinical trial of 5-hydroxypicolinaldehyde thiosemicarbazone (5-HP; NSC 107392), with special reference to its iron chelating properties. *Cancer Chemother Rep* 1974; 58:207–212.
181. Agrawal KC, Sartorelli AC. The chemistry and biological activity of (α -(N)-heterocyclic carboxaldehyde thiosemicarbazones. *Prog Med Chem* 1978; 15:321–356.
182. Liu M-C, Lin T-S, Sartorelli AC. Chemical and biological properties of cytotoxic (α -(N)-heterocyclic carboxaldehyde thiosemicarbazones. In: Ellis GP, Luscombe DK, eds. *Progress in Medicinal Chemistry*, Volume 32. Elsevier, 1995:1–35.

Novel Methods for Assessing Transport of Iron Across Biological Membranes

Z. IOAV CABANTCHIK, SILVINA EPSZTEJN, and WILLIAM BREUER

Hebrew University of Jerusalem, Jerusalem, Israel

I. INTRODUCTION	539
II. FLUORESCENCE DETECTION OF METALS (FDM)	541
III. ASSESSMENT OF IRON TRANSPORT ACROSS MEMBRANE MODEL SYSTEMS	543
IV. ASSESSMENT OF TRANSEPITHELIAL TRANSPORT OF IRON	546
V. ASSESSMENT OF IRON TRANSPORT INTO LIVING CELLS	546
VI. ASSESSMENT OF LIP IN LIVING CELLS	550
A. Rationale	550
B. Advantages and Limitations of FDM for Assessing LIP	550
C. Selected Examples of LIP Determinations in Model Cells	552
D. Assessment of Fe Efflux from Cells	554
VII. FUTURE DIRECTIONS	555
ACKNOWLEDGMENTS	557
REFERENCES	557

I. INTRODUCTION

Iron transport across biological membranes is carried out by a variety of membrane transporters that act on different chemical forms of the metal (substrate) and deliver

it to different cell compartments. Unlike most other classes of water-soluble permeants, the ionic forms of iron (Fe) available for transport are present in aqueous media as distinctly different chemical species. Those comprise either complexes of Fe(II) and Fe(III) with anions (i.e., organic salts) or with polyfunctional ligands (i.e., chelates or siderophores). Other transportable forms are integrated into stable structures such as heme or into carrier proteins such as transferrin (Tf) and possibly also ferritin (FT). The diversity in substrate composition is complemented by a diversity of transport systems that recognize a particular form of the metal. Most of the iron transporters require auxiliary functions for substrate recognition, such as reductases for converting Fe(III) into the transportable Fe(II) or vice versa (23), oxidases for conversion of Fe(II) into Fe(III), and anion channels for maintenance of electroneutrality. Others comprise or depend on multistep reactions for translocating the metal to the final destination, such as the apparatus involved in Tf-receptor-mediated endocytosis (Tf-RME).

Various genes of mammalian iron transporters have been recently identified (2,3,11,12,14,19,28), and some elements in the noncoding regions of their mRNA have been defined as regulatory sites (14,19). However, the functional properties of the transporters per se have yet to be explored in heterologous expression systems and/or reconstituted proteoliposomes. Unfortunately, the available information about the membrane transport mechanisms of iron in native membranes is still scant. Even for the classical system of Tf-RME operating in animal cells (1,8,27), little is known about how iron is made available in endosomes (see Chapter 4) for translocation by the DMT1/Nramp-2) transporter or whether the latter operates electrogenically and in a manner dependent on Cl^- as the diffusing counterion and H^+ as a co-substrate (14). Among the factors limiting our knowledge about metal transport mechanisms is the lack of reliable methodologies for tracing heavy metals in cells and cell compartments in a manner that does not affect cellular integrity.

The study of the iron transport mechanisms in constitutive or genetically engineered systems (transfected cells or lines immortalized from transgenic animals) or in model membranes depends to a large extent on the possibility of measuring the transmembrane movement of a given form of the metal ion from one compartment to another. Classical means of tracing such movement are by exposing cells or vesicles to radioisotope-labeled substrates (e.g., inorganic or organic salts of ^{55}Fe or ^{59}Fe or radiolabeled Tf or FT) and sampling a particular compartment (cells or medium) after its physical separation. These means are limited when applied to ionic iron, due to its propensity for electrostatic adsorption to anionic surfaces (e.g., membranes) and precipitation as oxidized forms when inadequately complexed or solubilized by acids or chelators. In most published studies on iron transport, the parameter that has been followed is uptake or ingress of radiolabeled iron into cells or tissues. Although such studies yield kinetic parameters of iron uptake, they show variability from study to study due to the use of different experimental conditions, such as anion composition, pH, and partial O_2 tension. The latter undoubtedly have a major effect on the activity of the metal and its availability as substrate during the transport measurements. Moreover, the extent to which the kinetic parameters of uptake correspond to transport per se depends on whether the latter is indeed rate-limiting under any experimental condition. For cases in which Fe(II) has been specifically invoked as the translocated form of the metal, it is even difficult to ascertain

the actual concentration (or activity) of the substrate at any time point during the transport assay, even when reducing agents such as ascorbate are included.

An even higher degree of uncertainty exists regarding the active or labile forms of intracellular iron available for intracellular traffic (distribution, secretion, etc.). In most mammalian cells, the total cell iron level spans a wide range (20–100 μM), most of which is associated with proteins. Only a minor fraction (<1%) appears to be loosely bound (to a variety of ligands) in forms immediately available for metabolism, chelation, and possibly also for generation of free radicals. This fraction (<1 μM), referred to in this chapter as the cellular labile iron pool (LIP), was predicted by earlier studies of Jacobs and Chrichton (8,16) and approached experimentally by others (17,24).

The approach we have used for tracing iron in biological compartments is one that allows monitoring the metal in terms of its spatial and temporal distribution. We based the approach on fluorescence detection of metals (FDM), which uses fluorescence metalosensors, namely, fluorescent probes that undergo reversible spectroscopic changes upon binding of the metal. FDM is in principle applicable to solutions as well as to membrane model systems and to living cells appearing as individual entities or as functional units in a homogeneous or heterogeneous cell population.

II. FLUORESCENCE DETECTION OF METALS (FDM)

FDM depends on probes or metal-sensing devices that undergo swift changes in signal properties as a function of the metal concentration. A metal-binding moiety attached to a fluorophor can usually serve the purpose, provided the metal binding is fast, stable, and capable of modulating the fluorescence properties of the fluorophor in a reversible fashion. Fluorescent analogs of desferrioxamine (DFO) seemingly met the metal sensor criteria (18), since the specific binding of Fe(III) evoked a stoichiometric and marked (>90%) quenching of its fluorescence (18). Fluoresceinated derivatives of the chelators DFO (DFO-green or FL-DFO) or phenanthroline (phen-green or FL-phen) (Fig. 1) were prepared and are now offered commercially by Molecular Probes. The different probes differ in their iron-binding stoichiometry (1:1 for FL-DFO and 3:1 for FL-phen) and in their specificity for binding Fe(III) versus Fe(II), respectively. However, in practice, in ambient conditions the probes tightly complex both forms of the metal, either by oxidizing or reducing the lower-binding-affinity forms to the higher ones [e.g., in the presence of O_2 , DFO will rapidly oxidize Fe(II) to Fe(III), while FL-phen could slowly favor the reduction of Fe(III) to Fe(II)]. Although the quantitative relationship between metal binding and fluorescence quenching can be used for tracing iron in fluids and in cell-free systems, the relatively high metal-binding affinity of the chelator limits (but does not preclude) its use as an intracellular probe for iron dynamics (7,10). We have found the fluoresceinated analog of EDTA, calcein (CAL), to be a more versatile probe for monitoring iron dynamics, by detection of iron in living cells, in solutions, or in biological fluids (4–7,10). Moreover, although the probe is less iron-specific than DFO or even phen, it is also substantially less toxic to cells.

The unique properties of CAL comprise: (a) high quantum yield; (b) 1:1 stoichiometry of binding iron and commensurate quenching of fluorescence; (c) rapid on/off kinetics of metal binding; (d) relatively slow kinetics of Fe(III) binding in physiological solutions as compared to binding of Fe(II), despite the 10^{13} higher

Fluorescent metalosensors

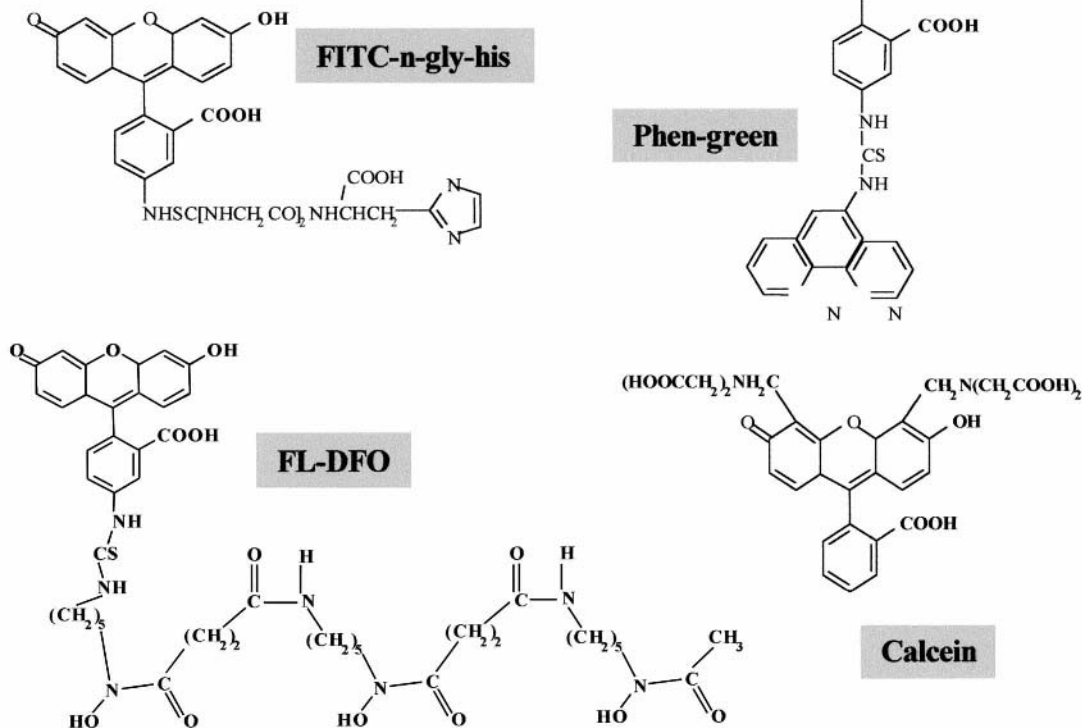


Figure 1 Chemical structures of fluorescent metalosensors. All the probes carry the green fluorescent fluorescein (FL) as the fluorophore conjugated to a metal-binding moiety or moieties: FITC-*n*-glyhis (or FL-glyhis) is obtained by reacting FITC (fluoresceinisothiocyanate) with *N*-gly-his, resulting in a Cu-binding probe, phen green (or FL-phen) is obtained by reacting isothiocyanophenanthroline with FL-amine [resulting in an Fe(II)-binding probe], and DFO-green (or FL-DFO) is obtained by reacting FITC with deferoxamine (DFO), yielding an Fe(III)-binding probe. Calcein (CAL), which is composed of FL conjugated with an EDTA-like moiety, can bind divalent and trivalent metals (4).

apparent affinity of CAL for Fe(III) than for Fe(II) (10^{27} as compared to 10^{14}); (e) fast conversion of Fe(II) into Fe(III) upon binding to CAL in ambient conditions and slower reversal upon reduction with ascorbate; (f) the possibility of loading the probe into cells as a hydrophobic precursor calcein-acetomethoxy ester (CAL-AM) and its retention within cells as free CAL; (g) relatively low toxicity of CAL loaded into mammalian cells; and (h) low selectivity for binding Fe as compared to Cu in solution, that is, compensated by the prevalence of Fe versus Cu in cells. The basic principles of CAL-based FDM are depicted in Fig. 2.

Because of the propensity of Fe(II) for oxidation in ambient conditions and physiological solutions, particularly when bound to solubilizing ligands, the initial binding of Fe(II) to CAL is immediately followed by a time-dependent oxidation (Fig. 3).

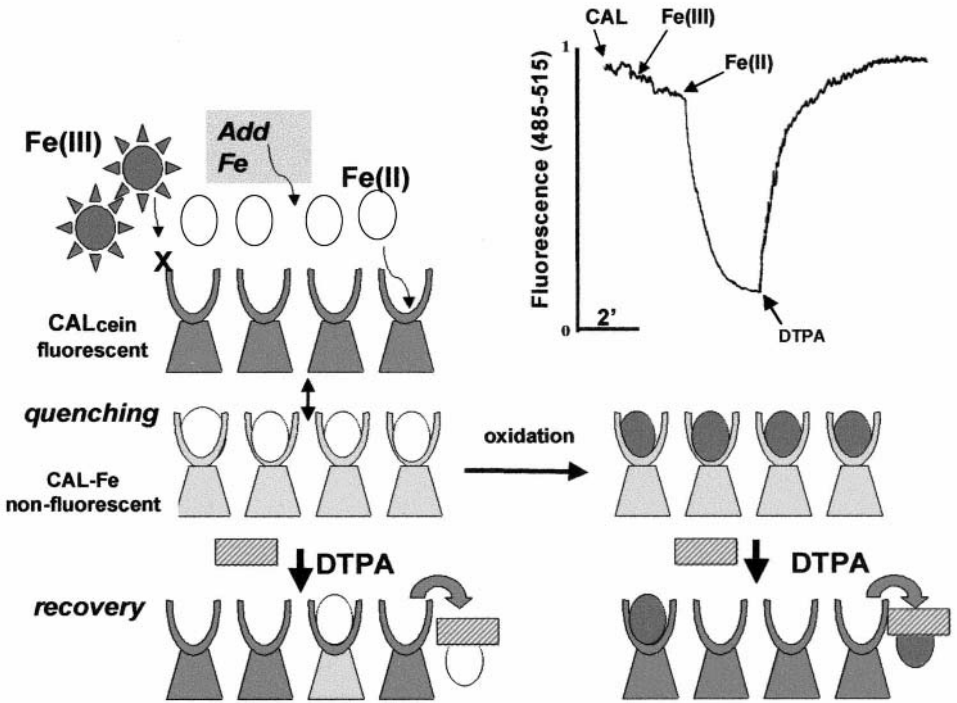


Figure 2 The principle of FDM using CAL as the metalosensor. The fluorescent CAL binds Fe(II) or Fe(III) (when solubilized with agents such as NTA). Fe(III) salts prepared in physiological media comprise ionic forms (filled stars) that are poorly accessible to CAL (indicated by X). In ambient conditions, Fe(II) (empty circles) binds CAL weakly but swiftly quenches fluorescence (measured at 480-nm excitation, 515-nm emission) while getting oxidized to Fe(III) (filled circles) and tightly bound. Thus, oxidation shifts the low-affinity CAL-Fe(II) to the high affinity CAL-Fe(III). Addition of excess DTPA (hatched rectangle) restores the original fluorescence by scavenging iron (II or III) from CAL-Fe.

The rate and degree of Fe(II) oxidation are likely to be less pronounced in cells, and even more so *in vivo*, due to both the intracellular reducing capacity and the lower O₂ partial pressure. To a first approximation, the relative levels of intracellular Fe(II) and Fe(III) can be deduced from the redox potential of the cells, which is largely dictated by the ratio of NADPH/NADP or GSH/GSSG (10,15).

III. ASSESSMENT OF IRON TRANSPORT ACROSS MEMBRANE MODEL SYSTEMS

Membrane vesicles can be used for studying the transport mechanism of iron (Fig. 4). For that purpose iron sensors such as CAL [or possibly FL-DFO and (or) FL-phen, not shown] are encapsulated into vesicles, e.g., resealed membrane ghosts isolated from human red blood cells or from human placental membranes. Although the highly anionic probes are relatively membrane-impermeant, that property needs to be assessed for each membrane preparation. This is done by suspending the probe-laden vesicles in the presence of probe-quenching antibodies (anti-CAL or anti-FL,

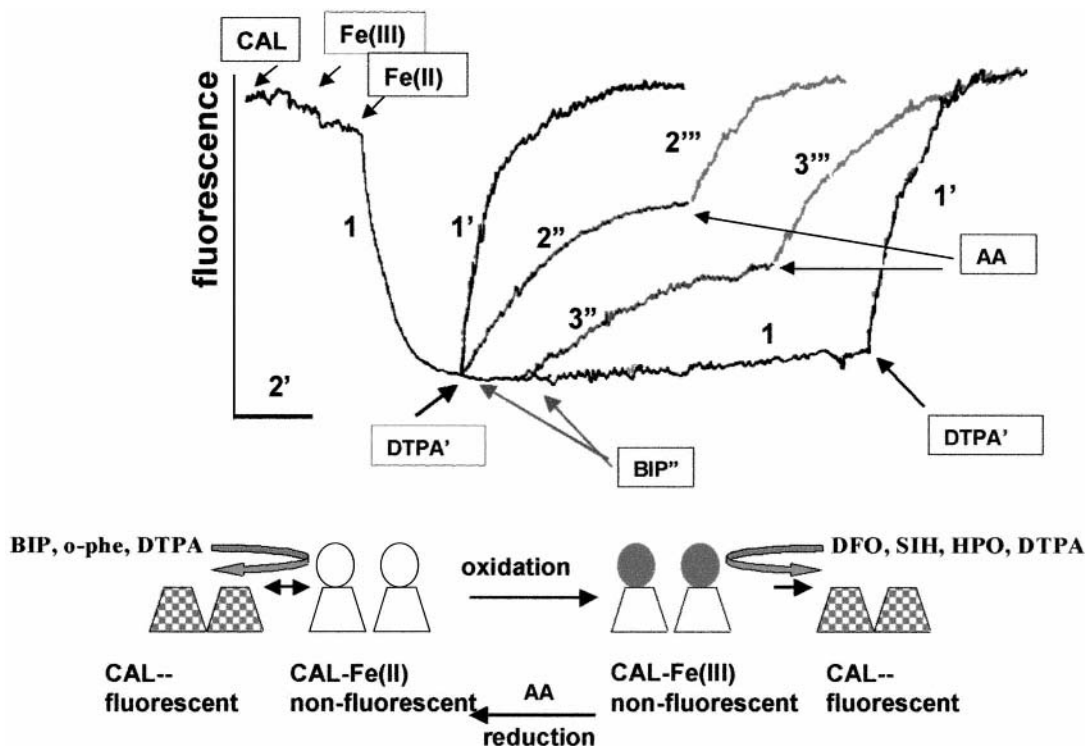


Figure 3 Oxidation of Fe(II) \rightarrow Fe(III) following Fe(II) binding to CAL in solution. The fluorescent CAL probe (100 nM) (filled trapezoid) swiftly binds Fe(II) (100 nM) (empty circle) in a physiological buffered salt solution (1), forming CAL-Fe (empty trapeze). Fe(III) is normally spared by CAL. The binding induces quenching of fluorescence and, in ambient conditions, also the oxidation of the Fe(II) into Fe(III) (filled circles). DTPA (1') added after quenching is almost complete fully restores the original fluorescence. However, the capacity of bipyridyl (BIP) or *o*-phenathroline (ophe) (100 μ M) for restoring the fluorescence (2'' or 3'') is partial and decreases with time, indicating oxidation of the CAL-bound iron(II) or CAL-Fe(II). Addition of 20 μ M dithionite (DT) (or ascorbate, not shown) reduces the CAL-bound iron(III), and weakens the metal binding, allowing BIP or ophe [iron(II) chelators] to scavenge the metal and restore fluorescence. Addition of the iron(III) chelators DFO, SIH, hydroxypyridinone, or others, restores the fluorescence from all quenched forms of CAL (in ambient conditions) by binding Fe(III).

respectively) and following fluorescence decay with time as an indicator of probe leakage. Influx of Fe(II) given as ferrous ammonium sulfate (FAS) is measured by following the time-dependent quenching of the fluorescence (Fig. 4). The latter can be taken as a direct measure for Fe(II)'s capacity to cross the membrane (i.e., membrane translocation) if it can be proven that the probe scavenges the metal within the vesicles and not in the medium, due to membrane leakage (4,10). The addition of the above antiprobe antibodies to the medium serves that purpose.

In typical experiments, human red blood cell ghosts (or any other vesicles) are loaded with the fluorescent probe (usually at 100 μ M during the resealing–rean-nealing process), washed from extravascular probe (by centrifugation, gel filtration,

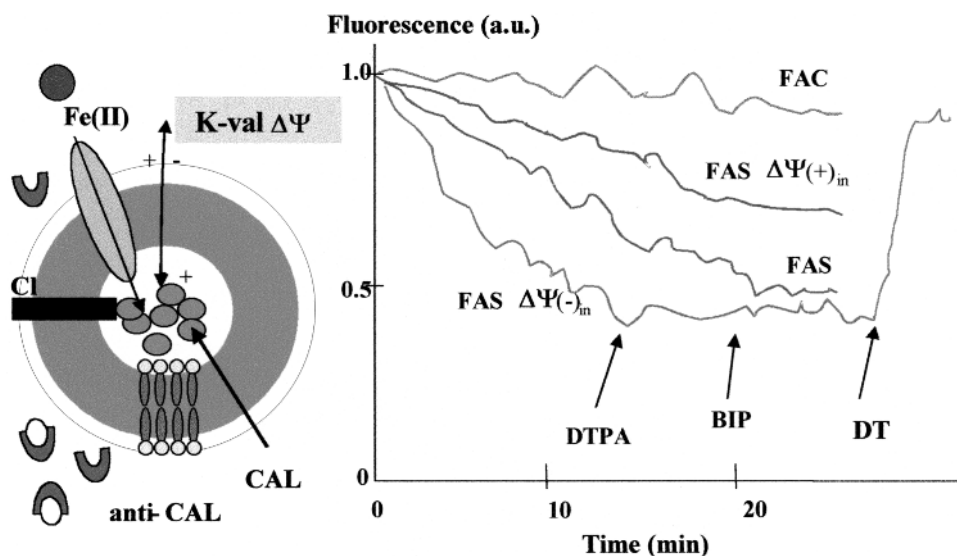


Figure 4 Iron uptake into membrane vesicles. Resealed ghosts (20- μ L packed human red cell ghosts) encapsulated with CAL (50 μ M) in Tris-NaCl (Tris 10 mM, NaCl 74 mM, KCl 75, pH 7.0, 37°C) and resuspended in the same medium containing anti-CAL antibodies. Upon exposure to FAS (20 μ M) but not FAC (50 μ M), there is a time-dependent fall of fluorescence that represents the entry of Fe(II) into the probe-enclosed compartment. Addition of 200 μ M DTPA stops Fe(II) influx, while addition of BIP has no effect unless the permeant reducing agent dithionite (DT, 500 μ M) is added. The latter leads to fluorescence recovery, due to reduction of the metal by DT and its scavenging by the permeant BIP. Substituting external Na^+ for K^+ ($K_{out}^+ \gg K_{in}^+$) and adding valinomycin (1 μ M) induces membrane depolarization [$\Delta\Psi(+)$] and decreases Fe(II) influx, whereas replacing the external K^+ by Na^+ ($K_{in}^+ > K_{out}^+$) hyperpolarizes the vesicle interior [$\Delta\Psi(-)$] and increases Fe(II) influx. Fluorescence is given as arbitrary units of intensity (a.u.)

or ion chromatography), and resuspended in a buffered salt solution containing the appropriate antiprobe antibodies (4×10^2). The vesicle suspensions are exposed to organic salts of either Fe(II) (FAS), Fe(III) ferric ammonium sulfate, (FAC), or other metals, and fluorescence is monitored with time. Figure 4 shows that Fe(II) but not Fe(III) gains access to the vesicle interior, that diethylenetriaminepentaacetic acid (DTPA) stops the influx, and that subsequent addition of permeating Fe(II) chelators such as α, α' -bipyridyl (BIP) or phen do not lead to fluorescence recovery, unless a permeant reductive agent such as dithionite (DT) is added (3). Thus, as the vesicles have no reductive capacity, the incoming Fe(II) oxidizes immediately upon binding to the probe. The intravesicular formation of CAL-Fe(III) is also corroborated by the differential response to a permeating chelator, salicylaldehyde isonicotinoylhydrazone (SIH) versus a nonpermeating chelator (DTPA) (not shown). The latter can also be used for stopping the influx of Fe(II), as well as for reversing the metal concentration gradient after a given accumulation of metal. However, Fe(II) efflux from vesicles can be obtained only if the intravesicular metal is reduced by addition of a permeant and strong reducing agent such as DT, and a favorable electrochemical potential is generated. Figure 4 demonstrates that Fe(II) influx is electrogenic to the

extent that it responds to changes in membrane potential (induced by adding valinomycin and modulating the K^+ -gradients inside versus outside the vesicles) and to anion substitution (gluconate for Cl^-). Similar experiments can be carried out with other fluorescence-modulating metals, particularly Cu. Finally, assuming the intravesicular concentration of probe is the same as that used during the resealing phase, the changes in fluorescence that reflect 1:1 binding of iron to probes such as FL-DFO can be easily transformed into concentration of Fe.

The method depicted in Fig. 4 can be applied for the parallel assessment of Fe(II) fluxes in a variety of experimental conditions using a 96-well plate and a fluorescence plate reader. The kinetic profiles of metal influx can be automatically transferred to a spreadsheet, normalized for the lowest (obtained with buffer alone, as control) and highest attainable (obtained in the presence of SIH) fluorescence levels, and plotted as a function of time.

IV. ASSESSMENT OF TRANSEPITHELIAL TRANSPORT OF IRON

The established human carcinoma Caco-2 cell line (13) is used for assessing iron absorption by intestinal epithelia in conjunction with FL-DFO or FL-green or CAL. Although derived from a colon carcinoma, Caco-2 cells display structural and functional characteristics of mature enterocytes and have been extensively employed as a model to study enterocyte epithelial biology (9). Caco-2 cells are grown for 7–10 days in transwell bicameral chambers with 3- μ m pore size, collagen-coated membranes (Costar, Cambridge), such that the membranes separate the upper apical from the lower basolateral compartment. Upon reaching confluence, the cells form tight junctions that are monitored electrically as a transepithelial electrical resistance (TEER) with a Millipore Millicell system. A resistance greater than 250 $\Omega \cdot \text{cm}^2$ is indicative of the formation of a tight monolayer. For studying trans-epithelial transport of Fe(II) from the apical to the basolateral side, FAS or FAC is added to the apical medium (top chamber) as a 20- μ M solution in HEPES buffered saline (HBS) medium, pH 7.0, and either FL-DFO (100 nM), CAL (100 nM), or FL-phen (300 nM) are added to the basolateral medium (lower chamber) (Fig. 5). The fluorescence can be monitored either directly and continuously by using a fluorescence plate reader while reading from the bottom side facing the basolateral surface, or samples can be taken from the lower compartment at given times and read in a spectrofluorimeter. Changes in the fluorescence intensity of the compartment facing the filter represent the appearance of iron crossing the basolateral membrane. In order to assess the tightness of the system, we use CAL-Fe (100 nM) in the lower compartment and the impermeant DFO (0.5 mM) in the upper compartment and verify that no DFO leaks through the system and reaches the lower solution. In the event of leakage, a time-dependent rise in fluorescence should result from DFO scavenging iron from the fluorescence-quenched CAL-Fe.

V. ASSESSMENT OF IRON TRANSPORT INTO LIVING CELLS

The major physiological substrate of cellular iron is Tf-bound iron, whereas non-Tf-bound iron (NTBI) is detected in pathological conditions of iron overload. Although the forms of NTBI have not been defined chemically, they probably represent a heterogeneous mixture of iron complexed to different serum components such as

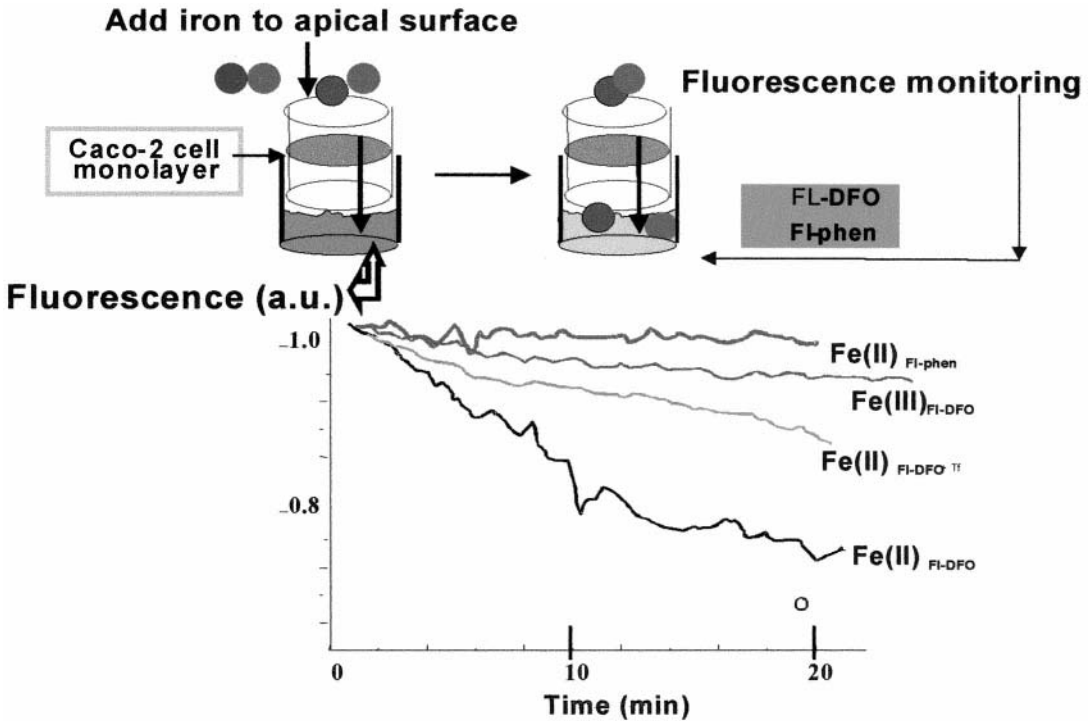


Figure 5 Transepithelial movement of iron. The fluorescent CAL, FL-DFO (100 nM) or FL-phen (300 nM) are added to the basolateral surface of Caco-2 cells (lower compartment) grown to confluence on collagen-coated filters in multiwell plates. To initiate the trans-epithelial flux of Fe(II) or Fe(III), either FAS or FAC (each at 20 μ M), is added to the apical surface and fluorescence in the lower compartment is recorded from the bottom of a 24-well culture plate (with a fluorescence plate reader, 485-nm excitation, 515-nm emission). As Fe(II) or Fe(III) emerges at the bottom layer binding to CAL, FL-DFO or FL-phen ensues and the fluorescence signal is quenched in a time-dependent manner.

citrate and amino acids. The NTBI composition probably varies qualitatively and quantitatively with the severity of iron overload. For assessing NTBI transport into cells, it is not obvious which form of iron should be used as substrate. For convenience, but not necessarily because of physiological or pathological relevance, most uptake studies rely on the use of organic salts of Fe(III) (citrate or ammonium citrate, nitrilotriacetic acid, etc.) or of Fe(II) (sulfate or ammonium sulfate or even ascorbate), usually in buffered saline medium.

For assessing Fe(II) ingress into living cells, the method based on FDM comprises the initial loading of CAL into cells via the nonfluorescent membrane-permeant acetomethoxy precursor, CAL-AM. Once inside cells, CAL-AM hydrolyzes enzymatically to yield fluorescent CAL, some of which binds iron associated with LIP. The intracellular concentrations of CAL generated are 1–10 μ M (10). Because some CAL might be surface-associated or might either egress or leak from some cells, we found it necessary to add fluorescence-quenching anti-CAL antibodies (anti-CAL) to the external medium, as in vesicle studies (Sec. III). The establishment of

a stable baseline in the presence of anti-CAL provides a measure for the tightness of the system in terms of cell integrity and membrane impermeability. For attached cells, it is possible to perfuse the system and focus the microscope-attached detection system on the cell layer for tracing intracellular iron with time. Figure 6 depicts iron transport into K562 cells using either Fe(II) or Tf-Fe(III) as substrate.

The results in Fig. 6 depict two iron transport properties of mammalian cells: (a) iron bound to Tf serves as the source and Tf-RME as the initial mechanism of iron delivery into the cytosol via endosomes, and (b) NTBI (artificially given as FAS) which is taken up by DMT1/Nramp2 directly into the cytosol. The iron transporter that might stimulate pathological NTBI entry into cells has not been identified

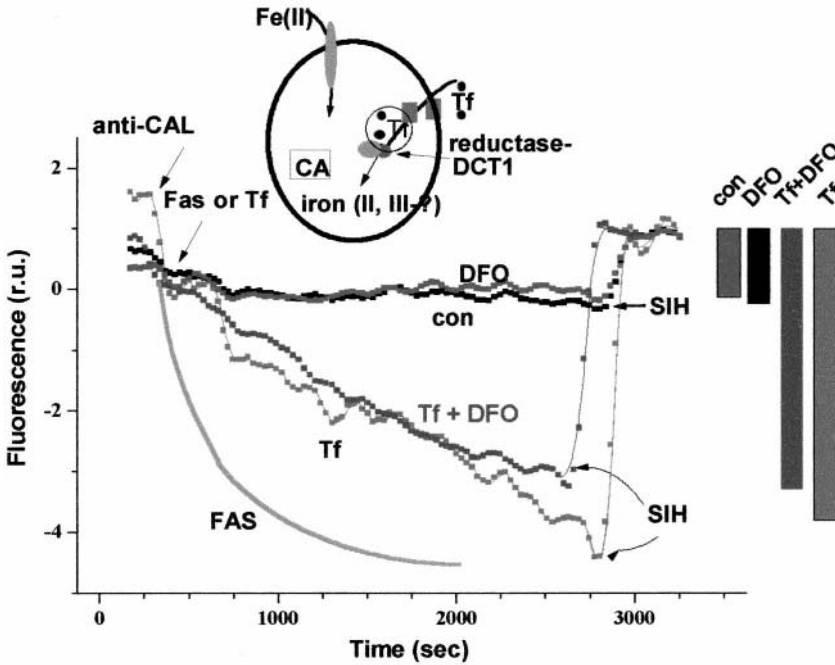


Figure 6 Iron influx into living cells grown in suspension. CAL-AM was added to cells in order to generate intracellular fluorescent CAL (filled circles), some of which binds iron (squares in the cell) associated with the labile (or chelatable) iron pool LIP, whereupon quenched CAL-Fe is formed. Anti-CAL antibodies are added in order to quench extracellular probe. A stable line is established in control cells (con) or in those treated with 50 μM DFO. When supplemented with SIH (100 μM), the fluorescence associated with those cells rises, indicating the release of intracellular CAL-Fe by SIH and providing a measure for LIP (see Fig. 8). The latter can be increased in a time-dependent manner by supplying the cells with 20 μM iron as Fe(II) or Tf (FAS or the Fe-saturated Tf, respectively). Fe(II) enters the cells via DMT1/Nramp2 and Tf-Fe by receptor-mediated endocytosis of Tf, both leading to a time-dependent decrease in the fluorescence signal, which can be restored by addition of the permeating SIH. The level of the latter attained at the point of addition of SIH is depicted as bars on the right. The height of each bar represents the level of fluorescence quenched by incoming iron, namely, the intracellular concentration of CAL-Fe, which for the control cells is ca. 300 nM.

for any disease of iron overload, or for conditions such as end-stage renal disease, in which erythropoietin-treated dialysis patients have to be supplemented with intravenous iron formulations, some of which produce transient iron overload (6). In K562 cells, iron derived from human Tf enters into the LIP and is visualized as a time-dependent decrease in fluorescence. The iron taken up by the cells is, in the short term, not accessible to the poorly permeant DFO. In MEL erythroleukemia cells (not shown), the quenching of cytosolic CAL is not observed when Tf serves as the iron source (unlike K562 cells), although Tf-bound radiolabeled iron is demonstrably taken up into these cells (Epsztejn, Glickstein, and Cabantchik, unpublished observations). On the other hand, when added as Fe(II), the metal that is taken up swiftly quenches the intracellular CAL fluorescence. The possibility that the bulk of the iron taken up via Tf in MEL cells (but not in K562 cells) initially bypasses the LIP, is in accordance with alternative pathways of intracellular iron traffic via direct organelle–organelle metal transfer (22) or shuttle protein-mediated transfer (26), as proposed for trafficking of Cu. However, with time, that putative delivery pathway is surpassed and iron starts to appear in the LIP (Epsztejn and Cabantchik, unpublished observations).

An important property seen in Fig. 6 is that the final level of fluorescence attained after addition of a permeant chelator such as SIH is similar for all the systems. The increment in fluorescence signal (FL, or the recovery of fluorescence), represents the cell iron originally bound by CAL (hence CAL-Fe), which is quantitatively related to the labile iron pool (LIP). Calculation of CAL-Fe and LIP demands knowledge of the intracellular concentration of CAL and the apparent K_d of the CAL-Fe complexes present in cells (see Table 1).

Table 1 Compilation of LIP Parameters Obtained with Various Cells Following Iron Loading and Chelator-Mediated Deprivation

Cells and treatments	[CAL] _{in} (μM)	[CAL-Fe] (μM)	[CAL] (μM)	[Fe] (μM)	[CAL-Fe + Fe] (μM)	NLIP
K562	2.8	0.29	2.51	0.025	0.315	0.113
K562 + DFO	2.8	0.15	2.75	0.012	0.162	0.058
U937	2.6	0.27	2.53	0.023	0.293	0.113
U937	9.3	1.60	8.70	0.040	1.640	0.176
U937 + DFO	15	1.05	13.95	0.017	1.067	0.071
U937 + FAC	6.1	2.40	4.70	0.112	2.512	0.412
Hepatocytes	3.7	0.70	3.00	0.051	0.751	0.203
Hepatocytes + DFO	4.6	0.20	4.40	0.010	0.210	0.046
Hepatocytes + FAC	2.9	2.10	0.80	0.578	2.678	0.923

The various parameters were calculated from data similar to those shown in Fig. 5 for K562 and in Fig. 3 for U937 cells. The representative experiments were chosen on the basis of similar [CAL]_{in} attained in the various cells. Rat hepatocytes (1 day in culture conditions), U937 cells, and K562 cells were incubated with either DFO (100 μM) or FAC (100 μM) for 18 h in full growth medium. [CAL]_{in} and [CAL-Fe] were determined experimentally for both treated and untreated cells. [Fe]_{in} values were determined experimentally for untreated cells using the K_d value of CAL-Fe of 0.22 μM (13). [Fe]_{in} for treated cells was calculated using the K_d values determined for untreated cells. N-LIP represents the total LIP measured with CAL, i.e., [Fe] + [CAL-Fe], normalized to the CAL level attained in cells, i.e., ([Fe] + [CAL-Fe])/[CAL]_{in} (13).

VI. ASSESSMENT OF LIP IN LIVING CELLS

LIP is the first cellular compartment populated by ionic iron entering cells, and it is the one from which iron is distributed to the other cell compartments or cell components. As a crossroads of iron traffic, LIP is surely to be heterogeneous and variable with time. However, as a regulated entity, cell LIP levels are likely to be maintained within certain limits. Thus, for the assessment of iron transport, it is important to have a measure of LIP both for defining the ionic gradients of the metal that are germane to the assessment of the transport mechanism, and for measuring transport per se.

A. Rationale

LIP comprises all the chelatable and rapidly exchangeable forms of cellular Fe whose liganded forms are collectively designated L-Fe, as depicted in Fig. 7 (10). All these forms are assumed to be in dynamic equilibrium with the soluble and free form of Fe(II), taking into account the spontaneous and mediated interconversions of Fe(II) and Fe(III). Addition of CAL shifts the equilibrium toward the CAL-bound form of iron, resulting in a proportional quenching of CAL fluorescence (Fig. 7a).

The CAL-Fe(II) form is apparently in equilibrium with Fe(II) present within or entering the cytoplasm, as observed by challenging cells with either permeant Fe(II) (FAS), diferric-Tf or Fe(II) or Fe(III) chelators (5,7,10). Addition of a membrane-permeant chelator will restore CAL fluorescence commensurately with the amount of Fe originally bound to CAL (Fig. 7). Thus, changes in “free” or soluble Fe(II), such as would occur during influx of Fe(II) from the medium, will be rapidly manifested as changes in CAL fluorescence intensity. The magnitude of the change, which is determined by addition of a permeant chelator in conjunction with measurements of total cell CAL, provides a means for calculating the amount of Fe bound to CAL, which we refer to as LIP(CAL-Fe) (Fig. 7b). Alternatively, Fe(II) can be estimated directly from the changes in CAL-fluorescence intensity by a calibration based on clamping the cell Fe(II) concentration by addition of the divalent metal ionophore A23187 in the presence of set concentrations of iron(II) (Fig. 7c). This method of measuring of LIP is analogous to routinely used methods for estimating changes in intracellular concentrations of ions such as Ca^{2+} and H^+ (i.e., pH) (25). We have demonstrated that, depending on experimental demands, measurements of LIP(CAL-Fe) and/or LIP(Fe) provide, separately or together, reliable measurements or estimates of the true LIP at discrete time points or continuously.

B. Advantages and Limitations of FDM for Assessing LIP

The major advantages of the above method are its application to living cells for:

1. *Monitoring LIP and changes in LIP either continuously (up to 1 h) or at periodic intervals*, with CAL being loaded into cells at each time point and LIP determined as above. In our experimental setup we can simultaneously monitor changes in LIP in four cell suspension systems using a four-cuvette rotating turret in equivalent controlled conditions.
2. *Monitoring LIP over a wide dynamic range of Fe concentrations*, spanning easily detectable intracellular (i.e., Fe quenchable) CAL concentrations from 0.1 μM and LIP(CAL-Fe) from 50 nM and upward. At this level,

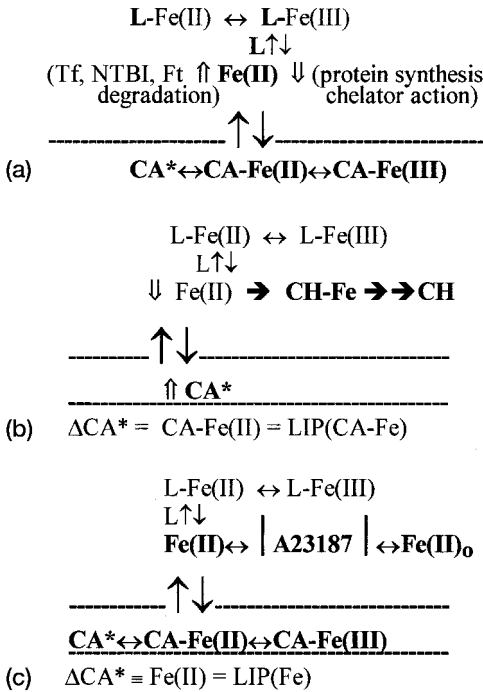


Figure 7 Dynamic equilibrium between Fe(II) and various cytosolic ligands (from Ref. 10). (a) Intracellular Fe can be increased (\uparrow) either by Tf or NTBI-mediated uptake of iron into cells or by FT degradation and lowered (\downarrow) either by metabolic utilization (heme and nonheme protein synthesis), chelation, or sequestration by FT. CAL loaded into cells, like resident low-affinity ligands (L), binds the free and soluble forms of Fe(II), some of which are oxidized to Fe(III). All these modalities were manifested as CAL fluorescence changes in solution and cells. CAL* and CAL denote the fluorescent (free) and quenched (iron-bound) forms of CAL, respectively, and Fe all the chelatable forms of iron which comprise the LIP. The broken line divides equilibrium reactions in the absence and presence of CAL. Panel (b) describes the equilibria in the presence of excess permeant chelator and highlights the key players in all the measurements; (c) describes the equilibration of intracellular Fe(II) with extracellular Fe(II)_{out}, mediated by the ionophore A23187, and highlights the components which play key roles in the calibration of changes in intracellular CAL in terms of Fe concentrations [LIP(Fe)]. The change in CAL* fluorescence which is elicited by addition of a chelator to (a) yields (b). In (b), the amount of fluorescence recovered (Δ fluorescence of CAL = Δ CAL*) is based on calibration of CAL-intracellular concentration, which provides an estimate of total CAL-bound iron, denoted LIP(CAL-Fe). In (c), Δ CAL* is converted into iron concentration based on calibration curves which relate CAL fluorescence quenching to Fe(II), thus providing an estimate of cytosolic Fe(II) [denoted as LIP(Fe)].

LIP(CAL-Fe) is almost equivalent to LIP(Fe) and the relative change elicited by the permeant chelator in resting cells is highest and sensitivity to Fe influx is near optimal. The range can be expanded by varying the concentrations of CAL, depending on the expected changes in LIP, i.e., increasing CAL for increased iron loads or decreasing CAL for iron depletion. An example is provided in Fig. 6, in which cells were exposed to Tf

or FAS, and Fe(II) influx was detected as a decrease in fluorescence followed continuously. The amount of Fe taken up is determined from the accumulated Δ LIP obtained by the addition of SIH.

3. *Measuring LIP in single cells* using the same apparatus but in conjunction with fluorescence microscope photometry. The method can be used to follow changes in individual glass-attached cells under perfusion, with the same degree of sensitivity as with cell suspensions (using 0.5×10^6 cells/mL) (4).
4. *On-line assessment of cell viability* or integrity, by following changes in fluorescence with time under stationary conditions. CAL leakage into anti-CAL antibody-containing medium is monitored as a time-dependent, irreversible (i.e., nonchelator-recoverable) reduction in fluorescence.

The limitations of the CAL-fluorescence-based LIP monitoring technique are:

1. *Variability of responses in some cell lines*, which demands the acquisition of calibration curves or look-up tables for each cell system, depending on its resting LIP levels and the magnitude of LIP changes induced by the various modulators.
2. *Possible contribution of metals other than iron* to changes in CAL-cell-associated fluorescence, particularly when evoked by extreme conditions of cell damage, such as following oxidative stresses. Thus far, we have not observed such a phenomenon in our experimental systems, although in cases of tissue damage, various metals, including Cu, might also be decompartmentalized or even released from cells.
3. *Chelatable iron pools that may not be accessible* to interact with CAL.
4. In the fluorescence imaging mode (conventional or confocal), resting LIP levels can only be measured in cells with CAL concentrations in the range of the free cytosolic Fe, due to inherent fluctuations in signal intensification. Although this can be partially overcome with cooled cameras, we have found that the method is applicable to cells with LIP(CAL-Fe) levels greater than $2 \mu\text{M}$.

C. Selected Examples of LIP Determinations in Model Cells

For routine measurements of LIP in cell suspension, one employs a conventional spectrofluorimeter with one to four cuvette holders and a stirring device. The same system can be used with cells grown on microscope cover slips that are positioned in standard cuvettes by appropriate holders. Alternatively, cells are placed in a perfusion chamber and analyzed by fluorescence microscopy-photometry or imaging. For the analysis, the following steps are taken.

Loading of cells is done by incubating cell suspensions or attached cells for 5 min at 37°C with 0.05 – $0.5 \mu\text{M}$ CAL-AM. These parameters (time, concentration, and temperature) determine the cytosolic CAL concentration and the sensitivity of the method, i.e., the level of iron responsiveness, which is inversely proportional to cytosolic CAL concentration. After washing, the cells can be kept in growth medium (no additives) at room temperature for up to 2 h. The target intracellular concentration of CAL is 1 – $5 \mu\text{M}$.

Fluorescence measurements are carried out in our laboratory in a PTI Felix Fluorescence Station (PTI Inc., Princeton, NJ) equipped with excitation and emission ratio facilities. When using cell suspensions, up to four systems can be followed simultaneously in equivalent conditions. The PTI system is also used as the excitation source in a fluorescence microscope (Nikon Diaphot) equipped with a 510-nm dichroic mirror and 520–560-nm emission filter set, and attached either to an ICCD camera (Hamamatsu) or a photomultiplier tube. Data analysis is done on computers interfaced to the above devices. Laser confocal microscopy is done with a Bio-Rad MRC-1024 system.

Estimation of LIP is described in Ref. 10. Cells are loaded with CAL to attain a cytosolic concentration of 1–5 μM , which binds a significant portion of the chelatable Fe and undergoes partial quenching. The cells are placed in minimal salt buffered medium (usually with 20 mM HEPES) with or without glucose (10 mM) but containing anti-CAL antibodies which, by quenching the fluorescence of CAL leaking out from cells, serve also as indicators of cell integrity. The amount of intracellular CAL quenched by intracellular Fe is revealed by addition of excess permeant chelators, which scavenge all the cytoplasmic iron, including the CAL-bound fraction. The amplitude of the chelator-mediated rise in fluorescence is equivalent to the amount of CAL-bound iron which is used for calculating either LIP(CAL-Fe) or LIP(Fe), depending on which method of calibration is applicable (see Fig. 8). Among the highly permeant and effective chelators used are BIP and SIH (5,7,10). The chelator-elicited change in fluorescence is converted either directly into change in CAL-Fe concentration (equivalent to bound Fe) using calibration curves of CAL and changes in Fe (equivalent to unbound Fe), or on the basis of calibration curves or look-up tables which relate quenching of CAL fluorescence to intracellular “free” Fe.

Calibration is based on measurements of changes in CAL-fluorescence, where LIP(CAL-Fe) is obtained by estimating the change in cell fluorescence elicited by addition of the permeant chelator SIH and the total CAL in cells is measured by permeabilizing cells (no anti-CAL present) with 1.5% octyl- β -D-glycoside in the presence of excess chelator, 500 μM DTPA. The fluorescence is followed after adding a known concentration of CAL. Calibrations of free Fe are performed by adding Fe(II) as FAS or Co(II) as CoCl_2 to CAL-loaded cells in the presence of ionophore A23187 (5–10 μM), and determining fluorescence intensities (Fig. 8). The value of the cell volume within the cuvette system used for the calculations of intracellular CAL are obtained experimentally by the [^3H] 3-*O*-methylglucoside tracer equilibration method described elsewhere (10) and counting the number of cells in a Coulter counter. Another mode of assessing LIP dynamics relates to the cellular capacity to restore LIP to homeostatic levels (1 to 3 h window) following an acute iron load (usually 10-min exposure to 50–100 μM FAS or 30-min exposure to 50–100 $\mu\text{g}/\text{mL}$ Tf). The marked rise in LIP is followed, after removal of the external iron source, by a time-dependent decay in LIP. The decay profiles depend on cellular capacities for utilizing the iron (e.g., erythroid cells use a substantial amount of incoming iron for heme synthesis) or liganding it by various mechanisms, such as sequestration by ferritin or other metal-binding moieties. The decay time provides a measure of the cell iron-buffering capacity, designated as LIP (IBC) (10,21). The FDM has allowed us to measure the dynamics of the LIP in various experimental conditions (10,21).

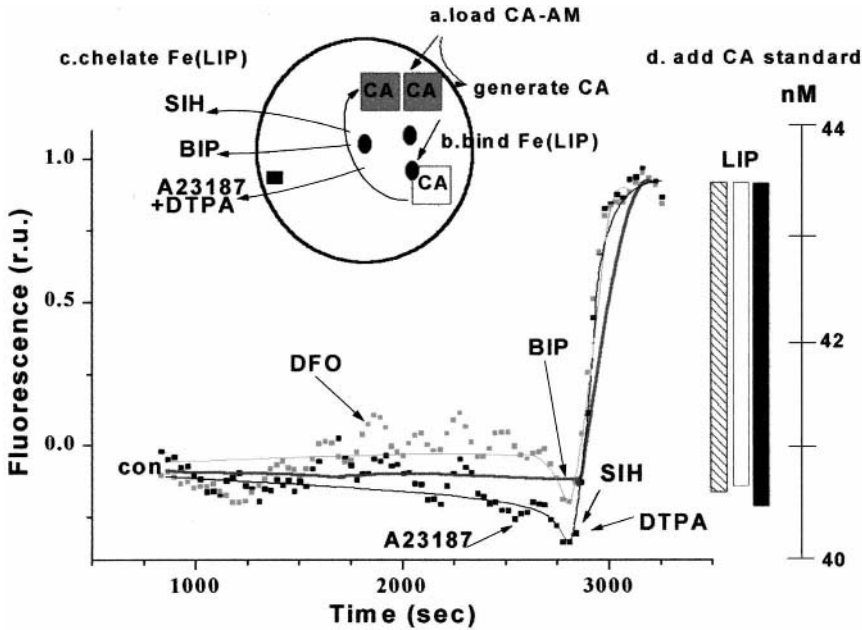


Figure 8 Steady-state LIP in cells grown in suspension (modified from Ref. 10). K562 cells (48 h culture, 5×10^5 cells/mL) were loaded with CAL-AM (0.25 μM for 5 min) (a) and resuspended in buffered HEPES medium. The generation of intracellular fluorescent CAL leads to binding of the probe to components of the LIP (b), whereupon a fraction of CAL fluorescence is quenched. Various permeant chelators are added in order to scavenge intracellular Fe and reveal the amount of CAL-Fe formed (c). Four identical systems of CAL-laden cells were monitored in parallel in terms of CAL fluorescence, and all systems but one (system 1) were supplemented with anti-CAL antibodies as described in previous figures. System 1 was used for calibrating the CAL signal, by adding CAL from a stock solution and generating a standard curve on top of the cell-associated signal (d). After a steady signal was attained, DFO was added to system 2 (final concentration 100 μM), in order to ascertain that all the CAL-bound iron was intracellular. In order to reveal the amount of iron (LIP) that binds to CAL in the cells (CAL-Fe), a permeant chelator (BIP or 100 μM) was added, leading to a rise in the fluorescence signal, ΔF . The same was done in the other systems by using either the permeant chelator SIH (100 μM) or DTPA (100 μM) in combination with the metal ionophore A23187 (2 μM). The ionophore subserves the translocation of the intracellular Fe(II) into the medium, where it is captured by the DTPA. The final levels of fluorescence attained were used for calculating the intracellular concentration of $[\text{CAL}]_i$, using the number of cells per milliliter in the system and the cell volume (10). The intracellular concentration of CAL-Fe was calculated as $\Delta F \times [\text{CAL}]_i$. LIP is calculated from the derived values of $[\text{CAL}]_i$, $[\text{CAL-Fe}]_i$, and the K_d of CAL-Fe measured in cells (13) (see Table 1).

D. Assessment of Fe Efflux from Cells

Iron efflux mechanisms operate primarily at the basolateral membrane of duodenocytes and in macrophages that process the hemoglobin released from phagocytosed cells (20). *Ireg1* or ferroportin has recently been proposed to be a gene coding for the putative iron efflux transporter [(21); see Chapter 7]. FDM can be used to trace

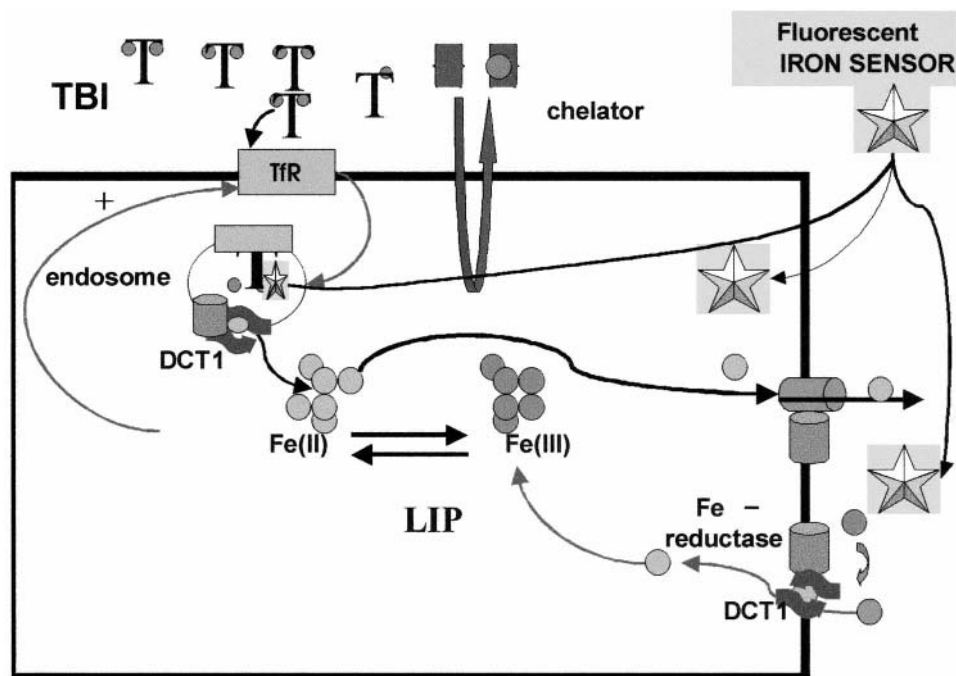


Figure 9 Cellular pools of chelatable iron and their assessment by FDM in combination with probe targeting. The scheme depicts the two major forms of iron acquired by cells, the physiological TBI (Tf or transferrin-bound iron) and one found in pathological iron overload, non-TBI (NTBI). TBI is delivered into cells by endocytosis of Tf via binding to its receptor R (TfR) followed by release, reduction to Fe(II), and translocation from the endosome via a putative transporter DMT1/Nramp2. NTBI ingress into cells is unclear. Ionic iron might be translocated into the cell via a process analogous to that of transport of iron from the endosome, which comprises both reduction and DMT1/Nramp2-mediated translocation. The transporters deliver iron to the cytosol, where they mix with the LIP of cells. The latter comprises both oxidation states of iron, weakly bound to a variety of both low- and high-molecular-weight ligands. From within the LIP, iron is distributed to all other cell compartments and components. The iron sensor consists of a metalosensitive probe that can be placed either intra- or extracellularly and used as a device to monitor changes in metal concentration in either compartment or in specific organelles. The sensor does not bind TBI or other forms of protein-bound iron (X). The sensors can be used to trace extracellular iron or iron associated with defined cellular compartments, particularly the cytosol, mitochondria, endosomes, and lysosomes. The later demands organellar targeting (see Fig. 10).

iron efflux from macrophages by using Tf-Fe as the iron substrate and FL-DFO or FL-Tf as the extracellular probe for iron that is processed by the cells and released into the medium.

VII. FUTURE DIRECTIONS

The fluoresceinated derivatives of EDTA, DFO, Tf, and phe might be considered first-generation probes for the detection of iron. As with fluorescent probes for the

detection of other inorganic ions such as Ca^{2+} , Mg^{2+} , H^+ , Cl^- , improved versions can be expected. Among the properties envisaged for future metalosensitive probes are: (a) enhanced specificity for iron and for other metals, (b) spectral fluorescence modulation by metal binding in order to carry out ratio fluorescence measurements, and (c) higher quantum yield. A potentially useful property of metalosensors is the possibility of targeting them to specific cell compartments or organelles for tracing the subcellular distribution of LIPs at precise locations within the cell (Fig. 9). Targeting strategies can be based on the unique properties of organelles and probes for selective accumulation of a probe in a particular organelle. Thus, the high negative membrane potential of mitochondria can be used for accumulating hydrophobic-cationic chelators and the acidity of lysosomes for accumulation of chelators with weak base properties (Fig. 10).

Notwithstanding its drawbacks, CAL, as well as the other fluoresceinated derivatives of DFO, Tf, and phe, are highly versatile probes that are likely to remain useful for the foreseeable future, particularly for the rapid and convenient screening of new iron chelators in solution, model cell systems, and living cells. Moreover, promising clinical applications of FDM using CAL and FL-DFO include monitoring serum NTBI and/or deranged cell LIP levels in hemochromatosis and thalassemia and assessing the efficacy of chelation therapy (6), and monitoring serum NTBI in intravenously iron-supplemented end-stage renal disease patients.

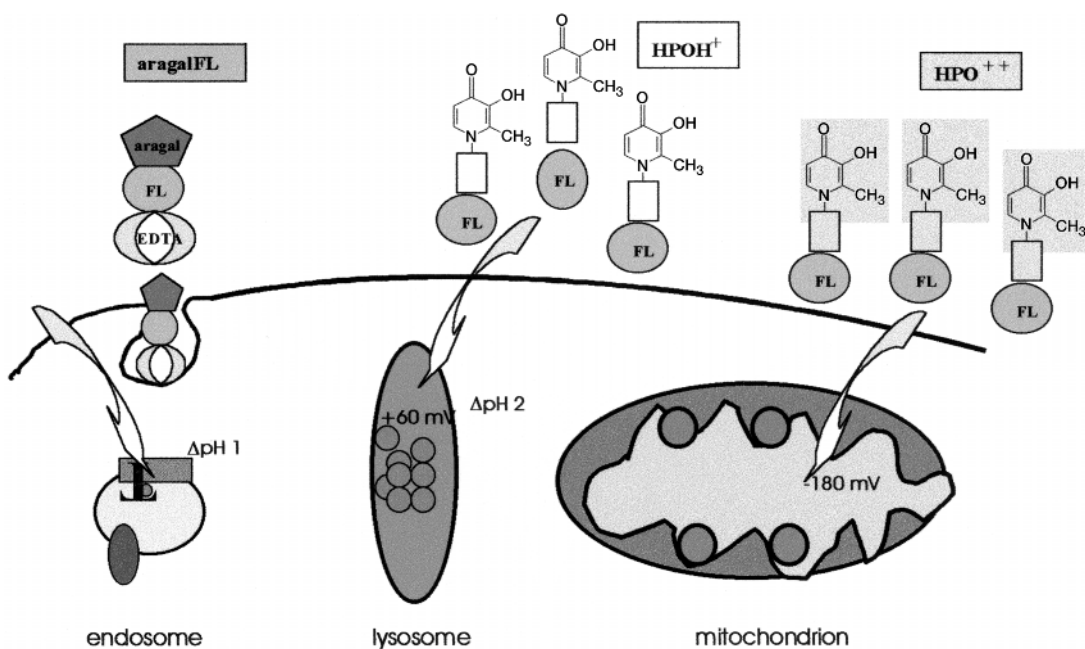


Figure 10 Targeting of dynamic fluorescent iron sensors to specific cell organelles. Hydroxypyridinones were selected for this study due to their 3:1 iron-binding stoichiometry, the possibility of coupling to them FL that renders them fluorescent, and the existence of a wide repertoire of derivatives with distinct chemical groups. Endosomal/lysosomal targeting is approached by endocytosis of macromolecules carrying FI-DFO or CAL.

ACKNOWLEDGMENTS

This work was supported in part by the Israel Science Foundation and the EEC (Biomed II).

REFERENCES

1. Aisen P, Wessling-Resnick M, Leibold EA. Iron metabolism. *Curr Opin Chem Biol* 1999; 3:200–206.
2. Andrews NC. The iron transporter DMT1. *Int J Biochem Cell Biol* 1999; 31:991–994.
3. Andrews NC, Fleming MD, Gunshin H. Iron transport across biologic membranes *Nutr Rev* 1999; 57:114–123.
4. Breuer VW, Epstejn S, Milgram P, Cabantchik ZI. Transport of iron and other related metals into cells as revealed by a fluorescent probe. *Am J Physiol* 1995; 268:1354–1361.
5. Breuer W, Epstejn S, Cabantchik ZI. Iron acquired from transferrin by K562 cells is delivered into a cytoplasmic pool of chelatable iron(II). *J Biol Chem* 1995; 270:24209–24215.
6. Breuer W, Hershko H, Cabantchik ZI. The importance of non-transferrin-bound iron in disorders of iron metabolism. *Transf Sci* 2000; 23:185–192.
7. Cabantchik ZI, Milgram P, Glickstein H, Breuer W. A method for assessing iron chelation in membrane model systems and in living mammalian cells. *Anal Biochem* 1995; 233:221–227.
8. Crichton RR. *Inorganic Biochemistry of Iron Metabolism*. New York, London, Toronto, Sydney, Tokyo, Singapore: Ellis Horwood.
9. Dix CJ, et al. The transport of vitamin B12 through polarized monolayers of the epithelial cell line Caco-2-cells. *Gastroenterology* 1990; 98:1272–1279.
10. Epsztejn S, Kakhlon O, Breuer W, Glickstein H, Cabantchik ZI. A fluorescence assay for the labile iron pool (LIP) of mammalian cells. *Anal Biochem* 1997; 248:31–40.
11. Fleming MD, Romano MA, Su MA, Garrick LM, Garrick MD, Andrews NC. Nramp2 is mutated in the anemic Belgrade (b) rat: Evidence of a role for Nramp2 in endosomal iron transport. *Proc Natl Acad Sci USA* 1998; 95:1148–1153.
12. Fleming MD, Trenor CC III, Su MA, et al. Microcytic anaemia mice have a mutation in Nramp2, a candidate iron transporter gene. *Nature Genet* 1997; 16:383–386.
13. Grasset E, Bernabeu J, Pinto M. Epithelial properties of human colonic carcinoma cell line Caco-2: Effect of secretagogues. *Am J Physiol* 1985; 248:C410–C418.
14. Gunshin H, Mackenzie B, Berger UV, Gunshin Y, Romero MF, Boron WF, Nussberger S, Hediger M. Cloning and characterization of a mammalian proton-coupled metal-ion transporter. *Nature* 1997; 388:482–488.
15. Halliwell B, Gutteridge MC. *Free Radicals in Biology and Medicine*. 3d ed. Oxford and New York: Oxford University Press, 1990.
16. Jacobs A. An intracellular transit iron pool. *Blood* 1977; 50:4331–4336.
17. Kozlov AV, Yegorov DY, Vladimirov YA, Azizova OA. Intracellular iron in liver tissue and liver homeogenate—Studies with electron paramagnetic resonance on the formation of paramagnetic complexes with desferal and nitric oxide. *Free Rad Biol Med* 1992; 13: 9–16.
18. Lytton SJ, Mester B, Libman J, Shanzer A, Cabantchik ZI. Monitoring of iron(III) removal from biological sources using a novel fluorescent siderophore. *Anal Biochem* 1992; 205:326–333.
19. McKie AT, Marciani P, Rolfs A, Brennan K, Wehr K, Barrow D, Miret S, Bomford A, Peters TJ, Farzaneh F, Hediger MA, Hentze MW, Simpson RJ. A novel duodenal iron-

- regulated transporter, IREG1, implicated in the basolateral transfer of iron to the circulation. *Mol Cell* 2000; 5:299–309.
20. Moura E, Noordermeer MA, Verhoeven N, Verheul AF, Marx JJ. Iron release from human monocytes after erythrophagocytosis in vitro: An investigation in normal subjects and hereditary hemochromatosis patients. *Blood* 1998; 92(7):2511–2519.
 21. Picard V, Epsztejn S, Santambrogio P, Cabantchik ZI, Beaumont C. Role of ferritin in the control of the labile iron pool in murine erythroleukemia cells. *J Biol Chem* 1998; 273(25):15382–15386.
 22. Richardson DR, Ponka P. The molecular mechanisms of the metabolism and transport of iron in normal and neoplastic cells. *Biochim Biophys Acta* 1997; 1331:1–40.
 23. Riedel HD, Remus AJ, Fitscher BA, Stremmel W. Characterization and partial purification of a ferrireductase from human duodenal microvillus membranes. *Biochem J* 1995; 309:745–748.
 24. Rothman RJ, Serroni A, Farber JL. Cellular pool of transient ferric iron, chelatable by deferoxamine and distinct from Ft, that is involved in oxidative cell injury. *Mol Pharmacol* 1992; 42:703–710.
 25. Tsien RY. Fluorescent probes of cell signaling. *Annu Rev Neurosci* 1989; 12:227–253.
 26. Vulpe CD, Kuo YM, Murphy TL, Cowley L, Askwith C, Libina N, Gitschier J, Anderson GJ. Hephaestin, a ceruloplasmin homologue implicated in intestinal iron transport, is defective in the sla mouse. *Nature Genet* 1999; 21:195–199.
 27. Wessling-Resnick M. Biochemistry of iron uptake. *Crit Rev Biochem Mol Biol* 1999; 1934:285–314.
 28. Yu J, Wessling-Resnick M. Structural and functional analysis of SFT, a stimulator of Fe transport. *J Biol Chem* 1998; 273:21380–21385.

Regulation of Intestinal Iron Transport

GREGORY J. ANDERSON

Queensland Institute of Medical Research, Brisbane, Queensland, Australia

CHRISTOPHER D. VULPE

University of California, Berkeley, California

I. INTRODUCTION	560
II. FACTORS THAT MODULATE IRON ABSORPTION	562
A. Iron Stores	563
B. Erythropoiesis	563
C. Hypoxia	564
D. Neonatal Life	564
III. SPATIAL AND TEMPORAL ASPECTS OF REGULATION	565
A. Specialization of the Proximal Small Intestine	565
B. The Delayed Response to Absorption Signals	565
IV. REGULATION OF INDIVIDUAL STEPS	566
A. The Rate-Limiting Step in Iron Absorption	566
B. Brush Border Uptake	567
C. Intracellular Events	569
D. Basolateral Transfer	570
E. Iron Delivery to the Plasma	571
V. MECHANISMS OF REGULATION	572
A. Role of Mucosal Iron Status	572
B. Regulation by Other Stimuli	573
C. Molecular Basis of Regulation	574
VI. RECEIVING AND TRANSDUCING SIGNALS FROM THE BODY	575

VII. SIGNALS FOR THE CONTROL OF IRON ABSORPTION	579
VIII. LOCAL REGULATION OF ABSORPTION—MUCOSAL BLOCK REVISITED	580
IX. SUMMARY AND FUTURE DIRECTIONS	582
REFERENCES	584

I. INTRODUCTION

The acquisition of dietary iron by the small intestine is a process which is tightly linked to the body's iron needs. Early studies of body iron turnover showed that humans have only a limited capacity to excrete iron (1), so the regulation of the body iron content must be achieved at the point of absorption. The daily intake of iron is finely tuned to replace the small amounts lost through the exfoliation of skin and gastrointestinal cells, and in bile and urine (2). In the adult human male, this represents approximately 1 mg of iron per day, while human females absorb 1.5–2 mg per day to account for the additional iron losses associated with menstrual bleeding. Although some other species are able to excrete somewhat greater quantities of iron than humans (3), the same basic factors which regulate iron absorption in people appear to operate in other mammals.

Iron is present in the diet in a wide range of forms, but in simplified terms the iron absorbed by the intestine can be considered as either inorganic ferrous (Fe^{2+}) or ferric (Fe^{3+}) iron, or as heme iron. Smaller amounts of iron may be absorbed bound to proteins, notably lactoferrin, but these will not be considered in this chapter. The initial stages in the absorption of heme and nonheme iron are different and heme iron is absorbed more efficiently (2,4), but once within the absorptive cells of the intestinal epithelium, the various forms of iron appear to enter a common "transit" pool, and their subsequent transfer to the body is similar (5).

It is convenient to divide the process of intestinal iron absorption into several phases or steps (Fig. 1). The first is the luminal phase—the processing of iron in the intestinal lumen which makes it available or unavailable for absorption. While the interactions between iron and various dietary constituents have a considerable influence on how much iron is absorbed and are the subject of an extensive literature (e.g., Ref. 6), they do not appear to be regulated by body iron requirements and will not be considered further here. The next stage is the brush border or uptake phase—the binding to and transport of iron across the brush border of the intestinal epi-

Figure 1 Factors that influence intestinal iron absorption. The amount of iron entering the body is ultimately determined by body iron requirements. Systemic stimuli act on the crypt cells to influence the expression of molecules involved in iron transport across the mature enterocytes, while various mucosal factors are important in mediating this response. The constituents of the diet also play a major role in influencing how much iron is absorbed.

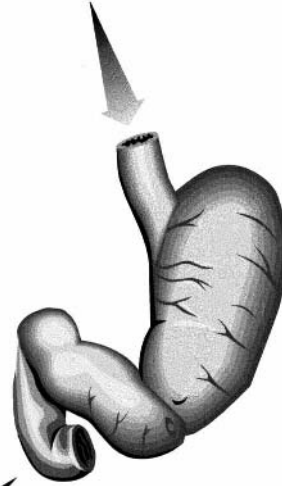
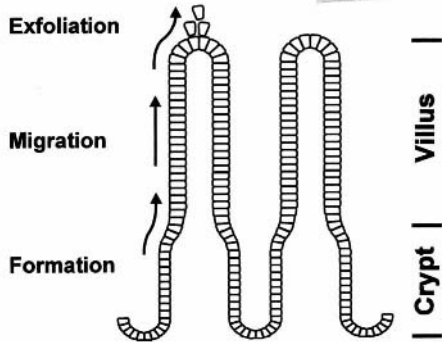
DIETARY IRON

Systemic

- Body iron stores
- Erythropoiesis
- Hypoxia
- Disorders
e.g. hemochromatosis
thalassemia

Mucosal

- Cell migration time
- Differentiation
- Surface area

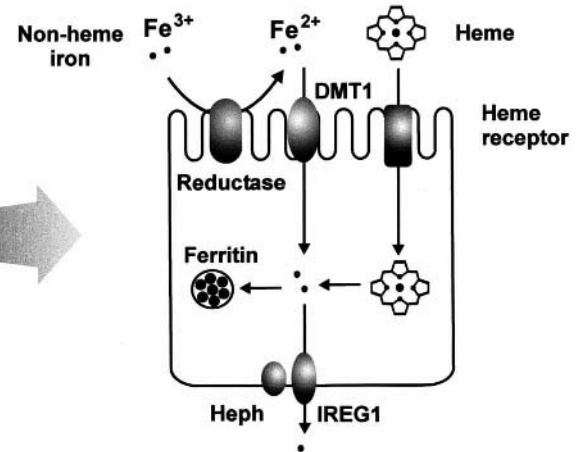


Luminal

- Amount
- Chemical form
- pH
- Chelation
- Other metals
- Intestinal motility

Cellular

- Iron content
- Gene expression
- mRNA stability
- Protein trafficking



thelial cell (or enterocyte). While the intestine can absorb iron in both the ferrous and ferric forms, there is a growing body of evidence that ferric iron must be reduced to the ferrous form before it can traverse the brush border and that a brush border enzyme, a ferric reductase, mediates this process (7–9). The membrane metal transporter DMT1 appears to be responsible for most of the brush border iron traffic and it utilizes ferrous iron as a substrate (10,11). However, other proteins may also be involved. For example, an iron transit pathway involving an integrin and a protein designated mobilferrin has been described (12). After crossing the brush border, iron enters an ill-defined intracellular phase prior to its passage across the basolateral membranes and into the circulation. Within the enterocyte, iron is probably chelated by low-molecular-weight organic acids such as citrate, but binding to protein ligands may also occur. Iron which is not transferred to the body is bound by ferritin within the enterocyte and ultimately is lost when the epithelial cells are sloughed at the villus tip. The movement of iron from the epithelial cells into the body is known as the basolateral or serosal transfer phase of iron absorption. The ceruloplasmin homolog hephaestin (13) is important for iron transfer, and strong circumstantial evidence suggests that the basolateral iron transporter Ireg1 is also required [(14–16); and see Chapter 7 for a detailed discussion]. In simplified terms, the transit of iron across the intestinal epithelium is usually discussed in terms of two stages: (a) iron uptake, the movement of iron from the lumen into the epithelial cells, and (b) iron transfer, the handling of iron within the enterocytes and its subsequent passage across the basolateral membranes into the body. More details on the specific components of the intestinal iron transport pathway may be found in other chapters in this volume. The following discussion will focus on the regulation of the transport steps and how they are affected by changes in body iron requirements.

II. FACTORS THAT MODULATE IRON ABSORPTION

The amount of iron entering the body at any one time is determined by the body's iron requirements. Consequently, changes in the two largest pools of iron within the body—storage iron and iron in the erythroid mass—exert the greatest influence on iron absorption. Absorption is increased when body iron stores are low, or when the erythropoietic rate is increased, and vice versa in times of iron sufficiency or when erythropoiesis is reduced. Other situations in which absorption is increased include chronic hypoxia, pregnancy, and in the newborn. Whether these disparate stimuli alter iron absorption via a common mechanism or whether more than one mechanism is involved has yet to be firmly established.

Most of the following discussion concerns nonheme iron absorption. The absorption of heme iron is also affected by variations in iron status and erythropoiesis, and in the same direction as the effects on nonheme iron, but the magnitude of the response for heme iron is smaller (17–20). After heme has entered the enterocyte and iron has been released from the protoporphyrin ring, the liberated iron follows the same pathway to the body as recently absorbed nonheme iron, and thus this component of intestinal iron transit would be regulated similarly for both forms of iron.

A. Iron Stores

Body iron stores appear to be the most important factor regulating nonheme iron absorption in the normal individual. In both humans (e.g., Refs. 21–26) and other animals (e.g., Refs. 27–32), an inverse relationship exists between iron stores and absorption, with depleted stores leading to increased absorption and elevated stores depressing the process. In discussing the ability of the body to alter its iron absorption to accommodate small variations in iron stores, normal iron losses, and the requirements of growth and menstruation, Finch has coined the term the “store regulator” (33). The store regulator has a limited capacity to alter absorption, of the order of 1–2 mg per day, but this is sufficient to cater for most day-to-day iron demands. Furthermore, the body appears to have an optimum level of storage iron; in a normal adult male this is approximately 1 g. If stores drop below this level, absorption is increased until they are replenished, whereas if stores are above this level absorption will decline until equilibrium is regained (20,26,34,35). Indeed, under normal conditions, once iron stores have reached the optimum level, it is difficult to induce the body to accumulate more even if the iron content of the diet is increased significantly. The increased iron absorption seen in pregnancy (36–38) is accompanied by a decrease in maternal iron stores (39), and thus may be a secondary reflection of maternal iron status.

The capacity of the body to regulate its iron levels by varying iron excretion is very limited, at least in humans (2). The daily losses of iron are small and obligate, and there does not appear to be an active excretion mechanism. Losses do seem to be lower in iron deficiency and higher when stores are replete or elevated (40), but this probably only reflects the fact that the epithelial cells that are sloughed each day contain levels of iron that reflect whole-body iron status due to the equilibrium that exists among all cells in the body; the losses are passive, not active.

B. Erythropoiesis

The other major physiological process influencing iron absorption is erythropoiesis. Within the body, the single most significant sink for iron is the erythroid marrow, where iron is utilized both to meet the metabolic requirements of developing red blood cells and for incorporation into newly synthesized hemoglobin. The rate of erythropoiesis has been shown to have a direct relationship to iron absorption in animal studies (21,27,41–43), and in humans, iron absorption is enhanced when erythropoiesis is stimulated by bleeding or acute hemolysis (21,44), or following androgen or erythropoietin treatment (18,45), and decreased following hypertransfusion (21) or radiation treatment (46). The capacity of the body to increase its absorption in response to an increased erythroid demand is very high, and in iron deficiency anemia, for example, individuals may absorb over 20 mg per day provided intestinal iron supply is sufficient (2,33). The magnitude of this response is far greater than that possible with the store regulator, and Finch has proposed a second regulatory pathway mediated by the “erythroid regulator” (33). This regulatory mechanism serves to protect the iron-hungry erythroid pathway from an inadequate iron supply. The strength of the erythropoietic effect on absorption is such that it can override the effect of the store regulator. Thus, in β -thalassemia, absorption

continues in the face of elevated body iron stores (44,47), and in the iron-loading disorder hemochromatosis, venesection therapy will stimulate absorption even though iron stores may be greatly elevated (48).

The rate of erythropoiesis per se is not a major determinant of iron absorption. In chronic hemolytic states in humans the absorption rate is usually normal (2), presumably because the return of iron to the marrow following red cell destruction is sufficiently rapid to meet the increased erythroid iron demand. However, once the ability to meet the marrow's requirements by catabolism of red cells or mobilization of storage iron is exceeded, an increase in iron absorption will result (33). In support of this, the absorption response in rats following erythropoietin treatment can be prevented by prior iron loading of the reticuloendothelial system using iron dextran (49). The situation is complicated in iron-loading anemias such as β -thalassemia and sideroblastic anemia, in which absorption is elevated despite the apparent adequacy of iron supply to the marrow. The common feature of these conditions is that erythropoiesis is markedly ineffective (2,47). The physiological response to ineffective erythropoiesis is a very high rate of iron uptake by the erythroid marrow as it perceives its iron supply to be inadequate. Consequently, the marrow continues to acquire iron at a very high rate that exceeds the rate at which iron can be recycled from the reticuloendothelial system. The body is unable to recognize that the recycled iron is not being used appropriately. Thus, it appears that adequacy of marrow iron supply and the rate of effective erythropoiesis are important determinants of iron absorption.

C. Hypoxia

Of other influences on iron absorption, perhaps the most extensively studied is hypoxia. It has been known for many years that absorption is increased under hypoxic conditions, and returns to normal after the hypoxic stimulus is removed (43,46,50). Part of the effect of low oxygen tensions can be ascribed to alterations in the rate of erythropoiesis, but a component of the response is independent of these effects (46,51–53). Indeed, an effect of hypoxia on iron absorption can be observed before a response from the erythroid marrow (50). This rapid response suggests that hypoxia may exert at least some of its influences directly on the intestinal enterocyte. However, the mechanism by which hypoxia effects intestinal iron transit has yet to be elucidated.

D. Neonatal Life

Changes in iron absorption are also found during postnatal development. In the immediate postnatal period, during suckling, iron absorption is greatly elevated (54–58). This occurs at a time when the iron requirements associated with rapid growth are particularly high, yet dietary iron availability is very limited. The neonate's intestine is thus specially adapted to extract as much iron as possible from the diet. The elevated iron absorption of neonates has been best studied in animals and appears to last from birth to about the time of weaning. After weaning, absorption drops nearly to adult levels, although it remains slightly elevated above the final adult level until growth has been completed. The mechanism of the high neonatal absorption is unknown. Most studies have suggested that specific iron uptake mechanisms are activated, but some have proposed that it may reflect the generalized high

level of macromolecule uptake which is characteristic of the immature intestine (54,59).

III. SPATIAL AND TEMPORAL ASPECTS OF REGULATION

A. Specialization of the Proximal Small Intestine

Quantitatively, the most important site of iron absorption is the proximal small intestine (duodenum and upper jejunum) (30,60–64). However, small amounts of iron may be absorbed from the stomach (65,66), ileum (60,67,68), and colon (68,69). The higher absorption across the proximal small intestine may be ascribed in part to luminal factors (such as the exposure of the proximal region to higher concentrations of dietary iron and a lower pH) and intestinal motility (2), but a number of studies suggest that it is an intrinsic property of the gut mucosa in this region (70–75). The recent demonstration that the brush border and basolateral iron transporters DMT1/Nramp2 and Ireg1, respectively, are expressed at high levels in the proximal small intestine but at much lower levels in the distal parts of the gastrointestinal tract provides a molecular explanation for this specialization (10,14,15,76). At the cellular level, iron absorption occurs through the differentiated epithelial cells of the mid- and upper villus, rather than across the immature crypt cells (77), and it is to these cells that the critical molecules of intestinal iron transit (DMT1/Nramp2, hephaestin, and Ireg1) are localized (10,13–16,76). Finally, there is some evidence that in times of increased body iron requirements there is anatomical adaptation of the small intestine to increase the effective absorptive area and consequently the capacity of the intestine to absorb iron. Thus, in hemolytic anemia a larger proportion of the villus enterocytes participate in absorption (78), in pregnancy villus size is increased (79), and in iron deficiency absorption extends more distally in the small intestine (62).

B. The Delayed Response to Absorption Signals

An understanding of the regulation of intestinal iron absorption requires an appreciation of the temporal aspects of the response of the small intestine to a stimulus to alter the process. Most of the factors which affect iron absorption (e.g., bleeding or changes in iron stores) do not do so instantaneously. Only after a lag period of 2–3 days is an alteration in absorption observed (e.g., Refs. 2,5,80–83). The probable cause of this delay in absorption relates to the life span and degree of differentiation of the intestinal epithelial cells. These cells are formed in the intestinal crypts, then migrate up the villus and differentiate into mature absorptive enterocytes that ultimately undergo apoptosis before being exfoliated at the villus tip, a process requiring 2–3 days. There is considerable evidence that the developing epithelial cells in the crypt receive signals from the body to alter absorption, but can only translate these signals into an absorption response after they have migrated up to the villus and differentiated into mature enterocytes. For example, one of the most important of these signals is the iron content of the crypt cells (this will be considered in more detail below). Autoradiographic studies (77,84,85) have clearly shown that orally administered radioactive iron (newly absorbed iron) is incorporated into the cells of the mid- to upper villus in the duodenum, but radioiron administered intravenously is localized to the cells of the intestinal crypts. This crypt cell iron is found progressively farther up the villus over a period of several days as the cells mature and

differentiate (84,85). Thus, while the crypt cells can take up iron from the body, the ability of mature enterocytes to take up circulating iron appears to be extremely limited. Most of the iron taken up by crypt cells is likely to be bound to plasma transferrin (Tf), and the localization of the transferrin receptor (TfR) to these cells supports the concept that they form an important interface with the body in controlling iron absorption. HFE, the protein mutated in hereditary hemochromatosis [(86); see Chapter 8], is known to play a role in the regulation of iron absorption, perhaps by interacting with the TfR, and its localization to the crypt cells reinforces their importance in regulating absorption (87). Taken together, these observations support the model that the delayed iron absorption response following a corporeal signal reflects the time it takes intestinal crypt cells to differentiate and migrate up the villus, and highlight the critical role of crypt enterocytes in sensing body iron requirements.

IV. REGULATION OF INDIVIDUAL STEPS

A. The Rate-Limiting Step in Iron Absorption

The debate as to whether brush border iron uptake or basolateral iron transfer is the rate-limiting step in iron absorption has not been resolved, and it appears likely that neither uptake nor transfer may be universally rate-limiting. The step which is rate-limiting in any one situation depends on the iron status of the individual, the nature of the signal for iron absorption, and the species studied. Since the amount of iron crossing the basolateral membranes cannot exceed that crossing the brush border membranes, basolateral transfer would seem the best candidate for the rate-limiting step.

Computer modeling of iron kinetics in the normal dog has indicated that a rate-limiting uptake step would best explain the distribution of luminally administered radioiron in animals with normal iron stores, and following bleeding to iron deficiency (29). However, in the normal human rate constants for both uptake and transfer were similar (88), and physiological studies have provided support for a rate-limiting transfer step. The response of iron absorption to changes in iron status in rats suggests that not only is serosal transfer rate-limiting, the effects are more restricted to the duodenum (36,61,64,74,89,90). In humans, both iron uptake and iron transfer are increased in iron deficiency, but the proportional increase in transfer is much greater (48,91). However, these findings are by no means universal, as both uptake and transfer are clearly elevated in iron deficiency (see below), and in many studies elevated uptake seems to be more important (61,92–96). Indeed, in a recent kinetic study, transfer was found to be neither iron-regulated nor rate-limiting (97). Discrepancies in experimental findings may reflect factors such as species differences and the nature of the intestinal preparation used. Furthermore, the demonstration that either uptake or transfer is increased or decreased per se does not imply that a particular step is rate-limiting, and only when more detailed kinetic studies are carried out can such conclusions be drawn.

Much of our understanding of the regulation of iron absorption has come from studying hereditary hemochromatosis (see Chapter 28). In this condition, the body continues to accumulate excessive amounts of iron from the gastrointestinal tract despite high body iron stores, suggesting that the small intestine is unable to rec-

ognize effectively that the body is iron-loaded. Despite this, iron absorption is still regulated in hemochromatosis, as increasing stores will depress absorption and phlebotomy therapy will increase it (48,98,99). However, the amount of iron required to produce a given reduction in iron absorption is much higher in hemochromatosis patients than it is in unaffected individuals. Various kinetic studies have shown clearly that the inappropriately high iron absorption in hereditary hemochromatosis is associated with an elevated rate constant for the transfer step (48,88,91). This conclusion is supported in a mouse model of hemochromatosis (the β_2 -microglobulin knockout mouse), although an elevation in uptake was also observed in this system (100). There is also some evidence for increased brush border uptake in duodenal biopsies from hemochromatosis patients but these studies could not distinguish between uptake and transfer, and no firm conclusion about which step was rate-limiting was possible (101–103). Overall, the available data support the concept that basolateral transfer is the rate-limiting step for absorption when the stimulus is altered body iron stores.

The relative importance of changes in uptake or transfer following other stimuli that alter iron absorption is also unclear. Some studies suggest that the increase in iron absorption following the stimulation of erythropoiesis can best be explained by a rate-limiting serosal transfer step (53,104), while kinetic analyses of iron absorption in acutely hemolyzed and polycythemic animals show that brush border uptake is rate-limiting (105,106), or that both uptake and transfer are stimulated (100). Hypoxia seems to exert several effects. Acute hypoxia stimulates the brush border uptake of ferric iron, but chronic hypoxia stimulates both uptake and transfer, the latter effect predominating from about one day after the period of hypoxia is commenced in mouse studies (32,53,75). The delayed response in chronic hypoxia may reflect changes in erythropoiesis.

Analysis of the expression of DMT1/Nramp2, the major brush border iron transporter, provides support for the notion that the uptake step of absorption is not rate-limiting for absorption, at least under some circumstances. Under conditions of iron deficiency, the expression of DMT1 is very high (10,76,107), and its increase relative to the iron-sufficient state far exceeds the increase in iron absorption induced by iron deficiency. Under iron-deficient conditions, basolateral transfer is likely to be rate-limiting, while brush border transporter expression is stimulated to a high level to maximize iron entry from the lumen and ensure a continued supply of iron to the basolateral transport machinery. A similar large increase in DMT1 (10- to 100-fold) has been reported in hemochromatosis (108), although absorption itself is only increased severalfold. Again the data suggest that brush border uptake is not rate-limiting, in agreement with earlier kinetic and physiological studies.

B. Brush Border Uptake

There is abundant evidence that brush border iron uptake is inducible by iron deficiency and decreases with iron overload (e.g., Refs. 24,72,92,109,110). This effect is seen on both nonheme and heme absorption, although the magnitude of the effect on heme absorption is smaller. Some studies have shown that stimulation of erythropoiesis will enhance brush border iron transport (100,110,111), but most studies suggest that the increase in the transfer step is more significant (45,53,104). Brush border uptake is also enhanced by acute hypoxia, but the effect appears to be re-

stricted to Fe^{3+} , as Fe^{2+} transport is not altered (32,53,75,112–115). Chronic hypoxia leads to increases in both uptake and transfer.

The identification of DMT1/Nramp2 as an important [and probably the major (10,11,116,117)] brush border iron transporter has provided considerable insight into how this step of iron absorption is regulated. The levels of both DMT1 mRNA and protein are elevated under conditions of chronic iron deficiency and depressed in iron-loaded states, and this provides an explanation for the alterations in iron transport that are observed under these conditions (10,76). As noted in the previous section, the expression of DMT1 is very sensitive to alterations in intracellular iron levels. The presence of a consensus iron-responsive element (IRE) in the 3'-untranslated region of the *DMT1* mRNA (see Chapter 6) provides a mechanism for this regulation via the iron-regulatory protein (IRP)/IRE system, and the mode of regulation is predicted to be similar to that of the TfR, where low iron levels stabilize the mRNA (10). Thus, under iron-deficient conditions, *DMT1* mRNA would be stabilized and more DMT1 protein would be translated. Recent evidence suggests that the level of DMT1 can be modulated via local changes in iron content in the mature enterocytes (118,119), but it is less clear whether changes in systemic iron metabolism have a direct influence on *DMT1* mRNA levels or whether the observed modulation is secondary to changes in local enterocyte iron levels. This will be considered in more detail below.

Perhaps as important as the level of DMT1 protein in determining the level of brush border iron uptake is the subcellular location of that protein. Several groups have provided evidence that under iron-sufficient conditions DMT1 shows a predominantly intracellular distribution, but that under iron-deficient conditions it can traffic rapidly to the brush border membrane (76,107,119). The combination of increased stability of *DMT1* message and rapid translocation to the brush border membrane under iron-deficient conditions provides a mechanism for rapidly enhancing iron uptake into the enterocytes in times of increased iron demand. If animals on an iron-deficient diet are transferred to a diet of higher iron content, DMT1 appears to be rapidly internalized by the enterocytes and then degraded (119). The mechanisms underlying the traffic of DMT1 in response to changes in cellular iron status are currently under investigation.

The modulation of DMT1 levels does not provide the only mechanism for regulating the entry of iron into duodenal enterocytes. Changes in the level of a brush border ferric reductase are also likely to be important. Most nonheme iron in the diet is in the ferric form rather than in the reduced ferrous state. Thus, to supply iron to DMT1, a ferrous ion transporter, the metal must first be reduced. Several biochemical studies have provided evidence for the existence of such a reductase and have shown that its activity is increased under conditions of body iron deficiency (8,9). This enzyme also appears to be induced in hemochromatosis, where iron absorption is elevated (120). Recently, a putative brush border ferric reductase has been cloned, and its expression shown to be enhanced under conditions known to stimulate iron absorption, such as iron deficiency and hypoxia (121). Alterations in the expression and/or activity of the ferric reductase in times of increased iron demand provides a mechanism for maximizing the utilization of ferric iron at the brush border and ensuring a continued supply of ferrous iron to DMT1. The effects of hypoxia in stimulating ferric iron uptake by the small intestine may relate to a direct effect on the ferric reductase.

C. Intracellular Events

The intracellular events following the brush border transit of iron are the least understood in the pathway of iron transport across the intestinal epithelium. However, the intracellular iron pool fulfills several key functions: first, it is the transit pool through which all absorbed iron must pass (both nonheme and heme iron); second, it provides a mechanism for sequestering any iron that does not cross the basolateral membrane and prevents it from accumulating to toxic levels; and third, it plays a regulatory role in modulating the local expression of molecules involved in the epithelial transit of iron. It may be too simplistic to think of iron in the enterocyte as constituting a single pool. It is conceivable that there is some functional compartmentalization of iron such that, for example, newly absorbed iron occupies a different compartment than the iron taken up by the cell when it was formed in the intestinal crypt. Many early studies (e.g., Refs. 63,122) investigated the distribution of newly absorbed radioiron in mucosal homogenates and found it to be incorporated into three main fractions. These were identified as ferritin, Tf (or a Tf-like protein), and a low-molecular-weight fraction. Ferritin is the most extensively studied of these and will be considered in more detail below. The significance of mucosal Tf remains unresolved. The *Tf* gene is not expressed in the intestinal epithelium, so the Tf detected in mucosal homogenates must be internalized plasma Tf or result from plasma Tf contamination during experimental procedures (123). The nature of the low-molecular-weight pool of iron in enterocytes is poorly understood, as it is in any other cell type. It is likely that this iron is sequestered by small organic acids such as citrate, but it may also be bound to as yet unidentified cellular proteins. Membrane-permeant iron chelators such as desferrioxamine are able to inhibit iron absorption, presumably by chelating iron in this intracellular pool (124–126).

Following the administration of an intraluminal dose of radioactive iron, radioactivity usually appears in the circulation within 15 s, and within minutes 60–80% of the total amount ultimately transferred will be present in the carcass (61). This initial phase of rapid iron uptake is followed by a slower rate of transfer which continues for 12–48 h (127,128), and there is evidence that the iron transferred during the latter phase has been stored in the absorptive cell in the form of ferritin (5,82,129). Some of this iron is not transferred to the body at all, but remains sequestered within the cell in ferritin, and is lost when the mucosal cell is sloughed at the end of its lifespan (82). In iron deficiency, not only is the total amount of iron absorbed greater, the fraction retained within the mucosal cell is much smaller, i.e., the rapid transfer pathway predominates (48,95). A similar predominance of the rapid transfer phase has been inferred in hemochromatosis, where the body continues to accumulate iron despite elevated body iron stores (48).

The demonstration that the mucosal ferritin concentration varies directly with body iron stores and inversely with iron absorption (63,89,130–132) has led to the suggestion that the protein may play an important role in the regulation of intestinal iron absorption. This relationship also implies that the mucosal ferritin level reflects the quantity of iron available to the mucosal cells when they are developing in the crypts. It has been argued that epithelial cells containing a large amount of ferritin, for example, may allow the passage of less iron because that ferritin is able to take up iron that is otherwise destined to pass to the body. The forced overexpression of ferritin in cultured cells can indeed generate an iron sink (133), but the relevance of

this observation *in vivo* is questionable and this explanation is likely to be an oversimplification. Mature enterocytes are able to synthesize ferritin in response to newly absorbed iron (82,134–139), so their ferritin level is not simply set at the time the enterocytes are formed in the intestinal crypts, although that may play a role. Also, any ferritin formed in the crypts as a reflection of body iron levels is likely to be iron-loaded and thus not a good candidate as a destination for newly absorbed iron. Finally, there are some situations where iron absorption is altered, such as in inflammation and following hemolysis, that are not associated with changes in mucosal ferritin synthesis (111,140). Taken together, these data suggest that ferritin most likely acts as a passive sink for iron which is not passed to the body, rather than playing an active role in withdrawing iron from a default stream destined to cross the basolateral membrane. Our current knowledge of the molecular basis of ferritin synthesis shows that ferritin mRNA is translated on demand in the face of increased intracellular iron levels, making it an ideal sink for unabsorbed iron.

D. Basolateral Transfer

The basolateral transfer step, like the brush border uptake step, appears to be modulated by changes in body iron demand. Transfer is elevated under iron-deficient conditions and depressed when body iron stores are elevated (36,48,89,91,95), and enhanced when erythropoiesis is stimulated (53,104). Chronic hypoxia will stimulate transfer, although this affect may be mediated by a stimulation of erythropoiesis (32,53). An increase in basolateral transfer also appears to be the major contributor to the elevated iron absorption found in hemochromatosis (48,88), and in hypotransferrinemic mice, systemic manipulations such as injection of Tf will reduce iron absorption and appear to exert their greatest effect on the transfer step (141). The proposal that basolateral transfer is particularly affected by systemic stimuli is supported by the observation that parenteral iron dextran administration will preferentially decrease transfer in mice (100). Some studies have also shown that serosal transfer can be depressed following the administration of an intraluminal dose of iron (e.g., Ref. 142), suggesting that this transport step may be regulated at least in part by local enterocyte iron concentrations, but one recent study has not shown such a decrease (118). This will be considered in more detail below.

The only molecule proven to be involved in the basolateral transfer of iron is hephaestin, since a defect in hephaestin in the *sla* mouse leads to a severe impairment in iron transfer and the subsequent accumulation of iron within enterocytes (13). Hephaestin itself is unlikely to be an iron transporter, since it contains only a single transmembrane domain, but it may interact with a transporter to facilitate iron movement across the basolateral membrane. The strongest candidate for a basolateral iron transport protein is Ireg1 [(14–16); see Chapter 7]. Although not yet definitively shown to play a role in intestinal iron transport, the localization of Ireg1 to the basolateral membrane, and its demonstrated role in cellular iron efflux in experimental systems, strongly supports such a role (14–16). Whether Ireg1 and hephaestin interact has yet to be determined. Ireg1 is suspected to transport ferrous iron, and it has been demonstrated that most iron that has recently crossed the intestinal epithelium is in this form (143).

The limited data that are available on hephaestin suggest that its expression is increased in iron deficiency and decreased in iron loading, although the range of

regulation is far smaller than that observed for DMT1/Nramp2 (144). The hephaestin mRNA does not contain a consensus IRE sequence, so regulation by IRP binding is unlikely. The expression of *Ireg1* is also inversely regulated by cellular iron content in the small intestine (14–16). Its range of regulation appears to be approximately two- to fivefold, somewhat larger than that of hephaestin but still far less than that observed for DMT1. *Ireg1* mRNA contains a consensus IRE motif in its 5'-untranslated region (UTR), but whether this plays a role in its regulation in the intestine is not clear (16). In other genes bearing a 5'-UTR IRE, such as the ferritin genes, the binding of IRPs under low-iron conditions leads to a block in translation and lower protein synthesis. However, the opposite direction of regulation is observed for *Ireg1* in the gut. Elucidation of the mechanisms by which *Ireg1*, and perhaps hephaestin, are regulated by iron may provide some clues to the regulation of the basolateral transport step. It is noteworthy that the range of regulation of these basolateral transfer components (in response to changes in body iron stores) more closely agrees with the observed physiological range of iron absorption than does the range of regulation of DMT1, and this provides further support for the concept that basolateral transfer plays a primary regulatory role in iron absorption under these conditions.

The finding that a copper-containing protein such as hephaestin is required for basolateral transport raises the possibility that copper could play a role in the control of iron movement across the intestinal epithelium. Indeed, Coppen and Davies (145) found that iron transfer, but not uptake, was diminished in copper-deficient rats. Copper depletion has also been shown to lead to anemia in several species (146,147), and much of this has been attributed to a deficiency of functional ceruloplasmin in the plasma. However, an additional deficiency in functional hephaestin in the small intestine could exacerbate the anemia by leading to a severe reduction in iron entry into the body.

E. Iron Delivery to the Plasma

After iron crosses the basolateral membrane it must make its way to the circulation, but the mechanism of this passage and whether it is regulated are not known. Undoubtedly, some of the iron that crosses the intestinal epithelium can be bound by extravascularized plasma apotransferrin and transported back to the blood vessels, but the transcapillary exchange rate of transferrin is insufficient to account for all the iron absorbed (74,148). Furthermore, the degree of saturation of transferrin with iron does not show any correlation with the rate of iron absorption (149–151), and hypotransferrinemic animals, which have negligible circulating transferrin, do not have impaired iron absorption (152–154). These studies raise questions about a carrier role for transferrin in this phase of iron absorption. It seems more likely that at least some newly absorbed iron passes to the circulation as a low-molecular-weight chelate, bound with low affinity to plasma proteins such as albumin, or specifically bound with high affinity to one or more as yet unidentified proteins.

Recent investigations using the intestinal cell line Caco-2 have raised the intriguing possibility that apotransferrin might bind to the basolateral membrane and be internalized, then acquire iron from the cells and return it to the serosal medium (155). Others have proposed a similar mechanism (12). The early studies of Levine et al. (150) and Evans and Grace (156) showed, respectively, that either isolated intestinal cells or intestinal cell plasma membranes which had been preloaded with

radioactive iron released this iron to Tf. Levine et al. (150) also demonstrated that iron-poor Tf bound to the mucosal cells with a higher affinity than diferric Tf. However, more recent studies have not been able to reproduce this observation and have shown that the transferrin receptor is not expressed on the surface of mature enterocytes (157–159). Until definitive data can be produced to demonstrate apotransferrin binding to mature enterocytes *in vivo*, the proposal that apotransferrin plays a physiologically important role in mediating basolateral iron release must remain speculative.

A final comment should be made on the potential role of ceruloplasmin in the passage of iron from the intestinal epithelium to the circulation. Ceruloplasmin has been shown to play a critical role in iron release from tissues (160) and, by virtue of its ferroxidase activity, it is able to facilitate the loading of iron onto plasma transferrin by oxidizing ferrous iron to the ferric form. It might be expected to play a similar role in loading newly absorbed iron onto apotransferrin in the interstitial fluid, most of which appears to be in the ferrous state, and one study has found evidence to support such a role (143). However, in several other studies ceruloplasmin appears to have little effect on iron absorption (145,161). It is possible that the role fulfilled by ceruloplasmin in iron release from many tissues is carried out by other molecules that act specifically at the mucosal level. Hephaestin is the obvious candidate, but earlier studies have suggested that xanthine oxidase may also be important (162).

V. MECHANISMS OF REGULATION

The mechanisms by which the intestinal epithelium responds to alterations in body iron demand to allow the passage of more or less iron remain relatively poorly characterized, although recent molecular advances are rapidly enhancing our understanding in this field. The largest body of evidence suggests that the iron content of the intestinal epithelium is an important determinant of absorption, but whether this is the sole factor or whether other factors are in operation remains a matter of conjecture. For example, the iron content of the epithelium may be an important determinant of absorption for the store regulator, but the erythroid regulator might act via a different mechanism.

A. Role of Mucosal Iron Status

Very early studies on iron homeostasis recognized the potential importance of the intestinal epithelial iron content in the control of absorption (1), but its role was articulated more clearly by Conrad and Crosby (77) some years later. They suggested that body iron requirements dictated the iron content of the epithelial cells at the time they were formed in the intestinal crypts, and that this in turn affected how much iron these cells would absorb after they had migrated up the villus and differentiated into mature enterocytes. Over time the details of this concept have been modified a little, but the basic theory has remained unchanged. It does not appear as though the iron concentration of the crypt cell per se is of prime importance, but rather, the way in which this cellular iron affects the synthesis of components of the iron transport machinery of the mature epithelial cell.

Many studies have shown that the mucosal iron content reflects body iron levels and that it is inversely proportional to the rate of iron absorption (30,31,84,111,163–

169). Thus, in iron deficiency the epithelial cell iron content is relatively low and iron absorption is elevated, while when iron stores are increased the epithelial iron level is increased and absorption declines. This relationship has not been confirmed in some studies (101,170–172), but overall the correlation is well supported. The discrepancies between the results of various groups may relate to species and methodological differences, e.g., the diets the animals were fed, whether they were starved before the study, or if epithelial cells were stripped from the underlying tissues or whole intestinal preparations used. Other studies have shown that iron absorption can be decreased following the parenteral administration of iron in various forms (27,100,173). This decrease was accompanied by an increase in epithelial iron levels and the absorption response was delayed for approximately 2 days, suggesting that the treatments were exerting their effects by changing the iron content of the crypt cells. Investigations with animals have also shown that an increased absorption in response to a low-iron diet can occur before overt changes in hepatic iron content (174–176), although absorption is still inversely correlated with mucosal iron content. These data and others (177) indicate that local changes in intestinal iron content can be important in regulating absorption.

The relationship between body and mucosal iron levels is also supported by the analysis of genes and proteins whose expression is regulated by cellular iron content. Thus, in iron deficiency the level of mucosal ferritin decreases and that of TfR, DMT1/Nramp2, and Ireg1 increases (14–16,108,168,178,179). The opposite is the case following iron loading. Since the regulation of most of these molecules is dependent on IRP activity, it is no surprise that the RNA-binding capacity of mucosal IRP is greatest in iron deficiency and is lower in iron overload (180,181). An excellent illustration of the role of the mucosal iron content in the control of iron absorption comes from the study of patients with hemochromatosis. In contrast to subjects with secondary iron overload, absorption in hemochromatosis patients continues despite an increase in body iron stores (95,101). One might expect that an elevated mucosal iron content would be found in hemochromatosis [as it is in secondary iron overload (102)], but this is not the case. In fact the level of mucosal iron is disproportionately low compared to body iron levels, as shown by measuring epithelial cell iron directly; by studying ferritin, TfR, DMT1, or Ireg1 expression; or by measuring IRP activity (14,108,132,157,182–184). Thus, the mucosal epithelium is relatively iron-deficient in hemochromatosis and the observed absorption is correspondingly high relative to body iron stores.

B. Regulation by Other Stimuli

Despite an enormous body of literature on intestinal iron absorption, relatively little effort has been devoted to understanding the mechanism of action of stimuli that alter absorption other than iron stores. Do stimuli such as increased erythropoiesis or changes in oxygen tension also affect the iron content of the epithelial cells, or do they act through other pathways? Support for an alternative pathway for the stimulation of iron absorption accompanying enhanced erythropoiesis comes from the demonstration that in iron loading anemias where the erythropoietic rate is high (e.g., β -thalassemia), absorption continues in the face of elevated body iron stores (44,47). Furthermore, experimental acute hemolysis in rats has been shown to increase iron absorption without a corresponding increase in mucosal TfR levels, sug-

gesting that a stimulation of erythropoiesis can, at least in part, alter iron absorption without changing the mucosal iron concentration (185).

Hypoxia demonstrates both short-term and longer-term enhancing effects on iron absorption and exerts most of its effects on ferric iron (53,113,114). The short-term effect occurs within hours and is likely to be due to a direct action on mature enterocytes rather than on nascent crypt cells (53,75). The later response probably reflects the delayed effect of hypoxia on erythropoiesis. Several studies have found that a hypoxic stimulus does not lead to alterations in mucosal iron content (32,75,168) [although one study noted an increase in mucosal iron when hypoxic rats were removed from a hypoxic environment (43)], so the mechanism of induction of transport is likely to be different from the intestinal response to changes in body iron stores. Changes in oxygen tension may have a direct bearing on the oxidation state of iron. Hypoxia most strongly affects Fe^{3+} uptake and, since this form of iron must initially be reduced to Fe^{2+} before it can be transported by DMT1, low oxygen tension may help to facilitate this reduction or increase the stability of the product. In the movement of iron through the enterocytes, the metal may undergo several oxidation–reduction steps and hypoxia could potentially modulate any of these. Chronic hypoxia will stimulate the expression of *Ireg1*, but whether this is through a direct or systemic mode of action is not clear (14).

C. Molecular Basis of Regulation

How are the components of intestinal iron transit regulated at the molecular level? The most extensively investigated mechanism for the regulation of proteins of iron metabolism is the IRE/IRP system and, as has been noted above, the regulation of the TfR, ferritin, and DMT1 in the intestinal epithelium is likely to occur by this mechanism. Although *Ireg1* mRNA contains an IRE in its 5'-untranslated region, recent data have suggested that this IRE may not be utilized in the small intestine since it is located too close to the mRNA cap site (16). In addition, *Ireg1* is upregulated under iron-deficient conditions in the small intestine, and not downregulated as would be expected if the IRE were operational (14–16). It is of interest that, in the liver, *Ireg1* expression is elevated under iron-loading conditions, so its 5'-IRE may be utilized in the liver even if it is not in the gut (16). Studies using cultured Caco-2 cells have shown that artificially disturbing the equilibrium of the IRE/IRP system by overexpressing a ferritin IRE can alter iron transport (186), but whether these cells provide an appropriate model for iron absorption *in vivo* is unclear.

A possible explanation for the control of iron transport protein synthesis in the small intestine is that signals from the body to alter absorption affect the capacity of mucosal IRPs to bind mRNA transcripts in the crypts. This mRNA-binding state is held until the cells migrate to the villus and differentiate, where the IRPs can bind to *DMT1*, ferritin, and possibly *Ireg1* and other mRNAs (181,187). However, this appears too simplistic and it is unlikely that this is the sole or indeed the major mechanism operating. The mRNA-binding ability of the IRPs is constantly being modulated by changes in cellular iron levels, and thus is most likely to be regulated by local rather than systemic regulatory effects. This has been shown in an elegant series of experiments by Schumann and colleagues (181), in which rats were treated with either intravenous or oral iron and then their intestinal mucosa was removed and carefully sectioned to provide tissue in a villus-to-crypt gradient. The measure-

ment of IRP activity showed that crypt cell IRP activity, but not villus cell IRP activity, would respond to intravenously administered iron, whereas only villus cell activity would respond to oral iron. These data suggest that it is unlikely that an “IRP-binding state” that has been set in the crypts would be retained after the epithelial cell had crossed the crypt/villus boundary. However, it is still possible that does occur, and that sufficient “preset” IRP does persist in differentiated cells, and is able to influence gene expression before changes in local iron concentration become important (187). The rate at which the capacity of IRPs to bind to RNA changes after the crypt cells migrate and differentiate, either through assembly/disassembly of its iron–sulfur cluster in the case of IRP1 or through degradation/synthesis in the case of IRP2, is an important consideration here but has yet to be investigated in detail.

In addition to the IRE/IRP system, other regulatory mechanisms that are in operation in the small intestine exert a considerable influence on iron absorption. The significance of transcriptional regulation of various genes of iron metabolism has often been overlooked in evaluating mechanisms for the control of iron absorption. DMT1, hephaestin, and Ireg1 are expressed at very low levels in the immature crypt cells, but after these cells traverse the crypt–villus boundary, high levels of mRNA (or protein) are seen (13–16,107). So, how can the levels of transport components be affected by body signals, which appear to act via the crypt cells, if they are not expressed in these cells and if IRP activity is too sensitive to local variations in cellular iron content to provide the major control mechanism? At the moment we do not know the answer, but perhaps the mechanism involves a transcriptional cascade which is activated in the crypts by systemic signals. Superimposed upon this would be the fine tuning of the system brought about by IRP-dependent control according to local cellular iron levels.

Another possibility which has yet to be explored in detail is that posttranslational modifications of DMT1, hephaestin, or Ireg1 play a role in their regulation in the small intestine. Each of these proteins is glycosylated, and this may play some role in their activity. Furthermore, hephaestin is predicted to be a copper-containing protein and that copper is necessary for its putative ferroxidase activity. In the absence of copper, hephaestin protein may still be produced, but it may not have biological activity.

Finally, variations in the subcellular localization of iron transport proteins in response to signals to alter iron absorption provides an additional level of regulation. As described above, DMT1 is found diffusely distributed in the cytoplasm (presumably associated with a cytoplasmic vesicular compartment) under iron-replete conditions, but in iron-deficient conditions there is a redistribution of the transporter to the brush border membrane (76,107,119). Thus, when the body requires iron, more DMT1 is expressed on the luminal membrane where it can participate in the absorption of new iron. Similarly, a recent study has shown that Ireg1 has a predominantly intracellular distribution under iron-sufficient conditions, but in iron deficiency it is strongly expressed on the basolateral membrane (16). Whether the localization of other proteins of iron transport varies in this way remains to be established. However, cytoskeletal inhibitors have been shown to decrease iron absorption when administered intraluminally (188), providing further evidence for the involvement of vesicle trafficking in iron absorption.

VI. RECEIVING AND TRANSDUCING SIGNALS FROM THE BODY

How does the intestinal crypt cell respond to an increased body demand for iron? The evidence that the crypt cell iron content plays an important role in this process has been summarized above, and it is reasonable to assume that alterations in the delivery of iron to these immature enterocytes can alter absorption. In iron deficiency, the crypt cells, like other cells in the body, are iron-deficient, and this leads to subsequent increases in the expression of various iron transport molecules in the mature enterocytes. The early autoradiographic studies of Conrad and Crosby (77,84) showed that only crypt cells and not villus cells could take up iron from the circulation, so understanding how the crypt cell receives iron is important for understanding how the body/intestine interface is working. Whether other stimuli, such as elevated erythropoiesis, can exert some effects directly on the mature enterocytes has yet to be established, but the 2- to 3-day delay in absorption response following an erythropoietic stimulus suggests otherwise.

The major route of iron uptake by developing enterocytes in the intestinal crypts is the receptor-mediated uptake of Tf by the TfR. Transferrin receptors are abundant on the basolateral membrane of the crypt enterocytes (157,158,185,189), and this reflects the high iron requirements of these rapidly dividing cells. As the enterocytes pass the crypt-villus junction and differentiate, transcription of the *TfR* gene is switched off (190), and residual receptor molecules appear to accumulate at intracellular sites and are degraded as the cells age (159,185). This provides a molecular explanation for the inability of mature enterocytes to take up iron via the TfR/Tf pathway (158,191). Under iron-deficient conditions, the concentration of TfRs in the crypt cells increases, and when body iron stores are high the receptor number is decreased (157,185). This shows that the iron status of the crypt cells reflects whole-body iron status and that alterations in receptor number help either to ensure an adequate supply of iron to these cells or to prevent the accumulation of iron in excess of metabolic requirements. Despite the higher receptor number in iron-deficient crypts, the amount of iron delivered to these cells remains low, as the saturation of plasma Tf with iron is also low in iron deficiency (169). Iron-loaded crypts may take up less iron through the Tf receptor pathway since receptor numbers are decreased, but under these conditions non-receptor-mediated Tf uptake may become important. There is some evidence that such a pathway exists in crypt cells (158).

It might be predicted that disruption of the TfR/Tf pathway would lead to an increase in iron absorption, as iron delivery to the crypt cells would be reduced and they would be relatively iron-deficient. This may be the mechanism underlying the elevated iron absorption found in congenital Tf deficiency (154,192), although the increased absorption could also result from the pronounced anemia in this condition. This has recently been examined in the atransferrinemic mouse, where it was shown that correction of the anemia alone was not sufficient to reduce absorption to control levels, whereas injections of Tf proved more effective (141). However, an earlier study, using slightly different methodology, concluded that the anemia was the major cause of enhanced iron absorption in these mice (193). The latter study did not examine the effects of Tf injections. Other studies have found that the mucosal iron concentration does not appear to be reduced in atransferrinemia (141,194), so the epithelial cells appear to be able to acquire sufficient iron from the body without Tf.

This iron could derive from the circulating non-transferrin-bound iron (NTBI) pool, which is high in atransferrinemia, as NTBI is readily taken up by cells. These data suggest that signals other than the mucosal iron content are operating to regulate absorption in these animals. Mice which are heterozygous for a targeted disruption of the *TfR* gene have fewer receptors and their tissues take up less iron by the receptor-mediated pathway (195). Thus, one might also expect the intestine to be relatively iron-deficient under these conditions, and that this, combined with the iron-deficient erythropoiesis in these animals, would lead to an increase in intestinal absorption. However, circumstantial evidence suggests this is not the case and that absorption is reduced. This could point to a previously unrecognized role for the TfR in the control of iron absorption (159), or it may be that alterations in the ratio between the TfR and HFE in the intestinal crypt cells bring about changes in absorption (117). Taken together, studies with atransferrinemic and TfR knockout mice have not provided clear support for a role for Tf and its receptor in the control of iron absorption, but there are a number of significant confounding factors which could be influencing the results.

An interesting recent study has proposed a role for apotransferrin in the regulation of absorption (196). A series of experiments in Caco-2 cells has suggested that apoTf can occupy a proportion of the cellular complement of TfRs and sequester them inside the cell. Thus, these cells would express fewer TfRs on their surface and would have a reduced capacity to take up Tf-bound iron. If such a system were operating in intestinal crypt cells, in iron-deficient conditions when the concentration of apoTf was higher, these cells would be relatively iron-deficient, and thus would absorb more iron on maturity. The physiological relevance of Tf saturation to the control of iron absorption is questionable, however, and whether such a mechanism operates in crypt cells *in vivo* remains to be established.

Further clues as to how the body communicates with the intestine to regulate iron absorption have come from the analysis of the inherited iron-overload disease hemochromatosis (see Chapters 8 and 28). In this disorder, absorption continues at increased levels despite substantial increases in body iron stores. In a normal individual, as iron stores increase, iron absorption decreases. This also happens in patients with hemochromatosis, but the level of body iron required to cause a given diminution in absorption is much greater than that required in a healthy individual (88,100). Thus the ability of the intestinal epithelium to respond to alterations in body iron stores is somewhat blunted in hemochromatosis. The main HFE mutation found in hemochromatosis patients leads to the amino acid substitution C282Y, and although it was originally thought that this mutation would lead to a functional knockout of HFE, recent data suggest that the mutant molecule retains some activity (197). Many aspects of the biology of HFE have yet to be resolved, but it is now clear that this protein is able to interact with the TfR [(87,198,199); see Chapter 8]. This interaction could lead to disturbances in the receptor-mediated delivery of Tf, and hence iron, to the crypt cells. The localization of HFE to the intestinal crypt cells supports its likely role in the regulation of iron absorption, although rather than being on the cell surface as expected, the molecular is predominantly found in a perinuclear distribution (87,200–202). Other aspects of the biology of HFE are more confusing. Its expression is not restricted to the small intestine and it is found in many tissues. Furthermore, its expression in most of these tissues, including the small intestine, is very low, much lower than that of the TfR. These observations have led

to the suggestion that the major role of HFE is not to alter the function of the TfR, but to affect iron delivery to the cell at an intracellular site, perhaps the endosome. The binding of HFE to the TfR would provide it with a means of getting to the correct intracellular location where it could exert these effects (203,204).

It is clear that HFE plays an important role in how the body signals the gut to modulate absorption, but the mechanism by which this is brought about is not clear. A number of investigators have conducted studies using cell lines transfected with HFE and the TfR, and most of these studies suggest that wild-type HFE will interfere with Tf/TfR-mediated iron uptake and thus reduce the delivery of iron to the cells (203,205–207). Overexpression of the C282Y mutant HFE, however, does not have this effect. The explanations for how the Tf cycle is disrupted vary, and include an effect of HFE on the affinity of the TfR for Tf (205); a direct competition between HFE and Tf for binding to the receptor (208); interfering with iron delivery from Tf-bound iron in the endosome (206); and an altered rate of recycling of the TfR (209). A perplexing issue, though, is the physiological relevance of these observations. These data suggest that when HFE is not bound to the TfR, cells will accumulate more iron via the TfR pathway. Since the most significant function of HFE seems to be modulating iron delivery to the intestinal crypt cells, this suggests that these cells might accumulate excess iron in hemochromatosis. The evidence that this does not happen, and that the crypt cells acquire less iron rather than more in hemochromatosis, is quite convincing, and has been described above. One explanation for the discrepancy may be that the studies using transfected cell lines are to some extent artefactual and that the levels of HFE achieved in these studies are supraphysiological. Another is that HFE may perform different functions in different cell types and the systems used have not been relevant to the biology of the intestinal crypt, although they may be relevant to cells such as hepatocytes that do accumulate iron in hemochromatosis. Support for the suggestion that the *in vitro* studies do not reflect the *in vivo* situation comes from studies of knockout mice with only one functional TfR allele (117,195). In these mice the ratio of HFE to TfR is increased and thus it mimics the situation where HFE is overexpressed in cultured cells. We would therefore expect the crypt cells to take up less iron and for iron absorption to be stimulated in these animals, but this does not appear to be the case. Alterations in the ratio between HFE and the TfR may also occur with variations in iron status. Some data suggest that expression of HFE is decreased in iron deficiency, although the range of regulation appears to be small (202,210). Reduced expression of HFE under iron-deficient conditions might mimic the situation in hemochromatosis, either by decreasing the ratio of HFE to TfR or by some TfR-independent pathway, but again the *in vitro* data are difficult to reconcile with observed physiological response if a decreased HFE/TfR ratio leads to increased iron uptake by the crypt cells, because absorption in these situations is increased, not decreased.

Despite our growing knowledge of HFE biology and the role of the TfR in crypt iron homeostasis, many aspects of how the crypt cells recognize body iron demands are obscure. It is possible that the crypt cell iron content is not the major factor influencing the expression of iron transport proteins and that the observed variations simply parallel alterations in some other factor. Under certain conditions, increasing erythropoiesis will increase iron absorption without apparently altering crypt cell iron levels (185), so perhaps other signals and response pathways need to be invoked. If variations in crypt cell iron content are important, they must be su-

perimposed on the already high iron requirements of the intestinal crypts, which comprise one of the most mitotically active cell populations in the body. Is the total iron content important, or is there some compartmentalization of the two iron pools? These issues have yet to be resolved.

VII. SIGNALS FOR THE CONTROL OF IRON ABSORPTION

The effective regulation of iron absorption requires the body to be able to supply an appropriate signal to the intestinal mucosa to program it to allow more or less iron to enter the circulation. This signal must reflect the body's iron requirements and must be able to act at a distance, since there is no physical or neuronal link between sites where stimuli to alter absorption may be generated, such as the erythroid marrow, and the intestine. The search for a circulating signal influencing iron absorption was stimulated by early studies showing that absorption was decreased when serum from iron-loaded rats was injected into normal rats (211). Support for a plasma-borne regulator has come from other infusion studies or experiments with parabiotic animals (212–214), but other workers have failed to find any evidence for a circulating factor (83,193,215,216).

The various plasma measures of iron status are the most obvious candidates for signals that regulate absorption, but numerous studies have failed to show any consistent correlation between iron absorption and parameters such as the serum iron concentration, hemoglobin concentration, total iron-binding capacity, Tf saturation, or plasma iron clearance (149,151,170,217–221). However, a subtle change in one or more of these parameters cannot be excluded as the potential messenger. There is some evidence that serum ferritin might provide the signal for iron absorption, as its level varies inversely with the magnitude of the absorption response (222,223). The heat-stable inhibitor of iron absorption described by MacDermott and Greenberger (211) in the serum of iron-loaded rats could be ferritin. Serum ferritin levels are also known to reflect accurately body iron stores (224). In addition, in infectious diseases, which are often associated with reduced iron absorption (2,225), serum ferritin levels are increased (224). However, this association remains circumstantial. One study designed to examine the direct effect of infusions of ferritin on iron absorption did not prove fruitful (226), but the short term of study and the use of tissue ferritin rather than serum ferritin limit the conclusions that can be drawn. Circulating TfR levels are elevated with increased erythropoietic activity and when iron stores are depleted (227,228), both situations in which iron absorption is increased, but a strong correlation between receptor levels and absorption has not been demonstrated. One could envisage, however, that circulating TfRs might interact with HFE on the surface of intestinal crypt cells to abrogate its function, so a role for this protein should not be discounted.

Of other candidate signals, much attention has centered on erythropoietin in view of the importance of erythropoiesis in iron absorption. However, a number of studies have suggested that erythropoietin is unlikely to provide a cue for absorption (46,51,53,214,229). Thus, following bleeding, iron absorption remains elevated in iron-deficient individuals long after the hemoglobin mass is restored to normal (41). In addition, erythropoietin levels are very high in aplastic anemia, but the rate of erythropoiesis is low and absorption is not elevated (230). Other proposed iron-absorption signals include a hepatocyte-derived factor (231) and a pituitary-derived

hormone (232), but these studies have yet to be confirmed. A comment should also be made on the potential role of cytokines in regulating iron absorption. In the anemia of chronic disease, the rate at which iron is delivered to the plasma from both the reticuloendothelial system and the intestinal mucosa is reduced (233). This reduction is likely to be mediated by cytokines, particularly the inflammatory mediator interleukin-1, so a role for cytokines in modulating absorption is possible. However, another inflammatory cytokine, interleukin-11, has been shown to stimulate iron absorption in rats (234). The mechanisms by which cytokines act on the intestinal epithelium have yet to be defined, but indirect stimulation or downregulation of molecules involved in cellular iron release, particularly Ireg1, could be involved.

Perhaps the most feasible hypothesis to explain the regulation of iron absorption is that proposed by Cavill and co-workers in 1975 (235) based on the plasma iron turnover [though Marx later suggested that taking the unsaturated iron binding capacity into account gives a more reliable parameter (236)]. Cavill et al. suggested that each tissue is able to donate iron to a labile plasma iron pool, and that the amount of iron donated is proportional to the iron stores of that tissue. Iron from this pool is bound by Tf and is used to meet the iron requirements of developing erythroid cells. The ability of the erythropoietic tissues to regulate their system for acquiring transferrin-bound iron in accordance with their requirements has been demonstrated *in vivo* in rats (237). In Cavill et al.'s hypothesis, if the Tf iron requirement is increased, then the amount of iron supplied by all tissues, including the gut, increases, and there would be a resultant increase in iron absorption. Evidence in support of this proposal has come from kinetic studies (238) and experiments in rats in which the requirement for Tf iron was increased by exchange transfusion with reticulocyte-rich blood (83,221). Under these conditions, iron donation from all tissues increased and there was an increase in iron absorption. However, similar studies in mice found little effect of increasing the reticulocyte level (216). Cavill et al.'s hypothesis, like all other proposals to explain how the body signals the gut to alter iron absorption, lacks a satisfying conclusion. How do cells recognize that they must donate iron to the plasma pool, and how is this brought about? Ireg1 may provide the answer to the second question, and as our knowledge of the biology of this protein increases, the answer to the first question may be revealed.

VIII. LOCAL REGULATION OF ABSORPTION—MUCOSAL BLOCK REVISITED

The regulation of intestinal iron absorption can occur at at least two levels: (a) modulation by systemic signals via the crypt cells, and (b) local regulation in the mature enterocyte by the luminal iron concentration. Overall, regulation at the crypt cell by systemic signals appears to be the most important pathway for the regulation of absorption, since the process must respond to body iron needs, and most of the discussion above has considered this pathway. That the body's response to changes in iron requirements is mediated by signals to the crypt is evidenced by the time it takes the absorptive process to respond to these signals. Superimposed on this, however, is the capacity of changes in the luminal iron concentration to alter rapidly the expression of components of iron transport in the mature enterocytes. Thus it appears that a combination of systemic and local control ultimately influences how much iron the epithelium will admit from the diet. Emerging molecular data are helping

to explain how enterocytes can respond to changes in the local iron concentration, but evidence that they have this capacity has been available for many years.

One of the earliest theories proposed to explain the regulation of iron absorption was the “mucosal block” theory of Hahn and co-workers (80,239). Their experiments with dogs indicated that the absorption of a test dose of iron could be inhibited by a “blocking” dose of iron given a short time previously. Many others have subsequently confirmed this observation (36,61,118,142,176,177,240,241). The biological significance of this phenomenon may be as a defense against excessive iron uptake. In fact, the lethal effect of a massive oral dose of iron can be prevented by several days of prior “conditioning” with smaller doses of iron (242). Hahn also recognized that the blocking effect on absorption can be determined by body iron requirements. Iron-deficient dogs absorbed relatively large amounts of iron, but iron-replete dogs absorbed much less, so absorption was “blocked” in the iron-replete state. Hahn’s explanation of these phenomena (both the local effect and the systemic effect) was that the amount of iron absorbed depended on the level of saturation of the mucosal cells with iron. Thus the mucosal cell was considered to contain a certain number of iron-binding sites which were required for absorption. When the body iron load was high, these sites were saturated with iron and no iron could cross the mucosal cell. Similarly, a prior blocking dose of iron would saturate the iron-binding sites and reduce the absorption of a subsequent dose. Ferritin best fits the description of Hahn’s iron-binding substance, and this was recognized over half a century ago by Granick (243), but ferritin is unlikely to play an active role in regulating iron absorption as discussed above.

Hahn’s theory was initially discounted as an adequate theory to explain iron absorption, largely because a total block to absorption could not be demonstrated [summarized by Crosby (244)], but his basic observations were sound and the concepts he proposed for how iron absorption is regulated were perhaps ahead of their time. His ability to interpret his findings was severely limited as he had no knowledge of the molecules involved in intestinal iron transit. Now that at least some of the molecules have been identified, his studies bear reexamination. Current data suggest that iron-binding or -storage proteins (i.e., ferritin) in the mucosa play a passive rather than an active role in iron absorption, and that it is the levels of transporters themselves that are important in regulating the amount of iron absorbed. So iron does not saturate a mucosal binding or carrier protein per se, as Hahn reasoned, but alters the level of transporter expression. The role of systemic signals that alter absorption on iron transporter expression in the gut has been considered above, and there is a growing body of evidence that DMT1 and Ireg1 expression in particular are responsive to changes in body iron requirements.

The influence of oral “blocking” doses of iron on transporter expression has been examined in some interesting recent studies that suggest that the mucosal block can be explained by variations in the expression of DMT1, and perhaps other iron transport proteins in the intestinal epithelium. A number of groups have shown that the administration of a blocking dose of iron decreases the brush border uptake step of absorption (36,61,118,142,176,241) and most, but not all (118), studies suggest that the transfer step is also decreased. The diminution of the uptake step can be explained by a rapid decrease in the expression of DMT1. Within 1–2 h of an intraluminal dose of iron, mucosal *DMT1* mRNA and protein levels are severely depleted and remain so for at least 7 h (118,119). Correspondingly rapid decreases

in IRP activity explain the decrease in the mRNA level (119,181). The demonstration that DMT1 protein also decreased in parallel with the message suggests that it is rapidly degraded in the presence of iron. Yeh and co-workers (119) also made the interesting observation that, soon after the administration of luminal iron, DMT1 on the brush border was internalized before being degraded. Since DMT1 appears to be the major molecule mediating the brush border uptake of iron (117), a decrease in its expression would be sufficient to explain a transient mucosal block.

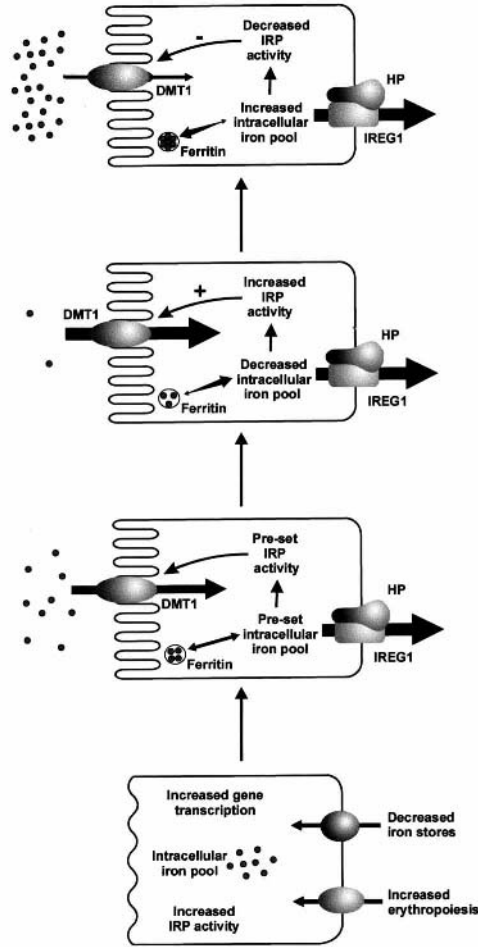
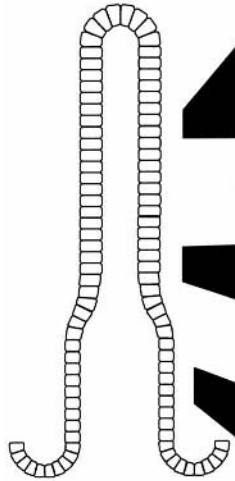
The ability of local changes in iron status to exert such a rapid and profound effect on DMT1 expression in mature enterocytes brings into question the value of modulating its expression via signals to the crypt. An alternative hypothesis is that systemic signals exert their primary effect on the transfer step, and that subsequent changes in the labile iron pool of the mature enterocytes will modulate the expression of DMT1. An important consideration in addressing this issue is whether the effects on DMT1 seen with supraphysiological blocking doses of iron are also manifest when mucosal iron levels vary within the physiological range. These are questions that can be answered experimentally and should prove an area of fruitful investigation over the next few years.

IX. SUMMARY AND FUTURE DIRECTIONS

In 1937 McCance and Widdowson (1) wrote "it is quite impossible to evolve a theory to cover the absorption and excretion of iron which does not conflict with some of the published findings." That statement is still as applicable today as it was almost 65 years ago. Since that time, several thousand papers have been published on intestinal iron absorption, and although our view of the process is now much more sophisticated than it was in 1937, we still have a great deal to learn about how iron traverses the intestinal epithelium and how this transport is regulated. Nevertheless, it is possible to provide a consensus model for nonheme iron absorption that most workers in the field would accept in principle, if not in all its details.

Dietary nonheme iron is presented to the intestinal epithelium in either the ferric or ferrous form. Ferrous iron is absorbed most efficiently, and it is likely that ferric iron must first be reduced by a brush border ferric reductase before it can be utilized. Ferrous iron then moves across the brush border membrane into the cytoplasm. The majority of this transit appears to be mediated by the multispanning membrane protein DMT1. Once within the enterocytes, iron is found in a low-molecular-weight transit pool, and iron which subsequently enters the circulation is

Figure 2 A model for the control of intestinal iron absorption in response to increased body iron demand. A stimulus to increase absorption will act on the newly formed crypt cells to program them to increase absorption ①. This programming or "presetting" of the absorption level may affect the iron content of the crypt cell, although other pathways may also be involved. Both stimulated IRP activity and transcriptional mechanisms are likely to increase the expression of brush border and basolateral iron transport components as the epithelial cells migrate out of the crypts and differentiate ②. As the cells migrate up the villus, local variations in enterocyte iron content (determined by a balance between basolateral efflux and influx from the lumen), ③ and ④, will alter brush border transport through modulation of IRP activity, but will have little effect on transfer across the basolateral membranes.



- ④ Increased dietary iron will decrease IRP activity and DMT1 expression. Transfer unchanged.
- ③ Local influences on iron content e.g. iron deficient diet, will stimulate IRP activity and DMT1 expression. Basolateral transfer unchanged.
- ② Expression of basolateral and brush border transport molecules in newly differentiated enterocytes reflects crypt programming.
- ① Systemic signals act on the crypt cells to increase IRP activity and stimulate transcription.

derived from this pool. Iron not required for absorption is incorporated into mucosal ferritin and is ultimately lost when these cells are sloughed from the villus tip. Movement of iron across the basolateral membranes and into the circulation probably involves the membrane iron exporter Ireg1, although this has yet to be confirmed. The membrane-bound ceruloplasmin homolog hephaestin is required for iron export from the intestinal epithelium, but whether it acts alone or in conjunction with other proteins such as Ireg1 is unclear.

The passage of iron across the intestinal epithelium is regulated by body iron requirements. The two main regulatory influences are the level of body iron stores and the rate of erythropoiesis, and evidence suggests that these two parameters affect absorption via different mechanisms. Whatever the mechanism, each of these stimuli appears to act initially on the intestinal crypt cells to ultimately alter the expression of molecules involved in iron transport in the mature enterocytes; i.e., the ability of mature intestinal epithelial cells to absorb more or less iron is established at the time they are formed in the crypts. Variations in the iron content of the crypt cell seem to provide one mechanism for altering the expression of iron transport molecules, but other signals are also likely to be important. Thus, in iron deficiency the crypt cells are relatively iron-depleted, and after they mature they take up more iron from the diet and export more into the circulation. Crypt-cell iron levels must alter the expression of iron transport genes indirectly, since those genes relevant for iron transit across mature enterocytes are not expressed in the crypts. Changes in gene expression could be brought about through the IRE/IRP system, via transcriptional mechanisms, or perhaps through multiple pathways. In addition to the influence of systemic signals on the adaptation of the intestine to iron needs, local variations in the iron content of mature enterocytes are also able to influence the expression of DMT1, ferritin, and perhaps Ireg1. A possible mechanism for the regulation of iron absorption is illustrated in Fig. 2.

The recent identification of a number of the critical molecules involved in intestinal iron transport promises to stimulate major advances in our understanding of this important physiological process over the next few years. How these molecules are modulated in response to signals known to alter absorption will clarify many aspects of the way in which the process is regulated. However, many significant issues are still to be addressed: Are other transporters or regulatory molecules involved? How does the body signal the intestine to change absorption? How are these signals received and interpreted by the crypt cells? What role does HFE play? What is the mechanism of heme iron absorption and how is it regulated? To address some of these issues we will need to learn more about the molecular and cellular biology of the known genes, and to define interactions between these molecules and novel components of the iron transport pathway(s). Perhaps the greatest challenge is understanding how iron absorption functions as an integrated component of whole body iron homeostasis. In vitro studies will be essential in helping to define the characteristics of the relevant molecules and their basic interactions with each other, but ultimately studies in humans and animal models are likely to lead to the most satisfying physiological conclusions.

REFERENCES

1. McCance RA, Widdowson EM. Absorption and excretion of iron. *Lancet* 1937; ii:680–684.

2. Bothwell TH, Charlton RW, Cook JD, Finch CA. Iron Metabolism in Man. Oxford, UK: Blackwell Scientific, 1979.
3. Finch CA, Ragan HA, Dyer IA, Cook JD. Body iron loss in animals. Proc Soc Exp Biol Med 1978; 159:335–338.
4. Bezwoda WR, Bothwell TH, Charlton RW, Torrance JD, MacPhail AP, Derman DP, Mayet F. The relative dietary importance of haem and non-haem iron. S Afr Med J 1983; 64:552–556.
5. Forth W, Rummel W. Iron absorption. Physiol Rev 1973; 53:724–792.
6. Hallberg L. Bioavailability of dietary iron in man. Annu Rev Nutr 1981; 1:123–147.
7. Parmley RT, Barton JC, Conrad ME, Austin RL. Ultrastructural cytochemistry of iron absorption. Am J Pathol 1978;93:707–727.
8. Wollenberg P, Rummel W. Dependence of intestinal iron absorption on the valency state of iron. Naunyn Schmiedebergs Arch Pharmacol 1987; 336:578–582.
9. Raja KB, Simpson RJ, Peters TJ. Investigation of a role for reduction in ferric iron uptake by mouse duodenum. Biochim Biophys Acta 1992; 1135:141–146.
10. Gunshin H, Mackenzie B, Berger UV, Gunshin Y, Romero MF, Boron WF, Nussberger S, Gollan JL, Hediger MA. Cloning and characterization of a mammalian proton-coupled metal-ion transporter. Nature 1997; 388:482–488.
11. Fleming MD, Trenor CC, Su MA, Foernzler D, Beier DR, Dietrich WF, Andrews NC. Microcytic anaemia mice have a mutation in *Nramp2*, a candidate iron transporter gene. Nature Genet 1997; 16:383–386.
12. Umbreit JN, Conrad ME, Moore EG, Latour LF. Iron absorption and cellular transport: the mobilferrin/paraferitin paradigm. Semin Hematol 1998; 35:13–26.
13. Vulpe CD, Kuo Y-M, Murphy TL, Cowley L, Askwith C, Libina N, Gitschier J, Anderson GJ. Hephaestin: A caeruloplasmin homologue implicated in intestinal iron transport and its defect in the *sla* mouse. Nat Genet 1999; 21:195–199.
14. McKie AT, Marciani P, Rolfs A, Brennan K, Wehr K, Barrow D, Miret S, Bomford A, Peters TJ, Farzaneh F, Hediger MA, Hentze MW, Simpson RJ. A novel duodenal iron-regulated transporter, IREG1, implicated in the basolateral transfer of iron to the circulation. Mol Cell 2000; 5:299–309.
15. Donovan A, Brownlie A, Zhou Y, Shepard J, Pratt SJ, Moynihan J, Paw BH, Drejer A, Barut B, Zapata A, Law TC, Brugnara C, Lux SE, Pinkus GS, Pinkus JL, Kingsley PD, Palis J, Fleming MD, Andrews NC, Zon LI. Positional cloning of zebrafish ferroportin1 identifies a conserved vertebrate iron exporter. Nature 2000; 403:776–781.
16. Abboud S, Haile DJ. A novel mammalian iron-regulated protein involved in intracellular iron metabolism. J Biol Chem 2000; 275:19906–19912.
17. Hallberg L, Bjorn Rasmussen E, Howard L, Rossander L. Dietary heme iron absorption. A discussion of possible mechanisms for the absorption-promoting effect of meat and for the regulation of iron absorption. Scand J Gastroenterol 1979; 14:769–779.
18. Skikne BS, Cook JD. Effect of enhanced erythropoiesis on iron absorption. J Lab Clin Med 1992; 120:746–751.
19. Roberts SK, Henderson RW, Young GP. Modulation of uptake of heme by rat small intestinal mucosa in iron deficiency. Am J Physiol 1993; 265:G712–G718.
20. Hunt JR, Roughhead ZK. Adaptation of iron absorption in men consuming diets with high or low iron bioavailability. Am J Clin Nutr 2000; 71:94–102.
21. Bothwell TH, Pirzio-Biroli G, Finch CA. Iron absorption. I. Factors influencing absorption. J Lab Clin Med 1958; 51:24–36.
22. Pirzio-Biroli G, Finch CA. Iron absorption. III. The influence of iron stores on iron absorption in the normal subject. J Lab Clin Med 1960; 55:216–220.
23. Heinrich HC, Bruggemann J, Gabbe EE, Glaser M. Correlation between diagnostic $^{59}\text{Fe}^{2+}$ -absorption and serum ferritin concentration in man. Z Naturforsch [C] 1977; 32:1023–1025.

24. Cox TM, Peters TJ. Cellular mechanisms in the regulation of iron absorption by the human intestine: Studies in patients with iron deficiency before and after treatment. *Br J Haematol* 1980; 44:75–86.
25. Magnusson B, Bjorn Rassmussen E, Hallberg L, Rossander L. Iron absorption in relation to iron status. Model proposed to express results to food iron absorption measurements. *Scand J Haematol* 1981; 27:201–208.
26. Gavin MW, McCarthy DM, Garry PJ. Evidence that iron stores regulate iron absorption — a setpoint theory. *Am J Clin Nutr* 1994; 59:1376–1380.
27. Barton JC, Conrad ME, Holland R. Iron, lead, and cobalt absorption: Similarities and dissimilarities. *Proc Soc Exp Biol Med* 1981; 166:64–69.
28. Cox TM, O'Donnell MW. Studies on the control of iron uptake by rabbit small intestine. *Br J Nutr* 1982; 47:251–258.
29. Nathanson MH, Muir A, McLaren GD. Iron absorption in normal and iron-deficient beagle dogs: Mucosal iron kinetics. *Am J Physiol* 1985; 249:G439–G448.
30. Conrad ME, Parmley RT, Osterloh K. Small intestinal regulation of iron absorption in the rat. *J Lab Clin Med* 1987; 110:418–426.
31. Huebers HA, Csiba E, Josephson B, Finch CA. Iron absorption in the iron-deficient rat. *Blut* 1990; 60:345–351.
32. Simpson RJ. Dietary iron levels and hypoxia independently affect iron absorption in mice. *J Nutr* 1996; 126:1858–1864.
33. Finch C. Regulators of iron balance in humans. *Blood* 1994; 84:1697–1702.
34. Sayers MH, English G, Finch C. Capacity of the store-regulator in maintaining iron balance. *Am J Hematol* 1994; 47:194–197.
35. Hallberg L, Hulthen L, Gramatkovski E. Iron absorption from the whole diet in men: How effective is the regulation of iron absorption? *Am J Clin Nutr* 1997; 66:347–356.
36. Manis JG, Schachter D. Active transport of iron by intestine: effects of oral iron and pregnancy. *Am J Med* 1962; 203:81–86.
37. Batey RG, Gallagher ND. Role of the placenta in intestinal absorption of iron in pregnant rats. *Gastroenterology* 1977; 72:255–259.
38. Batey RG, Gallagher ND. Study of the subcellular localization of ⁵⁹Fe and iron-binding proteins in the duodenal mucosa of pregnant and nonpregnant rats. *Gastroenterology* 1977;73:267–272.
39. Fenton V, Cavill I, Fisher J. Iron stores in pregnancy. *Br J Haematol* 1977; 37:145–149.
40. Dubach R, Moore CV, Callender S. Studies in iron transport and metabolism. IX. The excretion of iron as measured by the isotope technique. *J Lab Clin Med* 1955; 45:599–615.
41. Conrad ME, Crosby WH. The natural history of iron deficiency induced by phlebotomy. *Blood* 1962; 20:173–185.
42. Weintraub LR, Conrad ME, Crosby WH. The role of hepatic iron stores in the control of iron absorption. *J Clin Invest* 1964; 43:40–44.
43. Weintraub LR, Conrad ME, Crosby WH. Regulation of the intestinal absorption of iron by the rate of erythropoiesis. *Br J Haematol* 1965; 11:432–438.
44. Erlandson ME, Walden B, Stern G, Hilgartner MW, Wehman J, Smith CH. Studies on congenital hemolytic syndromes. IV. Gastrointestinal absorption of iron. *Blood* 1962; 19:359–378.
45. Murray MJ, Stein N. The effect of administered oestrogens and androgens on the absorption of iron by rats. *Br J Haematol* 1968; 14:407–409.
46. Mendel GA. Studies of iron absorption. I. The relationships between the rate of erythropoiesis, hypoxia and iron absorption. *Blood* 1961; 18:727–736.
47. Heinrich HC, Gabbe EE, Oppitz KH, Whang DH, Bender-Gotze C, Schafer KH, Schroter W, Pfau AA. Absorption of inorganic and food iron in children with heterozygous and homozygous beta-thalassemia. *Z Kinderheilkd* 1973; 115:1–22.

48. Powell LW, Campbell CB, Wilson E. Intestinal mucosal uptake of iron and iron retention in idiopathic haemochromatosis as evidence for a mucosal abnormality. *Gut* 1970; 11:727–731.
49. Adams PC, Chau LA, Lin E, Muirhead N. The effect of human recombinant erythropoietin on iron absorption and hepatic iron in a rat model. *Clin Invest Med* 1991; 14:432–436.
50. Hathorn MK. The influence of hypoxia on iron absorption in the rat. *Gastroenterology* 1971; 60:76–81.
51. Peschle C, Jori GP, Marone G, Condorelli M. Independence of iron absorption from the rate of erythropoiesis. *Blood* 1974; 44:353–358.
52. Peters TJ, Raja KB, Simpson RJ, Snape S. Mechanisms and regulation of intestinal iron absorption. *Ann NY Acad Sci* 1988; 526:141–147.
53. Raja KB, Simpson RJ, Pippard MJ, Peters TJ. *In vivo* studies on the relationship between intestinal iron (Fe^{3+}) absorption, hypoxia and erythropoiesis in the mouse. *Br J Haematol* 1988; 68:373–378.
54. Ezekiel E. Intestinal iron absorption by neonates and some factors affecting it. *J Lab Clin Med* 1967; 70:138–149.
55. Loh TT, Kaldor I. Intestinal iron absorption in suckling rats. *Biol Neonate* 1971; 17:173–186.
56. Gallagher ND, Mason R, Foley KE. Mechanisms of iron absorption and transport in neonatal rat intestine. *Gastroenterology* 1973; 64:438–444.
57. Srai SK, Debnam ES, Boss M, Epstein O. Age-related changes in the kinetics of iron absorption across the guinea pig proximal intestine *in vivo*. *Biol Neonate* 1988; 53:53–59.
58. Anderson GJ, Walsh MD, Powell LW, Halliday JW. Intestinal transferrin receptors and iron absorption in the neonatal rat. *Br J Haematol* 1991; 77:229–236.
59. Forbes GB, Reina JC. Effect of age on gastrointestinal absorption (Fe, Sr, Pb) in the rat. *J Nutr* 1972; 102:647–652.
60. Duthie HL. The relative importance of the duodenum in the intestinal absorption of iron. *Br J Haematol* 1964; 10:59–68.
61. Wheby MS, Jones LG, Crosby WH. Studies on iron absorption. Intestinal regulatory mechanisms. *J Clin Invest* 1964; 43:1433–1442.
62. Wheby MS. Site of iron absorption in man. *Scand J Haematol* 1970; 7:56–62.
63. Johnson G, Jacobs P, Purves LR. Iron binding proteins of iron-absorbing rat intestinal mucosa. *J Clin Invest* 1983; 71:1467–1476.
64. Chowrimootoo G, Debnam ES, Srai SK, Epstein O. Regional characteristics of intestinal iron absorption in the guinea-pig. *Exp Physiol* 1992; 77:177–183.
65. Dagg JH, Kuhn IN, Templeton FE, Finch CA. Gastric absorption of iron. *Gastroenterology* 1967; 53:918–922.
66. Rhodes J, Beton D, Brown DA. Absorption of iron instilled into the stomach, duodenum and jejunum. *Gut* 1968; 9:323–324.
67. Jacobs P, Bothwell TH, Charlton RW. Intestinal iron transport: Studies using a loop of gut with an artificial circulation. *Am J Physiol* 1966; 210:694–700.
68. Murray MJ, Delaney JP, Stein JP. Use of isolated subcutaneous intestinal loops for direct study of radioisotopes in dogs. *Am J Dig Dis* 1964; 9:684–689.
69. Chernelch M, Fawwaz R, Sargent T, Winchell HS. Effect of phlebotomy and pH on iron absorption from the colon. *J Nuclear Med* 1970; 11:25–27.
70. Dowdle EB, Schachter D, Schenker H. Active transport of ^{59}Fe by everted segments of rat duodenum. *Am J Physiol* 1960; 198:609–613.
71. Manis J, Schachter D. Active transport of iron by intestine: Features of the two-step mechanism. *Am J Physiol* 1962; 203:73–80.

72. Greenberger NJ, Balcerzak SP, Ackerman GA. Iron uptake by isolated intestinal brush borders: Changes induced by alterations in iron stores. *J Lab Clin Med* 1969; 73:711–721.
73. Richter GW, Lee YH. Absorption of iron from gut into blood: Sex- and time-related studies in rats. *Experientia* 1982; 38:583–585.
74. Schumann K, Osterloh K, Forth W. Independence of *in vitro* iron absorption from mucosal transferrin content in rat jejunal and ileal segments. *Blut* 1986; 53:391–400.
75. Raja KB, Bjarnason I, Simpson RJ, Peters TJ. *In vitro* measurement and adaptive response of Fe^{3+} uptake by mouse intestine. *Cell Biochem Funct* 1987; 5:69–76.
76. Canonne-Hergaux F, Gruenheid S, Ponka P, Gros P. Cellular and subcellular localization of the Nramp2 iron transporter in the intestinal brush border and regulation by dietary iron. *Blood* 1999; 93:4406–4417.
77. Conrad ME, Crosby WH. Intestinal mucosal mechanisms controlling iron absorption. *Blood* 1963; 22:406–415.
78. O’Riordan DK, Sharp P, Sykes RM, Srail SK, Epstein O, Debnam ES. Cellular mechanisms underlying the increased duodenal iron absorption in rats in response to phenylhydrazine-induced haemolytic anaemia. *Eur J Clin Invest* 1995; 25:722–727.
79. Southon S, Wright AJA, Fairweather Tait SJ. The effect of differences in dietary iron intake on ^{59}Fe absorption and duodenal morphology in pregnant rats. *Br J Nutr* 1989; 62:707–717.
80. Hahn PF, Bale WF, Ross JF, Balfour WN, Whipple GH. Radioactive iron absorption by gastro-intestinal tract. *J Exp Med* 1943; 78:169–188.
81. Weintraub LR, Conrad ME, Crosby WH. The significance of iron turnover in the control of iron absorption. *Blood* 1964; 24:19–24.
82. Charlton RW, Jacobs P, Torrance JD, Bothwell TH. The role of intestinal mucosa in iron absorption. *J Clin Invest* 1965; 44:543–554.
83. Rosenmund A, Gerber S, Huebers H, Finch C. Regulation of iron absorption and storage iron turnover. *Blood* 1980; 56:30–37.
84. Conrad ME, Weintraub LR, Crosby WH. The role of the intestine in iron kinetics. *J Clin Invest* 1964; 43:963–974.
85. Bedard YC, Pinkerton PH, Simon GT. Uptake of circulating iron by the duodenum of normal mice and mice with altered iron stores, including sex-linked anemia: High resolution radioautographic study. *Lab Invest* 1976; 34:611–615.
86. Feder JN, Gnirke A, Thomas W, Tsuchihashi Z, Ruddy DA, Basava A, Dormishian F, Domingo R, Ellis MC, Fullan A, Hinton LM, Jones NL, Kimmel BE, Kronmal GS, Lauer P, Lee VK, Loeb DB, Mapa FA, McClelland E, Meyer GA, Mintier GA, Moeller N, Moore T, Morikang E, Prass CE, Quintana L, Starnes SM, Schatzman RC, Brunke KJ, Drayna DT, Risch NJ, Bacon BR, Wolff RK. A novel MHC class I-like gene is mutated in patients with hereditary haemochromatosis. *Nature Genet* 1996; 13:399–408.
87. Waheed A, Parkkila S, Saarnio J, Fleming RE, Zhou XY, Tomatsu S, Britton RS, Bacon BR, Sly WS. Association of HFE protein with transferrin receptor in crypt enterocytes of human duodenum. *Proc Natl Acad Sci USA* 1999; 96:1579–1584.
88. McLaren GD, Nathanson MH, Jacobs A, Trevett D, Thomson W. Regulation of intestinal iron absorption and mucosal iron kinetics in hereditary hemochromatosis. *J Lab Clin Med* 1991; 117:390–401.
89. Savin MA, Cook JD. Mucosal iron transport by rat intestine. *Blood* 1980; 56:1029–1035.
90. Manis J. Intestinal iron-transport defect in the mouse with sex-linked anemia. *Am J Physiol* 1971; 220:135–139.
91. Marx JJ. Mucosal uptake, mucosal transfer and retention of iron, measured by whole-body counting. *Scand J Haematol* 1979; 23:293–302.

92. Wheby MS, Crosby WH. The gastrointestinal tract and iron absorption. *Blood* 1963; 22:416–428.
93. Pearson WN, Reich MB. In vitro studies of ⁵⁹Fe absorption from the rate of erythropoiesis. *J Nutr* 1965; 87:117–124.
94. Helbock JH, Saltman P. The transport of iron by rat intestine. *Biochim Biophys Acta* 1967; 135:979–990.
95. Boender CA, Verloop MC. Iron absorption, iron loss and iron retention in man: Studies after oral administration of a tracer dose of ⁵⁹FeSO₄ and ¹³¹BaSO₄. *Br J Haematol* 1969; 17:45–58.
96. Howad J, Jacobs A. Iron transport by rat small intestine in vitro: Effect of body iron status. *Br J Haematol* 1972; 23:595–603.
97. Schumann K, Elsenhans B, Forth W. Kinetic analysis of ⁵⁹Fe movement across the intestinal wall in duodenal rat segments ex vivo. *Am J Physiol* 1999; 276:G431–G440.
98. Williams R, Manenti F, Williams HS, Pitcher CS. Iron absorption in idiopathic haemochromatosis before, during, and after venesection therapy. *Br Med J* 1966; 2: 78–81.
99. Lynch SR, Skikne BS, Cook JD. Food iron absorption in idiopathic hemochromatosis. *Blood* 1989; 74:2187–2193.
100. Santos M, Clevers H, de Sousa M, Marx JJ. Adaptive response of iron absorption to anemia, increased erythropoiesis, iron deficiency, and iron loading in beta2-microglobulin knockout mice. *Blood* 1998; 91:3059–3065.
101. Cox TM, Peters TJ. Uptake of iron by duodenal biopsy specimens from patients with iron deficiency anaemia and primary haemochromatosis. *Lancet* 1978; i:123–124.
102. Cox TM, Peters TJ. In vitro studies of duodenal iron uptake in patients with primary and secondary iron storage disease. *Q J Med* 1980; 49:249–257.
103. Duane P, Raja KB, Simpson RJ, Peters TJ. *In vitro* uptake of iron from iron-ascorbate by human duodenal biopsies from control subjects and patients with idiopathic haemochromatosis. *Eur J Gastroenterol Hepatol* 1992; 4:661–666.
104. Hughes RT, Smith T, Hesp R, Hulme B, Dukes DC, Bending MB, Pearson J, Raja KB, Cotes PM, Pippard MJ. Regulation of iron absorption in iron loaded subjects with end stage renal disease: Effects of treatment with recombinant human erythropoietin and reduction of iron stores. *Br J Haematol* 1992; 82:445–454.
105. McLaren GD, Colville J, Nathanson MH. Mechanism of increased intestinal iron absorption in dogs with hemolytic anemia (abstr). *Blood* 1989; 74(suppl 1):138a.
106. McLaren GD, Colville J, Nathanson MH. Erythropoiesis and iron absorption: Decreased absorption and altered mucosal iron kinetics in dogs with increased red blood cell mass (abstr). *Blood* 1991; 78(suppl 1):88a.
107. Trinder D, Oates PS, Thomas C, Sadleir J, Morgan EH. Localisation of divalent metal transporter 1 (DMT1) to the microvillus membrane of rat duodenal enterocytes in iron deficiency, but to hepatocytes in iron overload. *Gut* 2000; 46:270–276.
108. Zoller H, Pietrangelo A, Vogel W, Weiss G. Duodenal metal-transporter (DMT-1, NRAMP-2) expression in patients with hereditary haemochromatosis. *Lancet* 1999; 353:2120–2123.
109. Thomson AB, Valberg LS. Kinetics of intestinal iron absorption in the rat: Effect of cobalt. *Am J Physiol* 1971; 220:1080–1085.
110. Acheson LS, Schultz SG. Iron influx across the brush border of rabbit duodenum: Effects of anemia and iron loading. *Biochim Biophys Acta* 1972; 255:479–483.
111. Sheehan RG, Frenkel EP. The control of iron absorption by the gastrointestinal mucosal cell. *J Clin Invest* 1972; 51:224–231.
112. Simpson RJ, Peters TJ. Fe²⁺ uptake by intestinal brush-border membrane vesicles from normal and hypoxic mice. *Biochim Biophys Acta* 1985; 814:381–388.

113. Simpson RJ, Raja KB, Peters TJ. Fe^{3+} transport by brush-border membrane vesicles isolated from normal and hypoxic mouse duodenum and ileum. *Biochim Biophys Acta* 1985; 814:8–12.
114. Simpson RJ, Raja KB, Peters TJ. Fe^{2+} uptake by mouse intestinal mucosa in vivo and by isolated intestinal brush-border membrane vesicles. *Biochim Biophys Acta* 1986; 860:229–235.
115. Raja KB, Simpson RJ, Peters TJ. Comparison of $^{59}\text{Fe}^{3+}$ uptake in vitro and in vivo by mouse duodenum. *Biochim Biophys Acta* 1987; 901:52–60.
116. Farcich EA, Morgan EH. Diminished iron acquisition by cells and tissues of Belgrade laboratory rats. *Am J Physiol* 1992; 262:R220–R224.
117. Levy JE, Montross LK, Andrews NC. Genes that modify the hemochromatosis phenotype in mice. *J Clin Invest* 2000; 105:1209–1216.
118. Oates PS, Trinder D, Morgan EH. Gastrointestinal function, divalent metal transporter-1 expression and intestinal iron absorption. *Pflügers Arch* 2000; 440:496–502.
119. Yeh KY, Yeh M, Watkins JA, Rodriguez-Paris J, Glass J. Dietary iron induces rapid changes in rat intestinal divalent metal transporter expression. *Am J Physiol* 2000; 279:G1070–G1079.
120. Raja KB, Pountney D, Bomford A, Przemioslo R, Sherman D, Simpson RJ, Williams R, Peters TJ. A duodenal mucosal abnormality in the reduction of Fe(III) in patients with genetic haemochromatosis. *Gut* 1996; 38:765–769.
121. McKie AT, Barrow D, Pountney D, Bomford A, Farzaneh F, Peters H, Raja K, Simpson RJ. Molecular cloning of a b-type cytochrome reductase implicated in iron absorption from the mouse duodenal mucosa. *World Congress on Iron Metabolism—Bioiron '99*, Sorrento, Italy, May 23–28, 1999.
122. Halliday JW, Powell LW, Mack U. Iron absorption in the rat: The search for possible intestinal mucosal carriers. *Br J Haematol* 1976; 34:237–250.
123. Osterloh KR, Simpson RJ, Peters TJ. The role of mucosal transferrin in intestinal iron absorption. *Br J Haematol* 1987; 65:1–3.
124. Jacobs A, Kaye MD, Trevett D. The chelation of iron during intestinal absorption. *J Lab Clin Med* 1969; 74:212–217.
125. Pippard MJ, Callender ST, Warner GT, Weatherall DJ. Iron absorption in iron-loading anaemias: Effect of subcutaneous desferrioxamine infusions. *Lancet* 1977; 2:737–739.
126. Levine DS, Huebers HA, Rubin CE, Finch CA. Blocking action of parenteral desferrioxamine on iron absorption in rodents and men. *Gastroenterology* 1988; 95:1242–1248.
127. Stewart WB, Gambino SR. Kinetics of iron absorption in normal dogs. *Am J Physiol* 1961; 201:67–70.
128. Brown EB, Rother ML. Studies of the mechanism of iron absorption. I. Iron uptake by the normal rat. *J Lab Clin Med* 1963; 62:357–373.
129. Worwood M, Jacobs A. The subcellular distribution of orally administered ^{59}Fe in rat small intestinal mucosa. *Br J Haematol* 1971; 20:587–597.
130. Cumming RL, Smith JA, Millar JA, Goldberg A. The relationship between body iron stores and ferritin turnover in rat liver and intestinal mucosa. *Br J Haematol* 1970; 18:653–658.
131. Halliday JW, Mack U, Powell LW. Duodenal ferritin content and structure. Relationship with body iron stores in man. *Arch Intern Med* 1978; 138:1109–1113.
132. Whittaker P, Skikne BS, Covell AM, Flowers C, Cooke A, Lynch SR, Cook JD. Duodenal iron proteins in idiopathic hemochromatosis. *J Clin Invest* 1989; 83:261–267.
133. Picard V, Epsztein S, Santambrogio P, Cabantchik ZI, Beaumont C. Role of ferritin in the control of the labile iron pool in murine erythroleukemia cells. *J Biol Chem* 1998; 273:15382–15386.

134. Smith JA, Drysdale JW, Goldberg A, Munro HN. The effect of enteral and parenteral iron on ferritin synthesis in the intestinal mucosa of the rat. *Br J Haematol* 1968; 14: 79–86.
135. Bernier GM, Schade SG, Conrad ME. Ferritin production in the rat small intestine. *Br J Haematol* 1970; 19:361–367.
136. Brittin GM, Raval D. Duodenal ferritin synthesis during iron absorption in the iron-deficient rat. *J Lab Clin Med* 1970; 75:811–817.
137. Brittin GM, Raval D. Duodenal ferritin synthesis in iron-replete and iron deficient rats: Response to small doses of iron. *J Lab Clin Med* 1971; 77:54–58.
138. Setsuda T, Ueda A. Study on the control mechanism of iron absorption in the intestinal mucosa in rat, particularly as viewed from its ferritin level as well as ATPase and ALPase activities. *Nippon Ketsueki Gakkai Zasshi* 1982; 45:711–720.
139. Ehtechami C, Elsenhans B, Forth W. Incorporation of iron from an oral dose into the ferritin of the duodenal mucosa and the liver of normal and iron-deficient rats. *J Nutr* 1989; 119:202–210.
140. Schade SG. Normal incorporation of oral iron into intestinal ferritin in inflammation. *Proc Soc Exp Biol Med* 1972; 139:620–622.
141. Raja KB, Pountney DJ, Simpson RJ, Peters TJ. Importance of anemia and transferrin levels in the regulation of intestinal iron absorption in hypotransferrinemic mice. *Blood* 1999; 94:3185–3192.
142. Benito P, House W, Miller D. Comparison of oral and intraperitoneal iron supplementation in anaemic rats: A re-evaluation of the mucosal block theory of iron absorption. *Br J Nutr* 1998; 79:533–540.
143. Wollenberg P, Mahlberg R, Rummel W. The valency state of absorbed iron appearing in the portal blood and ceruloplasmin substitution. *Biol Metals* 1990; 3:1–7.
144. Frazer DM, Cowley LL, Cleghorn GJ, Vulpe CD, Anderson GJ. Cloning of the rat hephaestin gene and its expression in the gastrointestinal tract (abstr). *J Gastroenterol Hepatol* 1999; 14(Oct suppl):A131.
145. Coppen DE, Davies NT. Studies on the roles of apotransferrin and caeruloplasmin (EC 1.16.3.1) on iron absorption in copper-deficient rats using an isolated vascularly- and lumenally-perfused intestinal preparation. *Br J Nutr* 1988; 60:361–373.
146. Lee GR, Nacht S, Lukens JN, Cartwright GE. Iron metabolism in copper-deficient swine. *J Clin Invest* 1968; 47:2058–2069.
147. Cohen NL, Keen CL, Hurley LS, Lonnerdal B. Determinants of copper-deficiency anemia in rats. *J Nutr* 1985; 115:710–725.
148. Morgan EH. The role of plasma transferrin in iron absorption in the rat. *Q J Exp Physiol Cogn Med Sci* 1980; 65:239–252.
149. Pollack S, Balcerzak SP, Crosby WH. Transferrin and the absorption of iron. *Blood* 1962; 21:33–38.
150. Levine PH, Levine AJ, Weintraub LR. The role of transferrin in the control of iron absorption: Studies on a cellular level. *J Lab Clin Med* 1972; 80:333–341.
151. Taylor P, Martinez Torres C, Leets I, Ramirez J, Garcia Casal MN, Layrisse M. Relationships among iron absorption, percent saturation of plasma transferrin and serum ferritin concentration in humans. *J Nutr* 1988; 118:1110–1115.
152. Bernstein SE. Hereditary hypotransferrinemia with hemosiderosis, a murine disorder resembling human atransferrinemia. *J Lab Clin Med* 1987; 110:690–705.
153. Craven CM, Alexander J, Eldridge M, Kushner JP, Bernstein S, Kaplan J. Tissue distribution and clearance kinetics of non-transferrin-bound iron in the hypotransferrinemic mouse: A rodent model for hemochromatosis. *Proc Natl Acad Sci USA* 1987; 84:3457–3461.
154. Simpson RJ, Lombard M, Raja KB, Thatcher R, Peters TJ. Iron absorption by hypotransferrinemic mice. *Br J Haematol* 1991; 78:565–570.

155. Alvarez-Hernandez X, Smith M, Glass J. The effect of apotransferrin on iron release from Caco-2 cells, an intestinal epithelial cell line. *Blood* 1998; 91:3974–3979.
156. Evans GW, Grace CI. Interaction of transferrin with iron-binding sites on rat intestinal epithelial cell plasma membranes. *Proc Soc Exp Biol Med* 1974; 147:687–689.
157. Banerjee D, Flanagan PR, Cluett J, Valberg LS. Transferrin receptors in the human gastrointestinal tract. Relationship to body iron stores. *Gastroenterology* 1986; 91:861–869.
158. Anderson GJ, Powell LW, Halliday JW. The endocytosis of transferrin by rat intestinal epithelial cells. *Gastroenterology* 1994; 106:414–422.
159. Oates PS, Thomas C, Morgan EH. Transferrin receptor activity and localisation in the rat duodenum. *Pflugers Arch* 2000; 440:116–124.
160. Harris ZL, Durlay AP, Man TK, Gitlin JD. Targeted gene disruption reveals an essential role for ceruloplasmin in cellular iron efflux. *Proc Natl Acad Sci USA* 1999; 96:10812–10817.
161. Brittin GM, Chee QT. Relation of ferroxidase (ceruloplasmin) to iron absorption. *J Lab Clin Med* 1969; 74:53–59.
162. Topham RW, Woodruff JH, Walker MC. Purification and characterization of the intestinal promoter of iron(3+)-transferrin formation. *Biochemistry* 1981; 20:319–324.
163. Kimura I, Tsuchida J, Kodani H. Iron metabolism of intestinal mucosa in various blood diseases. *Acta Med Okayama* 1964; 18:127–137.
164. Chirasiri L, Izak G. The effect of acute haemorrhage and acute haemolysis on the intestinal iron absorption in the rat. *Br J Haematol* 1966; 12:611–622.
165. Richmond VS, Worwood M, Jacobs A. The iron content of intestinal epithelial cells and its subcellular distribution: Studies on normal, iron-overloaded and iron-deficient rats. *Br J Haematol* 1972; 23:605–614.
166. Mattii R, Mielke CH, Levine PH, Crosby WH. Iron in the duodenal mucosa of normal, iron-loaded, and iron-deficient rats. *Blood* 1973; 42:959–966.
167. Adams PC, Zhong R, Haist J, Flanagan PR, Grant DR. Mucosal iron in the control of iron absorption in a rat intestinal transplant model. *Gastroenterology* 1991; 100:370–374.
168. McKie AT, Raja KB, Peters TJ, Farzaneh F, Simpson RJ. Expression of genes involved in iron metabolism in mouse intestine. *Am J Physiol* 1996; 271:G772–G779.
169. Oates PS, Morgan EH. Ferritin gene expression and transferrin receptor activity in intestine of rats with varying iron stores. *Am J Physiol* 1997; 273:G636–G646.
170. Allgood JW, Brown EB. The relationship between duodenal mucosal iron concentration and iron absorption in human subjects. *Scand J Haematol* 1967; 4:217–229.
171. Balcerzak SP, Greenberger NJ. Iron content of isolated intestinal epithelial cells in relation to iron absorption. *Nature* 1968; 220:270–271.
172. Pollack S, Campana T. The relationship between mucosal iron and iron absorption in the guinea pig. *Scand J Haematol* 1970; 7:208–211.
173. Schumann K, Elsenhans B, Ehtechami C, Forth W. Increased intestinal iron absorption in rats with normal hepatic iron stores. Kinetic aspects of the adaptive response to parenteral iron repletion in dietary iron deficiency. *Biochim Biophys Acta* 1990; 1033:277–281.
174. Pollack S, Kaufman RM, Crosby WH. Iron absorption: the effect of an iron deficient diet. *Science* 1964; 144:1015–1016.
175. Topham RW, Joslin SA, Prince JS. The effect of short-term exposure to low-iron diets on the mucosal processing of ionic iron. *Biochem Biophys Res Commun* 1985; 133:1092–1097.
176. Topham RW, Eads CE, Butler BF. Alterations in the mucosal processing of iron in response to very-short-term dietary iron depletion and repletion. *Biochem J* 1992; 284:877–884.

177. Hoglund S. Studies in iron absorption VI. Transitory effect of oral administration of iron on iron absorption. *Blood* 1969; 34:505–510.
178. Pietrangelo A, Rocchi E, Casalgrandi G, Rigo G, Ferrari A, Perini M, Ventura E, Cairo G. Regulation of transferrin, transferrin receptor, and ferritin genes in human duodenum. *Gastroenterology* 1992; 102:802–809.
179. Lombard M, Bomford AB, Polson RJ, Bellingham AJ, Williams R. Differential expression of transferrin receptor in duodenal mucosa in iron overload. Evidence for a site-specific defect in genetic hemochromatosis. *Gastroenterology* 1990; 98:976–984.
180. Rabie A, Simpson RJ, Bomford A, Cunningham Graham D, Peters TJ. Relationship between duodenal cytosolic aconitase activity and iron status in the mouse. *Biochim Biophys Acta* 1995; 1245:414–420.
181. Schumann K, Moret R, Kunzle H, Kuhn LC. Iron regulatory protein as an endogenous sensor of iron in rat intestinal mucosa. Possible implications for the regulation of iron absorption. *Eur J Biochem* 1999; 260:362–372.
182. Flanagan PR, Hajdu A, Adams PC. Iron-responsive element-binding protein in hemochromatosis liver and intestine. *Hepatology* 1995; 22:828–832.
183. Pietrangelo A, Casalgrandi G, Quaglino D, Gualdi R, Conte D, Milani S, Montosi G, Cesarini L, Ventura E, Cairo G. Duodenal ferritin synthesis in genetic hemochromatosis. *Gastroenterology* 1995; 108:208–217.
184. Fleming RE, Migas MC, Zhou X, Jiang J, Britton RS, Brunt EM, Tomatsu S, Waheed A, Bacon BR, Sly WS. Mechanism of increased iron absorption in murine model of hereditary hemochromatosis: Increased duodenal expression of the iron transporter DMT1. *Proc Natl Acad Sci USA* 1999; 96:3143–3148.
185. Anderson GJ, Powell LW, Halliday JW. Transferrin receptor distribution and regulation in the rat small intestine. Effect of iron stores and erythropoiesis. *Gastroenterology* 1990; 98:576–585.
186. Garate MA, Nunez MT. Overexpression of the ferritin iron-responsive element decreases the labile iron pool and abolishes the regulation of iron absorption by intestinal epithelial (Caco-2) cells. *J Biol Chem* 2000; 275:1651–1655.
187. Roy CN, Enns CA. Iron homeostasis: New tales from the crypt. *Blood* 2000; 96:4020–4027.
188. Johnson G, Jacobs P, Purves LR. The effects of cytoskeletal inhibitors on intestinal iron absorption in the rat. *Biochim Biophys Acta* 1985; 843:83–91.
189. Levine DS, Woods JW. Immunolocalization of transferrin and transferrin receptor in mouse small intestinal absorptive cells. *J Histochem Cytochem* 1990; 38:851–858.
190. Jeffrey GP, Basclain KA, Allen TL. Molecular regulation of transferrin receptor and ferritin expression in the rat gastrointestinal tract. *Gastroenterology* 1996; 110:790–800.
191. Oates PS, Thomas C, Morgan EH. Characterization of isolated duodenal epithelial cells along a crypt–villus axis in rats fed diets with different iron content. *J Gastroenterol Hepatol* 1997; 12:829–838.
192. Raja KB, Simpson RJ, Peters TJ. Intestinal iron absorption studies in mouse models of iron-overload. *Br J Haematol* 1994; 86:156–162.
193. Buys SS, Martin CB, Eldridge M, Kushner JP, Kaplan J. Iron absorption in hypotransferrinemic mice. *Blood* 1991; 78:3288–3290.
194. Pountney DJ, Konijn AM, McKie AT, Peters TJ, Raja KB, Salisbury JR, Simpson RJ. Iron proteins of duodenal enterocytes isolated from mice with genetically and experimentally altered iron metabolism. *Br J Haematol* 1999; 105:1066–1073.
195. Levy JE, Jin O, Fujiwara Y, Kuo F, Andrews NC. Transferrin receptor is necessary for development of erythrocytes and the nervous system. *Nature Genet* 1999; 21:396–399.
196. Nunez MT, Nunez-Millacura C, Beltran M, Tapia V, Alvarez-Hernandez X. Apotransferrin and holotransferrin undergo different endocytic cycles in intestinal epithelia (Caco-2) cells. *J Biol Chem* 1997; 272:19425–19428.

197. Levy JE, Montross LK, Cohen DE, Fleming MD, Andrews NC. The C282Y mutation causing hereditary hemochromatosis does not produce a null allele. *Blood* 1999; 94: 9–11.
198. Lebron JA, Bennett MJ, Vaughn DE, Chirino AJ, Snow PM, Mintier GA, Feder JN, Bjorkman PJ. Crystal structure of the hemochromatosis protein HFE and characterization of its interaction with transferrin receptor. *Cell* 1998; 93:111–123.
199. Parkkila S, Waheed A, Britton RS, Bacon BR, Zhou XY, Tomatsu S, Fleming RE, Sly WS. Association of the transferrin receptor in human placenta with HFE, the protein defective in hereditary hemochromatosis. *Proc Natl Acad Sci USA* 1997; 94:13198–13202.
200. Parkkila S, Waheed A, Britton RS, Feder JN, Tsuchihashi Z, Schatzman RC, Bacon BR, Sly WS. Immunohistochemistry of HLA-H, the protein defective in patients with hereditary hemochromatosis, reveals unique pattern of expression in gastrointestinal tract. *Proc Natl Acad Sci USA* 1997; 94:2534–2539.
201. Bastin JM, Jones M, O'Callaghan CA, Schimanski L, Mason DY, Townsend AR. Kupfer cell staining by an HFE-specific monoclonal antibody: Implications for hereditary haemochromatosis. *Br J Haematol* 1998; 103:931–941.
202. Byrnes V, Ryan E, O'Keane C, Crowe J. Immunohistochemistry of the Hfe protein in patients with hereditary hemochromatosis, iron deficiency anemia, and normal controls. *Blood Cells Mol Dis* 2000; 26:2–8.
203. Gross CN, Irrinki A, Feder JN, Enns CA. Co-trafficking of HFE, a nonclassical major histocompatibility complex class I protein, with the transferrin receptor implies a role in intracellular iron regulation. *J Biol Chem* 1998; 273:22068–22074.
204. Ramalingam TS, West AP Jr, Lebron JA, Nangiana JS, Hogan TH, Enns CA, Bjorkman PJ. Binding to the transferrin receptor is required for endocytosis of HFE and regulation of iron homeostasis. *Nature Cell Biol* 2000; 2:953–957.
205. Feder JN, Penny DM, Irrinki A, Lee VK, Lebron JA, Watson N, Tsuchihashi Z, Sigal E, Bjorkman PJ, Schatzman RC. The hemochromatosis gene product complexes with the transferrin receptor and lowers its affinity for ligand binding. *Proc Natl Acad Sci USA* 1998; 95:1472–1477.
206. Roy CN, Penny DM, Feder JN, Enns CA. The hereditary hemochromatosis protein, HFE, specifically regulates transferrin-mediated iron uptake in HeLa cells. *J Biol Chem* 1999; 274:9022–9028.
207. Roy CN, Carlson EJ, Anderson EL, Basava A, Starnes SM, Feder JN, Enns CA. Interactions of the ectodomain of HFE with the transferrin receptor are critical for iron homeostasis in cells. *FEBS Lett* 2000; 484:271–274.
208. Lebron JA, West AP Jr, Bjorkman PJ. The hemochromatosis protein HFE competes with transferrin for binding to the transferrin receptor. *J Mol Biol* 1999; 294:239–245.
209. Ikuta K, Fujimoto Y, Suzuki Y, Tanaka K, Saito H, Ohhira M, Sasaki K, Kohgo Y. Overexpression of hemochromatosis protein, HFE, alters transferrin recycling process in human hepatoma cells. *Biochim Biophys Acta* 2000; 1496:221–231.
210. Han O, Fleet JC, Wood RJ. Reciprocal regulation of HFE and Nramp2 gene expression by iron in human intestinal cells. *J Nutr* 1999; 129:98–104.
211. MacDermott RP, Greenberger NJ. Evidence for a humoral factor influencing iron absorption. *Gastroenterology* 1969; 57:117–125.
212. Reynafarje C, Ramos J. Influence of plasma filtrate containing erythropoietic factor on intestinal iron absorption in rats. *Proc Soc Exp Biol Med* 1962; 109:868–869.
213. Fischer DS, Price DC. A possible humoral regulator of iron absorption. *Proc Soc Exp Biol Med* 1963; 112:228–229.
214. Brittin GM, Haley J, Brecher G. Enhancement of intestinal iron absorption by a humoral effect of hypoxia in parabiotic rats. *Proc Soc Exp Biol Med* 1968; 128:178–184.

215. Beutler E, Bittenwieser E. The regulation of iron absorption. I. A search for humoral factors. *J Lab Clin Med* 1960; 55:274–280.
216. Raja KB, Simpson RJ, Peters TJ. Effect of exchange transfusion of reticulocytes on in vitro and in vivo intestinal iron (Fe^{3+}) absorption in mice. *Br J Haematol* 1989; 73: 254–259.
217. Wheby MS, Jones JG. Role of transferrin in iron absorption. *J Clin Invest* 1963; 42: 1007–1016.
218. Wheby MS, Umpierre G. Effect of transferrin saturation on iron absorption in man. *N Engl J Med* 1964; 271:1391–1395.
219. Hoglund S, Reizenstein P. Studies in iron absorption. IV. Effect of humoral factors on iron absorption. *Blood* 1969; 34:488–495.
220. Schade SG, Bernier GM, Conrad ME. Normal iron absorption in hypertransferrinaemic rats. *Br J Haematol* 1969; 17:187–190.
221. Finch CA, Huebers H, Eng M, Miller L. Effect of transfused reticulocytes on iron exchange. *Blood* 1982; 59:364–369.
222. Walters GO, Thompson W, Jacobs A, Wood CS. Iron stores and iron absorption. *Lancet* 1973; 2:1216.
223. Walters GO, Jacobs A, Worwood M, Trevett D, Thomson W. Iron absorption in normal subjects and patients with idiopathic haemochromatosis: Relationship with serum ferritin concentration. *Gut* 1975; 16:188–192.
224. Halliday JW, Powell LW. Serum ferritin and isoferritins in clinical medicine. *Prog Hematol* 1979; 11:229–266.
225. Conrad ME, Barton JC. Factors affecting iron balance. *Am J Hematol* 1981; 10:199–225.
226. Greenman J, Jacobs A. The effect of iron stores on iron absorption in the rat: The possible role of circulating ferritin. *Gut* 1975; 16:613–616.
227. Cook JD, Dassenko S, Skikne BS. Serum transferrin receptor as an index of iron absorption. *Br J Haematol* 1990; 75:603–609.
228. Kohgo Y, Niitsu Y, Kondo H, Kato J, Tsushima N, Sasaki K, Hirayama M, Numata T, Nishisato T, Urushizaki I. Serum transferrin receptor as a new index of erythropoiesis. *Blood* 1987; 70:1955–1958.
229. Krantz S, Goldwasser E, Jacobson LO. Studies on erythropoiesis. XIV. The relationship of humoral stimulation to iron absorption. *Blood* 1959; 14:654–661.
230. Schiffer LM, Brann I, Cronkite EP, Reizenstein P. Iron absorption and excretion in aregenerative anaemia. A collaborative Swedish-American whole body counter study. *Acta Haematol* 1966; 35:80–90.
231. Adams PC, Reece AS, Powell LW, Halliday JW. Hepatic iron in the control of iron absorption in a rat liver transplantation model. *Transplantation* 1989; 48:19–21.
232. Chow BF, Yeh SDJ, Eberspaecher H. Pituitary gland and iron absorption. *Endocrinology* 1963; 72:871–883.
233. Benn HP, Drews J, Randzio G, Jensen JM, Loffler H. Does active rheumatoid arthritis affect intestinal iron absorption? *Ann Rheum Dis* 1988; 47:144–149.
234. Baynes RD, Cook JD, Keith J. Interleukin-11 enhances gastrointestinal absorption of iron in rats. *Br J Haematol* 1995; 91:230–233.
235. Cavill I, Worwood M, Jacobs A. Internal regulation of iron absorption. *Nature* 1975; 256:328–329.
236. Marx JJ. Regulation of iron absorption in man. *Neth J Med* 1983; 26:194.
237. Intragumtornchai T, Huebers HA, Eng M, Finch CA. In vivo transferrin-iron receptor relationships in erythron of rats. *Am J Physiol* 1988; 255:R326–R331.
238. Nathanson MH, McLaren GD. Computer simulation of iron absorption: Regulation of mucosal and systemic iron kinetics in dogs. *J Nutr* 1987; 117:1067–1075.

239. Hahn PF, Bale WF, Lawrence EO, Whipple GH. Radioactive iron and its metabolism in anemia. *J Exp Med* 1939; 69:739–753.
240. O'Neil Cutting MA, Crosby WH. Blocking of iron absorption by a preliminary oral dose of iron. *Arch Intern Med* 1987; 147:489–491.
241. Wright AJ, Southon S, Fairweather Tait SJ. Measurement of non-haem iron absorption in non-anaemic rats using ⁵⁹Fe: can the Fe content of duodenal mucosal cells cause lumen or mucosal radioisotope dilution, or both, thus resulting in the underestimation of Fe absorption? *Br J Nutr* 1989; 62:719–727.
242. Weintraub LR, Conrad ME, Crosby WH. Control of iron absorption: An evaluation of the concept of mucosal block. *Blood* 1965; 26:887.
243. Granick S. Ferritin. IX. Increase of protein apoferritin in the gastrointestinal mucosa as a direct response to iron feeding. The function of ferritin in the regulation of iron absorption. *J Biol Chem* 1946; 164:737–746.
244. Crosby WH. Mucosal block. An evaluation of concepts relating to control of iron absorption. *Semin Hematol* 1966; 3:299–313.

Regulation of Systemic Iron Transport and Storage

PIERRE BRISSOT, CHRISTELLE PIGEON, and OLIVIER LORÉAL

University Hospital Pontchaillou, Rennes, France

I. INTRODUCTION	597
II. IRON DISTRIBUTION AND STORAGE	598
A. Iron Distribution	598
B. Iron Storage	601
C. Physiological Movement of Iron in the Body	602
III. REGULATION OF SYSTEMIC IRON TRANSPORT AND STORAGE	603
A. Regulation of Stores	604
B. Regulation of Distribution	605
ADDENDUM	609
REFERENCES	609

I. INTRODUCTION

The main characteristics of systemic iron transport and storage in humans may be explained by the following facts. (a) The high propensity of ferrous iron to be oxidized in aqueous solution to the insoluble ferric state under physiological conditions exposes the body to iron unavailability; this explains the necessity for iron to be transported linked to solubilizing molecules, such as transferrin. (b) Iron is an essential element in human metabolism, involved in many biological functions ranging from oxygen transport to various enzymatic reactions. This physiological importance of iron accounts for its wide organ and cellular distribution. It can also explain the capacity of the body to store iron in order to get access to an iron reserve in case of deficient external iron supply or excessive internal iron losses. (c) Iron ions, even

in tiny amounts, can damage tissues and organs through the production of hydroxyl radicals which can attack lipids, proteins, and nucleic acids. Therefore, iron needs to be sequestered within protection proteins, such as ferritin. (d) The human body is very sensitive to the consequences of iron deficiency as well as of iron excess, as illustrated by the fact that disorders of iron metabolism are among the most frequent diseases of humans. Consequently, the physiological iron balance is very tenuous in order to maintain bodily iron homeostasis.

II. IRON DISTRIBUTION AND STORAGE

A. Iron Distribution

1. Overview

The iron content in the human body is normally 3–4 g, corresponding to about 40 mg/kg weight in women and 50 mg/kg in men. About two-thirds of the body's iron content is incorporated into hemoglobin within erythroid precursors and mature red blood cells (see Chapter 26). Each erythrocyte contains about 10^9 atoms of iron, corresponding, at normal rates of turnover, to the incorporation of 2×10^{20} atoms of iron per day (2). Approximately 20% corresponds to stored iron, the main storage sites being the parenchymal cells of the liver and the reticuloendothelial macrophages (primarily those of the spleen). Ten percent are present in muscle fibers (in myoglobin) and in various tissues (as part of ferritin, enzymes, and cytochromes). In brain (see Chapter 20), the total amount of iron is around 60 mg (3): its distribution is variable, reaching its highest concentration in the globus pallidus ($13.5 \mu\text{mol/g}$ dry weight). Substantia nigra and putamen are also rich in iron (4). The kidney contains minimal iron (11 mg). A tiny—although functionally essential—amount of iron (3 mg) is present in the plasma, linked to transferrin.

2. Sources

Dietary iron represents, in a normal diet, a daily amount of 10–20 mg, of which only 1–2 mg is absorbed. Alimentary iron corresponds to two main physicochemical forms, organic or inorganic iron. Inorganic or nonheme iron is present in fruits and vegetables. Various dietary constituents, such as sugars, amino acids, and amines, enhance its absorption by rendering iron soluble at the alkaline pH of the small intestine. Ascorbic acid also stimulates iron absorption through both reduction of iron and formation of soluble iron-ascorbate chelates. Heme iron itself can promote nonheme iron absorption. Inorganic iron absorption is decreased by calcium and by compounds such as phytates (vegetables, bran), dietary fibers, and polyphenols (tea, coffee) which produce molecular aggregation or precipitation. Organic iron (or heme iron) is present in fish and meat. Its absorption is five times more efficient than that of nonheme iron. Organic iron, which is soluble in alkaline solutions, is not influenced by the various compounds available to affect the absorption of inorganic iron.

3. Transport

a. Plasma

Transferrin iron represents the major physiological form of circulating iron. Transferrin is a glycoprotein consisting of a single polypeptide chain with two binding

sites (each capable of binding one atom of ferric iron), and two branched carbohydrate chains (glycans). Circulating transferrin can exist in four molecular forms (apo-transferrin, monoferric A, monoferric B, diferric transferrin) but can be considered, physiologically, as a single homogeneous pool. The normal plasma concentrations are 20 $\mu\text{mol/L}$ for serum iron and 30 $\mu\text{mol/L}$ for transferrin (which corresponds to a transferrin saturation rate of approximately 30%).

Other forms of plasma iron include nonheme and heme iron. Ferritin-iron is likely to represent only a minute amount of total body iron, as the iron content of circulating ferritin is usually low. Serum ferritin levels are normally less than 200 ng/mL in men and 100 ng/mL in women. The so-called non-transferrin-bound iron is not significantly detectable in normal plasma, whereas it can reach significant concentrations in cases of iron overload. Its biochemical nature remains undefined, but it has been found to circulate complexed to low-molecular-weight compounds such as citrate and acetate. These species are probably heterogeneous (5), iron being also associated with macromolecules such as albumin.

Heme iron is carried as hemoglobin bound to haptoglobin, and as heme bound to hemopexin. Normally, the haptoglobin and hemopexin systems handle about 10% of erythrocyte destruction.

b. Cerebrospinal Fluid

Iron concentration in normal cerebrospinal fluid (CSF) is low, of the order of 0.8 $\mu\text{mol/L}$ (6), probably due to an efficient blood–brain barrier against plasma iron crossing. Transferrin levels vary, according to various authors (6–9) between 8 and 23 mg/L, but it is established that, in most normal CSFs, transferrin is fully saturated, and therefore other forms of iron must be present. This is supported by Gutteridge's data (10) showing, with a bleomycin assay, normal mean levels of non-transferrin-bound iron of $0.55 \pm 0.27 \mu\text{mol/L}$. Normal CSF contains approximately 10% of the levels of ferritin found in the serum (11).

4. Iron Utilization

Utilization of iron occurs at several levels. These include (a) the lifetime of the red cell, which represents, quantitatively, the major consumer of iron. Over 80% of the transferrin-bound iron leaving the plasma pool is delivered to erythroid precursors in the bone marrow, in order to produce haemoglobin. (b) Being part of myoglobin, iron plays a key role in muscle functioning. (c) Iron participates in many hepatic functions, such as the respiratory process and various enzymatic reactions (biotransformation, collagen synthesis, DNA synthesis). (d) In the brain, iron is required by neurons and glia for many functions, especially involving in the synthesis of various neurotransmitters, such as dopamine, serotonin, and GABA (12).

5. Iron Losses

Iron loss takes place mainly in the intestine, from the skin, and in the urine. The gastrointestinal tract is the major route of iron loss. Three intestinal iron pools can be distinguished, consisting of blood loss (0.3 mg/day), biliary iron excretion (0.5 mg/day), and exfoliated epithelial cells (0.4 mg/day). Skin losses occur from both desquamated cells and sweat (0.2–0.3 mg/day). Urinary elimination is about 0.1

mg/day. Globally, the total amount of lost iron approximately equals the amount absorbed (1–2 mg/day).

6. Physiological Variations

a. Variations in Sources

Dietary habits greatly influence the amount of absorbed iron (13). On the one hand, the degree of absorbed iron is increased in (red) meat eaters, (red) wine drinkers, and consumers of ascorbic acid (orange juice) and citric acid (citrus fruits). On the other hand, absorbed iron is decreased in vegetarians because of low heme iron content of the diet plus a high phytate intake, in tea drinkers (due to polyphenols), and in consumers of calcium-rich high-fiber diets.

b. Variations in Utilization

Gynecological events need to be considered in iron utilization. Indeed, during pregnancy, iron needs are increased due to several factors: (a) An enhancement of red blood cell mass by about 20% corresponds to 500 mg of iron. This expansion of maternal red cells is maximal toward weeks 20–25 of gestation. (b) The constitution of the blood-rich placenta requires additional iron, as does (c) the development of fetal tissues. Most fetal iron deposition occurs after week 30. On the whole, a pregnant woman needs 800 mg of iron (14,15) to ensure her iron balance. Lactation also consumes iron, the iron content of maternal milk ranging from 0.3 to 1.5 mg/L (16) (the absence of menstruation, however, attenuates iron loss during this period).

c. Variations in Losses

The usual median values of menstrual blood losses are 25–30 mL/month, corresponding to iron losses of 12.5–15 mg/month, i.e., 0.4–0.5 mg/day (15). Ten percent of women have menstruation volumes above 80 mL/month, corresponding to losses higher than 2.1 mg/day. Oral contraceptives may decrease the menstruations by 50%, whereas an intrauterine device can increase them by more than 100%. Menopause obviously suppresses iron loss due to menstruation, unless substitutive hormone-therapy is instituted.

7. Transport in Children

The iron content of a term newborn is 260–290 mg (15). The main feature of iron distribution in the newborn is that about 75% of this iron is in circulating hemoglobin because hemoglobin concentration is particularly high at birth. In the first two months of life, there are both a marked fall of hemoglobin concentration and a redistribution of iron to storage compartments. The iron needs are greatest by three to four months of age, due the doubling in body weight so that, by six months of age in term infants, iron stores become depleted, and the baby becomes dependent on external sources for maintenance of iron homeostasis (17,18).

Due to growth needs, iron requirements expressed per kilogram of body weight are 8–10 times as high in children as in adults. This is especially true during the sexual maturation phase. It has been estimated (15) that, during the year of maximal growth, an adolescent requires a net increase of 350 mg of iron. In female adolescents, the yearly gain of weight being less than in males, the iron requirement is

about 280 mg per year. Menstruations correspond to a yearly iron loss of about 175 mg (19).

B. Iron Storage

Two cell types are mainly involved in systemic iron storage, macrophages and hepatocytes.

1. Macrophages

Macrophages constitute the major iron storage site in the body (see Chapter 19). At the end of their lifespan, red blood cells are removed from the bloodstream by a specialized population of macrophages located predominantly in the spleen, but also present in the bone marrow and the liver (Kupffer cells) (20). Globally, the iron coming from catabolized erythrocytes is released from macrophages into the plasma according to biphasic kinetics: an early phase with a half-life on the order of half an hour is followed by a late phase corresponding to the release of the macrophagic storage in iron pool. The latter occurs with a half-life of about six days (21). With decreasing iron stores, the proportion of early-phase iron increases, whereas with increasing iron stores, the proportion of both early- and late-phase iron decreases. Erythrophagocytosis involves the process of hemoglobin catabolism, with globin undergoing proteolysis and heme reaching the endoplasmic reticulum of the macrophage where it is degraded by heme oxygenase. The iron generated through oxidative catabolism of heme is partly retained within the macrophage. There, iron is incorporated predominantly into ferritin molecules which are rich in L-subunits (22). When iron storage increases in the macrophage, the proportion of iron stored as hemosiderin progressively increases, as is also seen in hepatocytes. The other fraction of heme-derived iron is released into the bloodstream, where it is taken up by plasma apotransferrin. This release process represents the largest single flux of iron from cells into the vascular compartments (20). It has also been proposed that ferritin plays a role in the transfer of iron from Kupffer cells to hepatocytes (23).

2. Hepatocytes

Hepatocytes are the other major site of iron storage (see Chapter 25). Schematically, hepatocytic iron can be distributed among three main compartments: (a) The labile iron pool (LIP), also termed the transit iron pool, serves as an interface between the other two (functional and storage) pools. (b) The functional iron compartment can be divided into two subcompartments. One is the mitochondrial iron pool, which participates in heme formation and therefore in the synthesis of hemoproteins such as the cytochromes, which are involved in cellular respiratory processes. The extramitochondrial iron pool includes microsomal hemoproteins such as cytochrome P450 that are especially involved in xenobiotic biotransformation; peroxisomal haemoproteins such as peroxidases and catalases which act as free-radical scavengers; iron-dependent enzymes such as prolylhydroxylase (catalyzing a critical step of collagen biosynthesis), ribonucleotide reductase (catalyzing the reduction of ribo- to deoxyribonucleotides), and xanthine oxidase (catalyzing the oxidation of purines to uric acid, as well as the incorporation of copper into ceruloplasmin). (c) The storage iron compartment includes the ferritin and the hemosiderin subcompartments. Holo-ferritin is the principal form of iron storage in the physiological range. The iron is

localized within the hollow central part of apoferritin which forms a shell consisting of 24 subunits, designated H (for heavy or heart) and L (for light or liver), depending on their relative molecular weights (19,000–21,000) and the organs in which they predominate (see Chapter 5). L-ferritin appears to function primarily as an iron storage protein. Each apoferritin molecule can store up to 4500 atoms of iron in the ferric form as ferrihydrite (FeOOH). Iron enters (and leaves) the ferritin molecule through channels piercing the protein shell. The exact mechanism whereby iron is transported to the ferritin cavity remains under debate. One view, perhaps the most widely accepted, is that Fe(II) dimers bind to a ferroxidase center of the H chains, are oxidized into Fe(III) via a peroxodiferric intermediate (24), Fe(III) being then conveyed to the ferritin cavity. The other model considers that Fe(II) oxidation is carried out by ceruloplasmin (instead of ferritin) via its ferroxidase activity or by an intracellular analog of ceruloplasmin (25). The physiological mechanisms of iron release from the ferritin molecule also remain poorly understood. This release is known to be facilitated by reducing agents such as vitamin C and flavoproteins, but whether iron removal from ferritin is a reversible process or requires protein degradation remains to be defined. For a more detailed discussion of the molecular interactions of iron and ferritin, see Chapter 5.

Hemosiderin is a poorly defined molecule corresponding to a degradation product of ferritin, produced by the partial digestion of the protein and the release of iron, leading to the formation of insoluble aggregates. When the amount of storage iron increases, the hemosiderin content increases to a greater extent than does that of ferritin (26).

C. Physiological Movement of Iron in the Body

The movement of iron in the body is a heavy, multidirectional traffic. Although the impression may be that of a random diffusion, the overall process is in fact highly consistent and organized. Three main clues may help to explain these movements. The major one concerns the erythrocyte's life cycle. The bloodstream contains, in its plasma compartment, transferrin iron which is at the source of erythrocyte formation, and arrives from the gut (absorbed iron) and from the macrophages (following the degradation of senescent red blood cells). This plasma iron pool converges on the bone marrow in order to contribute to erythrocyte formation. In a cellular compartment, the erythrocytes are themselves heavily iron-loaded because of their hemoglobin content. At the end of their lifespan, the red blood cells are degraded within the macrophages, essentially of the spleen, and regenerate iron which returns to the plasma compartment. These movements are in fact unidirectional and constitute the red blood cell cycle (Fig. 1).

The second important clue to understanding iron traffic is related to the necessity for the nonerythroid cells, especially the hepatocytes and enterocytes, to adapt their iron content according to their own functional needs, and to the iron status of the body, thereby explaining a two-directional iron flux (entry of iron from the plasma into the cell and egress of cellular iron toward the plasma). The third clue is that iron metabolism in humans is a highly conservative one and corresponds to an almost closed circuit, with very little entry and exit of iron as indicated by the fact that the normal delivery entry (which equals the daily exit) represents only 0.02% of the total body iron.

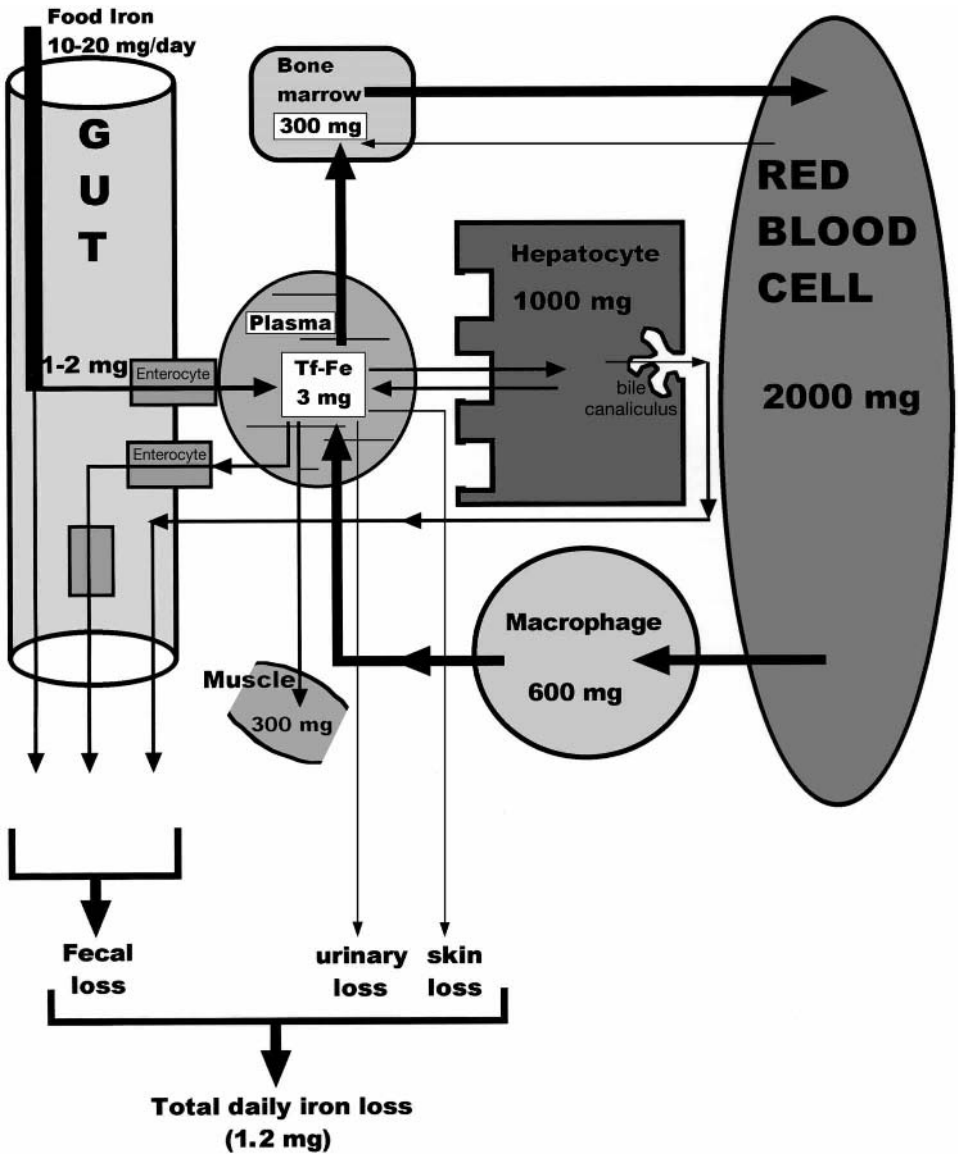


Figure 1 Schematic representation of iron distribution and storage in human body. (Tf = transferrin.)

III. REGULATION OF SYSTEMIC IRON TRANSPORT AND STORAGE

Adequate amounts of iron are required in each of the body's different compartments, and in each of the different cellular compartments. Modifications of iron distribution and storage may result in iron deficiency or iron excess in any of these different compartments, leading to deleterious effects (2). Therefore, iron transport and repar-

titioning, as well as iron storage, must be highly regulated. All these steps are primarily dependent on total body iron stores.

A. Regulation of Stores

To be distributed correctly among the different compartments, i.e., mainly the erythroid compartments in the normal situation, appropriate total iron stores must be maintained. For example, during iron overload, iron in excess is predominantly taken up by other organs, including the liver. Maintenance of a normal iron content is the result of an equilibrium between digestive iron absorption and iron losses. However, since iron losses are not clearly regulated, the stability of total iron body stores is related mainly to the amount of absorbed iron.

The total amount of iron absorbed daily can be modulated by different exogenous factors including the biochemical form of iron, with greater part of heme iron, and the amount of iron ingested. For the latter parameter, it has been well demonstrated that high quantities of ingested iron limit digestive uptake for several days and represent a "mucosal block." In addition, other nutritional factors, such as divalent cations, amino acids, lipids, sugars, and some vitamins, are able to enhance iron absorption. Conversely, some other nutrients induce a decrease in iron uptake in the duodenal mucosal cells. Furthermore, endogenous factors are able to modulate iron absorption. This is well illustrated during some physiological situations, including pregnancy and in growing children, where, due to high iron requirements, a high level of iron absorption is present in order to maintain adequate iron stores.

Pathological situations may also influence the rate of iron absorption. In iron deficiency, the amount of absorbed iron is increased. In addition, in some types of anemia there appears to be an unknown signal, independent of iron stores, which can lead to an increase of iron absorption. Thus, in thalassemia major and myelodysplastic syndromes (27,28), excessive iron content is related not only to blood transfusions, but also to iron hyperabsorption resulting from dyserythropoiesis.

Players which are involved in digestive iron absorption are suggested and (or) proven for several different pathological situations in rodents and humans. Indeed, several proteins, including DMT-1, Ireg1 (ferroportin), hephaestin, and HFE, which are described in detail in other chapters of this book, play important roles.

DMT-1 is involved in iron uptake by the enterocyte from the digestive lumen and is the first gate for iron ingress in the body [(29,30); see also Chapter 6]. During genetic hemochromatosis, it has been demonstrated that DMT-1 expression is increased and therefore could contribute to the hyperabsorption of iron leading to development of iron excess (31). In this situation, it is well known that the first target of this excessive iron is the liver, by a mechanism that will be described below. This hepatic iron overload reflects a strong modification of iron distribution within the body. Other organs, including heart and pancreas, are also affected by excessive iron deposition. Conversely, mutation in DMT-1 leads to a development of iron deficiency in *mk/mk* mice (30) and in Belgrade rats (32). Additionally, DMT-1 could play a role in intracellular iron metabolism by mediating the egress of iron from endocytic vesicles (32,33).

Recently, a protein named Ireg1 (34), or ferroportin (35), has been described (and see Chapter 7). This transmembrane protein is involved in the egress of iron at the enterocyte's basolateral side. Additionally, this protein could be expressed in

different compartments, could play a role in iron metabolism, and then in turn in iron distribution in a large variety of cells. However, Ireg-1 is not sufficient to ensure iron egress from the enterocyte. Indeed, besides Ireg-1, it has been demonstrated that hephaestin, a multicopper oxidase homolog to ceruloplasmin but with a perimembrane localization, plays a role in iron transfer to the apical medium. A defect of this protein leads to the development of the well-characterized sex-linked anemia in the mouse (36).

HFE, by its interaction with the transferrin receptor, could modulate enterocyte transferrin iron uptake at the basolateral pole of the enterocyte (37), and then secondarily influence the intracellular iron status. This could in turn lead to an adapted regulation of iron absorption, or conversely to a nonadapted iron absorption, as has been described for genetic hemochromatosis. In this disease, HFE is mutated (C282Y) and digestive iron hyperabsorption occurs (see Chapters 8 and 28). This effect of HFE could implicate IRP, which is involved in the control of enterocyte iron metabolism (38), through its potential interactions with the IRE sequences found in the 3'-UTR of DMT-1 (29), in transferrin receptor m-RNA, and in the 5'-UTRs of ferritin- (39) and Ireg1-mRNAs (34). Recent data demonstrate both that retention of transferrin-bound iron within the macrophages is lower in patients with C282Y hemochromatosis, and that this abnormality is corrected by transfection of the wild-type gene (40). These results suggest that macrophages could play a key role in the modulation of total body iron stores, due to their potential action on digestive iron absorption by an as yet unknown process.

From the above, it is clear that the enterocyte is not a simple gate for iron entry into the apical medium. It represents, in fact, the major step on which depend body stores of iron, and subsequently how the iron is distributed among different body compartments. This distribution favors the bone marrow compartment in the case of iron deficiency, and is related, for instance, to excessive iron losses. Conversely, it may favor the iron storage organs such as the liver in the case of iron excesses.

B. Regulation of Distribution

As soon as iron enters the plasma as new or recycled iron, it must be adequately distributed among the different organs. This repartition of iron depends on body stores of cellular iron. However, a modification of the iron distribution is also related to the changes in the biochemical plasmatic form of iron. In addition, some specific pathological situations may lead to abnormal distribution of iron.

1. Cellular Iron Stores

Generally, transferrin receptor expression at the cell membrane increases in cases of iron deficiency, and decreases in iron overload. This modulation of its expression is related to regulation through IRP activity, which is itself related to the intracellular iron content, especially the LIP (41). This phenomenon theoretically allows the cell to take up a greater amount of transferrin-iron in case of cellular iron deficiency and, conversely, to limit the iron ingress whenever there is cellular iron excess (Fig. 2).

In the latter case, cells which express transferrin receptor at a lower level will be relatively protected against iron excess development. In the special case of the liver, there is a contrast between the downregulation of the transferrin receptor ex-

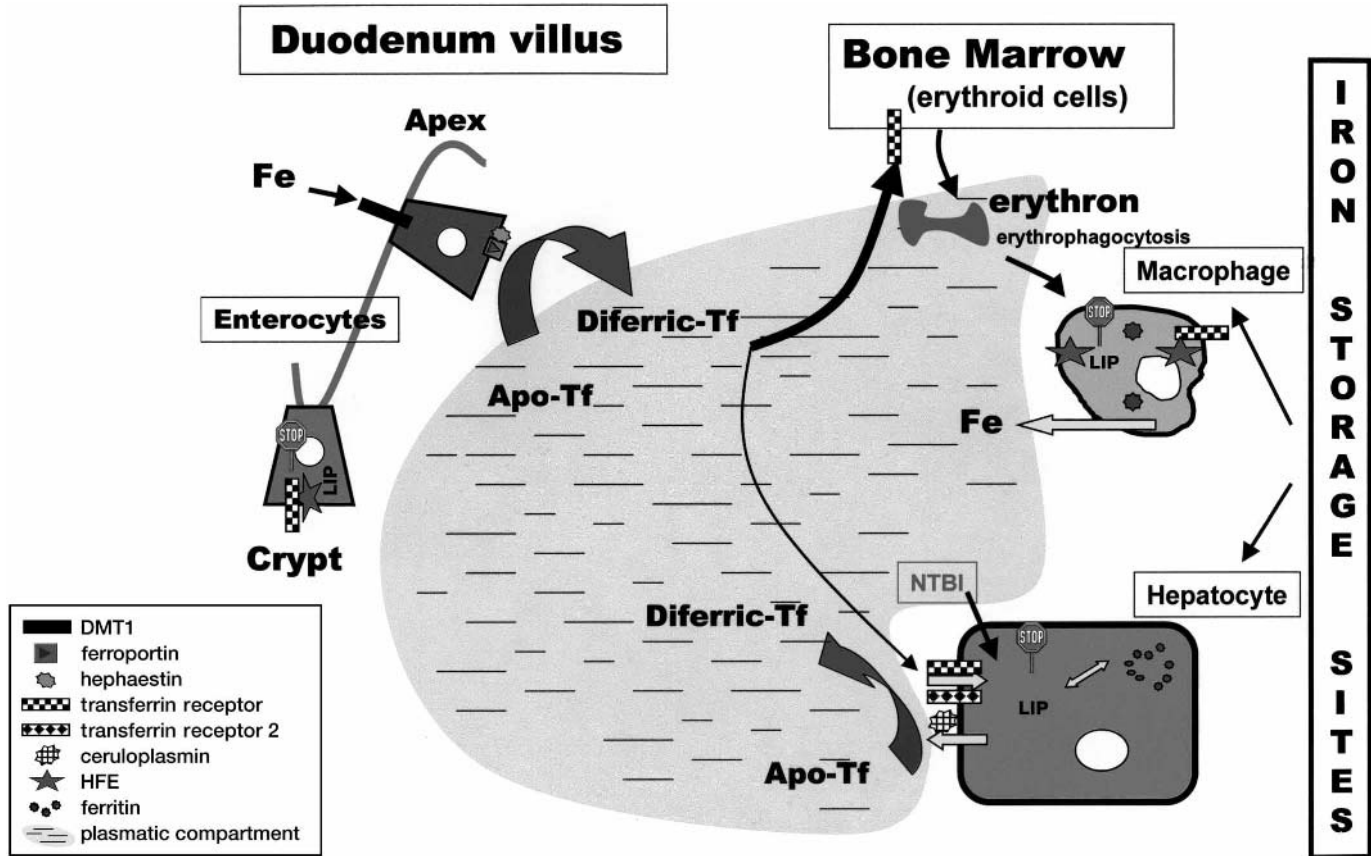


Figure 2 Schematic representation of pathways and proteins involved in the maintenance of body and cellular iron stores. The stop signal symbolizes the possible regulation of IRE containing mRNA expression by IRP when labile iron pool (LIP) varies. NTBI = non-transferrin-bound iron which is found in plasma in condition of iron overload. ApoTf = apotransferrin. DiferricTf = diferric-transferrin.

pression and the fact that this organ continues to take up iron, leading to iron overload. This could be partially related to the expression of a second form of transferrin receptor (transferrin receptor-2), which is not iron-regulated due to the absence of an IRE in the 3'-UTR of its mRNA. This recently described transferrin receptor (42) is expressed at especially high levels in the liver (43).

2. Role of the Biochemical Form of Iron

In the normal situation, transferrin is the most important plasmatic biochemical form of iron transport from one site to another. Other proteic transporters include hemopexin, haptoglobin, and ferritin. Transferrin-iron is distributed mainly to the erythroid compartments for hemoglobin synthesis. Transferrin iron uptake involves the fixation of ferric-transferrin to the transferrin receptor, the endocytosis of this couple, and thereafter iron dissociation from the transferrin within the endocytotic vesicles due to a pH decrease. Subsequently, recycling of transferrin and transferrin receptor to the cell membrane occur, whereas iron reaches the cytosol after having crossed the endocytic membrane under the effect of an iron transporter which could be DMT-1 (32,33).

However, in case of iron excess, the repartition of newly absorbed and recycling iron among the different organs is modified. Indeed, other organs are then involved directly in iron storage. This includes the liver, which is the main iron storage site, as well as the pancreas and heart (44). It must be pointed out that myeloencephalic structures, likely due to the blood-brain barrier membrane, are usually not, or only slightly, involved in iron overload, except in the case of aceruloplasminemia (see Chapter 30).

This localization of iron especially in the liver has been attributed mainly to the appearance of non-transferrin-bound iron (NTBI) in the plasma. Indeed, it has been demonstrated that this biochemical iron species is found in the serum of iron-overloaded patients, as well as in various pathological states. This form of iron is avidely taken up by those organs. This has been clearly demonstrated in the atransferrinemic mouse (44) and in the perfused rat liver (45,46). Thus, the liver is able to extract 70% of plasma NTBI during the first vascular passage. Moreover, in iron-overloaded rats, the biliary excretion of iron presented to the liver as NTBI is strongly decreased (47). Taken together, these phenomena could explain the predominant role of the liver in iron storage. Mechanisms of cellular uptake of NTBI are not clearly elucidated. They could involve a reduction step of iron to its Fe^{2+} form before being taken up by an iron transporter to cross the cell membrane (48). However, the proteins or enzymes involved have not yet been identified.

Ferritin could represent another way for iron delivery to the liver in case of iron overload with hyperferritinemia (49). Indeed, tissue ferritin is rapidly taken up by the liver in rats. This mechanism is saturable and could involve endocytosis. Whether this mechanism is regulated by cellular iron stores remains to be elucidated. Hepatic ferritin receptors have been isolated and partially purified (50,51). Sibille et al. (23) have described the role of Kupffer cells and hepatocytes in the metabolism of ferritin. Kupffer cells could release ferritin, which contains iron provided by erythron phagocytosis, and secondarily this ferritin is taken up by hepatocytes which degrade then degrade the ferritin in their lysosomes. Additionally, ferritin receptors have been described on hepatic stellate cells (52).

3. Abnormalities Not Primarily Iron-Related

Various pathological situations may influence iron distribution. The most prominent situation is inflammation, in which serum iron parameters may be altered. In an extreme situation, serum iron and transferrin saturation are decreased, ferritin values are increased, and in parallel a normocytic or microcytic anemia develops. In addition, iron stores increase especially in the liver, spleen, and bone marrow. The mechanisms accounting for these inflammation-related changes in iron levels are not well known. They could involve an inadequate response to erythropoietin that could play a role in the development of anemia and in a reduction of iron release into the plasma, which in turn leads to iron retention. Explanations of the iron retention have been reviewed (53). They include, first, a displacement of iron from transferrin to lactoferrin produced by granulocytes during inflammation, leading to preferential macrophagic iron uptake (although this might be true only at local sites of inflammation); and second, hyperferritinemia, which could be induced by inflammatory cytokines such as interleukin-1, interleukin-6, and tumor necrosis factor- α would lead to excessive iron storage.

Neurodegenerative diseases, including Alzheimer and Parkinson diseases, are of particular interest. Indeed, in classical iron overload situations such as genetic hemochromatosis or thalassemia major, the brain is globally protected against iron overload, probably because of the presence of the blood–brain barrier. However, in neurodegenerative diseases, excess iron deposition may be found in the brain, leading to increased neuronal lesions through oxidative stress. However, the detailed mechanisms leading to this excessive iron deposition remain to be elucidated (see Chapter 20).

Recently, a new entity in iron overload has been described, aceruloplasminemia (see Chapter 30). This disease is related to mutations and (or) deletions in the ceruloplasmin gene, a multicopper oxidase, which is involved in plasma copper transport (54). However, its main role is related to its ferroxidase activity. Clinical presentation includes hepatic iron overload which mimics growth hormone in its hepatocytic distribution, with a porto-centrolobular decreasing gradient. Surprisingly, however, there are extremely low levels of serum iron and low transferrin saturation. In addition, iron overload is also found in the brain, a phenomenon which is not observed in other classical iron-overload situations.

The biochemical effect of ceruloplasmin deficiency has been debated. From radioactive-iron kinetic studies in humans (55), and in the ceruloplasmin knockout mouse (56), it is now established that ceruloplasmin is required for the exit of iron from the cells. Its ferroxidase activity may permit the oxidation of Fe^{2+} to Fe^{3+} , outside the cell. The Fe^{3+} would then be taken in charge by transferrin. Therefore, the very special accumulation of iron in the brain observed in this disease is likely related to the absence of expression of ceruloplasmin in the brain. Indeed, it has been demonstrated that ceruloplasmin is expressed in the normal brain, especially by astrocytes as a glycosyl phosphatidylinositide-anchored form (57). In addition, expression of ceruloplasmin in brain could play a role in the nonspecific iron accumulation described in neurodegenerative diseases described above.

Together these data illustrate the complexity of iron metabolism due to numerous players operating in numerous biological compartments. Each of these players, if mutated, may be the molecular target which could favor the development of

an abnormality in iron distribution and/or storage. Furthermore, recent data clearly document the close relationship between copper and iron metabolisms and open a new field for the comprehension of iron metabolism.

ADDENDUM

Two new actors involved in iron metabolism have been identified during the printing of this book: (a) Dcytb (Duodenal cytochrome b), which exhibits ferric reductase activity in the brush-border membrane of mouse duodenal enterocytes and permits the subsequent transmembrane transport of Fe^{2+} by DMT1 (58); (b) Hfe, originally identified as a gene upregulated by iron overload in the liver (59), reported as nonexpressed in (USF2) knockout mice which develop multivisceral iron overload (60), suggesting its regulatory role in iron metabolism.

REFERENCES

1. Brissot P, Deugnier Y. Normal iron metabolism. In: McIntyre N, Benhamou JP, Bircher J, Rizzetto M, Rodes J, eds. *Oxford Textbook of Clinical Hepatology*. Oxford, UK: Oxford University Press, 1999:409–413.
2. Andrews NC. Disorders of iron metabolism. *N Engl J Med* 1999; 341:1986–1995.
3. Jacobs A, Worwood M. Normal iron metabolism. In: Powell LW, ed. *Metals and the Liver*. New York: Marcel Dekker, 1978:3–51.
4. Bradbury MWB. Transport of iron in the blood-brain-cerebrospinal fluid system. *J Neurochem* 1997; 69:443–454.
5. Loréal O, Gosriwatana I, Guyader D, Porter J, Brissot P, Hider RC. Determination of non-transferrin-bound iron in genetic hemochromatosis using a new HPLC-based method. *J Hepatol* 2000; 32:727–733.
6. Bleijenberg BG, Van Eijk HG, Leijnse B. The determination of nonheme iron and transferrin in cerebrospinal fluid. *Clin Chim Acta* 1979; 31:277–281.
7. Felgenhauer K. Protein size and cerebrospinal fluid. *Klin Wochenschr* 1974; 52:1158–1164.
8. Lamoureux G, Jolicoeur R, Giard N, St-Hilaire M, Duplantis F. Cerebrospinal fluid proteins in multiple sclerosis. *Neurology* 1975; 25:537–552.
9. Del Principe D, Menichelli A, Colistra C. The ceruloplasmin and transferrin systems in cerebrospinal fluid in acute leukaemia patients. *Acta Paediatr Scand* 1989; 78:327–328.
10. Gutteridge JMC. Hydroxyl radicals, iron, oxidative stress and neurodegeneration. *Ann NY Acad Sci* 1994; 738:201–213.
11. Campbell DR, Skikne BS, Cook JD. Cerebrospinal fluid ferritin levels in screening for meningism. *Arch Neurol* 1986; 43:1257–1260.
12. Crichton RR, Ward RJ. Iron homeostasis. In: Crichton RR, ed. *Metals Ions in Biological Systems*. 1998:633–665.
13. Skikne, Baynes RD. Iron absorption. In: Brock JH, Halliday JW, Pippard MJ, Powell LW, eds. *Iron Metabolism in Health & Disease*. London: Saunders, 1994:151–187.
14. Hercberg S. La carence en fer en nutrition humaine. Paris: Editions médicales internationales, 1988.
15. Allen LH. Pregnancy and iron deficiency: Unresolved issues. *Nutr Rev* 1997; 55:91–101.
16. Fransson GB, Lönnerdal B. Iron in human milk. *J Pediatr* 1980; 96:380–384.
17. Stekel A. Iron requirements in infancy and childhood. In: Stekel A, ed. *Iron Nutrition in Infancy and Childhood*. Nestlé Nutrition Workshop Series. Vol. 4. New York: Raven Press, 1984:1–10.

18. Yip R. Changes in iron metabolism with age. In: Brock JH, Halliday JW, Pippard MJ, Powell LW, eds. *Iron Metabolism in Health & Disease*. London: Saunders, 1994:427–448.
19. Hallberg L, Hogdahl AM, Nilsson L, Rybo G. Menstrual blood loss—A population study. *Acta Obstet Gynecol Scand* 1966; 45:25–56.
20. Brittenham GM. The red cell cycle. In: Brock JH, Halliday JW, Pippard MJ, Powell LW, eds. *Iron Metabolism in Health & Disease*. London: Saunders, 1994:31–62.
21. Fillet G, Beguin Y, Baldelli L. Model of reticuloendothelial iron metabolism in humans: Abnormal behaviour in idiopathic hemochromatosis and in inflammation. *Blood* 1989; 74:844–851.
22. Invernizzi R, Cazzola M, De Fazio P, Rosti V, Ruggeri G, Arosio P. Immunocytochemical detection of ferritin in human bone marrow and peripheral blood cells using monoclonal antibodies specific for the H and L subunit. *Br J Haematol* 1990; 76:427–432.
23. Sibille JC, Kondo H, Aisen P. Interactions between isolated hepatocytes and Kupffer cells in iron metabolism: A possible role for ferritin as an iron carrier protein. *Hepatology* 1998; 8:296–301.
24. Pereira AS, Small W, Krebs C, Tavares P, Edmodson DE, Theil EC, Huynh BH. Direct spectroscopic and kinetic evidence for the involvement of a peroxidodiferric intermediate during the ferroxidase reaction in fast ferritin mineralization. *Biochemistry* 1998; 37:9871–9876.
25. Reilly CA, Aust SD. Iron loading into ferritin by an intracellular ferroxidase. *Arch Biochem Biophys* 1998; 359:69–76.
26. Morgan EH, Walters MN. Iron storage in human disease. Fractionation of hepatic and splenic iron into ferritin and hemosiderin with histo-chemical correlations. *J Clin Pathol* 1963; 16:101–107.
27. Fargion S, Sampietro M, Cappellini MD. Thalassemias and their interactions with hemochromatosis. In: Barton JC, Edwards CQ, eds. *Hemochromatosis. Genetics, Pathophysiology, Diagnosis, and Treatment*. Cambridge, UK: Cambridge University Press, 2000:435–441.
28. Bottomley SS. Iron overload in sideroblastic and other non-thalassemic anemias. In: Barton JC, Edwards CQ, eds. *Hemochromatosis. Genetics, Pathophysiology, Diagnosis, and Treatment*. Cambridge, UK: Cambridge University Press, 2000:442–452.
29. Gunshin H, Mackenzie B, Berger UV, Gunshin Y, Romero MF, Boron WF, Nussberger S, Gollan JL, Hediger MA. Cloning and characterization of a mammalian proton-coupled metal-ion transporter. *Nature* 1997; 388:482–488.
30. Fleming MD, Trenor CC, Su MA, Foerzler D, Beier DR, Dietrich WF, Andrews NC. Microcytic anemia mice have a mutation in Nramp2, a candidate iron transporter gene. *Nature Genet* 1997; 16:383–386.
31. Zoller HZ, Pietrangello A, Vogel W, Weiss G. Duodenal metal-transporter (DMT-1, NRAMP-2) expression in patients with hereditary haemochromatosis. *Lancet* 1999; 353: 2120–2123.
32. Fleming MD, Romano MA, Su MA, Garrick LM, Garrick MD, Andrews C. Nramp2 is mutated in the anemic Belgrade (b) rat: Evidence for a role for Nramp2 in endosomal iron transport. *Proc Natl Acad Sci USA* 1998; 95:1148–1153.
33. Gruenheid S, Cannone-Hergaux F, Gauthier S, Hackam DJ, Grinstein S, Gros P. The iron transport protein NRAMP2 is an integral membrane glycoprotein that colocalizes with transferrin in recycling endosomes. *J Exp Med* 1999; 189:831–841.
34. McKie AT, Marciani P, Rolfs A, Brennan K, Wehr K, Barrow D, Miret S, Bomford A, Peters TJ, Farzaneh F, Hediger MW, Simpson RJ. A novel duodenal iron-regulated transporter, IREG1, implicated in the basolateral transfer of iron to the circulation. *Mol Cell* 2000; 5:299–309.

35. Donovan A, Brownlie A, Zhou Y, Shepard J, Pratt SJ, Moynihan J, Paw BH, Drejer A, Barut B, Zapata A, Law TC, Brugnara C, Lux SE, Pinkus GS, Pinckus JL, Kingsley PD, Palls J, Fleming MD, Andrews NC, Zon LI. Positional cloning of zebrafish ferroptin1 identifies a conserved vertebrate iron exporter. *Nature* 2000; 403:776–781.
36. Vulpe CD, Kuo YM, Murphy TL, Cowley L, Askwith C, Libina N, Gitschier J, Anderson GJ. Hephaestin, a ceruloplasmin homologue implicated in intestinal iron transport, is defective in the *sla* mouse. *Nature Genet* 1999; 21:195–199.
37. Waheed A, Parkkila S, Saarnio J, Fleming RE, Zhou XY, Tomatsu S, Britton RS, Bacon BR, Sly WS. Association of HFE protein with transferrin receptor in crypt enterocytes of human duodenum. *Proc Natl Acad Sci USA* 1999; 96:1579–1584.
38. Pietrangelo A, Casalgrandi G, Quaglino D, Gualdi R, Conte D, Milani S, Montosi G, Cesarini L, Ventura E, Cairo G. Duodenal ferritin synthesis in genetic hemochromatosis. *Gastroenterology* 1995; 108:208–217.
39. Casey JL, Hentze MW, Koeller DM, Caughman SW, Rouault TA, Klausner RD, Harford JB. Iron-responsive elements: regulatory RNA sequences that control mRNA levels and translation. *Science* 1988; 240:924–928.
40. Montosi G, Paglia P, Garuti C, Guzman CA, Bastin JM, Colombo MP, Pietrangelo A. Wild-type HFE protein normalizes transferrin iron accumulation in macrophages from subjects with hereditary hemochromatosis. *Blood* 2000; 96:1125–1129.
41. Zanninelli G, Loréal, Brissot P, Konjin A, Hider RC, Cabantchik I. The labile iron pool of hepatocytes is modulated in iron overload and chelator-induced iron deprivation. Submitted.
42. Kawabata H, Yang R, Hiramata T, Vuong PT, Kawano S, Gombart AF, Koeffler HP. Molecular cloning of transferrin receptor 2. A new member of the transferrin receptor-like family. *J Biol Chem* 1999; 274:20826–20832.
43. Fleming RE, Migas MC, Holden CC, Waheed A, Britton RS, Tomatsu S, Bacon BR, Sly WS. Transferrin receptor 2: Continued expression in mouse liver in the face of iron overload and in hereditary hemochromatosis. *Proc Natl Acad Sci USA* 2000; 97:2214–2219.
44. Craven CM, Alexander J, Eldridge M, Kushner JP, Bernstein S, Kaplan J. Tissue distribution and clearance kinetics of non-transferrin-bound iron in the hypotransferrinemic mouse: A rodent model for hemochromatosis. *Proc Natl Acad Sci USA* 1987; 84:3457–3461.
45. Brissot P, Wright TL, Ma WL, Weisiger RA. Efficient clearance of non-transferrin-bound iron by rat liver. Implications for hepatic iron loading in iron overload states. *J Clin Invest* 1985; 76:1463–1470.
46. Wright TL, Brissot P, Ma WL, Weisiger RA. Characterization of non-transferrin-bound iron clearance by rat liver. *J Biol Chem* 1986; 261:10909–1014.
47. Brissot P, Zanninelli G, Guyader D, Zeind J, Gollan J. Biliary excretion of non-transferrin-bound iron in rats: Pathogenetic importance in iron-overload disorders. *Am J Physiol* 1994; 267:G135–G142.
48. Jordan I, Kaplan J. The mammalian transferrin-independent iron transport system may involve a surface ferrireductase activity. *Biochem J* 1994; 302:875–879.
49. Anderson GJ, Ramm GA, Halliday JW, Powell LW. Ferritin metabolism in hemochromatosis. In: Barton JC, Edwards CQ, eds. *Hemochromatosis. Genetics, Pathophysiology, Diagnosis, and Treatment*. Cambridge, UK: Cambridge University Press, 2000: 145–156.
50. Mack U, Powell LW, Halliday JW. Detection and isolation of a hepatic membrane receptor for ferritin. *J Biol Chem* 1983; 258:4672–4675.
51. Adams PC, Powell LW, Halliday JW. Isolation of a human hepatic ferritin receptor. *Hepatology* 1988; 8:719–721.

52. Ramm GA, Britton RS, O'Neill R, Bacon BR. Identification and characterization of a receptor for tissue ferritin on activated rat lipocytes. *J Clin Invest* 1994; 94:9–15.
53. Brock JH. Iron in infection, immunity, inflammation and neoplasia. In: Brock JH, Halliday JW, Pippard MJ, Powell LW, eds. *Iron Metabolism in Health and Disease*. London: Saunders, 1994:353–389.
54. Yoshida K, Furihata K, Takeda S, Nakamura A, Yamamoto K, Morita H, Ikeda S, Shimizu N, Yanagisawa N. A mutation in the ceruloplasmin gene is associated with systemic hemosiderosis in humans. *Nature Genet* 1995; 9:267–272.
55. Miyajima H, Takahashi Y, Kamata T, Shimizu H, Sakai N, Gitlin JD. Use of desferrioxamine in the treatment of aceruloplasminemia. *Ann Neurol* 1997; 41:404–407.
56. Harris L, Durley AP, Kwong Man T, Gitlin JD. Targeted gene disruption reveals an essential role for ceruloplasmin in cellular iron efflux. *Proc Natl Acad Sci USA* 1999; 96:10812–10817.
57. Patel BN, David S. A novel glycosylphosphatidylinositol-anchored form of ceruloplasmin is expressed by mammalian astrocytes. *J Biol Chem* 1997; 272:20185–20190.
58. McKie AT et al. *Science* 2001; 291:1755–1759.
59. Pigeon C, Ilyin G, Courseland B, Leroyer P, Turlin B, Brissot P, Loréal O. A new mouse liver-specific gene, encoding a protein homologous to human antimicrobial peptide hepcidin, is overexpressed during iron overload. *J Biol Chem* 2001; 276:7811–7819.
60. Nicolas G et al. *Proc Natl Acad Sci USA* 2001; 98:8780–8785.

Regulation of Liver Iron Metabolism

GAETANO CAIRO

University of Milan, Milan, Italy

I. INTRODUCTION	614
II. LIVER IRON METABOLISM	614
A. Iron Uptake	614
B. Iron Storage	615
C. Iron Mobilization	615
III. PROTEINS OF IRON METABOLISM	616
A. Transferrin	616
B. Transferrin Receptor	618
C. Ferritin	620
D. Iron Regulatory Proteins	622
E. HFE	624
F. DMT1/Nramp2	624
G. SFT	625
H. Ceruloplasmin	625
I. Mitochondrial Aconitase	625
J. Hephaestin	626
K. Ferroportin1	626
L. Frataxin	626
M. Hemopexin	626
N. Haptoglobin	626
IV. PATHOBIOLOGY OF HEPATIC IRON METABOLISM	627
A. Iron Overload	627
B. Inflammation	628
C. Growth	629
D. Oxidative Stress, Ischemia/Reperfusion, and Hypoxia	630
V. CONCLUSIONS	632
REFERENCES	633

I. INTRODUCTION

The liver plays a pivotal role in systemic iron metabolism for at least four reasons: (a) hepatocytes synthesize and secrete virtually all circulating transferrin (Tf) (see Chapter 2), the protein that distributes this essential metal to cells requiring it, primarily erythroid precursors and proliferating cells; (b) the liver is the main long-term depository for iron and therefore represents a buffer compartment for detoxification as well as for recovery in case of acute body needs; (c) Kupffer cells participate in iron processing and recirculation from damaged or senescent erythrocytes, and only the bone marrow deals with more iron than the liver; (d) because of its anatomical position, the liver is particularly exposed to dietary iron, in both transferrin-bound and unbound forms, and is therefore susceptible to overload.

This chapter presents a brief overview of liver iron metabolism and examines in detail the regulation of the proteins, which are the individual components of intracellular iron pathways. Finally, the regulation of iron metabolism in the framework of hepatic pathophysiology is summarized.

II. LIVER IRON METABOLISM

Liver iron metabolism at the organ level consists of three main processes, which reflect similar steps at the cellular level: uptake, storage, and release (1). For both the single cell and the whole organ, the pathways of hepatic iron entry and deposition are relatively well understood, whereas the mechanisms and the regulation of iron efflux are still undefined. The liver is a complex organ, and all its cell types have a role in iron metabolism and in the three above processes, although their participation differs in the individual pathways. Most of the information available concerns hepatocytes, while knowledge of the role of sinusoidal cells is limited to that of resident hepatic macrophages (Kupffer cells). However, other liver cells may be involved in iron-related processes. For instance, the function of the fat-storing hepatic stellate cells (HSC) in iron metabolism is probably limited, but they are important participants in iron-mediated toxicity. In fact, being the major source of extracellular matrix components, they are responsible for fibrosis, the most common response to liver injury (2).

A. Iron Uptake

Like most animal cells, liver cells acquire iron by means of receptor-mediated Tf internalization (see Chapters 3 and 17). The major source of iron for hepatocytes under normal conditions is diferric Tf; the number of transferrin receptor (TfR) molecules on hepatocytes is quite large for cells with a low rate of proliferation. However, hepatocytes also take up non-transferrin-bound iron (NTBI) (see Chapter 18). The latter is defined as iron bound to low-molecular-weight ligands. It plays a significant role in iron overload of parenchymal cells in a number of organs, with the liver being a preferential site of accumulation. This occurs in severe iron-overload states such as in hereditary hemochromatosis (HH) and transfusional siderosis, when the plasma iron content exceeds the binding capacity of Tf. The hepatocyte possesses an additional mechanism to take up iron: heme bound to hemopexin and the complex between free hemoglobin and haptoglobin are cleared from the circulation through the interaction with specific receptors on liver parenchymal cells, but the physiolog-

ical importance of these iron sources for the liver is limited, as underscored by recent studies with knockout mice (see below). In addition, ferritin receptors have been detected on hepatocytes (3), but probably very little iron reaches the liver by this mechanism because the hepatic ferritin receptor appears to mediate the clearance of circulating ferritin, which is iron-poor. This pathway is possibly involved only in intrahepatic iron transport between Kupffer cells and hepatocytes (4), although the mechanisms for secretion and receptor-mediated internalization of ferritin have not been fully clarified.

On the other hand, as indicated by the prompt accumulation of iron in hepatic reticuloendothelial (RE) cells under conditions of increased catabolism of red blood cells (e.g., in transfusional siderosis), Kupffer cells acquire most of their iron by means of phagocytosis of effete erythrocytes, although TfR molecules have been detected on their cell surface (see below). Phagocytosed heme iron is freed from its linkage with hemoglobin in the vacuole and is then transported by a yet-unknown route to the endoplasmic reticulum, where it is degraded by heme oxygenase. Catabolized heme iron will then encounter two distinct fates. One, still undefined, is release to the extracellular space. The other is storage in ferritin.

B. Iron Storage

The importance of the liver as an iron storage compartment is undisputed, but the relative importance of the various hepatic cell types as iron repositories is less clear. Although it is recognized that hepatocytes store about 5% of total body iron content, the importance of Kupffer cells as an iron storage compartment has been debated (1). However, studies in murine experimental models, in which parenchymal or RE cells were targeted by means of dietary or parenteral iron overload, respectively (discussed in Ref. 2), have made clear that both cell types can accumulate large amounts of the metal, thus confirming evidence coming from the analysis of diseases of iron overload (5). Kupffer cells appear to be a storage site less subject to the toxic effect of iron than hepatocytes, but, when their storing capacity is overcome, they discharge some of their iron. Parenchymal deposition and organ damage ensue. Under normal iron loading, the metal in hepatic cells is stored in ferritin (see Chapter 5), but in iron-overload states hemosiderin derived from ferritin breakdown becomes the predominant storage site. Since hemosiderin is insoluble, iron sequestered in this degradation product is thought to be less easily available.

C. Iron Mobilization

Iron balance is essentially determined by intestinal absorption, because the body does not have a physiological or regulated pathway of iron excretion. Most cells tightly conserve iron, the notable exceptions being the enterocyte and the RE cells, which share a unique capacity to export and donate iron to circulating Tf constitutively. Kupffer cells therefore play an important role in iron cycling, as they release a considerable amount of iron derived from phagocytosed red cells to Tf, from which the metal is delivered throughout the body for reutilization, mainly by the bone marrow for hemoglobin synthesis. Iron release is a constitutive function of RE cells and occurs continuously under normal circumstances, but is also regulated in response to still undefined signals, probably deriving from the bone marrow (6). On the other hand, release from other tissue stores occurs only under conditions of

increased demand, such as with blood loss, pregnancy, etc., so that the storage reserve of hepatocytes functions as a buffer compartment to help alleviate states of iron deficiency. Iron excretion into the bile provides an alternative route of liver iron mobilization, though in this case the metal is not destined for reutilization but for disposal. Although accounting for a significant fraction of body iron elimination, however, this pathway is insufficient to prevent iron overload.

Iron removal from overloaded hepatocytes and hepatic macrophages can also be achieved by treatment with iron chelators (see Chapters 13 and 33), at present essentially represented by desferrioxamine. However, the molecular processes of iron mobilization, both physiological and drug-mediated, are similarly obscure. In contrast to the improvements in the molecular analysis of the regulatory pathways of cellular iron acquisition and storage, little progress has been made in defining the mechanisms underlying iron egress from the cell. Only recently has the gene coding for a membrane protein responsible for iron export [named ferroportin1 (7), Ireg1 (8), or MTP1 (9)] been cloned. Other proteins, such as hephaestin and ceruloplasmin, may work together with this transporter to load iron onto Tf (see below).

III. PROTEINS OF IRON METABOLISM

The field of iron metabolism has blossomed in the last several years, and the list of iron-related proteins has expanded as new proteins involved directly or indirectly in iron transport have been discovered and characterized. In addition, new details have been added to the knowledge of the functions of the proteins that have been known for years to be key players in iron homeostasis. Each of these is considered in more detail in separate chapters. Here the emphasis is on their role and regulation of in the mammalian liver. The main characteristics of these proteins are summarized in Table 1.

A. Transferrin

Tf is synthesized by several cell types during fetal development, but Tf production after birth is restricted to a few "sanctuary sites," i.e., sequestered areas such as the brain and the testis that are separated from the general circulation (9a), and to hepatocytes, which are the main source of serum Tf. Detailed analysis of the 5'-regulatory regions of the Tf gene has allowed a comprehensive knowledge of both the cis-acting DNA elements and the trans-activating factors that impart the liver-specific expression of this gene (10).

Hepatic Tf gene expression is upregulated by iron deficiency in rats through a transcriptional mechanism (11), whereas rat liver Tf mRNA levels are not affected in iron overload (12). Since iron chelators and hypoxia share the same transcriptional activator, known as hypoxia inducible factor (HIF-1), to induce target genes (13), the finding that Tf transcription is activated in hypoxic cells (14) suggests that transcriptional regulation by HIF-1 also has a major role in the regulation of Tf synthesis in response to changes in iron levels. The low serum Tf levels found in some patients with increased iron stores (15) suggested that hepatic Tf production is inhibited by iron. However, in agreement with the lack of inhibition found in experimental chronic overload (12), increased amounts of hepatic Tf mRNA have been found in patients with severe iron overload caused by both secondary and genetic siderosis (16). Fac-

Table 1 Proteins of Iron Metabolism Expressed in the Liver

	Function	Localization	Effect of iron on hepatic expression	Other regulatory stimuli	Pathobiological settings
Transferrin	Iron transport	Secreted	Positive	Hormones, hypoxia, cytokines	Alcoholism
Transferrin receptor	Iron uptake	Membrane	Negative	Growth, NO, hypoxia, cytokines	HH, cancer, inflammation
Ferritin	Iron storage	Cytoplasm	Positive	Growth, ROS, NO, hypoxia, cytokines	HH, cancer, inflammation, oxidative stress
IRPs	RNA binding	Cytoplasm	Negative	Growth, ROS, NO, hypoxia, cytokines	HH, cancer, inflammation, oxidative stress
Ceruloplasmin	Copper transport, iron oxidase	Secreted	Negative	Hormones, cytokines, copper	Wilson dis., inflammation, aceruloplasminemia
Mitochondrial aconitase	Krebs cycle	Mitochondria	Positive	NDA	NDA
HFE	Iron uptake	Membrane	Negative	NDA	HH
DMT1	Iron uptake	Membrane	?	NDA	NDA
SFT	Iron uptake	Membrane	?	NDA	HH
Ferroportin1/Ireg	Iron export	Membrane	NDA	NDA	NDA
Hemopexin	Heme binding	Secreted	NDA	Cytokines	Hemolysis, inflammation
Haptoglobin	Hemoglobin binding	Secreted	NDA	Cytokines	Hemolysis, inflammation
Frataxin	Intracellular iron transport	Mitochondria	NDA	NDA	NDA
Haephestin	Iron export	Membrane	NDA	NDA	NDA

The table lists the major function and localization of the proteins of iron metabolism expressed in liver cells. The modulating agents and pathobiological conditions possibly associated with altered hepatic expression are also indicated.

HH = hemochromatosis; NO = nitric oxide; ROS = reactive oxygen species; ? = conflicting results; NDA = no data available.

tors other than iron, such as nutritional status and/or hepatocellular damage, rather than a specific effect on Tf gene expression, likely play a role in lowering circulating Tf levels in patients with iron overload.

It has been reported that Tf is also regulated at the translational level with a 40–50% decrease in iron-loaded livers of transgenic mice (17). However, the proposed iron regulatory protein (IRP)-mediated translational inhibition (18) was not confirmed in experiments with recombinant IRP-1 (19).

Hepatic Tf synthesis can be modulated by signals other than iron, including oxygen, cytokines, hormones, and xenobiotics. Indeed, being a negative acute-phase reactant (20), the Tf gene has been shown to be transcriptionally downregulated in the liver of turpentine-treated rats (21), although little else is known of the molecular mechanisms underlying the effect of inflammatory mediators. Steroid hormones increase Tf mRNA transcription and protein synthesis in chicken liver (22), and Tf transcription is also stimulated by retinoic acid in a human hepatoma cell line (23). Moreover, Tf synthesis is transcriptionally suppressed by hypolipidemic peroxisome proliferators in both animals and cell lines, possibly resulting in reduced iron availability and/or altered transferrin-mediated differentiation processes (24). Recently, it has been demonstrated that HIF-1, which activates transcription in response to reduced oxygen concentration (13), upregulates Tf gene transcription in hepatoma cells exposed to hypoxia (14).

Derangement of iron metabolism with hepatic accumulation of the metal often accompanies alcoholic liver disease (discussed in Ref. 25). Moreover, a strong reduction of serum Tf levels is frequently detected in advanced alcoholic cirrhosis. This decline likely reflects a generalized defect in synthesis and/or secretion of hepatic proteins. Nevertheless, a specific abnormality of Tf has been found to be associated with chronic alcoholism. In fact, the presence of a partially desialylated protein, accounting for about 20% of circulating Tf, correlates strongly with alcohol ingestion. However, the presence of abnormally glycosylated Tf, although a useful marker of hepatocellular injury, has given no insights into the alterations of iron metabolism occurring in patients with alcoholic cirrhosis.

B. Transferrin Receptor

Transferrin receptor (TfR) binds diferric Tf at the cell surface and enters the cell, whereupon iron is released (for details see Chapters 3 and 4). Since hepatocytes are quiescent cells and also acquire iron by Tf-independent pathways (see Chapter 18), expression of TfR is not very high in the liver. However, since the number of receptor molecules is the rate-limiting step for iron entry into cells, the TfR plays a crucial role in the control of iron homeostasis, and its expression is tightly regulated. Iron controls TfR mRNA levels mainly through IRP-mediated posttranscriptional mechanisms involving the binding of IRP to iron responsive elements (IRE) in the 3'-untranslated region of TfR mRNA (see Chapters 3 and 9). This leads to high expression in conditions of iron deficiency and, conversely, to downregulation when iron is plentiful. Transcriptional induction mediated by HIF-1 (26) enhances the response to iron deficiency, allowing the cell to respond better to a situation that may severely affect important functions.

The expected regulation of TfR by iron has been found also in experimental models of manipulation of hepatic iron levels and in patients with liver iron overload.

The number of TfRs at the cell surface increased in rat hepatocytes treated with iron chelators (27), and TfR expression was downregulated by iron in a human hepatoma cell line and in human hepatocyte primary cultures (28). Regulation of TfR by iron also occurs *in vivo*, with higher and lower expression in iron-deficient and -replete rats, respectively (29,30). In addition, a cell-specific difference was described in rats fed an iron-enriched diet, in which a decrease in TfR in parenchymal cells was contrasted by an increase in Kupffer cells (30). A recent report described increased TfR protein levels in the livers of both iron-deficient and iron-loaded rats (31). However, interpretation of TfR upregulation in conditions of increased iron stores is difficult in view of the observed decrease in IRP activity and increase in ferritin content. The expected differences in hepatocyte TfR in relation to hepatic iron stores were found in humans with iron overload, including patients with HH (32,33). Molecular analysis established that the above differences were due to reduced levels of TfR mRNA (16). *In-situ* hybridization analysis in a small series of HH patients localized TfR mRNA predominantly to hepatocytes, but, unlike previous studies, did not detect significant differences between patients and normal controls, probably because subjects with a lower degree of iron overload were selected (34).

TfR expression also strongly correlates with cell growth, probably because it ensures iron is available to enzymes directly (e.g., ribonucleotide reductase) or indirectly (cytochromes, iron-sulfur proteins) involved in proliferation. In fact, an increased number of cell-surface TfR molecules has been detected in murine models of liver proliferation (35). Analysis of the underlying molecular mechanisms (36) has shown that this is due not only to redistribution of receptor molecules from the internal pool (37), but also to increased synthesis. Contrary to what has been described for mitogen-driven growth activation *in vitro* (38), transcriptional control is not involved in the activation of TfR *in vivo* during liver regeneration. Rather, IRP2-mediated posttranscriptional mechanisms accounted for the induction, suggesting the existence of changes in intracellular iron distribution, because total tissue iron content is unaffected (36). TfR upregulation has been detected not only in replicating liver cells but also in preneoplastic and neoplastic tissues. In fact, in both liver nodules and hepatocellular carcinomas arising in experimental models of liver carcinogenesis, TfR protein (39,40) and mRNA (41) levels are markedly increased. Whether this higher TfR expression results in enhanced iron uptake is still a matter of debate (39,41). This uncertainty prevents a clear understanding of whether the well-known absence of stainable iron in neoplastic liver foci is caused by impaired acquisition or increased consumption to sustain growth.

TfR has been shown to be involved in efficient uptake of hepatitis B virus by human activated T lymphocytes (42). TfR expressed on hepatocytes may therefore represent a doorway of cellular entry of HBV, and thus may play a role in this major hepatic disease.

TfR gene expression is also sensitive to oxygen tension, being upregulated in hepatoma cells grown under hypoxic conditions (43,44). While an IRP-mediated increase of TfR mRNA levels has been reported (43), another study, in agreement with findings in other cell types (45), showed transcriptional induction through the nuclear factor HIF-1 (44). The finding that TfR is among a variety of hypoxia-inducible genes has reinforced the strong link between iron metabolism and oxygen homeostasis. However, the biological significance of enhanced TfR synthesis in hy-

poxic hepatic cells remains to be determined, as the enhanced iron influx could be detrimental in the context of subsequent reoxygenation.

Cytokines and inflammatory stimuli have also been shown to induce TfR expression both in rat liver (46,47) and in hepatoma cells (48).

Regarding the expression of TfR in different liver cell types, rat Kupffer cells have TfR (49), although they express it at lower levels than do parenchymal cells and do so with considerable heterogeneity (50). Variable TfR positivity was also found in liver biopsies of patients with secondary iron overload (51), without any relationship with liver iron content. Moreover, no iron-induced downregulation of TfR was observed in iron-laden Kupffer cells (30). These findings may be related more to activation and (or) differentiation processes of macrophages than to iron per se, as the TfR number increases when monocytes mature into macrophages (52). No evidence is presently available for TfR expression in other liver cells.

The importance of TfR has been recently underlined by a genetic approach in which the mouse TfR gene was mutated. Homozygous mice with a functionally inactive allele die in utero, while heterozygous animals have severe abnormalities of erythropoiesis, but only a slight reduction of liver iron accumulation is seen, underscoring the importance of Tf (or TfR)-independent pathways of iron acquisition for liver cells (53).

Transferrin receptor 2 (TfR 2), a new member of the TfR family, has been recently identified and cloned (54). TfR 2 mRNA is particularly abundant in liver cells, but its expression pattern is not always correlated with that of TfR. This was also shown by the lack of modulation of TfR 2 mRNA in murine models of iron overload and deficiency, and is possibly the result of the absence of IRE in the 3' region (55). Interestingly, a mutation causing premature termination of TfR 2 translation has been recently detected in patients with non-HFE-linked HH (56).

C. Ferritin

Ferritin is an evolutionarily conserved, ubiquitous protein destined to store iron inside the cell. H and L chains assemble in a tissue-specific way to generate a family of isoferritins with different metabolism and functions. L-subunit-rich isoferritins predominate in iron-storing tissues, whereas H-subunit-rich ferritins are preferentially found in cells which rapidly take up and release iron (see Chapter 5; and Ref. 3). As the liver is a major site of iron accumulation, hepatic ferritin is L-rich, particularly in human liver, where H chains represent only about 5–10% of this protein (3). Rat liver ferritin is also composed predominantly of L subunits, with an L/H ratio of about 4:1. Since the L/H ratio at the mRNA level, paralleled by synthesis rate, is 2:1, it seems that the liver-specific isoferritin profile is determined by a combination of pre- and posttranslational mechanisms (57). Indeed, a relatively high transcription of the H gene in hepatic cells was found with another experimental approach, confirming the discrepancy between transcript levels and isoferritin composition (58).

In keeping with its role in iron storage and detoxification, ferritin content closely parallels intracellular iron levels (3), and increased hepatic ferritin accumulation in animals has been documented in a number of studies (reviewed in Refs. 3 and 59). In humans, increased amounts of hepatic (predominantly L) ferritin, closely correlated with iron content, were found in patients with siderosis (33,60). More recently, by means of in-situ analysis it has been demonstrated that excess ferritin is localized predominantly to hepatocytes (34).

Changes in iron availability regulate ferritin gene expression at multiple levels. Although the major control mechanism is translational (see below), transcriptional induction has also been documented (61,62). In rat liver, both acute (63) and long-term (12,64) iron administration induced a specific transcriptional activation of the L gene. Increased levels of L-ferritin mRNA have also been found in patients with severe iron overload (16), but not in HH patients with a lower hepatic iron concentration (34). In both murine and human livers, H-chain mRNA was unaffected by iron, whereas treatment of hepatic cells in culture induced both ferritin mRNAs (28). The differing results obtained *in vivo* (where iron entry in the hepatocyte is massive but slow) and *in vitro* seem to lend support to the biochemical data showing the role of the H and L subunits in fast iron exchange and storage, respectively.

Although also acting at the transcriptional level, iron increases ferritin synthesis primarily by allowing the translation of preexisting mRNA (65). In conditions of iron deficiency, interaction of IRP with conserved iron responsive elements (IRE) in the 5'-untranslated region of both H- and L-ferritin mRNAs blocks ferritin translation by preventing the interaction of the eIF4F initiation factor with the small ribosomal subunit (66). Conversely, when iron is abundant, IRP is inactive and ferritin translation can proceed; this mechanism allows the cell to fine-tune ferritin content with iron availability. Since the experiments by Munro and co-workers, who first established the molecular mechanisms underlying iron-mediated regulation of ferritin synthesis (reviewed in Refs. 59, 62, and 67), liver cells have been widely used to investigate the posttranscriptional control of ferritin expression. In both rat liver (68) and hepatoma cells (69), acute iron administration mobilized both ferritin-subunit mRNAs from the free pool to polyribosomes, whereas chronic overload changed the intracellular distribution of the L mRNA alone (70). In short, it seems possible to conclude that both the H and L subunits are induced by iron at the translational level, while increased transcription of the L gene alone may account for the preferential increase in L-subunit accumulation. However, the *cis*-acting sequences in the promoter regions of ferritin genes that respond to iron have not yet been identified.

Since cellular environmental conditions may require an adjustment in iron homeostasis without a change in the exogenous levels of the metal, ferritin responds to regulatory influences in addition to iron. In fact, hepatic ferritin synthesis has been shown to be stimulated *in vivo* by both inflammatory stimuli (46,64,71–73) and interleukin-6 (47), and by purified cytokines in cultured cells (48,74). Elevated ferritin synthesis is accompanied by modest increases of mRNA (46,64), but posttranscriptional control is probably predominant, although in an IRP-independent way. In fact, interleukin-6 causes a twofold enhancement of ferritin translation acting via sequences similar to those present in the 5'-UTR of acute-phase proteins but other than IRE (75). The effect of inflammatory agents is probably independent of changes in cellular iron content or distribution (46,74), whereas NO has been shown to be involved (46). In addition, treatment of human hepatoma cells with the acute-phase protein 1-antitrypsin has been shown to increase the abundance of H-chain mRNA, as well as ferritin content (76).

In non-neoplastic liver cell growth, *i.e.*, during liver regeneration, early work did not detect variations in the amount of ferritin 3 days after hepatectomy, although the iron content of the protein was reduced (77). The lack of variation found at late times of regeneration could have been caused by the fact that the significant decrease

of ferritin content found at earlier times is followed by a progressive reaccumulation (36). The latter is accompanied by a transcriptionally regulated twofold increase in the amount of H- and L-subunit mRNAs, as found in the liver of rats undergoing regeneration after CCl₄ administration (78). This finding was not in agreement with results obtained in liver regeneration after partial hepatectomy by Wu and colleagues (79), possibly reflecting different responses in the two models of regeneration. By contrast, the same authors detected a specific H-mRNA overexpression during development of hepatocellular carcinomas in rats treated with diethylnitrosamine (79). This seems more related to carcinogenesis than to iron storage, as also indicated by previous detection of very low ferritin levels in Morris rat hepatomas (77). Interestingly, treatment of rats with the cancer-chemopreventive agent dithiolethione induced H- and L-ferritin accumulation (80). Increased protein levels were associated with higher transcription of the corresponding genes, which was apparently independent of the intracellular iron levels and possibly related to the presence of antioxidant response elements in the promoter of the gene, as also suggested by the concomitant induction of heme oxygenase.

In consideration of the influence of intracellular iron levels on susceptibility to oxidative stress, ferritin, as an iron storage protein, plays an important role in the stress response. However, it has been alternatively presented either as a dangerous source of catalytically active iron (81) or as an effective intracellular iron chelator (82). We demonstrated that in the liver of rats subjected to oxidative stress by treatment with a glutathione-depleting drug (83) or by postischemic reperfusion (84), ferritin can represent either a pro- or an antioxidant in a time-dependent fashion. In agreement with other findings obtained both in rat liver (85,86) and in isolated hepatocytes (87), early ferritin degradation causes iron release and expansion of the labile iron pool. However, these events set in motion both transcriptional and post-transcriptional mechanisms aimed at reestablishing ferritin content, thus curbing the pro-oxidant challenge of the metal.

Recently, a useful in-vivo model to assess the biological significance of ferritin subunit has become available with the construction of H-subunit knockout mice (88). Homozygous deletion of the H gene results in embryonic lethality, whereas heterozygotes do not show apparent abnormalities in the various organs, including the liver.

D. Iron Regulatory Proteins

IRPs (IRP1 and IRP2), cytoplasmic proteins belonging to the aconitase superfamily, regulate iron metabolism by binding to IRE in the untranslated regions of target mRNAs (see Chapters 9 and 10; and Ref. 89). In conditions of iron deficiency, IRPs bind actively to IRE and simultaneously prevent ferritin mRNA translation and TfR mRNA degradation. Conversely, when iron in the cell is abundant, IRP1 is converted to a 4Fe-4S cluster-bearing form endowed with aconitase activity and loses RNA-binding capacity, while IRP2 is degraded by the proteasome. This results in TfR and ferritin mRNA destabilization and translation. IRPs maintain intracellular iron homeostasis by means of this coordinate and opposite regulation of the major proteins of iron metabolism.

Since the first report describing IRP, in which an S100 cytoplasmic extract prepared from rat liver was used to demonstrate an interaction between IRE sequences and specific proteins (90), a number of studies have addressed IRP expres-

sion and regulation in hepatic cells. IRP1 is quite abundant in liver cells (about 1 pmol/mg protein), in absolute terms and with respect to other tissues. Although, as in most other cells, in the liver there is a greater number of IRP1 than IRP2 molecules (91,92), the latter are easily detected by bandshift assays in extracts of rodent liver cells. The activity of both IRPs is repressed by increased liver iron load, but both initial evidence (90) and later findings (93,94) indicated that variations of IRP2 activity are more relevant. Conversely, treatment of rat hepatoma cells with an iron chelator (95) or maintenance of rats on a low-iron diet (94) increased the binding activity of both IRPs. Thorough investigation of hepatic IRP activity in response to graded physiological changes in dietary iron intake indicated that liver IRP activity is responsive to a range of dietary iron levels. In particular, IRPs were found to be affected more by iron deficiency than by iron excess (93). In addition, IRP2 was more sensitive than IRP1 to variations of iron in the diet (93,94).

An inverse relationship between hepatic iron concentration and IRP activity, with a significant IRP downregulation in HH and secondary iron overload patients, was also found in humans (96). Because human IRPs do not separate during bandshift analysis, the detected effect was on total (IRP1 plus IRP2) activity, but the finding that both the IRE-binding activity and the IRP content were affected might indicate increased IRP2 degradation, in view of the particular mechanism of IRP2 regulation (see above).

The recognition that the most important effects of nitric oxide (NO) are mediated by its interaction with iron and (or) iron proteins prompted investigations into the effect of NO and other reactive nitrogen species on IRPs activity. Most of the studies have investigated the effect of NO on macrophages, but a few have also addressed the interaction of the NO pathway with IRP in liver cells. Higher IRP2 activity, without significant changes in IRP1, was found in the livers of rats undergoing an acute inflammatory reaction following turpentine injection (46). A differential regulation of the two IRP was also demonstrated in cytokine-treated rat hepatoma cells, but in this case the activation was specific for IRP1 (97). Clearly, the in-vivo situation is complex and not entirely reproducible in cell culture, as also shown by the differential effects of cytokines and NO donors on the expression of TfR in rat hepatoma cells (97).

Iron is an absolute requirement for growing cells, and TfR expression is closely related to the rate of cell proliferation (52). Thus, IRP activity is also modulated by cell growth, and elevated IRP-binding activity has been detected in mitogenically stimulated cells (98–100). This could be the result of a reduction of iron availability caused by higher metal consumption or to specific gene activation (101).

In the liver, preferential activation of IRP2 has been shown to occur during liver regeneration, an in-vivo model of hepatic cell growth (36). Since during regeneration total liver iron content did not change appreciably (36), growth-dependent activation of IRP2 could be caused either by the higher sensitivity of this protein to small variations of iron availability (94) or by specific transcriptional activation, similar to that found in cells overexpressing the c-myc oncogene (101). The finding that IRP2 activity is higher in hepatoma cell lines than in the liver (94) is consistent with the results found in non-neoplastic hepatic cell growth.

Iron availability must be kept under strict control in order to prevent reactive oxygen species (ROS) from severely damaging a variety of target molecules essential for cell homeostasis. It is not surprising, therefore, that the activity of IRPs, as the

master regulators of cellular iron metabolism, is altered under conditions of oxidative stress. Considering the role of ferritin and TfR in iron chelation and uptake, one would expect up- and downregulation, respectively, of these two proteins in conditions of oxidative stress, and, therefore, a reduction of IRP activity. Indeed, ROS production *in vivo*, obtained either by pharmacological depletion of cellular thiols (83) or by postischemic reperfusion (84), has been shown to downregulate liver IRP activity. A specific effect of ROS on IRP-2 has been found after treatment with phorone, a drug that reduces glutathione concentration (83). The high susceptibility of IRP2 to changes in the redox status of the cell is probably due to its mechanism of regulation, i.e., proteolytic cleavage after direct oxidative modification of residues in the degradation domain (102). *In-vitro* treatment of liver lysates with xanthine/xanthine oxidase, which simultaneously generate H_2O_2 plus $O_2^{\cdot-}$, reproduced the inhibition of IRP activity found *in vivo* (103), thus suggesting that these ROS are involved directly in IRP regulation.

IRPs are also regulated by exposure to low oxygen tension, although conflicting results concerning the effects of hypoxia on IRP activity in human hepatoma cells have been reported (43,44). Because rodent IRP can be separated by bandshift analysis, use of mouse hepatoma cells allowed Leibold and co-workers to demonstrate that hypoxia differentially regulates the binding activity of the two IRPs, with a decrease of IRP-1 binding, accompanied by acquisition of aconitase activity, and an increase of IRP2 (104). The latter derives from enhanced protein stability, a mechanism involved also in the induction of HIF-1 (13). The significance of the opposite IRP1 and IRP2 response to hypoxia remains to be established, but this differential modulation may possibly account for the discrepancies noted above.

E. HFE

The HFE gene, which is mutated in the majority of patients with HH (see Chapters 8 and 28), encodes a MHC class I protein whose function in maintaining iron homeostasis is still not fully understood (5). HFE mRNA is transcribed in the liver (105), and immunohistochemistry with anti-HFE antibodies detected expression of this protein in cells lining the sinusoids (106,107) and in Kupffer cells (107), but not in parenchymal cells. Interestingly, staining for HFE was greatly reduced in the liver from an untreated patient homozygous for the C282Y mutation (107). This could help to explain the lack of iron deposition in Kupffer cells that is a hallmark distinguishing genetic from secondary hemochromatosis.

F. DMT1/Nramp2

Two technically and conceptually different approaches have recently led to the simultaneous identification of a long-sought divalent metal transporter (DMT1) which translocates iron across the apical membrane of enterocytes (see Chapter 6; and Refs. 108 and 109). Since the same protein is also involved in the movement of iron released from Tf across the endosomal membrane to enter the cytoplasm (110), it is not surprising that DMT1 expression is widespread; low levels of DMT1 mRNA (108) and protein (111) have also been detected in murine liver. Modest (108) or no (111) DMT1 induction is seen in the liver of iron-deficient animals, in contrast to the robust upregulation present in the duodenum. A recent study, which demonstrated a reduction of DMT1 protein levels in the liver of iron-depleted rats and an upreg-

ulation in iron overload (112), suggests that this membrane protein may be involved in NTBI uptake. No information is presently available on the expression of DMT1 in the different hepatic cell types.

G. SFT

A protein which facilitates transport of non-transferrin-bound iron (Stimulator of *Fe* Transport; SFT) has been identified by functional expression cloning (113). The SFT clone was isolated from a K562 cells cDNA library, but SFT is also expressed in the liver. Interestingly, and quite inexplicably since SFT expression is enhanced by iron chelation in nonhepatic and hepatic cell lines, SFT upregulation has been found in liver samples from HH patients, as compared to control subjects (114). At this time, the exact nature of this protein is uncertain, as corrections of initial sequence errors suggest a much smaller protein than at first thought (114a,114b).

H. Ceruloplasmin

Ceruloplasmin (Cp) provides a link between copper and iron metabolism (see, e.g., Chapter 30; also see Chapters 15 and 16). In fact, the ferroxidase activity of this copper-containing protein, synthesized mainly by liver cells, is necessary to incorporate iron into apotransferrin (115). Moreover, a role of Cp in release of iron from tissues was initially suggested by the finding that sideropenic anemia in copper-deficient animals with concomitant tissue iron overload could be reversed by Cp administration (116). More recently, this was supported by the results of clinical studies showing that hereditary Cp deficiency in humans leads to systemic hemosiderosis, including hepatic overload (reviewed in Chapter 30; and Ref. 117). The aceruloplasminemic phenotype has been faithfully reproduced in mice bearing a targeted disruption of the Cp gene (118). Further evidence of a connection between Cp and iron transport has been provided by the existence of a multicopper oxidase-based iron transport system in yeast (reviewed in Ref. 119) and by the recent identification of a new gene involved in duodenal iron absorption which codes for a membrane-bound copper oxidase highly homologous to Cp (120). Whether Cp, in addition to playing a role in the efflux of stored iron out of hepatocytes (118), is required for cellular iron uptake (121) is still a matter of debate (118). Not only has Cp a role in iron transport, but cellular iron status affects Cp expression, as demonstrated by increased Cp gene transcription in hepatoma cells treated with an iron chelator (121). This latter finding strengthens the argument for a relationship between Cp and iron metabolism.

In addition to iron, hepatic Cp expression is modulated by hormones and inflammatory stimuli. Transcriptionally mediated upregulation of Cp synthesis has been found in turpentine-treated syrian hamsters (122), and synthesis and secretion of Cp was enhanced in primary cultured rat hepatocytes treated with glucocorticoids (123). In addition, increased Cp activity accompanied by increased copper content has been observed in the serum of patients with primary biliary cirrhosis (124).

I. Mitochondrial Aconitase

Mitochondrial aconitase (m-Acon), a citric acid cycle enzyme, has an IRE in its 5'-untranslated region and is therefore subject to translational regulation by IRP, its

cytoplasmic counterpart, in response to changes in iron levels (89). As expected, then, a decrease in dietary uptake of iron caused a decline in the abundance of liver m-Acon, whereas an increase was seen when rats were fed an iron-enriched diet (125). Possibly because of a different IRE structure (126), the regulation of m-Acon is more limited, compared to Ft. This likely reflects the different biological functions of the two proteins.

J. Hephaestin

As mentioned above, a gene involved in intestinal absorption of iron has been recently cloned based on studies of the sex-linked anemia (sla) mouse. Termed hephaestin (120), its expression is high in duodenum, in keeping with its role in intestinal absorption. Low levels of hephaestin mRNA have been detected in mouse liver. However, its role and regulation in hepatic cells have yet to be characterized.

K. Ferroportin1

By an elegant approach that exploited the advantages of fishes to investigate defects of mammalian iron metabolism, the gene for ferroportin1—a basolateral iron exporter responsible for iron egress from the cell—has recently been cloned (7). Ferroportin1 mRNA is expressed at high levels not only in duodenal enterocytes but also in the liver; moreover, conspicuous amounts of protein in Kupffer cells were revealed by immunohistochemistry. Thus, this protein might have an important function not only in iron absorption but also in iron recycling by RE cells.

L. Frataxin

Frataxin is important for mitochondrial iron homeostasis (see Chapter 11; and Ref. 127), and has a prominent role in the nervous system and the heart, which most heavily depend on respiratory oxidation and are therefore more affected by a deficit of this mitochondrial protein. Although frataxin has been detected in the liver (128,129), no data are available about a specific role of this protein in the liver.

M. Hemopexin

Hemopexin (Hx) is a plasma glycoprotein with high affinity for heme. It is synthesized mainly in the liver (20). Analysis of Hx-deficient mice revealed no major abnormalities of iron metabolism; in particular, no differences in liver iron deposition were found between Hx-knockout mice and wild-type controls, although a protective role after hemolytic stress has been demonstrated, particularly in the kidney (130).

N. Haptoglobin

By binding to free hemoglobin, haptoglobin (Hp), an acute-phase protein produced primarily by liver cells, participates in systemic iron metabolism (131). It performs its role, however, mainly outside the liver. In fact, studies with Hp-knockout mice have revealed that its major function might be the amelioration of renal damage by the hemoglobin-driven lipid peroxidation that follows severe hemolysis (132).

IV. PATHOBIOLOGY OF HEPATIC IRON METABOLISM

This section summarizes the regulation of liver iron metabolism (i.e., the control of the expression of iron-related proteins) in pathobiology. Disturbances linked pathogenetically to excess body iron stores are distinguished from other disorders in which iron homeostasis is altered.

A. Iron Overload

It is clear that excess iron deposition is the major cause of iron-mediated hepatic damage, and this condition can be caused by both genetic [either HFE-linked (105) or not (133)] and acquired defects. Diseases of iron overload have been reviewed recently (5) and are also the subject of other chapters of this book (see Sec. IV). Here only the response of liver cells to iron is described.

The liver, when exposed to iron overload, reacts by restricting uptake and sequestering excess iron in newly formed ferritin. In fact, increased levels of iron in a labile pool downregulate IRPs (IRP2 in particular), which are key modulators of this response. Reduced IRP-binding activity causes both TfR mRNA destabilization and efficient ferritin mRNAs translation to take place. Liver cells add a selective increase of L-subunit gene transcription to the IRP-mediated control in order to produce ferritin shells enriched in L chains, which are better suited to long-term iron storage. This has been demonstrated not only in rodent models of iron loading or in iron-treated hepatic cell cultures, but also in patients with either genetic or secondary siderosis (16).

The basic scenario for the pathobiological response is one in which liver cells are faced with iron overload and try to prevent toxicity by limiting iron availability. If iron load progresses, in the long run these countermeasures are ineffective because the buffering capacity of ferritin becomes saturated and labile iron species lead to oxidative stress-mediated cell damage. Indeed, unabated NTBI uptake has been invoked to account for the accumulation of iron despite TfR downregulation (16). However, it has been recently demonstrated that liver cells express high levels of a second TfR which is not repressed by iron (55). This finding therefore gives potentially novel insights into the mechanisms of hepatic iron loading. The demonstration that the TfR2 gene is mutated in patients meeting diagnostic criteria for HH (56) is difficult to integrate into the current framework of iron metabolism but is certainly intriguing.

Regardless of the processes underlying iron entry, excess iron accumulation leads to hepatic fibrosis and cirrhosis (134). These are major causes of morbidity and mortality in their own right, and they additionally result in a dramatically increased risk for hepatocellular carcinoma. Numerous studies have addressed the molecular and cellular aspects of iron-induced liver damage and have clearly established a role for iron-mediated ROS generation and oxidant stress in the pathogenesis of liver injury (reviewed in Ref. 2). Studies with rodent models have shown that various pathways converge to trigger HSC activation, depending on differential cell localization of excess iron (e.g., in hepatocytes or Kupffer cells). The Kupffer cells, by producing ROS and (or) cytokines, have a key role as mediators of the fibrogenic response. HSC, although not directly sensitive to in-vivo iron overload, are essential players in iron-mediated toxicity and fibrogenesis, because their activation, charac-

terized by enhanced proliferation and acquisition of a myofibroblast-like phenotype, leads to higher deposition of extracellular matrix components.

Increased iron content has been associated with liver damage in clinical disorders other than genetic and acquired hemochromatoses. Mild to moderate liver iron overload is seen in patients with advanced chronic viral hepatitis, especially when caused by the hepatitis C virus. Excess iron deposition in the liver also seems to favor the persistence of viral infection and to have a negative effect on the response to interferon (135). A certain degree of hepatic iron accumulation provoked by alcohol, estrogens, viruses, or a combination of these factors is present in many patients with prophyria cutanea tarda (134), and there may be an association between an increased susceptibility to iron acquisition and an allelic HFE mutation (136). Iron probably amplifies the damaging effect of hepatotoxins, and this may explain these phenomena, but the underlying mechanisms are far from being understood.

Finally, it should be pointed out that hepatic iron overload is a feature very commonly observed in response to functional derangement or inactivation (as in knockout mice) of a number of proteins that are not always connected in a straightforward way to iron deposition. For example, lack of Cp (118), Tf (reviewed in Ref. 137), heme oxygenase-1 (138), or HFE (reviewed in Ref. 5) all lead to liver iron overload. Similarly, hepatic iron overload has been observed in human disorders as different as dismetabolic (139) and Zellweger (1) syndromes. It appears, therefore, that whenever one of the components of the integrated control of iron metabolism is altered, abnormal deposition of iron in the liver ensues. On the other hand, the role in hepatic iron deposition of other proteins commonly thought to be important physiological sources of iron for the liver (1) has been recently questioned by studies in Hp- (132) and Hx- (130) deficient mice (see above). These considerations on the one hand reinforce the idea that the liver is essential for maintenance of the body's iron homeostasis, and on the other hand clearly indicate that, despite recent impressive progress, much remains to be clarified about the regulation of systemic iron metabolism.

B. Inflammation

The liver plays an important role in systemic inflammation. This is related not only to its role in producing acute-phase reactants, but also to its ability to modulate iron metabolism and decrease circulating iron levels. Results of experiments provoking the acute-phase response *in vivo* (46,47,71,140), when interpreted in the context of data gleaned from cultured cells, allow us to construct a picture of the events occurring in the liver during acute inflammation. A biphasic response to experimental inflammation (71,140) begins with a translationally controlled early increase of ferritin synthesis, not mediated through the IRE/IRP interaction but through an acute box region (74,75). This is followed by an elevation of ferritin mRNAs. Activation of IRP binding (46,97) then causes decreased ferritin synthesis and elevated TfR mRNA levels. Later on, a decline in IRP activity allows a second wave of ferritin synthesis to start, while TfR mRNA returns to control levels. In experimental inflammation the first rise in rat liver ferritin synthesis occurs before the reduction of serum iron levels (140), suggesting that iron sequestration by newly made ferritin subunits is one of the mechanisms underlying hypoferrremia. However, the interleukin-mediated increase in TfR and the resulting enhanced uptake of Tf-bound iron may also

contribute to increasing hepatic iron deposition (47,48). Conversely, as NO reduces uptake of NTBI by HepG2 cells (141), this form of iron probably does not play a significant role in this context. Cytokines, which exploit NO as intracellular messenger (46,97), seem to be key players in the response of hepatic iron metabolism to inflammation. Indeed, TNF has been shown to specifically activate H-ferritin subunit transcription in an iron-independent fashion (142) and in hepatic cells IL-1 and IL-6 induce both H- and L-ferritin chains via an IRE-independent posttranscriptional mechanism (74,75). Conversely, increased IRP activity paralleled the rise in the amount of TfR transcripts in the livers of rats undergoing an acute inflammatory reaction following turpentine treatment (46). In summary, multiple independent regulatory pathways cooperate to modulate ferritin composition and content and TfR expression as important components of the inflammatory response. Ferritin and TfR are usually regulated in opposite manner by the IRE/IRP interaction. However, simultaneous induction of the two proteins by means of different pathways might be instrumental in the iron-withholding process that gives rise to the typical hypoferrremia associated with inflammatory states.

At present, it is difficult to distinguish the role of the different liver cell populations in the response of iron metabolism to inflammation. Most of the results reported above have been obtained in hepatocellular cell lines, but, for instance, Kupffer cells are probably very active, as deduced from investigation of iron metabolism in cytokine-treated macrophage cell lines. However, their role has not been assessed *in vivo* (e.g., in rats previously treated with gadolinium chloride) nor investigated in Kupffer cells maintained in primary culture.

C. Growth

Liver cells rarely divide in adults, but they can undergo regenerative growth after surgical removal, such as in partial hepatectomy, or necrotic loss of tissue mass caused by toxic injury. Hepatic regeneration is therefore an excellent example of controlled liver proliferation and a powerful model system to investigate growth control and hence to get insights into the processes leading to liver carcinogenesis. In particular, because iron is a necessary factor for cell multiplication, understanding the changes of iron metabolism in relation to proliferative stimuli may also help to unravel the role of the metal in malignant growth. This is relevant to human pathology because a large body of evidence from epidemiological, animal, and laboratory studies supports the positive relation between increased body iron stores and the risk of liver cancer.

In view of the above considerations, liver iron metabolism has been investigated in regenerating liver and in rodent models of hepatic carcinogenesis. As in a number of other types of growing cells, increased TfR expression, accompanied by higher Tf-iron uptake, has been found in rat liver preneoplastic nodules and hepatocellular carcinomas (41), probably in order to ensure sufficient iron to sustain cell proliferation. Similarly, high levels of TfR expression and IRP activity have been detected in regenerating liver cells. Intriguingly, in spite of the activation of IRP, the physiological repressor of its translation, ferritin synthesis also increases during regeneration. Analysis of the molecular mechanisms underlying this paradoxical contradiction of the opposite control of TfR and ferritin showed that liver regeneration triggers growth-dependent signals that activate ferritin gene transcription and, at the

same time, hamper the capacity of activated IRP to repress ferritin mRNA translation (78). Ferritin expression has been addressed by a number of studies in rodent models of hepatocarcinogenesis and in human hepatomas, but a unifying picture has not emerged. This is likely the result not only of the use of different techniques and models but also of the multiple regulatory mechanisms for this protein, which is affected by differentiation, growth rate, malignant transformation, iron status, etc. Recently, the finding that the genes for H ferritin and IRP2 are transcriptional targets of the c-myc oncogene convincingly indicated that alteration of iron metabolism is one of the mechanism c-myc uses to induce malignant cell transformation. In fact, transcriptionally controlled repression of H ferritin and activation of IRP2 result in amplification of the intracellular iron pool (101). This strongly support previous results showing the presence of H-rich ferritins and increased H-ferritin-chain mRNA levels in murine and human hepatomas (reviewed in Ref. 143). On the other hand, a decreased total ferritin content, represented mainly by the L chain, has been found in liver tumors, often despite increased L-mRNA content. It seems therefore that the normal characteristics of hepatic ferritin expression, such as low proportion of H chains and a high translational efficiency of L subunits, are partially lost in malignant liver cells. The mechanisms and the meaning of this alteration are presently obscure.

The biological basis of the association between iron and cancer probably rests in both oxidative stress-mediated DNA damage and availability of the metal to support rapid growth. Iron may therefore play a role both as an initiator in an early phase and, once malignant change has occurred, as a promoter that allows the transformed cell to fully express its potential of unrestricted growth. Full knowledge of the alterations of iron metabolism occurring during proliferation of normal and malignant cells may indicate new avenues to interfere with cancer development and progression.

D. Oxidative Stress, Ischemia/Reperfusion, and Hypoxia

These conditions represent different but related aspects of the interaction between iron homeostasis and oxygen. Reactive oxygen species (ROS) are unavoidable by-products of cell life in aerobic conditions, and they can impose substantial damage to a number of target molecules essential for cell homeostasis. However, if produced in controlled amounts, they also play a role in important physiological pathways such as signal transduction and redox regulation of cell proliferation and apoptosis. The cell keeps ROS levels under control also by means of the modulation of iron availability, because the appropriate sequestration of iron may allow the physiological roles of the relatively safe O_2^- and H_2O_2 to take place without the production of highly reactive $\cdot OH$. In consideration of this, cellular iron metabolism is sensitive to conditions of oxidative stress. Given the role of ferritin and TfR in iron chelation and uptake, their respective up- and downregulation under conditions of oxidative stress in order to limit iron availability may be anticipated. Indeed, it has been shown that various cell types react to a variety of stressful conditions by increasing ferritin synthesis (144–147), and H-subunit overexpression decreased the oxidative stress response (148). On the other hand, under conditions of oxidative stress, ferritin may release iron and therefore may also be considered a pro-oxidant. This effect has been noted in rat liver cells (85–87), but the role of ferritin is probably more complex. We have demonstrated that in rat liver subjected to oxidative stress ferritin can

initially represent a pro-oxidant because shell degradation by stress-activated proteases—more than reductive release of iron from intact shell, which probably occurs only under nonphysiological conditions—causes iron release at early times. This leads to an expansion of the “free” iron pool, which in turn downregulates IRP activity and also activates ferritin transcription through still unknown mechanisms (83,84). In this way, increased translation of a higher number of transcripts leads to reconstitution of the previous liver ferritin content and the protein can thus function as a physiological antioxidant. The regulation of hepatic TfR expression under conditions of oxidative stress has not been addressed so far, but the fall of IRP activity may suggest that a downregulation of TfR, aimed at preventing further iron uptake, will occur. Furthermore, based also on results in other cell types (149), a downmodulation of surface TfR by oxidative stress in liver cells may be anticipated; this response is probably regulated at the posttranslational level by changes in phosphorylation-dependent microtubule-based transport resulting in altered intravesicular trafficking (150).

The involvement of free-radical generation in the pathogenesis of liver injury is well established: iron overload (see above) and alcohol abuse are probably the most common conditions in which oxidative stress-mediated liver damage occurs. Moreover, free-radical reactions have been implicated in the mechanism of action of many xenobiotics. Therefore, given its role in drug detoxification, the liver is often the target of acute toxicity by oxidative stress, as exemplified by poisoning by paracetamol overdose, which, through rapid depletion of glutathione, causes massive hepatocellular necrosis. Furthermore, iron metabolism and detoxification of xenobiotics are often intertwined, as shown for the potentiating effect of iron on the hepatic toxicity of dioxin (151). It is therefore apparent that further insights into the response of hepatic iron metabolism to oxidative stress will provide advances in a field with important clinical applications.

Liver ischemia occurring during vascular occlusions, shock, and liver transplantation, together with the additional damage caused by reperfusion, may impose an anoxic or hypoxic injury on liver cells so severe as ultimately to cause organ failure. Whereas the events occurring during the posts ischemic reperfusion may be assimilated in a condition of oxidative stress (see above) and are therefore reasonably well understood, the modulation of liver iron metabolism under hypoxic conditions can be inferred only by extrapolating results obtained mainly in cell cultures. As outlined above, in hypoxic murine hepatoma cells, IRP-1 activity declines whereas IRP-2 activity and content are upregulated. The functional consequence of this divergent modulation on target mRNAs is presently unclear. Regardless of the divergent results about the molecular basis underlying the response (43,44), TfR upregulation in hypoxic hepatoma cells is undisputed. The effect of low oxygen tension on ferritin expression is less clear. In fact, in Hep3B cells exposed to hypoxia, ferritin synthesis and content were decreased, accompanied by IRP upregulation (43). On the other hand, the amount of ferritin was found unchanged *in vivo* during liver ischemia (84). Indeed, unmodified or even increased ferritin content is more consistent with results obtained in a model mimicking conditions of organ storage for transplants, which demonstrated that cultured liver cells exposed to a prolonged period of cold hypoxia accumulate low-molecular-weight iron (152).

Tf and TfR are among the increasing number of genes induced under conditions of low oxygen by means of the nuclear factor HIF-1. Indeed, Tf synthesis is induced

in hypoxic hepatoma cells (14), and serum Tf levels are higher in animals maintained under hypoxia (153). The finding that HIF-1 is activated during liver ischemia (154) may suggest that expression of proteins of iron metabolism such as Tf and TfR may also be transcriptionally induced *in vivo* by the absence of blood supply. While the meaning of Tf induction in this condition is clear—i.e., to enhance plasma iron transport capacity in a condition of stimulated erythropoiesis—the interpretation in physiological terms of increased TfR levels in hypoxic liver cells is less obvious. Indeed, a higher amount of free iron could trigger ROS formation during reoxygenation or postischemic reperfusion, even in spite of a possible elevated ferritin content. The finding that in erythroid cells the hypoxic response of TfR is increased compared with that of hepatoma cells might offer an explanation. Hypoxia seems to modulate TfR expression at multiple levels in a cell-specific way. Unidirectional activation, through enhanced transcription and unchanged mRNA stability, occurs in erythroid cells, whereas in hepatic cells the two controls are divergent and reduced IRP activity counteracts in part higher transcription, eventually resulting in a smaller rise of TfR mRNA (26). One can speculate whether the HIF-1-mediated transcriptional response, so important to provide bone marrow cells with plenty of iron for erythropoiesis, has been evolutionarily maintained in liver cells, but has been blunted by means of a posttranscriptional control to prevent excessive entry of the metal.

V. CONCLUSIONS

Not surprisingly, given the key importance of iron homeostasis for a variety of physiological and pathological functions, the processes of acquisition, storage, and transport of this essential metal are turning out to be complex and requiring the involvement of an increasing number of proteins (see Table 1). At both the cellular and systemic levels, a critical balance is needed, aimed at keeping adequate iron levels for important cell functions while avoiding the toxic events associated with an expanded iron pool. This requires a complicated regulation which is far from being completely understood, and this is particularly true for a complex organ such as the liver. Furthermore, proteins of iron metabolism are specific preferential targets of a number of factors other than iron, which may modify iron metabolism. This regulation may replace or supplement iron-dependent control in order to fine-tune iron homeostasis in such a way as to allow liver cells to respond or adapt to stressful events. These observations have clear clinical ramifications, and not just in relation to the control of body iron homeostasis. Iron is clearly involved in a number of other pathobiological settings concerning the liver, in addition to iron overload.

In conclusion, results about the multifaceted regulation of liver iron metabolism have been recently accumulating at an impressive rate, but, notably in the case of the liver, an integrated view of the regulation of liver iron metabolism remains for future studies to determine. It is easy to predict that insights will be provided in particular by *in-vivo* studies; a genetic approach using gene targeting technology to produce knockout and knockin mice will be especially helpful to this purpose. This effort will contribute toward a better understanding of the mechanisms underlying the physiology and pathophysiology of liver iron metabolism and hence toward the molecular characterization of the liver disorders in which iron is involved.

REFERENCES

1. Young SP, Aisen P. The liver and iron. In: Arias IM, Boyer JL, Fausto N, Jakoby WB, Schachter DA, Shafritz DA, eds. *The Liver: Biology and Pathobiology*. New York: Raven Press, 1994:597–617.
2. Pietrangelo A. Metals, oxidative stress, and hepatic fibrogenesis. *Semin Liver Dis* 1996; 16:13–30.
3. Harrison PM, Arosio P. The ferritins: Molecular properties, iron storage function and cellular regulation. *Biochim Biophys Acta* 1996; 1275:161–203.
4. Sibille JC, Kondon H, Aisen P. Interaction between isolated hepatocytes and Kupffer cells in iron metabolism: A possible role for ferritin as an iron carrier protein. *Hepatology* 1988; 8:296–301.
5. Andrews NC. Disorders of iron metabolism. *N Engl J Med* 1999; 341:1986–1995.
6. Fillet G, Beguin Y, Baldelli L. Model of reticuloendothelial iron metabolism in humans: Abnormal behavior in idiopathic hemochromatosis and in inflammation. *Blood* 1989; 74:844–851.
7. Donovan A, Brownlie A, Zhou Y, Shepard J, Pratt SJ, Moynihan J, Paw BH, Drejer A, Barut B, Zapata A, Law TC, Brugnara C, Lux SE, Pinkus GS, Pinkus JL, Kingsley PD, Palis J, Fleming MD, Andrews NC, Zon LI. Positional cloning of zebrafish ferroportin1 identifies a conserved vertebrate iron exporter. *Nature* 2000; 403:776–781.
8. McKie AT, Marciani P, Rolfs A, Brennan K, Wehr K, Barrow D, Miret S, Bomford A, Peters TJ, Farzaneh F, Hediger MA, Hentze MW, Simpson RJ. A novel duodenal iron-regulated transporter, Ireg1, implicated in the basolateral transfer of iron to the circulation. *Mol Cell* 2000; 5:299–309.
9. Abboud S, Haile DJ. A novel mammalian iron-regulated protein involved in intracellular iron metabolism. *J Biol Chem* 2000; 275:19906–19912.
- 9a. Kaplan J. Metal transport and unsafe sanctuary sites [editorial; comment]. *J Clin Invest* 1996; 98:3–4.
10. Zakin MM. Regulation of transferrin gene expression. *FASEB J* 1992; 6:3253–3258.
11. Idzerda RL, Huebers H, Finch CA, McKnight GS. Rat transferrin gene expression: Tissue specific regulation by iron deficiency. *Proc Natl Acad Sci USA* 1986; 83:3723–3727.
12. Pietrangelo A, Rocchi E, Schiaffonati L, Ventura E, Cairo G. Liver gene expression during chronic dietary iron overload in rats. *Hepatology* 1990; 11:798–804.
13. Semenza GL. Expression of hypoxia-inducible factor 1: Mechanisms and consequences. *Biochem Pharmacol* 2000; 59:47–53.
14. Rolfs A, Kvietikova I, Gassmann M, Wenger RH. Oxygen related transferrin expression is mediated by hypoxia-inducible factor-1. *J Biol Chem* 1997; 272:20055–20062.
15. Lipschitz DA, Cook JD, Finch CA. A clinical evaluation of serum ferritin as an index of iron stores. *N Engl J Med* 1974; 290:1213–1216.
16. Pietrangelo A, Rocchi E, Ferrari A, Ventura E, Cairo G. Regulation of hepatic transferrin, transferrin receptor and ferritin genes in human siderosis. *Hepatology* 1991; 14:1083–1089.
17. Cox LA, Adrian GS. Posttranscriptional regulation of chimeric human transferrin genes by iron. *Biochemistry* 1993; 32:4738–4745.
18. Cox LA, Kennedy MC, Adrian GS. The 5'-untranslated region of human transferrin mRNA, which contains a putative iron-regulatory element, is bound by purified iron-regulatory protein in a sequence-specific manner. *Biochem Biophys Res Commun* 1995; 212:925–932.
19. Henderson BR, Menotti E, Bonnard C, Kuhn LC. Optimal sequence and structure of iron responsive elements. Selection of RNA stem-loop with high affinity for iron regulatory factor. *J Biol Chem* 1994; 269:17481–17489.

20. Baumann H, Gauldie J. The acute phase response. *Immunol Today* 1994; 15:74–80.
21. Birch HE, Schreiber G. Transcriptional regulation of plasma protein synthesis during inflammation. *J Biol Chem* 1986; 261:8077–8080.
22. McKnight GS, Lee DC, Palmiter RD. Transferrin gene expression: Regulation of mRNA transcription in chick liver by steroid hormones and iron deficiency. *J Biol Chem* 1980; 255:148–153.
23. Hsu SL, Lin YF, Chou CK. Transcriptional regulation of transferrin and albumin genes by retinoic acid in human hepatoma cell line Hep3B. *Biochem J* 1992; 283:611–615.
24. Hertz R, Seckbach M, Zakin MM, Bar-Tana J. Transcriptional suppression of the transferrin gene by hypolipidemic peroxisome proliferators. *J Biol Chem* 1996; 271: 218–224.
25. Aisen P. Transferrin and the alcoholic liver. *Hepatology* 1985; 5:902–903.
26. Bianchi L, Tacchini L, Cairo G. HIF-1-mediated activation of transferrin receptor gene transcription by iron chelation. *Nucleic Acids Res* 1999; 27:4223–4227.
27. Muller-Eberhard U, Liem HH, Grasso JA, Giffhorn-Katz S, DeFalco MG, Katz NR. Increase in surface expression of transferrin receptors on cultured hepatocytes of adult rats in response to iron deficiency. *J Biol Chem* 1988; 263:14753–14756.
28. Hubert N, Lescoat G, Sciote R, Moirand R, Jego I, Leroyer P, Brissot P. Regulation of ferritin and transferrin receptor expression by iron in human hepatocyte cultures. *J Hepatol* 1993; 18:301–312.
29. Lu JP, Hayashi K, Awai M. Transferrin receptor expression in normal, iron-deficient and iron-overloaded rats. *Acta Pathol Jpn* 1989; 39:759–764.
30. Sciote R, Verhoeven G, van Eyken P, Cailleau J, Desmet VJ. Transferrin receptor expression in rat liver: Immunohistochemical and biochemical analysis of the effect of age and iron storage. *Hepatology* 1990; 11:416–427.
31. Basclain KA, Jeffrey GP. Coincident increase in periportal expression of iron proteins in the iron-loaded rat liver. *J Gastroenterol Hepatol* 1999; 14:659–668.
32. Sciote R, Paterson AC, Van den Oord JJ, Desmet VJ. Lack of hepatic transferrin receptor expression in hemochromatosis. *Hepatology* 1987; 7:831–837.
33. Lombard M, Bomford A, Hynes M, Naoumov NV, Roberts S, Crowe J, Williams R. Regulation of hepatic transferrin receptor in hereditary hemochromatosis. *Hepatology* 1989; 9:1–5.
34. Basclain KA, Shilkin KB, Withers G, Reed WD, Jeffrey GP. Cellular expression and regulation of iron transport and storage proteins in genetic haemochromatosis. *J Gastroenterol Hepatol* 1998; 13:624–634.
35. Hirose-Kumagai A, Sakai H, Akamatsu N. Increase of transferrin receptors in hepatocytes during rat liver regeneration. *Int J Biochem* 1984; 16:601–605.
36. Cairo G, Pietrangelo A. Transferrin receptor gene expression during rat liver regeneration. Evidence for post-transcriptional regulation by iron regulatory factorB, a second iron-responsive element-binding protein. *J Biol Chem* 1994; 269:6405–6409.
37. Hirose-Kumagai A, Akamatsu N. Change in transferrin receptor distribution in regenerating rat liver. *Biochem Biophys Res Commun* 1989; 164:1105–1112.
38. Neckers LM. Regulation of transferrin receptor expression and control of cell growth. *Pathobiology* 1991; 59:11–18.
39. Eriksson LC, Torndal UB, Andersson GN. The transferrin receptor in hepatocyte nodules: Binding properties, subcellular distribution and endocytosis. *Carcinogenesis* 1986; 7:1467–1474.
40. Park CI, Park YN, Jung WH. Transferrin receptor expression in hyperplastic lesions of hepatocyte in experimental hepatocarcinogenesis. *J Korean Med Sci* 1995; 10:183–188.
41. Pascale RM, De Miglio MR, Muroli MR, Simile MM, Daino L, Seddaiu MA, Pusceddu S, Gaspa L, Calvisi D, Manente G, Feo F. Transferrin and transferrin receptor

- gene expression and iron uptake in hepatocellular carcinoma in the rat. *Hepatology* 1998; 27:452–461.
42. Franco A, Paroli M, Testa U, Benvenuto R, Peschle C, Balsano F, Barnaba V. Transferrin receptor mediates uptake and presentation of hepatitis B envelope antigen by T lymphocytes. *J Exp Med* 1992; 175:1195–1205.
 43. Toth I, Yuan L, Rogers JT, Boyce H, Bridges KR. Hypoxia alters iron-regulatory protein-1 binding capacity and modulates cellular iron homeostasis in human hepatoma and erythroleukemia cells. *J Biol Chem* 1999; 274:4467–4473.
 44. Tacchini L, Bianchi L, Bernelli-Zazzera A, Cairo G. Transferrin receptor induction by hypoxia. HIF-1-mediated transcriptional activation and cell-specific post-transcriptional regulation. *J Biol Chem* 1999; 274:24142–24146.
 45. Lok CN, Ponka P. Identification of a hypoxia response element in the transferrin receptor gene. *J Biol Chem* 1999; 274:24147–24152.
 46. Cairo G, Pietrangelo A. Nitric-oxide-mediated activation of iron-regulatory protein controls hepatic iron metabolism during acute inflammation. *Eur J Biochem* 1995; 232:358–363.
 47. Kobune M, Kohgo Y, Kato J, Miyazaki E, Niitsu Y. Interleukin-6 enhances hepatic transferrin uptake and ferritin expression in rats. *Hepatology* 1994; 19:1468–1475.
 48. Hirayama M, Kohgo Y, Kondo H, Shintani N, Fujikawa K, Sasaki K, Kato J, Niitsu Y. Regulation of iron metabolism in HepG2 cells: A possible role for cytokines in the hepatic deposition of iron. *Hepatology* 1993; 18:874–880.
 49. Kumazawa M, Misaki M, Baba M, Shima T, Suzuki Y. Transferrin receptor on rat Kupffer cells in primary culture. *Liver* 1986; 6:138–144.
 50. Vogel W, Bomford A, Young S, Williams R. Heterogeneous distribution of transferrin receptors on parenchymal and nonparenchymal liver cells: biochemical and morphological evidence. *Blood* 1987; 69:264–270.
 51. Sciot R, Van Eyken P, Facchetti F, Callea F, Van der Steen K, Van Dijck H, Van Parijs G, Desmet VJ. Hepatocellular transferrin receptor expression in secondary siderosis. *Liver* 1989; 9:52–61.
 52. Testa U, Pelosi E, Peschle C. The transferrin receptor. *Crit Rev Oncog* 1993; 4:241–276.
 53. Levy JE, Jin O, Fujiwara Y, Kuo F, Andrews NC. Transferrin receptor is necessary for development of erythrocytes and the nervous system. *Nature Genet* 1999; 21:396–399.
 54. Kawabata H, Yang R, Hiramata T, Vuong PT, Kawano S, Gombart AF, Koeffler HP. Molecular cloning of transferrin receptor 2. A new member of the transferrin receptor-like family. *J Biol Chem* 1999; 274:20826–20832.
 55. Fleming RE, Migas MC, Holden CC, Waheed A, Britton RS, Tomatsu S, Bacon BR, Sly WS. Transferrin receptor 2: Continued expression in mouse liver in the face of iron overload and in hereditary hemochromatosis. *Proc Natl Acad Sci USA* 2000; 97:2214–2219.
 56. Camaschella C, Roetto A, Cali A, De Gobbi M, Garozzo G, Carella M, Majorano N, Totaro A, Gasparini P. The gene TFR2 is mutated in a new type of haemochromatosis mapping to 7q22. *Nature Genet* 2000; 25:14–15.
 57. Cairo G, Rappocciolo E, Tacchini L, Schiaffonati L. Expression of the genes for the ferritin H and L subunits in rat liver and heart. Evidence for tissue-specific regulations at pre- and post-translational levels. *Biochem J* 1991; 275:813–816.
 58. Bevilacqua MA, Giordano M, D'Agostino P, Santoro C, Cimino F, Costanzo F. Promoter for the human ferritin heavy chain-encoding gene (FERH): Structural and functional characterization. *Gene* 1992; 111:255–260.
 59. Munro HN, Linder MC. Ferritin: Structure, biosynthesis, and role in iron metabolism. *Physiol Rev* 1978; 58:317–396.

60. Beaumont C, Simon M, Smith PM, Worwood M. Hepatic and serum ferritin concentrations in patients with idiopathic hemochromatosis. *Gastroenterology* 1980; 79:877–883.
61. Cairo G, Bardella L, Schiaffonati L, Arosio P, Levi S, Bernelli-Zazzera A. Multiple mechanisms of iron-induced ferritin synthesis in HeLa cells. *Biochem Biophys Res Commun* 1985; 133:314–321.
62. Munro HN. Iron regulation of ferritin gene expression. *J Cell Biochem* 1990; 44:107–115.
63. White K, Munro HN. Induction of ferritin subunit synthesis by iron is regulated at both the transcriptional and translational levels. *J Biol Chem* 1988; 263:8938–8942.
64. Leggett BA, Fletcher LM, Ramm GA, Powell LW, Halliday JW. Differential regulation of ferritin H and L subunit mRNA during inflammation and long-term iron overload. *J Gastroenterol Hepatol* 1993; 8:21–27.
65. Zahringer J, Baliga BS, Munro HN. Novel mechanism for translational control in regulation of ferritin synthesis by iron. *Proc Natl Acad Sci USA* 1976; 73:857–861.
66. Muckenthaler M, Gray NK, Hentze MW. IRP-1 binding to ferritin mRNA prevents the recruitment of the small ribosomal subunit by the cap-binding complex eIF4F. *Mol Cell* 1998; 2:383–388.
67. Munro HN, Drysdale JW. Role of iron in the regulation of ferritin metabolism. *Fed Proc* 1970; 29:1469–1473.
68. Azia N, Munro HN. Both subunits of rat liver ferritin are regulated at a translational level by iron induction. *Nucleic Acids Res* 1986; 14:915–927.
69. Rogers J, Munro H. Translation of ferritin light and heavy subunit mRNAs is regulated by intracellular chelatable iron levels in rat hepatoma cells. *Proc Natl Acad Sci USA* 1987; 84:2277–2281.
70. Cairo G, Tacchini L, Schiaffonati L, Rappocciolo E, Ventura E, Pietrangelo A. Translational regulation of ferritin synthesis in rat liver. Effects of chronic dietary iron overload. *Biochem J* 1989; 264:925–928.
71. Konijn AM, Carmel N, Levy R, Hershko C. Ferritin synthesis in inflammation. II. Mechanism of increased ferritin synthesis. *Br J Haematol* 1981; 49:361–370.
72. Schiaffonati L, Rappocciolo E, Tacchini L, Bardella L, Arosio P, Cozzi A, Cantu GB, Cairo G. Mechanisms of regulation of ferritin synthesis in rat liver during experimental inflammation. *Exp Mol Pathol* 1988; 48:174–181.
73. Campbell CH, Solgonick RM, Linder MC. Translational regulation of ferritin synthesis in rat spleen: Effects of iron and inflammation. *Biochem Biophys Res Commun* 1989; 160:453–459.
74. Rogers JT, Bridges KR, Durmowicz GP, Glass J, Auron PE, Munro HN. Translational control during the acute phase response. Ferritin synthesis in response to interleukin-1. *J Biol Chem* 1990; 265:14572–14578.
75. Rogers JT. Ferritin translation by interleukin-1 and interleukin-6: The role of sequences upstream of the start codons of the heavy and light subunit genes. *Blood* 1996; 87:2525–2537.
76. Graziadei I, Weiss G, Bohm A, Werner-Felmayer G, Vogel W. Unidirectional upregulation of the synthesis of the major iron proteins, transferrin-receptor and ferritin, in HepG2 cells by the acute-phase protein alpha1-antitrypsin. *J Hepatol* 1997; 27:716–725.
77. Linder M, Munro HN, Morris HP. Rat ferritin isoproteins and their response to iron administration in a series of hepatic tumors and in normal and regenerating liver. *Cancer Res* 1970; 30:2231–2239.
78. Cairo G, Tacchini L, Pietrangelo A. Lack of coordinate control of ferritin and transferrin receptor expression during rat liver regeneration. *Hepatology* 1998; 28:173–178.

79. Wu CG, Groenink M, Bosma A, Reitsma PH, van Deventer SJH, Chamuleau RAFM. Rat ferritin-H: cDNA cloning, differential expression and localization during hepatocarcinogenesis. *Carcinogenesis* 1997; 18:47–52.
80. Primiano T, Kensler TW, Kuppusamy P, Zweier JL, Sutter TR. Induction of hepatic heme oxygenase-1 and ferritin in rats by cancer chemopreventive dithiolethiones. *Carcinogenesis* 1996; 17:2291–2296.
81. Reif DW. Ferritin as a source of iron for oxidative damage. *Free Radical Biol Med* 1992; 12:417–427.
82. Morel Y, Barouki R. Repression of gene expression by oxidative stress. *Biochem J* 1999; 342:481–496.
83. Cairo G, Tacchini L, Pogliaghi G, Anzon E, Tomasi A, Bernelli-Zazzera A. Induction of ferritin synthesis by oxidative stress. Transcriptional and post-transcriptional regulation by expansion of the “free” iron pool. *J Biol Chem* 1995; 270:700–703.
84. Tacchini L, Recalcati S, Bernelli-Zazzera A, Cairo G. Induction of ferritin synthesis in ischemic-reperfused rat liver: Analysis of the molecular mechanisms. *Gastroenterology* 1997; 113:946–953.
85. Powers RH, Stadnicka A, Kalbfleish JH, Skibba JL. Involvement of xanthine oxidase in oxidative stress and iron release during hyperthermic rat liver perfusion. *Cancer Res* 1992; 52:1699–1703.
86. Rikans LE, Ardinska V, Hornbrook KR. Age-associated increase in ferritin content of male rat liver: Implication for diquat-mediated oxidative injury. *Arch Biochem Biophys* 1997; 344:85–93.
87. Sakaida I, Kyle ME, Farber JL. Autophagic degradation of protein generates a pool of ferric iron required for the killing of cultured hepatocytes by an oxidative stress. *Mol Pharmacol* 1990; 37:435–442.
88. Ferreira C, Bucchini D, Martin ME, Levi S, Arosio P, Grandchamp B, Beaumont C. Early embryonic lethality of H ferritin gene deletion in mice. *J Biol Chem* 2000; 275:3021–3024.
89. Hentze MW, Kuhn LC. Molecular control of vertebrate iron metabolism: mRNA-based regulatory circuits operated by iron, nitric oxide, and oxidative stress. *Proc Natl Acad Sci USA* 1996; 93:8175–8182.
90. Leibold EA, Munro HN. Cytoplasmic protein binds in vitro to a highly conserved sequence in the 5′ untranslated region of ferritin heavy- and light-subunit mRNAs. *Proc Natl Acad Sci USA* 1988; 85:2171–2175.
91. Henderson BR, Seiser C, Kuhn LC. Characterization of a second RNA-binding protein in rodents with specificity for iron-responsive elements. *J Biol Chem* 1993; 268:27327–27334.
92. Guo B, Brown FM, Phillips JD, Yu Y, Leibold EA. Characterization and expression of iron regulatory protein 2 (IRP2): Presence of multiple IRP2 transcripts regulated by intracellular iron levels. *J Biol Chem* 1995; 270:16529–16535.
93. Chen OS, Schalinske KL, Eisenstein RS. Dietary iron intake modulates the activity of iron regulatory proteins and the abundance of ferritin and mitochondrial aconitase in rat liver. *J Nutr* 1997; 127:238–248.
94. Recalcati S, Conte D, Cairo G. Preferential activation of iron regulatory protein-2 in cell lines as a result of higher sensitivity to iron. *Eur J Biochem* 1999; 259:304–309.
95. Guo B, Yu Y, Leibold EA. Iron regulates cytoplasmic levels of a novel iron responsive element-binding protein without aconitase activity. *J Biol Chem* 1994; 269:24252–24260.
96. Flanagan PR, Hajdu A, Adams PC. Iron-responsive element-binding protein in hemochromatosis liver and intestine. *Hepatology* 1995; 22:828–832.
97. Phillips JD, Kinikini DV, Yu Y, Guo B, Leibold EA. Differential regulation of IRP1 and IRP2 by nitric oxide in rat hepatoma cells. *Blood* 1996; 87:2983–2992.

98. Testa U, Kuhn L, Petrini M, Quaranta MT, Pelosi E, Peschle C. Differential regulation of iron regulatory element-binding protein(s) in cell extracts of activated lymphocytes versus monocytes-macrophages. *J Biol Chem* 1991; 266:13925–13930.
99. Teixeira S, Kuhn LC. Post-transcriptional regulation of the transferrin receptor and 4F2 antigen heavy chain mRNA during growth activation of spleen cells. *Eur J Biochem* 1991; 202:819–826.
100. Seiser C, Teixeira S, Kuhn LC. Interleukin-2-dependent transcriptional and post-transcriptional regulation of transferrin receptor mRNA. *J Biol Chem* 1993; 268:13074–13080.
101. Wu KJ, Polack A, Dalla-Favera R. Coordinated regulation of iron-controlling genes, H-ferritin and IRP2, by c-MYC. *Science* 1999; 283:676–679.
102. Iwai K, Drake SK, Wehr NB, Weissman AM, LaVaute T, Minato N, Klausner RD, Levine RL, Rouault TA. Iron-dependent oxidation, ubiquitination, and degradation of iron regulatory protein 2: Implications for degradation of oxidized proteins. *Proc Natl Acad Sci USA* 1998; 95:4924–4928.
103. Cairo G, Castrusini E, Minotti G, Bernelli-Zazzera A. Superoxide and hydrogen peroxide-dependent inhibition of iron regulatory protein activity: A protective stratagem against oxidative injury [see comments]. *FASEB J* 1996; 10:1326–1335.
104. Hanson ES, Foot LM, Leibold EA. Hypoxia post-translationally activates iron-regulatory protein 2. *J Biol Chem* 1999; 274:5047–5052.
105. Feder JN, Gnirke A, Thomas W, Tsuchihashi Z, Ruddy DA, Basava A, Dormishian F, Domingo RJ, Ellis MC, Fullan A, Hinton LM, Jones NL, Limmel E, B, Kronmal GS, Lauer P, Lee VK, Loeb DB, Mapa FA, McClelland E, Meyer NC, Mintier GA, Moeller N, Moore T, Morikang E, Prass CE, Quintana L, Starnes SM, Schatzman RC, Brunke KJ, Drayna DT, Risch NJ, Bacon BR, Wolff RK. A novel MHC class I-like gene is mutated in patients with hereditary hemochromatosis. *Nature Genet* 1996; 13:399–408.
106. Parkkila S, Waheed A, Britton RS, Feder JN, Tsuchihashi Z, Schatzman RC, Bacon BR, Sly WS. Immunohistochemistry of HLA-H, the protein defective in patients with hereditary hemochromatosis, reveals unique pattern of expression in gastrointestinal tract. *Proc Natl Acad Sci USA* 1997; 94:2534–2539.
107. Bastin JM, Jones M, O'Callaghan CA, Schimanski L, Mason DY, Townsend AR. Kupffer cell staining by an HFE-specific monoclonal antibody: Implications for hereditary haemochromatosis. *Br J Haematol* 1998; 103:931–941.
108. Gunshin H, Mackenzie B, Berger UV, Gunshin Y, Romero MF, Boron WF, Nussberger S, Gollan JL, Hediger MA. Cloning and characterization of a mammalian proton-coupled metal-ion transporter. *Nature* 1997; 388:482–488.
109. Fleming MD, Trenor CC 3rd, Su MA, Foerzler D, Beier DR, Dietrich WF, Andrews NC. Microcytic anaemia mice have a mutation in Nramp2, a candidate iron transporter gene. *Nature Genet* 1997; 16:383–386.
110. Fleming MD, Romano MA, Su MA, Garrick LM, Garrick MD, Andrews NC. Nramp2 is mutated in the anemic Belgrade (b) rat: Evidence of a role for Nramp2 in endosomal iron transport. *Proc Natl Acad Sci USA* 1998; 95:1148–1153.
111. Canonne-Hergaux F, Gruenheid S, Ponka P, Gros P. Cellular and subcellular localization of the Nramp2 iron transporter in the intestinal brush border and regulation by dietary iron. *Blood* 1999; 93:4406–4417.
112. Trinder D, Oates PS, Thomas C, Sadleir J, Morgan EH. Localisation of divalent metal transporter 1 (DMT1) to the microvillus membrane of rat duodenal enterocytes in iron deficiency, but to hepatocytes in iron overload. *Gut* 2000; 46:270–276.
113. Gutierrez JA, Yu J, Rivera S, Wessling-Resnick M. Functional expression cloning and characterization of SFT, a stimulator of Fe transport. *J Cell Biol* 1997; 139:895–905.

114. Yu J, Yu ZK, Wessling-Resnick M. Expression of SFT (stimulator of Fe transport) is enhanced by iron chelation in HeLa cells and by hemochromatosis in liver. *J Biol Chem* 1998; 273:34675–34678.
- 114a. Wessling-Resnick M. Additions and corrections. *J Biol Chem* 1999; 274:35283.
- 114b. Wessling-Resnick M. Correction. *J Cell Biol* 1999; 139:275.
115. Askwith C, Kaplan J. Iron and copper transport in yeast and its relevance to human disease. *Trends Biochem Sci* 1998; 23:135–138.
116. Roeser HP, Lee GR, Nacht S, Cartwright GE. The role of ceruloplasmin in iron metabolism. *J Clin Invest* 1970; 49:2408–2417.
117. Harris ZL, Klomp LW, Gitlin JD. Aceruloplasminemia: An inherited neurodegenerative disease with impairment of iron homeostasis. *Am J Clin Nutr* 1998; 67:972S–977S.
118. Harris ZL, Durley AP, Man TK, Gitlin JD. Targeted gene disruption reveals an essential role for ceruloplasmin in cellular iron efflux. *Proc Natl Acad Sci USA* 1999; 96:10812–10817.
119. Radisky D, Kaplan J. Regulation of transition metal transport across the yeast plasma membrane. *J Biol Chem* 1999; 274:4481–4484.
120. Vulpe CD, Kuo YM, Murphy TL, Cowley L, Askwith C, Libina N, Gitschier J, Anderson GJ. Hephhaestin, a ceruloplasmin homologue implicated in intestinal iron transport, is defective in the sla mouse. *Nature Genet* 1999; 21:195–199.
121. Mukhopadhyay CK, Attieh ZK, Fox PL. Role of ceruloplasmin in cellular iron uptake. *Science* 1998; 279:714–717.
122. Gitlin JD. Transcriptional regulation of ceruloplasmin gene expression during inflammation. *J Biol Chem* 1988; 263:6281–6287.
123. Weiner AL, Cousins RJ. Hormonally produced changes in caeruloplasmin synthesis and secretion in primary cultured rat hepatocytes. *Biochem J* 1983; 212:297–304.
124. Sogawa K, Yamada T, Suzuki Y, Masaki T, Watanabe S, Uchida Y, Arima K, Nishioka M, Matsumoto K. Elevation of ceruloplasmin activity involved in changes of hepatic metal concentration in primary biliary cirrhosis. *Res Commun Chem Pathol Pharmacol* 1994; 84:367–370.
125. Chen OS, Schalinske KL, Eisenstein RS. Dietary iron intake modulates the activity of iron regulatory proteins and the abundance of ferritin and mitochondrial aconitase in rat liver. *J Nutr* 1997; 127:238–248.
126. Ke Y, Wu J, Leibold EA, Walden WE, Theil EC. Loops and bulge/loops in iron-responsive element isoforms influence iron regulatory protein binding. Fine-tuning of mRNA regulation? *J Biol Chem* 1998; 273:23637–23640.
127. Kaplan J. Friedreich's ataxia is a mitochondrial disorder. *Proc Natl Acad Sci USA* 1999; 96:10948–10949.
128. Campuzano V, Montermini L, Molto MD, Pianese L, Cossee M, Cavalcanti F, et al. Friedreich's ataxia: Autosomal recessive disease caused by an intronic GAA triplet repeat expansion [see comments]. *Science* 1996; 271:1423–1427.
129. Koutnikova H, Campuzano V, Foury F, Dolle P, Cazzalini O, Koenig M. Studies of human, mouse and yeast homologues indicate a mitochondrial function for frataxin. *Nature Genet* 1997; 16:345–351.
130. Tolosano E, Hirsch E, Patrucco E, Camaschella C, Navone R, Silengo L, Altruda F. Defective recovery and severe renal damage after acute hemolysis in hemopexin-deficient mice. *Blood* 1999; 94:3906–3914.
131. Baumann H, Morella KK, Wong GH. TNF-alpha, Il-1 beta, and hepatocyte growth factor cooperate in stimulating specific acute phase plasma protein genes in rat hepatoma cells. *J Immunol* 1993; 151:4248–4257.
132. Lim S, Kim H, Lim SK, Ali A, Lim YK, Wang Y, Chong SM, Costantini F, Baumann H. Increased susceptibility in Hp knockout mice during acute hemolysis. *Blood* 1998; 92:1870–1877.

133. Pietrangelo A, Montosi G, Totaro A, Garuti C, Conte D, Cassanelli S, Fraquelli M, Sardini C, Vasta F, Gasparini P. Hereditary hemochromatosis in adults without pathogenic mutations in the hemochromatosis gene. *N Engl J Med* 1999; 341:725–732.
134. Bonkovsky H. Iron and the liver. *Am J Med Sci* 1991; 301:32–43.
135. Bonkovsky H, Banner BF, Rothman AL. Iron and chronic viral hepatitis. *Hepatology* 1997; 25:759–768.
136. Piperno A, Vergani A, Malosio I, Parma L, Fossati L, Ricci A, Bovo G, Boari G, Mancina G. Hepatic iron overload in patients with chronic viral hepatitis: role of HFE gene mutations. *Hepatology* 1998; 28:1105–1109.
137. De Silva DM, Askwith CC, Kaplan J. Molecular mechanisms of iron uptake in eukaryotes. *Physiol Rev* 1996; 76:31–47.
138. Poss KD, Tonegawa S. Heme oxygenase 1 is required for mammalian iron reutilization. *Proc Natl Acad Sci USA* 1997; 94:10919–10924.
139. Mendler MH, Turlin B, Moirand R, Jouanolle AM, Sapey T, Guyader D, Le Gall JY, Brissot P, David V, Deugnier Y. Insulin resistance-associated hepatic iron overload. *Gastroenterology* 1999; 117:1155–1163.
140. Konijn AM, Hershko C. Ferritin synthesis in inflammation. I. Pathogenesis of impaired iron release. *Br J Haematol* 1977; 37:7–16.
141. Barisani D, Cairo G, Ginelli E, Marozzi A, Conte D. Nitric oxide reduces nontransferrin-bound iron transport in HepG2 cells. *Hepatology* 1999; 29:464–470.
142. Tsuji Y, Miller LL, Miller SC, Torti SV, Torti FM. Tumor necrosis factor-alpha and interleukin1-alpha regulate transferrin receptor in human diploid fibroblasts: Relationship to the induction of ferritin heavy chain. *J Biol Chem* 1991; 266:7257–7261.
143. Arosio P, Levi S, Cairo G, Cazzola M, Fargion S. Ferritin in malignant cells. In: Ponka P, Schulman HM, Woodworth RC, eds. *Iron Transport and Storage*. Boca Raton, FL: CRC Press, 1990:201–216.
144. Balla G, Jacob HS, Balla J, Rosenberg M, Nath KA, Apple F, Eaton JW, Vercellotti GM. Ferritin: A cytoprotective antioxidant stratagem of endothelium. *J Biol Chem* 1992; 267:18148–18153.
145. Vile GF, Tyrrell RM. Oxidative stress resulting from ultraviolet A irradiation of human skin fibroblasts leads to a heme oxygenase-dependent increase in ferritin. *J Biol Chem* 1993; 268:14678–14681.
146. Kwak EL, Larochelle DA, Beaumont C, Torti SV, Torti FM. Role for NF-kB in the regulation of ferritin H by tumor necrosis factor-alpha. *J Biol Chem* 1995; 270:15285–15293.
147. Lobreaux S, Thoirion S, Briat JF. Induction of ferritin synthesis in maize leaves by an iron-mediated oxidative stress. *Plant J* 1995; 8:443–449.
148. Epsztejn S, Glicksteon H, Picard V, Slotki IN, Breuer W, Beaumont C, Cabantchik ZI. H-ferritin subunit overexpression in erythroid cells reduces the oxidative stress response and induces resistance properties. *Blood* 1999; 94:3593–3603.
149. Malorni W, Testa U, Rainaldi G, Tritarelli E, Peschle C. Oxidative stress leads to a rapid alteration of transferrin receptor intravesicular trafficking. *Exp Cell Res* 1998; 241:102–116.
150. Runnegar M, Wei X, Berndt N, Hamm-Alvarez SF. Transferrin receptor recycling in rat hepatocytes is regulated by protein phosphatase 2A, possibly through effects on microtubule-dependent transport. *Hepatology* 1997; 26:176–185.
151. Smith AG, Clothier B, Robinson S, Scullion MJ, Carthew P, Edwards R, Luo J, Lim CK, Toledano M. Interaction between iron metabolism and 2,3,7,8-tetrachlorodibenzo-p-dioxin in mice with variants of the *Ahr* gene: A hepatic oxidative mechanism. *Mol Pharmacol* 1998; 53:52–61.
152. Punshon G, Fuller B. Changes in ferrozine detectable iron in liver cells during hypoxia and hypothermia. *Biochem Soc Trans* 1998; 26:S102.

153. Simpson RJ. Dietary iron levels and hypoxia independently affect iron absorption in mice. *J Nutr* 1996; 126:1858–1864.
154. Tacchini L, Radice L, Bernelli-Zazzera A. Differential activation of some transcription factors during rat liver ischemia, reperfusion and heat shock. *J Cell Physiol* 1999; 180:255–262.

Iron Utilization in Erythrocyte Formation and Hemoglobin Synthesis

PREM PONKA

Jewish General Hospital and McGill University, Montreal, Quebec, Canada

I. OVERVIEW OF ERYTHROPOIESIS	644
II. OVERVIEW OF ORGANISMAL IRON METABOLISM IN RELATIONSHIP TO ERYTHROPOIESIS	647
III. OVERVIEW OF CELLULAR IRON METABOLISM	651
IV. EXPERIMENTAL SYSTEMS TO STUDY ERYTHROID IRON METABOLISM	655
A. Reticulocytes	655
B. Erythroid Cell Lines	655
C. A Two-Phase Liquid Culture for Growing Human Erythroid Cells	656
D. K562 Cells	657
V. IRON METABOLISM AND HEME SYNTHESIS IN ERYTHROID CELLS	657
A. Heme Synthesis	657
B. Transferrin Receptors	660
C. Iron Is Targeted into Mitochondria in Erythroid Cells	662
VI. INTEGRATED VIEW: THE AVAILABILITY OF IRON CONTROLS HEMOGLOBINIZATION	666
ACKNOWLEDGMENTS	668
REFERENCES	668

I. OVERVIEW OF ERYTHROPOIESIS

Vertebrates depend on the circulation of body fluids for oxygen transport, and this function is fulfilled by hemoglobins encapsulated within red blood cells. Free hemoglobin in the bloodstream is very rapidly catabolized and, hence, one important function of erythrocytes is to prolong the hemoglobin's life span up to 120 days (in humans). Moreover, encasement within erythrocytes allows attainment of remarkably high hemoglobin concentrations of about 5 mM. Hemoglobin is a tetrameric protein composed of four globin polypeptide chains ($\alpha_2\beta_2$ in adults), each protein subunit having one heme molecule attached noncovalently to it (1). Heme* is a complex of protoporphyrin IX with ferrous iron that reversibly binds oxygen as the erythrocytes travel between the lungs and tissues. Hemoglobin also participates in the transport of CO_2 from tissues to the lungs and acts as a carrier of nitric oxide (NO). The binding of oxygen to iron in hemoglobin promotes the binding of NO to cysteine (93) in the β chain, forming *S*-nitrosohemoglobin (2). Deoxygenation of hemoglobin enhances the release of NO, a potent vasorelaxant, which increases blood flow and therefore O_2 transport into tissues. It may be of interest to mention that there is an example of a vertebrate, the arctic icefish, that lacks hemoglobin (3,4). The icefish transports oxygen to its tissues solely in physical solution, and the oxygen-carrying capacity of its blood is only one-tenth that of red-blooded teleosts (3).

There are about 24 trillion (2.4×10^{13}) erythrocytes in the blood of adults, and their total weight is about 2.4 kg. Red blood cells are produced at a rate of 2.3×10^6 cells per second by a dynamic and exquisitely regulated process that is part and parcel of the development of all blood cells, or hematopoiesis. In humans, hematopoiesis occurs in the bone marrow of the adult and in the liver of the developing fetus. In mice and rats, the spleen, in addition to the bone marrow, is an important site of erythropoiesis. The mature erythrocyte is the product of complex and highly regulated cellular and molecular processes that initiate at the level of the hematopoietic stem cells, which have the potential to develop into all morphologically and functionally distinct blood cells. Stem cells, which are present in hematopoietic tissues in very small numbers (<0.01%), are self-renewing, slowly cycling cells that express receptors for stem cell factor (SCF) also known as c-kit receptor (tyrosine-kinase type). Although regulation of stem cell proliferation and commitment is poorly understood, SCF and some other hematopoietic growth factors seem to be involved in the regulation. The process of commitment is characterized by restriction in the stem cell differentiation capacity leading to the formation of progenitor cells that differentiate along one lineage (5).

Progenitor cells committed to the erythroid lineage cannot be distinguished by morphologic criteria, but their existence and characteristics can be inferred from their capacity to generate colonies of hemoglobinized cells *in vitro* (6). The earliest functionally detectable erythroid precursor is known as the BFU-E (burst-forming unit, erythroid), an early descendant of the hematopoietic stem cell. The BFU-E is detected by its capacity to generate multiclustered colonies ("erythroid bursts") of hemoglobin-containing cells when marrow is incubated in semisolid medium. The development of BFU-E-type colonies requires supplementing of tissue culture media with

*Heme is ferroporphyrin IX; hemin is ferric protoporphyrin IX. In this chapter, the term "heme" is used as a generic expression denoting no particular iron valence state.

erythropoietin (Epo), granulocyte macrophage colony-stimulating factor (GM-CSF), and interleukin-3 (IL-3). BFU-E are relatively insensitive to Epo both in vitro (requiring a high concentration of the hormone to generate the bursts of erythropoietic colonies) and in vivo (the number of BFU-E is relatively unresponsive both to depressed and elevated oxygen-carrying conditions of the blood).

BFU-E in turn generate a class of more mature erythropoietic precursors, termed CFU-E (colony-forming units, erythroid). These cells are detected by virtue of their capability in cell culture to generate a small cluster of erythroid cells, which mature all the way to erythrocytes. The proliferative capacity of CFU-E is limited to four or five cell divisions, generating 16 to 32 progeny red cells. Virtually all CFU-E are proliferating, and they have an absolute requirement for Epo to maintain viability, undergo cell division, and differentiate into proerythroblasts. The number of CFU-E in vivo is extremely sensitive to the Epo titer; hence CFU-E are considerably depleted by hypertransfusion or polycythemia and augmented by anemia.

The first morphologically recognized erythroid element is the proerythroblast, which presumably is the immediate progeny of a CFU-E. Maturation of the proerythroblast to the circulating red cell involves four or five cell divisions; production of characteristic red cell proteins (hemoglobin and enzymes), surface antigens, and metabolic machinery; loss of replicative capacity and eventually of the nucleus itself; loss of organelles and acquisition of characteristic red cell morphological features. The process takes between 48 and 96 h, and one proerythroblast will give rise to 16 to 32 progeny erythrocytes. The proerythroblast stage is succeeded by basophilic erythroblast. This erythroblast is basophilic because of the high concentration of cytoplasmic ribosomes that accumulate in preparation for the onset of hemoglobin synthesis, which already occurs in these cells at a relatively low rate. The next cell, polychromatophilic erythroblast, displays increasingly deep staining for hemoglobin and a progressive decrease in the concentration of cytoplasmic ribosomes. Cell division continues until the orthochromatic erythroblast state, by which time the cytoplasm has lost much of its basophilia, although hemoglobin synthesis continues on relatively stable ribosome-globin mRNA complexes. At this stage the nucleus is expelled and the nuclear remnant is phagocytosed by macrophages, a process which leads to the generation of reticulocytes. These non-nucleated cells still contain active globin-synthesizing polyribosomes as well as mitochondria that produce heme. At this stage the reticulocytes are released into the circulation. During the first 24–36 h of circulation in the blood, the reticulocyte is transformed into the mature erythrocyte (6).

The maturation of reticulocytes is poorly understood and is characterized by progressive decrease in the number of polyribosomes and mitochondria, loss of hemoglobin synthetic capacity, including loss of transferrin receptors (TfR, see below), as well as by a decrease in size, and assumption of the biconcave disk shape. It is remarkable that reticulocyte maturation involves degradation of mitochondria and the complete removal of some proteins while preserving hemoglobin, carbonic anhydrase, as well as a large number of cytosolic and cytoskeletal proteins needed as life-support for mature erythrocytes. Breakdown of internal membranes, including those of mitochondria, is accomplished in part by erythroid 15-lipoxygenase (LOX), which, interestingly, contains one Fe per mole (7,8). Erythroid 15-LOX is unique in its ability to attack phospholipids and is the main factor in mitochondrial degradation during reticulocyte maturation. Somewhat surprisingly, the mRNA for erythroid 15-

LOX is the second most abundant reticulocyte mRNA (after globin mRNA). Although it is transcribed in erythroblasts, it is only activated for translation in peripheral reticulocytes (9). Interestingly, the 3'-untranslated region (UTR) of rabbit erythroid 15-LOX mRNA contains an unusual repeat structure consisting of a 19-nucleotide pyrimidine-rich motif (10,11). Recently Ostareck et al. (12) identified hnRNPs, K and E1, two highly abundant cytoplasmic proteins, as repressors responsible for masking rabbit 15-LOX mRNA during early erythroid cell development. Although hnRNP K and E1 bind to the repeated pyrimidine-rich motif present in the 3'-UTR of 15-LOX mRNA, they inhibit translation which is initiated at the 5' end. Once 15-LOX protein is translated, it attacks the membranes of various organelles, allowing release of proteins from the organelle lumen and access of proteases to both luminal and integral membrane proteins (13). It is conceivable that many other enzymes play a role in the cellular reorganization occurring at the reticulocyte stage of erythroid development. Recently identified examples (14) include two ubiquitin-conjugating enzymes (E2-20K and E2-230K) that are strongly induced during the maturation of erythroblasts into reticulocytes which do not seem to contain lysosomes (7). Johnstone and her co-workers (15–17) described yet another mechanism involved in protein disappearance during reticulocyte maturation. This group showed that reticulocytes lose TfR by “shedding.” The loss of TfRs seems to be preceded by the formation of multivesicular bodies containing encapsulated receptors. Fusion of multivesicular bodies with the plasma membrane leads to release of vesicles (exosomes), containing receptors whose extracellular domain is positioned externally, into the circulation. Although it is unknown how the above processes are triggered, it is tempting to speculate that reaching a threshold concentration of hemoglobin in reticulocytes represents a signal for their activation.

As already mentioned, Epo is essential for the proliferation, differentiation, and survival of the erythroid progenitors. The major function of hemoglobin within erythrocytes is to transport oxygen to the tissues and, hence, it makes perfect physiological sense that decreased oxygen tension triggers Epo production and vice versa. The gene for Epo, which is synthesized primarily in the kidney, contains a cis-acting hypoxia response element (HRE) that mediates transcriptional activation by hypoxia-inducible factor-1 (HIF-1) (18,19). HIF-1 is a heterodimeric basic-helix-loop-helix transcription factor consisting of HIF-1 α and HIF-1 β (identical to the aryl hydrocarbon nuclear translocator, ARNT) subunits. In hypoxia, HIF-1 α is stabilized against degradation via the ubiquitin-proteasome system, leading to the formation of HIF-1 α /ARNT heterodimers that activate Epo gene expression (18,19). It is of interest to mention that the iron chelator desferrioxamine (DFO) mimics the effects of hypoxia and activates HIF-1 and, consequently, Epo gene transcription (20).

The actions of Epo are mediated through specific high-affinity Epo receptors expressed on the membrane of target cells (BFU-E, CFU-E, and proerythroblasts). Binding of Epo induces dimerization and transphosphorylation of the Janus family kinase, JAK2, which then phosphorylates several tyrosine residues of the Epo receptor. Epo receptor phosphorylation creates docking sites for the SH2 domains of several signal transduction proteins, including STAT5. Phosphorylated STAT5 dissociates from the Epo receptor, dimerizes, and moves to the nucleus, where it activates transcription of the protein bclx. Bclx is an antiapoptotic protein that prevents programmed cell death of the erythroid progenitors, allowing the terminal differentiation program to be expressed (6,21). Although the exact mechanism by which Epo

regulates differentiation of erythroid cells is ill understood, it is well known that the major change associated with erythroid differentiation is the induction of hemoglobin synthesis. This involves de-novo induction of globin gene expression, an erythroid-specific event, and increases in heme biosynthesis and iron transport. Many of these aspects of terminal erythroid maturation are regulated by transcription factors such as GATA-1, NF-E2, and erythroid Krüppel-like factor (EKLF) (6,22).

It is remarkable that although three different and totally distinct pathways are involved in hemoglobin synthesis, virtually no intermediates, i.e., globin chains, porphyrin intermediates, or iron, accumulate in the developing erythroblasts and reticulocytes. This is achieved, at least in part, by a series of negative and positive feedback mechanisms in which heme plays a crucial role. In general, in erythroid cells heme inhibits cellular iron acquisition (reviewed in Refs. 23 and 24) and, consequently, heme synthesis and is essential for the synthesis of globin. The effect of heme on its own synthesis and iron metabolism will be discussed later; here I shall briefly describe the role of heme in globin synthesis. Numerous reports indicate that heme stimulates globin gene transcription and is probably involved in promoting some other aspects of erythroid differentiation. Hemin treatment of erythroid precursors leads to rapid accumulation of globin mRNA, whereas heme deficiency leads to a decrease in globin mRNA levels (25–29). These effects can probably be explained by heme-mediated upregulation of NF-E2-binding activity (29).

It has long been known that the translation of globin in intact reticulocytes and their lysates is dependent on the availability of heme (30–33). Heme deficiency inhibits protein synthesis in part through activation of the heme-regulated inhibitor (HRI). HRI is a cyclic AMP-independent protein kinase which specifically phosphorylates the α subunit (eIF-2 α) of eukaryotic initiation factor 2 (eIF-2). Phosphorylation of eIF-2 α blocks initiation of protein synthesis. By contrast, hemin binds to HRI, and this association inhibits the enzyme by promoting formation of disulfide bonds, perhaps between two HRI subunits (33). Disulfide bond formation reverses the inhibition of globin synthesis seen during heme deficiency. The expression of HRI seems to be confined to erythroid cells (34) and, hence, HRI plays an important physiological role in the translation of globin and probably other proteins synthesized in erythroid cells.

In conclusion, in erythroid cells iron is not only the substrate for the synthesis of hemoglobin but also participates in its regulation. The iron protoporphyrin complex appears to enhance globin gene transcription, is essential for globin translation, and supplies the prosthetic group for hemoglobin assembly. Moreover, heme may be involved in the expression (at transcriptional as well as translational levels) of numerous other erythroid-specific proteins.

II. OVERVIEW OF ORGANISMAL IRON METABOLISM IN RELATIONSHIP TO ERYTHROPOIESIS

Iron is a precious metal for the organism because of its unsurpassed versatility as a biological catalyst. It is involved in a broad spectrum of essential biological functions such as oxygen transport (hemoglobin), electron transfer (mitochondrial heme and nonheme iron proteins essential for energy production), and DNA synthesis (ribonucleotide reductase), to name just a few. However, the chemical properties of iron which allow this versatility also lead to the paradoxical situation that acquisition by

the organism of the fourth most abundant element in the earth's crust is exceedingly difficult. At pH ~ 7.4 and physiological oxygen tension, relatively soluble ferrous iron is readily oxidized to ferric ion, which is susceptible to hydrolysis, forming virtually insoluble ferric hydroxides. The concentration of aquated Fe^{3+} in aqueous solutions (pH ≈ 7.4) cannot exceed 10^{-17} M. Moreover, unless it is bound to specific ligands, iron plays a key role in the formation of harmful oxygen radicals which ultimately cause peroxidative damage to vital cell structures (35). Because of this virtual insolubility and potential toxicity, specialized mechanisms and molecules for the acquisition, transport, and storage of iron in a soluble nontoxic form have evolved to meet cellular and organismal iron requirements. Moreover, organisms are equipped with remarkable mechanisms that prevent the expansion of the catalytically active intracellular iron pool, while maintaining sufficient concentrations of the metal for metabolic use.

In vertebrates, iron is transported within the body between sites of absorption, storage, and utilization by the plasma glycoprotein transferrin (Tf) which binds Fe(III) very tightly but reversibly. $\text{Fe(III)}_2\text{-Tf}$ is recognized by specific cell membrane Tf receptors (TfR) which are crucial for cellular iron acquisition. Following its intracellular release from Tf-TfR complexes, iron enters functional compartments or is stored in ferritin. Iron represents 55 and 45 mg per kilogram of body weight in adult men and women, respectively. Normally, about 60–70% of total body iron is present in hemoglobin in circulating erythrocytes. Myoglobin, cytochromes, and other iron-containing enzymes comprise a further 10%, and the remaining 20–30% is stored in ferritin. Although iron bound to transferrin is less than 0.1% (~ 3 mg) of total body iron, dynamically it is the most important iron pool, with the highest rate of turnover (36).

The turnover of Tf iron is roughly 30 mg/24 h and, normally, about 80% of this iron is transported to the bone marrow for hemoglobin synthesis in developing erythroid cells (Fig. 1). As already mentioned, from these sites reticulocytes are released into the circulation, where, within about 24 h, they develop into mature erythrocytes which circulate in the blood for about 120 days. Senescent erythrocytes are phagocytosed by macrophages of the reticuloendothelial system where the heme moiety is split from hemoglobin and catabolized enzymatically via heme oxygenase (HO). Hence, *in vivo*, macrophages, in contrast to the majority of cells in the organism, do not seem to acquire significant amounts of iron from Tf (36). Nevertheless, it is possible that a low level of iron acquisition via the Tf-TfR pathway occurs in macrophages *in vivo* and that this mechanism serves a signaling role informing macrophages about body iron status and this, in turn, determines how much iron should be released from them.

Iron, which is liberated from its confinement within the protoporphyrin ring inside macrophages, is returned almost quantitatively to the circulation (37). It seems that the quantity of iron leaving reticuloendothelial cells (macrophages) is directly proportional to the input of hemoglobin into the cells, and that stimulation of erythropoiesis is followed by an increased iron release from macrophages. However, the mechanism involved in the regulation of macrophage iron output is unknown, since neither plasma iron nor Epo can be directly and exclusively responsible for the control. In patients with aplastic anemia, iron release is low, despite high Epo levels. Iron release in patients with hemolytic anemia or after phlebotomy can be increased four- to sixfold without significant changes in plasma iron concentration (37).

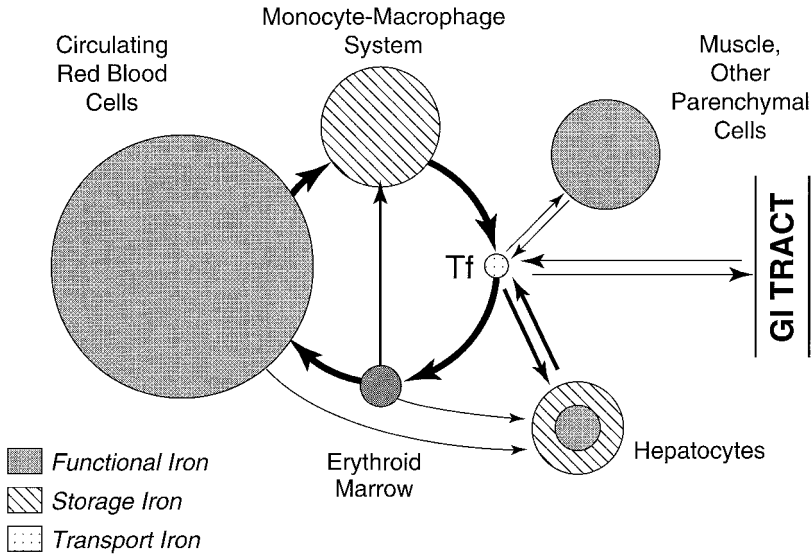


Figure 1 Body iron supply and storage. The figure shows a schematic representation of the routes of iron movement in the adult. The area of each circle is proportional to the amount of iron contained in the compartment, and the width of each arrow is proportional to the daily flow of iron from one compartment to another. (Reprinted from Ref. 176 with permission.)

As part of their physiological function, hepatocytes also show some spontaneous release of iron in a form that binds to plasma Tf. Iron mobilization from isolated hepatocytes is inversely related to the oxygen tension (38), and if such a phenomenon occurs also *in vivo*, this can be expected to have important physiological and pathophysiological implications. Either hypoxia itself, or Epo increased by hypoxia, may promote hepatocyte iron release to satisfy increased demand for iron by the expanded erythron.

Many questions on the mechanisms and controls involved in the release of macrophage and hepatocyte iron, to make it available for erythropoiesis, remain unanswered. Nevertheless, a number of recent studies have provided important new clues that promise to enhance our understanding of the recycling of hemoglobin iron by macrophages. First, Poss and Tonegawa (39) generated mice lacking functional HO-1 (i.e., isoform of HO inducible by heme and oxidative stress, as opposed to isoform 2, which is constitutive) and showed that the mice developed an anemia with abnormally low plasma iron. This finding provides direct evidence that HO-1 plays a key role in recycling hemoglobin iron. Moreover, HO-1-deficient mice developed conspicuous nonheme iron loading in the hepatocytes, macrophages, and some other cells. This finding is unexpected and suggests a link between iron release from the cells and HO-1 activity. Further support for this idea comes from a recent study (40) which showed that the induction of HO-1 was associated with a significant increase in iron transport by a newly identified iron-ATPase which has been proposed to play a role in iron release from the cells. Second, Donovan et al. (41) reported the identification of the transporter required for exporting iron from the enterocytes into the blood plasma. This exporter was identified by cloning a mutant gene in

zebrafish that results in iron-deficient erythropoiesis. The normal allele of this gene has been termed *ferroportin 1*, and the authors subsequently identified its homologs in both mouse and humans. They showed that ferroportin 1 mRNA is present in tissues involved in iron export, namely, the zebrafish yolk sac and intestine as well as mouse placenta, intestine, and macrophages. Hence, it seems highly likely that ferroportin 1 is the macrophage iron exporter. McKie et al. (42) and Abboud and Haile (43) independently reported cloning of mouse genes *Ireg1* and *MTP1*, respectively, which seem to be identical to mouse *ferroportin 1*. All these groups provided some evidence that the protein products of the genes identified by them may function as iron exporters.

Third, studies of patients with a recently identified genetic deficiency of ceruloplasmin (a blue copper-containing plasma protein with ferroxidase activity) indicate that this protein plays an important role in controlling iron release from cells. Patients with hereditary aceruloplasminemia have low plasma iron levels, but marked iron accumulation is evident in the liver, brain, pancreas, spleen, heart, and kidney (44,45). Moreover, ceruloplasmin knockout mice exhibit a severe impairment of iron efflux from the reticuloendothelial system and hepatocytes (46). Hence, it is conceivable that ceruloplasmin may facilitate iron export, presumably via ferroportin 1, by promoting the oxidation of Fe(III) at the side facing toward the blood. In this context it is of interest to mention that a multicopper oxidase, termed hephaestin, is required for efficient export of iron from the intestine (47). In fact, hephaestin was identified (47) during a quest to explain the molecular pathogenesis of mouse sex-linked anemia (*sla*), which has long been known to be caused by an impaired transfer of iron across the basolateral membrane of enterocytes. Importantly, hephaestin is a ceruloplasmin homolog but, unlike ceruloplasmin, it is a membrane protein (see Chapter 23). Hence, it is clear that copper-containing ferroxidases have crucial roles in the export of iron from the cell and in making this metal available for erythropoiesis.

These are exciting new developments, but much further research is needed to delineate the intricate molecular and functional relationships among HO-1, ferroportin 1, and ceruloplasmin/hephaestin. In particular, it will be highly important to determine whether and how these proteins modulate iron release in response to physiological and pathophysiological stimuli such as Epo, hypoxia and, perhaps, to other factors.

Considering the overall theme of this chapter, several important features marking organismal iron metabolism have to be highlighted. First, iron turnover is virtually an internal event in the body, and most of the iron turning over is used for the synthesis of heme in erythroid cells. Iron exchange with nonerythroid tissues (namely, the liver) represents only about 17% of the total plasma iron turnover. Normally, only 1 mg of dietary iron is absorbed per 24 h (~3% of Fe turnover), and the organismal iron balance is maintained by a daily loss of approximately 1 mg via nonspecific mechanisms (mostly cell desquamation) (see Fig. 1). Second, as discussed elsewhere in this volume (see Chapter 18), at least some nonerythroid cells can acquire non-Tf-bound iron (NTBI), and this process likely operates *in vivo* only in severely iron-overloaded patients who have NTBI in their plasma. However, hemoglobin synthesis is stringently dependent on Tf as a source of iron for erythroid cells. *In-vitro* studies with erythroid cells have provided clear evidence that the only physiological chelator that can provide iron for hemoglobin synthesis is Tf. Even

when these cells incorporate iron bound to some low-molecular-weight chelators (e.g., citrate), this uptake is mediated by cell-associated Tf (48). An absolute requirement for Tf by erythroid cells *in vivo* is demonstrated by the observations that humans (49) and mice (50) with hereditary atransferrinemia have severe hypochromic microcytic anemias associated with generalized iron overload. Moreover, mice that are homozygous for atransferrinemia die shortly after birth, unless transfused with erythrocytes or administered Tf (50), indicating that non-Tf iron sources cannot be used for hemoglobin synthesis. Third, erythrocytes contain about 45,000-fold more heme iron (20 mmol/L) than nonheme iron (440 nmol/L; ref. 51). The fact that all iron for hemoglobin synthesis comes from Tf and that this delivery system operates so efficiently, leaving mature erythrocytes with negligible amounts of nonheme iron, suggests that the iron transport machinery in erythroid cells is an integral part of the heme biosynthesis pathway. It seems reasonable to propose that the evolutionary forces that led to the development of highly hemoglobinized erythrocytes also dramatically affected numerous aspects of iron metabolism in developing erythroid cells, making them unique in this regard.

III. OVERVIEW OF CELLULAR IRON METABOLISM

Iron, in both its heme and nonheme forms, is present and exerts its function in every cell in the body and most cells, except for highly differentiated cells such as erythrocytes, leukocytes, keratinocytes, etc., have the capacity to acquire iron. As already described, hemoglobin-synthesizing cells are the major consumers of Tf-borne iron and, after their development into erythrocytes, they contain up to 70% of total body iron. Hence, to fully comprehend the peculiar regulation of iron metabolism in hemoglobin-synthesizing cells, its unique aspects have to be compared with those encountered in nonerythroid cells. Obviously, some aspects of iron metabolism in erythroid and nonerythroid cells are very similar or identical, but some are very different. This and the following sections will attempt to clarify these issues.

“Traditional” proteins involved in iron metabolism include Tf, TfR, and ferritin, but a remarkable flurry of activity in the past several years has identified a large number of novel genes whose products emerge as important players in iron metabolism (Table 1). Both the “classical” and novel proteins are covered extensively in other chapters, and in the following text I shall focus on the role these proteins may or may not play in erythropoiesis. One obvious aspect of erythroid-cell iron metabolism needs to be stressed at the beginning: iron transport by these cells is unilateral and, therefore, proteins likely to be involved in iron release from the cells, such as ferroportin1, ceruloplasmin, and hephaestin (see Table 1), presumably do not operate in erythroid cells. Similarly, the protein product of *HFE*, whose mutation is responsible for hereditary hemochromatosis, is unlikely to play any role in erythroid cells, since it does not seem to be expressed in them (76,77).

With some notable exceptions (e.g., macrophages, see above), physiologically, virtually all the cells in the organism take up iron from Tf. Iron uptake from Tf is reasonably well understood and, highly likely, the basic molecular mechanisms of iron acquisition via Tf-TfR pathway are similar in both erythroid and nonerythroid cells. The current view on iron acquisition via TfR-mediated endocytosis is depicted schematically in Fig. 2 (reviewed in Refs. 23 and 51). Until recently, the mechanism of iron transport across the endosomal membrane was elusive, but in 1997 two

Table 1 Overview of Proteins Involved in Iron Metabolism

Protein	Function	Role in erythroid cells	References
Tf ^a	Fe(III) carrier in plasma	Yes	51,52
TfR	Membrane receptor for Fe ₂ -Tf	Yes	53
TfR2	As “classical” TfR (?); different tissue distribution	Unknown	54,55
HFE	Unknown; binds TfR; restricted expression (enterocytes, macrophages)	No	56,57
Huntingtin	Trafficking of TfR	Unknown	57a
Ferritin (H and L)	Cellular Fe storage	Yes	51,58
Mitochondrial ferritin	Protection of mitochondria against Fe toxicity (?)	Yes	58a
IRP (1 and 2)	Fe “sensors”; binds to IREs	Yes	51,59–61
Nramp2/DCT1/DMT1	Membrane transporter for Fe ²⁺ (endosomes, enterocytes)	Yes	62–65
Duodenal cytochrome b (Dcytb)	Ferric reductase (provides Fe ²⁺ for DMT1 in duodenum)	Unknown	66
Ferroportin 1/Ireg1/MTP1	Fe export from cells	No	41–43
Ceruloplasmin (Cp)	Regulation of Fe export from somatic cells	No	67
Hephaestin	Regulation of Fe export from enterocytes (membrane-bound Cp homolog)	No	47
Sideroflexin 1	Mitochondrial transport function related to Fe metabolism	Yes	67a
ABC7	Nonheme Fe export from mitochondria (?)	Unlikely	68
Frataxin	Control of Fe export from mitochondria (?)	Unlikely	69,70
ABC-me	Mitochondrial transport function related to heme synthesis	Yes	71
ALA-S2/eALA-S	First enzyme of heme synthesis; erythroid-specific (translational induction by Fe)	Yes	23,24,72
Ferrochelatase	Last enzyme of heme synthesis; Fe ²⁺ insertion into protoporphyrin IX	Yes	23,73
Heme oxygenase 1	Recycling of Hb Fe	Indirect	74

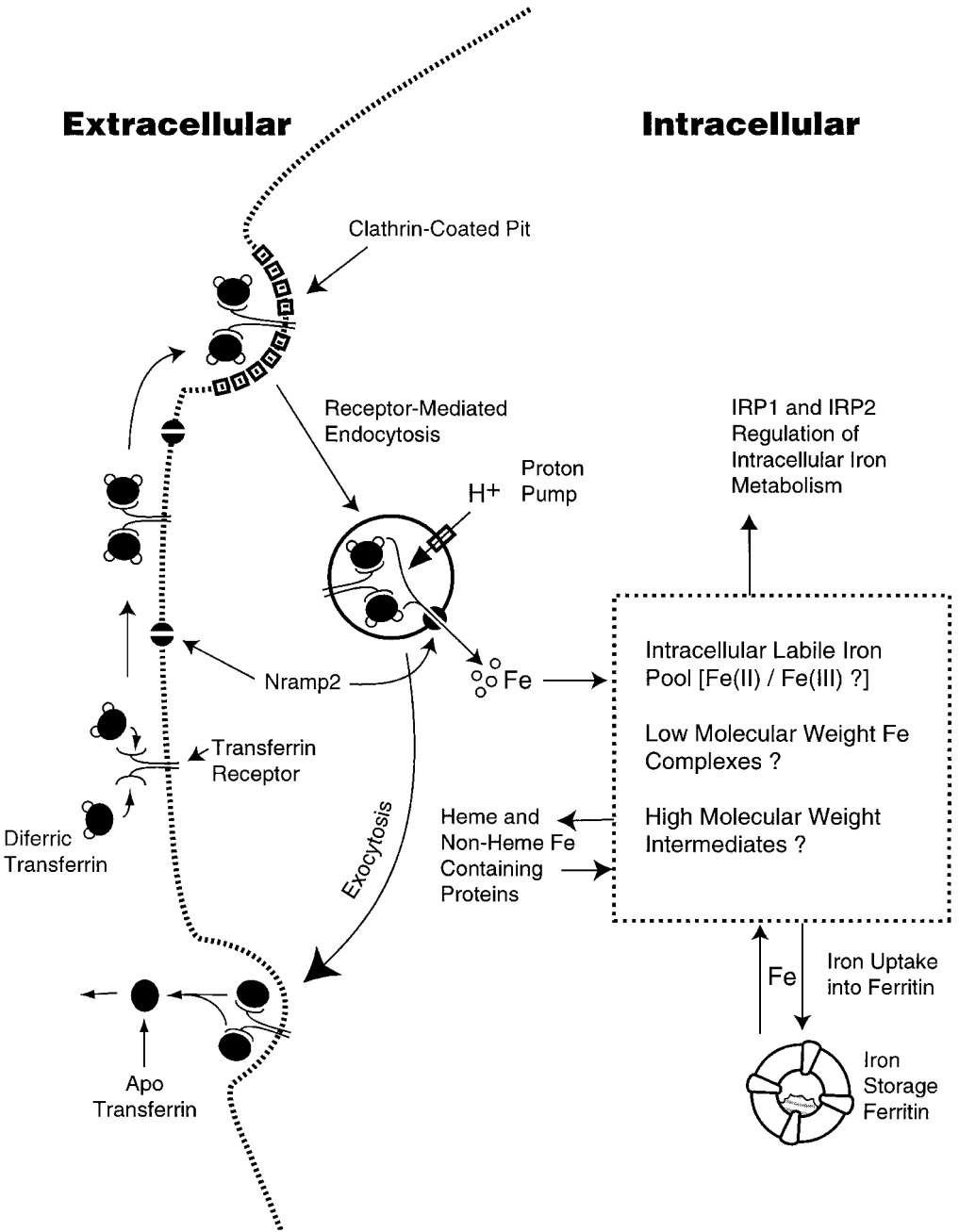
^aLactoferrin (75) and melanoTf (51) are other members of the “Tf family”; they do not seem to play any role in erythroid cell Fe metabolism.

groups identified a compelling candidate for an endosomal iron transporter (62,63). The transporter Nramp2 (also known as DCT1, divalent cation transporter 1, ref. 63, or DMT1, divalent metal transporter), is encoded by a gene that belongs to the *Nramp* (“*Natural resistance associated macrophage protein*”) family of genes identified by Gros et al. (78). Mutation of *Nramp2* causes decreased iron uptake by erythroid cells (and possibly other cells) in mice with microcytic anemia (*mk/mk*) (62), and in anemic Belgrade (*b/b*) rats (64). Importantly, Nramp2/DMT1/DCT1 is also involved in the dietary absorption of inorganic iron (see Chapter 23). Since the substrate for Nramp2/DCT1/DMT1 is ferrous iron (63), reduction of Fe(III) must occur in endosomes, but nothing is known about the mechanism of this process. McKie et al. (66) recently isolated a cDNA which encoded a plasma membrane di-heme protein in mouse duodenal membrane that exhibited ferric reductase activity. This protein belongs to the cytochrome b561 family of plasma membrane reductases, and it seems important to examine whether this or a similar b-type cytochrome is involved in Fe(III) reduction within endosomes. Following its escape from endosomes, iron is then transported to intracellular sites of use and/or storage in ferritin, but this aspect of iron metabolism, including the nature of the elusive intermediary pool of iron and its cellular trafficking, remains enigmatic. Only in erythroid cells does some evidence exist for a specific targeting of iron toward mitochondria (23) that are sites of heme production by ferrochelatase, the enzyme which inserts iron into protoporphyrin IX (see below).

The above conclusion is based on the observation that inhibition of heme synthesis in erythroid cells leads to mitochondrial iron accumulation (also see below). This phenomenon may, perhaps, be linked to another erythroid-specific control in which “uncommitted” heme inhibits iron acquisition from Tf (79–86) and, consequently, heme synthesis (23,87). Unfortunately, it is still unresolved whether heme inhibits Tf endocytosis (83,84) or iron release from Tf (85). Interestingly, heme does not inhibit iron uptake by reticulocytes from the Belgrade rat (82) and, hence, it would be of interest to examine whether heme affects Nramp2 function.

Although the chemical nature of the labile iron pool is unknown, sensitive control mechanisms exist that monitor iron levels in this pool and prevent its expansion, while still making the metal available for iron-dependent proteins and enzymes. In general, enlargement of the intracellular transit iron pool leads to a stimulation of ferritin synthesis and to a decrease in the expression of TfRs and the opposite scenario develops when this pool is depleted of iron. Interestingly, a single genetic regulation system is responsible for these changes in expression of structurally unrelated proteins, ferritin and TfR (reviewed in Refs. 23, 51, and 59–61). Pivotal players in this regulation are iron regulatory proteins (IRP1 and IRP2) which “sense” iron levels in the labile pool. IRPs control the synthesis of TfR and ferritin by binding to iron-responsive elements (IREs) that are located in the 3'-UTR and the 5'-UTR of their respective mRNAs. When cellular iron is scarce, IRPs bind to the IREs and this association blocks the translation of ferritin mRNA and stabilizes TfR mRNA. The expansion of the labile iron pool inactivates IRP1 binding to the IREs and leads to a degradation of IRP2, resulting in an efficient translation of ferritin and rapid degradation of TfR mRNA (for details, see Chapter 9).

The brilliance and elegance of the IRE/IRP regulatory system is seductively powerful, and numerous recent reviews seem to suggest that the IRE/IRP-dependent mechanism is involved in the coordinated regulation of iron uptake and storage by



all cells. However, some specialized cells and tissues have specific requirements for iron and appear to display distinct regulation of its uptake and, possibly, intracellular trafficking. In at least some instances, cells evolved mechanisms that can override some aspects of the IRE/IRP control system, and one notable example of this is the erythroid cell (see Sec. V).

IV. EXPERIMENTAL SYSTEMS TO STUDY ERYTHROID IRON METABOLISM

A. Reticulocytes

Ehrlich was probably the first investigator to describe reticulocytes, in 1881, but only the advent of isotopes, together with pivotal experiments of several groups in the late 1940s and 1950s made them an indispensable tool for studying hemoglobin synthesis and iron metabolism. Using ^{15}N -glycine, Shemin and Rittenberg (88) were the first to demonstrate heme synthesis in reticulocytes, and the uptake of Tf-bound iron by reticulocytes was first reported by Walsh et al. (89). In 1959 Jandl and co-workers (90) showed that treatment of reticulocytes with trypsin abolished iron uptake from Tf and inferred the existence of membrane receptors for Tf. The advantage of reticulocytes, which have been widely used ever since, is that they are the only system of pure erythroid cells available and they are easily obtained from the peripheral blood of anemic individuals. As already pointed out, reticulocytes do not contain DNA but still contain mitochondria, ribosomes, and mRNA (7). Hence, they can only be used to investigate the posttranscriptional aspects of heme synthesis and iron transport. Nevertheless, reticulocytes, in which over 90% of the iron taken up from Tf is used for heme synthesis (91–93), are extremely valuable for investigating mechanisms and controls operating in fully induced hemoglobin-synthesizing cells.

B. Erythroid Cell Lines

Murine erythroleukemia (MEL) cells are virus-transformed erythroid cells blocked in a relatively early stage of differentiation, and were derived from mice infected

Figure 2 Schematic representation of iron uptake from Tf via TfR-mediated endocytosis in mammalian cells. Extracellular $\text{Fe}_2\text{-Tf}$ is bound by the membrane-bound TfR and internalized via receptor-mediated endocytosis into an endosome. Iron is released from Tf by a decrease in pH and is then transported through the membrane by Nramp2/DCT1/DMT1. Physiologically, all iron in the circulation is Tf-bound and, therefore, Nramp2 expressed at the plasma membrane of erythroid and perhaps other cells has no substrate. Obviously, Nramp2 can assume its function of Fe^{2+} transporter only following its recruitment into endosomes where it co-localizes with TfR. Since reticulocytes acquire Fe^{2+} at rates that are much higher than those of iron uptake from Tf (Zhang A-S, Canonne-Hergeaux F, Gros P, Ponka P, unpublished results), Nramp2 is not a limiting factor in iron uptake via a Tf-dependent pathway in these cells. Once the iron has passed through the membrane, it then enters a very poorly characterized compartment known as the intracellular labile iron pool. Apo-Tf remains bound to the TfR and is then released by exocytosis. Iron that enters the cell can be used for metabolic functioning or can be stored in ferritin. It is thought that iron in the intracellular Fe pool modulates the activity of iron regulatory proteins 1 and 2 (IRP1 and IRP2). (Adapted from Ref. 51 and used with permission.)

with the Friend virus complex (94). Friend and her co-workers (95) successfully established a number of cell lines from the spleens of infected mice, which when grown in culture display a low level of erythroid differentiation ($\leq 1\%$), the extent of which can be enormously enhanced by dimethylsulfoxide (96) or numerous other chemical inducers (97). MEL cell differentiation is characterized by (a) an increase in the enzymes of the heme biosynthetic pathway (reviewed in Ref. 23), (b) an increase in TfR expression and iron uptake (98–101), and (c) an increase in globin mRNA (25), all of which lead to the accumulation of large amounts of hemoglobin. This differentiation process, which is accompanied by the onset of terminal cell division (i.e., the loss of capacity for proliferation), in many ways parallels that of normal erythroid development and, therefore, provides a model system to investigate transcriptional aspects of iron transport and heme synthesis during terminal erythroid differentiation.

However, there are drawbacks in the use of MEL cells as a model of normal erythroid differentiation. First, MEL cells are insensitive to the physiological inducer of erythroid differentiation, Epo (102). Second, since MEL cells are transformed cells, they have high numbers of TfR and seem to contain higher than average levels of ferritin (103). Therefore, the basal level of iron transport, and the amount of iron stored in uninduced MEL cells, is considerably higher than what would be found in the normal physiological equivalent, the proerythroblast.

Koury et al. (104) developed a procedure to procure a large number of developmentally synchronized, relatively pure erythroid cells from the spleens of mice infected with the anemia strain of Friend virus (FVA cells). Unlike the MEL cells, FVA cells are responsive to Epo, which induces the synthesis of hemoglobin, red cell-specific membrane proteins (104–106), and TfR (107). FVA cells are highly useful for investigating erythroid-specific aspects of iron metabolism, but working with them requires rather cumbersome cell separation by centrifugal elutriation.

Busfield and Klinken (108) developed an erythroid cell line (J2E) that differentiates in response to Epo and that was recently exploited to investigate some aspects of iron metabolism (109). However, Epo induction of J2E cells is not associated with a conspicuous increase in hemoglobin levels in these cells (109).

C. A Two-Phase Liquid Culture for Growing Human Erythroid Cells

More recently, Fibach et al. (110) described a liquid suspension culture that supports the growth and maturation of human erythroid progenitors. This procedure consists of two phases. In the first phase, peripheral blood mononuclear cells, which contain erythroid progenitors, are cultured for 1 week in the presence of a combination of growth factors, but in the absence of Epo. During this phase, early erythroid-committed progenitors (BFU-E) proliferate and differentiate into CFU-E-like progenitors. In the second phase, Epo is included in the medium and the CFU-E-like progenitors continue to proliferate and mature into orthochromatic erythroblasts and then enucleated erythrocytes. This system was used to examine various aspects of iron metabolism (111,112) and appears to be very useful for examining gene expression in erythroid precursors following their exposure to Epo (113,114). However, the procedure is somewhat laborious, and the development of erythroid cells during the second phase takes much longer than in vivo (10–15 days versus 4–5 days).

D. K562 Cells

K562 cells, which are very popular for the study of iron metabolism, are sometimes referred to as a human equivalent of MEL cells. However, they are not an appropriate model of normal erythroid differentiation. Although K562 cells are inducible for hemoglobin synthesis by hemin (115), Epo is unable to induce their differentiation (116). Moreover, K562 cells are ill-defined cells originating from a patient with chronic myelogenous leukemia (117) that synthesize only embryonic or fetal types of hemoglobin upon heme treatment (118). Obviously, no meaningful conclusion regarding erythroid-specific regulation of TfR expression can be made from studies using K562 cells treated with heme, which is known to dramatically downregulate TfR mRNA levels (119) by increasing intracellular iron concentrations.

V. IRON METABOLISM AND HEME SYNTHESIS IN ERYTHROID CELLS

Erythroid cells have by far the greatest need for iron, which is used for hemoglobin synthesis with remarkable efficiency and speed (23). On a per-cell basis the rate of heme synthesis in the immature erythroid cells is at least an order of magnitude higher than in the liver, the second highest heme producer in the organism. Such an exceptionally high capacity of immature erythroid cells to synthesize heme is primarily a result of the unique control of iron metabolism as well as the distinct enzyme of heme biosynthesis, 5-aminolevulinic acid synthase (ALA-S). Because of such an intimate link between iron metabolism and heme synthesis, an overview of this process has to be included in this review.

A. Heme Synthesis

In erythroid cells heme is synthesized by enzymatic mechanisms identical to those occurring in all other cells in the organism (Fig. 3). It is well established that heme biosynthesis involves eight enzymes, four of which are cytoplasmic and the rest mitochondrial. The first step occurs in the mitochondria and involves the condensation of succinyl CoA and glycine to form 5-aminolevulinic acid (ALA) catalyzed by ALA-S. The next four biosynthetic steps take place in the cytosol. ALA dehydratase (ALA-D) converts two molecules of ALA to a monopyrrole porphobilinogen (PBG). Two subsequent enzymatic steps convert 4 molecules of PBG into the cyclic tetrapyrrole uroporphyrinogen III, which is then decarboxylated to form coproporphyrinogen III. The final three steps of the biosynthetic pathway, including the insertion of Fe(II) into protoporphyrin IX by ferrochelatase, occur in the mitochondria.

All mammalian heme pathway enzymes have been cloned, and analysis of the genes and their corresponding mRNAs and protein products has revealed several distinct features of some of these enzymes in erythroid cells (reviewed in Refs. 23 and 24). There are two different genes for the first pathway enzyme, ALA-S. One of these is expressed ubiquitously (*ALA-S1*, or housekeeping *ALA-S*) and is encoded on chromosome 3 (120), while the expression of the other is specific to erythroid cells (*ALA-S2*, or erythroid *ALA-S*) and is encoded on the X chromosome (121). These two genes encode the ubiquitous and erythroid-specific mRNAs for ALA-S and, consequently, two corresponding isoforms of the enzyme. No tissue-specific isozyme is known for ALA-D, but there are subtle differences in 5'-UTRs in "house-

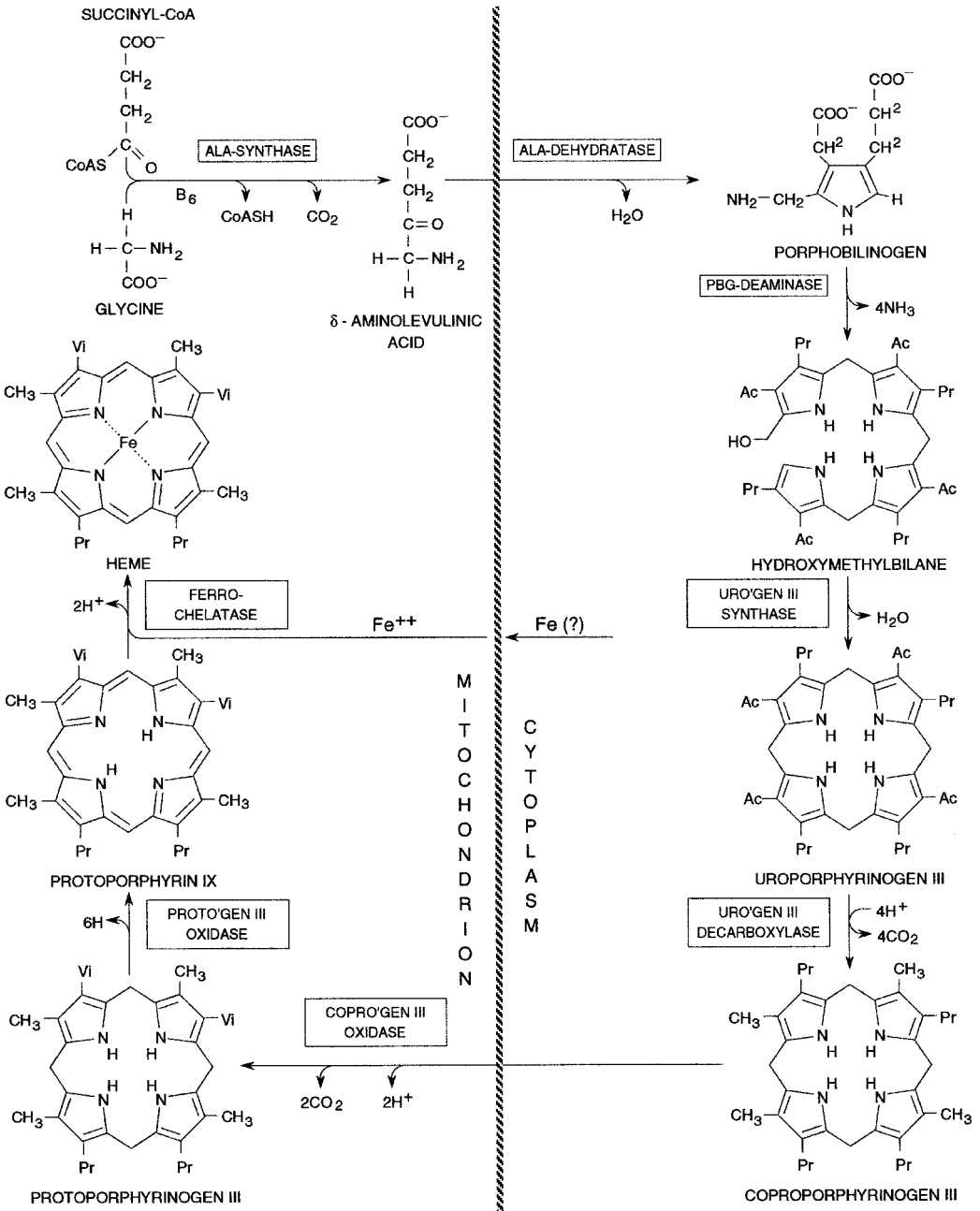


Figure 3 The pathway of heme biosynthesis. *B₆*, pyridoxal-5'-phosphate; URO'GEN, uroporphyrinogen; COPRO'GEN, coproporphyrinogen; PROTO'GEN, protoporphyrinogen; Ac, acetate; Pr, propionate; Vi, vinyl. (Adapted and reprinted with permission from DF Bishop and RJ Desnick. Assays of the heme biosynthetic enzymes (Preface). Enzyme 28:91-93, 1982.)

keeping” and erythroid ALA-D mRNAs (122). PBG deaminase (PBG-D) exists in two isoforms differing in their N terminus, one being present in all cells while the other is expressed only in erythroid cells. However, these isoforms arise from differential splicing of a single gene and from two mRNAs which differ solely in their 5' ends (123). There is no evidence that the ubiquitous and the erythroid enzymes would be different in the rest of the pathway. However, variations in mRNAs, caused by the alternative use of the two polyadenylation signals, have been reported for ferrochelatase (124). Interestingly, the preferential utilization of the upstream polyadenylation signal appears to be an erythroid-specific characteristic of ferrochelatase gene expression (125). Importantly, murine (126) and human (127) ferrochelatase were shown to contain a [2Fe–2D] cluster which seems to be essential for enzyme activity or plays either a redox or regulatory role. Recently, Taketani et al. (127a) demonstrated that the iron–sulfur cluster in mammalian ferrochelatase is involved in the regulation of heme biosynthesis at the terminal step. These authors found that in desferrioxamine-treated K562 cells the amount of ferrochelatase decreased with a concomitant decrease in enzyme activity; addition of iron to desferrioxamine-containing cultures resulted in restoration of ferrochelatase activity.

ALA-S plays an important regulatory role in heme synthesis in both nonerythroid and erythroid cells. A detailed discussion of the control of heme synthesis in nonerythroid cells is beyond the scope of this review, but it is important to point out that ALA-S1 is the rate-limiting step in the nonerythroid heme pathway (for details, see Refs. 23 and 24). In contrast to *ALA-S1*, the promoter of the human erythroid-specific *ALA-S2* gene contains several erythroid-specific cis-acting elements, including GATA-1, the CACCC box, and the NF-E2-binding sites (23,72). Hence, it is highly likely that erythroid-specific transcription factors control and induce *ALA-S2* transcription in concert with the induction of other erythroid-specific genes.

A crucial link between *ALA-S2* and iron was provided by the discovery of an IRE in the 5'-UTR of *ALA-S2* mRNA (128–130). As expected, iron has consequently been shown to translationally induce the expression of *ALA-S2* (131) and to stimulate ALA production in erythroid cells (132). There are several important implications for this finding. First, since the translation of *ALA-S2* mRNA depends on the availability of iron, in erythroid cells it is iron acquisition rather than ALA production which is the rate-limiting step in heme synthesis. In fact, a step in iron transport, localized between the TfR and ferrochelatase, limits and thus controls the rate of heme synthesis in erythroid cells. This conclusion is based on experiments with lipophilic iron-chelates that, when added in relatively high concentrations, can stimulate heme synthesis in erythroid cells above the level seen in the presence of saturating concentrations of Fe₂-Tf (101,133,134). Second, this regulatory mechanism guarantees a coupling of levels of protoporphyrin IX (which is toxic) with iron availability. Third, the existence of an IRE in *ALA-S2* mRNA indicates that the IRE/IRP mechanism does play an important role in erythroid cells. However, it should be immediately obvious that exactly those IRE/IRP-dependent mechanisms that drive *ALA-S2* synthesis would downregulate TfR mRNA. Hence, since TfR mRNA levels are well known to increase during erythroid differentiation, this increase is highly likely independent of the IRE/IRP mechanism. This important issue will be discussed further in the following subsection.

B. Transferrin Receptors

TfRs are discussed extensively in this volume (see Chapter 3) and elsewhere (53), and here I shall focus on TfR with regard to their relevance to erythroid differentiation.

With the exception of mature erythrocytes and some other terminally differentiated cells, TfRs are probably expressed on all cells but their levels vary greatly, developing erythroid cells showing very high densities of TfR. As already pointed out, erythroid heme synthesis is critically dependent on iron uptake from Tf that is mediated by high levels of TfR in erythroid cells. This is not only exemplified by numerous in-vitro and in-vivo models demonstrating upregulation of TfR levels during erythroid differentiation (109,134–137), but also by recent studies exploiting TfR knockout mice (138). Transgenic animals with no functional receptors die in utero, and mice containing only one functional copy of the TfR develop hypochromic microcytic anemia (138). This finding strongly suggests that normal hemoglobini- zation of erythroblasts on the one hand requires “full” transcriptional activation of the TfR and, on the other hand, is limited by TfR levels. Clearly, posttranscriptional mechanisms, involving the IRE/IRP system, are unable to maintain the TfR at adequate levels if only one allele contains a functional receptor gene. Recently, a homolog of TfR, designated TfR2, has been identified and shown to mediate iron uptake from Tf (54). It is interesting that TfR2 mRNA does not contain IREs and hence, as expected, its expression is not negatively regulated by iron. TfR2 mRNA is expressed predominantly in the liver, and high levels of this transcript were also found in K562 cells, which, as explained above, cannot be regarded as “proper” erythroid cells. It will be important to examine whether TfR2 is expressed in hemoglobin-synthesizing cells. Disruption of mouse TfR is lethal in utero (138), indicating that TfR2 is unable to compensate the loss of “classical” TfR and, thus, the “classical” TfR is indispensable for hemoglobini- zation.

The early erythroid progenitor cell has only a few TfR, the levels of which increase significantly in CFU-E-type progenitors (139,140). Following the induction of erythroid differentiation by Epo, TfR expression gradually increases, reaching a maximum of about 800,000 molecules per polychromatophilic erythroblast, followed by a slight decrease with further maturation (141). Similarly, an increase in TfR and iron uptake is observed in response to treatment of MEL cells with chemical inducers, such as dimethylsulfoxide (98–101,136). There are still very high numbers of receptors on orthochromatic erythroblasts and reticulocytes (100,000–500,000 per cell, probably depending on their maturity), neither of which is capable of cell division. During the maturation of reticulocytes to erythrocytes, the cells lose all activities of the components of the hemoglobin-synthesizing system (7), including TfR. It has already been mentioned that TfR may be released from reticulocytes by “shedding” (15–17), but it is not known whether this is the only mechanism involved in their disappearance.

1. Transcriptional Regulation of TfR Expression During Erythroid Differentiation

Although erythroid cells are probably the most widely used model to study various aspects of iron metabolism, the mechanism of the induction of TfR during erythroid differentiation is not fully understood. As discussed above, iron modulates TfR ex-

pression in nonerythroid cells in a negative-feedback manner at the level of mRNA stabilization that affects steady-state TfR mRNA levels. However, in hemoglobin-synthesizing cells, TfR mRNA levels are only slightly affected by high iron concentrations (136), suggesting that TfR expression is regulated differently in erythroid and nonerythroid cells. This relative insensitivity of TfR mRNA to the destabilizing effects of iron may be due to the high rate of TfR gene transcription (109,135,136). Recently, the Ets-1 transcription factor was shown to stimulate the TfR transcription in avian immature erythroid cells, via an Ets-binding site in the promoter region (137). Ets-1 is the cellular homolog of c-Ets, the causative component of avian erythroblastosis virus E26 (142), and may be involved in controlling the transcription of several genes expressed in erythroid cells.

More recently, our group characterized the TfR promoter activities in MEL cells (143). We demonstrated that the TfR promoter activities increased six- to eight-fold in MEL cells induced to differentiate into hemoglobin-synthesizing cells. This was mediated by a minimal region within -118 to $+14$. Mutation of either an EBS or an AP-1-like motif within this region, but not disruption of the adjacent GC rich/SP-1 sequence, inhibited the inducible promoter activities. Our data suggest that the linked EBS and AP-1-like site are critical for the transcriptional regulation of TfR expression during MEL cell differentiation. However, it is also possible that some unidentified regulatory elements may also be responsible for coordinating the expression of TfR with overall hemoglobin synthesis.

When discussing the transcriptional control of TfR expression, it is pertinent to mention that our group recently identified a functional HRE in the TfR gene which contains a binding site for HIF-1 and that is involved in transcriptional upregulation of TfR in response to hypoxia (144). HIF-1 is well known to transcriptionally induce not only the Epo gene, as already mentioned, but also a wide range of genes encoding proteins that represent an important physiological adaptation to hypoxia (18,19). There is no doubt that Epo-mediated mechanisms directly stimulate TfR expression (23) and, hence, the effect of hypoxia on TfR expression can be only partial. However, it cannot be ruled out that both Epo and hypoxia can cooperate to drive maximal expression of TfR under severe hypoxic conditions. The presence of the HIF-1-binding site in the TfR was independently reported by Cairo and his co-workers (145).

2. The IRE/IRP System Is Not Involved in TfR Upregulation in Erythroid Cells

The aforementioned experiments strongly suggest that TfR is induced transcriptionally during erythroid differentiation. Moreover, levels of active IRP1 remain virtually unchanged when MEL cells are induced to synthesize hemoglobin, indicating that IRP1 probably does not play a role in the increase of TfR mRNA during erythroid differentiation (136). However, a recent report (146) has suggested that Epo enhances the binding affinity of IRP1 in K562 cells and MEL cells, associated with an increase in TfR mRNA levels. These conflicting reports, together with the well-known fact that neither K562 nor MEL cells differentiate upon exposure to Epo (see above), led our group (147) to reexamine the mechanism by which TfR increase in these as well as in Epo-sensitive cells. As expected, in our experiments Epo failed to induce erythroid differentiation in either K562 or MEL cells. Moreover, Epo did not activate IRP1, increase IRP2 levels, or enhance TfR mRNA levels in either K562 or MEL

cells. We also studied FVA cells (see above) that undergo terminal differentiation when cultured with Epo. We found that Epo-induced differentiation of FVA cells was associated with a marked progressive increase in TfR mRNA that occurred without changes in binding activity of IRPs. Moreover, Epo treatment of FVA cells caused a significant increase in transcription of TfR gene (147). These results provide strong evidence that the induction of TfR expression in hemoglobin-synthesizing cells is independent of the IRE/IRP regulatory system and is due mainly to changes in transcription rates.

3. Heme Enhances TfR Expression in Erythroid Cells

In nonerythroid cells, heme decreases TfR mRNA levels (119) via the IRE/IRP system (23). However, IRP-binding activity is not regulated by heme itself, but rather by iron released from heme due to the action of HO (148). Somewhat surprisingly, in erythroid cells, heme appears to be needed for maintaining a high rate of TfR synthesis. Cox et al. (149) documented that inhibition of heme synthesis by succinylacetone (SA, an inhibitor of ALA-D, the second enzyme of heme synthesis) depresses TfR synthesis in reticulocytes, and that this can be restored by the addition of heme. Similarly, Johnstone and co-workers (150) found that heme was essential for optimal expression of TfR in chicken erythroid cells. On the other hand, heme synthesis inhibitors were shown to strongly inhibit TfR expression at both the mRNA (136,151,152) and protein (136) levels in nucleated erythroid cells, but had little effect on the expression of the TfR in cells that did not synthesize hemoglobin (136).

More recently, our group demonstrated that treatment of MEL cells with heme precursors ALA and protoporphyrin IX increased TfR mRNA levels and that this increase was accompanied by an enhanced uptake of Tf by the cells (153). In addition, we showed that succinylacetone (SA) and N-methyl protoporphyrin (an inhibitor of ferrochelatase) prevented, respectively, the ALA-mediated or protoporphyrin IX-mediated enhancement of TfR mRNA. Hence, the enhancing effect on TfR mRNA required the conversion of ALA and protoporphyrin IX into heme. Interestingly, control and ALA-treated MEL cells contained identical levels of IRP1 (153), indicating that endogenous heme (derived from added ALA) stimulated TfR expression by an IRE/IRP1-independent mechanism. The mechanism of heme action on TfR expression in erythroid cells remains to be determined, but it may be related to a general dependence of the erythroid differentiation program on the availability of heme.

C. Iron Is Targeted into Mitochondria in Erythroid Cells

As already discussed (see p. 653), it is generally believed that, after crossing endosomal membranes, iron enters the "labile intermediate pool" from which it is available for mitochondrial heme synthesis, for its insertion into iron-dependent proteins and enzymes, and for storage in ferritin. It has been proposed that iron in this pool may be complexed to citrate, sugars, some amino acids, and nucleotides (154), but the real chemical nature of this metabolically and kinetically active pool is ill defined. The only abiding certainty is that this iron can be intercepted by strong chelators. However, this does not necessarily mean that the iron is complexed to low-molecular-weight ligands; it may equally well be bound to yet-unidentified membrane-associated carriers.

The role of ferritin as a mediator involved in intracellular translocation of iron for the synthesis of heme is controversial. Although ferritin has been postulated to act as an intermediate for heme synthesis in erythroid cells, several studies failed to show that ^{59}Fe from ^{59}Fe -ferritin could be incorporated into hemoglobin (reviewed in Refs. 51 and 155). When heme synthesis is inhibited in erythroid cells incubated with ^{59}Fe -Tf, very little (93) or no (156) ^{59}Fe accumulates in ferritin. More importantly, when heme synthesis is restored in these cells, no ^{59}Fe from ^{59}Fe -ferritin can be used for heme synthesis (93). Furthermore, MEL cells overexpressing H-ferritin subunits show significantly inhibited synthesis of heme (157), suggesting that ferritin in excess traps intracellular iron and restricts its availability for heme synthesis.

As already pointed out, the delivery of Tf-borne iron to hemoglobin occurs with extremely high efficiency, since after only a 3-min incubation of reticulocytes with ^{59}Fe -Tf, about 80% of cell-associated ^{59}Fe can be found in heme (93). This can be explained, at least in part, by a specific targeting of iron toward mitochondria in hemoglobin-synthesizing cells. In erythroid cells, the vast majority of iron released from endosomes must cross both the outer and the inner mitochondrial membranes to reach ferrochelatase. Importantly, in hemoglobin-synthesizing cells, iron acquired from Tf continues to flow into mitochondria, even when the synthesis of protoporphyrin IX is markedly suppressed [e.g., by isonicotinic acid hydrazide (INH) or SA] (92,93,156,158,159). The chemical nature of the iron which accumulates in mitochondria is unknown, but it is possible that iron in excess may be stored in recently identified mitochondrial ferritin (58a). A certain proportion of this nonheme iron accumulated in mitochondria is in a form readily available for heme synthesis when protoporphyrin IX formation is restored (92,93,156,158). Under these conditions, heme is quickly transported out of the mitochondria to combine with globin chains in the cytosol, suggesting that the majority of iron taken up by erythroid mitochondria can leave the organelle only after it is inserted into protoporphyrin IX. In contrast to erythroid cells, in nonerythroid cells iron in excess of metabolic needs ends up in cytosolic ferritin. The above observations strongly suggest that in erythroid cells some specific mechanisms and controls are involved in mitochondrial iron and heme metabolism.

Based on the facts that Tf-bound iron is extremely efficiently used for hemoglobin synthesis, that iron is targeted into erythroid mitochondria, and that virtually no cytoplasmic iron transport intermediate can be identified in reticulocytes, a new hypothesis of intracellular iron transport has been suggested (23). This model proposes that after iron is released from Tf in the endosome, it is passed directly from endosomal protein to mitochondrial protein until it reaches ferrochelatase in the mitochondrion. Such a transfer of iron between proteins could be mediated by the direct interaction of the endosome with the mitochondrion (Fig. 4).

Recently, our group provided some evidence supporting this hypothesis (160). We specifically labeled reticulocyte endosomes with ^{59}Fe bound to Tf and followed its incorporation into heme. We found that the transfer of endosomal ^{59}Fe into heme was very rapid (minutes) and required an unrestricted supply of protoporphyrin. Both ferrous (dipyridyl) and ferric (salicylaldehyde isonicotinoyl hydrazone, SIH) iron chelators can intercept ^{59}Fe during its translocation from ^{59}Fe -endosomes to protoporphyrin IX when reticulocytes are incubated at 37°C. However, very little intracellular ^{59}Fe can be acquired by the chelators when they are added during the lysis (4°C) of ^{59}Fe -reticulocytes. In other words, at any given time during the transfer of

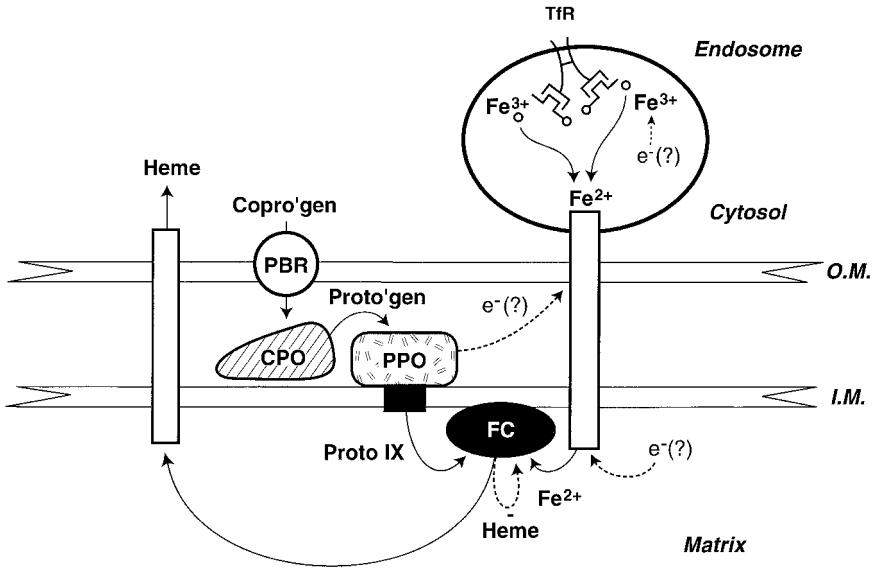


Figure 4 A model for the terminal mitochondria-associated steps in the heme biosynthesis pathway. Three terminal enzymes, coproporphyrinogen III oxidase (CPO), protoporphyrinogen III oxidase (PPO), and ferrochelatase (FC), are associated with the inner mitochondrial membrane. Coproporphyrinogen III (Copro'gen) uptake by mitochondria may be mediated by peripheral-type benzodiazepine receptors (PBR) (177). The ligand carrying iron toward mitochondria is unknown. It has been recently proposed that, in erythroid cells, there may be direct interaction of the endosome with the mitochondrion followed by the transfer of iron through membrane-bound transporters to ferrochelatase (“the kiss-and-run” hypothesis of cellular iron transfer) (23). Only ferrous iron (Fe^{2+}) can be used by ferrochelatase, but neither the site where iron reduction occurs nor the source of electrons (e^-) are known; it is tempting to speculate that only one reduction step, occurring in endosomes (see Fig. 2), is required for Fe^{2+} translocation from endosomes to ferrochelatase. This model proposes that an iron “channel” is involved in iron transport from endosomes toward ferrochelatase and that a specific transporter is involved in the exit of heme from mitochondria. O.M., outer mitochondrial membrane; I.M., inner mitochondrial membrane. (Adapted from Ref. 23 and used with permission.)

^{59}Fe from endosomes toward ferrochelatase, the vast majority of ^{59}Fe is bound to components that bind ^{59}Fe with a stronger affinity than dipyrindyl or SIH. Even more important, we found that myosin light-chain kinase inhibitor, wortmannin, as well as the calmodulin antagonist, W-7, caused significant inhibition of ^{59}Fe incorporation from ^{59}Fe -Tf-labeled endosomes into heme. Both agents are known to inhibit the microfilament motor, myosin, appearing to be involved in intracellular movement of endosomes. These results, together with confocal microscopy studies (using Tf and mitochondria labeled by distinct fluorescent markers), suggest that in erythroid cells a transient mitochondrion–endosome interaction may be involved in iron translocation to ferrochelatase (Fig. 4).

As pointed out above, the substrate for the endosomal transporter, Nramp2/DCT1/DMT1 is Fe^{2+} , the redox form of iron in which it is also translocated across the mitochondrial membrane toward ferrochelatase (161). These facts make the above

hypothesis quite attractive, since ferrous ions would bypass an oxygen-rich cytosol in hemoglobin-synthesizing cells. Recently, Scott and Eaton (162) showed that trace amounts of “free” iron in combination with cellular reducing equivalents oxidize hemoglobin. This report strongly suggests that a pool of free iron is capable of establishing a self-amplifying and self-propagating redox reaction with hemoglobin that can eventually lead to red cell destruction. Hence, the chaperone-like function of endosomes may be one of the mechanisms that keeps concentrations of reactive iron at extremely low levels. The intricate and highly organized structure of the intracellular matrix (163), together with the extremely rapid incorporation of iron into hemoglobin, argues against freely diffusible and potentially toxic cytosolic iron pool, and suggests a more tightly coordinated and efficient mechanism.

Mitochondrial iron accumulation in erythroid cells treated with heme synthesis inhibitors requires some additional discussion. This phenomenon has its in-vivo equivalent in a human disease, sideroblastic anemia. The hallmark of this anemia is the ring sideroblast, a pathological erythroid precursor containing excessive deposits of nonheme iron within mitochondria, which shows perinuclear distribution accounting for the ringed appearance (164). In some sideroblastic anemias caused genetically or following drug treatment, heme synthesis defects can clearly be identified. Classical examples are sideroblastic anemias caused by a defect in the *ALA-S2* gene or in patients treated by the antituberculosis drug INH, which inhibits ALA-S activity (164). Interestingly, Levi et al. (58a) recently demonstrated that erythroblasts of patients with defective *ALA-S2* contain high levels of mitochondrial ferritin that could not be detected in normal erythroblasts. However, it is rather surprising that no sideroblast formation is seen in either zebrafish erythroblasts with defective *ALA-S2* (165) or in hematopoietic cells of the *ALA-S2*-null mutant embryos (166). These observations suggest that erythroid cells derived from tissues of early phylogenetic or ontogenetic origin have a different mode of regulation of their intracellular iron metabolism.

Importantly, in some sideroblastic anemias, in particular the primary acquired ones, there is little evidence of inhibited protoporphyrin formation. Recently, a point mutation in mitochondrial DNA coding for one of the subunits of cytochrome c oxidase has been demonstrated in hematopoietic cells of a patient with primary acquired sideroblastic anemia (167). It has been suggested that defective cytochrome c oxidase is responsible for the reduced availability of ferrous iron for ferrochelatase, leading to Fe(III) accumulation in mitochondria.

Somewhat surprisingly, several families were reported in which a nonprogressive spinocerebellar syndrome (ataxia) and sideroblastic anemia segregated together in an X-linked recessive fashion (168). Recently, Allikmets et al. (169) demonstrated that a mutation in a gene encoding an ATP-binding cassette (ABC) transporter, known as *ABC7*, causes X-linked sideroblastic anemia and ataxia. The *ABC7* gene (68) is an ortholog of the yeast *ATM1* gene whose product localizes to the mitochondrial inner membrane. Importantly, yeast strains deficient for the *ATM1* gene have been shown to accumulate high levels of “free” iron in mitochondria (170). This, together with a recent report by Kispal et al. (171), suggests that the *Atm1p* transporter, and possibly its human counterpart, are involved in the export of mitochondrial nonheme iron. It is not immediately obvious how a defect in the nonheme iron export can cause sideroblastic phenotype, since iron seems to be able to leave erythroid mitochondria only after being inserted into protoporphyrin IX (for details,

see Ref. 23). Possibly, the ABC7 protein defect manifests itself in early erythroid progenitors, before significant heme biosynthesis is induced, and iron-laden mitochondria are carried onto hemoglobin-synthesizing erythroblasts.

Another important recent development is the identification (67a) of a novel gene, termed *sideroflexin 1* (*sfxn1*), whose mutation is responsible for the hematological and skeletal abnormalities of *flexed-tail* (*ff*) mice. These animals have hypochromic red blood cells with remnants of mitochondria containing deposits of nonheme iron. *Sfxn1* is localized in mitochondria and is predicted to have five transmembrane domains (67a). Hence, *sfxn1* may be a channel or carrier molecule, but its role in heme synthesis or iron metabolism has not yet been defined.

The unique nature of iron metabolism in the mitochondria of erythroid cells is further emphasized by the fact that mitochondria in nonerythroid cells do not accumulate nonheme iron even in severely iron-overloaded individuals. However, recent research has revealed that nonheme iron accumulates in mitochondria in cardiomyocytes of patients with Friedreich's ataxia (69,70; Massimo Pandolfo, personal communication), the most common of the hereditary ataxias. Friedreich's ataxia is caused by a deficiency of frataxin, a nuclear-encoded mitochondrial protein that seems to play a role in mitochondrial iron homeostasis (for details, see Chapter 11). Importantly, disruption of a gene in *Saccharomyces cerevisiae*, which is homologous with the human frataxin gene, leads to mitochondrial iron accumulation in the yeast (172,173). This seems to suggest that frataxin is somehow involved in the release of nonheme iron from mitochondria. However, since Friedreich's ataxia patients do not have mitochondrial iron loading in their erythroblasts, it is tempting to speculate that frataxin levels will decrease (which may be significant to keep mitochondrial Fe for heme synthesis) during erythroid differentiation.

VI. INTEGRATED VIEW: THE AVAILABILITY OF IRON CONTROLS HEMOGLOBINIZATION

Erythropoiesis is a remarkably complex process that comprises both differentiation of erythroid cells from hemopoietic progenitor cells and induction of hemoglobin in these cells. The synthesis of hemoglobin is accomplished by three independent but mutually well-coordinated pathways: globin synthesis, protoporphyrin IX synthesis, and iron acquisition and translocation that depends on the expression of TfR. During differentiation all three pathways are either transcriptionally induced de novo (globin) or transcriptionally increased (heme synthesis enzymes and TfR). Although not yet documented experimentally, it can be postulated that erythroid differentiation will also augment further but less defined steps in the erythroid pathway, including the endosomal (Nramp2) and mitochondrial iron-transporting systems. In addition, a change ("differentiation") in mitochondria can be predicted that allows a specific targeting of iron into this organelle, but currently it is impossible to foresee whether such an alteration is qualitative (induction of new proteins) or simply a quantitative one. Notwithstanding this, some changes in mitochondria during erythroid differentiation have already been defined. First, the induction of ALA-S2 is associated with a decrease in the "housekeeping" ALA-S1 (174). Second, the erythroid transcription factor GATA-1 has recently been shown to induce a novel mitochondrial ABC transporter termed ABC-me (71). ABC-me localizes to the inner mitochondrial membrane and is postulated to transport yet to be identified substrate(s) from the

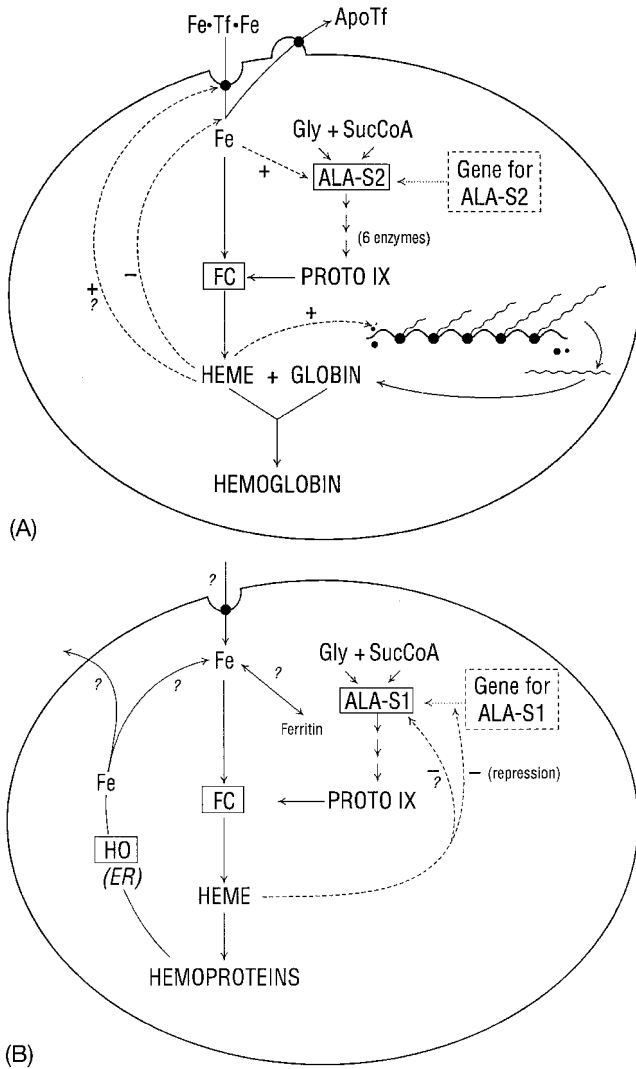


Figure 5 Distinct aspects of heme synthesis regulation in erythroid (A) and nonerythroid (B) cells. Differences in iron metabolism and in genes for ALA-S probably account for the differences in the rate of heme synthesis and its regulation in erythroid cells. In erythroid cells, heme inhibits cellular iron acquisition from Tf but does not inhibit either activity or the synthesis of ALA-S2. Because the 5'-UTR of ALA-S2 mRNA contains an IRE, the availability of iron controls ALA-S2 translation, the rate of ALA formation, and, consequently, the overall rate of heme synthesis in hemoglobin-synthesizing cells. Heme is also essential for globin translation and may also be involved in globin gene transcription. In contrast, in nonerythroid cells, the removal of iron from Tf is not regulated by intracellular heme and the ubiquitous ALA-S1 mRNA does not contain the IRE, so iron availability does not control the overall heme synthesis rate. Gly, glycine; PROTO IX, protoporphyrin IX; HO, heme oxygenase; FC, ferrochelatase; ER, endoplasmic reticulum. (Reprinted from Ref. 23 with permission.)

matrix into the intermembrane space. Importantly, ABC-me overexpression enhances hemoglobin synthesis in MEL cells. Hence, it seems likely that ABC-me mediates critical mitochondrial transport functions related to heme synthesis (71). Moreover, it can also be assumed that erythroid differentiation is associated with the induction of a heme transporter involved in the export of heme from the mitochondria to the cytosol. Furthermore, a cytosolic heme-binding protein may be needed to safely carry heme in the cytosol. Taketani et al. (175) recently purified a novel heme-binding protein (termed p22 HBP) and identified its cDNA. p22 HBP (both mRNA and protein) is induced during erythroid differentiation, and antisense oligonucleotides to p22 HBP decrease heme biosynthesis in induced MEL cells (175).

Hence, based on the experimental evidence and above discussions, it can be proposed that one aspect of erythroid differentiation involves an “iron metabolism switch” during which the erythroid-specific pathway and control mechanisms are turned on, leading to their prevalence in erythroblasts and eventually total predominance in reticulocytes.

Once all the machinery required for hemoglobin synthesis is induced, its formation is controlled by a series of exquisite mechanisms depicted in Fig. 5A. In contrast to nonerythroid cells (Fig. 5B), in erythroid cells heme does not inhibit either the activity or the synthesis of ALA-S, but does inhibit cellular iron acquisition from Tf (see above). This negative feedback is likely to explain the mechanism by which the availability of Tf iron limits the heme synthesis rate, and also clarifies why the system transporting iron to ferrochelatase operates so efficiently, leaving normally mature erythrocytes with negligible amounts of nonheme iron. Since the 5'-UTR of ALA-S2 mRNA contains the IRE, the availability of iron controls ALA-S2 translation, the rate of ALA formation, and, consequently, the overall rate of heme synthesis in hemoglobin-synthesizing cells. Moreover, a positive-feedback mechanism in which heme maintains a high rate of TfR synthesis (see Sec. V.B.3.) may be one of the mechanisms that keeps heme synthesis at “maximum levels.” Because the availability of Tf-bound iron limits erythroid heme synthesis (23), and because heme is required for globin mRNA translation (32), the overall hemoglobin synthesis rate appears to be controlled by the capacity of erythroid cells to acquire iron from Tf. Hence, it is tempting to speculate that erythroid cells with their high requirement for iron, whose biological availability is so limited, have evolved regulatory mechanisms in which iron controls hemoglobinization.

ACKNOWLEDGMENTS

This work was supported in part by the Canadian Institutes of Health Research. The author would like to acknowledge Dr. Kostas Pantopoulos and Dr. Joan Buss for their critical review of this manuscript and for many valuable suggestions. The author also thanks Ms. Sandy Fraiberg for excellent editorial assistance.

REFERENCES

1. Perutz MF. Molecular anatomy, physiology and pathology of hemoglobin. In: Stamatoyannopoulos G, Nienhuis AW, Leder P, Majerus PW, eds. *The Molecular Basis of Blood Diseases*. Philadelphia: Saunders, 1987:127–178.

2. Stampler JS, Jia L, Eu JP, McMahon TJ, Demchenko IT, Bonaventura J, Gernert K, Piantadosi CA. Blood flow regulation by S-nitrosohemoglobin in the physiological oxygen gradient. *Science* 1997; 276:2034–2037.
3. Ruud JT. Vertebrates without erythrocytes and blood pigment. *Nature* 1954; 173:848–859.
4. Cocca E, Ratnayake-Lecamwasam M, Parker SK, Camardella L, Ciaramella M, di Prisco G, Detrich HW 3rd. Genomic remnants of alpha-globin genes in the hemoglobinless antarctic icefishes. *Proc Natl Acad Sci USA* 1995; 92:1817–1821.
5. Williams DA. Stem cell model of hematopoiesis. In: Hoffman R, Benz EJ Jr, Shattil SJ, Furie B, Cohen HJ, Silberstein LE, McGlave P, eds. *Hematology: Basic Principles and Practice*, 3d ed. New York, London: Churchill Livingstone, 2000:126–138.
6. Papayannopoulou T, Abkowitz J, D'Andrea A. Biology of erythropoiesis, erythroid differentiation and maturation. In: Hoffman R, Benz EJ Jr, Shattil SJ, Furie B, Cohen HJ, Silberstein LE, McGlave P, eds. *Hematology: Basic Principles and Practice*, 3d ed. New York, London: Churchill Livingstone, 2000:202–219.
7. Rapoport SM. *The Reticulocyte*. Boca Raton, FL: CRC Press, 1986.
8. Rapoport SM, Schewe T. The maturational breakdown of mitochondria in reticulocytes. *Biochim Biophys Acta* 1986; 864:471–495.
9. Thiele BJ, Andree H, Hohne M, Rapoport SM. Lipoyxygenase mRNA in rabbit reticulocytes. Its isolation, characterization and translational repression. *Eur J Biochem* 1982; 129:133–141.
10. Fleming J, Thiele BJ, Chester J, O'Prey J, Janetzki S, Aitken A, Anton IA, Rapoport SM, Harrison PR. The complete sequence of the rabbit erythroid cell-specific 15-lipoyxygenase mRNA: Comparison of the predicted amino acid sequence of the erythrocyte lipoyxygenase with other lipoyxygenases. *Gene* 1989; 79:181–188.
11. Ostareck-Lederer A, Ostareck DH, Standart N, Thiele BJ. Translation of 15-lipoyxygenase mRNA is inhibited by a protein that binds to a repeated sequence in the 3' untranslated region. *EMBO J* 1994; 13:1476–1481.
12. Ostareck DH, Ostareck-Lederer A, Wilm M, Thiele BJ, Mann M, Hentze MW. mRNA silencing in erythroid differentiation: hnRNP K and hnRNP E1 regulate 15-lipoyxygenase translation from the 3' end. *Cell* 1997; 89:597–606.
13. Van Leyen K, Duvoisin RM, Engelhardt H, Wiedmann M. A function for lipoyxygenase in programmed organelle degradation. *Nature* 1998; 395:392–395.
14. Wefes I, Mastrandrea LD, Haldeman M, Koury ST, Tamburlin J, Pickart CM, Finley D. Induction of ubiquitin-conjugating enzymes during terminal erythroid differentiation. *Proc Natl Acad Sci USA* 1995; 92:4982–4986.
15. Pan BT, Johnstone RM. Fate of the transferrin receptor during maturation of sheep reticulocytes in vitro: Selective externalization of the receptor. *Cell* 1983; 33:967–978.
16. Johnstone RM. The Jeanne Manery-Fisher Memorial Lecture 1991. Maturation of reticulocytes: Formation of exosomes as a mechanism for shedding membrane proteins. *Biochem Cell Biol* 1992; 70:179–190.
17. Ahn J, Johnstone RM. Origin of a soluble truncated transferrin receptor. *Blood* 1993; 81:2442–2452.
18. Semenza GL. Regulation of mammalian O₂ homeostasis by hypoxia-inducible factor 1. *Annu Rev Cell Dev Biol* 1999; 15:551–578.
19. Ebert BL, Bunn HF. Regulation of the erythropoietin gene. *Blood* 1999; 94:1864–1877.
20. Wang GL, Semenza GL. Desferrioxamine induces erythropoietin gene expression and hypoxia-inducible factor 1 DNA-binding activity: Implications for models of hypoxia signal transduction. *Blood* 1993; 82:3610–3615.

21. Constantinescu SN, Ghaffari S, Lodish HF. The erythropoietin receptor: Structure, activation and intracellular signal transduction. *Trends Endocrinol Metab* 1999; 10: 18–23.
22. Andrews NC, Orkin SH. Transcriptional control of erythropoiesis. *Curr Opin Hematol* 1994; 1:119–124.
23. Ponka P. Tissue-specific regulation of iron metabolism and heme synthesis: Distinct control mechanisms in erythroid cells. *Blood* 1997; 89:1–25.
24. Ponka P. Cell biology of heme. *Am J Med Sci* 1999; 318:241–256.
25. Ross J, Ikawa Y, Leder P. Globin messenger-RNA induction during erythroid differentiation of cultured leukemia cells. *Proc Natl Acad Sci USA* 1972; 69:3620–3623.
26. Ross J, Sautner D. Induction of globin mRNA accumulation by hemin in cultured erythroleukemia cells. *Cell* 1976; 8:513–520.
27. Dabney BJ, Beudet AL. Increase in globin chains and globin mRNA in erythroleukemia cells in response to hemin. *Arch Biochem Biophys* 1977; 179:106–112.
28. Fuchs O, Ponka P, Borova J, Neuwirt J, Travnicek M. Effect of heme on globin messenger RNA synthesis in spleen erythroid cells. *J Supramol Struct Cell Biochem* 1981; 15:73–81.
29. Sassa S, Nagai T. The role of heme in gene expression. *Int J Hematol* 1996; 63:167–178.
30. Bruns GP, London IM. The effect of hemin on the synthesis of globin. *Biochem Biophys Res Commun* 1965; 18:236–242.
31. Zucker WV, Schulman HM. Stimulation of globin chain initiation by hemin in the reticulocyte cell-free system. *Proc Natl Acad Sci USA* 1968; 59:582–589.
32. London IM, Levin DH, Matts RL, Thomas NSB, Petryshyn R, Chen J-J. Regulation of protein synthesis. In: Boyer PD, ed. *The Enzymes*. Vol. 18. New York: Academic Press, 1987:359–380.
33. Chen J-J, London IM. Regulation of protein synthesis by heme-regulated eIF-2 alpha kinase. *Trends Biochem Sci* 1995; 20:105–108.
34. Crosby JS, Lee K, London IM, Chen J-J. Erythroid expression of the heme-regulated eIF-2 α kinase. *Mol Cell Biol* 1994; 14:3906–3914.
35. Gutteridge JM, Halliwell B. Iron toxicity and oxygen radicals. *Ballières Clin Haematol* 1989; 2:195–256.
36. Bothwell TA, Charlton RW, Cook JD, Finch CA. *Iron Metabolism in Man*. Oxford, UK: Blackwell Scientific, 1979.
37. Hershko C. Storage iron regulation. *Progr Hematol* 1977; 10:105–148.
38. Baker E, Vicary FR, Huehns ER. Iron release from isolated hepatocytes. *Br J Haematol* 1981; 47:493–504.
39. Poss KD, Tonegawa S. Heme oxygenase 1 is required for mammalian iron reutilization. *Proc Natl Acad Sci USA* 1997; 94:10919–10924.
40. Baranano DE, Wolosker H, Bae BI, Barrow RK, Snyder SH, Ferris CD. A mammalian iron ATPase induced by iron. *J Biol Chem* 2000; 275:15166–15173.
41. Donovan A, Brownlie A, Zhou Y, Shepard J, Pratt SJ, Moynihan J, Paw BH, Drejer A, Barut B, Zapata A, Law TC, Brugnara C, Lux SE, Pinkus GS, Pinkus JL, Kingsley PD, Palis J, Fleming MD, Andrews NC, Zon LI. Positional cloning of zebrafish ferroportin 1 identifies a conserved vertebrate iron exporter. *Nature* 2000; 403:776–781.
42. McKie AT, Marciani P, Rolfs A, Brennan K, Wehr K, Barrow D, Miret S, Bomford A, Peters TJ, Farzaneh F, Hediger MA, Hentze MW, Simpson RJ. A novel duodenal iron-regulated transporter, IREG1, implicated in the basolateral transfer of iron to the circulation. *Mol Cell* 2000; 5:299–309.
43. Abboud S, Haile DJ. A novel mammalian iron-regulated protein involved in intracellular iron metabolism. *J Biol Chem* 2000; 275:19906–19912.

44. Yoshida K, Furihata K, Takeda S, Nakamura A, Yamamoto K, Morita H, Hiyamuta S, Ikeda S, Shimizu N, Yanagisawa N. A mutation in the ceruloplasmin gene is associated with systemic hemosiderosis in humans. *Nature Genet* 1995; 9:267–272.
45. Harris ZL, Takahashi Y, Miyajima H, Serizawa M, MacGillivray RT, Gitlin JD. Aceruloplasminemia: Molecular characterization of this disorder of iron metabolism. *Proc Natl Acad Sci USA* 1995; 92:2539–2543.
46. Harris ZL, Durley AP, Man TK, Gitlin JD. Targeted gene disruption reveals an essential role for ceruloplasmin in cellular iron efflux. *Proc Natl Acad Sci USA* 1999; 96:10812–10817.
47. Vulpe CD, Kuo YM, Murphy TL, Cowley L, Askwith C, Libina N, Gitschier J, Anderson GJ. Hephaestin, a ceruloplasmin homologue implicated in intestinal iron transport, is defective in the sla mouse. *Nature Genet* 1999; 21:195–199.
48. Hemmaplardh D, Morgan EH. The mechanism of iron exchange between synthetic iron chelators and rabbit reticulocytes. *Biochim Biophys Acta* 1974; 373:84–99.
49. Hamill RL, Woods JC, Cook BA. Congenital atransferrinemia. A case report and review of the literature. *Am J Clin Pathol* 1991; 96:215–218.
50. Bernstein SE. Hereditary hypotransferrinemia with hemosiderosis, a murine disorder resembling human atransferrinemia. *J Lab Clin Med* 1987; 110:690–705.
51. Richardson DR, Ponka P. The molecular mechanisms of the metabolism and transport of iron in normal and neoplastic cells. *Biochim Biophys Acta* 1997; 1331:1–40.
52. Ponka P, Beaumont C, Richardson DR. Function and regulation of transferrin and ferritin. *Semin Hematol* 1998; 35:35–54.
53. Ponka P, Lok CN. The transferrin receptor: role in health and disease. *Int J Biochem Cell Biol* 1999; 31:1111–1137.
54. Kawabata H, Yang R, Hirama T, Vuong PT, Kawano S, Gombart AF, Koeffler HP. Molecular cloning of transferrin receptor 2. A new member of the transferrin receptor-like family. *J Biol Chem* 1999; 274:20826–20832.
55. Fleming RE, Migas MC, Holden CC, Waheed A, Britton RS, Tomatsu S, Bacon BR, Sly WS. Transferrin receptor 2: Continued expression in mouse liver in the face of iron overload and in hereditary hemochromatosis. *Proc Natl Acad Sci USA* 2000; 97:2214–2219.
56. Feder JN, Gnirke A, Thomas W, Tsuchihashi Z, Ruddy DA, Basava A, Dormishian F, Domingo R Jr, Ellis MC, Fullan A, Hinton LM, Jones NL, Kimmel BE, Kronmal GS, Lauer P, Lee VK, Loeb DB, Mapa FA, McClelland E, Meyer NC, Mintier GA, Moeller N, Moore T, Morikang E, Prass CE, Quintana L, Starnes SM, Schatzman RC, Brunke KJ, Drayna DT, Risch NJ, Bacon BR, Wolff RK. A novel MHC class I-like gene is mutated in patients with hereditary haemochromatosis. *Nature Genet* 1996; 13:399–408.
57. Lebron JA, Bennett MJ, Vaughn DE, Chirino AJ, Snow PM, Mintier GA, Feder JN, Bjorkman PJ. Crystal structure of the hemochromatosis protein HFE and characterization of its interaction with transferrin receptor. *Cell* 1998; 93:111–123.
- 57a. Hilditch-Maguire P, Trettel F, Passani LA, Auerbach A, Perischetti F, MacDonald ME. Huntingtin: An iron-regulated protein essential for normal nuclear and perinuclear organelles. *Hum Mol Genet* 2000; 9:2789–2797.
58. Harrison PM, Arosio P. The ferritins: Molecular properties, iron storage function and cellular regulation. *Biochim Biophys Acta* 1996; 1275:161–203.
- 58a. Levi S, Corsi B, Bosisio M, Invernizzi R, Volz A, Sanford D, Arosio P, Drysdale J. A human mitochondrial ferritin encoded by an intronless gene. *J Biol Chem* 2001; 270:24437–24440.
59. Hentze MW, Kühn LC. Molecular control of vertebrate iron metabolism: mRNA-based regulatory circuits operated by iron, nitric oxide, and oxidative stress. *Proc Natl Acad Sci USA* 1996; 93:8175–8182.

60. Rouault T, Klausner R. Regulation of iron metabolism in eukaryotes. *Curr Top Cell Regul* 1997; 35:1–19.
61. Mikulits W, Schranzhofer M, Beug H, Müllner EW. Post-transcriptional control via iron-responsive elements: The impact of aberrations in hereditary disease. *Mutat Res* 1999; 437:219–230.
62. Fleming MD, Trenor CC 3rd, Su MA, Foerzler D, Beier DR, Dietrich WF, Andrews NC. Microcytic anaemia mice have a mutation in Nramp2, a candidate iron transporter gene. *Nature Genet* 1997; 16:383–386.
63. Gunshin H, Mackenzie B, Berger UV, Gunshin Y, Romero MF, Boron WF, Nussberger S, Gollan JL, Hediger MA. Cloning and characterization of a mammalian proton-coupled metal-ion transporter. *Nature* 1997; 388:482–488.
64. Fleming MD, Romano MA, Su MA, Garrick LM, Garrick MD, Andrews NC. Nramp2 is mutated in the anemic Belgradre (b) rat: Evidence of a role for Nramp2 in endosomal iron transport. *Proc Natl Acad Sci USA* 1998; 95:1148–1153.
65. Canonne-Hergaux F, Gruenheid S, Ponka P, Gros P. Cellular and subcellular localization of the Nramp2 iron transporter in the intestinal brush border and regulation by dietary iron. *Blood* 1999; 93:4406–4417.
66. McKie AT, Barrow D, Latunde-Dada GO, Rolfs A, Sager G, Mudaly E, Mudaly M, Richardson C, Barlow D, Bomford A, Peters TJ, Raja KB, Shirali S, Hediger MA, Farzaneh F, Simpson RJ. An iron-regulated ferric reductase associated with the absorption of dietary iron. *Science* 2001; 291:1755–1759.
67. Gitlin JD. Aceruloplasminemia. *Pediatr Res* 1998; 44:271–276.
- 67a. Fleming MD, Campagna DR, Haslett JN, Trenor CC 3rd, Andrews NC. A mutation in a mitochondrial transmembrane protein is responsible for the pleiotropic hematological and skeletal phenotype of flexed-tail (*fff*) mice. *Genes Dev* 2001; 15:652–657.
68. Csere P, Lill R, Kispal G. Identification of a human mitochondrial ABC transporter, the functional orthologue of yeast *Atm1p*. *FEBS Lett* 1998; 441:266–270.
69. Rotig A, de Lonlay P, Chretien D, Foury F, Koenig M, Sidi D, Munnich A, Rustin P. Aconitase and mitochondrial iron-sulphur protein deficiency in Friedreich ataxia. *Nature Genet* 1997; 17:215–217.
70. Pandolfo M. Molecular pathogenesis of Friedreich ataxia. *Arch Neurol* 1999; 56:1201–1208.
71. Shirihai OS, Gregory T, Yu C, Orkin SH, Weiss MJ. ABC-me: A novel mitochondrial transporter induced by GATA-1 during erythroid differentiation. *EMBO J* 2000; 19:2492–2502.
72. Sadlon TJ, Dell'Oso T, Surinya KH, May BK. Regulation of erythroid 5-aminolevulinate synthase expression during erythropoiesis. *Int J Biochem Cell Biol* 1999; 31:1153–1167.
73. Ferreira GC. Ferrochelatase. *Int J Biochem Cell Biol* 1999; 31:995–1000.
74. Maines MD. The heme oxygenase system: A regulator of second messenger gases. *Annu Rev Pharmacol Toxicol* 1997; 37:517–554.
75. Nuijens JH, van Berkel PH, Schanbacher FL. Structure and biological actions of lactoferrin. *J Mammary Gland Biol Neoplasia* 1996; 1:285–295.
76. Basti JM, Jones M, O'Callaghan CA, Schimanski L, Mason DY, Townsend AR. Kupfer cell staining by an HFE-specific monoclonal antibody: Implications for hereditary haemochromatosis. *Br J Haematol* 1998; 103:931–941.
77. Feeney GP, Worwood M. Expression of HFE detected in a wide range of cells, but not erythroid cells. Presented at the World Congress on Iron Metabolism (BIOIRON '99), Sorrento, Italy, May 23–28, 1999, Abstr. 215.
78. Cellier M, Prive G, Belouchi A, Kwan T, Rodrigues V, Chia W, Gros P. Nramp defines a family of membrane proteins. *Proc Natl Acad Sci USA* 1995; 92:10089–10093.

79. Ponka P, Neuwirt J. Regulation of iron entry into reticulocytes. I. Feedback inhibitory effect of heme on iron entry into reticulocytes and on heme synthesis. *Blood* 1969; 33:690–707.
80. Ponka P, Neuwirt J. Regulation of iron entry into reticulocytes. II. Relationship between hemoglobin synthesis and entry of iron into reticulocytes. *Biochim Biophys Acta* 1971; 230:381–392.
81. Schulman HM, Martinez-Medellin J, Sidloi R. The reticulocyte-mediated release of iron and bicarbonate from transferrin: Effect of metabolic inhibitors. *Biochim Biophys Acta* 1974; 343:529–534.
82. Garrick LM, Edwards JA, Hoke JE. The effect of hemin on globin synthesis and iron uptake by reticulocytes of the Belgrade rat. *FEBS Lett* 1978; 93:109–114.
83. Iacopetta B, Morgan E. Heme inhibits transferrin endocytosis in immature erythroid cells. *Biochim Biophys Acta* 1984; 805:211–216.
84. Cox TM, O'Donnell MW, Aisen P, London IM. Hemin inhibits internalization of transferrin by reticulocytes and promotes phosphorylation of the membrane transferrin receptor. *Proc Natl Acad Sci USA* 1985; 82:5170–5174.
85. Ponka P, Schulman HM, Martinez-Medellin J. Haem inhibits iron uptake subsequent to endocytosis of transferrin in reticulocytes. *Biochem J* 1988; 251:105–109.
86. Hradilek A, Neuwirt J. Inhibition of cellular iron uptake by haem in mouse erythro-leukaemia cells. *Br J Haematol* 1989; 73:410–415.
87. Ponka P, Schulman HM. Regulation of heme synthesis in erythroid cells: Hemin inhibits transferrin iron utilization but not protoporphyrin synthesis. *Blood* 1985; 65: 850–857.
88. Shemin D, Rittenberg D. Biological utilization of glycine for the synthesis of proto-porphyrin of hemoglobin. *J Biol Chem* 1946; 166:621–625.
89. Walsh RJ, Thomas ED, Chow SK, Fluharty RH, Finch CA. Iron metabolism: Heme synthesis in vitro by immature erythrocytes. *Science* 1949; 110:396–398.
90. Jandl JH, Inman JK, Simmons RL, Allen DW. Transfer of iron from serum iron-binding protein to human reticulocytes. *J Clin Invest* 1959; 38:161–185.
91. Martinez-Medellin J, Schulman HM. The kinetics of iron and transferrin incorporation into rabbit erythroid cells and the nature of stromal-bound iron. *Biochim Biophys Acta* 1972; 264:272–274.
92. Ponka P, Wilczynska A, Schulman HM. Iron utilization in rabbit reticulocytes. A study using succinylacetone as an inhibitor of heme synthesis. *Biochim Biophys Acta* 1982; 720:96–105.
93. Richardson DR, Ponka P, Vyoral D. Distribution of iron in reticulocytes after inhibition of heme synthesis with succinylacetone: Examination of the intermediates involved in iron metabolism. *Blood* 1996; 87:3477–3488.
94. Friend C. Cell-free transmission in adult Swiss mice of a disease having the characteristics of leukemia. *J Exp Med* 1957; 105:307–318.
95. Friend C, Patuleia MC, De Harven E. Erythrocytic maturation in vitro of murine (Friend) virus-induced leukemic cells. *Natl Cancer Inst Monogr* 1966; 22:505–522.
96. Friend C, Scher W, Holland JG, Sato T. Hemoglobin synthesis in murine virus-induced leukemia cells in vitro: Stimulation of erythroid differentiation by dimethyl sulfoxide. *Proc Natl Acad Sci USA* 1971; 68:378–382.
97. Marks PA, Rifkind RA. Erythroleukemia differentiation. *Annu Rev Biochem* 1978; 47:419–448.
98. Hu HY, Gardner J, Aisen P. Inducibility of transferrin receptors on Friend erythro-leukemic cells. *Science* 1977; 197:559–561.
99. Yeoh GC, Morgan EH. Dimethyl sulphoxide induction of transferrin receptors on Friend erythro-leukemia cells. *Cell Differ* 1979; 8:331–343.

100. Wilczynska A, Schulman HM. Friend erythroleukemia cell membrane transferrin receptors. *Can J Biochem* 1980; 58:935–940.
101. Laskey JD, Ponka P, Schulman HM. Control of heme synthesis during Friend cell differentiation: Role of iron and transferrin. *J Cell Physiol* 1986; 129:185–192.
102. Ben-David Y, Bernstein A. Friend virus-induced erythroleukemia and the multistage nature of cancer. *Cell* 1991; 66:831–834.
103. Drysdale JW, Adelman TG, Arosio P, Casareale D, Fitzpatrick P, Harzard JT, Yokota M. Human isoferritins in normal and disease states. *Semin Hematol* 1977; 14:71–88.
104. Koury MJ, Sawyer ST, Bondurant MC. Splenic erythroblasts in anemia-inducing Friend disease: A source of cells for studies of erythropoietin-mediated differentiation. *J Cell Physiol* 1984; 121:526–532.
105. Koury MJ, Bondurant MC, Rama SS. Changes in erythroid membrane proteins during erythropoietin-mediated terminal differentiation. *J Cell Physiol* 1987; 133:438–448.
106. Koury MJ, Bondurant MC. Maintenance by erythropoietin of viability and maturation of murine erythroid precursor cells. *J Cell Physiol* 1988; 137:65–74.
107. Sawyer ST, Krantz SB. Transferrin receptor number, synthesis, and endocytosis during erythropoietin-induced maturation of Friend virus-infected erythroid cells. *J Biol Chem* 1986; 261:9187–9195.
108. Busfield SJ, Klinken SP. Erythropoietin-induced stimulation of differentiation and proliferation in J2E cells is not mimicked by chemical induction. *Blood* 1992; 80:412–419.
109. Busfield SJ, Tilbrook PA, Callus BA, Spadaccini A, Kühn L, Klinken SP. Complex regulation of transferrin receptors during erythropoietin-induced differentiation of J2E erythroid cells—Elevated transcription and mRNA stabilisation produce only a modest rise in protein content. *Eur J Biochem* 1997; 249:77–84.
110. Fibach E, Manor D, Oppenheim A, Rachmilewitz EA. Proliferation and maturation of human erythroid progenitors in liquid culture. *Blood* 1989; 73:100–103.
111. Vaisman B, Fibach E, Konijn AM. Utilization of intracellular ferritin iron for hemoglobin synthesis in developing human erythroid precursors. *Blood* 1997; 90:831–838.
112. Meyron-Holtz EG, Vaisman B, Cabantchik ZI, Fibach E, Rouault TA, Hershko C, Konijn AM. Regulation of intracellular iron metabolism in human erythroid precursors by internalized extracellular ferritin. *Blood* 1999; 94:3205–3211.
113. Gubin AN, Njoroge JM, Bouffard GG, Miller JL. Gene expression in proliferating human erythroid cells. *Genomics* 1999; 59:168–177.
114. Pope SH, Fibach E, Sun J, Chin K, Rodgers GP. Two-phase liquid culture system models normal human adult erythropoiesis at the molecular level. *Eur J Haematol* 2000; 64:292–303.
115. Rutherford TR, Clegg JB, Weatherall DJ. K562 human leukaemic cells synthesise embryonic haemoglobin in response to haemin. *Nature* 1979; 280:164–165.
116. Baliga BS, Mankad M, Shah AK, Mankad VN. Mechanism of differentiation of human erythroleukaemic cell line K562 by hemin. *Cell Prolif* 1993; 26:519–529.
117. Lozzio CB, Lozzio BB. Human chronic myelogenous leukemia cell line with positive Philadelphia chromosome. *Blood* 1975; 45:321–334.
118. Rutherford T, Clegg JB, Higgs DR, James RW, Thompson J, Weatherall DJ. Embryonic erythroid differentiation in the human leukemic cell line K562. *Proc Natl Acad Sci USA* 1981; 78:348–352.
119. Rouault T, Rao K, Harford J, Mattia E, Klausner RD. Hemin, chelatable iron, and the regulation of transferrin receptor biosynthesis. *J Biol Chem* 1985; 260:14862–14866.
120. Cotter PD, Drabkin HA, Varkony T, Smith DI, Bishop DF. Assignment of the human housekeeping delta-aminolevulinic acid synthase gene (ALAS1) to chromosome band 3p21.1 by PCR analysis of somatic cell hybrids. *Cytogenet Cell Genet* 1995; 69:207–208.

121. Cotter PD, Willard HF, Gorski JL, Bishop DF. Assignment of human erythroid delta-aminolevulinate synthase (ALAS2) to a distal subregion of band Xp11.21 by PCR analysis of somatic cell hybrids containing X; autosome translocations. *Genomics* 1992; 13:211–212.
122. Bishop TR, Miller MW, Beall J, Zon LI, Dierks P. Genetic regulation of delta-aminolevulinate dehydratase during erythropoiesis. *Nucleic Acids Res* 1996; 24:2511–2518.
123. Beaumont C, Porcher C, Picat C, Nordmann Y, Grandchamp B. The mouse porphobilinogen deaminase gene. Structural organization, sequence, and transcriptional analysis. *J Biol Chem* 1989; 264:14829–14834.
124. Taketani S, Nakahashi Y, Osumi T, Tokunaga R. Molecular cloning, sequencing, and expression of mouse ferrochelatase. *J Biol Chem* 1990; 265:19377–19380.
125. Chan RY, Schulman HM, Ponka P. Expression of ferrochelatase mRNA in erythroid and non-erythroid cells. *Biochem J* 1993; 292:343–349.
126. Ferreira GC, Franca R, Lloyd SG, Pereira AS, Moura I, Moura JJ, Huynh BH. Mammalian ferrochelatase, a new addition to the metalloenzyme family. *J Biol Chem* 1994; 269:7062–7065.
127. Dailey HA, Finnegan MG, Johnson MK. Human ferrochelatase is an iron-sulfur protein. *Biochemistry* 1994; 33:403–407.
- 127a. Taketani S, Adachi Y, Nakahashi Y. Regulation of the expression of human ferrochelatase by intracellular iron levels. *Eur J Biochem* 2000; 267:4685–4692.
128. Dierks P. Molecular biology of eukaryotic δ -aminolevulinate synthase. In: HA Dailey, ed. *Biosynthesis of Heme and Chlorophylls*. New York: McGraw-Hill, 1990:201–233.
129. Cox TC, Bawden MJ, Martin A, May BK. Human erythroid 5-aminolevulinate synthase: Promoter analysis and identification of an iron-responsive element in the mRNA. *EMBO J* 1991; 10:1891–1902.
130. Dandekar T, Stripecke R, Gray NK, Goossen B, Constable A, Johansson HE, Hentze MW. Identification of a novel iron-responsive element in murine and human erythroid delta-aminolevulinic acid synthase mRNA. *EMBO J* 1991; 10:1903–1909.
131. Melefors O, Goossen B, Johansson HE, Stripecke R, Gray NK, Hentze MW. Translational control of 5-aminolevulinate synthase mRNA by iron-responsive elements in erythroid cells. *J Biol Chem* 1993; 268:5974–5978.
132. Vyoral D, Schulman HM, Ponka P. Role of iron in the control of erythroid δ -aminolevulinic acid (ALA) synthase. *Blood* 1993; 82(suppl 1):8a.
133. Ponka P, Schulman HM. Acquisition of iron from transferrin regulates reticulocyte heme synthesis. *J Biol Chem* 1985; 260:14717–14721.
134. Schmidt JA, Marshall J, Hayman MJ, Ponka P, Beug H. Control of erythroid differentiation; Possible role of the transferrin cycle. *Cell* 1986; 46:41–51.
135. Chan LN, Gerhardt EM. Transferrin receptor gene is hyperexpressed and transcriptionally regulated in differentiating erythroid cells. *J Biol Chem* 1992; 267:8254–8259.
136. Chan RY, Seiser C, Schulman HM, Kühn LC, Ponka P. Regulation of transferrin receptor mRNA expression. Distinct regulatory features in erythroid cells. *Eur J Biochem* 1994; 220:683–692.
137. Sieweke MH, Tekotte H, Frampton J, Graf T. MafB is an interaction partner and repressor of Ets-1 that inhibits erythroid differentiation. *Cell* 1996; 85:49–60.
138. Levy JE, Jin O, Fujiwara Y, Kuo F, Andrews NC. Transferrin receptor is necessary for development of erythrocytes and the nervous system. *Nature Genet* 1999; 21:396–399.
139. Sieff C, Bicknell D, Caine G, Robinson J, Lam G, Greaves MF. Changes in cell surface antigen expression during hemopoietic differentiation. *Blood* 1982; 60:703–713.

140. Lesley J, Hyman R, Schulte R, Trotter J. Expression of transferrin receptor on murine hematopoietic progenitors. *Cell Immunol* 1984; 83:14–25.
141. Iacopetta BJ, Morgan EH, Yeoh GC. Transferrin receptors and iron uptake during erythroid cell development. *Biochim Biophys Acta* 1982; 687:204–210.
142. Janknecht R, Nordheim A. Gene regulation by Ets proteins. *Biochim Biophys Acta* 1993; 1155:346–356.
143. Lok CN, Ponka P. Identification of an erythroid active element in the transferrin receptor gene. *J Biol Chem* 2000; 275:24185–24190.
144. Lok CN, Ponka P. Identification of a hypoxia response element in the transferrin receptor gene. *J Biol Chem* 1999; 274:24147–24152.
145. Tacchini L, Bianchi L, Bernelli-Zazzera A, Cairo G. Transferrin receptor induction by hypoxia. HIF-1-mediated transcriptional activation and cell-specific post-transcriptional regulation. *J Biol Chem* 1999; 274:24142–24146.
146. Weiss G, Houston T, Kastner S, Johrer K, Grunewald K, Brock JH. Regulation of cellular iron metabolism by erythropoietic activation of iron-regulatory protein and upregulation of transferrin receptor expression in erythroid cells. *Blood* 1997; 89:680–687.
147. Ponka P, Zhang A-S, Kim S, Koury MJ. Regulation of transferrin receptor expression in erythroid cells: Erythropoietin does not affect iron-regulatory proteins but increases transferrin receptor gene transcription. Submitted.
148. Eisenstein RS, Garcia-Mayol D, Pettingell W, Munro HN. Regulation of ferritin and heme oxygenase synthesis in rat fibroblasts by different forms of iron. *Proc Natl Acad Sci USA* 1991; 88:688–692.
149. Cox TM, O'Donnell MW, Aisen P, London IM. Biosynthesis of the transferrin receptor in rabbit reticulocytes. *J Clin Invest* 1985; 76:2144–2150.
150. Grdisa M, Mathew A, Johnstone RM. Expression and loss of the transferrin receptor in growing and differentiating HD3 cells. *J Cell Physiol* 1993; 155:349–357.
151. Battistini A, Coccia EM, Marziali G, Bulgarini D, Scalzo S, Fiorucci G, Romeo G, Affabris E, Testa U, Rossi GB, Peschle C. Intracellular heme coordinately modulates globin chain synthesis, transferrin receptor number, and ferritin content in differentiating Friend erythroleukemia cells. *Blood* 1991; 78:2098–2103.
152. Hradilek A, Fuchs O, Neuwirt J. Inhibition of heme synthesis decreases transferrin receptor expression in mouse erythroleukemia cells. *J Cell Physiol* 1992; 150:327–333.
153. Lok CN, Ponka P. Role of heme in transferrin receptor expression in erythroid cells. *Blood* 1997; 90(suppl 1):6a.
154. Jacobs A. Low molecular weight intracellular iron transport compounds. *Blood* 1997; 90:433–439.
155. Ponka P, Richardson DR. Can ferritin provide iron for hemoglobin synthesis? *Blood* 1997; 89:2611–2613.
156. Adams ML, Ostapiuk I, Grasso JA. The effects of inhibition of heme synthesis on the intracellular localization of iron in rat reticulocytes. *Biochim Biophys Acta* 1989; 1012:243–253.
157. Picard V, Renaudie F, Porcher C, Hentze MW, Grandchamp B, Beaumont C. Overexpression of the ferritin H subunit in cultured erythroid cells changes the intracellular iron distribution. *Blood* 1996; 87:2057–2064.
158. Borova J, Ponka P, Neuwirt J. Study of intracellular iron distribution in rabbit reticulocytes with normal and inhibited heme synthesis. *Biochim Biophys Acta* 1973; 320:143–156.
159. Garrick LM, Gniecko K, Liu Y, Cohan DS, Grasso JA, Garrick MD. Iron distribution in Belgrade rat reticulocytes after inhibition of heme synthesis with succinylacetone. *Blood* 1993; 81:3414–3421.

160. Zhang A-S, Sheftel AD, Ponka P. Intracellular kinetics of iron in reticulocytes: Evidence for endosome involvement in iron targeting to mitochondria. Submitted.
161. Lange H, Kispal G, Lill R. Mechanism of iron transport to the site of heme synthesis inside yeast mitochondria. *J Biol Chem* 1999; 274:18989–18996.
162. Scott MD, Eaton JW. Thalassaemic erythrocytes: Cellular suicide arising from iron and glutathione-dependent oxidation reactions? *Br J Haematol* 1995; 91:811–819.
163. Penman S. Rethinking cell structure. *Proc Natl Acad Sci USA* 1995; 92:5251–5257.
164. May A, Fitzsimons E. Sideroblastic anaemia. *Ballières Clin Haematol* 1994; 7:851–879.
165. Brownlie A, Donovan A, Pratt SJ, Paw BH, Oates AC, Brugnara C, Witkowska HDE, Sassa S, Zon LI. Positional cloning of the zebrafish *sauternes* genes: A model for congenital sideroblastic anaemia. *Nature Genet* 1998; 20:244–250.
166. Nakajima O, Takahashi S, Harigae H, Furuyama K, Hayashi N, Sassa S, Yamamoto M. Heme deficiency in erythroid lineage causes differentiation arrest and cytoplasmic iron overload. *EMBO J* 1999; 18:6282–6289.
167. Gattermann N, Retzlaff S, Wang YL, Hofhaus G, Heinisch J, Aul C, Schneider W. Heteroplasmic point mutations of mitochondrial DNA affecting subunit I of cytochrome c oxidase in two patients with acquired idiopathic sideroblastic anemia. *Blood* 1997; 90:4961–4972.
168. Pagon RA, Bird TD, Detter JC, Pierce I. Hereditary sideroblastic anaemia and ataxia: An X linked recessive disorder. *J Med Genet* 1985; 22:267–273.
169. Allikmets R, Raskind WH, Hutchinson A, Schueck ND, Dean M, Koeller DM. Mutation of a putative mitochondrial iron transporter gene (*ABC7*) in X-linked sideroblastic anemia and ataxia (*XLSA/A*). *Hum Mol Genet* 1999; 8:743–749.
170. Kispal G, Csere P, Guiard B, Lill R. The ABC transporter *Atm1p* is required for mitochondrial iron homeostasis. *FEBS Lett* 1997; 418:346–350.
171. Kispal G, Csere P, Prohl C, Lill R. The mitochondrial proteins *Atm1p* and *Nfs1p* are essential for biogenesis of cytosolic Fe/S proteins. *EMBO J* 1999; 18:3981–3989.
172. Babcock M, de Silva D, Oaks R, Davis-Kaplan S, Jiralerspong S, Montermini L, Pandolfo M, Kaplan J. Regulation of mitochondrial iron accumulation by *Yfh1p*, a putative homolog of frataxin. *Science* 1997; 276:1709–1712.
173. Radisky DC, Babcock MC, Kaplan J. The yeast frataxin homologue mediates mitochondrial iron efflux. Evidence for a mitochondrial iron cycle. *J Biol Chem* 1999; 274:4497–4499.
174. Fujita H, Yamamoto M, Yamagami T, Hayashi N, Sassa S. Erythroleukemia differentiation. Distinctive responses of the erythroid-specific and the nonspecific delta-aminolevulinic synthase mRNA. *J Biol Chem* 1991; 266:17494–17502.
175. Taketani S, Adachi Y, Kohno H, Ikehara S, Tokunaga R, Ishii T. Molecular characterization of a newly identified heme-binding protein induced during differentiation of murine erythroleukemia cells. *J Biol Chem* 1998; 273:31388–31394.
176. Brittenham GM. The red cell cycle. In: Brock JH, Halliday JW, Pippard MJ, Powell LW, eds. *Iron Metabolism in Health and Disease*. London: Saunders, 1994:31–62.
177. Taketani S, Kohno H, Okuda M, Furukawa T, Tokunaga R. Induction of peripheral-type benzodiazepine receptors during differentiation of mouse erythroleukemia cells. A possible involvement of these receptors in heme biosynthesis. *J Biol Chem* 1994; 269:7527–7531.

Animal Models of Iron Transport and Storage Disorders

NANCY C. ANDREWS

Children's Hospital and Harvard Medical School, Boston, Massachusetts

I. INTRODUCTION	679
II. RODENT MODELS	680
A. Spontaneous Mutations	681
B. Induced Mutations	685
C. The Belgrade (<i>b</i>) Rat	690
III. A ZEBRAFISH MODEL	690
IV. CONCLUSIONS	691
REFERENCES	693

I. INTRODUCTION

Investigation of animal models has contributed to our understanding of iron metabolism for more than half a century. Initially, studies of anemic animals in laboratory colonies allowed detailed characterization of their physiology. More recently, molecular biology has changed the nature of animal studies, by allowing positional cloning of spontaneously mutated genes, and targeted mutagenesis of the genome, particularly in the mouse. The combination of physiology and molecular analysis has been powerful in moving the field forward. Several key proteins in iron transport (DMT1, hephaestin, and Ireg1/ferroportin1) were identified through positional cloning of mutations in laboratory animals. Mouse models of hemochromatosis, aceruloplasminemia, and heme oxygenase 1 deficiency have given critical insights into the patho-

genesis of human diseases. This chapter describes existing animal models, and how they have helped elucidate iron metabolism.

It should be mentioned that animals have also been used extensively in experiments involving dietary manipulation, to study induced iron deficiency and iron overload. However, information gleaned from those experiments will be presented elsewhere. This chapter will deal exclusively with models carrying heritable mutations affecting iron metabolism.

II. RODENT MODELS

Mouse mutants have provided the greatest body of information about iron metabolism. Initially maintained by mouse fanciers, and more recently by biological laboratories, mouse colonies allow the rapid identification of new mutations. Spontaneous mutations affecting iron metabolism typically result in iron deficiency anemia, which is readily observed as pallor (Fig. 1). Examination of a peripheral blood smear helps to distinguish those anemias due to iron deficiency from those due to other causes, e.g., hemolysis secondary to enzymatic or cytoskeletal defects of erythrocytes. To date, six mouse mutations have been shown to result in abnormalities of iron transport and utilization: *mk*, *sla*, *hpx*, *f*, *fsn/hea*, and *hbd*. The mutation and the gene affected by the mutation have been reported for all of those except *fsn/hea* and *hbd*. In addition to the mouse mutations, there is one spontaneous rat mutation that results in iron deficiency anemia. Remarkably, this mutation affecting the Belgrade (*b*) rat



Figure 1 Anemic mouse mutants. The figure shows a litter of newborn mice. Two mice in the center of the figure are noticeably pale; they are homozygous for the *f* mutation. The pallor is particularly obvious in the feet and tail. Three unaffected *f*/+ littermates have normal color. The photograph was taken by Dr. Mark Fleming in our laboratory.

is identical to that seen in the *mk* mouse. Physiological studies of the *b* rat have been somewhat different from those carried out on the *mk* mouse, producing complementary data.

A. Spontaneous Mutations

1. Microcytic Anemia (*mk*)

Microcytic anemia mice (gene symbol *mk*) was initially described in 1964 at the Jackson Laboratory (1). An autosomal recessive mutation resulted in poor viability, runting, characteristic skin lesions, and microcytic anemia (2). The anemia is apparent during fetal development. It is similar to that seen in iron deficiency, with decreased cell volume, marked hypochromia, anisocytosis, poikilocytosis, and abundant target forms. Body iron stores are low and the serum transferrin saturation is decreased (3). Reciprocal bone marrow transplantation studies established that homozygous *mk* mice have defects in iron transport in at least two tissues (4). Irradiated normal mice, transplanted with bone marrow from homozygous *mk* mutant mice, developed hypochromic, microcytic anemia similar to *mk* mutant mice, in spite of good splenic iron stores. This indicated that there is a defect in iron uptake by erythroid precursor cells. Conversely, irradiated *mk* mice, transplanted with bone marrow from normal mice, were anemic owing to poor intestinal iron absorption. In these latter mice the anemia was corrected by parenteral administration of iron, bypassing a defect in intestinal absorption.

These defects were studied in more detail. The reticulocyte percentage is increased in *mk* homozygotes. It is associated with increased splenic destruction of newly formed erythrocytes (5). Reticulocytes from normal animals take up significantly more iron than reticulocytes from *mk* homozygotes, though the ability to incorporate internalized iron into heme is indistinguishable (6). The serum transferrin appears normal in *mk* mice, because *mk* plasma was as effective as wild-type plasma for delivery of transferrin bound iron to wild-type cells.

Intestinal iron transport in homozygous *mk* mutant mice was studied by intragastric instillation of radiolabeled iron followed by whole-body counting, and by incubation of iron-containing solutions in isolated gut loops (7). In spite of their anemia, *mk* mice absorbed less of an intragastric ferric citrate dose than did wild-type controls. Mucosal iron uptake was diminished in *mk* gut loops. However, iron that did enter the intestinal mucosal cells was efficiently transferred to the plasma. Serosal transfer was actually enhanced in *mk* animals, consistent with induction of basolateral enterocyte iron transfer in the setting of anemia.

Taken together, these results suggested that the *mk* gene encodes a protein that is essential for transmembrane iron transport in at least two cell types, the developing erythroid precursor and the absorptive enterocyte. In both instances it mediates cellular iron import. Speculating that the gene product might be a ferrous ion transporter protein, Fleming and colleagues undertook positional cloning of the *mk* gene. They set up a backcross panel that produced 1000 progeny with meiotic events that could be analyzed to determine the location of *mk* in the mouse genome. They confirmed classical mapping studies that had placed *mk* on mouse chromosome 15 (8), and refined the map position relative to anonymous microsatellite markers (9). They found that *mk* was nonrecombinant with a known gene of unknown function, *Nramp2*, and identified a single missense mutation that converted amino acid 185

from glycine to arginine (*G185R*). Simultaneously, Gunshin and colleagues isolated rat *Nramp2* cDNA (called DCT1 in their study) using a *Xenopus* oocyte expression cloning strategy designed to identify iron transporters (10). Later studies demonstrated that wild-type *Nramp2* conferred iron uptake capability on transfected mammalian cells, but the *G185R* mutant form of *Nramp2* had little if any iron transport activity (11). Together, these results confirm that *Nramp2* is the *mk* gene product, and that it functions as a transmembrane iron transporter. To explain the phenotype of *mk* mutant mice, *Nramp2* must be operative in both erythroid precursors and intestinal cells.

Most investigators now refer to *Nramp2* as DMT1, for *divalent metal transporter 1*, better to describe its function. The murine gene symbol has been changed to *Slc11a2*.

2. Sex-Linked Anemia (*sla*)

The sex-linked anemia (*sla*) mutation of mice was produced by X-irradiation (12). Young *sla/Y* males and *sla/sla* females have hypochromic, microcytic erythrocytes, and hypoferrremia associated with decreased body iron stores (13,14). In contrast to the anemia of *mk* mice, however, the *sla* anemia is corrected by parenteral iron treatment, and there is no primary defect in erythropoiesis (15,16). The *sla* defect exclusively affects intestinal and placental iron transport (17). Iron transport studies using everted duodenal sacs showed that mucosal uptake was normal, but serosal (basolateral) transfer was greatly reduced (18,19). Excess nonheme iron can be visualized in enterocytes (20). Heterozygous females show a partial defect (19). Interestingly, radiolabeled iron administered parenterally also accumulates within developing enterocytes, suggesting that the block in iron egress also leads to inappropriate retention of iron from plasma (21). The *sla* defect appears to be exclusive for iron; it does not affect enteric transport of zinc (22).

Reasoning that the *sla* gene product was likely to encode a protein that is important for basolateral iron transfer in the intestine, Vulpe, Anderson, and co-workers undertook positional cloning of the *sla* gene. Fortunately, they were simultaneously searching for ceruloplasmin homologs among expressed sequence tags (ESTs), because ceruloplasmin is a ferroxidase that is important for iron egress from cells. They found a cDNA sequence predicted to encode a membrane-bound ceruloplasmin homolog. When they discovered that the gene for this protein mapped to the region of mouse chromosome X that contained the *sla* gene, they searched for and found a deletion mutation within its coding sequence that was unique to *sla* mice (23). Postulating that this protein served as a ferroxidase involved in iron export, they named it hephaestin, after the Greek god Hephaestus, who forged iron.

Hephaestin is expressed at low levels in many tissues, and at high levels in the small intestine (23). It is primarily found in enterocytes of the mid to upper villus; little is present in the intestinal crypts. The deletion mutation presumably renders the protein nonfunctional, though this has not been formally tested. Hephaestin is postulated to oxidize ferrous iron to the ferric form, aiding in its transfer from the enterocyte to plasma transferrin. It is not yet known, however, whether hephaestin localizes to the basolateral membrane of the enterocyte.

Mice carrying the *sla* mutation for hephaestin recover from anemia as they grow older, though their liver iron stores are always lower than in wild-type mice (M. D. Fleming, J. E. Levy, and N. C. Andrews, unpublished observations). There

are several possible explanations for this. First, it may be that hephaestin plays a more important role in placental iron transfer than in intestinal iron transfer. Alternatively, it may be that it is not essential at any time, but rather that it facilitates iron transport and therefore appears more important during periods when growth is most rapid. Ceruloplasmin might be able to serve the same function when hephaestin is absent. Finally, it is possible that the *sla* mutation does not result in a null allele, but rather creates a hypofunctional or dominant negative protein.

3. Hypotransferrinemia (*hpx*)

To date, only one spontaneously occurring mouse mutation has served as a direct model for a human disorder. Mice that are homozygous for hypotransferrinemia (*hpx*) are severely deficient in serum transferrin (24), and phenotypically similar to human patients with atransferrinemia (25–29). In both mice and humans, heterozygosity for the defect results in half-normal levels of serum transferrin, and homozygosity leads to profound transferrin deficiency. As a result, iron deficiency anemia associated with tissue iron overload begins before birth. Blood smears are hypochromic and microcytic, with marked anisocytosis, poikilocytosis, and target forms. The liver and pancreas are preferred sites for iron deposition, but all nonhematopoietic tissues become siderotic (24,30,31). The murine disorder is lethal by 2 weeks of age unless animals are given purified transferrin or red blood cell transfusions in the newborn period (24). Exogenous transferrin has a short half-life in *hpx* serum, lasting less than 2 days (32). However, it stimulates erythropoiesis enough to sustain the animals. The treated animals have subtle changes in the central nervous system, with decreased cell numbers and mild architectural disorganization, particularly in the hippocampus and cerebellum (33). This suggests that cells of the nervous system may be particularly sensitive to inadequate or fluctuating transferrin levels. Interestingly, animals that are rescued with early treatment do not need further hematological support after they have reached adulthood (31). They remain severely anemic, develop massive iron overload, and show generalized cachexia, but can survive untreated for at least 5 months.

Early studies indicated that a protein that was immunologically indistinguishable from transferrin was present at approximately 2% normal levels in *hpx* mice (24). Classical mapping studies positioned the *hpx* mutation close to or within the murine transferrin gene (24). An abnormally spliced transferrin transcript was detected in nuclear RNA from *hpx* mice, suggesting a defect in splicing signals (34). The mutation was recently identified as a single-nucleotide change in the splice donor site following transferrin exon 16 (31). Splicing is inhibited, but low-level activation of an upstream cryptic splice site creates an mRNA encoding a protein with a nine-amino acid deletion near the carboxyl terminus. This explains why transferrin from *hpx* mice appeared biochemically indistinguishable from that of wild-type mice in early studies (24). This protein is expressed at very low levels. It is not known whether it can bind iron or transferrin receptor (TfR). No normal transferrin mRNA can be detected in *hpx* homozygotes, and no mRNA resulting from the cryptic splice event can be detected in wild-type mice (31).

The phenotype of *hpx* mice offers insight into the role of the transferrin cycle in iron delivery. The fact that these animals become massively iron-overloaded indicates that the transferrin cycle is not required for intestinal iron uptake or cellular iron uptake in most tissues. Conversely, their profound iron deficiency anemia un-

derscores the importance of transferrin cycle iron uptake in developing erythroid precursors. As discussed below, targeted disruption of the murine TfR gene leads to similar conclusions (35). Hypotransferrinemic mice absorb a far greater amount of dietary iron than do normal mice (36,37). The stimulus for increased iron absorption is not understood on a molecular level. Transferrin itself does not seem to be part of the signal (38). It is likely that increased absorption is a response to increased erythropoietic drive, through a mediator that has not yet been identified. This has been referred to as the “erythroid regulator” of iron absorption (39,40). The mediator may be a circulating protein, but efforts for plasma transfer of the mediator from one animal to another have been unsuccessful (38).

4. Flexed Tail (*f*)

The autosomal recessive flexed tail (*f*) mutation was discovered by Hunt in 1927 (41). Homozygous *f* mice have a triad of findings including hypochromic, siderocytic anemia (the most consistent sign), tail flexures, and white belly spots (42). It has been proposed that the anemia is the primary problem, and that the other findings are secondary (43). The anemia is unusual in that it begins during the embryonic period, starts to improve at the time bone marrow hematopoiesis begins (embryonic day 16), and resolves almost completely by 6 weeks of life (44). It is also unusual because the circulating erythrocytes contain visible iron deposits in the cytoplasm, hence the name siderocytes (45). While several common anemias are characterized by sideroblasts (i.e., nucleated erythroid precursor cells containing iron granules), siderocytes are uncommon. Interestingly, bone marrow examination shows that *f* mice do not have sideroblasts; the iron granules appear only after nuclear expulsion (M. D. Fleming and N. C. Andrews, unpublished data). Normal rodents and human infants have some circulating siderocytes before birth (46,47), but the siderotic granules are much smaller, and there are far fewer siderocytes than seen in *f* animals (48). Siderocytes are rarely detectable in wild-type adult mice. In contrast, adult *f* mice have approximately 3% siderocytes, probably resulting from a low level of ongoing fetal-type erythropoiesis (48). The *f* defect can be elicited in adult *f* mice when erythropoiesis is stressed. When hematopoietic cells from *f* mice are used for engraftment of irradiated recipient mice, they produce smaller splenic colonies that show decreased incorporation of radiolabeled iron into hemoglobin when compared on a per-cell basis (49). Although some investigators proposed that *f* animals have a defect in heme biosynthesis, later studies discounted that possibility. Definitive understanding of the role of the *f* gene product in erythropoiesis and iron metabolism must await identification of the *f* gene.

5. Flaky Skin/Hereditary Erythroblastic Anemia (*fsn/hea*)

The autosomal recessive flaky skin mutation (*fsn*) arose spontaneously in an inbred mouse colony in 1984 (50). The mutation, which mapped to the distal portion of mouse chromosome 17, was initially recognized on the basis of a psoriasis-like skin phenotype accompanied by runting. The animals were also noted to have hypochromic, normocytic anemia that worsened as they aged. Blood smears from *fsn* mice showed anisocytosis and poikilocytosis, with many circulating nucleated red blood cells. Although osmotic fragility was normal, hyperbilirubinemia was present in the context of certain genetic backgrounds, suggesting increased hemolysis (50).

The animals have marked extramedullary hematopoiesis in the liver and spleen. Absence of macrophage iron stores and increased erythrocyte protoporphyrin levels suggested that *fsn* mice have abnormal iron metabolism (50). Intestinal absorption of radiolabeled iron appeared to be increased, but the iron did not distribute normally to sites of erythropoiesis. Surprisingly, a significant fraction of the radiolabeled iron dose appeared to be excreted in the urine 24 h after administration.

The iron phenotype of *fsn* mice has not been characterized further, and the *fsn* gene has not been identified. Interestingly, however, the *fsn* mutation has been shown to be allelic with another mouse mutation, hereditary erythroblastic anemia (*hea*) (51). Mice with the *hea* mutation die by 15–25 days of life from severe anemia characterized by polychromasia, anisocytosis, and poikilocytosis. Large numbers of immature cells, including orthochromatophilic erythroblasts and myeloid precursors, are present in the circulation of *hea* mice. Iron parameters have not been reported for *hea* mice.

6. Hemoglobin Deficit (*hbd*)

The hemoglobin deficit mutation (*hbd*; also called “hemoglobin deficient”) arose spontaneously in an inbred mouse strain in Germany and was recognized as an anemia with autosomal recessive inheritance (52). Although the animals are viable and fertile, they have marked hypochromic, microcytic anemia with abundant target forms. No siderocytes or sideroblasts are seen. Free erythrocyte protoporphyrin and serum iron levels are elevated, suggesting a defect in red-cell iron metabolism (53). The anemia is present at birth, persists throughout life, and is not corrected by parenteral iron therapy (52). The enzymes of heme biosynthesis appear to be intact, placing the defect at the level of erythroid iron procurement.

The transferrin cycle has been studied in reticulocytes from *hbd* homozygotes (54). Double labeling with ¹²⁵I-transferrin and ⁵⁹Fe demonstrated that transferrin binding and uptake were normal, but less iron was retained within the cell. This suggests that the initial steps of the transferrin cycle occur normally, but there is a problem in intracellular iron trafficking. Bone marrow transplantation experiments have confirmed that there is an intrinsic bone marrow defect causing the *hbd* anemia (55). The *hbd* gene has not yet been identified, but it maps to mouse chromosome 19 (56).

B. Induced Mutations

Over the past 15 years it has become possible to deliberately mutate the mouse genome, to inactivate and alter genes in their normal chromosomal context. Targeted disruption of iron-related genes has offered new insights into their functions and physiological roles. The most instructive mutants are discussed below.

1. Transferrin Receptor Knockout

The cell surface transferrin receptor (TfR) is important for cellular uptake of iron bound to circulating transferrin (reviewed in Ref. 40). This process, termed the transferrin cycle, brings iron into specialized endosomes within the cell. Nramp2/DMT1 subsequently carries iron across the endosomal membrane to the cytoplasm. Mammalian TfRs are homodimers of glycosylated 90-kDa polypeptides containing a small N-terminal cytoplasmic domain, a single transmembrane domain, and a large, extra-

cellular ligand-binding domain. TfRs are abundant on the surfaces of developing erythroid precursors, activated lymphocytes, and tumor cells. Other differentiated cells express very little TfR protein. A proteolytic cleavage product of the TfR, termed soluble TfR or serum TfR (sTfR), is detectable in the plasma. Levels of sTfR increase in iron deficiency and in disorders characterized by ineffective erythropoiesis (57).

To determine which cell types require the transferrin cycle for iron uptake, gene targeting was used to inactivate the TfR gene (35). The targeting strategy was designed to modify a murine TfR allele (gene symbol *Tfrr*) such that no membrane bound or soluble TfR protein could be produced. This mutation was transmitted through the mouse germline, and mutant animals were analyzed (35). All animals homozygous for the disrupted TfR allele (*Tfrr*-/-) died in utero from severe anemia. The anemia became apparent in some *Tfrr*-/- embryos as early as embryonic day 9.5 (E9.5). Other embryos were not visibly anemic until E10.5. No *Tfrr*-/- embryos survived past E12.5. Hematopoietic progenitor cells from *Tfrr*-/- yolk sacs did not form normal erythroid colony formation in vitro. In addition to the anemia, *Tfrr*-/- embryos had increased apoptotic cell death in the neuroepithelium, associated with kinking of the developing neural tube. However, their development was otherwise normal. These results led to the conclusion that the transferrin cycle is important for erythropoiesis and development of the nervous system, but dispensable for the differentiation of other issues, at least through E12.5.

Animals heterozygous for the targeted TfR allele (*Tfrr*+/-) also showed phenotypic abnormalities. They were not anemic, but their erythrocytes were microcytic (35). Although liver and spleen iron stores were decreased when compared with wild-type controls, the microcytosis did not appear to result from systemic iron deficiency. Rather, it was associated with decreased levels of cell surface TfR on developing erythroid precursors, suggesting an intrinsic defect in iron uptake by those cells.

Taken together, these results confirm the importance of the transferrin cycle in erythropoiesis. It is interesting that absence of the TfR results in embryonic lethality, whereas severe transferrin deficiency in homozygous *hpx* mice does not. There are several possible explanations for this difference. First, *hpx* mice produce a small amount of an aberrant transferrin protein. It is possible that the mutant protein delivers enough iron to erythroid precursors to prevent prenatal death from anemia. Alternatively, it may be that non-transferrin-bound iron is more available for non-transferrin cycle uptake pathways than is the transferrin-bound iron circulating in animals lacking TfR. Other uptake mechanisms may be more efficient when iron is not tightly complexed to protein.

2. *Hfe* Knockout/Knock-in

The *Hfe* gene is the primary site of mutations in patients with hereditary hemochromatosis. Most patients with classical hemochromatosis are homozygous for a unique missense mutation converting amino acid 282 of the HFE protein from cysteine to tyrosine (C282Y) [(58); see also Chapters 8 and 28]. A subset of the remaining hemochromatosis patients have other mutations in *Hfe* (59–61). As discussed elsewhere in this volume, HFE resembles an atypical major histocompatibility (MHC) class I protein, and binds β_2 -microglobulin. While this homology is intriguing, it has not yielded any insight into the mechanism by which HFE regulates intestinal iron absorption. HFE forms a protein–protein complex with TfR, resulting in decreased

affinity for transferrin (62). However, the role of the HFE-TfR complex in vivo has not been definitively determined.

Three groups have produced mutations in the murine *Hfe* gene (35–65). The first goal was to determine whether hemochromatosis results from a gain or loss of protein function. Targeted disruption of *Hfe* causes iron loading in a pattern similar to that seen in human hemochromatosis patients. Thus, hemochromatosis results from a loss of protein function. The C282Y mutation prevents formation of an intramolecular disulfide bond, perturbing the conformation of HFE and preventing its association with β_2 -microglobulin (66). To determine whether this mutation totally inactivates HFE or simply interferes with its function, Levy and co-workers introduced the C282Y point mutation into an otherwise intact murine *Hfe* gene by targeted mutagenesis (64). They found that mice homozygous for the C282Y mutation also develop iron overload, but to a lesser extent than *Hfe*-null mice. Like human patients, both types of *Hfe*-mutant mice have normal iron levels at birth, followed by rapid iron loading that appears to plateau as the animals age. Interestingly, *Hfe*-mutant mice do not develop the same type of tissue damage seen in human patients; fibrosis cannot be detected in liver or heart, and diabetes does not develop (J. E. Levy and N. C. Andrews, unpublished data).

In addition to establishing that hemochromatosis is due to a partial loss of HFE function, these gene targeting experiments provide useful models for studying the pathophysiology of the disease. By crossing *Hfe*-mutant mice with *mk* mice and *sla* mice, it has been established that iron loading occurs through transport pathways involving Nramp2/DMT1 and hephaestin, respectively (67). The iron-overload phenotype of animals homozygous for *Hfe* mutations is exacerbated by coexisting mutations in either β_2 -microglobulin or TfR genes (67). These observations are intriguing, and place constraints on models of HFE function.

3. β_2 -Microglobulin Knockout

The gene encoding β_2 -microglobulin (*B2m*) was disrupted by targeted mutagenesis in mice to study its role in the immune system (68,69). Predictably, *B2m*-null mice lack MHC class I antigens, and have perturbations of T-cell maturation. Interestingly, they also have abnormalities in iron metabolism. Several years after the mutation was first made, DeSousa and colleagues made the important observation that *B2m*-null mice develop tissue iron overload similar to that seen in hemochromatosis (70). This finding was particularly important because it was made before the *Hfe* gene was identified. It led to the correct prediction that the hemochromatosis gene would be a class I-like molecule.

The iron phenotype of *B2m*-null mice is very similar to that of *Hfe* mutant mice. They have increased intestinal iron absorption, associated with increased serum transferrin saturation and tissue iron deposition, particularly in hepatocytes (70). Interestingly, when *B2m*-null mice are lethally irradiated and transplanted with normal mouse hematopoietic cells, their tissue iron redistributes from hepatic parenchymal cells to macrophages. However, increased intestinal iron absorption persists (70). Intriguingly, when *Hfe*-null mice and *B2m*-null mice are bred to produce compound mutant animals lacking both HFE and β_2 -microglobulin, iron loading is more severe than in animals lacking HFE alone (67). This suggests that there may be another class I-like molecule, in addition to HFE, that interacts with β_2 -microglobulin to regulate iron metabolism.

4. Heme Oxygenase Knockouts

Heme oxygenases catalyze the degradation of heme to biliverdin, carbon monoxide, and free iron. There are at least two physiologically important heme oxygenases in mammals. Heme oxygenase 1 is induced by heme and by oxidative stress. Heme oxygenase 2 is constitutively expressed at high levels in most tissues. These enzymes are thought to play roles in a variety of physiological functions, including neurotransmission and protection against oxidative stress. Heme oxygenase probably also functions in iron metabolism. Most of the body's utilizable iron comes through a macrophage-recycling pathway in which red cell hemoglobin is degraded to release iron. Heme oxygenase probably catalyzes heme degradation. Furthermore, dietary absorption of heme iron involves a heme catabolism step, presumably within the absorptive enterocytes of the intestine.

Heme oxygenase 1 deficiency has been reported in one patient (71). A young boy presented with growth delay, rash, recurrent fevers, hematuria, and proteinuria associated with hepatomegaly and asplenia. He had marked intravascular hemolysis resulting in anemia. Surprisingly, however, his serum haptoglobin levels were high, and bilirubin levels were low. He had clear evidence of systemic endothelial cell damage. Iron deposition was apparent in the liver and kidneys. Different mutations were found in each of his heme oxygenase 1 alleles, leading to a total deficiency of heme oxygenase protein.

This phenotype is remarkably similar to that observed in mice with heme oxygenase 1 deficiency. Targeted disruption of the murine heme oxygenase 1 gene deleted approximately 85% of the coding sequence to generate a null allele (72). Only a small fraction of the homozygous null animals survive to weaning age. The null mice are smaller than their littermates, but otherwise indistinguishable until approximately 5 months of age. At that time they appear ill, with microcytic anemia, hypoferremia, iron accumulation in the liver and kidneys, and premature mortality. Hepatic iron is present in both parenchymal cells and Kupffer cells. In contrast to the human patient, the spleens are present, but do not show iron accumulation. There is evidence of chronic systemic inflammation and endothelial cell damage, suggesting a component of anemia of chronic inflammation. In contrast, mice deficient in the constitutive enzyme, heme oxygenase 2, do not show an iron phenotype under normal conditions. These findings are consistent with a role for heme oxygenase 1 in cellular iron metabolism, but they do not suggest a straightforward model for its role. Other mechanisms may be involved in removing iron from heme for reuse.

5. Ceruloplasmin Knockout

Ceruloplasmin, a multicopper oxidase, has been suspected of having a role in iron metabolism since its ferroxidase activity was characterized almost 40 years ago (73). A clue to its function came from studies of copper-deficient pigs that developed iron deficiency anemia. Administration of ceruloplasmin corrected the anemia (74). It has gradually become clear that a major function of ceruloplasmin is to aid in exporting iron from cells. Human patients who are homozygous for mutations in the ceruloplasmin gene have a distinct iron-loading phenotype, with accumulation of the metal in the liver, macrophages, pancreas, and central nervous system [(75–79); see also Chapter 30]. At present there is no effective treatment for this disorder. Patients suffer

from progressive neurodegenerative disease, diabetes, and hepatic siderosis. Aceruloplasminemia is fatal in middle age as a consequence of iron deposition in the basal ganglia. Importantly, affected patients have no obvious defect in copper metabolism per se, emphasizing the fact that the copper moieties in ceruloplasmin are important for its enzymatic activity, and not for plasma copper transport.

Targeted disruption of the murine ceruloplasmin gene has provided a mouse model of aceruloplasminemia and allowed careful study of its pathogenesis. A portion of the gene encoding critical copper-associated residues was removed to create a null allele (80). Heterozygous mice are not affected. Homozygous null mice have little or no detectable serum ferroxidase activity. They are normal at birth, but develop iron overload on standard mouse chow, with liver and spleen iron levels 3–6 times normal by 1 year of life. Both hepatocytes and macrophages are affected; marked reticuloendothelial iron accumulation is particularly noticeable in the spleen.

Ferroketic studies indicated that there is a defect in iron efflux from recycling endothelial macrophages (80). This was corrected by administration of exogenous ceruloplasmin. Similarly, when normal and ceruloplasmin-deficient mice were phlebotomized to induce anemia, ceruloplasmin-deficient mice could not increase their plasma iron turnover to compensate for the anemia, as normal animals could. Iron was not effectively mobilized from reticuloendothelial cells or hepatocytes. Thus, ceruloplasmin appears to function systemically in a manner analogous to the function proposed for its homolog, hephaestin, in absorptive intestinal cells (23).

These studies confirm the importance of ceruloplasmin in normal iron metabolism. They provide *in vivo* evidence against the hypothesis that ceruloplasmin is important for cellular iron uptake (81). It will be interesting to analyze compound mutant animals, lacking both ceruloplasmin and hephaestin, to determine whether mice can survive when neither of these proteins is present to provide ferroxidase activity.

6. H-Ferritin Knockout

Ferritin is ubiquitously expressed in prokaryotic and eukaryotic cells. It serves the essential function of sequestering iron within cells, to prevent toxicity. Mammalian holoferritin is a 24-subunit multimer made up of varying ratios of L-ferritin and H-ferritin polypeptides, and containing up to 4000 atoms of iron (reviewed in Ref. 82; see also Chapter 5). H-ferritin has a ferroxidase activity that is important for iron incorporation (83).

The gene encoding H-ferritin (*Fth*) has been inactivated by targeted disruption in mice (84). H-ferritin is essential for early embryonic development. Embryos can survive at least until the 64-cell stage, but no homozygous *Fth*^{-/-} embryos can be found at embryonic day 9.5 (84). This suggests that L-ferritin alone cannot substitute after maternal ferritin is depleted. In contrast, heterozygous mice lacking one *Fth* allele are viable and grossly indistinguishable from their normal littermates. Interestingly, they have half-normal levels of ferritin mRNA and protein in all tissues examined, indicating that there is no corresponding increase in expression of the intact ferritin allele at the level of transcription or translation. The absence of a phenotype in these animals indicates that, in spite of lower levels, the amount of H-ferritin produced is not limiting. Further insights may be gleaned from future studies of animals lacking L-ferritin.

C. The Belgrade (*b*) Rat

In 1969, an anemic rat model with microcytic red blood cells was described in Yugoslavia (85). This animal, the Belgrade (*b*) rat, has high serum iron levels associated with decreased iron uptake by reticulocytes and decreased hemoglobin production (86). Edwards and co-workers used an elegant double-labeling experiment to demonstrate that this defect is distal to the transferrin cycle (87). They bound ^{59}Fe to ^{125}I -labeled transferrin, and allowed the holotransferrin to be taken up by reticulocytes in vitro. At 60 min the uptake of transferrin was significantly greater in the *b* reticulocytes, but the retention of radiolabeled iron was significantly less. This study was subsequently reproduced by others (54,88). In-vivo experiments extended these observations, by showing that erythroid precursors in *b* animals had decreased iron uptake (89). The defect had to be either in unloading of iron from transferrin within transferrin cycle endosomes, or export of iron from those endosomes to the cytoplasm. Accordingly, treatment of erythroid precursors with a lipophilic iron chelate, ferric salicylaldehyde isonicotinoyl hydrazone, restored hemoglobin synthesis in *b* cells by bypassing the transferrin cycle to deliver iron directly to the cytoplasm (90).

Subsequently, it was discovered that *b* animals also have decreased intestinal iron absorption, and it was proposed that the *b* defect altered a transmembrane iron carrier protein (91,92). Intriguingly, *b* animals also develop manganese deficiency, due to decreased absorption of dietary manganese (93).

All of these findings were explained when it was discovered that the *b* rat, like the *mk* mouse, has a deleterious mutation in the gene encoding the iron transporter DMT1 (94). Remarkably, the mutation in *b* animals results in the same amino acid substitution, G185R, introducing a charged, bulky amino acid into the fourth predicted transmembrane domain of the transporter protein. The *b* DMT1 molecule, similar to the *mk* DMT1 molecule, has very little iron transport capability when expressed in transfected cells (11,94). These results complement the understanding of DMT1 that was gleaned from studying *mk* animals. DMT1 is important for transmembrane iron transport in both absorptive enterocytes and transferrin cycle endosomes in rodents. While it is very likely that it has similar importance in humans, this has not yet been formally proven. To date, no mutations have been reported in the human gene encoding DMT1.

III. A ZEBRAFISH MODEL

The *weissherbst* (*weh*) mutation in the zebrafish *Danio rerio* results in a severe hypochromic anemia (95). Two independent alleles (*weh*^{h238} and *weh*^{tp85c}) were produced and identified as part of a large-scale screen for ethyl nitrosourea-induced mutations (96). The erythroid cells in both mutants are normal in number at 33 and 48 h postfertilization, but severely deficient in hemoglobin (95). After that time there is a progressive decrease in red cell numbers, though some hemoglobin is detected at 72 h postfertilization. Animals with the *weh*^{h238} allele are more severely affected than those with the *weh*^{tp85c} allele. The red cells are abnormal, with immature features and persistence of embryonic globin mRNA expression. Nonhematopoietic organogenesis is intact. All mutant animals die between day 7 and day 14 of development,

apparently from severe anemia (95). It was found that *weh* mutants had 4- to 9-fold less iron in their erythroid cells than did normal zebrafish at the same stage. The mutation resulted in lower levels of circulating iron, rather than an erythroid iron-utilization defect, because injected iron dextran fully rescued the phenotype.

The *weh* gene was identified by positional cloning (95). It encodes a protein of 562 amino acids, now called ferroportin1. The *weh*^{th238} allele contains a missense mutation that results in premature translational termination at codon 361. The *weh*^{lp85} allele contains a missense mutation changing amino acid 167 from leucine to phenylalanine. Zebrafish ferroportin1 mRNA is not expressed in erythroid cells, consistent with the observation that injected iron dextran rescues the anemia phenotype. It is expressed in the yolk syncytial layer surrounding the developing embryo. Nutrients must pass through this layer to be transferred from the yolk to the embryo. At 18 h postfertilization, the site of greatest ferroportin1 expression corresponds to the portion of the yolk syncytial layer that lies just below the developing hematopoietic cells in the intermediate cell mass. Later, it is in the region of the yolk syncytial layer over which blood flows. These results suggest that ferroportin1 is involved in transport of iron from the yolk to the embryo. Injection of ferroportin1 mRNA into *weh* mutant embryos partially rescues the mutant phenotype, confirming that ferroportin1 is the *weh* gene product. Expression of ferroportin1 in *Xenopus* oocytes has shown that the protein is involved in export of iron from cells (95). A similar result was obtained by a second group, who reported cloning of mammalian *ferroportin1* (termed *Ireg1* in their report) by subtractive isolation of mRNAs involved in iron transport [(97); see also Chapter 7]. They further showed that the ferroportin1 mRNA contains a bona-fide iron-responsive RNA element in its 5'-untranslated region, suggesting that its expression is regulated by intracellular iron concentration at the level of translation. More ferroportin1 mRNA is detectable in intestinal samples from mice subjected to iron deficiency or hypoxia (97).

Mammalian ferroportin1 is widely expressed, but levels are particularly high in murine intestine, placenta, liver, spleen, and kidney (95,97). It is not expressed in erythroid precursors. Immunohistochemical staining demonstrates that mouse ferroportin1 is localized along the basolateral membrane of absorptive duodenal enterocytes, and on the basal surface of the placental syncytiotrophoblast adjacent to the fetal circulation. Both locations are consistent with a role in cellular iron export (95). Ferroportin1 is also highly expressed in mammalian liver and spleen macrophages, suggesting a role in iron recycling. Thus, it is present in most cell types known to have important iron export functions: the absorptive duodenal enterocyte, the placental syncytiotrophoblast, and the iron-handling reticuloendothelial macrophage.

IV. CONCLUSIONS

Over the past 4 years, genetic analyses of mice, rats, and zebrafish have contributed substantially to our understanding of iron metabolism. New genes have been identified, and known genes have been characterized *in vivo*. These efforts have been important for progress in this field. Iron transport is difficult to study biochemically, because transport molecules are often highly hydrophobic proteins expressed at low levels. Furthermore, a true understanding of iron homeostasis requires manipulation of living animals; the basis of iron balance will never be worked out from test-tube

Table 1 Animal Models with Inherited Defects in Iron Metabolism

Mutation	Chromosome	Gene symbol	Comments
Mouse			
Microcytic anemia (<i>mk</i>)	15	<i>Slc11a2</i>	G185R mutation in DMT1 transmembrane iron transporter
Sex-linked anemia (<i>sla</i>)	X	<i>heph</i>	Deletion mutation in hephaestin membrane-associated ferroxidase
Hypotransferrinemia (<i>hpx</i>)	9	<i>Trf</i>	Splice donor mutation in transferrin plasma iron carrier
Flexed tail (<i>f</i>)	13	<i>sfxn1</i>	Frameshift mutation in sideroflexin mitochondrial membrane protein; function unknown
Flaky skin/hereditary erythroblastic anemia (<i>fsn/hea</i>)	17	<i>fsn, hea</i>	Gene not yet known, <i>hea</i> a more severe allele than <i>fsn</i> ; hemolytic anemia, perturbed iron metabolism
Hemoglobin deficit	19	<i>hbd</i>	Gene not yet known
Transferrin receptor knockout	16	<i>Trfr</i>	Targeted disruption of <i>Trfr</i>
Hfe knockout/knock-in	13	<i>Hfe</i>	Mouse model of hemochromatosis; targeted disruption, introduction of C282Y mutation
Beta-2 microglobulin knockout	2	<i>B2m</i>	Mouse model of hemochromatosis; targeted disruption
Heme oxygenase knockouts	8	<i>Hmox1</i>	Targeted disruption
	16	<i>Hmox2</i>	Targeted disruption
Ceruloplasmin knockout	9	<i>Cp</i>	Targeted disruption
H-ferritin knockout	19	<i>Fth</i>	Targeted disruption
Rat			
Belgrade (<i>b</i>) rat	7	<i>Nramp2</i>	G185R mutation in DMT1 transmembrane iron transporter (import)
Zebrafish			
<i>Weissherbst</i> (<i>weh</i>)		<i>Fpn1</i>	Missense and termination mutations in ferroportin 1 transmembrane iron transporter (export)

experiments alone. The animal models described in this chapter offer new tools for investigating this question. The current list of known mutants of iron metabolism, shown in Table 1, will almost certainly be expanded over the next few years as more animal models of human iron-related diseases are discovered and generated. Breeding of mutants to each other, as has already been done with *Hfe* mutant mice (67), will help elucidate the functional relationships among the proteins of iron metabolism.

REFERENCES

1. Nash DJ, Kent E, Dickie MM, Russell ES. The inheritance of "mick," a new anemia in the house mouse [abstr]. *Am Zool* 1964; 4:404–405.
2. Russell ES, McFarland EC, Kent EL. Low viability, skin lesions, and reduced fertility associated with microcytic anemia in the mouse. *Transplant Proc* 1970; 2:144–151.
3. Bannerman RM, Edwards JA, Kreimer-Birnbaum M, McFarland E, Russell ES. Hereditary microcytic anaemia in the mouse; studies in iron distribution and metabolism. *Br J Haematol* 1972; 23:235–245.
4. Harrison DE. Marrow transplantation and iron therapy in mouse hereditary microcytic anemia. *Blood* 1972; 40:893–901.
5. Landaw SA, Russell ES, Bernstein SE. Splenic destruction of newly-formed red blood cells and shortened erythrocyte survival in mice with congenital microcytosis. *Scand J Haematol* 1970; 7:516–524.
6. Edwards JA, Hoke JE. Red cell iron uptake in hereditary microcytic anemia. *Blood* 1975; 46:381–388.
7. Edwards JA, Hoke JE. Defect of intestinal mucosal iron uptake in mice with hereditary microcytic anemia. *Proc Soc Exp Biol Med* 1972; 141:81–84.
8. McFarland EC, Russell ES. Microcytic anemia (*mk*) has been located close to Ca on chromosome 15. *Mouse News Lett* 1975; 53:35.
9. Fleming MD, Trenor CC, Su MA, et al. Microcytic anemia mice have a mutation in *Nramp2*, a candidate iron transporter gene. *Nature Genet* 1997; 16:383–386.
10. Gunshin H, Mackenzie B, Berger UV, et al. Cloning and characterization of a mammalian proton-coupled metal-ion transporter. *Nature* 1997; 388:482–488.
11. Su MA, Trenor CC, Fleming JC, Fleming MD, Andrews NC. The G185R mutation disrupts function of iron transporter *Nramp2*. *Blood* 1998; 92:2157–2163.
12. Falconer DS, Isaacson JH. The genetics of sex-linked anaemia in the mouse. *Genet Res* 1962; 3:248–250.
13. Grewal MD. A sex-linked anaemia in the mouse. *Genet Res* 1962; 3:238–247.
14. Bannerman RM, Cooper RG. Sex-linked anemia: A hypochromic anemia of mice. *Science* 1966; 151:581–582.
15. Bennett M, Pinkerton PH, Cudkowicz G, Bannerman RM. Hemopoietic progenitor cells in marrow and spleen of mice with hereditary iron deficiency anemia. *Blood* 1968; 32:908–921.
16. Pinkerton PH, Bannerman RM, Doebelin TD, Benisch BM, Edwards JA. Iron metabolism and absorption studies in the X-linked anaemia of mice. *Br J Haematol* 1970; 18:211–228.
17. Kingston PJ, Bannerman CE, Bannerman RM. Iron deficiency anaemia in newborn *sla* mice: A genetic defect of placental iron transport. *Br J Haematol* 1978; 40:265–276.
18. Edwards JA, Bannerman RM. Hereditary defect of intestinal iron transport in mice with sex-linked anemia. *J Clin Invest* 1970; 49:1869–1871.
19. Manis J. Intestinal iron-transport defect in the mouse with sex-linked anemia. *Am J Physiol* 1971; 220:135–139.
20. Pinkerton PH. Histological evidence of disordered iron transport in the X-linked hypochromic anaemia of mice. *J Pathol Bacteriol* 1968; 95:155–165.
21. Bedard YC, Pinkerton PH, Simon GT. Uptake of circulating iron by the duodenum of normal mice and mice with altered iron stores, including sex-linked anemia. High resolution radioautographic study. *Lab Invest* 1976; 34:611–615.
22. Flanagan PR, Haist J, MacKenzie I, Valberg LS. Intestinal absorption of zinc: Competitive interactions with iron, cobalt and copper in mice with sex-linked anemia (*sla*). *Can J Physiol Pharmacol* 1984; 62:1124–1128.
23. Vulpe CD, Kuo YM, Murphy TL, et al. Hephaestin, a ceruloplasmin homologue impli-

- cated in intestinal iron transport, is defective in the sla mouse. *Nature Genet* 1999; 21: 195–199.
24. Bernstein SE. Hereditary hypotransferrinemia with hemosiderosis, a murine disorder resembling human atransferrinemia. *J Lab Clin Med* 1987; 110:690–705.
 25. Heilmeyer L, Keller W, Vivell O, et al. Congenital transferrin deficiency in a seven-year old girl. *German Med Monthly* 1961; 86:1745–1751.
 26. Heilmeyer L. Atransferrinemias [German]. *Acta Haematol* 1966; 36:40.
 27. Goya N, Miyazaki S, Kodate S, Ushio B. A family of congenital atransferrinemia. *Blood* 1972; 40:239–245.
 28. Hamill RL, Woods JC, Cook BA. Congenital atransferrinemia: A case report and review of the literature. *Am J Clin Pathol* 1991; 96:215–218.
 29. Hayashi A, Wada Y, Suzuki T, Shimizu A. Studies on familial hypotransferrinemia: Unique clinical course and molecular pathology. *Am J Hum Genet* 1993; 53:201–213.
 30. Craven CM, Alexander J, Eldridge M, et al. Tissue distribution and clearance kinetics of non-transferrin-bound iron in the hypotransferrinemic mouse: A rodent model for hemochromatosis. *Proc Natl Acad Sci USA* 1987; 84:3457–3461.
 31. Trenor CC, Campagna DR, Sellers VM, Andrews NC, Fleming MD. The molecular defect in hypotransferrinemic mice. *Blood* 2000; in press.
 32. Raja KB, Simpson RJ, Peters TJ. Plasma clearance of transferrin in control and hypotransferrinaemic mice: Implications for regulation of transferrin turnover. *Br J Haematol* 1995; 89:177–180.
 33. Dickinson T, Connor JR. Histological analysis of selected brain regions of hypotransferrinemic mice. *Brain Res* 1994; 635:169–178.
 34. Huggenvik JI, Craven CM, Idzerda RL, et al. A splicing defect in the mouse transferrin gene leads to congenital atransferrinemia. *Blood* 1989; 74:482–486.
 35. Levy JE, Jin O, Fujiwara Y, Kuo F, Andrews NC. Transferrin receptor is necessary for development of erythrocytes and the nervous system. *Nature Genet* 1999; 21:396–399.
 36. Simpson RJ, Lombard M, Raja KB, Thatcher R, Peters TJ. Iron absorption by hypotransferrinaemic mice. *Br J Haematol* 1991; 78:565–570.
 37. Raja KB, Simpson RJ, Peters TJ. Intestinal iron absorption studies in mouse models of iron overload. *Br J Haematol* 1994; 86:156–162.
 38. Buys SS, Martin CB, Eldridge M, Kushner JP, Kaplan J. Iron absorption in hypotransferrinemic mice. *Blood* 1991; 78:3288–3290.
 39. Finch C. Regulators of iron balance in humans. *Blood* 1994; 84:1697.
 40. Andrews NC. Medical progress: Disorders of iron metabolism. *N Engl J Med* 1999; 341:1986–1995.
 41. Hunt HR, Mixter R, Permar D. Flexed tail in the mouse, *Mus musculus*. *Genetics* 1933; 18:335–366.
 42. Clark FH. The inheritance and linkage relations of a new recessive spotting mutation in the house mouse. *Genetics* 1934; 19:365–393.
 43. Gruneberg H. The anaemia of flexed-tail mice: I. Static and dynamic haematology. *J Genet* 1942; 43:45–68.
 44. Russell ES, Thompson MW, McFarland EC. Analysis of effects of *W* and *f* genic substitutions on fetal mouse hematology. *Genetics* 1968; 58:259–270.
 45. Gruneberg H. Siderocytes: A new kind of erythrocytes. *Nature* 1941; 148:114.
 46. Gruneberg H. “Siderocytes” in man? *Lancet* 1941; 241:172.
 47. Gruneberg H. Siderocytes in man. *Nature* 1941; 148:469.
 48. Gruneberg H. The anemia of flexed-tailed mice. II. Siderocytes. *J Genet* 1942; 44:246–270.
 49. Thompson MW, McCulloch EA, Siminovitch L, Till JE. The cellular basis for the defect in haemopoiesis in flexed-tailed mice. I. The nature and persistence of the defect. *Br J Haematol* 1966; 12:152–160.

50. Beamer WG, Pelsue SC, Shultz LD, Sundberg JP, Barker JE. The flaky skin (*fsn*) mutation in mice: Map location and description of the anemia. *Blood* 1995; 86:3220–3226.
51. White RA, Hummel GS, Copple A, et al. Characterization and chromosomal mapping of the hereditary erythroblastic anemia (*hea*) mouse mutation: A potential iron transport defect [abstr]. *Blood* 1998; 92(suppl 1):326a.
52. Scheufler VH. Eine weitere Mutante der Hausmaus mit Anämie (*hbd*). *Z Versuchstierk* 1969; 11:348–353.
53. Bannerman RM, Garrick LM, Rusnak-Smalley P, Hoke JE, Edwards JA. Hemoglobin deficit: An inherited hypochromic anemia in the mouse. *Proc Soc Exp Biol Med* 1986; 182:52–57.
54. Garrick LM, Edwards JA, Hoke JE, Bannerman RM. Diminished acquisition of iron by reticulocytes from mice with hemoglobin deficit. *Exp Hematol* 1987; 15:671–675.
55. Bloom ML, Simon-Stoos KL. The hemoglobin-deficit mouse: Analysis of phenotype and hematopoiesis in the transplant model. *Blood* 1997; 90:2062–2067.
56. Bloom ML, Simon-Stoos KL, Mabon ME. The hemoglobin-deficit mutation is located on mouse chromosome 19. *Mammal Genome* 1998; 9:666–667.
57. Cook JD. The measurement of serum transferrin receptor. *Am J Med Sci* 1999; 318:269–276.
58. Feder JN, Gnirke A, Thomas W, et al. A novel MHC class I-like gene is mutated in patients with hereditary haemochromatosis. *Nature Genet* 1996; 13:399–408.
59. Barton JC, Sawada-Hirai R, Rothenberg BE, Acton RT. Two novel missense mutations of the *HFE* gene (I105T and G93R) and identification of the S65C mutation in Alabama hemochromatosis probands. *Blood Cells Mol Dis* 1999; 25:147–155.
60. Mura C, Ragueues O, Ferec C. *HFE* mutations analysis in 711 hemochromatosis probands: Evidence for S65C implication in mild form of hemochromatosis. *Blood* 1999; 93:2502–2505.
61. Wallace DF, Dooley JS, Walker AP. A novel mutation of *HFE* explains the classical phenotype of genetic hemochromatosis in a C282Y heterozygote. *Gastroenterology* 1999; 116:1409–1412.
62. Lebron JA, Bjorkman PJ. The transferrin receptor binding site on HFE, the class I MHC-related protein mutated in hereditary hemochromatosis. *J Mol Biol* 1999; 289:1109–1118.
63. Zhou XY, Tomatsu S, Fleming RE, et al. *HFE* gene knockout produces mouse model of hereditary hemochromatosis. *Proc Natl Acad Sci USA* 1998; 95:2492–2497.
64. Levy JE, Montross LK, Cohen DE, Fleming MD, Andrews NC. The C282Y mutation causing hereditary hemochromatosis does not produce a null allele. *Blood* 1999; 94:9–11.
65. Bahram S, Gilfillan S, Kuhn LC, et al. Experimental hemochromatosis due to MHC class I HFE deficiency: Immune status and iron metabolism. *Proc Natl Acad Sci USA* 1999; 96:13312–13317.
66. Waheed A, Parkkila S, Zhou XY, et al. Hereditary hemochromatosis: Effects of C282Y and H63D mutations on association with beta2-microglobulin, intracellular processing, and cell surface expression of the HFE protein in COS-7 cells. *Proc Natl Acad Sci USA* 1997; 94:12384–12389.
67. Levy JE, Montross LK, Andrews NC. Genes that modify the hemochromatosis phenotype in mice. *J Clin Invest* 2000; in press.
68. Zijlstra M, Bix M, Simister NE, et al. Beta 2-microglobulin deficient mice lack CD4-8+ cytolytic T cells. *Nature* 1990; 344:742–746.
69. Koller BH, Marrack P, Kappler JW, Smithies O. Normal development of mice deficient in beta 2M, MHC class I proteins, and CD8+ T cells. *Science* 1990; 248:1227–1230.
70. Santos M, Schilham MW, Rademakers LHPM, et al. Defective iron homeostasis in beta2-microglobulin knockout mice recapitulates hereditary hemochromatosis in man. *J Exp Med* 1996; 184:1975–1985.

71. Yachie A, Niida Y, Wada T, et al. Oxidative stress causes enhanced endothelial cell injury in human heme oxygenase-1 deficiency. *J Clin Invest* 1999; 103:129–135.
72. Poss KD, Tonegawa S. Heme oxygenase 1 is required for mammalian iron reutilization. *Proc Natl Acad Sci USA* 1997; 94:10919–10924.
73. Osaki S, Johnson DA, Frieden E. The possible significance of the ferrous oxidase activity of ceruloplasmin in normal human serum. *J Biol Chem* 1966; 241:2746–2751.
74. Lee GR, Nacht S, Lukens JN, Cartwright GE. Iron metabolism in copper-deficient swine. *J Clin Invest* 1968; 47:2058–2069.
75. Morita H, Ikeda S, Yamamoto K, et al. Hereditary ceruloplasmin deficiency with hemosiderosis: A clinicopathological study of a Japanese family. *Ann Neurol* 1995; 37: 646–656.
76. Yoshida K, Furihata K, Takeda S, et al. A mutation in the ceruloplasmin gene is associated with systemic hemosiderosis in humans. *Nature Genet* 1995; 9:267–272.
77. Harris ZL, Takahashi Y, Miyajima H, et al. Aceruloplasminemia: Molecular characterization of this disorder of iron metabolism. *Proc Natl Acad Sci USA* 1995; 92:2539–2543.
78. Harris ED. The iron-copper connection: The link to ceruloplasmin grows stronger. *Nutr Rev* 1995; 53:170–173.
79. Harris ZL, Klomp LW, Gitlin JD. Aceruloplasminemia: An inherited neurodegenerative disease with impairment of iron homeostasis. *Am J Clin Nutr* 1998; 67:972S–977S.
80. Harris ZL, Durley AP, Man TK, Gitlin JD. Targeted gene disruption reveals an essential role for ceruloplasmin in cellular iron efflux. *Proc Natl Acad Sci USA* 1999; 96:10812–10817.
81. Mukhopadhyay CK, Attieh ZK, Fox PL. Role of ceruloplasmin in cellular iron uptake. *Science* 1998; 279:714–717.
82. Aisen P, Wessling-Resnick M, Leibold EA. Iron metabolism. *Curr Opin Chem Biol* 1999; 3:200–206.
83. Levi S, Luzzago A, Cesareni G, et al. Mechanism of ferritin iron uptake: Activity of the H-chain and deletion mapping of the ferro-oxidase site. A study of iron uptake and ferro-oxidase activity of human liver, recombinant H-chain ferritins, and two H-chain deletion mutants. *J Biol Chem* 1988; 263:18086–18092.
84. Ferreira C, Bucchini D, Martin ME, et al. Early embryonic lethality of H ferritin gene deletion in mice. *J Biol Chem* 2000; 275:3021–3024.
85. Sladic-Simic D, Martinovich PN, Zivkovic N, et al. A thalassemia-like disorder in Belgrade laboratory rats. *Ann NY Acad Sci* 1969; 165:93–99.
86. Edwards JA, Garrick LM, Hoke JE. Defective iron uptake and globin synthesis by erythroid cells in the anemia of the Belgrade laboratory rat. *Blood* 1978; 51:347–357.
87. Edwards JA, Sullivan AL, Hoke JE. Defective delivery of iron to the developing red cell of the Belgrade laboratory rat. *Blood* 1980; 55:645–648.
88. Bowen BJ, Morgan EH. Anemia of the Belgrade rat: Evidence for defective membrane transport of iron. *Blood* 1987; 70:38–44.
89. Edwards J, Huebers H, Kunzler C, Finch C. Iron metabolism in the Belgrade rat. *Blood* 1986; 67:623–628.
90. Garrick LM, Gniecko K, Hoke JE, et al. Ferric-salicylaldehyde isonicotinoyl hydrazone, a synthetic iron chelate, alleviates defective iron utilization by reticulocytes of the Belgrade rat. *J Cell Physiol* 1991; 146:460–465.
91. Farcich EA, Morgan EH. Diminished iron acquisition by cells and tissues of Belgrade laboratory rats. *Am J Physiol* 1992; 262:R220–R224.
92. Oates PS, Morgan EH. Defective iron uptake by the duodenum of Belgrade rats fed diets of different iron contents. *Am J Physiol* 1996; 270:G826–G832.
93. Chua AC, Morgan EH. Manganese metabolism is impaired in the Belgrade laboratory rat. *J Comp Physiol* 1997; 167:361–369.

94. Fleming MD, Romano MA, Su MA, et al. Nramp2 is mutated in the anemic Belgrade (b) rat: Evidence of a role for Nramp2 in endosomal iron transport. *Proc Natl Acad Sci USA* 1998; 95:1148–1153.
95. Donovan A, Brownlie A, Zhou Y, et al. Positional cloning of zebrafish ferroportin1 identifies a conserved vertebrate iron exporter [in process citation]. *Nature* 2000; 403: 776–781.
96. Haffter P, Granato M, Brand M, et al. The identification of genes with unique and essential functions in the development of the zebrafish, *Danio rerio*. *Development* 1996; 123:1–36.
97. McKie AT, Marciani P, Rolfs A, et al. A novel duodenal iron-regulated transporter, IREG1, implicated in the basolateral transfer of iron to the circulation. *Mol Cell* 2000; 5:299–309.

Hemochromatosis

Diagnosis and Management Following the Discovery of the Gene

PAUL C. ADAMS

University of Western Ontario, London, Ontario, Canada

I.	INTRODUCTION	700
II.	HISTORY OF HEMOCHROMATOSIS	700
III.	CLINICAL FEATURES OF HEMOCHROMATOSIS	701
	A. Liver Disease	701
	B. Diabetes in Hemochromatosis	702
	C. Cardiac Disease in Hemochromatosis	703
	D. Arthropathy of Hemochromatosis	703
	E. Endocrine Abnormalities	704
	F. Pigmentation of the Skin	704
	G. Fatigue	704
IV.	DIAGNOSIS OF HEMOCHROMATOSIS	704
	A. Underdiagnosis of Hemochromatosis	704
	B. Diagnostic Tests for Hemochromatosis	705
V.	TREATMENT OF HEMOCHROMATOSIS	713
VI.	POPULATION SCREENING FOR HEMOCHROMATOSIS	714
	A. Target Populations to Screen for Hemochromatosis	714
	B. Cost Models of Screening for Hemochromatosis	714
	C. Phenotypic Screening for Hemochromatosis	714
	D. Genetic Population Screening for Hemochromatosis	715
VII.	DIFFERENTIAL DIAGNOSIS OF HEMOCHROMATOSIS	716
	A. Iron Overload in Alcoholic and Viral Hepatitis	716
	B. Porphyria Cutanea Tarda	717

C. Iron-Loading Anemias	718
D. Miscellaneous Iron-Overload Syndromes	718
VIII. SUMMARY	719
REFERENCES	719

I. INTRODUCTION

Hemochromatosis is the most common genetic disease in populations of European ancestry. Despite estimates in different countries ranging from 1 in 100 to 1 in 300, many physicians consider hemochromatosis to be a rare disease. The diagnosis can be elusive because of the nonspecific nature of the symptoms. With the discovery of the hemochromatosis gene in 1996 (1) came new insight into the pathogenesis of the disease, and new diagnostic strategies.

A fundamental issue that has arisen since the discovery of the *HFE* gene is whether the disease "hemochromatosis" should be defined strictly on phenotypic criteria such as the degree of iron overload (transferrin saturation, ferritin, liver biopsy, hepatic iron concentration, or iron removed by venesection therapy), or whether the condition should be defined as a familial disease in Europeans most commonly associated with the C282Y mutation of the *HFE* gene and varying degrees of iron overload. Since the genetic test has been widely used as a diagnostic tool, most studies now utilize a combination of phenotypic and genotypic criteria for the diagnosis of hemochromatosis. It is important to realize that there are many causes of iron overload other than hemochromatosis (Table 1).

II. HISTORY OF HEMOCHROMATOSIS

In 1865, Trousseau described an association among cirrhosis of the liver, diabetes, pancreatic disease, and pigmentation of the skin. These clinical features are associated with advanced disease and are now uncommonly seen by clinicians. The term hemochromatosis was used by Von Recklinghausen in 1889 because he suspected that the increased pigment came from the blood. Many variations in the nomenclature have been suggested (e.g., *HFE*-linked hemochromatosis, hereditary hemochromatosis, iron overload disease). In 1935, Sheldon published his classic monograph on 311 cases (2). The relative roles of genes and alcoholism were debated for many years, but the familial aspects of the disease were clearly elucidated in pedigree studies by Simon in Brittany, France, in 1977, including a close linkage of the disease to the human leukocyte antigen (HLA) complex on chromosome 6 (3). Genetic studies concentrated on this region of the chromosome, but informative genetic recombinations were rarely found. The hemochromatosis gene (*HFE*) was finally discovered a long distance from the HLA complex by Mercator Genetics in 1996 (1). This discovery led to the development of a simple genetic blood test which has demonstrated that more than 90% of typical hemochromatosis patients are homozygous for the C282Y mutation of the *HFE* gene (4). The relationship between the *HFE* gene and the iron overload of hemochromatosis has been discussed previously (5).

Table 1 Differential Diagnosis of Iron Overload

HFE-related hemochromatosis
C282Y homozygotes (95%)
C282Y/H63D compound heterozygotes (4%)
H63D homozygotes (1%)
Non-HFE-related hemochromatosis
Familial (rarely described in Italy)
Nonfamilial (may be a heterogeneous collection of conditions resulting in iron overload)
Juvenile hemochromatosis (young adults with cardiac and endocrine dysfunction) (17)
Neonatal hemochromatosis (96)
Miscellaneous iron overload
African-American iron overload (90,97)
African iron overload (87)
Polynesian iron overload (91)
Transfusional iron overload
Insulin resistance-related iron overload (15)
Aceruloplasminemia (98)
Alcoholic siderosis
Iron overload secondary to end-stage cirrhosis (32)
Porphyria cutanea tarda (85)
Post-portacaval shunt (88)

Most patients with hemochromatosis can trace their ancestry to Northern Europe. Because of the high prevalence of hemochromatosis in Brittany, it has been hypothesized that the original couple with hemochromatosis were born in Brittany around 800 A.D. Since the Vikings were exploring this area extensively during those years, it is possible that some of the original genes were of Nordic ancestry. Further evidence for this hypothesis comes from the high prevalence of the *HFE* gene in Iceland, which was explored by the Vikings but not by French explorers (6). We are left now with a biblical concept that all patients today with hemochromatosis descended from this original couple with hemochromatosis.

III. CLINICAL FEATURES OF HEMOCHROMATOSIS

A. Liver Disease

Although hemochromatosis is often classified as a liver disease, it should be emphasized that it is a systemic, genetic disease with multisystem involvement. The liver has been central to both the diagnosis and prognosis of hemochromatosis. Hepatic iron deposition is common in hemochromatosis because it is the first stop on the pathway after enhanced intestinal iron absorption. The liver has a great capacity to accumulate iron within hepatocytes, initially without any obvious sequelae in terms of clinical symptoms or abnormal liver biochemistry. Since hepatic iron presumably accumulates from birth in this genetic disease, one would predict a relationship between iron and age. However, this may only apply serially within an individual patient, since the correlation coefficient between age and hepatic iron concentration was not significant in 410 homozygotes ($r = 0.07$, $p = 0.12$) (7).

Hepatomegaly remains one of the more common physical signs in hemochromatosis, but it may not be present in the young asymptomatic homozygote. In older studies in which patients presented with clinical features of chronic liver disease in the fifth or sixth decade, cirrhosis was invariably present. As patients are detected as young adults through pedigree studies or population screening studies, the prevalence of cirrhosis is much lower. In a study of 410 homozygotes from Canada and France, 22% had cirrhosis of the liver at the time of diagnosis. The mean serum aspartate amino transferase (AST) and alanine amino transferase (ALT) measurements were within the normal range in these 410 patients. Cirrhotic patients and patients with concomitant alcohol abuse were more likely to have abnormal liver enzymes (7). A study of the critical hepatic iron concentration associated with cirrhosis in C282Y homozygotes using receiver operating characteristic curve analysis suggested that the critical iron concentration was 283 $\mu\text{mol/g}$ (normal, 0–35) (8). However, there were many patients with much higher liver iron concentrations that did not have cirrhosis. Liver damage at lower iron concentrations was usually associated with other risk factors, such as alcohol abuse or chronic viral hepatitis. Therefore, it seems likely that there are factors other than iron overload that contribute to cirrhosis in hemochromatosis. It should also be emphasized that women can have significant liver involvement in hemochromatosis. In a study of 176 women, matched with males for year of birth, there was no difference in the hepatic iron concentration (9). Hepatocellular carcinoma has been described in 18.5% of cirrhotic patients with hemochromatosis (10). It has rarely been described in noncirrhotic hemochromatosis patients. The relative risk is approximately 200-fold, which is similar to cirrhotic patients with chronic viral hepatitis. The effect of iron-depletion therapy has usually been stabilization of the liver disease. This may account for the relatively small number of C282Y homozygotes that have required liver transplantation. Reversal of cirrhosis has rarely been described with iron depletion (11). This has been previously questioned on the basis of sampling errors, but evidence is increasing in other liver diseases (e.g., treatment of chronic viral hepatitis) that cirrhosis can be reversed. Posttreatment liver biopsies have been uncommonly reported (12), nor are they recommended.

B. Diabetes in Hemochromatosis

The presence of diabetes in hemochromatosis is related directly to the presence of liver disease (7). Many patients with cirrhosis of any etiology have glucose intolerance or diabetes, and this is true of hemochromatosis as well. Earlier morphological studies of iron deposition in the pancreas suggested pancreatic damage as the cause of diabetes. However, subsequent studies have demonstrated that high circulating insulin levels (insulin resistance secondary to liver disease) is more common than low circulating insulin levels related to islet cell damage. Metabolic studies of insulin and glucose have not clearly demonstrated a reversal of these changes with iron depletion. This is consistent with the clinical observation that diabetes rarely resolves with therapy (13,14). Insulin resistance in obese patients has also been associated with iron overload in patients without the typical genetic profile for hemochromatosis (15). Most of these cases have a moderate elevation in serum ferritin, with a normal transferrin saturation.

C. Cardiac Disease in Hemochromatosis

Cardiac disease in hemochromatosis includes both cardiomyopathy and arrhythmias. In a series of 410 patients, cardiac disease was present in only 10% of probands and 3% of discovered cases (7). Dyspnea is the most common symptom associated with the cardiomyopathy. The cardiac iron concentration is significantly lower than the liver iron concentration. Transvenous cardiac biopsies have occasionally missed the diagnosis of hemochromatosis and should not be considered to exclude the diagnosis. There have been uncommon cases of young adults who present with life-threatening cardiac disease. These cases have been called “juvenile hemochromatosis,” and preliminary studies suggest that they are not homozygous for the *HFE* gene (16). The putative gene for juvenile hemochromatosis has been localized to chromosome 1 in several Italian pedigrees, but the gene has not yet been identified (17). These patients can also have life-threatening ventricular arrhythmias requiring implantable defibrillators or potentially hepatotoxic medications such as amiodarone.

D. Arthropathy of Hemochromatosis

Arthralgias are perhaps the most common symptom of hemochromatosis. Joint complaints have been found in 32% of probands and 21% of discovered cases (7). The classical description is in the proximal interphalangeal joints of the hands, but wrists, shoulders, knees, and feet are commonly affected. The features of the arthropathy are more similar to osteoarthritis and less commonly involve chondrocalcinosis. Radiological features are often nonspecific, but on occasion the diagnosis is suggested by an astute radiologist. Joint complaints are particularly common in women with hemochromatosis. Arthritis has been demonstrated to be the major factor affecting quality of life in hemochromatosis (18). Since arthritis is common, it has been difficult to attribute the arthritis to hemochromatosis in an aging population (19). The prevalence of arthritis in women with and without hemochromatosis is illustrated in Fig. 1.

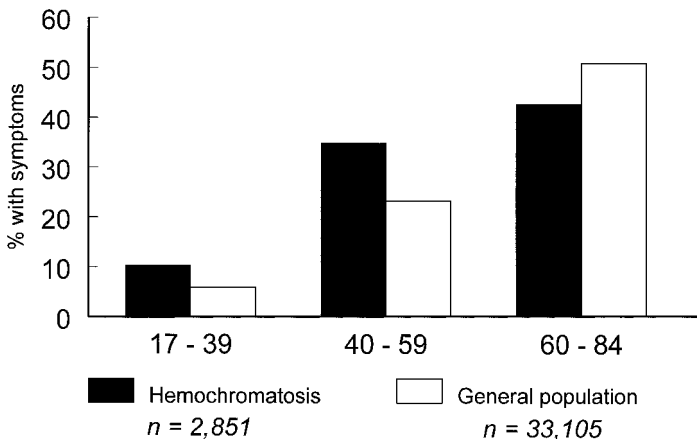


Figure 1 The prevalence of arthritis in hemochromatosis is compared to the general population in women in various age ranges. [Adapted from a survey of 2,851 hemochromatosis patients and 33,105 patients in the general population (19).]

E. Endocrine Abnormalities

The most common symptom of endocrine dysfunction in men with hemochromatosis is impotence. This has been estimated to be present in 40% of cases and is almost universal in male cirrhotic patients. Most cases will have low luteinizing and follicle-stimulating hormones and testosterone levels. Amenorrhea can occur in women. Hypothyroidism is a less common endocrine manifestation of hemochromatosis. Hemochromatosis patients are predisposed to osteoporosis. This is likely related to the low testosterone levels, as well as an independent effect of cirrhosis. Many patients will receive testosterone supplementation without a major effect on their impotence, but may possibly experience an improvement in bone density (20): The effect of androgens, potentially increasing the risk of hepatocellular carcinoma in a cirrhotic patient, is another consideration in the clinical management. The benefits of sildenafil (Viagra) have not been specifically studied for impotence in hemochromatosis.

F. Pigmentation of the Skin

The characteristic pigmentation of hemochromatosis is caused by melanin, not by iron. In the late stages of hemochromatosis, iron can be found in the sweat glands and in the basal layers of the epidermis. The prevalence of pigmentation depends to an extent on the age of the patient and the eye of the beholder. For example, it seems to be more apparent after review of the serum ferritin. It was estimated to be present in 47% of proband cases and 18% of discovered cases (7), but like all signs and symptoms of hemochromatosis, it is decreasing with earlier diagnosis.

G. Fatigue

Although it is nonspecific, fatigue is one of the most common symptoms of hemochromatosis. The presence of fatigue often leads to biochemical iron studies; the physician who was expecting a low value is surprised to find iron overload. Since more than half of patients attending a general medical clinic complain of fatigue, this has been one of the most difficult symptoms to attribute to hemochromatosis. Screening projects within chronic fatigue syndrome clinics have not demonstrated an enhanced case detection of hemochromatosis.

IV. DIAGNOSIS OF HEMOCHROMATOSIS

A paradox of genetic hemochromatosis is the observation that the disease is underdiagnosed in the general population, and overdiagnosed in patients with secondary iron overload.

A. Underdiagnosis of Hemochromatosis

Preliminary population studies using genetic testing have demonstrated a prevalence of homozygotes of 1 in 100 in Ireland (6) and 1 in 189 Australia (21). The fact that many physicians consider hemochromatosis to be rare implies either a lack of penetrance of the gene (nonexpressing homozygotes) or a large number of patients who remain undiagnosed in the community. Until larger genetic population studies allows us to estimate the percentage of homozygotes without iron overload, it is reasonable to assume that both of these factors are contributory.

A major problem in the diagnosis of hemochromatosis is the lack of symptoms and the nonspecific nature of symptoms. An elderly patient who presents with arthralgia and diabetes is not often considered to have genetic hemochromatosis. Many patients assume that the routine blood tests done frequently at ambulatory clinics test their iron status, but in fact this is uncommonly the case unless iron deficiency is suspected. The presenting features vary depending on age and gender, but fatigue is the most common complaint. Women are more likely to have fatigue, arthralgia, and pigmentation rather than liver disease (9).

B. Diagnostic Tests for Hemochromatosis

1. Serum Iron

As the disease is characterized by iron overload, it seems intuitive that the serum iron would be elevated in hemochromatosis. This is true in most, but not all, cases. Serum iron can vary throughout the day, and we have estimated that approximately 5–10% of our homozygotes have had a normal serum iron (22). The assay for serum iron is widely available and is readily automated. A large population screening study in Minnesota, using an automated serum iron measurement, reported a prevalence of only one in 300 for hemochromatosis (23). This is much lower than for other population screening studies in North America.

2. Transferrin Saturation

The transferrin saturation is the ratio of serum iron to total iron-binding capacity. It is a two-step test that is widely available. Transferrin saturation has a sensitivity of greater than 90% for hemochromatosis. The sensitivity of transferrin saturation is lower in population screening studies designed to detect C282Y homozygotes. A fasting value has even greater predictive value but may not always be practical. Transferrin saturation is elevated even in young adults with hemochromatosis before the development of iron overload and a rising ferritin. The threshold to pursue further diagnostic studies has varied from 45% to 62% in previous studies; a lower threshold picks up more patients with hemochromatosis but also leads to more investigations in patients without hemochromatosis. A higher threshold leads to fewer investigations overall, with a greater possibility of missing some patients.

3. Unbound Iron-Binding Capacity (UIBC)

The UIBC is a one-step colorimetric assay that has been used in many reference laboratories to calculate the transferrin saturation. It is an inexpensive test compared to transferrin saturation and has been demonstrated to be a promising initial screening test for hemochromatosis.

4. Serum Ferritin

The relationship between serum ferritin and total-body iron stores has been clearly established by strong correlations with hepatic iron concentration and amount of iron removed by venesection (24). However, ferritin can be elevated secondary to chronic inflammation and histiocytic neoplasms. A major diagnostic dilemma in the past was whether the serum ferritin was related to hemochromatosis or to another underlying liver disease such as alcoholic liver disease, chronic viral hepatitis, or nonalcoholic steatohepatitis. It is likely that some of these difficult cases will now be resolved by

genetic testing. It is important to realize that the sensitivity of both transferrin saturation and ferritin have been established primarily in tertiary referral centers for hemochromatosis. Abnormalities in these tests were used as part of the diagnostic criteria, and this introduces a bias that nevertheless increases the sensitivity of these tests.

5. Iron Removed by Venesection

Since hemochromatosis has usually been diagnosed when symptoms developed in the fifth or sixth decade, patients had significant iron overload at the time of diagnosis. The weekly removal of 500 mL of blood (0.25 g iron) was well tolerated, often for years, without the development of significant anemia. If a patient became anemic (hemoglobin <10 g/dL) after only 6 venesections, it suggested mild iron overload incompatible with the diagnosis of hereditary hemochromatosis. These guidelines may no longer apply as population and pedigree studies uncover patients in the second and third decades (25). At our center, only 71% of C282Y homozygotes would have met the arbitrary criteria that more than 5 g of iron (20 venesections) have been removed without anemia (26). This is another historical diagnostic criterion for hemochromatosis which will no longer be as relevant in the era of genetic testing.

6. Liver Biopsy

Liver biopsy had previously been the gold standard diagnostic test for hemochromatosis. Liver biopsy has shifted from a major diagnostic tool to a method of estimating prognosis and concomitant disease. The need for liver biopsy seems less clear now in the young asymptomatic C282Y homozygote, where there is a low clinical suspicion of cirrhosis based on history, physical examination, and liver biochemistry. A large study conducted in France and Canada suggested that C282Y homozygotes with a serum ferritin of less than 1000 $\mu\text{g/L}$, a normal aspartate aminotransferase (AST), and without hepatomegaly have a very low risk of cirrhosis. In this multivariate model, it was more difficult to predict the presence of cirrhosis than its absence (27). Patients with cirrhosis have a 5.5-fold relative risk of death compared to noncirrhotic hemochromatosis patients (12,28). Cirrhotic patients are also at increased risk of hepatocellular carcinoma. The mean age of hepatocellular carcinoma is 68 in our series, but has been lower in Italian patients with concomitant viral hepatitis (29). Although early detection has been clearly demonstrated by serial ultrasound and α -fetoprotein determination, curative treatment options remain limited. An elderly cirrhotic patient may not withstand a major resection, and the residual cirrhotic liver remains a fertile ground for new tumor development. Organ shortages often preclude the possibility of immediate liver transplantation, which has shown promising results in solitary tumors less than 5 cm in diameter. Screening for hepatocellular carcinoma is a time- and resource-intensive program, and in the area of hemochromatosis resources may be better utilized if directed toward early diagnosis for the disease, in the precirrhotic stage, with early venesection therapy to prevent cirrhosis and hepatocellular carcinoma.

Liver biopsy is considered in typical C282Y homozygotes with liver dysfunction, and in iron-overloaded patients without the typical C282Y mutation. Simple C282Y heterozygotes, compound heterozygotes (C282Y/H63D), and patients with

other risk factors (alcohol abuse, chronic viral hepatitis) with moderate to severe iron overload (ferritin >1000 $\mu\text{g/L}$) may be considered for liver biopsy.

7. Hepatic Iron Concentration and Hepatic Iron Index

The traditional method of assessing iron status by liver biopsy utilizes the semi-quantitative staining method of Perl. This is adequate when there is no iron staining or massive parenchymal iron overload. However, when moderate iron overload is present, the degree of iron overload can be difficult to interpret. Iron concentration can be measured using atomic absorption spectrophotometry. This can be done on a piece of paraffin-embedded tissue so special preparation is not required at the time of the biopsy. An advantage of cutting the tissue from the block is that one is more certain that the tissue assayed is the same as the tissue examined under the microscope. For example, a piece of tissue set aside for iron analysis at the time of the biopsy may represent intercostal muscle rather than liver tissue. The normal reference range for hepatic iron concentration is 0–35 $\mu\text{mol/g}$ (<2000 $\mu\text{g/g}$). The hepatic iron concentration ($\mu\text{mol/g}$ dry weight) divided by age in years is the hepatic iron index. This was demonstrated by Bassett et al. to be a useful test in differentiating the patient with genetic hemochromatosis from the patient with alcoholic siderosis (30). The index remains a useful test in this clinical setting but has been extrapolated to be a diagnostic criterion for hemochromatosis. A threshold of 1.9 for the hepatic iron index had a 91% sensitivity for hemochromatosis, and the area under the receiver operating characteristic curve was 0.94 (0.9–0.99; 95% confidence interval) (31). Early diagnosis in population screening and pedigree studies have demonstrated many homozygotes with a hepatic iron index less than 1.9 (7). Increasing awareness of the concept of moderate iron overload in cirrhosis of any etiology has demonstrated many patients without hemochromatosis but having a hepatic iron index greater 1.9 (32). The hepatic iron index will become less useful with the advent of genetic testing. The comment on liver biopsy reports that a hepatic iron index greater than 1.9 confirms a diagnosis of genetic hemochromatosis should be strongly discouraged, though it will remain a tool to aid the clinician with clinical judgment in an individual case. It may be most useful in the unusual hemochromatosis patient who is negative by conventional genetic testing but clinically seems to have genetic hemochromatosis.

8. Imaging Studies of the Liver

Magnetic resonance imaging (MRI) can demonstrate moderate to severe iron overload of the liver. The technology is advancing, and it is possible that eventually it may be as precise as direct analytical hepatic iron determination (33). Proponents of MRI to alleviate the need for liver biopsy have emphasized the noninvasive nature of the test for the diagnosis. However, as discussed previously, the role of liver biopsy has now shifted from a diagnostic tool to a prognostic tool. It is likely that the presence of an elevated ferritin with a positive genetic test would satisfy the non-invasive desires of the clinician more than an MRI study. The MRI can also demonstrate the clinical features of cirrhosis such as nodularity of the liver, ascites, portal hypertension, and splenomegaly, as well as hepatocellular carcinoma. These features can be more readily assessed by abdominal ultrasound at a lower cost. Dual-energy computerized tomography (CT) scanning can also quantitate liver iron concentration, but is not widely used. Magnetic susceptibility has been studied using a supercon-

ducting quantum interference device (SQUID) machine, but the technology is not widely available.

9. HLA Typing and DNA Microsatellite Studies

HLA-A typing has been used for over two decades within pedigree studies in hemochromatosis (34). Although 70% of homozygotes carry the HLA-A3 antigen, it was not a useful diagnostic test except for pedigree studies. It is anticipated that with the advent of true genetic testing for hemochromatosis, the use of surrogate genetic testing such as HLA typing will be reserved for pedigree studies in unusual cases that are negative for the hemochromatosis gene. Microsatellite markers on chromosome 6 (D6S105) were DNA markers used as surrogate genetic tests before the discovery of the gene and are unlikely now to be useful in clinical practice except in atypical cases (35,36).

10. Genetic Testing for Hemochromatosis

A major advance which stems from the discovery of the hemochromatosis gene is the use of a diagnostic genetic test. The original publication reported that 83% of a group of patients with suspected hemochromatosis had the characteristic C282Y mutation of the *HFE* gene. A more detailed analysis of the non-C282Y cases revealed other explanations for the iron overload, in some cases resulting in >90% of the typical hemochromatosis patients being C282Y homozygotes (37). In the original report, the gene was called *HLA-H*, but this name was later changed to *HFE* (1; see also Chapter 8). The C282Y mutation is also reported as 845A in some laboratories, reflecting the base-pair change rather than the amino acid change. Subsequent studies in well-defined hemochromatosis pedigrees reported that 90–100% of typical hemochromatosis patients had the C282Y mutation (4,26,31,38,39). The prevalence of the C282Y mutation in different populations is illustrated in Table 2. The presence of a single mutation in most patients is in marked contrast to other genetic diseases, in which multiple mutations have been discovered (e.g., cystic fibrosis, Wilson disease, α_1 -anti-trypsin deficiency). A second minor mutation, H63D, was also described in the original report (1). This mutation does not cause the same intracellular trafficking defect of the HFE protein. Compound heterozygotes (C282Y/H63D), and less commonly H63D homozygotes, may resemble C282Y homozygotes with mild to moderate iron overload (40). Other putative hemochromatosis mutations such as S65C (41,42) and IVS3+1G (43) have not been clearly established in large studies to explain iron overload in non-C282Y homozygotes. It is likely that more mutations will be found, but they will be relevant to only a minority of patients.

The genetic test can be done using a variety of techniques. For laboratories familiar with polymerase chain reaction (PCR)-based DNA testing, restriction enzyme digestion analysis may be the easiest test to perform. However, for large-volume testing, methods using oligonucleotide ligation assay, Taqman, dot-blot hybridization, or light cyler methods may be more appropriate. The cost of supplies for the test is low and the actual charges for the test have ranged from (CAD) \$13 to (CAD) \$220 per sample. The test results in patients being classified as normal (wild-type), heterozygotes, or homozygotes for the C282Y mutation. The H63D mutation may be used as a secondary screen in iron-loaded patients who are heterozygotes for the C282Y mutation. The interpretation of the test in several settings is shown in Table 3. A new polymorphism in intron 4 of the *HFE* gene (5569A) was

Table 2 Prevalence of Hemochromatosis in Genotypic Screening Studies

Year	Population sample	Location	Initial test	Liver biopsy	Prevalence	Ref.
1997	Stored DNA samples	Europe; Africa; Asia; Australasia	C282Y, H63D	No	Highest in Northern Europe	(6)
1997	Neonates	Brisbane, Australia	C282Y	No	1 in 150	(69)
1998	Employees	Dublin, Ireland	C282Y	No	1 in 45	(99)
1998	General population	Busselton, Australia	TS, Ferritin, C282Y	Yes	1 in 189	(21)
1998	Hospital patients	Brisbane, Australia	UIBC	No	1 in 300	(70)
1998	Blood donors	London, Canada	UIBC, C282Y	No	1 in 327	(47)
1998	Electoral roll	Christchurch, NZ	TS, C282Y	Yes	1 in 200	(100)
1998	Stored DNA samples (buccal smear)	Scarborough, Maine	C282Y	No	1 in 143	(101)
1998	Blood donors	Barcelona, Spain	C282Y, H63D	No	1 in 512	(102)
1998	Female health-care workers	Salzburg, Austria	C282Y	No	1 in 234	(103)
1999	Employees	North Carolina, USA	TS, ferritin	Yes	1 in 656	(74)
1999	Hospital employees	Oslo, Norway	TS, ferritin, C282Y	No	1 in 252	(104)

Table 3 Interpretation of Genetic Testing for Hemochromatosis

<i>C282Y homozygote</i>	This is the classical genetic pattern which is seen in >90% of typical cases. Expression of disease ranges from no evidence of iron overload to massive iron overload with organ dysfunction. Siblings have a 1-in-4 chance of being affected and should have genetic testing. For children to be affected, the other parent must be at least a heterozygote. If iron studies are normal, false-positive genetic testing or a nonexpressing homozygote should be considered.
<i>C282Y/H63D compound heterozygote</i>	This patient carries one copy of the major mutation and one copy of the minor mutation. Most patients with this genetic pattern have normal iron studies. A small percentage of compound heterozygotes have been found to have mild to moderate iron overload. Severe iron overload is usually seen in the setting of another concomitant risk factor (alcoholism, viral hepatitis).
<i>C282Y heterozygote</i>	This patient carries one copy of the major mutation. This pattern is seen in about 10% of the Caucasian population and is usually associated with normal iron studies. In rare cases the iron studies are high, in the range expected in a homozygote rather than a heterozygote. These cases may carry an unknown hemochromatosis mutation, and liver biopsy is helpful to determine the need for venesection therapy.
<i>H63D homozygote</i>	This patient carries two copies of the minor mutation. Most patients with this genetic pattern have normal iron studies. A small percentage of these cases have been found to have mild to moderate iron overload. Severe iron overload is usually seen in the setting of another concomitant risk factor (alcoholism, viral hepatitis).
<i>H63D heterozygote</i>	This patient carries one copy of the minor mutation. This pattern is seen in about 20% of the Caucasian population and is usually associated with normal iron studies. This pattern is so common in the general population that the presence of iron overload may be related to another risk factor. Liver biopsy may be required to determine the cause of the iron overload and the need for treatment in these cases.
<i>No HFE mutations</i>	Other hemochromatosis mutations will likely be discovered in the future. If iron overload is present without any HFE mutations, a careful history for other risk factors must be reviewed, and liver biopsy may be useful to determine the cause of the iron overload and the need for treatment. Most of these cases are isolated, nonfamilial cases.

independently reported by two laboratories to lead to false positive genetic testing in which a C282Y heterozygote appears to be a homozygote (44,45). This should be considered during the evaluation of a non-expressing C282Y homozygote. The correct diagnosis can be confirmed by direct DNA sequencing. The risk of a false-positive genetic test can be minimized by using primers that do not include the 5569A polymorphism site, lower annealing temperatures, and the use of proofreading enzymes.

The genetic test can also be done on DNA extracted from paraffin-embedded tissue such as liver explants. Studies of explanted livers have demonstrated that many liver transplant patients classified as having hemochromatosis are negative for the C282Y mutation (46). This suggests that those patients may have had iron overload secondary to chronic liver disease rather than hemochromatosis. Therefore any interpretation of iron reaccumulation post-liver transplant for hemochromatosis must be cautious.

Genetic discrimination is a major concern with the widespread use of genetic testing. A positive genetic test even without iron overload could disqualify a patient

for health insurance or life insurance. In the case of hemochromatosis, the advantages of early diagnosis of a treatable disease outweigh the disadvantages of genetic discrimination.

a. Genotypic–Phenotypic Correlation in Hemochromatosis

If we define the presence of homozygosity for the C282Y mutation as the new gold standard for hemochromatosis, it provides for the first time a benchmark for the assessment of the phenotypic diagnostic tools that have been used for decades. Transferrin saturation, ferritin, hepatic iron index, and iron removed by venesection were studied in putative homozygotes who had been previously evaluated at this medical center. Patients were homozygous for the C282Y mutation in 122/128 cases (95%). In C282Y homozygotes, the hepatic iron index was >1.9 in 91.3%, transferrin saturation >55% in 90%, serum ferritin >300 $\mu\text{g/L}$ in 96% of men, >200 $\mu\text{g/L}$ in 97% of women, and iron removed was >5 g in 70% of men and 73% of women. There were 4 homozygotes for C282Y with no biochemical evidence of iron overload. The sensitivity of the phenotypic tests in decreasing order was serum ferritin > hepatic iron index > transferrin saturation > iron removed by venesection. Although the genetic test is useful in the diagnostic algorithm, this study demonstrated both iron-loaded patients without the mutation and homozygous patients without iron overload (26).

b. Nonexpressing Homozygotes

As genetic testing becomes more widespread, there is an increasing number of persons who have been found with the *HFE* gene without iron overload. They include siblings within well-defined hemochromatosis pedigrees (26). A well-defined example of this phenomenon was a 59-year-old brother of a woman with well-documented hemochromatosis (C282Y homozygote). He had a normal serum ferritin and transferrin saturation. There was no history of occult blood loss; and occult blood in stool, colonoscopy, and anti-endomysial antibody for celiac disease were all negative. Liver biopsy was performed with no stainable iron and a low normal hepatic iron concentration (26). The prevalence of these nonexpressing homozygotes is not yet determined from population studies, but this may explain the wide discrepancy between the gene frequency and the clinician's perception that this is an uncommon disease. The prevalence of iron overload as determined by serum ferritin is compared in voluntary blood donors and relatives of known proband cases in Fig. 2.

In a study of 5211 blood donors, only 75% of C282Y homozygotes had an elevated transferrin saturation, and among these only 3/16 (19%) had an elevated ferritin (47). In another population screening study in non-blood donors in France, 50% of the female C282Y homozygotes had a normal transferrin saturation (48).

Patients who are homozygous for the C282Y mutation should be considered at risk of developing iron overload, but if there are no abnormalities in transferrin saturation or ferritin in adulthood, it seems more likely that they are nonexpressing homozygotes rather than patients who will develop iron overload later in life. It seems appropriate, at the present time, to repeat the serum ferritin and transferrin saturation every 5 years in non-iron-loaded C282Y homozygotes, to learn more about the natural history of their disease. It is important to exclude a false-positive genetic test result, as discussed previously. In most nonexpressing homozygotes, there has been no evidence of chronic blood loss or reduced dietary intake of iron. The study

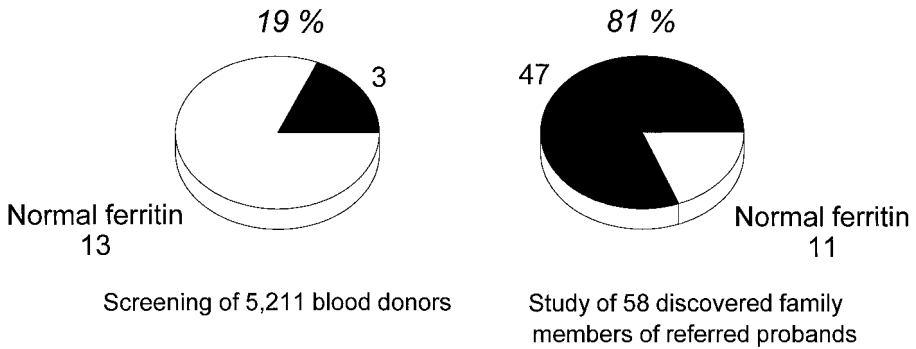


Figure 2 A comparison of the percentage of C282Y homozygotes with an elevated ferritin in voluntary blood donors and family members of referred probands.

of the nonexpressing homozygote may provide additional information about new genes that counteract the effect of the hemochromatosis gene.

c. Family Studies in Hemochromatosis

Once the proband case is identified and confirmed with the genetic test for the C282Y mutation, family testing is imperative. Siblings have a 1 in 4 chance of carrying the gene and should be screened with the genetic test (C282Y and H63D mutation), transferrin saturation, and serum ferritin. Phenotypic expression can vary widely among siblings, and we have identified identical twins with hemochromatosis with a marked difference in iron loading, which suggests that environmental factors are contributory. Patients are usually very concerned about their children and may have difficulty with the concept of autosomal recessive transmission. The risk to a child is dependent on the prevalence of heterozygotes in the community and is probably greater than 1 in 20, and much lower if the spouse is non-Caucasian. A cost-effective strategy now possible with the genetic test is to test the spouse for the C282Y mutation to assess the risk in the children (49). If the spouse is not a C282Y heterozygote or homozygote, the children will be obligate heterozygotes. This assumes paternity and excludes another gene or mutation causing hemochromatosis. This strategy is particularly advantageous where the children are geographically separated or may be under a different health-care system. Genetic testing in general raises many ethical questions, such as about premarital testing, in-utero testing, and paternity issues, which have not been tested yet in hemochromatosis. Preliminary studies at our center have demonstrated that genetic testing is well accepted by patients and does not lead to an increase in anxiety.

If an isolated heterozygote is detected by genetic testing, it is recommended to test siblings. Extended family studies are less revealing than a family study with a homozygote, but are more likely to uncover a homozygote than random population screening.

It is important to remember that there will be patients with a clinical picture indistinguishable from genetic hemochromatosis who will be negative for the C282Y mutation. Most of these patients will be isolated cases, although a few cases of familial iron overload have been reported with negative C282Y testing (50). In these cases, it may be prudent to do HLA-A typing to facilitate the study of siblings. A

negative C282Y test should alert the physician to question the diagnosis of genetic hemochromatosis and reconsider secondary iron overload related to cirrhosis, alcohol, viral hepatitis, or iron-loading anemias. If no other risk factors are found, the patient should begin venesection treatment similar to any other hemochromatosis patient.

V. TREATMENT OF HEMOCHROMATOSIS

The therapy of hemochromatosis continues to be the medieval approach of periodic bleeding. At our center, patients attend an ambulatory-care facility and the venesections are performed by a nurse using a kit containing a 16-gauge straight needle and a collection bag. Blood is removed with the patient in the reclining position over 15–30 min. Hemoglobin is measured at the time of each venesection. If hemoglobin levels decrease to less than 100 g/L the venesection schedule is modified to remove 500 mL every other week. Venesections are continued until the serum ferritin is approximately 50 $\mu\text{g/L}$. The concomitant administration of a salt-containing beverage is a simple method of maintaining plasma volume during the venesection. Maintenance venesections after iron depletion of 3–4 venesections per year are done in most patients, although the rate of iron reaccumulation is highly variable (51). The transferrin saturation will remain elevated in many treated patients and will not normalize unless the patient become iron-deficient. The prognosis of hemochromatosis is primarily dependent on the presence of cirrhosis at the time of diagnosis (Fig. 3).

Chelation therapy with desferrioxamine is not recommended for hemochromatosis. The therapy is expensive, inefficient, cumbersome, and potentially toxic. Oral chelators such as deferiprone have side effects such as agranulocytosis and possible hepatotoxicity (52). Patients are advised to avoid oral iron therapy and alcohol abuse, but there are no dietary restrictions; patients should be informed that much of the iron in “iron-fortified” foods is in an inexpensive form with poor bioavailability.

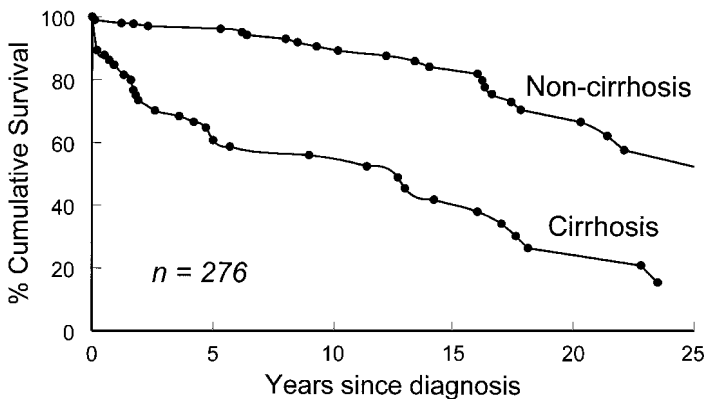


Figure 3 Actuarial survival of C282Y homozygotes among cirrhotic and noncirrhotic patients.

VI. POPULATION SCREENING FOR HEMOCHROMATOSIS

Identification of persons at risk of developing the sequelae of hemochromatosis is the preferred approach. The plan should be to screen a population of asymptomatic individuals, with no personal or family history to suggest that they are at higher risk of the disease than the rest of the population. Such a plan aims to detect disease in presymptomatic individuals in order to provide more effective treatment in the early stages of disease (53–55). Since screening programs are initially associated with increased health-care costs, it is imperative that planning of screening protocols consider all the risks and benefits, and the diagnostic strategy relevant to the disease being considered prior to implementation. Population screening for hemochromatosis meets most of the criteria established by the World Health Organization for screening for medical disease (56).

A. Target Populations to Screen for Hemochromatosis

It is inadequate to wait for the onset of symptoms to diagnose hemochromatosis. Many of the symptoms are unrecognized, and organ damage is usually present at the time of clinical presentation (25). In our database, 43% of males had cirrhosis of the liver—a generally irreversible complication—at the time of diagnosis. In contrast, among the asymptomatic siblings who were then investigated, cirrhosis was present in only 6%. In a series of 37 patients with hemochromatosis who required liver transplantation in the United States, the diagnosis of hemochromatosis was unsuspected at the time of transplant in 13/37 (35%) (57). The ideal patient to screen is the young adult with European ancestry.

B. Cost Models of Screening for Hemochromatosis

There have previously been three published studies using decision analysis to predict the cost effectiveness of screening for hemochromatosis. Two of these studies used hypothetical cohorts and estimates available from the literature and concluded that screening for hemochromatosis would be a strategy that would result in cost savings (58,59). The study by Phatak et al. concluded that screening for hemochromatosis in a Caucasian male population has a favourable cost-effectiveness ratio under a wide range of assumptions, and that there is an urgent need for large prospective screening strategies to test this hypothesis (59). We created a decision analysis model based on 30 years of clinical practice with hemochromatosis patients. The cost of detecting hemochromatosis in the presymptomatic stage was compared to the cost of treating the complications when they occurred. This study concluded that it was essential that the initial phenotypic screening test be low-cost (<CAD\$8), in order to eliminate the possibility of screening with transferrin saturation if cost savings were sought. The cost effectiveness of screening was apparent even if only 20% of cases developed life-threatening symptoms. As a result of this analysis we proceeded with a screening study in blood donors using the unbound iron-binding capacity as a low-cost, phenotypic screening test, and then confirmed the diagnosis by (60). Prospective cost studies are in progress to assess the validity of these models.

C. Phenotypic Screening for Hemochromatosis

Sporadic screening studies have been performed to establish the utility of various tests and the prevalence of hemochromatosis in a target population. Target popula-

tions have included blood donors (60–63), hospital inpatients (23,64), outpatients (65), bank employees (66), diabetics (67), and army recruits (68). Initial testing and test thresholds also varied and have included serum iron, UIBC, transferrin saturation, ferritin, and combinations of these tests. All of these studies have used phenotypic screening rather than genotypic screening. The prevalence of hemochromatosis in most of these studies is similar to studies using genetic testing, which suggests that most cases will show biochemical expression of the disease.

D. Genetic Population Screening for Hemochromatosis

A large study was done on 2375 Australian neonates which demonstrated a prevalence of 1 in 150 babies homozygous for the C282Y mutation (69). A study in Western Australia demonstrated a frequency in adults of 1 in 189 (21). In this study, inhabitants of Busselton, Western Australia, had annual examinations and blood tests as part of a long-term epidemiological project. When 12 C282Y homozygotes were discovered in the screening study, it was possible to determine the serum ferritin concentration in samples drawn 4 years previously. This is a fascinating glimpse into the natural history of untreated hemochromatosis detected at an early stage in the asymptomatic population. The serum ferritin levels in these homozygotes are shown in Figure 4. It is apparent that most, but not all, of these homozygotes were accumulating iron over the observation period. Another large study screened 5211 Canadian blood donors and directly compared transferrin saturation, UIBC, and C282Y genotype. In this study, the UIBC detected more homozygotes than the transferrin saturation, and did so at a lower cost and with fewer false-positive cases (47).

Since many patients without iron overload have now been described as homozygous for the C282Y mutation, the role of the genetic test as the initial screening test will depend very much on the prevalence of the nonexpressing homozygote in the general population. The preferred approach for screening at the present time is initial screening for iron overload with transferrin saturation or UIBC, with C282Y genotyping as the second-line test in those with abnormal iron tests. An example of this approach is a study in which 5182 hospital patients were screened for UIBC

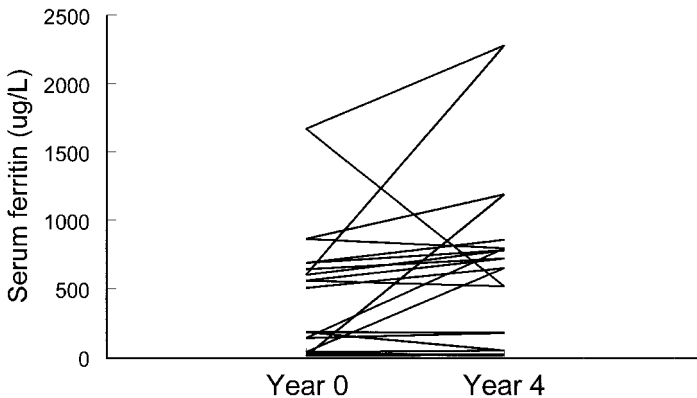


Figure 4 Serum ferritin in untreated C282Y homozygotes observed over a 4-year period. [Adapted from a population survey screening for hemochromatosis in Busselton, Australia (21).]

and then those with a UIBC $<30 \mu\text{mol/L}$ had C282Y genetic testing (70). This approach allows the genetic testing to focus on those with iron abnormalities. A strong case for initial screening with the genetic test can be made in countries with a high prevalence of disease, a low cost of the genetic test, and a lower risk of genetic discrimination (e.g., Ireland).

Periodic health examination in asymptomatic people has been discouraged by many health-care systems. Screening in diabetes and arthritis clinics has also been studied (67,71,72). By the time diabetes is present, organ damage is also evident, and arthritis is a common cause of an elevation in serum ferritin. This elevation will increase the number of false-positive patients who will go on to have invasive testing. The use of genetic testing in an arthritis clinic would likely improve the screening algorithm.

Screening in the workplace has now been successfully completed in several large corporations, confirming the expectedly high prevalence of hemochromatosis (66,73,74). At the present time, it seems likely that studies based on population screening will continue using combinations of phenotypic and genotypic testing. The challenge for the future will be to devise an optimal method of both sampling the population and obtaining financial support from healthcare systems.

VII. DIFFERENTIAL DIAGNOSIS OF HEMOCHROMATOSIS

A. Iron Overload in Alcoholic and Viral Hepatitis

1. Prevalence

Biochemical markers of iron overload are very commonly found in hepatitis C. Increases in serum iron are present in 36% of patients, increased transferrin saturation is present in 18–31%, and serum ferritin is elevated in 30–55%. Despite these parameters, most of these patients have a normal hepatic iron concentration. Iron overload has been reported less commonly with chronic hepatitis B (75). Genetic testing in hepatitis C patients has not identified a higher prevalence of heterozygotes for hemochromatosis in patients with iron abnormalities (76). Iron overload in hepatitis C is most likely a sequela of the disease.

Iron overload has been well known to occur in alcoholic liver disease, most commonly with alcoholic hepatitis accompanied by cirrhosis. Elevations in transferrin saturation and ferritin are common. In contrast to those with hepatitis C, many of these patients will have increased hepatic iron concentration, though not to the same degree as patients with genetic hemochromatosis (77,78).

Emerging genetic studies with explanted livers do not support the hypothesis that iron overload in end-stage cirrhosis, alcoholic liver disease, or chronic viral hepatitis can be readily explained by heterozygosity for the hemochromatosis gene (46). In a study of 447 explanted livers, 8.5% had hepatic iron concentrations in the range associated with hemochromatosis yet did not appear to have genetic hemochromatosis (32). The clinician should be cautious in assigning the diagnosis of genetic hemochromatosis to a patient with end-stage cirrhosis who is negative for the C282Y mutation. In a study of 303 explanted livers there was no increase in the prevalence of C282Y heterozygotes compared to a control population of 5211 blood donors (79). This suggests that heterozygotes are not at increased risk of other liver diseases likely to lead to liver transplantation.

2. Diagnostic Studies

At the time of initial assessment, abnormal iron studies in an alcoholic patient or one with viral hepatitis raises the possibility of genetic hemochromatosis. The liver enzymes are usually much higher in viral hepatitis than in hemochromatosis, and patients with alcoholic liver disease may have the typical AST/ALT ratio of 3:1. However, the possibility exists that the patient may have concomitant hemochromatosis (78).

The most common test to resolve this issue has been the liver biopsy. Iron staining can give a semiquantitative assessment on the degree of iron overload. Distribution of iron can also be helpful. Secondary iron overload usually has a patchy distribution, including overload of Kupffer cells, whereas hemochromatosis has a more diffuse parenchymal iron overload. The typical features of alcoholic liver disease (Mallory's hyaline, polymorphonuclear infiltrate, and fatty change) with patchy iron overload should strongly suggest secondary iron overload rather than hemochromatosis. The hepatic iron index (hepatic iron concentration/age) has a sensitivity of approximately 91% for hemochromatosis and is still a useful test for distinguishing alcoholic siderosis from genetic hemochromatosis. Iron overload in chronic viral hepatitis with cirrhosis can result in a hepatic iron index $>1.9 \mu\text{mol/g dry wt/yr}$, leading to an incorrect diagnosis of hemochromatosis.

It is likely that genetic testing (C282Y mutation on chromosome 6 of the *HFE* gene) will be a powerful diagnostic test in this setting that will replace the hepatic iron index and possibly even the liver biopsy. The use of genetic testing in this setting has resulted in a wide array of genetic test results, including simple C282Y heterozygotes and H63D heterozygotes. The genetic test result is often reported in a form that is cryptic to both the referring physician and the patient. As a result, many patients with alcoholic or viral liver disease are left with the impression that they have genetic hemochromatosis, and inappropriate treatment may be initiated.

3. Clinical Implications

Iron-reduction therapy has been shown in most studies to reduce ALT in hepatitis C without any effects on HCV-RNA. Reports suggesting that decreasing iron burden prior to interferon therapy increases the sustained response rates have been inconclusive (80,81). Since most of the hepatitis C patients in these studies have hepatic iron concentrations within the normal range, the rationale for iron-reduction therapy is unclear. Another point of view is that any excess iron is too much, and venesection is an easy, inexpensive, and well-tolerated therapy.

Yet another perspective on this problem is that mild to moderate iron overload is a sequela of the severity of the hepatitis C. Therefore it is not surprising that patients with more severe disease have a worse response to interferon therapy, and it is unlikely that iron-reduction therapy will change the severity of the disease.

B. Porphyrria Cutanea Tarda

Even prior to the use of genetic testing there were several well-defined pedigrees which had some members with hemochromatosis and other members with porphyria cutanea tarda (PCT) (82,83). Patients with PCT have been described to be both heterozygotes and homozygotes for the C282Y mutation (84) and H63D mutation (85). However, there continue to be patients with PCT with moderate iron overload

who are negative for the C282Y and H63D mutations. It has been estimated that over 40% of European and Australian PCT patients carry at least one *HFE* mutation (86). At this time it seems unlikely that *HFE* mutations can explain all of the iron abnormalities of PCT. A more likely explanation is that some patients with *HFE* mutations will accumulate iron, which then brings out the clinical manifestations of PCT in a patient who is genetically predisposed to porphyria.

C. Iron-Loading Anemias

The presence of anemia at the time of initial presentation with iron overload should immediately suggest that a blood problem may be the cause of the iron overload. Many chronic anemias such as thalassemia or hereditary spherocytosis can cause iron overload that is indistinguishable from *HFE*-linked hemochromatosis on liver biopsy. The additional risk factor of multiple blood transfusions will increase iron predominantly in the reticuloendothelial cells in a liver biopsy, and will increase the risk of chronic viral hepatitis. Management in this group of patients is often guided by liver biopsy and measurement of hepatic iron concentration. A trial of venesection therapy is warranted in a patient with mild anemia. Patients with significant anemia will require chelation therapy.

D. Miscellaneous Iron-Overload Syndromes

Dietary iron overload had previously been considered to be the cause of the iron overload seen in the African Bantu population, which consumes beer brewed in iron pots. However, new data support a genetic locus which differs from the *HFE* gene as a major factor in African iron overload (87).

Patients who have undergone portacaval shunting operations have been found to have mild to moderate iron overload. This is unlikely to be related only to cirrhosis, since serial biopsies have been reported in some patients before and after surgery (88). The mechanism of iron deposition after portacaval shunting remains poorly defined.

Hypocerculoplasminemia has been described in association with iron overload in Japanese patients who also have diabetes and neurological problems (89).

Another group of patients has been described in Brittany with mild to moderate iron overload without evidence of the C282Y mutation. The characteristic features of this group of patients included an elevated serum ferritin, normal transferrin saturation, hyperlipidemia, obesity, and insulin resistance (15). Other reports from Italy have suggested that similar patients often are heterozygotes for C282Y or the H63D mutation.

There have been several reports of iron overload in African-American patients that differs from hemochromatosis (90). Isolated family studies of iron-loading diseases from China and Polynesia have also been described (91,92). Further studies are needed to define the prevalence, pathophysiology, and clinical consequences of these conditions.

Neonatal hemochromatosis is a rare life-threatening disease presenting with decompensated liver disease shortly after birth. Most infants are the products of complicated pregnancies, and often there are multiple other medical problems. This has raised the question as to whether the iron overload is the cause or the result of the multiorgan problems. A genetic locus has been identified in some cases which is

not the *HFE* gene. Therapies have included a cocktail of antioxidants and desferrioxamine and emergency liver transplantation, but most cases are fatal (93).

The clinical implication of these unusual iron-overload diseases is that C282Y genetic testing will not detect these patients and venesection therapy should be guided by histological demonstration of significant iron overload in a liver biopsy specimen.

A syndrome characterized by hyperferritinemia without iron overload associated with cataracts has been found to be related to a mutation in the iron-responsive element of the L-ferritin mRNA. It is an autosomal dominant syndrome that can be confused with hemochromatosis because of the high ferritin (94,95).

VIII. SUMMARY

Hemochromatosis is a common and often underdiagnosed disease. Early diagnosis and treatment results in an excellent long-term prognosis. The development of a diagnostic genetic test has improved the feasibility of the goal of prevention of morbidity and mortality from hemochromatosis.

REFERENCES

1. Feder JN, Gnirke A, Thomas W, Tsuchihashi Z, Ruddy DA, Basava A, et al. A novel MHC class I-like gene is mutated in patients with hereditary hemochromatosis. *Nature Genet* 1996; 13:399–408.
2. Sheldon JH. *Haemochromatosis*. Oxford Medical Publications 1935; 164–340.
3. Simon M, Bourel M, Genetet B, Fauchet R. Idiopathic hemochromatosis. Demonstration of recessive transmission and early detection by family HLA typing. *N Engl J Med* 1977; 297:1017–1021.
4. Bacon BR, Powell L, Adams PC, Kresina T, Hoofnagle J. Molecular medicine and hemochromatosis: At the crossroads. *Gastroenterology* 1999; 116:193–207.
5. Andrews NC. Disorders of iron metabolism. *N Engl J Med* 1999; 341:1986–1995.
6. Merryweather-Clarke A, Pointon J, Sherman J, Robson K. Global prevalence of putative haemochromatosis mutations. *J Med Genet* 1997; 34:275–278.
7. Adams PC, Deugnier Y, Moirand R, Brissot P. The relationship between iron overload, clinical symptoms and age in 410 patients with genetic hemochromatosis. *Hepatology* 1997; 25:162–166.
8. Adams PC. Is there a threshold of hepatic iron concentration causing cirrhosis in hemochromatosis? *Am J Gastro* 2001; 96:567–569.
9. Moirand R, Adams PC, Bicheler V, Brissot P, Deugnier Y. Clinical features of genetic hemochromatosis in women compared to men. *Ann Intern Med* 1997; 127:105–110.
10. Adams PC. Hepatocellular carcinoma in hereditary hemochromatosis. *Can J Gastroenterol* 1993; 7:37–41.
11. Powell LW, Kerr JF. Reversal of “cirrhosis” in idiopathic haemochromatosis following long-term intensive venesection therapy. *Australas Ann Med* 1970; 19:54–57.
12. Niederau C, Fischer R, Purschel A, Stremmel W, Haussinger D, Strohmeyer G. Long-term survival in patients with hereditary hemochromatosis. *Gastroenterology* 1996; 110:1107–1119.
13. Hramiak I, Finegood D, Adams PC. Factors affecting glucose tolerance in hereditary hemochromatosis. *Clin Invest Med* 1997; 20:110–118.
14. Niederau C, Berger M, Stremmel W, Starke A, Strohmeyer G, Ebert R, et al. Hyperinsulinaemia in non-cirrhotic haemochromatosis: Impaired hepatic insulin degradation. *Diabetologia* 1984; 26:441–444.

15. Mendler MH, Turlin B, Moirand R, Jouanolle AM, Sapey T, Guyader D, et al. Insulin resistance-associated hepatic iron overload. *Gastroenterology* 1999; 117:1155–1163.
16. Kaltwasser JP, Schalk KP, Werner E. Juvenile hemochromatosis. *Ann NY Acad Med Sci* 1988; 526:339–341.
17. Roetto A, Totaro A, Cazzola M, Cicilano M, Bosio S, Ascola G, et al. Juvenile hemochromatosis locus maps to chromosome 1q. *Am J Hum Genet* 1999; 64:1388–1393.
18. Adams PC, Speechley M. The effect of arthritis on the quality of life in hereditary hemochromatosis. *J Rheumatol* 1996; 23:707–710.
19. McDonnell S, Preston B, Jewell S, Barton J, Edwards C, Adams P, et al. A survey of 2,851 patients with hemochromatosis: Symptoms and response to treatment. *Am J Med* 1999; 106:619–625.
20. Diamond T, Stiel D, Posen S. Osteoporosis in hemochromatosis: Iron excess, gonadal deficiency, or other factors? *Ann Intern Med* 1989; 110:430–436.
21. Olynyk J, Cullen D, Aquilia S, Rossi E, Summerville L, Powell LW. A population-based study of the clinical expression of the hemochromatosis gene. *N Engl J Med* 1999; 341:718–724.
22. Adams PC, Valberg LS. Evolving expression of hereditary hemochromatosis. *Semin Liv Dis* 1996; 16:47–54.
23. Balan V, Baldus W, Fairbanks V, Michels V, Burritt M, Klee G. Screening for hemochromatosis: A cost-effectiveness study based on 12,258 patients. *Gastroenterology* 1994; 107:453–459.
24. Brissot P, Bourel M, Herry D, Verger J-P, Messner M, Beaumont C, et al. Assessment of liver iron content in 271 patients: A reevaluation of direct and indirect methods. *Gastroenterology* 1981; 80:557–565.
25. Adams PC, Kertesz AE, Valberg LS. Clinical presentation of hemochromatosis: A changing scene. *Am J Med* 1991; 90:445–449.
26. Adams PC, Chakrabarti S. Genotypic/phenotypic correlations in genetic hemochromatosis: Evolution of diagnostic criteria. *Gastroenterology* 1998; 114:319–323.
27. Guyader D, Jacquelinet C, Moirand R, Turlin B, Mendler M, Chaperon J, et al. Non-invasive prediction of fibrosis in C282Y homozygous hemochromatosis. *Gastroenterology* 1998; 115:929–936.
28. Adams PC, Speechley M, Kertesz AE. Long-term survival analysis in hereditary hemochromatosis. *Gastroenterology* 1991; 101:368–372.
29. Fargion S, Mandelli C, Piperno A, Cesana B, Fracanzani AL, Fraquelli M, et al. Survival and prognostic factors in 212 Italian patients with genetic hemochromatosis. *Hepatology* 1992; 15:655–659.
30. Bassett ML, Halliday JW, Powell LW. Value of hepatic iron measurements in early hemochromatosis and determination of the critical iron level associated with fibrosis. *Hepatology* 1986; 6:24–29.
31. Adams PC, Bradley C, Henderson AR. Evaluation of the hepatic iron index as a diagnostic criterion in hereditary hemochromatosis. *J Lab Clin Med* 1997; 130:509–514.
32. Ludwig J, Hashimoto E, Porayko M, Moyer T, Baldus W. Hemosiderosis in cirrhosis: A study of 447 native livers. *Gastroenterology* 1997; 112:882–888.
33. Bonkovsky HL, Rubin RB, Cable EE, Davidoff A, Rijcken TH, Stark DD. Hepatic iron concentration: Noninvasive estimation by means of MR imaging techniques. *Radiology* 1999; 212:227–234.
34. Adams PC, Kertesz AE. Human leukocyte antigen typing of siblings in hereditary hemochromatosis: A cost approach. *Hepatology* 1992; 15:263–268.
35. Jazwinska EC, Pyper WR, Burt MJ, Francis JL, Goldwurm S, Webb SI, et al. Haplotype analysis in Australian hemochromatosis patients: Evidence for a predominant ancestral haplotype exclusively associated with hemochromatosis. *Am J Hum Genet* 1995; 56:428–433.

36. Stone C, Pointon JJ, Jazwinska EC, Halliday JW, Powell LW, Robson KJH, et al. Isolation of CA dinucleotide repeats close to d6s105; linkage disequilibrium with haemochromatosis. *Hum Mol Genet* 1994; 3:2043–2046.
37. Shaheen N, Bacon BR, Grimm I. Clinical characteristics of hereditary hemochromatosis patients who lack the C282Y mutation. *Hepatology* 1998; 28:526–529.
38. Jouanolle A-M, Gandon G, Jezequel P, Blayau M, Campion ML, Mosser J, et al. Haemochromatosis and HLA-H. *Nature Genet* 1996; 14:251–252.
39. The UK Haemochromatosis Consortium. A simple genetic test identifies 90% of UK patients with haemochromatosis. *Gut* 1997; 41:841–845.
40. Bacon BR, Schratz C, Britton RS, Wolff RK. Presence of the hemochromatosis genotype in patients with liver disease. *Gastroenterology* 1997; 112:A1218.
41. Mura C, Ragueneas O, Ferec C. HFE mutations analysis in 711 hemochromatosis probands: Evidence for S65C implication in mild form of hemochromatosis. *Blood* 1999; 93:2502–2505.
42. Arya N, Chakrabarti S, Hegele R, Adams PC. HFE S65C variant is not associated with an increased transferrin saturation in voluntary blood donors. *Blood Cells Mol Dis* 1999; 25:354–357.
43. Wallace DF, Dooley JS, Walker AP. A novel mutation of HFE explains the classical phenotype of genetic hemochromatosis in a C282Y heterozygote. *Gastroenterology* 1999; 116:1409–1412.
44. Jeffrey G, Chakrabarti S, Hegele R, Adams PC. Polymorphism in intron 4 of HFE may cause overestimation of C282Y homozygote prevalence in haemochromatosis. *Nature Genet* 1999; 22:325–326.
45. Somerville M, Sprysak K, Hicks M, Elyas B, Vichen-Wyhony L. An HFE intronic variant promotes misdiagnosis of hereditary hemochromatosis. *Am J Hum Genet* 1999; 65:924–926.
46. Minguillan J, Lee R, Britton R, Wolff R, Demetris A, Bacon B, et al. Genetic markers for hemochromatosis in patients with cirrhosis and iron overload. *Hepatology* 1997; 26:158A.
47. Adams PC, Kertesz AE, McLaren C, Barr R, Bamford A, Chakrabarti S. Population screening for hemochromatosis: A comparison of unbound iron binding capacity, transferrin saturation and C282Y genotyping in 5,211 voluntary blood donors. *Hepatology* 2000; 31:1160–1164.
48. David V, Moirand R, LeGall J-Y, Deugnier Y, Jouanolle AM. Preliminary studies before systematic screening of hemochromatosis: Prevalence and penetrance of C282Y homozygosity. *Am J Hum Genet* 1999; 65:A213.
49. Adams PC. Implications of genotyping of spouses to limit investigation of children in genetic hemochromatosis. *Clin Genet* 1998; 53:176–178.
50. Pietrangelo A, Montosi G, Totaro A, Garuti C, Conte D, Cassanelli S, et al. Hereditary hemochromatosis in adults without pathogenic mutations in the hemochromatosis gene. *N Engl J Med* 1999; 341:725–732.
51. Adams PC. Factors affecting rate of iron mobilization during venesection therapy for hereditary hemochromatosis. *Am J Hematol* 1998; 58:16–19.
52. Olivieri N, Brittenham G, McLaren C, Templeton DM, Cameron R, McClelland R, et al. Long-term safety and effectiveness of iron-chelation therapy with deferiprone for thalassemia major. *N Engl J Med* 1998; 339:417–423.
53. Edwards CQ, Kushner JP. Screening for hemochromatosis. *N Engl J Med* 1993; 328:1616–1620.
54. Adams PC. Population screening for hemochromatosis. *Gut* 2000; 46:301–303.
55. Powell LW. Hemochromatosis: The impact of early diagnosis and therapy. *Gastroenterology* 1996; 110:1304–1307.

56. Adams PC, Gregor JC, Kertesz AE, Valberg LS. Screening blood donors for hereditary hemochromatosis: Decision analysis model based on a thirty-year database. *Gastroenterology* 1995; 109:177–188.
57. Kowdley K, Kaur S, Hassanien T. Primary liver cancer and survival in patients undergoing orthotopic liver transplantation for hemochromatosis. *J Liver Transplant Surg* 1995; 1:237–241.
58. Buffone GJ, Beck JR. Cost-effectiveness analysis for evaluation of screening programs: Hereditary hemochromatosis. *Clin Chem* 1994; 40:1631–1636.
59. Phatak PD, Guzman G, Woll JE, Robeson A, Phelps CE. Cost-effectiveness of screening for hereditary hemochromatosis. *Arch Intern Med* 1994; 154:769–776.
60. Adams PC, Kertesz AE, Barr R, Bamford A, Chakrabarti S. Population screening for hemochromatosis with the unbound iron binding capacity. *Gastroenterology* 1998; 114: A1199.
61. Edwards CQ, Griffin LM, Goldgar D, Drummond C, Skolnick MH, Kushner JP. Prevalence of hemochromatosis among 11,065 presumably healthy blood donors. *N Engl J Med* 1988; 318:1355–1362.
62. Velati C, Piperno A, Fargio S, Colombo S, Fiorelli G. Prevalence of idiopathic hemochromatosis in Italy: Study of 1301 blood donors. *Haematologica* 1990; 75:309–312.
63. Wiggers P, Dalhoj J, Kiaer H, Ring-Larsen H, Hyltoft Petersen P, Blaabjerg O, et al. Screening for haemochromatosis: Prevalence among Danish blood donors. *J Intern Med* 1991; 230:265–270.
64. Hallberg L, Bjorn-Rasmussen E, Jungner I. Prevalence of hereditary haemochromatosis in two Swedish urban areas. *J Intern Med* 1989; 225:249–255.
65. Baer DM, Simons JL, Staples RL, Rumore GJ, Morton CJ. Hemochromatosis screening in asymptomatic ambulatory men 30 years of age and older. *Am J Med* 1995; 98:464–468.
66. Leggett BA, Halliday JW, Brown NN, Bryant S, Powell LW. Prevalence of haemochromatosis amongst asymptomatic Australians. *Br J Haematol* 1990; 74:525–530.
67. O'Brien T, Barrett B, Murray DM, Dinneen S, O'Sullivan DJ. Usefulness of biochemical screening of diabetic patients for hemochromatosis. *Diabet Care* 1990; 13:532–534.
68. Olsson KS, Marsell R, Ritter B, Olander B, Akerblom A, Ostergard H, et al. Iron deficiency and iron overload in Swedish male adolescents. *J Intern Med* 1995; 237: 187–194.
69. Cullen LM, Sommerville L, Glassick TCDHG, Powell LW, Jazwinska EC. Neonatal screening for the hemochromatosis defect. *Blood* 1997; 90:4236–4237.
70. Hickman P, Hourigan L, Powell LW, Cordingley F, Dimenski G, Ormiston BSJFW, et al. Automated measurement of unsaturated iron binding capacity is an effective screening strategy for C282Y homozygous hemochromatosis. *Gut* 2000; 46:405–409.
71. Porter DR, Sturrock RD, Capell HA. The use of serum ferritin estimation in the investigation of anaemia in patients with rheumatoid arthritis. *Clin Exp Rheumatol* 1994; 12:179–182.
72. Kaye TB, Guay AT. Increased serum ferritin levels in patients with diabetes mellitus. *Mayo Clin Proc* 1994; 69:498–499.
73. Smith BN, Kantrowitz W, Grace ND, Greenberg MS, Patton TJ, Ookubo R, et al. Prevalence of hereditary hemochromatosis in a Massachusetts corporation: Is Celtic origin a risk factor? *Hepatology* 1997; 25:1439–1446.
74. Stave G, Mignogna J, Powell G, Hunt C. Evaluation of a workplace hemochromatosis screening program. *Am J Prev Med* 1999; 16:303–306.
75. Cohen C, Berson SD, Shulman G, Budgeon LR. Liver iron stores and hepatitis B antigen status. *Cancer* 1985; 56:2202–2204.

76. Hezode C, Cazeneuve C, Coue O, Roudot-Thoraval F, Lonjon I, Bastie A, et al. Liver iron accumulation in patients with chronic active hepatitis C: Prevalence and role of hemochromatosis gene mutations and relationship with hepatic histological lesions. *J Hepatol* 1999; 31:979–984.
77. LeSage GD, Baldus WP, Fairbanks VF, Baggenstoss AH, McCall JT, Moore SB, et al. Hemochromatosis: Genetic or alcohol-induced? *Gastroenterology* 1983; 84:1471–1477.
78. Adams PC, Agnew S. Alcoholism in hereditary hemochromatosis revisited: Prevalence and clinical consequences among homozygous siblings. *Hepatology* 1996; 23:724–727.
79. Alanen K, Chakrabarti S, Rawlins J, Howson W, Jeffrey G, Adams PC. Prevalence of the C282Y mutation of the hemochromatosis gene in liver transplant recipients and donors. *Hepatology* 1999; 30:665–669.
80. Boucher E, Bourienne A, Adams PC, Turlin B, Brissot P, Deugnier Y. Liver iron concentration and distribution during therapy for chronic hepatitis C. *Gut* 1997; 41: 115–120.
81. Bacon BR. Iron and hepatitis C. *Gut* 1997; 41:127–128.
82. Edwards CQ, Griffen LM, Goldgar DE, Skolnick MH, Kushner JP. HLA-linked hemochromatosis alleles in sporadic porphyria cutanea tarda. *Gastroenterology* 1989; 97: 972–981.
83. Beaumont C, Fauchet R, Phung LN, De Verneuil H, Gueguen M, Nordmann Y. Porphyria cutanea tarda and HLA-linked hemochromatosis. Evidence against a systemic association. *Gastroenterology* 1987; 92:1833–1838.
84. Beutler E. Genetic irony beyond haemochromatosis: Clinical effects of HLA-H mutations. *Lancet* 1997; 349:296–297.
85. Bonkovsky HL, Poh-Fitzpatrick M, Pimstone N, Obando J, Di Bisceglie A, Tattrie C, et al. Porphyria cutanea tarda, hepatitis C, and HFE gene mutations in North America. *Hepatology* 1998; 27:1661–1669.
86. Stuart K, Busfield F, Jazwinska E, Gibson P, Butterworth L, Cooksley W, et al. The C282Y mutation in HFE is common in Australian patients and can act independently of HCV to precipitate porphyria cutanea tarda. *Hepatology* 1997; 26:606A.
87. Gordeuk V, Mukiibi J, Hasstedt SJ, Samowitz W, Edwards CQ, West G, et al. Iron overload in Africa. Interaction between a gene and dietary iron content. *N Engl J Med* 1992; 326:95–100.
88. Adams PC, Bradley C, Frei JV. Hepatic iron and zinc concentrations after portacaval shunting for nonalcoholic cirrhosis. *Hepatology* 1994; 19:101–105.
89. Morita H, Ikeda S, Yamamoto K, Morita S, Yoshida K, Nomoto S, et al. Hereditary ceruloplasmin deficiency with hemosiderosis: A clinicopathological study of a Japanese family. *Ann Neurol* 1995; 37:646–656.
90. Wurapa RK, Gordeuk V, Brittenham G, Khiyami A, Schechter GP, Edwards CQ. Primary iron overload in African Americans. *Am J Med* 1996; 100:9–18.
91. Eason RJ, Adams PC, Aston CE, Searle J. Familial iron overload with possible autosomal dominant inheritance. *Austral NZ J Med* 1990; 20:226–230.
92. Oliver M, Scully L, Guiraudon C, Adams PC. Non-HLA linked hemochromatosis in a Chinese woman. *Dig Dis Sci* 1995; 40:1589–1591.
93. Egawa H, Berquist W, Garcia-Kennedy R, Cox K, Knisely AS, Esquivel CO. Rapid development of hepatocellular siderosis after liver transplantation for neonatal hemochromatosis. *Transplantation* 1997; 62:1511–1513.
94. Cazzola M, Bergamaschi G, Tonon L, Arbustini E, Grasso M, Vercesi E, et al. Hereditary hyperferritinemia-cataract syndrome: Relationship between phenotypes and specific mutations in the iron-responsive element of ferritin light-chain mRNA. *Blood* 1997; 90:814–821.
95. Girelli D, Corrocher R, Biscelglia L, Olivieri O, Zelante L, Panozzo G, et al. Hereditary hyperferritinemia-cataract syndrome caused by a 29-base pair deletion in the iron responsive element of ferritin L-subunit gene. *Blood* 1997; 90:2084–2088.

96. Knisely AS, Magid MS, Dische MR, Cutz E. Neonatal hemochromatosis. *Birth Defects* 1987; 23:75–102.
97. Barton JC, Edwards CQ, Bertoli LF, Shroyer TW, Hudson SL. Iron overload in African Americans. *Am J Med* 1995; 99:616–623.
98. Harris ZL, Takahashi Y, Miyajima H, Serizawa M, MacGillivray RT, Gitlin JD. Aceruloplasminemia: Molecular characterization of this disorder of iron metabolism. *Proc Natl Acad Sci USA* 1995; 92:2539–2543.
99. Ryan E, Byrnes V, Flanagan A, Crowe J. Haemochromatosis—An Irish disease. *Hepatology* 1998; 28:527A.
100. Burt MJ, George PM, Upton J, Collett J, Frampton C, Chapman T, et al. The significance of haemochromatosis gene mutations in the general population: Implications for screening. *Gut* 1998; 43:830–836.
101. Bradley L, Johnson D, Palomaki G, Haddow J, Robertson N, Ferrie R. Hereditary haemochromatosis mutation frequencies in the general population. *J Med Screen* 1998; 5:34–36.
102. Sanchez M, Bruguera M, Bosch J, Rodes J, Ballesta F, Oliva R. Prevalence of the Cys282Tyr and His63Asp HFE gene mutations in Spanish patients with hereditary hemochromatosis and in controls. *J Hepatol* 1998; 29:725–728.
103. Datz C, Haas T, Rinner H, Sandhofer F, Patsch W, Paulweber B. Heterozygosity for the C282Y mutation in the hemochromatosis gene is associated with increased serum iron, transferrin saturation, and hemoglobin in young women: A protective role against iron deficiency. *Clin Chem* 1998; 44:2429–2432.
104. Distant S, Berg JP, Lande K, Haug E, Bell H. High prevalence of the hemochromatosis-associated Cys282Tyr HFE gene mutation in a healthy Norwegian population in the city of Oslo, and its phenotypic expression. *Scand J Gastroenterol* 1999; 34:529–534.

Transfusional Iron Overload

NANCY F. OLIVIERI

University of Toronto, Toronto, Ontario, Canada

I. INTRODUCTION	726
II. MECHANISMS OF TISSUE DAMAGE	726
A. Non-Transferrin-Bound Iron	726
B. Chelatable Tissue Iron	727
C. Pathological and Clinical Consequences	727
III. LIVER	727
A. Process of Liver Iron Accumulation and Damage	728
B. Factors Influencing Development of Liver Disease	728
IV. HEART	729
A. Pathology and Pathophysiology	729
B. Clinical Presentation	730
C. Detection of Cardiac Dysfunction	730
V. OTHER ORGANS	731
A. Hypothalamic/Pituitary Axis	731
B. Pancreas	732
C. Thyroid and Parathyroid	732
D. Adrenal	733
E. Lung	733
VI. ASSESSMENT OF IRON OVERLOAD	734
A. Serum or Plasma Ferritin Concentrations	734
B. Hepatic Iron Measurement	734
VII. TRANSFUSIONAL IRON LOADING IN SICKLE CELL DISEASE: AN UNSTUDIED PROBLEM	735

VIII. ASSESSING EFFECTIVENESS OF THERAPY	735
A. Cardiac Disease	736
B. Safety of Deferiprone	736
C. Deferiprone Hepatotoxicity	737
D. Combination Therapy with Deferoxamine and Deferiprone	737
REFERENCES	738

I. INTRODUCTION

Although transfusional iron loading is an important feature of other diseases, this process most often complicates the course of severe thalassemia, the most common monogenic disorder worldwide, in which regular transfusions are usually required from infancy. Regular transfusions present to the body the problem of handling iron from the resulting load of erythrocytes, and this unique source of iron poses a pathophysiological challenge. It is on studies in thalassemia that much of our understanding with respect to the pathology and pathophysiology, rate of accumulation, clinical presentation, detection, and assessment of transfusional iron overload has been established; and from which have been provided the most secure conclusions regarding treatment with iron-chelating agents. Therefore, transfusional iron overload will be discussed with reference to the severe thalassemia syndromes.

In humans approximately 0.5% of total body iron is acquired or lost daily. Because people cannot increase the rate of iron excretion, the state of iron balance is regulated by the control of intestinal iron absorption, itself influenced both by the amount of body storage iron and the level of erythropoietic activity (1).

Tissue iron overload has been recognized as a complication of thalassemia for many years (2–6). It is now clear that in this disorder excess iron is derived from intestinal absorption as well as from transfusions, the former predominating in patients with intermediate forms of thalassemia in whom there is increased rate of absorption from the gastrointestinal tract, and the latter common in regularly transfused children. Sixfold increases in iron absorption may be observed in untransfused patients (7–10) and appear to be correlated both with body storage iron (indicating an abnormal mechanism of iron absorption in this disorder) and with the magnitude of increased erythropoiesis (11). This heightened absorption, which may lead to increases in body iron burden of up to 5 g per year (9,10), is corrected after adequate transfusion (7,12–15).

II. MECHANISMS OF TISSUE DAMAGE

A. Non-Transferrin-Bound Iron

The toxicity of iron is mediated, in part, by its catalysis of reactions which generate free hydroxyl radicals, propagators of oxygen-related damage (16,17). Hydroxyl radicals induce lipid peroxidation of cellular organelles including mitochondria, lysosomes, and sarcoplasmic membranes. Evidence of peroxidant damage has been demonstrated in vivo in the tissues of iron-loaded animals (18) and of thalassemic patients

(19). Iron not bound to storage or transport proteins is particularly toxic. In normal individuals, tight binding of plasma iron to transferrin prevents the catalytic activity of iron in free-radical production (20). In very heavily iron-loaded patients, transferrin becomes fully saturated and a non-transferrin-bound fraction of iron (NTBI) becomes detectable in plasma (21). NTBI may accelerate the formation of free hydroxyl radical and facilitate the rate of uptake of iron by tissues [summarized in Ref. (20)]. The effectiveness of iron-chelating therapy, prescribed for iron-loaded patients, depends in part on its ability to bind NTBI over sustained periods, thereby ameliorating iron-catalyzed toxicity of free radicals.

B. Chelatable Tissue Iron

Following delivery to cells by transferrin, iron is immediately available for chelation from a low-molecular-weight iron pool through which all intracellular traffic of iron passes (16,20,22). When this pool is large, it may be toxic to cells without the capacity to generate iron storage proteins. Excess iron is deposited in reticuloendothelial cells, where it appears to be relatively harmless, or in parenchymal tissues, where it may cause significant damage (20,22).

The advances in free-radical chemistry which have clarified the toxic properties of iron have been summarized previously (23), and the effects of free-radical damage mediated by iron have been reviewed recently (16). Free hydroxyl radicals, and possibly other oxygen-derived species, may cause considerable damage by the degradation of DNA and hyaluronic acid, and by membrane peroxidation (20,24). Although there are several defense mechanisms against free-radical damage, including such first-line antioxidant systems as superoxide dismutase, catalase, and glutathione peroxidase, in heavily iron-loaded patients these appear inadequate to prevent oxidative damage.

C. Pathological and Clinical Consequences

In several early pathological studies in patients with thalassemia, the most striking finding was the widespread deposition of iron, with varying degrees of organ fibrosis in the heart, liver, and endocrine glands, the most important sites of iron accumulation (4,6,25–32). The pathologic and clinical consequences of iron loading in these organs are discussed below.

III. LIVER

The liver is the principal iron storage organ of the body; in young iron-loaded adults, liver disease remains a common cause of death (33). Iron produces hepatocellular injury, with progression to fibrosis and cirrhosis, through the promotion of free-radical-mediated lipid peroxidation and mitochondrial dysfunction (16). Liver biopsies from thalassemic infants, children, and adolescents have described both the light and electron microscopic appearances of the tissue damage mediated by progressive iron deposition (34–38). These studies suggest that the primary cirrhotic factor may be excessive collagen deposition, induced by iron-promoted catalysis of collagen synthesis, or decreased collagen breakdown from lysosomal blockade resulting from iron overload. As well, human liver cells in culture upregulate the transport of NTBI in response to iron loading, a factor that may be of considerable importance

in generating iron-induced liver damage (39). Viral infection (40) and alcohol ingestion (41) may accelerate the development of iron-induced liver damage.

A. Process of Liver Iron Accumulation and Damage

Electron microscopic studies of infants aged less than 18 months revealed early excessive deposition of collagen in association with evidence of increased iron content, prior to morphological evidence of cellular injury. A relationship between the increased iron content of these specimens and the excessive collagen was suggested. Hepatic fibrosis has been reported in several infants in whom liver biopsies (but not liver iron) were obtained in early studies (35,42–44). In transfused patients after infancy, iron deposition is both parenchymal and reticulendothelial in distribution; by late childhood, liver damage is associated with hepatocytes apparently totally filled with iron-laden lysosomes, with destruction of normal architecture (34). Fibrosis, initially interhepatic, progresses to capillarization of sinusoids and cirrhosis with ongoing transfusions. Finally, hepatocytes disappear within connective tissue scars containing clumps of hemosiderin. In older transfused children, fibrosis has commonly been observed after the age of 3 years (4,25,44–48). As survival became extended in thalassemia, frank cirrhosis was observed during the second decade of life (49–52) and, in some studies, it was noted as early as 8 years of age (50). Screening tests were of limited value; changes in liver enzymes were not regularly observed (44).

B. Factors Influencing Development of Liver Disease

1. Age

Although some studies suggested that cirrhosis was not common prior to the age of 6 (48) or 10 (49) years of age, other series noted fibrosis as early as 3 years of age and cirrhosis in some patients by the age of 8, with virtually all patients demonstrating cirrhosis by the age of 16 years (50). One study of 16 patients aged 3 to 17 years observed that all but two patients (both aged 3 years at the time of biopsy) had moderate to massive fibrosis or cirrhosis (52). Another later series suggested that fibrosis is observed in 90% of transfused, irregularly chelated patients over the age of 5 years (53), an incidence confirmed in more recent studies (54). These data are of concern given that both hepatic fibrosis and cirrhosis may be underestimated by a factor of 2 if less than three samples of liver are drawn (55).

2. Previous Splenectomy

Although it has been suggested that the spleen is a major target of iron deposition (56) and that iron loading and fibrosis of the liver may be accelerated following splenectomy (48), these findings have been challenged by other studies (57), including those reporting a low splenic iron content in transfused, nonchelated patients (58).

3. Iron Content of Liver

The iron content at which significant fibrosis or cirrhosis may develop is uncertain. An exponential relationship between iron content and fibrosis has been noted in a series of 52 biopsies in transfused patients (49). Hepatic iron is reported to increase

by 1.7 mg/g dry weight of tissue for every gram of total body storage iron (59). In addition, human liver cells in culture upregulate the transport of NTBI in response to iron loading, a factor that may accelerate liver iron loading and damage in transfused patients (39); see also Chapter 18.

In the earliest studies, in which a small number of hepatic iron concentrations were measured, fibrosis was present only in those patients whose hepatic iron exceeded 7.6 mg/g dry weight (48). Although hepatic iron concentrations of approximately 12.5 mg/g dry weight were suggested to be associated with moderate or severe hepatic fibrosis (51), later observations from the same group reported that a lower threshold of risk, approximately 7 mg/g, may be significant (60). These studies appear to confirm those in which a threshold for the development of hepatic fibrosis above 7 mg/g dry weight has been identified in patients with hereditary hemochromatosis (61).

IV. HEART

The etiology of iron-mediated cardiac disease, the leading cause of death, in regularly transfused patients with thalassemia is multifactorial, occurring secondary to iron overload but also to other factors including chronic anemia and pulmonary disease (summarized in Ref. 62).

A. Pathology and Pathophysiology

Most of the information available on the pathology of the iron-loaded myocardium comes from autopsy studies, most published in the era prior to iron-chelating therapy in erratically transfused patients (30–32,63). Commonly observed was diffuse, gross rust-brown staining of the heart, right and left ventricular hypertrophy and dilatation, and a greatly increased cardiac weight. Pericarditis was a commonly reported finding (48,64–66); analysis of pericardial fluid was not helpful in identifying its cause. Of interest, pericarditis was not reported in a large autopsy series of nonthalassemic patients who had cardiac iron loading and anemia (31). Estimations of myocardial iron content reported gross elevations—up to 20 times normal concentrations—but with 10-fold marked variation in cardiac iron content (31,67). The preferential deposition of iron in the left ventricular septum and free wall, with maximal concentration in the left ventricular epicardium (31) and only later involving the remainder of the myocardium, may explain the preservation of systolic ventricular function until late in the course of the disease. Even in many patients who died of cardiac arrhythmias, iron deposition in the conduction system appeared to be relatively mild (31,67). Also noted were extensive myocardial fiber disruption and fibrosis (3), the latter varying from minimal (48) to variable (67,68) to extensive (3), often unrelated to myocardial iron content (67,69). In the two youngest children with thalassemia reported to have developed fatal cardiac disease, at ages 8 and 10 years, respectively (48), cardiac fibrosis was absent or minimal, despite the presence of hepatic cirrhosis. The observation of minimal fibrosis despite heavy myocardial iron loading prompted the observation that iron deposition alone may not produce a fibrous tissue reaction (65). Later studies, which observed that fibrosis was often associated with cardiac iron loading, challenged these findings (70).

The precise mechanisms of iron-related cardiac dysfunction are debated. Myocardial iron deposition appears to be primarily confined to the myocyte (68,71). In

transfusional iron overload, transferrin receptors are downregulated (72), but augmented transport of non-transferrin-bound iron in response to iron loading may aggravate cardiac iron loading (73). These results suggest that a vicious circle may be created whereby iron loading exacerbates the uptake of the most toxic fraction of iron, leading to cardiac damage and further iron loading, as described in liver cells (39).

From autopsy studies it is clear that the heart can accommodate less iron than the liver, possibly because cardiac cells have relatively smaller amounts of storage protein and heightened sensitivity to iron-induced oxygen radicals. Very low levels of myocardial iron may interfere directly with diastolic function (74), a process which resembles the effect of hypercalcemia and is characterized by inadequate relaxation, spontaneous early depolarization, and subsequent failure of contractility (75). Higher concentrations of iron promote the conversion of superoxide and hydrogen peroxide into the highly toxic free hydroxyl radicals through the Haber-Weiss reaction (16,20). Increased lipid peroxidation may target the lysosomal membranes of myocytes, increasing their fragility, leading to the disruption of the sarcolemmal membrane and inhibition of the mitochondrial respiratory chain (16,76). The effects of iron may be augmented by the reduction of ferric iron to ferrous iron and the addition of low concentrations of ascorbic acid, and are inhibited by high concentrations of ascorbic acid, alpha tocopherol, and deferoxamine (16).

B. Clinical Presentation

Prior to deferoxamine therapy, death from iron-induced cardiac disease was commonly reported as early as the first decade of life (48,64,67). In irregularly transfused patients, asymptomatic and progressive cardiac enlargement was noted around the age of 10 years. This was often followed shortly by an attack of pericarditis in nearly half the patients, of unknown etiology but occurring out of season for a typical viral etiology. Pericarditis was not influenced by antibiotic therapy and was frequently recurrent and self-limited (77). Pericarditis was often followed by the appearance of atrial arrhythmias and first-degree heart block. Later, right and left ventricular failure and serious disturbances of rhythm and conduction developed. The peak incidence of cardiac failure was between the ages of 10 and 15 years and in most patients was noted prior to age 20 years. The duration of life after the onset of failure was less than 3 months in over half of patients; one-third died within 1 month of the appearance of cardiac failure (3,64,67).

In this era, in adequately chelated, asymptomatic patients, subtle abnormalities of both systolic and diastolic function may be multifactorial in origin (78). The onset of clinical cardiac failure is to be anticipated in any transfused patient over the age of 15 years whose hepatic iron exceeds 15 mg/g dry weight (79). Lung disease and myocarditis may aggravate iron-induced cardiac disease (80); conversely, iron-promoted free-radical formation may contribute to the pathogenesis of infectious myocarditis (81,82).

C. Detection of Cardiac Dysfunction

Diagnosis of cardiac disease prior to its clinical presentation in transfusional iron overload may be challenging. Systolic function, cardiac dimensions, and myocardial wall thickness are usually normal until there are unequivocal symptoms of cardiac

failure. Both electrocardiograms and standard echo-cardiograms may be normal late in the course of iron-induced cardiac disease. While widely applied, these tests are not sufficiently sensitive to detect preclinical cardiac dysfunction (summarized in Ref. 22). While normal at rest, the iron-loaded ventricle may demonstrate systolic ventricular dysfunction during exercise (83) or following dolbutamine stimulation (74). The measurement of the left ventricular end-systolic-pressure dimension (LVPD_{ES}) to assess contractility, which has shown dysfunction in transfused patients (84), has not been widely applied.

Most studies of myocardial biopsy demonstrate a heterogenous distribution of myocardial iron (70,71,85). This limits the use of this technique in the serial systematic evaluation of cardiac iron loading *in vivo*, and prevents direct correlation with values of cardiac iron estimated by other techniques, including magnetic resonance imaging (22). Magnetic resonance imaging (MRI) does not provide accurate determination of hepatic iron in patients with severe iron loading, hepatic fibrosis, or both (86), and is likely to have similar limitations in the quantitation of cardiac iron. Magnetic susceptometry has not yet been applied for the evaluation of cardiac iron. While abnormalities have been detected by ultrasonic analysis (87), this approach has not been widely used. The value of measurement of serum atrial natriuretic peptide (85) and of the variability of blood pressure and heart rate (88) in the identification of preclinical cardiac involvement requires further experience. Similarly, further studies are awaited on the value of decreased antioxidant activity of apolipoprotein E, related to the frequency of the apolipoprotein E4 allele and proposed as a genetic risk for left ventricular failure in thalassemia (89). In summary, none of the methods used to assess early myocardial impairment has been rigorously and prospectively tested (78).

V. OTHER ORGANS

Iron loading of the tissues in transfused patients affects the endocrine organs (4,6,90–92). In the present era, the most common endocrine abnormalities appear to be hypogonadotropic hypogonadism and diabetes mellitus; lower frequencies of hypothyroidism, hypoparathyroidism, and adrenal insufficiency are reported.

A. Hypothalamic/Pituitary Axis

1. Pathology

The hypothalamic/pituitary axis is particularly vulnerable to the effects of iron loading. Disproportionally marked iron loading is observed in the anterior, compared to the posterior, pituitary, with preferential localization of iron within the gonadotrophs that secrete luteinizing hormone. Marked reduction in gonadotrophs and secretory granules has been reported (93–95) and is supported by the loss of anterior pituitary volume observed by MRI scanning (96). Iron within the testes is usually confined to the vessel walls, leaving the germinal epithelium and interstitial Leydig cells uninvolved (94,95,97); occasionally, iron within the tubular cells is associated with interstitial fibrosis and decreased numbers of Leydig cells (98,99). While ovarian iron deposition has been implicated in infertility in one patient (100), the major mechanism involved in failure of sexual maturation appears to be selective central hypogonadism, and rarely end-organ unresponsiveness (52,101–105). Failure of lin-

ear growth has been attributed to central hypogonadism (100,101,103,105) but may also be impaired through other actions of iron. Iron may interfere with the production of insulin-like growth factor (106–108), impaired growth hormone response to growth hormone-releasing hormone (109), abnormalities in growth hormone secretion (110), and a postreceptor defect in growth hormone action (111,112). Contributing factors include a reduced level of secretion of adrenal androgen (113,114), zinc deficiency (115), and free-hemoglobin-induced inhibition of cartilage growth (116).

2. Clinical Findings

Arrest or failure of puberty occurs in approximately 50% of transfused male and female patients with thalassemia; secondary amenorrhea is noted in 23% of females (92). Within the anterior pituitary, unlike the heart and liver, the consequences of iron deposition may be irreversible. There are no reports in the literature describing improvement in potency or fertility after reduction of iron load in transfusional iron overload, although this has been reported in primary hemochromatosis (97,117). Iron-chelating therapy likely has a positive impact on the prevention of gonadal dysfunction (92,118,119). Recent studies have suggested that body iron burdens corresponding to hepatic iron concentrations of 9 to 13 mg/g dry weight are associated with a high risk of development of pituitary failure (120), but prospective studies should provide more secure conclusions with respect to thresholds of risk for this complication.

B. Pancreas

1. Endocrine

Diabetes mellitus has been reported in 4–6% of transfused thalassemia patients (92). Early and progressive loss of β -cell mass, manifested by decreased insulin release in response to secretagogues before the development of significant insulin resistance, has been described in iron-loaded patients (121,122). Both the observed relationship between diabetes and the severity and duration of iron overload (123), as well as a reported reduction in the frequency of diabetes in adequately chelated patients (79), suggests that iron-mediated damage is the major factor in producing diabetes in transfusional iron overload. Attributed to both impaired secretion of insulin secondary to chronic pancreatic iron overload (4,123–127) and insulin resistance (128–131), diabetes has also been linked temporally to episodes of acute viral hepatitis (123,132).

2. Exocrine

Damage to the exocrine pancreas (133) also occurs in patients with transfusional iron overload in whom echogenicity of the pancreas, decreased size of the gland, and decreased serum concentrations of trypsin and lipase have been reported. Most of these findings correlated with age and the duration of transfusion therapy.

C. Thyroid and Parathyroid

Glandular atrophy and fibrosis leading to hyposecretion of thyroid and parathyroid hormone is observed in approximately 4–6% of transfused patients. Although clinical signs of thyroid impairment are uncommon, it has been suggested that a substantial

proportion of patients have subclinical disease (134). Hypoparathyroidism of variable severity is observed generally in poorly chelated patients, associated with other complications of iron overload (135). Subclinical hypoparathyroidism may also be relatively common (136). Supporting the role of iron is the observation that thyroid and hypoparathyroid dysfunction has declined in prevalence in the era of iron-chelating therapy (137).

D. Adrenal

In transfused patients, iron loading within the adrenal gland, primarily in the zona glomerulosa cells, may be marked. Although abnormalities of adrenal function including reduction in baseline and peak stimulated levels of DHEA-S, and low levels of adrenal androgen secretion with normal glucocorticoid reserve (114), may be measurable (138), these are rarely associated with adrenal failure (98,99,113,139).

No quantitative studies are available to indicate the levels of body storage iron which may be associated with the development of iron-induced thyroid, parathyroid, or adrenal dysfunction.

E. Lung

1. Pathophysiology

Over the past two decades the role of chronic iron deposition in the lungs has been increasingly recognized. Iron deposition may provoke pulmonary hypertension and right ventricular strain, dilatation, and failure (140). In some (141) but not all studies (142,143), parameters of lung disease have been correlated with increasing age and the duration and degree of iron overload. In autopsy studies, massive accumulation of hemosiderin in alveolar phagocytes within the perivascular and supporting framework of the lungs has been described (48,144). Fibrosis has been reported as an inconsistent finding (144–146) and, when noted, as unrelated to the degree of vascular sclerosis or chronic pneumonitis (146). Deposition of hemosiderin and lipofuscin, the latter believed to result from iron catalysis of lipid peroxidation within the respiratory epithelium, tracheal, and bronchial cells, has been observed (146). These changes are reported to increase in severity with age and duration of disease, as does ferrugination of alveolar septa, blood vessels, and bronchial walls (146). Sclerotic vascular lesions and emboli have been recognized and attributed to platelet thrombi (32,146). A variety of mechanisms have been proposed to account for this pathology. They include tissue damage due to the generation of free hydroxyl radicals secondary to iron deposition, ferrugination of connective tissue resulting in reduced capillary compliance (146), and other less well defined abnormalities of the alveolar capillary membrane (142). Abnormal growth and development of the alveolus, secondary either to intrinsic disease or related to transfusionally acquired iron, has also been proposed as a contributing factor (142). Pulmonary disease due to recurrent pulmonary thromboembolic episodes, and deferoxamine toxicity (147), may also play roles.

2. Clinical Manifestations

Possibly as a result of these pathological processes, small-airway obstruction, hyperinflation, and hypoxemia have been commonly described as significant findings

in patients with thalassemia (148–151). Evidence for a primarily restrictive pattern of lung disease, with isolated abnormalities consistent with obstructive airways disease, has also been presented (141,144,150,152,153). Studies of total lung capacity have given inconsistent results (144,148,149), as have the effects of transfusion on pulmonary function (151).

In summary, restrictive lung dysfunction, leading to parenchymal disease and desaturation, may be the most common pulmonary abnormality in transfused patients. Ultimately, pulmonary hypertension and right ventricular dysfunction, as reported in the earliest pathological series (32,48) may cause right ventricular cardiac failure (140,150). The effects of transfusion and chelating therapy on pulmonary function require further study.

VI. ASSESSMENT OF IRON OVERLOAD

A. Serum or Plasma Ferritin Concentrations

While statistically significant correlations between the serum ferritin and liver iron concentration in iron-overloaded patients have been observed (154), even these early studies reported an initial steep rise in ferritin, after which the rate of increase was less marked. Later studies indicated that a plasma ferritin concentration of about 4000 $\mu\text{g/L}$ probably reflects the upper physiological limit of the rate of its synthesis, and that higher concentrations are caused by the release of intracellular ferritin from damaged cells (155). Several other factors, including ascorbate deficiency, infection, hepatic damage, hemolysis, and ineffective erythropoiesis, probably determine the level of circulating ferritin [(156,157), and summarized in (22)]. In patients with a wide range of body iron burden, the 95% prediction interval for hepatic iron concentration, given the plasma ferritin concentration, was so broad as to restrict greatly the clinical usefulness of a single determination of plasma ferritin as a predictor of body iron stores. Only 57% of the variability in plasma ferritin concentration could be explained by variation in hepatic storage iron (158).

B. Hepatic Iron Measurement

Because the magnitude of the body iron burden is the principal determinant of clinical outcome in transfusional iron overload, its accurate assessment is of primary importance. Careful studies indicate that, in the absence of focal lesions, hepatic nonheme iron distribution is uniform (159). Studies suggesting an uneven hepatic distribution of iron (160) at autopsy do not appear to be confirmed *in vivo*, either in older studies of patients with hemochromatosis (161) or in more recent ones in thalassemic patients phlebotomized following bone marrow transplantation. In this latter group a striking linear relationship between the changes in liver iron concentration in noncirrhotic liver samples of 1 mg or more in dry weight, and body storage iron mobilized by venesection, has been reported (162). Furthermore, a striking relationship has also been observed between liver iron concentration determined by biopsy and that assessed by magnetic susceptometry, a modality which evaluates the iron content of the liver as a whole (163). Two caveats are to be emphasized. In cirrhotic samples, iron deposition may be nonuniform; and specimens of at least 0.4 mg dry weight are needed for accurate biochemical measurement of hepatic iron (164).

Overall, the preponderance of evidence confirms that in transfusional iron overload, hepatic iron distribution is usually uniform, and liver biopsy provides the definitive information with respect to quantitative body iron stores (1). Determination of hepatic iron through liver biopsy performed under ultrasound guidance is safe and permits rational adjustment of iron-chelating therapy (165). Magnetic susceptometry provides a direct measure of hepatic storage iron that is quantitatively equivalent to that determined by biopsy (163) over a range of iron concentrations (158). Presently, magnetic susceptometry is available in only two centers worldwide. By contrast, the more widely available modality of magnetic resonance imaging fails to provide accurate quantitation of hepatic iron in patients with severe iron overload, hepatic fibrosis, or both (86).

VII. TRANSFUSIONAL IRON LOADING IN SICKLE CELL DISEASE: AN UNSTUDIED PROBLEM

While widely described in patients with thalassemia (22), complications associated with transfusional iron overload remain less so in patients with sickle cell disease, in whom the indications for transfusions continue to expand. Early studies suggested the pattern of iron-induced tissue damage, as observed in other transfused patients, either does not occur, or is most unusual in sickle cell anemia, allegedly because of the element of inflammation associated with sickle cell disease that may fix a large portion of iron in reticuloendothelial cells (166). Later studies have suggested that liver injury in transfused patients with sickle cell disease is less severe than in thalassemia (167). But other studies do not support these findings. The first detailed study of pathological findings in this disorder observed patchy, variable iron deposits in the reticuloendothelial system, but did not relate these findings to the previous administration of transfusions (168). The first recognition of iron deposits related to transfusions led to recommendation that complications of iron overload might develop in sickle cell anemia (47) two decades later. Later studies identified fibrosis and advanced cirrhosis in transfused patients with sickle cell disease (169,170). One large study of the cardiac pathology of transfused and nontransfused patients identified a single patient with sickle cell disease with the highest iron content of any heart reported (171). In another report of patients with sickle cell anemia 14 to 22 years of age, transfused 8 to 11 years (172), abnormal liver histology, increased liver enzymes, alterations in cardiac function, and pericardial effusions, similar to those findings in repeatedly transfused patients with other disorders, suggest that transfusional iron overload in sickle cell anemia is as toxic as in other disorders.

VIII. ASSESSING EFFECTIVENESS OF THERAPY

The effectiveness of deferoxamine, and the principles of its use in the treatment of iron overload, have been recently detailed in several recent comprehensive reviews [(22,137); see also Chapter 33]. More uncertain is the status of the iron-chelating agent 1,2-dimethyl-3-hydroxypridin-4-one (deferiprone). An excellent review of the evidence for deferiprone's safety and effectiveness has recently been published (173). It appears that all studies which have evaluated body iron burden quantitatively have confirmed that, in most patients, this drug is inadequately effective in controlling body iron (174–177).

In summary, five peer-reviewed studies published to date have utilized liver iron concentration to evaluate the effectiveness of deferiprone (174–178). Conclusions that short-term therapy exerted a favorable effect on iron balance in a cohort of patients (178) do not appear to be applicable to long-term therapy in this same group (176), in whom more than one-third were noted to have liver iron concentrations exceeding the threshold for cardiac disease and premature death. While two studies published in the same year did not obtain pre-deferiprone liver irons (174,175), both did quantitate liver iron concentrations after several years of deferiprone. In these studies, 88% and 54% of patients, respectively, exceeded the threshold for complications of iron overload, while 59% and 18%, respectively, exceeded the threshold for premature death, leading to increasing concern about an apparent loss of efficacy of deferiprone (174). In the most recent study, mean hepatic iron increased by 25% over baseline in 20 patients treated with 1 year of deferiprone (177). Eighty-five percent of patients exceeded the threshold for complications of iron overload, while 65% exceeded that for premature death. Although pre- and post-deferiprone liver biopsies were obtained, hepatic histology was not reported. The conclusions of this study are controversial: the authors, citing one study which reported that hepatic iron is heterogeneously distributed (160), argued that the poor outcome could, therefore, not be considered conclusive (177). As noted above, however, a substantial body of work demonstrates that body iron burden and hepatic iron are indeed closely correlated in patients with transfusional iron overload (48,49,51,60,61,162).

A. Cardiac Disease

In a retrospective study that followed studies of an animal model of iron overload (179), the combination of treatment with a compound closely related to deferiprone (1,2-diethyl-3-hydroxypyridin-4-one) and iron overload was associated with increased cardiac iron accumulation both initially and with chronic therapy, and with the development of cardiac fibrosis. In another animal species, chronic deferiprone was associated with myocardial necrosis in the absence of iron overload (180). At least five patients in human trials have died from cardiac disease and another patient developed tachycardia requiring drug withdrawal during deferiprone therapy, leading to recommendations against use of deferiprone in patients at risk of cardiac disease (175).

B. Safety of Deferiprone

Two publications arising out of a 1-year trial of deferiprone (designed originally to evaluate deferiprone-associated bone marrow toxicity and joint toxicity) have now been published (181,182). In the first report, it was found that serum ferritin concentrations rose significantly in all patients with initial ferritins less than 2500 $\mu\text{g/L}$, whereas in the later report mean serum ferritin concentration was said not to have changed in this group. Also, in the first report, levels of serum alanine aminotransferase were noted to have doubled in 48% of patients, changes proposed to be unrelated to hepatitis C status; later, the authors suggested that these elevations were more common in hepatitis C-infected patients (182). Recently, another abstract (183) has raised further concerns with respect to the lack of long-term effectiveness of deferiprone in this group of patients. For the first time in this cohort, the serum

ferritin has been reported to have increased in 55% of the patients, while 37% of the original group to date have been withdrawn from deferiprone. Nearly 50% have withdrawn because of increasing iron stores (183).

C. Deferiprone Hepatotoxicity

1. Animal Studies

Studies of an animal model of iron overload reported that the combination of treatment with 1,2-diethyl-3-hydroxypyridin-4-one and iron overload was associated with increased iron accumulation in the liver over the long term despite short-term efficacy (179), findings generally recapitulated in the human studies with deferiprone (176,184). Recently, it has been noted that deferiprone may accelerate the progression of hepatic fibrosis in some animals (185).

2. Human Trials

The only long-term trial which prospectively obtained pre- and post-deferiprone liver biopsies has observed that deferiprone accelerated the progression of hepatic fibrosis (176). In this study, a panel of hepatopathologists retrospectively examined liver biopsies from deferiprone-treated patients and compared the findings to liver biopsies obtained from deferoxamine-treated patients. Progression of fibrosis was identified in 36% of deferiprone-treated patients, but in none of the deferoxamine-treated group. The estimated median time to progression of fibrosis was 3.2 years; the estimated odds of progression of fibrosis increased by 5.8-fold with each additional year of deferiprone. Extensive debate of these findings (186–190) has not resolved the issue. In other studies that obtained liver biopsies, two did not collect pre-deferiprone biopsies (174,175), while a third study did not report the results of liver histology (177); no study has obtained serial liver biopsies in deferiprone-treated patients. In one of these studies (175) the authors reported that no fibrosis was present in any hepatitis C-negative patient, a surprising observation given the ages, simultaneous iron-related complications (iron-induced cardiac failure and diabetes), and hepatic iron concentrations (mean, 17 mg/g dry weight) reported in this group. However, a later study, from the same center reported hepatic cirrhosis in several patients of similar advanced age, who had a median liver iron less than half this value (60).

Subsequent studies consistent with findings of hepatocellular damage during exposure to deferiprone continue to emerge. The latest report from the original 1-year safety trial now indicates that the mean serum alanine aminotransferase has increased significantly in this cohort (183). Because this observation is inconsistent with a report published less than 7 months previously (182), it raises serious concerns with respect to hepatotoxicity during long-term therapy. Another recent report of the hepatic histology of the patients enrolled in this trial (191) unfortunately selected only 17% of the original cohort for examination after the minimal period of treatment required to refute deferiprone's liver toxicity (176).

D. Combination Therapy with Deferoxamine and Deferiprone

One study (192) examined the effectiveness of a combination of deferiprone and deferoxamine (the latter at fully therapeutic doses administered 7 days per week) in five patients treated for a mean of 10 months; in four of the patients, the total length

of therapy was 1 year or less. In parallel, these investigators had increased the dose of deferiprone simultaneously with adding deferoxamine to deferiprone therapy. Not unexpectedly, during administration of fully therapeutic doses of deferoxamine, a significant decline in serum ferritin was noted; urine iron excretion studies during administration of both agents reportedly demonstrated additive effects. These findings were reported as an improvement in iron status. These observations provide limited contribution to the understanding of the usefulness of combination therapy because of the use of different dosing regimens of deferiprone, the co-administration of therapeutic doses of deferoxamine, the short-term nature of the combined therapy, and the failure to quantitate body iron burden in most patients. In another study, following treatment with a combination of deferiprone and 2 days of deferoxamine per week (193), liver iron in 77% of the patients still exceeded the threshold for premature death; no data on liver histology were provided. The conclusion that negative balance can be achieved with this regimen seems to this author to be unsupported by the data provided in these studies.

REFERENCES

1. Brittenham GM. Disorders of iron metabolism: deficiency and overload. In: Hoffman R, Benz EJ, Shattil SJ, Furie B, Cohen HJ, Silberstein LE, eds. *Hematology: Basic Principles and Practice*. New York: Churchill Livingstone, 1994:492–523.
2. Whipple GH, Bradford WL. Racial or familial anemia of children. Associated with fundamental disturbances of bone and pigment metabolism (Cooley-Von Jaksch). *Am J Dis Child* 1932; 44:336.
3. Howell J, Wyatt JP. Development of pigmentary cirrhosis in Cooley's anaemia. *Arch Pathol* 1953; 55:423–431.
4. Ellis JT, Schulman I, Smith CH. Generalized siderosis with fibrosis of liver and pancreas in Cooley's (Mediterranean) anemia; with observations on the pathogenesis of the siderosis and fibrosis. *Am J Pathol* 1954; 30:287–309.
5. Erlandson ME, Golubow J, Wehman J, Smith CH. Metabolism of iron, calcium and magnesium in homozygous thalassemia. *Ann NY Acad Sci* 1964; 119:769–775.
6. Fink HE. Transfusion hemochromatosis in Cooley's anemia. *Ann NY Acad Sci* 1964; 119:680–685.
7. Heinrich HC, Gabbe EE, Oppitz KH, et al. Absorption of inorganic and food iron in children with heterozygous and homozygous beta-thalassemia. *Z Kinderheilkd* 1973; 115:1–22.
8. De Alarcon PA, Donovan ME, Forbes GB, Landau SA, Stockman JA. Iron absorption in the thalassemia syndromes and its inhibition by tea. *N Engl J Med* 1979; 300:5–8.
9. Pippard MJ, Warner GT, Callender ST, Weatherall DJ. Iron absorption and loading in β -thalassaemia intermedia. *Lancet* 1979; ii:819–821.
10. Pippard MJ, Weatherall DJ. Iron absorption in non-transfused iron loading anaemias: Prediction of risk for iron loading, and response to iron chelation treatment, in β thalassaemia and congenital sideroblastic anaemias. *Haematologica* 1984; 17:17–24.
11. Pootrakul P, Kitcharoen K, Yansukon P, et al. The effect of erythroid hyperplasia on iron balance. *Blood* 1988; 71:1124–1129.
12. Larizza P, Ventura S, Matioli G, Sulis E, Aresu G. Contributo alla conoscenza dell'anemia talassemica; ricerche condotte con l'ausilio de Fe^{59} . *Haematologica* 1958; 43:517–562.
13. Erlandson ME, Walden B, Stern G, Hilgartner MW, Wehman J, Smith CH. Studies on congenital hemolytic syndromes. IV Gastrointestinal absorption of iron. *Blood* 1962; 19:359.

14. Bannerman RM. Iron absorption in thalassaemia. *Br J Haematol* 1964; 10:490.
15. Necheles TF, Allen DM, Finkel HE. *Clinical Disorders of Hemoglobin Structure and Synthesis*. New York: Appleton Century Crofts, 1969.
16. Hershko C, Link G, Cabantchik I. Pathophysiology of iron overload. *Ann NY Acad Sci* 1998; 850:191–201.
17. Halliwell B, Gutteridge JM. Oxygen toxicity, oxygen radicals, transition metals and disease. *Biochem J* 1984; 219:1–14.
18. Bacon BR, Tavil AS, Brittenham GM, Park CH, Recknagel RO. Hepatic lipid peroxidation *in vivo* in rats with chronic iron overload. *J Clin Invest* 1983; 71:429–439.
19. Heys AD, Dormandy TL. Lipid peroxidation in iron loaded spleens. *Clin Sci* 1981; 60:295–230.
20. Hershko C, Konijn AM, Link G. Iron chelators for thalassaemia. *Br J Haematol* 1998; 101:399–406.
21. Hershko C, Graham G, Bates CW, Rachmilewitz ES. Non-specific serum iron in thalassaemia: An abnormal serum iron fraction of potential toxicity. *Br J Haematol* 1978; 40:255–263.
22. Olivieri NF, Brittenham GM. Iron-chelating therapy and the treatment of thalassaemia. *Blood* 1997; 89:739–761.
23. Gutteridge JMC, Halliwell B. Iron toxicity and oxygen radicals. *Clin Haematol* 1989; 2:195–256.
24. Slater TF. Free radical mechanisms in tissue injury. *Biochem J* 1984; 222:1–15.
25. Whipple GH, Bradford WL. Mediterranean disease-thalassaemia (erythroblastic anemia of Cooley); associated pigment abnormalities simulating hemochromatosis. *J Pediatr* 1936; 9:279–311.
26. Aastaldi G, Tolentino P, Sacchetti G. *La talassemia (Morbo di Cooley e forme affini)*. Biblioteca 'Haematologica'. Vol. XII. Pavia: Tipografia del libro, 1951.
27. Sansone G, Russo C, Zunin C, Salomone P. Studio clinico ed anatomo-patologico di due bambini con anemia di Cooley deceduti per reazione transfusionale. *Minerva Pediatr* 1955; 7:1005.
28. Chaptal J, Jean R, Pays A. Hemachromatose secondaire de la maladie de Cooley, etude clinique, biologique et anatomique. *Pediatric* 1967; 19:677–693.
29. Putignano A, Caruso G, Tannoia N. Cooley in adulta. Studio clinico e anatomopatologico di un case, *Atti del v° Congresso Microticimie*, Cosenza, 1973. Istituto Italiano di Medicina Sociale, Roma.
30. Modell CB, Matthews R. Thalassaemia in Britain and Australia. In: Bergsma D, Cerami A, Peterson CH, Graziano JH, eds. *Birth Defects: Original Article Series*. Vol. XII. New York: Liss, 1976:13–29.
31. Buja LM, Roberts WC. Iron in the heart: etiology and clinical significance. *Am J Med* 1971; 51:209–221.
32. Sonakul D, Peacharee P, Thakerngpol K. Pathologic findings in 76 autopsy cases of thalassaemia. *Birth Defects: Original Articles Series* 1988; 23:157–176.
33. Zurlo MF, De Stefano P, Borgna-Pignatti C, et al. Survival and causes of death in thalassaemia major. *Lancet* 1989; ii:27–30.
34. Iancu TC, Neustein HB, Landing BH. The liver in thalassaemia major: Ultrastructural observations. In: *Iron Metabolism*. Ciba Symposium No. 51. Amsterdam: Excerpta Medica, 1977:293–316.
35. Iancu TC, Landing BH, Neustein HB. Pathogenic mechanisms in hepatic cirrhosis of thalassaemia major: Light and electron microscopic studies. *Pathol Annu* 1977; 12:171–200.
36. Iancu TC, Neustein HB. Ferritin in human liver cells of homozygous β -thalassaemia: Ultrastructural observations. *Br J Haematol* 1977; 37:527–535.

37. Masera G, Jean G, Conter V, Terzoli S, Mauri RA, Cazzaniga M. Sequential study of liver biopsy in thalassaemia. *Arch Dis Child* 1980; 55:800–802.
38. Iancu TC. Ultrastructural pathology of iron overload. *Clin Haematol* 1989; 2:475–495.
39. Parkes JG, Randell EW, Olivieri NF, Templeton DM. Modulation by iron loading and chelation of the uptake of non-transferrin-bound iron by human liver cells. *Biochim Biophys Acta* 1995; 1243:373–380.
40. Piperno A, Fargion S, D'Alba R, et al. Liver damage in Italian patients with hereditary hemochromatosis is highly influenced by hepatitis B and C virus infection. *J Hepatol* 1992; 16:364–368.
41. Tsukamoto H, Horne W, Kamimura S, et al. Experimental liver cirrhosis induced by alcohol and iron. *J Clin Invest* 1995; 96:620–630.
42. Wollstein M, Kreidel KV. Familial hemolytic anemia of childhood—von Jaksch. *Am J Dis Child* 1930; 39:115–130.
43. Koch LA, Shapiro B. Erythroblastic anemia; review of cases reported showing roentgenographic changes in bones and 5 additional cases. *Am J Dis Child* 1932; 44:318–335.
44. Panizon F, Vullo C. Sulla enoluzione della siderosi e fibrosi epatica nella malattia di Cooley. *Studio biotico su 20 casi. Acta Paediat. Lat.* 1952; 10:71.
45. Cooley TB, Witwer ER, Lee P. Anemia in children with splenomegaly and peculiar changes in bones; report of cases. *Am J Dis Child* 1927; 34:347.
46. Baty JM, Blackfan KD, Diamond LK. Blood studies in infants and in children. I. Erythroblastic anemia: a clinical and pathologic study. *Am J Dis Child* 1932; 43:667–704.
47. Frumin AM, Waldman S, Morris P. Exogenous hemochromatosis in Mediterranean anemia. *Pediatrics* 1952; 9:290–294.
48. Witzleben CL, Wyatt JP. The effect of long-survival on the pathology of thalassaemia major. *J Pathol Bacteriol* 1961; 82:1–12.
49. Risdon AR, Barry M, Flynn DM. Transfusional iron overload: The relationship between tissue iron concentration and hepatic fibrosis in thalassaemia. *J Pathol* 1975; 116:83–95.
50. Jean G, Terzoli S, Mauri R, et al. Cirrhosis associated with multiple transfusions in thalassaemia. *Arch Dis Child* 1984; 59:67–70.
51. Aldouri MA, Wonke B, Hoffbrand AV, et al. Iron state and hepatic disease in patients with thalassaemia major treated with long term subcutaneous desferrioxamine. *J Clin Pathol* 1987; 40:1352–1359.
52. Maurer HS, Lloyd-Still JD, Ingrisano C, Gonzalez-Crussi F, Honig CR. A prospective evaluation of iron chelation therapy in children with severe β -thalassaemia: A six-year study. *Am J Dis Child* 1988; 142:287–292.
53. Angelucci E, Baronciani D, Lucarelli G, et al. Liver iron overload and liver fibrosis in thalassaemia. *Bone Marrow Transplant* 1993; 1:29–31.
54. Thakerngpol K, Fucharoen S, Boonyaphipat P, et al. Liver injury due to iron overload in thalassaemia: Histopathologic and ultrastructural studies. *Biometals* 1996; 9:177–183.
55. Maharaj B, Maharaj RJ, Leary WP, et al. Sampling variability and its influence on the diagnostic yield of percutaneous needle biopsy of the liver. *Lancet* 1986; 1:523–525.
56. Lukens JN, Neuman LA. Excretion and distribution of iron during chronic deferoxamine therapy. *Blood* 1971; 38:614–622.
57. Risdon RA, Flynn DM, Barry M. The relation between liver iron concentration and liver damage in transfusional iron overload in thalassaemia and the effect of chelation therapy. *Gut* 1973; 14:421.
58. Borgna-Pignatti C, de Stefano P, Bongo IG, Avato F, Cazzola M. Spleen iron content is low in thalassaemia. *Am J Pediatr Hematol/Oncol* 1984; 6:340–343.

59. Prieto J, Barry M, Sherlock S. Serum ferritin in patients with iron overload and with acute and chronic liver disease. *Gut* 1974; 15:343.
60. Telfer P, Hoffbrand A, Prescott E, Wonke B. Long term followup of thalassemic patients after liver biopsy: Quantitative liver iron estimation and risk of complications of transfusional iron overload. 7th International Conference on Thalassemia and the Haemoglobinopathies, Bangkok, Thailand, 1999.
61. Niederau C, Fischer R, Purschel A, Stremmel W, Haussinger D, Strohmeyer G. Long-term survival in patients with hereditary hemochromatosis. *Gastroenterology* 1996; 110: 1304–1307.
62. Olivieri NF. The beta-thalassemias [published erratum appears in *N Engl J Med* 1999; 341(18):1407]. *N Engl J Med* 1999; 341:99–109.
63. Sonakul D, Pacharee P, Wasi P, Fucharoen S. Cardiac pathology in 47 patients with beta thalassaemia/haemoglobin E. *SE Asian J Trop Med Public Health* 1984; 15:554–563.
64. Engle MA, Erlandson M, Smith CH. Late cardiac complications of chronic severe refractory anaemia with haemochromatosis. *Circulation* 1964; 30:698.
65. Arnett EN, Nienhuis AW, Henry WL, Ferrans VJ, Redwood DR, Roberts WC. Massive myocardial hemosiderosis: A structure-function conference at the National Heart and Lung Institute. *Am Heart J* 1975; 90:777–787.
66. Finch S, Finch C. Idiopathic hemochromatosis, and iron storage disease. *Medicine (Baltimore)* 1955; 34:381–430.
67. Schellhammer PF, Engle MA, Hagstrom JWC. Histochemical studies of the myocardium and conduction system in acquired iron-storage disease. *Circulation* 1967; 35: 631–637.
68. Engle MA. Cardiac involvement in Cooley's anemia. *Ann NY Acad Sci* 1964; 119: 694–702.
69. Keschner H, Gables C. The heart in hemochromatosis. *So Med J* 1951; 44:927–930.
70. Lombardo T, Tamburino C, Bartoloni G, et al. Cardiac iron overload in thalassemic patients: An endomyocardial biopsy study. *Ann Hematol* 1995; 71:135–141.
71. Fitchett DH, Coltart DJ, Littler WA, et al. Cardiac involvement in secondary haemochromatosis: A catheter biopsy study and analysis of myocardium. *Cardiovasc Res* 1980; 14:719–724.
72. Leibold EA, Guo B. Iron-dependent regulation of ferritin and transferrin receptor expression by the iron-responsive element binding protein. *Annu Rev Nutr* 1992; 12: 345–368.
73. Parkes JG, Hussain RA, Olivieri NF, Templeton DM. Effects of iron loading on uptake, speciation, and chelation of iron in cultured myocardial cells. *J Lab Clin Med* 1993; 122:36–47.
74. Spirito P, Lupi G, Melevendi C, Veechio C. Restrictive diastolic abnormalities identified by Doppler echocardiography in patients with thalassemia major. *Circulation* 1990; 82: 88–94.
75. Liu P, Olivieri N. Iron overload cardiomyopathies: New insights into an old disease. *Cardiovasc Drugs Ther* 1994; 8:101–110.
76. Link G, Pinson A. Heart cells in culture: A model of myocardial iron overload and chelation. *J Lab Clin Med* 1985; 106:147–153.
77. Orsini A, Louchet E, Raybaud C, Brusquet Y, Perrimond H. Les pericardites de la maladie de Cooley. *Pediatric* 1970; 15:831–842.
78. Jessup M, Manno CS. Diagnosis and management of iron-induced heart disease in Cooley's anemia. *Ann NY Acad Sci* 1998; 850:242–250.
79. Brittenham GM, Griffith PM, Nienhuis AW, et al. Efficacy of deferoxamine in presenting complications of iron overload in patients with thalassemia major [see comments]. *N Engl J Med* 1994; 331:567–573.

80. Kremastinos DT, Tiniakos G, Theodorakis GN, Katritsis DG, Toutouzas PK. Myocarditis in beta-thalassemia major. A cause of heart failure. *Circulation* 1996; 91:66–71.
81. Hiraoka Y, Kishimoto C, Takada H, et al. Role of oxygen derived free radicals in the pathogenesis of coxsackievirus B3 myocarditis in mice. *Cardiovasc Res* 1993; 27:957–961.
82. Suzuki H, Matsumori A, Matoba Y, et al. Enhanced expression of superoxide dismutase messenger RNA in viral myocarditis. An SH-dependent reduction of its expression and myocardial injury. *J Clin Invest* 1993; 91:2727–2733.
83. Leon MB, Borer JS, Bacharach SL, Green MV, Benz EJ, Griffith P, Nienhuis AW. Detection of early cardiac dysfunction in patients with severe beta-thalassemia and chronic iron overload. *N Engl J Med* 1979; 301:1143–1148.
84. Borow KM, Propper R, Bierman FZ, Grady S, Inati A. The left ventricular end-systolic pressure-dimension relation in patients with thalassemia major. A new non-invasive method for assessing contractile state. *Circulation* 1982; 66:980–985.
85. Derchi G, Bellone P, Forni GL, et al. Cardiac involvement in thalassaemia major: Altered atrial natriuretic peptide levels in asymptomatic patients. *Eur Heart J* 1992; 13: 1368–1372.
86. Angelucci E, Giovagnoni A, Valeri G, et al. Limitations of magnetic resonance imaging in measurement of hepatic iron. *Blood* 1997; 90:4736–4742.
87. Lattanzi F, Bellotti P, Picano E, et al. Quantitative ultrasonic analysis of myocardium in patients with thalassemia major and iron overload. *Circulation* 1993; 87:748–754.
88. Veglio F, Melchio R, Rabbia F, et al. Blood pressure and heart rate in young thalassemia major patients. *Am J Hypertens* 1998; 11:539–547.
89. Economou-Petersen E, Aessopos A, Kladi A, et al. Apolipoprotein E epsilon4 allele as a genetic risk factor for left ventricular failure in homozygous beta-thalassemia. *Blood* 1998; 92:3455–3459.
90. Erlandson ME, Brilliant R, Smith CH. Comparison of sixty-six patients with thalassemia major and thirteen patients with thalassemia intermedia: Including evaluations of growth, development, maturation and prognosis. *Ann NY Acad Sci* 1964; 119:727–735.
91. Bannerman RM, Keusch G, Kreimer-Birnbaum M, Vance VK, Vaughan S. Thalassemia intermedia, with iron overload, cardiac failure, diabetes mellitus, hypopituitarism and porphyrinuria. *Am J Med* 1967; 42:476–486.
92. Italian Working Group on Endocrine Complications in Non-endocrine Diseases. Multicentre study on prevalence of endocrine complications in thalassemia major. *Clin Endocrinol* 1995; 42:581–586.
93. Bergeron C, Kovacs K. Pituitary siderosis. A histologic, immunocytologic, and ultrastructural study. *Am J Pathol* 1978; 93:295–309.
94. Peillon F, Racadot J. [Histopathological in the hypophysis in 6 cases of hemochromatosis]. *Ann Endocrinol (Paris)* 1969; 30:800–807.
95. Sheldon J. Haemochromatosis. London: Oxford University Press, 1935.
96. Chatterjee R, Katz M, Oatridge A, Bydder GM, Porter JB. Selective loss of anterior pituitary volume with severe pituitary-gonadal insufficiency in poorly compliant male thalassaemic patients with pubertal arrest. *Ann NY Acad Sci* 1998; 850:479–482.
97. Siemons LJ, Mahler CH. Hypogonadotropic hypogonadism in hematochromatosis: Recovery of reproductive function after iron depletion. *J Clin Endocrinol Metab* 1987; 62:585.
98. Canale VC, Steinherz P, New M, Erlandson M. Endocrine function in thalassemia major. *Ann NY Acad Sci* 1974; 232:333–345.
99. Kuo B, Zaino E, Roginsky MS. Endocrine function in thalassemia. *J Clin Endocrinol Metab* 1968; 28:805–808.

100. Costin G, Kogut MD, Hyman CB, Ortega JA. Endocrine abnormalities in thalassemia major. *Am J Dis Child* 1979; 133:497–502.
101. Kletsky OA, Costin G, Marrs RP, Bernstein G, March CM, Mishell DR. Gonadotrophin insufficiency in patients with thalassemia major. *J Clin Endocrinol Metab* 1979; 48: 901–905.
102. De Sanctis V, Vullo C, Katz M, Wonke B, Tanas R, Bagni B. Gonadal function in patients with beta thalassaemia major. *J Clin Pathol* 1988; 41:133–137.
103. Wang C, Tso SC, Todd D. Hypogonadotropic hypogonadism in severe beta-thalassemia: Effect of chelation and pulsatile gonadotrophin-releasing hormone therapy. *J Clin Endocrinol Metab* 1989; 68:511–516.
104. Chatterjee R, Katz M, Cox TF, Porter JB. A prospective study of the hypothalamic-pituitary axis in thalassaemic patients who developed secondary amenorrhoea. *Clin Endocrinol* 1993; 39:287–296.
105. Landau H, Matoth I, Landau-Cordova Z, Goldfarb A, Rachmilewitz EA, Glaser B. Cross-sectional and longitudinal study of the pituitary-thyroid axis in patients with thalassaemia major. *Clin Endocrinol* 1993; 38:55–61.
106. Saenger P, Schwartz E, Markenson AL, et al. Depressed serum somatomedin activity in beta-thalassemia. *J Pediatr* 1980; 96:214–218.
107. Herington AC, Werthe GA, Matthews RN, Burger HG. Studies on the possible mechanism for deficiency of nonsuppressible insulin-like activity in thalassemia major. *J Clin Endocrinol Metab* 1981; 52:393–398.
108. Werther GA, Matthews RN, Burger HG, Herington AC. Lack of response of nonsuppressible insulin-like activity to short term administration of human growth hormone in thalassemia major. *J Clin Endocrinol Metab* 1981; 53:806–809.
109. Pintor C, Cella SG, Manso P, et al. Impaired growth hormone (GH) response to GH-releasing hormone in thalassemia major. *J Clin Endocrinol Metab* 1986; 62:263–267.
110. Shehadeh N, Hazani A, Rudolf MCJ, Benderly A, Hochberg Z. Neurosecretory dysfunction of growth hormone secretion in thalassaemia major. *Acta Paediatr Scand* 1990; 79:790–795.
111. Scacchi M, Damesi L, De Martin M, et al. Treatment with biosynthetic growth hormone of short thalassaemic patients with impaired growth hormone secretion. *Clin Endocrinol* 1991; 35:335–339.
112. Wonke B, Hoffbrand AV, Bouloux P, Jensen C, Telfer P. New approaches to the management of hepatitis and endocrine disorders in Cooley's anemia. *Ann NY Acad Sci* 1998; 850:232–241.
113. McIntosh N. Endocrinopathy in thalassaemia major. *Arch Dis Child* 1976; 51:195–201.
114. Sklar CA, Lew LQ, Yoon DJ, David R. Adrenal function in thalassemia major following long-term treatment with multiple transfusions and chelation therapy. Evidence for dissociation of cortisol and adrenal androgen secretion. *Am J Dis Child* 1987; 141: 327–330.
115. Arcasoy A, Cavdar A, Cin S, et al. Effects of zinc supplementation on linear growth in beta thalassemia (a new approach). *Am J Hematol* 1987; 24:127–136.
116. Vassilopoulou-Sellin R, Oyedeji CO, Foster PL, Thompson MM, Saman NA. Haemoglobin as a direct inhibitor of cartilage growth *in vitro*. *Horm Metab Res* 1989; 21: 11.
117. Kelly TM, Edwards CQ, Meikle AW, Kushner JP. Hypogonadism in hemochromatosis: Reversal with iron depletion. *Ann Intern Med* 1984; 101:629.
118. Bronspegel-Weintrob N, Olivieri NF, Tyler NF, Andrews D, Freedman MH, Holland FJ. Effect of age at the start of iron chelation therapy on gonadal function in β -thalassemia major. *N Engl J Med* 1990; 323:713.

119. Jensen CE, Tuck SM, Old J, et al. Incidence of endocrine complications and clinical disease severity related to genotype analysis and iron overload in patients with β -thalassaemia. *Eur J Haematol* 1997; 59:76–81.
120. Olivieri NF. Personal observation 2001.
121. Karahyan E, Stoyaniva A, Mouldzhiev I, Ivanov I. Secondary diabetes in children with thalassaemia major (homozygous thalassemia). *Folio Med Plovdiv* 1994; 35:29–34.
122. Soliman AT, el-Banna N, Al Salmi I, Asfour M. Insulin and glucagon responses to provocation with glucose and arginine in prepubertal children with thalassemia major before and after long-term blood transfusion. *J Trop Pediatr* 1996; 42:291–296.
123. De Sanctis V, Zurlo MG, Senesi E, Boffa C, Cavallo L, Di Gregorio F. Insulin dependent diabetes in thalassaemia. *Arch Dis Child* 1988; 63:58–62.
124. Lassman MN, Genel M, Wise JK, Hendler R, Felig P. Carbohydrate homeostasis and pancreatic islet cell function in thalassemia. *Blood* 1974; 80:65–69.
125. Costin G, Kogut MD, Hyman C, Ortega JA. Carbohydrate metabolism and pancreatic islet-cell function in thalassemia major. *Diabetes* 1977; 26:230–240.
126. Saudek CD, Hemm RM, Peterson CM. Abnormal glucose tolerance in beta-thalassemia major. *Metabolism* 1977; 26:43–52.
127. Zuppinger K, Molinari B, Hirt A, et al. Increased risk of diabetes mellitus in beta-thalassaemia major. *Hel Paediatr Acta* 1979; 4:197–207.
128. Dandona P, Hussain MAM, Varghese Z, Politis D, Flynn DM, Hoffbrand AV. Insulin resistance and iron overload. *Ann Clin Biochem* 1983; 20:77–79.
129. Merkel PA, Simonson DC, Amiel SA, et al. Insulin resistance and hyperinsulinemia in patients with thalassemia major treated by hypertransfusion. *N Engl J Med* 1988; 318:809–814.
130. Dmochowski K, Finegood DT, Francombe WH, Tyler B, Zinman B. Factors determining glucose tolerance in patients with thalassemia major. *J Clin Endocrinol Metab* 1993; 77:478–483.
131. Cavello-Perin P, Pacini B, Cerutti F, et al. Insulin resistance and hyperinsulinemia in homozygous β -thalassemia. *Metabolism* 1995; 44:281–286.
132. De Sanctis V, D'Ascola G, Wonke B. The development of diabetes mellitus and chronic liver disease in long term chelated β -thalassaemic patients. *Postgrad Med J* 1986; 62:831–836.
133. Gullo L, Corcioni E, Brancati C, Bria M, Pezzelli R, Sprovieri G. Morphologic and functional evaluation of the exocrine pancreas in beta-thalassemia. *Pancreas* 1993; 8:176–180.
134. Magro S, Puzzon P, Consarino C, et al. Hypothyroidism in patients with thalassemia syndromes. *Acta Haematol* 1990; 84:72–76.
135. De Sanctis V, Vullo C, Bagni B, Chiccoli L. Hypoparathyroidism in β -thalassemia major. Clinical and laboratory observations in 24 patients. *Acta Haematol* 1992; 88:105–108.
136. Pratico G, Di Gregorio F, Caltabiano L, Palano GM, Caruso-Nicoletti M. Calcium phosphate metabolism in thalassemia. *Pediatr Med Chir* 1998; 20:265–268.
137. Gabutti V, Piga A. Results of long-term iron-chelating therapy. *Acta Haematol* 1996; 95:26–36.
138. Lassman MN, O'Brien RT, Pearson HA, et al. Endocrine evaluation in thalassemia major. *Ann NY Acad Sci* 1974; 232:226.
139. Vullo C, De Sanctis V, Katz M, et al. Endocrine abnormalities in thalassemia. *Ann NY Acad Sci* 1990; 612:293–310.
140. Koren A, Garty I, Antonelli D, Katzuni E. Right ventricular cardiac dysfunction in β -thalassemia major. *Am J Dis Child* 1987; 141:93–96.

141. Factor JM, Pottipati SR, Rappaport I, Rosner IK, Lesser ML, Giardini PJ. Pulmonary function abnormalities in thalassemia major and the role of iron overload. *Am J Respir Crit Care Med* 1994; 149:1570–1574.
142. Tai DYH, Wang YT, Lou J, Wang WY, Mak KH, Cheng HK. Lungs in thalassaemia major patients receiving regular transfusion. *Eur Respir J* 1996; 9:1389–1394.
143. Luyt DK, Richards GA, Roode H, Dowdeswell RJ, van Rensburg AJ, Reinach SG. Thalassemia: Lung function with reference to iron studies and reactive oxidant status. *Pediatr Hematol Oncol* 1993; 10:13–23.
144. Cooper DM, Mansell AL, Weiner MA, et al. Low lung capacity and hypoxemia in children with thalassemia major. *Am Rev Respir Dis* 1980; 121:639–646.
145. Fung KP, Chow OK, So SY, Yuen PM. Pulmonary function in thalassemia major. *J Pediatr* 1987; 111:534–537.
146. Landing BH, Nadorra R, Hyman CB, Ortega JA. Pulmonary lesions of thalassaemia major. *Perspect Pediatr Pathol* 1987; 11:82–96.
147. Freedman MH, Olivieri NF, Grisaru D, McLuskey I, Thorner P. Pulmonary syndrome in patients receiving intravenous deferoxamine infusions. *Am J Dis Child* 1990; 144:565–569.
148. Keens TG, O'Neal MH, Ortega JA, Hyman CB, Platzker ACG. Pulmonary function abnormalities in thalassemia patients on a hypertransfusion program. *Pediatrics* 1980; 65:1013–1017.
149. Hoyt RW, Scarpa N, Wilmott RW, Cohen A, Schwartz E. Pulmonary function abnormalities in homozygous β -thalassemia. *J Pediatr* 1986; 109:452–455.
150. Grisaru D, Rachmilewitz EA, Mosseri M, et al. Cardiopulmonary assessment in beta-thalassemia major. *Chest* 1990; 98:1138–1142.
151. Santamaria F, Villa MP, Werner B, Cutrera R, Barreto M, Ronchetti R. The effect of transfusion on pulmonary function in patients with thalassemia major. *Pediatr Pulmonol* 1994; 18:139–143.
152. Grant GP, Graziano JH, Seaman C, Mansell AL. Cardiorespiratory response to exercise in patients with thalassemia major. *Am Rev Respir Dis* 1987; 136:92–97.
153. Bacalo A, Kivity S, Heno N, Greif J, Topilsky M. Blood transfusion and lung function in children with thalassemia major. *Chest* 1992; 101:362–370.
154. Letsky EA, Miller F, Worwood M, Flynn DM. Serum ferritin in children with thalassaemia regularly transfused. *J Clin Pathol* 1974; 27:652–655.
155. Worwood M, Cragg SJ, McLaren C, Ricketts C, Economidou J. Binding of serum ferritin to concanavalin A: Patients with homozygous β thalassaemia and transfusional iron overload. *Br J Haematol* 1980; 46:409–416.
156. Roeser HP, Halliday JW, Sizemore DEA. Serum ferritin in ascorbic acid deficiency. *Br J Haematol* 1980; 45:457–466.
157. Baynes R, Bezwoda W, Bothwell T, Khan Q, Mansoor N. The non-immune inflammatory response: Serial changes in plasma iron, iron-binding capacity, lactoferrin, ferritin and C-reactive protein. *Scand J Clin Lab Invest* 1986; 46:695–704.
158. Brittenham GM, Cohen AR, McLaren C, et al. Hepatic iron stores and plasma ferritin concentration in patients with sickle cell anemia and thalassemia. *Am J Hematol* 1993; 42:81–85.
159. Overmoyer BA, McLaren CE, Brittenham GM. Uniformity of liver density and non-heme (storage) iron distribution. *Arch Pathol Lab Med* 1987; 111:549–554.
160. Ambu R, Crisponi G, Sciort R, et al. Uneven hepatic iron and phosphorus distribution in beta-thalassemia. *J Hepatol* 1995; 23:544–549.
161. Barry M, Flynn DN, Letsky EA, Risdon RA. Long-term chelation therapy in thalassaemia major: Effect on liver iron concentration, liver histology and clinical progress. *Br Med J* 1974; i:16–20.

162. Angelucci E, Brittenham GM, McLaren CE, et al. Hepatic iron concentration and total body iron stores in thalassemia major. *N Engl J Med* 2000; 343:327–331.
163. Brittenham GM, Farrell DE, Harris JW, Feldman ES, Danish EH. Magnetic-susceptibility measurement of human iron stores. *N Engl J Med* 1982; 307:1671–1675.
164. Olynk J, O’Neil R, Britton R, Bacon B. Determination of hepatic iron concentration in fresh and paraffin-embedded tissue: Diagnostic implications. *Gastroenterology* 1994; 106:674–677.
165. Olivieri NF, Brittenham GM. Iron-chelating therapy and the treatment of thalassemia [see comments] [published erratum appears in *Blood* 1997; 89(7):2621]. *Blood* 1997; 89:739–761.
166. Finch CA, Lee MY, Leonard JM. Continuous RBC transfusions in a patient with sickle cell disease. *Arch Intern Med* 1982; 142:279–282.
167. Harmatz P, Butensky E, Quirolo K, et al. Severity of iron overload in patients with sickle cell disease receiving chronic red blood cell transfusion therapy. *Blood* 2000; 96:76–79.
168. Diggs L, Ching R. Pathology of sickle cell anemia. *So Med J* 1934; 27:839–845.
169. Green T, Conley C, Berthrong M. The liver in sickle cell anemia. *Bull Johns Hopkins Hosp* 1953; 92:99–127.
170. Bogoch A, Casselman W, Margolies M, et al. Liver disease in sickle cell anemia. A correlation of clinical, biochemical, histological and histochemical observations. *Am J Med* 1955; 19:583–609.
171. Buja LM, Roberts WC. Iron in the heart. Etiology and clinical significance. *Am J Med* 1971; 51:209–221.
172. Cohen A, Kron E, Brittenham GM. Toxicity of transfusional iron overload in sickle cell anemia. *Blood* 1984; 64:47a.
173. Pippard MJ, Weatherall DJ. Oral iron chelation therapy for thalassaemia: an uncertain scene [in process citation]. *Br J Haematol* 2000; 111:2–5.
174. Tondury P, Zimmermann A, Nielsen P, Hirt A. Liver iron and fibrosis during long-term treatment with deferiprone in Swiss thalassaemic patients. *Br J Haematol* 1998; 101: 413–415.
175. Hoffbrand AV, al-Refaie F, Davis B, et al. Long-term trial of deferiprone in 51 transfusion-dependent iron overloaded patients. *Blood* 1998; 91:295–300.
176. Olivieri NF, Brittenham GM, McLaren CE, et al. Long-term safety and effectiveness of iron chelation therapy with deferiprone for thalassemia major. *N Engl J Med* 1998; 339:417–423.
177. Mazza P, Anurri B, Lazzari G, et al. Oral iron chelating therapy. A single center interim report on deferiprone (L1) in thalassemia. *Haematologica* 1998; 83:496–501.
178. Olivieri NF, Brittenham GM, Matsui D, et al. Iron-chelation therapy with oral deferiprone in patients with thalassemia major. *N Engl J Med* 1995; 332:918–922.
179. Carthew P, Smith AG, Hider RC, Dorman B, Edwards RE, Francis JE. Potentiation of iron accumulation in cardiac myocytes during the treatment of iron overload with the hydroxypyridinone iron chelator CP94. *Biometals* 1994; 7:267–271.
180. Wong A, Alder V, Robertson D, et al. Liver iron depletion and toxicity of the iron chelator deferiprone (L1, CP20) in the guinea pig. *Biometals* 1997; 10:247–256.
181. Cohen A, Galanello R, Piga A, Vullo C, Tricta F. A multi-center safety trial of the oral iron chelator deferiprone. In: Cohen AR, ed. *Cooley’s Anemia Seventh Symposium*. Vol. 850. New York: The New York Academy of Sciences, 1998; 223–226.
182. Cohen AR, Galanello R, Piga A, DiPalma A, Vullo C. Safety profile of the oral iron chelator deferiprone: A multicentre study. *Br J Haematol* 2000; 108:305–312.
183. Cohen A, Galanello R, Piga A, Gamberini R, DeSanctis V, Tricta F. Long-term safety and efficacy of the oral iron chelator deferiprone. *Blood* 2000; 96:443a [abstr].

184. Tondury P, Kontoghiorghes GJ, Ridolfi-Luthy AR, et al. L1 (1,2-dimethyl-3-hydroxy-pyrid-4-one) for oral iron chelation in patients with beta-thalassaemia major. *Br J Haematol* 1990; 76:550–553.
185. Hershko C, Link G, Konijn A. Ability of deferiprone to protect tissues from non-transferrin-bound iron (NTBI) toxicity. 9th International Conference on Oral Chelation in the Treatment of Thalassemia and Other Diseases, Hamburg, Germany, 1999.
186. Cohen A, Martin M. Iron chelation with oral deferiprone in patients with thalassemia. *N Engl J Med* 1998; 339:1713.
187. Grady RW, Giardina P. Iron chelation with oral deferiprone in patients with thalassemia. *N Engl J Med* 1998; 339:1713.
188. Stella M, Giovanni P, Maggio A. Iron chelation with oral deferiprone in patients with thalassemia. *N Engl J Medicine* 1998; 339:1712.
189. Wonke B, Telfer P. Iron chelation with oral deferiprone in patients with thalassemia. *N Engl J Med* 1998; 339:1712.
190. Tricta F, Spino M. Iron Chelation with oral deferiprone in patients with thalassemia. *N Engl J Med* 1998; 339:1710.
191. Wanless I, Sweeney G, Dhillon A, et al. Absence of deferiprone-induced hepatic fibrosis: A multi-center study. *Blood* 2000; 96:606a [abstr].
192. Wonke B, Wright C, Hoffbrand AV. Combined therapy with deferiprone and desferrioxamine. *Br J Haematol* 1998; 103:361–364.
193. Aydinok Y, Nisli G, Kavakli K, Coker C, Kantar M, Cetingul N. Sequential use of deferiprone and desferrioxamine in primary school children with thalassaemia major in Turkey. *Acta Haematol* 1999; 102:17–21.

Aceruloplasminemia

NATHAN E. HELLMAN

Washington University School of Medicine, St. Louis, Missouri

Z. LEAH HARRIS

Johns Hopkins University, Baltimore, Maryland

I. INTRODUCTION	749
II. CERULOPLASMIN	750
III. ACERULOPLASMINEMIA	750
IV. ACERULOPLASMINEMIC MICE	752
V. CONCLUSION	758
ACKNOWLEDGMENTS	758
REFERENCES	758

I. INTRODUCTION

The last decade has witnessed the identification and characterization of multiple proteins involved in both copper and iron trafficking. Among these, a family of multicopper oxidases essential for iron metabolism has emerged. These multicopper oxidases possess the ability to reduce dioxygen in a four-electron reduction to water while simultaneously providing one-electron oxidation of the reducing substrate. Ubiquitously expressed and with highly conserved copper ligands, these proteins are characterized by the presence of three spectroscopically distinct copper ions (1). In vertebrate species, ceruloplasmin (Cp) is the predominant multicopper oxidase responsible for the ferroxidation of ferrous iron (Fe^{2+}) to ferric iron (Fe^{3+}). The recent characterization of a disease of iron overload, aceruloplasminemia, resulting from

mutations in the ceruloplasmin gene has further confirmed the essential role of ceruloplasmin in iron metabolism (2). The development of a murine model of this disease has allowed elucidation of the mechanisms by which ceruloplasmin regulates iron efflux (3).

II. CERULOPLASMIN

Ceruloplasmin is an α_2 -glycoprotein, synthesized and secreted predominantly by hepatocytes, containing 95% of the copper present in serum (4). Type I copper sites impart a sky-blue hue to the purified protein. Multiple functions have been ascribed to ceruloplasmin: a primary ferroxidase, an antioxidant, and an acute-phase reactant. Serum concentrations of ceruloplasmin increase during infection, inflammation, and injury secondary to effects on hepatic ceruloplasmin gene expression (5).

Human ceruloplasmin is a 19-exon, single-copy, 40-kb gene in the haploid human genome (6). It results in the production of two transcripts, 3.7 kb and 4.2 kb, secondary to differential polyadenylation. Each transcript is translated into a 132-kDa protein (1046 amino acids) with 6 copper atoms tightly incorporated during the biosynthetic process (7). Additionally, there are two forms of ceruloplasmin, a secreted form and a glycosylphosphatidylinositol-linked form (8). In the absence of available copper for incorporation into the secreted protein, an apoprotein is made at the same synthetic rate. However, in the absence of incorporated copper this apoprotein has a half-life of 4–5 h, compared to the holoprotein half-life of 4–5 days (9,10).

X-ray crystallography and elucidation of the structure of human ceruloplasmin have revealed details of the ligand structure essential for function (11). Three of the six copper atoms occupy mononuclear sites in domains 2, 4, and 6. The remaining three copper atoms exist in a trinuclear copper cluster at the interface of domains 1 and 6. It is this trinuclear copper cluster that is essential for ceruloplasmin oxidase activity (12).

Copper, bound either to albumin or histidine, enters the hepatocyte via the copper transporter 1 (CTR1), where the copper chaperone HAH1 escorts the copper to the Wilson disease P-type ATPase (13). This ATPase, which is essential for the movement of copper into the secretory pathway (trans-Golgi network) for either incorporation into ceruloplasmin or excretion into bile (14) (Fig. 1). The absence of copper within the secretory pathway as a result of either (a) a mutation in the Wilson disease P-type ATPase or (b) copper deficiency resulting in an apoceruloplasmin being produced that is rapidly degraded.

III. ACERULOPLASMINEMIA

Recently, patients have been identified who lack circulating serum ceruloplasmin secondary to mutations in their ceruloplasmin gene (2,15–21). These mutations in the ceruloplasmin gene cause insulin-dependent diabetes mellitus, and retinal and neurological degeneration in adulthood secondary to alterations in iron trafficking. Presenting symptoms include a Parkinson-like movement disorder, dysarthria, ataxia, dystonia, and dementia (22,23). Aceruloplasminemia represents a novel disorder of systemic and central nervous system iron overload resulting from abnormal iron accumulation in the brain, liver, and pancreas.

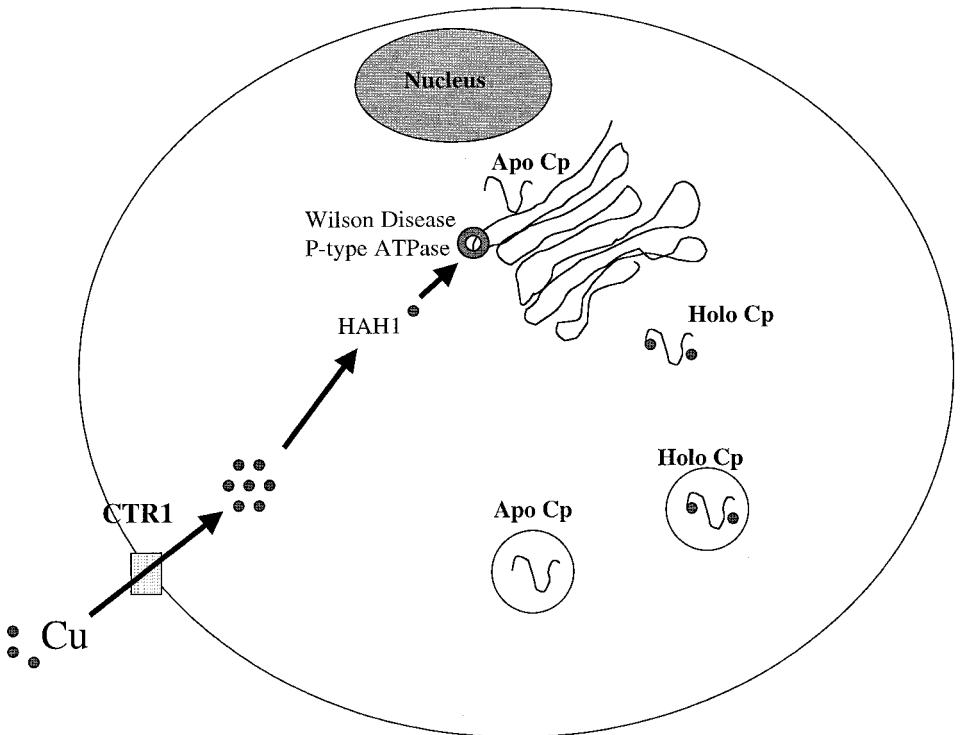


Figure 1 A model of copper trafficking into the hepatocyte.

T2-weighted magnetic resonance imaging (MRI) studies reveal iron accumulation in the basal ganglia and substantia nigra (24). Postmortem examinations of brains from affected individuals confirm iron accumulation throughout the basal ganglia, as manifested by neuronal dropout and loss, and iron accumulation in both neurons and microglia (24). In addition, despite normal cortical architecture on gross histological examination of the brain, cavitory degeneration within the basal ganglia and substantia nigra has been identified (24).

Examinations of other organs reveal iron accumulation in the liver in both hepatocytes and Kupffer cells (cells of the reticuloendothelial system). Histological review of liver tissue from aceruloplasminemic patients reveals normal architecture without evidence of fibrosis, cirrhosis, or any hepatocellular damage classically associated with the copper deposition of Wilson disease (24). Selective pancreatic β -cell iron accumulation within islets of Langerhans can be identified by Perl's stain, and patients have ineffective insulin production as a result (25).

Through the use of sophisticated animal models, genetics is now revealing molecular details of the pathways of iron influx. However, little or nothing is known about the mechanisms of cellular iron efflux. It is the understanding of this process, iron efflux, which will become essential for treatment of iron-overload syndromes. Aceruloplasminemia represents a newly recognized disorder of iron storage. Despite the recognition of this disease, the precise role of ceruloplasmin is unclear. Earlier attempts using the classic nutritional studies of Cartwright and Freiden had suggested

a role as a primary ferroxidase but were clouded by the effects of copper deficiency (26–29).

A relationship between iron and copper metabolism had been established earlier in experiments by E. B. Hart et al., demonstrating that in anemia unresponsive to iron administration, copper administration promoted iron incorporation into red blood cells (30). Only in the presence of copper could these iron-deficient animals utilize the iron they were receiving. Interestingly, a similar pattern of copper delivery has been identified in baker's yeast, *Saccharomyces cerevisiae* (Fig. 2). FET3, a multi-copper oxidase and ceruloplasmin homolog, is intimately dependent on copper incorporation to oxidize substrates (31,32). In order for iron to be stored in yeast it must be oxidized to ferric iron, and yeast rely on FET3 and its associated permease, the transmembrane protein FTR1, to accomplish this (33).

IV. ACERULOPLASMINEMIC MICE

In order to understand the role of ceruloplasmin in iron biology, a ceruloplasmin-null mouse was developed. To generate a murine model of aceruloplasminemia by homologous recombination, we designed a gene targeting strategy based on the human Matsumoto mutation, where the last 100 amino acids of the ceruloplasmin protein are predicted to be absent secondary to a splice-site mutation (15). This is predicted to disrupt the interface between the amino terminus and the carboxy terminus that is essential for the appropriate alignment of the trinuclear copper cluster.

To confirm that transcription of ceruloplasmin was disrupted in the ceruloplasmin knockout ($Cp^{-/-}$) mouse, Northern blot analysis was performed on total RNA isolated from murine liver and brain (Fig. 3A). No detectable mRNA was found in the tissue from $Cp^{-/-}$ mice compared to the ceruloplasmin wild-type ($Cp^{+/+}$) mice. Like patients who have absent circulating serum ceruloplasmin, the $Cp^{-/-}$ mouse lacks circulating serum ceruloplasmin. Heterozygote mice ($Cp^{+/-}$) have half-normal detectable circulating serum ceruloplasmin (3) (Fig. 3B). Screening of successfully targeted recombinant alleles was performed by both Southern blot analysis and polymerase chain reaction amplification (PCR) (Figs. 3C and 3D). Additionally, $Cp^{-/-}$ mice lack appreciable oxidase activity as measured by *o*-dianisidine oxidation, or ferroxidase activity as determined by the formation of Fe^{3+} -transferrin. The small amount of activity detected (<3% $Cp^{+/+}$) is consistent with other nonenzymatic oxidants present in the serum (3) (Fig. 3E).

To determine the effect of overwhelming nonenzymatic serum oxidants and making the ferroxidation capabilities of ceruloplasmin rate-limiting, we followed serum iron concentrations in wild-type and knockout mice following an infusion of heat-damaged red blood cells (DRBC). It was important to deliver the iron in a form that would be taken up selectively by the reticuloendothelial system. Following an infusion of DRBC delivering 2–3 mg iron/g body weight, wild-type mice ($Cp^{+/+}$) were able to handle the increased iron load and mobilize iron bound to transferrin for delivery from the reticuloendothelial system to the bone marrow 3 h following the injection. Knockout mice ($Cp^{-/-}$) did not mobilize iron, and their serum iron concentrations remained constant throughout the experiment (Fig. 4A).

To determine the effect of ceruloplasmin in mediating this observed iron release, purified human holoceruloplasmin was prepared and each mouse was injected via the tail vein with 20% equivalent of normal circulating ceruloplasmin. When

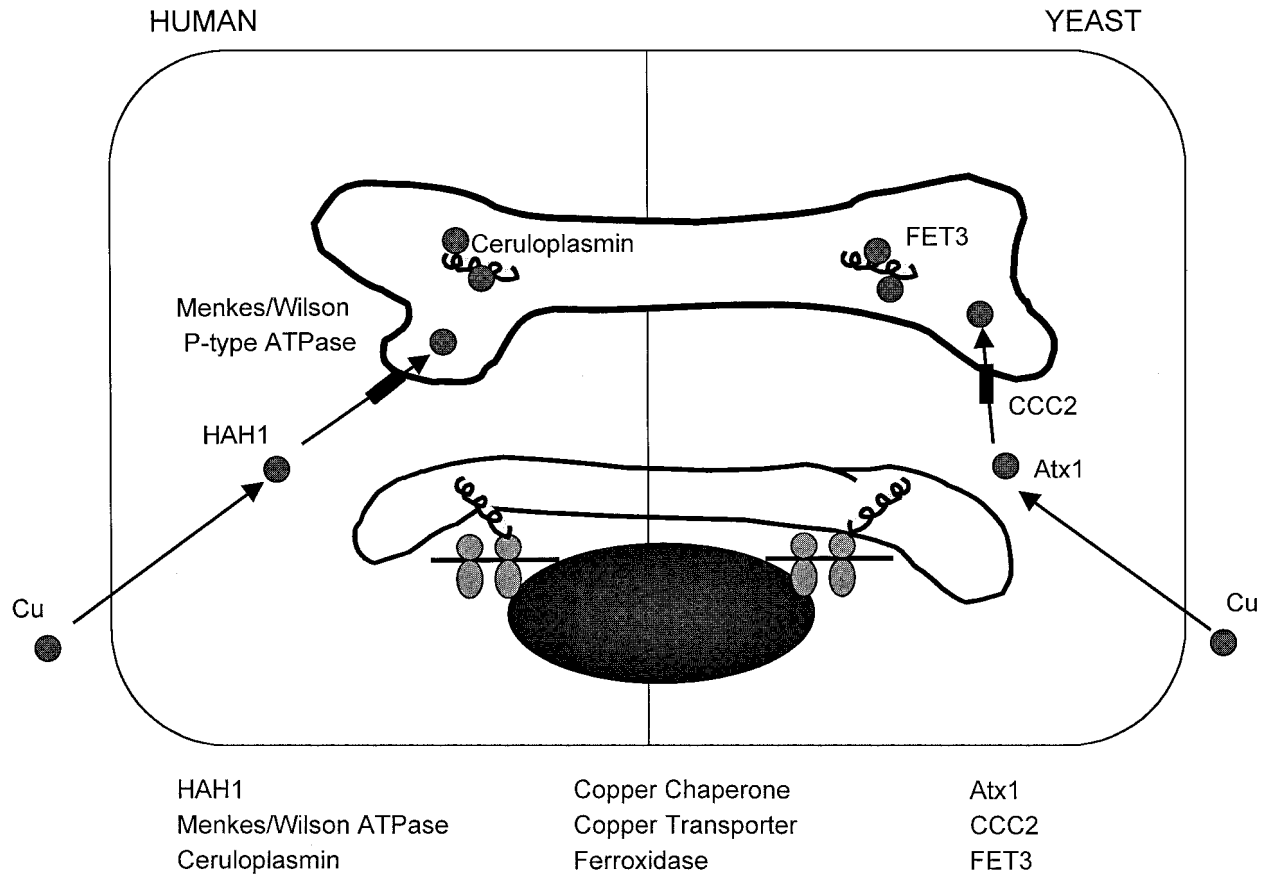


Figure 2 A model of yeast and human copper proteins.

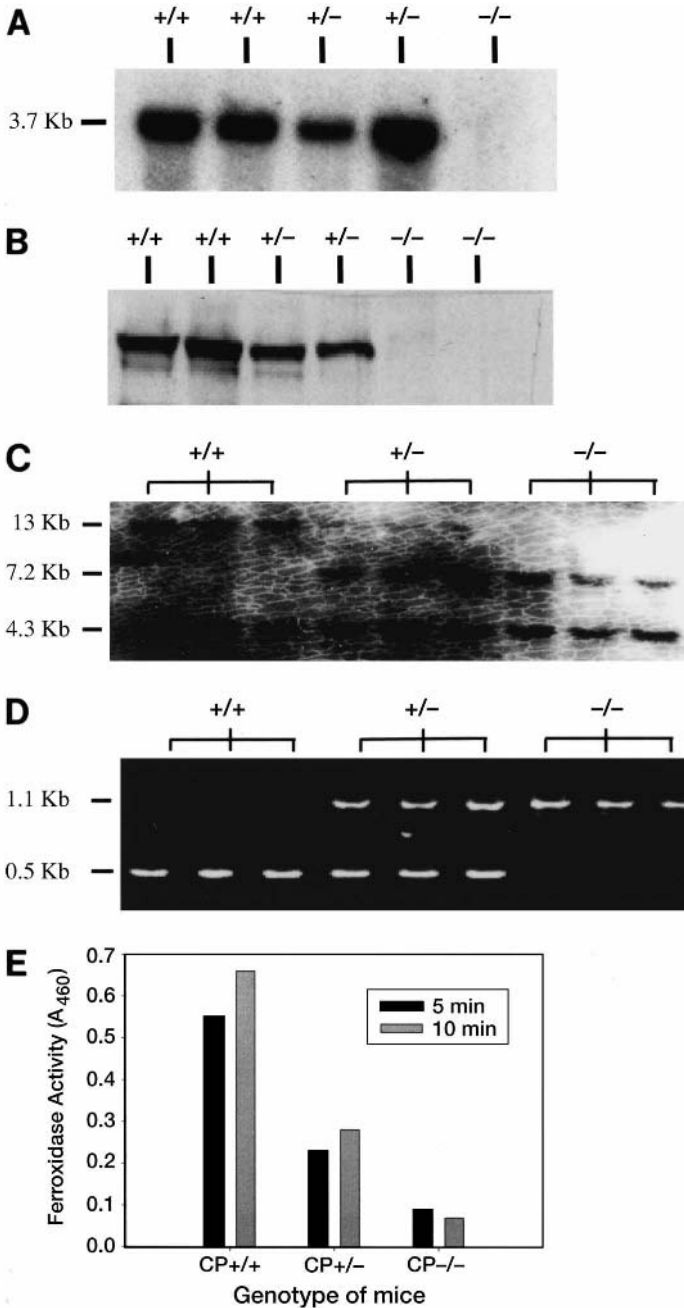


Figure 3 (A) Northern blot analysis reveals a 3.7-kb transcript from RNA isolated from liver from $Cp^{+/+}$, $Cp^{+/-}$, and $Cp^{-/-}$ mice. (B) Western blot analysis using a polyclonal antibody of serum from $Cp^{+/+}$, $Cp^{+/-}$, and $Cp^{-/-}$ mice. (C) Southern blot analysis from DNA isolated from $Cp^{+/+}$, $Cp^{+/-}$, and $Cp^{-/-}$ mice revealing 13-kb and 4.3-kb bands for $Cp^{+/+}$, 13-kb, 7.2-kb, and 4.3-kb bands for $Cp^{+/-}$, and 7.2-kb and 4.3-kb bands for $Cp^{-/-}$. (D) PCR amplification products from tail genomic DNA corresponding to a 0.5-kb fragment from exon 16 to exon 17 in $Cp^{+/+}$ and a 1.0-kb fragment from exon 16 to the Neo cassette in $Cp^{-/-}$. (E) Ferroxidase activity in $Cp^{+/+}$, $Cp^{+/-}$, and $Cp^{-/-}$ mice.

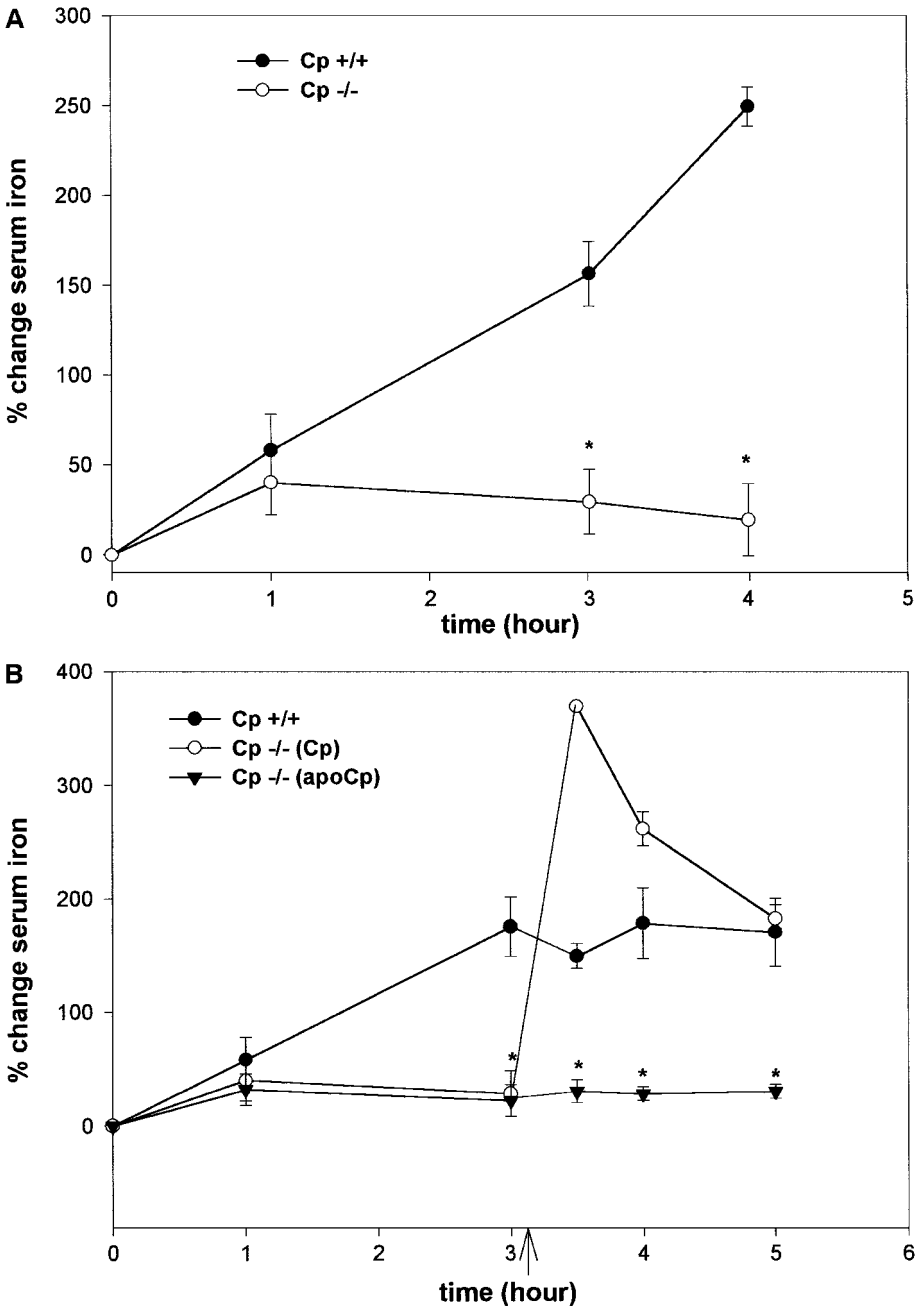


Figure 4 (A) Effect of damaged red blood cell infusion on percent change of total serum iron concentration in $Cp^{+/+}$ and $Cp^{-/-}$ mice. (B) Effect of the administration of holoceruloplasmin (Cp) and apoceruloplasmin (apoCp) on percent change of total serum iron concentrations following the infusion of damaged red blood cells in $Cp^{+/+}$ and $Cp^{-/-}$ mice. (C) Effect of severe anemia on total serum iron concentration in $Cp^{+/+}$ and $Cp^{-/-}$ mice and the effect of the infusion of holoceruloplasmin (Cp) and apoceruloplasmin (apoCp) on the percent change of total serum iron concentration in phlebotomized mice. [Reproduced with permission of Harris et al. (3).]

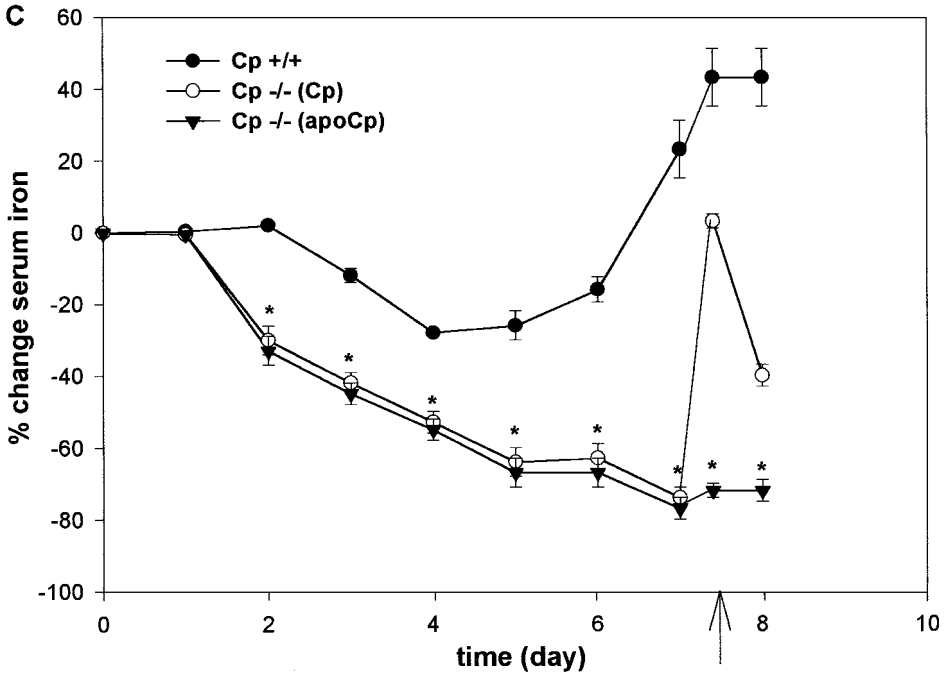


Figure 4 Continued

purified human ceruloplasmin was administered to both wild-type ($Cp^{+/+}$) and knock-out ($Cp^{-/-}$) mice, a rapid iron efflux was observed in the knockout ($Cp^{-/-}$) mice which peaked at 30 min following the ceruloplasmin infusion and remained elevated for the hour following. These results were not observed when these mice were given apoceruloplasmin (heat-inactivated holoceruloplasmin) (Fig. 4B).

To continue to test the hypothesis that ceruloplasmin regulates iron efflux under conditions that saturate nonenzymatic serum oxidants, mice were made anemic by daily serial bleeding of 15% of their circulating total volume. In such mice, the delivery of iron from reticuloendothelial stores to the bone marrow to correct the anemia would be made dependent on the availability of ceruloplasmin. Following serum iron concentrations in these same mice daily revealed the ability of wild-type ($Cp^{+/+}$) mice to effectively mobilize iron stores and traffic iron bound to transferrin to the bone marrow for new red cell synthesis. The knockout ($Cp^{-/-}$) mice were unable to increase the amount of iron released from their reticuloendothelial stores to meet the demand placed by the anemia. In fact, the serum iron concentrations of the knockout ($Cp^{-/-}$) mice continued to drop as the bleeding progressed. On day 7 of bleeding, mice received a tail-vein infusion of purified human ceruloplasmin calculated to restore 20% equivalent of normal circulating serum ceruloplasmin. Within 30 min of the holoceruloplasmin infusion, knockout ($Cp^{-/-}$) mice serum iron concentrations elevated to wild-type ($Cp^{+/+}$) levels, while wild-type ($Cp^{+/+}$) serum iron levels remained constant (Fig. 4C). There was no observed effect of apoceruloplasmin injection on serum iron concentrations in either group of mice (3).

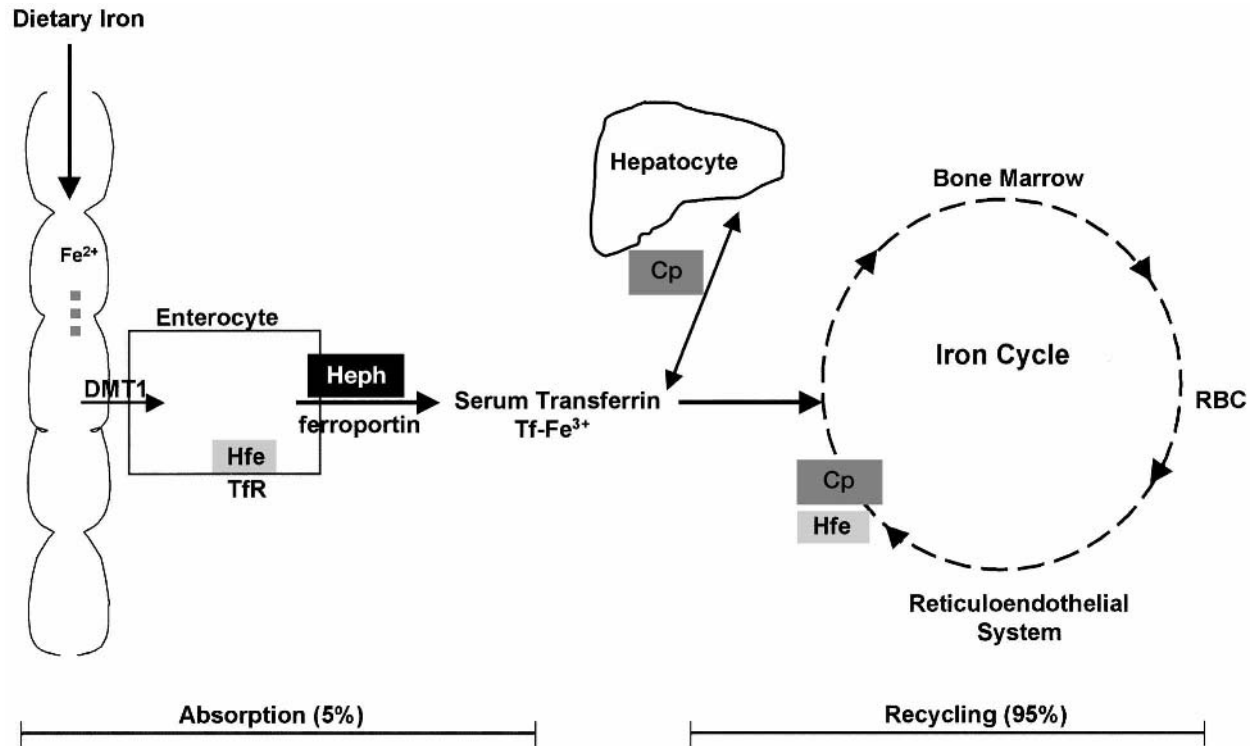


Figure 5 The iron cycle. The proteins critical for iron absorption and trafficking are shown. Emphasis is placed on the multicopper oxidases, hephaestin (Heph), and ceruloplasmin (Cp). DMT1, divalent metal transporter; Hfe, hereditary hemochromatosis gene product; TfR, transferrin receptor; RBC, red blood cell.

V. CONCLUSION

Following absorption across the gastrointestinal tract, the majority of iron is bound to serum transferrin and delivered to the bone marrow for incorporation into hemoglobin in erythrocytes. The mechanisms of intestinal iron absorption have been well studied and involve a complex interplay among the brush border transporter, DMT1/Nramp2, the hemochromatosis gene product (Hfe), the transferrin receptor (TfR), ferroportin, and hephaestin (34–36). Only 5% of the daily iron requirement is absorbed from the diet, as the remaining 95% is met by the recycling of iron from senescent red blood cells within the reticuloendothelial system. Iron homeostasis is achieved when equivalent amounts of iron utilized for erythropoiesis are returned to the plasma from the reticuloendothelial system (Fig. 5). Although this process represents the single greatest daily efflux of tissue iron, virtually nothing is known about the mechanisms underlying this process of cellular iron trafficking.

Studies now reveal that ceruloplasmin functions as a “gatekeeper” of iron efflux from the reticuloendothelial system. The recent discovery and molecular characterization of aceruloplasminemia reveals an essential role for the copper-containing serum protein, ceruloplasmin, in iron metabolism. The ceruloplasmin-null mouse suggests that in the absence of serum ceruloplasmin, nonenzymatic oxidation of ferrous to ferric iron is sufficient to maintain an adequate level of ferric iron bound to transferrin for completion of the red cell cycle, albeit with an associated slow accumulation of iron within the reticuloendothelial compartment. However, under circumstances that make ceruloplasmin rate-limiting by exceeding the capacity of alternative nonenzymatic ferroxidases, there is an increase in serum ferrous iron, an increase in nontransferrin ferrous iron uptake into tissues, and a decrease in iron efflux. Thus, aceruloplasminemia represents a disorder of iron efflux manifest as iron overload in the central nervous system and parenchymal tissues and reveals an essential role for ceruloplasmin in iron metabolism.

ACKNOWLEDGMENTS

These studies were supported by National Institutes of Health Grant DK02462 (ZLH). ZLH was a Scholar of the Child Health Research Center of Excellence at Washington University School of Medicine (HD33688).

REFERENCES

1. Malmstrom BG. Early and more recent history in the research of multi-copper oxidases. In: Messerschmidt A, ed. *Multi-Copper Oxidases*. River Edge, NJ: World Scientific, 1997:1–22.
2. Harris ZL, Takahashi Y, Miyajima H, Serizawa M, MacGillivray RTA, Gitlin JD. Aceruloplasminemia: Molecular characterization of this disorder of iron metabolism. *Proc Natl Acad Sci USA* 1995; 92:2539–2543.
3. Harris ZL, Durley AP, Man TK, Gitlin JD. Targeted gene disruption reveals an essential role for ceruloplasmin in cellular iron efflux. *Proc Natl Acad Sci USA* 1999; 96:10812–10817.
4. Harris ZL, Klomp LWJ, Gitlin JD. Aceruloplasminemia: an inherited neurodegenerative disease with impaired iron homeostasis. *Am J Clin Nutr* 1998; 67:972S–977S.
5. Gitlin JD. Transcriptional regulation of ceruloplasmin gene expression during inflammation. *J Biol Chem* 1988; 263:6281–6287.

6. Harris ZL, Morita H, Gitlin JD. The biology of human ceruloplasmin. In: Messerschmidt A, ed. *Multi-Copper Oxidases*. River Edge, NJ: World Scientific, 1997:285–305.
7. Gitlin JD. Aceruloplasminemia. *Pediatr Res* 1998; 44:271–275.
8. Patel BN, David S. A novel glycosylphosphatidylinositol-anchored form of ceruloplasmin is expressed by mammalian astrocytes. 1997; 272:20185–20190.
9. Holtzman NA, Guamnitz BM. Identification of an apoceruloplasmin-like substance in the plasma of copper-deficient rats. *J Biol Chem* 1970; 245:2350–2353.
10. Holtzman NA, Guamnitz BM. Studies of the rate of release and turnover of ceruloplasmin and apoceruloplasmin in rat plasma. *J Biol Chem* 1970; 245:2354–2358.
11. Zaitseva I, Zaitsev V, Cara G, Mojtkov K, Bar B, Lindley PF. The x-ray structure of human ceruloplasmin at 3.1 Å resolution: Nature of the copper centers. *J Biol Inorg Chem* 1996; 1:15–23.
12. Calabrese L, Carbonaro M, Giovanni M. Presence of coupled trinuclear copper cluster in mammalian ceruloplasmin is essential for efficient electron transfer to oxygen. *J Biol Chem* 1993; 264:6183–6187.
13. Hamza I, Schaefer M, Klomp LWJ, Gitlin JD. Interaction of the copper chaperone HAH1 with the Wilson disease protein is essential for copper homeostasis. *Proc Natl Acad Sci USA* 1999; 96:13363–13368.
14. Hung IH, Suzuki M, Yamaguchi Y, Yuan DS, Klausner RD, Gitlin JD. Biochemical characterization of the Wilson disease protein and functional expression in yeast *Saccharomyces cerevisiae*. *J Biol Chem* 1997; 272:21461–21466.
15. Yoshida K, Furihata K, Takeda S, Nakamura A, Yamamoto K, Hiyamuta S, Ikeda S, Shimizu N, Yanagisawa N. A mutation in the ceruloplasmin gene is associated with systemic hemosiderosis in humans. *Nature Genet* 1995; 9:267–272.
16. Daimon M, Kato T, Kawanami T, Tominaga M, Igarashi M, Yamatani K, Sasaki H. A nonsense mutation of the ceruloplasmin gene in hereditary ceruloplasmin deficiency with diabetes mellitus. *Biochem Biophys Res Commun* 1995; 217:89–95.
17. Takahashi Y, Miyajima H, Shirabe S, Nagataki S, Suenaga A, Gitlin JD. Characterization of a nonsense mutation in the ceruloplasmin gene resulting in diabetes and neurodegenerative disease. *Hum Mol Genet* 1996; 5:81–84.
18. Harris ZL, Migas MC, Hughes AE, Logan JI, Gitlin JD. Familial dementia due to a frameshift mutation in the caeruloplasmin gene. *Q J Med* 1996; 89:355–359.
19. Okamoto N, Wada S, Oga T, Kawabata Y, Baba Y, Habu D, Takeda Z, Wada Y. Hereditary ceruloplasmin deficiency with hemosiderosis. *Hum Genet* 1996; 97:755–758.
20. Yazaki M, Yoshida K, Nakamura A, Furihata K, Yonekawa M, Okabe T, Yamashita N, Ohta M, Ikeda S. A novel splicing mutation in the ceruloplasmin gene responsible for hereditary ceruloplasmin deficiency with hemosiderosis. *J Neurol Sci* 1998; 156:30–34.
21. Hellman NE, Schaefer M, Gehrke S, Stegen P, Hoffman WJ, Gitlin JD, Stremmel W. Aceruloplasminemia in the differential diagnosis of hepatic iron excess. *Gut* 2000; 47: 858–860.
22. Miyajima H, Nishimura Y, Mizoguchi K, Sakamoto M, Shimizu T, Honda N. Familial apoceruloplasmin deficiency associated with blepharospasm and retinal degeneration. *Neurology* 1987; 37:761–767.
23. Logan JI, Harveyson KB, Wisdom GB, Hughes AE, Archbold GP. Hereditary caeruloplasmin deficiency, dementia and diabetes mellitus. *Q J Med* 1994; 87:663–670.
24. Morita H, Ikeda S, Yamamoto K, Morita S, Yoshida K, Nomoto S, Kato M, Yanagisawa N. Hereditary ceruloplasmin deficiency with hemosiderosis: A clinicopathological study of a Japanese family. *Ann Neurol* 1995; 37:646–656.
25. Kato T, Daimon M, Kawanami T, Ikezawa Y, Sasaki H, Maeda K. Islet changes in hereditary ceruloplasmin deficiency. *Hum Pathol* 1997; 28(4):499–502.
26. Osaki S, Johnson DA, Freiden E. The possible significance of the ferrous oxidase activity of ceruloplasmin in normal human serum. *J Biol Chem* 1966; 241:2746–2751.

27. Lee GR, Nacht S, Lukens JN, Cartwright GE. Iron metabolism in copper deficient swine. *J Clin Invest* 1968; 47:2058–2069.
28. Roeser HP, Lee GR, Nacht S, Cartwright GE. The role of ceruloplasmin in iron metabolism. *J Clin Invest* 1970; 49:2408–2417.
29. Osaki S, Johnson DA, Freiden E. The mobilization of iron from the perfused mammalian liver by a serum copper enzyme, ferroxidase I. *J Biol Chem* 1971; 246:3018–3023.
30. Hart EB, Steenbock H, Waddell J, Elvehjem CA. Iron in nutrition. VII. Copper as a supplement to iron for hemoglobin building in the rat. *J Biol Chem* 1928; 77:797–812.
31. Askwith C, Eide D, VanHo A, Bernard PS, Li L, Davis-Kaplan S, Sipe DM, Kaplan J. The FET3 gene of *S. cerevisiae* encodes a multicopper oxidase required for ferrous iron uptake. *Cell* 1994; 76:403–410.
32. Yuan DS, Stearman R, Dancis A, Dunn T, Beeler T, Klausner RD. The Menkes/Wilson disease gene homologue in yeast provides copper to a ceruloplasmin-like oxidase required for iron uptake. *Proc Natl Acad Sci USA* 1995; 92:2632–2636.
33. Stearman R, Yuan DS, Yamaguchi-Iwa Y, Klausner RD, Dancis A. A permease-oxidase complex involved in high-affinity iron uptake in yeast. *Science* 1996; 271:1552–1557.
34. Andrews NC. Disorders of Iron Metabolism. *N Engl J Med* 1999; 341:1986–1995.
35. Donovan A, Brownlie A, Zhou Y, Shepard J, Pratt SJ, Moynihan J, Paw BH, Drejer A, Barut B, Zapata A, Law TC, Brugnara C, Lux SE, Pinkus GS, Pinkus JL, Kingsley PD, Palis J, Fleming MD, Andrews NC, Zon LI. Positional cloning of zebrafish ferroportin1 identifies a conserved vertebrate iron exporter. *Nature* 2000; 403:776–781.
36. Vulpe CD, Kuo YM, Murphy TL, Cowley L, Askwith C, Libina N, Gitschier J, Anderson GJ. Hephaestin, a ceruloplasmin homologue implicated in intestinal iron transport, is defective in the sla mouse. *Nat Genet* 1999; 21:195–199.

Hereditary Hyperferritinemia Cataract Syndrome

CAROLE BEAUMONT

INSERM U409, Faculté de Médecine Xavier Bichat, Paris, France

DOMENICO GIRELLI

University of Verona, Verona, Italy

I. INTRODUCTION	762
II. CLINICAL PRESENTATION OF HHCS PATIENTS	762
III. HHCS: A TRANSLATIONAL PATHOLOGY	763
A. Regulation of Ferritin Synthesis	763
B. IRE Mutations and Deletions	763
C. Clinical Consequences of L-Ferritin Overexpression	765
IV. IS THERE A PHENOTYPE–GENOTYPE CORRELATION?	769
V. CONTEXT OF HHCS AMONG THE HEREDITARY CATARACTS	769
A. Prevalence of IRE Mutations in Cases of Isolated Hyperferritinemia	770
B. Differential Diagnosis in Iron-Overload Disorders	770
VI. CONCLUSIONS	771
ACKNOWLEDGMENTS	771
REFERENCES	771

I. INTRODUCTION

The hereditary hyperferritinemia cataract syndrome (HHCS) was discovered simultaneously by our groups in France and in Italy in 1995. This genetic disease, of autosomal dominant transmission, had remained undetected until then, probably because serum ferritin determination is not of current practice in ophthalmology departments. The elucidation of the molecular basis of this genetic disorder, which rapidly followed identification of the disease, revealed a number of interesting points. First, it led to the discovery of a new gene responsible for hereditary cataract, a very heterogeneous condition with multiple causative genes. Second, the mutations which have been identified in this syndrome impair the translational regulatory element which regulates ferritin synthesis and leads to the unregulated overexpression of normal L-ferritin subunit. It is the only pathological condition known so far which affects this major regulator of iron homeostasis. Finally, this syndrome gives some clue to the origin of serum ferritin, which has been the subject of much controversy.

II. CLINICAL PRESENTATION OF HHCS PATIENTS

The first three families were referred to us following the intriguing observation of a co-segregation of hyperferritinemia and cataract, in several individuals over two or three generations (1,2). These two symptoms were transmitted in the autosomal dominant mode. The probands were initially suspected to have hemochromatosis, because of marked hyperferritinemia found during routine laboratory examinations. One of them was a blood donor, a category in which the biochemical markers of iron metabolism are frequently checked. However, in the probands and in all the affected members, serum iron values and transferrin saturation were normal to low, contrasting with the persistently elevated serum ferritin levels. A history of cataract was also present in the three probands and in all members within the families who had hyperferritinemia. A carefully collected family history, together with biochemical evaluation of the first-degree relatives, were the simple clues to the identification of a new genetic disease, although a logical link between the two manifestations was not immediately apparent. No other symptoms or signs were noted in affected subjects from these families.

These observations were rapidly followed by elucidation of the molecular basis of the disease. Mutations were identified in a translational regulatory element present in the first exon of the L-ferritin gene (3,4). Although this syndrome remained a French-Italian story for some time, with the identification of several new families in our countries, a number of additional case reports have now been described in the United Kingdom, Germany, Spain, Sweden, the United States, and Canada, suggesting that HHCS may be widely distributed throughout the world, and not sporadic or restricted to the Mediterranean.

With the increasing awareness of the high prevalence of genetic hemochromatosis in the white populations, an evaluation of the biochemical markers of iron metabolism, including serum ferritin, is now frequently prescribed by general practitioners. Also, a high serum ferritin level is a relatively common finding during in-hospital practice, with previously considered "unexplained" cases accounting for up to nearly 10% of the total (5). Physicians should now always consider HHCS in the diagnostic workup of these patients, particularly to avoid further unnecessary and

potentially dangerous procedures (see below). Similarly, cataract is one of the most common ocular pathologies (6), and serum ferritin measurement should be performed when assessing patients with a history of early-onset cataract.

III. HHCS: A TRANSLATIONAL PATHOLOGY

A. Regulation of Ferritin Synthesis

Multiple isoferritins are found in tissues, which are made from the assembly of various proportions of both H- and L-ferritin subunits in the protein shell (see Chapter 5). The respective amounts of these two subunits in tissues result from complex transcriptional and translational regulations. Differences in the stability between the two subunits is also likely to modify the tissue H- and L-ferritin contents. Multiple transcriptional regulatory elements have been identified upstream of the H-ferritin gene which regulate gene transcription following various stimuli, such as cytokines, oxidative stress, changes in the cell cycle, or differentiation status (7). Very little is known about the transcriptional regulation of the L-ferritin gene, but few conditions other than iron accumulation seem to affect L-ferritin gene transcription. Translation of both H- and L-mRNAs depends on the iron status of the cells and is regulated by interaction between the iron-responsive element (IRE), present in the 5'-noncoding region of both H- and L-ferritin mRNAs, and the cytoplasmic iron regulatory proteins (IRPs) (see Chapter 9). These complex regulatory systems are necessary to maintain the right balance between H and L subunits in the cells, and to form functional ferritin heteropolymers adapted to cellular iron status. Attempts to overexpress the H-ferritin subunits by transfection into various cell types have shown that this subunit can act as a suppresser of cell proliferation in some cell types (8), whereas in other cells it has an antioxidant effect with little limitation on cell growth (9,10). Conversely, complete inactivation of the H-ferritin gene by homologous recombination in the mouse was found to be lethal at an early stage during embryonic development, suggesting that both ferritin subunits are required for proper detoxification and storage of iron (11). HHCS brought about some evidence that overexpression of the L-ferritin subunit has almost no effect on intracellular iron metabolism in most cell types and only affects lens transparency, in an age-dependent manner and probably independently of iron.

B. IRE Mutations and Deletions

In the first two families described above, point mutations were identified in the iron-responsive element of the L-ferritin gene. These mutations affected two different nucleotides of the IRE loop and consisted of an A40→G (3) and a G41→C (4) change at the heterozygous state (numbering starts at the cap site of the L-ferritin mRNA). Following identification of these first two mutations, and based on the rather unexpected association of the two major symptoms, it was initially proposed that this syndrome could result from the co-segregation of two different mutated genes. However, the identification by both our groups and by many other investigators of additional mutations, clearly demonstrated that this syndrome is due to mutations in the L-ferritin gene present on chromosome 19q13.3-qter.

The G41→C mutation has remained unique so far, whereas several additional families with the A40→G mutation have been found both in France (12) and in Italy (13).

Several new mutations have also been described, and all but one [G51→C, (14)] affect the first half of the IRE structure (Fig. 1). Another nucleotide of the loop has been found mutated in at least seven different families, with a C39→U (13,15–17). This mutation impairs a C-G base pairing which has been shown to be important for RNA-binding affinity (18). The bulge in the middle of the stem also appears as frequently mutated, especially on G32, where all three possible mutations have been found (16,19,20). This G32 nucleotide has been found mutated in at least nine different families. Nucleotides of the stem, between the loop and the bulge, have also been found mutated (Fig. 1), including the unpaired cytosine of the bulge (21). Finally, two mutations linked on the same allele have been found on the more distal part of the IRE structure (17,22). In addition, two deletions have been described

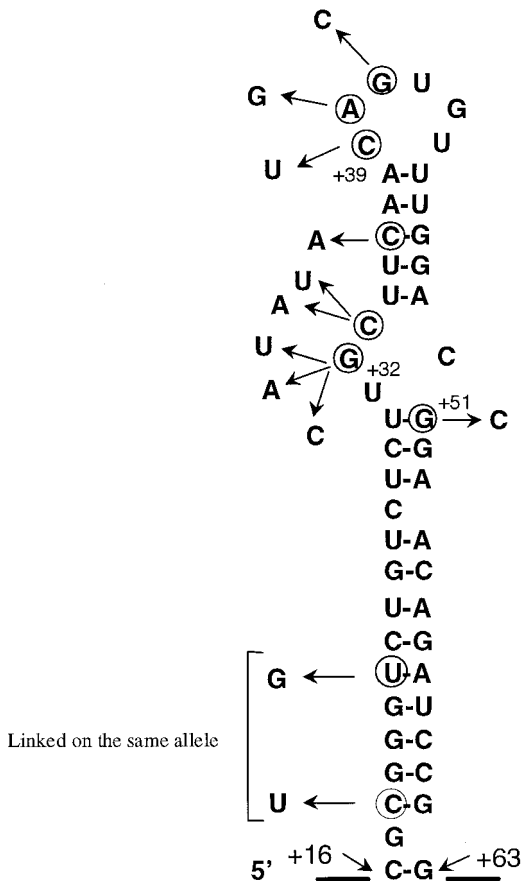


Figure 1 Nucleotide sequence of the IRE in the L-ferritin mRNA and point mutations which have been found in HHCS patients. Numbers are from the cap site of the L-ferritin mRNA.

which removed either the first half of the IRE [del 10–38 (23)] or the second half [del 42–57 (24)]. It is possible that the inverted repeats made by the two halves of the IRE stem might favor intrachromosomal rearrangements and subsequent deletions. The large number of different mutations which have been identified in unrelated individuals, taken together with the observation made by us (17) and others (25) that some of these mutations are neomutations, suggest that the IRE structure of the L-ferritin gene is a hot spot for mutations.

C. Clinical Consequences of L-Ferritin Overexpression

1. Upregulated L-Ferritin Synthesis

a. Tissue Ferritin

Tissue ferritin content is highly regulated by iron through IRE–IRP interactions. It is clear that in HHCS patients, the presence of L-ferritin mRNA molecules bearing a mutated IRE leads to the uncontrolled production of L-ferritin subunits, independently of the cell iron status. It has been shown by several authors that mutated IREs have highly reduced binding affinities for both IRP1 and IRP2 (19,26). Therefore, they fail to repress ferritin synthesis when iron entry into the cells is limited, so that L-ferritin synthesis becomes constitutive. Lymphoblastoid cell lines established from patients with IRE mutations have L-ferritin contents between 1400 and 2300 ng/mg total protein, whereas control cell lines have 80–100 ng of L-ferritin/mg protein (27). In addition, treatment of the cells with iron or deferoxamine did not change the rate of synthesis of L-ferritin(3) nor the L-ferritin content of these cells (27), to normal cells where ferritin synthesis was normally regulated. Several reports have also described elevated L-ferritin levels in tissues from HHCS patients. Amorphous iron-free deposits have been observed in a liver biopsy from a HHCS patient and found to consist mostly of L-rich ferritin molecules (17). Blood mononuclear cells from HHCS patients were also found to contain 10-fold more ferritin than normal cells (22). Finally, the lens of one patient with the A41→G mutation was also analyzed and exhibited a substantial accumulation of L chains, with an L:H ratio of more than 200:1 (as compared to 3–6:1 in control lens) (27). This is the most striking difference with iron-overload disorders, which are also accompanied by elevated levels of L-ferritin in tissues and serum, following iron-mediated stimulation of ferritin synthesis. However, in these conditions, there is probably no excess ferritin production in the lens, where iron does not accumulate due to blood–brain barrier protection.

b. Serum Ferritin

The hallmark of HHCS is the presence of elevated serum ferritin levels, associated with normal to low serum iron and transferrin saturation. Normal serum ferritin values are within the range 50–350 $\mu\text{g/L}$, with slight variations with age and sex. Elevated serum ferritin values are considered a good index of increased iron stores, although several other clinical conditions can also give rise to increased serum ferritin levels, such as cancer, inflammation, and infection (28). In HHCS patients with IRE mutations, abnormal serum ferritin levels are a constant finding, although important fluctuations can be observed with time for the same individual or among several individuals within a family. For instance, one affected member of the family with the interstitial 29-bp deletion of the IRE (del 10–38) had a progressive reduction

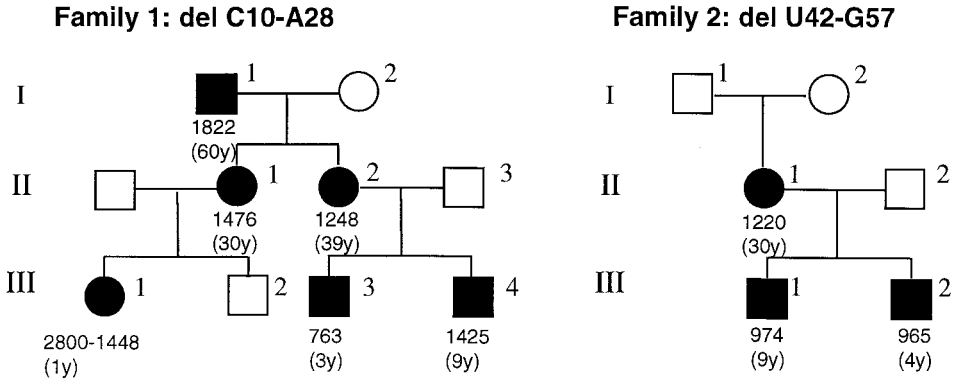


Figure 2 Pedigree of two families with an interstitial deletion of the iron-responsive element in the L-ferritin mRNA. Affected members in family 1 have a 29-bp deletion of the IRE, from C10 to A28 (23), whereas affected members in family 2 have a 16-bp deletion, from U42 to G57 (24). Black symbols denote the presence of cataract, and the numbers in brackets refer to the age of the individuals at the time the HHCS was diagnosed. Serum ferritin levels are indicated below the symbols and are expressed in micrograms per liter.

in ferritin levels, from 2800 ng/L at birth to 1400 ng/L at about 1 year of age (Fig. 2, family 1, individual III1). Furthermore, ferritin values ranged between 760 and 2800 $\mu\text{g/L}$ among the different members of the family. We recently reported a relatively large series of families including a total of about 50 affected subjects (13). A marked phenotypic variability was noted in terms of both serum ferritin levels and the severity of cataract. Again, a clear association with other clinical manifestations did not become apparent.

The origin of serum ferritin has been the subject of several controversies. Serum ferritin is mostly composed of L subunits which are partially glycosylated (29). This glycosylation suggests that L-ferritin could be secreted through the endoplasmic reticulum, although this has never been formally proven. The L-ferritin mRNAs in the cells could be distributed between membrane-bound ribosomes and free ribosomes, and a stretch of hydrophobic amino acid in the N-terminal part of the molecule could act as a signal peptide, targeting L-ferritin for secretion. Some authors have proposed that serum ferritin might be encoded by a different gene, but this gene has never been cloned (30). However, the presence of elevated serum ferritin levels in patients with an IRE mutation in the L-ferritin gene on chromosome 19q13.3-qter clearly demonstrates that, at least in this pathology, serum ferritin derives from the same gene as tissue ferritin. This is also supported by the finding that there is a good correlation between serum ferritin levels and L-ferritin in monocytic cells in both controls and HHCS patients (22).

c. Iron Stores

Whereas serum ferritin levels often parallel the body iron stores, the paradoxical hallmark of HHCS is a substantial increase in serum ferritin that, by definition, is independent of the amount of iron in the cells. This marker not being useful, other indicators of iron metabolism have to be taken into account in these patients. A systematic study on iron stores in HHCS has not yet been reported. Nonetheless,

important information can be inferred by the number of case reports in the literature. In all HHCS patients reported so far, serum iron and transferrin saturation levels were found to be generally normal—sometimes low, but never increased. Before the recognition of HHCS, several affected subjects were submitted to liver iron biopsy because of a suspected iron-overload disorder. In these subjects, the stainable iron by the Perl's method was reported normal or scanty. In some circumstances, a bone marrow biopsy was also performed, again showing normal to low tissue iron (1,16). Finally, only trace amounts of iron were detected in the HHCS lens, similarly to control lens (27). Taken together, these observations suggest that iron stores in HHCS patients are generally normal, if not low in certain subgroups.

Biochemical studies on HHCS lymphoblastoid cell lines have shown that these cells accumulated nonfunctional H₀-L₂₄ homopolymers. Also, the remaining pool of isoferritins shifted toward L-chain-rich molecules (27). The H chain is known to be essential for iron uptake into the ferritin cavity, because of its ferroxidase activity that is not shared by the L chain (31,32); see also Chapter 5. Moreover, a minimum of 30% H chains seems to be required for optimal iron incorporation into the ferritin molecule. Thus it is possible to speculate that the formation of iron deposits in HHCS individuals, rather than being increased, could be at least slightly less efficient than in normal, depending on the degree of L-chain overproduction. In-vitro experiments found the cellular iron uptake of HHCS to be similar to that of control cells (27). On the other hand, it is interesting to note that when HHCS subjects were submitted to inappropriate therapy with phlebotomy, they invariably developed an iron-deficient, microcytic anemia after the removal of very few (2–5) units of blood. On these occasions, serum ferritin levels remained as high as before the development of anemia. An adequate cycle of oral iron therapy corrected the anemia, demonstrating that iron absorption and the response of erythropoiesis to iron depletion and subsequent repletion are normal in HHCS. In our recent series, 4 of 10 probands were initially referred to our hematology units because of mild iron-deficient anemia with “paradoxical” hyperferritinemia. A condition associated with blood loss (erosive gastritis, tendency to hypermenorrhea, etc.) was often documented in the history of these patients, although it was not always impressive. In other cases, patients were identified because they developed mild anemia during pregnancy or soon after they had enrolled as regular blood donors. Whether this simply reflects a selection bias or a true tendency of HHCS patients to become iron-deficient in response to relatively mild stimuli remains to be elucidated.

2. Age of Onset and Features of the Cataract

For yet unknown reasons, the lens appears to be the only tissue in which L-ferritin accumulation leads to a clinically relevant abnormality. Initially, the cataract in HHCS was thought to be “congenital,” as the probands from the first families reported severe visual symptoms since their infancy. Later, with the increasing number of observations, it became clear that the severity of cataract is quite variable. Lens opacities can be serious enough to require surgical correction in the second or third decade, or mild enough to have no detectable effect on visual acuity. In the latter situation, only an accurate examination by a slit lamp is able to demonstrate its presence. Recently, we had the opportunity to follow the ophthalmologic pattern of a newborn from the family with one of the apparently most severe genotypes, i.e., a 29-bp deletion removing most of the 5'-IRE sequence (patient III1 in Fig. 2).

Despite a marked hyperferritinemia (1448–1920) $\mu\text{g/L}$, well-defined lens opacities were not detectable either at birth or at 1-year examination, indicating that cataract in HHCS is not congenital (13). In addition, in several affected members from the same family, cataract was found at a very broad range of age. The ophthalmologic pattern showed a progression from sparse, dustlike deposits (“pulverulent” cataract) in a 6-year-old boy to well-defined “sunflower” opacities in his 26-year-old aunt (Fig. 3). The latter pattern was quite similar to that observed at slit-lamp examination in unoperated, symptomatic adults from other families. Taken together, these morphological observations suggest that an age-related evolution of the lens opacities might occur in HHCS. This may be due either to the progressive accumulation of L-ferritin itself, or to interaction with other(s) yet unknown environmental factors. It is interesting to note that transgenic mice that overexpress L-ferritin, and have a 10-fold increase in their lens L-ferritin content, do not develop cataracts, even after 18 months (C. Beaumont, unpublished).

The observation of a substantial variability in cataract severity seen within subjects sharing the same genotype may support a role for additional environmental factors. Nevertheless, the ultimate mechanism leading to cataract formation in HHCS remains puzzling. When we analyzed specimens from cataract surgery in an HHCS patient and age-matched controls, we found the HHCS lens to contain about 10-fold more L-ferritin than controls (27). In HHCS lenses, ferritin accounted for a significantly higher proportion of total proteins (near 0.15%, versus 0.01% in controls), but probably this is still too low to account for loss of transparency. Unfortunately, only qualitative information could be obtained because of the phacoemulsification technique, which is widely used in modern cataract surgery. The technique implies ultrasound-mediated lens fragmentation and aspiration, thus preventing any reliable immunohistochemical analysis. It has been speculated that L-chain accumulation in the lens may induce cataract formation by altering the delicate equilibrium among other water-soluble proteins (i.e., crystallins) or, alternatively, by an unbalance in the antioxidant properties of the lens.

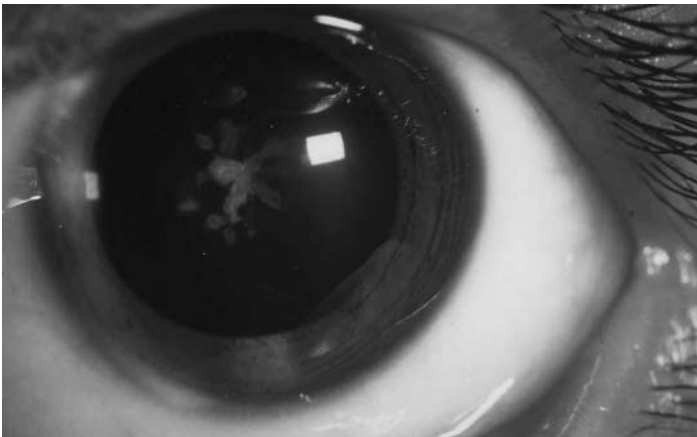


Figure 3 Slit-lamp examination of the lens of a 26-year-old HHCS patient carrying the G41C mutation. When viewed by retroillumination, the “sunflower” cataract is seen associated with cortical opacities.

IV. IS THERE A PHENOTYPE–GENOTYPE CORRELATION?

Taking into account all the mutations and deletions that have been described in the literature, the associated serum ferritin values for HHCS patients are generally between 600 and 2700 $\mu\text{g/L}$. Some evidence has been put forward for a possible correlation between IRE mutations and serum ferritin levels. These conclusions were based on in-vitro studies of the thermo-denaturation profile and dissociation constant of the IRE-IRP complex performed for several mutated IREs (26). However, as mentioned previously, serum ferritin levels fluctuate with time for a given individual, and important differences are observed among members of the same family. This also applies to mutations that have been found to severely impair IRE-binding affinity. In addition, it is surprising that patients with a partial deletion of the IRE have serum ferritin concentrations which are not necessarily higher than those found in patients with point mutations. In the family with the C10–A28 deletion, serum ferritin was between 700 and 2000 $\mu\text{g/L}$ (Fig. 2, family 1), and in the family with the U42–G57 deletion, a ferritinemia of the patients between 960 and 1200 $\mu\text{g/L}$ was recorded (Fig. 2, family 2). In these cases, it is tempting to speculate that the loss of between 16 and 29 nucleotides impairs the mRNA stability and that this altered mRNA does not contribute to ferritin overproduction to the same extent as an mRNA molecule with a point mutation. Differential stability of the various mRNA could account for the apparent variability in disease penetrance.

However, based on our experience and on data of the literature (22), it seems that at least the genotype corresponding to the presence of two mutations linked on the same allele repeatedly gives a milder phenotype, in terms of both serum ferritin values and severity of cataract. These two mutations, which are very distal on the IRE stem, have an important effect on the thermal denaturation profile of the IRE, although the mutated IRE retains almost wild-type affinity for IRP1 and IRP2 binding (26). This mutated allele, which has been found in two different families, has a very mild phenotype. Serum ferritin levels are moderately elevated (400–600 $\mu\text{g/L}$), and the cataract remains asymptomatic until later stages. Multiple dustlike spots were visible only upon slit-lamp examination, and there was no loss of visual acuity.

For all the other mutations, important variability has been observed in terms of serum ferritin levels and both age of onset and severity of cataract. Obviously, additional genetics or environmental factors are likely to affect the phenotype of this syndrome.

V. CONTEXT OF HHCS AMONG THE HEREDITARY CATARACTS

In recent years, dramatic progress has been made in identifying the cause of a number of inherited cataracts in humans (33). For example, specific mutations in several genes coding for crystallins, the major structural proteins of the lens, (γE -crystallin, $\beta\text{B}2$ -crystallin, $\beta\text{3A}1$ -crystallin, and αA -crystallin) or other lens-related proteins (connexins 50 and 46), have been associated with human autosomal dominant cataracts (34–39). Inability of these lens crystallins to interact in a close and orderly fashion, causing them to aggregate or precipitate and scatter light, are plausible mechanisms in this condition. HHCS represents an interesting example of hereditary cataract associated to a genetic defect involving a gene apparently unrelated to the lens. From a practical standpoint for ophthalmologists, as compared to the above-

mentioned conditions, HHCS has the peculiarity of being easily identified by a simple biochemical assay (serum ferritin, with genetic testing needed only for confirmation), rather than by complex and expensive techniques of molecular biology. However, it is likely that HHCS accounts for only a small proportion of hereditary cataracts. A preliminary screen of families recently diagnosed in an ophthalmology department in Paris failed to detect HHCS patients among 10 families with hereditary cataract.

A. Prevalence of IRE Mutations in Cases of Isolated Hyperferritinemia

The authors have used two different approaches to estimate the prevalence of IRE mutations among cases of isolated hyperferritinemia and in the general population. Patients with isolated hyperferritinemia in the absence of iron overload are not uncommon in hematology clinics. Over the past two years, 36 patients have been referred to us for unexplained elevated serum ferritin levels ranging from 600 to 4000 $\mu\text{g/L}$, in the absence of any signs of iron overload. The presence or absence of a cataract was poorly documented in most cases. We amplified by polymerase chain reaction, and then sequenced, the first exon of the L-ferritin gene in each of these patients. For 12 patients, a mutation could be identified in the IRE of the L-ferritin gene, and signs of cataract were always found, although in some cases the cataract was asymptomatic and had not been detected before. For the remaining 24 patients, no IRE mutation was present. Most of these patients were over 50 years of age, with serum ferritin levels ranging from 1500 to 4000 $\mu\text{g/L}$, and some had a cataract diagnosed recently. In addition, 30% of them were heterozygous for the H63D mutation of the HFE gene, but had no signs of iron overload (C. Beaumont, unpublished). It is likely that the cataract was age-related, but the origin of the hyperferritinemia remains unexplained. Some of them could represent a dysmetabolic syndrome, a new condition characterized by normal transferrin saturation, hyperferritinemia, and mild iron overload (40).

The incidence of HHCS in the general population is probably also very low. A preliminary screening was undertaken of about 3500 blood donors, in whom serum ferritin measurement was done as part of their yearly medical examination. We found 47 subjects with ferritin above the established cutoff (350 ng/mL in males, 300 ng/mL in females). No data on ferritin levels in first-degree relatives could be obtained in the majority of these subjects. Among the subjects, 43 of 47 agreed to have a slit-lamp examination, and in 14 of them there were some spotty opacities in the lens. From 11 we obtained DNA and so could examine the IRE by DGGE, but no abnormalities were found. Although blood donors are not a good representation of the general population, these data suggest an incidence of HHCS below 1 in 3000 (D. Girelli, unpublished).

B. Differential Diagnosis in Iron-Overload Disorders

It is essential for the clinician to keep HHCS in mind when facing subjects with hyperferritinemia, especially to avoid unnecessary invasive diagnostic procedures such as liver biopsy. Liver biopsy is currently recommended for prognostic stratification in subjects with suspected genetic hemochromatosis and serum ferritin levels $\geq 1000 \mu\text{g/L}$, to verify whether cirrhosis is present or not. In these patients, however,

transferrin saturation is invariably very high, distinct from the typical HHCS subject. To distinguish HHCS from an iron-overload disorder is also important to avoid treatment-related morbidity, i.e., phlebotomy-induced iron deficiency anemia (see above). To address the correct diagnosis is generally easy, as an accurate personal and family history, together with ferritin measurement in first-degree relatives, may suffice in most cases. On the other hand, since de-novo mutation/deletion can also occur, HHCS should be taken into account also in sporadic cases of early-onset cataract. Moreover, a slit-lamp examination of the lens should always be performed in subjects with apparently “unexplained” hyperferritinemia and a personal or family history negative for cataract, to identify those patients with asymptomatic cataract associated with “mild” forms of HHCS. When the diagnosis of HHCS is established in family members by combining data from history, ferritin measurements, and ophthalmological examination, this may suffice for practical purposes. Atypical patients need the demonstration of the presence of a mutation in the L-ferritin IRE. Since several, often “private,” mutations have been found, sequencing of the L-ferritin IRE by sending DNA samples to referral centers is generally needed.

VI. CONCLUSIONS

The hereditary hyperferritinemia cataract syndrome is a genetic disease of autosomal dominant transmission. It is due to heterozygous mutation/deletion in the iron-responsive element of the L-ferritin gene on chromosome 19q13.3-qter. Mutated L-ferritin mRNAs are highly translated, regardless of iron status, leading to ferritin overexpression in tissues and serum. Surprisingly, the only symptoms in the patient is a progressive early-onset cataract and possibly an unusually high tendency to develop anemia. The mechanism leading to lens opacification remains to be elucidated. IRE mutations probably account for a small proportion of hereditary cataracts, but, although HHCS has now been described in several countries in Europe and North America, its frequency is probably still underestimated. This syndrome demonstrates that IRE/IRP interactions on ferritin message are important to limit ferritin production in the absence of iron, and that when this interaction is impaired due to the presence of a mutation in the IRE, the L-ferritin mRNA is efficiently translated.

From a general standpoint, HHCS represents an interesting and almost unique model of human translational pathology, in which an altered gene expression is due to mutations in a translational regulatory element. The discovery of additional diseases sharing the same molecular pathophysiology is probably still to come.

ACKNOWLEDGMENTS

This work was supported in part by Telethon-Italy (Grant E.749).

REFERENCES

1. Girelli D, Olivieri O, De Franceschi L, Corrocher R, Bergamaschi G, Cazzola M. A linkage between hereditary hyperferritinaemia not related to iron overload and autosomal dominant congenital cataract. *Br J Haematol* 1995; 90:931–934.
2. Bonneau D, Winter-Fuseau I, Loiseau MN, Amati P, Berthier M, Orio D, Beaumont C. Bilateral cataract and high serum ferritin: A new dominant genetic disorder? *J Med Genet* 1995; 32:778–779.

3. Beaumont C, Leneuve P, Devaux I, Scoazec JY, Berthier M, Loiseau MN, Grandchamp B, Bonneau D. Mutation in the iron responsive element of the L ferritin mRNA in a family with dominant hyperferritinaemia and cataract. *Nature Genet* 1995; 11:444–446.
4. Girelli D, Corrocher R, Bisceglia L, Olivieri O, De, Franceschi L, Zelante L, Gasparini P. Molecular basis for the recently described hereditary hyperferritinemia-ataract syndrome: A mutation in the iron-responsive element of ferritin L-subunit gene (the “Verona mutation”). *Blood* 1995; 86:4050–4053.
5. Lee MH, Means RT Jr. Extremely elevated serum ferritin levels in a university hospital: Associated diseases and clinical significance. *Am J Med* 1995; 98:566–571.
6. World Health Organization. Use of intraocular lenses in cataract surgery in developing countries. *Bull World Health Organ* 1991; 69:657.
7. Ponka P, Beaumont C, Richardson DR. Function and regulation of transferrin and ferritin. *Semin Hematol* 1998; 35:35–54.
8. Wu KJ, Polack A, Dalla-Favera R. Coordinated regulation of iron-controlling genes. H-ferritin and IRP2, by c-MYC. *Science* 1999; 283:676–679.
9. Picard V, Renaudie F, Porcher C, Hentze MW, Grandchamp B, Beaumont C. Overexpression of the ferritin H subunit in cultured erythroid cells changes the intracellular iron distribution. *Blood* 1996; 87:2057–2064.
10. Epsztejn S, Glickstein H, Picard V, Slotki IN, Breuer W, Beaumont C, Cabantchik ZI. H-ferritin subunit overexpression in erythroid cells reduces the oxidative stress response and induces multidrug resistance properties. *Blood* 1999; 94:3593–3603.
11. Ferreira C, Bucchini D, Martin ME, Levi S, Arosio P, Grandchamp B, Beaumont C. Early embryonic lethality of H ferritin gene deletion in mice. *J Biol Chem* 2000; 275:3021–3024.
12. Aguilar-Martinez P, Biron C, Masméjean C, Jeanjean P, Schved JF. A novel mutation in the iron responsive element of ferritin L-subunit gene as a cause for hereditary hyperferritinemia-ataract syndrome. *Blood* 1996; 88:1895.
13. Girelli D, Zecchina G, Tinazzi E, Ciciliano M, Piperno A, Bisceglia L, et al. Molecular, biochemical, and clinical findings in a series of families with the hereditary hyperferritinemia-ataract syndrome (abstr). *Blood* 1999;94(suppl 1):644a.
14. Camaschella C, Zecchina G, Lockitch G, Roetto A, Arosio P, Levi S. A new G51C mutation in the IRE of L-ferritin in hyperferritinemia cataract syndrome decreases the binding affinity of the mutant IRE to IRP (abstr). *Blood* 1999;94(suppl 1):407a.
15. Mumford AD, Vulliamy T, Lindsay J, Watson A. Hereditary hyperferritinemia-ataract syndrome: Two novel mutations in the L-ferritin iron-responsive element. *Blood* 1998; 91:367–368.
16. Cicilano M, Zecchina G, Roetto A, Bosio S, Infelise V, Stefani S, Mazza U, Camaschella C. Recurrent mutations in the iron regulatory element of L-ferritin in hereditary hyperferritinemia-ataract syndrome. *Haematologica* 1999; 84:489–492.
17. Beaumont C. Le syndrome héréditaire cataracte-hyperferritinémie. *Hépatogastro* 2000; in press.
18. Henderson BR, Menotti E, Bonnard C, Kuhn LC. Optimal sequence and structure of iron-responsive elements. Selection of RNA stem-loops with high affinity for iron regulatory factor. *J Biol Chem* 1994; 269:17481–17489.
19. Martin ME, Fargion S, Brissot P, Pellat B, Beaumont C. A point mutation in the bulge of the iron-responsive element of the L ferritin gene in two families with the hereditary hyperferritinemia-ataract syndrome. *Blood* 1998; 91:319–323.
20. Kato GJ, Casella F. L-ferritin-Baltimore-1: A novel mutation in the iron response element (C32G) as a cause of the hyperferritinemia-ataract syndrome (abstr). *Blood* 1999; 94(suppl 1):407a.
21. Balas A, Aviles MJ, Garcia-Sanchez F, Vicario JL. Description of a new mutation in the L-ferritin iron-responsive element associated with hereditary hyperferritinemia-ataract syndrome in a Spanish family. *Blood* 1999; 93:4020–4021.

22. Cazzola M, Bergamaschi G, Tonon L, Arbustini E, Grasso Vercesi E, Barosi G, Bianchi PE, Cairo G, Arosio P. Hereditary hyperferritinemia-cataract syndrome: Relationship between phenotypes and specific mutations in the iron-responsive element of ferritin light-chain mRNA. *Blood* 1997; 90:814–821.
23. Girelli D, Corrocher R, Bisceglia L, Olivieri O, Zelante L, Panozzo G, Gasparini P. Hereditary hyperferritinemia-cataract syndrome caused by a 29-base pair deletion in the iron responsive element of ferritin L-subunit gene. *Blood* 1997; 90:2084–2088.
24. Cattan D, Aygalenq P, Milon B, Hetet G, Beaumont C. Hereditary hyperferritinemia-cataract syndrome by a 16 base pair deletion in the iron responsive element of ferritin L-subunit gene (abstr). *Gastroenterology* 1999;116:
25. Arosio C, Fossati L, Vigano M, Trombini P, Cazzaniga G, Piperno A. Hereditary hyperferritinemia cataract syndrome: A de novo mutation in the iron responsive element of the L-ferritin gene. *Haematologica* 1999; 84:560–561.
26. Allerson CR, Cazzola M, Rouault TA. Clinical severity and thermodynamic effects of iron-responsive element mutations in hereditary hyperferritinemia-cataract syndrome. *J Biol Chem* 1999; 274:26439–26447.
27. Levi S, Girelli D, Perrone F, Pasti M, Beaumont C, Corrocher R, Albertini A, Arosio P. Analysis of ferritins in lymphoblastoid cell lines and in the lens of subjects with hereditary hyperferritinemia-cataract syndrome. *Blood* 1998; 91:4180–4187.
28. Torti SV, Torti FM. Iron and ferritin in inflammation and cancer. *Adv Inorg Biochem* 1994; 10:119–137.
29. Worwood M, Dawkins S, Wagstaff M, Jacobs A. The purification and properties of ferritin from human serum. *Biochem J* 1976; 157:97–103.
30. Tran TN, Eubanks SK, Schaffer KJ, Zhou CY, Linder MC. Secretion of ferritin by rat hepatoma cells and its regulation by inflammatory cytokines and iron. *Blood* 1997; 90:4979–4986.
31. Levi S, Luzzago A, Cesareni G, Cozzi A, Franceschinelli F, Albertini A, Arosio P. Mechanism of ferritin iron uptake: Activity of the H-chain and deletion mapping of the ferro-oxidase site. A study of iron uptake and ferro-oxidase activity of human liver, recombinant H-chain ferritins, and of two H-chain deletion mutants. *J Biol Chem* 1988; 263:18086–18092.
32. Levi S, Santambrogio P, Cozzi A, Rovida E, Corsi B, Tamborini E, Spada S, Albertini A, Arosio P. The role of the L-chain in ferritin iron incorporation. Studies of homo and heteropolymers. *J Mol Biol* 1994; 238:649–654.
33. Ionides A, Francis P, Berry V, Mackay D, Bhattacharya S, Shiels A, Moore A. Clinical and genetic heterogeneity in autosomal dominant cataract. *Br J Ophthalmol* 1999; 83:802–808.
34. Brakenhoff RH, Henskens HA, van Rossum MW, Lubsen NH, Schoenmakers JG. Activation of the gamma E-crystallin pseudogene in the human hereditary. Coppock-like cataract. *Hum Mol Genet* 1994; 3:279–283.
35. Stephan DA, Gillanders E, Vanderveen D, Freas-Lutz D, Wistow G, Baxevanis AD, Robbins CM, VanAuken A, Quesenberry MI, Bailey-Wilson J, Juo SH, Trent JM, Smith L, Brownstein MJ. Progressive juvenile-onset punctate cataracts caused by mutation of the gammaD-crystallin gene. *Proc Natl Acad Sci USA* 1999; 96:1008–1012.
36. Litt M, Carrero-Valenzuela R, LaMorticella DM, Schultz DW, Mitchell TN, Kramer P, Maumenee IH. Autosomal dominant cerulean cataract is associated with a chain termination mutation in the human beta-crystallin gene CRYBB2. *Hum Mol Genet* 1997; 6:665–668.
37. Litt M, Kramer P, LaMorticella DM, Murphey W, Lovrien EW, Weleber RG. Autosomal dominant congenital cataract associated with a missense mutation in the human alpha crystallin gene CRYAA. *Hum Mol Genet* 1998; 7:471–474.

38. Shiels A, Mackay D, Ionides A, Berry V, Moore A, Bhattacharya S. A missense mutation in the human connexin50 gene (GJA8) underlies autosomal dominant “zonular pulverulent” cataract, on chromosome 1q. *Am J Hum Genet* 1998; 62:526–532.
39. Mackay D, Ionides A, Kibar Z, Rouleau G, Berry V, Moore A, Shiels A, Bhattacharya S. Connexin46 mutations in autosomal dominant congenital cataract. *Am J Hum Genet* 1999; 64:1357–1364.
40. Moriand R, Mortaji AM, Loreal O, Paillard F, Brissot P, Deugnier Y. A new syndrome of liver iron overload with normal transferrin saturation. *Lancet* 1997; 349:95–97.

Other Disorders of Increased Iron Absorption Iron Overload in Africans and African Americans

FITZROY W. DAWKINS and VICTOR R. GORDEUK

Howard University College of Medicine, Washington, D.C.

I. INTRODUCTION	775
II. AFRICAN DIETARY IRON OVERLOAD	776
A. Epidemiology	776
B. Etiology	777
C. Pathophysiology	778
D. Diagnosis and Treatment	779
E. Future Directions	780
III. IRON OVERLOAD IN AFRICAN AMERICANS	780
A. Epidemiology	780
B. Etiology	781
C. Pathophysiology	781
D. Diagnosis and Treatment	781
E. Future Directions	782
ACKNOWLEDGMENT	782
REFERENCES	783

I. INTRODUCTION

Three main forms of systemic iron overload are found around the world: *HFE* hemochromatosis in European-derived populations, dietary iron overload in sub-Saharan Africa, and iron overload related to thalassemia major and intermedia condi-

tions in populations extending from the Mediterranean to Southeast Asia. Each of these conditions seems to have a hereditary component, to share the mechanism of the excessive absorption of food iron, and to be a relatively common condition. In addition to these geographically common forms of iron overload, many blood transfusions given to patients with a variety of refractory anemias will lead to iron overload because of the iron contained in the transfused hemoglobin. Most of these conditions are covered in other chapters of this volume. In this chapter, we will examine issues of African dietary iron overload and iron overload in African Americans.

II. AFRICAN DIETARY IRON OVERLOAD

Iron overload has been recognized in sub-Saharan Africa for over 70 years (1). The condition is known as “dietary iron overload,” for the consumption of a traditional fermented beverage rich in iron is strongly associated with the development of iron loading (2). Two observations are important in characterizing iron overload in Africa. (a) The condition is distinct from alcoholic liver disease, although the excess iron is often derived from a traditional beer that contains alcohol. Hepatic iron concentrations do not exceed 90–180 $\mu\text{mol/g}$ dry weight in alcoholic liver disease (3,4). In iron overload in Africans, liver iron concentrations often exceed these levels (5–8), and the histological changes associated with alcohol are almost always absent (8,9). (b) While the clinical manifestations of African iron overload and *HFE* hemochromatosis are similar, the pattern of iron accumulation in iron overload in Africans differs from that of *HFE* hemochromatosis in Caucasians. Iron deposition is prominent both in macrophages and in hepatic parenchymal cells in African iron overload (10,11). By contrast, *HFE* hemochromatosis is marked by relatively reduced amounts of iron in macrophages (11,12). This raises the possibility that two distinct metabolic defects are responsible for the two conditions.

A. Epidemiology

Since Professor A. S. Strachan of the University of the Witwatersrand first described African iron overload in Johannesburg, South Africa, in 1929 (1), iron overload has been reported in at least 15 countries. These include the eastern African countries of Ethiopia (13), Kenya (14), Tanzania (15), and Uganda (16); the west African countries of Ghana (17,18) and Nigeria (19); the central African countries of Malawi, Mozambique (20), Zambia (21), and Zimbabwe (22–24); the west-central African countries of Angola (20) and Zaire (1); and the southern African countries of Botswana, Lesotho (7), South Africa (5), and Swaziland (8).

Iron overload seems to be more common in sub-Saharan Africa than is *HFE* hemochromatosis in populations of European ancestry. In fact, the prevalence of iron overload may exceed 10% among adult males in some rural African populations, while the homozygous state for *HFE* hemochromatosis is estimated to be from 0.2% to 0.5% in European populations (25). In 1959 and 1960, an autopsy study of adult black South Africans was conducted in Baragwanath Hospital in Johannesburg. Twenty-one percent of males and 7% of females who came to autopsy had hepatic iron concentrations exceeding 360 $\mu\text{mol/g}$ dry weight (normal range < 30) (6). This degree of iron loading is comparable to Caucasians with advanced *HFE* hemochro-

matosis and carries a high risk of cirrhosis. By 1979, however, the results of another autopsy series at the same institution suggested that the prevalence of dietary iron overload had declined in urban blacks (7). The explanation given was that there was a decline in the use of home-brewed traditional beer in favor of commercially prepared alcoholic beverages. However, the same study showed that the prevalence of iron overload remained substantial, with 11% of males and 5% of females having hepatic iron concentrations more than 360 $\mu\text{mol/g}$.

In the 1980s, two community surveys conducted in rural areas of Zimbabwe and South Africa showed that iron overload remains an important public health challenge. These studies were different in two respects from the previous autopsy series. First, they were community-based studies conducted with living subjects. Second, indirect measures of iron status, transferrin saturation and serum ferritin concentration, were used to screen apparently healthy subjects. In the Zimbabwe study, in which more than 500 people were enrolled, 21% of traditional beer-drinking males older than 45 years had a high serum ferritin concentration and a transferrin saturation in excess of 70% (9). This combination of elevations in indirect measures of iron status suggests a risk for toxic iron overload. Based on similar criteria, the prevalence of potentially severe iron overload was 16.5% among rural males in South Africa (8).

Studies in the 1990s continued to show that dietary iron overload is an important problem in Africa. In a different rural Zimbabwe community from that studied in the 1980s, 4 of 28 men (14.3%) who gave a history of the consumption of traditional beer had the combination of an elevated serum ferritin concentration and a transferrin saturation over 70% (26). A high prevalence of iron overload was also found in an urban autopsy study from Harare, Zimbabwe (27). The series included 107 males and 28 females who experienced violent death or death due to suicide. Twenty-three percent of the subjects had hepatic iron stores in excess of the normal range, and 5% had concentrations of hepatic iron more than 180 $\mu\text{mol/g}$ dry weight or five times the upper limit of normal.

B. Etiology

The relationship between dietary iron and African iron overload was recognized in the 1950s, and for many years high dietary iron was thought to be the exclusive etiology. The excess dietary iron is present in a traditional fermented beverage that is prepared at home from locally grown grains (2). The brewing process requires 7 days, and the typical container is a nongalvanized steel drum. The concentration of ferrous iron in the supernatant of this opaque traditional beer is usually more than 40 mg/L (26). In contrast, the iron content of commercially prepared beer in the United States is less than 0.2 mg/L, and the total iron content of a typical Western diet is 10–15 mg/day. The alcohol content of the traditional beer in Africa tends to be low compared to commercially prepared beer, and liver biopsies from patients with iron overload rarely show changes suggestive of alcoholic liver disease (8,9).

Some evidence indicates that iron overload in sub-Saharan Africa may be related to a genetic defect as well as to increased dietary iron. In a Zimbabwe community survey conducted in the 1980s, it was noted that only a minority of the traditional beer drinkers developed iron overload (9), and this led to the hypothesis that there may be an inborn error of metabolism to explain the development of iron

overload. Two pedigree studies have been conducted to investigate this hypothesis. In the first study, 36 Zimbabwean and Zambian families were chosen because of index subjects with iron overload, and 234 family members were studied using transferrin saturation as a marker of iron status. Among 99 family members who gave a history of traditional beer consumption, transferrin saturations had a bimodal distribution: 55 of the transferrin saturation values fell within the normal range and 44 were elevated. Likelihood analysis was consistent with both a genetic effect as well as an effect of increased dietary iron on transferrin saturation (21). In the most likely model, increased dietary iron raised the mean transferrin saturation from 30% to 81% in subjects who were heterozygous for the iron-loading locus.

In a second pedigree study, 351 subjects from 45 Zimbabwean, South African, and Swazi families were studied. In that study, both transferrin saturation and serum ferritin concentration were used as markers of iron status, and they were determined in duplicate on blood samples that were obtained in the morning after supplementation with vitamin C and abstinence from alcohol. Transferrin saturation values again showed a bimodal distribution in relatives who gave a history of traditional beer consumption. For both transferrin saturation and serum ferritin concentration, segregation analysis was consistent with an interaction between a postulated iron-loading gene and dietary iron content in determining iron status (28). In the most likely genetic model, the transferrin saturation would be 75% and the serum ferritin 985 $\mu\text{g/L}$ in a 40-year-old male with an estimated traditional beer consumption of 10,000 L who is a heterozygote for the putative iron-loading locus. At the same time, the transferrin saturation would be 36% and serum ferritin concentration 233 $\mu\text{g/L}$ in a man of identical age and traditional beer consumption who is unaffected by the putative iron-loading mutation.

The postulated iron-loading locus in Africans with iron overload appears to be different from the *HFE* gene that is responsible for most primary iron overload in Caucasians. In the first pedigree study described above, the postulated iron-loading locus was not linked to the HLA locus on the short arm of chromosome 6 (21), while the *HFE* gene is linked to this locus. In the second pedigree study, 25 of the family members with a high probability for having the postulated iron-loading locus were tested for the C282Y and H63D mutations in the *HFE* gene, and all were negative (29).

C. Pathophysiology

The original 1929 autopsy study reported high deposits of iron in both the liver and spleen in patients with African iron overload (1). Subsequent studies have been more specific, showing that iron deposits are prominent both in hepatocytes and in macrophages of the liver, spleen, and bone marrow (27,30,31). The pattern of iron deposition in hepatic tissue in African iron overload differs from the distribution seen with *HFE* hemochromatosis in Caucasians, in which the macrophages are relatively spared of iron loading (30). The typical changes of alcohol-induced hepatic damage are almost always absent in African dietary iron (8,9,32).

Portal fibrosis and cirrhosis are prominent complications of African iron overload (10). These complications are especially prominent after a threshold hepatic iron concentration of about 360 $\mu\text{mol/g}$ dry weight has been reached (normal < 30) (6). Recent studies suggest an association between African iron overload and hepa-

tocellular carcinoma (33–35). The incidence of hepatocellular carcinoma in southern Africa is high, and major risk factors include hepatitis B and C viral infections and dietary exposure to aflatoxin B1 and mycotoxin. In a case-control study that controlled for these known factors, the population attributable risk of iron overload in the development of hepatocellular carcinoma was 29%, while that of hepatitis B virus infection was 69% (34). Another study raised the possibility that African iron overload poses a risk for hepatocellular carcinoma even in the absence of cirrhosis (35).

A recent study examined serum non-transferrin-bound iron and its possible correlation with hepatic dysfunction in African iron overload (36). All plasma iron is bound to transferrin under normal conditions. Non-transferrin-bound iron has been reported in several forms of iron overload, but was not previously investigated in African iron overload. This abnormal iron fraction is probably toxic, but this has not been demonstrated previously. In 25 African subjects with biopsy-proven iron overload, abnormal fractions of non-transferrin-bound iron were frequently present in the serum. Furthermore, the presence and magnitude of the non-transferrin-bound iron fractions correlated with elevations in the hepatic enzymes, alanine, and aspartate amino transferases. This study thus suggested that non-transferrin-bound iron may contribute to hepatocellular damage in African iron overload.

D. Diagnosis and Treatment

The typical presentation of African iron overload is a middle-aged or older adult with hepatomegaly and a history of the consumption of traditional, home-brewed beer (32). Other clinical findings that may be associated with African iron overload are summarized in Table 1. Once African iron overload is suspected, the finding of an elevated serum ferritin concentration provides further evidence of the diagnosis (32). The transferrin saturation may also be elevated (32), and circulating transferrin receptor concentrations tend to be low (37). Because the serum ferritin concentration and transferrin saturation may be perturbed by inflammatory processes and hepatocellular damage, the diagnosis should be confirmed by liver biopsy or bone marrow

Table 1 Clinical Findings That May Be Associated with African Iron Overload

Finding	Reference
Hepatic portal fibrosis and cirrhosis	Isaacson et al., 1961 (10)
Diabetes mellitus	Seftel et al., 1961 (52)
Idiopathic heart failure	MacPhail et al., 1979 (7)
Ascorbic acid deficiency	Seftel et al., 1966 (53)
Osteoporosis	Seftel et al., 1966 (53)
Hepatocellular carcinoma	Mandishona et al., 1999 (34)
Esophageal carcinoma	Isaacson et al., 1985 (54)
Infections	
Bacterial peritonitis	Buchanan, 1970 (55)
Amebiasis	Bothwell et al., 1984 (56)
Tuberculosis	Gordeuk et al., 1996 (33)

biopsy if possible. Such direct measures of iron status demonstrate abnormally increased iron stores in macrophages (26,31) and, in the case of liver biopsy, hepatocytes (32). Neither anemia nor erythrocytosis is a typical feature of African iron overload.

Two methods for treating iron overload are available: phlebotomy and iron chelation therapy. Because African iron overload is not characterized by anemia, phlebotomy is the preferred method of treatment (38). During phlebotomy therapy, 500 mL of blood (representing about 225 mg of iron) is removed once or twice per week until a state of mild iron deficiency is induced as evidenced by a decline in the mean corpuscular volume or serum ferritin concentration. Because of the association between African iron overload and the consumption of traditional beer, preventive efforts should be directed at reducing or eliminating the consumption of this beverage. Another possible approach is to develop methods to modify the method of preparation so as to reduce the iron content.

E. Future Directions

One challenge is to identify the putative gene that is involved in the pathogenesis of African iron overload. If an African iron-loading gene is found, there will be benefits related to the possibility of early diagnosis and prevention, but also controversial issues related to genetic screening and counseling. Advances in our understanding of the molecular biology and biochemistry of iron metabolism would also be expected to derive from finding such a locus. Another challenge is to identify the best laboratory test for screening for African iron overload. While transferrin saturation is recognized as the best nongenetic screening tool for *HFE* hemochromatosis in Caucasians, the preferred test for screening for African iron overload has not been established. Also, the clinical picture of African iron overload is not completely described, and further research in this regard is needed.

III. IRON OVERLOAD IN AFRICAN AMERICANS

A. Epidemiology

As reviewed in the previous section, dietary iron overload is well documented in sub-Saharan Africa, and recent data suggest that there may be an inborn error of iron metabolism associated with this condition. Although the African-American population originated in Africa, there has been a paucity of data regarding primary iron overload in African Americans. After the first description of an African American with "hemochromatosis" in 1950 (39), only four additional cases of primary iron overload had been reported by 1990 (40–42). In the 1990s, at least 21 additional cases were described (43–47).

The prevalence of primary iron overload in African Americans is not known, but there is some evidence that the condition may be more common than is presently recognized. (a) The second National Health and Nutrition Examination Survey, conducted between 1976 and 1980, did not make a systematic attempt to identify this illness. Nevertheless, 2 of 518 (0.4%) adult African Americans in whom both transferrin saturation and serum ferritin concentration were determined had both an elevated serum ferritin concentration and a transferrin saturation above 70%, a combination that is suggestive of primary iron overload (42). (b) A survey of 326

hospitalized African Americans who died and went to autopsy found that 4 (1.2%) had elevations in hepatic concentration that were similar to those observed in homozygous HFE hemochromatosis (45). (c) An analysis of the distribution of transferrin saturation values from 808 African Americans studied in the second National Health and Nutrition Survey was consistent with population genetics for a major locus that affects iron status. The results were consistent with the possibility that homozygotes for such a locus might constitute between 0.5% and 1.0% of those surveyed (48).

B. Etiology

The African-American population does not typically ingest foods with a high concentration of ferrous iron comparable to the traditional beer of sub-Saharan Africa. Nevertheless, the practice of fortifying flour with iron in the United States may promote iron loading (49), and the chronic ingestion of vitamin preparations that contain iron could also be a factor in increasing iron stores. In general, there is a high consumption of meat in the United States compared to Africa, and this practice would also tend to increase iron stores in the population. Heme iron, such as that present in myoglobin, is the form of dietary iron that is best absorbed from the gastrointestinal tract. Despite these considerations, whether certain dietary practices might be related to the development of iron overload in African Americans is not known.

The possibility that the hemochromatosis gene responsible for primary iron overload in Caucasians could also be etiologically related to iron overload in African Americans has been suggested (43). However, homozygosity for the C282Y mutation of the *HFE* gene has not yet been described in published cases of primary iron overload in African Americans (Table 2). Furthermore, the frequency of the C282Y mutation in the African-American population is much lower than the frequency in the Caucasian population. The combined results of two studies which screened a total of 228 African Americans give a gene frequency of 0.0136 for the C282Y mutation in the *HFE* gene (47,50). For comparison, the gene frequency of the C282Y mutation is about 0.064 in the Caucasian population (51). These gene frequencies would correlate with 17 C282Y homozygotes per 100,000 in the African-American population and 410 C282Y homozygotes per 100,000 in the Caucasian population. Thus, the C282Y mutation would only rarely be a cause of primary iron overload in African Americans, and studies to identify a different genetic mutation appear to be in order. It seems possible that a common genetic defect might underlie African iron overload and iron overload in African Americans.

C. Pathophysiology

Iron tissue deposition in African Americans with iron overload is present in both parenchymal cells and macrophages (44,45), and this pattern seems to parallel that found in African iron overload. As shown in Table 2, cirrhosis and a variety of malignancies have been common findings in the published cases of African Americans with primary iron overload.

D. Diagnosis and Treatment

The 25 published cases of primary iron overload in African Americans are summarized in Table 2. In general, the clinical findings are similar to those found with both

Table 2 Summary of Clinical Characteristics of 25 Published^a Cases of African Americans with Possible Primary Iron Overload^b

Characteristic	No. with observation available	Result	Normal range
Age (years)	24	50 (27–69)	
Sex (male:female)	24	18:6	1:1
C282Y homozygote	6	0 (0)	
Transferrin saturation (%)	19	86 (29–100)	20–45
Serum ferritin ($\mu\text{g/L}$)	19	1567 (242–4639)	20–200
Hepatic iron concentration ($\mu\text{mol/g}$ dry weight)	14	222 (104–684)	<30
Hepatic iron index	10	4.8 (1.6–20.2)	<1.0
Hepatocellular iron grade	12	3+ (2+–4+)	0–1+
Macrophage iron present; no. (%)	16	14 (87.5%)	—
Iron mobilized by phlebotomy (grams)	8	6.8 (4.6–22.7)	<1.5
Cirrhosis; no. (%)	18	10 (56)	Absent
Cardiomyopathy; no. (%)	17	2 (12)	Absent
Arthritis; no. (%)	17	5 (29)	Absent
Diabetes mellitus; no. (%)	17	5 (29)	Absent
Impotence or decreased libido; no. (%)	17	4 (24)	Absent
Malignancy; no. (%)	17	7 (41)	Absent

^aKrainin et al., 1950 (39); McDonald et al., 1960 (40), Rosner et al., 1981 (41); Expert Scientific Working Group, 1984 (42); Conrad, 1991 (43); Barton et al., 1995 (44); Wurapa et al., 1996 (45); Castro et al., 1998 (46); Monaghan et al., 1998 (47).

^bResults in median (and range) unless otherwise indicated.

African iron overload and *HFE* hemochromatosis. Of note, none of the six patients who were tested was either homozygotic or heterozygotic for the C282Y mutation in the *HFE* gene. Also, macrophage iron deposition was a common finding along with hepatocyte iron accumulation. Because primary iron overload in African Americans is not associated with anemia, phlebotomy is the appropriate treatment. In one young man who presented with severe cardiomyopathy, there was full reversal with phlebotomy (45).

E. Future Directions

The prevalence and clinical consequences of primary iron overload in African Americans should be defined. Also, the etiology needs to be clearly established, in particular, whether a genetic defect is involved. Therefore, careful clinical epidemiological studies and the genetic investigation of family pedigrees are needed.

ACKNOWLEDGMENT

This work was supported in part by a Research Scientist Award from the National Heart, Lung and Blood Institute of the National Institutes of Health (UH1-HL03679-03).

REFERENCES

1. Strachan AS. Haemosiderosis and haemochromatosis in South African natives with a comment on the etiology of haemochromatosis. M.D. thesis, University of Glasgow, Glasgow, Scotland, 1929.
2. Bothwell TH, Seftel H, Jacobs P, Torrance JD, Baumslag N. Iron overload in Bantu subjects. Studies on the availability of iron in Bantu beer. *Am J Clin Nutr* 1964; 14:47–51.
3. Chapman RW, Morgan MY, Laulich M, Hoffbrand AV, Sherlock S. Hepatic iron stores and markers of iron overload in alcoholics and patients with idiopathic hemochromatosis. *Dig Dis Sci* 1982; 27:909–916.
4. Bassett ML, Halliday JW, Powell LW. Value of hepatic iron measurement in early hemochromatosis and determination of the critical iron level associated with fibrosis. *Hepatology* 1986; 6:24–29.
5. Bothwell TH, Bradlow BA. Siderosis in the Bantu. A combined histopathological and chemical study. *Arch Pathol* 1960; 70:279–292.
6. Bothwell TH, Isaacson C. Siderosis in the Bantu. A comparison of incidence in males and females. *Br Med J* 1962; 1:522–524.
7. MacPhail AP, Simon MO, Torrance JD, et al. Changing patterns of dietary iron overload in black South Africans. *Am J Clin Nutr* 1979a; 32:1272–1278.
8. Friedman BM, Baynes RD, Bothwell TH, et al. Dietary iron overload in southern African rural blacks. *S Afr Med J* 1990; 78:301–305.
9. Gordeuk VR, Boyd RD, Brittenham GM. Dietary iron overload persists in rural sub-Saharan Africa. *Lancet* 1986; 1:1310–1313.
10. Isaacson C, Seftel HC, Keeley KJ, Bothwell TH. Siderosis in the Bantu: The relationship between iron overload and cirrhosis. *J Lab Clin Med* 1961; 58:845–853.
11. Brink B, Disler P, Lynch S, Jacobs P, Charlton R, Bothwell T. Patterns of iron storage in dietary iron overload and idiopathic hemochromatosis. *J Lab Clin Med* 1976; 88:725–731.
12. Valberg LS, Simon JB, Manley PN, et al. Distribution of storage iron as body iron stores expand in patients with hemochromatosis. *J Lab Clin Med* 1975; 86:479–489.
13. Hofvander Y, Olding L, Westermarck P. Liver changes in medicolegal autopsies in Addis Abbaba, Ethiopia. *Acta Med Scand* 1972; 191:167–170.
14. Senba M, Nakamura T, Itakura H. Statistical analysis of relationship between iron accumulation and hepatitis B surface antigen. *Am J Clin Pathol* 1985; 84:340–342.
15. Haddock DRW. Bantu siderosis in Tanzania. *E Afr Med J* 1965; 42:67–73.
16. Owor R. Hemosiderosis in Uganda: Autopsy study. *E Afr Med J* 1974; 51:388–391.
17. Edington GM. Haemosiderosis and anaemia in the Gold Coast African. *W Afr Med J* 1954; 3:66–70.
18. Edington GM. Nutritional siderosis in Ghana. *Central Afr J Med* 1959; 5:186–189.
19. Isah HS, Fleming AF. Anaemia and iron status of symptom-free adult males in northern Nigeria. *Ann Trop Med Parasitol* 1985; 79:479–484.
20. Gerritsen T, Walker ARP. Serum iron and iron-binding capacity in the Bantu. *S Afr Med J* 1953; 27:577–581.
21. Gordeuk VR, Mukiibi J, Hasstedt SJ, et al. Iron overload in Africa: Interaction between a gene and dietary iron content. *N Engl J Med* 1992; 326:95–100.
22. Buchanan WM. Bantu siderosis with special reference to Rhodesian Africans. *Univ College Rhodesia Faculty Med Res Ser* 1967; 1:5–30.
23. Buchanan WM. Siderosis in Rhodesian Africans. *Central Afr J Med* 1966; 12:199.
24. Buchanan WM. Bantu siderosis—A review. *Central Afr J Med* 1969; 15:105.
25. Gordeuk VR. Hereditary and nutritional iron overload. *Balliere's Clin Haematol* 1992; 5:169–186.

26. Moyo VM, Gangaidzo IT, Gomo ZAR, et al. Traditional beer consumption and the iron status of spouse pairs from a rural community in Zimbabwe. *Blood* 1997; 89:2159–2166.
27. Gangaidzo IT, Moyo VM, Saungweme T, et al. High prevalence of iron overload in urban Africans in the 1990's. *Gut* 1999; 45:278–283.
28. Moyo VM, Mandishona E, Hasstedt SJ, et al. Evidence of genetic transmission in African iron overload. *Blood*, 1998; 91:1076–1082.
29. McNamara L, MacPhail AP, Gordeuk VR, Hasstedt SJ, Rouault T. Is there a link between African iron overload and the described mutations of the hereditary haemochromatosis gene? *Br J Haematol* 1998; 102:1176–1178.
30. Bothwell TH, Abrahams C, Bradlow BA, Charlton RW. Idiopathic and Bantu hemochromatosis. *Arch Pathol* 1965; 79:163.
31. Gale E, Torrance J, Bothwell T. The quantitative estimation of total iron stores in human bone marrow. *J Clin Invest* 1963; 42:1076–1082.
32. MacPhail AP, Mandishona E, Bloom P, Paterson AC, Rouault TA, Gordeuk VR. Measurements of iron status and survival in African iron overload. *S Afr Med J* 1999; 89: 966–972.
33. Gordeuk V, McLaren CE, MacPhail AP, Deichsel G, Bothwell TH. Associations of iron overload in Africa with hepatocellular carcinoma and tuberculosis: Strachan's 1929 thesis revisited. *Blood* 1996; 87:3470–3476.
34. Mandishona E, MacPhail AP, Gordeuk VR, Kedda M-A, Rouault T, Kew MC. Dietary iron overload as a risk factor for hepatocellular carcinoma in black Africans. *Hepatology* 1998; 27:1563–1566.
35. Mayo VM, Makunike R, Gangaidzo IT, et al. African iron overload and hepatocellular carcinoma. *Eur J Hematol* 1998; 60:28–34.
36. McNamara L, MacPhail AP, Mandishona E, Bloom P, Paterson AP, Rouault TA, Gordeuk VR. Non-transferrin bound iron and hepatic dysfunction in African dietary iron overload. *J Gastroenterol Hepatol* 1999; 14:126–132.
37. Khumalo H, Gomo ZAR, Moyo VM, Gangaidzo IT, Saungweme T, Kiire CF, Rouault TA, Gordeuk VR. Serum transferrin receptors are decreased in the presence of iron overload. *Clin Chem* 1998; 44:40–44.
38. Speight ANC, Cliff J. Iron storage disease of the liver in Dar Es Salaam; a preliminary report on venesection therapy. *E Afr Med J* 1974; 51:895–902.
39. Krainin P, Kahn BS. Hemochromatosis: Report of a case in a Negro; discussion of iron metabolism. *Ann Intern Med* 1950; 33:452–462.
40. MacDonald RA, Mallory GK. Hemochromatosis and hemosiderosis. *Arch Intern Med* 1960; 105:686–700.
41. Rosner IA, Askari AD, McLaren GD, et al. Anthroopathy, hypouricemia and normal serum iron studies in hereditary hemochromatosis. *Am J Med* 1981; 70:870–874.
42. Expert Scientific Working Group. Assessment of the Iron Nutritional Status of the U.S. Population Based on Data Collected in the Second National Health and Nutrition Examination Survey, 1976–1980. Washington, DC: Center for Food Safety and Applied Nutrition, Food and Drug Administration, 1984.
43. Conrad ME. Sick cell disease and hemochromatosis. *Am H Hematol* 1991; 38:150–152.
44. Barton JC, Edwards CQ, Bertoli LF, Shroyer TW, Hudson SL. Iron overload in African Americans. *Am J Med* 1995; 99:616–623.
45. Wurapa RK, Gordeuk VR, Brittenham GM, Khyami A, Schechter GP, Edwards CQ. Primary iron overload in African Americans. *Am J Med* 1996; 100:9–18.
46. Castro O, Hasan A, Kaur K, Loyevsky M, Gordeuk V. Hemochromatosis in non-transfused African-American patient with sickle cell anemia (abstr). *Blood* 1998; 92.

47. Monaghan KG, Rybicki EA, Shurafa M, Feldman GL. Mutation analysis of the *HFE* gene associated with hereditary hemochromatosis in African Americans. *Am J Hematol* 1998; 58:213–217.
48. Gordeuk VR, McLaren CE, Looker AC, Hasselblad V, Brittenham GM. Distribution of transferrin saturation in the African-American population. *Blood* 1998; 91:2175–2179.
49. Olsson KS, Vaisaner M, Konar J, Bruce A. The effects of withdrawal of food iron fortification in Sweden as studied with phlebotomy in subjects with genetic hemochromatosis. *Eur J Clin Nutr* 1997; 51:782–786.
50. Marshall DS, Linfert DR, Tsongalis GJ. Prevalence of the C282Y and H63D polymorphisms in a multi-ethnic control population. *Int J Mol Med* 1999; 4:389–393.
51. Feder JN, Gnirke A, Thomas W, et al. A novel MHC class I-like gene is mutated in patients with hereditary haemochromatosis. *Nature Genet* 1996; 13:399–408.
52. Seftel HC, Keeley KJ, Isaacson C, Bothwell TH. Siderosis in the Bantu: The clinical incidence of hemochromatosis in diabetic subjects. *J Lab Clin Med* 1961; 58:837.
53. Seftel HC, Malkin C, Schmaman A, Abrahams C, Lynch SR, Charlton RW, Bothwell TH. Osteoporosis, scurvy, and siderosis in Johannesburg Bantu. *Br Med J* 1966; 1:642.
54. Isaacson C, Bothwell TH, MacPhail AP, Simon M. The iron status of urban black subjects with carcinoma of the oesophagus. *S Afr Med J* 1985; 67:591–593.
55. Buchanan WM. Peritonitis and Bantu siderosis. *S Afr Med J* 1970; 44:43–44.
56. Bothwell TH, Adams EB, Simon M, Isaacson C, Simjee AE, Kallichurum S, Gathiram. The iron status of Black subjects with amoebiasis. *S Afr Med J* 1984; 65:601–604.

Iron Chelation

CHAIM HERSHKO*Shaare Zedek Medical Center, Jerusalem, Israel***GABRIELA LINK and AVRAHAM M. KONIJN***Hebrew University, Jerusalem, Israel*

I. INTRODUCTION	788
II. PATHOPHYSIOLOGY OF TRANSFUSIONAL IRON OVERLOAD	788
III. CHELATABLE IRON POOLS	790
A. Role of Iron Stores in Reticuloendothelial and Parenchymal Cells	790
IV. IRON CHELATION WITH DEFEROXAMINE	791
A. Pharmacokinetics of Deferoxamine	791
B. Results of Long-Term Deferoxamine Treatment	792
C. Method of Treatment	792
D. Deferoxamine Toxicity	793
E. Impact on Survival	794
F. Pregnancy and Deferoxamine	795
V. DEVELOPMENT OF ORALLY EFFECTIVE CHELATORS	795
A. Deferiprone (L1)	795
B. Pyridoxal Isonicotinoyl Hydrazone (PIH)	802
C. Desferrithiocin Analogs	803
D. The Polyanionic Amines (HBED)	803
E. The Substituted Polyaza Compounds (IRCO11)	804
F. Bis-Hydroxyphenyl-Triazole (ICL 670A)	805
VI. CO-ADMINISTRATION OF CHELATORS: THE “SHUTTLE EFFECT”	805

VII. CURRENT ISSUES IN CHELATOR DEVELOPMENT	807
ACKNOWLEDGMENTS	808
REFERENCES	808

I. INTRODUCTION

Iron research in the last few years has yielded exciting new insights into the understanding of normal iron homeostasis. Much of this research is reviewed in other chapters of the present volume. However, normal physiology offers little protection from the toxic effects of pathological iron accumulation, because nature did not equip us with an effective mechanism of iron excretion. Excess iron can be effectively removed by phlebotomy in hereditary hemochromatosis, but this method cannot be applied to chronic anemias associated with iron overload. In these diseases, iron chelating therapy is the only method available for preventing early death caused mainly by myocardial and hepatic iron toxicity. In the following, we shall discuss the abnormalities of iron metabolism associated with thalassemia major (the most common form of “iron-loading anemia”); examine the results of long-term deferoxamine (DFO) therapy in thalassemia; and, finally, review the development of new, orally effective iron chelators which may be considered for present or future use. The use of chelators for controlling disease by iron deprivation in conditions unrelated to iron overload, such as reperfusion injury, prevention of anthracycline cardiotoxicity, or inhibition of cell proliferation, has been reviewed elsewhere (1).

II. PATHOPHYSIOLOGY OF TRANSFUSIONAL IRON OVERLOAD

Iron balance in normal subjects is characterized by an efficient recycling of wastage iron derived from senescent erythrocytes. Only a fraction of the daily iron requirement is contributed by intestinal absorption (2). The primary abnormality in thalassemia major is a wasteful, ineffective erythropoiesis resulting in a 10- to 15-fold expansion of the erythroid bone marrow (3) and a drastic increase in hemoglobin catabolism. Iron accumulation is the consequence of blood transfusions as well as of increased iron absorption caused by erythropoietic activity. The role of increased iron absorption is illustrated by the severe iron overload encountered in patients with thalassemia intermedia who have never received blood transfusions. The combination of iron overload and increased outpouring of catabolic iron from the reticuloendothelial system overwhelms the iron-carrying capacity of transferrin, resulting in the emergence of toxic nontransferrin-bound plasma iron (NTBI).

Although our original description of a chelatable, low-molecular-weight plasma iron fraction in thalassemic patients with severe iron overload (4) was greeted with initial scepticism, its existence has been confirmed by many subsequent studies using a variety of methods. NTBI promotes the formation of free hydroxyl radicals and accelerates the peroxidation of membrane lipids *in vitro* (5). Long-term treatment with DFO or deferiprone (L1) in thalassemic patients results in a marked decrease in their NTBI levels (6). More recently, Porter et al. (7) have shown that plasma

NTBI is removed by intravenous DFO therapy in a biphasic manner and that upon cessation of DFO infusion it reappears rapidly, lending support to the continuous, rather than intermittent, use of DFO in high-risk patients. The rate of low-molecular-weight iron uptake by cultured rat heart cells is over 300 times that of transferrin iron (8). Moreover, unlike transferrin iron uptake, which is inhibited at high tissue iron concentrations by downregulation of transferrin receptor production, non-transferrin iron uptake is increased by high tissue iron (9). Such uptake results in increased myocardial lipid peroxidation and abnormal contractility, and these effects are reversed by *in vitro* treatment with DFO (10). Recognition of NTBI as a potentially toxic component of plasma iron in thalassemic siderosis has important practical implications for designing better strategies for the effective administration of DFO and other iron chelating drugs.

Without iron chelating therapy, the accumulation of iron will progress relentlessly, and when about 20 g of iron have been retained in the body, significant clinical manifestations of iron toxicity may be anticipated (11). The most important complications of transfusional siderosis are cardiac, hepatic, and endocrine disease. Pathological findings in the heart include dilated, thickened ventricular walls with particularly heavy iron deposits in the ventricles, epicardium, and papillary muscles. These cellular deposits induce increased membrane lipid peroxidation in the sarcolemma, resulting in impaired Na,K,ATPase activity (12), increased lysosomal fragility (13), and, in particular, impaired mitochondrial inner-membrane respiratory chain activity (14). It is possible to demonstrate early myocardial dysfunction in asymptomatic patients using a MUGA scan (15) or dobutamine stress echocardiography (16). With progressive cardiac siderosis, symptomatic heart failure and life-threatening arrhythmias will develop. Myocardial siderosis is the single most important cause of mortality in inadequately treated thalassemics.

Hepatic fibrosis is a common complication of thalassemia and, similar to cardiac problems, its incidence is age-related. It has been proposed that patients with liver iron concentrations below 15 mg/g dry weight may have a prolonged survival free of the clinical complications of iron overload (17). Iron overload per se is responsible for the development of cirrhosis in many cases. However, the coexistence of chronic hepatitis B or C, with an incidence ranging from 8.7% to 70% of thalassemic patients in various geographic areas (11), underlines the complexity of this problem. Endocrine problems caused by direct accumulation of iron in endocrine glands or indirectly through the hypothalamic–pituitary axis are common. Stunted growth, delayed puberty, hypothyroidism, hypoparathyroidism, and diabetes mellitus are all well-established complications of transfusional siderosis (18). Because diabetes and hypothyroidism appear when most endocrine cells are destroyed and replaced by fibrosis, these complications are rarely reversible. The prevalence of insulin-dependent diabetes mellitus has been shown to decline, and the age of onset of diabetes has increased over the years. This is attributable to improved iron chelation therapy. Poor compliance with DFO treatment, the severity of iron overload, and the presence of liver fibrosis and cirrhosis are major risk factors for the development of diabetes (19).

Short trunk, with or without short stature, is common in thalassemia. In a multicenter study of 476 Italian patients, abnormal shortening of the trunk was found in 40% of patients and short stature in 18%. The cause of these abnormalities is multifactorial. Thalassemia per se may cause spinal growth impairment starting in

infancy, but this is aggravated subsequently by hypogonadism in pubertal age (20). Further aggravation of skeletal shortening may be caused by platyspondylosis associated with DFO toxicity.

III. CHELATABLE IRON POOLS

Current models of iron acquisition, sequestration, and storage by mammalian cells are based on a regulated adjustment of membrane transferrin receptor and cytosolic ferritin levels. Iron in transit between these two iron-binding proteins is believed to exist in a weakly bound low-molecular-weight complex which is also available for interaction with iron chelating drugs (21). This chelatable labile iron pool (LIP) is assumed to be sensed by a cytosolic iron-responsive protein (IRP) which coordinately represses ferritin mRNA translation and increases transferrin receptor mRNA stability (22). Efficient regulatory mechanisms prevent fluctuations in the size of the labile iron pool under conditions of moderate iron deprivation and iron loading. However, massive iron loading results in uncontrollable expansion of the chelatable pool, which fails to be matched by the sequestering capacity of cellular ferritin (23). This expanded LIP is an obvious target of intracellular iron chelation by drugs that are able to cross the barrier of the cytoplasmic membrane.

A. Role of Iron Stores in Reticuloendothelial and Parenchymal Cells

Although excess iron may be deposited in almost all tissues, most of it is found in association with two cell types: reticuloendothelial (RE) cells in the spleen, liver, and bone marrow; and parenchymal tissues represented by hepatocytes, endocrine cells, and the myocardium. In contrast to RE cells, in which iron accumulation is relatively harmless, parenchymal siderosis may result in significant organ damage. The source of iron and the proportion retained in ferritin stores or recycled into the circulation from the two cell types is quite different. RE cells have a limited ability to assimilate transferrin iron, and they derive iron from the catabolism of hemoglobin in nonviable erythrocytes (24). Most of this catabolic iron is recycled to plasma transferrin or NTBI within a few hours. In contrast, hepatic parenchymal cells maintain a dynamic equilibrium with plasma transferrin, with iron uptake predominating when transferrin saturation is high, and release when serum iron and transferrin saturation is low. Unlike RE cells, the turnover of parenchymal iron stores is extremely low. In general, iron overload associated with increased intestinal absorption such as hereditary hemochromatosis results in predominant parenchymal siderosis, whereas in iron overload caused by multiple blood transfusions the primary site of siderosis is the RE cells. Considerable redistribution of iron may take place subsequently.

Experimental and clinical observations indicate that the urinary excretion of chelated iron derives mainly from RE cells. Studies in hypertransfused rats have shown that, in contrast to hepatocellular radio-iron excretion, which is confined entirely to the bile, most of the radio-iron excreted from RE cells is recovered in the urine. Moreover, when DTPA or IRCO11, water-soluble synthetic chelators that do not enter cells easily, are employed in the same experimental model, there is no enhancement at all of hepatocellular iron excretion, but the enhancement of urinary

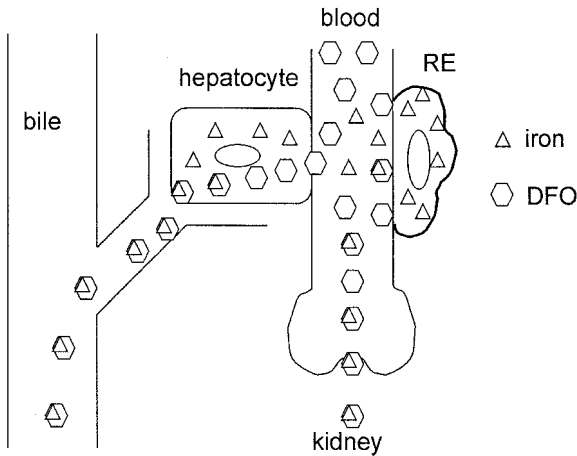


Figure 1 Deferoxamine (DFO) promotes the excretion of iron by two alternative mechanisms: (left) in-situ interaction with hepatocellular iron with subsequent biliary excretion, and (right) interaction with iron derived from red blood cell breakdown in the reticuloendothelial (RE) system directly, or following its release into circulation as NTBI, with subsequent urinary excretion.

RE radio-iron excretion is similar to, or higher than, that observed previously with DFO (25). Hence, DFO acquires iron for chelation by one of two alternative mechanisms: (a) an in-situ interaction with hepatocellular iron that subsequently results in biliary excretion, or (b) chelation of iron derived from red blood cell (RBC) catabolism in the RE system directly or following its release into the plasma in the form of NTBI with subsequent urinary excretion (Fig. 1).

IV. IRON CHELATION WITH DEFEROXAMINE

The iron chelating compound DFO was discovered accidentally, as a by-product of antibiotic research by scientists at the Swiss Federal Institute of Technology in Zurich and at Ciba in Basel. As described by Keberle in the volume dedicated to the presentation of the 1991 Pharmaceutical of the Year Award to DFO by the *Munchener Medizinische Wochenschrift* (26), DFO was first considered as a compound for the treatment of iron deficiency anemia. However, after discovering that its absorption is limited, but following its parenteral administration all iron bound to it is excreted in the urine, it occurred to the investigators that it might be useful for promoting iron excretion, instead of absorption. Although DFO has been available for treating transfusional iron overload since the early 1960s, the era of modern and effective iron chelating therapy started only 20 years ago, with the introduction of subcutaneous DFO infusions by portable pumps. Today, long-term DFO therapy is an integral part of the management of thalassemia and other transfusion-dependent anemias, with a major impact on patient well-being and survival.

A. Pharmacokinetics of Deferoxamine

The pharmacokinetics of DFO and its main metabolite obtained by oxidative deamination (DFO-met B) have been studied in thalassemic patients after intravenous

infusion at a dose of 50 mg/kg/24 h (27). DFO is eliminated from the blood in a bi-exponential manner. The initial phase indicates a rapid distribution, followed by a slower elimination phase. The terminal half-life is about 3 h, and the volume of distribution 1.88 L/kg. The major metabolite, DFO-met B, has a half-life of 1.3 h and is usually present at a lower concentration than DFO.

The ratio of DFO-met B to total DFO (deferoxamine and ferrioxamine) is determined by the availability of chelatable iron (28). It is directly correlated with the therapeutic index, i.e., the mean daily dose of DFO (mg/kg) divided by serum ferritin ($\mu\text{g/L}$). This is attributed to the fact the iron-bound DFO is resistant to catabolism and thus, in patients with excessive doses of DFO relative to a limited amount of chelatable iron, more DFO will be converted into metabolite B. However, this ratio reflects only the availability of chelatable iron and not an intrinsic, qualitative difference in DFO catabolism in patients at high risk of developing toxic complications of DFO.

B. Results of Long-Term Deferoxamine Treatment

The introduction of DFO for the treatment of transfusional iron overload had a major impact on the survival and well-being of thalassemic patients. Although this has never been proven by prospective, randomized clinical studies, and such randomized studies are no longer justified ethically, the beneficial effects of long-term DFO treatment are clearly demonstrated by comparison of treatment outcome with historical controls. Experience with long-term DFO therapy in thalassemic patients has been the subject of a number of excellent recent reviews (29,30).

C. Method of Treatment

The effect of treatment, measured by urinary iron excretion, is directly proportional to the severity of iron overload. Hence, treatment in subjects without iron overload will result in limited iron excretion. However, treatment should not be introduced too late if the objective is the prevention of iron toxicity. It should be started when serum ferritin levels reach about 1000 $\mu\text{g/L}$, which usually occurs after the first 10–20 transfusions (28). DFO is infused through a thin s.c. needle inserted to the arm or abdomen nightly, connected to a portable pump over 8–12 h, 5–7 times per week at a daily dose of 20–60 mg/kg. A urinary iron excretion of 0.5 mg/kg/day is usually sufficient to ensure negative iron balance.

Although prolonged subcutaneous DFO infusion is universally recognized as the optimal method of treatment, twice-daily s.c. injections may yield similar amounts of urinary iron (31). A new delivery system for continuous DFO infusion has been introduced by Baxter, allowing continuous 48-h s.c. or continuous 24-h i.v. delivery for 7 days each week (32). This technology allows effective removal of toxic free iron (i.e., NTBI) from the plasma, causes a significant decrease in serum ferritin levels within 4 weeks, and improves patient compliance compared to conventional s.c. DFO pumps. Compliance with the new disposable Baxter device allowing continuous DFO delivery for 48 or 120 h in a group of 26 thalassemic patients from Turkey has been quite satisfactory (33).

In order to overcome the need for continuous s.c. infusion of DFO for efficient iron chelation, a new salt of DFO has been developed by Novartis with properties suitable for formulation as an injectable depot to be used for bolus s.c. injections

(ICL749B) once every 1 or 2 days. In this manner, a smaller dose of DFO would be delivered over a longer time period, thus reducing the wastage of nonutilized free DFO which, under usual conditions, may be up to 90% of the drug. Initial single-dose pharmacokinetic studies indicated that doses of 5–12 mg/kg of ICL749B corresponded to 40 mg of DFO by infusion (34). These promising initial results prompted the establishment of a large-scale multicenter clinical trial at 10 centers located in Italy, Greece, and Great Britain, in which the same compound was given daily for 14 consecutive days (35). Unfortunately, and for reasons that are unclear, the continued use of depot ICL749B yielded iron excretion rates which did not reach the efficiency of standard s.c. DFO.

Response to treatment may be assessed by serum ferritin measurements, liver biopsies, computed tomography, or magnetic susceptibility [using a superconducting quantum interference device (SQUID)] (36). Serum ferritins are disproportionately low in patients with coexistent ascorbate deficiency (37) and high in active liver disease or inflammation. Nevertheless, serum ferritin is the most accessible and inexpensive tool for the long-term monitoring of chelating efficiency, and protection from cardiac complications may be achieved when serum ferritin levels are kept below 2500 $\mu\text{g/L}$ (38).

D. Deferoxamine Toxicity

DFO is remarkably nontoxic, but a number of complications may arise from excessive dosage, in particular in subjects with limited iron overload. These complications are dose-dependent, although their mechanism is poorly understood. A decreased growth rate was first noted by Piga et al. (39), in particular in young children with low serum ferritin levels. The term “deferoxamine-induced bone dysplasia” was coined by Brill et al. to underline the importance of DFO as a cause of skeletal abnormalities in thalassemic patients (40).

Abnormal skeletal growth is manifested in vertebral flattening and rickets-like metaphyseal bone deformities most commonly seen in the distal ulnar, radial, and tibial bones (41,42). Improved growth rates are usually resumed upon decreasing DFO dosage. Delaying chelation therapy until age 3 years and using minimal effective doses of DFO resulted in the complete avoidance of further metaphyseal abnormalities in new patients (43).

Similarly, a high-frequency sensorineural hearing loss has been observed in well-chelated young patients with low serum ferritin levels (44). Reducing DFO dosage was followed by recovery in patients with mild hearing defects but not in those with severe auditory impairment. At very high DFO doses, ocular, pulmonary, and renal toxicities have also been described (45–47). None of these complications precludes continued chelation therapy. They are preventable if proper monitoring to detect early signs of toxicity is practiced. Since they are dose-dependent and inversely related to the degree of iron overload, their risk can be minimized by proper dose adjustment. One such method is limiting the daily dose to a DFO-to-ferritin ratio of 0.025 per kilogram of body weight (48).

Local hypersensitivity to s.c. DFO infusion is occasionally encountered. This has been successfully treated in patients considered to be allergic to DFO by high-dose i.v. therapy (49). The absence of allergic episodes after 1 year of i.v. therapy supports the hypothesis that the so-called allergy to s.c. DFO is related to a direct

effect on dermal mast cells and is not an immunological reaction. The shift from s.c. to i.v. therapy was associated with a striking improvement in compliance and a 74% decrease in serum ferritin within 1 year (49).

A rare but serious complication of DFO is *Yersinia* sepsis, occurring when a nonvirulent organism utilizes chelated iron as a virulence factor (see Chapter 16). It occurs in 0.7% of chelated patients. Prompt diagnosis of *Yersinia* sepsis may limit the severity of this life-threatening complication (50).

E. Impact on Survival

The impact of DFO treatment on life expectancy is eloquently demonstrated by comparison of survival in well-chelated versus poorly chelated patients. In a major study of 1127 thalassemic patients at seven Italian teaching hospitals, it was shown that 70% of patients born before 1970 and hence prior to the modern era of chelation survived to the age of 20 years, compared to 88% of patients born after 1970 and therefore receiving effective chelation from an early age (11). Most of the improvement in survival was attributed to decreased death from cardiac disease. This cohort-of-birth-related improvement in survival is reflected in a mirror-like inverse decrease in cardiac mortality, supporting the assumption that prevention of cardiac deaths is the most important beneficial effect of DFO therapy. A subsequent update on this group of patients (51) has shown that the prevalence of heart failure and diabetes declines with subsequent birth cohorts. Conversely, hypothyroidism is becoming more frequent. Overall, diabetes was present in 5.4%, heart failure in 6.4%, thrombosis in 1.1%, HIV infection in 1.8%, and hypogonadism in 55% of those reaching pubertal age. This update on the cohort of patients described in earlier reports confirms the remarkable improvement in life expectancy comparing successive cohorts of thalassemic patients. This improvement is due mainly to decreased cardiac mortality. Conversely, mortality caused by other complications of thalassemia has not decreased. Improved survival in well-chelated thalassemic patients has been reported in several other major studies from the United Kingdom (53) and North America (17,38,54). The increasing incidence with age of hypothyroidism, and the emergence of HIV as a significant cause of mortality, has also been noticed in a group of thalassemic patients living in the New York area (52).

The strongest direct evidence supporting the beneficial effect of DFO on hemosiderotic heart disease is the reversal of established myocardopathy in some far advanced cases. Earlier experience in hereditary hemochromatosis has shown that the cardiomyopathy of iron overload is potentially curable by effective iron mobilization through phlebotomy. However, in transfusional hemosiderosis the course of established myocardial disease was uniformly fatal and, until recently, believed to be nonresponsive to iron chelating therapy. Several reports indicate that these patients may still be responsive to aggressive chelating treatment. Marcus et al. (55) described the reversal of established symptomatic myocardial disease in 3 of 5 patients by continuous high-dose (85–200 mg/kg/day) i.v. DFO therapy, although at the cost of severe but reversible retinal toxicity. Reversal of symptomatic cardiomyopathy has been reported by others, without significant drug toxicity (56,57). Continuous 24-h ambulatory i.v. infusion of DFO through central venous ports, using standard portable infusion pumps, or with the new Baxter delivery system (32), is a very effective method for the rapid reversal of established hemosiderotic heart disease. In addition,

it is an excellent tool for improving patient compliance, allowing uninterrupted delivery of DFO and the effective depletion of very large iron stores.

F. Pregnancy and Deferoxamine

The chance of uneventful pregnancy and normal delivery in patients who are well chelated, on a prolonged hypertransfusion program, and with normal left ventricular function on echocardiography, is excellent. Of 22 pregnancies, including one with twins, 21 ended with the delivery of healthy newborn infants by elective Caesarean section (58). Although the use of DFO is generally avoided during pregnancy, a review of the world literature has disclosed 40 cases in whom DFO was given at various stages of pregnancy without any evidence of a teratogenic effect (59).

V. DEVELOPMENT OF ORALLY EFFECTIVE CHELATORS

In spite of the proven efficacy of DFO, not all patients are willing to cope with the rigorous requirements of the long-term use of portable pumps. In addition, the high cost of this treatment is a serious obstacle to its more widespread use. In view of these considerations, there is a great need for the development of alternative, orally effective iron chelating drugs. Within recent years more than 100 candidate compounds have been screened in animal models. These efforts have led to the identification of several interesting compounds, a few of which may be of possible clinical usefulness. The present discussion will be limited to the most important of these compounds, including deferiprone (earlier known as L1), pyridoxal isonicotinoyl hydrazone (PIH), desferrithiocin analogs, the polyanionic amines, the substituted polyaza compounds, and bishydroxyphenyl thiazole.

A. Deferiprone (L1)

Of all the new iron chelating drugs available today, only deferiprone has been used as a substitute for DFO in clinical trials involving many hundreds of patients. The family of 3-hydroxypyrid-4-one bidentate chelators, designed by Hider and colleagues (60,61), binds to iron in a 3:1 ratio with a stability constant of 10^{37} , about six orders of magnitude higher than DFO (see Chapter 13). The most important compound of this family is 1,2-dimethyl-3-hydroxypyrid-4-one (deferiprone). Although clinical reports on the use of deferiprone in thalassemic and other patients were published as early as 1987, detailed animal studies on toxicity and on pharmacokinetics only became available subsequently. The pharmacology and clinical efficacy of deferiprone has been the subject of several reviews (62–65).

1. Animal Toxicity

At a daily dose of 200–300 mg/kg (i.e., 3–4 times the dose recommended for patients) given for several months, deferiprone caused bone marrow aplasia in mice, rats, dogs, and monkeys, involution of lymphatic tissues, and adrenal steatosis. These alterations were associated with high rates of mortality (66,67). As shown below, clinical experience with deferiprone indicates that zinc deficiency is a common complication of deferiprone treatment (68). Zinc is essential for the formation and function of the immune system. Zinc deprivation results in thymic atrophy, impaired function of macrophages and T cells, inability to respond to antigens, and impaired

resistance to infection (69). It also leads to gonadal atrophy and congenital malformations. Thus, it is quite likely that some of the most impressive toxic effects of deferiprone observed in animal studies of drug tolerability were caused by concurrent zinc deficiency and were not a direct consequence of deferiprone toxicity.

In view of animal toxicity data, in 1993 Ciba-Geigy announced the discontinuation of its efforts to develop deferiprone for clinical use (70). This decision has been contested on the grounds that deferiprone should continue to be available for patients with severe transfusional iron overload who are unable or unwilling to use DFO (71). It was also felt that toxicity of any chelator should be tested in iron-loaded, not in normal, animals.

2. Paradoxical Aggravation of Iron Toxicity—A Current Controversy

Unlike DFO, which is a hexadentate chelator combining with iron at a 1:1 ratio to form a stable inert complex, deferiprone is a bidentate chelator requiring a 3:1 molar ratio of chelator to iron, $[\text{Fe-L}_3]$. Thus, in theory, at suboptimal drug concentrations the charged partial dissociation products $[\text{Fe-L}_1]^{2+}$ or $[\text{Fe-L}_2]^+$ complexes may be formed that are less effective than $[\text{Fe-L}_3]$ in iron mobilization and may promote, instead of preventing, iron-induced peroxidative damage.

The possible paradoxical aggravation of iron toxicity by chelating treatment with deferiprone was explored in an in-vitro system by Cragg et al. (72). Iron-loaded HepG2 cells were used to monitor iron-catalyzed oxidative hydrogen peroxide-mediated DNA damage and its modification by iron chelators. DNA damage in iron-loaded cells was aggravated by deferiprone when added prior to hydrogen peroxide treatment. By contrast, deferiprone exerted a protective effect when chelating treatment was maintained during incubation with hydrogen peroxide. Moreover, DFO, the standard reference drug for iron-chelating treatment, had no effect at all. In view of these complex interactions, the authors underlined the need for further animal studies to verify the risk of potentiating peroxidative damage by deferiprone in the clinical setting.

Increased rates of myocardial iron accumulation and hepato- and cardiotoxicity have been described as occurring in iron-loaded gerbils following treatment with diethyl-3-hydroxypyrid-4-one (CP94), a compound closely related to deferiprone (73). However, CP94 (diethyl-3-hydroxypyrid-4-one) and deferiprone (dimethyl-3-hydroxypyrid-4-one) are quite different in their biological activity, and CP94 has long been abandoned as a candidate iron chelator because of its increased toxicity in vivo. Hence, in order to explore its potential to aggravate iron toxicity, it was important to repeat the studies reported by Carthew et al. (73) using deferiprone instead of CP94. We have studied 8-week-old gerbils (*Psamomys obesus*), iron-loaded by weekly injections of iron-dextran resulting in a more than a 10-fold increase in plasma iron, over 90% of which was not transferrin-bound, and a 100-fold increase in liver iron (74). This regimen was associated with considerable toxicity manifested in massive parenchymal necrosis, occasional cirrhosis, and a median survival of only 10 weeks. Response to iron chelating therapy judged by liver iron concentrations and mitochondrial respiratory enzyme activity was slightly better for DFO compared with deferiprone. However, both drugs failed to prevent iron-reduced hepatocellular necrosis and mortality. This failure is explained by the extreme degree of iron loading required for the Carthew model, exceeding many times the chelating

capacity of both deferiprone and DFO at a dose of 200 mg/kg/day. We could find no evidence of a paradoxical increase in iron toxicity following deferiprone therapy.

In another study aimed at exploring the effect of drug concentrations on cytoprotective action, we (75) have compared DFO and deferiprone in their ability to mobilize heart cell iron and preserve mitochondrial respiratory complex activity in normal and iron-loaded rat heart cells in culture. At drug concentrations ranging from 0.01 to 0.3 mM, the ability of DFO and deferiprone to prevent or reverse the toxic effects of iron in iron-loaded heart cells was identical. We could find no evidence of a paradoxical increase in iron toxicity at suboptimal deferiprone concentrations.

The toxicity of deferiprone was also examined in normal and iron-loaded (carbonyl iron) guinea pigs by Wong et al. (76). Animals were treated with 50 mg/kg/day deferiprone 6 days per week for over 8 months. In contrast with normal animals, in whom deferiprone caused focal hepatic, myocardial, and musculo-skeletal necrosis, decreased white cell counts, and abnormal electroretinograms, iron loading had a protective effect against deferiprone toxicity, suggesting that such toxicity is largely explained by depletion of essential cellular iron pools. There was no indication at all of increased iron toxicity in deferiprone-treated animals.

Taken together, although these in-vivo and in-vitro studies do not entirely exclude the possibility that under specific conditions deferiprone may aggravate the toxic effect of iron, there is little or no evidence in these experimental models to substantiate such a claim.

3. Pharmacokinetics

Pharmacokinetic studies in humans have shown that peak plasma deferiprone concentrations (C_{\max}) are achieved within 1 h or less of oral administration (77,78). Food intake decreases the rate of absorption, but not its total extent (79). At the recommended dose of 75 mg/kg/day the C_{\max} is 11 mg/L when the drug is given at 6-h intervals, and 35 mg/L when it is given at 12-h intervals (78). In thalassemic patients, the volume distribution of deferiprone is 1.6–1.7 L/kg (78). Table 1 describes the pharmacokinetics of deferiprone and DFO together. By comparison with DFO administered by continuous i.v. infusion, peak concentrations (C_{\max}) of deferiprone are much higher. However, it is worth recalling that oral deferiprone treatment offers only intermittent drug levels, whereas the presence of DFO given by continuous i.v. infusion is constant. The volume distribution of the two compounds and their elimination half-lives ($t_{1/2\beta}$) are comparable.

Table 1 Pharmacokinetics of DFO and Deferiprone

	Deferoxamine (27) ^a	Deferiprone (77,78) ^b
C_{\max}	7.4 μM	76–159 μM
t_{\max}	n.a.	0.5–1.0 h
Volume distribution	1.9 L/kg	1.7 L/kg
Elimination half-life, $t_{1/2\beta}$	3.1 h	1.3–2.7 h

^ai.v., 50 mg/kg/day, continuous.

^bp.o., 75 mg/kg/day, q6h.

Glucuronidation is an important mechanism of drug inactivation and is more efficient in humans than in rats, a difference that may explain the observed discrepancies in drug efficacy and toxicity between clinical and animal studies (60,80). The glucuronidated conjugate lacks chelating properties (81). It is excreted mainly in the urine, in company with the free and the iron-bound parent compound (82). The elimination half-life ($t_{1/2\beta}$) of deferiprone in iron-loaded thalassemic patients (2.3 h) is longer than in healthy volunteers (1.3 h) (83). The excretion of the glucuronide is slower than of the parent compound (77) and is further impaired by abnormal renal function.

4. Clinical Evaluation

The results of long-term iron chelating therapy with deferiprone in thalassemic patients (84–86) have been summarized in several reviews (62–65), and the combined experience of the four major European and Canadian groups pioneering the clinical use of deferiprone has been described in a report of the International Study Group for Oral Iron Chelators (ISGOIC) (68). The study involved 84 patients, 74 with thalassemic major or intermedia, representing a total of 167 patient-years of deferiprone treatment. Compliance was rated as excellent in 48%, intermediate in 36%, and poor in 16% of patients. On a deferiprone dose of 73–81 mg/kg/day, urinary iron excretion was stable, at around 0.5 mg/kg/day, with no indication of a diminishing response with time. Serum ferritin showed a very steady decrease with time from an initial mean ± 1 S.D. of 4207 ± 3118 to 1779 ± 1154 after 48 months ($p < 0.001$). Seventeen patients abandoned deferiprone therapy. Major complications of deferiprone requiring permanent discontinuation of treatment included agranulocytosis (three), severe nausea (four), arthritis (two), and persistent liver dysfunction (one). The remaining patients abandoned treatment because of low compliance (three) and conditions unrelated to deferiprone toxicity. Lesser complications permitting continued deferiprone treatment included transient mild neutropenia (four), zinc deficiency (12), transient increase in liver enzymes (37), moderate nausea (three), and arthropathy (16). There was no treatment-associated mortality. Two patients died, both while off treatment: one of hemosiderotic heart disease, and the other of *Pneumocystis carinii* pneumonia with AIDS. This study demonstrates the efficacy of deferiprone in long-term use for the treatment of transfusional iron overload, but also underlines the complications associated with such treatment.

Subsequent experience with thalassemic patients on long-term deferiprone treatment has been reported by Olivieri et al. (87,88), Hoffbrand et al. (89), and Tondury et al. (90), as well as in a report of a major multicenter study employing the Apotex formulation of deferiprone, involving 187 patients from Cagliari, Torino, Ferrara, Philadelphia, and Toronto (the LA-02 study) (91,92). All patients received a daily deferiprone dose of 75 mg/kg (Table 2). The mean duration of treatment was 1.61 years for the study reported by Tricta, and 7.14 for that of Tondury, with the rest ranging from a mean of 3.28 to 4.60 years. Comparing these data with the ISGOIC study terminated in mid-1994, one can see that, with the exception of the Tondury study, there was little or no overlap with the patients participating in the earlier report, indicating a high turnover rate of the patient populations. Likewise, with the exception of the Olivieri and Tondury studies, there was no evidence of a consistent decrease in mean serum ferritins or liver iron concentrations comparing pretreatment values with subsequent measurements. The proportion of patients in

Table 2 Clinical Response to Deferiprone Treatment

	Tricta and Spino	Olivieri et al.	Hoffbrand et al.	Tondury et al.
Year (Ref.)	1997 (91)	1998 (87)	1998 (89)	1998 (90)
No. of patients	187	18	51	11
Dose (mg/kg/day)	75	75	75	75
Duration (years)	1.61 ± 0.79	4.60 ± 0.30	3.28 ± 0.77	7.14 ± 1.28
Ferritin (μg/L)				
Initial	2525 ± 1816	4455 ± 841	2937 ± 2028	4786 ± 3241
Final	2495 ± 1719	2831 ± 491	2323 ± 1286	1813 ± 1246
Liver Fe (mg/g)				
Initial	10.0 ± 6.2	16.6 ± 2.3	n.a.	n.a.
Final	10.4 ± 4.3	12.2 ± 1.5	17.4 ± 8.8	8.7 ± 4.9
% >15 mg/g	n.a.	39	59	18

whom liver iron concentrations remained above 15 mg/g dry weight (identified in previous studies as the limit above which a significant risk of cardiac complications continues to exist) was 18% (90), 37% (87), and 59% (89). Agranulocytosis developed in six patients and transient neutropenia in 19. Although the mechanism of neutropenia is unknown, in some cases it is clearly an immune reaction to deferiprone, as illustrated by the simultaneous development of agranulocytosis, systemic vasculitis, alterations in humoral and cell-mediated immune function, and the presence of circulating immune complexes (93).

In three of the above four reports the proportion of patients abandoning treatment has been specified (Table 3). Of a total of 92 patients, 36 (39%) discontinued deferiprone therapy. Six patients died. Of particular concern is the observation that four of the patients died with congestive heart failure due to iron overload, a complication which was shown previously to be prevented by effective deferoxamine therapy. Other important causes of deferiprone discontinuation were agranulocytosis

Table 3 Causes of Discontinuing Deferiprone Treatment

	Olivieri et al.	Hoffbrand et al.	Tondury et al.	Total	
				<i>n</i>	%
No. of patients	26	51	15	92	100
Stopped drug	7	25	4	36	39.1
Died	0	5	1	6	6.5
Agranulocytosis	2	1	0	3	3.3
Neutropenia	1	2	0	3	3.3
Nausea	0	5	0	5	5.4
Poor response	1	5	2	8	8.7
Protocol violation	2	0	0	2	2.2
Arthropathy	0	5	0	5	5.4
Other	1	2	1	4	4.3

or neutropenia (six patients), arthropathy (five patients), nausea (five patients), or unsatisfactory response to deferiprone (five patients) [defined as low compliance (two patients), rising serum ferritin levels (four patients), a request to resume DFO (one patient), or a change of residence (one patient)].

Thus, by comparison with the ISGOIC study summarizing deferiprone experience prior to June 1994, these recent reports indicate a higher rate of treatment discontinuation (39% versus 20%), failure to decrease serum ferritin and liver iron concentrations to levels assuring significant cardioprotection in a substantial proportion of cases, and, indeed, the continued presence of cardiac mortality, a complication of transfusional iron overload which has already been largely eliminated by effective DFO treatment. A recent meta-analysis of nine clinical trials providing data on 129 iron-overloaded patients (94) has shown that after a mean of 16 months, 75% of patients with severe iron overload had a decrease in serum ferritin as compared with baseline, and 51.8% achieved a negative iron balance. Other reports from Near Eastern countries describe a high compliance rate in patients not previously compliant with DFO treatment, and a significant decrease in serum ferritin within the first year of deferiprone treatment (95).

The failure to achieve a steady decrease in storage iron with deferiprone may be explained by the difference in efficacy between the two drugs on a weight-per-weight basis. As shown by a metabolic balance study comparing combined urinary and fecal iron excretion in thalassemic patients receiving either 60 mg/kg DFO or 75 mg/kg p.o. deferiprone, mean iron excretion on deferiprone was only 65% of that on DFO (96). However, in some patients deferiprone was as effective as, or better than, DFO.

Collectively, these data imply that oral deferiprone treatment alone will not ensure sufficient protection in all patients, and that close monitoring is required to identify patients in whom additional conventional chelating treatment with DFO is indicated. In patients with unsatisfactory response to deferiprone, a number of options are available. The dose of deferiprone may be increased from the standard 75 mg/kg/day to 83 or 100 mg/kg/day. Alternatively, deferiprone given daily may be combined with DFO 5 days per week. Such measures resulted in a decrease in serum ferritin in all 13 patients previously failing to respond to standard deferiprone treatment (97). The effect of combined DFO and deferiprone on urinary iron excretion appear to be additive, and no toxic side effects have been observed. Improved results were also reported following alternate use of deferiprone and DFO (101).

5. Deferiprone Hepatotoxicity

Concerns related to the accelerated development of hepatic fibrosis have been expressed based on observations made in patients on long-term deferiprone therapy at the Toronto Hospital for Sick Children (87). Because in thalassemia viral hepatitis is an important cause of cirrhosis, one should focus on hepatitis C virus (HcV)-negative patients to evaluate the potential hepatotoxicity of deferiprone (Table 4). Of the 14 evaluable patients from the Toronto study, five developed progression of hepatic fibrosis on deferiprone treatment. Four of these patients were HcV positive. Only one of the eight HcV-negative Toronto patients developed progression of hepatic fibrosis. By comparison, none of the 25 HcV-negative patients reported collectively by Tondury et al. (90), Hoffbrand et al. (89), and Galanello et al. (98) developed this complication. No evidence of progression of fibrosis was found among any

Table 4 Proportion of HCV-Negative Patients Developing Grade III–IV Fibrosis

	Olivieri et al.	Tondury et al.	Hoffbrand et al.	Galanello et al.
Year (Ref.)	1998 (87)	1998 (90)	1998 (89)	1999 (98)
No. of patients	8	5	12	8
Dose (mg/kg/day)	75	75	75	75
Duration (years)	1.6–4.0	4.5–8.5	2.0–4.0	1.5–2.2
Liver Fe (mg/g)	13.8 ± 1.3	11.2 ± .0	17.4 ± 5.5	n.a.
Patients developing fibrosis	1/8	0/5	0/12	0/8

of the 29 patients, both HcV-positive and -negative, represented among the children who participated in the LA-02 study, and receiving deferiprone for a mean duration of 22 to 26 months, studied prospectively by repeated liver biopsies by Piga (99) and by Galanello (98). The effect of long-term deferiprone treatment on liver histology was also examined by Berdoukas et al. (100). Repeat liver biopsies were performed at an interval of about 1 year in 14 patients treated with deferiprone, and these were compared with those of 22 patients receiving DFO. The authors concluded that deferiprone appears to stabilize liver iron and that it does not significantly increase liver fibrosis.

Although these findings appear to be reassuring, the potential hepatotoxicity of deferiprone is still an issue of intense controversy. This important question is likely to determine the future of deferiprone in clinical medicine and needs urgent clarification by reviewing the hepatic status of all other patients on long-term deferiprone treatment, such as the remaining members of the large group of patients who participated in the Italian-American multicenter (LA-02) trial (91,92).

The results of deferiprone therapy in nonthalassemic patients, such as those with myelodysplasia (MDS), are quite similar to those with thalassemia: negative iron balance was achieved in 56% of patients, and the main causes of discontinuation of treatment were nausea and arthralgia (102). An unexpected bonus of iron chelating therapy with deferiprone or DFO in MDS was a significant decrease in transfusion requirement and increased erythroid activity documented by serum transferrin receptor levels. This is attributed to improved endogenous erythropoietin production (103). In addition, removal of red blood cell membrane free iron from thalassemic RBC by deferiprone has resulted in normalization of the increased KCI co-transport and decreased intracellular K⁺ content found in these cells (104).

6. New Hydroxypyridone Derivatives

An important cause of limited efficiency of deferiprone in humans is its rapid conjugation with glucuronide, inhibiting the iron-binding function of the 3-hydroxyl group. Hence, present ligand design is aimed at the development of compounds resisting inactivation by extensive conjugation with glucuronide or sulfate (105). The efficacy/toxicity ratio of hydroxypyridone derivatives may be improved by introducing bulky substituents on the 2-position of the pyridone ring. Such compounds show a limited interaction with nonheme iron enzymes such as lipoxygenase and ribonucleotide reductase, are less active in inducing apoptosis, but retain their ability to

mobilize intracellular iron effectively (106). In an effort to improve chelating efficiency and minimize toxicity, ester prodrugs of hydroxypyridinone have been designed by Liu et al. (107). Their partition coefficient and rates of hydrolysis at pH 2 and 7.4 have been correlated with their ability to promote hepatocellular radioiron excretion in rats. Of the various prodrugs tested, the picolinic and nicotinic ester derivatives appeared to offer the best potential for in-vivo efficiency.

B. Pyridoxal Isonicotinoyl Hydrazone (PIH)

PIH was introduced by Ponka et al., who recognized its ability to mobilize iron from ⁵⁹Fe-labeled reticulocytes (108). PIH is a tridentate chelator with a molecular weight of 287. At physiological pH, PIH is mainly in its neutral form, which allows it access across cell membranes and absorption from the gut (109). At pH 7.4 and a ligand concentration of 1 mmol/L, the pM value of PIH is 27.7, which is less than 28.6 for DFO. It would be worthwhile, therefore, to examine whether PIH may, or may not, be able to donate chelated iron to DFO (110), to act as a “shuttle” when the two chelators are co-administered. The selectivity of PIH for iron is comparable with that of DFO.

In hypertransfused rats (111), PIH is able to remove parenchymal and RE iron with equal efficiency, and practically all chelated iron is excreted through the bile. Its in-vivo chelating efficiency is equal to, or slightly better than, that of DFO; and its oral and parenteral effectiveness is similar. No evidence of toxicity has been found at doses up to 500 mg/kg/day. However, long-term (10 weeks) PIH treatment in rats failed to increase iron excretion (112). It is possible that this failure was caused by the hydrolysis of PIH into pyridoxal, and the corresponding acid hydrazide, at the low pH of the stomach (113).

Studies of patients with iron overload who were treated with PIH at a dose of 30 mg/kg/day have shown a modest net iron excretion of 0.12 ± 0.07 mg/kg/day (114), which is much less than the mean value of 0.5 mg/kg/day required to achieve negative iron balance in most cases. Nevertheless, it was estimated that this degree of iron excretion may be sufficient for achieving a negative iron balance in non-transfusion-dependent patients with iron-loading anemias. Although the results of this pilot study in thalassemic patients were generally regarded as evidence for the limited value of PIH in the treatment of thalassemia, several arguments have been raised in favor of PIH in a recent review (115) by Richardson and Ponka. First, the dose of 30 mg/kg used in the above study was much less than the effective doses of 125–500 mg/kg employed in experimental animals. Second, PIH was given to patients after calcium carbonate as a powder in gelatin capsules. This may have prevented acid hydrolysis of PIH, but also could drastically limit its absorption because of the low solubility of PIH in aqueous solution at a neutral pH (116).

Other Schiff base compounds are readily formed with pyridoxal, and a large number of such derivatives have been studied (108,111). One of the most effective of these, pyridoxal-pyrimidinyl-ethoxycarbonyl methbromide (PPH15), is able to remove 79% of hepatocellular radioiron stores in hypertransfused rats, following a single parenteral dose of 200 mg/kg, and its oral effectiveness exceeds that of parenteral DFO. Although results of preliminary toxicity studies in rats have been encouraging, subsequent studies in Cebus monkeys disclosed significant toxicity, precluding the use of this drug for clinical purposes. A variety of PIH analogs has been

prepared and evaluated by Ponka and his group (115). One of the most promising of these is PBH (pyridoxal-benzoyl hydrazone). It is 280% more effective than PIH, with a pK of 39.7 at neutral pH and 1 mmol/L (116). These improved features are attributed to its greater lipophilicity.

Progress in the development of PIH and its derivatives for clinical use has been painfully slow. The reasons for this have been reviewed by Richardson and Ponka (115): (a) PIH is not a proprietary (patentable) agent and therefore its attractiveness for industry is severely limited; (b) interest in recent years in deferiprone has left limited space for further development of other, alternative orally efficient chelators; (c) toxicologic and pharmacokinetic studies, although vitally important for drug development, are not sufficiently attractive to allow support by competitive governmental granting agencies; (d) on the other hand, the FDA is increasingly insistent on further toxicologic and pharmacokinetic studies as a precondition for human trials, which places the academic clinical investigator in a difficult situation; and (e) to these serious limitations one may add the high likelihood that the limited apparent efficacy of PIH in the single clinical study performed so far may have discouraged further efforts in this direction. Clearly, the therapeutic potential of PIH and its derivatives still awaits extensive and careful evaluation.

C. Desferrithiocin Analogs

Desferrithiocin is a very effective but toxic oral chelator identified in 1980 as a natural siderophore isolated from *Streptomyces*. Studies in a number of animal species have shown that desferrithiocin is about three times as effective as DFO. Some of its analogs have recently been found to be less toxic than the parent compound. In particular, desmethyl desferrithiocin shows minimal side effects relative to the parent compound while maintaining its iron-clearing properties in vivo in rats and Cebus monkeys (117). Desazadesmethyl desferrithiocin analogs have also shown promising features (118). Structural modifications, including the introduction of hydroxy, carboxy, or methoxy groups on the aromatic ring, alteration of the thiazoline ring, increasing the distance between the ligand donor atoms, and benz-fusion of the aromatic rings have been undertaken. These structural modifications have an impact on the rate of iron clearance and drug toxicity. These compounds were first screened for biological effect in bile duct-cannulated rodents and, if found promising, in iron-loaded primates, and subsequently submitted to formal toxicity studies. Although some favored compounds have already been identified, no clinical studies are available as yet (119,120).

D. The Polyanionic Amines (HBED)

N,N'-bis (2-hydroxybenzoyl)-ethylenediamine-*N,N'*-diacetic acid (HBED) is a very powerful polyanionic amine synthesized over 30 years ago by Martell's laboratory (121). It was rediscovered in recent years in the ongoing search for orally effective new chelators. It forms a hexadentate ligand with ferric iron with its secondary or tertiary nitrogens and hydroxyl and carboxyl groups. The affinity constant of HBED for Fe(III) is 39.6, and its affinity for other metals is relatively low. Conversion of the carboxylic groups of HBED to methyl esters results in a marked improvement in its intestinal absorption and a further increase in iron excretion.

HBED and dimethyl-HBED are remarkably nontoxic, and their LD₅₀ in rats is in excess of 800 mg/kg. Our studies in hypertransfused rats (122) have shown that at the dose range of 25–50 mg/kg HBED and dimethyl-HBED were 12–15 times more effective than DFO. Iron balance studies performed in a smaller number of thalassemic patients treated with HBED (123) have shown increased iron excretion following oral treatment in both the urine and stool. Daily total iron excretion with 40 mg/kg/day HBED was 6–11 mg, but no further increase in excretion was achieved at a dose of 80 mg/kg/day. These limited amounts of iron excretion represented 28–48% of the excretion needed for achieving negative iron balance. Because the pro-drug dimethyl-HBED showed improved absorption and bioavailability in animal studies, this compound is now regarded as a promising candidate for clinical evaluation.

There are several methods that may improve the efficacy of HBED. Its subcutaneous administration to iron-loaded *Cebus apella* monkeys resulted in iron excretion rates which were almost three times higher than identical doses of DFO (124). Moreover, when oral HBED (80 mg/kg/day) was used in combination with deferiprone (75 mg/kg/day), iron excretion exceeded the combined effect of the two drugs by 148–227%, and a negative iron balance was achieved. This synergistic effect was interpreted as the product of a “shuttle” and “sink” phenomenon wherein deferiprone, a small molecule with better access to the intracellular chelatable pool, would deliver chelatable iron to HBED (125). Thus, it would be possible to use HBED in patients either subcutaneously, as single injections twice weekly, as a more convenient alternative to DFO delivered by pump, or orally in combination with deferiprone.

E. The Substituted Polyaza Compounds (IRCO11)

The substituted cyclic polyaza compound IRCO11 was synthesized by Israel Resources Corporation Ltd., Haifa, Israel (126). IRCO11 has a number of promising features: (a) it is a hexadentate chelator binding Fe(III) at a 1:1 ratio and therefore without the risk of possible toxic intermediate complexes; (b) IRCO11 is water-soluble, and its stability constant with Fe(III) is over 1000 times that of DFO; (c) its acute LD₅₀ in mice exceeds 4.0 mmol/kg, compared to 0.44 mmol/kg for DFO; and (d) unlike DFO, polyaza compounds with the structure of IRCO11 do not contain any readily hydrolyzable covalent bonds, and are anticipated to resist biotransformation in vivo.

In contrast to DFO, which promotes the excretion of both hepatocellular and RE iron, the major source of iron mobilized by IRCO11 is iron derived from the catabolism of RBC hemoglobin in the RE system (24). Because in thalassemia the contribution of RBC catabolism to the influx of iron to the plasma is incomparably higher than that of all other sources combined, it is reasonable to assume that RBC catabolism is the predominant source of the toxic and readily chelatable non-transferrin-bound plasma iron (NTBI) compartment. Thus IRCO11, with its superior ability to interact with catabolic RBC iron, may not only improve the rate of urinary iron excretion in thalassemia, but possibly also offer better protection of vital tissues from peroxidative damage by preventing the formation or eliminating NTBI. Since IRCO11 is a water-soluble compound, its membrane permeability is limited, but it may be regarded as a useful parent compound for a wide spectrum of polyaza analogs. Substitution of its synthetic arms by more lipophilic ligands may result in

improved interaction with hepatocellular iron stores, and possibly also better oral activity. Such studies are presently underway.

F. Bis-Hydroxyphenyl-Triazole (ICL 670A)

ICL 670A is a member of a new class of tridentate iron-selective synthetic chelators, the bis-hydroxyphenyl-triazoles produced by Novartis. ICL 670A (formerly CGP 72 670: 4-[3,5-bis-(hydroxyphenyl)-[1,2,4]triazol-1-yl]-benzoic acid (127)) has been evaluated together with 44 compounds of the triazole series and about 700 other compounds of five additional chemical classes. ICL 670A has emerged from this screening process as the best compound combining oral effectiveness and low toxicity. ICL 670A has an affinity for ferric iron which is three log units higher than deferiprone, and the ligand is stable both in vivo and in vitro.

In a 12-week study in iron-loaded rats, ICL 670A was twice as effective orally as s.c. DFO. In the iron-loaded marmoset, iron excretion was predominantly fecal. At the higher dose range the effect of a single dose continued up to 48 h. Iron excretion was predominantly fecal and iron-selective, without increasing copper or zinc excretion. At equimolar doses, it was 10 times more effective than deferiprone. At the effective oral dose of 22 mg/kg no adverse effects were seen after 4 weeks of treatment. At very high doses, nephrotoxicity was seen in both rats and marmosets, but this was much less in iron-loaded animals (128).

Phase I clinical trials with ICL 670A are in progress. In these studies, the safety and efficacy of ICL 670A will be evaluated in thalassemic patients starting with a dose of 2.5 mg/kg and gradually escalating to 80 mg/kg. These studies will also include detailed pharmacokinetics including area under the curve (AUC), C_{\max} , t_{\max} , and $t_{1/2}$. These studies will be followed by repeated-dose safety trials and iron-balance metabolic studies (129).

VI. CO-ADMINISTRATION OF CHELATORS: THE “SHUTTLE EFFECT”

Observations on the comparative ability of DFO and a hydroxypyridinone chelator (CP094) to cross cellular membranes are pertinent to the issue of probable differences in the chelatable iron pools interacting with DFO and deferiprone (130). These studies, conducted in the rat visceral yolk sac, showed that hydroxypyridones cross the plasma and lysosomal membranes rapidly, whereas DFO is incapable of crossing the same membranes, and enters cells only by endocytosis. These in-vitro studies lend strong support to the concept that DFO and deferiprone tap different iron pools, and that their concurrent use may result in an additive, or synergistic, effect on iron excretion (Fig. 2).

The combination of a weak chelator which has a better ability to penetrate cells with a stronger chelator that penetrates cells poorly but yields more efficient urinary excretion may result in a synergistic effect through iron shuttling between the two compounds. Such a “shuttle effect” was first proposed by Grady. Metabolic balance studies performed by Grady et al. in thalassemic patients have shown that when deferiprone is given during DFO treatment (at time 0, 4, and 8 h of an 8-h infusion), a synergistic effect is achieved with total iron excretion 2.4 to 3.4 times higher than with DFO alone (131). These data suggest an interaction between deferiprone and

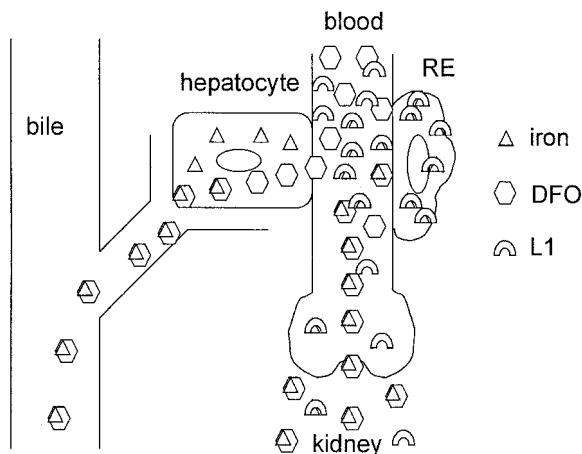


Figure 2 This cartoon is a modification of Fig. 1, describing the putative “shuttle effect” of deferiprone (L1) on DFO-induced iron excretion. The shuttle hypothesis assumes that the two chelators tap different chelatable iron pools. If deferiprone is more efficient in penetrating RE cells, it will facilitate the egress of RE iron and then yield it to extracellular DFO to enhance the urinary excretion of DFO-iron (ferrioxamine).

DFO, and may have important implications to the design of new strategies in iron chelating treatment.

A shuttle effect was directly demonstrated by following the fate of chelated plasma iron in thalassemic patients receiving combined DFO and deferiprone therapy (132). Deferiprone treatment resulted in the temporary accumulation of chelated iron in the plasma peaking at 2 h. The addition of DFO to deferiprone treatment resulted in the transfer of chelated iron from deferiprone to DFO and an increase in total chelated iron in the serum. This chain of events indicates improved in-vivo chelating efficiency utilizing chelatable iron first mobilized by deferiprone and transferred subsequently to DFO.

Improved chelating efficiency and improved compliance with combined deferiprone and DFO regimen has been reported by several groups. Wonke et al. (97) described the effect of combining DFO with deferiprone treatment in thalassemic patients. Deferiprone was given daily, and DFO 5 days per week. This has resulted in a decrease in serum ferritin in all 13 patients previously failing to respond to standard deferiprone treatment. The effect of combined DFO and deferiprone on urinary iron excretion appeared to be additive, and no toxic side effects have been observed.

Combination treatment using a lowered daily dose of deferiprone (50 mg/kg/day) and DFO by subcutaneous infusion (50 mg/kg/day) twice weekly in 28 patients resulted in a marked decrease in the incidence of gastrointestinal symptoms and arthropathy, and a decrease of serum ferritin from 3724 to 1790 $\mu\text{g/L}$ within 16 ± 9 months (133). Others have reported improved compliance when DFO was given over the weekend for 2 days, alternating with deferiprone for 4 days per week (101), although the 6-month study period did not allow firm conclusions regarding cumulative efficacy.

Table 5 Possible Advantages of Combined Chelation Therapy

-
1. Decreasing drug toxicity
 2. Allowing optimal conditions for 3:1 complex formation with deferiprone
 3. Preventing the production of NTBI by RE cells
 4. New and more effective application of weak or ineffective oral chelators: HBED, PIH, DHB
-

It is possible that co-administration of deferiprone and DFO will achieve nothing more than the combination of their separate effects. However, several possible additional benefits are worth exploring (Table 5). (a) Since the toxic side effects of the two compounds are different, and some of them are dose-dependent, co-treatment may allow dose reduction and diminishing drug toxicity. (b) Decreasing the chelatable iron pool by DFO may shift the proportion of chelatable iron to deferiprone closer to the optimal 1:3 molar ratio, allowing optimal conditions for deferiprone's effect. (c) DFO has a limited access to RE iron stores but may be able to interact indirectly with reticuloendothelial iron by the shuttling effect deferiprone. Such an interaction may prevent the production of the toxic NTBI originating from RBC hemoglobin breakdown in the reticuloendothelial system. (d) If the shuttling concept is validated, it may be utilized for the co-administration of other drug combinations. For example, Grady et al. have already shown that the co-administration of deferiprone and HBED greatly enhances the oral effectiveness of HBED (125). (e) Likewise, it would be worthwhile to reexamine the clinical effectiveness of PIH (see above) or dihydroxybenzoic acid (DHB), which are weak oral chelators unable by themselves to induce a negative iron balance, in the context of combined chelating treatment with DFO. (f) In-vitro observations on the antimalarial effect of iron chelators suggest that co-administration of lipophilic chelators with easy access to the intracellular parasite, together with extracellular DFO, may result in a synergistic parasitocidal effect (134). This approach could be utilized in clinical studies of iron chelators in malaria.

VII. CURRENT ISSUES IN CHELATOR DEVELOPMENT

Undoubtedly, DFO remains the drug of choice for the management of transfusional siderosis in thalassemic patients. However, its high cost and the inconvenience of its parental administration by portable pumps are major limitations underlying the need for developing alternative orally effective new iron chelating drugs. In the search for new and improved chelators, it is useful to remember some of the basic principles determining the safety and efficacy of iron chelators as defined in an important recent review by Hider et al. (136) (and see Chapter 13):

1. Stability of the chelator-iron complex is determined not only by the affinity of the drug for Fe(III), but also by the nature of the interaction. Hexadentate chelators bind Fe(III) at a 1:1 ratio, forming a neutral, stable complex that prevents iron from participating in harmful reactions and producing hydroxyl radicals. By contrast, bidentate chelators such as deferiprone require three molecules to one ferric iron to form a stable, neutral complex. Hence, at suboptimal concentrations of deferiprone, when either tissue iron concentrations are very high or drug concentrations are too

low, incomplete 1:1 or 2:1 complexes may be formed which may result in enhanced mobilization of potentially toxic iron. Thus, hexadentate chelators would, on theoretical grounds, be generally preferable to bidentate or tridentate chelators.

2. Partition coefficient, i.e., the relative solubility in water and lipids, determines the ability to cross lipid membranes. Chelators with partition coefficients of 0.05 to 1.0 will have efficient gastrointestinal absorption. Increasing lipophilicity will result in efficient drug clearance from the portal circulation by the liver. Unfortunately, increasing lipophilicity also improves the penetration of the blood-brain and placental barriers and increases drug toxicity (137).

3. Molecular weight is a critical feature in designing new chelators with improved oral efficacy. New chelators with excellent in-vitro interaction with chelatable iron in cell cultures or following their parenteral administration may be ineffective if their size interferes with their intestinal absorption. To achieve greater than 70% absorption, the molecular weight should be less than 300. Thus, by virtue of their lower molecular weights, bidentate and tridentate ligands are predicted to have higher absorption efficiency than hexadentates.

4. Prodrugs are an excellent solution for a number of requirements in the development of oral chelators. Lipophilic esters represent an attractive model of non-toxic orally effective iron chelators. Such nonpolar prodrugs would be efficiently absorbed and subsequently cleared from the portal system by the liver. Following conversion into the active hydrophilic metabolite, they may chelate liver iron in situ to be excreted in the bile or, following release into the systemic circulation, would interact with non-transferrin-bound plasma iron and be excreted into the urine. Because of their gradual absorption, iron excretion may be improved severalfold. Protection against the harmful effects of circulating NTBI is optimal when the chelator is permanently present in the plasma. This effect, similar to continuous s.c. or i.v. drug infusion, may be achieved conveniently by employing orally effective prodrugs in slow-release preparations.

Iron chelating therapy has changed the quality of life and life expectancy of thalassemic patients. However, the high cost and rigorous requirements of DFO therapy and the significant toxicity of deferiprone underline the need for the continued development of new and improved orally effective iron chelators. Such development, as well as the evolution of improved strategies for iron chelating therapy, require better understanding of the pathophysiology of iron toxicity and the mechanism of action of iron chelating drugs.

ACKNOWLEDGMENTS

This work was supported by the Israel Science Foundation administered by the Israel Academy of Sciences and Humanities and grant DK54199 of the NIDDK.

REFERENCES

1. Hershko C. Control of disease by selective iron depletion: A novel therapeutic strategy utilizing iron chelators. *Clin Haematol* 1994; 7:965–1000.
2. Cook JD, Marsaglia G, Eschbach JW. Ferrokinesics: A biologic model for plasma iron exchange in man. *J Clin Invest* 1970; 49:197–205.
3. Hershko C, Rachmilewitz EA. Mechanism of desferrioxamine-induced iron excretion in thalassemia. *Br J Haematol* 1979; 42:125–132.

4. Hershko C, Graham G, Bates GW, Rachmilewitz EA. Non-specific serum iron in thalassaemia: An abnormal serum iron fraction of potential toxicity. *Br J Haematol* 1978; 40:255–263.
5. Gutteridge JMC, Rowley DA, Griffiths E, Halliwell B. Low-molecular-weight iron complexes and oxygen radical reactions in idiopathic haemochromatosis. *Clin Sci* 1985; 68:463–467.
6. Al-Refai FN, Wickens DG, Wonke B, Kontoghiorghes GJ, Hoffbrand AV. Serum non-transferrin-bound iron in beta-thalassaemia major patients treated with desferrioxamine and L1. *Br J Haematol* 1992; 82:431–436.
7. Porter JB, Abeyasinghe RR, Marshall L, Hider RC, Singh S. Kinetics of removal and reappearance of non-transferrin-bound plasma iron with deferoxamine therapy. *Blood* 1996; 88:705–713.
8. Link G, Pinson A, Hershko C. Heart cells in culture: A model of myocardial iron overload and chelation. *J Lab Clin Med* 1985; 106:147–153.
9. Randell EW, Parkes JG, Olivieri NF, Templeton DM. Uptake of non-transferrin-bound iron by both reductive and nonreductive processes is modulated by intracellular iron. *J Biol Chem* 1994; 269:16046–16053.
10. Link G, Athias P, Grynberg A, Pinson A, Hershko C. Effect of iron loading on transmembrane potential, contraction and automaticity of rat ventricular muscle cells in culture. *J Lab Clin Med* 1989; 113:103–111.
11. Gabutti V, Borgna-Pignatti C. Clinical manifestations and therapy of transfusional haemosiderosis. *Clin Haematol* 1994; 7:919–940.
12. Link G, Pinson A, Hershko C. The ability of orally effective iron chelators dimethyl- and diethyl-hydroxypyrid-4-one and of deferoxamine to restore sarcolemmal thiolic enzyme activity in iron-loaded heart cells. *Blood* 1994; 83:2692–2697.
13. Link G, Pinson A, Hershko C. Iron loading of cultured cardiac myocytes modifies sarcolemmal structure and increases lysosomal fragility. *J Lab Clin Med* 1993; 121:127–134.
14. Link G, Tirosh R, Pinson A, Hershko C. Role of iron in the potentiation of anthracycline toxicity: Identification of heart cell mitochondria as the site of iron-anthracycline interaction. *J Lab Clin Med* 1996; 127:272–278.
15. Aldouri MA, Wonke B, Hoffbrand AV, Flynn DM, Ward SE, Agnew JE, Hilson AJ. High incidence of cardiomyopathy in beta-thalassaemia patients receiving regular transfusion and iron chelation: Reversal by intensified chelation. *Acta Haematol* 1990; 83:113–117.
16. Mariotti E, Agostini A, Angelucci E, et al. Cardiac study by dobutamine stress echocardiography in thalassaemic patients. *Bone Marrow Transplant* 1993; 12(suppl 1):14–15.
17. Brittenham GM, Griffith PM, Nienhuis AW, et al. Efficacy of deferoxamine in preventing complications of iron overload in patients with thalassaemia major. *N Engl J Med* 1994; 331:567–569.
18. De Sanctis V, Pintor C, Aliquo MC. Prevalence of endocrine complications in patients with β -thalassaemia major: An Italian multicenter study. In: Pintor C, Muller EE, Loche S, New MI (eds). *Advances in Pediatric Endocrinology*, Berlin: Springer-Verlag, 1992: 127–133.
19. Gamberini MR, Fortini M, Gilli G, Testa MR, De Sanctis V. Epidemiology and chelation therapy effects on glucose homeostasis in thalassaemic patients. *J Pediatr Endocrinol Metab* 1998; 11:867–869.
20. Caruso-Nicoletti M, De Sanctis V, Capra M, et al. Short stature and body proportion in thalassaemia. *J Pediatr Endocrinol Metab* 1998; 11:811–816.
21. Rothman RJ, Serroni A, Farber JL. Cellular pool of transient ferric iron, chelatable by deferoxamine and distinct from ferritin, that is involved in oxidative cell injury. *Mol Pharmacol* 1992; 42:703–710.

22. Klausner RD, Rouault TA, Harford JB. Regulating the fate of mRNA: The control of cellular iron metabolism. *Cell* 1993; 72:19–28.
23. Breuer W, Epsztejn S, Cabantchik ZI. Dynamics of the cytosolic chelatable iron pool of K562 cells. *FEBS Lett* 1997; 382:304–308.
24. Hershko C, Weatherall JD. Iron chelating therapy. *CRC Crit Rev Clin Lab Sci* 1988; 26(4):303–345.
25. Rivkin G, Link G, Simhon E, Cyjon RL, Klein JY, Hershko C. IRCO11, a new synthetic chelator with selective interaction with catabolic red blood cell iron. Evaluation in hypertransfused rats with hepatocellular and reticuloendothelial radioiron probes and in iron-loaded rat heart cells in culture. *Blood* 1997; 90:4180–4187.
26. Keberle H. From antibiotic to chelating agent. In: Gross K, Aumiller J, Gelzer J, eds. *Desferrioxamine: History, Clinical Value, Perspectives*. MMV Medizin-Verlag, 1992: 26–36.
27. Lee P, Mohammed N, Marshall L, Abeyasinghe RD, Hider RC, Porter JB, Singh S. Intravenous infusion pharmacokinetics of desferrioxamine in thalassaemic patients. *Drug Metabol Disp* 1993; 21:640–644.
28. Porter JB, Faherty A, Stallibrass L, Brookman L, Hassan L, Howes C. A trial to investigate the relationship between DFO pharmacokinetics and metabolism and DFO-related toxicity. *Ann NY Acad Sci* 1998; 850:485–487.
29. Gabutti V, Piga A. Results of long-term iron-chelating therapy. *Acta Haematol* 1996; 95:26–36.
30. Olivieri NF, Brittenham GM. Iron chelating therapy and the treatment of thalassemia. *Blood* 1997; 89:739–761.
31. Borgna-Pignatti C, Cohen A. Evaluation of a new method of administration of the iron chelating agent deferoxamine. *J Pediatr* 1997; 130:86–88.
32. Araujo A, Kosaryan M, MacDowell A, Wickens D, Puri S, Wonke B, Hoffbrand AV. A novel delivery system for continuous desferrioxamine infusion in transfusional iron overload. *Br J Haematol* 1996; 93:835–837.
33. Canatan D, Temimhan N, Dincer N, Ozsancak A, Oguz N, Temimhan M. Continuous desferrioxamine infusion by an infusor in thalassaemia major. *Acta Paediatr* 1999; 88: 550–552.
34. Alberti D, Piga A, Porter JB, Hassan I. Desferrioxamine depot (CGH 749B): A new formulation allowing the prospect of a daily s.c. injection (abstr 39). 8th International Conference, Oral Chelation in the Treatment of Thalassaemia and Other Diseases, Corfu, 1997.
35. Cappellini MD, Alberti D, Dimitrijevic S. A new depot formulation of desferrioxamine (ICL749B) given as subcutaneous bolus injection in transfusion dependent β -thalassaemic patients: Update on the dosage-finding program (abstr 25). *Bioiron 99: World Congress on Iron Metabolism, Sorrento, Naples, Italy, May 23–28, 1999*.
36. Brittenham GM, Farrell DE, Harris DE, Feldman ES, Danish EH, Muir DA, Tripp JH, Bellon EM. Magnetic susceptibility measurement of human iron stores. *N Engl J Med* 1982; 307:1671–1675.
37. Chapman RWG, Hussain MAM, Gorman A, Laulich M, Politis D, Flynn DM, Sherlock S, Hoffbrand AV. Effect of ascorbic acid deficiency on serum ferritin concentration in patients with beta thalassaemia. *J Clin Pathol* 1982; 35:481–486.
38. Olivieri NF, Nathan DG, MacMillan JH, Wayne AS, Liu PP, McGee A, Martin M, Koren G, Cohen AR. Survival in medically treated patients with homozygous β -thalassaemia. *N Engl J Med* 1994; 331:574–578.
39. Piga A, Luzzatto L, Capalbo P, Gambotto S, Tricta F, Gabutti V. High-dose desferrioxamine as a cause of growth failure in thalassaemic patients. *Eur J Haematol* 1988; 40:380–381.

40. Brill PW, Winchester P, Giardina PJ, Cunningham-Rundles S. Deferoxamine-induced bone dysplasia in patients with thalassemia major. *Am J Radiol* 1991; 156:561–565.
41. Olivieri NF, Koren G, Harris J, Khattak S, Freedman MH, Templeton DM, Baily JD, Reilly BJ. Growth failure and bony changes induced by deferoxamine. *Am J Pediatr Hematol Oncol* 1992; 14:48–56.
42. De-Sanctis V, Pinamonti A, Di-Palma A, Sprocati M, Atti G, Gamberini MR, Vullo C. Growth and development in thalassaemia major patients with severe bone lesions due to desferrioxamine. *Eur J Pediatr* 1996; 155:368–372.
43. Naselli A, Vignolo M, Di Battista E, Garzia P, Forni GL, Traverso T, Aicardi G. Long-term follow-up of skeletal dysplasia in thalassaemia major. *J Pediatr Endocrinol Metab* 1998; 11:817–825.
44. Olivieri NF, Buncic RJ, Chew E, Gallanti T, Harrison RV, Kennan N, Logan N, Mitchell D, Ricci G, Skarf B, Taylor M, Freedman MH. Visual and auditory neurotoxicity in patients receiving sub-cutaneous deferoxamine infusions. *N Engl J Med* 1986; 314: 869–873.
45. Arden GB, Wonke B, Kennedy C, Huehns ER. Ocular changes in patients undergoing long-term desferrioxamine treatment. *Br J Ophthalmol* 1984; 68:873–877.
46. Koren G, Bentur Y, Strong D, Harvey E, Klein J, Baumal R, Spielberg SP, Freedman MH. Acute changes in renal function associated with deferoxamine therapy. *Am J Dis Child* 1989; 143:1077–1080.
47. Freedman MH, Grisaru D, Olivieri N, MacLusky I, Thorner PS. Pulmonary syndrome in patients with thalassemia major receiving intravenous deferoxamine infusions. *Am J Dis Child* 1990; 144:565–569.
48. Porter JB, Jaswon MB, Huehns ER, East CA, Hazell JW. Desferrioxamine ototoxicity: Evaluation of risk factors in thalassaemic patients and guidelines for safe dosage. *Br J Haematol* 1989; 73:403–409.
49. Lombardo T, Ferro G, Frontini V, Percolla S. High-dose intravenous desferrioxamine (DFO) delivery in four thalassaemic patients allergic to subcutaneous DFO administration. *Am J Hematol* 1996; 51:90–92.
50. Gallant T, Freedman MH, Vellend H, Francombe WH. *Yersinia* sepsis in patients with iron overload treated with deferoxamine. *N Engl J Med* 1986; 314:1643.
51. Borgna-Pignatti C, Rugolotto S, De Stefano P, Piga A, Di Gregorio F, Gamberini MR, Sabato V, Melevendi C, Cappellini MD, Verlato G. Survival and disease complications in thalassemia major. *Ann NY Acad Sci* 1998; 850:227–231.
52. Calleja EM, Shen JY, Lesser M, Grady RW, New MI, Giardina PJ. Survival and morbidity in transfusion-dependent thalassaemic patients on subcutaneous desferrioxamine chelation. *Ann NY Acad Sci* 1998; 850:469–470.
53. Hoffbrand AV, Wonke B. Results of long-term subcutaneous desferrioxamine therapy. *Bailliere's Clin Haematol* 1989; 2:345–359.
54. Giardina PJ, Grady RW, Ehlers KH, Burstein S, Graziano JH, Markenson AL, Hiltgartner MW. Current therapy of Cooley's anemia. A decade of experience with subcutaneous desferrioxamine. In: Bank A, ed. *Sixth Cooley's Anemia Symposium*, Ann NY Acad Sci 1990; 612:275–285.
55. Marcus RE, Davies SC, Bantock HM, Underwood SR, Walton S, Huehns ER. Desferrioxamine to improve cardiac function in iron-overloaded patients with thalassaemia major. *Lancet* 1984; 1:392.
56. Hyman CB, Agness CL, Rodriguez-Funes R, Zednikova M. Combined subcutaneous and high-dose intravenous deferoxamine therapy of thalassemia, *Ann NY Acad Sci* 1985; 445:293–303.
57. Cohen AR, Martin M, Schwartz E. Current treatment of Cooley's anemia. Intravenous chelation therapy. In: Bank A, ed. *Sixth Cooley's Anemia Symposium*, Ann NY Acad Sci 1990; 612:286–292.

58. Aessopos A, Karabatsos F, Farmakis D, Katsantoni A, Hatziliami A, Youssef J, Karagiorga M. Pregnancy in patients with well-treated beta-thalassemia: Outcome for mothers and newborn infants. *Am J Obstet Gynecol* 1999; 180:360–365.
59. Singer ST, Vichinsky EP. Deferoxamine treatment during pregnancy: Is it harmful? *Am J Hematol* 1999; 60:24–26.
60. Hider RC, Singh S, Porter JB, Huehns ER. The development of hydroxypyridin-4-ones as orally active iron chelators. In: Bank A, ed. Sixth Cooley's Anemia Symposium, Ann NY Acad Sci 1990; 612:327–328.
61. Kontoghiorghes GJ. Design, properties, and effective use of the oral chelator L1 and other ketohydroxypyridines in the treatment of transfusional iron overload in thalassemia. In: Bank A, ed. Sixth Cooley's Anemia Symposium, Ann NY Acad Sci 1990; 612:339–350.
62. Diav-Citrin O, Koren G. Oral iron chelation with deferiprone. *Pediatr Clin N Am* 1997; 44:235–247.
63. Barman Balfour JA, Foster RH. Deferiprone. A review of its clinical potential in iron overload in β -thalassemia major and other transfusion-dependent diseases. *Drugs* 1999; 58:553–578.
64. Olivieri NF. Long-term therapy with deferiprone. *Acta Haematol* 1996; 95:37–48.
65. Al-Refaie FN, Hoffbrand AV. Oral iron-chelating therapy: The L1 experience. *Clin Haematol* 1994; 7:941–964.
66. Grady RW, Srinivasan R, Dunn JB, Coursey MP, Lemert RF, Calvano SE, Hilgartner MW. Evidence of toxicity due to 1,2-dimethyl-3-hydroxypyrid-4-one (L1) in normal rats. *Drugs Today, Suppl. A.* 1992; 28:73–80.
67. Ziel R, Junker Walker U, Pfaar U, Vogel B, Bentley P, Schnebli HP. Toxicological and metabolic studies with CGP 37 391 (L1). 5th International Conference on Thalassaemias and the Haemoglobinopathies, Nicosia, Cyprus, 1993: abstr 191.
68. Al-Refaie FN, Hershko C, Hoffbrand AV, Kosaryan M, Olivieri NF, Tondury P, Wonke B. Results of long-term deferiprone (L1) therapy: A report of the International Study Group on Oral Iron Chelators. *Br J Haematol* 1995; 91:224–229.
69. Vallee BL, Falchuk KH. The biochemical and pathological basis of zinc physiology. *Physiol Rev* 1993; 73:79–88.
70. Berdoukas V, Bentley P, Frost H, Schnebli HP. Toxicity of iron chelator L1. *Lancet* 1993; 341:1088.
71. Hershko C. Development of iron chelator L1. *Lancet* 1993; 341:1088–1089.
72. Cragg L, Hebbel RP, Miller W, Solovey A, Selby S, Enright H. The iron chelator L1 potentiates oxidative damage in iron-loaded liver cells. *Blood* 1998; 92:632–638.
73. Carthew P, Smith AG, Hider RC, Dorman B, Edwards RE, Francis JE. Potentiation of iron accumulation in cardiac myocytes during the treatment of iron overload in gerbils with the hydroxypyridone iron chelator CP94. *Biometals* 1994; 7:267–271.
74. Hershko C, Link G, Konijn AM. Relative effectiveness of deferoxamine (DFO) and deferiprone (L1) in protecting iron-loaded Gerbils from non-transferrin-bound iron (NTBI) toxicity. American Society of Hematology, Forty-First Annual Meeting, New Orleans, LA, December 3–7, 1999, *Blood* 94(Suppl. 1): abstr 1870.
75. Link G, Konijn AM, Hershko C. Cardioprotective effect of alpha-tocopherol, ascorbate, deferoxamine, and deferiprone: Mitochondrial function in cultured, iron-loaded heart cells. *J Lab Clin Med* 1999; 133:179–188.
76. Wong A, Alder V, Robertson D, Papadimitriou J, Maserei J, Berdoukas V, Kontoghiorghes G, Taylor E, Baker E. Liver iron depletion and toxicity of the iron chelator deferiprone (L1, CP20) in the guinea pig. *Biometals* 1997; 10:247–256.
77. Al-Refaie FN, Sheppard LN, Nortey P, Wonke B, Hoffbrand AV. Pharmacokinetics of the oral iron chelator deferiprone (L1) in patients with iron overload. *Br J Haematol* 1995; 89:403–407.

78. Fassos FF, Klein J, Fernandes D, et al. The pharmacokinetics and pharmacodynamics of the oral chelator deferiprone (L1) in relation to hemoglobin levels. *Int J Clin Pharmacol Ther* 1996; 34:288–292.
79. Matsui D, Klein J, Hermann C, et al. Relationship between the pharmacokinetics and iron excretion pharmacodynamics of the new oral iron chelator 1,2-dimethyl-3-hydroxy-pyrid-4-one in patients with thalassemia. *Clin Pharmacol Ther* 1991; 50:294–298.
80. Porter JB, Abeysinghe RD, Hoyes KP, Barra C, Huehns ER, Brooks PN, Blackwell MP, Araneta M, Brittenham G, Singh S, Dobbin P, Hider RC. Contrasting interspecies efficacy and toxicology of 1,2-diethyl-3-hydroxypyrid-4-one, CP94, relates to differing metabolism of the iron chelating site. *Br J Haematol* 1993; 85:159–168.
81. Singh S, Epemolu RO, Dobbin PS, et al. Urinary metabolic profiles in human and rat of 1,2-dimethyl and 1,2-diethyl-substituted 3-hydroxypyrid-4-ones. *Drug Metab Disp* 1992; 20:256–261.
82. Kontoghiorghes GJ, Goddard JG, Bartlett AN, et al. Pharmacokinetic studies in humans with the oral iron chelator 1,2-dimethyl-3-hydroxypyrid-4-one. *Clin Pharmacol Ther* 1990; 48:255–261.
83. Stobie S, Tyberg J, Matsui D, et al. Comparison of the pharmacokinetics of 1,2-dimethyl-3-hydroxypyrid-4-one (L1) in healthy volunteers, with and without co-administration of ferrous sulfate, to thalassemia patients. *Int J Clin Pharmacol Ther Toxicol* 1993; 31:602–605.
84. Olivieri NF, Brittenham JM, Matsui D, Berkovitch M, Blendis LM, Cameron RG, McLelland RA, Liu PP, Templeton DM, Koren G. Iron-chelation therapy with oral deferiprone in patients with thalassemia major. *N Engl J Med* 1995; 332:918–922.
85. Tondury P, Kontoghiorghes GJ, Ridolfi-Luthy A, Hirt A, Hoffbrand AV, Lottenbach AM, Sonderegger T, Wagner HP. L1 (1,2-dimethyl-3-hydroxypyrid-4-one) for oral iron chelation in patients with beta-thalassaemia major. *Br J Haematol* 1990; 76:550–553.
86. Agarwal MB, Gupte SS, Viswanathan C, Ramanathan J, Desai N, Puniyani RR, Chhablani AT. Long-term assessment of efficacy and safety of L1, an oral iron chelator, in transfusion dependent thalassaemia: Indian trial. *Br J Haematol* 1992; 82:460–466.
87. Olivieri NF, Brittenham GM, McLaren CE, Templeton DM, Cameron RG, McClelland RA, Burt AD, Fleming KA. Long-term safety and effectiveness of iron-chelation therapy with deferiprone for thalassemia major. *N Engl J Med* 1998; 339:417–423.
88. Olivieri NF, Brittenham GM. Final results of the randomized trial of deferiprone (L1) and deferoxamine (DFO). Thirty-Ninth Annual Meeting, American Society of Hematology, San Diego, CA, *Blood* 1997(Suppl 1): abstr 1161.
89. Hoffbrand AV, Al-Refaie F, Davis B, et al. Long-term trial of deferiprone in 51 transfusion-dependent iron overloaded patients. *Blood* 1998; 91:295–300.
90. Tondury P, Zimmermann A, Nielsen P, Hirt A. Liver iron and fibrosis during long-term treatment with deferiprone in Swiss thalassaemic patients. *Br J Haematol* 1998; 101: 413–415.
91. Tricta F, Spino M. Deferiprone: The long term cumulative experience (abstr). 8th International Conference, Oral Chelation in the Treatment of Thalassaemia and Other Disease, Corfu, 1997.
92. Cohen A, Galanello R, Piga A, Vullo C, Tricta F. A multi-center safety trial of the oral iron chelator deferiprone. Cooley's Anemia Seventh Symposium, *Ann NY Acad Sci* 1998; 850:223–226.
93. Castriota-Scanderberg A, Sacco M. Agranulocytosis, arthritis and systemic vasculitis in a patient receiving the oral iron chelator L1 (deferiprone). *Br J Haematol* 1997; 96: 254–255.
94. Addis A, Loebstein R, Koren G, Einarson TR. Meta-analytic review of the clinical effectiveness of oral deferiprone (L1). *Eur J Clin Pharmacol* 1999; 55:1–6.

95. Taher A, Chamoun FM, Koussa S, Saad MA, Khoriaty AI, Neeman R, Mourad FH. Efficacy and side effects of deferiprone (L1) in thalassemia patients not compliant with desferrioxamine. *Acta Haematol* 1999; 101:173-177.
96. Grady RW, Hilgartner MW, Giardina PJ. Deferiprone: Its efficacy relative to that of desferal. Thirty-Eighth Annual Meeting, American Society of Hematology, Orlando, FL, Blood 1996(suppl 1): abstr 1230.
97. Wonke B, Wright C, Hoffbrand AV. Combined therapy with deferiprone and desferrioxamine. *Br J Haematol* 1998; 103:361-364.
98. Galanello R, De Virgiliis S, Agus A, Carta E, Cao A, Mancosu MG, Faa G. Sequential liver fibrosis grading during deferiprone treatment in patients with thalassemia major. 9th International Conference on Oral Chelation in the Treatment of Thalassaemia and Other Diseases, Hamburg, March 25-28, 1999: abstr 50.
99. Piga A, Facello S, Pucci A, Pietribiasi F, Zimmermann A. The assessment of liver fibrosis in thalassemia major during chelation therapy. 9th International Conference on Oral Chelation in the Treatment of Thalassaemia and Other Diseases, Hamburg, March 25-28, 1999: abstr 49.
100. Berdoukas VA, Lindeman R, Eagle C, Bohane TD, Tobias VH, de Silva K, Painter D, Fraser I. Liver assessment in a group of transfusion dependent patients treated with deferiprone and compared to a group of patients treated with desferrioxamine. American Society of Hematology. Forty-First Annual Meeting, New Orleans, LA, December 3-7, 1999, *Blood* 94(suppl 1): abstr 3283.
101. Aydinok Y, Nisli G, Kavakli K. Alternate use of deferiprone and desferrioxamine in primary school children with thalassaemia major. *Br J Haematol* 1999; 106:252-253.
102. Kersten MJ, Lange R, Smeets ME, Vreugdenhil G, Roozendaal KJ, Lameijer W, Goudsmit R. Long-term treatment of transfusional iron overload with the oral iron chelator deferiprone (L1): A Dutch multicenter trial. *Ann Hematol* 1996; 73:247-252.
103. Jensen PD, Heickendorff L, Pedersen B, Bendix-Hansen K, Jensen FT, Christensen T, Boesen AM, Ellegaard J. The effect of iron chelation on haemopoiesis in MDS patients with transfusional iron overload. *Br J Haematol* 1996; 94:288-299.
104. De Franceschi L, Shalev O, Piga A, Collell M, Olivieri O, Corrocher R, Hebbel RP, Brugnara C. Deferiprone therapy in homozygous human beta-thalassemia removes erythrocyte membrane free iron and reduces KC1 cotransport activity. *J Lab Clin Med* 1999; 133:64-69.
105. Hider RC, Choudhury R, Rai BL, Dehkordi LS, Singh S. Design of orally active iron chelators. *Acta Haematol* 1996; 95:6-12.
106. Porter JB, Kayyali RS, Hider RC. Improved efficacy-toxicity ratios with oral iron chelators (abstr). 8th International Conference, Oral Chelation in the Treatment of Thalassaemia and Other Disease, Corfu, 1997.
107. Liu ZD, Liu DY, Hider RC. Synthesis, physicochemical properties and biological evaluation of aromatic ester prodrugs of 1-(2'-hydroxyethyl)-2-ethyl-3-hydroxypyridin-4-one (CP102): Orally active iron chelators with clinical potential. *J Pharm Pharmacol* 1999; 51:555-564.
108. Ponka P, Borova J, Neuwirth J, Fuchs O, Necas E. A study of intracellular iron metabolism using pyridoxal isonicotinoyl hydrazone and other synthetic chelating agents. *Biochim Biophys Acta* 1979; 586:278-297.
109. Richardson DR, Baker E. The release of iron and transferrin from the human melanoma cell. *Biochim Biophys Acta* 1991; 1091:294-302.
110. Ponka P, Schulman HM, Wilczynska A. Ferric pyridoxal isonicotinoyl hydrazone can provide iron for heme synthesis in reticulocytes. *Biochim Biophys Acta* 1982; 718: 151-158.
111. Hershko C, Avramovici-Grisaru S, Link G, Gelfand L, Sarel S. Mechanism of in vivo iron chelation by pyridoxal isonicotinoyl hydrazone and other imino derivatives of pyridoxal. *J Lab Clin Med* 1981; 98:99-107.

112. Williams A, Hoy T, Pugh A, Jacobs A. Pyridoxal complexes as potential chelating agents for oral therapy in transfusional iron overload. *J Pharm Pharmacol* 1982; 34: 730–732.
113. Richardson DR, Wis Vitolo L, Baker E, Webb J. Pyridoxal isonicotinoyl hydrazone and analogues. Study of their stability in acidic, neutral and basic aqueous solutions by ultraviolet-visible spectrophotometry. *Biol Metals* 1989; 2:69–76.
114. Brittenham GM. Pyridoxal isonicotinoyl hydrazone: An effective iron chelation after oral administration. *Semin Hematol* 1990; 27:112–116.
115. Richardson DR, Ponka P. Pyridoxal isonicotinoyl hydrazone and its analogs: Potential orally effective iron-chelating agents for the treatment of iron overload disease. *J Lab Clin Med* 1998; 131:306–314.
116. Vitolo LMW, Hefter GT, Clare BW, Webb J. Iron chelators of the pyridoxal isonicotinoyl hydrazone class Part 2. Formation constants with iron(III) and iron(II). *Inorg Chim Acta* 1990; 170:171–174.
117. Bergeron RJ, Streiff RR, Creary EA, Daniels RD, King W, Luchetta G, Wiegand J, Moerker T, Peter HH. A comparative study of the iron-clearing properties of desferri-rithiocin analogues with desferrioxamine B in a Cebus monkey model. *Blood* 1993; 81: 2166–2173.
118. Bergeron RJ, Wiegand J, Weimar WR, Vinson JR, Bussenius J, Yao GW, McManis JS. Desazadesmethyl-desferri-rithiocin analogues as orally effective iron chelators. *J Med Chem* 1999; 42:95–108.
119. Bergeron RJ, Wiegand J, McManis JS, McCosar BH, Weimar WR, Brittenham GM, Smith RE. Effects of C-4 stereochemistry and C-4' hydroxylation on the iron clearing efficiency and toxicity of desferri-rithiocin analogues. *J Med Chem* 1999; 42:2432–2440.
120. Bergeron RJ, Weimar WR, Wiegand J. Pharmacokinetics of orally administered desferri-rithiocin analogs in Cebus apella primates. *Drug Metab Disp* 1999; 27:1496–1498.
121. L'Epplattenier F, Murase I, Martell AE. New multidentate ligands. VI. Chelating tendencies of N,N'-Di(2-hydroxybenzoyl) ethylenediamine-N,N'-diacetic acid. *J Am Chem Soc* 1967; 89:837–843.
122. Hershko C, Grady RW, Link G. Phenolic ethylenediamine derivatives: A study of orally effective iron chelators. *J Lab Clin Med* 1984; 103:337–346.
123. Grady RW, Salbe AD, Hilgartner MW, Giardina PJ. Results from a phase I clinical trial of HBED. *Adv Exp Med Biol* 1994; 356:351–359.
124. Bergeron RJ, Wiegand J, Brittenham GM. HBED: The continuing development of a potential alternative to deferoxamine for iron-chelating therapy. *Blood* 1999; 93:370–375.
125. Grady RW, Giardina PJ. Oral iron chelation: A potential role for HBED in combination therapy. American Society of Hematology, Forty-First Annual Meeting, New Orleans, LA, December 3–7, 1999, *Blood* 94(suppl 1):abstr 3293.
126. Winchell HS, Klein JY, Simhon ED, Cyjon RL, Klein O, Zaklad H. Compounds with chelation affinity and selectivity for first transition series elements: Use in medical therapy and diagnosis. Patent Cooperative Treaty (PCT) document 1996: 96/10785.
127. Acklin P, Lattmann R, Buhlmayer P, Crowe A, Faller B, Jin Y, Nick HP, Sergejew T, Spanka C, Wong A, Zbinden P, Schnebli HP. CGP72670, a potent orally active iron chelator. *Chimia* 1998; 52:446–451.
128. Schnebli HP. CGP 72 670: A new, potent, orally active iron chelator. ISH-EHA Combined Haematology Congress, Amsterdam, The Netherlands, 4–8 July, *Br J Haematol* 1998; 102:abstr O-1121.
129. Galanello R, Loehrer F, Alberti D, Piga A. A novel oral iron chelator (ICL 670A): Update on a phase I single dose safety study. The 7th International Conference on Thalassaemia and the Haemoglobinopathies, Bangkok, Thailand, 31 May–4 June 1999: abstr S1704.

130. Cable H, Lloyd JB. Cellular uptake and release of two contrasting iron chelators. *J Pharm Pharmacol* 1999; 51:131–134.
131. Grady RW, Berdoukas VA, Rachmilewitz EA, Giardina PJ. Iron chelation therapy: A better approach. The 7th International Conference on Thalassaemia and the Haemoglobinopathies. Bangkok, Thailand, 31 May–4 June 1999: abstr 0018.
132. Breuer W, Ronson A, Abramov A, Pootrakul P, Hershko C, Cabantchik IZ. Non-transferrin-bound iron (NTBI) in sera of thalassaemic patients during oral chelation treatment. American Society of Hematology, Forty-First Annual Meeting, New Orleans, LA, December 3–7, 1999, *Blood* 94(suppl 1):abstr 1869.
133. Agarwal MB, Rajadhyaksha G, Sameer A. Deferiprone: How to make it work more widely, effectively and without adverse effect: an Indian study. The 7th International Conference on Thalassaemia and the Haemoglobinopathies, Bangkok, Thailand, 31 May–4 June 1999: abstr S1304.
134. Cabantchik ZI, Glickstein H, Golenser J, Loyevsky M, Tsafack A. Iron chelators: Mode of action of antimalarials. *Acta Haematol* 1996; 95:70–77.
135. Hider RC, Choudhuri R, Rai BL, Dehkordi LS, Singh S. Design of orally active iron chelators. *Acta Haematol* 1996; 95:6–12.
136. Porter JB, Huehns ER, Hider RC. The development of iron chelating drugs. *Clin Haematol* 1989; 2:257–292.
137. Porter JB, Morgan J, Hoyes KP, Burke LC, Huehns ER, Hider RC. Relative oral efficacy and acute toxicity of hydroxypyridin-4-one iron chelators in mice. *Blood* 1990; 76:2389–2396.

Index

- ABC7*, 218, 262, 665
ABC transporters, 218, 262, 266, 387, 397–400, 402–404, 416, 665, 666
Aceruloplasminemia, 458, 498, 501, 608, 625, 650, 679, 689, 749–758
Aconitase:
 bacterial, 216, 217, 221, 239, 414, 416, 417
 cytosolic, 215, 217, 218, 221–224, 262, 622
 matrix, 264
 mitochondrial, 84, 210, 213, 215, 216, 221, 223, 238, 244, 246, 248, 468, 500, 625, 626
African Bantu siderosis, 718, 775–782
 treatment of, 779, 780
AFT1/Aft1p, 380, 382–384
AHA genes, 362
ALAS (*see* 5-Aminolevulinic acid synthetase)
Albumin, 453, 524, 571, 599, 750
Alcohol, 702, 705, 707, 713, 716, 717, 728, 776–781
 α -Fetoprotein, 706
 α -Tocopherol, 730
Aluminum, 23, 31, 323, 489
Alzheimer's disease, 488, 500, 501, 518, 608
5-Aminolevulinic acid synthetase, 84, 210, 213, 215, 218, 238, 244–246, 473, 657, 659, 662, 665, 666, 668
Anemia (*see also* Animal models; Iron deficiency; Thalassemia):
 iron deficiency, 79, 159, 360, 471, 563, 680, 791
 hemolytic, 80, 648, 688
 other, 459, 476, 478, 492, 521, 564, 571, 576, 579, 605, 608, 625, 645, 651, 653, 684, 688, 689, 691, 706, 718, 756, 767, 775–782, 788
 sideroblastic, 218, 262, 564, 665
Animal models, 491, 584, 607, 632, 679–692, 736, 737, 749, 751, 796, 797, 802–804 (*see also* Belgrade rat; β_2 -microglobulin, knockout mouse; Ceruloplasmin, knockout mouse; Ferritin, H chain, knockout mouse; Flexed-tail mouse; Heme oxygenase, knockout mouse; Hemopexin, knockout mouse; *HFE/HFE*, knockout mouse; *hpx*; Microcytic mouse; *sla*; Transferrin receptor, knockout mouse)
Antioxidant-responsive element, 141, 622
AP-1, 661
Apoptosis, 630, 686, 801
Arabidopsis thaliana, 129, 139, 143, 245, 361–368
Arctic icefish, 644
ARE (*see* Antioxidant-responsive element)
ARN genes, 376, 384, 385

- Arthritis, 716
- Ascorbic acid, 29, 144, 157, 368, 379, 455, 457, 474, 495, 598, 730, 734
- Astrocytes, 147, 494, 608
- Ataxia, 218, 262, 665, 750 (*see also* Friedrich's ataxia)
- ATF/Atf, 379
- ATM1/Atm1p, 218, 262, 387, 665
- ATP, 24, 30, 166, 221, 367, 386, 399, 400, 402, 488, 502
- ATP binding cassette (*see* ABC transporters)
- Atransferrinemia, 576, 577, 607, 651, 683 (*see also* Hypotransferrinemia)
- Atx1p, 382
- b* (*see* Belgrade rat)
- Basal ganglia, 689, 750, 751
- Bathophenanthroline disulfonate, 377, 457, 458
- bclx, 646
- Belgrade rat, 159, 166, 436, 459, 492, 493, 497, 500, 604, 653, 680, 681, 689
- β_2 -microglobulin, 81, 82, 166, 199 (*see also* HFE/HFE, association with) knockout mouse, 193, 472, 567, 687
- BFU-E (*see* Burst-forming units—erythroid)
- Blood-brain barrier, 331, 336, 341, 346, 428, 435, 488–493, 496, 497, 499, 502, 599, 607, 608, 765, 808
- Bone marrow, 87, 147, 159, 165, 182, 428, 429, 434, 526, 599, 601, 615, 644, 648, 684, 736, 756, 758, 778, 779, 788, 790, 795
- BPS (*see* Bathophenanthroline disulfonate)
- Brain, 434, 650, 688, 750, 751 (*see also* Basal ganglia; Blood-brain barrier; Cerebellum; Cerebrospinal fluid; Choroid plexus; Dentate nucleus; Globus pallidus; Pon; Putamen; Striatum; Substantia nigra; Thalamus) cells (*see* Astrocytes, Neurons, Oligodendrocytes) iron transport in, 435, 487–502, 598, 608 (*see also* Blood-brain barrier) developmental aspects of, 490, 491
- Breast cancer, 513, 515, 526 (*see also* MCF-7 cells)
- brz*, 363, 368
- BSD/Bsd, 384
- Burst-forming units—erythroid, 644–646, 656
- CaCo2 cells, 140, 163, 179, 180, 191, 546, 571, 574, 577
- Cadmium, 135, 156, 158, 367, 383
- Calcein, 146, 541–554, 556
- Calcium, 31, 181, 261, 336, 455, 470, 550, 552, 555, 598, 600, 802
- Calcium channels, 455, 459
- Calmodulin, 644
- Cancer, 629
- Cancer cells, 510–528 (*see also* Breast cancer; Hepatoma cells; Melanoma cells; Chelating agents, therapeutic use in cancer)
- Carbonic anhydrase, 645
- Cardiac myocytes, 223, 515, 729
- Catalase, 29, 30, 144, 208, 414, 601, 727
- Cataract (*see* Hereditary hyperferritinemia cataract syndrome)
- CCC2, 380, 382
- CCH, 366
- CDC, 383
- Central nervous system (*see* Brain)
- Cerebellum, 498–500, 683
- Cerebrospinal fluid, 488, 494–496, 499, 500, 599
- Ceruloplasmin, 167, 181–183, 379, 380, 454, 458, 460, 497, 498, 510, 521, 524, 562, 571, 572, 601, 602, 605, 608, 616, 625, 650, 651, 682, 683, 688, 689, 718, 749–758 gene structure of, 750 knockout mouse, 625, 650, 688, 752, 756 structure of, 750
- CFU-E (*see* Colony-forming units—erythroid)
- Chang cells, 459
- Chaperone, 387 copper, 382, 750
- Chelating agents, 17, 20–26, 101, 222, 321–351, 360, 366, 414, 433, 441, 456, 474, 540, 541, 550, 553, 556, 616, 619, 623, 650, 662, 689 (*see also* Deferiprone; Deferoxamine; Hydroxybenzyl ethylenediamine diacetic acid; Hydroxypyridinones; ICL670A; Isonicotinyl derivatives; Pyridoxal isonicotinyl hydrazones; Siderophores) absorption of, molecular weight dependence, 333, 346, 808 bidentate, 274, 284, 326 ff., 807 bioavailability of, 334, 342, 808

[Chelating agents]

hexadentate, 274, 281, 324, 328–333, 335, 336, 338, 341, 807

orally active, 322, 328, 331, 333, 334, 336, 337, 339, 344–346, 350, 713, 795–808

partition coefficients of, 331, 336, 346, 808

release of iron from Tf by, 98–103, 106

therapeutic use of:

in cancer, 510, 515, 526, 528

in demyelinating disease, 502

in iron overload, 556, 616, 713, 728, 729, 735, 737, 738, 788–808

in malaria, 807

in other disorders, 788

thermodynamic stability with Fe, 328–331, 807

toxicity of, 334–346, 733, 736, 802–808
(*see also* Deferiprone, toxicity of;
Deferoxamine, toxicity of)

chlonerva, 363, 364, 366

Chloride, 50, 100, 103–108, 111, 114, 115, 117, 382, 540, 546, 555

CHO cells, 438, 439, 514, 519

Choroid plexus, 499, 500

Chromium, 3, 4, 31, 32, 305

Cir, 407

Cirrhosis, 618, 627, 702, 704, 706, 713, 714, 716, 727, 734, 737, 751, 770, 778, 779, 781, 789, 796, 800

Citric acid, 22, 23, 25, 26, 30, 101, 102, 135, 142, 306, 366, 376, 378, 379, 402, 406, 415, 417, 418, 456, 457, 474, 495, 515, 516, 519, 547, 562, 569, 599, 600, 602, 625, 651, 662, 681

c-kit, 644

Cobalt, 2–4, 15, 156, 453, 455, 459–461, 553

Colony-forming units—erythroid, 645, 646, 656, 660

Copper, 2–4, 24, 31, 156, 158, 167, 181, 182, 248, 323, 336, 342, 366, 379–385, 389, 454, 455, 458, 459, 474, 519, 521, 526, 542, 546, 549, 571, 575, 601, 605, 608, 609, 625, 689, 749, 750, 752

deficiency of, 521, 571, 625, 688, 752

transporter of (*see* CTR/CTR)

COS cells, 474

Cox17p, 381

CTR/CTR, 379–381, 750

Cytokines, 191, 222, 238, 437, 438, 467–470, 472, 475–477, 580, 608, 618, 623, 629 (*see also* Interleukins)

DCT1 (*see* DMT1/Nramp2)

Deferiprone, 22, 102, 112, 344, 345, 349–351, 457, 458, 461, 713, 735–738, 795–808

pharmacokinetics of, 797, 798, 801

toxicity of, 735–738, 795–801, 807, 808

Deferoxamine, 22, 28, 30, 33, 34, 163, 217, 220, 264, 275, 283, 284, 289, 299, 302, 305–307, 322–324, 325, 333–337, 339, 342, 376, 402, 456, 460, 461, 470, 514, 516, 521, 526, 527, 659, 713, 719, 730, 735, 737, 738, 765, 791–797, 799–808

fluorescent analogs of, 541, 543, 555, 556

pharmacokinetics of, 791, 792, 797

toxicity of, 733, 793, 794, 807

Demyelinating disease, 501, 502

Dentate nucleus, 500

Desferrioxamine (*see* Deferoxamine)

Desferrithiocin, 342, 795, 803

DFO (*see* Deferoxamine)

dgl, 363, 368

Diabetes, 256, 687, 689, 702, 716, 718, 731, 737, 751, 789, 794

Dietary iron (*see* Iron, dietary intake of)

Divalent cation transporter (DCT1) (*see* DMT1/Nramp2)

Divalent metal transporter (DMT1) (*see* DMT1/Nramp2)

DMT1/Nramp2, 42, 84, 156–170, 182–185, 199–201, 214, 215, 238, 244–246, 376, 383, 434, 436, 437, 440, 441, 459, 471, 472, 474, 478, 488, 493–495, 497, 500, 510, 516, 540, 548, 562, 565, 567, 568, 571, 573–575, 581, 582, 584, 604, 607, 624, 625, 653, 664, 666, 679, 681, 682, 685, 687, 689, 758

isoforms of, 165, 214

Doxorubicin, 528

DTPA, 339, 414, 452, 456, 545, 553

DtxR, 415, 416

Duodenal loop, 159, 176

Duodenum, 156–158, 165, 167, 168, 175, 177, 180, 182, 193, 194, 197, 199–201, 245, 434, 436, 475, 565, 624, 626, 653 (*see also* Duodenal loop; Iron, intestinal transport of)

- EDTA, 17, 20, 22, 24, 25, 30, 34, 101, 102, 106, 109, 142, 246, 298, 299, 333, 541, 555
- Electrophoretic mobility shift, 163, 223
- Endocrine system, 704, 727, 731–733, 789, 794
- Endoplasmic reticulum, 615
- Endosome, 72, 73, 79, 97, 166, 195, 367, 382, 385, 430, 431, 433–437, 440, 441, 462, 489, 493, 497, 502, 510, 516, 540, 578, 607, 624, 651, 653, 663, 664, 689
- Enterobactin, 275, 280, 289, 291–294, 299, 300, 302, 303, 305–307, 324, 329, 330, 384, 397, 407, 410
- Enterocyte, 44, 53, 163, 167, 168, 181, 185, 195, 197, 199, 213, 214, 333, 434, 436, 472, 546, 562, 564, 565, 566, 568, 569, 570, 572, 574, 576, 580, 581, 582, 584, 602, 604, 605, 624, 626, 649, 681, 682, 688, 690, 691
- Erythroblast, 645–647, 656, 660, 666, 685
- Erythrocyte, 598, 599, 601, 602, 614, 615, 644, 645, 648–651, 656, 660, 665, 666, 668, 680, 681, 684, 685, 689, 726, 758, 780, 788, 791, 801, 804, 807
- Erythroid differentiation (*see* Erythropoiesis)
- Erythroid precursor, 428, 429, 431, 434, 564, 580, 598, 599, 614, 644–647, 655, 656, 659–662, 665, 666, 668, 681, 684, 686, 689–691
- Erythropoiesis, 431, 562–564, 567, 570, 573, 574, 576, 578–580, 584, 604, 646–648, 650, 651, 661, 666, 668, 684, 685, 726, 756, 767, 788
- ineffective, 429, 564, 604, 632, 686, 734
- Erythropoietin, 460, 461, 549, 563, 564, 579, 608, 645, 646, 648–650, 656, 657, 660–662
- Estrogen, 515
- Ets, 661
- exb* genes, 405
- Exb proteins, 407, 410, 412, 413, 417
- Exchangeable iron pool (*see* Labile iron pool)
- f* (*see* Flexed-tail mouse)
- FAC (*see* Ferric ammonium citrate)
- fbp*/*Fbp*, 403, 412
- fec*/*Fec*, 417–419
- Fenton reaction (*incl.* Haber-Weiss chemistry), 29–31, 208, 219, 263, 414, 456, 457, 475, 730
- FepA, 407, 410
- FER*, 363
- Ferric ammonium citrate, 163, 515, 516, 545–547, 549
- Ferric hydroxide, 20, 35, 136, 359, 360, 376, 648
- Ferric reductase, 156, 157, 168, 360–363, 376–379, 388, 389, 454, 457, 458, 562, 568, 653
- Ferrihydrite, 134–136, 602
- Ferrioxamine (*see* Deferoxamine)
- Ferrireductase (*see* Ferric reductase)
- Ferritin:
- bacterial, 126, 127, 129–135, 143, 239, 387
 - endocytosis of, 525
 - ferroxidase activity of, 127–130, 133, 136–138, 145, 146, 767
 - functions of, 142–148, 367, 525, 569, 570, 602, 662, 663
 - genes, 139, 368
 - chromosomal locations of, 128, 139
 - glycosylation of, 147
 - H chain, 128, 130–133, 136–142, 145–148, 211, 215, 220, 239, 246, 471, 474, 511, 525, 602, 620–622, 629, 663, 689, 763, 765, 767
 - knockout mouse, 622, 630, 689
 - receptor for, 147, 471
 - horse spleen, 130, 133, 135, 137, 138
 - iron core of, 133–138
 - formation of, 135–138, 368
 - L chain, 128, 130–133, 136–141, 145–148, 210, 211, 215, 239, 246, 249, 381, 471, 474, 511, 525, 601, 602, 620–622, 627, 629, 630, 689, 719, 766 (*see also* Hereditary hyperferritinemia cataract syndrome)
 - M chain, 128, 137, 239
 - mRNA, 84, 141, 142, 162, 239
 - non-IRP-dependent regulation of, 475–477, 629
 - regulation of translation by IRPs, 84, 140–142, 211–215, 248, 571, 621, 627, 630
 - plant, 126–129, 135, 139, 143, 148, 239, 367, 368
 - post-transcriptional regulation of (*see* Ferritin, mRNA):

- [Ferritin]
 in plants, 368
 receptors for, 477, 615
 serum/plasma, 427, 495, 511, 524, 525,
 599, 615, 702, 705, 711, 712, 715,
 716, 719, 734, 736, 738, 761–771,
 777, 792–794, 798, 800, 806
 structure of, 126, 128, 130–134
 transcriptional regulation of, 140, 141,
 368, 475, 621, 629, 631
 Ferrochelataase, 34, 213, 264, 266, 653, 657,
 659, 662–664
 Ferroportin, 156, 170, 213, 215, 238, 244–
 246, 366, 370, 604, 616, 626, 650,
 651, 691, 758 (*see also* Ireg1)
 Ferroxidase, 167, 181, 182, 184, 185, 380,
 381, 385, 388, 458, 497, 540, 572,
 575, 602, 608, 650, 682, 689, 752,
 758 (*see also* Ceruloplasmin; Ferritin,
 ferroxidase activity of; *FET/Fet*)
 Fe-S clusters (*see* Iron-sulfur clusters)
FET/Fet, 167, 365, 376, 379, 380, 382–388,
 457, 458, 521, 752
feu genes, 217, 245
fhu genes, 400
 Fhu proteins, 400–403, 407, 410–412, 418,
 420
 Fibroblasts, 76, 145, 163, 191, 256, 264,
 438, 476, 511, 516
 Fibrosis, 687, 727, 733, 789
 liver, 614, 627, 687, 727–729, 731, 735,
 737, 751, 778, 789, 800, 801 (*see*
also Cirrhosis)
fiol⁺, 381
fip1⁺, 381
 Fiu, 407
 Flavin, 362, 377, 378, 414, 415, 602
 Flavoprotein (*see* Flavin)
 Flexed-tail mouse, 665, 666, 680, 684
fos, 526
 Frataxin, 255–266, 386, 500, 626, 666
frd genes, 362, 363
FRE/Fre, 377–381, 388, 457
 Friedrich's ataxia, 255–259, 261–266, 386,
 488, 500, 501, 666
FRO genes, 362, 363
fsn/hea, 680, 684, 685
FTH/Fth, 376, 385, 689
 FTR1, 167, 381, 385, 386, 457, 752
fur genes, 143, 414, 415
 Fur, 403, 406, 413–415, 417
 FVA cells, 656, 662
 Gadolinium, 629
 Gallium, 323, 402, 489, 514, 516, 519, 526
 GATA factors, 647, 659, 666
GEF genes, 382
 Globin, 644, 645, 647, 656, 663, 668
 Globin genes, 647
 Globus pallidus, 500, 598
 Glutathione, 336, 543, 622, 631
 Glutathione peroxidase, 727
 GM-CSF, 645
 gp91^{phox}, 362, 377, 457
 Haber-Weiss chemistry (*see* Fenton reaction)
 HAH1, 750
 Hallervorden-Spatz disease, 500, 501
 Haptoglobin, 396, 403, 404, 405, 407, 428,
 599, 607, 614, 626, 688
has/Has, 405, 406
hbd, 680, 685
 HBED (*see* Hydroxybenzyl ethylenediamine
 diacetic acid)
 Heart, 156, 256, 264, 265, 602, 604, 607,
 626, 650, 687, 703, 727, 729–731,
 735–737, 789, 794, 798–800
 HeLa cells, 142, 146, 191, 196, 197, 257,
 454, 456
hem/Hem, 404, 406
 Hematopoiesis, 79, 684, 685 (*see also*
 Erythropoiesis)
 Hematopoietic stem cells, 644
 Heme, 145, 146, 157, 165, 213, 260, 377,
 378, 386, 396, 403–407, 419, 428,
 437, 440, 560, 562, 567, 568, 598,
 599, 601, 604, 615, 644, 645, 649,
 651, 664, 781
 synthesis of, 147, 238, 264, 266, 386,
 510, 647, 650, 653, 655, 656, 659,
 662, 663, 665, 666, 668, 684, 685
 Heme-binding protein (p22 HBP), 668
 Heme oxygenase, 145, 415, 601, 615, 622,
 628, 648, 649, 650, 662, 679, 688
 knockout mouse, 688
 Heme-regulated inhibitor, 647
 Heme-responsive factor, 141
 Hemin, 217, 404, 644, 667, 657
 Hemochromatosis, 166, 182, 190, 436, 439,
 469, 492, 500, 501, 556–559, 573,
 577, 578, 604, 605, 608, 614, 619,
 620, 623, 625, 627, 628, 679, 686,
 687, 700–719, 729, 732, 734, 770,
 776, 778, 780, 788, 790, 794 (*see*
also HFE/HFE)

- [Hemochromatosis]
 diagnosis of, 704–719
 genetic testing for, 708–712
 screening for, 714–716
 treatment of, 713–716
- Hemoglobin, 1, 10, 29, 85, 213, 396, 403–407, 428, 478, 554, 563, 579, 598–601, 607, 614, 615, 626, 644–646, 648, 649, 656, 663, 665, 666, 684, 685, 758, 804, 807
 deficiency of (*see hbd*)
 synthesis of, 645, 647, 650, 651, 656, 657, 660–664, 668, 690
- Hemolysis, 573, 734 (*see also* Anemia, hemolytic)
- Hemopexin, 51, 428, 599, 607, 614, 626
 knockout mouse, 626, 628
- Hemosiderin, 524, 601, 602, 615, 728, 733
- Hep3B cells, 163, 460, 631
- Hepatic iron index (*see* Liver, iron concentration in)
- Hepatic stellate cells, 607, 614, 627
- Hepatitis, viral, 628, 716, 728, 732, 779, 800 (*see also* Hepatitis B virus; Hepatitis C virus)
- Hepatitis B virus, 619, 716, 779, 789
- Hepatitis C virus, 628, 716, 717, 736, 737, 779, 789, 800, 801
- Hepatocellular carcinoma (*see* Hepatoma cells)
- Hepatocyte, 197, 347, 348, 428, 429, 431, 434, 437–441, 451–462, 471, 498, 513, 515, 598, 602, 607, 614–616, 618–622, 625, 627, 649, 650, 689, 701, 728, 750, 751, 776, 778, 790
- Hepatoma cells, 87, 141, 142, 222, 437–441, 460, 514, 521, 526, 618–625, 627, 629–632, 704, 706, 779 (*see also* HepG2 cells; Hep3B cells; Chang cells)
- HepG2 cells, 87, 453, 456, 458–460, 462, 521, 524, 629, 796
- Hephaestin, 156, 167, 170, 182, 185, 199, 454, 458, 562, 565, 570–572, 575, 604, 605, 616, 626, 650, 651, 679, 682, 683, 687, 689, 758
- Hereditary hemochromatosis (*see* Hemochromatosis)
- Hereditary hyperferritinemia cataract syndrome, 145, 146, 210, 211, 249, 761–771
- HFE/HFE*, 72, 78–80, 87, 166–170, 180, 190–201, 434, 436, 472, 566, 577, 578, 584, 604, 620, 624, 627, 651, 686, 687, 700, 701, 703, 758, 776–778, 780–782
 association of:
 with β_2 -microglobulin, 81, 82, 190, 193, 194, 196, 472, 686, 687
 with transferrin receptor, 78–82, 87, 193, 194, 195, 199, 201, 433, 472, 566, 577–579, 605, 686, 687
 gene structure, 190–192
 knockout mouse, 167, 190, 201, 214
 mutations in, 190, 192, 193, 197–201, 628, 686, 687, 700, 702, 705, 706, 708, 710–712, 715, 717–719, 777, 781, 782
 protein structure, 192, 193
- hgp/Hgp*, 405
- HIF (*see* Hypoxia-inducible factor)
- HHCS (*see* Hereditary hyperferritinemia cataract syndrome)
- Hippocampus, 498, 499, 683
- HIS3*, 380, 381
- hit* genes, 403
- H-kininogen, 147
- hmu/Hmu*, 404, 406
- Hpu proteins, 405
- hpx* mouse, 168, 182, 183, 492, 497, 680, 682
- HRE (*see* Hypoxia-responsive element)
- HRF (*see* Heme-responsive factor)
- HRI (*see* Heme-regulated inhibitor)
- Hsp70, 259, 386
- Huntington's disease, 488, 501
- Hut proteins, 405
- Hux proteins, 406
- Hydrogen peroxide, 84, 138, 142, 143, 145, 146, 208, 220, 221, 335, 386, 414, 415, 474, 624, 630, 796
- Hydroxamate, 21, 22, 30, 32–34, 101, 274, 275, 279–287, 294–296, 302, 307, 323–327, 329, 334–337, 384, 389, 397, 400, 407
- Hydroxybenzyl ethylenediamine diacetic acid, 20, 34, 339, 340, 343, 803, 804, 807
- Hydroxyl radical (*see* Oxygen, reactive species)
- Hydroxypyridinones, 22, 101, 274, 284, 300, 302, 306, 326–328, 331–336, 340, 343–351, 736, 737, 795, 796, 801, 802 (*see also* Deferiprone)

- Hyperferritinemia, 608
- Hypotransferrinemia, 182, 184, 570, 571, 576, 683, 684 (*see also hpx mouse*)
- Hypoxia, 85, 182, 216, 218, 219, 223–225, 238, 383, 460, 474, 562, 564, 567, 568, 570, 574, 616, 619, 624, 631, 632, 646, 649, 650, 661 (*see also Hypoxia-inducible factor; Hypoxia-responsive element*)
- Hypoxia-inducible factor (HIF), 85, 223–225, 460, 461, 616, 618, 619, 624, 631, 632
- Hypoxia-responsive element (HRE), 460, 461
- ICL670A, 805
- IDS* genes, 364
- Immune system, 467–473, 477, 525, 795, 799 (*see also Lymphocytes; Reticuloendothelial system*)
- Indium, 31
- Infection, 44, 159, 168, 396, 404, 426, 499, 628, 730, 734, 750, 765, 794, 798 (*see also Hepatitis; Inflammation*)
- Inflammation, 74, 144, 348, 384, 608, 618, 621, 623, 628, 629, 688, 735, 750, 765
- Insulin, 702, 732
- Insulin-like growth factor, 732
- Integrin, 180, 181, 562
- Interferon/IFN- γ , 468–470, 477, 478, 628, 717
- Interleukins, 437, 468–470, 476, 477, 513, 629, 645 (*see also Cytokines*)
- IRE, 83, 84, 87, 139, 142, 145–147, 156, 160–168, 182–185, 209–217, 237–249, 416, 417, 437, 458, 460, 462, 468, 473, 474, 477, 478, 511, 513, 516, 605, 607, 618, 620–622, 625, 628, 653, 655, 659, 661, 662, 668
- structure of, 209–211, 238, 239, 244–249, 626
- Ireg1, 156, 167–170, 182–185, 213–215, 223, 238, 246, 367, 554, 562, 565, 570, 571, 573–575, 580, 581, 584, 604, 605, 616, 650, 679
- Iron:
- abundance of, 3–5, 156, 648
 - cellular content of, 541, 549
 - cellular uptake of, 179, 180, 196, 197, 201, 209
 - in bacteria, 209, 360, 395–420
- [Iron]
- in mammalian cells, 427–441, 451–462, 789 (*see also Iron, intestinal transport of; Brain, iron transport in*)
 - in plants, 209, 359–369, 376
 - in yeast, 375–379
 - other fungi, 129, 159, 360, 376, 388, 389
 - Saccharomyces cerevisiae*, 142, 143, 218, 360, 364–366, 375–388, 521, 666
 - pH dependence of, 158, 163, 540
 - voltage dependence of, 156, 158
 - dietary intake of, 144, 156, 159, 163, 165, 168, 177, 193, 195, 197–201, 452, 758, 775–780
 - efflux of/release from cells, 181, 183, 453, 458, 521, 524, 527, 614–616, 625, 626, 649, 651, 750, 751
 - electrochemistry of, 27–31 (*see also Iron, redox potentials of*)
 - electronic configuration, 5–10, 14, 15, 25, 33, 274, 275, 302
 - fluorescence detection of, 541–546
 - hydrolysis of, 18–20, 29, 360, 361, 648
 - intestinal transport of, 157, 159, 166–170, 175–185, 190, 193, 367, 516, 560–584, 650, 726, 758, 775–782, 788, 790
 - in infectious/inflammatory disease, 579, 580
 - nutritional factors, 598, 600, 604
 - regulation by body iron stores, 176, 560–569, 573, 576, 604
 - ionic radii of, 8
 - Lewis acidity of, 16, 323
 - ligand binding, 16–18, 20–26, 31–34, 296–298, 328, 339, 342, 350
 - ligand-exchange kinetics, 31–34, 305, 335, 350, 541
 - loss from body, 560, 563, 597–601, 788
 - magnetic properties of, 10–13
 - non-transferrin-bound, 157, 442, 451–462, 492, 494, 496, 519, 540, 546–548, 556, 571, 577, 599, 607, 614, 625, 627, 629, 650, 726, 727, 729, 730, 779, 788–792, 796, 804, 808
 - plasma (*see Iron, serum*)
 - redox potentials of, 27–30, 262, 264, 274, 296, 298, 299, 322, 324, 335, 377, 406

- [Iron]
 serum, 22, 181, 264, 452, 453, 598, 599,
 605, 607, 608, 648–650, 689, 705,
 715, 727, 789, 796, 806
 systemic homeostasis, 597–609, 648, 650,
 726, 758
 toxicity of, 84, 143, 147, 156, 208, 215,
 360, 369, 379, 386, 451, 452, 470,
 568, 648, 665, 726, 727, 730, 735,
 788, 789, 792, 796, 797, 804, 808
- Iron deficiency, 156, 157, 159, 168, 184,
 362–367, 385, 431, 474, 488, 491,
 494, 498, 562, 568, 573, 576, 598,
 604, 605, 618, 619, 623, 624, 680
 (*see also* Anemia)
- Iron overload, 336, 437, 598, 604, 605, 607,
 608, 614–616, 618, 619–621, 623–
 625, 627, 628, 631, 632, 650, 651,
 680, 683, 688, 689, 701, 717, 718
 (*see also* Aceruloplasminemia;
 African Bantu siderosis; Animal
 models; Atransferrinemia; Chelating
 agents, therapeutic use of;
 Hemochromatosis)
 transfusional, 614, 615, 725–738, 788,
 789, 799, 800, 807 (*see also*
 Thalassemia)
- Iron-regulatory proteins (*see* IRP)
- Iron-responsive elements (*see* IRE)
- Iron-sulfur clusters, 84, 208, 213, 214–218,
 220–225, 244, 256, 262–264, 266,
 416, 500, 510, 513, 619, 622
- IRP, 78, 83, 145, 146, 156, 167, 196, 208–
 225, 238, 239, 244–249, 437, 438,
 458, 460, 461, 468, 472–474, 516,
 568, 571, 573–575, 582, 584, 605,
 618, 619, 621, 623–625, 627, 628,
 630, 631, 655, 659, 661, 662, 763,
 769, 771, 790 (*see also* IRP1, IRP2)
- IRP1, 83, 84, 163, 208–213, 215–225, 246,
 247, 257, 262, 417, 460, 462, 474,
 477, 478, 511, 513, 575, 622–624,
 631, 653, 661, 662, 765, 769
- IRP2, 83, 84, 146, 163, 208–213, 218–220,
 222–225, 238, 239, 244, 248, 460,
 474, 511, 513, 525, 575, 622–624,
 627, 630, 631, 653, 661, 765, 769
- IRT/IRT, 362, 363, 366, 367
- Isonicotinyl derivatives, 545, 546, 549, 552,
 553, 663, 690 (*see also* Pyridoxal
 isonicotinyl hydrazones)
- Iut, 407
- J2E cells, 656
- Janus kinases, 646
- jun*, 526
- K562 cells, 87, 147, 222, 458, 514, 521,
 548, 549, 625
- Kaposi's sarcoma, 526
- Kidney, 650, 688
- KISAB, 106, 115–117
- Kupffer cell, 437, 438, 475, 601, 607, 614,
 615, 619, 620, 624, 626, 627, 629,
 688, 717, 751
- L1 (*see* Deferiprone)
- Labile iron pool, 144–146, 211, 458, 469,
 510, 541, 547, 549–556, 569, 601,
 605, 622, 627, 631, 664, 653, 662,
 665, 727, 790, 804
- Lactoferrin, 42–44, 47, 50, 53, 56, 96, 100,
 274, 396, 403, 407, 412, 471, 472,
 475, 478, 488, 490, 560, 608
 antimicrobial activity of, 43, 274, 396,
 412, 478
- Lbp proteins, 412
- Lead, 156, 158, 474
- Leu1, 387
- Leukemia, 514, 521, 526
- Lipoxygenase, 645, 646, 801
- Liver, 45, 46, 87, 138, 141, 147, 156,
 181, 184, 192, 193, 197, 199, 245,
 256, 261, 331, 334, 336, 342, 345–
 348, 403, 428, 429, 574, 598, 601,
 604–607, 614–632, 644, 650, 660,
 682, 685–689, 691, 702, 705, 731,
 727–730, 735, 737, 750, 776, 789,
 790, 793, 798, 801
 biopsy, 700, 706, 707, 717, 718, 727, 728,
 734, 735, 737, 765, 770, 779, 793
 iron concentration in, 700–702, 705, 707,
 716–718, 728, 731, 732, 734–738,
 776, 778, 789, 796, 798–800
 transplantation, 706, 710, 716, 719
- LOX (*see* Lipoxygenase)
- Lymphocytes, 467–473, 475, 513, 686
- Lymphoma, 514
- Lysosome, 74, 144, 348, 384, 432, 440, 607,
 726–728, 789
- Macrophages, 165, 429, 434, 437, 472–479,
 598, 602, 605, 616, 623, 629, 648,
 649, 651, 685, 688, 691 (*see also*
 Reticuloendothelial system)

- Magnesium, 26, 157, 261, 336, 413, 455, 555
- Magnetic resonance imaging, 707, 731, 750
- Magnetic susceptometry, 708, 734, 735, 793
- Manganese, 156, 158, 162, 261, 363, 366, 367, 383, 384, 413–415, 418, 453, 455, 459, 689
- MCF-7 cells, 513, 515
- Melanoma cells, 45, 96, 438, 440, 514, 517, 519, 521, 526
- Melanotransferrin, 42, 45, 96, 490, 517–519
- MEL cells, 655–657, 660–663, 666, 668
- Menadione, 220
- Microcytic mouse, 159, 459, 604, 653, 680, 681, 682
- Mitochondria, 181, 208, 213, 218, 221, 255–266, 386, 387, 437, 601, 626, 645, 647, 655, 657, 662–666, 726, 727, 730, 789, 796
- mk* (see Microcytic mouse)
- Mobilferrin, 180, 181, 562
- Molecular weight:
dependence of blood-brain barrier transport, 336
dependence of intestinal Fe transport, 333
- MRI (see Magnetic resonance imaging)
- MTP-1, 494, 650
- MTPT, 44
- myc*, 84, 141, 146, 219, 220, 525, 623, 630
- Myeloperoxidase, 478
- Myofibroblast, 628
- Myoglobin, 29, 404, 598, 599, 648, 781
- NAD(P)(H), 362, 377, 378, 441, 457, 543
- Neonate, 562, 564, 600
- Neoplastic cells/tissue, 509–528, 619, 621, 623, 629
- Neuroblastoma, 514, 524–526
- Neurodegenerative disease, 147, 158, 225, 257, 416, 488, 495, 498, 500, 501, 689, 718 (see also
Aceruloplasminemia; Alzheimer's disease; Friedrich's ataxia; Huntington's disease; Parkinson's disease)
- Neurons, 435, 498, 499, 599
- Neutrophils, 471, 478, 479
- Nickel, 3, 4, 24, 31, 156, 455, 459
- Nitric oxide and nitrogen radicals, 84, 219, 220–222, 225, 238, 396, 414, 437, 438, 460–462, 474, 477, 516, 621, 623, 644
- Nitric oxide synthases, 460–462, 477, 629
- Nitrotriacetate, 20–22, 24, 51, 101, 102, 109, 457, 470, 474, 515, 516, 521, 524
- Nitrogen radicals (see Nitric oxide and nitrogen radicals)
- Nramp1, 159, 162, 168, 182, 367, 471
- Nramp2 (see DMT1/Nramp2)
- Nramp homologs, 366, 367
- NTBI (see Iron, non-transferrin-bound)
- Oligodendrocytes, 491, 498, 499, 501, 502
- Ovotransferrin, 42, 43, 47, 50, 51, 96, 100, 109
- Oxidative stress, 84, 141–146, 220, 221, 415, 416, 622, 624, 627, 630, 631, 649, 789, 804 (see also Oxygen)
- Oxohydroxide, 135–137 (see also Ferrihydrite)
- Oxygen, 1, 4, 10, 148, 220, 223–225, 238, 249, 321, 322, 335, 378–380, 573, 574, 597, 618, 619, 624, 630, 631, 644–647, 649, 664 (see also Hypoxia; Oxidative stress)
reactive species/oxidative stress, 29–31, 146, 157, 165, 208, 213, 217, 220, 221, 223–225, 264, 265, 322, 335, 368, 379, 386, 396, 414, 451, 473, 475, 478, 488, 500, 515, 521, 528, 598, 601, 608, 623, 624, 627, 630, 632, 649, 726, 727, 730, 733, 788, 796, 807
- p22^{phox}, 377, 457
- Pancreas, 650, 685, 688, 702, 732, 750, 751 (see also Diabetes)
- Parkinson's disease, 44, 157, 488, 490, 500, 501, 608
- Phlebotomy, 648, 767, 771, 780, 782
- Phorbol ester, 141, 217
- Phosphatase, 221, 223, 224
- Phosphorylation, 217, 221, 223, 224, 468
- phu/Phu*, 404–406
- PIH (see Pyridoxal isonicotinyl hydrazones)
- Pinocytosis, 514, 515, 519
- Placenta, 428, 429, 431, 434–436, 600, 650, 682, 808
- Platinum, 379
- pM/pFe value, 17, 22–25, 296–300, 328, 330–332, 339, 342, 344, 349, 350
definition of, 17, 296, 330
- Polycythemia, 645

- Polyelectrolytes, 458
 Pons, 498, 499
 Porphyria cutanea tarda, 628, 717, 718
 Porphyrin, 9, 10, 28, 33, 34, 213, 334, 386,
 562, 644, 647, 648, 657, 659, 662,
 663, 665, 666, 685
 Potassium, 546, 801
 Pregnancy, 562, 563, 565, 795 (*see also*
 Placenta)
 Proerythroblast (*see* Erythroblast)
 Proteasome, 218, 219, 224, 513
 Protein kinase C, 217
 Proteoglycan, 440
 Proton transport, 97, 132, 158, 166, 168,
 360–363, 367, 376, 384, 412, 459,
 471, 540
 Protoporphyrins (*see* Porphyrin)
 P-type ATPase, 360, 382, 387, 750
 Putamen, 598
 Pyoverdinin, 287, 288, 419, 420
 Pyridoxal isonicotinyl hydrazones, 526, 527,
 795, 802, 803, 807
- Rab proteins, 462
 RAW264.7 cells, 221, 222
 Respiratory burst, 362, 479 (*see also*
 gp91^{phox}, p22^{phox})
 Reticulocytes, 79, 166, 431, 435, 492, 580,
 645–648, 655, 660, 662, 663, 668,
 681, 685, 802
 Reticuloendothelial system, 165, 197, 199,
 222, 429, 434, 437, 467–479, 564,
 615, 626, 648, 650, 689, 691, 718,
 727, 728, 735, 751, 752, 756, 758,
 790, 791, 802, 804, 807 (*see also*
 Macrophages)
 Rhodium, 305
 Rhodotorulic acid, 280, 289, 294, 299, 304
 Ribonucleotide reductase, 5, 6, 85, 334, 468,
 521, 601, 619, 647, 801
- Saxophilins, 42, 45
 Sertoli cells, 513
 SFT, 625
sfu/*Sfu*, 402
sfxn (*see* Flexed-tail mouse)
shu/*Shu*, 404–406
 Sick cell disease, 735
 Sideroflexin (*sfxn*) (*see* Flexed-tail mouse)
 Siderophores, 43, 274–308, 324, 333, 335,
 341, 360, 364, 365, 376, 384, 388,
 389, 396–400, 406, 407, 410, 411,
 [Siderophores]
 413, 419 (*see also* Desferrithiocin;
 Enterobactin; Pyoverdinin;
 Rhodotorulic acid)
 Siderosis (*see* Iron overload)
sit genes (bacterial), 403
SIT genes (yeast), 384
 Skin pigmentation, 704, 705
sla/*SLA*, 167, 182, 626, 650, 680, 682
slc11a2, 682
SMF genes, 376, 383, 384
 Sodium, 360
 Speciation plots, 326, 350
 Spleen, 165, 192, 428, 429, 475, 495, 514,
 598, 601, 602, 608, 644, 650, 585,
 686, 688, 689, 691, 728, 778, 790
 Splenectomy, 728
 SQUID (*see* Magnetic susceptometry)
SSQ/*Ssq*, 386, 387
 STAT5, 646
 Stellate cells (*see* Hepatic stellate cells)
 Stem cells (*see* Hematopoietic stem cells)
 Stem cell factor, 644
 Striatum, 498–500
 Strontium, 261
 Substantia nigra, 498–500, 598, 750, 751
 Succinate dehydrogenase, 84, 213, 215, 238,
 244
 Superoxide (*see* Oxygen, reactive species)
 Superoxide dismutase, 30, 208, 378, 381,
 414, 415, 727
 Symport, 376, 384 (*see also* Proton
 transport)
- Tbp proteins, 412–413
 Terbium, 135
 Thalamus, 498, 499
 Thalassemia, 80, 322, 346, 452, 469, 470,
 556, 563, 564, 573, 604, 608, 718,
 726–729, 731, 732, 734, 735, 788,
 789, 791, 792, 794, 798, 800, 801,
 804, 806–808
Toll, 245
 Ton proteins, 402, 404, 407, 410–414, 417,
 420
 Tpn proteins, 403, 406
 Transcytosis, 490, 491, 493, 494
 Transferrin-like proteins, 42, 45, 46, 180,
 403, 488
 Transferrin receptor, 43, 51, 72–87, 97, 99,
 146, 165–170, 180, 192–196, 199,
 209, 210, 214, 215, 223, 238, 245,
 428, 433, 438, 439, 441, 468, 470,

- [Transferrin receptor]
 473–478, 488, 489, 492–494, 498,
 502, 519, 521, 568, 572, 573, 578,
 614, 618, 619, 623, 624, 629, 645,
 649, 653, 656, 660, 662, 666, 683,
 684, 686, 758, 779, 790 (*see also*
 HFE, association with transferrin
 receptor)
 biosynthesis of, 75, 76
 crystal structure of, 80, 100
 endocytosis of, 72–74, 77, 97, 156, 195,
 430–437, 439, 440, 462, 469, 477,
 489, 494, 510, 514, 515, 519, 540,
 548, 576, 607, 614, 651
 exocytosis of, 74, 76, 77, 97, 492
 gene, 82, 83, 577
 knockout mouse, 577, 620, 660, 685
 mRNA, 83–85, 162, 210, 239, 458, 619,
 629
 translational regulation of by IRP, 83,
 84, 214, 220, 460, 475, 516, 568,
 618, 631, 619
 post-translational modification of, 75, 76,
 432
 shedding, 646, 660
 soluble form of, 79, 686, 801
 transcriptional regulation of, 85, 460,
 475, 477, 618, 619, 632, 660–662,
 666
 Transferrin receptor-like protein, 515
 Transferrin receptor-2, 42, 85–87, 245, 440,
 454, 474, 514, 515, 607, 620, 627,
 660
 Transferrins:
 functions of, 43, 96, 428
 genes/genetics of, 46, 569
 iron release from, 50, 51, 56, 72, 77, 96–
 117, 430, 441, 607, 689
 methods for determining, 98, 99
 pH effect, 97, 101, 106–108, 115–117,
 166, 195, 430, 431, 433, 440, 489,
 510, 515
 recombinant, 47, 51
 expression systems for, 51–56
 redox potential, 28, 30
 serum/plasma, 42, 43, 51–54, 96, 274,
 428, 429, 432, 518, 519, 616,
 632
 [Transferrins]
 saturation of, 430, 474, 571, 579, 599,
 608, 618, 700, 702, 705, 711, 712,
 715, 716, 765, 767, 777, 779
 site-directed mutagenesis of, 52, 47, 51,
 53, 54, 56, 97, 104–107, 109–115
 stability constants, 22, 165
 structure of, 46 ff., 96
 synthesis of, 616, 618, 631
 Transferrin saturation (*see* Transferrin,
 serum/plasma, saturation of)
 Transfusions (*see* Iron overload,
 transfusional)
 Transit iron pool (*see* Labile iron pool)
 Tumor necrosis factor, 608, 629

 Ubiquinone, 265
 Ubiquitin(ation), 218, 219, 224
UTRI, 378

 Vacuole, 142, 143, 387, 388, 615
 Vanadium, 4, 300
 Vct proteins, 407
 Viu proteins
 Vitamin B₁₂, 410
 Vitamin E, 265
vps mutants, 382

weh, 184, 690, 691
 Weissherbst (*see weh*)
 Wilson disease, 750, 751

 Xanthine oxidase, 572, 601, 624

 Yeast, 44, 53, 54, 162, 167, 170, 209, 217,
 218, 256, 259, 261–264, 266, 362,
 363, 367, 375, 381 (*see also* Iron,
 cellular uptake of)
Yersinia, 403–406, 413, 794
yfe genes, 403
YFH/Yfh, 256, 259, 261–264, 386–388
ys, 364, 365, 368

 Zebrafish, 650, 690, 691 (*see also weh*)
 Zinc, 2, 3, 14, 24, 156, 158, 323, 334–336,
 339, 343, 363, 366, 367, 403, 413,
 415, 453, 455, 459, 474, 519, 795,
 796, 798
ZIP genes, 366, 367
ZRT genes, 366, 367